Scientific and Technical Aerospace Reports

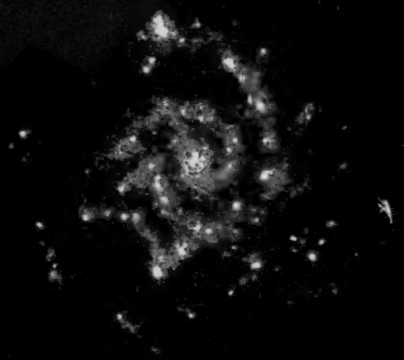

An Abstract Journal

Volume 32, Number 12
December 1994
N94-36441 to N94-37856

The NASA STI Program ... in Profile

Since its founding, NASA has been dedicated to the advancement of aeronautics and space science. The NASA Scientific and Technical Information (STI) Program plays a key part in helping NASA maintain this important role.

The NASA STI Program provides access to the NASA STI Database, the largest collection of aeronautical and space science STI in the world. The Program is also NASA's institutional mechanism for disseminating the results of its research and development activities.

Specialized services that help round out the Program's diverse offerings include creating custom thesauri, translating material to or from 34 foreign languages, building customized databases, organizing and publishing research results ... even providing videos.

For more information about the NASA STI Program, you can:

- **Phone** the NASA Access Help Desk at (301) 621-0390
- **Fax** your question to the NASA Access Help Desk at (301) 621-0134
- **E-mail** your question via the **Internet** to help@sti.nasa.gov
- **Write** to:

NASA Access Help Desk
NASA Center for AeroSpace Information
800 Elkridge Landing Road
Linthicum Heights, MD 21090-2934

Scientific and Technical Aerospace Reports

Scientific and Technical Aerospace Reports (STAR), is published each month as a major product of the NASA Scientific and Technical Information (STI) Program.

Inside this issue you will find:

- **Front Matter** containing a typical citation and abstract sample explaining the standard format, including codes for ordering reports
- **An Abstract Section** containing citations and abstracts of reports and publications that provide comprehensive coverage of worldwide aerospace-related topics including aeronautics and space science technology. *STAR* lists published and publicly available reports entered into the NASA STI Database during the four weeks preceding publication of this issue. These citations and abstracts are listed by subject categories.
- **An Index Section**
  - Subject
  - Personal author
  - Corporate source
  - Contract number
  - Report number
- **An Appendix** containing a guide for ordering cited reports, registering with the NASA STI Program, and using the available products and services. Additionally, price schedules, phone numbers, and addresses are included in this information packed section.

NASA also sponsors the companion journal, *NASA Open Volumes on Aerospace (NOVA)*, which lists abstracts of the open literature on aerospace subjects available worldwide. *NOVA* is for internal NASA use only, available from the NASA Center for AeroSpace Information (CASI).

Entries found in *STAR* are available through the NASA online retrieval service, RECON, and through DIALOG as the Aerospace Database.

The NASA STI Program gathers information through national and international agreements and exchanges and makes this information available to the NASA community and to the public in many forms through various outlets.

For additional information on the NASA STI Program, call the NASA Access Help Desk at (301) 621-0390, or write to:

NASA Center for AeroSpace Information
800 Elkridge Landing Road
Linthicum Heights, Maryland 21090-2934

US ISSN 0036-8741

This publication was prepared by the NASA Center for AeroSpace Information,
800 Elkridge Landing Road, Linthicum Heights, MD 21090-2934, (301) 621-0390.

Volume 32 Number 12 / December 1994

TABLE OF CONTENTS

AERONAUTICS For related information see also *Astronautics.*

01 AERONAUTICS (GENERAL) **4381**

02 AERODYNAMICS **4381**
Includes aerodynamics of bodies, combinations, wings, rotors, and control surfaces; and internal flow in ducts and turbomachinery. For related information see also *34 Fluid Mechanics and Heat Transfer.*

03 AIR TRANSPORTATION AND SAFETY **4384**
Includes passenger and cargo air transport operations; and aircraft accidents. For related information see also *16 Space Transportation* and *85 Urban Technology and Transportation.*

04 AIRCRAFT COMMUNICATIONS AND NAVIGATION **4385**
Includes digital and voice communication with aircraft; air navigation systems (satellite and ground based); and air traffic control. For related information see also *17 Space Communications, Spacecraft Communications, Command and Tracking* and *32 Communications and Radar.*

05 AIRCRAFT DESIGN, TESTING AND PERFORMANCE **4386**
Includes aircraft simulation technology. For related information see also *18 Spacecraft Design, Testing and Performance* and *39 Structural Mechanics.* For land transportation vehicles see *85 Urban Technology and Transportation.*

06 AIRCRAFT INSTRUMENTATION **4387**
Includes cockpit and cabin display devices; and flight instruments. For related information see also *19 Spacecraft Instrumentation* and *35 Instrumentation and Photography.*

07 AIRCRAFT PROPULSION AND POWER **4387**
Includes prime propulsion systems and systems components, e.g., gas turbine engines and compressors; and onboard auxiliary power plants for aircraft. For related information see also *20 Spacecraft Propulsion and Power, 28 Propellants and Fuels,* and *44 Energy Production and Conversion.*

08 AIRCRAFT STABILITY AND CONTROL **4388**
Includes aircraft handling qualities; piloting; flight controls; and autopilots. For related information see also *05 Aircraft Design, Testing and Performance.*

09 RESEARCH AND SUPPORT FACILITIES (AIR) **4389**
Includes airports, hangars and runways; aircraft repair and overhaul facilities; wind tunnels; shock tubes; and aircraft engine test stands. For related information see also *14 Ground Support Systems and Facilities (Space).*

ASTRONAUTICS For related information see also *Aeronautics.*

12 ASTRONAUTICS (GENERAL) **4391**
For extraterrestrial exploration see *91 Lunar and Planetary Exploration.*

13 ASTRODYNAMICS ..... **N.A.**
Includes powered and free-flight trajectories; and orbital and launching dynamics.

14 GROUND SUPPORT SYSTEMS AND FACILITIES (SPACE) **4391**
Includes launch complexes, research and production facilities; ground support equipment, e.g., mobile transporters; and simulators. For related information see also *09 Research and Support Facilities (Air).*

15 LAUNCH VEHICLES AND SPACE VEHICLES ..... **N.A.**
Includes boosters; operating problems of launch/space vehicle systems; and reusable vehicles. For related information see also *20 Spacecraft Propulsion and Power.*

16 SPACE TRANSPORTATION **4392**
Includes passenger and cargo space transportation, e.g., shuttle operations; and space rescue techniques. For related information see also *03 Air Transportation and Safety* and *18 Spacecraft Design, Testing and Performance.* For space suits see *54 Man/System Technology and Life Support.*

17 SPACE COMMUNICATIONS, SPACECRAFT COMMUNICATIONS, COMMAND AND TRACKING **4392**
Includes telemetry; space communications networks; astronavigation and guidance; and radio blackout. For related information see also *04 Aircraft Communications and Navigation* and *32 Communications and Radar.*

N.A.—No abstracts were assigned to this category for this issue.

18 SPACECRAFT DESIGN, TESTING AND PERFORMANCE **4392**
Includes satellites; space platforms; space stations; spacecraft systems and components such as thermal and environmental controls; and attitude controls. For life support systems see *54 Man/System Technology and Life Support.* For related information see also *05 Aircraft Design, Testing and Performance, 39 Structural Mechanics,* and *16 Space Transportation.*

19 SPACECRAFT INSTRUMENTATION **4397**
For related information see also *06 Aircraft Instrumentation* and *35 Instrumentation and Photography.*

20 SPACECRAFT PROPULSION AND POWER **4398**
Includes main propulsion systems and components, e.g., rocket engines; and spacecraft auxiliary power sources. For related information see also *07 Aircraft Propulsion and Power, 28 Propellants and Fuels, 44 Energy Production and Conversion,* and *15 Launch Vehicles and Space Vehicles.*

CHEMISTRY AND MATERIALS

23 CHEMISTRY AND MATERIALS (GENERAL) **4399**

24 COMPOSITE MATERIALS **4400**
Includes physical, chemical, and mechanical properties of laminates and other composite materials. For ceramic materials see *27 Nonmetallic Materials.*

25 INORGANIC AND PHYSICAL CHEMISTRY **4406**
Includes chemical analysis, e.g., chromatography; combustion theory; electrochemistry; and photochemistry. For related information see also *77 Thermodynamics and Statistical Physics.*

26 METALLIC MATERIALS **4414**
Includes physical, chemical, and mechanical properties of metals, e.g., corrosion; and metallurgy.

27 NONMETALLIC MATERIALS **4421**
Includes physical, chemical, and mechanical properties of plastics, elastomers, lubricants, polymers, textiles, adhesives, and ceramic materials. For composite materials see *24 Composite Materials.*

28 PROPELLANTS AND FUELS **4428**
Includes rocket propellants, igniters and oxidizers; their storage and handling procedures; and aircraft fuels. For related information see also *07 Aircraft Propulsion and Power, 20 Spacecraft Propulsion and Power,* and *44 Energy Production and Conversion.*

29 MATERIALS PROCESSING **4430**
Includes space-based development of products and processes for commercial application. For biological materials see *55 Space Biology:*

ENGINEERING For related information see also *Physics.*

31 ENGINEERING (GENERAL) **4430**
Includes vacuum technology; control engineering; display engineering; cryogenics; and fire prevention.

32 COMMUNICATIONS AND RADAR **4432**
Includes radar; land and global communications; communications theory; and optical communications. For related information see also *04 Aircraft Communications and Navigation* and *17 Space Communications, Spacecraft Communications, Command and Tracking.* For search and rescue see *03 Air Transportation and Safety,* and *16 Space Transportation.*

33 ELECTRONICS AND ELECTRICAL ENGINEERING **4436**
Includes test equipment and maintainability; components, e.g., tunnel diodes and transistors; microminiaturization; and integrated circuitry. For related information see also *60 Computer Operations and Hardware* and *76 Solid-State Physics.*

34 FLUID MECHANICS AND HEAT TRANSFER **4441**
Includes boundary layers; hydrodynamics; fluidics; mass transfer and ablation cooling. For related information see also *02 Aerodynamics* and *77 Thermodynamics and Statistical Physics.*

35 INSTRUMENTATION AND PHOTOGRAPHY **4445**
Includes remote sensors; measuring instruments and gauges; detectors; cameras and photographic supplies; and holography. For aerial photography see *43 Earth Resources and Remote Sensing.* For related information see also *06 Aircraft Instrumentation* and *19 Spacecraft Instrumentation.*

36 LASERS AND MASERS **4447**
Includes parametric amplifiers. For related information see also *76 Solid-State Physics.*

37 MECHANICAL ENGINEERING **4450**
Includes auxiliary systems (nonpower); machine elements and processes; and mechanical equipment.

38 QUALITY ASSURANCE AND RELIABILITY **4453**
Includes product sampling procedures and techniques; and quality control.

39 STRUCTURAL MECHANICS **4455**
Includes structural element design and weight analysis; fatigue; and thermal stress. For applications see *05 Aircraft Design, Testing and Performance* and *18 Spacecraft Design, Testing and Performance.*

GEOSCIENCES For related information see also *Space Sciences.*

42 GEOSCIENCES (GENERAL) ..... **N.A.**

43 EARTH RESOURCES AND REMOTE SENSING **4461**
Includes remote sensing of earth resources by aircraft and spacecraft; photogrammetry; and aerial photography. For instrumentation see *35 Instrumentation and Photography.*

44 ENERGY PRODUCTION AND CONVERSION **4461**
Includes specific energy conversion systems, e.g., fuel cells; global sources of energy; geophysical conversion; and windpower. For related information see also *07 Aircraft Propulsion and Power, 20 Spacecraft Propulsion and Power,* and *28 Propellants and Fuels.*

45 ENVIRONMENT POLLUTION **4463**
Includes atmospheric, noise, thermal, and water pollution.

46 GEOPHYSICS **4468**
Includes aeronomy; upper and lower atmosphere studies; ionospheric and magnetospheric physics; and geomagnetism. For space radiation see *93 Space Radiation.*

47 METEOROLOGY AND CLIMATOLOGY **4471**
Includes weather forecasting and modification.

48 OCEANOGRAPHY **4475**
Includes biological, dynamic, and physical oceanography; and marine resources. For related information see also *43 Earth Resources and Remote Sensing.*

LIFE SCIENCES

51 LIFE SCIENCES (GENERAL) **4477**

52 AEROSPACE MEDICINE **4480**
Includes physiological factors; biological effects of radiation; and effects of weightlessness on man and animals.

53 BEHAVIORAL SCIENCES **4482**
Includes psychological factors; individual and group behavior; crew training and evaluation; and psychiatric research.

54 MAN/SYSTEM TECHNOLOGY AND LIFE SUPPORT **4486**
Includes human engineering; biotechnology; and space suits and protective clothing. For related information see also *16 Space Transportation.*

55 SPACE BIOLOGY ..... **N.A.**
Includes exobiology; planetary biology; and extraterrestrial life.

MATHEMATICAL AND COMPUTER SCIENCES

59 MATHEMATICAL AND COMPUTER SCIENCES (GENERAL) ..... **N.A.**

60 COMPUTER OPERATIONS AND HARDWARE **4489**
Includes hardware for computer graphics, firmware, and data processing. For components see *33 Electronics and Electrical Engineering.*

61 COMPUTER PROGRAMMING AND SOFTWARE **4489**
Includes computer programs, routines, algorithms, and specific applications, e.g., CAD/CAM.

62 COMPUTER SYSTEMS **4497**
Includes computer networks and special application computer systems.

63 CYBERNETICS **4499**
Includes feedback and control theory, artificial intelligence, robotics and expert systems. For related information see also *54 Man/System Technology and Life Support.*

64 NUMERICAL ANALYSIS **4502**
Includes iteration, difference equations, and numerical approximation.

65 STATISTICS AND PROBABILITY **4506**
Includes data sampling and smoothing; Monte Carlo method; and stochastic processes.

66 SYSTEMS ANALYSIS **4507**
Includes mathematical modeling; network analysis; and operations research.

67 THEORETICAL MATHEMATICS **4507**
Includes topology and number theory.

PHYSICS For related information see also *Engineering.*

70 PHYSICS (GENERAL) **4508**
For precision time and time interval (PTTI) see *35 Instrumentation and Photography*; for geophysics, astrophysics or solar physics see *46 Geophysics, 90 Astrophysics*, or *92 Solar Physics.*

71 ACOUSTICS **4510**
Includes sound generation, transmission, and attenuation. For noise pollution see *45 Environment Pollution.*

72 ATOMIC AND MOLECULAR PHYSICS **4510**
Includes atomic structure, electron properties, and molecular spectra.

73 NUCLEAR AND HIGH-ENERGY PHYSICS **4521**
Includes elementary and nuclear particles; and reactor theory. For space radiation see *93 Space Radiation.*

74 OPTICS **4523**
Includes light phenomena and optical devices. For lasers see *36 Lasers and Masers.*

75 PLASMA PHYSICS **4526**
Includes magnetohydrodynamics and plasma fusion. For ionospheric plasmas see *46 Geophysics.* For space plasmas see *90 Astrophysics.*

76 SOLID-STATE PHYSICS **4532**
Includes superconductivity. For related information see also *33 Electronics and Electrical Engineering* and *36 Lasers and Masers.*

77 THERMODYNAMICS AND STATISTICAL PHYSICS **4539**
Includes quantum mechanics; theoretical physics; and Bose and Fermi statistics. For related information see also *25 Inorganic and Physical Chemistry* and *34 Fluid Mechanics and Heat Transfer.*

SOCIAL SCIENCES

80 SOCIAL SCIENCES (GENERAL) **4540**
Includes educational matters.

81 ADMINISTRATION AND MANAGEMENT **4540**
Includes management planning and research.

82 DOCUMENTATION AND INFORMATION SCIENCE **4540**
Includes information management; information storage and retrieval technology; technical writing; graphic arts; and micrography. For computer documentation see *61 Computer Programming and Software.*

83 ECONOMICS AND COST ANALYSIS ..... **N.A.**
Includes cost effectiveness studies.

84 LAW, POLITICAL SCIENCE AND SPACE POLICY ..... **N.A.**
Includes NASA appropriation hearings; aviation law; space law and policy; international law; international cooperation; and patent policy.

85 URBAN TECHNOLOGY AND TRANSPORTATION **4546**
Includes applications of space technology to urban problems; technology transfer; technology assessment; and surface and mass transportation. For related information see *03 Air Transportation and Safety, 16 Space Transportation,* and *44 Energy Production and Conversion.*

SPACE SCIENCES For related information see also *Geosciences.*

88 SPACE SCIENCES (GENERAL) ..... **N.A.**

89 ASTRONOMY **4546**
Includes radio, gamma-ray, and infrared astronomy; and astrometry.

90 ASTROPHYSICS **4548**
Includes cosmology; celestial mechanics; space plasmas; and interstellar and interplanetary gases and dust. For related information see also *75 Plasma Physics.*

91 LUNAR AND PLANETARY EXPLORATION **4549**
Includes planetology; and manned and unmanned flights. For spacecraft design or space stations see *18 Spacecraft Design, Testing and Performance.*

92 SOLAR PHYSICS **4549**
Includes solar activity, solar flares, solar radiation and sunspots. For related information see also *93 Space Radiation.*

93 SPACE RADIATION **4549**
Includes cosmic radiation; and inner and outer earth's radiation belts. For biological effects of radiation see *52 Aerospace Medicine.* For theory see *73 Nuclear and High-Energy Physics.*

GENERAL

Includes aeronautical, astronautical, and space science related histories, biographies, and pertinent reports too broad for categorization; histories or broad overviews of NASA programs.

99 GENERAL **4550**

SUBJECT INDEX **I-1**

PERSONAL AUTHOR INDEX **I-81**

CORPORATE SOURCE INDEX **I-91**

CONTRACT NUMBER INDEX **I-105**

REPORT NUMBER INDEX **I-109**

APPENDIX **A-1**

TYPICAL CITATION AND ABSTRACT

NASA SPONSORED — ON MICROFICHE

ACCESSION NUMBER → **N94-12270*#** United Technologies Corp., West Palm Beach, FL. ← CORPORATE SOURCE
Pratt and Whitney.

TITLE → **ADVANCED CONTROL FOR AIRBREATHING ENGINES, VOLUME 1: PRATT AND WHITNEY**

AUTHOR → J. A. Ralph Jul. 1993 83 p ← PUBLICATION DATE

CONTRACT OR GRANT → (Contract NAS3-25952; RTOP 505-62-61)

REPORT NUMBERS → (NASA-CR-189203; E-8006; NAS 1.26:189203) Avail: CASI HC A05/MF A01 ← AVAILABILITY SOURCE AND PRICE CODE

The application of advanced control concepts to air breathing engines may yield significant improvements in aircraft/engine performance and operability. Screening studies of advanced control concepts for air breathing engines were conducted by three major domestic aircraft engine manufacturers to determine the potential impact of concepts on turbine engine performance and operability. The purpose of the studies was to identify concepts which offered high potential yet may incur high research and development risk. A target suite of proposed advanced control concepts was formulated and evaluated in a two phase study to quantify each concept's impact on desired engine characteristics. To aid in the evaluation specific aircraft/engine combinations were considered: a Military High Performance Fighter mission, a High Speed Civil Transport mission, and a Civil Tiltrotor mission. Each of the advanced control concepts considered in the study are defined and described. The concept potential impact on engine performance was determined. Relevant figures of merit on which to evaluate the concepts are determined. Finally, the concepts are ranked with respect to the target aircraft/engine missions. A final report describing the screening studies was prepared by each engine manufacturer. Volume 1 of these reports describes the studies performed by Pratt & Whitney. Author (revised)

VOLUME 32 NUMBER 12 / December 1994

Scientific and Technical Aerospace Reports

A Monthly Publication of the National Aeronautics and Space Administration

01 AERONAUTICS (GENERAL)

N94-36648*# National Aeronautics and Space Administration. Hugh L. Dryden Flight Research Facility, Edwards, CA.
PRELIMINARY ANALYSIS FOR A MACH 8 CROSSFLOW TRANSITION EXPERIMENT ON THE PEGASUS (R) SPACE BOOSTER
Leslie Gong, W. Lance Richards, Richard C. Monaghan, and Robert D. Quinn Nov. 1993 23 p Presented at the Society for Experimenal Mechanics, Structural Testing Technology at High Temperature 2 Conference, Ojai, CA, 8-10 Nov. 1993
(RTOP 505-70-91)
(NASA-TM-104272; H-1954; NAS 1.15:104272) Avail: CASI HC A03/MF A01

A boundary-layer transition is proposed for a future flight mission of the air-launched Pegasus space booster. The flight experiment requires attaching a glove assembly to the wing of the first-stage booster. The glove design consists of a spring and hook attachment system which allows for thermal growth of a steel 4130 skin. The results from one- and two-dimensional thermal analyses of the initial design are presented. Results obtained from the thermal analysis using turbulent flow conditions showed a maximum temperature of approximately 305 C and a chordwise temperature gradient of less than 8.9 C/cm for the critical areas in the upper glove skin. The temperatures obtained from these thermal analyses are well within the required temperature limits of the glove. Author (revised)

N94-37117* National Aeronautics and Space Administration, Washington, DC.
AERONAUTICAL ENGINEERING: A CONTINUING BIBLIOGRAPHY WITH INDEXES (SUPPLEMENT 307)
Aug. 1994 118 p
(NASA-SP-7037(307); NAS 1.21:7037(307)) Avail: CASI HC A06

This bibliography lists 338 reports, articles, and other documents introduced into the NASA scientific and technical information system in Aug. 1994. Subject coverage includes: design, construction and testing of aircraft and aircraft engines; aircraft components, equipment, and systems; ground support systems; and theoretical and applied aspects of aerodynamics and general fluid dynamics. Author

N94-37332*# National Aeronautics and Space Administration. Ames Research Center, Moffett Field, CA.
TRENDS: A FLIGHT TEST RELATIONAL DATABASE USER'S GUIDE AND REFERENCE MANUAL
M. J. Bondi, W. S. Bjorkman, and J. L. Cross Jun. 1994 286 p See also N90-25149
(RTOP 505-59-36)
(NASA-TM-108806; A-94042; NAS 1.15:108806) Avail: CASI HC A13/MF A03

This report is designed to be a user's guide and reference manual for users intending to access rotocraft test data via TRENDS, the relational database system which was developed as a tool for the aeronautical engineer with no programming background. This report has been written to assist novice and experienced TRENDS users. TRENDS is a complete system for retrieving, searching, and analyzing both numerical and narrative data, and for displaying time history and statistical data in graphical and numerical formats. This manual provides a 'guided tour' and a 'user's guide' for the new and intermediate-skilled users. Examples for the use of each menu item within TRENDS is provided in the Menu Reference section of the manual, including full coverage for TIMEHIST, one of the key tools. This manual is written around the XV-15 Tilt Rotor database, but does include an appendix on the UH-60 Blackhawk database. This user's guide and reference manual establishes a referrable source for the research community and augments NASA TM-101025, TRENDS: The Aeronautical Post-Test, Database Management System, Jan. 1990, written by the same authors. Author (revised)

N94-37352 Naval Postgraduate School, Monterey, CA.
PLANNING GERMAN ARMY HELICOPTER MAINTENANCE AND MISSION ASSIGNMENT M.S. Thesis
Achim Sgaslik Mar. 1994 106 p Limited Reproducibility: More than 20% of this document may be affected by microfiche quality
(AD-A280483) Avail: CASI HC A06

German Army light helicopter transportation regimens operate 45 Bell UH-1D helicopters to support demanding missions throughout Europe. Maintenance period scheduling, major exercise and regular mission assignment decisions directly influence the readiness of the helicopter fleet. Currently, all planning is done manually, which is unstructured and time consuming. This thesis describes a decision support system designed to assist with maintenance planning and mission assignment. The yearly maintenance and event scheduling problem and the short term mission assignment tasks are formulated and solved as elastic mixed integer linear programs. Resulting yearly schedules and short term sortie plans are both generated in a fraction of the time previously required with solution quality superior to their manual counterparts. DTIC

02 AERODYNAMICS

Includes aerodynamics of bodies, combinations, wings, rotors, and control surfaces; and internal flow in ducts and turbomachinery.

For related information see also *34 Fluid Mechanics and Heat Transfer.*

N94-36466# EMA, Mansfield, TX.
ROTORWASH ANALYSIS HANDBOOK. VOLUME 1: DEVELOPMENT AND ANALYSIS Final Report
Samuel W. Ferguson Jun. 1994 336 p Prepared for Systems Control Technology, Inc., Arlington, VA
(Contract DTFA01-87-C-00014)
(SCT-93RR-17-Vol-1; DOT/FAA/RD-93-31-Vol-1) Avail: CASI HC A15/MF A03

Rotorcraft operations at heliports and airports are investigated to better understand and quantify the potential hazards associated with various types of rotorwash flow fields. Mathematical models for the various types are developed. These mathematical models are used in conjunction with hazard analysis models to develop an analysis methodology for evaluation of the potential for rotorwash-related mishaps in various operational scenarios. Correlation of all developed mathematical models with flight test, scale-model, and laboratory test data is provided wherever possible. Heliport design examples using the developed analysis methodology and the associated ROTWASH computer program are provided. Documentation, a program listing, and a user's guide are provided for version 2.1 of the FORTRAN 77-based ROTWASH computer program in report appendices (see Volume 2 of this report). An extensive bibliography of rotorwash related technical documents is also provided. Author (revised)

N94-36467# EMA, Mansfield, TX.
ROTORWASH ANALYSIS HANDBOOK. VOLUME 2: APPENDIXES Final Report
Samuel W. Ferguson Jun. 1994 192 p Prepared for Systems Control Technology, Inc., Arlington, VA
(Contract DTFA01-87-C-00014)
(SCT-93RR-17-Vol-2; DOT/FAA/RD-93-31-Vol-2) Avail: CASI HC A09/MF A02

Documentation, a program listing, and a user's guide are provided for version 2.1 of the FORTRAN 77-based ROTWASH computer program in report appendices. An extensive bibliography of rotorwash related technical documents is also provided. This listing is subdivided into different rotorwash topics. A companion report, entitled 'Evaluation of Rotorwash Characteristics for Tiltrotor and Tiltwing Aircraft in Hovering Flight,' DOT/FAA/RD-90/16, evaluates rotorwash characteristics of 11 different types of tiltrotor and tiltwing aircraft for comparison purposes. Another companion report, entitled 'Analysis of Rotorwash Effects in Helicopter Mishaps,' DOT/FAA/RD-90/17, presents an analysis of several of the more common types of rotorwash related helicopter mishaps. Much of the information provided in this second companion report is updated by this report. A third report, DOT/FAA/RD-90/25, 'Rotorwash Computer Model - User's Guide,' is replaced by this more comprehensive report and its updated version of the ROTWASH computer program. Author

N94-36686*# National Aeronautics and Space Administration. Lewis Research Center, Cleveland, OH.
MIXING AND NOISE BENEFIT VERSUS THRUST PENALTY IN SUPERSONIC JETS USING IMPINGEMENT TONES
Ganesh Raman (NYMA, Inc., Brook Park, OH.) and Edward J. Rice May 1994 17 p Proposed for presentation at the 30th Joint Propulsion Conference, Indianapolis, IN, 27-29 Jun. 1994; sponsored by AIAA, ASME, SAE, and ASEE
(Contract NAS3-27186; RTOP 537-02-22)
(NASA-TM-106583; E-8844; NAS 1.15:106583; AIAA Paper 94-2955)
Avail: CASI HC A03/MF A01

This paper reports the results of an experimental investigation on the effect of impingement tones generated by obstacles of various geometries on the spreading of a supersonic jet flow. A rectangular supersonic jet was produced using a convergent-divergent nozzle that was operated near its design point (with shocks minimized). The immersion of obstacles in the flow produced an intense impingement tone which then propagated upstream (as feedback) to the jet lip and excited the antisymmetric hydrodynamic mode in the jet, thus setting up a resonant self-sustaining loop. The violent flapping motion of the jet due to excitation of the antisymmetric mode, combined with the unsteady wakes of the obstacles, produced large changes in jet mixing. It was possible to control the frequency and amplitude of the impingement tone excitation by varying the nozzle-to-obstacle distance and the obstacle immersion. By proper shaping of the obstacles it was possible to reduce the thrust penalty significantly.
Author

N94-36687*# Eloret Corp., Palo Alto, CA.
EXPERIMENTAL INVESTIGATION OF NOZZLE/PLUME AERODYNAMICS AT HYPERSONIC SPEEDS Final Technical Report, 1 Aug. 1987 - 31 Jan. 1994
David W. Bogdanoff, Jean-Luc Cambier, and Perikles Papadopoulos 29 Apr. 1994 15 p
(Contract NCC2-487)
(NASA-CR-195829; NAS 1.26:195829) Avail: CASI HC A03/MF A01

Much of the work involved the Ames 16-Inch Shock Tunnel facility. The facility was reactivated and upgraded, a data acquisition system was configured and upgraded several times, several facility calibrations were performed and test entries with a wedge model with hydrogen injection and a full scramjet combustor model, with hydrogen injection, were performed. Extensive CFD modeling of the flow in the facility was done. This includes modeling of the unsteady flow in the driver and driven tubes and steady flow modeling of the nozzle flow. Other modeling efforts include simulations of non-equilibrium flows and turbulence, plasmas, light gas guns and the use of non-ideal gas equations of state. New experimental techniques to improve the performance of gas guns, shock tubes and tunnels and scramjet combustors were conceived and studied computationally. Ways to improve scramjet engine performance using steady and pulsed detonation waves were also studied computationally. A number of studies were performed on the operation of the ram accelerator, including investigations of in-tube gasdynamic heating and the use of high explosives to raise the velocity capability of the device. Author (revised)

N94-36729# Air Force Inst. of Tech., Wright-Patterson AFB, OH. School of Engineering.
AN AERODYNAMIC AND STATIC-STABILITY ANALYSIS OF THE HYPERSONIC APPLIED RESEARCH TECHNOLOGY (HART) MISSILE Ph.D. Thesis
Kenneth J. Moran Apr. 1994 124 p
(AD-A280631; AFIT/DS/AA/94-3) Avail: CASI HC A06/MF A02

The flow about the complete Hypersonic Applied Research Technology (HART) missile is simulated for inviscid, laminar, and turbulent conditions and Mach numbers from 2 to 6. An explicit, second-order-accurate, flux-difference-splitting, algorithm is implemented and employed to solve the Navier-Stokes equations. The equations are solved using a finite volume methodology. The aerodynamic and static-stability characteristics are investigated to determine if conventional supersonic missile configurations can be flown at Mach numbers higher than 5. The effects of nosetip blunting and boundary-layer condition are demonstrated. The structure of the flow near the fins is significantly affected by the turbulent transport of momentum in regions of blocked cross flow. Turbulence and the blockage phenomenon cause bleeding around the fin leading edges. Ultimately, this results in lower fin effectiveness and reduced static stability. The aerodynamic characteristics of the HART missile are predicted at Mach numbers beyond the experimental free-flight testing capabilities. The current predictions indicated that the pitching-moment coefficient decreases with increasing Mach number much less than previous numerical computations. The present results also suggest that the clipped-delta-fin configuration is stable beyond Mach 7. DTIC

N94-36741*# National Aeronautics and Space Administration. Langley Research Center, Hampton, VA.
A SHADOWGRAPH STUDY OF SPACE TRANSPORTATION SYSTEM (STS): THE SPACE SHUTTLE LAUNCH VEHICLE (SSLV)
A. M. Springer Jun. 1994 95 p
(NASA-RP-1341; M-752; NAS 1.61-1341) Avail: CASI HC A05/MF A01

A shadowgraph study of the space transportation system (STS), the space shuttle launch vehicle, is presented. The shadowgraphs presented in this study were obtained over the past 10 years from wind tunnel tests performed in the NASA Marshall Space Flight Center's 14-Inch Trisonic Wind Tunnel during the space shuttle development program. Shadowgraphs of the STS at various angles-of-attack and roll angles are shown for the Mach range of 0.6 to 4.96. The major flow field phenomena over the mated vehicle configuration are shown in these shadowgraphs. Shadowgraphs are also presented for the orbiter without the lower stack (reentry configuration) and the lower stack without the orbiter. A short study of external tank nose geometry effects on the mated vehicles flow field is presented. These shadowgraphs are used in the aerothermodynamic analysis of the external flow conditions the launch vehicle encounters during the ascent stage of flight. Author

N94-36942*# National Aeronautics and Space Administration. Langley Research Center, Hampton, VA.
AUTOMATIC PROCEDURES FOR COMPUTING COMPLETE CONFIGURATION GEOMETRY FROM INDIVIDUAL COMPONENT DESCRIPTIONS
Raymond L. Barger and Mary S. Adams Jul. 1994 14 p
(RTOP 509-10-11-01)
(NASA-TM-4607; L-17395; NAS 1.15:4607) Avail: CASI HC A03/MF A01

Procedures are derived for developing a complete airplane surface geometry starting from component descriptions. The procedures involve locating the intersection lines of adjacent components and omitting any regions for which part of one surface lies within the other. The geometry files utilize the wave-drag (Harris) format, and output files are written in Hess format. Two algorithms are used: one, if both intersecting surfaces have airfoil cross sections; the other, if one of the surfaces has circular cross sections. Some sample results in graphical form are included.
Author

N94-36944*# National Aeronautics and Space Administration. Hugh L. Dryden Flight Research Center, Edwards, CA.

CONTROLLING FOREBODY ASYMMETRIES IN FLIGHT: EXPERIENCE WITH BOUNDARY LAYER TRANSITION STRIPS

David F. Fisher and Brent R. Cobleigh Washington Jul. 1994 22 p Presented at the 6th Biennial Flight Test Conference, Colorado Springs, CO, 20-23 Jun. 1994

(RTOP 505-68-71)

(NASA-TM-4595; H-1992; NAS 1.15:4595; AIAA Paper 94-1826)

Copyright Avail: CASI HC A01/MF A01

The NASA Dryden Flight Research Center has an ongoing program to investigate aircraft flight characteristics at high angles of attack. As part of this investigation, longitudinal boundary layer transition strips were installed on the F-18 HARV forebody, a preproduction F/A-18 radome with a nose-slice tendency, and the X-31 aircraft forebody and noseboom to reduce asymmetric yawing moments at high angles of attack. The transition strips were effective on the F-18 HARV at angles of attack above 60 deg. On the preproduction F/A-18 radome at an angle of attack near 50 deg the strips were not effective. When the transition strips were installed on the X-31 noseboom, a favorable effect was observed on the yawing moment dynamics but the magnitude of the yawing moment was not decreased. Author

N94-36950*# National Aeronautics and Space Administration. Langley Research Center, Hampton, VA.

AUTOMATIC COMPUTATION OF EULER-MARCHING AND SUBSONIC GRIDS FOR WING-FUSELAGE CONFIGURATIONS

Raymond L. Barger, Mary S. Adams, and Ramki R. Krishnan Jul. 1994 20 p

(RTOP 509-10-11-01)

(NASA-TM-4573; L-17364; NAS 1.15:4573) Avail: CASI HC A03/MF A01

Algebraic procedures are described for the automatic generation of structured, single-block flow computation grids for relatively simple configurations (wing, fuselage, and fin). For supersonic flows, a quasi two-dimensional grid for Euler-marching codes is developed, and some sample results in graphical form are included. A type of grid for subsonic flow calculation is also described. The techniques are algebraic and are based on a generalization of the method of transfinite interpolation. Author

N94-36966*# National Aeronautics and Space Administration. Langley Research Center, Hampton, VA.

NAVIER-STOKES AND POTENTIAL THEORY SOLUTIONS FOR AHELICOPTER FUSELAGE AND COMPARISON WITH EXPERIMENT

Mark S. Chaffin (Vigyan Research Associates, Inc., Hampton, VA.) and John D. Berry (Army Aviation Systems Command, Hampton, VA.) Jun. 1994 31 p Prepared in cooperation with Army Aviation Systems Command, Hampton, VA

(Contract NAS1-19672; RTOP 505-59-36-01; RTOP 023-10-01-01)

(NASA-TM-4566; L-17325; NAS 1.15:4566; ATCOM-TR-94-A-013) Avail: CASI HC A03/MF A01

A thin-layer Navier-Stokes code and a panel method code are used to predict the flow over a generic helicopter fuselage. The computational results are compared with pressure data at four experimental conditions. Both methods produce results that agree with the experimental pressure data. However, separation patterns and other viscous flow features from the Navier-Stokes code solution are shown that cannot be easily modeled with the panel method. Author

N94-37219 Michigan State Univ., East Lansing, MI. Dept. of Mechanical Engineering.

UNSTEADY FLOW FIELD OF LARGE-AMPLITUDE PITCHING AIRFOILS Final Technical Report, Jul. 1992 - Nov. 1993

Manoochehr M. Koochesfahani 1 Feb. 1994 33 p Limited Reproducibility: More than 20% of this document may be affected by microfiche quality

(Contract AF-AFOSR-0417-89)

(AD-A280444; AFOSR-94-0355TR) Avail: Issuing Activity (Defense Technical Information Center (DTIC))

This research program investigated the physical mechanisms involved in the onset of leading edge separation when airfoils pitch to high angles of attack. Both constant pitch rate and variable pitch rate motions were considered. The highlights of results from a combined experimental and computational effort are described in this report. The conclusions from this research indicate the need for boundary-layer resolved measurements of the flow behavior near the leading edge and the evolution of the reverse flow regions on the suction surface. Furthermore, the deliberate shaping of the pitch trajectory for the purpose of optimization of separation delay is suggested as one way to manage the flow and aerodynamic behavior of an airfoil. DTIC

N94-37283*# National Aeronautics and Space Administration. Lewis Research Center, Cleveland, OH.

A METHOD FOR FLOW SIMULATION ABOUT COMPLEX GEOMETRIES USING BOTH STRUCTURED AND UNSTRUCTURED GRIDS

James R. DeBonis Jul. 1994 60 p

(RTOP 537-02-23)

(NASA-TM-106633; E-8955; NAS 1.15:106633) Avail: CASI HC A04/MF A01

A computational fluid dynamics code which utilizes both structured and unstructured grids was developed. The objective of this study was to develop and demonstrate the ability of such a code to achieve solutions about complex geometries in two dimensions. An unstructured grid generator and flow solver were incorporated into the PARC2D structured flow solver. This new unstructured grid generator capability allows for easier generation and manipulation of complex grids. Several examples of the grid generation capabilities are provided. The coupling of different grid topologies and the manipulation of individual grids is shown. Also, grids for realistic geometries, a NACA 0012 airfoil and a wing/nacelle installation, were created. The flow over a NACA 0012 airfoil was used as a test case for the flow solver. Eight separate cases were run. They were both the inviscid and viscous solutions for two freestream Mach numbers and airfoil angle of attacks of 0 to 3.86 degrees. The Mach numbers chosen were for a subsonic case, Mach 0.6, and a case where supersonic regions and a shock wave exists, Mach 0.8. These test case conditions were selected to match experimentally obtained data for code comparison. The results show that the code accurately predicts the flow field for all cases. Author

N94-37378*# National Aeronautics and Space Administration. Hugh L. Dryden Flight Research Center, Edwards, CA.

MEASUREMENT UNCERTAINTY AND FEASIBILITY STUDY OF A FLUSH AIRDATA SYSTEM FOR A HYPERSONIC FLIGHT EXPERIMENT

Stephen A. Whitmore and Timothy R. Moes Washington Jun. 1994 18 p Presented at the Applied Aerodynamics Conference, Colorado Springs, CO, 20-23 Jun. 1994

(RTOP 505-68-40)

(NASA-TM-4627; H-2010; NAS 1.15:4627; AIAA Paper 94-1930)

Copyright Avail: CASI HC A03/MF A01

Presented is a feasibility and error analysis for a hypersonic flush airdata system on a hypersonic flight experiment (HYFLITE). HYFLITE heating loads make intrusive airdata measurement impractical. Although this analysis is specifically for the HYFLITE vehicle and trajectory, the problems analyzed are generally applicable to hypersonic vehicles. A layout of the flush-port matrix is shown. Surface pressures are related airdata parameters using a simple aerodynamic model. The model is linearized using small perturbations and inverted using nonlinear least-squares. Effects of various error sources on the overall uncertainty are evaluated using an error simulation. Error sources modeled include boundarylayer/viscous interactions, pneumatic lag, thermal transpiration in the sensor pressure tubing, misalignment in the matrix layout, thermal warping of the vehicle nose, sampling resolution, and transducer error. Using simulated pressure data for input to the estimation algorithm, effects caused by various error sources are analyzed by comparing estimator outputs with the original trajectory. To obtain ensemble averages the simulation is run repeatedly and output statistics are compiled. Output errors resulting from the various error sources are presented as a function of Mach number. Final uncertainties with all modeled error sources included are presented as a function of Mach number. Author

N94-37395*# National Aeronautics and Space Administration. Hugh L. Dryden Flight Research Center, Edwards, CA.

PRESSURE-SENSING PERFORMANCE OF UPRIGHT CYLINDERS IN A MACH 10 BOUNDARY-LAYER

Steven Johnson and Kelly Murphy Washington Jul. 1994 25 p

(RTOP 505-70-00)
(NASA-TM-4633; H-1977; NAS 1.15:4633) Avail: CASI HC A03/MF A01

An experimental research program to provide basic knowledge of the pressure-sensing performance of upright, flushported cylinders in a hypersonic boundary layer is described. Three upright cylinders of 0.25-, 0.5- and 1.0-in. diameters and a conventional rake were placed in the test section sidewall boundary layer of the 31 Inch Mach 10 Wind Tunnel at NASA Langley Research Center, Hampton, Virginia. Boundary-layer pressures from these cylinders were compared to those measured with a conventional rake. A boundary-layer thickness-to-cylinder-diameter ratio of 8 proved sufficient to accurately measure an overall pressure profile and ascertain the boundary-layer thickness. Effects of Reynolds number, flow angularity, and shock wave impingement on pressure measurement were also investigated. Although Reynolds number effects were negligible at the conditions studied, flow angularity above 10 deg significantly affects the measured pressures. Shock wave impingement was used to investigate orifice-to-orifice pressure crosstalk. No crosstalk was measured. The lower pressure measured above the oblique shock wave impingement showed no influence of the higher pressure generated at the lower port locations.
Author

N94-37505*# National Aeronautics and Space Administration. Langley Research Center, Hampton, VA.
SUBSONIC AERODYNAMIC CHARACTERISTIC OF SEMISPAN COMMERCIAL TRANSPORT MODEL WITH WING-MOUNTED ADVANCED DUCTED PROPELLER OPERATING IN REVERSE THRUST
Zachary T. Applin, Kenneth M. Jones, Brenda E. Gile, and P. Frank Quinto Jul. 1994 114 p
(RTOP 535-03-10-02)
(NASA-TP-3427; L-1782; NAS 1.60:3427) Avail: CASI HC A06/MF A02

A test was conducted in the Langley 14 by 22 Foot Subsonic Tunnel to determine the effect of the reverse-thrust flow field of a wing-mounted advanced ducted propeller on the aerodynamic characteristics of a semispan subsonic high-lift transport model. The advanced ducted propeller (ADP) model was mounted separately in position alongside the wing so that only the aerodynamic interference of the propeller and nacelle affected the aerodynamic performance of the transport model. Mach numbers ranged from 0.14 to 0.26; corresponding Reynolds numbers ranged from 2.2 to 3.9 x 10(exp 6). The reverse-thrust flow field of the ADP shielded a portion of the wing from the free-stream airflow and reduced both lift and drag. The reduction in lift and drag was a function of ADP rotational speed and free-stream velocity. Test results included ground effects data for the transport model and ADP configuration. The ground plane caused a beneficial increase in drag and an undesirable slight increase in lift. The ADP and transport model performance in ground effect was similar to performance trends observed for out of ground effect. The test results form a comprehensive data set that supports the application of the ADP engine and airplane concept on the next generation of advanced subsonic transports. Before this investigation, the engine application was predicted to have detrimental ground effect characteristics. Ground effect test measurements indicated no critical problems and were the first step in proving the viability of this engine and airplane configuration.
Author (revised)

N94-37511*# Tennessee Univ. Space Inst., Tullahoma, TN.
SUPERSONIC LAMINAR FLOW CONTROL RESEARCH Semiannual Report No. 1, Jan. - Jun. 1994
C. F. Lo 1994 5 p
(Grant NAG2-881)
(NASA-CR-196260; NAS 1.26:196260) Avail: CASI HC A01/MF A01

The objective of the research is to understand supersonic laminar flow stability, transition and active control. Some prediction techniques will be developed or modified to analyze laminar stability. The effects of supersonic laminar flow with distributed heating and cooling on active control will be studied. The primary tasks of the research applying to the NASA/Ames POC and LFSWT's nozzle design with laminar flow control are as follows: (1) supersonic laminar boundary layer stability and transition prediction; (2) effects of heating and cooling for supersonic laminar flow control; and (3) POC and LFSWT nozzle design with heating and cooling effects combining wall contour and length changes.
Author

N94-37577*# National Aeronautics and Space Administration. Marshall Space Flight Center, Huntsville, AL.
AERODYNAMIC CHARACTERISTICS OF THE NATIONAL LAUNCH SYSTEM (NLS) 1 1/2 STAGE LAUNCH VEHICLE
A. M. Springer and D. C. Pokora Washington May 1994 57 p
(NASA-TP-3488; M-751; NAS 1.60:3488) Avail: CASI HC A04/MF A01

The National Aeronautics and Space Administration (NASA) is studying ways of assuring more reliable and cost effective means to space. One launch system studied was the NLS which included the I 1/2 stage vehicle. This document encompasses the aerodynamic characteristics of the 1 1/2 stage vehicle. To support the detailed configuration definition two wind tunnel tests were conducted in the NASA Marshall Space Flight Center's 14x14-Inch Trisonic Wind Tunnel during 1992. The tests were a static stability and a pressure test, each utilizing 0.004 scale models. The static stability test resulted in the forces and moments acting on the vehicle. The aerodynamics for the reference configuration with and without feedlines and an evaluation of three proposed engine shroud configurations were also determined. The pressure test resulted in pressure distributions over the reference vehicle with and without feedlines including the reference engine shrouds. These pressure distributions were integrated and balanced to the static stability coefficients resulting in distributed aerodynamic loads on the vehicle. The wind tunnel tests covered a Mach range of 0.60 to 4.96. These ascent flight aerodynamic characteristics provide the basis for trajectory and performance analysis, loads determination, and guidance and control evaluation.
Author

03 AIR TRANSPORTATION AND SAFETY

Includes passenger and cargo air transport operations; and aircraft accidents.

For related information see also *16 Space Transportation* and *85 Urban Technology and Transportation.*

N94-36530 Boeing Commercial Airplane Co., Seattle, WA.
WORLD JET AIRPLANE INVENTORY AT YEAR-END 1993
Mar. 1994 127 p See also PB93-174324
(PB94-164993) Avail: Issuing Activity (National Technical Information Service (NTIS))

The Marketing Department of Boeing Commercial Airplane Group publishes the World Jet Airplane Inventory. The document contains data on the world commercial jet airplane fleet (including some military derivatives) and reflects the status of this fleet as accurately as possible as of December 31, 1993. (Any fleet changes that have occurred since year-end 1993 will not be reflected in these data). World Jet Airplane Inventory is composed of a selected number of reports from JETTRACK, a computer-based jet airplane inventory systems. Fleet data in this system are obtained from many different sources, including airframe manufacturers, airplane owners and operators, governments, and trade publications. The document provides details for announced orders, deliveries, and inventories for all commercial jet airplanes built in the United States and Western Europe with a capacity of 60 seats or more. In addition, the year-end 1993 inventory data in Sections 5 and 7 include operators of the Soviet built Tupolev TU-134, TU-154, TU-204, Ilyushin IL-62 IL-86, IL-96 and Yakovlev Yak-42 airplanes.
NTIS

N94-37131 Federal Aviation Administration, Washington, DC. Office of Civil Aviation Security.
CRIMINAL ACTS AGAINST CIVIL AVIATION, 1993 Annual Report
1993 106 p Limited Reproducibility: More than 20% of this document may be affected by microfiche quality
(AD-A280694) Avail: CASI HC A06

Since 1986, the Federal Aviation Administration's Office of Civil Aviation Security has been publishing an annual report entitled Criminal Acts Against Civil Aviation. This report is a compilation of criminal incidents against civil aviation aircraft and interests worldwide. As in last year's publication, the 1993 issue contains feature articles and geographic overviews. Incidents are summarized in the overviews, and the feature articles focus on specific aviation-related issues or case histories. There is also a section in which incidents are compared for the 5-year period, 1989 to 1993. Charts, graphs, and maps appear throughout the publication. In one minor change from last year's format, an incident chronology appears at the beginning of

each geographic overview section. In addition, an asterisk has been added to incidents which are not counted in statistics but are reported for information. This is to distinguish them from those incidents which are counted in statistics. DTIC

N94-37604# Starmark Corp., Arlington, VA.
COMPOSITE HELICOPTER ACCIDENT PROFILES: DEFICIENT CREW/AIRCRAFT PERFORMANCE
David L. Green Jul. 1994 115 p Prepared for Systems Control Technology, Inc., Arlington, VA
(Contract DTFA01-87-C-00014)
(SCT-90RR-46; DOT/FAA/RD-94/22) Avail: CASI HC A06/MF A02

The purpose of this report is twofold. First, the unique characteristics of a wide variety of helicopter operations which ended in a collision with terrain features or man-made obstructions were analyzed. Special emphasis was given to operations during difficult visual conditions. Second, this report provides the reader with systematic insights into the affiliated technical and operational aspects of helicopter flight operations which contributed to this category of accident. The report explores the way helicopters are flown in the low airspace and employs composite accident summaries as points of departure to both illustrate and substantiate the analysis which in turn identifies opportunities for improved flight safety and productivity in the National Airspace System (NAS). The included analysis deals with a series of rotorcraft accidents involving terrain and obstruction strikes. The common characteristics of these accidents support the need for specific changes. Each composite accident is illustrated and treated to an analysis which often allows the reader to focus on one characteristic in isolation. The summaries of these composite accidents and supporting analysis are included in the report to provide a common information base for the FAA analysts and industry engineers to support the need for additional equipment, new procedures, new products, additional training, and regulatory change. This technical report contains pertinent data and testing/guidance material needed to support those elements of the agency charged with performance of regulatory actions and the development of advisory materials and standards. Author

N94-37706# Boeing Commercial Airplane Co., Seattle, WA. Technology and Product Development - Payloads.
AIRCRAFT COMMAND IN EMERGENCY SITUATIONS PROTOTYPE DEVELOPMENT USERS MANUAL Final Report
Gregory E. Grimstad Jun. 1994 77 p Original contains color illustrations
(Contract DTFA03-89-C-00061)
(DOT/FAA/CT-94/24) Avail: CASI HC A05/MF A01

This project involved assembly of the hardware and development of the software identified in ACES Phase 1 Concept Development contract study. The assembled system allows three critical stages in responding to an aircraft inflight smoke/fire event to be examined. These stages are (1) sensing (data gathering), (2) establishing the alerting criteria to maintain quick response while reducing false alarms (data analysis), and (3) methods of providing assistance to the crew, both flight deck and cabin, in responding to an inflight event. Four smoke/particle sensors are linked to a computer via a high speed data acquisition and control system. On the computer reside alerting logic functions and the capability to emulate the flight deck and cabin attendant displays. In addition, a thermal system that allows both location and temperature of numerous zones on a single fiber optic cable to be known was identified as a means to reduce false alarms and monitor hidden areas of an aircraft. The primary objective of the ACES system concept is to provide the capability to reduce the time required for the flight crew to make a decision to land the aircraft during an inflight smoke/fire event. Author (revised)

N94-37767 Department of the Navy, Washington, DC.
CANOPY BREAKING DEVICE Patent
Frederick C. Guill, inventor (to Navy) 12 Apr. 1994 7 p Filed 17 Mar. 1993
(AD-D016294; US-Patent-5,301,904; US-Patent-Appl-SN-035780; US-Patent-Class-244-129.1) Avail: US Patent and Trademark Office

An aircraft canopy breaking device is described, having means for penetrating the canopy glazing material upon application of an applied force from the rising ejection seat to the penetrating means. The device further comprises prepositioning means for prepositioning the penetrating means at a fixed distance from the canopy glazing material, shielding the penetrating means from inadvertently contacting the canopy glazing material, other material or personnel, and compressing whereby upon application of a force the penetrating means contacts the canopy glazing material causing crack propagation in the canopy glazing material. DTIC

04 AIRCRAFT COMMUNICATIONS AND NAVIGATION

Includes digital and voice communication with aircraft; air navigation systems (satellite and ground based); and air traffic control.

For related information see also *17 Space Communications, Spacecraft Communications, Command and Tracking* and *Communications and Radar.*

N94-37013*# Boston Univ., MA.
AN ERROR-RESISTANT LINGUISTIC PROTOCOL FOR AIR TRAFFIC CONTROL Final Report, Jan. - Sep. 1989
Steven Cushing 1989 48 p Prepared in cooperation with Stonehill Coll., North Easton, MA
(Grant NAG2-564)
(NASA-CR-196098; NAS 1.26:196098) Avail: CASI HC A03/MF A01

The research results described here are intended to enhance the effectiveness of the DATALINK interface that is scheduled by the Federal Aviation Administration (FAA) to be deployed during the 1990's to improve the safety of various aspects of aviation. While voice has a natural appeal as the preferred means of communication both among humans themselves and between humans and machines as the form of communication that people find most convenient, the complexity and flexibility of natural language are problematic, because of the confusions and misunderstandings that can arise as a result of ambiguity, unclear reference, intonation peculiarities, implicit inference, and presupposition. The DATALINK interface will avoid many of these problems by replacing voice with vision and speech with written instructions. This report describes results achieved to date on an on-going research effort to refine the protocol of the DATALINK system so as to avoid many of the linguistic problems that still remain in the visual mode. In particular, a working prototype DATALINK simulator system has been developed consisting of an unambiguous, context-free grammar and parser, based on the current air-traffic-control language and incorporated into a visual display involving simulated touch-screen buttons and three levels of menu screens. The system is written in the C programming language and runs on the Macintosh II computer. After reviewing work already done on the project, new tasks for further development are described. Author

N94-37830# Department of the Navy, Washington, DC.
MARKER BEACON CASE Patent Application
Frederick F. Hiltz, inventor (to Navy) and Charles E. Wilson, inventor (to Navy) 23 Mar. 1994 79 p
(AD-D016322; US-Patent-Appl-SN-216559; Navy-Case-74641) Avail: CASI HC A05/MF A01

A multifunctional case that is suitable for storing, carrying or launching a marker beacon is presented. The launching could be in a dense jungle to place the marker beacon atop tree branches to make it visible from the air, or the case may be adapted for launching at sea. The case has a triggering mechanism for launching the marker beacon. It has alignment means that comprises a first alignment position for inhibiting a launch when storing or carrying the marker beacon within the case. The alignment means has a second position for placing the marker beacon in position to be launched. The launching takes place upon activation of a triggering mechanism that forms part of the case. DTIC

N94-37839 Department of the Navy, Washington, DC.
SYSTEM FOR BROADCASTING MARKER BEACON SIGNALS AND PROCESSING RESPONSES FROM SEEKING ENTITIES Patent Application
Frederick F. Hiltz, inventor (to Navy) and Charles E. Wilson, inventor (to Navy) 23 Mar. 1994 84 p Limited Reproducibility: More than 20% of this document may be affected by microfiche quality

(AD-D016313; US-Patent-Appl-SN-216567; Navy-Case-74643) Avail: CASI HC A05

The present invention relates to a surface deployed navigational beacon, which is nominally secure from nonfriendly forces. More particularly the beacon is capable of user selection of any of a plurality of codes to modulate a transmitted radio signal. The signal is used by the navigational entity to determine direction to the beacon, as well as to distinguish a particular beacon from others which may be deployed within the same broad area. The beacon has the capability of receiving selected coded radio signals sent from the navigating entity. One received signal results in a signal being sent back to the navigating entity from the beacon for the purpose of providing slant range distance between the beacon and the navigating entity. Another signal received by the beacon from the navigating entity is employed to trigger a flare, integral to the beacon assembly, for backup visual/infrared navigational purposes. DTIC

05 AIRCRAFT DESIGN, TESTING AND PERFORMANCE

Includes aircraft simulation technology.

For related information see also *18 Spacecraft Design, Testing and Performance* and *39 Structural Mechanics*.For land transportation vehicles see *85 Urban Technology and Transportation*.

N94-36465 Air Univ., Maxwell AFB, AL. Airpower Research Inst.
AIRCRAFT BATTLE DAMAGE REPAIR FOR THE 1990'S AND BEYOND
Darrell H. Holcomb 20 Jul. 1994 55 p Limited Reproducibility: More than 20% of this document may be affected by microfiche quality
(AD-A278635; AU-ARI-93-4) Avail: Issuing Activity (Defense Technical Information Center (DTIC))

Combat aircraft that are damaged and sitting on the ground are completely useless to air component commanders. The goal of the United States Air Force's Aircraft Battle Damage Repair (ABDR) Program is to rapidly restore these damaged aircraft to some level of combat capability. To be effective, the repairs must allow the aircraft to return to combat in time to affect the outcome of the battle. Effective battle damage repair capability can truly be a force multiplier. This research project suggests methods to improve the Air Force's ability to provide this critical service to operational field commanders. Recent changes to the way the Air Force accomplishes its mission necessitate improvements to the ABDR Program. New technology, defense downsizing, and the introduction of composite wings all affect the Air Force and consequently its aircraft battle damage repair philosophy. A comprehensive review of the current ABDR Program with emphasis on areas of improvement is therefore in order. This study begins with a review of the ABDR Program and is followed by a brief historical background of battle damage repair, an outline of the current USAF program status, and a description of basic repair techniques and philosophies. Next is a comparison of different approaches to ABDR by other military services. The study then identifies both technical and programmatic challenges which the program must address to remain viable. The final chapter contains conclusions, recommendations for improvements, and highlights of areas requiring further research. DTIC

N94-36644*# National Aeronautics and Space Administration. Hugh L. Dryden Flight Research Facility, Edwards, CA.
CORRELATION OF ANALYTICAL AND EXPERIMENTAL HOT STRUCTURE VIBRATION RESULTS
Michael W. Kehoe and Vivian C. Deaton Aug. 1993 21 p Presented at the SEM Structural Testing Technology at High Temperatures 2 Conference, Ojai, CA, 8-10 Nov. 1993
(RTOP 505-63-50)
(NASA-TM-104269; H-1943; NAS 1.15:104269) Avail: CASI HC A03/MF A01

High surface temperatures and temperature gradients can affect the vibratory characteristics and stability of aircraft structures. Aircraft designers are relying more on finite-element model analysis methods to ensure sufficient vehicle structural dynamic stability throughout the desired flight envelope. Analysis codes that predict these thermal effects must be correlated and verified with experimental data. Experimental modal data for aluminum, titanium, and fiberglass plates heated at uniform, nonuniform, and transient heating conditions are presented. The data show the effect of heat on each plate's modal characteristics, a comparison of predicted and measured plate vibration frequencies, the measured modal damping, and the effect of modeling material property changes and thermal stresses on the accuracy of the analytical results at nonuniform and transient heating conditions. Author

N94-36767*# National Aeronautics and Space Administration. Langley Research Center, Hampton, VA.
FORWARD SWEEP, LOW NOISE ROTOR BLADE Patent Application
Thomas F. Brooks, inventor (to NASA) 2 May 1994 8 p
(NASA-Case-LAR-14569-1; NAS 1.71:LAR-14569-1; US-Patent-Appl-SN-238044) Avail: CASI HC A02/MF A01

A forward-swept, low-noise rotor blade includes an inboard section, an aft-swept section, and a forward-swept outboard section. The rotor blade reduces the noise of rotorcraft, including both standard helicopters and advanced systems such as tiltrotors. The primary noise reduction feature is the forward sweep of the planform over a large portion of the outer blade radius. The rotor blade also includes an aft-swept section. The purpose of the aft-swept region is to provide a partial balance to pitching moments produced by the outboard forward-swept portion of the blade. The noise source showing maximum noise reduction is blade-vortex interaction (BVI) noise. Also reduced are thickness, noise, high speed impulsive noise, cabin vibration, and loading noise. NASA

N94-37256*# National Aeronautics and Space Administration. Langley Research Center, Hampton, VA.
OPTIMIZATION FOR MINIMUM SENSITIVITY TO UNCERTAIN PARAMETERS
Jocelyn I. Pritchard (Army Vehicle Structures Lab., Hampton, VA.), Howard M. Adelman, and Jaroslaw Sobieszczanski-Sobieski Jul. 1994 10 p Presented at 5th AIAA/USAF/NASA/ISSMO Symposium on Multidisciplinary Analysis and Optimization, Panama City, FL, 7-9 Sep. 1994 Prepared in cooperation with Army Vehicle Structures Lab., Hampton, VA
(RTOP 505-63-36-06)
(NASA-TM-109139; NAS 1.15:109139; ARL-MR-157) Avail: CASI HC A02/MF A01

A procedure to design a structure for minimum sensitivity to uncertainties in problem parameters is described. The approach is to minimize directly the sensitivity derivatives of the optimum design with respect to fixed design parameters using a nested optimization procedure. The procedure is demonstrated for the design of a bimetallic beam for minimum weight with insensitivity to uncertainties in structural properties. The beam is modeled with finite elements based on two dimensional beam analysis. A sequential quadratic programming procedure used as the optimizer supplies the Lagrange multipliers that are used to calculate the optimum sensitivity derivatives. The method was perceived to be successful from comparisons of the optimization results with parametric studies. Author (revised)

N94-37636*# National Aeronautics and Space Administration. Langley Research Center, Hampton, VA.
STABILITY ANALYSIS OF AN F/A-18 E/F CABLE MOUNT M ODEL
Nancy Thompson and Moses Farmer Jun. 1994 24 p
(RTOP 505-63-50-13)
(NASA-TM-108989; NAS 1.15:108989) Avail: CASI HC A03/MF A01

A full-span F/A-18 E/F cable mounted wind tunnel model is part of a flutter clearance program at the NASA Langley Transonic Dynamics Tunnel. Parametric analysis of this model using GRUMCBL software was conducted to assess stability for wind tunnel tests. Two configurations of the F/A-18 E/F were examined. The parameters examined were pulley-cable friction, mach number, dynamic pressure, cable geometry, center of gravity location, cable tension, snubbing the model, drag, and test medium. For the nominal cable geometry (Cable Geometry 1), Configuration One was unstable for cases with higher pulley-cable friction coefficients. A new cable geometry (Cable Geometry 3) was determined in which Configuration One was stable for all cases evaluated. Configuration Two with the nominal center of gravity position was found to be unstable for cases with higher pulley-cable friction coefficients; however, the model was stable when the center of gravity moved forward 1/2. The model was tested using the cable mount system during the initial wind tunnel entry and was stable as predicted. Author

N94-37762*# National Aeronautics and Space Administration. Langley Research Center, Hampton, VA.
ORDERING DESIGN TASKS BASED ON COUPLING STRENGTHS
James L. Rogers, Jr. and Christina L. Bloebaum Jul. 1994 12 p Presented at 5th MDO-AIAA/NASA/USAF/ISSMO Conference, Panama City, FL, 7-9 Sep. 1994
(Grant NSF DDM-93-09706; RTOP 505-63-50-06)
(NASA-TM-109137; NAS 1.15:109137) Avail: CASI HC A03/MF A01

The design process associated with large engineering systems requires an initial decomposition of the complex system into modules of design tasks which are coupled through the transference of output data. In analyzing or optimizing such a coupled system, it is essential to be able to determine which interactions figure prominently enough to significantly affect the accuracy of the system solution. Many decomposition approaches assume the capability is available to determine what design tasks and interactions exist and what order of execution will be imposed during the analysis process. Unfortunately, this is often a complex problem and beyond the capabilities of a human design manager. A new feature for DeMAID (Design Manager's Aid for Intelligent Decomposition) will allow the design manager to use coupling strength information to find a proper sequence for ordering the design tasks. In addition, these coupling strengths aid in deciding if certain tasks or couplings could be removed (or temporarily suspended) from consideration to achieve computational savings without a significant loss of system accuracy. New rules are presented and two small test cases are used to show the effects of using coupling strengths in this manner. Author

N94-36618# Dornier-Werke G.m.b.H., Friedrichshafen (Germany).
LANDING OF AN UNMANNED HELICOPTER ON A MOVING PLATFORM. HIGH ACCURACY NAVIGATION AND TRACKING
Hans-Peter Engelbert and Johannes Schroeder *In* AGARD, Pointing and Tracking Systems May 1994 9 p (For primary document see N94-36616 12-18)
Copyright Avail: CASI HC A02/MF A02

06 AIRCRAFT INSTRUMENTATION

Includes cockpit and cabin display devices; and flight instruments.

For related information see also *19 Spacecraft Instrumentation* and *35 Instrumentation and Photography.*

N94-36933*# Lockheed Engineering and Sciences Co., Houston, TX.
SPACE GENERIC OPEN AVIONICS ARCHITECTURE (SGOAA) STANDARD SPECIFICATION
Richard B. Wray and John R. Stovall Jun. 1994 95 p Supersedes LESC-30354-B, issued December 1993
(Contract NAS9-19100)
(NASA-CR-188290; NAS 1.26:188290; LESC-30354-C) Avail: CASI HC A05/MF A01

This standard establishes the Space Generic Open Avionics Architecture (SGOAA). The SGOAA includes a generic functional model, processing structural model, and an architecture interface model. This standard defines the requirements for applying these models to the development of spacecraft core avionics systems. The purpose of this standard is to provide an umbrella set of requirements for applying the generic architecture models to the design of a specific avionics hardware/software processing system. This standard defines a generic set of system interface points to facilitate identification of critical services and interfaces. It establishes the requirement for applying appropriate low level detailed implementation standards to those interfaces points. The generic core avionics functions and processing structural models provided herein are robustly tailorable to specific system applications and provide a platform upon which the interface model is to be applied. Derived from text

N94-37401*# General Electric Co., Cincinnati, OH. Aircraft Engines
FIBER OPTIC (FLIGHT QUALITY) SENSORS FOR ADVANCED AIRCRAFT PROPULSION Final Report, Jan. 1990 - Jun. 1994
Gary L. Poppel Jul. 1994 90 p
(Contract NAS3-25805; RTOP 505-62-50)
(NASA-CR-191195; NAS 1.26:191195; R94AEB175) Avail: CASI HC A05/MF A01

Development of flight prototype, fiber-optic sensing system components for measuring nine sensed parameters (three temperatures, two speeds, three positions, and one flame) on an F404-400 aircraft engine is described. Details of each sensor's design, functionality, and environmental testing, and the electro-optics architecture for sensor signal conditioning are presented. Eight different optical sensing techniques were utilized. Design, assembly, and environmental testing of an engine-mounted, electro-optics chassis unit (EOU), providing MIL-C-1553 data output, are related. Interconnection cables and connectors between the EOU and the sensors are identified. Results of sensor/cable/circuitry integrated testing, and installation and ground testing of the sensor system on an engine in October 1993 and April 1994 are given, including comparisons with the engine control system's electrical sensors. Lessons learned about the design, fabrication, testing, and integration of the sensor system components are included. Author

N94-37658*# Boeing Commercial Airplane Co., Seattle, WA. Flight Deck Research.
SYNTHETIC VISION DISPLAY EVALUATION STUDIES Final Report
David M. Regal and David H. Whittington Aug. 1994 67 p
(Contract NAS1-19360; RTOP 537-08-20-01)
(NASA-CR-194963; NAS 1.26:194963) Avail: CASI HC A04/MF A01

The goal of this research was to help us understand the display requirements for a synthetic vision system for the High Speed Civil Transport (HSCT). Four experiments were conducted to examine the effects of different levels of perceptual cue complexity in displays used by pilots in a flare and landing task. Increased levels of texture mapping of terrain and runway produced mixed results, including harder but shorter landings and a lower flare initiation altitude. Under higher workload conditions, increased texture resulted in an improvement in performance. An increase in familiar size cues did not result in improved performance. Only a small difference was found between displays using two patterns of high resolution texture mapping. The effects of increased perceptual cue complexity on performance was not as strong as would be predicted from the pilot's subjective reports or from related literature. A description of the role of a synthetic vision system in the High Speed Civil Transport is provide along with a literature review covering applied research related to perceptual cue usage in aircraft displays. Author

07 AIRCRAFT PROPULSION AND POWER

Includes prime propulsion systems and systems components, e.g., gas turbine engines and compressors; and onboard auxiliary power plants for aircraft.

For related information see also *20 Spacecraft Propulsion and Power, 28 Propellants and Fuels,* and *44 Energy Production and Conversion.*

N94-37448*# National Aeronautics and Space Administration. Lewis Research Center, Cleveland, OH.
PREDICTION OF FILM COOLING ON GAS TURBINE AIRFOILS
Vijay K. Garg and Raymond E. Gaugler Jul. 1994 31 p Presented at the 39th International Gas Turbine and Aeroengine Congress and Exposition, The Hague, Netherlands, 13-16 Jun. 1994; sponsored by ASME
(RTOP 505-62-52)
(NASA-TM-106653; E-8965; NAS 1.15:106653) Avail: CASI HC A03/MF A01

A three-dimensional Navier-Stokes analysis tool has been developed in order to study the effect of film cooling on the flow and heat transfer characteristics of actual turbine airfoils. An existing code (Arnone et al., 1991) has been modified for the purpose. The code is an explicit, multigrid, cell-centered, finite volume code with an algebraic turbulence model. Eigenvalue scaled artificial dissipation and variable-coefficient implicit residual smoothing are used with a full-multigrid technique. Moreover, Mayle's transition criterion (Mayle, 1991) is used. The effects of film cooling have been incorporated into the code in the form of appropriate boundary conditions at the hole locations on the airfoil surface. Each hole exit is represented by several control volumes, thus providing an ability to study the effect of hole shape on the film-cooling characteristics. Comparison is

fair with near mid-span experimental data for four and nine rows of cooling holes, five on the shower head, and two rows each on the pressure and suction surfaces. The computations, however, show a strong spanwise variation of the heat transfer coefficient on the airfoil surface, specially with shower-head cooling. Author

08 AIRCRAFT STABILITY AND CONTROL

Includes aircraft handling qualities; piloting; flight controls; and autopilots.

For related information see also *05 Aircraft Design, Testing and Performance*.

N94-36733# Air Force Inst. of Tech., Wright-Patterson AFB, OH. School of Engineering.

MIXED H2/H-INFINITY OPTIMIZATION WITH MULTIPLE H INFINITY CONSTRAINTS M.S. Thesis

Julio C. Ullauri Jun. 1994 136 p

(AD-A280572; AFIT/GAE/ENY/94J-04) Avail: CASI HC A07/MF A02

A general mixed H2/H-infinity optimal control design with multiple H-infinity constraints is developed and applied to two systems, one SISO and the other MIMO. The SISO design model is normal acceleration command following for the F-16. This design constitutes the validation for the numerical method, for which boundaries between the H2 design and the H-infinity constraints are shown. The MIMO design consists of a longitudinal aircraft plant (short period and phugoid modes) with stable weights on the H2 and H-infinity transfer functions, and is linear-time-invariant. The controller order is reduced to that of the plant augmented with the H2 weights only. The technique allows singular, proper (not necessarily strictly proper) H-infinity constraints. The analytical nature of the solution and a numerical approach for finding suboptimal controllers which are as close as desired to optimal is developed. The numerical method is based on the Davidon-Fletcher-Powell algorithm and uses analytical derivatives and central differences for the first order necessary conditions. The method is applied to a MIMO aircraft longitudinal control design to simultaneously achieve Nominal Performance at the output and Robust Stability at both the input and output of the plant. DTIC

N94-36820*# National Aeronautics and Space Administration. Langley Research Center, Hampton, VA.

GAIN WEIGHTED EIGENSPACE ASSIGNMENT

John B. Davidson and Dominick Andrisani, II May 1994 32 p

(RTOP 505-64-30-01)

(NASA-TM-109130; NAS 1.15:109130) Avail: CASI HC A03/MF A01

This report presents the development of the gain weighted eigenspace assignment methodology. This provides a designer with a systematic methodology for trading off eigenvector placement versus gain magnitudes, while still maintaining desired closed-loop eigenvalue locations. This is accomplished by forming a cost function composed of a scalar measure of error between desired and achievable eigenvectors and a scalar measure of gain magnitude, determining analytical expressions for the gradients, and solving for the optimal solution by numerical iteration. For this development the scalar measure of gain magnitude is chosen to be a weighted sum of the squares of all the individual elements of the feedback gain matrix. An example is presented to demonstrate the method. In this example, solutions yielding achievable eigenvectors close to the desired eigenvectors are obtained with significant reductions in gain magnitude compared to a solution obtained using a previously developed eigenspace (eigenstructure) assignment method. Author

N94-36965*# Washington Univ., Seattle, WA. Dept. of Mechanical Engineering.

MULTIRATE FLUTTER SUPPRESSION SYSTEM DESIGN FOR THE BENCHMARK ACTIVE CONTROLS TECHNOLOGY WING Final Report, 16 Jun. 1991 - 15 Jun. 1994

Martin C. Berg and Gregory S. Mason 1994 79 p

(Contract NCC1-156)

(NASA-CR-196112; NAS 1.26:196112) Avail: CASI HC A05/MF A01

To study the effectiveness of various control system design methodologies, the NASA Langley Research Center initiated the Benchmark Active Controls Project. In this project, the various methodologies will be applied to design a flutter suppression system for the Benchmark Active Controls Technology (BACT) Wing (also called the PAPA wing). Eventually, the designs will be implemented in hardware and tested on the BACT wing in a wind tunnel. This report describes a project at the University of Washington to design a multirate flutter suppression system for the BACT wing. The objective of the project was two fold. First, to develop a methodology for designing robust multirate compensators, and second, to demonstrate the methodology by applying it to the design of a multirate flutter suppression system for the BACT wing. The contributions of this project are (1) development of an algorithm for synthesizing robust low order multirate control laws (the algorithm is capable of synthesizing a single compensator which stabilizes both the nominal plant and multiple plant perturbations; (2) development of a multirate design methodology, and supporting software, for modeling, analyzing and synthesizing multirate compensators; and (3) design of a multirate flutter suppression system for NASA's BACT wing which satisfies the specified design criteria. This report describes each of these contributions in detail. Section 2.0 discusses our design methodology. Section 3.0 details the results of our multirate flutter suppression system design for the BACT wing. Finally, Section 4.0 presents our conclusions and suggestions for future research. The body of the report focuses primarily on the results. The associated theoretical background appears in the three technical papers that are included as Attachments 1-3. Attachment 4 is a user's manual for the software that is key to our design methodology. Derived from text

N94-37014*# National Aeronautics and Space Administration. Langley Research Center, Hampton, VA.

DESIGN AND EVALUATION OF A STOCHASTIC OPTIMAL FEED-FORWARD AND FEEDBACK TECHNOLOGY (SOFFT) FLIGHT CONTROL ARCHITECTURE

Aaron J. Ostroff and Melissa S. Proffitt Jun. 1994 20 p

(RTOP 505-64-30-01)

(NASA-TP-3419; L-17273; NAS 1.60:3419) Avail: CASI HC A03/MF A01

This paper describes the design and evaluation of a stochastic optimal feed-forward and feedback technology (SOFFT) control architecture with emphasis on the feed-forward controller design. The SOFFT approach allows the designer to independently design the feed-forward and feedback controllers to meet separate objectives and then integrate the two controllers. The feed-forward controller has been integrated with an existing high-angle-of-attack (high-alpha) feedback controller. The feed-forward controller includes a variable command model with parameters selected to satisfy level 1 flying qualities with a high-alpha adjustment to achieve desired agility guidelines, a nonlinear interpolation approach that scales entire matrices for approximation of the plant model, and equations for calculating feed-forward gains developed for perfect plant-model tracking. The SOFFT design was applied to a nonlinear batch simulation model of an F/A-18 aircraft modified for thrust vectoring. Simulation results show that agility guidelines are met and that the SOFFT controller filters undesired pilot-induced frequencies more effectively during a tracking task than a flight controller that has the same feedback control law but does not have the SOFFT feed-forward control. Author

N94-37059*# National Aeronautics and Space Administration. Langley Research Center, Hampton, VA.

PREDICTING THE EFFECTS OF UNMODELED DYNAMICS ON AN AIRCRAFT FLIGHT CONTROL SYSTEM DESIGN USING EIGENSPACE ASSIGNMENT

Eric N. Johnson (George Washington Univ., Washington, DC.), John B. Davidson, and Patrick C. Murphy Jun. 1994 40 p

(RTOP 505-64-52-01)

(NASA-TM-4548; L-17333; NAS 1.15:4548) Avail: CASI HC A03/MF A01

When using eigenspace assignment to design an aircraft flight control system, one must first develop a model of the plant. Certain questions arise when creating this model as to which dynamics of the plant need to be included in the model and which dynamics can be left out or approximated. The answers to these questions are important because a poor choice can lead to closed-loop dynamics that are unpredicted by the design model. To alleviate this problem, a method has been developed for predicting the effect of not including certain dynamics in the design model on the final closed-loop eigenspace. This development provides insight as to which

characteristics of unmodeled dynamics will ultimately affect the closed-loop rigid-body dynamics. What results from this insight is a guide for eigenstructure control law designers to aid them in determining which dynamics need or do not need to be included and a new way to include these dynamics in the flight control system design model to achieve a required accuracy in the closed-loop rigid-body dynamics. The method is illustrated for a lateral-directional flight control system design using eigenspace assignment for the NASA High Alpha Research Vehicle (HARV). Author

N94-37259*# Calspan Corp., Arnold AFS, TN.
STRENGTH EVALUATION OF SOCKET JOINTS Final Report
Larry C. Rash Hampton, VA NASA Jun. 1994 43 p
(Contract NAS1-19385; RTOP 505-59-85-01)
(NASA-CR-4608; NAS 1.26:4608) Avail: CASI HC A03/MF A01

This report documents the development of a set of equations that can be used to provide a relatively simple solution for identifying the strength of socket joints and for most cases avoid the need of more lengthy analyses. The analytical approach was verified by comparison of the contact load distributions to results obtained from a finite element analysis. The contacting surfaces for the specific joint in this analysis are in the shape of frustrums of a cone and are representative of the tapered surfaces in the socket-type joints used to join segments of model support systems for wind tunnels. The results are in the form of equations that can be used to determine the contact loads and stresses in the joint from the given geometry and externally applied loads. Equations were determined to define the bending moments and stresses along the length of the joints based on strength and materials principles. The results have also been programmed for a personal computer and a copy of the program is included.
Author (revised)

09 RESEARCH AND SUPPORT FACILITIES (AIR)

Includes airports, hangars and runways; aircraft repair and overhaul facilities; wind tunnels; shock tubes; and aircraft engine test stands.

For related information see also *14 Ground Support Systems and Facilities (Space)*.

N94-36763# Federal Aviation Administration, Washington, DC. Office of Airport Planning and Programming.
ACCOMPLISHMENTS UNDER THE AIRPORT IMPROVEMENT PROGRAM Annual Report No. 12, Fiscal Year 1993
1993 124 p
(AD-A280661; DOT/FAA/PP-94-2) Avail: CASI HC A06/MF A02

Annual report of the Airport Improvement Program (AIP) for the fiscal year ending September 30, 1993, is the twelfth report of activity under authority granted by the Airport and Airway Improvement Act of 1982, as amended. Section 521 of the Airport and Airway Improvement Act of 1982, as amended, requires that the Secretary of Transportation submit an annual report to Congress describing the accomplishments of the airport grant program. DTIC

N94-36826*# National Aeronautics and Space Administration. Langley Research Center, Hampton, VA.
INTERNALLY DAMPED, SELF-ARRESTING VERTICAL DROP-WEIGHT APPARATUS Patent Application
Damodar R. Ambur, inventor (to NASA), Chunchu B. Prasad, inventor (to NASA), William A. Waters, inventor (to NASA), Robert W. Stockum, inventor (to NASA), and Manfred A. Walter, inventor (to NASA) 20 May 1994 19 p
(NASA-Case-LAR-15003-1; NAS 1.71:LAR-15003-1;
US-Patent-Appl-SN-250141) Avail: CASI HC A03/MF A01

A vertical dropped-weight impact test machine has a dropped-weight barrel vertically supported on upper and lower support brackets. The dropped-weight barrel is chambered to receive a dropped-weight assembly having a latch pin at its upper end, a damping unit in the middle, and a tup at its lower end. The tup is adapted for gathering data during impact testing. The latch pin releasably engages a latch pin coupling assembly. The latch pin coupling assembly is attached to a winch via a halyard for raising and lowering the dropped-weight assembly. The lower end of the dropped-weight barrel is provided with a bounce-back arresting mechanism which is activated by the descending passage of the dropped-weight assembly. After striking the specimen, the dropped-weight assembly rebounds vertically and is caught by the bounce-back arresting mechanism. The damping unit of the dropped-weight assembly serves to dissipate energy from the rebounding dropped-weight assembly and prevents the dropped-weight assembly from rebounding from the self-arresting mechanism. NASA

N94-36945*# Notre Dame Univ., IN. Dept. of Aerospace and Mechanical Engineering.
EXPERIMENTAL UNCERTAINTY AND DRAG MEASUREMENTS IN THE NATIONAL TRANSONIC FACILITY Final Report
Stephen M. Batill Jun. 1994 125 p
(Contract NCC1-177; RTOP 505-59-54-01)
(NASA-CR-4600; NAS 1.26:4600) Avail: CASI HC A06/MF A02

This report documents the results of a study which was conducted in order to establish a framework for the quantitative description of the uncertainty in measurements conducted in the National Transonic Facility (NTF). The importance of uncertainty analysis in both experiment planning and reporting results has grown significantly in the past few years. Various methodologies have been proposed and the engineering community appears to be 'converging' on certain accepted practices. The practical application of these methods to the complex wind tunnel testing environment at the NASA Langley Research Center was based upon terminology and methods established in the American National Standards Institute (ANSI) and the American Society of Mechanical Engineers (ASME) standards. The report overviews this methodology. Author

N94-36967*# Worcester Polytechnic Inst., MA. Dept. of Mechanical Engineering.
DESIGN AND DEVELOPMENT OF EXPERIMENTAL FACILITIES FOR SHORT DURATION, LOW-GRAVITY COMBUSTION AND FIRE EXPERIMENTS Final Report
Vahid Motevalli 30 Jun. 1994 198 p Original contains color illustrations
(Contract NCC3-312)
(NASA-CR-196107; NAS 1.26:196107) Avail: CASI HC A09/MF A03; 2 functional color pages

This report contains the results of three projects conducted by undergraduate students from Worcester Polytechnic Institute at the NASA's Lewis Research Center under a NASA Award NCC3-312. The students involved in these projects spent part of the summer of 1993 at the Lewis Research Center (LeRC) under the direction of Dr. Howard Ross, head of the Combustion group and other NASA engineers and scientists. The Principal Investigator at Worcester Polytechnic Institute was Professor Vahid Motevalli. Professor Motevalli served as the principal project advisor for two of the three projects which were in Mechanical Engineering. The third project was advised by Professor Duckworth of Electrical and Computer Engineering, while Professor Motevalli acted as the co-advisor. These projects provided an excellent opportunity for the students to participate in the cutting edge research and engineering design, interact with NASA engineers and gain valuable exposure to a real working environment. Furthermore, the combustion group at LeRC was able to forward their goals by employing students to work on topics of immediate use and interest such as experimental research projects planned for the space shuttle, the future space station, or to develop demonstration tools to educate the public about LeRC activities. Derived from text

N94-37159# Sandia National Labs., Albuquerque, NM. Contamination-Free Mfg. Research Center.
REAL-TIME SAW MEASUREMENTS OF NVR IN CLEANROOM AND IN MICROENVIRONMENT
Alan Y. Liang, Dale C. McIntyre, Richard D. Lujan, Steve M. Thornberg, and Susan F. A. Bender 1994 8 p Presented at the 40th Annual Technical Meeting and Exposition of the Institute of Environmental Sciences (IES), Rosemont, IL, 1-6 May 1994
(Contract DE-AC04-94AL-85000)
(DE94-011937; SAND-94-0478C; CONF-940510-6) Avail: CASI HC A02/MF A01

Using a real-time, surface acoustic wave (SAW) sensing instrument supplied by Femtometrics, we have measured organic contamination, or nonvolatile residues (NVR), in both a cleanroom and a microenvironment.

To demonstrate the 'real-time' NVR detectability and sensitivity of the SAW instrument, controlled contamination experiments with photoresist material were also conducted. In addition, two cleaning methods for removing contamination from used sensors have been evaluated. One technique uses the on-board temperature varying capability of the SAW instrument, while the other technique utilizes a uv-ozone cleaner for the sensor cleaning. Preliminary results from SAW measurements in the cleanroom and in a microenvironment and tests to evaluate sensor cleaning techniques are presented in this report. A concluding summary with an assessment of the current SAW instrument and potential future applications for this technology is also presented. DOE

N94-37163 Air Force Inst. of Tech., Wright-Patterson AFB, OH. School of Engineering.

CALIBRATION AND INITIAL TESTING OF A NEW HYDRAULIC SIMULATOR Final Report

Cristian A. Puebla 6 Jun. 1994 174 p Limited Reproducibility: More than 20% of this document may be affected by microfiche quality

(AD-A280632; AFIT/GA/ENY/94J-1) Avail: CASI HC A08

In the present research, the flow field associated with the ejection of a crew capsule from the fuselage of a high speed generic aircraft was experimentally investigated by means of the modified gas hydraulic analogy. For this, an existing hydraulic simulator was calibrated and modified to adapt it to the needs of the experiment. The analogy was evaluated for a five-sided capsule alone, and good quantitative agreement with the 2-D shock-expansion theory was obtained. It was found that the size of the model played a key role in the determination of good quantitative data. The analysis of the capsule interacting with a fuselage was made considering it at fixed vertical positions from the fuselage and moving with respect to the fuselage at different constant speeds. A clear difference in water depth ratio distribution on the surfaces of the capsule was found between the static and dynamic conditions and also differences occurred for the various velocities of separation. The agreement between theory and experiment was fair. It was concluded that larger models are needed to get good quantitative agreement between theory and experiment and that any separation study should be made applying a dynamical model. DTIC

N94-37424# Systems Control Technology, Inc., Arlington, VA.

ANALYSIS OF VERTIPORT STUDIES FUNDED BY THE AIRPORT IMPROVEMENT PROGRAM (AIP) Final Report

Deborah J. Peisen, William T. Sampson, Linda J. LaBelle, Brian M. Sawyer, J. Richard Ludders, Stephen V. Berardo, Richard J. Dyment, Samuel W. Ferguson, Robert M. Winick, and Clifford R. Bragdon May 1994 111 p

(Contract DTFA01-93-C-00030)

(SCT-93RR-21; DOT/FAA/RD-93/37) Avail: CASI HC A06/MF A02

It is expected that Advanced Vertical Flight (AVF) aircraft such as the Civil TiltRotor (CTR) will become viable, important vehicles for the relief of both ground and airport congestion. Furthermore, it is expected this will lead to expanded use of rotorcraft for scheduled passenger service. To prepare for this eventuality, the FAA in 1988 funded a program of vertiport feasibility studies. Thirteen locations, encompassing a range of cities, states, and regions, applied for and received funds. Canada conducted its own study. The purpose of these studies was to facilitate the use of AVF aircraft by identifying areas in the United States where the potential for missions using these aircraft is greatest so that infrastructure requirements could be identified and implemented in a timely manner. This report evaluates the fourteen studies to portray an overview of the status of potential scheduled passenger service and required vertiport development within the United States, Puerto Rico, and Canada. The report also evaluates the methodologies and assumptions used in these studies to reach conclusions regarding the feasibility of AVF aircraft service in these areas. Most studies concluded that the primary mission would be short-haul passenger service between city centers and major urban areas. Some studies, particularly in the lesser developed areas (Puerto Rico and Alaska), concluded that small package delivery and cargo missions were also feasible. Final conclusions and recommendations include suggestions for planning guidelines specifically for vertiports/large heliports developed primarily for passenger operations. Author

N94-37443*# National Aeronautics and Space Administration. Lyndon B. Johnson Space Center, Houston, TX.

ENGINEERING DIRECTORATE TECHNICAL FACILITIES CATALOG

Joseph E. Maloy Jan. 1993 331 p Revised

(NASA-TM-109895; JSC-19295; NAS 1.15:109895) Avail: CASI HC A15/MF A03

The Engineering Directorate Technical Facilities Catalog is designed to provide an overview of the technical facilities available within the Engineering Directorate at the National Aeronautics and Space Administration (NASA), Lyndon B. Johnson Space Center (JSC) in Houston, Texas. The combined capabilities of these engineering facilities are essential elements of overall JSC capabilities required to manage and perform major NASA engineering programs. The facilities are grouped in the text by chapter according to the JSC division responsible for operation of the facility. This catalog updates the facility descriptions for the JSC Engineering Directorate Technical Facilities Catalog, JSC 19295 (August 1989), and supersedes the Engineering Directorate, Principle test and Development Facilities, JSC, 19962 (November 1984). Derived from text

N94-37450*# Old Dominion Univ., Norfolk, VA. Dept. of Aerospace Engineering.

LARGE ANGLE MAGNETIC SUSPENSION TEST FIXTURE Progress Report, period ending 30 Apr. 1994

Colin P. Britcher Jul. 1994 21 p

(Grant NAG1-1056)

(NASA-CR-196138; NAS 1.26:196138) Avail: CASI HC A03/MF A01

Over the past few decades, research has proven the feasibility of the concept of noncontacting magnetic bearing systems which operate with no wear or vibration. As a result, magnetic bearing systems are beginning to emerge as integral parts of modern industrial and aerospace systems. Further applications research is still required. NASA has loaned an existing magnetic bearing device, the Annular Suspension and Pointing System (ASPS), to ODU to permit student design teams the opportunity to pursue some of these studies. The ASPS is a protoype for a high-accuracy space payload pointing and vibration isolation system. The project objectives are to carry out modifications and improvements to the ASPS hardware to permit recommissioning in a 1-g (ground-based) environment. Following recommissioning, new applications will be studied and demonstrated, including a rotary joint for solar panels. The first teams designed and manufactured pole shims to reduce the air-gaps and raise the vertical force capability as well as on control system studies. The most recent team concentrated on the operation of a single bearing station, which was successfully accomplished with a PC-based digital controller. The paper will review the history and technical background of the ASPS hardware, followed by presentation of the progress made and the current status of the project. Author

N94-37522*# National Aeronautics and Space Administration. Lewis Research Center, Cleveland, OH.

NASA LEWIS WIND TUNNEL MODEL SYSTEMS CRITERIA

Ronald H. Soeder and Henry C. Haller Jul. 1994 23 p

(RTOP 505-62-84)

(NASA-TM-106565; E-8742; NAS 1.15:106565) Avail: CASI HC A03/MF A01

This report describes criteria for the design, analysis, quality assurance, and documentation of models or test articles that are to be tested in the aeropropulsion facilities at the NASA Lewis Research Center. The report presents three methods for computing model allowable stresses on the basis of the yield stress or ultimate stress, and it gives quality assurance criteria for models tested in Lewis' aeropropulsion facilities. Both customer-furnished model systems and in-house model systems are discussed. The functions of the facility manager, project engineer, operations engineer, research engineer, and facility electrical engineer are defined. The format for pretest meetings, prerun safety meetings, and the model criteria review are outlined Then, the format for the model systems report (a requirement for each model that is to be tested at NASA Lewis) is described, the engineers that are responsible for developing the model systems report are listed, and the time table for its delivery to the facility manager is given. Author

N94-37755# Loral Systems, Inc., Orlando, FL. Advanced Distributed Simulation Technology Program Office.

ADVANCED DISTRIBUTED SIMULATION TECHNOLOGY ADVANCED ROTARY WING AIRCRAFT. SOFTWARE PROGRAMMER'S MANUAL VISUAL SYSTEM MODULE

Robert R. Anschuetz, II 7 Apr. 1994 13 p
(Contract N61339-91-D-0001)
(AD-A280260; ADST/TR/94-003256) Avail: CASI HC A03/MF A01

The purpose of this document is to provide information needed by a programmer to understand the instruction set architecture of the specified host and target computers. The Software Programmer's Manual provides information that may be used to interpret, check out, troubleshoot, or modify existing software on the host and target computers. Section 1 outlines the scope of the document. Section 2 describes the documents referenced in this specification. Section 3 outlines the software programming environment. Section 4 describes the programming information relative to the host and target computers. Section 5 provides general design notes. DTIC

N94-37756# Loral Systems, Inc., Orlando, FL. Advanced Distributed Simulation Technology Program Office.
ADVANCED DISTRIBUTED SIMULATION TECHNOLOGY ADVANCED ROTARY WING AIRCRAFT. SYSTEM/SEGMENT SPECIFICATION. VOLUME 4: SIMULATION SYSTEM MODULE RAH-66 KIT
Roger Branson and Robert R. Anschuetz, II 31 Mar. 1994 9 p
(Contract N61339-91-D-0001)
(AD-A280261; ADST/TR/94-003276-Vol-4) Avail: CASI HC A02/MF A01

The ADST ARWA System/Segment Specification establishes the functional requirements for the Advanced Rotary Wing Aircraft (ARWA) Simulator System (SS). Volume 4 describes the requirements for the Simulator System Module (SSM) with respect to the aircraft specific models for the RAH-66 Comanche aircraft. The RAH-66 Kit component provides aircraft simulation for flight dynamics, flight controls, propulsion, navigation/communication, sensors, aircraft survivability equipment, and weapons. DTIC

12 ASTRONAUTICS (GENERAL)

For extraterrestrial exploration see *91 Lunar and Planetary Exploration.*

N94-36999# Joint Publications Research Service, Arlington, VA.
JPRS REPORT: CENTRAL EURASIA. AVIATION AND COSMONAUTICS, NO. 4, APRIL 1993
25 Feb. 1994 31 p Transl. into ENGLISH from various Russian articles
(JPRS-UAC-94-003) Avail: CASI HC A03/MF A01

Translated articles cover the following topics: development of Russian space science in coming decades viewed; problems, prospects of Russian space science for the long term; comparison of features of Space Shuttle and Energiya/Buran systems; and unusual case of g-force pickup countered successfully in flight. Author

N94-37000# Joint Publications Research Service, Arlington, VA.
JPRS REPORT: CENTRAL EURASIA. AVIATION AND COSMONAUTICS, NO. 5, MAY 1993
15 Mar. 1994 22 p Transl. into ENGLISH from various Russian articles
(JPRS-UAC-94-004) Avail: CASI HC A03/MF A01

Translated articles cover the following topics: mathematical modeling assists investigations of flight accidents; and SLBM conversion for civilian launches continues. Author

N94-37001# Joint Publications Research Service, Arlington, VA.
JPRS REPORT: CENTRAL EURASIA. AVIATION AND COSMONAUTICS, NO. 6, JUNE 1993
28 Mar. 1994 17 p Transl. into ENGLISH from various Russian articles
(JPRS-UAC-94-005) Avail: CASI HC A03/MF A01

Translated articles cover the following topics: profiles of Russian RSR and Lockheed SR-71 reconnaissance aircraft; and the commercial and military uses of the French SPOT satellite. Author

N94-37002# Joint Publications Research Service, Arlington, VA.
JPRS REPORT: SCIENCE AND TECHNOLOGY. CENTRAL EURASIA: SPACE
16 May 1994 33 p Transl. into ENGLISH from various Russian articles
(JPRS-USP-94-004) Avail: CASI HC A03/MF A01

Translated articles cover the following topics: use of geodesic satellites for solving basic and applied problems; state and prospects of the development of space-based geodesic and navigation systems; experience in the creation of planetary models of the Earth's gravity field with the Geo-IK; determination of detailed characteristics of geopotential over the world ocean with the Geo-IK; the effects of exposure to factors associated with open space on the substructure and optical characteristics of light-absorbing thermal-regulating coatings; work proceeding on Spectrum-X-Gamma Astronomy satellite project; details on DoronaS-I Solar Research Satellite; methods of spacecraft, space debris observation; hypersonic propulsion tests support 'Orel' Aerospace Plane project; NPO Molniya designer urges hydrocarbon-fueled aerospace plane project; and opposing views of Russian space cooperation with the U.S. Author

N94-37003# Joint Publications Research Service, Arlington, VA.
JPRS REPORT: SCIENCE AND TECHNOLOGY. CENTRAL EURASIA: SPACE
21 Jun. 1994 17 p Transl. into ENGLISH from various Russian articles
Avail: CASI HC A03/MF A01

Translated articles cover the following topics: determination of the gravitational constant from particle motion on a satellite near the libration point; using the moon's gravity in a flyby of asteroids that are approaching earth's orbit; analytic method for computing motion in halo orbit and shielding spacecraft against solar radiation in 'Relikt-2' project; most rapid maneuvers of spacecraft; possibilities for remote diagnosis of auroral and aeronomic characteristics from spacecraft using new type of spectrophotometric imaging system; principles for designing small autonomous spacecraft; analysis of the possibility of mitigating the danger of asteroids to the earth via the impact of a spacecraft; numerical modeling of impacts of meteorites; scientific discoveries made by Granat satellite; quasisatellite orbits for experiments involving refinement of the gravitational constant; Russia, European scientists discuss asteroid, planetary missions; use of passive spacecraft for increasing accuracy of fundamental geodetic parameters; possibilities of using passive spacecraft for solving problems in geodesy, geophysics, and geodynamics; accuracy in determining coordinates of points by observing navigational artificial earth satellites of GLONASS type; and atmospheric refraction correction methods in space geodesy and navigation. CASI

13 ASTRODYNAMICS

Includes powered and free-flight trajectories; and orbital and launching dynamics.

No abstracts in this category.

14 GROUND SUPPORT SYSTEMS AND FACILITIES (SPACE)

Includes launch complexes, research and production facilities; ground support equipment, e.g., mobile transporters; and simulators.

For related information see also *09 Research and Support Facilities (Air).*

N94-37225 Air Force Inst. of Tech., Wright-Patterson AFB, OH. School of Engineering.
DESIGN AND ANALYSIS OF A MODE B AND MODE JD SATELLITE EARTH STATION M.S. Thesis
Dennis J. Hance Jun. 1994 167 p Limited Reproducibility: More than 20% of this document may be affected by microfiche quality
(AD-A280417; AFIT/GE/ENG/94J-02) Avail: CASI HC A08

This thesis focuses on the design, integration, and analysis of an amateur radio service mode B and mode JD satellite earth station. Preliminary designs were investigated to determine the optimum configuration for the earth station. Modern digital modems, cabling structures, an 80386-based computer system, satellite tracking software, transmission and reception antennas, preamplifiers, and sophisticated performance measurement

technologies were integrated into a functioning earth station. Initially, component availability and station design dictated the selection and acquisition of the requisite station equipment, integration of the transmitter, receiver preamplifiers, antennas, and computer equipment followed. Preliminary testing of the various components in the integration station occupied a significant amount of time. Empirical test tracking of different amateur and commercial satellites verified proper operation of the earth station. Results are discussed throughout this thesis. DTIC

15 LAUNCH VEHICLES AND SPACE VEHICLES

Includes boosters; operating problems of launch/space vehicle systems; and reusable vehicles.

For related information see also *20 Spacecraft Propulsion and Power.*

No abstracts in this category.

16 SPACE TRANSPORTATION

Includes passenger and cargo space transportation, e.g., shuttle operations; and space rescue techniques.

For related information see also *03 Air Transportation and Safety* and *18 Spacecraft Design, Testing and Performance.* For space suits see *54 Man/System Technology and Life Support.*

N94-37026# General Accounting Office, Washington, DC. National Security and International Affairs Div.

SPACE SHUTTLE: INCOMPLETE DATA AND FUNDING APPROACH INCREASE COST RISK FOR UPGRADE PROGRAM. REPORT TO CONGRESSIONAL REQUESTERS

David R. Warren, Lee Edwards, James Beard, and Terry Wyatt May 1994 32 p

(GAO/NSIAD-94-23; B-254253) Avail: CASI HC A03/MF A01; also available from GAO, PO Box 6015, Gaithersburg, MD 20884-6015

The space shuttle is the only U.S. launch system capable of carrying people to and from space. It has operated for over 10 years and is likely to be used well into the next century. As the shuttle ages, NASA will be faced with increased need to update and replace various components due to obsolescence or to enhance safety. A review is presented of the shuttle program to determine (1) the assumptions NASA has made regarding the length of time the current shuttle fleet will be in operation and (2) NASA's processes and criteria for selecting needed safety and obsolescence upgrades. Derived from text

17 SPACE COMM., SPACECRAFT COMM., COMMAND & TRACKING

Includes telemetry; space communications networks; astronavigation and guidance; and radio blackout.

For related information see also *04 Aircraft Communications and Navigation* and *32 Communications and Radar.*

N94-36726# Naval Postgraduate School, Monterey, CA.

PRELIMINARY PANSAT GROUND STATION SOFTWARE DESIGN AND USE OF AN EXPERT SYSTEM TO ANALYZE TELEMETRY M.S. Thesis

Gregory W. Lawrence Mar. 1994 130 p

(AD-A280600) Avail: CASI HC A07/MF A02

The Petite Amateur Navy Satellite (PANSAT) is a communications satellite designed to be used by civilian amateur radio operators. A master ground station is being built at the Naval Postgraduate School. This computer system performs satellite commands, displays telemetry, trouble-shoots problems, and passes messages. The system also controls an open loop tracking antenna. This paper concentrates on the telemetry display, decoding, and interpretation through artificial intelligence (AI). The telemetry is displayed in an easily interpretable format, so that any user can understand the current health of the satellite and be cued as to any problems and possible solutions. Only the master ground station has the ability to receive all telemetry and send commands to the spacecraft; civilian ham users do not have access to this information. The telemetry data is decommutated and analyzed before it is displayed to the user, so that the raw data will not have to be interpreted by ground users. The analysis will use CLIPS imbedded in the code, and derive its inputs from telemetry decommutation. The program is an expert system using a forward chaining set of rules based on the expected operation and parameters of the satellite. By building the rules during the construction and design of the satellite, the telemetry can be well understood and interpreted after the satellite is launched and the designers may no longer be available to provide input to the problem. DTIC

N94-37386*# National Aeronautics and Space Administration. Lyndon B. Johnson Space Center, Houston, TX.

PROGRESS IN NAVIGATION FILTER ESTIMATE FUSION AND ITS APPLICATION TO SPACECRAFT RENDEZVOUS

J. Russell Carpenter 13 Jul. 1994 81 p

(NASA-TM-104794; S-768; NAS 1.15:104794) Avail: CASI HC A05/MF A01

A new derivation of an algorithm which fuses the outputs of two Kalman filters is presented within the context of previous research in this field. Unlike other works, this derivation clearly shows the combination of estimates to be optimal, minimizing the trace of the fused covariance matrix. The algorithm assumes that the filters use identical models, and are stable and operating optimally with respect to their own local measurements. Evidence is presented which indicates that the error ellipsoid derived from the covariance of the optimally fused estimate is contained within the intersections of the error ellipsoids of the two filters being fused. Modifications which reduce the algorithm's data transmission requirements are also presented, including a scalar gain approximation, a cross-covariance update formula which employs only the two contributing filters' autocovariances, and a form of the algorithm which can be used to reinitialize the two Kalman filters. A sufficient condition for using the optimally fused estimates to periodically reinitialize the Kalman filters in this fashion is presented and proved as a theorem. When these results are applied to an optimal spacecraft rendezvous problem, simulated performance results indicate that the use of optimally fused data leads to significantly improved robustness to initial target vehicle state errors. The following applications of estimate fusion methods to spacecraft rendezvous are also described: state vector differencing, and redundancy management. Author

18 SPACECRAFT DESIGN, TESTING AND PERFORMANCE

Includes satellites; space platforms; space stations; spacecraft systems and components such as thermal and environmental controls; and attitude controls.

For life support systems see *54 Man/System Technology and Life Support.* For related information see also *05 Aircraft Design, Testing and Performance, 39 Structural Mechanics,* and *16 Space Transportation.*

N94-36616# Advisory Group for Aerospace Research and Development, Neuilly-Sur-Seine (France). Guidance and Control Panel.

POINTING AND TRACKING SYSTEMS [SYSTEMES D'ACQUISITION ET DE POURSUITE AUTOMATIQUES]

May 1994 188 p In ENGLISH and FRENCH The 57th symposium was held in Seattle, WA, 12-15 Oct. 1993

(AGARD-CP-539; ISBN-92-835-0741-X) Copyright Avail: CASI HC A09/MF A02

This volume contains the 19 unclassified papers, presented at the Guidance and Control Panel Symposium held in Seattle, the United States from the 12th to the 15th of October, 1993. The papers presented cover the following areas: (1) overview of pointing and tracking systems and techniques; (2) optical pointing and tracking systems; (3) weapon control and mechanical systems; (4) pointing and tracking algorithms; and (5) sensor fusion. For individual titles, see N94-36617 through N94-36634.

N94-36617# McDonnell-Douglas Aerospace, Saint Louis, MO.
ICAAS PILOTED SIMULATION RESULTS **c32**
R. J. Landy, P. J. Halski, and R. P. Meyer *In* AGARD, Pointing and Tracking Systems May 1994 14 p (For primary document see N94-36616 12-18)
Copyright Avail: CASI HC A03/MF A02

This paper reports piloted simulation results from the Integrated Control and Avionics for Air Superiority (ICAAS) piloted simulation evaluations. The program was to develop, integrate, and demonstrate critical technologies which will enable United States Air Force tactical fighter 'blue' aircraft to achieve superiority and survive when outnumbered by as much as four to one by enemy aircraft during air combat engagements. Primary emphasis was placed on beyond visual range (BVR) combat with provisions for effective transition to close-in combat. The ICAAS system was developed and tested in two stages. The first stage, called low risk ICAAS, was defined as employing aircraft and avionics technology with an initial operational date no later than 1995. The second stage, called medium risk ICAAS, was defined as employing aircraft and avionics technology with an initial operational date no later than 1998. Descriptions of the low risk and medium risk simulation configurations are given. Normalized (unclassified) results from both the low risk and medium risk ICAAS simulations are discussed. The results show the ICAAS system provided a significant improvement in air combat performance when compared to a current weapon system. Data are presented for both current generation and advanced fighter aircraft. The ICAAS technologies which are ready for flight testing in order to transition to the fighter fleet are described along with technologies needing additional development. Author (revised)

N94-36618# Dornier-Werke G.m.b.H., Friedrichshafen (Germany).
LANDING OF AN UNMANNED HELICOPTER ON A MOVING PLATFORM. HIGH ACCURACY NAVIGATION AND TRACKING **c05**
Hans-Peter Engelbert and Johannes Schroeder *In* AGARD, Pointing and Tracking Systems May 1994 9 p (For primary document see N94-36616 12-18)
Copyright Avail: CASI HC A02/MF A02

Drones are of great importance for reconnaissance and surveillance in military applications. In regard to maritime drones Dornier demonstrated the automatic landing of a drone on a moving ship motion simulator in December 1991. The landing accuracy is determined by the tracking process. The tracking is performed by a laser tracker, which measures the drone position relative to the ship. Not only the drone but also the ship is equipped with an INS (Inertial Navigation System). The landing computations are performed in earth-fixed coordinates, whereby the earth-fixed positions are delivered by the INS. The determination of the drone position results from a combination of measurement values from the airborne INS and data from the ship laser tracker. The combination of the different information in the drone is performed in a Kalman-filter. The concept was verified in an experimental program. During the experimental program 13 flights were performed. The tracking accuracy was approximately 0.2 m. Author

N94-36619# Diehl G.m.b.H. und Co., Roethenbach (Germany). Optoelectronics Div.
POINTING AND TRACKING CONCEPT FOR A HIGH ENERGY LASER WEAPON APPLICATION **c36**
M. Noll and B. Warm *In* AGARD, Pointing and Tracking Systems May 1994 10 p (For primary document see N94-36616 12-18)
Copyright Avail: CASI HC A02/MF A02

In order to profit from the advantages of a higher energy laser weapon for air defense tasks against aircraft, helicopters or missiles, a suitable laser source and a high-accuracy tracking and pointing system is required. The following publication describes a possible pointing and tracking concept for a laser weapon in order to compensate for the most important factors of disturbance and solve the problems faced when engaging airborne targets. In addition to describing the influence of the effects occurring during the laser beam propagation through the atmosphere and the methods for its compensation, this article will focus on the concept and the characteristics of the tracking and pointing system and its components, designed for a high energy laser weapon application. Finally, this publication gives a detailed description of the functional link of the essential subsystems and components of the pointing and tracking concept for high energy laser weapon applications. Author

N94-36620# Thomson-TRT Defense, Guyancourt (France).
LASER DESIGNATION PODS OPTIMIZED CONCEPT FOR DAY/NIGHT OPERATIONS [PODS DE DESIGNATION LASER UN CONCEPT OPTIMISE POUR LES OPERATIONS JOUR/NUIT] **c36**
Yves Huguenin *In* AGARD, Pointing and Tracking Systems May 1994 7 p In FRENCH (For primary document see N94-36616 12-18)
Copyright Avail: CASI HC A02/MF A02

The conception of an optimized laser guided weapon that can be used at any time requires some technologies which, today, are not always compatible within the same equipment. From the 'day' ATLIS concept, Thomson-CSF developed a complementary 'night' pod. This convertible laser designation pod is the result of technical and operational optimization. Transl. by FLS

N94-36621# Thermo Electron Technologies Corp., San Diego, CA.
ADAPTIVE OPTICS FOR LASER BEAMFORMING IN THE ATMOSPHERE **c36**
M. LeFebvre, L. Cuellar, D. Sandler, and S. Stahl *In* AGARD, Pointing and Tracking Systems May 1994 10 p (For primary document see N94-36616 12-18)
Copyright Avail: CASI HC A02/MF A02

We report on the operational and performance of an integrated 1 meter adaptive optics system for compensation of atmospheric distortion of optical wavefronts. A visible artificial laser guide star (frequency-doybled Nd:YAG laser with wavelength of 0.532 microns) is used as the source for the reference wavefront. A shearing interferometer which uses a narrow optical bandwidth and has 500 subapertures is employed to sense wavefront distortion. These measurements are used to compute a conjugate wavefront to the distorted input light. The computed conjugate is then imprinted on a deformable mirror which consists of 500 square mirror segments. The effectiveness of the compensation is measured two ways: by imaging stars with a high resolution CCD camera in a narrow spectral bandwidth centered at 0.532 microns from which the point spread function is computed, or by collecting illuminator light reflected from a remote object with a photomultiplier tube. Atmospheric experiments are under way to test the performance of the integrated system. The results of these tests are very promising, yielding short-exposure stellar images which contain discernible energy at the diffraction limit of 0.1 arcsec, as well as a noticable improvement in the amount of light reflected from a remote target. Author

N94-36622# GEC-Marconi Avionics Ltd., Basilon, Essex (England).
INFRARED SEARCH AND TRACK DEMONSTRATOR PROGRAMME **c74**
W. D. McGinn, C. J. Tucker, and S. Nallanthighal *In* AGARD, Pointing and Tracking Systems May 1994 10 p (For primary document see N94-36616 12-18)
Copyright Avail: CASI HC A02/MF A02

The objective of the infrared search and track (IRST) program is to develop demonstration hardware which will be capable of long range detection and tracking of air targets in an airborne environment. This paper describes each of the major subsystems of the IRST equipment, which comprises the pointing system, the thermal imaging systems and the signal processing system. The various modes of operation are outlined which provide the capability to search for, detect and track multiple targets; to display imagery of a selected target and to provide passive ranging information. The equipment will be flown in an experimental Tornado aircraft and the installation and proposed trials are also described. A description of the ground proving equipment is also included. Author

N94-36623# Naval Air Warfare Center, Warminster, PA. Aircraft Div.
ADVANCED HELMET TRACKING TECHNOLOGY DEVELOPMENTS FOR NAVAL AVIATION **c54**
James H. Brindle *In* AGARD, Pointing and Tracking Systems May 1994 15 p (For primary document see N94-36616 12-18)
Copyright Avail: CASI HC A03/MF A02

There is a critical need across the Services to improve the effectiveness of aircrew within the crewstation by capitalizing on the natural psycho-motor skills of the pilot through the use of a variety of helmet-mounted visual display and control techniques. This has resulted in considerable interest and significant ongoing research and development efforts on the part of the Navy, as well as the Army and the Air Force, in the technology

building blocks associated with this area, such as advanced head tracking technologies, helmet-mounted display optics and electronics, and advanced night vision or image intensification technologies. Advanced multi-mode visually-coupled systems combine the attributes of image intensification with those of the helmet-mounted display capabilities for symbology and thermal sensor presentation. Examples of this class of system could be something as simple as the night vision goggle HUD, or NVG-HUD, which combines head tracking, image intensification, and simple symbology overlay, to the more complex multi-mode systems with high resolution miniature CRT's. This class of systems is capable of presenting to the pilot correlated, spatially-referenced information from both the image intensification technology, as well as a dynamic, high fidelity symbology overlay, and correlated thermal sensor imagery. Derived from text

N94-36624# General Electric Co. Ltd., Edinburgh (Scotland). Display Systems Group.

ADVANCES IN HELMET TRACKERS **c54**

W. M. Aspin *In* AGARD, Pointing and Tracking Systems May 1994 4 p (For primary document see N94-36616 12-18)

Copyright Avail: CASI HC A01/MF A02

The object of this paper is to describe in general, some recent developments in helmet tracking devices and, to detail the design of a particular optically based system. Author

N94-36625# Draper (Charles Stark) Lab., Inc., Cambridge, MA.

INERTIAL PSEUDO STAR REFERENCE UNIT **c74**

Michael F. Luniewicz, Dale T. Woodbury, Jerold P. Gilmore, and Tze T. Chien *In* AGARD, Pointing and Tracking Systems May 1994 14 p (For primary document see N94-36616 12-18)

Copyright Avail: CASI HC A03/MF A02

Advanced space systems for earth observation sensing and defense applications share a common objective: high-resolution monitoring. They require subsystems that accurately provide precise line-of-sight (LOS) pointing of the monitoring sensor with extreme jitter suppression and a precision attitude control system. To address this objective, Draper has developed a pointing system, the Inertial Pseudo Star Reference Unit (IPSRU). The IPSRU effort is a DARPA and SDI sponsored program at Draper under contract with the USAF Phillips Laboratory. The IPSRU implements a collimated light source mounted on a wide-band, extremely low-noise inertially stabilized platform. The collimated light beam becomes, in effect, a jitter-stabilized pseudo star. In addition, its direction in inertial space can be pointed at a precise rate by commands applied to the platform. Derived from text

N94-36626# Thomson-CSF, Bagneux (France). Div. Systemes Electronique.

HIGH ACCURACY CONTROL ALGORITHM APPLICATION TO A TRACKING TURRET **c61**

P. Nicodeme and P. Poulain *In* AGARD, Pointing and Tracking Systems May 1994 11 p (For primary document see N94-36616 12-18)

Copyright Avail: CASI HC A03/MF A02

The aim of the application described in this paper is to provide high accuracy control to a servomotor driven tracking turret. The system principles and requirements (target tracking and pointing capabilities for static and dynamic working) are presented. Then, the functional structure of the servos system to be controlled is explained: (1) mechanical system; (2) motor and electronics; and (3) digital computer for servo loops. The steps of the study to obtain robust, 'modern' and accurate control laws are detailed: (1) mechanical modelization for computer simulation; (2) motor and electronic representation; (3) simplified linear transfers identification (methods to obtain linear transfer; results for this particular application); and (4) design of high capability controllers. For this servo application, two 'new control methods' are presented for various hardware configuration of the turret (with or without a mechanical structure damping system such as a tachometer loop): (1) 'Model Based Predictive Control' with the 'Predictive Functional Control' method and the associated computer aided design tool; and (2) H-infinity controllers and the CAD tool. The basic principles of the two methods are explained and the way to obtain control laws are presented. Then, some simulation results obtained with these control laws for various pointing scenarios are discussed: (1) fixed or low speed target; (2) dynamic capability (gathering from an initial position to the turret, high speed passing target); and (3) stability and robustness (disturbance robustness, mechanical characteristic variation). The constraints and advantages of the various control laws are compared and discussed. Then, some trial results are summarized in a brief description. As a conclusion of the paper, the compliance of the results obtained by these methods with high accuracy requirements for pointing and tracking systems is discussed. Author (revised)

N94-36627# McDonnell-Douglas Aerospace, Saint Louis, MO.

AEROSERVOELASTIC STABILIZATION CONSIDERATIONS FOR POINTING AND TRACKING SYSTEMS **c37**

Peter Y. Cheng and Ralph E. Lambert *In* AGARD, Pointing and Tracking Systems May 1994 6 p (For primary document see N94-36616 12-18)

Copyright Avail: CASI HC A02/MF A02

The high gain, wide bandwidth precision tracking/pointing systems used on advanced aircraft necessitate the consideration of aeroservoelasticity (ASE) early in the design process. Aircraft control systems are designed to meet stability, performance and, in the case of manned aircraft, handling qualities criteria defined by the Mil-Spec requirements. As digital controllers are introduced, airframes are made statically unstable, and as the push for increased dynamic response continues, the aeroservoelastic influences become increasingly important in the overall system performance. At times, the ASE considerations may dominate the rigid body control law design effort. This paper summarizes an approach to the ASE stabilization of a fighter aircraft when used as the integral part of a high bandwidth manual or automatic fire control tracking system. The same approach can be applied to standard manual control aircraft where a more thorough ASE analysis is desired. Author

N94-36628# Universitaet der Bundeswehr Muenchen, Neubiberg (Germany). Fakultaet fuer Luft-und Raumfahrttechnik.

TWO-AXIS CAMERA PLATFORM FOR MACHINE VISION **c63**

J. Schiehlen and E. D. Dickmanns *In* AGARD, Pointing and Tracking Systems May 1994 6 p (For primary document see N94-36616 12-18)

Copyright Avail: CASI HC A02/MF A02

Mobile robots operating autonomously have to perceive their environment; many advantages favor using a vision sensor. The concept of dynamic vision is an adequate solution to this problem. The ability to track moving objects is essential. Therefore, a two axis camera platform is described having several modes of operation, which can be mounted on a mobile robot. An active vision system is presented, including the design of the pan-tilt head and the controller. Problems arising due to image processing delays, robots' own motion and platform actuator disturbances, e.g. friction, are treated. An aircraft application for vision based autonomous landing is given. Author

N94-36629# GEC-Marconi Avionics Ltd., Basilon, Essex (England). Navigation and Electro-Optic Systems Div.

MULTIPLE TARGET TRACK-WHILE-SCAN IN THE AIRBORNE EO ENVIRONMENT **c32**

J. MacLean and M. G. McGuigan *In* AGARD, Pointing and Tracking Systems May 1994 12 p (For primary document see N94-36616 12-18)

Copyright Avail: CASI HC A03/MF A02

Since early 1991, the Electro-Optic Systems Department (EOSD) of GEC Marconi Avionics Ltd. (GMAv) has been collaborating closely with radar systems designers from GMAv's Radar System Division (RSD) to develop Multiple Target Track-While-Scan (MTTWS) algorithms for tracking applications involving the use of electro-optical sensors. This work has progressed to the stage where simulations of EO-adapted MTTWS systems are now available and are implemented in representative processing hardware. The paper gives a general 'top level' overview of the EO-adapted MTTWS design, including functional block diagrams and a description of each of its three key elements. Illustrative diagrams show the detection data path and the important decision-making processes involved in correctly identifying possible airborne targets from clutter and noise. Examples of the MTTWS simulation output are also given. This information is presented in the form of pseudo-IR imagery overlaid with the relevant track information to give an 'at-a-glance' view of system performance. A number of interesting examples effectively serve to demonstrate 'general' system performance, and superior system performance in non-standard/testing conditions. The

paper hints at further extending performance in the integration of airborne radar and EO sensors, and discusses the related key issue of accurate inertial stabilization and referencing. Author

N94-36630# McMaster Univ., Hamilton (Ontario). Communications Research Lab.
MULTITARGET TRACK INITIATION USING A MODIFIED HOUGH TRANSFORM **c32**
T. Lo, J. Litva, H. Leung, and A. W. Bridgewater *In* AGARD, Pointing and Tracking Systems May 1994 8 p (For primary document see N94-36616 12-18)
Copyright Avail: CASI HC A02/MF A02

A modified Hough transform is proposed for multitarget track initiation. The proposed technique can initiate target tracks using data from as few as three scans. Simulated data as well as real radar plot data are used to test the initiator. Results show that its performance is superior to the conventional Hough transform in terms of false track rate without degradation in the probability of track detection. Author

N94-36631# Defence Research Establishment Ottawa, Ottawa (Ontario).
RADAR TRACKING IN MULTIPATH: TECHNIQUES FOR IMPROVED PERFORMANCE **c32**
R. M. Turner, E. Riseborough, and E. Bosse *In* AGARD, Pointing and Tracking Systems May 1994 8 p (For primary document see N94-36616 12-18)
Copyright Avail: CASI HC A02/MF A02

The low-elevation tracking performance of naval fire-control radars may be degraded by specular multipath. Performance can be significantly improved provided the radar has sufficient frequency agility and the appropriate signal processing is used. This paper examines the performance of a number of alternative techniques: monopulse averaged over a group frequencies within the agile band, monopulse with averaging weighted according to the signal-to-noise ratio and the use of a detailed propagation model in a maximum likelihood estimation technique called the Refined Maximum Likelihood (RML) method. Simulation results are presented to show that moderate improvement can be obtained by using monopulse with frequency averaging with a better improvement given by weighted averaging, the degree of improvement increasing with agile bandwidth. Where very precise height tracking of targets in a specular multipath is required, the RML technique is best. While RML was originally developed for antenna array signal processing, it can be applied to the two sub antennas of a phase monopulse system provided a sufficient degree of frequency agility is available. In this latter application, the technique has been designated RMONO for Refined monopulse. The basis of the RML technique is presented followed by an evaluation of its performance using results obtained from two experimental trials. Author

N94-36632# Alenia Aeronautica, Turin (Italy). System Technology Dept.
STUDIES AND SIMULATIONS ON SENSOR FUSION AND CUEING FOR FIGHTER APPLICATION **c54**
M. Avalle *In* AGARD, Pointing and Tracking Systems May 1994 8 p (For primary document see N94-36616 12-18)
Copyright Avail: CASI HC A02/MF A02

A method to implement the sensor fusion and sensor cueing on an advanced fighter aircraft is described in this paper. Starting from a short introduction concerning the general aspects and theory of sensor fusion, the paper presents some choices adopted during the development of the sensor fusion process at ALENIA DVD System Technology Dept. Sensor cueing will be also introduced and some particular cases of interest for a fighter aircraft will be discussed. The performances of the adopted solutions are then discussed on the basis of some experimental results obtained using a simulation tool. An evaluations of the overall sensor fusion process performance and some considerations about possible alternatives will conclude the work. Author

N94-36633# British Aerospace Defence Ltd., Preston (England). Military Aircraft Div.
SENSOR DATA FUSION FOR AIR TO AIR SITUATION AWARENESS BEYOND VISUAL RANGE **c66**
C. A. Noonan, M. E. Everett, and R. C. Freeman *In* AGARD, Pointing and Tracking Systems May 1994 8 p (For primary document see N94-36616 12-18)
Copyright Avail: CASI HC A02/MF A02

A modern tactical aircraft is faced with ever increasing threats and, to be effective against them, it needs to know what and where they are as early as possible during any encounter. It must do this day and night, in all weather, in hostile countermeasure environments and in the presence of clutter. Tactical aircraft receive large amounts of information from multiple sensors and data communications systems. To allow the crew to manage the aircraft and ensure its mission is fulfilled, the information must be aligned, correlated, consolidated and presented to them in a meaningful form. The paper introduces a model of tactical situation awareness processing which comprises sensors, data fusion, situation assessment and sensor management. The purpose of each component of the model and the relationships between them are discussed. The requirements placed on sensor data fusion by air to air sensing are discussed, and so is the way in which they are dominated by particular features of the tactical aircraft platform and its mission. The influence of these factors on the design of air to air situation awareness systems is considered. A computer test harness, developed by BAe Defence, Military Aircraft Division, is described, along with built-in tools which calculate test statistics. The harness was developed as part of a program of studies carried out by the Mission Systems group of the Design Quality and R&D team within the Systems Engineering Department at BAe's Warton unit in Lancashire, U.K. Examples of the results which were obtained when an air to air sensor data fusion model was evaluated are reproduced. These take the form of graphs and diagrams representing test statistics and offer a means by which different solutions to various data fusion problems may be compared under identical conditions. Author

N94-36634# Paramax Electronic, Inc., Montreal (Quebec).
CONTACT LEVEL FUSION OF RADAR AND IRST CONTACTS ON ALMOST ELECTROMAGNETICALLY SILENT PLATFORM **c32**
Francois Begin, Marc-Alain Simard, and Pierre Valin *In* AGARD, Pointing and Tracking Systems May 1994 9 p (For primary document see N94-36616 12-18)
Copyright Avail: CASI HC A02/MF A02

The fusion of data coming from dissimilar sensors (passive/active) such as the IRST and radar raises the problem of the coordinate system used in the computation of the state vector. In single sensor tracking the IRST tracks are usually computed using an angle and angle rate coordinate system. In radar tracking, the state vector and the covariance matrix are generally computed in cartesian coordinates. Recent papers have shown the advantage of the modified spherical coordinates over cartesian coordinates in tracking passively AAW targets. It is thus natural to investigate if this advantage exists for fused sensors in an almost electromagnetically silent situation. Due to the missing range of the IRST, at the contact level fusion, the cartesian form of the 'purely' linear Kalman filter cannot be used directly without making non rigorous modifications. In this case, a linearized measurement matrix (H) can be used in a modified Kalman filter. This research pursues two goals: first, it analyzes the pertinence of the spherical and modified spherical coordinate formulation of the extended Kalman filter over the cartesian coordinate formulation and second, it evaluates the extent to which the platform can stay electromagnetically silent without damaging the quality of the tracking. The analysis shows the feasibility of data fusion in all three coordinate systems. The investigations are showing equivalent or better performances for the extended Kalman filter in cartesian coordinates. Sparse radar contacts are interleaved with regular IRST contacts, the former providing occasional range measurements to be fused with the regular more accurate angular information of the IRST. Author

N94-36825*# National Aeronautics and Space Administration. Marshall Space Flight Center, Huntsville, AL.
GLOBAL POSITIONING SYSTEM SYNCHRONIZED ACTIVE LIGHT AUTONOMOUS DOCKING SYSTEM Patent Application
Richard Howard, inventor (to NASA) et al 1 Aug. 1994 37 p
(NASA-Case-MFS-28853-1; NAS 1.71:MFS-28853-1;
US-Patent-Appl-SN-283728) Avail: CASI HC A03/MF A01

A Global Positioning System Synchronized Active Light Autonomous Docking System (GPSSALADS) for automatically docking a chase vehicle with a target vehicle comprises at least one active light emitting target which is operatively attached to the target vehicle. The target includes a

three-dimensional array of concomitantly flashing lights which flash at a controlled common frequency. The GPSSALADS further comprises a visual tracking sensor operatively attached to the chase vehicle for detecting and tracking the target vehicle. Its performance is synchronized with the flash frequency of the lights by a synchronization means which is comprised of first and second internal clocks operatively connected to the active light target and visual tracking sensor, respectively, for providing timing control signals thereto, respectively. The synchronization means further includes first and second Global Positioning System receivers operatively connected to the first and second internal clocks, respectively, for repeatedly providing simultaneous synchronization pulses to the internal clocks, respectively. In addition, the GPSSALADS includes a docking process controller means which is operatively attached to the chase vehicle and is responsive to the visual tracking sensor for producing commands for the guidance and propulsion system of the chase vehicle. NASA

N94-36990*# Computer Technology Associates, Inc., Hampton, VA.
CHARACTERIZATION OF SPACECRAFT AND ENVIRONMENTAL DISTURBANCES ON A SmallSat
Thomas A. Johnson, Dung Phu Chi Nguyen, Vince Cuda, and Doug Freesland Jul. 1994 85 p
(Contract NAS1-18936; RTOP 233-01-01-01)
(NASA-CR-194915; NAS 1.26:194915) Avail: CASI HC A05/MF A01

The objective of this study is to model the on-orbit vibration environment encountered by a SmallSat. Vibration control issues are common to the Earth observing, imaging, and microgravity communities. A spacecraft may contain dozens of support systems and instruments each a potential source of vibration. The quality of payload data depends on constraining vibration so that parasitic disturbances do not affect the payload's pointing or microgravity requirement. In practice, payloads are designed incorporating existing flight hardware in many cases with nonspecific vibration performance. Thus, for the development of a payload, designers require a thorough knowledge of existing mechanical devices and their associated disturbance levels. This study evaluates a SmallSat mission and seeks to answer basic questions concerning on-orbit vibration. Payloads were considered from the Earth observing, microgravity, and imaging communities. Candidate payload requirements were matched to spacecraft bus resources of present day SmallSats. From the set of candidate payloads, the representative payload GLAS (Geoscience Laser Altimeter System) was selected. The requirements of GLAS were considered very stringent for the 150 - 500 kg class of payloads. Once the payload was selected, a generic SmallSat was designed in order to accommodate the payload requirements (weight, size, power, etc.). This study seeks to characterize the on-orbit vibration environment of a SmallSat designed for this type of mission and to determine whether a SmallSat can provide the precision pointing and jitter control required for earth observing payloads. Author

N94-37009# National Oceanographic Data Center, Washington, DC. Ingest Systems Branch.
NOAA POLAR SATELLITE CALIBRATION: A SYSTEM DESCRIPTION
Cecil A. Paris Feb. 1994 67 p
(NOAA-TR-NESDIS-77) Avail: CASI HC A04/MF A01

The operational processing of polar satellite data has undergone many evolutionary changes since the launch of TIROS-N in 1978. These changes have resulted in both functional and organizational changes within NESDIS. In general, corporate knowledge of the detailed steps involved in processing satellite data has been greatly diminished. The following describes several factors contributing to our current situation: decreasing staff/budget and non-replacement of key positions, prompting centralization of many separate functions into one functional element; re-hosting of applications software from the original TIROS-N satellite processing subsystem to an IBM mainframe system (all capabilities inherent to the current system were not transferred in totality to the new system); the lack of properly documented software, procedures, and methodologies associated with detailed, step-by-step processing of satellite data, i.e. pre-launch, early orbit support, in-flight calibration, etc. In efforts to mitigate any further erosion of our knowledge base of operational satellite data processing with respect to calibration, this report is intended to document the instructional guidelines for processing of pre-launch and in-flight calibration data for instruments aboard the NOAA Polar-orbiting Operational Environmental Satellites (POES). Its purpose is to familiarize the reader--the user and managers of satellite acquired environmental data or data systems--with the basic operational technology, terminology and status of the NOAA polar satellite calibration system. Thus, a very brief description of calibration, radiometry, POES instrumentation, and procedures for prelaunch, early-orbit, in-flight, and post-launch support have been included as these subjects pertain to operational calibration. Author (revised)

N94-37257# General Accounting Office, Washington, DC. National Security and International Affairs Div.
SPACE STATION: IMPACT OF THE EXPANDED RUSSIAN ROLE ON FUNDING AND RESEARCH. REPORT TO THE RANKING MINORITY MEMBER, SUBCOMMITTEE ON OVERSIGHT OF GOVERNMENT MANAGEMENT, COMMITTEE ON GOVERNMENTAL AFFAIRS, US SENATE
David Warren, Frank Degnan, Lee Edwards, Richard Eiserman, Mona Zadjura, Vijay Barnabas, Elaine Coleman, John Gilchrist, Wendy Smythe, and Mae Jones Jun. 1994 15 p
(GAO/NSIAD-94-220; B-257654) Avail: CASI HC A03/MF A01; also available from GAO, PO Box 6015, Gaithersburg, MD 20884-6015

An examination is made on the impact of Russian participation in NASA's space station program. This interim report deals with whether expanded Russian participation will (1) reduce space station funding requirements by $2 billion, as estimated by NASA, and (2) improve the station's capabilities for conducting research. Results at this time are that (1) NASA's estimated savings in the space station program would be largely offset by an estimated $1.4 billion in increased funding requirements accounted for in other parts of NASA's budget and (2) some of NASA's $2 billion savings may not be attributable to Russian participation. Russian participation in the space station would substantially increase overall station research resources. CASI

N94-37260*# National Aeronautics and Space Administration. Langley Research Center, Hampton, VA.
OPTIMAL CONTROL THEORY DETERMINATION OF FEASIBLE RETURN-TO-LAUNCH-SITE ABORTS FOR THE HL-20 PERSONNEL LAUNCH SYSTEM VEHICLE
Kevin E. Dutton Jul. 1994 24 p
(RTOP 506-59-61-04)
(NASA-TP-3449; L-17343; NAS 1.60:3449) Avail: CASI HC A03/MF A01

The personnel launch system (PLS) being studied by NASA is a system to complement the space shuttle and provide alternative access to space. The PLS consists of a manned spacecraft launched by an expendable launch vehicle (ELV). A candidate for the manned spacecraft is the HL-20 lifting body. In the event of an ELV malfunction during the initial portion of the ascent trajectory, the HL-20 will separate from the rocket and perform an unpowered return to launch site (RTLS) abort. This work details an investigation, using optimal control theory, of the RTLS abort scenario. The objective of the optimization was to maximize final altitude. With final altitude as the cost function, the feasibility of an RTLS abort at different times during the ascent was determined. The method of differential inclusions was used to determine the optimal state trajectories, and the optimal controls were then calculated from the optimal states and state rates. Author

N94-37349 Virginia Polytechnic Inst. and State Univ., Blacksburg, VA. Dept. of Engineering Science and Mechanics.
MODELING AND CONTROL OF INTELLIGENT FLEXIBLE STRUCTURES Final Report, 15 Jun. 1990 - 14 Dec. 1993
Daniel J. Inman 26 Mar. 1994 207 p Limited Reproducibility: More than 20% of this document may be affected by microfiche quality
(Grant AF-AFOSR-0181-91)
(AD-A280478; AFOSR-94-0353TR) Avail: CASI HC A10

The research effort reported here summarizes the issues and discoveries of a three year effort to examine the modeling and control of intelligent structures for aerospace applications. Intelligent structures or smart structures or, more appropriately, active structures are defined here in a narrow sense as structures with highly integrated sensors and actuators (piezoceramic elements in this case). The major control thrust is vibration suppression. The issues of interest are (a) is the complexity of a smart structure control system worth it, (b) how detailed must modeling be to produce effective results, and (c) does the choice of a control law make a significant difference on the response. The results show clearly that improved

models and complex control strategies form the most effective combination. The results show three experimental examples which clearly indicate the usefulness and advantages of smart structures over conventional vibration suppression methodologies. In particular, active structures improve overall efficiency in cases involving both flexible and rigid body control. In addition, some tangent results on nonlinear control, control in the presence of uncertainties, and control of thermoelastic systems are presented. DTIC

N94-37351 Pennsylvania State Univ., University Park, PA. Dept. of Aerospace Engineering.
CONFIGURATIONAL EVOLUTION DYNAMICS AND STABILITY DURING IN-SITU DEVELOPMENT OF LARGE ORBITING SPACECRAFT Final Technical Report, 15 Jan. 1991 - 14 Jan. 1994
Anthony K. Amos 22 Apr. 1994 51 p Limited Reproducibility: More than 20% of this document may be affected by microfiche quality
(Grant AF-AFOSR-0155-91)
(AD-A280482; AFOSR-94-0361TR) Avail: CASI HC A04

This report documents the objectives, major tasks, and approaches of the research project and the progress made over the three year span of the effort. The primary objective is the search for understanding of and analytical simulation capability for the effects of flexibility and configuration evolution on the on-orbit dynamics and stability of orbiting spacecraft. The approach is described in terms of the modeling and analysis of isolated deployment and assembly mechanisms, the modeling and analysis of coupled orbital-attitude-vibration dynamics of orbiting spacecraft, and the integration of the two for on-orbit system performance simulation. Details of the modeling and analysis efforts are described and sample results obtained during the course of the research are presented and discussed. DTIC

N94-37502*# National Aeronautics and Space Administration. Langley Research Center, Hampton, VA.
APPROXIMATE ANALYSIS FOR REPEATED EIGENVALUE PROBLEMS WITH APPLICATIONS TO CONTROLS-STRUCTURE INTEGRATED DESIGN
Sean P. Kenny and Gene J. W. Hou Jun. 1994 30 p
(RTOP 233-01-01-05)
(NASA-TP-3439; L-17232; NAS 1.60:3439) Avail: CASI HC A03/MF A01

A method for eigenvalue and eigenvector approximate analysis for the case of repeated eigenvalues with distinct first derivatives is presented. The approximate analysis method developed involves a reparameterization of the multivariable structural eigenvalue problem in terms of a single positive-valued parameter. The resulting equations yield first-order approximations to changes in the eigenvalues and the eigenvectors associated with the repeated eigenvalue problem. This work also presents a numerical technique that facilitates the definition of an eigenvector derivative for the case of repeated eigenvalues with repeated eigenvalue derivatives (of all orders). Examples are given which demonstrate the application of such equations for sensitivity and approximate analysis. Emphasis is placed on the application of sensitivity analysis to large-scale structural and controls-structures optimization problems. Author

N94-37504*# Lockheed Engineering and Sciences Co., Hampton, VA.
REFERENCE MANUAL FOR THE THERMAL ANALYST'S HELP DESK EXPERT SYSTEM
Rachel A. Ormsby Jul. 1994 201 p
(Contract NAS1-19000; RTOP 477-50-00-01)
(NASA-CR-194941; NAS 1.26:194941) Avail: CASI HC A10/MF A03

This document provides technical information and programming guidance for the maintenance and future development of the Thermal Analyst's Help Desk. Help Desk is an expert system that operates within the EXSYSTM expert system shell, and is used to determine first approximations of thermal capacity for spacecraft and instruments. The five analyses supported in Help Desk are: (1) surface area required for a radiating surface, (2) equilibrium temperature of a surface, (3) enclosure temperature and heat loads for a defined position in orbit, (4) enclosure temperature and heat loads over a complete orbit and, (5) selection of appropriate surface properties. The two geometries supported by Help Desk are a single flat plate and a rectangular box enclosure. The technical information includes the mathematical approach and analytical derivations used in the analyses such as: radiation heat balance, view factor calculation, and orbit determination with coordinate transformation. The programming guide for developers describes techniques for enhancement of Help Desk. Examples are provided showing the addition of new features, user interface development and enhancement, and external program interfaces. Author

N94-37506*# George Washington Univ., Hampton, VA.
EVALUATION OF GPS POSITION AND ATTITUDE DETERMINATION FOR AUTOMATED RENDEZVOUS AND DOCKING MISSIONS M.S. Thesis
Marc D. DiPrinzio and Robert H. Tolson Jul. 1994 86 p
(Contract NCC1-104; RTOP 225-99-00-01)
(NASA-CR-4614; NAS 1.26:4614) Avail: CASI HC A05/MF A01

The use of the Global Positioning System for position and attitude determination is evaluated for an automated rendezvous and docking mission. The typical mission scenario involves the chaser docking with the target for resupply or repair purposes, and is divided into three sections. During the homing phase, the chaser utilizes coarse acquisition pseudorange data to approach the target; guidance laws for this stage are investigated. In the second phase, differential carrier phase positioning is utilized. The chaser must maintain a quasiconstant distance from the target, in order to resolve the initial integer ambiguities. Once the ambiguities are determined, the terminal phase is entered, and the rendezvous is completed with continuous carrier phase tracking. Attitude knowledge is maintained in all phases through the use of the carrier phase observable. A Kalman filter is utilized to estimate all states from the noisy measurement data. The effects of selective availability and cycle slips are also investigated.
Author (revised)

N94-37580*# Dayton Univ., OH. Dept. of Engineering Management and Systems.
OPERATIONS AND SUPPORT COST MODELING OF CONCEPTUAL SPACE VEHICLES Annual Report, Jun. 1993 - Jul. 1994
Charles Ebeling Aug. 1994 97 p
(Grant NAG1-1327)
(NASA-CR-196299; NAS 1.26:196299) Avail: CASI HC A05/MF A02

The University of Dayton is pleased to submit this annual report to the National Aeronautics and Space Administration (NASA) Langley Research Center which documents the development of an operations and support (O&S) cost model as part of a larger life cycle cost (LCC) structure. It is intended for use during the conceptual design of new launch vehicles and spacecraft. This research is being conducted under NASA Research Grant NAG-1-1327. This research effort changes the focus from that of the first two years in which a reliability and maintainability model was developed to the initial development of an operations and support life cycle cost model. Cost categories were initially patterned after NASA's three axis work breakdown structure consisting of a configuration axis (vehicle), a function axis, and a cost axis. A revised cost element structure (CES), which is currently under study by NASA, was used to established the basic cost elements used in the model. While the focus of the effort was on operations and maintenance costs and other recurring costs, the computerized model allowed for other cost categories such as RDT&E and production costs to be addressed. Secondary tasks performed concurrent with the development of the costing model included support and upgrades to the reliability and maintainability (R&M) model. The primary result of the current research has been a methodology and a computer implementation of the methodology to provide for timely operations and support cost analysis during the conceptual design activities. Derived from text

19 SPACECRAFT INSTRUMENTATION

For related information see also *06 Aircraft Instrumentation* and *35 Instrumentation and Photography.*

N94-36988*# Johns Hopkins Univ., Baltimore, MD. Dept. of Electrical and Computer Engineering.
RECEIVER DESIGN, PERFORMANCE ANALYSIS, AND EVALUATION FOR SPACE-BORNE LASER ALTIMETERS AND SPACE-TO-SPACE LASER RANGING SYSTEMS Interim Progress Report, 16 Oct. 1993 - 14 Apr. 1994
Frederic M. Davidson, Xiaoli Sun, and Christopher T. Field May 1994 90 p

(Grant NAG5-2232)
(NASA-CR-194747; NAS 1.26:194747) Avail: CASI HC A05/MF A01

Accomplishments in the following areas of research are presented: receiver performance study of spaceborne laser altimeters and cloud and aerosol lidars; receiver performance analysis for space-to-space laser ranging systems; and receiver performance study for the Mars Environmental Survey (MESUR). Derived from text

20 SPACECRAFT PROPULSION AND POWER

Includes main propulsion systems and components, e.g., rocket engines; and spacecraft auxiliary power sources.

For related information see also *07 Aircraft Propulsion and Power, 28 Propellants and Fuels, 44 Energy Production and Conversion,* and *15 Launch Vehicles and Space Vehicles.*

N94-36445 Naval Research Lab., Washington, DC.
UVPI IMAGING FROM THE LACE SATELLITE: THE LOW COST LAUNCH VEHICLE (LCLV) ROCKET PLUME Interim Report
H. W. Smathers, D. M. Horan, J. G. Cardon, E. R. Malaret, L. Perez, T. Tran, and J. E. Brandenburg 24 Sep. 1993 116 p Limited Reproducibility: More than 20% of this document may be affected by microfiche quality
(AD-A278785; NRL/FR/8121-93-9545) Avail: Issuing Activity (Defense Technical Information Center (DTIC))

The Ultraviolet Plume Instrument (UVPI) is a small, plume-tracking instrument flown on the Naval Research Laboratory's Low-power Atmospheric Compensation Experiment (LACE) satellite. The plume camera has a relatively narrow field of view, 0.184 deg by 0.137 deg, and observes sources through any of four filters with passbands of 195 to 295 nm, 200 to 320 nm, 235 to 350 nm, and 300 to 320 nm. The LCLV (Low Cost Launch Vehicle) was launched from Wallops Island, Virginia, before sunrise on 6 February 1991. The third stage, powered by an Aries solid-fuel rocket motor, reached a 117-km altitude and was successfully detected and tracked by the UVPI from a range of 450 to 550 km. The spectral radiance and spectral radiant intensities of the missile plumes were extracted from these images for the four passbands. DTIC

N94-36821*# National Aeronautics and Space Administration. Lewis Research Center, Cleveland, OH.
REVIEW OF ADVANCED RADIATOR TECHNOLOGIES FOR SPACECRAFT POWER SYSTEMS AND SPACE THERMAL CONTROL
Albert J. Juhasz and George P. Peterson Jun. 1994 25 p
(RTOP 583-02-21)
(NASA-TM-4555; E-8263; NAS 1.15:4555) Avail: CASI HC A03/MF A01

A two-part overview of progress in space radiator technologies is presented. The first part reviews and compares the innovative heat-rejection system concepts proposed during the past decade, some of which have been developed to the breadboard demonstration stage. Included are space-constructable radiators with heat pipes, variable-surface-area radiators, rotating solid radiators, moving-belt radiators, rotating film radiators, liquid droplet radiators, Curie point radiators, and rotating bubble-membrane radiators. The second part summarizes a multielement project including focused hardware development under the Civil Space Technology Initiative (CSTI) High Capacity Power program carried out by the NASA Lewis Research Center and its contractors to develop lightweight space radiators in support of Space Exploration Initiative (SEI) power systems technology. Author

N94-36951*# National Aeronautics and Space Administration. Lewis Research Center, Cleveland, OH.
OPERATIONAL ENVIRONMENTS FOR ELECTRICAL POWER WIRING ON NASA SPACE SYSTEMS
Mark W. Stavnes (NYMA, Inc., Brook Park, OH.), Ahmad N. Hammoud (NYMA, Inc., Brook Park, OH.), and Robert W. Bercaw Jun. 1994 40 p
(Contracts NAS3-27186; NAS3-25266; RTOP 323-15-03)
(NASA-TM-106655; E-8968; NAS 1.15:106655) Avail: CASI HC A03/MF A01; 3 functional color pages

Electrical wiring systems are used extensively on NASA space systems for power management and distribution, control and command, and data transmission. The reliability of these systems when exposed to the harsh environments of space is very critical to mission success and crew safety. Failures have been reported both on the ground and in flight due to arc tracking in the wiring harnesses, made possible by insulation degradation. This report was written as part of a NASA Office of Safety and Mission Assurance (Code Q) program to identify and characterize wiring systems in terms of their potential use in aerospace vehicles. The goal of the program is to provide the information and guidance needed to develop and qualify reliable, safe, lightweight wiring systems, which are resistant to arc tracking and suitable for use in space power applications. This report identifies the environments in which NASA spacecraft will operate, and determines the specific NASA testing requirements. A summary of related test programs is also given in this report. This data will be valuable to spacecraft designers in determining the best wiring constructions for the various NASA applications. Author

N94-37433# General Atomic Co., San Diego, CA.
CONCEPTUAL DESIGN: TFE VERIFICATION PROGRAM Final Report
Mar. 1994 82 p
(Contract DE-AC03-86SF-16298; GA Proj. 3450)
(DE94-012469; GA-A21590) Avail: CASI HC A05/MF A01

This report documents the TFE conceptual design, which provided the design guidance for the TFE verification program. The primary goals of this design effort were: (1) establish the conceptual design of an in-core thermionic reactor for a 2 Mw(e) space nuclear power system with a 7-year operating lifetime; (2) demonstrate scalability of the above concept over the output power range of 500 kW(e) to 5 MW(e); and (3) define the TFE which is the basis for the 2 MW(e) reactor design. This TFE specification provided the basis for the test program. These primary goals were achieved. The technical approach taken in the conceptual design effort is discussed in Section 2, and the results are discussed in Section 3. The remainder of this introduction draws a perspective on the role that this conceptual design task played in the TFE verification program. DOE

N94-37514# General Atomic Co., San Diego, CA.
TFE VERIFICATION PROGRAM Semiannual Report, period ending 30 Sep. 1993
Jan. 1994 107 p
(Contract DE-AC03-86SF-16298)
(DE94-009870; GA-A-21511) Avail: CASI HC A06/MF A02 (US Sales Only)

This is the final semiannual progress report for the Thermionic Fuel Elements (TFE) verification. A decision was made in August 1993 to begin a Close Out Program on October 1, 1993. Final reports summarizing the design analyses and test activities of the TFE Verification Program will be written, stand-alone documents for each task. The objective of the semiannual progress report is to summarize the technical results obtained during the latest reporting period. The information presented herein includes evaluated test data, design evaluations, the results of analyses and the significance of results. DOE

N94-37764*# Colorado State Univ., Fort Collins, CO. Dept. of Mechanical Engineering.
CHARACTERISTICS OF IONS EMITTED FROM HIGH-CURRENT HOLLOW CATHODES Final Report
Ikuya Kameyama Aug. 1994 93 p
(Grant NAG3-1206; RTOP 232-02-02)
(NASA-CR-195372; E-9055; NAS 1.26:195372) Avail: CASI HC A05/MF A01

Energy distributions of ions emanating from high-current, xenon hollow cathodes were obtained using an electrostatic energy analyzer. Ions with energies greater than maximum potential differences between electrodes were observed. This result is consistent with previous retarding-potential-analyzer data, but the electrostatic-energy-analyzer data show much more complicated structures. In order to characterize these distributions, simple Gaussian distributions were used and mean energies, energy dispersions, and ion populations of the Gaussian-distribution components are presented to illustrate the trends of high-energy-ion characteristics with discharge conditions. The energy of ions emanating from cathodes appears to increase as discharge current is increased, ambient pressure is reduced, or cathode flow rate is reduced. In addition, higher discharge currents, lower ambient pressures, and higher cathode flow rates cause the ion populations in the high-energy tails of the distribution to

increase. The visual appearances of the cathode-discharge plasmas observed with different discharge currents and orifice-bore shapes and sizes are correlated with the characteristics of the emitted ions.
Author (revised)

23 CHEMISTRY AND MATERIALS (GENERAL)

N94-37106 Harvard Univ., Cambridge, MA. Dept. of Chemistry.
TERT-BUTYLALUMOXANES: SYNTHETIC ANALOGS FOR METHYLALUMOXANE (MAO) AND NEW CATALYTIC ROUTES TO POLYOLEFINS AND POLYKETONES
Andrew R. Barron 15 Jun. 1994 9 p Limited Reproducibility: More than 20% of this document may be affected by microfiche quality
(Contract N00014-91-J-1934)
(AD-A280511) Avail: CASI HC A02

Alkyl alumoxanes, the products from the partial hydrolysis of aluminum trialkyls, have been shown to be active catalysts and co-catalysts for a variety of polymerization processes. Despite industrial usage, no one has been able to isolate individual compounds and demonstrate a structure activity correlation. The purpose of this study is to: (a) isolate single alumoxane species, (b) determine the function of alumoxanes in Ziegler Natta Catalysis, and (c) develop new polymers, employing these catalysts.
DTIC

N94-37134 State Univ. of New York, Stony Brook, NY. Dept. of Chemistry.
CYCLIZATION OF BIS-URETHANES AS A NEW METHOD FOR THE SYNTHESIS OF 5-SUBSTITUTED, 6-MEMBERED CYCLIC UREAS Technical Report No. 8, Jun. 1993 - May 1994
Kathy J. Fordon, Christopher G. Crane, and Cynthia J. Burrows 31 May 1994 4 p Submitted for publication Limited Reproducibility: More than 20% of this document may be affected by microfiche quality
(Contract N00014-88-K-0315)
(AD-A280232) Avail: Issuing Activity (Defense Technical Information Center (DTIC))

A new method of synthesis of 5-substituted, 6-membered cyclic ureas was found in which urethane derivatives of 1,3-diaminopropane were cyclized using Cs2CO3.
DTIC

N94-37214 Pittsburgh Univ., Pittsburgh, PA. Materials Research Center.
[STATUS REVIEW AND ACCOMPLISHMENTS OF THE MATERIALS RESEARCH CENTER AT THE UNIVERSITY OF PITTSBURGH] Final Report, 1 Nov. 1991 - 28 Feb. 1994
D. M. Hercules, F. S. Pettit, and G. Mayer 29 Apr. 1994 364 p Limited Reproducibility: More than 20% of this document may be affected by microfiche quality
(Contract AF-AFOSR-0441-91)
(AD-A280422; AFOSR-94-0354TR) Avail: CASI HC A16

The research and related activities at the Materials Research Center (MRC) of the University of Pittsburgh under AFOSR Grant 91-0441 are summarized. The research program has progressed in four technical areas. Nine projects under the heading of High-Performance Materials are discussed and include degradation of intermetallics and composites at elevated temperatures, deformation behavior of alloys during processing and service, and development of polymers with improved mechanical properties through microstructure control. Thirteen projects have involved Electro-optics. The development of new organic optoelectronic materials employing the design and synthesis of molecules, polymers, and molecular clusters is described and the tailoring of materials in specific device structures, such as IR detectors, light emitters, or filters is discussed. Five projects involve investigations related to Biotechnology where bioactive proteins as smart materials, viral proteins as templates for bioactive materials, and molecular recognition elements have been studied. In the catalysis technical area, the results from studies on decomposition of nerve gases, and catalysts related to alternate fuels are presented. Educational aspects of the Center are also summarized. New equipment capabilities are reviewed, as well as internal and external collaborations of the MRC. Finally, the future plans for the MRC are addressed.
DTIC

N94-37315*# National Aeronautics and Space Administration. Lewis Research Center, Cleveland, OH.
COPPER-CONTAINING CERAMIC PRECURSOR SYNTHESIS: SOLID-STATE TRANSFORMATIONS AND MATERIALS TECHNOLOGY
Aloysius F. Hepp, William E. Eckles, Stan A. Duraj, Maria T. Andras, Phillip E. Fanwick, Robert M. Richman, Michael L. Sabat, Michael B. Power, Edward M. Gordon, and Andrew Barron Jul. 1994 8 p Meeting held in Boston, MA, 29 Nov. - 3 Dec. 1993; sponsored by the Materials Research Society
(Contracts NCC3-162; NCC3-246; NCC3-249; NAS3-23709; NCC3-281; RTOP 233-01-0A)
(NASA-TM-106556; E-8716; NAS 1.15:106556) Avail: CASI HC A02/MF A01

Three copper systems with relevance to materials technology are discussed. In the first, a CuS precursor, Cu4S1O (4-methylpyridine)(sub 4)-(4-MePy), was prepared by three routes: reaction of Cu2S, reaction of CuBr-SMe2, and oxidation of copper powder with excess sulfur in 4-methylpyridine by sulfur. In the second, copper powder was found to react with excess thiourea (H2NC(S)NH2) in 4-methylpyridine to produce thiocyanate (NCS(-)) complexes. Three isolated and characterized compounds are: Cu(NCS)(4-MePy)(sub 2), a polymer, (4-MePy-H)(Cu(NCS)(sub 3)(4-MePy)(sub 2)), a salt, and t-Cu(NCS)(sub 2)(4-MePy)(sub 4). Finally, an attempt to produce a mixed-metal sulfide precursor of Cu and Ga in N-methylimidazole (N-MeIm) resulted in the synthesis of a Cu-containing polymer, Cu(SO4)(N-MeIm). The structures are presented; the chemistry will be briefly discussed in the context of preparation and processing of copper-containing materials for aerospace applications.
Author (revised)

N94-37531 Direction des Recherches, Etudes et Techniques, Paris (France). Centre de Documentation de l'Armement.
THE 1ST INTERNATIONAL SYMPOSIUM ON ORGANIC PHOTOCHROMISM: MOLECULES AND SYSTEMS
1994 116 p Conference held in Iles des Embiez, France, 12-16 Sep. 1993
(PB94-179488) Avail: Issuing Activity (National Technical Information Service (NTIS))

The document contains the abstracts from the International Symposium on Organic Photochromism 1993 (ISOP 93), held September 12-16, 1993 in Iles des Embiez, Var, France. It includes the organization and sponsorship, general schedule of the working sessions, and list of the contributed papers as well.
NTIS

N94-37614*# Boeing Defense and Space Group, Seattle, WA.
EVALUATION OF SEALS AND LUBRICANTS USED ON THE LONG DURATION EXPOSURE FACILITY Report, Oct. 1989 - Dec. 1993
H. W. Dursch, B. K. Keough, and H. G. Pippin Jun. 1994 107 p
(Contracts NAS1-18224; NAS1-19247; RTOP 506-43-61-02; RTOP 233-03-02-04)
(NASA-CR-4604; NAS 1.26:4604) Avail: CASI HC A06/MF A02

This report described results from testing and analysis of seals and lubricants subsequent to the 69-month low-earth-orbit (LEO) exposure on the Long Duration Exposure Facility (LDEF). Results show that if the materials were shielded from exposure to LDEF's external environment, the 69-month exposure to LEO resulted in minimal changes to material properties. However, if the materials were exposed to LDEF's exterior environments (atomic oxygen, solar radiation, meteoroids, and/or space debris), a variety of events occurred, ranging from no material change, to changes in properties, to significant erosion of the material.
Author

N94-37650# Harvard Univ., Cambridge, MA. Dept. of Chemistry.
TERT-BUTYLALUMOXANES: SYNTHETIC ANALOGS FOR METHYLALUMOXANE (MAO) AND NEW CATALYTIC ROUTES TO POLYOLEFINS AND POLYKETONES
C. J. Harlan, Mark R. Mason, and Andrew R. Barron 16 Jun. 1994 47 p
(Contract N00014-91-J-1934)
(AD-A280532; TR-4-ONR) Avail: CASI HC A03/MF A01

The hydrolysis of Al(Bu-t)3 in toluene using the hydrated salt, Al2(SO4)3.14(H20), results in the formation of the dimeric hydroxide ((Bu-t)2Al(mu-OH))2 (1) and Al4(Bu-t)7(mu 3-O)2(mu-OH) (2) as the major and minor products, respectively. Compound 1 may also be prepared by

the addition of water to a refluxing toluene solution of Al(Bu-t)3. Compound 1 is remarkably stable to thermolysis and is converted slowly to a mixture of alumoxane species. Dissolution of compound 1 in MeCN or THF yields the hydrogen-bound trimeric complexes ((Bu-t)2Al(mu-OH))3.n(MeCN) n = 1(3), 2 and ((Bu-t)2Al(mu-OH))3.2(THF), respectively. The large scale synthesis of alumoxanes from the low temperature thermolysis of the trimeric hydroxide, ((Bu-t)2Al(mu-OH))3, allows for the isolation of the penta-aluminum compound Al5(Bu-t)7(mu 3-O)2(mu-OH)2 (4) and the heptameric alumoxane ((Bu-t)Al(mu 3-O))7 (5). The structure of compound 4 is consistent with the condensation of ((Bu-t)2Al(mu-OH))3 with ((Bu-t)2Al(mu-OH))2. Thermolysis of 4 yields an alumina gel. The structural relationship of 4 with respect to the structures reported for nonalkyl alumoxanes and alumina gels is discussed. Reaction of ((Bu-t)2Ga(mu-OH))3 with Al(Bu-t)3 in toluene yields the octameric alumoxane Ga(Bu-t)3 and ((Bu-t)A1(mu3-O))8 (6), as the major isolable products. Mass spectrometry indicates the incorporation of low levels of gallium (less than 8%) into samples of 6 made by this route. The molecular structures of compounds 2, 4, and 6 have been determined by x-ray crystallography. DTIC

24 COMPOSITE MATERIALS

Includes physical, chemical, and mechanical properties of laminates and other composite materials.

For ceramic materials see *27 Nonmetallic Materials*.

N94-36456# Sandia National Labs., Albuquerque, NM.
A MIXTURE MODEL FOR SHOCK COMPRESSION OF POROUS MULTI-COMPONENT REACTIVE MATERIALS
M. R. Baer 1993 4 p Presented at the 14th International Conference of the International Association for the Advancement of High Pressure Science and Technology, Colorado Springs, CO, 27 Jun. - 2 Jul. 1993
(Contract DE-AC04-76DP-00789)
(DE93-017638; SAND-93-1395C; CONF-930676-9) Avail: CASI HC A01/MF A01

A multiphase mixture model is presented to describe shock compression of highly porous, multi-component powders. Volume fractions are represented as independent kinematic variables and thermodynamically-admissible phase interaction constitutive models are formulated in the context of a three phase system. Numerical solutions of the multiphase flow equations simulated impact on a porous layer of mixed powders of Al and Fe2O3. The multiphase model predicts dispersive compaction waves which have features similar to observed time-resolved pressure measurements. DOE

N94-36509# Oak Ridge National Lab., TN.
METAL-CARBON NANOSTRUCTURES
A. A. Puretzky, R. L. Hettich, Chang-Ming Jin, R. E. Haufler, R. N. Compton, and A. A. Tuinman 1993 12 p Presented at the International Symposium on Local Order in Condensed Matter Physics, Jekyll Island, GA, 14-17 Jun. 1993
(Contract DE-AC05-84OR-21400)
(DE94-009177; CONF-9306218-1) Avail: CASI HC A03/MF A01

Ultrafine particles formed by XeCl laser photolysis of M(CO6), M = V, Cr, Mo, and W, have been analyzed by Fourier transform mass spectrometry and other techniques. Novel metal carbide clusters, (MoC4)(sub n), n = 1 (minus) 4 and (WC4)(sub m), m = 1 (minus) 8, were detected and studied. The material produced by photolysis of V(CO6) shows a series of vanadium-oxygen clusters, V(sub x)O(sub 2x+2), x = 2 (minus) 10. No clusters of any type were detected in the photolysis product of Cr(CO6). Structures based on the experimental evidence are proposed and discussed in light of their chemical reactivity. DOE

N94-36649# Advisory Group for Aerospace Research and Development, Neuilly-Sur-Seine (France). Structures and Materials Panel.
CHARACTERISATION OF FIBRE REINFORCED TITANIUM MATRIX COMPOSITES [LA CARACTERISATION DES MATERIAUX COMPOSITES A MATRICE DE TITANE RENFORCES PAR FIBRES]
Feb. 1994 260 p In ENGLISH and FRENCH The 77th Meeting was held in Bordeaux, France, 27-28 Sep. 1993 Original contains color illustrations
(AD-A2775206; AGARD-R-796; ISBN-92-835-0735-5) Copyright Avail: CASI HC A12/MF A03

The combination of stiffness, strength, and high temperature resistance provided by fiber reinforced titanium matrix composites offers major benefits for aircraft engine and airframe applications, where these materials could be used to reduce weight or improve performance. This workshop on the subject of characterization of titanium composites was intended to provide a forum for the exchange of information in this important area. Characterization in this case refers to the understanding of the behavior of the composites as it relates to the ability to predict their performance in real-life applications. It covers various topics that include mechanical test techniques, NDE methods, life prediction models, and other factors that will affect the level of confidence with which these relatively new materials will be accepted for application. For individual titles, see N94-36650 through N94-36670.

N94-36650# Wright Lab., Wright-Patterson AFB, OH. Materials Directorate.
POSSIBILITIES AND PITFALLS IN AEROSPACE APPLICATIONS OF TITANIUM MATRIX COMPOSITES
James M. Larsen, Stephan M. Russ, and J. Wayne Jones *In* AGARD, Characterisation of Fibre Reinforced Titanium Matrix Composites Feb. 1994 21 p Sponsored by Systran Corp. (For primary document see N94-36649 12-24)
(AF Proj. 2302)
Copyright Avail: CASI HC A03/MF A03

High-temperature, light-weight materials represent enabling technology in the continued evolution of high-performance aerospace vehicles and propulsion systems being pursued by the U.S. Air Force. In this regard, titanium matrix composites (TMC's) appear to offer unique advantages in terms of a variety of weight-specific properties at high temperatures. However, a key requirement for eventual structural use of these materials is a balance of mechanical properties that can be suitably exploited by aircraft and engine designers without compromising reliability. An overview of the current capability of titanium matrix composites is presented, with an effort to assess the balance of properties offered by this class of materials. Emphasis is given to life-limiting cyclic and monotonic properties and the roles of high-temperature, time-dependent deformation and environmental effects. An attempt is made to assess the limitations of currently available titanium matrix composites with respect to application needs and to suggest avenues for improvements in key properties. Author

N94-36651# McDonnell-Douglas Corp., Saint Louis, MO.
APPLICATIONS OF TITANIUM MATRIX COMPOSITE TO LARGE AIRFRAME STRUCTURE
Timothy M. Wilson *In* AGARD, Characterisation of Fibre Reinforced Titanium Matrix Composites Feb. 1994 31 p (For primary document see N94-36649 12-24)
Copyright Avail: CASI HC A03/MF A03

Advanced Titanium Matrix Composite (TMC) materials are being developed for structures that must withstand high temperatures, possess high stiffness and be lighter. Scale-up of the TMC material system from the laboratory environment to large structural components has required significant advancements in design, manufacturing and assembly technology. Numerous large scale, TMC components have been developed, fabricated and tested to verify the feasibility of structural/material concepts for hypersonic vehicles. These articles include thick laminate TMC wing structure, minimum gage TMC fuselage sections, and integrated TMC fuselage/cryogenic tank structure. A summary of the development and testing of these articles is presented. Author (revised)

N94-36652# Textron Specialty Materials, Lowell, MA.
SCS-6 (TM) FIBER REINFORCED TITANIUM
Jim Henshaw *In* AGARD, Characterisation of Fibre Reinforced Titanium Matrix Composites Feb. 1994 6 p (For primary document see N94-36649 12-24)
Copyright Avail: CASI HC A02/MF A03

The low weight structurally efficient SCS-6 Fiber Reinforced Titanium, as produced by Textron Specialty Materials, is a material awaiting the development of production applications. A multitude of airframe and engine parts have been produced for test and developmental purposes and a production facility has been established to fabricate preforms, intermediary products, and component shapes. Author

N94-36653# AEA Technology, London (England).
PROCESSING OF TITANIUM MATRIX COMPOSITES
E. A. Feest and J. Cook *In* AGARD, Characterisation of Fibre Reinforced Titanium Matrix Composites Feb. 1994 9 p Prepared in cooperation with United Kingdom Atomic Energy Authority, Harwell, England (For primary document see N94-36649 12-24)
Copyright Avail: CASI HC A02/MF A03

European experience in the processing of monofilament reinforced Ti matrix composites is briefly reviewed. Results on fiber coating developments on foil- and PVD-based processing routes are presented. Issues addressed include fiber handling, fiber property measurement, residual stresses in fiber and matrix, fiber coating formulation and deposition, MMC consolidation, and composite properties. Progress towards economically viable matrix deposition via sputter ion plating is reported. Author

N94-36654# Academy of Sciences (USSR), Moscow (USSR). Inst. of Aviation Materials.
COMPOSITES BASED ON TITANIUM WITH EXTERNAL AND INTERNAL REINFORCEMENT
A. I. Khorev *In* AGARD, Characterisation of Fibre Reinforced Titanium Matrix Composites Feb. 1994 8 p (For primary document see N94-36649 12-24)
Copyright Avail: CASI HC A02/MF A03

The possibility of the efficient increase of the specific elasticity modulus and the specific strength of materials as well as aerospace vehicles by means of developing composites based on titanium with external and internal reinforcement was considered. Author

N94-36655# British Petroleum Co. Ltd., Sunbury-on-Thames (England). Research and Engineering Centre.
MANUFACTURE AND PROPERTIES OF SIGMA FIBRE REINFORCED TITANIUM
J. G. Robertson *In* AGARD, Characterisation of Fibre Reinforced Titanium Matrix Composites Feb. 1994 8 p (For primary document see N94-36649 12-24)
Copyright Avail: CASI HC A02/MF A03

Titanium Matrix Composites have long been known to offer potential for use in aeroengine components. The cost of producing the fiber and fabricating components has delayed large scale developments because of concern over long term component costs. The slow development pace has, in turn, kept the fiber and composite price high through low demand. Composite manufacturing routes using foil and filament wound fiber has been used for many years. The difficulties of maintaining a suitable fiber distribution during hot isostatic pressing and the availability of cheap foil have effectively put this technique on the shelf. However excellent fiber distributions have been achieved even in difficult geometries by a BP proprietary process. Mechanical properties comparable with the most expensive routes can be achieved with this, one of the cheapest manufacturing routes. Author

N94-36656# Deutsche Forschungs- und Versuchsanstalt fuer Luft- und Raumfahrt, Cologne (Germany). Inst. for Materials Science.
PROPERTIES OF TMC PROCESSED BY FIBRE COATING AND HIPING
H. J. Dudek and R. Leucht *In* AGARD, Characterisation of Fibre Reinforced Titanium Matrix Composites Feb. 1994 7 p (For primary document see N94-36649 12-24)
Copyright Avail: CASI HC A02/MF A03

SiC-fiber reinforced titanium alloys (Ti6A14V and IMI834) were processed by fiber coating and hot isostatic pressing (HIPing). Composites with a well consolidated microstructure, with a fiber volume fraction between 0.2 to 0.6, with a narrow fiber distance distribution and a fine globular grain structure were obtained. Tensile properties according to the rule of mixture are measured with values of the ultimate tensile strength for the 0.4 SiC-Ti6A14V-composite of 2.4 GPa at room temperature and for the 0.37 SiC-IMI834-composite of 1.3 GPa at 900 C. Fatigue properties were measured under loading conditions of R = -1. Different crack initiation effects for different matrix properties and stress amplitudes were observed. Author

N94-36657# Office National d'Etudes et de Recherches Aerospatiales, Paris (France). Materials Dept.
FIBRE-MATRIX INTERFACE PROPERTIES IN TI-MATRIX COMPOSITES: CHEMICAL COMPATIBILITY AND MICROMECHANICAL BEHAVIOUR
A. Vassel, R. Mevrel, J. P. Favre, and J. F. Stohr *In* AGARD, Characterisation of Fibre Reinforced Titanium Matrix Composites Feb. 1994 11 p Sponsored by Defence Research Establishment, Toronto (For primary document see N94-36649 12-24)
Copyright Avail: CASI HC A03/MF A03

Silicon carbide reinforced titanium alloys or titanium aluminides are challenging materials for engine discs applications in the temperature range 650-800 C. The main problems concerning fiber-matrix compatibility, i.e. fiber coating degradation through diffusion controlled mechanisms and fiber-matrix mechanical behavior are reviewed based on recent studies. It is also shown how two micromechanical tests, the fragmentation and the push-out test may be correlated. With the help of a 1D shear-lag type model, taking fiber-matrix debonding into account, a good fit is obtained between measured and computed values of the fiber-matrix load-transfer mean shear-stress. Author

N94-36658# Naval Air Warfare Center, Warminster, PA. Aircraft Div.
OXIDATION BEHAVIOR OF TITANIUM ALUMINIDE MATRIX MATERIALS
Jeffrey Cook, Eun U. Lee, William E. Frazier, Thu-Ha T. Mickle, and Jeffrey Waldman *In* AGARD, Characterisation of Fibre Reinforced Titanium Matrix Composites Feb. 1994 12 p Sponsored by ONR (For primary document see N94-36649 12-24)
Copyright Avail: CASI HC A03/MF A03

Oxidation tests were performed on titanium aluminide alloys of three different compositions to determine their oxidation properties under isothermal and cyclic conditions. The TiAl/Ti3Al alloy and the Al3Ti exhibited roughly parabolic behavior between 900 and 1100 C, while the TiAl oxidized in a linear fashion. Rate constants and activation energies were calculated for each material, and based on these the rate-controlling processes and mechanisms were determined. Author

N94-36659# Dayton Univ. Research Inst., OH.
METHODOLOGIES FOR THERMAL AND MECHANICAL TESTING OF TMC MATERIALS
George A. Hartman and Dennis J. Buchanan *In* AGARD, Characterisation of Fibre Reinforced Titanium Matrix Composites Feb. 1994 9 p (For primary document see N94-36649 12-24)
Copyright Avail: CASI HC A02/MF A03

An overview of test techniques currently being used at the Air Force Materials Directorate/MLLN laboratories for elevated temperature testing of TMC materials is presented. Methods for test system alignment/specimen gripping, specimen heating, temperature measurement, and displacement measurement are discussed in detail. In some cases, the interdependence of choices made in each of these areas is also discussed. A description of a complete system used to perform a variety of thermal and mechanical tests on TMC materials is presented. Selected results from tests using this system with TMC materials are presented. Author

N94-36660# Dayton Univ. Research Inst., OH.
ULTRASONIC NONDESTRUCTIVE CHARACTERIZATION METHODS FOR THE DEVELOPMENT AND LIFE PREDICTION OF TITANIUM MATRIX COMPOSITES
Prasanna Karpur, David A. Stubbs, Theodore E. Matikas, Mark P. Blodgett, and S. Krishnamurthy *In* AGARD, Characterisation of Fibre Reinforced Titanium Matrix Composites Feb. 1994 12 p (For primary document see N94-36649 12-24)
(Contracts F33615-89-C-5612; F33615-91-C-5606; F33615-92-C-5663)
Copyright Avail: CASI HC A03/MF A03

Titanium matrix composites (TMC's) are currently being developed for high strength and high stiffness applications with improved elevated operating temperature behavior. In order to provide guidelines for the development of new TMC's with the desired properties and to ensure reliable use, a thorough understanding of material behavior is required which necessitates the development and use of appropriate nondestructive evaluation (NDE) methods. This work outlines the concurrent use of NDE during composites development as well as material behavior studies of TMC's. The paper presents results based on various ultrasonic techniques developed in the

Materials Directorate, Wright Laboratory of the U.S. Air Force for the evaluation of different aspects of development and use of TMC's to tailor the properties for a particular application. Author (revised)

N94-36661# Defence Research Agency, Farnborough, Hampshire (England).
METAL MATRIX COMPOSITES: ANALYSIS OF SIMPLE SPECIMENS AND MODEL COMPONENTS UNDER CREEP AND FATIGUE LOADING
G. F. Harrison, B. Morgan, P. H. Tranter, and M. R. Winstone *In* AGARD, Characterisation of Fibre Reinforced Titanium Matrix Composites Feb. 1994 15 p (For primary document see N94-36649 12-24)
Copyright Avail: CASI HC A03/MF A03

The paper presents the results of a limited test program to establish the mechanical behavior of titanium metal matrix composite (MMC) laboratory specimens under tensile, low cycle fatigue (LCF), and creep loading conditions at 600 C. Using a micromechanical model, finite element stress analyses have been undertaken to evaluate local stresses under the various loading conditions. Good agreement was obtained only after the inclusion of procedures to calculate the residual stresses induced in cooling from the composite consolidation temperature to the test temperature. Additionally, as part of a collaborative component evaluation study, model discs manufactured by Rolls-Royce plc have been subjected to spin testing. These LCF results have been correlated via a macromechanical model which accounts for the orthotropic behavior of the MMC reinforced region of the disc. Author

N94-36662# Wright Lab., Wright-Patterson AFB, OH.
RESIDUAL STRENGTH AND LIFE PREDICTION TECHNIQUES FOR Ti MMC
J. Harter, D. Harmon, and R. Post *In* AGARD, Characterisation of Fibre Reinforced Titanium Matrix Composites Feb. 1994 6 p (For primary document see N94-36649 12-24)
Copyright Avail: CASI HC A02/MF A03

To date, the fatigue crack growth behavior of metal matrix composites (MMC) has been generally limited to data obtained from relatively small coupons (approximately 150 mm x 25 mm). Although self similar crack growth has been observed in some cases, many observers have noted various complex crack growth phenomena. Behaviors such as fiber bridging and extensive crack branching have been reported in several papers. The purpose of this paper is to present the results of several static and crack growth tests on larger titanium based MMC center cracked coupons (406 mm x 63.5 mm). The use of larger specimens has allowed for more observations during stable crack growth and is much more representative of actual applications. Author

N94-36663*# National Aeronautics and Space Administration. Lewis Research Center, Cleveland, OH.
PROCESS/COMPOSITE CONCURRENT TAILORING OF SiC/Ti COMPOSITES
C. C. Chamis and D. A. Saravanos *In* AGARD, Characterisation of Fibre Reinforced Titanium Matrix Composites Feb. 1994 7 p (For primary document see N94-36649 12-24)
Copyright Avail: CASI HC A02/MF A03

Recent work on the prediction of optimal processing and material characteristics for improved fatigue behavior of metal and intermetallic matrix composites (MMC's/IMC's) is summarized. The method is incorporated into the MMLT (Metal Matrix Laminate Tailoring) code. Excellent correlations between predictions for the isothermal fatigue life of the SCS-6/Ti-24Al-11Nb composite and experimental data are obtained at various temperatures and stress ranges. Finally, the optimal processing conditions for improved isothermal fatigue life of the composite are evaluated and the attained isothermal fatigue life improvements are shown. Author (revised)

N94-36664*# Massachusetts Univ., Lowell, MA. Dept. of Mechanical Engineering.
MICROMECHANICAL MODELING OF DAMAGE GROWTH IN TITANIUM BASED METAL-MATRIX COMPOSITES
James A. Sherwood and Howard M. Quimby *In* AGARD, Characterisation of Fibre Reinforced Titanium Matrix Composites Feb. 1994 9 p (For primary document see N94-36649 12-24)
(Contract NCC3-218)
Copyright Avail: CASI HC A02/MF A03

The thermomechanical behavior of continuous-fiber reinforced titanium based metal-matrix composites (MMC) is studied using the finite element method. A thermoviscoplastic unified state variable constitutive theory is employed to capture inelastic and strain-rate sensitive behavior in the Timetal-21s matrix. The SCS-6 fibers are modeled as thermoplastic. The effects of residual stresses generated during the consolidation process on the tensile response of the composites are investigated. Unidirectional and cross-ply geometries are considered. Differences between the tensile responses in composites with perfectly bonded and completely debonded fiber/matrix interfaces are discussed. Model simulations for the completely debonded-interface condition are shown to correlate well with experimental results. Author

N94-36665# Birmingham Univ. (England). School of Metallurgy and Materials.
CRACK GROWTH UNDER CYCLE LOADING IN FIBRE REINFORCED TITANIUM METAL MATRIX COMPOSITES
P. Bowen *In* AGARD, Characterisation of Fibre Reinforced Titanium Matrix Composites Feb. 1994 16 p Sponsored by Science Research Council; Rolls-Royce Ltd.; and British Petroleum Co. Ltd. (For primary document see N94-36649 12-24)
Copyright Avail: CASI HC A03/MF A03

This review paper considers the experimental characterization of crack growth from unbridged defects in fiber reinforced titanium metal matrix composites subjected to cyclic loading by the use of fracture mechanics parameters. The conditions under which parameters such as the nominal applied stress intensity range, Delta-K(sub app), the nominal maximum stress intensity factor, K(sub max), and the effective stress intensity range, Delta-K(sub eff), are of use, and their experimental measurement are considered. Effects of fiber fracture, stress intensity factor range, mean stress, loading configuration (bending versus tension), test temperature, and fiber-matrix interfacial strength on fatigue crack growth resistance are highlighted. Finally, a possible approach to the prediction of crack arrest in such composites is outlined. Author (revised)

N94-36666*# National Aeronautics and Space Administration. Langley Research Center, Hampton, VA.
PREDICTION OF THERMAL AND MECHANICAL STRESS-STRAIN RESPONSES OF TMC'S SUBJECTED TO COMPLEX TMF HISTORIES
W. S. Johnson and M. Mirdamadi *In* AGARD, Characterisation of Fibre Reinforced Titanium Matrix Composites Feb. 1994 6 p (For primary document see N94-36649 12-24)
Copyright Avail: CASI HC A02/MF A03

This paper presents an experimental and analytical evaluation of cross-plied laminates of Ti-15V-3Cr-3Al-3Sn (Ti-15-3) matrix reinforced with continuous silicon-carbide fibers (SCS-6) subjected to a complex TMF loading profile. Thermomechanical fatigue test techniques were developed to conduct a simulation of a generic hypersonic flight profile. A micromechanical analysis was used. The analysis predicts the stress-strain response of the laminate and of the constituents in each ply during thermal and mechanical cycling by using only constituent properties as input. The fiber was modeled as elastic with transverse orthotropic and temperature-dependent properties. The matrix was modeled using a thermoviscoplastic constitutive relation. The fiber transverse modulus was reduced in the analysis to simulate the fiber-matrix interface failures. Excellent correlation was found between measured and predicted laminate stress-strain response due to generic hypersonic flight profile when fiber debonding was modeled. Author

N94-36667# AEA Technology, London (England).
PRE-STANDARDISATION WORK ON FATIGUE AND FRACTURE TESTING OF TITANIUM MATRIX COMPOSITES
J. H. Tweed, J. Cook, N. L. Hancox, R. J. Lee, and R. F. Preston *In* AGARD, Characterisation of Fibre Reinforced Titanium Matrix Composites Feb. 1994 10 p Sponsored by Dept. of Trade and Industry (For primary document see N94-36649 12-24)
Copyright Avail: CASI HC A02/MF A03

This paper presents work on development of test techniques for S-N fatigue, fatigue crack growth, and fracture toughness of titanium matrix composites. Work has concentrated on eight-ply unidirectional Ti-6-4/SM1240 from BP Metal Composites with some preliminary work on eight-ply unidirectional Ti-6-4/SCS-6 from Textron Speciality Materials. For S-N fatigue testing, an approach, used successfully for the Textron material,

consistently gave failures in the tab region for BP material. Transverse fracture toughness of Ti/SiC sheets has been determined using a double cantilever beam test. Care has to be taken to restrain specimen twisting. For two BP materials, the transverse fracture toughness correlated with the static strength values. Author

N94-36668*# National Aeronautics and Space Administration. Langley Research Center, Hampton, VA.

ASTM AND VAMAS ACTIVITIES IN TITANIUM MATRIX COMPOSITES TEST METHODS DEVELOPMENT

W. S. Johnson, D. M. Harmon, P. A. Bartolotta, and S. M. Russ *In* AGARD, Characterisation of Fibre Reinforced Titanium Matrix Composites Feb. 1994 17 p (For primary document see N94-36649 12-24)

Copyright Avail: CASI HC A03/MF A03

Titanium matrix composites (TMC's) are being considered for a number of aerospace applications ranging from high performance engine components to airframe structures in areas that require high stiffness to weight ratios at temperatures up to 400 C. TMC's exhibit unique mechanical behavior due to fiber-matrix interface failures, matrix cracks bridged by fibers, thermo-viscoplastic behavior of the matrix at elevated temperatures, and the development of significant thermal residual stresses in the composite due to fabrication. Standard testing methodology must be developed to reflect the uniqueness of this type of material systems. The purpose of this paper is to review the current activities in ASTM and Versailles Project on Advanced Materials and Standards (VAMAS) that are directed toward the development of standard test methodology for titanium matrix composites. Author (revised)

N94-36669# Societe Nationale d'Etude et de Construction de Moteurs d'Aviation, Evry (France).

DEVELOPMENT OF MECHANICAL TESTING METHODS FOR TITANIUM MATRIX COMPOSITES (TRACTION-OGLIGO-CYCLIC FATIGUE) [DEVELOPPEMENT DE METHODES D'ESSAIS MECANIQUES POUR CMM A BASE TITANE (TRACTION-FATIGUE OLIGOCYCLIQUE)]

B. Dambrine and M. Hartley *In* AGARD, Characterisation of Fibre Reinforced Titanium Matrix Composites Feb. 1994 15 p In FRENCH Original contains color illustrations (For primary document see N94-36649 12-24)

Copyright Avail: CASI HC A03/MF A03

The performance objectives proposed for the next generation of military engines (thrust/mass ratio approximately equals 15) suggest extreme conditions of usage of titanium alloys in the compressor discs, while not allowing any consideration for the mass objectives. The composite materials with metal matrices (titanium base matrix reinforced by long fibers of silicon carbide) exhibit characteristics that appear to be encouraging for the construction of compressor discs (rigidity, endurance at high temperature). A complete understanding of the characteristics of fiber reinforced titanium matrix composites is a qualifying condition to the initiation and to the validation of calculation methods on the expected life of the components. The first step is to study their conduct, on laboratory samples, while in a state of traction or oligo-cyclic fatigue. The elements leading to the development of the tests are presented. Transl. by FLS

N94-36670# National Physical Lab., Teddington (England). Div. of Materials Metrology.

MODELLING AND TESTING FIBRE REINFORCED TITANIUM FOR DESIGN PURPOSES

L. N. McCartney *In* AGARD, Characterisation of Fibre Reinforced Titanium Matrix Composites Feb. 1994 10 p (For primary document see N94-36649 12-24)

Copyright Avail: CASI HC A02/MF A03

A review is given on some aspects of designing with continuous fiber reinforced titanium alloys. Issues that are addressed are as follows: (1) Need for multiaxial constitutive relations describing behavior of fiber reinforced titanium for monotonic loading at different temperatures, unloading at different temperatures, cyclic changes in load and temperature both in and out of phase, and general thermomechanical loading. Linear, yielding, incremental plasticity and time dependent deformations are considered. (2) Need for reliable failure criteria that take account of the micromechanisms that contribute to the failure event. (3) Role that micromechanical modeling can play in the development of reliable constitutive relations and design methods. (4) Need for validated test methods to measure the parameters that appear in the constitutive relations that are used for design purposes. Author (revised)

N94-36730# Duncan Technologies, Inc., Newcastle, CA.

STRUCTURAL COMPOSITE CONSTRUCTION MATERIALS MANUFACTURED FROM MUNICIPAL SOLID WASTE Final Report, 20 Sep. 1993 - 21 Mar. 1994

David B. Duncan and Randall L. Bickford 20 Apr. 1994 68 p

(Contract DACA88-93-C-0013)

(AD-A280635; CERL-P1-01) Avail: CASI HC A04/MF A01

Work was performed to assess alternatives and opportunities for the development of innovative construction materials made from recycled paper fiber and thermoplastic materials. The identification of such composites will create a stable market for recovered waste plastics and paper while providing a new material for applications. The goals were to identify methods and processes to produce composite materials with suitable properties and to evaluate the economics of the process and the markets they can compete in. Materials research was performed to identify possible composite compositions and chemical treatments that would enhance the interfacial strength between paper fibers and the thermoplastic matrix. Screening tests were performed to select the most promising options. Tensile tests were performed on several composites made of paper and polystyrene or high density polyethylene. Economic and market analyses were performed to assess the viability of these composites as a product. The data indicate that paper fibers are too weak to create a composite with suitable strength properties. In addition the available market is saturated and very difficult to compete in. The use of chopped glass fibers in a thermoplastic matrix as a fiberglass replacement may be a more promising strategy. Further investigation of this alternative is recommended. DTIC

N94-36752*# National Aeronautics and Space Administration. Lewis Research Center, Cleveland, OH.

NiAl-BASE COMPOSITE CONTAINING HIGH VOLUME FRACTION OF AlN FOR ADVANCED ENGINES Patent Application

Mohan Hebsur, inventor (to NASA), John D. Whittenbeger, inventor (to NASA), and Carl F. Lowell, inventor (to NASA) 5 May 1994 41 p

(NASA-Case-LEW-15818-1; NAS 1.71:LEW-15818-1;

US-Patent-Appl-SN-238767) Avail: CASI HC A03/MF A01

A particulate reinforced NiAl-AlN composite alloy has a NiAl matrix and greater than about 13 volume percent fine particles of AlN within the matrix. The particles preferably have a diameter from about 15 nanometers to about 50 nanometers. The particulate reinforced NiAl-AlN composite alloy may be prepared by cryomilling prealloyed NiAl in liquid nitrogen using grinding media having a diameter of from about 2 to 6 mm at an impeller speed of from about 450 RPM to about 800 RPM. The cryomilling may be done for a duration of from about 4 hours to about 20 hours to obtain a cryomilled powder. The cryomilled powder may be consolidated to form the particulate reinforced NiAl-AlN composite alloy. The particulate reinforced alloy can further include a toughening alloy. The toughening alloy may include NiCrAlY, FeCrAlY, and FeAl. NASA

N94-36956*# National Aeronautics and Space Administration. Lewis Research Center, Cleveland, OH.

DETECTION OF DELAMINATIONS IN COMPOSITE BEAMS USING PIEZOELECTRIC SENSORS

Dimitris A. Saravanos (Ohio Aerospace Inst., Brook Park.), Victor Birman (Missouri Univ., Saint Louis, MO.), and Dale A. Hopkins Jun. 1994 21 p Presented at the 35th Structures, Structural Dynamics and Materials Conference, Hilton Head, SC, 18-21 Apr. 1994; sponsored by AIAA, ASME, ASCE, AHS, and ASC

(Contract NCC3-208; RTOP 505-63-5B)

(NASA-TM-106611; E-8894; NAS 1.15:106611; AIAA Paper 94-1754)

Avail: CASI HC A03/MF A01

This paper investigates the feasibility of a proposed technique for detecting delamination using piezoelectric layers or patches embedded or bonded to a composite structure. Variations in the voltage generated in the piezoelectric layers indicates the presence and location of delamination, when the structure is excited either externally or via actuators. The theoretical foundations of a method for predicting the dynamic response of delaminated composite beams with piezoelectric layers are described. The governing equations are presented for the case of external vibroacoustic excitation,

as well as, for the case of locally induced vibrations by some of the embedded piezoelectric elements. An exact solution is developed within the limits of linear laminate theory. Applications illustrate the feasibility of delamination detection in cantilever beams. The results illustrate that the proposed technique may provide accurate detection of the presence, size, and location of a delamination. Author

N94-37010# Joint Publications Research Service, Arlington, VA.
JPRS REPORT: SCIENCE AND TECHNOLOGY. CENTRAL EURASIA: MATERIALS SCIENCE
16 Dec. 1993 25 p Transl. into ENGLISH from various Russian articles (JPRS-UMS-93-008) Avail: CASI HC A03/MF A01

Translated articles cover the following topics: ionospheric plasma's interaction with spacecraft materials and equipment; experimental investigation into effect of space factors on graphite epoxy composite durability: effect of gaseous chlorine on metallized graphite epoxy composite state; effect of interface on properties of Ti-W fiber composite under uniaxial tension conditions; distribution of titanium in the structure of various components of superconducting composites based on Nb3Sn; effect of gallium alloying on the structure and properties of a superconducting composite with Nb2Sn; experimental study concerning effect of cosmic-space factors on durability of carbon-plastic materials: laws governing accumulation of corrosion products from metallized carbon-plastic; experimental study concerning effect of cosmic-space factors on durability of carbon-plastics: low-energy electrons, x rays, ultraviolet light; wear resistance of ceramic materials based on silicon carbide and nitride; heating of aluminum particles with oxide sheaths by high-intensity laser radiation; growing thin films of metal oxides by ion-beam sputtering; principal trends in improving Al-Li alloy quality for welded aircraft structures; controlling aluminum alloy structure by adding disperse silicon carbide particles to melt; effect of hot deformation and heat treatment on complex nickel-based superalloy structure formation; and change in the structure and mechanical properties of a solid alloy as a function of the temperature of infiltration of the titanium carbide framework by nickel alloys. CASI

N94-37044 Virginia Polytechnic Inst. and State Univ., Blacksburg, VA. Dept. of Materials Engineering.
FEASIBILITY OF (IMC)(SUB d)-REINFORCED METAL MATRIX COMPOSITES Final Technical Report
S. G. Fisherman May 1994 21 p Limited Reproducibility: More than 20% of this document may be affected by microfiche quality
(Contract N00014-93-1-0539)
(AD-A280626) Avail: Issuing Activity (Defense Technical Information Center (DTIC))

A series of metal matrix composites were produced by co-extruding TiB2-reinforced near-gamma titanium aluminide intermetallic composites (IMC) within matrices of two commercial titanium alloy compositions. The components of the composites were produced or obtained in powder form, homogeneously blended, and deformation-processed at 1038 C in an attempt to evolve an aligned metal matrix composite microstructure via the principles of commensurate deformation. The IMC's, which were ultimately blended within the metallic matrix, are characterized by in situ-synthesized TiB2; the particulate is highly faceted, single crystalline, and has an average diameter of approximately 0.4 utm. The results of this feasibility study indicate that while the (IMC)-reinforced composites can be successfully produced by extrusion, the extent of deformation in the titanium aluminide intermetallic composite component is much less than that which would be predicted if it deformed equally with the titanium matrix phase. While the expected effect of IMC strength (as varied by the percentage of TiB2 synthesized within the IMC) on the ability to deform the IMC at high temperatures was not observed, the extent to which the IMC deforms was found to be enhanced by higher flow stresses in the titanium matrix phase. Recommendations based upon the experiences of the present work include creating a more deformable IMC-reinforcing phase by extruding at a higher homologous temperature, e.g., by alternatively utilizing the trialuminide Al3Ti as a matrix for the IMC-reinforcement in the titanium matrices. DTIC

N94-37088# Pennsylvania State Univ., University Park, PA. Dept. of Engineering Science and Mechanics.
USING NONEQUILIBRIUM ALLOYING TECHNIQUES FOR CORROSION INHIBITION IN Gr/Al AND Gr/Mg METAL MATRIX COMPOSITES Annual Technical Report, 1 Apr. 1993 - 31 Mar. 1994
B. A. Shaw, W. C. Moshier, R. G. Wendt, P. L. Miller, and A. E. Krebs 15 Jun. 1994 73 p
(Contract N00014-91-J-1196)
(AD-A280529) Avail: CASI HC A04/MF A01

Metal matrix composites (MMC's) have been heavily studied over the past thirty years. During that period, many proposals have been made to develop a matrix alloy that was compatible with the reinforcing phase. However, for one reason or another, the technology has continued to focus on conventional alloys and fabrication practices. Although tremendous advances have been made on composite materials, the basic technology remains similar to systems studied twenty years ago. This work represents the first new program where new alloys are being developed for graphite reinforced composites which are tailored to a novel processing technology for manufacturing corrosion resistant graphite reinforced composites. DTIC

N94-37105 Fiber Materials, Inc., Biddeford, ME.
THE DEVELOPMENT OF SHORT, HIGH SURFACE AREA ACTIVATED CARBON FIBERS Final Report, Jan. - Oct. 1993
J. Herrick May 1994 29 p Limited Reproducibility: More than 20% of this document may be affected by microfiche quality
(Contract DAAK60-93-C-0015)
(AD-A280509; NATICK-TR-94/020) Avail: CASI HC A03

This program was designed to develop short (0.03-0.04 inch), activated carbon fibers that possessed a Brunauer, Emmet and Teller (BET) surface area over 1500 sq.meters/gram. Several precursor fibers, including Kevlar(TM), phenolic, rayon, pitch and polyacrylonitrile (PAN), were carbonized and then activated under nitrogen with excess quantities of potassium hydroxide to temperatures of 900-950 C. The type of precursor fiber and processing conditions affected the resulting activated carbon fiber surface area and strength. The highest surface areas were obtained when the maximum activation temperature was significantly (e.g.,100 C) higher than the carbonization temperature. Eliminating the steel tumblers in the rotary activation furnace and reducing the rotation speed resulted in less damage to the fibers and the retention of original fiber lengths. Kevlar fibers activated under optimized conditions yielded the best combination of fiber properties with BET surface area of approximately 2000 M(2)/gram and the retention of fiber strength. Over 50 grams of this activated fiber were made for evaluation by the U.S. Army Natick Research, Development and Engineering Center. DTIC

N94-37205# Oak Ridge National Lab., TN. Metals and Ceramics Div.
SOME CONSIDERATIONS FOR MODELING THE CREEP BEHAVIOR OF COMPOSITE MATERIALS
Edgar Lara-Curzio and Mattison K. Ferber 1994 11 p Presented at the 18th Annual Conference on Composites and Advanced Ceramics, Cocoa Beach, FL, 9-14 Jan. 1994
(Contract DE-AC05-84OR-21400)
(DE94-012112; CONF-940135-6) Avail: CASI HC A03/MF A01

A simple treatment of the mechanics of creep in unidirectional composites is presented with the objective of stressing the need for using appropriate constitutive equations when modeling the behavior of the constituents. It is demonstrated that pseudo-constitutive relations, such as those obtained from constant stress creep experiments for example, can not be used to describe the mechanical behavior of the constituents when modeling the creep of composites. By describing the mechanical behavior of the composite constituents using linear viscoelastic models, an analysis is presented to assess the type of errors which are incurred when inappropriate constitutive relations are used. Other considerations for modeling the creep behavior of ceramic matrix composites are discussed. DOE

N94-37232 Pennsylvania State Univ., University Park, PA.
BASIC SOLUTIONS TO CARBON/CARBON OXIDATION: SCIENCE AND TECHNOLOGY Annual Technical Report, 15 Apr. 1993 - 14 Apr. 1994
Tan R. Harrison, T.-C. Chung, Ljubisa Radovic, Carlo Pantano, and Peter A. Thrower 13 May 1994 49 p Limited Reproducibility: More than 20% of this document may be affected by microfiche quality
(Contract F49620-93-1-0311)
(AD-A280447; AFOSR-94-0364TR) Avail: CASI HC A03

The attached report addresses the first year of a program aimed at developing basic solutions to carbon/carbon composite oxidation. In particular, one primary thrust is the development of boron containing carbons

through pyrolysis of boron containing polymers. Additionally, a basic understanding of the oxidation mechanisms in carbons and boron containing carbons is being sought. Several new boron containing precursors have been synthesized, which can be converted to B/C materials after pyrolysis. In particular, polyacrylonitrile (PAN) has been copolymerized with a boron-containing monomer (vinylcatecholborane.) Approximately 68% of the original boron is retained after pyrolysis yielding a product with 3.4% boron. The 1,4-polybutadiene (PBD) has been hyborated to contain large amounts of boron. Model compounds have been used to prepare polydyne with considerable amounts of boron. In the latter two cases, direct analysis for % boron is not yet available. Preliminary TGA data suggests that PBD containing boron results in a more stable structure. DTIC

N94-37289# Los Alamos National Lab., NM.
MECHANICAL BEHAVIOR OF MoSi2 AND MoSi2 COMPOSITES
J. J. Petrovic 1994 27 p Presented at the International Conference on High-Temperature Intermetallics, San Diego, CA, 16-19 May 1994
(Contract W-7405-eng-36)
(DE94-013116; LA-UR-94-1730; CONF-940598-1) Avail: CASI HC A03/MF A01

MoSi2 is a key member of the new class high temperature structural silicide materials. Important features of the mechanical behavior of MoSi2 and MoSi2 composites are reviewed. The mechanical properties of MoSi2 single crystals, polycrystalline MoSi2, and MoSi2-based composites are discussed in association with properties such as elevated temperature deformation and low temperature fracture toughness. Interrelationships between single crystal, polycrystal, and composite mechanical behavior are identified. DOE

N94-37318*# National Aeronautics and Space Administration. Lewis Research Center, Cleveland, OH.
CARBON-CARBON HEAT PIPE TESTING AND EVALUATION
Albert J. Juhasz and Richard D. Rovang Jul. 1994 8 p Presented at the 29th Intersociety Energy Conversion Engineering Conference, Monterey, CA, 7-12 Aug. 1994; sponsored by AIAA, IEEE, ASME, and SAE
(Contract NAS3-25209; RTOP 233-02-08)
(NASA-TM-106630; E-8929; NAS 1.15:106630; AIAA Paper 94-4065)
Avail: CASI HC A02/MF A01

This report discusses development and proof-of-concept testing of a new lightweight carbon-carbon (C-C) space radiator heat pipe developed under the NASA Civil Space Technology Initiative (CSTI) High Capacity Power Program. The heat pipe was filled with potassium working fluid and tested for 11 hours including startup from ambient temperature with the working fluid initially in the frozen state to near 700 K condenser temperature. Steady-state heat pipe input power during testing was facility limited to about 300 watts, representing about 50 percent of the design input power. Post test inspection showed the heat pipe to be in excellent condition after eight thermal cycles from ambient to steady-state operating temperature. Potential applications, ranging from small spacecraft heat rejection to aircraft and terrestrial uses, are discussed. Author

N94-37320*# National Aeronautics and Space Administration. Langley Research Center, Hampton, VA.
A METHODOLOGY TO PREDICT DAMAGE INITIATION, DAMAGE GROWTH AND RESIDUAL STRENGTH IN TITANIUM MATRIX COMPOSITES
J. G. Bakuckas, Jr. (Galaxy Scientific Corp., Pleasantville, NJ.) and W. S. Johnson Jul. 1994 44 p Presented at the ASTM Symposium on Life Prediction Methodology for Titanium Matrix Composites, Hilton Head, SC, 23-24 Mar. 1994
(RTOP 505-63-50-04)
(NASA-TM-109135; NAS 1.15:109135) Avail: CASI HC A03/MF A01

In this research, a methodology to predict damage initiation, damage growth, fatigue life, and residual strength in titanium matrix composites (TMC) is outlined. Emphasis was placed on micromechanics-based engineering approaches. Damage initiation was predicted using a local effective strain approach. A finite element analysis verified the prevailing assumptions made in the formulation of this model. Damage growth, namely, fiber-bridged matrix crack growth, was evaluated using a fiber bridging (FB) model which accounts for thermal residual stresses. This model combines continuum fracture mechanics and micromechanics analyses yielding stress-intensity factor solutions for fiber-bridged matrix cracks. It is assumed in the FB model that fibers in the wake of the matrix crack are idealized as a closure pressure, and an unknown constant frictional shear stress is assumed to act along the debond length of the bridging fibers. This frictional shear stress was used as a curve fitting parameter to the available experimental data. Fatigue life and post-fatigue residual strength were predicted based on the axial stress in the first intact 0 degree fiber calculated using the FB model and a three-dimensional finite element analysis. Author

N94-37370# Oak Ridge National Lab., TN.
METHODOLOGIES FOR THE THERMOMECHANICAL CHARACTERIZATION OF CONTINUOUS-FIBER CERAMIC MATRIX COMPOSITES: A REVIEW OF TEST METHODS
E. Lara-Curzio, M. K. Ferber, and M. G. Jenkins 1994 22 p Presented at the 39th International Symposium of the Society for the Advancement of Material and Process Engineering and Exhibition, Anaheim, CA, 11-14 Apr. 1994
(Contract DE-AC05-84OR-21400)
(DE94-012111; CONF-940412-5) Avail: CASI HC A03/MF A01

Requirements for thermomechanical characterization of ceramic matrix composite materials are reviewed. Feasibility of adapting existent room temperature test methods for polymer and metal matrix composites to test ceramic matrix composites at room and elevated temperatures is investigated. DOE

N94-37460*# National Aeronautics and Space Administration. Lewis Research Center, Cleveland, OH.
TENSILE STRENGTH OF SIMULATED AND WELDED BUTT JOINTS IN W-Cu COMPOSITE SHEET
Thomas J. Moore and Gordon K. Watson Washington Jun. 1994 27 p
(RTOP 505-63-12)
(NASA-TM-4584; E-8709; NAS 1.15:4584) Avail: CASI HC A03/MF A01

The weldability of W-Cu composite sheet was investigated using simulated and welded joints. The welded joints were produced in a vacuum hot press. Tensile test results showed that simulated joints can provide strength and failure mode data which can be used in joint design for actual weldments. Although all of the welded joints had flaws, a number of these joints were as strong as the W-Cu composite base material. Author

N94-37471*# Massachusetts Inst. of Tech., Cambridge. Technology Lab. for Advanced Composites.
MODELING OF OUTGASSING AND MATRIX DECOMPOSITION IN CARBON-PHENOLIC COMPOSITES Semiannual Report, Jan. - Jun. 1994
Hugh L. McManus Jul. 1994 52 p
(Grant NAG8-295)
(NASA-CR-196319; NAS 1.26:196319) Avail: CASI HC A04/MF A01

Work done in the period Jan. - June 1994 is summarized. Two threads of research have been followed. First, the thermodynamics approach was used to model the chemical and mechanical responses of composites exposed to high temperatures. The thermodynamics approach lends itself easily to the usage of variational principles. This thermodynamic-variational approach has been applied to the transpiration cooling problem. The second thread is the development of a better algorithm to solve the governing equations resulting from the modeling. Explicit finite difference method is explored for solving the governing nonlinear, partial differential equations. The method allows detailed material models to be included and solution on massively parallel supercomputers. To demonstrate the feasibility of the explicit scheme in solving nonlinear partial differential equations, a transpiration cooling problem was solved. Some interesting transient behaviors were captured such as stress waves and small spatial oscillations of transient pressure distribution. CASI

N94-37627# Sandia National Labs., Albuquerque, NM.
MICROMECHANICAL MODELING OF ADVANCED MATERIALS
S. A. Silling, P. A. Taylor, J. L. Wise, and M. D. Furnish Apr. 1994 57 p
(Contract DE-AC04-94AL-85000)
(DE94-011249; SAND-94-0129) Avail: CASI HC A04/MF A01

Funded as a laboratory-directed research and development (LDRD)

project, the work reported here focuses on the development of a computational methodology to determine the dynamic response of heterogeneous solids on the basis of their composition and microstructural morphology. Using the solid dynamics wavecode CTH, material response is simulated on a scale sufficiently fine to explicitly represent the material's microstructure. Conducting 'numerical experiments' on this scale, the authors explore the influence that the microstructure exerts on the material's overall response. These results are used in the development of constitutive models that take into account the effects of microstructure without explicit representation of its features. Applying this methodology to a glass-reinforced plastic (GRP) composite, the authors examined the influence of various aspects of the composite's microstructure on its response in a loading regime typical of impact and penetration. As a prerequisite to the microscale modeling effort, they conducted extensive materials' testing on the constituents, S-2 glass and epoxy resin (UF-3283), obtaining the first Hugoniot and spall data for these materials. The results of this work are used in the development of constitutive models for GRP materials in transient-dynamics computer wavecodes. DOE

N94-37633*# State Univ. of New York, Buffalo, NY. Dept. of Mechanical and Aerospace Engineering.

PROBABILITY TECHNIQUES FOR RELIABILITY ANALYSIS OF COMPOSITE MATERIALS

Robert C. Wetherhold and Anthony M. Ucci Jul. 1994 45 p

(Grant NAG3-862; RTOP 510-01-50)

(NASA-CR-195294; E-8664; NAS 1.26:195294) Avail: CASI HC A03/MF A01

Traditional design approaches for composite materials have employed deterministic criteria for failure analysis. New approaches are required to predict the reliability of composite structures since strengths and stresses may be random variables. This report will examine and compare methods used to evaluate the reliability of composite laminae. The two types of methods that will be evaluated are fast probability integration (FPI) methods and Monte Carlo methods. In these methods, reliability is formulated as the probability that an explicit function of random variables is less than a given constant. Using failure criteria developed for composite materials, a function of design variables can be generated which defines a 'failure surface' in probability space. A number of methods are available to evaluate the integration over the probability space bounded by this surface; this integration delivers the required reliability. The methods which will be evaluated are: the first order, second moment FPI methods; second order, second moment FPI methods; the simple Monte Carlo; and an advanced Monte Carlo technique which utilizes importance sampling. The methods are compared for accuracy, efficiency, and for the conservativism of the reliability estimation. The methodology involved in determining the sensitivity of the reliability estimate to the design variables (strength distributions) and importance factors is also presented. Author

N94-37653*# Virginia Polytechnic Inst. and State Univ., Blacksburg, VA. Center for Composite Materials and Structures.

A SIMPLE EVALUATION OF THERMALLY-INDUCED STRESES IN THE VICINITY OF THE STITCH IN A THROUGH-THICKNESS REINFORCED CROSS-PLY LAMINATE Interim Report No. 97, 1 Jan. - 31 Dec. 1992

M. W. Hyer, H. H. Lee, and T. W. Knott Jun. 1994 48 p

(Grant NAG1-343)

(NASA-CR-196317; NAS 1.26:196317; VPI-E-94-05; CCMS-94-05) Avail: CASI HC A03/MF A01

The stresses in the vicinity of a single stitch through the thickness of an infinite cylindrical cross-ply laminate subjected to a unit temperature decrease are computed. Interest centers on the potential for microcracking in the vicinity of the through-thickness reinforcement. The infinite cylindrical cross-ply model is a simplification which leads to a tractable axisymmetric formulation, but which retains many of the three-dimensional features of the problem. In the model the stitch is a through-thickness cylinder consisting of fibers and resin and the laminate consists of plies with fibers oriented radially and plies with with fibers oriented circumferentially. Here only a (0/90)2's laminate is examined. Both glass and kevlar stitches are considered, as is the possibility of resin pockets forming near the stitch. The results indicate that the presence of a resin pocket can alter the stress state in the vicinity of the stitch. In particular, the sign of a peak in the radial stress that occurs at the outside of the laminate changes from compression to tension when resin pockets are considered. Also, with a resin pocket the state of stress at a slight distance from the stitch can be more severe than at the interface between the stitch and the adjoining material. This worsening of conditions slightly away from the stitch can be attributed to points where three materials, namely resin, 0 deg. layers, and 90 deg. layers, coincide, so-called trimaterial points. Author

25 INORGANIC AND PHYSICAL CHEMISTRY

Includes chemical analysis, e.g., chromatography; combustion theory; electrochemistry; and photochemistry.

For related information see also *77 Thermodynamics and Statistical Physics.*.

N94-36450# Dow Corning Corp., Carrollton, KY.

METHYL CHLORIDE VIA OXYHYDROCHLORINATION OF METHANE

Jan. 1994 114 p

(Contract DE-AC22-91PC-91030)

(DE94-010691; DOE/PC-91030/T8) Avail: CASI HC A06/MF A02

The purpose of this contract is to develop a process for converting light alkane gases to methyl chloride via oxyhydrochlorination using highly selective, stable catalysts in fixed-bed reactors designed to remove the large amount of heat generated, so as to control the reaction temperature. Further, the objective is to obtain the engineering data base necessary for developing a commercially feasible process and to evaluate the economics of the process. Several key technology areas were evaluated this quarter. The catalyst definition effort focused on the determination of the role of the Li and La promoters that have been found to be useful in enhancing Cu based oxyhydrochlorination of methane catalysts. Initial experiments show that the La acts to provide a much more active catalyst than the Cu only case. The role of the Li is ambiguous at this point. The Li enhances the stability of the La promoted catalyst, but gives only marginal improvement by itself This work will be continued, with additional emphasis on the analysis of the catalysts to determine the structural role that the promoters may play. The separation unit operation definition made significant progress by demonstrating in a laboratory system that a process solvent may be used to remove the product CH3Cl from the reactor effluent stream. To date the data has been qualitative, but clear. Work will continue to gather the information possible in the laboratory to help with PDU design. An extensive amount of testing was performed on the chosen process solvent, Multitherm. A comprehensive review of all the thermal testing and associated FTIR, UV/VIS, and physical property testing is included in this report. This work shows that Multitherm should give the desired stability and solubility that are necessary to make the separation unit operation successful. DOE

N94-36453# Edgerton, Germeshausen and Grier, Inc., Idaho Falls, ID.

MOLECULAR BEAM SURFACE ANALYSIS

A. D. Appelhans, J. C. Ingram, G. S. Groenewold, D. A. Dahl, and J. E. Delmore Sep. 1993 68 p

(Contract DE-AC07-76ID-01570)

(DE94-010773; EGG-CMRE-11006) Avail: CASI HC A04/MF A01

The Molecular Beam Surface Analysis (MBSA) program is developing both laboratory-based and potentially field-portable chemical analyses systems taking advantage of new surface analysis technology developed at the Idaho National Engineering Laboratory (INEL). The objective is to develop the means to rapidly detect and identify, with high specificity and high sensitivity, nonvolatile and low volatile organics found in Chemical Weapons (CW) and High Explosives (HE) feedstocks, agents, and decomposition products on surfaces of plants, rocks, paint chips, filters, smears of buildings, vehicles, equipment, etc.. Ideally, the method would involve no sample preparation and no waste generation, and would have the potential for being implemented as a field-portable instrument. In contrast to existing analytical methods that rely on sample volatility, MBSA is optimized for nonvolatile and low volatile compounds. This makes it amenable for rapidly screening field samples for CW agent decomposition products and feedstock chemicals and perhaps actual agents. In its final configuration (benchtop size) it could be operated in a non-laboratory environment (such as an office building) requiring no sample preparation chemistry or chemical supplies. It could also be included in a mobile laboratory used in on-site, or remote site cooperative surveys, or in a standard laboratory, where it would provide fast screening of samples at minimal cost. DOE

N94-36458# Lawrence Livermore National Lab., Livermore, CA.
FLUIDS AT HIGH SHOCK PRESSURES AND TEMPERATURES AND SOME THOUGHTS ABOUT FUTURE POSSIBILITIES
W. J. Nellis Aug. 1993 5 p Presented at the 14th International Conference of the International Association for the Advancement of High Pressure Science and Technology, Colorado Springs, CO, 27 Jun. - 2 Jul. 1993
(Contract W-7405-eng-48)
(DE94-003625; UCRL-JC-115052; CONF-930676-65) Avail: CASI HC A01/MF A01

Shock compression achieves high pressures and temperatures in molecular liquids. High pressures cause high densities in compressible liquid specimens; high temperatures are achieved because the process is adiabatic by virtue of the fast nature of the compression. To illustrate representative effects, the author restricts the discussion to the diatomic fluids of hydrogen and nitrogen. Liquid hydrogen undergoes little or no dissociation, while nitrogen undergoes substantial dissociation in shock-compression experiments. Thus, results for these two similar diatomic fluids are complementary. The initial specimens are liquid but the states achieved by shock compression are supercritical. Thus, the high-pressure data are for the fluid phase. Since vibrational and electronic relaxation times of fluid hydrogen and nitrogen are short compared to the duration of an experiment, these shock-compressed fluids are in thermal equilibrium. Recent experiments to measure electric conductivities and temperatures of liquid hydrogen shock-compressed up to Mbar pressures are described and contrasted with results for liquid nitrogen. Some thoughts about future possibilities for high-pressure shock experiments are discussed. DOE

N94-36462# Sandia National Labs., Albuquerque, NM.
RICH METHANE/AIR FLAMES: BURNING VELOCITIES, EXTINCTION LIMITS, AND FLAMMABILITY LIMIT
M. N. Bui-Pham and J. A. Miller 1994 19 p Presented at the 25th International Symposium on Combustion, Irvine, CA, 31 Jul. - 5 Aug. 1994
(Contract DE-AC04-76DR-00789)
(DE94-004340; SAND-94-8483C; CONF-940711-1) Avail: CASI HC A03/MF A01

A theoretical investigation has been conducted to establish a reliable chemical kinetic mechanism that can determine the extinction limit of opposed-flow, strained, rich premixed methane-air flames. In the process of developing this kinetic representation for rich methane-air flames, we found that the heat of formation of (sup 1)CH2 = 102.5 kcal/mole, which is 1 kcal/mole higher than the currently available thermochemical data, gives the best agreement with experimental data on burning velocities for equivalence ratios between 0.5 and 1.7. Employing this value for Delta-H(sub f(sup 1)CH2) in our calculations, the extinction stretch rate, K(sub ex), was found to be K(sub ex) = 2250 sec(exp -1) for phi = 1.0, K(sub ex) = 2000 sec(exp -1) for phi = 1.1, and K(sub ex) = 1400 sec(exp -1) for phi = 1.2. These results agree better with experiments than those using a lower heat of formation of singlet methylene. In comparison with previous calculations made by Kee et al., our predictions are basically the same except that our extinction stretch rate is slightly higher at phi = 1.0 and that our location of the maximum extinction stretch rate is closer to that found in experiments. In addition, we establish the rich flammability limit using two different criteria to be approximately between phi = 1.61 and phi = 1.68, which agrees very well with an experimental value of phi = 1.67. DOE

N94-36475# Massachusetts Inst. of Tech., Cambridge. Dept. of Chemical Engineering.
DIRECT CATALYTIC DECOMPOSITION OF NITRIC OXIDE
M. Flytzani-Stephanopoulos, A. F. Sarofim, and Yan-Ping Zhang 1993 10 p
(Contract DE-FG22-91PC-91293)
(DE94-005025; DOE/PC-91293/8) Avail: CASI HC A02/MF A01

Six Cu-ZSM-5 catalysts with different Cu exchange levels were prepared according to our earlier reports. Experimental tests have suggested that the active sites of Cu-ZSM-5 catalysts for nitric oxide decomposition are square planar four-coordinated Cu2+ cations. Conversion of NO into N2 and O2 increases linearly with the amount of square planar four-coordinated Cu2+, and the turn over frequency of the NO decomposition over the catalysts is not sensitive to total Cu ion-exchanged levels in Cu-ZSM-5 catalysts at the same experimental conditions. Co-cation promoter effect in metal ion modified Cu-ZSM-5 catalyst is discussed in terms of higher turnover frequency of NO decomposition than that for Cu-ZSM-5 with the same amount of Cu exchange level. Parent ZSM-5 zeolites were dealuminated after they had been treated in a gaseous mixture of 20 percent H2O-4 percent O2-He at 750 C for 20 hours. Cu exchange process and BET measurements showed that the dealuminated ZSM-5 materials had only 15 percent of Cu exchange capacity and negligible micropore volume. DOE

N94-36482# Sandia National Labs., Albuquerque, NM.
RICH FLAMMABILITY LIMITS IN CH3OH/CO/DILUENT MIXTURES
M. N. Bui-Pham, A. E. Lutz, J. A. Miller, M. Desjardin, D. M. OShaughnessey, and R. J. Zondlak 1994 22 p Presented at the 25th International Symposium on Combustion: Western States Section of the Combustion Institute Spring Meeting, Irvine, CA, 31 Jul. - 5 Aug. 1994; Davis, CA, 21-22 Mar. 1994 Prepared in cooperation with Dow Chemical Co., Midland, MI
(Contract DE-AC04-94AL-85000)
(DE94-004341; SAND-94-8484C; WSS/CI-94-015; CONF-940711-2; CONF-940397-1) Avail: CASI HC A03/MF A01

This research, a joint project between Sandia National Laboratories/California and Dow Chemical Company/Midland, is intended to examine existing flame modeling capability developed at Sandia to model experimental data for rich flammability limits. System studied is methanol/carbon monoxide/diluent mixtures, where the diluent is either nitrogen or carbon dioxide at pressures of 1, 11, and 21 atm, respectively. Critical oxygen concentration needed to sustain a flame was measured in a spherical vessel with a central ignition source for several mixtures and pressures. Burning velocities of one dimensional, planar, freely propagating premixed flames were calculated to determine minimum oxygen concentration required for these flames to propagate. This minimum O2 concentration was found to be consistently larger than that observed in experiments; however, effects of pressure and diluent composition agreed well with experimental data. Attempts were made to model the spherical vessel experiment directly, which resulted in qualitative agreement with experimental data and steady flame predictions. In addition, the rich flammability limit was calculated for pure methanol-air flames to be at an equivalence ratio of approximately 2.1, and extinction occurs at K(sub ex) = 1670 sec(exp -1) for the opposed-flow, strained, stoichiometric methanol-air case. DOE

N94-36529# Vietnam National Atomic Energy Commission, Hanoi. Inst. of Nuclear Science.
METHOD OF N-15 ANALYSIS BY MASS-SPECTROSCOPY ON ION IMPLANTER MPB-200
Van Thuan Vo, Duc Nhan Dang, Phuc Nguyen, Tien Dung Nguyen, and Van Dach Nguyen 22 Nov. 1993 11 p
(DE94-618203; VAEC-B-020) Avail: CASI HC A03/MF A01 (US Sales Only)

The industrial implanter MPB-200 has been modified to a light-isotope mass spectrometer. Mass-resolution has been improved by combination of quadrupole focusing system and a collimator with additional scattering shielding. Single beam method has been set up, in which mass-spectrum are obtained by scanning magnetic field of the separator. A start-stop control system has been added to operate automatically the magnet and registration system, from which signals are transferred to a XT/AT computer for saving and analysis. The mass-resolution is satisfactory for analysis of light isotopes with mass number A less than 40. A testing measurement has been done with standard samples of natural and enriched N-15 isotope, at acceleration energy of 50 keV, beam current less than 100 nA, vacuum of 4x10E-6 and collimator's shell of 1 mm. Obtained resolution and background condition allowed to achieve a good linear dependence of relative isotope ratio data vs real abundance in the range from natural 0.365 percent to 5.0 percent with a 3 percent error (96 percent of reliability). Routine N-15 may achieve 5 to 10 percent accuracy by a 7-10 minutes measurement for every sample. Sensitivity of the mass-spectrometer is better almost by one order in comparing with one of emission spectrometers. The new mass-spectroscopy system is applied to research in agriculture, biology and environmental study. DOE

N94-36537*# National Aeronautics and Space Administration. Lewis Research Center, Cleveland, OH.

DETERMINATION OF COPPER IN TAP WATER USING SOLID-PHASE SPECTROPHOTOMETRY

Carol M. Hill (Akron Univ., OH.), Kenneth W. Street, Warren H. Philipp, and Stephen P. Tanner May 1994 12 p Presented at the 1993 Pittsburgh Conference on Analytical Chemistry and Applied Spectroscopy, Atlanta, GA, 13 Mar. 1993 Original contains color illustrations

(NASA-TM-106480; E-8410; NAS 1.15:106480) Avail: CASI HC A03/MF A01; 1 functional color page

A new application of ion exchange films is presented. The films are used in a simple analytical method of directly determining low concentrations of Cu(2+) in aqueous solutions, in particular, drinking water. The basis for this new test method is the color and absorption intensity of the ion when adsorbed onto the film. The film takes on the characteristic color of the adsorbed cation, which is concentrated on the film by many orders of magnitude. The linear relationship between absorbance (corrected for variations in film thickness) and solution concentration makes the determinations possible. These determinations agree well with flame atomic absorption determinations. Author

N94-36559# Brookhaven National Lab., Upton, NY.

DIPOLE FORBIDDEN VIBRATIONAL MODES FOR NO AND CO ON Cu OBSERVED IN THE FAR IR

C. J. Hirschmugl, P. Dumas, M. Suhren, and Y. J. Chabal 1993 7 p Presented at the 7th Vibrations at Surfaces, Santa Margherita, Italy, 13-17 Jun. 1993

(Contract DE-AC02-76CH-00016; NSF INT-90-16771)

(DE94-003199; BNL-49557; CONF-9306281-1) Avail: CASI HC A02/MF A01

IRRAS spectra of NO/Cu(111) and ((radical)3 (times) (radical)3) R30(degrees) coverage of CO/Cu(111) in the range 3000-180 cm(sup -1) show both the adsorbate internal modes and features assigned to the hindered rotational modes. These dipole-forbidden features are characterized by asymmetric (mostly negative) absorption lineshapes and are accompanied by a change in broadband absorption. The shape and intensity of this broadband absorption is well accounted for by a scattering model. DOE

N94-36735# Materials Research Society, Pittsburg, PA.

GAS-PHASE AND SURFACE CHEMISTRY IN ELECTRONIC MATERIALS PROCESSING. MATERIALS RESEARCH SOCIETY SYMPOSIUM PROCEEDINGS, VOLUME 334

T. J. Mountziaris, G. R. Paz-Pujalt, F. T. Smith, and P. R. Westmoreland Jan. 1994 571 p Symposium held in Boston, MA, 29 Nov. - 2 Dec. 1993

(Contracts N00014-94-1-0511; DAAH04-93-G-0516)

(AD-A280586) Avail: CASI HC A24/MF A04

The papers are organized in six sections. Part I contains papers on silicon and carbon systems. In addition to papers discussing silicon and silicon oxide deposition it includes several papers on diamond film growth. The chemistry underlying the growth and doping of III-V and II-VI compound semiconductors is covered in Part II together with several studies discussing new precursors. Part III contains papers on metallization. The deposition of dielectric and transitional layers is the topic of Part IV. Part V contains papers on etching of thin films. Finally, Part VI covers special topics, such as deposition on patterned substrates, reactor design, heteroepitaxy and selective epitaxy. DTIC

N94-36989*# Research Inst. for Advanced Computer Science, Moffett Field, CA.

COMPUTATIONAL CHEMISTRY RESEARCH Semiannual Status Report, Jan. - Jul. 1987

Eugene Levin 1987 53 p

(Contract NCC2-431)

(NASA-CR-196120; NAS 1.26:196120) Avail: CASI HC A04/MF A01

Task 41 is composed of two parts: (1) analysis and design studies related to the Numerical Aerodynamic Simulation (NAS) Extended Operating Configuration (EOC) and (2) computational chemistry. During the first half of 1987, Dr. Levin served as a member of an advanced system planning team to establish the requirements, goals, and principal technical characteristics of the NAS EOC. A paper entitled 'Scaling of Data Communications for an Advanced Supercomputer Network' is included. The high temperature transport properties (such as viscosity, thermal conductivity, etc.) of the major constituents of air (oxygen and nitrogen) were correctly determined. The results of prior ab initio computer solutions of the Schroedinger equation were combined with the best available experimental data to obtain complete interaction potentials for both neutral and ion-atom collision partners. These potentials were then used in a computer program to evaluate the collision cross-sections from which the transport properties could be determined. A paper entitled 'High Temperature Transport Properties of Air' is included. Derived from text

N94-37031 Hunter Coll., New York, NY. Dept. of Physics and Astronomy.

SODIUM-23 NMR AND COMPLEX IMPEDANCE STUDIES OF GEL ELECTROLYTES BASED ON POLY(ACRYLONITRILE) Interim Technical Report No. 9, period ending Jul. 1993

S. G. Greenbaum, J. Li, P. E. Stallworth, F. Croce, and S. Slane 29 Apr. 1994 32 p Limited Reproducibility: More than 20% of this document may be affected by microfiche quality

(Contract N00014-92-J-1629)

(AD-A280330) Avail: Issuing Activity (Defense Technical Information Center (DTIC))

Highly conducting gel electrolytes prepared from mixtures of poly(acrylonitrile) (PAN), ethylene carbonate (EC), propylene carbonate (PC), and NaClO4 have been studied by complex impedance, differential scanning calorimetry (DSC) and Na-23 nuclear magnetic resonance (NMR) spectroscopy. Ionic motional correlation times spanning nearly five orders of magnitude, probed by temperature-dependent dynamical features of the Na-23 quadrupole-broadened NMR lineshape, are strongly influenced by the single glass transition temperature observed in the gel electrolyte. Dielectric measurements of mixtures of PAN, EC, and PC suggest that the polar nitrile group in PAN may interact with Na+ ions in the gel. All results are consistent with the conclusion that PAN provides stability to the gel network down to the immediate vicinity of the Na+ ions, rather than acting as a rigid framework for regions of liquid electrolyte. DTIC

N94-37056# California Univ., Berkeley. Lawrence Berkeley Lab, CA.

NONLINEAR OPTICAL SPECTROSCOPY FOR SURFACE STUDIES

Y. R. Shen Jan. 1994 7 p Presented at the OE/LASE 1994: Conference on Optics, Electro-Optics, and Laser Applications in Science and Engineering, Los Angeles, CA, 22-29 Jan. 1994

(Contract DE-AC03-76SF-00098)

(DE94-011623; LBL-35306; CONF-940142-39) Avail: CASI HC A02/MF A01

Infrared-visible sum-frequency generation as a versatile surface vibrational spectroscopic tool is described. Applications to neat water interfaces and hydrogen adsorption on diamond are used as illustrative examples. DOE

N94-37091# Sandia National Labs., Albuquerque, NM.

A DYNAMIC MODEL OF A LINEAR ACTUATOR BASED ON POLYMER HYDROGEL

D. Brock (Massachusetts Inst. of Tech., Cambridge.), Woojin Lee (Massachusetts Inst. of Tech., Cambridge.), D. Segalman, and W. Witkowski 1994 13 p Presented at the 2nd International Conference on Intelligent Materials, Williamsburg, VA, 5-8 Jun. 1994

(Contract DE-AC04-94AL-85000)

(DE94-010800; SAND-93-3822C; CONF-940691-2) Avail: CASI HC A03/MF A01 (US Sales Only)

The design and analysis of a series of linear actuators based on polymer hydrogel is presented. The actuators use arrays of pH sensitive gel fibers together with a fluid irrigation system to locally and rapidly regulate the composition of the solution. A dynamic model is constructed for one of the linear actuators, which includes the polymer gel, fluidic system, and transmission mechanics. Emphasis in the design and mechanical modeling of the actuators is placed on the complete system including not only the polymer gel, but also on the containment system, irrigation scheme, and servo valving system. DOE

N94-37095# Chicago Univ., Chicago, IL.

BOND SELECTIVE CHEMISTRY BEYOND THE ADIABATIC APPROXIMATION

L. J. Butler 22 Feb. 1994 5 p
(Contract DE-FG02-92ER-14305)
(DE94-012486; DOE/ER-14305/2) Avail: CASI HC A01/MF A01

Developing predictive ability for branching between energetically allowed chemical reaction pathways is important for design of efficient combustion processes and the development/utilization of new fuels. The work in the second year investigates the central role played by coupling between electronic states in polyatomic molecules in the selective branching between energetically allowed fragmentation pathways. Five projects are described: dynamics in Franck-Condon and exit channels regions of dissociating H2S (emission spectra upon tunable excitation 199-203 nm); selective C-Br bond fission in 1,3-bromoiodopropane (intramolecular distance dependence of coupling between electronic configurations); testing adiabatic predictions for the C-S:S-H bond fission branching in CH3SH; competition between bond fission channels and H2 elimination in CH(sub 3)NH(sub 2); and determination of absolute C-C: C-X (X=Br, Cl) branching ratios in bromoacetone and chloroacetone photolysis using acetyl chloride photodissociation. DOE

N94-37132# Wisconsin Univ., Milwaukee, WI.
AN INVESTIGATION OF MOLYBDENUM AND MOLYBDENUM OXIDE CATALYZED HYDROCARBON FORMATION REACTIONS
1994 25 p
(Contract DE-FG02-92ER-14289)
(DE94-013700; DOE/ER-14289/2) Avail: CASI HC A03/MF A01

Equipment construction includes: uv source, vacuum system with mass spectrometer, Auger analyzer, fast sample transfer cell, and infrared spectrometer detector. Mo and Mo oxide catalysts were tested for activity for olefin (propylene) metathesis. Higher hydrocarbons were also formed in this reaction in parallel with metathesis products. Surface chemistry experiments were carried out on metallic surfaces in ultrahigh vacuum, photoelectron MoO2 and its reduction, and Mo(CO)(sub 6) adsorption on alumina. Identification of surface species using near-edge x-ray adsorption fine structure is discussed. DOE

N94-37145 Nebraska Univ., Lincoln, NE. Dept. of Chemistry.
SOLUTION CHARACTERIZATION OF POLY(ISOBORNYL METHACRYLATE) IN TETRAHYDROFURAN
X. Q. Zhang and C. H. Wang 1994 7 p Repr. from Journal of Polymer Science. Part B: Polymer Physics, v. 32, 1994 6 p Sponsored by ONR Limited Reproducibility: More than 20% of this document may be affected by microfiche quality
(AD-A280497; TR-29-ONR) Avail: Issuing Activity (Defense Technical Information Center (DTIC))

Thermodynamic and hydrodynamic properties of dilute solutions of poly(isobornyl methacrylate) (PIMA) in tetrahydrofuran (THF) were characterized by using viscosity, static, and dynamic light scattering measurements. PIMA samples were different molecular weight were obtained by fractional precipitation of PIMA solution. Chain dimension parameters (R(g) and R(H)), together with second virial coefficient A2 and intrinsic viscosity ETA, were used to calculate various solution parameters characterizing polymer chains in polymer solutions. The experimental results are compared with calculation, indicating that PIMA behaves as a flexible coil in THF. DTIC

N94-37161# Sandia National Labs., Albuquerque, NM. Microsensor R/D Dept.
NEW MATERIALS AND MULTIDIMENSIONAL CLUSTER ANALYSIS FOR SAW CHEMICAL SENSOR ARRAYS
Antonio J. Ricco, Gordon C. Osbourn, John W. Bartholomew, Richard M. Crooks, Chuanjing Xu, and Ronald E. Allred 1994 4 p Presented at the 1994 Solid-state Sensor and Actuator Workshop, Hilton Head, SC, 13-16 Jun. 1994
(Contract DE-AC04-94AL-85000)
(DE94-012066; SAND-94-0240C; CONF-9406166-1) Avail: CASI HC A01/MF A01

We use six-element arrays of 97-MHz ST-quartz surface acoustic wave (SAW) devices to detect changes in thin-film mass and mechanical properties resulting from sorption of analytes by films representing two new classes of chemical sensor interface: self-assembled monolayers (SAM's) and plasma-grafted films (PGF's). While these materials do not display exceptional chemical selectivity, various combinations of the seven different SAM's and eight PGF's examined to produce distinct response patterns for each of 13 analytes. The analytes include aliphatic, aromatic, and chlorinated hydrocarbons; alcohols; ketones; organophosphonates; and water. Evaluation of the SAW array data using multidimensional cluster analysis techniques show that each chemical species can be correctly identified 100% of the time over the 9% to 49% of saturation range using data from many combinations of four or more films. DOE

N94-37168# Wisconsin Univ., Madison, WI. Dept. of Chemistry.
INFRARED SPECTROSCOPY OF ORGANIC FREE RADICALS RELATED TO COMBUSTION PROCESSES
J. C. Weisshaar 1994 5 p
(Contract DE-FG02-92ER-14306)
(DE94-012481; DOE/ER-14306/2) Avail: CASI HC A01/MF A01

Experiments were done to resolve internal rotor states in parent cations of aromatic molecules cooled in skimmed, pulsed nozzle expansion. Internal rotation of methyl and silyl groups attached to aromatic rings was studied. S(sub 1)-S(sub 0) spectra were measured using one-color R2PI (resonant two-photon ionization). Ab initio calculations using the GAUSSIAN package were performed. For various neutral and cationic ground states with threefold or sixfold barriers, effects of different levels of theory on calculated barrier height and phase were tested. The HF/6-31G* level of theory was used to calculate V(sub 6) and V(sub 3) for a variety of S(sub 0) molecules. Distortions of the phenyl ring and precession of rotor axis as the methyl group rotates are discussed. DOE

N94-37199# California Univ., Berkeley. Lawrence Berkeley Lab, CA. Energy and Environment Div.
SOME EFFECTS OF HEAT RELEASE IN PREMIXED FLAMES
I. G. Shepherd Mar. 1994 18 p Presented at the Wester States Section of the Combustion Institute Spring Meeting, Davis, CA, 21-22 Mar. 1994
(Contract DE-AC03-76SF-00098)
(DE94-011346; LBL-35318; CONF-940397-2) Avail: CASI HC A03/MF A01

Numerical and experimental results are presented to illustrate some hydrodynamic effects of heat release in premixed flames. The heat release is represented by a simple model which treats the flame front as a two dimensional line source of volume. The velocity and strain rate induced in the flow field are determined and the numerical solution for the case of a laminar double kernel ignition is obtained. Of primary interest is the strain induced in the reactants between the expanding flame kernels and, for heat release rates typical of hydrocarbon flames, the strain rate at the plane of symmetry midway between the kernels up to 150 s(exp -1). The effects of kernel size, density ratio across the flame front, and laminar burning velocity are studied. For the case of turbulent combustion the velocity induced in the reactant stream is measured in a plane parallel to the flame holder of an open premixed turbulent V-shaped flame. A divergent flow field, with a strain rate of 50 s(exp -1), is induced by the heat release in the flame zone and the consequences of this for determining the turbulent burning velocity in this and similar systems are reviewed. DOE

N94-37221# Sandia National Labs., Albuquerque, NM.
INFLUENCES OF FLAME-VORTEX INTERACTIONS ON FORMATION OF OXIDES OF NITROGEN IN CURVED METHANE-AIR DIFFUSION FLAMELETS
J. M. Card (Sandia National Labs., Livermore, CA.), R. Ryden (Volvo Flygmotor A.B., Trollhaettan, Sweden.), and F. A. Williams (California Univ., San Diego, La Jolla, CA.) 1994 20 p Presented at the 25th Combustion Symposium, Irvine, CA, 1 Aug. 1994
(Contract DE-AC04-76DR-00789)
(DE94-005105; SAND-94-8501C; CONF-940838-4) Avail: CASI HC A03/MF A01

To improve knowledge of production rates of nitrogen oxides in turbulent diffusion flames in reaction-sheet regimes, an analytical investigation is made of the structure of a parabolic flamelet. The mixture-fraction field, scalar dissipation rate, and gas velocity relative to the flamelet in the vortex are related to flame curvature at the parabolic tip. Flame structure for major species and temperature is described by rate-ratio asymptotics based on two-step and three-step reduced chemical-kinetic mechanisms. Production rates by prompt, thermal, and nitrous-oxide mechanisms are obtained from one-step reduced-chemistry approximations that employ steady

states for all reaction intermediaries. For sufficiently large streamwise separation distances between isoscalar surfaces, it is found that equilibrium conditions are closely approached near the flame tip, and the thermal mechanism dominates there, but the prompt mechanism always dominates in the wings, away from the tip, where the highest rates of scalar dissipation occur. Increasing the tip curvature increases the Peclet number and the prompt contribution while decreasing the thermal contribution. At 1 atm and ambient temperatures of 300 K, the prompt mechanism always dominates the total production rate in the parabolic flamelet, and, perhaps surprisingly, the rate of the nitrous-oxide mechanism is faster than that of the thermal mechanism and varies with the tip curvature and with scalar dissipation in the same manner as that of the prompt mechanism, different from that of the thermal mechanism. The conclusion reached is that Zel'dovich NO is relatively insignificant in hydrocarbon-air mixtures in reaction-sheet regimes. DOE

N94-37222# Sandia National Labs., Albuquerque, NM.
FINITE-RATE CHEMISTRY AND TRANSIENT EFFECTS IN DIRECT NUMERICAL SIMULATIONS OF TURBULENT NON-PREMIXED FLAMES
S. Mahalingam (Colorado Univ., Boulder, CO.), J. H. Chen (Sandia National Labs., Kirtland AFB, NM.), and L. Vervisch (Institut National des Sciences Appliquees, Routen, France.) 1994 18 p Presented at the 25th Combustion Symposium, Irvine, CA, 1 Aug. 1994
(Contract DE-AC04-76DP-00789)
(DE94-005250; SAND-94-8507C; CONF-940838-5) Avail: CASI HC A03/MF A01

Three-dimensional Direct Numerical Simulations (DNS) of turbulent non-premixed flames including finite-rate chemistry and heat release effects were performed. Two chemical reaction models were considered: (1) a single-step global reaction model in which the heat release and activation energy parameters are chosen to model methane-air combustion, and (2) a two-step reaction model to simulate radical production and consumption and to compare against the single-step model. The model problem consists of the interaction between an initially unstrained laminar diffusion flame and a three-dimensional field of homogeneous turbulence. Conditions ranging from fast chemistry to the pure mixing limit were studied by varying a global Damkoehler number. Results suggest that turbulence-induced mixing acting along the stoichiometric line leads to a strong modification of the inner structure of the turbulent flame compared with a laminar strained flame, resulting in intermediate species concentrations well above the laminar prediction. This result is consistent with experimental observations. Comparison of the response of the turbulent flame structure due to changes in the scalar dissipation rate with a steady strained laminar flame reveals that unsteady strain rates experienced by the turbulent flame may be responsible for the observed high concentrations of reaction intermediates. DOE

N94-37250*# Alabama Univ., Huntsville, AL.
SPRAY COMBUSTION MODEL IMPROVEMENT STUDY, 1 Final Technical Report, 11 Sep. - 11 Dec. 1991
C. P. Chen, Y. M. Kim, and H. M. Shang Mar. 1993 197 p
(Contract NAS8-38609)
(NASA-CR-196122; NAS 1.26:196122; UAH-5-32753) Avail: CASI HC A09/MF A03

This study involves the development of numerical and physical modeling in spray combustion. These modeling efforts are mainly motivated to improve the physical submodels of turbulence, combustion, atomization, dense spray effects, and group vaporization. The present mathematical formulation can be easily implemented in any time-marching multiple pressure correction methodologies such as MAST code. A sequence of validation cases includes the nonevaporating, evaporating and—burnin dense—sprays. Author

N94-37284# New Mexico Univ., Albuquerque, NM. Dept. of Chemistry.
DEVELOPMENT OF IMMOBILIZED LIGANDS FOR ACTINIDE SEPARATIONS
R. T. Paine 1994 37 p
(Contract DE-FG04-88ER-13915)
(DE94-012714; DOE/ER-13915/T4) Avail: CASI HC A03/MF A01

Primary goals during this grant period were to (1) synthesize new bifunctional chelating ligands, (2) characterize the structural features of the Ln and An coordination complexes formed by these ligands, (3) use structural data to iteratively design new classes of multifunctional ligands, and (4) explore additional routes for attachment of key ligands to solid supports that could be useful for chromatographic separations. Some highlights of recently published work as well as a summary of submitted, unpublished and/or still in progress research are outlined. DOE

N94-37286# Georgia Univ., Aiken, SC.
MODELING OF FORCED CVI FOR TUBE FABRICATION
T. L. Starr and A. W. Smith May 1994 14 p Prepared for Oak Oak Ridge National Lab., TN
(Contract DE-AC05-84OR-21400)
(DE94-012718; ORNL/Sub-85-55901/04) Avail: CASI HC A03/MF A01

The forced flow/thermal gradient chemical vapor infiltration process (FCVI) can be used for fabrication of tube-shaped components of ceramic matrix composites. Recent experimental work at Oak Ridge National Laboratory (ORNL) includes process and materials development studies using a small tube reactor for tubes 20 cm long and 2.5 cm ID. Adaption of FCVI for this geometry involves significant changes in fixturing as compared to disk-shaped preforms previously fabricated. The authors have used this computer model of the CVI process to simulate tube densification and to identify process modifications that will decrease processing time. DOE

N94-37296# Los Alamos National Lab., NM.
THE HYDROGENOLYSIS AND ISOMERIZATION OF LIGHT HYDROCARBONS OVER Pt CATALYSTS
S. Anderson (New Mexico Univ., Albuquerque, NM.), A. K. Datye (New Mexico Univ., Albuquerque, NM.), and M. T. Paffett 1994 4 p Presented at the 15th Conference on Catalysis of Organic Reactions, Phoenix, AZ, 2-5 May 1994
(Contract W-7405-eng-36)
(DE94-013142; LA-UR-94-1871; CONF-940504-1) Avail: CASI HC A01/MF A01

There is evidence that metallic Pt, unlike Ni and Rh, has the ability to isomerize light hydrocarbons in the presence of hydrogen. The nature of the active site for the isomerization is still unclear though. It has been shown that the morphology of a silica supported Pt particles can be controlled by heating in different atmospheres and that annealing in hydrogen produces cubo-octahedral particles. The reaction of n-butane with H2 was carried out over two silica supported Pt catalysts of different particle sizes and a Pt(III) single crystal. Comparison of the product distribution between the two supported and the single crystal sample are the focus of this paper. DOE

N94-37357# Argonne National Lab., IL.
[ACTIVITIES OF THE CHEMICAL TECHNOLOGY DIVISION] Annual Technical Report, 1993
J. E. Battles, K. M. Myles, J. J. Laidler, and D. W. Green Apr. 1994 198 p
(Contract W-31-109-eng-38)
(DE94-013050; ANL-94/15) Avail: CASI HC A09/MF A03

Chemical Technology (CMT) Division this period conducted research and development in the following areas: advanced batteries and fuel cells; fluidized-bed combustion and coal-fired magnetohydrodynamics; treatment of hazardous waste and mixed hazardous/radioactive waste; reaction of nuclear waste glass and spent fuel under conditions expected for an unsaturated repository; separating and recovering transuranic elements, concentrating radioactive waste streams with advanced evaporators, and producing Mo-99 from low-enriched uranium; recovering actinide from IFR core and blanket fuel in removing fission products from recycled fuel and disposing removal of actinides in spent fuel from commercial water-cooled nuclear reactors; and physical chemistry of selected materials in environments simulating those of fission and fusion energy systems. The division also conducts basic research in catalytic chemistry associated with molecular energy resources and novel ceramic precursors; materials chemistry of superconducting oxides, electrified metal/solution interfaces, molecular sieve structures, thin-film diamond surfaces, effluents from wood combustion, and molten silicates; and the geochemical processes involved in water-rock interactions. The Analytical Chemistry Laboratory in CMT also provides a broad range of analytical chemistry support. DOE

N94-37365# Sandia National Labs., Albuquerque, NM.
SAW CHEMICAL SENSOR ARRAYS USING NEW THIN-FILM MATERIALS
A. J. Ricco, Chuan-Jing Xu, R. M. Crooks, and R. E. Allred 1994 5 p Presented at the 5th International Meeting on Chemical Sensors, Rome, Italy, 11-14 Jul. 1994
(Contract DE-AC04-94AL-85000)
(DE94-011940; SAND-94-0241C; CONF-940775-1) Avail: CASI HC A01/MF A01

We have used two classes of materials, self-assembled monolayers (SAM's) and plasma-grafted films (PGF's), as new chemically sensitive layers for an array of 97-MHz surface acoustic wave (SAW) delay-line-based devices. Responses of these materials to each of 14 different analytes, representing the classes of saturated alkane, aromatic hydrocarbon, chlorinated hydrocarbon, alcohol, ketone, organophosphonate, and water, have been evaluated using our six-SAW device array. Results reveal a qualitative 'chemical orthogonality' of the films that is very promising for pattern recognition analysis. DOE

N94-37372# Wisconsin Univ., Madison, WI. Dept. of Chemical Engineering.
THERMODYNAMIC AND KINETIC ASPECTS OF SURFACE ACIDITY
J. A. Dumesic 1994 8 p
(Contract DE-FG02-84ER-13183)
(DE94-012351; DOE/ER-13183/9) Avail: CASI HC A02/MF A01

During the past year, the research involved studies of solid acidity, role of acidity in methylamine synthesis reactions, and catalytic cracking of hydrocarbons. Studies were completed of the acidity of ZSM-5 catalysts, in which effects of non-framework aluminum species on acidity of Broensted acid sites associated with the framework were explored. It was found that microcalorimetric studies of ammonia adsorption at 423 K can be used to determine acid strength distributions of high surface area catalysts. Effects of Sn(2+) and Sn(4+) on acid and base sites of alumina were investigated; the former cation neutralizes the acid and base sites. Results of microcalorimetric, infrared spectroscopic, and reaction kinetic studies are being brought together to describe the factors controlling methylamine synthesis and related reactions over acid catalysts. The catalytic cracking studies involved developing a kinetic model for isobutane cracking over acidic Y zeolites. DOE

N94-37380 Argonne National Lab., IL.
ANALYTICAL ELECTRON MICROSCOPY EXAMINATION OF SOLID REACTION PRODUCTS IN LONG-TERM TEST OF SRL 200 WASTE GLASSES
E. C. Buck, J. A. Fortner, J. K. Bates, X. Feng, N. L. Dietz, C. R. Bradley, and B. S. Tani 1993 10 p Presented at the Fall Meeting of the Materials Research Society (MRS), Boston, MA, 29 Nov. - 3 Dec. 1993 Limited Reproducibility: More than 20% of this document may be affected by microfiche quality
(Contract W-31-109-eng-38)
(DE94-005482; ANL/CMT/CP-79802; CONF-931108-38) Avail: CASI HC A02

Alteration phases, found on the leached surfaces and present as colloids in the leachates of 200-based frit (fully active and simulated) nuclear waste glass, reacted under static test conditions, at a surface area to leachate volume ratio of 20,000 m(sup -1) for 15 days to 728 days, have been examined by analytical electron microscopy. The compositions of the secondary phases were determined using x-ray energy dispersive spectroscopy and electron energy loss spectroscopy, and structural analysis was accomplished by electron diffraction. Long-term samples of simulated glass, which had undergone an acceleration of reaction after 182 days, possessed a number of silicate secondary phases, including; smectite (iron silicate and potassium iron alumina-silicate), weeksite (uranium silicate), zeolite (calcium potassium alumino-silicate), tobermorite (calcium silicate), and a pure silica phase. However, uranium silicates and smectite have also been observed in tests, which have not undergone the acceleration of reaction, in both the leachate and leached layer, suggesting that these phases are not responsible for the acceleration of reaction. DOE

N94-37409# Midwest Research Inst., Cary, NC.
COMBUSTION CHARACTERIZATION OF METHYLAL IN RECIPROCATING ENGINES
L. Dodge and D. Naegeli Jun. 1994 25 p Prepared for Midwest Research Inst., Golden, CO
(Contract DE-AC02-83CH-10093)
(DE94-006949; NREL/TP-425-6345) Avail: CASI HC A03/MF A01

Methylal, CH3OCH2OCH3, also known as dimethoxy-methane, is unique among oxygenates in that it has a low autoignition temperature, no carbon-carbon bonds, and is soluble in middle distillate fuels. Because of these properties, methylal has been shown to be a favorable fuel additive for reducing smoke in diesel engines. Recent measurements of ignition delay times indicate that methylal has a cetane number in the range of 45-50, which is compatible with diesel fuels. Engine tests have shown that adding methylal to diesel fuel significantly reduces smoke emissions. Gaseous emissions and combustion efficiencies obtained with methylal/diesel fuel blends remain essentially the same as those measured using neat diesel fuel. Lubricity measurements of methylal/diesel fuel blends with a ball on cylinder lubrication evaluator (BOCLE) show that methylal improves the lubricity of diesel fuel. Even though additions of methylal lower the fuel viscosity, the results of the BOCLE tests indicate that the methylal/diesel fuel blends cause less pump wear than neat diesel fuel. The one drawback is that methylal has a low boiling point (42 C) and a relatively high vapor pressure. As a result, it lowers the flash point of diesel fuel and causes a potential fuel tank flammability hazard. One solution to this increased volatility is to make polyoxymethylenes with the general formula of CH3O(CH(2)O)(sub x)CH3 where x is greater than 2. The molecules are similar to methylal, but have higher molecular weights and thus higher viscosities and substantially lower vapor pressures. Therefore, their flash points will be compatible with regular diesel fuel. The polyoxymethylenes are expected to have combustion properties similar to methylal. It is theorized that by analogy with hydrocarbons, the ignition quality (i.e., cetane number) of the polyoxymethylenes will be better than that of methylal. DOE

N94-37412# Sandia National Labs., Livermore, CA.
EFFECTS OF TWO-PHASE FLOW ON THE DEFLAGRATION OF POROUS ENERGETIC MATERIALS
S. B. Margolis and F. A. Williams 1994 23 p Presented at the 1994 Joint USA-Russia Energetic Material Technology Symposium, Livermore, CA, 18-25 May 1994
(Contract DE-AC04-94AL-85000)
(DE94-011423; SAND-94-1190C; CONF-9405136-8) Avail: CASI HC A03/MF A01

The combustion behavior of energetic materials (e.g., solid propellants) has long been of interest in the fields of propulsion and pyrotechnics. In many such applications, it is becoming increasingly clear that two-phase flow effects play an important role, especially since, during combustion, most homogeneous solid propellants develop thin multi-phase layers at their surfaces in which finite-rate exothermic reactions occur. In addition, there is a growing interest in the behavior of porous energetic solids, since even initially dense materials can develop significant void fractions if, at any time, they are exposed to abnormal thermal environments. The deflagration characteristics of such 'damaged' materials may then differ significantly from those of the pristine material due, at least in part, to gas flow in the solid/gas preheat region. The presence of gas in the porous solid in turn results in a more pronounced two-phase effect in the multi-phase surface layer, such as in the liquid melt region of nitramine propellants, which thus tend to exhibit extensive bubbling in an exothermic foam layer. The present analysis is largely applicable to this latter class of propellants. DOE

N94-37431# California Univ., Davis, CA. Dept. of Chemical Engineering and Materials Science.
SUPERACID CATALYSIS OF LIGHT HYDROCARBON CONVERSION Quarterly Report No. 2, 25 Nov. 1993 - 26 Feb. 1994
B. C. Gates 1994 6 p Prepared for Delaware Univ., Newark, DE
(Contract DE-AC22-93PC-92116)
(DE94-011132; DOE/PC-92116/T2) Avail: CASI HC A02/MF A01

The primary objectives of this report are (1) to explain briefly the procedures used in the preparation of the first solid superacids to be used in the research, namely, sulfated zirconia promoted by iron and/or manganese and (2) to describe the completion of construction and initial testing of the flow reactor system to be used in catalyst testing. DOE

N94-37439# Argonne National Lab., IL. Chemistry Div.
PHOTOCHEMISTRY WITHOUT PROTONS. RADICAL CATION CHEMISTRY IN ZEOLITES
A. D. Trifunac and M. V. Barnabas 1994 4 p
(Contract W-31-109-eng-38)
(DE94-012631; ANL/CHM/PP-77910) Avail: CASI HC A01/MF A01

The interconversion of the C7H8 molecular framework, especially norbornadiene (NBD) and quadricyclane (Q), has been considered for photochemical energy storage. Actually, very little was known about the details of these carbon-skeleton transformations, and only one radical cation species (NBD(+) center dot) was characterized. The authors have undertaken a thorough study of these systems using zeolite matrices. They have shown that zeolites have exceptional properties, allowing unprecedented control of chemical reactivity. In the attached scheme, they outline some of the species they were able to characterize. The crucial aspect of the zeolite matrix is that one can tune the matrix-radical cation interaction by varying the matrix polarity. The ZSM-5 zeolites of identical structure with different Si/Al ratio are ideally suited for such study. Without discussing all the transformations, the authors point that several processes, such as the reverse Diels-Alder reaction, are known to occur by involvement of highly excited states. Such reactions in zeolites means that sites in the zeolite matrix are able to stabilize high electronic states of ions, significantly lowering the potential energy barrier for such reactions. Thus, they are able to thermally drive otherwise photodriven reactions. DOE

N94-37462# SRI International Corp., Menlo Park, CA.
DEVELOPMENT OF DURABLE HIGH-TEMPERATURE CATALYSTS FOR NATURAL GAS COMBUSTION: CATALYTIC MATERIALS (CATMAT (TRADE NAME)) PROPERTIES DATABASE Topical Report No. 3, 1 Jul. 1991 - 28 Feb. 1994
Bernard J. Wood and Jon G. McCarty Feb. 1994 79 p See also PB93-226447
(Contract GRI 5091-260-2233)
(PB94-171824; SRI-PYH-2976; GRI-94/0086) Copyright Avail: CASI HC A05/MF A01

The report describes the development and functions of the initial version of a catalytic materials properties database that the authors have named CATMAT. The CATMAT menus, data structure, screen and reporting layout, and part of the properties data were developed by Fourth Floor Databases, Inc., using the 4th Dimension database management software by ACI US, Inc. The database and compiled properties data, which are intended for use by catalytic combustion device designers, include thermomechanical properties of substrate, supporting oxides, and active catalytic materials. A user manual for this initial version is attached to this report as an appendix. The initial set of data includes some 85 materials with properties in tabular and parametric form. NTIS

N94-37491# Northwestern Univ., Evanston, IL. Dept. of Engineering Sciences and Applied Mathematics.
STABILITY AND DYNAMICS OF SPATIO-TEMPORAL STRUCTURES
H. Riecke May 1994 10 p
(Contract DE-FG02-92ER-14303)
(DE94-013035; DOE/ER-14303/2) Avail: CASI HC A02/MF A01

Goal is to contribute to understanding of localized spatial and spatio-temporal structures far from thermodynamic equilibrium. Here we report on our progress in the study of the following three classes of systems: (1) We have studied cellular flame structures arising in a circular burner. Using numerical computations we have found a number of traveling-wave structures in which different cells undergo different motion. Most strikingly, we have found a localized wave traveling through the array of steady cells. Results are interpreted using various asymptotic approaches. They are in qualitative agreement with recent experiments. (2) We have continued our investigation of localized waves in binary-mixture convection. Starting from the extended Ginzburg-Landau equations introduced earlier, we have derived equations of motion for interacting fronts connecting the conductive and the convective state. These equations reveal a repulsive interaction between the fronts which implies a new localization mechanism for waves. It is solely due to the long-wavelength mode specific to the extended Ginzburg-Landau equations. The stability properties of the resulting localized waves are in qualitative agreement with very recent experiments. (3) We have extended our investigation of domain structures to include their temporal evolution. DOE

N94-37533# China Nuclear Information Centre, Beijing (China).
THE DETERMINATION OF HYDROGEN IN SODIUM BY VACUUM EXTRACTION
Lin-Kun Qi (Academia Sinica, Beijing, China.), Gang Wan (Academia Sinica, Beijing, China.), Xi-Meng Wen (Academia Sinica, Beijing, China.), Shi-Ping Sun (Academia Sinica, Beijing, China.), and un-Teng Jia (Academia Sinica, Beijing, China.) May 1993 8 p In CHINESE
(DE94-620278; CNIC-00759; IAE-0119) Avail: CASI HC A02/MF A01 (US Sales Only)

A method to determine the hydrogen in sodium is introduced. The sodium sample, which is less than 7 g, is put into a thin iron capsule in argon atmosphere, the capsule is sealed by electron beam welding and heated to 700 C in a vacuum system with pressure less than 10(exp -5) Pa, then the hydrogen released from the vacuum system can be determined. The determining limit by this method is 20 to approx. 150 (mu)g and the standard deviation is 20%. This method uses electron beam welding to replace the argon arc welding and combines the off-line sampling with on-line measuring. It is an easier off-line measurement to determine hydrogen in sodium. DOE

N94-37534# China Nuclear Information Centre, Beijing (China).
STUDY ON EXTRACTION BEHAVIOR OF TRPO WITH DIFFERENT COMPOSITION
Rong-Zhu Jiao, Da-Zhu Yang, and Wei-Be Zhang Jun. 1993 7 p In CHINESE
(DE94-620287; CNIC-00758; TSHUNE-0068) Avail: CASI HC A02/MF A01 (US Sales Only)

The structures of four kinds of TRPO (trialkyl phosphine oxide) were studied by infrared spectrometry and gas chromatography mass spectrometry. The ratio of alkyl phosphorus compounds with different molecular weight was determined. The extraction behavior of americium and nitric acid and the third phase formation condition of TRPO (mixed) have been studied and its melting point has been measured. Results show that the extractant (TRPO) produced by Jinan Phosphate Factory in China has been proved to be a competitive one and may have wide application in the future. DOE

N94-37542# Sandia National Labs., Albuquerque, NM.
IRON HYDROUS TITANIUM OXIDE CATALYSTS FOR THE DEHYDROGENATION OF ETHYLBENZENE TO STYRENE
E. P. Boespflug and A. G. Sault Feb. 1994 13 p Presented at the Spring Meeting of the AIChE, Atlanta, GA, 17-21 Apr. 1994
(Contract DE-AC04-94AL-85000)
(DE94-010381; SAND-93-2070C; CONF-940433-3) Avail: CASI HC A03/MF A01

Hydrous titanium oxide (HTO) supports are amorphous, high surface area materials which can be loaded with highly dispersed catalytically active metals by ion exchange. Fe/HTO catalysts possess significant activity and selectivity for the dehydrogenation of ethylbenzene (EB) to styrene at 873 K. The most active Fe/HTO incorporates silicon into the HTO support to stabilize surface area. Conversions obtained with the best Fe/HTO catalysts studied to date are only 50-70% as great as those obtained with commercial bulk iron oxide catalysts. However, at least two potential improvements to the Fe/HTO catalysts have been identified which could increase activity significantly. First, previous work with HTO supports has shown that iron loadings can be at least doubled from the nominal 2 wt% iron loadings used in this study. Second, the Fe/HTO shrinks by 37% to 58% during reaction, decreasing the volume of the catalytic zone and thus reactant residence times compared to the residence time using bulk iron oxides. Several strategies are proposed for pre-shrinking the HTO's to allow more active sites to be loaded into a given reactor volume. In addition to their potential superiority in bulk form, HTO's can also be coated as thin films on a wide variety of substrates. Formation of such catalytically active films on membrane surfaces offers potential advantages in catalytic membrane reactor applications. DOE

N94-37546# Oak Ridge National Lab., TN.
THE APPLICATION OF MAXIMUM ENTROPY TO Z-CONTRAST IMAGING IN A STEM
A. J. McGibbon and S. J. Pennycook Mar. 1994 3 p Presented at the 13th International Congress on Electron Microscopy, Paris, France,

17-22 Jul. 1994
(Contracts DE-AC05-84OR-21400; DE-AC05-76OR-00033)
(DE94-011470; CONF-940766-2) Avail: CASI HC A01/MF A01

Maximum entropy (Gull and Skilling, IEE Proceedings, 131F, 646 (1984)) is an image processing routine based on Bayesian probability which can produce a 'most likely' image from original data given a particular point spread function. By combining maximum entropy and analysis with incoherent Z-contrast imaging, it is possible to retrieve crystal lattice information at atomic resolution from directly acquired experimental data without the need for preconceived structures. Results are given for simulated and experimentally acquired Z-contrast images of semiconductors (graded SiGe, (110) Si, (110) GaAs) at 300 kV. DOE

N94-37623# Massachusetts Univ., Amherst, MA. Dept. of Chemical Engineering.
PROBING FLAME CHEMISTRY WITH MBMS, THEORY, AND MODELING
P. R. Westmoreland Apr. 1994 13 p
(Contract DE-FG02-91ER-14192)
(DE94-011224; DOE/ER-14192/3) Avail: CASI HC A03/MF A01

Propene/oxygen/argon flames have been mapped and modeled at fuel-lean (phi = 0.229;30 Torr) conditions and fuel-rich conditions (phi = 1.64;35 Torr). Objective is to establish kinetics of combustion and molecular-weight growth in C3 hydrocarbon flames as part of an ongoing study of flame chemistry. In the past year, we made extensive re-measurements of temperature because previous modeling suggested that the temperature profiles were wrong. The new measurements changed only slightly from the previous measurements. Instead, continued modeling of the lean propane flame and of ethene flames revealed that the problem was inadequacies in the earlier reaction set. Corrections from the literature and from theoretical kinetics resolved nearly all the problems except for allyl, which was overpredicted by 20 to 30 times. This error is corrected by identifying a new reaction of allyl + O2 with a rate constant of 3(+/-1) x 10(exp 12) at 1000-1700 K, probably forming propenal + OH. DOE

N94-37630 California Univ., Berkeley. Lawrence Berkeley Lab, CA.
OPTICAL SPECTROSCOPY OF A NITROGEN-HYDROGEN COMPLEX IN ZnSe
J. A. Wolk, J. W. Ager, III, K. J. Duxstad, E. E. Haller, N. R. Taskar, D. R. Dorman, and D. J. Olego Feb. 1994 6 p Presented at the Fall Meeting of the Materials Research Society, Boston, MA, 29 Nov. - 3 Dec. 1993 Limited Reproducibility: More than 20% of this document may be affected by microfiche quality
(Contract DE-AC03-76SF-00098)
(DE94-011622; LBL-34997; CONF-931108-101) Avail: CASI HC A02

We have observed two local vibrational modes related to H bonded to N acceptors in ZnSe samples grown by metal organic vapor phase epitaxy. The modes have been seen in both infrared and Raman spectroscopy. The new mode seen at 3194 cm(exp -1) is assigned to an N-H stretching vibrational mode and the mode found at 783 cm(exp -1) is tentatively assigned to an N-H wagging, vibrational mode. Polarized Raman spectroscopy was used to determine that the symmetry of the defect complex is C(sub 3v), which implies that the H atom is in either a bonding or anti-bonding position. DOE

N94-37711# Sandia National Labs., Albuquerque, NM.
EFFECTS OF MOLECULAR TRANSPORT ON TURBULENCE-CHEMISTRY INTERACTIONS IN A HYDROGEN-ARGON-AIR JET DIFFUSION FLAME
S. Menon, W. H. Calhoon, Jr., G. Goldin, and A. R. Kerstein 1994 23 p Presented at the 25th International Symposium on Combustion, Irvine, CA, 31 Jul. - 5 Aug. 1994
(Contract DE-AC04-76DR-00789)
(DE94-005107; SAND-94-8510C; CONF-940711-3) Avail: CASI HC A03/MF A01

A numerical simulation of entrainment, turbulent advection, molecular import and chemical kinetics in a turbulent diffusion flame is used to investigate effects of molecular transport on turbulence-chemistry interactions. A full finite-rate chemical mechanism is used to represent the combustion of a hydrogen-argon mixture issuing into air. Results based on incorporation of differential diffusion and variable Lewis number are compared to cases with the former effect, or both-effects, suppressed. Significant impact on radical species production and on NO emission index (based on a reduced mechanism for thermal NO) is found. A reduced mechanism for hydrogen-air combustion, omitting both effects and incorporating other simplifications, performs comparably except that its NO predictions agree well with the case of full chemistry and molecular transport, possibly due to cancellation of errors. DOE

N94-37713# Texas Univ., Austin, TX. Dept. of Chemistry.
MORPHOLOGICAL ASPECTS OF SURFACE REACTIONS
J. M. White 10 Jan. 1994 6 p
(Contract DE-FG03-93ER-14334)
(DE94-011208; DOE/ER-14334/T1) Avail: CASI HC A02/MF A01

This work focuses on substrate morphology and on fragments synthesized by thermal, electron, and photon activation. The following work is complete: (1) Low energy electron diffraction, Auger electron spectroscopy and scanning tunneling microscopy were used to determine the local morphology of rhodium films on titania. (2) A new tool was developed for diagnosing surface reactions that involve C-H bond cleavage -- predosed oxygen TPD (POTPD), a technique based on scavenging surface H(a) by small amounts of preadsorbed 0(a) to form water. (4) For (pi)-bonded benzene on Ag(111), exposure to low energy electrons results in selective decomposition Of C(sub 6)D(sub 6)(a) to surface D atoms and phenyl fragments, which recombine and desorb as biphenyl between 275-390 K. Similarly, vinyl fragments have been prepared from ethylene. These fragments open the way for kinetic and spectroscopic characterization of interesting hydrocarbon reactions on transition metals. (5) Using Fourier transform infra-red spectroscopy, we have studied how coadsorbates, particularly carbon monoxide, inhibit the decomposition of ethylidyne. The experiments were done in an ambient pressure of CO in order to maintain a sizable coverage into the temperature regime where ethylidyne normally decomposes. One aspect of our present work involves morphological studies of Rh on planar TiO2 surfaces using scanning tunneling microscopy and scanning electron microscopy. The objective is to measure, in some cases in real-time, how the surface morphology changes as oxidation and reduction processes are carried out. In another interesting project, we are preparing spectroscopically significant and reasonably pure concentrations of methyl groups on Pt(111) by exposing physisorbed methane to controlled doses of low energy electrons. DOE

N94-37754# Colorado State Univ., Fort Collins, CO.
DIOSMACYCLOALKANES AS MODELS FOR THE FORMATION OF HYDROCARBONS FROM SURFACE METHYLENES
J. R. Norton 25 Apr. 1994 17 p
(Contract DE-FG02-84ER-13299)
(DE94-011211; DOE/ER-13299/10) Avail: CASI HC A03/MF A01

Assignment of the vibrational modes of Os(sub 2)(CO)(sub 8)(CHCH(sub 3)) and Os(CO)(sub 4)(C(sub 2)H(sub 4)) has given fingerprint vibrational spectra for the following species when chemisorbed on metal catalyst surfaces: ethylidene and ethylene bound in a metallacyclopropane mode. The formation and fragmentation of diosmacyclobutanes have been shown to involve slippage of the outgoing olefin onto a single osmium, and associative exchange of the olefin from that site. The incorporation of vinylcyclopropane without rearrangement has confirmed the absence of a diradical intermediate. The anomalous stability of the diosmacyclobutane derived from trans-2-butene has proven due to greater destabilization (by the substituent methyls) of the slipped intermediate than of the ground state. Reaction of an osmacyclobutane with 1,3- or 1,2-dienes (allenes) gives 1,2 rather than 1,4 addition to the diosmium unit. Treatment of Os(CO)(sub 4)(C(sub 2)H(sub 4)) with triflic acid results in the formation of Os(CO)(sub 4)(C(sub 2)H(sub 5))OTf. The authors have found that the reaction of an aryl iodine(III) reagent with propargyl stannanes or silanes results in o-iodo propargyl arenes. DOE

N94-37761 Department of the Navy, Washington, DC.
CHEMILUMINESCENT MICROEMULSIONS Patent
Richard Thompson, inventor (to Navy) 29 Mar. 1994 5 p Filed 6 Oct. 1988 Supersedes AD-D013911
(AD-D016292; US-Patent-5,298,197; US-Patent-Appl-SN-253635; US-Patent-Class-252-700) Avail: US Patent and Trademark Office

The invention is directed to a light producing microemulsion formed in the presence of a surfactant/cosurfactant pair from an oil phase medium having at least an oxalate derivative and a fluorescer compound dissolved in it and an aqueous phase medium containing at least an oxidant dissolved

in it. The light produced in such a microemulsion can be used to analyze aqueous oxidant-containing samples by comparing the amount of light produced by a microemulsion formed from a known quantity of an oxidant to a similar sample containing an unknown quantity of an oxidant. The comparison can be made by any well known photosensitive means and can be computerized. DTIC

26 METALLIC MATERIALS

Includes physical, chemical, and mechanical properties of metals, e.g., corrosion; and metallurgy.

N94-36461# Los Alamos National Lab., NM.
FIRST RESULTS FROM THE LOS ALAMOS PLASMA SOURCE ION IMPLANTATION EXPERIMENT
D. J. Rej, R. J. Faehl, R. J. Gribble, I. Henins, P. Kodali, M. Nastasi, W. A. Reass, J. Tesmer, K. C. Walter, and B. P. Wood et al 1993 7 p Presented at the Fall Meeting of the Materials Research Society, Boston, MA, 29 Nov. - 3 Dec. 1993
(Contract W-7405-eng-36)
(DE94-003931; LA-UR-93-4218; CONF-931108-10) Avail: CASI HC A02/MF A01

A new facility is operational at Los Alamos to examine plasma source ion implantation on a large scale. Large workpieces can be treated in a 1.5-m-diameter, 4.6-m-long plasma vacuum chamber. Primary emphasis is directed towards improving tribological properties of metal surfaces. First experiments have been performed at 40 kV with nitrogen plasmas. Both coupons and manufactured components, with surface areas up to 4 sq m, have been processed. Composition and surface hardness of implanted materials are evaluated. Implant conformality and dose uniformity into practical geometries are estimated with multidimensional particle-in-cell computations of plasma electron and ion dynamics and Monte Carlo simulations of ion transport in solids. DOE

N94-36517# Instituto de Pesquisas Energeticas e Nucleares, Sao Paulo (Brazil).
SINTERING OF DIOXIDE PELLETS IN AN OXIDIZING ATMOSPHERE (CO2) M.S. Thesis
G. R. T. Santos 1992 90 p
(DE94-613046; INIS-BR-3209) Avail: CASI HC A05/MF A01 (US Sales Only)

This work consists of the study of the sintering process of UO2 pellets in an oxidizing atmosphere. Sintering tests were performed in a CO2 atmosphere and the influence of temperature and time on the pellets density and microstructure were verified. The results obtained were compared to those from the conventional sintering process and its efficiency was confirmed. DOE

N94-36525# Rautarukki Oy, Raahe, Oulu (Finland).
MINERALOGY AND METALLURGICAL PROPERTIES OF IRON ORE SINTER BASED ON MAGNETITE FINES Ph.D. Thesis
K. Heinaenen 1993 122 p Prepared in cooperation with Helsinki Univ., Finl and
(DE94-763309; NEI-FI-217) Avail: CASI HC A06/MF A02

This study has shown that sintering is primarily a mineralogical process even though it is traditionally considered as being controlled by chemical analyses. The effect of the mineralogy of the sinter mix on the mineralogy of the finished sinter is, in some extreme cases, quite clear and easily understood. The mineralogy of sinter based on magnetite fines differs completely from that of sinter made of hematite ores, even when they have the same chemical composition. In the author's opinion, this is due to the fact that in the sintering process the material is only partly melted and the first liquid phase to form is then of crucial importance to the mineralogy of the sinter. Magnetite reacts easily with SiO2 forming a fayalite melt, whereas hematite forms a calcium ferrite melt with CaO. Sinter based on magnetite fines contains 40-60 percent magnetite and 10-30 percent hematite, the slag phase consisting mainly of vitreous silicate with very little calcium ferrites. Sinters made of hematite ores contain 30-50 percent hematite, 10-20 percent magnetite and much more calcium ferrites than vitreous slag. The correlation between sinter mineralogy and metallurgical test results has been studied on process sinters made by the Rautaruukki sinter plant at Raahe. In this study, the mineral composition of the sinters has been determined by four different methods, the chemical composition of the minerals has been analyzed in different sinters and the distribution of the main chemical components between different minerals has been calculated. DOE

N94-36534 Maison de la Mecanique, Courbevoie, Ile-de-France (France).
STRATEGIC CHOICES IN SURFACE TREATMENTS [TRAITEMENTS DE SURFACE CHOIX STRATEGIQUES]
7 Jul. 1993 137 p In FRENCH Sponsored by Direction des Recherches, Etudes et Techniques and Centre de Documentation de l'Armement Prepared in cooperation with Centre Technique des Industries Mecaniques, Saint Etienne, France
(PB94-170669) Avail: Issuing Activity (National Technical Information Service (NTIS))

Selected papers from a day-long industry-sponsored symposium on future trends and priorities in surface treatments are reprinted here. Topics include: Multipurpose Coatings Produced by Physical Processes; Industrial Applications of a New Generation of Wear-Resisting and Anti-Corrosion Processes; Improving the Mechanical Properties of Case-Hardened and Carbon-Nitrided Layers Via Pre-Stress Shot Blasting; Multipurpose Surface Treatment Concepts Applied to Tools; Multipurpose Polymer Coating Systems (Anti-Corrosion and Self-Lubricating); Beam Modulation and Full Quenching; From 2D-3D Numerical Models to Induction Industrial Applications for Surface Treatments; and ANVAR (National Agency for the Application of Research) Surface Treatment Programs. NTIS

N94-36541# Vietnam National Atomic Energy Commission, Hanoi.
PRODUCTION OF AMORPHOUS METAL LAYERS USING ION IMPLANTATION AND INVESTIGATION OF THE RELATED MODIFICATION OF SOME SURFACE PROPERTIES
Dac Luc Hoang and Hoang Lam Vu 29 Nov. 1993 12 p
(DE94-617509; VAEC-B-021) Avail: CASI HC A03/MF A01 (US Sales Only)

Amorphous layers were produced by implanting B(+) ions into Al at 50 keV. The modification of the electrochemical corrosion resistance and the mechanical strength of implanted specimen was investigated. DOE

N94-36543# Atomic Energy of Canada Ltd., Chalk River (Ontario). Nuclear Labs.
MITIGATION OF HARMFUL EFFECTS OF WELDS IN ZIRCONIUM ALLOY COMPONENTS
C. E. Coleman, G. L. Doubt, R. W. L. Fong, J. H. Root, J. W. Bowden, S. Sagat, and R. T. Webster Oct. 1993 31 p Presented at the 10th International ASTM Symposium on Zirconium in the Nuclear Industry, Baltimore, MD, 21-24 Jun. 1993
(DE94-619033; AECL-10950; CONF-930611; COG-93-376) Avail: CASI HC A03/MF A01 (US Sales Only)

Welding produces local residual tensile stresses and changes in texture in components made from zirconium alloys. In the heat-affected zone in tubes or plates, the basal plane normals are rotated into the plane of the component and perpendicular to the direction of the weld. Thin-walled zircaloy-2 tubes containing an axial weld do not reach their full strength, because they always fail prematurely in the weld when pressurized to failure in a fixed-end burst test. Reinforcing the weld by increasing its thickness by 25 percent moves the failure to the parent metal, improves the biaxial strength of the tube by 20 to 25 percent, and increases the total elongation by 200 to 450 percent. In components made from Zr-2.5Nb, the texture in the heat-affected zone promotes delayed hydride cracking (DHC) driven by tensile residual stress. Although the texture is not much affected by heat-treatments below 630 C and large grain interaction stresses remain as a result of mixed textures, macro-residual tensile stresses can be relieved by heat-treatment to the point where the probability of cracking is very low. DOE

N94-36544# Atomic Energy of Canada Ltd., Chalk River (Ontario). Nuclear Labs.
MODELLING IRRADIATION CREEP OF ZIRCONIUM ALLOYS
N. Christodoulou, A. R. Causey, C. H. Woo, C. Tome, R. J. Klassen, and R. A. Holt Sep. 1993 24 p
(DE94-619055; AECL-10823; COG-93-84) Avail: CASI HC A03/MF A01 (US Sales Only)

The effect of texture and dislocation structure on irradiation creep of Zircaloy-2 (irradiated at about 340 K) and Zr-2.5Nb alloys (irradiated at about 558 K) is studied by means of a self-consistent model. The model relates the creep behavior of polycrystals to that of single crystals by taking into account the crystallographic texture, dislocation density, grain shape and the intergranular stresses generated due to the crystallographic anisotropy. Three independent creep compliances of the polycrystal obtained from creep tests on a reference material are used to derive the single crystal creep compliances. These are used to calculate the polycrystalline compliances for the remaining materials. At low irradiation temperatures the predicted polycrystalline compliances agree well with the measured values. The observed behavior can be described by a climb-assisted glide mechanism, in which the creep strain is accommodated mainly by prismatic slip, with smaller contributions from basal and pyramidal slip systems. At higher irradiation temperatures, the self-consistent approach can also describe well the creep behavior of Zr-2.5Nb samples. DOE

N94-36553# Pacific Northwest Lab., Richland, WA.
CHARACTERIZATION AND PROCESSING OF SINTERED PRODUCTS FROM NANO-CRYSTALLINE POWDERS GENERATED BY THE RTDS METHOD
J. G. Darab, M. F. Buehler, J. C. Linehan, and D. W. Matson Aug. 1993 17 p Presented at the 24th Annual Meeting of the Fine Particle Society, Chicago, IL, 24-28 Aug. 1993
(Contract DE-AC06-76RL-01830)
(DE94-004765; PNL-SA-22235; CONF-9308160-2) Avail: CASI HC A03/MF A01

Large quantities of nano-crystalline zirconium oxide/oxyhydroxide and nickel-chromium oxide/oxyhydroxide particles agglomerated and sieved into +320/-200 mesh powders have been produced using the rapid thermal decomposition of solutes (RTDS) method. Green compacts (approximately 40 percent theoretical density) prepared by cold-pressing the RTDS powders at pressures of 140-280-MPa were heated to form dense (86-91 percent theoretical density) ZrO2 or Ni50Cr50 components. Dimensional changes in the compacts during heating were used to extract information about the sintering kinetics in these systems. At 800C, grain-boundary diffusion coupled with some surface diffusion are the dominant mechanisms contributing toward the observed densification in the ZrO2 system. The mechanism-independent activation energy for densification was determined to be 81-kJ/mol for the ZrO2 system and 56-kj/mol for the NiCr system. DOE

N94-36563# Atomic Energy of Canada Ltd., Chalk River (Ontario). Nuclear Labs.
PRECIPITATION IN Zr-2.5 Nb ENHANCED BY PROTON IRRADIATION
C. D. Cann, C. B. So, R. C. Styles, and C. E. Coleman Aug. 1993 16 p Presented at The Evolution of Microstructure in Metals During Irradiation Conference, Muskoka, Ontario, 29 Sep. - 2 Oct. 1992
(DE94-619056; AECL-10877; CONF-9209447; COG-93-205) Avail: CASI HC A03/MF A01

A 3.6 MeV proton irradiation of annealed Zr-2.5Nb has been performed to determine whether proton irradiation will enhance the precipitation of Nb-rich beta-phase precipitates within the alpha-grains. A transmission electron microscope examination of a foil after irradiation at 770 K for 18 h and at 720 K for 264.5 h to a total damage of 0.94 dpa revealed a fine dispersion of precipitates within the alpha-grains. Electron diffraction analysis of the precipitates found they have lattice plane spacings consistent with the Nb-rich beta-phase. This result is in agreement with the beta-phase precipitation observed following neutron irradiation, and thus it supports the use of proton irradiation to simulate neutron-irradiation effects in Zr-2.5Nb. DOE

N94-36564# Atomic Energy Commission, Damascus (Syria).
IRRADIATION EFFECTS IN Fe-30 PERCENT Ni ALLOY DURING Ar ION IMPLANTATION
Mohamad Soukieh and Ali Al-Mohamad Dec. 1993 41 p
(DE94-619057; AECS-PH-S/FRSR-77) Avail: CASI HC A03/MF A01 (US Sales Only)

The use of metallic thin films for studying the processes which take place during ion irradiation has recently increased. For example, ion implantation is widely used to study the structural defects in transition metallic thin films such as (Fe, Ni, Co), because it can simulate the effects occurring in nuclear reactors during neutron irradiation especially the swelling of reactor materials. The swelling of metals and alloys is strongly related to the material structure and to the irradiation conditions. The general feature of formation of structural defects as a function of irradiation dosage and annealing temperature is well known. However, the detailed mechanisms are still not well understood. For example, the swelling of iron alloy with 30-35 percent nickel is very small in comparison with other Ni concentrations, and there is no clear information on the possibility of phase transitions in Fe-Ni alloys during irradiation. The aim of this work is to study the phase-structural changes in Fe-30 percent Ni implanted by high dose of argon ions. The effect of irradiation with low energy argon ions (40 KeV), and fluences of 10(exp 15) to 10(exp 17) ions/cm squared on the deposited thin films of Fe-30 percent Ni alloy was investigated using RBS and TEM techniques. The thicknesses of these films were about 65 +/- 10 nm deposited on ceramic, KBr, and Be foils substrates. Gas bubble formation and profile distribution of the implanted argon ions were investigated. Formation of an ordered phase Fe(sub 3) Ni during irradiation appears to inhibit gas bubble formations in the film structure. DOE

N94-36809*# Virginia Univ., Charlottesville, VA. Dept. of Materials Science and Engineering.
NASA-UVA LIGHT AEROSPACE ALLOY AND STRUCTURES TECHNOLOGY PROGRAM (LA2ST) Progress Report, 1 Jan. - 30 Jun. 1994
Richard P. Gangloff 25 Jul. 1994 364 p
(Grant NAG1-745)
(NASA-CR-196290; NAS 1.26:196290; UVA/528266/MSE94/116) Avail: CASI HC A16/MF A03

The NASA-UVA Light Aerospace Alloy and Structures Technology (LA2ST) Program was initiated in 1986 and continues with a high level of activity. Projects are being conducted by graduate students and faculty advisors in the Department of Materials Science and Engineering, as well as in the Department of Civil Engineering and Applied Mechanics, at the University of Virginia. This work is funded by the NASA-Langley Research Center under Grant NAG-1-745. Here, we report on progress achieved between January 1 and June 30, 1994. These results were presented at the Fifth Annual NASA LA2ST Grant Review Meeting held at the Langley Research Center in July of 1994. The objective of the LA2ST Program is to conduct interdisciplinary graduate student research on the performance of next generation, lightweight aerospace alloys, composites, and thermal gradient structures in collaboration with NASA-Langley researchers. Specific technical objectives are presented for each research project. We generally aim to produce relevant data and basic understanding of material mechanical response, environmental/corrosion behavior, and microstructure; new monolithic and composite alloys; advanced processing methods; new solid and fluid mechanics analyses; measurement and modeling advances; and a pool of educated graduate students for aerospace technologies. Derived from text

N94-36811*# Illinois Univ., Urbana-Champaign, IL. Dept. of Mechanical and Industrial Engineering.
USE OF ROTATION TO SUPPRESS THERMOSOLUTAL CONVECTION IN DIRECTIONALLY SOLIDIFIED BINARY ALLOYS Final Technical Report
Arne J. Pearlstein 15 Jul. 1994 238 p
(Grant NAG3-1121)
(NASA-CR-196372; NAS 1.26:196372; UILU-ENG-94-4008) Avail: CASI HC A11/MF A03

Effects of rotation on onset of convection during plane-front directional solidification of Pb-Sn and the pseudobinary system mercury cadmium telluride (Hg(1-x)Cd(x)Te), and on dendritic solidification of Pb-Sn have been studied by means of linear stability analysis. Incorporating Coriolis and centrifugal accelerations into the momentum equation of Coriell et al., we find that under realistic processing conditions, a large degree of stabilization can be achieved using modest rotation rates for both Pb-Sn and mercury cadmium telluride. At a growth velocity of 5 micron/sec and nominal liquid-side temperature gradient of 200 K/cm in Pb-Sn, rotation at 500 rpm results in a hundredfold increase in the critical Sn concentration. Large increases in the maximum allowable growth velocity at fixed melt composition are also attainable with modest rotation rates. The effect is amplified under conditions of reduced gravitational acceleration. For

Hg(1-x)Cd(x)Te, we have also studied the nonrotating case. The key differences are due to the existence of a composition range for Hg(1-x)Cd(x)Te in which the melt density has a local maximum as a function of temperature. When the melt solidifies by cooling from below, the liquid density may initially increase with distance above the interface, before ultimately decreasing as the melt temperature increases above the value at which the local density maximum occurs. In contrast to the Pb-Sn case where density depends monotonically on temperature and composition, for Hg(1-x)Cd(x)Te there exists a critical value of the growth velocity above which plane-front solidification is unstable for all bulk CdTe mole fractions. Again, rotation leads to significant inhibition of onset. We identify the predicted stabilization with the Taylor-Proudman mechanism by which rotation inhibits thermal convection in a single-component fluid heated from below. In a binary liquid undergoing solidification, rotation inhibits the onset of buoyancy-driven convection, and has no effect on the short-wavelength morphological instability. At large growth velocities, the plane-front interface between liquid and solid becomes unstable with respect to a morphological instability and solidification occurs dendritically, with a mushy zone of dendrites and interdendritic fluid separating the solid from the melt. For the Pb-Sn system, rotation substantially suppresses the onset of convection in the mushy zone and in the overlying liquid, holding open the promise that rotation can suppress freckling and other macrosegregation defects.
Author (revised)

N94-36954*# Tennessee Univ., Knoxville, TN.
PROCESSING AND MECHANICAL PROPERTIES OF NiAl-BASED IN-SITU COMPOSITES Ph.D. Thesis Final Report
David Ray Johnson May 1994 204 p
(Grant NAG3-876; RTOP 505-63-52)
(NASA-CR-195333; E-8864; NAS 1.26:195333) Avail: CASI HC A10/MF A03

In-situ composites based on the NiAl-Cr eutectic system were successfully produced by containerless processing and evaluated. The NiAl-Cr alloys had a fibrous microstructure while the NiAl-(Cr,Mo) alloys containing 1 at. percent or more molybdenum exhibited a lamellar structure. The NiAl-28Cr-6Mo eutectic displays promising high temperature strength while still maintaining a reasonable room temperature fracture toughness when compared to other NiAl-based materials. The Laves phase NiAlTa was used to strengthen NiAl and very promising creep strengths were found for the directionally solidified NiAl-NiAlTa eutectic. The eutectic composition was found to be near NiAl-15.5Ta (at. percent) and well aligned microstructures were produced at this composition. An off-eutectic composition of NiAl-14.5Ta was also processed, consisting of NiAl dendrites surrounded by aligned eutectic regions. The room temperature toughness of these two phase alloys was similar to that of polycrystalline NiAl even with the presence of the brittle Laves phase NiAlTa. Polyphase in-situ composites were generated by directional solidification of ternary eutectics. The systems investigated were the Ni-Al-Ta-X (X=Cr, Mo, or V) alloys. Ternary eutectics were found in each of these systems and both the eutectic composition and temperature were determined. Of these ternary eutectics, the one in the NiAl-Ta-Cr system was found to be the most promising. The fracture toughness of the NiAl-(Cr,Al)NiTa-Cr eutectic was intermediate between those of the NiAl-NiAlTa eutectic and the NiAl-Cr eutectic. The creep strength of this ternary eutectic was similar to or greater than that of the NiAl-Cr eutectic. Author

N94-36993*# National Aeronautics and Space Administration. Langley Research Center, Hampton, VA.
LET SPECTRA OF FRAGMENTED 600-MeV/A IRON BEAM ON ALUMINUM AND POLYETHYLENE: A PRELIMINARY ANALYSIS
Judy L. Shinn, John W. Wilson, E. V. Benton, I. Csige, A. L. Frank, and E. R. Benton May 1994 17 p
(RTOP 199-45-16-11)
(NASA-TP-3436; L-17342; NAS 1.60:3436) Avail: CASI HC A03/MF A01

An iron beam experiment recently conducted at the Lawrence Berkeley Laboratory Bevalac by Benton et al. provides an opportunity for verifying the new Green's function computer code (GRNTRN) and assessing the related nuclear database. The iron beam with 600 MeV/A at extraction traversed a series of beam transport elements, lead foil, and several triggering devices before impacting the target. Of these, only the 2.24 g/sq cm lead foil and target are considered in the transport analysis with an assumed (inferred from calibration) beam energy of 557 MeV/A. A thin layer of CR-39 plastic nuclear track detector (PNTD) was placed in front of the target to monitor the incident flux and a stack of four PNTD's placed behind to measure the linear energy transfer (LET) distribution of the transported beam. Test data are analyzed for three separate targets: 2 g/sq cm aluminum, 5-cm polyethylene, and 8-cm polyethylene. The two-layer GRNTRN results were mapped into the detector response function for comparison with the measured LET spectra. Reasonable agreement is obtained. Future research and analysis can be improved by using a more accurate isotope set or including other important media which significantly alter the beam. The assumption that the fragmentation cross sections are too small for aluminum is inconclusive because the production of fragments by 2 g/sq cm aluminum can be more significantly affected by the fragment contribution originating from the media in front of the target than that currently considered in the analysis. Author

N94-37030# Clemson Univ., SC. Dept. of Mechanical Engineering.
PROCESS SIMULATION AND MODELING FOR ADVANCED INTERMETALLIC ALLOYS Final Report, 1 Sep. 1989 - 31 Aug. 1993
H. J. Rack 1 Jun. 1994 233 p
(Contract N00014-89-J-3166)
(AD-A280327) Avail: CASI HC A11/MF A03

This final report summarizes the technical effort for contract 'Process Simulation and Modeling for Advanced Intermetallic Alloys' undertaken under N0001489-J-3166 (R&T Project Number: DU 89005) at Clemson University with H. J. Rack, Professor of Mechanical Engineering and Metallurgy acting as Principal Investigator. The report contains two major parts, phase stability (Part 1) and high temperature deformation processing (Part 2). Part 1 contains nine (9) papers describing the high temperature phase stability of Ti-Al-Nb and Ti-Al-V intermetallic alloys, primary attention being focused on the temperature regimes normally associated with deformation processing. Part 2 contains three (3) papers which demonstrate the utility of combining phase equilibria studies with dynamic material modeling to simulate and model the high temperature deformation processing response of alpha + beta and alpha(sub 2) + beta titanium alloys. DTIC

N94-37074# Bulgarian Academy of Sciences, Sofia. Inst. za Yadrena Izsledvaniya i Yadrena Energetika.
DATA COMPATIBILITY FOR VARIOUS CHARPY-TESTS [PODKHOD ZA OPREDELYSNE SYVMESTIMOST NA DANNI OT RAZLICHNI SHARPI IZPITANIYA]
T. Petrova 1993 6 p In BULGARIAN Presented at the 2nd Conference on Metrology Assurance of Nuclear Energy: From Theory to Practical Applications, Varna, Bulgaria, 30 May - 1 Jun. 1993
(DE94-617534; INIS-MF-13795; CONF-9305325) Avail: CASI HC A02/MF A01 (US Sales Only)

An approach is proposed for determination of mechanical properties alteration of the irradiated metals. It consists in comparing the metal condition before and after the irradiation. The base material is tested in so called 'cold' cells, while the irradiated samples - in 'hot' ones. As long as the tests could be carried out in different laboratories, having at their disposal different Charpy test machines (with different parameters), from metrological point of view it is necessary to perform benchmark investigations in order to verify the compatibility of data obtained. They should include: comparison of the results, obtained in different 'cold' cells or in different 'hot' cells; comparison of the results, obtained in 'cold' and 'hot' cells; comparison of the results, obtained with or without electron filtration after the amplifier; comparison of the on-line and off-line results. Such benchmark investigations would enable the utilization of the results accumulated in data bank from all available experiments for a further complete assessment and for analysis of the metal state of the reactor pressure vessel. DOE

N94-37080# Westinghouse Electric Corp., West Mifflin, PA.
IRRADIATION ASSISTED STRESS CORROSION CRACKING OF HTH ALLOY X-750 AND ALLOY 625
W. J. Mills, M. R. Lebo, R. Bajaj, J. J. Kearns, R. C. Hoffman, and J. J. Korinko 1994 32 p Presented at the 1994 Meeting of the International Collaborative Group on Irradiation-Assisted Stress Corrosion Cracking, Stevenson, WA, 30 Mar. - 1 Apr. 1994 Prepared in cooperation with Bettis Atomic Power Lab., Pittsburgh, PA
(Contracts DE-AC11-93PN-38195; DE-AC11-89PN-38014)

(DE94-012667; WAPD-T-3034; CONF-9403119-1) Avail: CASI HC A03/MF A01

In-reactor testing of bolt-loaded precracked compact tension specimens was performed in 360 C water to determine effect of irradiation on the SCC behavior of HTH Alloy X-750 and direct aged Alloy 625. Out-of-flux and autoclave control specimens provided baseline data. Primary test variables were stress intensity factor, fluence, chemistry, processing history, and prestrain. Results for the first series of experiments were presented at a previous conference. Data from two more recent experiments are compared with previous results; they confirm that high irradiation levels significantly reduce SCC resistance in HTH Alloy X-750. Heat-to-heat differences in IASCC were related to differences in boron content, with low boron heats showing improved SCC resistance. The in-reactor SCC performance of Alloy 625 was superior to that for Alloy X-750, as no cracking was observed in any Alloy 625 specimens even though they were tested at very high K(sub 1) and fluence levels. A preliminary SCC usage model developed for Alloy X-750 indicates that in-reactor creep processes, which relax stresses but also increase crack tip strain rates, and radiolysis effects accelerate SCC. Hence, in-reactor SCC damage under high flux conditions may be more severe than that associated with postirradiation tests. In addition, preliminary mechanism studies were performed to determine the cause of IASCC In Alloy X-750. DOE

N94-37116# Lehigh Univ., Bethlehem, PA.
ROBOTIC WELD OVERLAY COATINGS FOR EROSION CONTROL
B. F. Levin, J. N. Dupont, and A. R. Marder 21 Apr. 1994 23 p
(Contract DE-FG22-92PC-92542)
(DE94-013477; DOE/PC-92542/T6) Avail: CASI HC A03/MF A01

The erosion of materials by the impact of solid particles has received increasing attention during the past twenty years. Recently, research has been initiated with the event of advanced coal conversion processes in which erosion plays an important role. The resulting damage, termed solid particle erosion (SPE), is of concern primarily because of the significantly increased operating costs which result in material failures. Reduced power plant efficiency due to solid particle erosion of boiler tubes and waterwalls has led to various methods to combat SPE. One method is to apply coatings to the components subjected to erosive environments. Protective weld overlay coatings are particularly advantageous in terms of coating quality. The weld overlay coatings are essentially immune to spallation due to a strong metallurgical bond with the substrate material. By using powder mixtures, multiple alloys can be mixed in order to achieve the best performance in an erosive environment. However, a review of the literature revealed a lack of information on weld overlay coating performance in erosive environments which makes the selection of weld overlay alloys a difficult task. The objective of this project is to determine the effects of weld overlay coating composition and microstructure on erosion resistance. These results will lead to a better understanding of erosion mitigation in circulated fluidized beds. DOE

N94-37122 Army Research Lab., Watertown, MA. Materials Directorate.
THERMOMECHANICAL STUDIES OF TUNGSTEN HEAVY ALLOYS Final Report
Kenneth F. Ryan and Robert J. Dowding May 1994 22 p Limited Reproducibility: More than 20% of this document may be affected by microfiche quality
(AD-A280250; ARL-TR-447) Avail: CASI HC A03

This report describes the ongoing thermomechanical studies of tungsten heavy alloys at the Materials Directorate of the Army Research Laboratory. Building upon previous work, the data obtained has been correlated to microstructural features before and after testing and evaluated using well known constitutive relations. In past efforts a 91% tungsten heavy alloy was examined. This work examines the effect of strain rate and temperature on a 91% and a 97% heavy alloy and a commercially pure (100%) tungsten. The apparent occurrence of dynamic recrystallization is also discussed. DTIC

N94-37138 Army Armament Research, Development and Engineering Center, Watervliet, NY.
CHROMIUM/MOLYBDENUM ALLOY PLATING. PART 1: THE ELECTRODEPOSITION OF LOW CONTRACTION CHROMIUM/MOLYBDENUM ALLOYS USING UNIPOLAR (ON/OFF) PULSE PLATING Final Report
Mark D. Miller and Stephen Langston Mar. 1994 19 p Limited Reproducibility: More than 20% of this document may be affected by microfiche quality
(AD-A280236; ARCCB-TR-94011) Avail: Issuing Activity (Defense Technical Information Center (DTIC))

The microstructure and mechanical properties of a pulse-plated low contraction (LC) chromium/molybdenum (Cr/Mo) alloy deposit were evaluated and compared to both pulse-plated LC chromium and direct (dc)-plated LC chromium. Molybdenum concentrations as high as approximately 2.4 percent were obtained at a pulsing frequency of 5 Hz (100 ms on-time/100 ms off-time). This represents nearly a 300 percent increase over the percent molybdenum obtained in a dc-plated LC Cr/Mo alloy deposit. However, pulse-plated LC Cr/Mo deposits were generally poor in quality with deposits that were frequently cracked and nodular in appearance. Hardness values as high as 900 KHN (50 gm load) were obtained for the pulse-plated LC Cr/Mo alloy deposit. This hardness represents an 18 percent increase over the maximum reported hardness obtained in a dc-plated LC chromium deposit. The maximum cathode current efficiency (CCE) obtained while pulse plating an LC Cr/Mo alloy was 7.3 percent. This is nearly 52 percent less than the reported CCE obtained when dc plating LC chromium. DTIC

N94-37153# Brookhaven National Lab., Upton, NY. Energy Efficiency and Conservation Div.
INTERFACES OF HIGH-PROTECTION PERFORMANCE POLYARYLS-COATED ZINC PHOSPHATED STEELS
Toshifumi Sugama 1994 11 p Presented at the Tri-Service Conference on Corrosion, Orlando, FL, 21-24 Jun. 1994
(Contract DE-AC02-76CH-00016)
(DE94-011732; BNL-60347; CONF-9406167-1) Avail: CASI HC A03/MF A01

To evaluate the ability of polyaryl thermoplastic coatings such as poly phenylene sulfide (PPS) and poly phenyl ether ether ketone (PEEK) to protect zinc phosphate (ZnPh)-treated steels from corrosion in a wet, harsh environment (1.0 wt % H2SO4, 3.0 wt % NaCl, and 96.0 wt % water at temperature from 250 to 200 C), we exposed them in autoclave to determine performance in heating-cooling cyclic fatigue tests (1 cycle = 12 hr at 200 C + 12 hr at 25 C) for up to 90 cycles. Although no changes in appearance were seen in the PEEK specimens after 60 cycles, extension to 90 cycles caused delamination of the coating film from the ZnPh; the major reason was the degradation of the PEEK polymer caused by its hydrothermal-catalyzed esterification. In urea hydrogen peroxide (UHP)-modified PPS-coating systems, chemical reactions at the interfaces between the PPS and Zn in the ZnPh layer led to the formation of a ZnS reaction product, which enhanced the ZnPh-to-PPS adhesive bond; correspondingly, there were no signs of peeling nor separation of the coating after 90 cycles. In addition, because these intermediate reaction products are insoluble at high pH, they minimized the rate of delamination of the PPS coating caused by the cathodic reaction, H2O + 1/2O2 + 2e(-) yields 2OH(-), at the corrosion side of a defect in the film. In contrast, PEEK coatings containing nonreactive ZnPh underwent cathodic delamination because of the susceptibility of ZnPh to alkali dissolution. DOE

N94-37304# Oak Ridge National Lab., TN. Metals and Ceramics Div.
ELEMENTAL MAPPING OF SEGREGATION IN STAINLESS STEELS WITH AN IMAGING FILTER
J. Bentley and E. A. Kenik 1994 3 p Presented at the 13th International Congress on Electron Microscopy, Paris, France, 17-22 Jul. 1994
(Contract DE-AC05-84OR-21400)
(DE94-012659; CONF-940766-4) Avail: CASI HC A01/MF A01

Two types of solute segregation was studied in 300-series stainless steels. Elemental mapping was performed at 200 kV with Gatan Imaging Filters (GIFs) attached to electron microscopes. Results show that a GIF can be used to study solute segregation in stainless steels, that image acquisition and processing are straightforward and rapid, but that large probe currents and low specimen drift rates are essential. DOE

N94-37367# Sandia National Labs., Albuquerque, NM.
THE INFLUENCE OF VAR PROCESSES AND PARAMETERS ON WHITE SPOT FORMATION IN ALLOY 718
B. K. Damkroger, J. B. Kelley, M. E. Schlienger, J. A. VanDen Avyle, R. L.

Williamson, and F. J. Zanner 1994 12 p Presented at the International Symposium on Superalloys 718, 625, 706 and Derivatives, Pittsburgh, PA, 27-29 Jun. 1994
(Contract DE-AC04-94AL-85000)
(DE94-012071; SAND-94-1267C; CONF-940663-1) Avail: CASI HC A03/MF A01

Significant progress has occurred lately regarding the classification, characterization, and formation of white spots during vacuum arc remelting (VAR). White spots have been generally split into three categories: discrete white spots, which are believed to be associated with undissolved material which has fallen in from the shelf, crown, or torus regions; dendritic white spots, usually associated with dendrite clusters having fallen from the electrode; and solidification white spots, believed to be caused by local perturbations in the solidifications conditions. Characteristics and proposed formation mechanisms of white spots are reviewed and discussed in context of physical processes occurring during VAR, such as fluid flow and arc behavior. Where possible, their formation mechanisms will be considered with respect to specific operating parameters. In order to more fully understand the formation of solidification white spots, an experimental program has been begun to characterize the solidification stability of Alloy 718 and variants with respect to changes in growth rate and thermal environment. A description of the experimental program and preliminary results are included. DOE

N94-37385# Japan Atomic Energy Research Inst., Tokyo (Japan).
EXAMINATION OF WELDABILITY OF Ni-Cr-W SUPERALLOYS
Hirokazu Tsuji, Hajime Nakajima, Teiichiro Saito, and Tamao Takatsu Jul. 1993 93 p
(DE94-719014; JAERI-M-93-150) Avail: CASI HC A05/MF A01

Research and development have been carried out on the new Ni-Cr-W superalloy as a structural material for process heating high-temperature gas-cooled reactors with coolant outlet temperatures of around 1000 C, and the optimum chemical composition has already been proposed. For the application of the newly developed Ni-Cr-W superalloy to the structural components, the soundness and the reliability of the structures with weldments must be secured. Hence, weldability of Ni-Cr-W superalloys was examined. The results of the present study can be summarized as follows: (1) Susceptibility to cracking in the weldments of Ni-Cr-W superalloys is extremely high. (2) Susceptibility to cracking in the weldments of the alloy containing titanium is lower than that of the alloy free from titanium. (3) Heat treatment conditions affect susceptibility to cracking in the weldments of Ni-Cr-W superalloys significantly. Based on the results obtained, it has been concluded that the alloy with the same chemical composition as that of the base metal cannot be applied as the filler metal for welding of the newly developed Ni-Cr-W superalloy. Basic data on the weldability of Ni-Cr-W superalloys will be accumulated furthermore, and then research and development will be performed with a view to developing a filler metal for welding of the alloy applying the technique of minor alloying element adjustment. DOE

N94-37396# Oak Ridge National Lab., TN.
ATOMIC LEVEL CHARACTERIZATION OF DEFECTS IN MICROALLOYED NiAl: AN ATOM PROBE INVESTIGATION
R. Jayaram and M. K. Miller 1994 3 p Presented at the Microscopy Society of America and Microbeam Analysis Society Joint Meeting, New Orleans, LA, 31 Jul. - 5 Aug. 1994
(Contracts DE-AC05-84OR-21400; DE-AC05-76OR-00033)
(DE94-012732; CONF-940753-8) Avail: CASI HC A01/MF A01

Since mechanical behavior is largely controlled by the microstructure (particularly dislocations, substitutional solutes, and solute segregation to grain boundaries) atom probe field ion microscopy is well suited to studying such microstructural features. The atom probe has been used to explain changes in yield stress when NiAl is doped with B, C, Be, or Zr/Mo. It showed that the beneficial effect of B segregation is masked by formation of ultrafine, deleterious second-phase particles. Be occupied Al sites almost exclusively. Zr segregated to both grain boundaries and dislocations. DOE

N94-37398# Oak Ridge National Lab., TN.
AEM AND AES OF RADIATION-INDUCED SEGREGATION IN PROTON-IRRADIATED STAINLESS STEELS
E. A. Kenik, R. D. Carter, D. L. Damcott, M. Atzmon, and G. S. Was 1994 3 p Presented at the Microscopy Society of America and Microbeam Analysis Society Joint Meeting, New Orleans, LA, 31 Jul. - 5 Aug. 1994
(Contract DE-AC05-84OR-21400)
(DE94-012734; CONF-940753-9) Avail: CASI HC A01/MF A01

In order to avoid complications from long-term induced radioactivity of neutron-irradiated specimens, 4 type 304L alloys were irradiated to 1 dpa with 3.4 MeV protons at 400 C. Analytical electron microscopy and Auger electron spectrometry were used to measure composition at and near grain boundaries in controlled purity alloys. As a result of the narrow RIS profiles (less than 20 nm width) at grain boundaries induced in these materials by low temperature irradiation and the finite size of the excited volume for x-ray microanalysis, the measured profiles are convolutions of these two factors. DOE

N94-37399# Oak Ridge National Lab., TN.
THE EFFECT OF REACTIVE ELEMENTS ON THE SEGREGATION BEHAVIOR AND MICROSTRUCTURE OF ALPHA-Al2O3 SCALES ON BETA-NiAl
K. B. Alexander and B. A. Pint 1994 3 p Presented at the Microscopy Society of America and Microbeam Analysis Society Joint Meeting, New Orleans, LA, 31 Jul. - 5 Aug. 1994
(Contract DE-AC05-84OR-21400)
(DE94-012739; CONF-940753-10) Avail: CASI HC A01/MF A01

In order to improve oxidation resistance, small amounts of oxygen-active or 'reactive' elements (RE) such as Y, Zr, Hf, and Ce are added to chromia- and alumina-forming high-temperature alloys. As an alternative to a system where the RE-ion supply is self-limiting (Y-implant), it was desired to study effect of RE source-removal on microstructure and grain boundary segregation levels. Beta-NiAl doped with 0.23 wt% Zr was oxidized in oxygen at 1500 C for 50 h. Upon cooling, the scale spalled into pieces; these spalled alpha-Al2O3 scales were then annealed in air at 1500 C for 1 and 50 h. Specimens were fabricated parallel to metal/scale interface, and grain boundary chemistries were determined using x-ray energy dispersive spectrometry. Results show that no qualitative change in microstructural scale or zirconia particle size/density occurs after annealing, which is consistent with the model in which the gas-interface microstructure development depends on a continuous supply of zirconia diffusing from the metal interface towards the gas interface. DOE

N94-37410# Ames Lab., IA.
CHARACTERIZATION OF MECHANICAL PROPERTIES DEGRADATION USING SMALL PUNCH TESTING TECHNIQUE
J. Kameda 1994 16 p Presented at the 4th Conference on Fossil Plant Inspection, Palo Alto, CA, 18-20 Jan. 1994
(Contract W-7405-eng-82)
(DE94-011202; IS-M-787; CONF-940185-1) Avail: CASI HC A03/MF A01

A small punch (SP) testing technique developed at Ames Laboratory and its application to mechanical properties degradation evaluation are summarized. It has been clearly demonstrated on ferritic alloys that the SP test is capable of examining the intergranular embrittling potency of segregated P, Sn and Sb causing temper embrittlement, and the effects of neutron irradiation and post-irradiation annealing, giving rise to changes in the hardness and intergranular solute segregation, on the fracture properties in terms of the ductile-brittle transition temperature (DBTT). A linear relationship between the DBTT's obtained by the SP and Charpy V-notched tests has been theoretically and experimentally established. In model Al alloy substrates coated with Ni-P amorphous (10 (mu)m thick) and overlaying ceramics (0-1.0 (mu)m thick), the global and local fracture properties were well characterized by the SP test together with acoustic emission techniques. DOE

N94-37416# Japan Atomic Energy Research Inst., Tokyo (Japan).
CREEP-FATIGUE INTERACTION PROPERTY OF A NICKEL-BASE HEAT-RESISTANT ALLOY HASTELLOY XR IN SIMULATED HTGR HELIUM GAS ENVIRONMENT
Hirokazu Tsuji (Japan Atomic Energy Research Inst., Tokyo, Japan.) and Hajime Nakajima (Japan Atomic Energy Research Inst., Tokyo, Japan.) Oct. 1993 25 p
(DE94-737934; JAERI-M-93-187) Avail: CASI HC A03/MF A01 (US Sales Only)

The properties of Hastelloy XR, which is an alloy developed as the

structural material for high-temperature components of the HTTR, under creep-fatigue interaction conditions were examined by performing a series of axial strain controlled fully reversed fatigue tests in the simulated HTGR helium gas environment at 700, 800, 900 and 950 C. Two types of evaluation techniques, i.e., the life fraction rule and the ductility exhaustion one, were applied for the evaluation of the creep damage during the tensile strain holding. The fatigue life reduction due to the strain holding is observed even at hold times of 6 seconds, and the saturation point of the fatigue life reduction shifts to the shorter hold time side with increasing temperature. The life fraction rule predicts an excessively conservative value for the creep damage. The ductility exhaustion rule can predict the fatigue life under the effective creep condition much more successfully than the life fraction one. DOE

N94-37420# Oak Ridge National Lab., TN.
MECHANICAL BEHAVIOR AND PHASE STABILITY OF NIAL-BASED SHAPE MEMORY ALLOYS
E. P. George, C. T. Liu, J. A. Horton, H. Kunsmann, T. King, and M. Kao 1993 5 p Presented at the International Union of Materials Research Societies on Advanced Materials, Tokyo, Japan, 31 Aug. - 4 Sep. 1993
(Contract DE-AC05-84OR-21400)
(DE94-012336; CONF-9308122-18) Avail: CASI HC A01/MF A01

NiAl-based shape memory alloys (SMA's) can be made ductile by alloying with 100-300 wppm B and 14-20 at.% Fe. The addition of Fe has the undesirable effect that it lowers the temperature (A(sub p)) of the martensite yields austenite phase transformation. Fortunately, however, A can be raised by lowering the 'equivalent' amount of Al in the alloy. In this way a high A(sub p) temperature of approximately 190 C has been obtained without sacrificing ductility. Furthermore, a recoverable strain of 0.7% has been obtained in a Ni-Al-Fe alloy with A(sub p) temperature of approximately 140 C. Iron additions do not suppress the aging-induced embrittlement that occurs in NiAl alloys at 300-500 C as a result of Ni5Al3 precipitation. Manganese additions (up to 10 at.%) have the effect of lowering A(sub p), degrading hot workability, and decreasing room-temperature ductility. DOE

N94-37438# Georgia Univ., Athens. Dept. of Chemistry.
PHOTODISSOCIATION AND SPECTROSCOPY OF GAS PHASE BIMETALLIC CLUSTERS Final Report, 15 Sep. 1990 - 14 Sep. 1993
Michael A. Duncan 1993 10 p
(Contract DE-FG09-90ER-14156)
(DE94-012607; DOE/ER-14156/9) Avail: CASI HC A02/MF A01

Focus is the study of gas phase metal clusters to evaluate their potential to model fundamental interactions on metal surfaces. Chemical bonding between component atoms in metal clusters and 'physisorption' on cluster surfaces are studied. Electronic spectra, vibrational frequencies, and bond dissociation energies are measured for both neutral and ionized clusters using laser/mass spectrometry. Interest is on bimetallic cluster systems and how they compare to pure metal clusters. The following were studied: Bi/Cr, Bi/Fe, Pb/Sb, Ag2-rare gas, Ag-Al, Ag-K, Ag-Na, Ag-Li, and Ag3. DOE

N94-37442# Argonne National Lab., IL. Energy Technology Div.
DEVELOPMENT OF INTERMETALLIC COATINGS FOR FUSION POWER APPLICATIONS
J.-H. Park, T. Domenico, G. Dragel, and R. Clark Mar. 1994 23 p Presented at the 3rd International Symposium on Fusion Nuclear Technology, Los Angeles, CA, 27 Jun. - 1 Jul. 1994
(Contract W-31-109-eng-38)
(DE94-012647; ANL/ET/CP-81527; CONF-940664-1) Avail: CASI HC A03/MF A01

In the design of liquid-metal cooling systems, corrosion resistance of structural materials and magnetohydrodynamic (MHD) force and its subsequent influence on thermal hydraulics and corrosion are major concerns. The objective of this study is to develop stable corrosion-resistant electrical insulator coatings at the liquid-metal / structural-material interface, with emphasis on electrically insulating coatings that prevent adverse MHD-generated currents from passing through the structural walls. Vanadium and V-base alloys are potential materials for structural applications in a fusion reactor. Insulator coatings inside the tubing are required when the system is cooled by liquid metals. Various intermetallic films were produced on V, V-5Ti, V-20Ti, V-5Cr-5Ti, V-15Cr-5Ti, Ti, and Types 304 and 316 stainless steel. The intermetallic layers were developed by exposure of the materials to liquid lithium of 3-5 at.% and containing dissolved metallic solutes at temperatures of 416 to 860 C. Subsequently, electrical insulator coatings were produced by reaction of the reactive layers with dissolved nitrogen in liquid lithium or by air oxidation under controlled conditions at 600 to 1000 C. These reactions converted the intermetallic layers to electrically insulating oxide/nitride or oxynitride layers. This coating method could be applied to a commercial product. The liquid metal can be used over and over because only the solutes are consumed within the liquid metal. The technique can be applied to various shapes because the coating is formed by liquid-phase reaction. This paper will discuss initial results on the nature of the coatings and their in-situ electrical resistivity characteristics in liquid lithium at high temperatures. DOE

N94-37459*# National Aeronautics and Space Administration. Lewis Research Center, Cleveland, OH.
MODELLING OF SURFACES. PART 1: MONATOMIC METALLIC SURFACES USING EQUIVALENT CRYSTAL THEORY
Guillermo Bozzolo (Analex Corp., Brook Park, OH.), John Ferrante, and Agustin M. Rodriguez Jul. 1994 37 p
(Contract NAS3-26776; RTOP 505-90-53)
(NASA-TM-106680; E-9020-Pt-1; NAS 1.15:106680) Avail: CASI HC A03/MF A01

We present a detailed description of equivalent crystal theory focusing on its application to the study of surface structure. While the emphasis is in the structure of the algorithm and its computational aspects, we also present a comprehensive discussion on the calculation of surface energies of metallic systems with equivalent crystal theory and other approaches. Our results are compared to experiment and other semiempirical as well as first-principles calculations for a variety of fcc and bcc metals. Author

N94-37465# Japan Atomic Energy Research Inst., Tokyo (Japan).
CREEP PROPERTIES WITH SHORT PERIOD EXCESSIVE LOADINGS ON A NICKEL-BASE HEAT-RESISTANT ALLOY HASTELLOY XR
Hirokazu Tsuji (Japan Atomic Energy Research Inst., Tokai, Japan.), Hajime Nakajima (Japan Atomic Energy Research Inst., Tokai, Japan.), Tatsuhiko Tanabe, and Yuji Nakasone Jul. 1993 74 p In JAPANESE
(DE94-718965; JAERI-M-93-144) Avail: CASI HC A04/MF A01

A series of constant load and temperature creep tests and constant temperature creep tests with short period excessive loadings was carried out on a nickel-base heat-resistant alloy Hastelloy XR, which was developed for applications in the High-Temperature Engineering Test Reactor (HTTR), at temperatures ranging from 900 to 1000 C in order to examine the creep behaviors of the alloy under such conditions. The excessive loading levels were the design stress intensity values Sm for Hastelloy XR indicated in the HTTR high-temperature structural design code. Five to six time excessive loadings did not cause significant changes of the minimum creep rate or the time to onset of tertiary creep. About ten time excessive loadings did not cause significant changes of the time to rupture or the rupture elongation. The above-mentioned results suggest that the design stress intensity values Sm for Hastelloy XR have been determined reasonably. DOE

N94-37503*# National Aeronautics and Space Administration. Lewis Research Center, Cleveland, OH.
PHYSICAL AND MECHANICAL METALLURGY OF NIAl
Ronald D. Noebe, Randy R. Bowman, and Michael V. Nathal Washington Apr. 1994 44 p Submitted for publication
(RTOP 510-01-50)
(NASA-TP-3398; E-7713; NAS 1.60:3398) Avail: CASI HC A03/MF A01

Considerable research has been performed on NiAl over the last decade, with an exponential increase in effort occurring over the last few years. This is due to interest in this material for electronic, catalytic, coating and especially high-temperature structural applications. This report uses this wealth of new information to develop a complete description of the properties and processing of NiAl and NiAl-based materials. Emphasis is placed on the controlling fracture and deformation mechanisms of single and polycrystalline NiAl and its alloys over the entire range of temperatures for which data are available. Creep, fatigue, and environmental resistance of this material are discussed. In addition, issues surrounding alloy design, development of NiAl-based composites, and materials processing are addressed. Author

N94-37516 Argonne National Lab., IL.
SCANNING X-RAY DIFFRACTION: A TECHNIQUE WITH HIGH COMPOSITIONAL RESOLUTION FOR STUDYING PHASE FORMATION IN CO-DEPOSITED THIN FILMS
T. I. Selinder, D. J. Miller, K. E. Gray, M. A. Beno, and G. S. Knapp Apr. 1994 7 p Presented at the Spring Meeting of the Materials Research Society, San Francisco, CA, 4-8 Apr. 1994 Limited Reproducibility: More than 20% of this document may be affected by microfiche quality
(Contract W-31-109-eng-38)
(DE94-011496; ANL/MSD/CP-82716; CONF-940411-15) Avail: CASI HC A02

Investigation of the formation of new metastable phases in alloy thin films requires ways of quickly determining the crystalline structure of samples with different compositions. We report a novel technique for acquiring structural information from films intentionally grown with a composition gradient. For example, binary metal alloy films were deposited using a phase-spread sputtering method. In this way essentially the entire composition range could be grown in a single deposition. By using a narrow incident x-ray beam and a translating sample stage combined with a position sensitive x-ray detector technique, detailed information of the metastable phase diagram can be obtained rapidly. Compositional resolution of the order of +/- 0.2% can be achieved, and is limited by the brightness of the x-ray source. Initial results from studies of phase formation in Zr-Ta alloys are presented. Extensions of the analysis technique to ternary systems are discussed. DOE

N94-37548# Oak Ridge National Lab., TN.
RESIDUAL STRESSES IN A MULTI-PASS WELD IN AN AUSTENITIC STAINLESS STEEL PLATE BEFORE AND AFTER THERMAL STRESS RELIEF
S. Spooner, X. L. Wang, C. R. Hubbard, and S. A. David 1994 6 p Presented at the 4th International Conference on Residual Stress (ICRS-4), Baltimore, MD, Jun. 1994
(Contract DE-AC05-84OR-21400)
(DE94-013278; CONF-940692-4) Avail: CASI HC A02/MF A01

Changes in residual stresses due to thermal stress relief were determined in a welded 1/2 in. thick 304 stainless steel plate from two residual stress maps determined with the neutron diffraction technique. The 304 stainless plate was made from two 6 x 12 x 1/2 in. pieces joined along the length by a gas tungsten arc welding process. Multi-pass welds were made with a semiautomatic welding machine employing cold-wire feed of type 308 stainless steel filler alloy. The thermal stress relief treatment consisted of heating to 1150 F, holding for one hour at temperature and then air cooling. Strain components were measured along the weld direction (longitudinal), perpendicular to the weld line in the plate (transverse), and normal to the plate. Measurements were confined to the plane bisecting the weld at the center of the plate. The strain components were converted to stresses assuming that the measured strains were along the principal axes of the strain tensor. Parameters used in the calculation were E=224 GPa and v=0.25. As-welded longitudinal stresses are compressive in the base metal and become strongly tensile through the heat affected zone and into the fusion zone. The transverse stresses follow the longitudinal trend but with a lower magnitude while the normal stresses are small throughout. The stress relief treatment reduced the magnitudes of all the stresses. In the weld zone the longitudinal stress was lowered by 30% and the spatial range of residual stresses was reduced as well. DOE

N94-37552# Argonne National Lab., Idaho Falls, ID.
CHARACTERIZATION OF NUCLEAR TRANSMUTATIONS IN MATERIALS IRRADIATED TEST FACILITIES
I. C. Gomes and D. L. Smith May 1994 28 p Presented at the 3rd International Symposium on Fusion Nuclear Technology, Los Angeles, CA, 27 Jun. - 1 Jul. 1994
(Contract W-31-109-eng-38)
(DE94-013309; ANL/TD/CP-82061; CONF-940664-9) Avail: CASI HC A03/MF A01

This study presents a comparison of nuclear transmutation rates for candidate fusion first wall/blanket structural materials in available, fission test reactors with those produced in a typical fusion spectrum. The materials analyzed in this study include a vanadium alloy (V-4Cr-4Ti), a reduced activation martensitic steel (Fe-9Cr-2WVTa), a high conductivity copper alloy (Cu-Cr-Zr), and the SiC compound. The fission irradiation facilities considered include the EBR-II fast reactor, and two high flux mixed spectrum reactors, HFIR (High Flux Irradiation Reactor) and SM-3 (Russian reactor). The transmutation and dpa rates that occur in these test reactors are compared with the calculated transmutation and dpa rates characteristic of a D-T fusion first wall spectrum. In general, past work has shown that the displacement damage produced in these fission reactors can be correlated to displacement damage in a fusion spectrum; however, the generation of helium and hydrogen through threshold reactions ((n,x, alpha) and (n,xp)) are much higher in a fusion spectrum. As shown in this study, the compositional changes for several candidate structural materials exposed to a fast fission reactor spectrum are very low, similar to those for a characteristic fusion spectrum. However, the relatively high thermalized spectrum of a mixed spectrum reactor produces transmutation rates quite different from the ones predicted for a fusion reactor, resulting in substantial differences in the final composition of several candidate alloys after relatively short irradiation time. DOE

N94-37578*# National Aeronautics and Space Administration. Marshall Space Flight Center, Huntsville, AL.
THE CORROSION PROTECTION OF SEVERAL ALUMINUM ALLOYS BY CHROMIC ACID AND SULFURIC ACID ANODIZING
M. D. Danford Washington Jun. 1994 26 p
(NASA-TP-3490; M-753; NAS 1.60:3490) Avail: CASI HC A03/MF A01

The corrosion protection afforded 7075-T6, 7075-T3, 6061-T6, and 2024-T3 aluminum alloys by chromic acid and sulfuric acid anodizing was examined using electrochemical techniques. From these studies, it is concluded that sulfuric acid anodizing provides superior corrosion protection compared to chromic acid anodizing. Author

N94-37582*# Boeing Defense and Space Group, Philadelphia, PA.
A COMPARISON OF GRAPHITE/EPOXY TAPE LAMINATES AND 2-D BRAIDED COMPOSITES MECHANICAL PROPERTIES Final Report
Pierre J. Minguet and Christian K. Gunther Jul. 1994 53 p
(Contract NAS1-19247; RTOP 510-02-12-09)
(NASA-CR-4610; NAS 1.26:4610) Avail: CASI HC A04/MF A01

A comparison of the in-plane mechanical properties of unidirectional composite tape laminates and of two dimensional triaxially braided composite was conducted. The tape laminate layups were designed to match the percentage of axial fibers and the angle of the bias tows in the braided composite. The material system used for the laminates is AS4/3501-6 which was chosen as the closest available match to AS4/1895 used for the braids. This report documents the results of the testing of the laminates and compares these results with data previously obtained for the braided composite. The strength and stiffness properties measured here include tension, open-hole tension, filled-hole tension, compression, and open-hole compression, all of these in both the longitudinal and transverse direction, as well as in-plane shear and bearing. Author

N94-37678# Lawrence Livermore National Lab., Livermore, CA.
EXPLORATORY STUDY ON H13 STEEL DIES
A. J. Sunwoo Apr. 1994 11 p
(Contract W-7405-eng-48)
(DE94-012118; UCRL-ID-117158) Avail: CASI HC A03/MF A01

Ultrahigh-strength H13 steel is a recommended die material for aluminum die casting; dies made from H13 steel can be safely water-cooled during hot working operations without cracking. However, after time the dies exhibited surface cracking and excessive wear. Erosive wear also occurs owing to high pressure injection of molten Al. An exploratory study was made of the causes for surface cracking of H13 dies. Results suggest that surface cracking is caused by interrelated factors, internal to the die material as well as externally induced conditions. DOE

N94-37758# Colorado School of Mines, Golden, CO.
MECHANICAL PERFORMANCE OF AUSTEMPERED DUCTILE IRON Final Report, Feb. - Dec. 1993
David K. Matlock and George Krauss Apr. 1994 36 p
(Contract NSF EEC-91-47146)
(AD-A280452; ARL-CR-117) Avail: CASI HC A03/MF A01

Plates of Austempered Ductile Iron (ADI) containing, in mass pct, 3.7 C. 2.7 Si, 0.97 Ni and 0.27 Mn were heat treated to ASTM 897 Grade 1 and 3 tensile properties and subjected to tensile testing at temperatures between -80 and 120 deg C. Room temperature yield and ultimate tensile

strengths met specifications but values of elongation were lower than expected. The retained austenite contents contributed to lowered yield strengths during low temperature testing and increased ultimate tensile strengths and ductilities during high temperature testing. These changes in properties were related to the effects of temperature on the strain-induced transformation of austenite to martensite. The lower than expected ductility of the ADI specimens was related to microporosity, differences in graphite nodule distributions, differences in strain hardening related to austenite stability, and the ductile-to-brittle fracture transition of the matrix ferrite with decreasing temperature. DTIC

N94-37323# British Columbia Univ., Vancouver. Dept. of Metals and Materials Engineering.
ALTERNATE MELTING AND REFINING ROUTES
Alec Mitchell *In* AGARD, Impact of Materials Defects on Engine Structures Integrity Apr. 1993 8 p (For primary document see N94-37321 12-38)
Copyright Avail: CASI HC A02/MF A02

N94-37324# Wright Lab., Wright-Patterson AFB, OH. Materials Dirctorate.
PROCESS ENHANCEMENTS OF SUPERALLOY MATERIAL
Ronald H. Williams, Kristine A. Lark, Sharon Vukelich, Donald R. Parille, and Richard W. Salkeld *In* AGARD, Impact of Materials Defects on Engine Structures Integrity Apr. 1993 6 p (For primary document see N94-37321 12-38)
Copyright Avail: CASI HC A02/MF A02

N94-37325# Imphy S.A., Imphy (France).
THE CONTROL OF CLEANNESS IN POWDER METALLURGY MATERIALS FOR TURBINE DISKS
G. Raisson *In* AGARD, Impact of Materials Defects on Engine Structures Integrity Apr. 1993 14 p (For primary document see N94-37321 12-38)
Copyright Avail: CASI HC A03/MF A02

N94-37326# Forge Societe Nationale d'Etude et de Construction de Moteurs d'Aviation, Gennevilliers (France).
MAINTAINING CONSTANT STANDARDS DURING THE FORGING PROCESS [MAITRISE DE LA REPRODUCTIBILITE DU PROCEDE DE FORGEAGE]
F. Chevet and M. Caralp *In* AGARD, Impact of Materials Defects on Engine Structures Integrity Apr. 1993 23 p In FRENCH (For primary document see N94-37321 12-38)
Copyright Avail: CASI HC A03/MF A02

N94-37328# Defence Research Agency, Farnborough, Hampshire (England).
DEFECTS AND THEIR EFFECTS ON THE INTEGRITY OF NICKEL BASED AEROENGINE DISCS
G. F. Harrison, P. H. Tranter, and L. Grabowski *In* AGARD, Impact of Materials Defects on Engine Structures Integrity Apr. 1993 16 p (For primary document see N94-37321 12-38)
Copyright Avail: CASI HC A03/MF A02

27 NONMETALLIC MATERIALS

Includes physical, chemical, and mechanical properties of plastics, elastomers, lubricants, polymers, textiles, adhesives, and ceramic materials.

For composite materials see *24 Composite Materials*.

N94-36474# Allied-Signal Aerospace Co., Kansas City, MO.
REPLACEMENT OF SILICONE POLYMER A WITH SILICONE POLYMER B AND THE SUBSEQUENT CHARACTERIZATION OF THE NEW CELLULAR SILICONE MATERIALS
J. W. Schneider Apr. 1994 58 p
(Contract DE-AC04-76DP-00613)
(DE94-010105; KCP-613-5266) Avail: CASI HC A04/MF A01

The purpose of this project is to replace silicone polymer A with silicone polymer B produced by Vendor B. Silicone polymer B and the resulting B-50 cellular silicone have been used to produce cushions for the W87 program. Approximately 5.5 years of stress relaxation aging study data as well as actual part surveillance data have been collected, characterizing the stockpile life performance of the B-50 cellular silicone cushion material. Process characterization of new cellular silicone materials as a result of replacing silicone polymer A with silicone polymer B has been completed. Load deflection requirements for the new cellular silicone materials based on silicone polymer B have been met. The silicone polymer B based cellular silicone materials must be compounded at densities of approximately 0.03 g/cu cm less than the silicone polymer A based cellular silicone materials in order to achieve the same load deflection requirements has also been demonstrated. The change in silicone polymers from A to B involved a decrease in volatile content as well as a decrease in part shrinkage. DOE

N94-36637*# Deformation Control Technology, Inc., Cleveland, OH.
MODELING OF THERMAL BARRIER COATINGS Final Report
B. L. Ferguson, G. J. Petrus, and T. M. Krauss 12 Nov. 1992 157 p
(Contract NAS3-26664; RTOP 505-63-5A)
(NASA-CR-195365; E-9033; NAS 1.26:195365) Avail: CASI HC A08/MF A02

The project examined the effectiveness of studying the creep behavior of thermal barrier coating system through the use of a general purpose, large strain finite element program, NIKE2D. Constitutive models implemented in this code were applied to simulate thermal-elastic and creep behavior. Four separate ceramic-bond coat interface geometries were examined in combination with a variety of constitutive models and material properties. The reason for focusing attention on the ceramic-bond coat interface is that prior studies have shown that cracking occurs in the ceramic near interface features which act as stress concentration points. The model conditions examined include: (1) two bond coat coefficient of thermal expansion curves; (2) the creep coefficient and creep exponent of the bond coat for steady state creep; (3) the interface geometry; and (4) the material model employed to represent the bond coat, ceramic, and superalloy base. Author (revised)

N94-36641*# Albany International Research Corp., Mansfield, MA.
FLAME RESISTANT FIBROUS STRUCTURES DEVELOPMENT Final Report
Robert J. Coskren Sep. 1992 4 p
(Contract NAS9-17635)
(NASA-CR-185700; NAS 1.26:185700) Avail: CASI HC A01/MF A01

The purpose of the current program was (1) to investigate potentially useful new polymers, both for fire safety and mechanical properties, (2) to produce fibers from these polymers if necessary, and (3) to produce sufficient quantities of qualified fibrous structures, composites, or laminates for use in various areas of the Space Shuttle and Space Station Programs. During the past six years, development efforts have been expended in several major areas in support of Space Shuttle missions and Space Station Freedom projects. The summarized results of several of these major efforts are included in this report. Derived from text

N94-36952*# National Aeronautics and Space Administration. Lewis Research Center, Cleveland, OH.
ATOMIC OXYGEN TREATMENT FOR NON-CONTACT REMOVAL OF ORGANIC PROTECTIVE COATINGS FROM PAINTING SURFACES
Sharon K. Rutledge, Bruce A. Banks, and Michael Cales Jul. 1994 8 p
Presented at Materials Issues in Art and Archaeology IV, Cancun, Mexico, 16-20 May 1994 Sponsored by Materials Research Society
(Contract NCC3-19; RTOP 233-01-0E)
(NASA-TM-106650; E-8958; NAS 1.15:106650) Avail: CASI HC A02/MF A01

Current techniques for removal of varnish (lacquer) and other organic protective coatings from paintings involve contact with the surface. This contact can remove pigment, or alter the shape and location of paint on the canvas surface. A thermal energy atomic oxygen plasma, developed to simulate the space environment in low Earth orbit, easily removes these organic materials. Uniform removal of organic protective coatings from the surfaces of paintings is accomplished through chemical reaction. Atomic oxygen will not react with oxides so that most paint pigments will not be affected by the reaction. For paintings containing organic pigments, the exposure can be carefully timed so that the removal stops just short of

the pigment. Color samples of Alizarin Crimson, Sap Green, and Zinc White coated with Damar lacquer were exposed to atomic oxygen. The lacquer was easily removed from all of the samples. Additionally, no noticeable change in appearance was observed after the lacquer was reapplied. The same observations were made on a painted canvas test sample obtained from the Cleveland Museum of Art. Scanning electron microscope photographs showed a slight microscopic texturing of the vehicle after exposure. However, there was no removal or disturbance of the paint pigment on the surface. It appears that noncontact cleaning using atomic oxygen may provide a viable alternative to other cleaning techniques. It is especially attractive in cases where the organic protective surface cannot be acceptably or safely removed by conventional techniques. Author

N94-36958# Loyola Coll., Baltimore, MD. International Technology Research Inst.

ADVANCED MANUFACTURING TECHNOLOGY FOR POLYMER COMPOSITE STRUCTURES IN JAPAN Final Report

Dick J. Wilkins, Moto Ashizawa, Jon B. DeVault, Dee R. Gill, Vistasp M. Karbhari, Joseph S. McDermott, Michael J. DeHaemer, Geoffrey M. Holdridge, and Karen Hagerman Apr. 1994 264 p

(Grant NSF ENG-91-11333)

Avail: CASI HC A12/MF A03

This report covers Japanese research and development in the manufacturing of polymer composite structures. The study was supported by the National Science Foundation, the Department of Energy, the Army Research Office, and the Air Force Office of Scientific Research. Manufacturing technologies covered include lamination, pultrusion, filament winding, compression molding, thermoforming, and liquid molding (RTM, SRIM, etc.). Applications covered include aerospace (civil and military), civil engineering, automotive, and industrial. In addition, the report covers developments in composite materials, manufacturing and processing science, and composite product and process development methods. The report is based on site visits in Japan conducted in the fall of 1992, with updates provided by the panel's Japanese hosts in 1993 and early 1994. The panel concluded that the same basic manufacturing technologies are practiced in both the United States and Japan. However, Japanese companies implement these technologies with greater respect for detail, leading directly to the high quality evident in their operations and parts, also reducing errors and costs. The panel observed impressive Japanese efforts to reduce composite detail part count, a high level of excellence in co-curing, and an emphasis on dry-fiber preforming. Author (revised)

N94-37025*# Southwest Texas State Univ., San Marcos, TX. Dept. of Chemistry.

HIGHLY FLUORINATED POLYMERS Semiannual Status Report, 1 Jan. - 30 Jun. 1994

1994 5 p

(Grant NAG1-631)

(NASA-CR-196270; NAS 1.26:196270) Avail: CASI HC A01/MF A01

Work in the following areas is discussed: fluorinated poly(ether-ketone)s containing phosphorus; polyacrylates containing highly polar fluorinated pendant groups; and polyalkylene- and arylene-difluoroterephthalates.

Derived from text

N94-37055# Argonne National Lab., IL.

SCOPING ECONOMICS FOR THE COMMERCIAL MANUFACTURE OF METALLOCENE CATALYSTS

N. F. Brockmeier 26 May 1994 20 p Presented at the MetCon 1994: Worldwide Metallocene Catalyst/Processes Conference, Houston, TX, 25-27 May 1994

(Contract W-31-109-eng-38)

(DE94-011526; ANL/ES/CP-82657; CONF-9405150-1) Avail: CASI HC A03/MF A01

This study assumes that commercial-scale production of propylene-based isotactic polymers with metallocene catalyst systems will become a reality. The challenge that must be overcome for commercial success with these propylene polymers is to discover a metallocene system recipe that will give sufficient catalyst activity along with the requisite stereo-selectivity at reasonable cost. Anticipating such a discovery, it is assumed here that the economics are well-represented by a catalyst system that consists in part of a silylene-bridged cyclopentadienyl zirconocene made in a batchwise process having an annual capacity of 15,000 pounds. Activation will be achieved with a cocatalyst such as methylaluminoxane (MAO), coated in conjunction with the catalyst on a support such as silica. The MAO at an estimated $100/lb contributes $1800/lb cost to the finished catalyst with an assumed recipe of 18:1 mass ratio of MAO to zirconocene. Based on a 20% return on investment, the selling price for the supported zirconocene system is estimated to be $2915/lb. The required capital investment to make 735,000 lb/yr of the total supported system is 9 million dollars. These estimates have +/- 50% range of uncertainty. Payback period for this plant in a sold-out condition is three years. The catalyst system cost in ethylene-propylene copolymer is 3.9 cents per pound with a productivity of 75,000 lb polymer/lb of zirconocene. An Appendix includes some economic details. DOE

N94-37068# Argonne National Lab., IL.

TURNING SOOT INTO DIAMONDS WITH MICROWAVES

D. M. Gruen, A. R. Krauss, J. Luo, X. Pan, and S. Liu 1994 6 p Presented at the 29th Microwave Power Symposium, Chicago, IL, 25-27 Jul. 1994

(Contract W-31-109-eng-38)

(DE94-013426; ANL/CHM/CP-82961; CONF-940782-1) Avail: CASI HC A02/MF A01

Growth of diamond films using fullerene precursors in an argon microwave plasma without the addition of hydrogen or oxygen has recently been accomplished. Microwave discharges (2.45 GHz) were generated in C60-containing Ar. The gas mixtures were produced by flowing Ar over fullerene-containing soot at a variety of temperatures. Optical spectroscopy shows that the spectrum is dominated by the d(exp 3) Pi(sub g) - a(exp 3) Pi(sub u) Swan bands of C2 and particularly the Delta nu = -2, -1.0, +1, and +2 sequences. C2 is one of the products of C60 fragmentation brought about, at least in part, by collisionally-induced dissociation. The nanocrystalline films were characterized with scanning and high-resolution transmission electron microscopy, x-ray diffraction, and Raman spectroscopy. Assuming a linear dependence on carbon concentration, a growth rate at least six times higher than commonly observed using methane as a precursor would be predicted at a carbon content of 1% based on C60. Energetic and mechanistic arguments are advanced to rationalize this result based on C2 as the growth species. DOE

N94-37104 Army Construction Engineering Research Lab., Champaign, IL.

EVALUATION OF FLAME-SPRAYED POLYMER COATINGS FOR CIVIL WORKS NAVIGATION STRUCTURES Final Report

Timothy D. Race Apr. 1994 27 p Limited Reproducibility: More than 20% of this document may be affected by microfiche quality

(AD-A280507; CERL-FM-94/07) Avail: CASI HC A03

Provisions of the Clean Air Act Amendments of 1990 will further restrict the use of high solvent-content paints beginning in 1996, requiring the U.S. Army Corps of Engineers to replace some of the coatings now used to protect steel from corrosion in atmospheric and immersion exposures. To address this problem, the U.S. Army Construction Engineering Research Laboratories (USACERL) has experimented with several low-and zero-volatile emissions coating technologies. This report documents laboratory and field tests to evaluate the performance of flame-sprayed polymer coatings for potential use on Corps of Engineers navigation structures. Laboratory tests included salt and fresh water immersion, water resistance, atmospheric weathering, and ultraviolet (UV) condensation. Exposed test panels were evaluated for blistering, surface rust, adhesion, gloss retention, and rust undercutting. Plastic coatings were also evaluated for impact resistance. Standard Corps of Engineers coating formulations were used as experimental controls. Because of their relatively poor performance in these tests compared to the standard coating systems, flame-sprayed polymer coatings are not recommended at this time. DTIC

N94-37121 Utah State Univ., Logan, UT. Dept. of Chemistry and Biochemistry.

POLY(P-PHENYLENE) DERIVATIVES NEW HIGH PERFORMANCE NONLINEAR OPTICAL POLYMERS Technical Report No. 16, 1 Jun. 1993 - 31 May 1994

Michael E. Wright and Edward G. Toplikar 28 May 1994 3 p Limited Reproducibility: More than 20% of this document may be affected by microfiche quality

(Contract N00014-91-J-1625)
(AD-A280248) Avail: CASI HC A01

NLO polymers (NLOPS) based on the poly(p-phenylene) (PPP) backbone were prepared in the study. The thermal stability for the new materials is presented. The polymer displayed a Tg of 220 C. The TGA scan of the material indicated reasonable thermal stability to 300 C. A thin film of the material was supported on a glass slide and heated at 200 C and monitored by UV-vis spectroscopy. These experiments indicated less than 10% loss of the absorption band due to the NLO-phore (i.e. chromophore) over a period of 24 h. DTIC

N94-37133 Utah State Univ., Logan, UT. Dept. of Chemistry and Biochemistry.
ORGANIC NLO POLYMERS. 2: MAIN-CHAIN AND GUEST-HOST CHI(2)NLO POLYMERS: NLO-PHORE STRUCTURE VERSUS POLING Technical Report, 1 Jun. 1993 - 31 May 1994
Michael E. Wright, Sanjoy Mullick, Hilary S. Lackritz, and Lee-Yin Liu 28 May 1994 35 p Submitted for publication Limited Reproducibility: More than 20% of this document may be affected by microfiche quality
(Contract N00014-91-J-1625)
(AD-A280230) Avail: Issuing Activity (Defense Technical Information Center (DTIC))

Several new dipolar main-chain X (2) nonlinear optical (NLO) polymers were prepared in the study. The NLO-phores, based on alkoxy substituted alpha-cyanoacrylates, were also placed as monomeric guests within a poly(methyl methacrylate) host. Polar alignment of the NLO-phores by corona poling and their relaxation behavior was monitored by detecting the optical signal resulting from second harmonic generation. By making small variations in the structure of the NLO-phore, it was found that when hydrogen-bonding groups are rigidly coupled to the NLO-phore they are very effective for retaining polar asymmetry induced by poling and induced no deleterious effects on the alignment process. For main-chain NLOP's, it appears that for optimum alignment the bonding-axis and the polar-axis should not be parallel. DTIC

N94-37144 Nebraska Univ., Lincoln, NE. Dept. of Chemistry.
HOLOGRAPHIC GRATING RELAXATION STUDIES OF PROBE DIFFUSION IN AMORPHOUS POLYMERS
Jiulin Xia and C. H. Wang 15 Jun. 1994 29 p Sponsored by ONR Limited Reproducibility: More than 20% of this document may be affected by microfiche quality
(AD-A280496; TR-27-ONR) Avail: CASI HC A03

Probe diffusion of camphorquinone, thymorquinone and diacetyl is studied by the laser induced holographic grating relaxation (HRG) technique in polymers. It is shown that the probe diffusion coefficient decreases as the probe size increases. The presence of plasticizer enhances the rate of probe diffusion whereas crosslinker retards the diffusion. Probe diffusion is also studied by varying of polymer properties such as Tg, molecular weight and chain conformation. Temperature dependent studies show that except for the very low molecular weight poly(methylmethacrylate), all diffusion coefficients fit well to the WLF equation. Probe diffusion of camphorquinone is found to be much slower in poly(vinyl acetate) than in other polymers. This result is correlated with the outstanding damping property of the polymer. DTIC

N94-37147 Queens Univ., Kingston (Ontario). Dept. of Chemistry.
OPTICALLY INDUCED HIGH EFFICIENCY GRATINGS IN AZO POLYMER FILMS
P. Rochon, J. Mao, A. Natansohn, and E. Batalla 17 Jun. 1994 3 p Limited Reproducibility: More than 20% of this document may be affected by microfiche quality
(Contract N00014-93-1-0615)
(AD-A280505; TR-14-ONR) Avail: CASI HC A01

Going beyond the usual orientation of azobenzene groups within amorphous polymers, an increased amount of incident light may produce physical gratings of the order of magnitude of the wavelength. The diffraction efficiency of such gratings can reach 28% or even more. The surface profile of the grating can be observed with an atomic force microscope. Such gratings can be used to couple beams optically into the film and out of the film, as well as for waveguides. DTIC

N94-37148 Utah State Univ., Logan, UT. Dept. of Chemistry and Biochemistry.
ORGANIC NONLINEAR OPTICAL (NLO) POLYMERS. 4: THERMALLY STABLE NLO POLYMERS Report, 1 Jun. 1993 - 31 May 1994
Michael E. Wright and Edward G. Toplikar 22 May 1994 4 p Limited Reproducibility: More than 20% of this document may be affected by microfiche quality
(Contract N00014-91-J-1625)
(AD-A280196; TR-15) Avail: CASI HC A01

NLO polymers (NLOP's) based on the poly(p-phenylene) (PPP) backbone were prepared in the study. Starting from readily synthesized NLO-phore/monomers, homopolymerization afforded low molecular weight PPP's with the NLO-phore attached to the polymer backbone through a sulfone linkage. The thermal and linear optical behavior of the new materials is discussed in the paper. DTIC

N94-37151 Utah State Univ., Logan, UT. Dept. of Chemicstry and Biochemistry.
ORGANIC NLO POLYMERS. 5: HOMOPOLYMERIZATION OF INDOLE BASED NLO-PHORE: A HETEROCYCLE CHI(2)NLO MAIN-CHAIN POLYMER Technical Report, 1 Jun. 1993 - 31 May 1994
Michael E. Wright, Isabel McFarland, Hilary S. Lackritz, and Lee-Yin Liu 28 May 1994 4 p Submitted for publication Limited Reproducibility: More than 20% of this document may be affected by microfiche quality
(Contract N00014-91-J-1625)
(AD-A280229) Avail: Issuing Activity (Defense Technical Information Center (DTIC))

The paper describes the synthesis of main-chain NLOP's from indole-based NLO-phores/monomers. Homopolymers were prepared and spun cast into thin films. Corona poling of the samples produced materials which exhibited SHG signal (approx. 1 pm/V) with enhanced stability in comparison to related guest/host systems. DTIC

N94-37179 Utah State Univ., Logan, UT. Dept. of Chemistry and Biochemistry.
ORGANOMETALLIC NLO POLYMERS. 4: ORGANOMETALLIC MAIN-CHAIN, SIDE-CHAIN, AND GUEST-HOST POLYMERS: A STUDY OF THEIR ORIENTATION AND RELAXATION USING SECOND HARMONIC GENERATION Technical Report No. 20
Michael E. Wright, Edward G. Toplikar, Hilary S. Lackritz, and John T. Kerney 28 May 1994 34 p Limited Reproducibility: More than 20% of this document may be affected by microfiche quality
(Contract N00014-91-J-1625)
(AD-A280347) Avail: Issuing Activity (Defense Technical Information Center (DTIC))

tructure-property relationships for local polymer mobility and the net orientation of the organometallic NLO-phores have been investigated using second harmonic generation (SHG). The methacrylate organometallic derivatives were prepared and polymerized with methylmethacrylate. Corona poling and SHG measurements were made under a variety of carefully controlled experimental conditions. In the case of the covalently bound ferrocenyl NLO-phore, temporal stability was greatest for the smaller acceptor group CH=C(CN)2. DTIC

N94-37181 New Mexico Univ., Albuquerque, NM.
INTERACTION EFFECTS OF CRACKS, FLAWS AND DAMAGE IN CERAMIC Final Report, Sep. 1992 - Mar. 1994
Howard L. Schreyer and Ming L. Wang 4 May 1994 102 p Limited Reproducibility: More than 20% of this document may be affected by microfiche quality
(Contract AF-AFOSR-0419-91)
(AD-A280368; AFOSR-94-0352TR) Avail: Issuing Activity (Defense Technical Information Center (DTIC))

It is generally recognized that the nature of grain boundaries and microstructures affects the properties and behavior of ceramics. One of the objectives of this research is to study the fracture process of the ceramic in real time and to measure the strain field in the vicinity of the crack including the bridging zones. A fast-scanning electron microscope (FSEM) for dynamic microscopy applications was used to capture the fracture events in the ceramic. This equipment captures images at high speed. The SEM chamber was also modified to accommodate an in-situ tension-compression loading device to fracture ceramics. The fracture mode

was predominantly intergranular. No indication of a microcrack-cloud zone was observed in the FSEM results. Grain bridging was observed along the entire crack interface and over the entire propagation distance. DTIC

N94-37184 Washington State Univ., Pullman, WA. Dept. of Physics.
DEFECT INITIATION/GROWTH AND ENERGY DISSIPATION INDUCED BY DEFORMATION AND FRACTURE Final Technical Report, 15 Dec. 1992 - 14 Dec. 1993
J. T. Dickinson 15 May 1994 50 p Limited Reproducibility: More than 20% of this document may be affected by microfiche quality
(Contract F49620-91-C-0093)
(AD-A280411; AFOSR-94-0357TR) Avail: Issuing Activity (Defense Technical Information Center (DTIC))

Based on our capabilities to (a) detect and characterize particle release from surfaces on fast time scales, (b) to measure rapid electrical transients and (c) to obtain high resolution topographical information utilizing scanning tunneling and atomic force microscopy, we have investigated a number of defect initiation and growth processes which ultimately leads to fracture and energy dissipation. We employ dynamic methods as well as post-fracture examination in polymers, ceramics, metals, and interfaces. We have examined mechanisms, with interpretation and connections between these results and the creation and evolution of defects in materials under mechanical stress. The information we have acquired with our techniques has important implications concerning dissipation of energy (e.g., plastic deformation, microcracking, crack branching, and crack deflection) which play critical roles in controlling the strength and toughness of materials. DTIC

N94-37185 Queens Univ., Kingston (Ontario). Dept. of Chemistry.
AZOBENZENE-CONTAINING POLYMERS: SOME OPTOELECTRONIC PROPERTIES
A. Natansohn and P. Rochon 17 Jun. 1994 4 p Limited Reproducibility: More than 20% of this document may be affected by microfiche quality
(Contract N00014-93-1-0615)
(AD-A280448; TR-16-ONR) Avail: CASI HC A01

Orientation of azobenzenes in polymers depends on the neighboring unit in the same polymer and on the thermodynamic tendency of the polymer to form oriented domains. These two factors are briefly discussed in the context of current work. DTIC

N94-37204# Sandia National Labs., Albuquerque, NM. Contamination-Free Mfg. Research Center.
DEVELOPMENT OF HIGH SENSITIVITY TECHNIQUES FOR CHARACTERIZING OUTGASSING OF POLYMERIC CONSTRUCTION MATERIALS FOR MICROENVIRONMENTS
Dale C. McIntyre, Steven M. Thornberg, Alan Y. Liang, Susan F. A. Bender, and Richard D. Lujan 1994 8 p Presented at the 40th Annual Technical Meeting and Exposition of the Institute of Environmental Sciences (IES), Rosemont, IL, 1-6 May 1994
(Contract DE-AC04-94AL-85000)
(DE94-012068; SAND-94-1278C; CONF-940510-7) Avail: CASI HC A02/MF A01

Further reductions in particulate contamination in semiconductor device manufacturing environments will be required to meet the future challenges of producing devices with decreased dimensions. Using pods (microenvironments) to provide very clean environments on a local (wafer level) scale is an alternative that may reduce the technological demands and cost of providing comparable contamination levels in an entire clean-room manufacturing facility. It has been demonstrated that pods can provide wafer environments that have lower and less variable levels of particulate contamination than conventional clean-room manufacturing environments. However, there have also been indications that outgassed constituents from polymeric pod materials can condense on wafers during storage. A standard technique to evaluate outgassing of polymers is needed so that: (1) manufacturers can make reliable comparisons of the outgassing potential of materials being considered for use and (2) microenvironment users can make judgments on the relative outgassing threats from different manufacturers' products. The goal of the work that is summarized below has been to develop standard high sensitivity (10-100 ppb) testing techniques for evaluation of outgassing from polymeric pod materials in a temperature range from 30 to 75 C. This paper will briefly review outgassing data from polycarbonate materials that was obtained using thermal desorption combined with detection using gas chromatography/mass spectroscopy with volatile preconcentration or using a flame ionization detector (FID). Although the focus of this program has been on developing techniques to evaluate pod materials of construction, the techniques that have been evaluated may be useful for characterizing outgassing from other polymeric materials found in cleanrooms. DOE

N94-37223# Rensselaer Polytechnic Inst., Troy, NY. Dept. of Chemical Engineering.
MICROSCOPIC IMAGE PROCESSING SYSTEMS FOR MEASURING NONUNIFORM FILM THICKNESS PROFILES
A. H. Liu, J. L. Plawsky, S. DasGupta, and P. C. Wayner, Jr. 1994 7 p Presented at the 10th International Heat Transfer Conference, Brighton, England, 14-18 Aug. 1994
(Contract DE-FG02-89ER-14045)
(DE94-005336; DOE/ER-14045/8; CONF-940809-4) Avail: CASI HC A02/MF A01

In very thin liquid films, transport processes are controlled by the temperature and the interfacial intermolecular force field which is a function of the film thickness profile and interfacial properties. The film thickness profile and interfacial properties can be measured most efficiently using a microscopic image processing system (IPS) to record the intensity pattern of the reflected light from the film. There are two types of IPS: an image analyzing interferometer (IAI) and/or an image scanning ellipsometer (ISE). The ISE is a novel technique to measure the two dimensional thickness profile of a nonuniform, thin film, from 1 nm up to several microns in a steady state as well as in a transient state. It is a full field imaging technique which can study every point on the surface simultaneously with high spatial resolution and thickness sensitivity, i.e., it can measure and map the 2-D film thickness profile. Using the ISE, the transient thickness profile of a draining thin liquid film was measured and modeled. The interfacial conditions were determined in situ by measuring the Hamaker constant. The ISE and IAI systems are compared. DOE

N94-37227 Queens Univ., Kingston (Ontario). Dept. of Chemistry.
THERMAL CIS-TRANS ISOMERIZATION RATES OF AZOBENZENES BOUND IN THE SIDE CHAIN OF SOME COPOLYMERS AND BLENDS
C. Barrett, A. Natansohn, and P. Rochon 17 Jun. 1994 29 p Limited Reproducibility: More than 20% of this document may be affected by microfiche quality
(Contract N00014-93-1-0615)
(AD-A280451; TR-15-ONR) Avail: CASI HC A03

Copolymers of 4'-((2-(acryloyloxy) ethyl)ethylamino)-4-nitrozaobenzene (DR1A) with methyl methacrylate (MMA) and of the respective methacrylate monomer (DRIM) with MMA were cast as films and subjected to a pump/relax procedure to analyze the thermal cis-trans isomerization behavior of the azo groups. Blends of polyDR1A with polyMMA were also used in a similar manner. All samples show a fast isomerization process due to strained cis isomers, trapped below the glass transition temperature of the film, followed by a slower isomerization process. The homopolymers, all blends, and the copolymers with very low azo concentrations can be analyzed by a monoexponential decay for the slow process. The isomerization of all other copolymers is analyzed as a sum of three monoexponential processes, in which each process is the isomerization of an azo-centered triad. The rate constants found for the individual processes indicate that isomerization is faster when more azo groups are neighboring the central azo group in the triad. This is proof for neighboring effect on motion of the azo groups, even in these completely amorphous samples. DTIC

N94-37300*# National Aeronautics and Space Administration. Lewis Research Center, Cleveland, OH.
THERMAL-OXIDATIVE PRETREATMENT AND EVALUATION OF POLY (HEXAFLUOROPROPENE OXIDE) FLUIDS
K. J. L. Paciorek (Technolube Products Co., Vernon, CA.), S. R. Masuda (Technolube Products Co., Vernon, CA.), W-H. Lin (Technolube Products Co., Vernon, CA.), W. R. Jones, Jr., and L. S. Helmick Jul. 1994 20 p Proposed for presentation at the Tribology Conference, Lahaina, HI, 16-19 Oct. 1994; sponsored by the Society of Tribologists and Lubrication Engineers and ASME
(RTOP 233-02-0D)
(NASA-TM-106659; E-8974; NAS 1.15:106659) Avail: CASI HC A03/MF A01

Two commercial poly(hexafluoropropene oxide) fluids were thermally pretreated at 343 C in pure oxygen. IR and NMR spectra indicate that this pretreatment was effective in removing hydrogen end-capped impurities. Decrease in the quantity of volatile material produced during thermal oxidative decomposition and increase in the thermal decomposition temperature indicated improvement in the stability of the fluids. However, this pretreatment failed to render the fluids completely stable in oxidizing atmospheres at 316 C in the presence of metal alloys. Author

N94-37317# Los Alamos National Lab., NM.
LOW TEMPERATURE ATMOSPHERIC PRESSURE CHEMICAL VAPOR DEPOSITION OF GROUP 14 OXIDE FILMS
D. M. Hoffman (Houston Univ., TX.), L. M. Atagi, Wei-Kan Chu, Jia-Rui Liu, Zong-Shuang Zheng, and R. R. Rubiano 1994 7 p Presented at the Spring Meeting of the Materials Research Society, San Francisco, CA, 4-8 Apr. 1994
(Contract W-7405-eng-36)
(DE94-013115; LA-UR-94-1733; CONF-940411-24) Avail: CASI HC A02/MF A01

Depositions of high quality SiO2 and SnO2 films from the reaction of homoleptic amido precursors M(NMe(sub 2))4 (M = Si,Sn) and oxygen were carried out in an atmospheric pressure chemical vapor deposition r. The films were deposited on silicon, glass and quartz substrates at temperatures of 250 to 450C. The silicon dioxide films are stoichiometric (O/Si = 2.0) with less than 0.2 atom % C and 0.3 atom % N and have hydrogen contents of 9 plus/minus 5 atom %. They are deposited with growth rates from 380 to 900 angstrom/min. The refractive indexes of the SiO2 films are 1.46, and infrared spectra show a possible Si-OH peak at 950 cm(sup-1). X-Ray diffraction studies reveal that the SiO2 film deposited at 350C is amorphous. The tin oxide films are stoichiometric (O/Sn = 2.0) and contain less than 0.8 atom % carbon, and 0.3 atom % N. No hydrogen was detected by elastic recoil spectroscopy. The band gap for the SnO2 films, as estimated from transmission spectra, is 3.9 eV. The resistivities of the tin oxide films are in the range 10(exp -2) to 10(exp -3) Omega-cm and do not vary significantly with deposition temperature. The tin oxide film deposited at 350C is cassitterite with some (101) orientation. DOE

N94-37373# Air-Conditioning and Refrigeration Technology Inst., Inc., Arlington, VA.
MATERIALS COMPATIBILITY AND LUBRICANT RESEARCH ON CFC-REFRIGERANT SUBSTITUTES
S. R. Szymurski, M. Hawley, G. C. Hourahan, and D. S. Godwin Apr. 1994 66 p
(Contract DE-FG02-91CE-23810)
(DE94-012352; DOE/CE-23810/38) Avail: CASI HC A04/MF A01

The Materials Compatibility and Lubricants Research (MCLR) program supports critical research to accelerate the introduction of CFC and HCFC refrigerant substitutes. The MCLR program addresses refrigerant and lubricant properties and materials compatibility. Primary elements of the work include data collection and dissemination, materials compatibility testing, and methods development. The work is guided by an Advisory Committee consisting of technical experts from the refrigeration and air-conditioning industry and government agencies. The Air-Conditioning and Refrigeration Technology Institute, Inc., (ARTI) manages and contracts multiple research projects and a data collection and dissemination effort. Detailed results from these projects are reported in technical reports prepared by each subcontractor. DOE

N94-37421# Air-Conditioning and Refrigeration Technology Inst., Inc., Arlington, VA.
SEALED TUBE COMPARISONS OF THE COMPATIBILITY OF DESICCANTS WITH REFRIGERANTS AND LUBRICANTS Quarterly Technical Progress Report, Jan. - Mar. 1994
Jay E. Field (Spauschus Associates, Inc., Stockbridge, GA.) Apr. 1994 19 p
(Contract DE-FG02-91CE-23810)
(DE94-012371; DOE/CE-23810/38A) Avail: CASI HC A03/MF A01

Continuing environmental concerns mandate replacement of CFC's with alternate refrigeration fluids. At this time relatively little testing has been reported in the literature for compatibility of desiccants in these new working fluids. Using bench scale test methods generally accepted throughout the industry today, this work will provide data necessary to assess the compatibility or virtually all of the currently used desiccant types, both bead and molded core, with thirteen refrigerant/lubricant combinations. The desiccants are tested by exposure to refrigerant and lubricant in sealed, glass tubes in accordance with ASHRAE/ANSI Standard 97-1989. After aging, the liquid phase is evaluated for acid anion formation, change in color, and presence of halide ions, the gas phase is analyzed for refrigerant decomposition by gas chromatography, and the desiccants are evaluated for changes in crush strength and for retention of acids and halide ions. Metal catalysts, also present in the sealed tubes, are visually examined for corrosion, copper plating, and appearance changes. DOE

N94-37422# Lawrence Livermore National Lab., Livermore, CA.
AN AMORPHOUS FLUOROPOLYMER: NEXT GENERATION OPTICAL COATING CANDIDATE
R. Chow, G. E. Loomis, M. K. Spragge, E. L. Lindsey, F. Rainer, R. L. Ward, and M. R. Kozlowski May 1994 12 p Presented at the International Symposium on Optical Interference Coatings, Grenoble, France, 6-14 Jun. 1994
(Contract W-7405-eng-48)
(DE94-012386; UCRL-JC-115222; CONF-9406168-1) Avail: CASI HC A03/MF A01

Antireflective (AR) and high reflector (HR) optical coatings were made by physical vapor deposition (PVD) of Teflon AF2400, a perfluorinated amorphous polymer. The AR had the highest laser damage thresholds recorded for PVD coatings at the Lawrence Livermore National Laboratory damage facility. The HR was a multilayer of ZnS and AF2400. The bandwidth was 550 mn, centered at 1064 mn. Single layers of Teflon AF2400 deposited by PVD were characterized optically. The refractive index could be intentionally reduced below the bulk value by varying either deposition rate or substrate temperature. Scanning electron microscopy and nuclear magnetic resonance observations indicated that morphological changes caused the variations in the refractive index rather than compositional changes. DOE

N94-37423# Argonne National Lab., IL. Energy Technology Div.
DEVELOPMENT OF NONDESTRUCTIVE EVALUATION METHODS AND PREDICTION OF EFFECTS OF FLAWS ON THE FRACTURE BEHAVIOR OF STRUCTURAL CERAMICS
W. A. Ellingson, J. P. Singh, E. A. Sivers, D. L. Holloway, T. D. Jacobs, S. L. Dieckman, and D. Singh May 1994 12 p Presented at the 8th Annual Conference on Fossil Energy Materials, Oak Ridge, TN, 10-12 May 1994
(Contract W-31-109-eng-38)
(DE94-012466; ANL/ET/CP-82303; CONF-9405143-3) Avail: CASI HC A03/MF A01

In the NDE area, specimens with different cloth lay-up orientations were examined by a 3-D x-ray microtomography device and image processing to measure and map in-plane fiber orientations. Results show detection sensitivity to better than +/- 3 degrees. We establish detection of 3-D braid/weave fiber orientation and spacing. Another NDE method, muitinuclear (C-13, Si-29, and B-11) NMR spectroscopy, is being developed to determine the chemical state of the fiber surface and its potential impact on fiber pullout. We have conducted initial studies to investigate sensitivity to bulk composition of the matrix materials (a,b, amorphous phase, silica, and oxynitride concentration). The first Si-29 NMR experiments focused on methods to enhance the signal from the surface by selectively reducing surface relaxation. Additionally, we have determined that there is sufficient sensitivity of B-11 NMR for monitoring fiber coatings. DOE

N94-37482 Department of the Navy, Washington, DC.
CARBORANE-SILOXANE OR SILANE-UNSATURATED HYDROCARBON BASED POLYMERS Patent
Teddy M. Keller, inventor (to Navy) and Leslie J. Henderson, inventor (to Navy) 21 Dec. 1993 8 p Filed 30 Nov. 1992
(AD-D016220; US-Patent-5,272,237; US-Patent-Appl-SN-983194) Avail: US Patent and Trademark Office

This invention relates to a new class of novel linear inorganic/organic hybrid polymers of varying molecular weight that are useful for making high temperature, oxidatively stable thermosets, and these novel linear polymers are in themselves oxidatively stable at high temperatures between 600 - 1000 C. These new materials have repeat units that contain at least one alkynyl group and at least one bis(silyl or siloxanyl)carboranyl group

within the backbone of these novel linear polymers. These novel linear polymers can be further polymerized to form thermosets and ceramics.
DTIC

N94-37490# Air-Conditioning and Refrigeration Technology Inst., Inc., Arlington, VA.
INFORMATION ON ALTERNATIVE REFRIGERANTS AND LUBRICANTS: THE ARTI REFRIGERANT DATABASE
J. M. Calm 1993 3 p Presented at the 1993 International CCFC and Halon Alternatives Conference, Washington, DC, 20-22 Oct. 1993
(Contract DE-FG02-91CE-23810)
(DE94-009997; DOE/CE-23810/25; CONF-9310191-2) Avail: CASI HC A01/MF A01

A database has been established to locate property, performance, compatibility, safety, and other data on alternative refrigerants. It also addresses associated lubricants, retrofit procedures and experience, and test and analysis methods to quality refrigerants and refrigerant-lubricant combinations. The goal is to facilitate access to information, to assist industry in developing equipment using environmentally-safer fluids and practices. As the computerized version of the database enters its second year, the scope is being broadened to further address the needs of refrigerant users. The underlying purpose is to accelerate phase out of chemical compounds of environmental concern.
DOE

N94-37510*# San Jose State Univ., CA. Dept. of Materials Engineering.
DEVELOPMENT OF PROCESSING TECHNIQUES FOR ADVANCED THERMAL PROTECTION MATERIALS Annual Progress Report, 1 Jun. 1993 - 31 May 1994
Guna S. Selvaduray 15 May 1994 9 p
(Grant NAG2-848)
(NASA-CR-196261; NAS 1.26:196261) Avail: CASI HC A02/MF A01

The effort, which was focused on the research and development of advanced materials for use in Thermal Protection Systems (TPS), has involved chemical and physical testing of refractory ceramic tiles, fabrics, threads and fibers. This testing has included determination of the optical properties, thermal shock resistance, high temperature dimensional stability, and tolerance to environmental stresses. Materials have also been tested in the Arc Jet 2 x 9 Turbulent Duct Facility (TDF), the 1 atmosphere Radiant Heat Cycler, and the Mini-Wind Tunnel Facility (MWTF). A significant part of the effort hitherto has gone towards modifying and upgrading the test facilities so that meaningful tests can be carried out. Another important effort during this period has been the creation of a materials database. Computer systems administration and support have also been provided. These are described in greater detail below.
Author

N94-37520*# National Aeronautics and Space Administration. Lewis Research Center, Cleveland, OH.
PROPERTIES OF PERFLUOROPOLYETHERS FOR SPACE APPLICATIONS
William R. Jones, Jr. Jun. 1994 23 p Proposed for presentation at the ASME/STLE Tribology Conference, Lahaina, HI, 16-19 Oct. 1994; sponsored by ASME and the Society of Tribologists and Lubrication Engineers
(RTOP 233-02-0D)
(NASA-TM-106616; E-8899; NAS 1.15:106616) Avail: CASI HC A03/MF A01

The perfluoropolyether (PFPE) class of liquid lubricants has been used for space applications for over two decades. At first, these fluids performed satisfactorily as early spacecraft placed few demands on their performance. However, as other spacecraft components have become more reliable and lifetimes have been extended, PFPE lubricant deficiencies have been exposed. Therefore, the objective of this paper is to review the PFPE properties that are important for successful long term operation in space.
Author

N94-37537# Sandia National Labs., Albuquerque, NM.
RESIDUAL STRESS AND RAMAN SPECTRA OF LASER DEPOSITED HIGHLY-TETRAHEDRAL-COORDINATED-AMORPHOUS-CARBON FILMS
T. A. Friedmann, M. P. Siegal, D. R. Tallant, R. L. Simpson, and F. Dominguez 1994 6 p Presented at the Spring Meeting of the Materials Research Society, San Francisco, CA, 4-8 Apr. 1994
(Contract DE-AC04-94AL-85000)
(DE94-012067; SAND-94-1019C; CONF-940411-18) Avail: CASI HC A02/MF A01

We are studying carbon thin films by using a pulsed excimer laser to ablate pyrolytic graphite targets to form highly tetrahedral coordinated amorphous carbon (alpha)t-C films. These films have been grown on room temperature p-type Si (100) substrates without the intentional incorporation of hydrogen. In order to understand and optimize the growth of (alpha)t-C films, parametric studies of the growth parameters have been performed. We have also introduced various background gases (H2, N2, and Ar) and varied the background gas pressure during deposition. The residual compressive stress levels in the films have been measured and correlated to changes in the Raman spectra of the (alpha)t-C band near 1565 cm(exp -1). The residual compressive stress falls with gas pressure, indicating a decreasing atomic sp(exp 3)-bonded carbon fraction. We find that reactive gases such as hydrogen and nitrogen significantly alter the Raman spectra at higher pressures. These effects are due to a combination of chemical incorporation of nitrogen and hydrogen into the film as well as collisional cooling of the ablation plume. In contrast, films grown in non-reactive Ar background gases show much less dramatic changes in the Raman spectra at similar pressures.
DOE

N94-37712# Ames Lab., IA.
PERFLUORODIETHOXYMETHANE ON NICKEL AND NICKEL OXIDE SURFACES Ph.D. Thesis
J. Jacobson 3 Mar. 1994 55 p
(Contract W-7405-eng-82)
(DE94-011200; IS-T-1678) Avail: CASI HC A04/MF A01

The interaction of perfluorodiethoxymethane with a nickel single crystal, Ni(100); a nickel crystal with chemisorbed oxygen, Ni(100)-c(2x2)O; and a nickel crystal with nickel oxide crystallites, NiO(100) is investigated in an ultra high vacuum environment using thermal desorption spectroscopy and high resolution electron energy loss spectroscopy. Nickel, a component of hard disk drives and stainless steel, is used to represent metal surfaces in these 'real' systems. Perfluorodiethoxymethane is used in this study as a model compound of industrial perfluoropolyether lubricants. These lubricants are known for their exceptional stability, except in the presence of metals. Perfluorodiethoxymethane contains the acetal group (-OCF(sub 2)O-), believed to be particularly vulnerable to attack in the presence of Lewis acids. Since the surfaces studied show increasing Lewis acidity at the nickel atom sites, one might expect to see increasing decomposition of perfluorodiethoxymethane due to acidic attack of the acetal group. No decomposition of perfluorodiethoxymethane is observed on the clean Ni(100) surface, while more research is needed to determine whether a small decomposition pathway is observed on the oxygenated surfaces, or whether sample impurities are interfering with results. The strength of the bonding of perfluorodiethoxymethane to the surface is found to increase as the nickel atoms sites become more acidic in moving from Ni(100) to Ni (100)-c(2x2)O to NiO (100).
DOE

N94-37714# Spire Corp., Bedford, MA.
GAS MICROSTRIP DETECTORS ON RESISTIVE PLASTIC SUBSTRATES
M. S. Dixit (Carleton Univ., Ottawa, Ontario.), F. G. Oakham (Carleton Univ., Ottawa, Ontario.), J. C. Armitage (Carleton Univ., Ottawa, Ontario.), J. Dubeau (Carleton Univ., Ottawa, Ontario.), D. Karlen (Carleton Univ., Ottawa, Ontario.), G. C. Stuart (Carleton Univ., Ottawa, Ontario.), S. C. Taylor (Carleton Univ., Ottawa, Ontario.), I. Shipsey (Purdue Univ., West Lafayette, IN.), E. Johnson, and A. Greenwald 1993 26 p Presented at the 3rd London Conference on Position-Sensitive Detectors, London, England, 6-10 Sep. 1993
(Contract DE-FG02-92ER-81463)
(DE94-011336; CONF-9309256-5) Avail: CASI HC A03/MF A01

Plastics are desirable as substrates for gas microstrip detectors (GMD's) because of their flexibility, low density and long radiation length. GMD's have been fabricated on white Tedlar which has bulk electrical conductivity and ion-implanted Upilex which has a thin electrically conductive layer on the surface of an insulator. The effect of back plane voltage on the gain of such GMD's is investigated. Three 200 (mu)m pitch, ion-implanted Upilex GMD's were recently tested in a high intensity beam at CERN. The anode signals were read out using fast, low noise, high gain amplifiers. Preliminary results of the test are presented.
DOE

N94-37725# Sandia National Labs., Livermore, CA.
COMPILATION OF DIAMOND-LIKE CARBON PROPERTIES FOR BARRIERS AND HARD COATINGS
D. A. Outka, Wen L. Hsu, K. Phillips, D. R. Boehme, N. Y. C. Yang, D. K. Ottesen, H. A. Johnsen, W. M. Clift, and T. J. Headley May 1994 53 p (Contract DE-AC04-76DR-00789)
(DE94-012139; SAND-94-8219B) Avail: CASI HC A04/MF A01

Diamond-like carbon (DLC) is an amorphous form of carbon which resembles diamond in its hardness, lubricity, and resistance to chemical attack. Such properties make DLC of interest for use in barrier and hard coating technology. This report examines a variety of properties of DLC coatings. This includes examining substrates on which DLC coatings can be deposited; the resistance of DLC coatings to various chemical agents; adhesion of DLC coatings; and characterization of DLC coatings by electron microscopy, FTIR, sputter depth profiling, stress measurements and nanoindentation. DOE

N94-37773 Department of the Navy, Washington, DC.
FLUORINATED RESINS WITH LOW DIELECTRIC CONSTANT Patent
James R. Griffith, inventor (to Navy) and Henry S. Hu, inventor (to Navy) 8 Mar. 1994 7 p Filed 26 Feb. 1992 Supersedes AD-D015810
(AD-D016303; US-Patent-5,292,927; US-Patent-Appl-SN-841944; US-Patent-Class-560-221) Avail: US Patent and Trademark Office

A highly fluorinated benzene compound is reacted with acryloyl chloride to yield a fluorinated liquid product which is used to impregnate a reinforcing structure. Upon impregnation, the liquid material is polymerized at about 55 C to produce a reinforced polymeric structure, which can be a circuit board. The polymer has dielectric constant of about 2.1, which is very low compared to the polymers used presently. DTIC

N94-37778 Department of the Navy, Washington, DC.
SYNTHESIS OF PHTHALONITRILE RESINS CONTAINING ETHER AND IMIDE LINKAGES WITH AROMATIC DIAMINE CURING AGENT Patent
Teddy M. Keller, inventor (to Navy) 22 Feb. 1994 8 p Filed 30 Jul. 1992
(AD-D016309; US-Patent-5,292,854; US-Patent-Appl-SN-921776; US-Patent-Class-528-170) Avail: US Patent and Trademark Office

Imide-containing phthalonitrile monomers are prepared from a phthalonitrile and an aromatic dianhydride. The monomer and a method for preparing the monomer is disclosed. These monomers are synthesized into heat resistant polymers and copolymers with aromatic ring structure incorporating imide and ether linkages. The synthesis of the high temperature thermosetting polymers and copolymers is also disclosed. DTIC

N94-37779 Department of the Navy, Washington, DC.
SUBSTITUTED SILYL-TERMINATED COMPOUNDS AND POLYMERS THEREOF Patent
Kreisler S. Lau, inventor (to Navy), Abraham L. Landis, inventor (to Navy), and Thomas K. Dougherty, inventor (to Navy) 8 Mar. 1994 11 p Filed 10 Aug. 1992
(AD-D016310; US-Patent-5,292,851; US-Patent-Appl-SN-926625; US-Patent-Class-528-38) Avail: US Patent and Trademark Office

The general purpose of the present invention is to provide a new group of compounds from which oligomers may be derived or formed for subsequent use in forming novel polymer-ceramic networks which are resistant to high temperatures and are easy to process. These compounds and the novel processes for forming them possess most, if not all, of the advantages of the above prior art compounds while overcoming their above-mentioned significant disadvantages. The above-described general purpose of the present invention is accomplished by providing a new group of compounds terminated with substituted silyl groups. DTIC

N94-37818 Department of the Navy, Washington, DC.
CARBORANE-(SILANE OR SILOXANE)-UNSATURATED HYDROCARBON BASED THERMOSETTING POLYMERS Patent
Teddy M. Keller, inventor (to Navy) and Leslie J. Henderson, inventor (to Navy) 8 Mar. 1994 14 p Filed 17 Dec. 1992 Supersedes AD-D015718
(AD-D016311; US-Patent-5,292,779; US-Patent-Appl-SN-991940; US-Patent-Class-522-99) Avail: US Patent and Trademark Office

This invention relates to a new class of novel inorganic-organic hybrid polymers that are formed from linear inorganic-organic hybrid polymers of varying molecular weight. These new high temperature oxidatively stable thermosetting polymers are formed from linear polymeric materials having repeat units that contain at least one alkynyl group for cross-linking purposes and at least one bis(sily or siloxanyl)carboranyl group. These novel organoboron thermoset polymers contain an unsaturated cross-linked hydrocarbon moiety. DTIC

N94-37829 Department of the Navy, Washington, DC.
SURFACE MODIFICATION OF POLYMERS WITH SELF-ASSEMBLED MONOLAYERS THAT PROMOTE ADHESION, OUTGROWTH AND DIFFERENTIATION OF BIOLOGICAL CELLS Patent Application
Alan Rudolph, inventor (to Navy), David A. Stenger, inventor (to Navy), Barry J. Spargo, inventor (to Navy), and Chin-Chang Chu, inventor (to Navy) 28 Apr. 1994 56 p Limited Reproducibility: More than 20% of this document may be affected by microfiche quality
(AD-D016321; US-Patent-Appl-SN-234034; Navy-Case-75846) Avail: CASI HC A04

The present invention relates to a method of patterned adhesion, outgrowth and differentiation of biological cells. More particularly, the present invention relates to a method of patterned adhesion, outgrowth and differentiation of endothelial cells to form longitudinally-oriented neo-vascular capillaries. DTIC

N94-37831# Department of the Navy, Washington, DC.
DOUBLE NETWORK ELASTOMERS AND METHOD OF MAKING SAME Patent Application
C. M. Roland, inventor (to Navy) and P. G. Santangelo, inventor (to Navy) 29 Mar. 1994 24 p
(AD-D016323; US-Patent-Appl-SN-219318; Navy-Case-75421) Avail: CASI HC A03/MF A01

A process for modifying elastomeric structures to improve mechanical properties involves subjecting a pre-cured shape of elastomeric material to an orientation technique to result in an oriented elastomeric material; and curing the oriented elastomeric material while maintaining the orientation of the elastomeric material under conditions effective to result in an elastomeric structure having a predetermined crosslink density and enhanced modulus, the magnitude of orientation being sufficient to result in the enhanced modulus. Typically, the orientation techniques used may include uniaxial extension, biaxial extension, simple shear, planar shear, and inflation. The elastomeric material be capable of strain induced crystallization or incapable of strain induced crystallization. The enhanced modulus is obtained while at least maintaining failure performance of the elastomeric structure, and the conditions during the curing are sufficient to maintain a constant crosslink density in the double network elastomer while the modulus is enhanced. DTIC

N94-37854 Helsinki Univ. of Technology, Espoo (Finland). Dept. of Technical Physics.
PRESSURE DEPENDENCE OF THE CONDUCTIVITY AND MAGNETOCONDUCTANCE IN ORIENTED IODINE-DOPED POLYACETYLENE
M. Reghu, K. Vaekiparta, Y. Cao, and D. Moses 11 Nov. 1993 28 p Limited Reproducibility: More than 20% of this document may be affected by microfiche quality
(PB94-184488; TKK-F-A719) Avail: Issuing Activity (National Technical Information Service (NTIS))

A comprehensive study of the conductivity and magnetoconductivity has been carried out for directions both parallel and perpendicular to the chain axis, as a function of pressure, temperature and magnetic field. The room temperature conductivity increases up to 4 kbar, and at higher pressures the conductivity gradually decreases. At 8 kbar, the temperature dependence of conductivity and the anisotropy in conductivity have decreased by factors of 1.4 and 1.6, respectively. This indicates that the interchain transport is enhanced by pressure. The critical region near the M-I transition, in directions both parallel and perpendicular to the chain axis, is from 180 to 60 K; in this temperature regime the reduced activation energy function is temperature independent. The temperature dependence of the conductivity in the temperature regime 60 K - 2 K indicates that inelastic electron-electron scattering is the dominant scattering process. However, at temperatures below 2 K, the temperature dependence of conductivity arises from the residual electron-electron interaction in this disordered metal. NTIS

28 PROPELLANTS AND FUELS

Includes rocket propellants, igniters, and oxidizers; their storage and handling procedures; and aircraft fuels.

For related information see also *07 Aircraft Propulsion and Power, 20 Spacecraft Propulsion and Power,* and *44 Energy Production and Conversion.*

N94-36505 Sandia National Labs., Albuquerque, NM.
ADVANCED THERMALLY STABLE, COAL-DERIVED, JET FUELS DEVELOPMENT PROGRAM. EXPERIMENT SYSTEM AND MODEL DEVELOPMENT Annual Report, Oct. 1992 - Sep. 1993
E. A. Klavetter, S. J. Martin, W. Trott, and T. J. OHern Dec. 1993 50 p Limited Reproducibility: More than 20% of this document may be affected by microfiche quality
(Contract DE-AC04-94AL-85000; DA Proj. 3048)
(AD-A278968; WL-TR-94-2003) Avail: Issuing Activity (Defense Technical Information Center (DTIC))

A program entitled 'Thermally Stable Jet Fuels Development' was initiated in FY89 by the U.S. Air Force, Aero Propulsion and Power Directorate, working jointly with the Department of Energy, Pittsburgh Energy Technology Center. Thermal stability of aviation fuels is of concern because of the potential operation problems arising from fuel degradation under thermal stress conditions. Sandia National Laboratories has been conducting efforts to develop instrumentation for monitoring characteristics of jet fuel degradation and solids deposition and develop models of those mechanisms from the data acquired using that instrumentation. This report describes the instrumentation development, data acquisition, and model parameter determination. DTIC

N94-36972 Naval Postgraduate School, Monterey, CA.
VALIDATION AND IMPLEMENTATION OF OPTICAL DIAGNOSTICS FOR PARTICLE SIZING IN ROCKET MOTORS M.S. Thesis
Paul V. Gomes Dec. 1993 45 p Limited Reproducibility: More than 20% of this document may be affected by microfiche quality
(AD-A278581) Avail: Issuing Activity (Defense Technical Information Center (DTIC))

Aluminum oxide particles of known size distribution were cast into a solid propellant which burned at temperatures less than the melting point of Al2O3. Thus, particles of known size distribution existed at the nozzle inlet and in the plume. Malvern particle sizing instruments were used to make measurements at these two location using a windowed subscale motor and the results were compared to the known distribution. In the motor, measurements were limited due to disruptive flow from the window purge gas. However, the unaffected larger modes were properly measured. In the plume, the measurements of the modes were quite accurate, but low signal strength resulted in some inaccuracies for the mass contained in each mode. A phase Doppler particle analyzer was adapted to an existing plume probe. Initial measurements at two radial locations were in good agreement with the expected size distribution. DTIC

N94-37052# Sandia National Labs., Albuquerque, NM.
DDT MODELING AND SHOCK COMPRESSION EXPERIMENTS OF POROUS OR DAMAGED ENERGETIC MATERIALS
M. R. Baer, M. U. Anderson, and R. A. Graham 1994 18 p Presented at the 1994 Joint USA-Russia Energetic Material Technology Symposium, Livermore, CA, 18-25 May 1994
(Contract DE-AC04-94AL-85000)
(DE94-011419; SAND-94-1188C; CONF-9405136-6) Avail: CASI HC A03/MF A01

In this presentation, we present modeling of DDT in porous energetic materials and experimental studies of a time-resolved, shock compression of highly porous inert and reactive materials. This combined theoretical and experimental study explores the nature of the microscale processes of consolidation, deformation, and reaction which are key features of the shock response of porous or damaged energetic materials. The theoretical modeling is based on the theory of mixtures in which multiphase mixtures are treated in complete nonequilibrium allowing for internal boundary effects associated mass/momentum and energy exchange between phases, relative flow, rate-dependent compaction behavior, multistage chemistry, and interphase boundary effects. Numerous studies of low-velocity impacts using a high resolution adaptive finite element method are presented which replicate experimental observations. The incorporation of this model into multimaterial hydrocode analysis will be discussed to address the effects of confinement and its influence on accelerated combustion behavior. The experimental studies will focus on the use of PVDF piezoelectric polymer stress-rate gauge to precisely measure the input and propagating shock stress response of porous materials. In addition to single constituent porous materials, such as granular HMX, we have resolved shock waves in porous composite intermetallic powders that confirm a dispersive wave nature which is highly morphologically and material dependent. This document consists of viewgraphs from the poster session. DOE

N94-37201# Sandia National Labs., Albuquerque, NM.
A FULLY COUPLED THERMAL, CHEMICAL, MECHANICAL COOKOFF MODEL
M. L. Hobbs, M. R. Baer, and R. J. Gross 1994 8 p Presented at the 1994 Joint USA-Russia Energetic Material Technology Symposium, Livermore, CA, 18-25 May 1994
(Contract DE-AC04-94AL-85000)
(DE94-011432; SAND-94-1197C; CONF-9405136-2) Avail: CASI HC A02/MF A01

Cookoff modeling of confined energetic materials involves the coupling of thermal, chemical, and mechanical effects. In the past, modeling has focussed on the prediction of thermal runaway with little regard to the effects of mechanical behavior of the energetic material. To address the mechanical response of the energetic material, a constitutive submodel has been developed which can be incorporated into thermal-chemical-mechanical analysis. This work presents development of this submodel and its incorporation into a fully coupled one-dimensional, thermal-chemical-mechanical computer code to simulate thermal initiation of energetic materials. Model predictions include temperature, chemical species, stress, strain, solid/gas pressure, solid/gas density, yield function, and gas volume fraction. Sample results from a scaled aluminum tube filled with RDX exposed to a constant temperature bath at 500 K will be displayed. The micromechanical submodel is based on bubble mechanics which describes nucleation, decomposition, and elastic/plastic mechanical behavior. This constitutive material description requires input of temperatures and reacted fraction of the energetic material as provided by the reactive heat flow code, XCHEM, and the mechanical response is predicted using a quasistatic mechanics code, SANTOS. A parametric sensitivity analysis indicates that a small degree of decomposition causes significant pressurization of the energetic material, which implies that cookoff modeling must consider the strong interaction between thermal-chemistry and mechanics. This document consists of view graphs from the poster session. DOE

N94-37202# Sandia National Labs., Albuquerque, NM.
PROCESSING SOLID PROPELLANTS FOR RECYCLING
L. L. Whinnery, S. K. Griffiths, J. L. Handrock, and J. Lipkin 1994 18 p Presented at the 1994 Joint USA-Russia Energetic Material Technology Symposium, Livermore, CA, 18-25 May 1994
(Contract DE-AC04-94AL-85000)
(DE94-011433; SAND-94-1198C; CONF-9405136-3) Avail: CASI HC A03/MF A01

Rapid evolution in the structure of military forces worldwide is resulting in the retirement of numerous weapon systems. Many of these systems include rocket motors containing highly energetic propellants based on hazardous nitrocellulose/nitroglycerin (NC/NG) mixtures. Even as the surplus quantities of such material increases, however, current disposal methods -- principally open burning and open detonation (OB/OD) -- are coming under close scrutiny from environmental regulators. Environmentally conscious alternatives for disposal of propellant and explosives are thus receiving renewed interest. Recycle and reuse alternatives to OB/OD appear particularly attractive because some of the energetic materials in the inventories of surplus weapon systems represent potentially valuable resources to the commercial explosives and chemical industries. The ability to reclaim such resources is, therefore, likely to be a key requirement of any successful technology of the future in rocket motor demilitarization. This document consists of view graphs from the poster session. DOE

N94-37243# Sandia National Labs., Albuquerque, NM.
HYDROGEN STORAGE FOR VEHICULAR APPLICATIONS: TECHNOLOGY STATUS AND KEY DEVELOPMENT AREAS

S. L. Robinson and J. L. Handrock Apr. 1994 47 p
(Contract DE-AC04-94AL-85000)
(DE94-011626; SAND-94-8229) Avail: CASI HC A03/MF A01

The state-of-the-art of hydrogen storage technology is reviewed, including gaseous, liquid, hydride, surface adsorbed media, glass microsphere, chemical reaction, and liquid chemical technologies. The review of each technology includes a discussion of advantages, disadvantages, likelihood of success, and key research and development activities. A preferred technological path for the development of effective near-term hydrogen storage includes both cur-rent DOT qualified and advanced compressed storage for down-sized highly efficient but moderate range vehicles, and liquid storage for fleet vehicle applications. Adsorbate media are also suitable for fleet applications but not for intermittent uses. Volume-optimized transition metal hydride beds are also viable for short range applications. Long-term development of coated nanoparticulate or metal matrix high conductivity magnesium alloy, is recommended. In addition, a room temperature adsorbate medium should be developed to avoid cryogenic storage requirements. Chemical storage and oxidative schemes present serious obstacles which must be addressed for these technologies to have a future role. DOE

N94-37402# Department of Energy, Washington, DC.
ALTERNATIVE FUEL INFORMATION: FACTS ABOUT CNG AND LPG CONVERSION
K. OConnor 1994 8 p
(Contract DE-AC02-83CH-10093)
(DE94-006888; DOE/CH-10093/315) Avail: CASI HC A02/MF A01

As new environmental and energy related laws begin to take effect, increasing numbers of alternative fuel vehicles (AFV's) will be required in federal, state, municipal, and private fleets across the country. The National Energy Policy Act of 1992 and the Clean Air Act Amendments of 1990, along with several new state and local laws, will require fleet managers to either purchase original equipment manufacturer (OEM) vehicles, which are produced by automakers, or convert existing vehicles to run on alternative fuels. Because there is a limited availability and selection of OEM vehicles, conversions are seen as a transition to the time when automakers will produce more AFV's for public sale. A converted vehicle is any vehicle that originally was designed to operate on gasoline, and has been altered to run on an alternative fuel such as compressed natural gas (CNG) or propane (liquefied petroleum gas -- LPG), the two most common types of fuel conversions. In the United States, more than 25,000 vehicles already have been converted to COG, and 300,000 have been converted to LPG. DOE

N94-37403# Department of Energy, Washington, DC.
ALTERNATIVE FUEL INFORMATION: GLOSSARY
1994 15 p
(Contract DE-AC02-83CH-10093)
(DE94-006889; DOE/CH-10093/316) Avail: CASI HC A03/MF A01

This short document contains definitions of acronyms and definitions of terms used in papers on the use of alternative fuels in automobiles. DOE

N94-37404# Department of Energy, Washington, DC.
ALTERNATIVE FUEL INFORMATION: STATE ALTERNATIVE FUEL LAWS AND INCENTIVES
1994 20 p
(Contract DE-AC02-83CH-10093)
(DE94-006892; DOE/CH-10093/319) Avail: CASI HC A03/MF A01

Laws and incentives related to the use of alternative fuels in automobiles are listed for most states of USA. DOE

N94-37413# Sandia National Labs., Livermore, CA.
THERMAL DECOMPOSITION REACTIONS OF HMX AND RDX AND THEIR IMPORTANCE IN PREDICTING COOKOFF HAZARDS
R. Behrens, Jr. and S. Bulusu 1994 30 p Presented at the 1994 Joint USA-Russia Energetic Material Technology Symposium, Livermore, CA, 18-25 May 1994
(Contract DE-AC04-94AL-85000)
(DE94-011430; SAND-94-1191C; CONF-9405136-11) Avail: CASI HC A03/MF A01

To develop robust models for predicting the response of munitions under abnormal conditions associated with cookoff, it is necessary to be able to accurately characterize the following: the time to ignition, the location of the ignition point within the munition, and the combustive behavior of the damaged energetic material after ignition. For the response of the munition, as controlled by these parameters, will determine whether its response will be characterized by a relatively mild deflagration or whether it will be characterized by a more damaging detonation. Several of the underlying properties of the energetic materials used in munitions that must be understood in order to accurately characterize these parameters are the chemical and physical changes that occur in these energetic materials as they are heated. The chemical changes involve overcoming the forces that tend to stabilize these materials, such as binding within the crystal lattice or intermolecular hydrogen bonding, and their transformation to less stable forms, such as mixtures of gases with high energy content. The physical changes typically involve phase changes of the material. One significant phase change is the slow transformation of the energetic materials from the solid reactant to gas phase products. This transformation can lead initially to the formation of high pressure gas bubbles within the solid particles and ultimately to changes in the porosity and gas permeability of the energetic material formulation. The presence of these reactive gases within high pressure bubbles can lead to increased hot spot formation of the material if it is compressed. The increased porosity can lead to significant increases in the burn rates of these materials at high pressures. DOE

N94-37426# Midwest Research Inst., Golden, CO. National Renewable Energy Lab.
COMPARATIVE ALTERNATIVE/CLEAN FUELS PROVISIONS OF THE CLEAN AIR ACT AMENDMENTS OF 1990 AND THE ENERGY POLICY ACT OF 1992
1994 6 p
(Contract DE-AC02-83CH-10093)
(DE94-006887; DOE/CH-10093/314) Avail: CASI HC A02/MF A01

This is a summary side-by-side comparison of the fleet provisions and incentives under the Clean Air Act Amendments of 1990 (Public Law 101-549) and the Energy Policy Act of 1992 (Public Law 102-486). For more information on how to comply, contact your regional Department of Energy and Environmental Protection Agency support offices in addition to your state energy office. DOE

N94-37427# Lawrence Livermore National Lab., Livermore, CA.
CHEETAH: A FAST THERMOCHEMICAL CODE FOR DETONATION
L. E. Fried Nov. 1993 24 p
(Contract W-7405-eng-48)
(DE94-012586; UCRL-ID-115752) Avail: CASI HC A03/MF A01

For more than 20 years, TIGER has been the benchmark thermochemical code in the energetic materials community. TIGER has been widely used because it gives good detonation parameters in a very short period of time. Despite its success, TIGER is beginning to show its age. The program's chemical equilibrium solver frequently crashes, especially when dealing with many chemical species. It often fails to find the C-J point. Finally, there are many inconveniences for the user stemming from the program's roots in pre-modern FORTRAN. These inconveniences often lead to mistakes in preparing input files and thus erroneous results. We are producing a modern version of TIGER, which combines the best features of the old program with new capabilities, better computational algorithms, and improved packaging. The new code, which will evolve out of TIGER in the next few years, will be called 'CHEETAH.' Many of the capabilities that will be put into CHEETAH is inspired by the thermochemical code CHEQ. The new capabilities of CHEETAH are: calculate trace levels of chemical compounds for environmental analysis; kinetics capability: CHEETAH will predict chemical compositions as a function of time given individual chemical reaction rates. Initial application: carbon condensation; CHEETAH will incorporate partial reactions; CHEETAH will be based on computer-optimized JCZ3 and BKW parameters. These parameters will be fit to over 20 years of data collected at LLNL. We will run CHEETAH thousands of times to determine the best possible parameter sets; CHEETAH will fit C-J data to JWL's, and also predict full-wall and half-wall cylinder velocities. DOE

N94-37446*# Atlantic Research Corp., Gainesville, VA. Propulsion Div.
NASA RELOAD PROGRAM Final Report, 25 Sep. 1990 - 31 Jan. 1993
Marshall Byington 12 Apr. 1993 80 p
(Contract NAS8-38668)
(NASA-CR-193972; NAS 1.26:193972) Avail: CASI HC A05/MF A01

Atlantic Research Corporation (ARC) contracted with NASA to manufacture and deliver thirteen small scale Solid Rocket Motors (SRM). These motors, containing five distinct propellant formulations, will be used for plume induced radiation studies. The information contained herein summarizes and documents the program accomplishments and results. Several modifications were made to the scope of work during the course of the program. The effort was on hold from late 1991 through August, 1992 while propellant formulation changes were developed. Modifications to the baseline program were completed in late-August and Modification No. 6 was received by ARC on September 14, 1992. The modifications include changes to the propellant formulation and the nozzle design. The required motor deliveries were completed in late-December, 1992. However, ARC agreed to perform an additional mix and cast effort at no cost to NASA and another motor was delivered in March, 1993. Author

N94-37768 Department of the Navy, Washington, DC.
INTERFEROMETRIC JFTOT TUBE DEPOSIT MEASURING DEVICE Patent
Robert E. Morris, inventor (to Navy) and Robert Wagner, inventor (to Navy) 8 Mar. 1994 166 p Filed 30 Jun. 1992 Supersedes AD-D015599
(AD-D016295; US-Patent-5,293,218; US-Patent-Appl-SN-906903; US-Patent-Class-356-382) Avail: US Patent and Trademark Office

Jet fuels are tested for thermal stability by passing the fuel over a heated metal tube and measuring the amount of residue deposited as a film on the tube as a result of chemical changes to the fuel. The thickness distribution and volume of a deposited film on a tube are calculated by scanning the length of the tube with an optical probe, shining light onto the tube, measuring the intensity of reflected light of a preselected wavelength from the tube, and correlating the reflected light intensity with positions on the tube. The tube is then partially rotated, and the process is repeated until the entire surface of the tube is scanned. The volumes of each longitudinal slice of the tube are summed to give the total deposit volume on the tube. DTIC

29 MATERIALS PROCESSING

Includes space-based development of products and processes for commercial applications.

For biological materials see *55 Space Biology*.

N94-36806*# Rockwell International Corp., Downey, CA.
CRYOGENIC FLUID MANAGEMENT TECHNOLOGIES FOR SPACE TRANSPORTATION. ZERO G THERMODYNAMIC VENT SYSTEM Final Report
1994 64 p
(Contract NAS8-39202)
(NASA-CR-193981; NAS 1.26:193981; SSD-94M0038) Avail: CASI HC A04/MF A01

Long term storage of subcritical cryogens in space must address the problem of thermal stratification in the storage tanks, liquid acquisition devices, and associated feed systems. Due to the absence of gravity induced body forces, thermal stratification in zero-g is more severe than commonly experienced in a one-g environment. If left uncontrolled, the thermal gradients result in excessive tank pressure rise and the formation of undesirable liquid/vapor mixtures within the liquid bulk, liquid acquisition system, and propellant transfer lines. Since external heat leakage cannot be eliminated, a means of minimizing the thermal stratification in the ullage gas, liquid, and feed system is required. A subsystem which minimizes the thermal stratification and rejects the environmental heat leakage in an efficient manner is therefore needed for zero-g subcritical cryogenic systems. In ground based storage systems the ullage gas location is always known (top of the tank) and therefore direct venting of gases as a means of heat rejection is easily accomplished. In contrast, because the ullage location in a zero-g environment is not easily predictable, heat rejection through direct gaseous venting is difficult in space (requires liquid settling, or surface tension devices). A means of indirect venting through the use of a thermodynamic vent system (TVS) is therefore required. A thermodynamic vent system allows indirect venting of vapor through heat exchange between the vented fluid and the stored fluid. The objective is to ensure that only gas and not liquid is vented, in order to minimize the propellant losses. Consequently, the design of a TVS is a critical enabling technology for future applications such as solar thermal and electric propulsion, single-stage-to-orbit vertical landers and upper stages, and any space based operations involving subcritical cryogenics. To bridge this technology gap NASA MSFC initiated an effort to build and verify through ground tests a zero-g liquid hydrogen TVS. The primary objective of the zero-g TVS contract (Contract NAS8-39202) was to design a zero-g vent system that is innovative, simple, efficient, lightweight, and can be characterized through one-g tests. The TVS concept defined by Rockwell International was selected by NASA for further design evaluation. The 30 month activity was initiated in November 1991 and concluded on May 1994. Derived from text

31 ENGINEERING (GENERAL)

Includes vacuum technology; control engineering; display engineering; cryogenics; and fire prevention.

N94-36444# Lawrence Livermore National Lab., Livermore, CA.
MODIL CRYOCOOLER PRODUCIBILITY DEMONSTRATION PROJECT RESULTS
G. E. Cruz and R. M. Franks 24 Jun. 1993 56 p
(Contract W-7405-eng-48)
(DE93-019213; UCRL-ID-112216) Avail: CASI HC A04/MF A01

The production of large quantities of spacecraft needed by SDIO will require a cultural change in design and production practices. Low rates of production and the need for exceedingly high reliability have driven the industry to custom designed, hand crafted, and exhaustingly tested satellites. These factors have mitigated against employing design and manufacturing cost reduction methods commonly used in tactical missile production. Additional challenges to achieving production efficiencies are presented by the SDI spacecraft mission requirement. IR sensor systems, for example, are comprised of subassemblies and components that require the design, manufacture, and maintenance of ultra precision tolerances over challenging operational lifetimes. These IR sensors demand the use of reliable, closed loop, cryogenic refrigerators or active cryocoolers to meet stringent system acquisition and pointing requirements. The authors summarize some spacecraft cryocooler requirements and discuss their observations regarding Industry's current production capabilities of cryocoolers. The results of the Lawrence Livermore National Laboratory (LLNL) Spacecraft Fabrication and Test (SF and T) MODIL's Phase I producibility demonstration project are presented. The current project that involves LLNL and industrial participants is discussed. DOE

N94-36447# Sandia National Labs., Albuquerque, NM.
ADVANCES IN RAPID PROTOTYPING
C. L. Atwood, G. D. McCarty, B. T. Pardo, and E. A. Bryce 1993 8 p Presented at the Society of Manufacturing Engineers (SME) Rapid Prototyping and Manufacturing 1994 Conference, Dearborn, MI, 26-28 Apr. 1994
(Contract DE-AC04-94AL-85000)
(DE94-010075; SAND-93-3862C; CONF-9404133-1) Avail: CASI HC A02/MF A01

Recent advances in stereolithography and selective laser sintering have had a significant impact on the overall quality of parts produced using these rapid prototyping processes. The development and implementation of 3D System's QuickCast(trademark) resin and software for building investment casting patterns have proven to be major steps toward fabricating highly accurate patterns with very good surface finishes. Sandia uses patterns generated from rapid prototyping processes to reduce the cycle time and cost of fabricating prototype parts in support of a Sandia National Laboratories managed program called FASTCAST. As participants in the Beta test program for QuickCast(trademark) resin and software, they experienced a steep learning curve and were able to build accurate parts in a short period of time. It is now possible, using this technology, to produce highly accurate prototype parts as well as acceptable first article and small lot size production parts. They use the selective laser sintering (SLS) process to fabricate prototype wax patterns for investment casting. DTM Corporation recently introduced the use of their polycarbonate material for fabricating investment casting patterns. The polycarbonate material is processed significantly faster, with improved strength, dimensional stability, and without a support structure during the

build process. Sandia is currently changing from investment casting wax to polycarbonate for the fabrication of investment casting patterns using the SLS process. This presentation will focus on the successes with these new materials from the standpoints of application, accuracy, surface finish, and post processing. Also presented will be examples of parts manufactured by these processes. DOE

N94-36943*# National Aeronautics and Space Administration. Lewis Research Center, Cleveland, OH.
NEURAL NETWORK FOR POSITIONING SPACE STATION SOLAR ARRAYS
Ronald E. Graham and Paul P. Lin Jun. 1994 8 p Proposed for presentation at the Symposium on Automatic Control in Aerospace, Palo Alto, CA, 12-16 Sep. 1994; sponsored by the International Federation of Automatic Control
(NASA-TM-106656; E-8969; NAS 1.15:106656) Avail: CASI HC A02/MF A01

As a shuttle approaches the Space Station Freedom for a rendezvous, the shuttle's reaction control jet firings pose a risk of excessive plume impingement loads on Freedom solar arrays. The current solution to this problem, in which the arrays are locked in a feathered position prior to the approach, may be neither accurate nor robust, and is also expensive. An alternative solution is proposed here: the active control of Freedom's beta gimbals during the approach, positioning the arrays dynamically in such a way that they remain feathered relative to the shuttle jet most likely to cause an impingement load. An artificial neural network is proposed as a means of determining the gimbal angles that would drive plume angle of attack to zero. Such a network would be both accurate and robust, and could be less expensive to implement than the current solution. A network was trained via backpropagation, and results, which compare favorably to the current solution as well as to some other alternatives, are presented. Other training options are currently being evaluated. Author (revised)

N94-37029 Utah Univ., Salt Lake City, UT. Dept. of Physics.
MINIATURE THERMOACOUSTIC REFRIGERATOR Final Report
Orest G. Symko 21 Apr. 1994 21 p Limited Reproducibility: More than 20% of this document may be affected by microfiche quality
(Contract N00014-91-J-2015)
(AD-A280326) Avail: Issuing Activity (Defense Technical Information Center (DTIC))

A miniature thermoacoustic refrigerator was developed for cooling electronic components. The refrigerator is driven at 5,000 Hz by a piezoelectric driver and it consists of an acoustic resonator, a stack, and copper heat exchangers. The working fluid is pressurized helium gas between 10 to 20 atmospheres. Sound was produced with different piezoelectric drivers, a monomorph, a bimorph, and Tonpilz driver to achieve the highest intensity possible. Since the operating frequency is high, the refrigerator is compact, being about 10 cm long. Temperature differences of 12 C across the stack were achieved at sound levels of 160 dB. The performance of the refrigerator scaled with frequency according to existing models of thermoacoustic heat engines. DTIC

N94-37090 Nevada Univ. System, Reno, NV. Atmospheric Sciences Center.
FUNDAMENTALS STUDIES OF RADIAL WAVE THERMOACOUSTIC ENGINES Summary Report, 1 Oct. 1993 - 31 May 1994
W. Patrick Arnott Jun. 1994 38 p Limited Reproducibility: More than 20% of this document may be affected by microfiche quality
(Contract N00014-93-J-1131)
(AD-A280534) Avail: CASI HC A03

Research on radial wave thermoacoustic sound sources and refrigerators is described. Theoretical analysis and a computer program to implement it, were developed for acoustic quantities such as pressure, particle velocity, etc, and energy fluxes for thermoacoustic engines in the lowest radial mode of a cylindrical resonator. The program is currently most useful for computing prime mover operation both below, at, and beyond onset of oscillation. A short stack approximation was derived to compare the theoretical promise of thermoacoustic engines in the longitudinal and radial standing waves of cylindrical resonators. Results to date indicate radial wave engines are worth pursuing. DTIC

N94-37254*# National Aeronautics and Space Administration. Lewis Research Center, Cleveland, OH.
NUMERICAL ANALYSIS OF AN IMPINGING JET REACTOR FOR THE CVD AND GAS-PHASE NUCLEATION OF TITANIA
Suleyman A. Gokoglu, Gregory D. Stewart, Joshua Collins, and Daniel E. Rosner Jun. 1994 12 p Presented at the 1993 Fall Meeting, Boston, MA, 29 Nov. - 3 Dec. 1993; sponsored by the Materials Research Society
(Grant NGT-5-0377; RTOP 962-22-00)
(NASA-TM-106619; E-8905; NAS 1.15:106619) Avail: CASI HC A03/MF A01

We model a cold-wall atmospheric pressure impinging jet reactor to study the CVD and gas-phase nucleation of TiO2 from a titanium tetra-iso-propoxide (TTIP)/oxygen dilute source gas mixture in nitrogen. The mathematical model uses the computational code FIDAP and complements our recent asymptotic theory for high activation energy gas-phase reactions in thin chemically reacting sublayers. The numerical predictions highlight deviations from ideality in various regions inside the experimental reactor. Model predictions of deposition rates and the onset of gas-phase nucleation compare favorably with experiments. Although variable property effects on deposition rates are not significant (approximately 11 percent at 1000 K), the reduction rates due to Soret transport is substantial (approximately 75 percent at 1000 K). Author (revised)

N94-37452# Oak Ridge National Lab., TN.
REFRIGERATION AND AIR-CONDITIONING TECHNOLOGY WORKSHOP
P. J. Lewis, ed. and D. M. Counce, ed. 1993 274 p Workshop held at the Oak Ridge National Laboratory, Breckenridge, CO, 23-25 Jun. 1993
(Contract DE-AC05-84OR-21400)
(DE94-010813; ORNL-6797; CONF-9306166) Avail: CASI HC A12/MF A03

The Alternative Fluorocarbon Environmental Acceptability Study (AFEAS), a consortium of fluorocarbon manufacturers, and the U.S. Department of Energy (DOE) are collaborating on a project to evaluate the energy use and global warming impacts of CFC alternatives. The goal of this project is to identify technologies that could replace the use of CFC's in refrigeration, heating, and air-conditioning equipment; to evaluate the direct impacts of chemical emissions on global warming; and to compile accurate estimates of energy use and indirect CO2 emissions of substitute technologies. The first phase of this work focused on alternatives that could be commercialized before the year 2000. The second phase of the project is examining not-in-kind and next-generation technologies that could be developed to replace CFC's, HCFC's, and HFC's over a longer period. As part of this effort, Oak Ridge National Laboratory held a workshop on June 23-25, 1993. The preliminary agenda covered a broad range of alternative technologies and at least one speaker was invited to make a brief presentation at the workshop on each technology. Some of the invited speakers were unable to participate, and in a few cases other experts could not be identified. As a result, those technologies were not represented at the workshop. Each speaker was asked to prepare a five to seven page paper addressing six key issues concerning the technology he/she is developing. These points are listed in the sidebar. Each expert also spoke for 20 to 25 minutes at the workshop and answered questions from the other participants concerning the presentation and area of expertise. The primary goal of the presentations and discussions was to identify the developmental state of the technology and to obtain comparable data on system efficiencies. DOE

N94-37523# Joint Publications Research Service, Arlington, VA.
JPRS REPORT: SCIENCE AND TECHNOLOGY. CENTRAL EURASIA: ENGINEERING AND EQUIPMENT
26 Oct. 1993 33 p Transl. into ENGLISH from various Russian articles
(JPRS-UEQ-93-007) Avail: CASI HC A03/MF A01

Translated articles cover the following topics: transient gas dynamic processes in ramjet engines; aerodynamic characteristics of delta wings with detached leading edge shock wave at hypersonic flight velocities; effect of atmospheric density gradient on aerodynamic stabilization; measurement of target radar scattering characteristics using frequency synthesized signals; assessing survivability and ensuring safety of large axial-flow compressor blades; procedure for experimentally determining transient aerodynamic forces caused by flat vane cascade; analysis of aerodynamic interaction of profile and vortex; laser machine for balancing dynamically adjusted gyros; use of heat pumps in solar heat supply systems;

numerical simulation of deflagration transition to detonation in homogeneous combustible fuel mixture; and investigation of chemically nonequilibrium flow about bodies allowing for vibrational relaxation. CASI

N94-37524# Joint Publications Research Service, Arlington, VA.
JPRS REPORT: SCIENCE AND TECHNOLOGY. CENTRAL EURASIA: ENGINEERING AND EQUIPMENT
18 Nov. 1993 28 p Transl. into ENGLISH from various Russian articles (JPRS-UEQ-93-008) Avail: CASI HC A03/MF A01

Translated articles cover the following topics: measurement of gravitation interaction parameters on satellite; gravitational constant measurement during particle motion in neighborhood of libration points; simulation of dynamics of a high-velocity spinning flexible flying vehicle; anomaly estimation accuracy of inertial navigation system; observability in probe navigation problem; interaction of gyro system oscillation frequencies; imperfect shell dynamics and oscillation control; and variational principle of creep theory for prestressed body analysis. CASI

N94-37538# Joint Publications Research Service, Arlington, VA.
JPRS REPORT: SCIENCE AND TECHNOLOGY. CENTRAL EURASIA: ENGINEERING AND EQUIPMENT
15 Jul. 1993 47 p Transl. into ENGLISH from various Russian articles (JPRS-UEQ-93-005) Avail: CASI HC A03/MF A01

Translated articles cover the following topics: formulation of programmed aircraft motion control; floated-type linear acceleration integrated gyro with electromagnetic sensor suspension; ensuring unity of monitoring facilities and methods during life cycle stage of aviation engineering products; methods for forming rational requirements for monitoring fullness of functional systems and aircraft as whole; electron gun with ribbon beam; investigation of effect of airfoil vibrations on its edge noise; bending stability of composite cylindrical shell with longitudinal stiffening ribs; numerical investigation of conical shell flutter; intermediate asymptotics in nonlinear shell dynamics; dynamic stability critical load estimate of shells with holes; heat exchange on tip fins in hypersonic flow; boundary layer laminarization of vibrating wing; nonplanar airfoils with minimum induced drag; supersonic flow about cone under heat influx in vicinity of vertex; aero- and thermo-dynamics of high-altitude flight; discharge characteristics of converging-diverging nozzles with cylindrical minimal cross section path; experimental investigation of supersonic flow over wedges with longitudinal slots on windward side; on limit of motion of systems with dry friction; asymptotic integration of dynamic equations of elasticity theory in case of thin shells; dynamic electroelasticity problem for inhomogeneous cylinder; solution of linear and nonlinear boundary problems of shell and plate theory based on lines method; nonlinear elastic state near elliptic hole in orthotropic spherical shell; acoustic shock wave interaction with cylindrical piezoelectric ceramic shell located near planar boundary; analysis of straining characteristics of glass-reinforced plastic parabolic shells; experimental investigation into strained state of ribbed cylindrical shell under pulse loading; effect of elastic wave inertia during cylindrical shell rotation; clean room technology devices and systems; on effect of normal vibrations on tractive-gripping properties of walking machines; and electromechanical effect of high-current discharges on shell structures. CASI

32 COMMUNICATIONS AND RADAR

Includes radar; land and global communications; communications theory; and optical communications.

For related information see also *04 Aircraft Communications and Navigation* and *17 Space Communications, Spacecraft Communications, Command and Tracking.* For search and rescue see *03 Air Transportation and Safety,* and *16 Space Transportation.*

N94-36443# Los Alamos National Lab., NM.
TIPC USER MANUAL
T. A. Kelley, R. A. Roussel-Dupre, E. M. D. Symbalisty, and W. B. Clodius Nov. 1993 52 p
(Contract W-7405-eng-36)
(DE94-004470; LA-12644-M) Avail: CASI HC A04/MF A01

The Translonospheric Propagation Code (TIPC) computer program executes tasks related to the detection of vhf and uhf signals following propagation through the ionosphere. These tasks include: transionospheric propagation, signal detection, signal processing, delta time of arrival study, delta time of arrival uncertainty study, and signal reconstruction. The parameters needed to accomplish each task are defined and the process of using TIPC in each of these tasks is explained step-by-step. TIPC is also capable of saving these parameter values defined for the specific task. In addition, subroutine descriptions are identified. DOE

N94-36471# Sandia National Labs., Albuquerque, NM.
RADIALLY COMBINED 30 W, 14-16 GHz AMPLIFIER
F. Sechi (Microwave Power, Inc., Santa Clara, CA.), M. Bujatti (Microwave Power, Inc., Santa Clara, CA.), R. Knudson, and R. Bugos 1994 4 p Presented at the 1994 Institute of Electrical and Electronics Engineers (IEEE) Microwave Theory Technique Symposium, San Diego, CA, 23-27 May 1994
(Contract DE-AC04-94AL-85000)
(DE94-010078; SAND-94-0709C; CONF-9405112-2) Avail: CASI HC A01/MF A01

The paper describes a highly integrated 30 W power amplifier for a Synthetic Aperture Radar, operating in the 14-16 GHz band. The use of a waveguide radial combiner, a microstrip power divider and direct microstrip to waveguide miniaturized ceramic technology, leads to an unusually compact and accessible structure, well suited for commercial production. DOE

N94-36473 Navy Personnel Research and Development Center, San Diego, CA.
EVALUATION OF A TOOL FOR PRODUCING AND PRESENTING INTERACTIVE VIDEODISC JOB AIDS Final Report, Mar. 1991 - Sep. 1992
Hervey W. Stern Mar. 1994 26 p Limited Reproducibility: More than 20% of this document may be affected by microfiche quality
(AD-A278599; NPRDC-TR-94-8) Avail: Issuing Activity (Defense Technical Information Center (DTIC))

Hyperlinks provide rapid access to databases that contain all forms of media, including motion video. The use of hypermedia to present job task procedural training is widely perceived to be an efficient means of presentation. A prototype video-based workstation was developed and used to explore videodisc job aid development and use issues. Job aids for torpedo and Ellison door maintenance tasks were developed and presented on the workstation. Development issues are discussed and the results of the use of the two task aids are presented. Alternatives to the hypermedia software used in this experiment are explored. DTIC

N94-36567 Rutherford Appleton Lab., Chilton (England). Radio Communications Research Unit.
CHILBOLTON ADVANCED METEOROLOGICAL RADAR: A TOOL FOR MULTI-DISCIPLINARY ATMOSPHERIC RESEARCH
M. Thurai, J. D. Eastment, K. L. Morgan, and J. W. F. Goddard Feb. 1994 32 p
(PB94-167467; RAL-94-011) Avail: Issuing Activity (National Technical Information Service (NTIS))

The Chilbolton Advanced Meteorological Radar is used not only for propagation studies, but for cloud physics, hydrology, meteorology, and environment related programs. We describe here recent developments, which include the implementation of polarization-diversity techniques as well as added phase and Doppler capabilities. Section 2 deals with the reasons for developing the switched polarization method, whilst section 3 deals with its hardware realization. Some aspects of the theory behind the signal processing are considered in section 4, together with their software implementation and a brief description of the overall system. Finally, section 5 outlines the parameters measured by the Chilbolton Radar and gives examples of areas where the data are currently being used. NTIS

N94-36743# Army Research Lab., Watertown, MA. Materials Directorate.
PROCESSING, PACKAGING, AND CHARACTERIZATION OF ELECTROCERAMIC MATERIALS FOR PHASED ARRAY ANTENNAS Final Report
L. C. Sengupta, E. Ngo, S. Stowell, M. E. ODay, and R. Lancto May 1994 24 p
(AD-A280251; ARL-TR-448) Avail: CASI HC A03/MF A01

As a part of an effort to optimize the electronic device performance in

the ceramic phase shifter, various composites of BSTO combined with other nonelectrically active oxide ceramics have been formulated. In general, the composites have reduced dielectric constants and loss tangents and have high tunabilities, which reduce the overall impedance mismatch and the insertion loss of the device. The combination of electronic properties of these materials offer substantially higher operating frequencies, 10 GHz and above. Grain size and phase analysis have examined use SEM and x ray diffraction. The packaging of the phase shifter materials, electroding materials, electrode shapes, and encapsulation materials will be discussed. DTIC

N94-36753# International Centre for Theoretical Physics, Trieste (Italy).
INTENSITY OF WAVES DIFFRACTED FROM SYMMETRICAL PROFILE LAMELLAR GRATINGS
S. Chakrabarti and J. N. Chakravorty Aug. 1993 15 p
(DE94-611101; IC-93/267) Avail: CASI HC A03/MF A01 (US Sales Only)

We derive the expression for the intensity of the diffracted waves from a symmetrical profile lamellar grading (SLG). Such symmetrical structure may improve the performance of an ordinary lamellar grating. If suitably designed, its applicability may be extended to the millimeter to radio wave regions apart from the normal optical and near infrared region in which it is mostly used. Such millimeter wave SLG can have significant application in astronomy and astrophysics. By proper choice of geometrical parameters, an SLG may be used as a microwave antenna in space communication as well. DOE

N94-36754 Secure Solutions, Inc., La Jolla, CA.
ANALYSIS OF END-TO-END ENCRYPTION AND TRAFFIC FLOW CONFIDENTIALITY OPTIONS
20 Apr. 1994 98 p Limited Reproducibility: More than 20% of this document may be affected by microfiche quality
(Contract N00039-93-C-0099)
(AD-A278612; Rept-102-94-007U) Avail: Issuing Activity (Defense Technical Information Center (DTIC))

The report describes the utility of traffic flow confidentiality options that may be employed to reduce the risk of exposure to traffic analysis. This introduction to the report provides background information on why this research effort was initiated, the scope and objectives of the study, the approach used, and the organization of the report. Naval command and control systems are hosted on ship, submarine, shore, airborne, and space platforms that operate in a variety of environments. Diverse communication networks are used to support these command and control systems. These networks operate from the Extremely Low Frequency (ELF) to Extremely High Frequency (EHF) bands and employ both point-to-point and broadcast transmission techniques. A major thrust in Naval command and control is to interconnect these networks for the purpose of sharing information and improving the survivability of the overall network. DTIC

N94-36756 Alliance for Telecommunications Industry Solutions, Washington, DC. Standards Committee T1 Telecommunications.
NETWORK SURVIVABILITY PERFORMANCE Interim Report, FY 1991-FY 1992
Nov. 1993 88 p See also AD-M000332 Limited Reproducibility: More than 20% of this document may be affected by microfiche quality
(AD-A278746; TR-24) Avail: Issuing Activity (Defense Technical Information Center (DTIC))

This technical report has been developed to address the survivability of telecommunications networks including services. It responds to the need for a common understanding of, and assessment techniques for network survivability, availability, integrity, and reliability. It provides a basis for designing and operating telecommunications networks to user expectations for network survivability and a foundation for continuing industry activities in the subject area. This report focuses on the survivability of both public and private networks and covers a wide range of users. Two frameworks are established for quantifying and categorizing service outages, and for classifying network survivability techniques and measures. The performance of the network survivability techniques is considered; however, recommended objectives are not established for network survivability performance. DTIC

N94-36757 Alliance for Telecommunications Industry Solutions, Washington, DC. Standards Committee T1 Telecommunications.
NETWORK SURVIVABILITY PERFORMANCE (COMPUTER DISKETTE)
Nov. 1993 1 p See also AD-A278746
(AD-M000332; TR-24; NONP-DTIC-DK-94-14636) Avail: Issuing Activity (Defense Technical Information Center (DTIC))

File characteristics: Data file; 1 file. Physical description: 1 computer diskette; 3 1/2 in.; high density; 2.0MB. System requirements: Mac; Word. This technical report has been developed to address the survivability of telecommunications networks including services. It responds to the need for a common understanding of, and assessment techniques for network survivability, availability, integrity, and reliability. It provides a basis for designing and operating telecommunication networks to user expectations for network survivability. DTIC

N94-36810*# Nebraska Univ., Lincoln, NE. Coll. of Engineering and Technology.
[STUDIES ON IMAGE COMPRESSION AND IMAGE RECONSTRUCTION] Semiannual Status Report, 15 Dec. 1993 - 15 Jun. 1994
Khalid Sayood, Sekhar Nori, and A. Araj 15 Jun. 1994 106 p
(Grant NAG5-1612)
(NASA-CR-196304; NAS 1.26:196304) Avail: CASI HC A06/MF A02

During this six month period our works concentrated on three, somewhat different areas. We looked at and developed a number of error concealment schemes for use in a variety of video coding environments. This work is described in an accompanying (draft) Masters thesis. In the thesis we describe application of this techniques to the MPEG video coding scheme. We felt that the unique frame ordering approach used in the MPEG scheme would be a challenge to any error concealment/error recovery technique. We continued with our work in the vector quantization area. We have also developed a new type of vector quantizer, which we call a scan predictive vector quantization. The scan predictive VQ was tested on data processed at Goddard to approximate Landsat 7 HRMSI resolution and compared favorably with existing VQ techniques. A paper describing this work is included. The third area is concerned more with reconstruction than compression. While there is a variety of efficient lossless image compression schemes, they all have a common property that they use past data to encode future data. This is done either via taking differences, context modeling, or by building dictionaries. When encoding large images, this common property becomes a common flaw. When the user wishes to decode just a portion of the image, the requirement that the past history be available forces the decoding of a significantly larger portion of the image than desired by the user. Even with intelligent partitioning of the image dataset, the number of pixels decoded may be four times the number of pixels requested. We have developed an adaptive scanning strategy which can be used with any lossless compression scheme and which lowers the additional number of pixels to be decoded to about 7 percent of the number of pixels requested! A paper describing these results is included. Derived from text

N94-36931*# Notre Dame Univ., IN. Dept. of Electrical Engineering.
ERROR CONTROL TECHNIQUES FOR SATELLITE AND SPACE COMMUNICATIONS Semiannual Status Report
Daniel J. Costello, Jr. Aug. 1994 236 p
(Grant NAG5-557)
(NASA-CR-196302; NAS 1.26:196302) Avail: CASI HC A11/MF A03

Brief summaries of research in the following areas are presented: (1) construction of optimum geometrically uniform trellis codes; (2) a statistical approach to constructing convolutional code generators; and (3) calculating the exact performance of a convolutional code. Derived from text

N94-36955*# National Aeronautics and Space Administration. Lewis Research Center, Cleveland, OH.
A NOVEL TRANSITION BETWEEN RECTANGULAR WAVEGUIDE AND LAYERED RIDGE DIELECTRIC WAVEGUIDE
George E. Ponchak, Nihad I. Dib, and Linda P. B. Katehi Jun. 1994 7 p Proposed for presentation at European Microwave Conference, Cannes, France, 5-8 Sep. 1994 Sponsored by Institute of Electrical Engineers and Institute of Electrical and Electronics Engineers
(RTOP 307-51-00)
(NASA-TM-106661; E-8977; NAS 1.15:106661) Avail: CASI HC A02/MF A01

A novel transition between rectangular waveguide and layered ridge dielectric waveguide (LRDW) is reported. The transition is also suitable for use with image guide, insulated image guide, dielectric ridge waveguide and other open dielectric waveguides. Both experimental and theoretical data are presented which compare the new transition to three transitions reported in the literature. Author

N94-37032 Boston Univ., MA. Dept. of Electrical Computer and Systems Engineering.
SEGMENT-BASED ACOUSTIC MODELS FOR CONTINUOUS SPEECH RECOGNITION Progress Report, 1 Jan. - 31 Mar. 1994
Mari Ostendorf and J. R. Rohlicek 11 May 1994 14 p Limited Reproducibility: More than 20% of this document may be affected by microfiche quality
(Contract N00014-92-J-1778)
(AD-A280332) Avail: Issuing Activity (Defense Technical Information Center (DTIC))

This research aims to develop new and more accurate stochastic models for speaker-independent continuous speech recognition by extending previous work in segment-based modeling and by introducing a new hierarchical approach to representing intra-utterance statistical dependencies. These techniques, which have high computational costs because of the large search space associated with higher order models, are made feasible through rescoring a set of HMM-generated N-best sentence hypotheses. We expect these different modeling techniques to result in improved recognition performance over that achieved by current systems, which handle only frame-based observations and assume that these observations are independent given an underlying state sequence. In the past quarter, our focus has been on developing the theory and initial implementation behind high level models and search algorithms to accommodate these models. DTIC

N94-37127 Communications Research Centre, Ottawa (Ontario).
VHF ADAPTIVE ANTENNA DEVELOPMENT TASK Final Report
Robert W. Jenkins, U. A. Tenne-Sens, and Brian Lisson Jun. 1993 64 p Limited Reproducibility: More than 20% of this document may be affected by microfiche quality
(AD-A280320; CRC-93-003) Avail: Issuing Activity (Defense Technical Information Center (DTIC))

The work of the VHF adaptive antenna development task is reported. An adaptive-antenna test bed was assembled, including a programmable real-time signal processing system. Power-ratio inversion (PRI) and eigenvector-weighting (EV) adaptive algorithms were investigated analytically and by means of simulation, and implemented in two-element form on the real-time processor. These algorithms tend to separate incoming signals into different output channels according to their relative strengths, and do not require a priori information on the communications being received. DTIC

N94-37141# Air Force Inst. of Tech., Wright-Patterson AFB, OH. School of Engineering.
NOISE REDUCTION FOR SPEECH ENHANCEMENT USING NON-LINEAR WAVELET PROCESSING M.S. Thesis
Hassan Dehmani Jun. 1994 201 p
(AD-A280469; AFIT/GCE/ENC/94J-1) Avail: CASI HC A10/MF A03

The problem of speech enhancement presents many obstacles in the speech processing field. This thesis develops several speech de-noising systems that can be used in the time, Fourier, and wavelet domains. We present two thresholding techniques: soft and hard. The application of these thresholding techniques to noisy speech data is discussed. The combination of both wavelets and the Fourier domains with noisy phase restoration proves to yield the best results in terms of intelligibility. Informal listening tests were conducted in order to compare the effects and differences between the speech de-noising systems. DTIC

N94-37162# Defence Research Establishment Ottawa, Ottawa (Ontario).
ARRAY ELEMENT GAIN AND PHASE ESTIMATION IN THE PRESENCE OF INTERFERENCE
Eric K. Hung Dec. 1993 30 p
(AD-A280381; DREO-12111) Avail: CASI HC A03/MF A01

Presented is a method to estimate the element gains and phases of a sensor array when interfering signals, including specular multipath, are present. A movable calibration source is used. The element gains are derived from the relative output powers at the array elements. The element phases are obtained by transforming the array snapshots to make the source direction appear fixed and then maximizing a function constructed with the transformed snapshots. Computer simulations produce highly accurate estimates of element gains and phases when the signal directions are known and the signal-to-noise ratio is reasonably high. When the directions are not known, the set of element phase estimates contains an additional component which produces a bias in direction estimates. DTIC

N94-37183 Syracuse Univ., NY. Dept. of Electrical and Computer Engineering.
DISTRIBUTED DETECTION THEORY AND DATA FUSION Final Report, 15 Jan. 1993 - 14 Jan. 1994
Pramod K. Varshney Mar. 1994 5 p Limited Reproducibility: More than 20% of this document may be affected by microfiche quality
(Contract F49620-93-1-0122)
(AD-A280410; ECETR-1; AFOSR-94-0365TR) Avail: Issuing Activity (Defense Technical Information Center (DTIC))

Design of distributed order statistic constant false alarm rate (OS-CFAR) detection systems with data fusion was investigated. Its performance for different fusion rules and for a variety of nonhomogeneous backgrounds such as clutter edges and interfering targets was analyzed. Issues related to sampling and quantization in distributed detection systems were addressed. Sampling schemes for signal detection based on Ali-Silvey distance measures were derive. Performance enhancement over uniform sampling was shown. A number of collaborative research projects with Rome Laboratory engineers were performed. The most notable one was the development of a prototype of an expert system CFAR (ES-CFAR) processor. This processor intelligently selects the CFAR algorithm based upon the observed characteristics of the environment. Substantial performance improvement over a conventional CFAR processor was demonstrated. DTIC

N94-37206# Argonne National Lab., IL. Decision and Information Sciences Div.
A TWO-LEVEL FORMAL SPECIFICATION OF A DEFENSE COMMUNICATIONS SYSTEM
G. H. Chisholm and R. A. Kemmerer Apr. 1994 30 p
(Contract W-31109-eng-38)
(DE94-012117; ANL/DIS/TM-13) Avail: CASI HC A03/MF A01

Computer systems are being used in critical situations with sensitive data, which makes it very important to ensure that these systems perform as desired. The defense communications system contains particularly sensitive data. A two-level ASLAN formal specification of a defense communications system is presented. The ASLAN model is designed to enhance the understanding of critical requirements and demands of the defense communications system. For the top-level (high-level) specifications, the structural details of the actual network are abstracted to allow more time for examining the interactions between the sites and the network. At this level, DataGrams move through the network, although the actual routing decisions are not specified. More details are added in the second-level specification. At this level, structure is added to the network. DOE

N94-37218 Federal Aviation Administration, Atlantic City, NJ.
TERMINAL DOPPLER WEATHER RADAR (TDWR) BUILD 5 TEST AND EVALUATION MASTER PLAN (TEMP)
Elizabeth Turcich and Robert Cranston May 1994 81 p Limited Reproducibility: More than 20% of this document may be affected by microfiche quality
(AD-A280426; DOT/FAA/CT-TN94/2) Avail: CASI HC A05

This document presents the Terminal Doppler Weather Radar (TDWR), Build 5 enhancement, Test and Evaluation Master Plan (TEMP). This Build 5 TEMP identifies Operational Test and Evaluation (OT&E) objectives, responsibilities, resources, schedules, and critical test issues. The Build 5 enhancement consists of a Build 5A which provides connectivity to the Low Level Wind Shear Alert System (LLWAS) 2, and a Build 5B which provides connectivity to an LLWAS III. Build 5A displays LLWAS 2 wind data along with TDWR hazardous weather data on TDWR Geographic Situation Displays (GSD) and Ribbon Display Terminals (RDT). Build 5B provides additional capabilities such as having a Microburst Shear Integration

Algorithm (MSIA), TDWR/LLWAS 3 Integration Algorithm, 15-day archiving and TDWR, LLWAS 2 and LLWAS 3 data integration. DTIC

N94-37255*# Illinois Univ., Urbana-Champaign, IL. Electromagnetics Lab.

BASELINE ANTENNA DESIGN FOR SPACE EXPLORATION INITIATIVE Final Report

Y. L. Chen, M. A. Nasir, S. W. Lee, and Afroz Zaman May 1993 77 p
(Contract NCC3-216)
(NASA-CR-196298; NAS 1.26:196298) Avail: CASI HC A05/MF A01

A key element of the future NASA Space Exploration Initiative (SEI) mission is the lunar and Mars telecommunication system. This system will provide voice, image, and data transmission to monitor unmanned missions to conduct experiments, and to provide radiometric data for navigation. In the later half of 1991, a study was conducted on antennas for the Mars Exploration Communication. Six antenna configurations were examined: three reflector and three phased array. The conclusion was that due to wide-angle scan requirement, and multiple simultaneous tracking beams, phased arrays are more suitable. For most part, this report studies phased array antenna designs for two different applications for Space Exploration Initiative. It also studies one design for a tri-reflector type antenna. These antennas will be based on a Mars orbiting satellite. Derived from text

N94-37391# Sandia National Labs., Albuquerque, NM.

IMAGING TARGETS EMBEDDED IN A LOSSY HALF SPACE WITH SYNTHETIC APERTURE RADAR

A. W. Doerry, B. C. Brock, B. Boverie, and D. Cress 1994 5 p
Presented at the International Geoscience and Remote Sensing Symposium, Pasadena, CA, 8-12 Aug. 1994
(Contract DE-AC04-94AL-85000)
(DE94-010807; SAND-93-3898C; CONF-940814-1) Avail: CASI HC A01/MF A01

This paper addresses theoretical aspects of forming images from an airborne Synthetic Aperture Radar (SAR) of targets buried below the earth's surface. Soil is generally a lossy, dispersive medium, with wide ranging variability in these attributes depending on soil type, moisture content, and a host of other physical properties. Focussing a SAR subsurface image presents new dimensions of complexity relative to its surface-image counterpart, even when the soil's properties are known. This paper treats the soil as a lossy, dispersive half space, and presents a practical model for the radar echo-delay time to point scatterers within it. This model is then used to illustrate effects of refraction, dispersion, and attenuation on a SAR's phase histories, and the resulting image. Various data collection geometries and processing strategies are examined for both 2-Dimensional and 3-Dimensional SAR images. The conclusions from this work are that (1) focussing a SAR image must generally take into account both refraction and dispersion; (2) resolving targets at different depths in lossy soils requires perhaps unprecedented sidelobe attenuation, that for some soils may only be achievable with specialized window functions; (3) the impulse response of the soil itself places a practical limit on the usable bandwidth of the radar; and (4) dynamic ranges and sensitivities will need to be orders of magnitude greater than typical surface-imaging SAR's, leading to significant impact on SAR parameters, for example compressing the usable range of Pulse Repetition Frequencies (PRF's). DOE

N94-37393# Los Alamos National Lab., NM.

NRL HF PROPAGATION MEASUREMENTS BETWEEN GUADELOUPE AND PROVIDENCIALES DURING THE CRRES EXERCISES

1994 8 p
(Contracts W-7405-eng-36; DE-AI32-92AL-82529)
(DE94-012078; LA-SUB-94-79) Avail: CASI HC A02/MF A01

During this experiment series, scientists from NRL and LANL deployed high frequency radio transmitters on the Caribbean island of Guadeloupe and receiving equipment on the island of Providenciales in the Turks and Caicos Islands. The objective of these tests was twofold: (1) to determine the effect of injecting chemical agents known to affect the ambient plasma into a region of the ionospheric F layer subject to 'heating' by HF radiowaves; and (2) to assess the effect of the combined chemical and radiowave modification on HF skywave propagation through the modified ionosphere. Successful NRL channel probe measurements were made during experiments AA-3a (HF Induced Ionospheric Striations) and AA-4 (Ionospheric Focussed Heating). This report is intended to provide a brief description of some of the salient observational results from these two experiments. DOE

N94-37461*# West Virginia State Coll., Charleston, VA.

MAGNETIC EARTH IONOSPHERE RESONANT FREQUENCIES (NASA-MEIRF PROJECT) Progress Report

Jun. 1994 98 p
(Grant NAG5-1267)
(NASA-CR-196303; NAS 1.26:196303) Avail: CASI HC A05/MF A02

During this current reporting period, the project has focused on completing Phase 1 of the field monitoring work and documenting research results. Highlights of these efforts include presentations of papers at the annual joint meeting of the American Physical Society/American Association of Physics Teachers, April 18-22, 1994, in Crystal City, Virginia, and at the International Space, Time, and Gravitation Conference and Etoiles de L'Ecole Polytechnique Symposium, May 23-28, 1994, in St. Petersburg, Russia. Field measurements of the background ultra low frequency (ULF) electromagnetic spectrum in the New Mexico and Texas regions show interesting differences. Included are papers entitled 'Triplet Solution of the Twin Paradox' and 'Classical Electron Mass and Fields, Part 3.' CASI

N94-37736# Argonne National Lab., IL.

A GRAPHIC VIEW OF GEOMETRIC DIMENSIONING AND TOLERANCING

R. A. C. Swanson 1994 9 p
(Contract W-31-109-eng-38)
(DE94-011478; ANL/TD/CP-82680) Avail: CASI HC A02/MF A01

This paper points out a weakness frequently encountered in communication between Engineering Documents and Manufacturing Practices. In addition this paper gives an overview of a symbolic language designed to provide important communication between the Engineering Document and the Manufacturing process for every part and assembly. It will define the application of the characters used. Unlike the English language where the same word can have several meanings, the characters used in this symbolic language have only one. DOE

N94-37771 Department of the Navy, Washington, DC.

MTI COMPATIBLE COHERENT SIDELOBE CANCELLER Patent

Bernard L. Lewis, inventor (to Navy) 22 Mar. 1994 7 p Filed 23 Aug. 1974
(AD-D016300; US-Patent-5,296,865; US-Patent-Appl-SN-499962; US-Patent-Class-342-384) Avail: US Patent and Trademark Office

A system for instrumenting time sampled interference suppression, particularly in a side-lobe canceller system, is described. Interference signals are sampled just before a radar transmits on command of a sample gate or radar pulse, with main and auxiliary channel signals being delayed by the time between two successive samples. The two samples are then combined to allow interpolation such that weighting functions can be formed to adjust the delayed auxiliary signal so that interference in the delayed main channel signal can be suppressed at all times. By sampling just prior to radar transmission and interpolating between samples, cross modulation of clutter, and antenna scan error can be reduced in order that a side-lobe canceller system may be used compatibly with Moving Target Indicators (MTI). DTIC

N94-37813 National Defence Research Establishment, Stockholm (Sweden).

KONRAD: WIDE BAND DIGITAL HF RECEIVER

F. Oscarsson Jan. 1994 35 p See also PB94-149176 Limited Reproducibility: More than 20% of this document may be affected by microfiche quality
(PB94-184686; FOA-C-30745-3.6) Avail: Issuing Activity (National Technical Information Service (NTIS))

Electronic support measures (ESM) and spread spectrum techniques, i.e. direct sequence (DS) or frequency hopping (FH), in the HF band require a high dynamic range as well as a large instantaneous bandwidth in the receiver. This report describes an experimental digital receiver utilizing digitally implemented quadrature splitting and baseband translation. It is shown that the use of digital quadrature splitting improves the image rejection and that oversampling and digital filtering improves the dynamic range. The receiver is built of standard components which give a beneficial

cost/performance ratio. The focus is on the analog hardware of the experimental digital receiver named KONRAD. The report also serves as the manual for this receiver. NTIS

N94-37835# Department of the Navy, Washington, DC.
WAVEFRONT SIMULATOR FOR EVALUATING RF COMMUNICATION ARRAY SIGNAL PROCESSORS Patent Application
Steven B. Minarik, inventor (to Navy) 23 Oct. 1993 38 p
(AD-D016281; US-Patent-Appl-SN-145352; Navy-Case-75055) Avail: CASI HC A03/MF A01

A wavefront simulator that emulates plane wave propagation from multiple transmitting antennas is used to evaluate, in both a static and a dynamic manner, an array processor used in RF communications to determine the location of transmitting antennas and possibly to perform beamforming for cancelling the energy of an interfering transmitter. The wavefront simulator generates time delay signals, giving the appearance of being emitted from different transmitters or sources, and simulates those signals as being received by an antenna array associated with the array processor. The array processor utilizes the time delay signals to calculate, e.g., the angle of arrival of the signals from the emitting antennas. DTIC

N94-36617# McDonnell-Douglas Aerospace, Saint Louis, MO.
ICAAS PILOTED SIMULATION RESULTS
R. J. Landy, P. J. Halski, and R. P. Meyer *In* AGARD, Pointing and Tracking Systems May 1994 14 p (For primary document see N94-36616 12-18)
Copyright Avail: CASI HC A03/MF A02

N94-36629# GEC-Marconi Avionics Ltd., Basilon, Essex (England). Navigation and Electro-Optic Systems Div.
MULTIPLE TARGET TRACK-WHILE-SCAN IN THE AIRBORNE EO ENVIRONMENT
J. MacLean and M. G. McGuigan *In* AGARD, Pointing and Tracking Systems May 1994 12 p (For primary document see N94-36616 12-18)
Copyright Avail: CASI HC A03/MF A02

N94-36630# McMaster Univ., Hamilton (Ontario). Communications Research Lab.
MULTITARGET TRACK INITIATION USING A MODIFIED HOUGH TRANSFORM
T. Lo, J. Litva, H. Leung, and A. W. Bridgewater *In* AGARD, Pointing and Tracking Systems May 1994 8 p (For primary document see N94-36616 12-18)
Copyright Avail: CASI HC A02/MF A02

N94-36631# Defence Research Establishment Ottawa, Ottawa (Ontario).
RADAR TRACKING IN MULTIPATH: TECHNIQUES FOR IMPROVED PERFORMANCE
R. M. Turner, E. Riseborough, and E. Bosse *In* AGARD, Pointing and Tracking Systems May 1994 8 p (For primary document see N94-36616 12-18)
Copyright Avail: CASI HC A02/MF A02

N94-36634# Paramax Electronic, Inc., Montreal (Quebec).
CONTACT LEVEL FUSION OF RADAR AND IRST CONTACTS ON ALMOST ELECTROMAGNETICALLY SILENT PLATFORM
Francois Begin, Marc-Alain Simard, and Pierre Valin *In* AGARD, Pointing and Tracking Systems May 1994 9 p (For primary document see N94-36616 12-18)
Copyright Avail: CASI HC A02/MF A02

33 ELECTRONICS AND ELECTRICAL ENGINEERING

Includes test equipment and maintainability; components, e.g., tunnel diodes and transistors; microminiaturization; and integrated circuitry.

For related information see also *60 Computer Operations and Hardware* and *76 Solid-State Physics*.

N94-36514# Los Alamos National Lab., NM.
PULSED FIELD MAGNETS AT THE UNITED STATES NATIONAL HIGH MAGNETIC FIELD LABORATORY
L. J. Campbell, D. M. Parkin, J. E. Crow, H. J. Schneider-Muntau, and N. S. Sullivan 1993 16 p Presented at the Todai Symposium on Frontiers in High Magnetic Fields, Tokyo, Japan, 10-12 Nov. 1993
(Contract W-7405-eng-36)
(DE94-002624; LA-UR-93-3553; CONF-9311109-1) Avail: CASI HC A03/MF A01

The pulsed field facility of the National High Magnetic Field Laboratory (NHMFL) consists of four components. Those components now available are: (1) explosive driven flux compression; (2) capacitor-driven magnets; and (3) a 20 T superconducting magnet. The fourth component, a 60 T quasi-continuous magnet, has been designed and is scheduled for installation in early 1995. All magnets have He-4 cryostats giving temperatures from room temperature (RT) to 2.2-1.5 K. Dilution refrigerators for the superconducting 20 T magnet and the 50 T pulsed magnet will be installed by early 1994. A wide range of experiments has been completed within the past year. DOE

N94-36532 Science Research Council, Chilton (England).
FIRST RESULTS FROM A PROTOTYPE LEVEL-1 CALORIMETER TRIGGER SYSTEM FOR LHC, RD 27 (UK) COLLABORATION
I. P. Brawn, R. E. Carney, J. Garvey, R. J. Staley, and A. T. Watson Dec. 1993 12 p Presented at the 4th Conference on Calorimetry in High Energy Physics, Isola d'Elba, Italy, 19-25 Sep. 1993 See also N94-18845 Prepared in cooperation with Rutherford Appleton Lab., Chilton, England; Birmingham Univ., England; Westfield Coll., London, England; and European Organization for Nuclear Research, Geneva Switzerland
(PB94-167475; RAL-93-086) Avail: Issuing Activity (National Technical Information Service (NTIS))

As part of the RD27 collaboration, we have studied the problem of level-1 calorimetric triggering and have developed an algorithm to identify electromagnetic energy clusters. This algorithm has been incorporated into a prototype CMOS Application-Specific Integrated Circuit (ASIC) running as a pipelined processor at up to 67 MHz. In order to verify the operation of the processor in a realistic environment, a multi-ASIC demonstrator system has been constructed and used to instrument small regions of two prototype electromagnetic calorimeters in CERN test beams. We present here details of the demonstrator system and analysis of the data which have been taken so far. The results show that the demonstrator system performs successfully and recognizes electromagnetic clusters efficiently at LHC (Large Hadron Collider) rates. NTIS

N94-36557# Sandia National Labs., Albuquerque, NM.
HIGH TEMPERATURE SUPERCONDUCTING DIGITAL CIRCUITS AND SUBSYSTEMS
J. S. Martens, A. Pance, S. R. Whiteley, K. Char, M. F. Johansson, L. Lee, V. M. Hietala, J. R. Wendt, S. Y. Hou, and J. Phillips 1993 4 p Presented at the GOMAC 1993: Government Microcircuit Application Conference, New Orleans, LA, 1-4 Nov. 1993
(Contract DE-AC04-76DP-00789)
(DE94-001207; SAND-93-1060C; CONF-9311101-3) Avail: CASI HC A01/MF A01

The advances in the fabrication of high temperature superconducting devices have enabled the demonstration of high performance and useful digital circuits and subsystems. The yield and uniformity of the devices is sufficient for circuit fabrication at the medium scale integration (MSI) level with performance not seen before at 77 K. The circuits demonstrated to date include simple gates, counters, analog to digital converters, and shift registers. All of these are mid-sized building blocks for potential applications

in commercial and military systems. The processes used for these circuits and blocks will be discussed along with observed performance data.
DOE

N94-36781*# National Aeronautics and Space Administration. Langley Research Center, Hampton, VA.
ELECTRICALLY CONDUCTIVE, THERMALLY INSULATING CRYOGENIC CURRENT LEADS Patent Application
Stephanie A. Wise, inventor (to NASA) and Matthew W. Hooker, inventor (to NASA) 15 Mar. 1994 8 p
(NASA-Case-LAR-14964-1-CU; NAS 1.71:LAR-14964-1-CU;
US-Patent-Appl-SN-215793) Avail: CASI HC A02/MF A01

An electrically conductive, thermally insulating current lead assembly has been developed for cryogenic systems. This lead assembly consists of thick film elements of high temperature superconductive materials deposited onto a low thermal conductivity substrate. The superconductor elements provide current transport but minimize heat transfer. The substrate provides the mechanical durability necessary for cryogenic and other environments.
NASA

N94-36819*# National Aeronautics and Space Administration. Lewis Research Center, Cleveland, OH.
EVALUATION OF SOME SLOW-WAVE VANE STRUCTURES FOR AMINIATURE TRAVELING-WAVE TUBE AT 30 GHz
Frank Kavanagh (Analex Corp., Brook Park, OH.), Ben Ebihara, Thomas M. Wallett, and James A. Dayton, Jr. Jun. 1994 11 p
(Contract NAS3-25776; RTOP 235-01-1C)
(NASA-TM-106654; E-8967; NAS 1.15:106654) Avail: CASI HC A03/MF A01

The dispersion characteristics of six vane type slow wave structures were experimentally measured near 1 GHz to determine applicability in an electrostatically focused 30 GHz miniature traveling wave tube (TWT). From the measured results, the trapezoidal vane structure appeared to be the most promising exhibiting an interaction impedance equal to 337.9 ohms at beta(L)/pi equal to 0.3. A 30 GHz trapezoidal vane structure with coupling irises was fabricated using electrical discharge machining (EDM). This structure, however, was too lossy for a short electrostatically focused tube, but several of the structures are amenable to a tube with permanent magnetic focusing.
Author (revised)

N94-37033 Microelectronics Center of North Carolina, Research Triangle Park, NC.
FIELD EMITTER ARRAY RF AMPLIFIER DEVELOPMENT PROJECT PHASE ONE, CATHODE TECHNOLOGY DEVELOPMENT Special Technical Report, 21-26 Jan. 1994
W. D. Palmer and Gary E. McGuire 31 Jan. 1994 5 p Limited Reproducibility: More than 20% of this document may be affected by microfiche quality
(Contract MDA972-91-C-0028)
(AD-A280334; P9350017-STR3) Avail: Issuing Activity (Defense Technical Information Center (DTIC))

MCNC has duplicated and improved upon test results documented in the special technical report dated 17 Jan. 94. Tables detailing the measured 1 GHz modulation of the field emitter array anode current are included, as is a printout of an oscilloscope screen displaying our best results. A net power gain at 1 GHz of +7.74 dB was observed with 161.9 micro-A of modulated anode current at a DC bias current of 1.8 mA. Continued improvement is expected.
DTIC

N94-37035# Microelectronics Center of North Carolina, Research Triangle Park, NC.
FIELD EMITTER ARRAY RF AMPLIFIER DEVELOPMENT PROJECT. PHASE 1, OPTION 1
W. D. Palmer and Gary E. McGuire 25 Feb. 1994 6 p
(Contract MDA972-91-C-0028)
(AD-A280377; P9350017-STR4) Avail: CASI HC A02/MF A01

We have demonstrated anode current modulation at 1 GHz as reported in the special technical report of 31 Jan. 94. Eighty microns A peak of anode current modulated at 1 GHz was observed with only 2.02 V peak RF modulation on the gate electrode at a DC gate bias voltage of 118 V and DC anode emission current of 1.8 mA. The bias current is about 2 microns A per tip, which is in the acceptable range for RF amplification suggested in the literature. The measured RF performance is consistent with DC current-voltage measurements shown in the report. This data was collected on a small field emitter device with 1197 tips on 4 micrometer columns in order to minimize the field emitter array cell capacitance. The RF input power level was 0.14 W peak. The measured input impedance of the device at 1 GHz, 28 Omega, is quite high, indeed much higher than that reported for competing device structures. We believe that this silicon-based process is easily scalable to larger arrays which should result in net RF gain. We also believe that this demonstration shows that RF modulation of field emitter devices is feasible.
DTIC

N94-37053# Argonne National Lab., IL.
SODIUM/NICKEL-CHLORIDE BATTERY DEVELOPMENT
L. Redey, J. Prakash, D. R. Vissers, and E. J. Dowgiallo 28 Feb. 1994 4 p Presented at the 1993 Automotive Technology Development Contractors' Meeting, Dearborn, MI, 18-21 Oct. 1993
(Contract W-31-109-eng-38)
(DE94-011481; ANL/CMT/CP-82684; CONF-9310169-3) Avail: CASI HC A01/MF A01

The performance of the Ni/NiCl2 positive electrode for the Na/NiCl2 battery has been significantly improved compared to that of our earlier electrodes, representative for 1990. This improvement has been achieved by lowering the impedance and increasing the usable capacity through the use of chemical additives and a tailored electrode morphology. The improved electrode has excellent performance even at 250 C and can be recharged within one hour. The performance of this new electrode was measured by the conventional interrupted galvanostatic method and under simulated driving profiles. These measurements were used to project the performance of 40 to 60 kWh batteries built with this new electrode combined with the already highly developed sodium/beta(double prime)-alumina negative electrode. These calculated results yielded a specific power of 150-400 W/kg and a specific energy of 110-200 Wh/kg for batteries with single-tube and bipolar cell designs. This high performance, along with the high cell voltage, midtemperature operation, fast recharge capability, and short-circuited failure mode of the electrode couple, makes the Na/NiCl2 battery attractive for electric vehicle applications.
DOE

N94-37107 Microelectronics Center of North Carolina, Research Triangle Park, NC.
FIELD EMITTER ARRAY RF AMPLIFIER DEVELOPMENT PROJECT. PHASE 1, OPTION 1 Special Report, period ending 12 Jan. 1994
W. Devereux Palmer and Gary E. McGuire 17 Jan. 1994 8 p Limited Reproducibility: More than 20% of this document may be affected by microfiche quality
(Contract MDA972-91-C-0028)
(AD-A280513) Avail: CASI HC A02

MCNC is pleased to report successful demonstration of continuous-wave modulation of field emitter array anode current at 1 GHz. A 1, 1 97-tip array produced a net signal gain of 0.84 dB with DC anode current of 172 microA Based on test performance data, MCNC has satisfied all of the performance milestones for Phase 1 of the ARPA Field Emitter Array RF Amplifier Development Project. We understand that competing programs have also met the criteria, but by comparison with the data that has been published, we have exceeded their performance in many respects. As better data is collected, it will be promptly reported. Based on these preliminary results, we feel that the device produced at MCNC is the best choice for high-frequency operation.
DTIC

N94-37108 Microelectronics Center of North Carolina, Research Triangle Park, NC.
FIELD EMITTER ARRAY RF AMPLIFIER DEVELOPMENT PROJECT. CATHODE TECHNOLOGY DEVELOPMENT. PHASE 1 Final Report, 9 Sep. 1991 - 15 May 1994
W. Devereux Palmer and Gary E. McGuire Jun. 1994 40 p Limited Reproducibility: More than 20% of this document may be affected by microfiche quality
(Contract MDA972-91-C-0028; ARPA Order 8162)
(AD-A280515) Avail: CASI HC A03

This document presents the results of Phase I of the Field Emitter Array RF Amplifier Development Project. The primary goal of the Phase I performance period was the development of field emission cathodes with the following characteristics: 5 mA total emission current, 5 A/sq cm current

density, operation at an applied voltage of less than 250 V, greater than 1 hour lifetime, and emission current modulation at 1 GHz or greater. The basic fabrication process for silicon field emitter arrays was defined during the first 18 months of the contract performance period. During the final 12 months of the contract, the process was refined using statistical process control, with the goal of maximizing electrical yield on large arrays. The resulting devices met each of the program performance criteria. Arrays of up to 232,630 emitters, the largest field emitter arrays in any material to date, were successfully fabricated and electrically tested. The emission currents measured from these devices were the highest reported in the literature for silicon field emitter arrays. Techniques for further enhancing performance through the deposition of low work function and metal coatings were developed. Recommended directions for further research were defined for implementation under ARPA leadership. DTIC

N94-37111# Argonne National Lab., IL. Energy Technology Div.
FABRICATION AND PROPERTIES OF Ag-CLAD Bi-2223 CONDUCTORS AND MAGNETS
U. Balachandran, A. N. Iyer, P. Haldar, J. G. Hoehn, Jr., and L. R. Motowidlo Apr. 1994 6 p Presented at the International Workshop on Superconductivity: Critical Current of High-Temperature Superconductors and Related Topics, Kyoto, Japan, 6-9 Jun. 1994
(Contract W-31-109-eng-38)
(DE94-011502; ANL/ET/CP-81945; CONF-940651-3) Avail: CASI HC A02/MF A01

Significant progress has been made in fabricating Ag-clad Bi-2223 tapes that are suitable for practical applications. Long lengths (approximately 100 m) of tapes with high transport critical current density (J(sub c)) were fabricated by the powder-in-tube technique, starting with partially reacted precursor powders. The tapes were given appropriate heat treatment, and growth of the 2223 phase at each step of the heat treatment was studied. At 77 K, J(sub c) values of greater than 4 x 10(exp 4) A/sq cm and approximately 1.5 x 10(exp 4) A/sq cm have been achieved in short-length and approximately 70-m-long tapes, respectively. Compact and robust pancake coils were fabricated from the tapes by the wind-and-react method. Pancake coils were stacked in series to make magnets. The coils and magnets were characterized as a function of applied magnetic fields at various temperatures. A magnet containing 10 pancake coils (approximately 480 m of conductor) generated magnetic fields as high as 2.6, 1.8, 0.53, and 0.36 T at 4.2, 27, 64, and 77 K, respectively. Progress in the manufacturing of long lengths of Bi-2223 conductors and their performance are presented. DOE

N94-37190# Sandia National Labs., Albuquerque, NM.
SINGLE EVENT MIRRORING AND SENSE AMPLIFIER DESIGNS FOR ENHANCED SE TOLERANCE OF DRAMS
Kush Gulati (Vanderbilt Univ., Nashville, TN.) and Lloyd W. Massengill (Vanderbilt Univ., Nashville, TN.) 1994 6 p Presented at the 31st Annual International Nuclear and Space Radiation Effects Conference, Tucson, AZ, 18-22 Jul. 1994
(Contract DE-AC04-94AL-85000)
(DE94-010397; SAND-94-0534C; CONF-940726-11) Avail: CASI HC A02/MF A01

This paper investigates the applicability of existing SRAM SEU hardening techniques to conventional CMOS cross-coupled sense amplifiers used in DRAM structures. We propose a novel SEU mirroring concept and implementation for hardening DRAMs to bitline hits. Simulations indicate a 24-fold improvement in critical charge during the sensing state using a 10K T-Resistor scheme and a 28-fold improvement during the highly susceptible high impedance state using 2pF dynamic capacitance coupling. DOE

N94-37196# Sandia National Labs., Albuquerque, NM.
A PROPOSED SEU TOLERANT DRAM CELL
Ghasi R. Agrawal (Vanderbilt Univ., Nashville, TN.) and Lloyd W. Massengill (Vanderbilt Univ., Nashville, TN.) 1994 6 p Presented at the 31st Annual International Nuclear and Space Radiation Effects Conference, Tucson, AZ, 18-22 Jul. 1994
(Contract DE-AC04-94AL-85000)
(DE94-010758; SAND-94-0533C; CONF-940726-10) Avail: CASI HC A02/MF A01

A novel DRAM cell technology consisting of an access transistor and a bootstrapped storage capacitor with an integrated breakdown diode is proposed. This design offers considerable resistance to single event cell hits. The information change packet is shielded from an SE hit by placing the vulnerable node in a self-compensating standby state. The proposed cell is comparable in size to a conventional DRAM cell, but simulations show an improvement in critical charge of two orders of magnitude. DOE

N94-37213# Lawrence Livermore National Lab., Livermore, CA.
TIME-DEPENDENT SIMULATIONS OF FILAMENT PROPAGATION IN PHOTOCONDUCTING SWITCHES
P. W. Rambo, W. S. Lawson, C. D. Capps, and R. A. Falk May 1994 6 p Presented at the 3rd International Workshop on Computational Electronics, Portland, OR, 18-20 May 1994
(Contract W-7405-eng-48)
(DE94-012146; UCRL-JC-116301; CONF-9405147-2) Avail: CASI HC A02/MF A01

The authors present a model for investigating filamentary structures observed in laser-triggered photoswitches. The model simulates electrons and holes in two-dimensional cylindrical (r-z) geometry, with realistic electron and hole mobilities and field dependent impact ionization. Because of the large range of spatial and temporal scales to be resolved, they are using an explicit approach with fast, direct solution of the field equation. A flux limiting scheme is employed to avoid the time-step constraint due to the short time for resistive relaxation in the high density filament. Self-consistent filament propagation with speeds greater than the carrier drift velocity are observed in agreement with experiments. DOE

N94-37239# Oak Ridge National Lab., TN.
ORNL SUPERCONDUCTING TECHNOLOGY PROGRAM FOR ELECTRIC POWER SYSTEMS
R. A. Hawsey, comp. Apr. 1994 63 p
(Contract DE-AC05-84OR-21400)
(DE94-011471; ORNL/HTSPC-5) Avail: CASI HC A04/MF A01

The Oak Ridge National Laboratory (ORNL) Superconducting Technology Program is conducted as part of a national effort by the US Department of Energy's Office of Energy Efficiency and Renewable Energy to develop the technology base needed by US industry for commercial development of electric power applications of high-temperature superconductivity. The two major elements of this program are conductor development and applications development. This document describes the major research and development activities for this program together with related accomplishments. The technical progress reported was summarized from information prepared for the FY 1993 Annual Program Review held July 28--29, 1993. This ORNL program is highly leveraged by the staff and other resources of US industry and universities. In fact, nearly three-fourths of the ORNL effort is devoted to industrial competitiveness projects with private companies. Interlaboratory teams are also in place on a number of industry-driven projects. Patent disclosures, working group meetings, staff exchanges, and joint publications and presentations ensure that there is technology transfer to US industry. Working together, the collaborative teams are making rapid progress in solving the scientific and technical issues necessary for the commercialization of long lengths of practical high-temperature superconductor wire and wire products. DOE

N94-37241# Phytron Instruments, Inc., Mountain View, CA.
A CHARGE DISTRIBUTION ANALYSIS INSTRUMENT FOR CATALYSIS AND MATERIAL SCIENCE APPLICATIONS
F. Freund and J. J. Plombon May 1994 11 p
(Contract DE-FG49-93CE-15566)
(DE94-011587; DOE/CE-15566/T2) Avail: CASI HC A03/MF A01

The instrument has four basic components: OEM analytical balance, pivot point and capacitor plates for sensing and controlling the position of the long inverted pendulum, gas confinement tower and high voltage bias electrodes, and furnace. Work during the second quarter has resulted in detailed design of the pivot point and capacitive sensing and control assembly to be attached onto the platen of a Denver Instruments A-series analytical balance. DOE

N94-37295# Los Alamos National Lab., NM.
THEORY OF METAL INSULATOR TRANSITION IN STRONGLY CORRELATED ELECTRON SYSTEMS
M. Gulacsi and K. S. Bedell 1994 15 p Presented at the 6th

International Symposium on Integrated Ferroelectrics, Monterey, CA, 14-16 Mar. 1994
(Contract W-7405-eng-36)
(DE94-013135; LA-UR-94-1853; CONF-9403120-2) Avail: CASI HC A03/MF A01

A comprehensive theory of the correlation driven metal insulator transition in 1D and 2D strongly correlated electron systems is given. In both the 1D and 2D Hubbard model the metal insulator transition encountered close to half filling is of Pokrovsky-Talapov type. An important consequence of this in the 2D Hubbard model is the break down of the Fermi liquid theory. We also describe in detail the properties of the Pokrovsky-Talapov transition in 2D ferroelectrics. DOE

N94-37302# California Univ., Berkeley. Lawrence Berkeley Lab, CA. Dept. of Materials Science and Mineral Engineering.
DEVELOPMENT OF LOW DIELECTRIC CONSTANT ALUMINA-BASED CERAMICS FOR MICROELECTRONIC SUBSTRATES Ph.D. Thesis
S. J. Wu May 1993 114 p
(Contract DE-AC03-76SF-00098)
(DE94-011360; LBL-32657) Avail: CASI HC A06/MF A02

The performance of high speed computers depends not only on IC chips, but also on the signal propagation speed between these chips. The signal propagation delay in a computer is determined by the dielectric constant of the substrate material to which the IC chips are attached. In this study, a ceramic substrate with a low dielectric constant (k approx. 5.0) has been developed. When compared with the traditional alumina substrate (k approx. 10.0), the new material corresponds to a 37% decrease in the signal propagation delay. Glass hollow spheres are used to introduce porosity (k = 1.0) to the alumina matrix in a controlled manner. A surface coating technique via heterogeneous nucleation in aqueous solution has been used to improve the high temperature stability of these spheres. After sintering at 1,400 C, isolated spherical pores are uniformly distributed in the almost fully dense alumina matrix; negligible amounts of matrix defects can be seen. All pores are isolated from each other. Detailed analyses of the chemical composition find that the sintered sample consists of alpha-alumina, mullite and residual glass. Mullite is the chemical reaction product of alumina and the glass spheres. Residual glass exists because current firing conditions do not complete the mullitization reaction. The dielectric constant of the sintered sample is measured and then compared with the predicted value using Maxwell's model. Mechanical strength is evaluated by a four-point bending test. Although the flexural strength decreases exponentially with porosity, samples with 34% porosity (k approx. 5.0) still maintain adequate mechanical strength for the proper operation of a microelectronic substrate. DOE

N94-37306# Lawrence Livermore National Lab., Livermore, CA.
THE 24/36/48 CATHODE STRIP CHAMBER LAYOUT FOR SSC GEM DETECTOR MUON SUBSYSTEM
F. C. Belser, J. W. Clements, J. A. Horvath, S. M. Pratuch, T. J. Wenaus, D. M. Wright, C. R. Wuest, F. Nimblett, J. Paradiso, and P. Sebelius et al 15 Dec. 1993 17 p
(Contract W-7405-eng-48)
(DE94-012676; UCRL-CR-117195; GEM/TN-93-518) Avail: CASI HC A03/MF A01

The '48/48/48' phi-segmentation design for the Cathode Strip Chambers in the GEM Detector produces a number of coverage 'gaps' in phi and theta. A revised '24/36/48' phi-segmentation layout provides increased geometric coverage and a significant reduction in the number of chambers in the detector. This will increase physics performance while reducing the labor costs associated with building and installing chambers in the GEM Detector. This paper documents the physical layout of the proposed change to the baseline chamber arrangement. DOE

N94-37363 Sandia National Labs., Albuquerque, NM.
EVALUATING PLASTIC ASSEMBLY PROCESSES FOR HIGH RELIABILITY APPLICATIONS USING HAST AND ASSEMBLY TEST CHIPS
J. A. Emerson, J. N. Sweet, and D. W. Peterson 1994 5 p Presented at the 44th Electronic Components and Technology Conference, Washington, DC, 1-4 May 1994 Limited Reproducibility: More than 20% of this document may be affected by microfiche quality
(Contract DE-AC04-94AL-85000)
(DE94-010750; SAND-94-0912C; CONF-940596-4) Avail: CASI HC A01

We demonstrate the use of HAST and Assembly Test Chips to evaluate the susceptability of epoxy molding compounds to moisture induced corrosion of Al conductors. We show that the procedure is sufficiently sensitive to discriminate between assembly processes used by different molding facilities. Our data show that the location in time of the 'knee' in the failure distribution is dependent on material properties of the epoxy. Reducing the failure rate in the early or 'extrinsic' region of the time-failure distribution is key to achieving high reliability. We examine the failure modes in the extrinsic region for test chips encapsulated with a number of high quality molding compounds in an attempt to better understand this region. DOE

N94-37501*# Case Western Reserve Univ., Cleveland, OH. Dept. of Physics.
THEORETICAL STUDIES OF THE TRANSPORT PROPERTIES IN COMPOUND SEMICONDUCTORS Final Technical Report
Benjamin Segall 1994 60 p
(Contract NCC3-55)
(NASA-CR-196109; NAS 1.26:196109) Avail: CASI HC A04/MF A01

This final report is an overview of the work done on Cooperative Agreement NCC 3-55 with the Solid State Technology Branch of the NASA-Lewis Research Center (LeRC). Over the period of time that the agreement was in effect, the principal investigator and, in the last three years, the co-principal investigator worked on a significant number of projects and interacted with members of the Solid State Technology (SST) branch in a number of different ways. For the purpose of this report, these efforts will be divided into five categories: 1) work directly with experimental electrical transport studies conducted by members of the SST branch; 2) theoretical work on electrical transport in compound semiconductors; 3) electronic structure calculations which are relevant to the electrical transport in polytypes of SiC and SiC-AlN alloys; 4) the electronic structure calculations of polar interfaces; and 5) consultative and supportive activities related to experiments and other studies carried out by SST branch members. Work in these categories is briefly discussed. Derived from text

N94-37513# Sandia National Labs., Albuquerque, NM.
ROLE OF BURN-IN DURING QUALIFICATION TESTING
M. R. Shaneyfelt, D. M. Fleetwood, J. R. Schwank, T. L. Meisenheimer, and P. S. Winokur 1994 5 p Presented at the 31st Annual International Nuclear and Space Radiation Effects Conference, Tucson, AZ, 18-22 Jul. 1994
(Contract DE-AC04-94AL-85000)
(DE94-007864; SAND-94-0448C; CONF-940726-8) Avail: CASI HC A01/MF A01

Significantly different radiation responses have been observed for both transistors and integrated circuits (IC's) with and without preirradiation burn-in. The hardness assurance implications of these results and possible changes to the—MIL-STD's will be presented. DOE

N94-37634*# Houston Univ., TX. Inst. for Beam Particle Dynamics.
PERMANENT SUPERCONDUCTING MAGNETS FOR SPACE APPLICATIONS Final Techical Report, 1 May 1993 - 30 Apr. 1994
Roy Weinstein 30 Jul. 1994 18 p
(Contract NAS9-592)
(NASA-CR-196293; NAS 1.26:196293) Avail: CASI HC A03/MF A01

Work has been done to develop superconducting trapped field magnets (TFM's) and to apply them to a bumper-tether device for magnetic docking of spacecraft. The quality parameters for TFM's are J(c), the critical current of the superconductor, and d, the diameter of the superconducting tile. During this year we have doubled d, for production models, from 1 cm to 2 cm. This was done by means of seeding, an improved temperature profile in processing, and the addition of 1 percent Pt to the superconductor chemistry. Using these tiles we have set increasing records for the fields' permanent magnets. Magnets fabricated from old 1 cm tiles trapped 1.52 Tesla at 77K, 4.0T at 65K and 7.0T at 55K. The second of these fields broke a 17 year old record set at Stanford. The third field broke our own record. More recently using 2 cm tiles, we have trapped 2.3T at 77K, and 5.3T at 65K. We expect to trap IOT at 55K in this magnet in the near future. We have also achieved increases in J(c) using a method we developed for seeding U-235, and subsequently bombarding with neutrons. This method doubles J(c). We have not yet fabricated magnets from these tiles. During

this year we have increased production yields from 15 percent to 95 percent. We have explored the properties of a magnetic bumper-tether for spacecraft. We have measured the bumper forces, and their dependence on time, distance, and the field of the ordinary ferromagnet (used together with a TFM). We have accounted for 85 percent of the collision energy, and its transformation to magnetic energy and heat energy. We have learned to control the relative bumper and tether forces by controlling TFM and ferromagnetic field strengths. Author (revised)

N94-37738# Los Alamos National Lab., NM.
FLUX CREEP: ITS DEPENDENCE ON CURRENT DENISTY AND RELATION TO CRITICAL CURRENT DENSITIES FROM TRANSPORT AND MAGNETIC MEASUREMENTS
M. P. Maley, P. J. Kung, J. H. Cho, and J. O. Willis 1994 5 p Presented at the International Workshop on Superconductivity: Critical Current of High-temperature Superconductors and Related Topics, Kyoto, Japan, 6-9 Jun. 1994
(Contract W-7405-eng-36)
(DE94-011701; LA-UR-94-1418; CONF-940651-2) Avail: CASI HC A01/MF A01

Thermally activated flux motion dominates the transport properties of High Temperature Superconductors (HTS) over a large portion of the H-T phase diagram. The activation energy for this flux motion is generally a non-linear function, U(J), of the current density. We discuss methods and results of U(J) determination for HTS materials and implications for the critical current densities inferred from magnetic hysteresis measurements. DOE

N94-37759 Army Construction Engineering Research Lab., Champaign, IL. Energy and Utilities Systems Div.
UNDERSTANDING AND MANAGING POWER SYSTEM HARMONICS Final Report
Franklin H. Holcomb and Steve J. Briggs Apr. 1994 57 p Limited Reproducibility: More than 20% of this document may be affected by microfiche quality
(AD-A280627; CERL-TR-FE-94/10) Avail: Issuing Activity (Defense Technical Information Center (DTIC))

The application of nonlinear electrical loads has increased dramatically in recent years. These loads include computers and other equipment with switch-mode power supplies (SUPS), high-efficiency fluorescent lighting systems with electronic ballasts, and adjustable-speed drives with power electronic convertors. All these loads have nonlinear voltage-current characteristics, and all produce harmonic distortion on the power system. Harmonic currents in the power system can cause unusual effects in the wiring and surrounding power equipment. These effects include the overheating of wires, circuit breakers, transformers, and other equipment, the nuisance tripping of breakers, the saturation of various magnetic components in the system, and the creation of voltage distortion for all joining and connecting loads. This report offers a comprehensive overview of power system harmonics. It includes the causes, effects, and mitigation procedures for harmonic voltages and currents. Field engineers and designers of new facilities will find this report useful. DTIC

N94-37769 Department of the Navy, Washington, DC.
MICROWAVE DETECTION OF A SUPERCONDUCTING INFRARED SENSOR Patent
James C. Culbertson, inventor (to Navy), Harvey S. Newman, inventor (to Navy), Jeffrey M. Pond, inventor (to Navy), Stuart A. Wolf, inventor (to Navy), and Ulrich Strom, inventor (to Navy) 8 Feb. 1994 12 p Filed 5 Mar. 1992
(AD-D016297; US-Patent-5,285,067; US-Patent-Appl-SN-846633; US-Patent-Class-250-336.2) Avail: US Patent and Trademark Office

Highly sensitive infrared detectors can be made from superconducting microstrip transmission lines, having a single ground plane, a dielectric substrate on the ground plane, and a thin film path of superconducting oxide on the substrate. These microstrip transmission lines can be fabricated into resonant or non-resonant structures. The detectors operate by detecting changes in a microwave signal transmitted through the microstrip, measures in the amplitude, frequency or time domains. An embodiment of this invention is an asymmetric ring interferometer, with or without a metal segment in the shorter leg of the interferometer. Another embodiment of this invention is a meander path transmission line, which, in certain configurations, may be used as a single element array with very high resolution in the direction parallel to the meander lines. DTIC

N94-37775 Department of the Navy, Washington, DC.
TIME-GATED IMAGING THROUGH DEFENSE-SCATTERING MATERIALS USING STIMULATED RAMAN AMPLIFICATION Patent
John F. Reintjes, inventor (to Navy), Michael D. Duncan, inventor (to Navy), Rita Mahon, inventor (to Navy), Lawrence L. Tankersley, inventor (to Navy), and Ronald W. Waynant, inventor (to Navy) 4 Jan. 1994 12 p Filed 31 Mar. 1992
(AD-D016305; US-Patent-5,275,168; US-Patent-Appl-SN-861213; US-Patent-Class-128-665) Avail: US Patent and Trademark Office

An apparatus for the time-gated optical examination of objects that are part of, embedded in or viewed through dense scattering materials is disclosed. In a preferred embodiment, the apparatus comprises: a light source for producing a first light pulse and a pump light pulse, each of the first and pump light pulses having a preselected pulse width at a preselected pump wavelength; a Raman generator for shifting the wavelength of the first light pulse to a preselected Stokes wavelength to form Stokes light; a first optical train for transmitting the Stokes light through the dense scattering material to obtain Stokes light comprised of a relatively small, image-bearing signal component including unscattered Stokes light or Stokes light with minimal deviation due to scattering, light followed in time by a relatively large amount of light scattered by the dense scattering material; a Raman amplifier; an optical system for transporting the Stokes light from the dense scattering material to the Raman amplifier; a variable delay path disposed between the light source and the Raman amplifier for varying the transit time of the pump pulse to cause the pump pulse to overlap in time with the signal component of Stokes light at the Raman amplifier, the Raman amplifier only amplifying the signal component of Stokes light that is overlapped in time by the pump pulse; and a two-dimensional detector for detecting the amplified signal component of Stokes light. DTIC

N94-37832# Department of the Navy, Washington, DC.
CROSSPOINT ANALOG DATA SELECTOR Patent Application
Chester Fedor, inventor (to Navy) and Kevin C. Fitzpatrick, inventor (to Navy) 8 Dec. 1993 31 p
(AD-D016326; US-Patent-Appl-SN-169923; Navy-Case-75641) Avail: CASI HC A03/MF A01

A crosspoint analog data selector for coupling data received on a predetermined number of input channel lines onto a predetermined lesser number of output channel lines is described. The crosspoint analog data selector includes a selector section and a control section. The selector section includes two or more crosspoint switch sections, each crosspoint switch section including a predetermined number of input terminals and a predetermined number of output terminals. Each output terminal is individually energizable. Each input terminal is connected to a different input channel line, such that none of the input channel lines are connected to input terminals of multiple crosspoint switch sections. Each output terminal is connected to one of the output channel lines such that each output channel line is connected to an output terminal of each of the crosspoint switch sections. DTIC

N94-37840 Department of the Navy, Washington, DC.
PHASE SHIFTER FOR DIRECTLY SAMPLED BANDPASS SIGNALS Patent Application
William M. Waters, inventor (to Navy) 31 Mar. 1994 19 p Limited Reproducibility: More than 20% of this document may be affected by microfiche quality
(AD-D016320; US-Patent-Appl-SN-220718; Navy-Case-75328) Avail: CASI HC A03

A phase shifter is comprised of a filter for shifting the phase of directly sampled bandpass signals without having to convert to complex (I,Q) form. An application requiring a plurality of appropriately phase shifted signals is a phased array antenna. In the operation of the filter, a sequence of directly sampled data is passed into an exemplary three-stage storage unit to sequentially store r(n+1), r(n) and r(n-1) data samples. The r(n) sample is multiplied by cos phi to develop an r(n) cos phi signal, where phi is the desired phase shift angle. At the same time, the r(n+1) and r(n-1) data samples are subtracted from each other and the result is multiplied by w(sub 1) sin phi to develop the value W(sub 1)(r (n+1) - r(n-1)) sin phi.

The value is added to r(n) cos phi to produce an estimated sample value r(n)', which is approximately equivalent to data directly sampled from a signal phase-shifted by phi. DTIC

N94-37851 Helsinki Univ. of Technology, Espoo (Finland). Lab. of Telecommunications Technology.
NEUROCONTROL OF A BROADBAND (ATM) CLOS' SWITCHING NETWORK
J. Ma, T. Antonelis, and K. Rahko 15 Oct. 1993 8 p Limited Reproducibility: More than 20% of this document may be affected by microfiche quality
(PB94-179389) Avail: CASI HC A02

The paper presents a neural network central controller which is used for assigning an optimal path arrangement to a three-stage Clos' packet switching network with input and output buffers. A close look at the architecture of the neural network is taken, and system behavior is shown. NTIS

34 FLUID MECHANICS AND HEAT TRANSFER

Includes boundary layers; hydrodynamics; fluidics; mass transfer; and ablation cooling.

For related information see also *02 Aerodynamics* and *77 Thermodynamics and Statistical Physics.*

N94-36519*# Pennsylvania State Univ., University Park, PA. Dept. of Mechanical Engineering.
HYPERSONIC SHOCK/BOUNDARY-LAYER INTERACTION DATABASE: NEW AND CORRECTED DATA (Diskette Supplement)
Gary S. Settles and Lori J. Dodson Apr. 1994 46 p Diskette supplement: MS-DOS 3.5-inch 2SHD
(Grant NAG2-781)
(NASA-CR-177638; A-94078; NAS 1.26:177638;
NONP-NASA-Suppl-DK-94-19641) Avail: CASI Set A06 (HC,DK)

An effort was begun in 1989 at the Penn State University Gas Dynamics Laboratory to perform a critical review of the available hypersonic data and to assemble a selected database for purposes of computational fluid dynamics (CFD) code validation and turbulence modeling. The effort was sponsored by the National Aero-Space Plane (NASP) Program through NASA Ames Research Center, and was part of an overall task to develop compressible turbulence models. NASA-CR-177577, a database report on hypersonic shock wave / turbulent boundary-layer interactions, was the product of phase 1 of that effort. Phase 2 produced a similar database, NASA-CR-177610, covering the topics of attached hypersonic boundary layers in pressure gradients and compressible turbulent mixing layers. The present report represents the result of the third and final phase: namely, recent additions and corrections to the hypersonic shock wave / turbulent boundary-layer interaction database originally given in NASA-CR-177577. Seven new datasets are presented, consisting of supersonic and hypersonic experiments using single- and double-fin shock wave generators and a compression corner shock wave generator. Finally, typographical and other errors occurring in NASA-CR-177577 have been corrected in a section of the present report, including clarification of some issues which were raised with regard to the original database by users in the interim. A 3.5-inch double-sided high-density diskette is also provided as a supplement to this document. This diskette contains the complete data-tables in machine-readable ASCII files, formatted for MS-DOS computers. Individual ASCII files are given for each of the datasets, with file names keyed to the first authors. Author (revised)

N94-36550# Morgantown Technology Center, WV.
MULTIPHASE FLOW WITH INTERPHASE EXCHANGES (MFIX) DOCUMENTATION THEORY GUIDE
M. Syamlal, W. Rogers, and T. J. OBrien Dec. 1993 49 p
(DE94-000087; DOE/METC-94-1004) Avail: CASI HC A03/MF A01

This report describes the MFIX (Multiphase flow with interphase exchanges) computer model. MFIX is a general-purpose hydrodynamic model that describes chemical reactions and heat transfer in dense or dilute fluid-solids flows, flows typically occurring in energy conversion and chemical processing reactors. MFIX calculations give detailed information on pressure, temperature, composition, and velocity distributions in the reactors. With such information, the engineer can visualize the conditions in the reactor, conduct parametric studies and what-if experiments, and, thereby, assist in the design process. The MFIX model, developed at the Morgantown Energy Technology Center (METC), has the following capabilities: (1) mass and momentum balance equations for gas and multiple solids phases; (2) a gas phase and two solids phase energy equations; (3) an arbitrary number of species balance equations for each of the phases; (4) granular stress equations based on kinetic theory and frictional flow theory; (5) a user-defined chemistry subroutine; (6) three-dimensional Cartesian or cylindrical coordinate systems; (7) nonuniform mesh size; (8) impermeable and semi-permeable internal surfaces; (9) user-friendly input data file; (10) multiple, single-precision, binary, direct-access, output files that minimize disk storage and accelerate data retrieval; and (11) extensive error reporting. This report, which is Volume 1 of the code documentation, describes the hydrodynamic theory used in the model: the conservation equations, constitutive relations, and the initial and boundary conditions. The literature on the hydrodynamic theory is briefly surveyed, and the bases for the different parts of the model are highlighted. DOE

N94-36646*# National Aeronautics and Space Administration. Lewis Research Center, Cleveland, OH.
A FLUX SPLITTING SCHEME WITH HIGH-RESOLUTION AND ROBUSTNESS FOR DISCONTINUITIES
Yasuhiro Wada (National Aerospace Lab., Tokyo, Japan.) and Meng-Sing Liou Jan. 1994 25 p Presented at the 32nd Aerospace Sciences Meeting and Exhibit, Reno, NV, 10-13 Jan. 1994; sponsored by AIAA
(Contract NCC3-233; RTOP 505-90-5K)
(NASA-TM-106452; E-8311; ICOMP-93-50; NAS 1.15:106452; AIAA Paper 94-0083) Avail: CASI HC A03/MF A01

A flux splitting scheme is proposed for the general nonequilibrium flow equations with an aim at removing numerical dissipation of Van-Leer-type flux-vector splittings on a contact discontinuity. The scheme obtained is also recognized as an improved Advection Upwind Splitting Method (AUSM) where a slight numerical overshoot immediately behind the shock is eliminated. The proposed scheme has favorable properties: high-resolution for contact discontinuities; conservation of enthalpy for steady flows; numerical efficiency; applicability to chemically reacting flows. In fact, for a single contact discontinuity, even if it is moving, this scheme gives the numerical flux of the exact solution of the Riemann problem. Various numerical experiments including that of a thermo-chemical nonequilibrium flow were performed, which indicate no oscillation and robustness of the scheme for shock/expansion waves. A cure for carbuncle phenomenon is discussed as well. Author

N94-36724# Air Force Inst. of Tech., Wright-Patterson AFB, OH. School of Engineering.
COMPUTATIONAL INVESTIGATION OF AN IMPROVED COWL CONCEPT FOR HYPERSONIC PROPULSIVE NOZZLES M.S. Thesis
Mark c. Butler Jun. 1994 187 p
(AD-A280596; AFIT/GAE/ENY/94J-1) Avail: CASI HC A09/MF A02

The effects of placing a gas generator into the cowl of a hypersonic nozzle/afterbody were investigated computationally. Gas generator mass flow and deflection angle effects were analyzed for two nozzle/cowl geometries; an experimentally validated nozzle/cowl configuration evaluated at off-design conditions and a generic hypersonic propulsive nozzle evaluated at more realistic on design conditions. A combination of Van Leer flux-vector splitting and Roe flux-difference splitting finite volume computational algorithms were used to solve the unsteady two-dimensional Navier-Stokes equations based on planar, laminar flow, perfect gas equation of state assumptions. For the low speed off-design cases analyzed, gas generator effects on nozzle wall pressure recovery were similar to geometric cowl extension and deflection effects. Nozzle wall pressure recovery increased with increased mass flow. Gas generator deflections towards the nozzle wall provided dramatic improvements in pressure recovery and only small penalties were paid for deflections away from the wall. As the combustor exit pressure and trajectory Mach number increased, the nozzle flow became increasingly dominated by large initial expansions which minimized the overall effects of the gas generator and tended to push the gas generator effects on nozzle wall pressure recovery further downstream. DTIC

N94-36808*# MCAT Inst., San Jose, CA.
TURBULENCE MODELING OF FREE SHEAR LAYERS FOR HIGH PERFORMANCE AIRCRAFT Final Report
Douglas Sondak Oct. 1993 11 p
(Contract NCC2-663)
(NASA-CR-196137; NAS 1.26:196137; MCAT-94-12) Avail: CASI HC A03/MF A01

In many flowfield computations, accuracy of the turbulence model employed is frequently a limiting factor in the overall accuracy of the computation. This is particularly true for complex flowfields such as those around full aircraft configurations. Free shear layers such as wakes, impinging jets (in V/STOL applications), and mixing layers over cavities are often part of these flowfields. Although flowfields have been computed for full aircraft, the memory and CPU requirements for these computations are often excessive. Additional computer power is required for multidisciplinary computations such as coupled fluid dynamics and conduction heat transfer analysis. Massively parallel computers show promise in alleviating this situation, and the purpose of this effort was to adapt and optimize CFD codes to these new machines. The objective of this research effort was to compute the flowfield and heat transfer for a two-dimensional jet impinging normally on a cool plate. The results of this research effort were summarized in an AIAA paper titled 'Parallel Implementation of the k-epsilon Turbulence Model'. Appendix A contains the full paper. Derived from text

N94-36817# Institute of Sound and Vibration Research, Southampton (England). Fluid Dynamics and Acoustics Group.
AN ALGORITHM FOR THE AUTOMATIC CONTROL OF BOUNDARY LAYER FLOW
P. A. Nelson and J.-L. Rioual May 1994 39 p
(ISVR-TR-233) Avail: Issuing Activity (Inst. of Sound and Vibration Research, Univ. of Southampton, Southampton SO9 5NH, England)

Interest has recently been renewed in the use of distributed suction for the production of laminar flow over substantial areas of the surface of aircraft wings and engine nacelles. Suction may be most efficiently applied by using a number of independently controllable panels through which fluid is withdrawn. It becomes necessary to determine the distribution of suction flowrates that results in a given streamwise location of boundary layer transition with minimum power consumed in providing suction. This problem is formulated here in terms of nonlinearly constrained optimization. An algorithm is presented which has proved successful in both experimental and numerical studies in determining the optimal suction distribution. Of particular concern in this work is the stability of the basic algorithm and the limits to its rate of convergence to the optimal solution. Author

N94-36934# Nordquist (Bruce O.), Troy, OH.
THE ALTERNATIVE FACES OF TURBULENT FLOW
1994 31 p
(TM-5-94) Avail: CASI HC A03/MF A01

This document presents selected conclusions from a series of articles based on the author's development of a mathematical equation for the Reynolds stress in parallel flow. Perhaps the most significant result from this series of articles is the requirement that there must be both a mathematical and physical continuum between viscous transport and turbulent transport. Otherwise the essential boundary conditions for turbulent flow cannot be properly applied to the problem. Within this concept, the originally developed equation represents a cross flow turbulent energy equation that is incorporated into the streamwise mean flow momentum equation, thereby yielding a totally complete and accurate mathematical representation of the mean velocity and its derivatives for both laminar and turbulent parallel flow. Author

N94-36957*# Scientific Research Associates, Inc., Glastonbury, CT.
A COMBINED EXPERIMENT/COMPUTATIONAL STUDY OF FLOW IN TURBINE BLADE COOLING PASSAGE
D. G. N. Tse, J. P. Kreskovsky, S. J. Shamroth, and D. B. McGrath May 1994 137 p Original contains color illustrations
(Contract NAS3-26251; RTOP 505-62-52)
(NASA-CR-4584; E-8243; NAS 1.26:4584) Avail: CASI HC A07/MF A02; 39 functional color pages

Laser velocimetry was utilized to map the velocity field in a serpentine turbine blade cooling passage at Reynolds and Rotation numbers of up to 25.000 and 0.48. These results were used to assess the combined influence of passage curvature and Coriolis force on the secondary velocity field generated. A Navier-Stokes code (NASTAR) was validated against incompressible test data and then used to simulate the effect of buoyancy. The measurements show a net convection from the low pressure surface to high pressure surface. The interaction of the secondary flows induced by the turns and rotation produces swirl at the turns, which persisted beyond 2 hydraulic diameters downstream of the turns. The incompressible flow field predictions agree well with the measured velocities. With radially outward flow, the buoyancy force causes a further increase in velocity on the high pressure surface and a reduction on the low pressure surface. The results were analyzed in relation to the heat transfer measurements of Wagner et al. (1991). Predicted heat transfer is enhanced on the high pressure surfaces and in turns. The incompressible flow simulation underpredicts heat transfer in these locations. Improvements observed in compressible flow simulation indicate that the buoyancy force may be important. Author

N94-36960*# Virginia Univ., Charlottesville, VA. Dept. of Computer Science.
RESEARCH IN PARALLEL COMPUTING Semiannual Report, 1 Jan. - 30 Jun. 1994
James M. Ortega and Charles Henderson Jul. 1994 7 p
(Grant NAG1-1529)
(NASA-CR-196267; NAS 1.26:196267; SEAS-UVA/528474/CS95/102)
Avail: CASI HC A02/MF A01

This report summarizes work on parallel computations for NASA Grant NAG-1-1529 for the period 1 Jan. - 30 June 1994. Short summaries on highly parallel preconditioners, target-specific parallel reductions, and simulation of delta-cache protocols are provided. CASI

N94-36969*# Calspan-Buffalo Univ. Research Center, NY.
EXPERIMENTAL MEASUREMENTS AND ANALYTICAL ANALYSIS RELATED TO GAS TURBINE HEAT TRANSFER. PART 1: TIME-AVERAGED HEAT-FLUX AND SURFACE-PRESSURE MEASUREMENTS ON THE VANES AND BLADES OF THE SSME FUEL-SIDE TURBINE AND COMPARISON WITH PREDICTION. PART 2: PHASE-RESOLVED SURFACE-PRESSURE AND HEAT-FLUX MEASUREMENTS ON THE FIRST BLADE OF THE SSME FUEL-SIDE TURBINE Final Report
May 1994 173 p
(Grant NAG3-581)
(NASA-CR-196296; NAS 1.26:196296; CUBRC-640II-Pt-1/2) Avail: CASI HC A08/MF A02

Time averaged Stanton number and surface-pressure distributions are reported for the first-stage vane row, the first stage blade row, and the second stage vane row of the Rocketdyne Space Shuttle Main Engine two-stage fuel-side turbine. Unsteady pressure envelope measurements for the first blade are also reported. These measurements were made at 10 percent, 50 percent, and 90 percent span on both the pressure and suction surfaces of the first stage components. Additional Stanton number measurements were made on the first stage blade platform blade tip, and shroud, and at 50 percent span on the second vane. A shock tube was used as a short duration source of heated and pressurized air to which the turbine was subjected. Platinum thin-film heat flux gages were used to obtain the heat flux measurements, while miniature silicon-diaphragm flush-mounted pressure transducers were used to obtain the pressure measurements. The first stage vane Stanton number distributions are compared with predictions obtained using a version of STAN5 and a quasi-3D Navier-Stokes solution. This same quasi-3D N-S code was also used to obtain predictions for the first blade and the second vane.
Author (revised)

N94-36992*# Rensselaer Polytechnic Inst., Troy, NY. Dept. of Chemical Engineering.
DETERMINATION OF THE DISPERSION CONSTANT IN A CONSTRAINED VAPOR BUBBLE THERMOSYPHON
Sunando. DasGupta, Joel L. Plawsky, and Peter C. Wayner, Jr. 1993 9 p
(Grant NAG3-1399)
(NASA-CR-196124; NAS 1.26:196124; RPI/CHE/NASA-5-23390-4) Avail: CASI HC A02/MF A01

The isothermal profiles of the extended meniscus in a quartz cuvette

were measured in a gravitational field using an image analyzing interferometer which is based on computer enhanced video microscopy of the naturally occurring interference fringes. The experimental results for heptane and pentane menisci were analyzed using the extended Young-Laplace equation. These isothermal results characterized the interfacial force field in-situ at the start of the heat transfer experiments by quantifying the dispersion constant, which is a function of the liquid-solid system and cleaning procedures. The experimentally obtained values of the disjoining pressure and the dispersion constants were compared to that predicted from the DLP theory and good agreements were obtained. The measurements are critical to the subsequent non-isothermal experiments because one of the major variables in the heat sink capability of the CVBT is the dispersion constant. In all previous studies of micro heat pipes the value of the dispersion constant has been 'guesstimated'. One of the major advantages of the current glass cell is the ability to view the extended meniscus at all times. Experimentally. we find that the extended Young-Laplace equation is an excellent model for the force field at the solid-liquid-vapor interfaces.
Author

N94-37050# California Univ., Berkeley. Lawrence Berkeley Lab, CA.
LARGE-SCALE THREE-DIMENSIONAL GEOTHERMAL RESERVOIR SIMULATION ON PC'S
E. Antunez, G. Moridis, and K. Pruess Jan. 1994 8 p Presented at the 19th Workshop on Geothermal Reservoir Engineering, Stanford, CA, 18-20 Jan. 1994
(Contract DE-AC03-76SF-00098)
(DE94-011374; LBL-35192; CONF-940120-2) Avail: CASI HC A02/MF A01

TOUGH2, Lawrence Berkeley Laboratory's general purpose simulator for mass and heat flow and transport, was enhanced with the addition of a set of preconditioned conjugate gradient solvers and ported to a PC. The code was applied to a number of large three dimensional (3-D) geothermal reservoir problems with up to 10,000 grid blocks. Four test problems were investigated. The first two involved a single-phase liquid system, and a two-phase system with regular Cartesian grids. The last two involved a two-phase field problem with irregular gridding with production from and injection into a single porosity reservoir, and a fractured reservoir. The code modifications to TOUGH2 and its setup in the PC environment are described. Algorithms suitable for solving large matrices that are generally nonsymmetric and nonpositive definite are reviewed. Computational work per time step and CPU time requirements are reported as function of problem size. The excessive execution time and storage requirements of the direct solver in TOUGH2 limits the size of manageable 3-D reservoir problems to a few hundred grid blocks. The conjugate gradient solvers significantly reduced the execution time and storage requirements making possible the execution of considerably larger problems (10,000+ grid blocks). It is concluded that the current PC's provide an economical platform for running large-scale geothermal field simulations that just a few years ago could only be executed on mainframe computers.
DOE

N94-37060*# Purdue Univ., West Lafayette, IN. Aerospace Sciences Lab.
HOLT FILM WALL SHEAR INSTRUMENTATION FOR BOUNDARY LAYER TRANSITION RESEARCH Final Report
Steven P. Schneider 18 Jul. 1994 3 p
(Grant NAG1-1201)
(NASA-CR-196040; NAS 1.26:196040) Avail: CASI HC A01/MF A01

Measurements of the performance of hot-film wall-shear sensors were performed to aid development of improved sensors. The effect of film size and substrate properties on the sensor performance was quantified through parametric studies carried out both electronically and in a shock tube. The results show that sensor frequency response increases with decreasing sensor size, while at the same time sensitivity decreases. Substrate effects were also studied, through parametric variation of thermal conductivity and heat capacity. Early studies used complex dual-layer substrates, while later studies were designed for both single-layer and dual-layer substrates. Sensor failures and funding limitations have precluded completion of the substrate thermal-property tests.
Author

N94-37128 Maryland Univ., College Park, MD.
A FUNDAMENTAL STUDY OF HYPERSONIC UNSTARTS Final Report, 1 Oct. 1991 - 30 Sep. 1993
Mark J. Lewis 29 May 1994 65 p Limited Reproducibility: More than 20% of this document may be affected by microfiche quality
(Contract F49620-92-J-0006)
(AD-A280506; AFOSR-94-0362TR) Avail: Issuing Activity (Defense Technical Information Center (DTIC))

Activities for the first year were primarily focused on laying the groundwork for accomplishing the ultimate goals of this investigation. Required hardware and software was obtained and implemented. Grid generators were tested and one was selected, as was the primary computational tool. Activities in the second year were directed towards beginning the three dimensional Euler, then Navier-Stokes calculations, to establish a steady-state time accurate baseline, which could then be perturbed to study the influence of downstream disturbances. Both Euler and laminar Navier-Stokes solutions were calculated.
DTIC

N94-37176# Argonne National Lab., IL.
SIMULATION OF THREE-DIMENSIONAL MULTI-PHASE FLOW CHARACTERISTICS IN THE DESWIRL SECTION OF THE CDIF MHD POWER TRAIN
S. L. Chang, S. A. Lottes, and M. Petrick 1994 11 p Presented at the 32nd Symposium on Engineering Aspects of Magnetohydrodynamics (SEAM-32), Pittsburgh, PA, 27-30 Jun. 1994
(Contract W-31-109-eng-38)
(DE94-012644; ANL/ES/CP-81789; CONF-9406163-1) Avail: CASI HC A03/MF A01

A three-dimensional, two-phase, turbulent flow computer code was used to predict flow characteristics of seed particles and coal gas in the deswirl section of the CDIF MHD power train system. Seed material which has a great effect on the overall performance of the MHD system is injected in the deswirl against the swirling coal gas flow coming from the first stage combustor. While testing the MHD system, excessive seed material (70 percent more than theoretical value) was required to achieve design operating conditions. Calculations show that the swirling coal gas flow turns a 90 degree angle to minimize the swirl motion before entering a second stage combustor and many seed particles are too slow to react to the flow turning and deposit on the walls of the deswirl section. Some seed material deposited on the walls is covered by slag layer and removed from the gas flow. The reduction of seed material in the gas flow decreases MHD power generation significantly. A computational experiment was conducted and its results show that seed injection on the wall can be minimized by simply changing the seed injection and an optimum location was identified. If seed is injected from the location of choice, the seed deposition is reduced by a factor of 10 compared to the original case.
DOE

N94-37195# Sandia National Labs., Albuquerque, NM. Computational Fluid Dynamics Dept.
FLOW VISUALIZATION FOR LAGRANGIAN PARTICLE METHODS
Michael W. Glass and Steven N. Kempka 1994 9 p Presented at the 1994 International American Vacuum Society Users Conference, Boston, MA, 2-4 May 1994
(Contract DE-AC04-94AL-85000)
(DE94-010757; SAND-94-0839C; CONF-9405139-1) Avail: CASI HC A02/MF A01

In particle methods, each particle represents a finite region over which there is a distribution of the field quantity of interest. The field value at any point is calculated by summing the distribution functions for all the particles. This summation procedure does not require the use of any connectivities to generate continuous fields. Various AVS modules and networks have been developed that enable us to visualize the results from particle methods. This will be demonstrated by visualizing a numerical simulation of a rising, chaotic bubble. In this fluid dynamics simulation, each particle represents a region with a specified vorticity distribution.
DOE

N94-37362 Texas Univ., Austin, TX. Inst. for Fusion Studies.
MOMENTUM-ENERGY TRANSPORT FROM TURBULENCE DRIVEN BY PARALLEL FLOW SHEAR
J. Q. Dong, W. Horton, R. D. Bengtson, and G. X. Li Apr. 1994 45 p Limited Reproducibility: More than 20% of this document may be affected by microfiche quality

(Contracts DE-FG05-80ET-53088; DE-FG05-88ER-53266)
(DE94-012765; DOE/ET-53088/657; IFSR-657) Avail: CASI HC A03

The low frequency E x B turbulence driven by the shear in the mass flow velocity parallel to the magnetic field is studied using the fluid theory in a slab configuration with magnetic shear. Ion temperature gradient effects are taken into account. The eigenfunctions of the linear instability are asymmetric about the mode rational surfaces. Quasilinear Reynolds stress induced by such asymmetric fluctuations produces momentum and energy transport across the magnetic field. Analytic formulas for the parallel and perpendicular Reynolds stress, viscosity, and energy transport coefficients are given. Experimental observations of the parallel and poloidal plasma flows on TEXT-U are presented and compared with the theoretical models. DOE

N94-37390# Lawrence Livermore National Lab., Livermore, CA.
EVOLUTION OF TURBULENT FIELDS IN EXPLOSIONS
A. L. Kuhl, J. B. Bell, R. E. Ferguson, K. Y. Chien, J. P. Collins, and M. L. Lyons Dec. 1993 22 p Presented at the Japanese National Symposium on Shock Waves, Chiba, Japan, 20-23 Jan. 1994
(Contract W-7405-eng-48)
(DE94-010405; UCRL-JC-115923; CONF-940181-1) Avail: CASI HC A03/MF A01

Explosions always contain turbulent mixing regions, e.g.: boundary layers, shear layers, wall jets and unstable interfaces. The inherent unsteadiness of turbulent mixing in explosions, and the lack of sufficient data, pose insurmountable difficulties for turbulence modeling of such flows. Proposed here is a direct numerical simulation approach where the three-dimensional (3-D) conservation laws are integrated via a high-order Godunov method. Adaptive Mesh Refinement (AMR) is used to capture the convective mixing processes on the computational grid. Then, an azimuthal-averaging operator is applied to the 3-D solution in order to extract the instantaneous mean and fluctuating components of the turbulent field. This methodology is applied to the numerical simulation of the turbulent wall jet and dusty boundary layer flow induced by a point explosion above a ground surface. Principal results include the evolution of the turbulent velocity field near the surface. During the wall jet phase, the mean profiles resemble our previous two-dimensional calculations, while the velocity fluctuation profiles and Reynolds stress profiles are qualitatively similar to measurements of self-preserving wall jets. During the boundary layer phase, the mean velocity profile evolved with time, e.g.: initially it agreed with measurements of a dusty boundary layer behind a shock; at intermediate times it resembled the dusty boundary layer profiles measured in a wind tunnel; while at late times, it approached a 1/7 power-law profile. Velocity fluctuation profiles were qualitatively similar to those measured for a turbulent boundary layer on a flat plate. The methodology can be used to predict the evolution of other turbulent fields such as dust clouds, axisymmetric jets, fireball instabilities, and dusty boundary layers in shock tube and wind tunnel flows. DOE

N94-37455*# National Aeronautics and Space Administration. Langley Research Center, Hampton, VA.
HYPERSONIC, NONEQUILIBRIUM FLOW OVER THE FIRE 2 FOREBODY AT 1634 SEC
Lin Hartung Chambers Jul. 1994 18 p
(RTOP 232-01-04-04)
(NASA-TM-109141; NAS 1.15:109141) Avail: CASI HC A03/MF A01

The numerical simulation of hypersonic flow in thermochemical nonequilibrium over the forebody of the FIRE 2 vehicle at 1634 sec in its trajectory is described. The simulation was executed on a Cray C90 with the program Langley Aerodynamic Upwind Relaxation Algorithm (LAURA) 4.0.2. Code setup procedures and sample results, including grid refinement studies, are discussed. This simulation relates to a study of radiative heating predictions on aerobrake type vehicles. Author (revised)

N94-37507*# National Aeronautics and Space Administration. Lewis Research Center, Cleveland, OH.
COUPLED MARANGONI-BENARD/RAYLEIGH-BENARD INSTABILITY WITH TEMPERATURE DEPENDENT VISCOSITY
J. Raymond Lee Skarda and Frances E. McCaughan Jul. 1994 12 p Proposed for presentation at the Winter Annual Meeting, Chicago, IL, 6-11 Nov. 1994; sponsored by ASME
(RTOP 674-24-05)
(NASA-TM-106646; E-8952; NAS 1.15:106646) Avail: CASI HC A03/MF A01

The onset of convection induced by coupled surface tension gradient and buoyancy forces is investigated with temperature dependent viscosity. Both surface tension and viscosity are assumed to vary linearly with temperature. The limiting case, Ma=0, is the buoyancy driven convection problem typically referred to as the Rayleigh-Benard stability problem. The other limiting case, Ra=0, is the surface tension (gradient) driven flow problem referred to as the Marangoni-Benard problem. The equations and boundary conditions obtained from the linear analysis are solved numerically as a generalized eigenvalue problem. Neutral stability curves for different viscosity slopes have been generated for the Marangoni-Benard and Rayleigh-Benard problems. It is shown that the curves can be collapsed to a single curve by appropriately scaling the results for each of the limiting cases. The critical Marangoni number is determined as a function of the slope of the viscosity temperature variation, epsilon, for different values of the Rayleigh number. When the viscosity decreases linearly with temperature, the coupled buoyancy-surface tension problem, including the limiting cases of Ra=0 and Ma=0, is found to be more stable than the constant viscosity case. Author (revised)

N94-37525*# Wales Univ., Swansea. Dept. of Civil Engineering.
UNSTRUCTURED GRID METHODS FOR THE SIMULATION OF 3D TRANSIENT FLOWS Final Report, 1 Jan. 1992 - 31 Dec. 1993
K. Morgan, J. Peraire, and J. Peiro 1 Jun. 1994 19 p
(Grant NAGw-2962)
(NASA-CR-196139; NAS 1.26:196139) Avail: CASI HC A03/MF A01

A description of the research work undertaken under NASA Research Grant NAGW-2962 has been given. Basic algorithmic development work, undertaken for the simulation of steady three dimensional inviscid flow, has been used as the basis for the construction of a procedure for the simulation of truly transient flows in three dimensions. To produce a viable procedure for implementation on the current generation of computers, moving boundary components are simulated by fixed boundaries plus a suitably modified boundary condition. Computational efficiency is increased by the use of an implicit time stepping scheme in which the equation system is solved by explicit multistage time stepping with multigrid acceleration. The viability of the proposed approach has been demonstrated by considering the application of the procedure to simulation of a transonic flow over an oscillating ONERA M6 wing. Derived from text

N94-37544# Pittsburgh Univ., Pittsburgh, PA. Dept. of Mechanical Engineering.
NUMERICAL STUDY OF THE FLOW OF GRANULAR MATERIALS DOWN AN INCLINED PLANE
K. R. Rajagopal 1994 19 p
(Contract DE-AC22-91PC-90180)
(DE94-010729; DOE/PC-90180/T10) Avail: CASI HC A03/MF A01

In the previous report the governing equations for the flow of granular materials down an inclined plane, modeled by the constitutive theory proposed by Boyle and Massoudi (1990), were derived. These equations are solved numerically subject to the appropriate boundary conditions. The effect of various non-dimensional parameters on the volume fraction and velocity are presented in the form of graphs. In this report we derive the governing equations for the flow of granular materials down an inclined plane using the continuum model proposed by Rajagopal and Massoudi (cf. Goodman and Cowin (1971, 1972), Rajagopal and Massoudi (1990)). Here, we study the effect of the various forms of the materials parameters (Beta's) as discussed in Cases 1, 2, and 3. The numerical solutions for case 1 and case 2 were presented in the earlier reports and case 3 is presented in the form of graphs for various nondimensional parameters. Also, the solutions from Cases 1, 2, and 3 are compared to see how the structure of the material parameters affect the velocity, volume fraction and temperature fields. DOE

N94-37605*# Institute for Computer Applications in Science and Engineering, Hampton, VA.
THE STABILIZING EFFECT OF COMPRESSIBILITY IN TURBULENT SHEAR FLOW Final Report
S. Sarkar (California Univ., San Diego, CA.) Jun. 1994 39 p

(Contract NAS1-19480; NAG1-1516; RTOP 505-90-52-01)
(NASA-CR-194932; NAS 1.26:194932; ICASE-94-46) Avail: CASI HC A03/MF A01

Direct numerical simulation of turbulent homogeneous shear flow is performed in order to clarify compressibility effects on the turbulence growth in the flow. The two Mach numbers relevant to homogeneous shear flow are the turbulent Mach number M(t) and the gradient Mach number M(g). Two series of simulations are performed where the initial values of M(g) and M(t) are increased separately. The growth rate of turbulent kinetic energy is observed to decrease in both series of simulations. This 'stabilizing' effect of compressibility on the turbulent energy growth rate is observed to be substantially larger in the DNS series where the initial value of M(g) is changed. A systematic companion of the different DNS cues shows that the compressibility effect of reduced turbulent energy growth rate is primarily due to the reduced level of turbulence production and not due to explicit dilatational effects. The reduced turbulence production is not a mean density effect since the mean density remains constant in compressible homogeneous shear flow. The stabilizing effect of compressibility on the turbulence growth is observed to increase with the gradient Mach number M(g) in the homogeneous shear flow DNS. Estimates of M(g) for the mixing and the boundary layer are obtained. These estimates show that the parameter M(g) becomes much larger in the high-speed mixing layer relative to the high-speed boundary layer even though the mean flow Mach numbers are the same in the two flows. Therefore, the inhibition of turbulent energy production and consequent 'stabilizing' effect of compressibility on the turbulence (over and above that due to the mean density variation) is expected to be larger in the mixing layer relative to the boundary layer in agreement with experimental observations. Author

N94-37606*# Institute for Computer Applications in Science and Engineering, Hampton, VA.
TOWARDS ENHANCING AND DELAYING DISTURBANCES IN FREE SHEAR FLOWS Final Report
W. O. Criminale (Washington Univ., Seattle, WA.), T. L. Jackson, and D. G. Lasseigne Jun. 1994 29 p Submitted for publication
(Contract NAS1-19480; RTOP 505-90-52-01)
(NASA-CR-194945; NAS 1.26:194945; ICASE-94-56) Avail: CASI HC A03/MF A01

The family of shear flows comprising the jet, wake, and the mixing layer are subjected to perturbations in an inviscid incompressible fluid. By modeling the basic mean flows as parallel with piecewise linear variations for the velocities, complete and general solutions to the linearized equations of motion can be obtained in closed form as functions of all space variables and time when posed as an initial value problem. The results show that there is a continuous as well as the discrete spectrum that is more familiar in stability theory and therefore there can be both algebraic and exponential growth of disturbances in time. These bases make it feasible to consider control of such flows. To this end, the possibility of enhancing the disturbances in the mixing layer and delaying the onset in the jet and wake is investigated. It is found that growth of perturbations can be delayed to a considerable degree for the jet and the wake but, by comparison, cannot be enhanced in the mixing layer. By using moving coordinates, a method for demonstrating the predominant early and long time behavior of disturbances in these flows is given for continuous velocity profiles. It is shown that the early time transients are always algebraic whereas the asymptotic limit is that of an exponential normal mode. Numerical treatment of the new governing equations confirm the conclusions reached by use of the piecewise linear basic models. Although not pursued here, feedback mechanisms designed for control of the flow could be devised using the results of this work. Author

N94-37635*# West Virginia Univ., Morgantown, VA. Dept. of Mechanical and Aerospace Engineering.
PROJECT JOVE Final Report
M. J. Lyell Aug. 1994 116 p
(Grant NAG8-149)
(NASA-CR-196292; NAS 1.26:196292) Avail: CASI HC A06/MF A02

The goal of this project is to investigate new areas of research pertaining to free surface-interface fluids mechanics and/or microgravity which have potential commercial applications. This paper presents an introduction to ferrohydrodynamics (FHD), and discusses some applications. Also, computational methods for solving free surface flow problems are presented in detail. Both have diverse applications in industry and in microgravity fluids applications. Three different modeling schemes for FHD flows are addressed and the governing equations, including Maxwell's equations, are introduced. In the area of computational modeling of free surface flows, both Eulerian and Lagrangian schemes are discussed. The state of the art in computational methods applied to free surface flows is elucidated. In particular, adaptive grids and re-zoning methods are discussed. Additional research results are addressed and copies of the publications produced under the JOVE Project are included. Author

N94-37724# Argonne National Lab., IL.
A NONCONSERVATIVE SCHEME FOR ISENTROPIC GAS DYNAMICS
Gui-Qiang Chen and Jian-Guo Liu 1994 21 p
(Contract W-31-109-eng-38)
(DE94-011488; ANL/MCS/PP-74001) Avail: CASI HC A03/MF A01

In this paper, we construct a second-order nonconservative for the system of isentropic gas dynamics to capture the physical invariant regions for preventing negative density, to treat the vacuum singularity, and to control the local entropy from dramatically increasing near shock waves. The main difference in the construction of the scheme discussed here is that we use piecewise linear functions to approximate the Riemann invariants w and z instead of the physical variables rho and m. Our scheme is a natural extension of the schemes for scalar conservation laws and it can be numerically implemented easily because the system is diagonalized in this coordinate system. Another advantage of using Riemann invariants is that the Hessian matrix of any weak entropy has no singularity in the Riemann invariant plane w-z, whereas the Hessian matrices of the weak entropies have singularity at the vacuum points in the physical plane p-m. We prove that this scheme converges to an entropy solution for the Cauchy problem with L(sup (infinity)) initial data. By convergence here we mean that there is a subsequent convergence to a generalized solution satisfying the entropy condition. As long as the entropy solution is unique, the whole sequence converges to a physical solution. This shows that this kind of scheme is quite reliable from theoretical view of point. In addition to being interested in the scheme itself, we wish to provide an approach to rigorously analyze nonconservative finite difference schemes. DOE

N94-37726# Sandia National Labs., Albuquerque, NM.
ANALYSIS OF ANELASTIC FLOW AND NUMERICAL TREATMENT VIA FINITE ELEMENTS
M. J. Martinez May 1994 44 p
(Contract DE-AC04-94AL-85000)
(DE94-012141; SAND-94-0320) Avail: CASI HC A03/MF A01

In this report, we reconsider the various approximations made to the full equations of motion and energy transport for treating low-speed flows with significant temperature induced property variations. This entails assessment of the development of so-called anelastic for low-Mach number flows outside the range of validity of the Boussinesq equations. An integral part of this assessment is the development of a finite element-based numerical scheme for obtaining approximate numerical solutions to this class of problems. Several formulations were attempted and are compared. DOE

35 INSTRUMENTATION AND PHOTOGRAPHY

Includes remote sensors; measuring instruments and gages; detectors; cameras and photographic supplies; and holography.

For aerial photography see *43 Earth Resources and Remote Sensing*. For related information see also *06 Aircraft Instrumentation*, and *19 Spacecraft Instrumentation*.

N94-36531 Rutherford Appleton Lab., Chilton (England).
EXPERIMENTAL CHARACTERISATION OF GAS MICROSTRIP DETECTORS. PART 1: GAIN CHARACTERISTICS
J. E. Bateman and J. F. Connolly Dec. 1993 22 p See also PB94-167095
(PB94-167087; RAL-93-090-Pt-1) Avail: Issuing Activity (National Technical Information Service (NTIS))

The results of a program of research into the experimental properties of gas microstrip detectors are reported. In this report, information on the gain characteristics of the devices is presented. NTIS

N94-36719 National Inst. of Standards and Technology, Gaithersburg, MD.
ELECTRONIC BALANCE AND SOME GRAVIMETRIC APPLICATIONS (THE DENSITY OF SOLIDS AND LIQUIDS, PYCNOMETRY AND MASS)
R. M. Schoonover, M.-S. Hwang, J. Taylor, and C. Smith 1993 26 p See also PB91-112854 Limited Reproducibility: More than 20% of this document may be affected by microfiche quality
(PB94-163052; NISTIR-5375) Copyright Avail: CASI HC A03

In recent years the electronic force balance has been perfected to a degree that it can replace the mechanical balance in both precision and capacity. Hence, the mechanical balance is rapidly disappearing from the scene. The work reported here describes the use of the electronic balance in some high precision gravimetric applications. The balance has been examined from the user's viewpoint and its use is illustrated in measuring solid and liquid densities and mass. The density assigned to a silicon crystal is in good agreement with its accepted value to within 2.4 ppm. Likewise, the water density measurements substantiate Kell's equation for the density of water near 23 C. NTIS

N94-36760# Defence Research Establishment Ottawa, Ottawa (Ontario).
LABORATORY EVALUATION OF THE STANDARD ELEKTRIK LORENZ (SEL) FIBRE-OPTIC RATE GYROSCOPE
M. F. Vinnins and L. D. Gallop Nov. 1993 58 p
(AD-A280191; DREO-1210) Avail: CASI HC A04/MF A01

A fibre-optic rate-sensing gyroscope (FOG) manufactured by Standard Elektrik Lorenz (SEL) was loaned to DREO for evaluation. The SEL FOG, model PMIDE, was designed for a drift rate of 10 to 100 deg/hr and consists of two units; a fibre-optic sensor and a support electronics unit. Laboratory tests were carried out in the DREO Inertial Navigation Laboratory and consisted of bias drift and scale factor over +/- 400 deg/sec as well as temperature sensitivity. Performance data obtained by DREO agreed closely with predicted performance although bias drift demonstrated wide deviations under thermal rate-transients. A permanent shift in bias drift and scale factor also occurred after extended testing at 50 C. A bias drift of 5.38 deg/hr +/- 0.68 deg/hr was achieved at 30 C and scale factor deviation was approximately 13,000 ppm over a rate range of 400 deg/sec. This instrument would be suitable for a low-performance Attitude and Heading Reference System (AHRS) application. DTIC

N94-36812*# Pennsylvania State Univ., University Park, PA. Dept. of Computer Science and Engineering.
A MODEL-BASED APPROACH FOR DETECTION OF RUNWAYS AND OTHER OBJECTS IN IMAGE SEQUENCES ACQUIRED USING AN ON-BOARD CAMERA Final Technical Report, 24 Jan. 1992 - 31 May 1994
Rangachar Kasturi, Sadashiva Devadiga, and Yuan-Liang Tang 18 Aug. 1994 125 p
(Grant NAG1-1371)
(NASA-CR-196424; NAS 1.26:196424) Avail: CASI HC A06/MF A02

This research was initiated as a part of the Advanced Sensor and Imaging System Technology (ASSIST) program at NASA Langley Research Center. The primary goal of this research is the development of image analysis algorithms for the detection of runways and other objects using an on-board camera. Initial effort was concentrated on images acquired using a passive millimeter wave (PMMW) sensor. The images obtained using PMMW sensors under poor visibility conditions due to atmospheric fog are characterized by very low spatial resolution but good image contrast compared to those images obtained using sensors operating in the visible spectrum. Algorithms developed for analyzing these images using a model of the runway and other objects are described in Part 1 of this report. Experimental verification of these algorithms was limited to a sequence of images simulated from a single frame of PMMW image. Subsequent development and evaluation of algorithms was done using video image sequences. These images have better spatial and temporal resolution compared to PMMW images. Algorithms for reliable recognition of runways and accurate estimation of spatial position of stationary objects on the ground have been developed and evaluated using several image sequences. These algorithms are described in Part 2 of this report. A list of all publications resulting from this work is also included. Derived from text

N94-36822*# National Aeronautics and Space Administration. Marshall Space Flight Center, Huntsville, AL.
AMPOULE FAILURE SENSOR TIME RESPONSE TESTING: EXPERIMENTS 2 AND 3
M. L. Johnson and D. A. Watring Jun. 1994 19 p
(NASA-TM-108458; NAS 1.15:108458) Avail: CASI HC A03/MF A01

The response time of an ampoule failure sensor exposed to a liquid or vapor gallium-arsenide (GaAs) and the corresponding breach time of the containing cartridge is investigated. The experiments were conducted in niobium-hafnium (WC-103) cartridges with an exterior silicide coating. These cartridges were built to flight specifications that were used in NASA's Crystal Growth Furnace during the first United States Microgravity Laboratory (USML-1) mission. The ampoule failure sensor is a chemical fuse made from a metal with which the semiconductor material reacts more rapidly than it does with the containing cartridge. In these experiments a platinum metal was used for the manufacture of the sensors. This technical report discusses the response time of two different sensor designs. The first design utilizes a helical wrapped wire and the second uses a single bare wire element. Experimental results indicate that both sensors are adequate in sensing the presence of molten or vapor GaAs with the latter having a 2-minute longer response time. In both experiments, the containing cartridge was breached within 185 minutes after ampoule rupture. Author

N94-37388# Lawrence Livermore National Lab., Livermore, CA.
ANGLE INTERFEROMETER CROSS AXIS ERRORS
J. B. Bryan, D. L. Carter, and S. L. Thompson Jan. 1994 18 p Presented at the 1994 CIRP General Assembly, Singapore, Singapore, 21-27 Aug. 1994
(Contract W-7405-eng-48)
(DE94-006190; UCRL-JC-112090; CONF-940854-1) Avail: CASI HC A03/MF A01

Angle interferometers are commonly used to measure surface plate flatness. An error can exist when the centerline of the double corner cube mirror assembly is not square to the surface plate and the guide bar for the mirror sled is curved. Typical errors can be one to two microns per meter. A similar error can exist in the calibration of rotary tables when the centerline of the double corner cube mirror assembly is not square to the axes of rotation of the angle calibrator and the calibrator axis is not parallel to the rotary table axis. Commercial double corner cube assemblies typically have non-parallelism errors of ten milli-radians between their centerlines and their sides and similar values for non-squareness between their centerlines and end surfaces. The authors have developed a simple method for measuring these errors and correcting them. DOE

N94-37723# Lawrence Livermore National Lab., Livermore, CA.
A FREON-FILLED, HOLOGRAPHIC BUBBLE CHAMBER AS A HIGH ENERGY PHOTON BURST SPECTROMETER
P. G. Dendooven (Jyvaskyla Univ., Finland.) and R. A. Lerche 26 Apr. 1994 10 p Presented at the 10th Topical Conference on High-Temperature Plasma Diagnostics, Rochester, NY, 8-12 May 1994
(Contract W-7405-eng-48)
(DE94-011645; UCRL-JC-116184; CONF-940552-2) Avail: CASI HC A02/MF A01

A small holographic, freon-filled bubble chamber is being built to measure the energy spectrum of high-energy photons (energy above a few 100 keV) emitted in a short burst (less than about 1 ms duration). The photon energy is calculated from the scattered electron's energy and direction in the case of Compton scattering or from the electron and positron energies in the case of pair production. Electron and positron energies are determined from the curvature of the tracks in a magnetic field. The use of freon results in a large photon interaction probability. Holography combines good spatial resolution with large depth of field. The main concern for the holographic system is the minimization of the bubble image size, so as to maximize the number of bubbles visible in one hologram. A high energy photon burst spectrometer has several potential applications in inertial confinement fusion research. DOE

36 LASERS AND MASERS

Includes parametric amplifiers.
For related information see also *76 Solid-State Physics.*

N94-36510# Los Alamos National Lab., NM.
A HIGH POWER MICROWAVE FREQUENCY MODULATED KrF LASER
R. C. Sze, A. McCown, and N. A. Kurnit 1994 8 p Presented at the 5th International Symposium on High Power Lasers and Applications, Vienna, Austria, 5-8 Apr. 1994
(Contract W-7405-eng-36)
(DE94-009303; LA-UR-94-802; CONF-9404135-1) Avail: CASI HC A02/MF A01

The authors report on the development of a 260mJ 248 nm KrF laser with 98.7 percent depth of modulation at 1.3 GHz and 77 percent depth of modulation at 2.6 GHz using a 1.3 GHz microwave source driving a Pockel's cell. Subsequent single-pass amplification of the modulated KrF source to the 1/4-joule level is shown to be straight forward with no noticeable degradation of the modulation depth. DOE

N94-36565# Atomic Energy of Canada Ltd., Chalk River (Ontario). Nuclear Labs.
AN EXTERNALLY HEATED COPPER VAPOUR LASER
P. A. Rochefort, F. C. Sopchyshyn, E. B. Selkirk, and L. W. Green Aug. 1993 70 p
(DE94-619484; AECL-10757) Avail: CASI HC A04/MF A01 (US Sales Only)

A pulsed Copper Vapor Laser (CVL), with a nominal 6 kHz repetition rate, was designed, built, and commissioned at Chalk River Laboratories. The laser was required for Resonant Ionization Mass Spectroscopy (RIMS) experiments and for projects associated with Atomic Vapour Laser Isotope Separation (AVLIS) studies. For the laser to operate, copper coupons positioned along the length of a ceramic tube must be heated sufficiently to create an appropriate vapor pressure. The AECL CVL uses an external heater element with a unique design to raise the temperature of the tube. The cylindrical graphite heating element is shaped to compensate for the large radiation end losses of the laser tube. The use of an external heater saves the expensive high-current-voltage switching device from heating the laser tube, as in most commercial lasers. This feature is especially important given the intermittent usage typical of experimental research. As well, the heater enables better parametric control of the laser output when studying the lasing of copper (or other) vapour. This report outlines the lasing process in copper vapor, describes in detail all three major laser sub-systems: the laser body; the laser tube heater; the high voltage pulsed discharge; and, reports parametric measurements of the individual sub-systems and the laser system as a whole. Also included are normal operating procedures to heat up, run and shut down the laser. DOE

N94-36946*# National Aeronautics and Space Administration. Langley Research Center, Hampton, VA.
OPTICAL POSITION MEASUREMENT FOR A LARGE GAP MAGNETIC SUSPENSION SYSTEM: DESIGN AND PERFORMANCE ANALYSIS
Sharon S. Welch, James I. Clemmons, Jr., Kevin J. Shelton, and Walter C. Duncan Jun. 1994 57 p
(RTOP 506-59-61-04)
(NASA-TP-3438; L-17257; NAS 1.60:3438) Avail: CASI HC A04/MF A01

An optical measurement system (OMS) has been designed and tested for a large gap magnetic suspension system (LGMSS). The LGMSS will be used to study control laws for magnetic suspension systems for vibration isolation and pointing applications. The LGMSS features six degrees of freedom and consists of a planar array of electromagnets that levitate and position a cylindrical element containing a permanent magnet core. The OMS provides information on the location and orientation of the element to the LGMSS control system to stabilize suspension. The hardware design of this optical sensing system and the tracking algorithms are presented. The results of analyses and experiments are presented that define the accuracy limits of the optical sensing system and that quantify the errors in position estimation. Author

N94-37051# Sandia National Labs., Albuquerque, NM.
A MORE EXACT ANALYSIS OF SANDIA LASER TRACKER DATA
G. S. Phipps May 1994 20 p
(Contract DE-AC04-94AL-85000)
(DE94-011411; SAND-94-0766) Avail: CASI HC A03/MF A01

The Sandia Laser Tracker (LT) systems illuminate a cooperative target with a diverged argon-ion laser beam and track the resulting bright target using a servo-controlled turning mirror. Raw data is digitally recorded in real time and analyzed later when more time is available. The recorded data consists of azimuth and elevation of the tracking mirror, tracking error signals, and range to the target. If the target is tracked perfectly, the error signals will always be zero. The data reduction for this simplified, zero-error condition can be accomplished with very few lines of code. To date, all data reduction for LT-1 has been done using this zero-error assumption. The more general data reduction problem using the tracking error signals is a much more involved calculation and is referred to as 'using the error foidback routine.' Detailed theory and vector analysis behind the data reduction and error decoupling algorithms used in the LT systems are described. Errors and corrections to the original document uncovered in over ten years of use are also noted and corrected. DOE

N94-37114# Lawrence Livermore National Lab., Livermore, CA.
GREATER THAN 100 WATT AVERAGE POWER AT 0.53 MICRON WITH 25 ns, 2.5 kHz REPETITION RATE PULSES FROM A SINGLE POWER OSCILLATOR
S. P. Velsko, B. Comaskey, G. F. Albrecht, and R. J. Beach Mar. 1994 7 p Presented at the 5th International Symposium on High Power Lasers and Applications, Vienna, Austria, 5-8 Apr. 1994
(Contract W-7405-eng-48)
(DE94-011641; UCRL-JC-116764; CONF-9404135-3) Avail: CASI HC A02/MF A01

We have generated approximately 100 watts of frequency doubled light from the output of an electro-optically Q-switched, diode-pumped Nd:YAG slab laser oscillator operating at an average power of 200 watts (2.5 kHz repetition rate, 80 mJ/pulse, 25 ns pulsewidth). The Q-switch was a compensated z-axis propagation LiNbO3 electro-optic modulator, and the frequency conversion crystal was a thin slab of KTP. In addition, Q-switched operation at an average power of approximately 250 watts with 26 ns pulsewidths has been demonstrated. DOE

N94-37137 Technology/Scientific Services, Inc., Dayton, OH.
SENSITIVITY AND SIGNAL TO NOISE RATIO IMPROVEMENT OF A ONE MICRON LADAR SYSTEM INCORPORATING A NEODYMIUM DOPED OPTICAL FIBER PREAMPLIFIER. LASER RADAR TESTBED Technical Report, 1 Aug. 1991 - 1 Nov. 1993
Michael S. Salisbury 28 Feb. 1994 73 p Limited Reproducibility: More than 20% of this document may be affected by microfiche quality
(AF Proj. 2004)
(AD-A280235; WL-TR-94-1075) Avail: CASI HC A04

In an effort to increase the signal to noise ratio of a continuous wave, one micron all solid state ladar system, a rare earth doped optical fiber amplifier has been investigated as a preamplifier for ladar return signals. This details the experimental system used and provides a theoretical analysis of the fiber amplifier's effect on heterodyne and direct detection. The SNR is plotted as a function of the return signal power, and a SNR threshold defines a minimum detectable signal power. The return signals required to attain the SNR threshold are compared for four cases: direct detection with and without the fiber amplifier, and heterodyne detection with and without the fiber amplifier. For direct detection, these results predict a sensitivity increase of 21.0 dB, yet for heterodyne detection the predicted sensitivity increase is only 4.0 dB. These SNR equations are then used to predict experimental improvements of 42.0 dB and 4.0 dB for the direct detection and heterodyne detection experiments, respectively. Experimentally measured increases in SNR are then compared to these predictions. Specifically, for direct detection a SNR increase of 36.5 dB has been measured, and for heterodyne detection the experimental work yielded an increase of 8.0 dB. DTIC

N94-37160# Lawrence Livermore National Lab., Livermore, CA. Advanced Development Group.
HIGH AVERAGE POWER PULSED PHASE CONJUGATE LASER WITH BIREFRINGENCE CORRECTION
M. W. Bowers, A. K. Hankla, and G. F. Jacobson May 1994 22 p Presented at the Conference on Lasers and Electro-Optics, Anaheim, CA,

8-13 May 1994 Revised
(Contract W-7405-eng-48)
(DE94-012062; UCRL-JC-115687-Rev-1; CONF-940582-1-Rev-1) Avail: CASI HC A03/MF A01

Nd:YAG rod lasers have been plagued with the inability to go to high average powers because of thermally induced birefringence and focusing. Several methods have been employed to correct for the birefringence and the thermal aberrations of such systems, but place stringent constraints on the laser heads and/or the system alignment. They have developed a scalable Nd:YAG master oscillator/power amplifier (MOPA) laser system which employs a novel phase conjugation scheme to correct both for the material and thermal distortions as well as the thermal birefringence in double pass amplifier systems. This method reduces the double pass depolarization from 42% to less than 2% and is easy to align. DOE

N94-37169# Atomic Energy Organization of Iran, Teheran. Laser Research Center.
ABSTRACTS OF 2ND INTERNATIONAL CONFERENCE ON LASERS AND THEIR APPLICATIONS Abstracts Only
1993 137 p Conference held in Teheran, Islamic Republic of Iran, 23-26 Aug. 1993
(DE94-617409; INIS-MF-13749; CONF-9308213) Avail: CASI HC A07/MF A02 (US Sales Only)

The following topics were covered at the second international conference on lasers and their applications in Iran: laser principle and technology; laser applications in spectroscopy; nonlinear optics; industry; medicine; and laser related techniques. DOE

N94-37198# Sandia National Labs., Albuquerque, NM. Electronic Processing Dept.
LASER DRILLING OF PRINTED WIRING BOARDS: SANDIA LDRD PROGRAM Final Report
James S. Arzigian May 1994 11 p
(Contract DE-AC04-94AL-85000)
(DE94-011004; SAND-94-0383) Avail: CASI HC A03/MF A01

Traditionally, electrical connections between layers of a printed wiring board are formed by mechanically drilling holes through all layers and then plating the resulting structure to provide electrical connections between the layers. The mechanical drilling process is very capital- and labor-intensive and is often a bottleneck in board production. The goal of this program was the development of laser drilling as an alternative to mechanical drilling. Cost advantages and the ability to produce smaller holes were both of interest. Although it had initially been intended to develop all processes at Sandia, suitable emerging processes and materials were identified in industry during the course of the work. Because of these industry efforts, it was decided to terminate the LDRD efforts after the first year of work and to pursue collaborative development efforts with industrial partners. A laser drilling facility is currently being developed at Sandia to pursue this work further. DOE

N94-37203# Lawrence Livermore National Lab., Livermore, CA.
DIODE ARRAY ALTERNATIVE TO PAINT REMOVAL SOLID-STATE CW LASER
Brian Comaskey 29 Dec. 1993 5 p
(Contract W-7405-eng-48)
(DE94-011482; UCRL-ID-117029) Avail: CASI HC A01/MF A01

The purpose of this memo is to highlight an alternative to the approach for cw laser paint removal. The point to be made is that a direct diode design is feasible and can be far more competitive than a solid-state laser based system. Through by-passing the use of a solid-state laser media, we immediately gain a factor of about five in system efficiency based on measured optical-to-optical efficiencies of our average power diode pumped lasers. This permits a massive reduction in system cooling requirements. It should be noted that cooling system size was the greatest concern voiced by Gordon McFadden at Hobart Lasers with regards to his Nd:YAG laser systems operated in field applications. Furthermore, with direct diode use far fewer diode packages will be needed to deliver a given amount of wattage on the target. This will largely eliminate the intimidating sticker shock and shorten (proportionally by the diode count) the required run-to-fail times demanded of the system. DOE

N94-37240# Lawrence Livermore National Lab., Livermore, CA.
FREQUENCY DOUBLING OF COPPER LASERS USING TEMPERATURE-TUNED ADP
W. A. Molander Mar. 1994 23 p
(Contract W-7405-eng-48)
(DE94-011542; UCRL-ID-117008) Avail: CASI HC A03/MF A01

The ability to generate high average power uv at 255 nm by frequency doubling the green line (510.6 nm) of copper lasers would greatly extend the utility of copper lasers. Material processing and microlithography are two areas of interest. The frequency-doubled copper laser could replace the KrF excimer laser, which has a similar wavelength (248 nm), in some applications. The frequency-doubled copper laser has a narrow linewidth and excellent beam quality at a competitive cost. Other attractive features are high reliability, low operating costs, and the absence of toxic gases. This paper will report recent progress in high-efficiency, high-average-power harmonic generation of the copper laser green line using noncritical phase matching in ADP. Frequency doubling of the yellow line (578.2 nm) and sum-frequency mixing of the two lines are also of interest. These processes, however, cannot be phase-matched in ADP and, therefore, will not be discussed here. The results reported and the issues identified here would be important in these other processes and also in many other frequency conversion schemes in the uv such as 4(omega) conversion of Nd(exp 3+):YAG lasers. DOE

N94-37244# Lawrence Livermore National Lab., Livermore, CA.
NEW HOLLOW-CATHODE ELECTRODE FOR HIGH-POWER COPPER LASERS
J. J. Chang, T. W. Alger, A. T. Anderson, and P. A. Arnold Mar. 1994 4 p Presented at the CLEO 1994 Conference on Lasers and Electro-Optics, Anaheim, CA, 8-13 May 1994
(Contract W-7405-eng-48)
(DE94-011637; UCRL-JC-116700; CONF-940582-4) Avail: CASI HC A01/MF A01

Multiple hollow-cathode slots were utilized on a profiled solid-copper electrode that extended stable glow discharge to higher pressures in copper lasers. This novel electrode design, which dramatically reduced discharge jitter and window contamination, has been run for more than 8000 hours with very little degradation. DOE

N94-37368# Maryland Univ., College Park, MD.
MICROWAVE GENERATION FOR MAGNETIC FUSION ENERGY APPLICATIONS
T. M. Antonsen, Jr., W. W. Destler, V. Granatstein, and B. Levush May 1994 12 p
(Contract DE-FG05-87ER-52147)
(DE94-012107; DOE/ER-52147/7) Avail: CASI HC A03/MF A01

This task involves the feasibility of high-power pulsed, high-efficiency, millimeter-wave free electron lasers (FEL) for ECR of thermonuclear plasmas. The research undertaken is to develop high average power FEL at voltage below IMV allowing for smaller and less costly power supplies. Linear amplification experiments employing a No. 56 period untapered wiggler have been conducted, and substantial small signal gain was observed at 95 GHz over a wide range of experimental conditions consistent with the prediction of one-dimensional numerical simulation. Progress is also reported on theoretical studies relating to the development of high-power gryotron and the ability to predict and improve the performance of various cavity designs. DOE

N94-37481 Department of the Navy, Washington, DC.
TWO-MICRON MODELOCKED LASER SYSTEM Patent
Leon Esterowitz, inventor (to Navy) and Joseph F. Pinto, inventor (to Navy) 21 Dec. 1993 7 p Filed 30 Oct. 1992
(AD-D016219; US-Patent-5,272,708; US-Patent-Appl-SN-968880; US-Patent-Class-372-20) Avail: US Patent and Trademark Office

A continuous wave modelocked laser is provided which generates output pulses having a duration in the picosecond range at a repetition rate in the MHz to GHz ranges. The laser includes a laser cavity defined by spaced, opposed reflective member forming a reflective path therebetween; a host laser crystal disposed in the cavity; an acousto-optic modulator disposed between the host laser crystal and one reflective member for modulating the output of the host laser crystal; and a birefringent filter, disposed in the laser cavity between the host laser crystal and the one

reflective member, for tuning the laser emission to any one of a plurality of wavelengths within a range between 1.86 micrometers and 2.14 micrometers. A pump source pumps the host laser crystal at a wavelength of substantially 785 nm. A collimating plano-convex lens is disposed so that the planar face thereof faces the laser crystal. A mechanical device adjusts the length of the reflective path by axially displacing the one reflective member in the laser cavity so as to match the cavity round trip time to the second harmonic of the drive frequency of the acoustic-optic modulator. DTIC

N94-37495# Los Alamos National Lab., NM.
RAMAN SCATTERING OF VARIABLE BANDWIDTH KrF RADIATION IN LONG AIR PATHS
N. A. Kurnit, D. C. Thompson, S. J. Thomas, A. W. McCown, D. S. Greene, C. Gossein, and H. S. Steele 1994 7 p Presented at the 4th International Workshop on KrF Laser Technology, Annapolis, MD, 2-5 May 1994
(Contract W-7405-eng-36)
(DE94-012912; LA-UR-94-1525; CONF-9405157-2) Avail: CASI HC A02/MF A01

Previous experiments to study Raman scattering of narrow- and broad-band KrF radiation in long air paths have been repeated with larger-area, higher-energy beams of wider bandwidth over longer air paths, and with a more-comprehensive diagnostic system. Parametric generation of Raman scattering has been observed with free-running bandwidth as well as with broader-band radiation and with a biharmonic pump. The effects of bandwidth on Raman threshold, output spectrum, and focusability will be reported. DOE

N94-37628# California Univ., Berkeley. Lawrence Berkeley Lab, CA.
LASER PROBING OF INTERFACES
Y. R. Shen Mar. 1994 7 p Presented at the NOVEL Laser Sources and Applications Workshop, San Jose, CA, 12-13 Nov. 1993
(Contract DE-AC03-76SF-00098)
(DE94-011300; LBL-35305; CONF-9311138-2) Avail: CASI HC A02/MF A01

In the past decade, the possibility of using lasers to probe surfaces and interfaces has attracted a great deal of attention. Such techniques have the advantages of being able to interrogate a surface or interface in a nondetrimental and remote sensing way. Optical second harmonic generation (SHG) and sum frequency generation (SFG) have turned out to be most effective and versatile. By symmetry, these second-order nonlinear optical processes are forbidden (under the electric dipole approximation) in media with an inversion center. They can therefore be highly surface specific. They are also capable of probing with high spatial, temporal, and spectral resolutions, suitable for in-situ studies of surfaces in hostile environment, and applicable to all interfaces accessible by light. Indeed, they have been successful in finding applications to a large variety of surface and interfacial problems: probing adsorption and desorption of molecules from surfaces, measuring average molecular orientation of adsorbates, monitoring surface symmetry and surface phase transitions, conducting surface microscopy and surface spectroscopy, and many others. Here, we discuss a few examples to illustrate the power of the techniques. DOE

N94-37722# Lawrence Livermore National Lab., Livermore, CA.
ADVANCED LASER DRIVER FOR SOFT X-RAY PROJECTION LITHOGRAPHY
L. E. Zapata, R. J. Beach, C. B. Dane, P. Reichert, J. N. Honig, and L. A. Hackel Mar. 1994 11 p Presented at the 5th International Symposium on High Power Lasers and Applications, Vienna, Austria, 5-8 Apr. 1994
(Contract W-7405-eng-48)
(DE94-011643; UCRL-JC-117000; CONF-9404135-2) Avail: CASI HC A03/MF A01

A diode-pumped Nd:YAG laser for use as a driver for a soft x-ray projection lithography system is described. The laser will output 0.5 to 1 J per pulse with about 5 ns pulse width at up to 1.5 kHz repetition frequency. The design employs microchannel-cooled diode laser arrays for optical pumping, zigzag slab energy storage, and a single frequency oscillator injected regenerative amplifier cavity using phase conjugator beam correction for near diffraction limited beam quality. The design and initial results of this laser's activation experiments are presented. DOE

N94-37733# Los Alamos National Lab., NM.
RECENT PROGRESS OF THE LOS ALAMOS ADVANCED FREE ELECTRON LASER
D. C. Nguyen, R. H. Austin, K. C. D. Chan, D. W. Feldman, J. C. Goldstein, S. M. Gierman, J. M. Kinross-Wright, S. H. Kong, J. G. Plato, and S. J. Russell et al 1994 31 p Presented at the OE/LASE 1994 Conference on Optics, Electro-Optics, and Laser Applications in Science and Engineering, Los Angeles, CA, 22-29 Jan. 1994
(Contract W-7405-eng-36)
(DE94-011654; LA-UR-94-1197; CONF-940142-37) Avail: CASI HC A03/MF A01

Many industrial and research applications can benefit from the availability of a compact, user-friendly, broadly tunable and high average power free electron laser (FEL). Over the past four years, the Los Alamos Advanced FEL has been built with these design goals. The key to a compact FEL is the integration of advanced beam technologies such as a high-brightness photoinjector, a high-gradient compact linac, and permanent magnet beamline components. These technologies enable the authors to shrink the FEL size yet maintain its high average power capability. The Advanced FEL has been in operation in the near ir (4-6 (mu)m) since early 1993. Recent results of the Advanced FEL lasing at saturation and upgrades to improve its average power are presented. DOE

N94-37737# Lawrence Livermore National Lab., Livermore, CA.
THE 250 WATT AVERAGE POWER ELECTRO-QUALITY Q-SWITCHED DIODE PUMPED POWER OSCILLATOR
S. P. Velsko, C. A. Ebbers, B. Comaskey, G. F. Albrecht, and S. C. Mitchell Apr. 1994 8 p Presented at the 9th Advanced Solid-State Lasers Meeting, Salt Lake City, UT, 7-10 Feb. 1994
(Contract W-7405-eng-48)
(DE94-011644; UCRL-JC-116999; CONF-940226-7) Avail: CASI HC A02/MF A01

We describe an electro-optically Q-switched, diode-pumped ND:YAG slab laser oscillator operating at an average power of greater than 250 watts. More than 100 watts of frequency doubled light has been demonstrated. DOE

N94-37772 Department of the Navy, Washington, DC.
HOLMIUM QUASI-TWO LEVEL LASER Patent
Steven R. Bowman, inventor (to Navy) and Barry J. Feldman, inventor (to Navy) 15 Feb. 1994 10 p Filed 30 Dec. 1992 Supersedes AD-D015706
(AD-D016302; US-Patent-5,287,378; US-Patent-Appl-SN-998347; US-Patent-Class-372-68) Avail: US Patent and Trademark Office

The directly pumped holmium (Ho) quasi-two level laser of the invention comprises a directly pumped holmium laser having a host material doped with an amount of holmium ions sufficient to produce an output laser emission at a wavelength of about 2.1 micrometer when the holmium laser is pumped by a pump beam at a wavelength of about 2 Jim and a pumping laser for producing the pump beam. In an exemplary embodiment, the pumping laser comprises a Cr,Tm:YAG laser pumped by a flashlamp. DTIC

N94-37777 Department of the Navy, Washington, DC.
INTRACAVITY-PUMPED 2.1 MICROMETER Ho(3+):YAGL ASER Patent
Leon Esterowitz, inventor (to Navy) and Robert S. Stoneman, inventor (to Navy) 22 Feb. 1994 8 p Filed 30 Dec. 1992 Supersedes AD-D015728
(AD-D016308; US-Patent-5,289,482; US-Patent-Appl-SN-998348; US-Patent-Class-372-41) Avail: US Patent and Trademark Office

In a preferred embodiment, a Tm(3+):YAG laser crystal and a Ho(3+):YAG laser crystal are placed within a reflective path of a laser cavity for intracavity pumping the Ho(3)+:YAG laser crystal. The Tm(3+):YAG laser crystal emits a substantially 2.0 micrometers laser emission after being resonantly end-pumped by a pump beam at a wavelength of about 785 nm and the substantially 2.0 micrometers laser emission is used to pump the Ho(3+):YAG laser crystal. The intracavity-pumped Ho(3+):YAG laser crystal emits an output laser emission at substantially 2.1 micrometers. The slope efficiency of the Ho(3+):YAG laser crystal output power is about 40% of the pump power absorbed by the Tm(3+):YAG laser crystal. DTIC

N94-37838# Department of the Navy, Washington, DC.
DIODE-PUMPED, CONTINUOUSLY TUNABLE, 2.3 MICRON CW LASER SPECIFICATION Patent Application
Leon Esterowitz, inventor (to Navy), Robert Stoneman, inventor (to Navy), and Joseph Pinto, inventor (to Navy) 29 Apr. 1994 26 p
(AD-D016312; US-Patent-Appl-SN-235844; Navy-Case-75724) Avail: CASI HC A03/MF A01

A room-temperature solid state laser for producing an output laser emission at any wavelength within a preselected range of wavelengths is disclosed. In a preferred embodiment, the laser comprises: a pump laser for emitting a CW pump beam at a preselected wavelength; a laser cavity defined by a first reflective element, an output coupler reflective element and a folded mirror disposed between the first reflective element and the output coupler reflective element to form a reflective path in the laser cavity; a laser crystal disposed in the laser cavity, the laser crystal being responsive to the CW pump beam at the preselected wavelength for producing a CW laser emission within a preselected range of wavelengths when the laser crystal is pumped by the CW pump beam at the preselected wavelength, the folded mirror operating to collimate the CW laser emission in the optical path between the folded mirror and the output coupler reflective element; and a tuning element disposed in the laser cavity between the folded mirror and the output coupler reflective element for tuning the collimated CW laser emission to any wavelength within the preselected range of wavelengths. DTIC

N94-36619# Diehl G.m.b.H. und Co., Roethenbach (Germany). Optoelectronics Div.
POINTING AND TRACKING CONCEPT FOR A HIGH ENERGY LASER WEAPON APPLICATION
M. Noll and B. Warm *In* AGARD, Pointing and Tracking Systems May 1994 10 p (For primary document see N94-36616 12-18)
Copyright Avail: CASI HC A02/MF A02

N94-36620# Thomson-TRT Defense, Guyancourt (France).
LASER DESIGNATION PODS OPTIMIZED CONCEPT FOR DAY/NIGHT OPERATIONS [PODS DE DESIGNATION LASER UN CONCEPT OPTIMISE POUR LES OPERATIONS JOUR/NUIT]
Yves Huguenin *In* AGARD, Pointing and Tracking Systems May 1994 7 p In FRENCH (For primary document see N94-36616 12-18)
Copyright Avail: CASI HC A02/MF A02

N94-36621# Thermo Electron Technologies Corp., San Diego, CA.
ADAPTIVE OPTICS FOR LASER BEAMFORMING IN THE ATMOSPHERE
M. LeFebvre, L. Cuellar, D. Sandler, and S. Stahl *In* AGARD, Pointing and Tracking Systems May 1994 10 p (For primary document see N94-36616 12-18)
Copyright Avail: CASI HC A02/MF A02

37 MECHANICAL ENGINEERING

Includes auxiliary systems (nonpower); machine elements and processes; and mechanical equipment.

N94-36645*# National Aeronautics and Space Administration. Lewis Research Center, Cleveland, OH.
HOT DYNAMIC TEST RIG FOR MEASURING HYPERSONIC ENGINE SEAL FLOW AND DURABILITY
Jeffrey H. Miller (Sverdrup Technology, Inc., Brook Park, OH.), Bruce M. Steinetz, Paul J. Sirocky, and Lawrence A. Kren Feb. 1994 19 p
(NASA-TM-106507; E-8031-1; NAS 1.15:10657) Avail: CASI HC A03/MF A01

A test fixture for measuring the dynamic performance of candidate high-temperature engine seal concepts was developed. The test fixture was developed to evaluate seal concepts under development for advanced hypersonic engines, such as those being considered for the National Aerospace Plane (NASP). The fixture can measure dynamic seal leakage performance from room temperature up to 840 C and air pressure differentials of to 0.7 MPa. Performance of the seals can be measured while sealing against flat or engine-simulated distorted walls. In the fixture, two seals are preloaded against the sides of a 0.3 m long saber that slides transverse to the axis of the seals, simulating the scrubbing motion anticipated in these engines. The capabilities of this text fixture along with preliminary data showing the dependence of seal leakage performance on high temperature cycling are covered. Author (revised)

N94-36721 Acurex Corp., Mountain View, CA.
LNG VEHICLE TECHNOLOGY, ECONOMICS, AND SAFETY ASSESSMENT Final Report, Apr. 1991 - Jun. 1993
Charles A. Powars, Carl B. Moyer, and Douglas D. Lowell Feb. 1994 198 p See also PB93-110088 Prepared for Gas Research Inst., Chicago, IL Limited Reproducibility: More than 20% of this document may be affected by microfiche quality
(Contract GRI-5091-292-2153)
(PB94-165487; GRI-94/0051) Avail: Issuing Activity (National Technical Information Service (NTIS))

Liquid natural gas (LNG) is an attractive transportation fuel because of its high heating value and energy density (i.e., Btu/lb. and Btu/gal.), clean burning characteristics, relatively low cost ($/Btu), and domestic availability. This research evaluated LNG vehicle and refueling system technology, economics, and safety. Prior and current LNG vehicle projects were studied to identify needed technology improvements. Life-cycle cost analyses considered various LNG vehicle and fuel supply options. Safety records, standards, and analysis methods were reviewed. The LNG market niche is centrally fueled heavy-duty fleet vehicles with high fuel consumption. For these applications, fuel cost savings can amortize equipment capital costs. NTIS

N94-36839*# National Aeronautics and Space Administration. Lyndon B. Johnson Space Center, Houston, TX.
PRELOAD RELEASE MECHANISM Patent Application
Robert M. Generoli, inventor (to NASA) (McDonnell-Douglas Corp., Houston, TX.) and Harry J. Young, inventor (to NASA) (McDonnell-Douglas Corp., Houston, TX.) 20 Apr. 1994 18 p
(NASA-Case-MSC-22327-1; NAS 1.71:MSC-22327-1;
US-Patent-Appl-SN-230571) Avail: CASI HC A03/MF A01

This invention relates to a preload release mechanism comprising a preload spring assembly adapted to apply a preload to a first connector member which is mounted on a support structure and adapted for connection with a second connector member on an object. The assembly comprises telescoped bushings and a preload spring. A tubular shaft extends through the spring assembly and openings in the first connector member and support structure, on which it is clamped. A plunger rod in the shaft is provided with a tip end and a recess in the rod near the other end thereof. A retainer precludes passage of the rod through the shaft in one direction and an end cap closes the bore of the shaft at the other end and provides a shoulder which extends radially of the shaft. A plunger return spring biases the plunger rod against the plunger retainer with the plunger tip protruding from the shaft and a spring assembly return spring engages at its ends the shoulder of the end cap and one end of the spring assembly. Detents received in lateral openings in the tubular shaft are held captive by the plunger rod and one end of the spring assembly to lock the spring assembly on the tubular shaft and apply a preload to the first connector member. Upon completion of the connection, detents and spring assembly are released by plunger contact with the object to be connected, thereby releasing the preload while the connection is maintained. NASA

N94-36953*# National Aeronautics and Space Administration. Lewis Research Center, Cleveland, OH.
VIBRATION SIGNATURE ANALYSIS OF A FAULTED GEAR TRANSMISSION SYSTEM
F. K. Choy (Akron Univ., OH.), S. Huang (Akron Univ., OH.), J. J. Zakrajsek, R. F. Handschuh, and D. P. Townsend Jun. 1994 16 p Presented at the 30th Joint Propulsion Conference, Indianapolis, IN, 27-29 Jun. 1994; sponsored by AIAA, ASME, SAE, and ASEE
(DA Proj. 1L1-62211-A-47-A; RTOP 505-62-36)
(NASA-TM-106623; E-8914; NAS 1.15:106623; ARL-TR-475; AIAA Paper 94-2937) Avail: CASI HC A03/MF A01

A comprehensive procedure in predicting faults in gear transmission systems under normal operating conditions is presented. Experimental data was obtained from a spiral bevel gear fatigue test rig at NASA Lewis Research Center. Time synchronous averaged vibration data was recorded

throughout the test as the fault progressed from a small single pit to severe pitting over several teeth, and finally tooth fracture. A numerical procedure based on the Winger-Ville distribution was used to examine the time averaged vibration data. Results from the Wigner-Ville procedure are compared to results from a variety of signal analysis techniques which include time domain analysis methods and frequency analysis methods. Using photographs of the gear tooth at various stages of damage, the limitations and accuracy of the various techniques are compared and discussed. Conclusions are drawn from the comparison of the different approaches as well as the applicability of the Wigner-Ville method in predicting gear faults. Author

N94-37070# Argonne National Lab., IL.
POTENTIAL BENEFITS OF OXYGEN-ENRICHED INTAKE AIR IN A VEHICLE POWERED BY A SPARK-IGNITION ENGINE
H. K. Ng and R. R. Sekar Apr. 1994 45 p
(Contract W-31-109-eng-38)
(DE94-013452; ANL/ESD/TM-64) Avail: CASI HC A03/MF A01

A production vehicle powered by a spark-ignition engine (3.1-L Chevrolet Lumina, model year 1990) was tested. The test used oxygen-enriched intake air containing 25 and 28% oxygen by volume to determine (1) if the vehicle would run without difficulties and (2) if emissions benefits would result. Standard Federal Test Procedure (FTP) emissions test cycles were run satisfactorily. Test results of catalytic converter-out emissions (emissions out of the converter) showed that both carbon monoxide and hydrocarbons were reduced significantly in all three phases of the emissions test cycle. Test results of engine-out emissions (emissions straight out of the engine, with the converter removed) showed that carbon monoxide was significantly reduced in the cold phase. All emission test results were compared with those for normal air (21% oxygen). The catalytic converter also had an improved carbon monoxide conversion efficiency under the oxygen-enriched-air conditions. Detailed results of hydrocarbon speciation indicated large reductions in 1,3-butadiene, formaldehyde, acetaldehyde, and benzene from the engine with the oxygen-enriched air. Catalytic converter-out ozone was reduced by 60% with 25%-oxygen-content air. Although NO(x) emissions increased significantly, both for engine-out and catalytic converter-out emissions, we anticipate that they can be ameliorated in the near future with new control technologies. The automotive industry currently is developing exhaust-gas control technologies for an oxidizing environment; these technologies should reduce NO(x) emissions more efficiently in vehicles that use oxygen-enriched intake air. On the basis of estimates made from current data, several production vehicles that had low NO(x) emissions could meet the 2004 Tier 2 emissions standards with 25%-oxygen-content air. DOE

N94-37188# Westinghouse Hanford Co., Richland, WA.
JUMPER CONNECTOR ANALYSIS
S. K. Kanjilal, M. R. Lindquist, and L. E. Ulbricht Feb. 1994 11 p Presented at the Pressure Vessel and Piping Conference, Minneapolis, MN, 19-23 Jun. 1994
(Contract DE-AC06-87RL-10930)
(DE94-010373; WHC-SA-2111; CONF-940613-8) Avail: CASI HC A03/MF A01

Jumper connectors are used for remotely connecting pipe lines containing transfer fluids ranging from hazardous chemicals to other nonhazardous liquids. The jumper connector assembly comprises hooks, hookpins, a block, a nozzle, an operating screw, and a nut. The hooks are tightened against the nozzle flanges by the operating screw that is tightened with a remotely connected torque wrench. Stress analysis for the jumper connector assembly (used extensively on the US Department of Energy's Hanford Site, near Richland, Washington) is performed by using hand calculation and finite-element techniques to determine the stress levels resulting from operating and seismic loads on components of the assembly. The analysis addresses loading conditions such as prestress, seismic, operating, thermal, and leakage. The preload torque-generated forces at which each component reaches its stress limits are presented in a tabulated format. Allowable operating loads for the jumper assembly are provided to prevent leakage of the assembly during operating cycles. DOE

N94-37319*# National Aeronautics and Space Administration. Lewis Research Center, Cleveland, OH.
EVALUATION OF THE EHL FILM THICKNESS AND EXTREME PRESSURE ADDITIVES ON GEAR SURFACE FATIGUE LIFE
Dennis P. Townsend and John Shimski Jul. 1994 10 p Proposed for presentation at the AUSTRIB 1994, Perth, Western Australia, 5-8 Dec. 1994; sponsored by the Institution of Engineers Australia
(DA Proj. 1L1-62211-A-47-A; RTOP 505-62-36)
(NASA-TM-106663; E-8979; NAS 1.15:106663; ARL-TR-477) Avail: CASI HC A02/MF A01

Surface pitting fatigue life tests were conducted with seven lubricants, using AISI 9310 spur gears. The test lubricants can be classified as synthetic polyol-esters with various viscosities and additive packages. The lubricant with a viscosity that provided a specific film thickness greater than one and with an additive package produced gear surface fatigue lives that were 8.6 times that for lubricants with a viscosity that provided specific film thickness less than one. Lubricants with the same viscosity and similar additive packages gave equivalent gear surface fatigue lives. Author

N94-37406# Midwest Research Inst., Golden, CO. National Renewable Energy Lab.
FUEL SAVINGS AND EMISSIONS REDUCTIONS FROM LIGHT DUTY FUEL CELL VEHICLES
J. Mark, J. M. Ohi, and D. V. Hudson, Jr. Apr. 1994 42 p
(Contract DE-AC02-83CH-10093)
(DE94-006909; NREL/TP-463-6157) Avail: CASI HC A03/MF A01

Fuel cell vehicles (FCV's) operate efficiently, emit few pollutants, and run on nonpetroleum fuels. Because of these characteristics, the large-scale deployment of FCV's has the potential to lessen U.S. dependence on foreign oil and improve air quality. This study characterizes the benefits of large-scale FCV deployment in the light duty vehicle market. Specifically, the study assesses the potential fuel savings and emissions reductions resulting from large-scale use of these FCV's and identifies the key parameters that affect the scope of the benefits from FCV use. The analysis scenario assumes that FCV's will compete with gasoline-powered light trucks and cars in the new vehicle market for replacement of retired vehicles and will compete for growth in the total market. Analysts concluded that the potential benefits from FCV's, measured in terms of consumer outlays for motor fuel and the value of reduced air emissions, are substantial. DOE

N94-37408# Sinor (J. E.) Consultants, Inc., Niwot, CO.
TECHNICAL EVALUATION AND ASSESSMENT OF CNG/LPG BI-FUEL AND FLEX-FUEL VEHICLE VIABILITY
J. E. Sinor May 1994 60 p Prepared for Midwest Research Inst., Golden, CO
(Contract DE-AC02-83CH-10093)
(DE94-006925; NREL/TP-425-6544) Avail: CASI HC A04/MF A01

This report compares vehicles using compressed natural gas (CNG), liquefied petroleum gas (LPG), and combinations of the two in bi-fuel or flex-fuel configurations. Evidence shows that environmental and energy advantages can be gained by replacing two-fuel CNG/gasoline vehicles with two-fuel or flex-fuel systems to be economically competitive, it is necessary to develop a universal CNG/LPG pressure-regulator-injector and engine control module to switch from one tank to the other. For flex-fuel CNG/LPG designs, appropriate composition sensors, refueling pumps, fuel tanks, and vaporizers are necessary. DOE

N94-37451*# National Aeronautics and Space Administration. Lewis Research Center, Cleveland, OH.
A METHOD FOR THERMAL ANALYSIS OF SPIRAL BEVEL GEARS
Robert F. Handschuh and Thomas P. Kicher Jul. 1994 8 p Proposed for presentation at the 1994 International Gearing Conference, Newcastle Upon Tyne, England, 7-9 Sep. 1994; sponsored by the UK National Gear Metrology Lab., Univ. of Newcastle Upon Tyne, and British Gear Assn.
(DA Proj. 1L1-61102-AH-45; RTOP 505-62-36)
(NASA-TM-106612; E-8895; NAS 1.15:106612; ARL-TR-457) Avail: CASI HC A02/MF A01

A modeling method for analyzing the three-dimensional thermal behavior of spiral bevel gears has been developed. The model surfaces are generated through application of differential geometry to the manufacturing process for face-milled spiral bevel gears. Contact on the gear surface is found by

combining tooth contact analysis with three-dimensional Hertzian theory. The tooth contact analysis provides the principle curvatures and orientations of the two surfaces. This information is then used directly in the Hertzian analysis to find the contact size and maximum pressure. Heat generation during meshing is determined as a function of the applied load, sliding velocity, and coefficient of friction. Each of these factors change as the point of contact changes during meshing. A nonlinear finite element program was used to conduct the heat transfer analysis. This program permitted the time- and position-varying boundary conditions, found in operation, to be applied to a one-tooth model. An example model and analytical results are presented. Author

N94-37457*# National Aeronautics and Space Administration. Lewis Research Center, Cleveland, OH.
DYNAMICS OF A SPLIT TORQUE HELICOPTER TRANSMISSION M.S. Thesis - Cleveland State Univ.
Timothy L. Krantz Jun. 1994 69 p
(DA Proj. 1L1-62211-A-47-A; RTOP 505-62-10)
(NASA-TM-106410; E-7881; NAS 1.15:106410; ARL-TR-291) Avail: CASI HC A04/MF A01

Split torque designs, proposed as alternatives to traditional planetary designs for helicopter main rotor transmissions, can save weight and be more reliable than traditional designs. This report presents the results of an analytical study of the system dynamics and performance of a split torque gearbox that uses a balance beam mechanism for load sharing. The Lagrange method was applied to develop a system of equations of motion. The mathematical model includes time-varying gear mesh stiffness, friction, and manufacturing errors. Cornell's method for calculating the stiffness of spur gear teeth was extended and applied to helical gears. The phenomenon of sidebands spaced at shaft frequencies about gear mesh fundamental frequencies was simulated by modeling total composite gear errors as sinusoid functions. Although the gearbox has symmetric geometry, the loads and motions of the two power paths differ. Friction must be considered to properly evaluate the balance beam mechanism. For the design studied, the balance beam is not an effective device for load sharing unless the coefficient of friction is less than 0.003. The complete system stiffness as represented by the stiffness matrix used in this analysis must be considered to precisely determine the optimal tooth indexing position. Author

N94-37512# General Electric Co., Schenectady, NY. Corporate Research and Development Center.
COAL-FUELED DIESEL TECHNOLOGY DEVELOPMENT: FUEL INJECTION EQUIPMENT FOR COAL-FUELED DIESEL ENGINES
R. N. Johnson and H. L. Hayden Jan. 1994 73 p
(Contract DE-AC21-88MC-23174)
(DE94-004088; DOE/MC-23174/3672) Avail: CASI HC A04/MF A01

The development of coal-fueled diesel engine technology by GE-Transportation Systems (GE-TS) required special fuel injection equipment due to the abrasive and corrosive nature of coal water slurries. GE-Corporate Research and Development (GE-CRD) undertook the design and development of fuel injectors, piston pumps, and check valves for this project. Components were tested at GE-CRD on a simulated engine cylinder, which included a cam-actuated jerk pump, prior to delivery to GE-TS for engine testing. DOE

N94-37515# Argonne National Lab., IL. Energy Systems Div.
STUDY OF JAPANESE ELECTRODYNAMIC-SUSPENSION MAGLEV SYSTEMS
J. L. He, D. M. Rote, and H. T. Coffey Apr. 1994 75 p
(Contract W-31-109-eng-38)
(DE94-011486; ANL/ESD-20) Avail: CASI HC A04/MF A01

This report presents the results of a study of the Japanese MLU magnetic levitation (maglev) system. The development of the MLU system is reviewed, and the dynamic circuit model then is introduced and applied to the figure-eight-shaped null-flux coil suspension system. Three different types of figure-eight-shaped null-flux suspension systems are discussed in detail: (1) the figure-eight-shaped null-flux coil suspension system without cross-connection; (2) the combined suspension and guidance system; and (3) the combined propulsion, levitation, and guidance system. The electrodynamic suspension maglev systems developed in Japan seem to be very promising and could result in a commercial application in the near future. DOE

N94-37521*# National Aeronautics and Space Administration. Lewis Research Center, Cleveland, OH.
AN ENHANCEMENT TO THE NA4 GEAR VIBRATION DIAGNOSTIC PARAMETER
Harry J. Decker, Robert F. Handschuh, and James J. Zakrajsek Jul. 1994 20 p Presented at the 18th Annual Meeting, Hershey, PA, 20-30 Jun. 1994; sponsored by the Vibration Institute
(DA Proj. 1L1-62211-A-47-A; RTOP 505-62-36)
(NASA-TM-106553; E-8708; NAS 1.15:106553; ARL-TR-389) Avail: CASI HC A03/MF A01

A new vibration diagnostic parameter for health monitoring of gears, NA4*, is proposed and tested. A recently developed gear vibration diagnostic parameter NA4 outperformed other fault detection methods at indicating the start and initial progression of damage. However, in some cases, as the damage progressed, the sensitivity of the NA4 and FM4 parameters tended to decrease and no longer indicated damage. A new parameter, NA4* was developed by enhancing NA4 to improve the trending of the parameter. This allows for the indication of damage both at initiation and also as the damage progresses. The NA4* parameter was verified and compared to the NA4 and FM4 parameters using experimental data from single mesh spur and spiral bevel gear fatigue rigs. The primary failure mode for the test cases was naturally occurring tooth surface pitting. The NA4* parameter is shown to be a more robust indicator of damage. Author

N94-37763*# Allison Engine Co., Indianapolis, IN. Gas Turbine Div.
ADVANCED TURBINE TECHNOLOGY APPLICATIONS PROJECT (ATTAP) Final Annual Report, 1991
Dec. 1992 87 p
(Contract DEN3-336; RTOP 778-32-21)
(NASA-CR-195367; E-9037; NAS 1.26:195367; DOE/NASA-0336-4; EDR-16624) Avail: CASI HC A05/MF A01

ATTAP activities during the past year included test-bed engine design and development, ceramic component design, materials and component characterization, ceramic component process development and fabrication, ceramic component rig testing, and test-bed engine fabrication and testing. Significant technical challenges remain, but all areas exhibited progress. Test-bed engine design and development included engine mechanical design, combustion system design, alternate aerodynamic designs of gasifier scrolls, and engine system integration aimed at upgrading the AGT-5 from a 1038 C (1900 F) metal engine to a durable 1372 C (2500 F) structural ceramic component test-bed engine. ATTAP-defined ceramic and associated ceramic/metal component design activities completed include the ceramic gasifier turbine static structure, the ceramic gasifier turbine rotor, ceramic combustors, the ceramic regenerator disk, the ceramic power turbine rotors, and the ceramic/metal power turbine static structure. The material and component characterization efforts included the testing and evaluation of seven candidate materials and three development components. Ceramic component process development and fabrication proceeded for the gasifier turbine rotor, gasifier turbine scroll, gasifier turbine vanes and vane platform, extruded regenerator disks, and thermal insulation. Component rig activities included the development of both rigs and the necessary test procedures, and conduct of rig testing of the ceramic components and assemblies. Test-bed engine fabrication, testing, and development supported improvements in ceramic component technology that permit the achievement of both program performance and durability goals. Total test time in 1991 amounted to 847 hours, of which 128 hours were engine testing, and 719 were hot rig testing. Author (revised)

N94-37766 Department of the Navy, Washington, DC.
DUAL VALVE PLATE TWO-WAY PRESSURE RELIEF VALVE Patent
Robert J. Angeli, inventor (to Navy) 1 Feb. 1994 7 p Filed 23 Feb. 1993
(AD-D016293; US-Patent-5,282,492; US-Patent-Appl-SN-023426; US-Patent-Class-137-493.4) Avail: US Patent and Trademark Office

There is disclosed a two-way valve which includes dual valve plates to be positioned between first and second chambers having varying pressure therein, to relieve excess pressure in either chamber by permitting fluid flow from one chamber to the other. The valve includes a body portion

having disposed therein dual valve plates. In the equilibrium state, the first valve plate is spring biased against the valve body in the direction of the first chamber to seal off any flow through the valve. The second valve plate is separately spring biased against the first valve plate in the direction of the second chamber, scaling off flow between the valve plates. When the pressure of the first chamber is greater than the pressure of the second chamber by a pre-determined amount, the first and second valve plates move away from the valve body permitting fluid flow from the first chamber to the second chamber. DTIC

N94-36627# McDonnell-Douglas Aerospace, Saint Louis, MO.
AEROSERVOELASTIC STABILIZATION CONSIDERATIONS FOR POINTING AND TRACKING SYSTEMS
Peter Y. Cheng and Ralph E. Lambert *In* AGARD, Pointing and Tracking Systems May 1994 6 p (For primary document see N94-36616 12-18)
Copyright Avail: CASI HC A02/MF A02

38 QUALITY ASSURANCE AND RELIABILITY

Includes product sampling procedures and techniques; and quality control.

N94-36452# Edgerton, Germeshausen and Grier, Inc., Idaho Falls, ID.
FOUR BEAM INTERFEROMETER MANUAL: OPERATING INSTRUCTIONS FOR THE INEL DIFFRACTION MOIRE INTERFEROMETER
V. A. Deason Nov. 1993 53 p
(Contract DE-AC07-76ID-01570)
(DE94-010772; EGG-APO-10944) Avail: CASI HC A04/MF A01

Moire interferometry is an interferometric method for measuring changes of in-plane geometry. It is essentially insensitive to out-of-plane topography or changes in that topography. Changes in geometry are referenced to a particular moment in time when the moire' sensor, a diffraction grating, was attached to the specimen. Distortions experienced by the specimen prior to that time are not directly detectable, although they may be inferred from specimen behavior or condition. In its most common form, moire interferometry is not well suited to large (greater than 50 mm square), curved (less than 300 mm diameter) or high temperature (greater than 200 C) regions. However, various efforts have been made to handle each of these conditions. In general, the moire' process is most straightforward for flat, 25 mm diameter regions of coverage and room temperature. Much smaller or larger regions require more specialized optics, which can become very expensive. This report will discuss various aspects of moire interferometry. In particular, a new four beam (bi-axial) interferometer is described in detail. Issues involved in safety, assembly, calibration and use are fully explained. DOE

N94-37150 California Univ., Davis, CA. Dept. of Electrical and Computer Engineering.
FAULT TOLERANCE IN OPTO-ELECTRONIC COMPUTING Semiannual Report
Ting-Ting Y. Lin 15 Apr. 1994 49 p Limited Reproducibility: More than 20% of this document may be affected by microfiche quality
(Contract N00014-91-J-1017)
(AD-A280219) Avail: CASI HC A03

This project has gotten some recognition in both fault modeling and testing of optical interconnects in a opto-electronic system. In the first part, we want to develop a new methodology for performance analysis of opto-electronic systems at a higher level. Our approach is to first identify possible failures in such interconnect implementations, and then extract information from the physical configuration and relate to the system performance parameters. In this way, system-level performance degradation can be estimated to construct design constraint for physical systems. In the second part on testing, we proposed an architecture which integrates the concept of concurrency and distributed test pattern generation for testing complex circuits on a planar layout. DTIC

N94-37321# Advisory Group for Aerospace Research and Development, Neuilly-Sur-Seine (France). Structures and Materials Panel.
IMPACT OF MATERIALS DEFECTS ON ENGINE STRUCTURES INTEGRITY [L'IMPACT DES DEFAUTS DES MATERIAUX SUR L'INTEGRITE DES STRUCTURES DES MOTEURS]
Apr. 1993 118 p In ENGLISH and FRENCH The 74th meeting was held in Patras, Greece, 27-28 May 1992
(AGARD-R-790; ISBN-92-835-0711-8) Copyright Avail: CASI HC A06/MF A02

Engine failures due to materials defects are rare, but are still a cause for concern to both manufacturers and lifting authorities. In these circumstances it is recognized that the introduction of higher strength materials, new production routes and improved non-destructive evaluation methods may have significant implications for engine lifing and safety. The impact of inherent defects on present and future component manufacture and on aircraft engine operation is considered. Materials processing and control aspects are reviewed, placing particular emphasis on nickel and titanium engine disc materials. Variations in engineers', scientists' and lawyers' interpretation of the work 'defect' was perhaps the most significant point to emerge from the meeting; so much so, that a small group agreed to develop a definition, and when established recommend it as standard AGARD materials technology. For individual titles, see N94-37322 through N94-37331.

N94-37322# Utah Univ., Salt Lake City, UT. Dept. of Mechanical Engineering.
HISTORY AND PROGNOSIS OF MATERIAL DISCONTINUITY EFFECTS ON ENGINE COMPONENTS STRUCTURAL INTEGRITY
David W. Hoeppner *In* AGARD, Impact of Materials Defects on Engine Structures Integrity Apr. 1993 8 p (For primary document see N94-37321 12-38)
Copyright Avail: CASI HC A02/MF A02

Ever since the development of aeroengines, 'defects' have been of significant concern to the assurance of structural integrity. Many of these issues have been the focus of recent Structures and Materials Panel (SMP) workshops and conferences. Although engine idealizations of materials being homogeneous, continuous, and 'free of defects' are invoked to make the complex issues of load, stress and strain, tractable, they were recognized as early as 1916, and later in the 1930's, as being oversimplistic and potentially in error. The epistemology of the role of discontinuities ('defects') in the design, selection, and lifing of critical aeroengine components is reviewed herein. Utilization of 'defect-free' and 'initiation' based fatigue criteria (as well as other time dependent failure modes such as creep, wear, etc.) have led to much success in the aeroengine industry. However, 'defects' also have led to numerous engine component failures in military and civilian aeroengines. And, as increasing demands are made on materials used in aeroengines, the role of 'defects' will, undoubtedly, become more important and critical. The history and prognosis of these issues is discussed with a review of on-condition lifing, defect-tolerant and damage-tolerant approaches, including, but not limited to, Engine Structural Integrity Program (ENSIP). The prognosis will suggest the need for the following: (1) development of increased understanding of the physics of failure processes of aeroengine materials; (2) integration of 'defect' considerations in the lifing methodologies from conceptual to detail design (the new paradigm of lifing); (3) assurance that knowledge of intrinsic materials behavior, including manufacturing specification and control, is a prime consideration in the defect-tolerant approach; (4) non-destructive inspection and evaluation should be one of many tools used to monitor and assure the state of the materials and should be a consideration in the lifing methodology at the earliest stage; (5) evaluation and integration of the role of extraneous influences, such as fretting, environmental attack, and the like, and how they are factored into the lifing procedure; and (6) development of consistent terminology with standardized definitions. Author

N94-37323# British Columbia Univ., Vancouver. Dept. of Metals and Materials Engineering.
ALTERNATE MELTING AND REFINING ROUTES c26
Alec Mitchell *In* AGARD, Impact of Materials Defects on Engine Structures Integrity Apr. 1993 8 p (For primary document see N94-37321 12-38)
Copyright Avail: CASI HC A02/MF A02

Although most research and development effort in turbine alloys has

been in the past directed towards the understanding and improvement of basic properties, it is a telling comment on the results that at present we can only manufacture the components with a reliability which, in the example case of a high pressure turbine disk, leads to a service life of less than one-fifth of the theoretical life of the alloy component. The purpose of this presentation is to examine the reasons for this situation and to indicate ways in which we can improve on it. We conclude that the techniques of melting, refining and casting which are now being developed have the potential to make a large change in the in-service life of turbine components without any significant change in the state of alloy development. Author

N94-37324# Wright Lab., Wright-Patterson AFB, OH. Materials Dirctorate.

PROCESS ENHANCEMENTS OF SUPERALLOY MATERIAL **c26**

Ronald H. Williams, Kristine A. Lark, Sharon Vukelich, Donald R. Parille, and Richard W. Salkeld *In* AGARD, Impact of Materials Defects on Engine Structures Integrity Apr. 1993 6 p (For primary document see N94-37321 12-38)

Copyright Avail: CASI HC A02/MF A02

Due to the ever-increasing demand for improvements in engine performance and better fuel efficiency, complex high pressure turbine (HPT) blade designs have been introduced into military engines. Greater emphasis has, therefore, been placed on increasing the structural integrity and life of engine components. Materials defects must be of a small enough size and sparse enough in population to enable the design of high thrust-to-weight ratio engines. This requirement has demanded the industry attainment of cleaner materials. In order to meet this requirement, possible process improvements were evaluated. Enhancements were incorporated into the melting and casting processes to reduce the size and number of dross defects within high pressure turbine blades. The accomplishment of this goal was through the efforts of a joint United States Air Force, Pratt & Whitney Task Force Team. Process implementation has been successful in reducing the remaining deleterious defects present in directionally solidified single crystal and polycrystalline nickel-base superalloy turbine blade materials. In conjunction with the introduction of melting and casting process improvements, the refinement of non-destructive inspection techniques was investigated. Author

N94-37325# Imphy S.A., Imphy (France).

THE CONTROL OF CLEANNESS IN POWDER METALLURGY MATERIALS FOR TURBINE DISKS **c26**

G. Raisson *In* AGARD, Impact of Materials Defects on Engine Structures Integrity Apr. 1993 14 p (For primary document see N94-37321 12-38)

Copyright Avail: CASI HC A03/MF A02

The origins of exogenous inclusions in powder metallurgy products are described and methodologies for assuring the quality of these alloys are reviewed. Elutriation, chemical dissolution, micrography, electron beam button melting, ultrasonic inspection, and other techniques are described and compared. CASI

N94-37326# Forge Societe Nationale d'Etude et de Construction de Moteurs d'Aviation, Gennevilliers (France).

MAINTAINING CONSTANT STANDARDS DURING THE FORGING PROCESS [MAITRISE DE LA REPRODUCTIBILITE DU PROCEDE DE FORGEAGE] **c26**

F. Chevet and M. Caralp *In* AGARD, Impact of Materials Defects on Engine Structures Integrity Apr. 1993 23 p In FRENCH (For primary document see N94-37321 12-38)

Copyright Avail: CASI HC A03/MF A02

The properties of aircraft engine discs made of a titanium and nickel alloy may be notably improved if deformations and temperatures are monitored during the forging process. On engines of recent fabrication, this optimization through thermomechanical treatment is also systematically applied. As an answer to this need SNECMA is using a monitoring system in its metal processing plant: monitoring devices positioned on the heat deformation machinery record and statistically document the important parameters. This new monitoring system, taking place at the time of fabrication, makes it possible to immediately detect any variance in the fabrication and to rapidly correct any possible abnormality. Thus checking and ensuring total duplication of the fabrication becomes systematic and the quality control checks on the finished project (strongly linked to the conditions of transformation) have improved. Finally, because of the knowledge that was thus gained on the forging process, our command of the thermomechanical treatments was improved. Variations in parameters which were not recorded in the past and had an important influence on the microstructure of the parts were observed. Transl. by FLS

N94-37327# Pratt and Whitney Aircraft, West Palm Beach, FL.

STATISTICAL CHARACTERIZATION OF RARE EVENTS **c65**

Charles Annis and Sharon Vukelich *In* AGARD, Impact of Materials Defects on Engine Structures Integrity Apr. 1993 10 p (For primary document see N94-37321 12-38)

Copyright Avail: CASI HC A02/MF A02

Inexpensive computing power has made computer-intensive methods, such as Monte Carlo simulation, available to a wide range of engineering problems, including risk assessments for structural components. Because well-designed structures have low probabilities of failure during their service lifetimes, it has become increasingly helpful to simulate the behavior of these unlikely events, so as to quantify the risk of failure. This paper considers the behavior of the 'tails' of the statistical distributions chosen to describe the behavior of life-controlling variables and their influence on the estimation of aggregate risk. It may seem obvious that the form of the probability distributions will necessarily have a profound influence on the resulting estimated probabilities of failure. What is perhaps less obvious are the subtle differences among candidate distributions in the range where most defining data will necessarily be obtained, namely between their fifth and ninety-fifth percentiles. We examine and compare several commonly used distributions: normal, log-normal 2- and 3-parameter Weibull, and Beta. Also considered here is the often used, but less often understood, concept of confidence associated with a probability of failure. Because it relies on knowing which one of several potential underlying probability distributions actually governs the observed behavior, it can result in a meaningless estimate of 'confidence', and thus presents the potential for a false sense of security. Author

N94-37328# Defence Research Agency, Farnborough, Hampshire (England).

DEFECTS AND THEIR EFFECTS ON THE INTEGRITY OF NICKEL BASED AEROENGINE DISCS **c26**

G. F. Harrison, P. H. Tranter, and L. Grabowski *In* AGARD, Impact of Materials Defects on Engine Structures Integrity Apr. 1993 16 p (For primary document see N94-37321 12-38)

Copyright Avail: CASI HC A03/MF A02

By specific reference to the powder metallurgy alloy API the paper examines the role of defects in generating local residual stress fields. The effects of defect size and location on crack initiation and low cycle fatigue life are discussed. It is shown that at stress levels consistent with those experienced by current engine components, defects can act under cyclic loading as crack nucleators from cycle 1. Methods of calculating appropriate stress intensity factors are briefly reviewed and it is shown that at existing turbine disc operating temperatures, a linear elastic fracture mechanics stress intensity factor can be used to calculate crack growth rates. Finally, the major lifting methods used for aeroengine discs are briefly reviewed, and attention is drawn to the specific problems created by the presence of macrostructural defects. Author

N94-37329# Fiat Aviazione S.p.A., Turin (Italy).

TURBINE DISKS: LIFING AGAINST DEFECTS AND MATERIALS DEVELOPMENT

E. Campo, G. Pasquero, Aldo Frediani, and Roberto Galatolo *In* AGARD, Impact of Materials Defects on Engine Structures Integrity Apr. 1993 12 p (For primary document see N94-37321 12-38)

Copyright Avail: CASI HC A03/MF A02

Structural integrity of turbine disks must be guaranteed with a high safety level. The Engine Structural Integrity Program as contained in NIL-STD-1783 is aimed to enhance disk safety. A major design requirement is the implementation of the Damage Tolerance concepts by assessing the disk life in presence of defects. This paper illustrates the MIL-STD-1893 impact on turbine design as well as on material requirements, putting more emphasis on induced discontinuity features than on evolutionary ones. Targets for future developments in lifing procedures as well as in innovative materials are defined taking into account possible differences in life management among NATO countries. Author

N94-37330# General Electric Co., Cincinnati, OH. Aircraft Engines.
SUBSTANTIATING POWDER METAL LIFE METHODOLOGIES FOR ENGINES
P. A. Domas *In* AGARD, Impact of Materials Defects on Engine Structures Integrity Apr. 1993 8 p (For primary document see N94-37321 12-38)
Copyright Avail: CASI HC A02/MF A02

The application of powder metal (PM) superalloys in aircraft turbine engine rotating components is prompted by performance driven high strength and creep resistance requirements. Fine grain, precipitation strengthened nickel-base alloys such as IN100, Rene'95, and Rene'88DT meet these requirements up to operating temperatures in the 1200-1300F (649-704C) range. In addition to burst and deformation limits, design constraints include durability (fatigue) and damage tolerance (crack growth resistance) capability to insure reliability and safety. Fatigue life for these alloys can be influenced by inhomogeneities (inclusions) intrinsic to the microstructure as the result of processing, and by perturbations of the surface integrity during component manufacture and subsequent usage. Understanding of PM fatigue behavior and substantiation of life assessment methodology must appropriately recognize these potential influences. New testing, modeling, and analysis schemes are necessitated in engineering development programs addressing generation and validation of life prediction techniques for these materials. This paper outlines one approach to substantiating PM fatigue life prediction that attempts to recognize homogeneous fatigue initiation by incorporating probabilistic models and development testing methods that address material volume and component feature effects. Complications and limitations being addressed in ongoing work are discussed. Author

N94-37331# Motoren- und Turbinen-Union Muenchen G.m.b.H., Munich (Germany).
PREDICTING DEFECT BEHAVIOUR
G. W. Koenig and J. W. Bergmann *In* AGARD, Impact of Materials Defects on Engine Structures Integrity Apr. 1993 11 p (For primary document see N94-37321 12-38)
Copyright Avail: CASI HC A03/MF A02

Fatigue is a statistical phenomenon with contributing factors which are statistical in nature too. Therefore probabilistic lifing concepts appear to be appropriate. Major components of any probabilistic lifting concept are: (1) microstructural characterization; (2) load history; and (3) material behavior. The results of any lifing model can only be as significant as the input data. This paper reviews some important aspects regarding input data which are necessary for the prediction of defect behavior by probabilistic models. Author

39 STRUCTURAL MECHANICS

Includes structural element design and weight analysis; fatigue; and thermal stress.

For applications see *05 Aircraft Design, Testing and Performance* and *18 Spacecraft Design, Testing and Performance.*

N94-36520 Rhode Island Univ., Kingston, RI. Dept. of Mechanical Engineering and Applied Mechanics.
STUDIES OF THE EFFECT OF MICROSTRUCTURE ON THE DYNAMIC BEHAVIOR OF GRANULAR AND PARTICULATE MEDIA Annual Report No. 1, Mar. 1993 - Feb. 1994
Arun Shukla and Martin H. Sadd Mar. 1994 157 p Limited Reproducibility: More than 20% of this document may be affected by poor print and microfiche quality
(Contract F40620-91-1-0209)
(AD-A279012; AFOSR-94-0267TR) Avail: Issuing Activity (Defense Technical Information Center (DTIC))

A combined experimental-numerical investigation is being conducted to study dynamic load transfer in particulate materials due to explosive loadings. The primary emphasis in the study is to relate the microstructural features of the particulate media to the load transfer process. The experimental techniques of dynamic photoelasticity is used to investigate the effect of cementation and of the particle shape on the local contact stress fields. The stiffness of the cement relative to that of the particle controls the location of the peak contact stresses. Strong cementation increases the load transfer velocity and also promotes fracture of the particles. The particle shapes as presently studied in this research program seem to have little influence on the load transfer process. The applicability of the fiber optic sensors and the speckle techniques to contact stress measurements is evaluated. Fiber optic sensors show promise of future applications to three dimensional problems. Discrete element numerical wave simulation has been conducted for saturated granular materials through the introduction of a new contact law using elastohydrodynamic theory. Pore fluid acts to decrease the wave speed and increase the attenuation. Future numerical studies will focus on additional changes of the interparticle contact response through cementation and particle shape effects. DTIC

N94-36561*# National Aeronautics and Space Administration. Lewis Research Center, Cleveland, OH.
A COUPLED/UNCOUPLED DEFORMATION AND FATIGUE DAMAGE ALGORITHM UTILIZING THE FINITE ELEMENT METHOD
Thomas E. Wilt (Toledo Univ., OH.) and Steven M. Arnold Mar. 1994 26 p
(Contract NCC3-248; RTOP 505-63-12)
(NASA-TM-106526; E-8652; NAS 1.15:106526) Avail: CASI HC A03/MF A01

A fatigue damage computational algorithm utilizing a multiaxial, isothermal, continuum based fatigue damage model for unidirectional metal matrix composites has been implemented into the commercial finite element code MARC using MARC user subroutines. Damage is introduced into the finite element solution through the concept of effective stress which fully couples the fatigue damage calculations with the finite element deformation solution. An axisymmetric stress analysis was performed on a circumferentially reinforced ring, wherein both the matrix cladding and the composite core were assumed to behave elastic-perfectly plastic. The composite core behavior was represented using Hill's anisotropic continuum based plasticity model, and similarly, the matrix cladding was represented by an isotropic plasticity model. Results are presented in the form of S-N curves and damage distribution plots. Author

N94-37015*# Nichols Research Corp., Huntsville, AL.
FRACTURE MECHANICS LIFE ANALYTICAL METHODS VERIFICATION TESTING Final Report
J. A. Favenesi, T. G. Clemmons, and T. J. Lambert Washington May 1994 56 p
(Contract NAS8-38103)
(NASA-CR-4602; M-748; NAS 1.26:4602) Avail: CASI HC A04/MF A01

Verification and validation of the basic information capabilities in NASCRAC has been completed. The basic information includes computation of K versus a, J versus a, and crack opening area versus a. These quantities represent building blocks which NASCRAC uses in its other computations such as fatigue crack life and tearing instability. Several methods were used to verify and validate the basic information capabilities. The simple configurations such as the compact tension specimen and a crack in a finite plate were verified and validated versus handbook solutions for simple loads. For general loads using weight functions, offline integration using standard FORTRAN routines was performed. For more complicated configurations such as corner cracks and semielliptical cracks, NASCRAC solutions were verified and validated versus published results and finite element analyses. A few minor problems were identified in the basic information capabilities of the simple configurations. In the more complicated configurations, significant differences between NASCRAC and reference solutions were observed because NASCRAC calculates its solutions as averaged values across the entire crack front whereas the reference solutions were computed for a single point. Author

N94-37102*# National Aeronautics and Space Administration. Langley Research Center, Hampton, VA.
ABILITY OF THE TOTAL STRAIN VERSION OF STRAINRANGE PARTITIONING TO CHARACTERIZE THERMOMECHANICAL FATIGUE BEHAVIOR
James F. Saltsman and Gary R. Halford Washington Jul. 1994 23 p
(RTOP 505-63-5B)
(NASA-TM-4556; E-7660; NAS 1.15:4556) Avail: CASI HC A03/MF A01

Strainrange partitioning (SRP) was originally developed on an inelastic strain basis for isothermal fatigue in the high-strain regime where the inelastic strainrange could be determined accurately. However, most

power-generating equipment operates in the regime where the inelastic strains are small and difficult to determine with any degree of accuracy. This shortcoming led to the development of the total strain version of SRP (TS-SRP). Power-generating equipment seldom operates under isothermal conditions, and isothermal life prediction methods cannot be depended on to predict the lives of anisothermal cycles. To overcome this shortcoming, a method was proposed for extending TS-SRP to characterize anisothermal fatigue behavior and to predict the lives of thermomechanical fatigue (TMF) cycles using appropriate anisothermal data. The viability of this method, referred to as TMF/TS-SRP, was demonstrated using TMF data for two high-temperature aerospace alloys. In this report, data from the literature are used to examine the ability of TMF/TS-SRP to characterize the failure and flow behavior of three low-strength, high-ductility alloys widely used for ground-based power-generating equipment. The three alloys are type 304 stainless steel, 1Cr-1Mo-0.25V steel, and 2.25Cr-1Mo steel. Because of the limited nature of the data, it was possible to evaluate the characterization, but not the predictive capability of TMF/TS-SRP.

Author (revised)

N94-37125 Utah State Univ., Logan, UT. Dept. of Mechanical Engineering.

LITERATURE REVIEW AND PRELIMINARY STUDIES OF FRETTING AND FRETTING FATIGUE INCLUDING SPECIAL APPLICATIONS TO AIRCRAFT JOINTS Final Report

David Hoeppner, Saeed Adibnazari, and Mark W. Moesser Apr. 1994 70 p Sponsored by FAA Limited Reproducibility: More than 20% of this document may be affected by microfiche quality

(AD-A280310; DOT/FAA/CT-93/2) Avail: Issuing Activity (Defense Technical Information Center (DTIC))

This report contains a review of the literature pertinent to fretting and fretting fatigue including special applications to aircraft joints. An introduction is given outlining the importance of fretting and fretting fatigue failures. Proposed mechanisms of fretting and fretting fatigue are then discussed. Research in the literature indicates there are three stages to fretting fatigue life. The first is a period of crack nucleation, usually by adhesion and plastic deformation of contacting asperities in relative motion. Several other possible mechanisms are discussed as well. In the second stage, propagation of nucleated cracks is determined by the stress resulting from the surface tractions imposed by fretting. The results of several investigations of the stress state and its effect on the propagation of nucleated cracks are discussed. The stress state can either dramatically increase early crack propagation rates or retard crack propagation, depending upon the specifics of the contact under study. The third stage is a period of crack propagation during which fretting contact stresses are not significant to crack propagation.

DTIC

N94-37186 Imperial Coll. of Science and Technology, London (England). Dept. of Chemistry.

THE CYCLIC FATIGUE BEHAVIOUR OF ADHESIVE JOINTS Interim Report No 4, Dec. 1993 - Jun. 1994

A. J. Kinloch and M. Fernando 10 Jun. 1994 6 p Limited Reproducibility: More than 20% of this document may be affected by microfiche quality

(Contract DAJA45-93-C-0008)

(AD-A280453; R/D-6869-MS-01) Avail: Issuing Activity (Defense Technical Information Center (DTIC))

We have continued the development and use of the electrical potential method for measuring the length of the crack and confirmed that this method gives accurate and reliable data. We have completed the fatigue testing of the aluminum-alloy substrates (BS 5083 grade), pretreated using various surface treatments, and bonded with the 'AF 163' film adhesive.

DTIC

N94-37253*# National Aeronautics and Space Administration. Langley Research Center, Hampton, VA.

ISSUES CONCERNING THE UPDATING OF FINITE-ELEMENT MODELS FROM EXPERIMENTAL DATA

Shane A. Dunn (Aeronautical Research Labs., Melbourne, Australia.) Jun. 1994 40 p

(RTOP 233-01-01-12)

(NASA-TM-109116; NAS 1.15:109116) Avail: CASI HC A03/MF A01

Some issues concerning the updating of dynamic finite-element models by incorporation of experimental data are examined here. It is demonstrated how the number of unknowns can be greatly reduced if the physical nature of the model is maintained. The issue of uniqueness is also examined and it is shown that a number of previous workers have been mistaken in their attempts to define both sufficient and necessary measurement requirements for the updating problem to be solved uniquely. The relative merits of modal and frequency response function (frf) data are discussed and it is shown that for measurements at fewer degrees of freedom than are present in the model, frf data will be unlikely to converge easily to a solution. It is then examined how such problems may become more tractable by using new experimental techniques which would allow measurements at all degrees of freedom present in the mathematical model.

Author (revised)

N94-37456*# National Aeronautics and Space Administration. Lewis Research Center, Cleveland, OH.

LAMINATED THIN SHELL STRUCTURES SUBJECTED TO FREE VIBRATION IN A HYGROTHERMAL ENVIRONMENT

Pascal K. Gotsis and James D. Guptill Jul. 1994 17 p

(RTOP 537-04-20)

(NASA-TM-106600; E-8874; NAS 1.15:106600) Avail: CASI HC A03/MF A01

Parametric studies were performed to assess the effects of various parameters on the free-vibration behavior (natural frequencies) of (+/-theta)(sub 2) angle-ply, fiber composite, thin shell structures in a hygrothermal environment. Knowledge of the natural frequencies of structures is important in considering their response to various kinds of excitation, especially when structures and force systems are complex and when excitations are not periodic. The three dimensional, finite element structural analysis computer code CSTEM was used in the Cray YMP computer environment. The fiber composite shell was assumed to be cylindrical and made from T300 graphite fibers embedded in an intermediate-modulus, high-strength matrix. The following parameters were investigated: the length and the laminate thickness of the shell, the fiber orientation, the fiber volume fraction, the temperature profile through the thickness of the laminate, and laminates with different ply thicknesses. The results indicate that the fiber orientation and the length of the laminated shell had significant effects on the natural frequencies. The fiber volume fraction, the laminate thickness, and the temperature profile through the shell thickness had weak effects on the natural frequencies. Finally, the laminates with different ply thicknesses had an insignificant influence on the behavior of the vibrated laminated shell. Also, a single through-the-thickness, eight-node, three dimensional composite finite element analysis appears to be sufficient for investigating the free-vibration behavior of thin, composite, angle-ply shell structures.

Author (revised)

N94-37541*# National Aeronautics and Space Administration. Langley Research Center, Hampton, VA.

ACTIVE COOLING FROM THE SIXTIES TO NASP

H. Neale Kelly (Analytical Services and Materials, Inc., Hampton, VA.) and Max L. Blosser Jul. 1994 61 p Presented at Current Technology for Thermal Protection Systems Workshop, Hampton, VA, 11-12 Feb. 1992

(RTOP 505-70-63-01)

(NASA-TM-109079; NAS 1.15:109079) Avail: CASI HC A04/MF A01

Vehicles, such as the X-15 or the National Aerospace Plane (NASP), traveling at hypersonic speeds through the earth's atmosphere experience aerodynamic heating. The heating can be severe enough that a thermal protection system is required to limit the temperature of the vehicle structure. Although several categories of thermal protection systems are mentioned briefly, the majority of the present paper describes convectively cooled structures for large areas. Convective cooling is a method of limiting structural temperatures by circulating a coolant through the vehicle structure. Efforts to develop convectively cooled structures during the past 30 years, from early engine structures which were intended to be tested on the X-15 to structural panels fabricated and tested under the NASP program, are described. Many of the lessons learned from these research efforts are presented.

Author

N94-37554*# Akron Univ., OH. Dept. of Mechanical and Polymer Engineering.

HIERARCHICALLY PARALLELIZED CONSTRAINED NONLINEAR SOLVERS WITH AUTOMATED SUBSTRUCTURING Final Report

Joe Padovan and Abel Kwang Jun. 1994 86 p

(Grant NAG3-1142; RTOP 505-63-5B)
(NASA-CR-194474; E-8615; NAS 1.26:194474) Avail: CASI HC A05/MF A01

This paper develops a parallelizable multilevel multiple constrained nonlinear equation solver. The substructuring process is automated to yield appropriately balanced partitioning of each succeeding level. Due to the generality of the procedure,—sequential, as well as partially and fully parallel environments can be handled. This includes both single and multiprocessor assignment per individual partition. Several benchmark examples are presented. These illustrate the robustness of the procedure as well as its capability to yield significant reductions in memory utilization and calculational effort due both to updating and inversion. Author (revised)

N94-37622# Sandia National Labs., Albuquerque, NM.
FATIGUE CASE STUDY AND LOADING SPECTRA FOR WIND TURBINES
H. J. Sutherland 1994 6 p Presented at the International Energy Agency Fatigue Experts Meeting, Bergen aan Zee, Netherlands, 21-22 Apr. 1994
(Contract DE-AC04-94AL-85000)
(DE94-010798; SAND-94-1078C; CONF-9404144-1) Avail: CASI HC A02/MF A01

The paper discusses two aspects of Sandia's Wind Energy Program. The first section of the paper presents a case study of fatigue in wind turbines. This case study was prepared for the American Society of Testing Material's (ASTM) Standard Technical Publication (STP) on fatigue education. Using the LIFE2 code, the student is lead through the process of cumulative damage summation for wind turbines and typical data are used to demonstrate the range of life estimates that will result from typical parameter variations. The second section summarizes the results from a workshop held by Sandia and the National Renewable Energy Laboratory (NREL) to discuss fatigue life prediction methodologies. This section summarizes the workshop discussions on the use of statistical modeling to deduce the shape and magnitude of the low-probability-of-occurrence, high-stress tail of the load distribution on a wind turbine during normal operation. DOE

N94-37670# Los Alamos National Lab., NM.
EXPERIMENTAL AND FINITE-ELEMENT SIMULATION RESULTS FOR A PLANE-STRAIN PUNCH-TEST USING ISOTROPIC AND ANISOTROPIC MATERIALS
P. J. Maudlin, M. G. Stout, R. Stevenson, and D. A. Stephenson 1994 6 p Presented at the World Congress on Computational and Applied Mathematics, Atlanta, GA, 11-15 Jul. 1994
(Contract W-7405-eng-36)
(DE94-011711; LA-UR-94-1238; CONF-940719-1) Avail: CASI HC A02/MF A01

Strength constitutive relationships that account for yield surface expansion (i.e., strain-rate hardening, strain hardening and thermal softening) and shape changes (anisotropy) are important for the simulation of metal cutting with Finite Element (FE) techniques. The behavior of 70:30 brass and pure Zn have been examined in the context of the symmetric plane-strain punch test shown in sectional view. This test can be viewed as a precursor orthogonal machining (metal-cutting) problem with a rake (alpha) and clearance angles of 0 degrees. Punch test simulations using an explicit continuum mechanics code are presented and compared to experimental profile and hardness data in the spirit of the work of Weinmann and Turkovich. The rate-dependent elastoplastic constitutive behavior, experimentally measured for these materials, is treated using von Mises and quadratic yield functions (f=0) for brass and Zn, respectively, in conjunction with the Mechanical Threshold Stress (MTS) flow stress (sigma) model. In this paper, we first describe the punch test, present the experimental data, review briefly the constitutive modeling used in the FE simulations, and then compare the simulation results and the experimental data. DOE

N94-37704*# National Aeronautics and Space Administration. Lewis Research Center, Cleveland, OH.
PROBABILISTIC ASSESSMENT OF SPACE NUCLEAR PROPULSION SYSTEM NOZZLE
Ashwin R. Shah (Sverdrup Technology, Inc., Brook Park, OH.), Richard D. Ball (Loral AeroSys, North Olmsted, OH.), and Christos C. Chamis Jun. 1994 14 p Presented at the 38th ASME International Gas Turbine and Aerospace Congress Exposition, Cincinnati, OH, 24-27 May 1994
(Contract NAS3-25266; RTOP 584-04-11)
(NASA-TM-106539; E-8682; NAS 1.15:106539) Avail: CASI HC A03/MF A01

In assessing the reliability of a space nuclear propulsion system (SNPS) nozzle, uncertainties associated with the following design parameters were considered: geometry, boundary conditions, material behavior, and thermal and pressure loads. A preliminary assessment of the reliability was performed using NESSUS (Numerical Evaluation of Stochastic Structures Under Stress), a finite-element computer code developed at the NASA Lewis Research Center. The sensitivity of the nozzle reliability to the uncertainties in the random variables was quantified. With respect to the effective stress, preliminary results showed that the nozzle spatial geometry uncertainties have the most significant effect at low probabilities whereas the inner wall temperature has the most significant effect at higher probabilities. Author

N94-37705# Sandia National Labs., Albuquerque, NM.
NUMERICAL SIMULATION OF DYNAMIC FRACTURE AND FAILURE IN SOLIDS
E. P. Chen 1994 4 p Presented at the International Symposium on Fracture and Strength of Solids, Xian, China, 4-8 Jul. 1994
(Contract DE-AC04-94AL-85000)
(DE94-010379; SAND-94-0247C; CONF-940771-1) Avail: CASI HC A01/MF A01

Numerical simulation of dynamic fracture and failure processes in solid continua using Lagrangian finite element techniques is the subject of discussion in this investigation. The specific configurations in this study include penetration of steel projectiles into aluminum blocks and concrete slabs. The failure mode in the aluminum block is excessive deformation while the concrete slab fails by hole growth, spallation, and scabbing. The transient dynamic finite element code LS-DYNA2D was used for the numerical analysis. The erosion capability in LS-DYNA2D was exercised to carry out the fracture and failure simulations. Calculated results were compared to the experimental data. Good correlations were obtained. DOE

N94-37796*# National Aeronautics and Space Administration. Langley Research Center, Hampton, VA.
WORKSHOP ON SCALING EFFECTS IN COMPOSITE MATERIALS AND STRUCTURES
Karen E. Jackson, comp. (Army Vehicle Structures Lab., Hampton, VA.) Jul. 1994 344 p Workshop held in Hampton, VA, 15-16 Nov. 1993; sponsored by NASA, Washington, Virginia Polytechnic Inst. and State Univ., and California Univ.
(RTOP 505-63-50-09)
(NASA-CP-3271; L-17414; NAS 1.55:3271) Avail: CASI HC A15/MF A03

This document contains presentations and abstracts from the Workshop on Scaling Effects in Composite Materials and Structures jointly sponsored by NASA Langley Research Center, Virginia Tech, and the Institute for Mechanics and Materials at the University of California, San Diego, and held at NASA Langley on November 15-16, 1993. Workshop attendees represented NASA, other government research labs, the aircraft/rotorcraft industry, and academia. The workshop objectives were to assess the state-of-technology in scaling effects in composite materials and to provide guidelines for future research. For individual titles, see N94-37797 through N94-37811.

N94-37797*# Cincinnati Univ., OH. Dept. of Aerospace Engineering and Engineering Mechanics.
DESIGN OF SCALED DOWN STRUCTURAL MODELS
George J. Simitses *In* NASA. Langley Research Center, Workshop on Scaling Effects in Composite Materials and Structures Jul. 1994 p 3-18
(For primary document see N94-37796 12-39)
(Grant NAG1-1280)
Avail: CASI HC A03/MF A03

In the aircraft industry, full scale and large component testing is a very necessary, time consuming, and expensive process. It is essential to find ways by which this process can be minimized without loss of reliability. One possible alternative is the use of scaled down models in testing and use of the model test results in order to predict the behavior of the larger system, referred to herein as prototype. This viewgraph presentation provides

justifications and motivation for the research study, and it describes the necessary conditions (similarity conditions) for two structural systems to be structurally similar with similar behavioral response. Similarity conditions provide the relationship between a scaled down model and its prototype. Thus, scaled down models can be used to predict the behavior of the prototype by extrapolating their experimental data. Since satisfying all similarity conditions simultaneously is in most cases impractical, distorted models with partial similarity can be employed. Establishment of similarity conditions, based on the direct use of the governing equations, is discussed and their use in the design of models is presented. Examples include the use of models for the analysis of cylindrical bending of orthotropic laminated beam plates, of buckling of symmetric laminated rectangular plates subjected to uniform uniaxial compression and shear, applied individually, and of vibrational response of the same rectangular plates. Extensions and future tasks are also described. Author (revised)

N94-37798*# Army Vehicle Structures Lab., Hampton, VA. Landing and Impact Dynamics Branch.

SUB-PLY LEVEL SCALING APPROACH INVESTIGATED FOR GRAPHITE-EPOXY COMPOSITE BEAM COLUMNS

Karen E. Jackson and Sotiris Kellas *In* NASA. Langley Research Center, Workshop on Scaling Effects in Composite Materials and Structures Jul. 1994 p 19-36 (For primary document see N94-37796 12-39)
Avail: CASI HC A03/MF A03

Scale model graphite-epoxy composite specimens were fabricated using the 'sub-ply level' approach and tested as beam-columns under an eccentric axial load to determine the effect of specimen size on flexural response and failure. In the current research project, although the fiber diameters are not scaled, the thickness of the pre-preg material itself has been scaled by adjusting the number of fibers through the thickness of a single ply. Three different grades of graphite-epoxy composite material (AS4/3502) were obtained from Hercules, Inc., in which the number of fibers through the thickness of a single ply was reduced (Grade 190 with 12 to 16 fibers, Grade 95 with 6 to 8 fibers, and Grade 48 with 3 to 4 fibers). Thus, using the sub-ply level approach, a baseline eight ply quasi-isotropic laminate could be fabricated using either the Grade 48 or Grade 95 material and the corresponding full-scale laminate would be constructed from Grade 95 or standard Grade 190 material, respectively. Note that in the sub-ply level approach, the number of ply interfaces is constant for the baseline and full-scale laminates. This is not true for the ply level and sublaminate level scaled specimens. The three grades of graphite-epoxy composite material were used to fabricate scale model beam-column specimens with in-plane dimensions of 0.5*n x 5.75*n, where n=1,2,4 corresponsing to 1/4, 1/2, and full-scale factors. Angle ply, cross ply, and quasi-isotropic laminate stacking sequences were chosen for the investigation and the test matrices for each laminate type are given. Specimens in each laminate family with the same in-plane dimensions but different thicknesses were tested to isolate the influence of the thickness dimension on the flexural response and failure. Also, specific lay-ups were chosen with blocked plies and dispersed plies for each laminate type. Specimens were subjected to an eccentric axial load until failure. The load offset was introduced through a set of hinges which were attached to the platens of a standard load test machine. Three sets of geometrically scaled hinges were used to ensure that scaled loading conditions were applied. This loading condition was chosen because it promotes large flexural deformations and specimens fail at the center of the beam, away from the grip supports. Five channels of data including applied vertical load, end shortening displacement, strain from gages applied back-to-back at the midspan of the beam, and rotation of the hinge from a bubble inclinometer were recorded for each specimen. The beam-column test configuration was used previously to study size effects in ply level scaled composite specimens of the same material system, sizes, and stacking sequences. Thus, a direct comparison between the two scaling approaches is possible. Ply level scaled beam-columns with angle ply, cross ply, and quasi-isotropic lay-ups exhibited no size dependencies in the flexural response, but significant size effects in strength. The reduction in strength with increasing specimen size was not predicted successfully by analysis techniques. It is anticipated that results from this investigation will lead to a better understanding of the strength scale effect in composite structures. Author (revised)

N94-37799*# Northrop Corp., Hawthorne, CA. Aircraft Div.

EFFECTS OF SCALE IN PREDICTING GLOBAL STRUCTURAL RESPONSE

Han-Pin Kan and R. B. Deo *In* NASA. Langley Research Center, Workshop on Scaling Effects in Composite Materials and Structures Jul. 1994 p 37-46 (For primary document see N94-37796 12-39)
(Contract NAS1-18842)
Avail: CASI HC A02/MF A03

In the course of previous composite structures test programs, the need for and the feasibility of developing analyses for scale-up effects has been demonstrated. The analysis techniques for scale-up effects fall into two categories. The first category pertains to developing analysis methods independently for a single, unique failure mode in composites, and using this compendium of analysis methods together with a global structural model to identify and predict the response and failure mode of full-scale built-up structures. The second category of scale-up effects pertains to similitude in structural validation testing. In this latter category, dimensional analysis is used to develop scale-up laws that enable extrapolation of sub-scale component test data to full-scale structures. This viewgraph presentation describes the approach taken and some developments accomplished in the first category of analysis for scale-up effects. Layup dependence of composite material properties severely limits the use of the dimensional analysis approach and these limitations are illustrated by examples. Author (revised)

N94-37800*# Rensselaer Polytechnic Inst., Troy, NY.

SCALING, ELASTICITY, AND CLPT

Eugene J. Brunelle *In* NASA. Langley Research Center, Workshop on Scaling Effects in Composite Materials and Structures Jul. 1994 p 47-56 (For primary document see N94-37796 12-39)
Avail: CASI HC A02/MF A03

The first few viewgraphs describe the general solution properties of linear elasticity theory which are given by the following two statements: (1) for stress B.C. on S(sub sigma) and zero displacement B.C. on S(sub u) the altered displacements u(sub i)(*) and the actual stresses tau(sub ij) are elastically dependent on Poisson's ratio nu alone: thus the actual displacements are given by u(sub i) = mu(exp -1)u(sub i)(*); and (2) for zero stress B.C. on S(sub sigma) and displacement B.C. on S(sub u) the actual displacements u(sub i) and the altered stresses tau(sub ij)(*) are elastically dependent on Poisson's ratio nu alone: thus the actual stresses are given by tau(sub ij) = E tau(sub ij)(*). The remaining viewgraphs describe the minimum parameter formulation of the general classical laminate theory plate problem as follows: The general CLT plate problem is expressed as a 3 x 3 system of differential equations in the displacements u, v, and w. The eighteen (six each) A(sub ij), B(sub ij), and D(sub ij) system coefficients are ply-weighted sums of the transformed reduced stiffnesses (bar-Q(sub ij))(sub k); the (bar-Q(sub ij))(sub k) in turn depend on six reduced stiffnesses (Q(sub ij))(sub k) and the material and geometry properties of the k(sup th) layer. This paper develops a method for redefining the system coefficients, the displacement components (u,v,w), and the position components (x,y) such that a minimum parameter formulation is possible. The pivotal steps in this method are (1) the reduction of (bar-Q(sub ij))(sub k) dependencies to just two constants Q(*) = (Q(12) + 2Q(66))/(Q(11)Q(22))(exp 1/2) and F(*) - (Q(22)/Q(11))(exp 1/2) in terms of ply-independent reference values Q(sub ij); (2) the reduction of the remaining portions of the A, B, and D coefficients to nondimensional ply-weighted sums (with 0 to 1 ranges) that are independent of Q(*) and F(*); and (3) the introduction of simple coordinate stretchings for u, v, w and x,y such that the process is neatly completed. Author (revised)

N94-37801*# Lockheed Advanced Development Co., Sunland, CA.

EXPERIMENTAL OBSERVATIONS OF SCALE EFFECTS ON BONDED AND BOLTED JOINTS IN COMPOSITE STRUCTURES

Glenn C. Grimes *In* NASA. Langley Research Center, Workshop on Scaling Effects in Composite Materials and Structures Jul. 1994 p 57-77 (For primary document see N94-37796 12-39)
Avail: CASI HC A03/MF A03

The objective is to observe size (scale) effects in (1) fiber dominated laminates and bolted joints, (2) adhesive (matrix) dominated bonded joints with fiber dominated laminate adherends, and (3) matrix dominated laminates. Selected literature on scale effects is reviewed with comments and test data from one source that is analyzed for predicted and actual scale

effects utilizing uniaxial loaded static strength, spectrum fatigue residual strength, and spectrum fatigue lifetime test results. Causes of scale effects are discussed, the results are summarized, and conclusions are made.
Author (revised)

N94-37802*# Naval Surface Warfare Center, Annapolis, MD. Composite Materials Program Office.
THE EFFECTS OF SPECIMEN SCALE ON THE COMPRESSION STRENGTH OF COMPOSITE MATERIALS
Eugene Thomas Camponeschi, Jr. *In* NASA. Langley Research Center, Workshop on Scaling Effects in Composite Materials and Structures Jul. 1994 p 81-99 (For primary document see N94-37796 12-39)
Avail: CASI HC A03/MF A03

This paper presents a number of observations on the effect of specimen scale on the compression response of composite materials. Work on this topic was motivated by observations that thick-walled, unstiffened carbon reinforced cylinders subjected to hydrostatic pressure were not reaching inplane laminate stress levels at failure expected from coupon level properties, while similar cylinders reinforced with fiberglass were. Results from a study on coupon strength of (0/0/90) laminates, reinforced with AS4 carbon fiber and S2 glass fiber, are presented and show that compression strength is not a function of material or specimen thickness for materials that have the same laminate quality (autoclave cured quality). Actual laminate compression strength was observed to decrease with increasing thickness, but this is attributed to fixture restraint effects on coupon response. The hypothesis drawn from the coupon level results is further supported by results from a compression test on a thick carbon reinforced coupon in a fixture with reduced influence on specimen response and from a hydrostatic test on an unstiffened carbon reinforced cylinder subjected to hydrostatic pressure with end closures designed to minimize their effect on cylinder response.
Author

N94-37803*# Delaware Univ., Newark, DE. Center for Composite Materials.
ON NATURE'S SCALING EFFECTS
Dick J. Wilkins *In* NASA. Langley Research Center, Workshop on Scaling Effects in Composite Materials and Structures Jul. 1994 p 101-118 (For primary document see N94-37796 12-39)
Avail: CASI HC A03/MF A03

This presentation afforded the opportunity to look back in the literature to discover scaling effects in nature that might be relevant to composites. Numerous examples were found in nature's approaches to wood, teeth, horns, leaves, eggs, feathers, etc. Nature transmits tensile forces rigidly with cohesive bonds, while dealing with compression forces usually through noncompressible hydraulics. The optimum design scaling approaches for aircraft were also reviewed for comparison with similitude laws. Finally, some historical evidence for the use of Weibull scaling in composites was reviewed.
Author

N94-37804*# Illinois Univ., Chicago, IL. Dept. of Civil Engineering, Mechanics and Metallurgy.
STRENGTH CHARACTERISTICS AND CRACK GROWTH BEHAVIOR OF A COMPOSITE WITH WELL ALIGNED FIBERS
John Botsis, C. Beldica, Ari G. Caliskan, and D. Zhao *In* NASA. Langley Research Center, Workshop on Scaling Effects in Composite Materials and Structures Jul. 1994 p 119-143 (For primary document see N94-37796 12-39)
(Grant AF-AFOSR-0493-92)
Avail: CASI HC A03/MF A03

Continuous fiber composites have shown tremendous promise in industrial applications. Their microstructures, however, are very complex and in many instances difficult to characterize. In this project, the fracture characteristics of a specially made fiber reinforced composite with different fiber spacing are investigated. The experimental results so far have shown that after an initial transient phase the crack speed reaches a steady phase, i.e., independent of the crack length. Within the steady crack growth phase debonding along the fibers in the bridging zone grows in a self-similar manner. During the steady phase the energy dissipation per cycle is constant. Afterwards, an increase of the energy dissipation is observed that is accompanied by a decrease in crack speed. This latter trend is presumed to be the result of relatively large amounts of energy dissipated in the bulk of the specimen. Using appropriate Green's function and computer simulations, the stress intensity factor at the crack tip is evaluated for various cases of bridging stresses. In this way the effects of specimen size and fiber spacing on the overall fracture behavior of the composite system are analyzed. The steady crack speed and the steady rate of debonding have a similar power dependence on stress level. Dimensional analysis demonstrates that the particular fracture process is not governed by dimensional invariance but on the detailed micromechanisms in the bridging zone.
Author

N94-37805*# Army Vehicle Structures Lab., Hampton, VA.
DAMAGE AND STRENGTH OF COMPOSITE MATERIALS: TRENDS, PREDICTIONS, AND CHALLENGES
T. Kevin OBrien *In* NASA. Langley Research Center, Workshop on Scaling Effects in Composite Materials and Structures Jul. 1994 p 145-159 (For primary document see N94-37796 12-39)
Avail: CASI HC A03/MF A03

Research on damage mechanisms and ultimate strength of composite materials relevant to scaling issues will be addressed in this viewgraph presentation. The use of fracture mechanics and Weibull statistics to predict scaling effects for the onset of isolated damage mechanisms will be highlighted. The ability of simple fracture mechanics models to predict trends that are useful in parametric or preliminary designs studies will be reviewed. The limitations of these simple models for complex loading conditions will also be noted. The difficulty in developing generic criteria for the growth of these mechanisms needed in progressive damage models to predict strength will be addressed. A specific example for a problem where failure is a direct consequence of progressive delamination will be explored. A damage threshold/fail-safety concept for addressing composite damage tolerance will be discussed.
Author (revised)

N94-37806*# National Aeronautics and Space Administration. Langley Research Center, Hampton, VA.
EFFECTS OF PLY THICKNESS ON THERMAL CYCLE INDUCED DAMAGE AND THERMAL STRAIN
Stephen S. Tompkins *In its* Workshop on Scaling Effects in Composite Materials and Structures Jul. 1994 p 161-177 (For primary document see N94-37796 12-39)
Avail: CASI HC A03/MF A03

An experimental study was conducted to determine the effects of ply thickness in composite laminates on thermally induced cracking and changes in the coefficient of thermal expansion, CTE. A graphite-epoxy composite material, P75/ERL 1962, in thin (1 mil) and thick (5 mils) prepregs was used to make cross-ply laminates, ((0/90)(sub n))s, with equal total thickness (n=2, n=10) and cross-ply laminates with the same total number of plies (n=2). Specimens of each laminate configuration were cycled up to 1500 times between -250 and 250 F. Thermally induced microdamage was assessed as a function of the number of cycles as was the change in CTE. The results showed that laminates fabricated with thin-plies microcracked at significantly different rates and reached significantly different equilibrium crack densities than the laminate fabricated with thick-ply and n=2. The CTE of thin-ply laminates was less affected by thermal cycling and damage than the CTE of thick-ply laminates. These differences are attributed primarily to differences in interply constraints. Observed effects of ply thickness on crack density was qualitatively predicted by a combined shear-lag stress/energy method.
Author (revised)

N94-37807*# Drexel Univ., Philadelphia, PA. Dept. of Mechanical Engineering.
SCALING EFFECTS OF DEFECTS IN FIBER-REINFORCED COMPOSITES
A. S. D. Wang *In* NASA. Langley Research Center, Workshop on Scaling Effects in Composite Materials and Structures Jul. 1994 p 179-195 (For primary document see N94-37796 12-39)
Avail: CASI HC A03/MF A03

Material defects may be introduced willingly or unwillingly during material manufacturing and structural component fabrication stages. Their presence in the material plays a dominant role in determining the material's strength and the associate failure mechanisms. In the sense that the size and the number of defects may increase with the volume of the material, the effect of dimensional scaling may manifest itself in the dependence of material strength on volume. Or, alternatively, there may exist a scaling effect of material defects. In fiber-reinforced composites, manufacturing or

fabrication defects may come in several forms: matrix voids, matrix microcracks, fiber misalignment, broken fibers, or interface disbonds, just to mention a few. These are interacting and competing defects in the sense that one type of defect may become dominant under one stress condition and another type of defect may become dominant under a different stress condition. This happens because the fiber reinforcement network, together with the distribution of defects, constitutes the prime microstructure of the composite, and there exist continued interactions between the evolving microstructure and the distribution of defects. In the process, the scaling effects of defects are complicated by this interaction. In this presentation, the scaling effects of defects in fiber-reinforced composites will be briefly discussed with the introduction of the concept of effective defects. It is then shown with the aid of some actual experimental and analysis results that the scaling effects are very much present, but they are regulated by the characteristic dimension of the composite microstructure due to the aforementioned microstructure-defect interaction effect. Author

N94-37808*# Martin Marietta Astro Space, Philadelphia, PA. Advanced Technology Div.

SIZE EFFECT IN COMPOSITE MATERIALS AND STRUCTURES: BASIC CONCEPTS AND DESIGN CONSIDERATIONS

Carl Zweben *In* NASA. Langley Research Center, Workshop on Scaling Effects in Composite Materials and Structures Jul. 1994 p 197-217 (For primary document see N94-37796 12-39)

Avail: CASI HC A03/MF A03

Composite materials display strength characteristics that are similar to those of brittle ceramics, whose strengths are known to decrease with increasing volume for a uniform state of stress (size effect) and also are dependent on stress distribution. These similarities raise the question of whether there is also a size effect in composite materials and structures. There is significant, but inconclusive experimental evidence for the existence of a size effect in composites. Macroscopic and micromechanical statistical models have been developed which predict a size effect and are in general agreement with experimental data. The existence of a significant size effect in composites would be of great importance. For example, it would mean that use of standard test coupons to establish design allowables for large structures could be very nonconservative. Further, it would be necessary to analyze the strength of large composite structures using statistical methods, as is done for ceramics. Author

N94-37809*# Cornell Univ., Ithaca, NY. Dept. of Theoretical and Applied Mechanics.

STATISTICAL SCALING RELATIONSHIPS AND SIZE EFFECTS IN THE STRENGTH AND CREEP RUPTURE OF FIBROUS COMPOSITES

S. Leigh Phoenix *In* NASA. Langley Research Center, Workshop on Scaling Effects in Composite Materials and Structures Jul. 1994 p 219-242 (For primary document see N94-37796 12-39)

Avail: CASI HC A03/MF A03

In this presentation we discuss a new theoretical model and supporting experimental results for the strength and lifetime in creep rupture of unidirectional, carbon fiber/epoxy matrix composites at ambient conditions. First we review the 'standard' Weibull/power-law methodology that has been standard practice. Then we discuss features of a recent model which build on the statistical aspects of fiber strength, micromechanical aspects of stress transfer around fiber breaks, and time-dependent creep of the matrix. The model is applied to 'microcomposites' consisting of seven fibers in a matrix for which strength and creep-rupture data are available. The model yields Weibull distributions in an envelope format for both strength and lifetime. The respective shape, scale and power-law parameters depend on such parameters as the Weibull shape parameter for fiber strength, the exponent for matrix creep, the effective load transfer length (which grows in time due to matrix creep) and the critical cluster size for failed fibers. The experimental results are consistent with the theory, though time-dependent debonding appears to be part of the failure process. Author

N94-37810*# Utah Univ., Salt Lake City, UT. Dept. of Mechanical Engineering.

SCALING OF IMPACT DAMAGE IN FIBER COMPOSITES

Stephen R. Swanson *In* NASA. Langley Research Center, Workshop on Scaling Effects in Composite Materials and Structures Jul. 1994 p 245-264 (For primary document see N94-37796 12-39)

Avail: CASI HC A03/MF A03

Impact damage in fiber composite structures remains of much concern, and is often the limiting factor in establishing allowable strain levels. The complexity of impact damage formation usually dictates that experiments are required, but scaling of results from small laboratory scale specimens to large structures introduces additional uncertainty into the analysis. This presentation gives the results of an analytical and experimental investigation intended to develop procedures for prediction of damage formation and subsequent strength loss, with particular emphasis on scaling of results with respect to structure size. The experimental investigation involved both drop-weight and airgun impact on carbon/epoxy plates and cylinders. Five sizes of plates ranging from 50 by 50 by 1.072 mm to 250 by 250 by 5.36 mm, and two sizes of cylinders with diameters of 96.5 and 319 mm, were employed in the experimental program. Impact tests were carried out over a range of impact conditions, and specimens were inspected for damage by C-scan and deplying. Analysis procedures were develcped for both quasistatic and dynamic impacts for both the plates and cylinders. As has been reported previously, comparison of predicted structural response and measured surface strains was quite good over the entire range of sizes employed in the program. The damage formation and strength loss after impact showed a number of interesting features that are significant with respect to scaling of size. The extent of delamination was observed to increase with specimen size more than would be expected if stresses controlled the delamination extent. This was explained on the basis that delamination is controlled by energy release rates, and thus incorporates the usual dependence on the absolute size characteristic of fracture mechanics. Additionally, the experiments indicated that delamination initiated at matrix cracks and is dependent on the absolute size of the ply group thicknesses. Both the initiation and propagation of delamination are seen to be controlled by fracture mechanics parameters, and thus show specific dependence on size that must be accounted for in extrapolating results from laboratory scale tests to full size structures. Author (revised)

N94-37811*# National Aeronautics and Space Administration. Langley Research Center, Hampton, VA.

IMPACT FORCE AS A SCALING PARAMETER

Clarence C. Poe, Jr. and Wade C. Jackson *In its* Workshop on Scaling Effects in Composite Materials and Structures Jul. 1994 p 305-338 (For primary document see N94-37796 12-39)

Avail: CASI HC A03/MF A03

The Federal Aviation Administration (FAR PART 25) requires that a structure carry ultimate load with nonvisible impact damage and carry 70 percent of limit flight loads with discrete damage. The Air Force has similar criteria (MIL-STD-1530A). Both civilian and military structures are designed by a building block approach. First, critical areas of the structure are determined, and potential failure modes are identified. Then, a series of representative specimens are tested that will fail in those modes. The series begins with tests of simple coupons, progresses through larger and more complex subcomponents, and ends with a test on a full-scale component, hence the term 'building block.' In order to minimize testing, analytical models are needed to scale impact damage and residual strength from the simple coupons to the full-scale component. Using experiments and analysis, the present paper illustrates that impact damage can be better understood and scaled using impact force than just kinetic energy. The plate parameters considered are size and thickness, boundary conditions, and material, and the impact parameters are mass, shape, and velocity. Author

42 GEOSCIENCES (GENERAL)

No abstracts in this category.

43 EARTH RESOURCES AND REMOTE SENSING

Includes remote sensing of earth resources by aircraft and spacecraft; photogrammetry; and aerial photography.

For instrumentation see *35 Instrumentation and Photography.*

N94-36464# Argonne National Lab., IL.

RESCALED BOX COUNTING FOR THE TOPOLOGICAL ANALYSIS OF SPATIAL DATA

C. Loehle 1994 22 p

(Contracts W-31-109-eng-38; DE-AC09-76SR-00819)

(DE94-009820; ANL/ER/PP-74856) Avail: CASI HC A03/MF A01

Topological analysis of surfaces of natural objects can provide information about surface features (ridges, fragmentation, dendritic patterns) and surface roughness. Box counting is a general method useful for such surfaces, but it is currently limited to cases where the x, y, and z directions are all in the same metric. A method, rescaled box counting, is presented for overcoming these limitations. The local first omnidirectional semivariance (lag 1) is calculated for boxes of different sizes. If the semivariance is not small for small box sizes, then the z data need to be scaled up to allow detection of a difference between patches that are significantly different. This rescaling converts the z metric into a distance equivalent (z units are converted into distances based on the horizontal distance over which a significant change in z is found to occur). Once rescaling is done, box counting can be used to quantify surface topology. DOE

N94-36827*# National Aeronautics and Space Administration, Washington, DC.

MODELING THE EARTH SYSTEM IN THE MISSION TO PLANET EARTH ERA

Sushel Unninayar and Kenneth H. Bergman Jul. 1993 140 p

(NASA-TM-109892; NAS 1.15:109892) Avail: CASI HC A07/MF A02

A broad overview is made of global earth system modeling in the Mission to Planet Earth (MTPE) era for the multidisciplinary audience encompassed by the Global Change Research Program (GCRP). Time scales of global system fluctuation and change are described in Section 2. Section 3 provides a rubric for modeling the global earth system, as presently understood. The ability of models to predict the future state of the global earth system and the extent to which their predictions are reliable are covered in Sections 4 and 5. The 'engineering' use of global system models (and predictions) is covered in Section 6. Section 7 covers aspects of an increasing need for improved transform algorithms and better methods to assimilate this information into global models. Future monitoring and data requirements are detailed in Section 8. Section 9 covers the NASA-initiated concept 'Mission to Planet Earth,' which employs space and ground based measurement systems to provide the scientific basis for understanding global change. Section 10 concludes this review with general remarks concerning the state of global system modeling and observing technology and the need for future research. CASI

N94-36919*# Aerojet Delft Corp., Azusa, CA.

EARTH OBSERVING SYSTEM/ADVANCED MICROWAVE SOUNDING UNIT-A (EOS/AMSU-A) SOFTWARE MANAGEMENT PLAN Final Report

Robert Schwantje 20 Jun. 1994 39 p

(Contract NAS5-32314; RTOP 422-00-00)

(NASA-CR-189362; NAS 1.26:189362; Rept-9803-1; Rept-10339; CDRL-008) Avail: CASI HC A03/MF A01

This document defines the responsibilites for the management of the like-cycle development of the flight software installed in the AMSU-A instruments, and the ground support software used in the test and integration of the AMSU-A instruments. Author (revised)

44 ENERGY PRODUCTION AND CONVERSION

Includes specific energy conversion systems, e.g., fuel cells; global sources of energy; geophysical conversion; and windpower.

For related information see also *07 Aircraft Propulsion and Power, 20 Spacecraft Propulsion and Power,* and *28 Propellants and Fuels.*

N94-36476# Midwest Research Inst., Golden, CO. National Renewable Energy Lab.

AMORPHOUS SILICON PHOTOVOLTAIC MANUFACTURING TECHNOLOGY, PHASE 2A

G. Duran (Utility Power Group, Chatsworth, CA.), K. Mackamul (Utility Power Group, Chatsworth, CA.), D. Metcalf (Utility Power Group, Chatsworth, CA.), and H. Volltrauer (Advanced Photovoltaic Systems, Inc., Princeton, NJ.) Apr. 1994 40 p

(Contract DE-AC02-83CH-10093)

(DE94-006895; NREL/TP-411-6470-Phase-2A) Avail: CASI HC A03/MF A01

Utility Power Group (UPG) and its lower-tier subcontractor, Advanced Photovoltaic Systems, Inc. (APS), continued work to develop their manufacturing lines. UPG focused on the automation of encapsulation and termination processes developed in Phase 1. APS focused on completion of the encapsulation and module design tasks while continuing process quality control, and automation projects. The goal is to produce 55-W (stabilized) EP50 modules in a new facility. DOE

N94-36511# Duke Univ., Durham, NC. Dept. of Mechanical Engineering and Materials Science.

NOVEL CARBON-ION FUEL CELLS

F. H. Cocks and H. LaViers 30 Jan. 1994 7 p

(Contract DE-FG22-93PC-93219)

(DE94-010716; DOE/PC-93219/T1) Avail: CASI HC A02/MF A01

Apparatuses are being constructed and supplies are being procured. Results of DTA runs on CeC2 and LaC2 were inconclusive. Literature searches continue to yield positive results. DOE

N94-36740# Midwest Research Inst., Golden, CO. National Renewable Energy Lab.

INTEGRATED GASIFICATION COMBINED CYCLE AND STEAM INJECTION GAS TURBINE POWERED BY BIOMASS JOINT-VENTURE EVALUATION

George J. Sterzinger (Economics, Environment and Regulation, Washington, DC.) May 1994 54 p

(Contract DE-AC02-83CH-10093)

(DE94-006905; NREL/TP-430-6080) Avail: CASI HC A04/MF A01

This report analyzes the economic and environmental potential of biomass integrated gasifier/gas turbine technology including its market applications. The mature technology promises to produce electricity at $55-60/MWh and to be competitive for market applications conservatively estimated at 2000 MW. The report reviews the competitiveness of the technology of a stand-alone, mature basis and finds it to be substantial and recognized by DOE, EPRI, and the World Bank Global Environmental Facility. DOE

N94-36805*# Creare, Inc., Hanover, NH. Engineering Research and Development.

PRELIMINARY DESIGN FOR A REVERSE BRAYTON CYCLE CRYOGENIC COOLER Final Report, Sep. 1990 - Dec. 1992

Walter L. Swift 10 Dec. 1993 79 p

(Contract NAS5-31281)

(NASA-CR-189341; NAS 1.26:189341; Creare-TN-508) Avail: CASI HC A05/MF A01

A long life, single stage, reverse Brayton cycle cryogenic cooler is being developed for applications in space. The system is designed to provide 5 W of cooling at a temperature of 65 Kelvin with a total cycle input power of less than 200 watts. Key features of the approach include high speed, miniature turbomachines; an all metal, high performance, compact heat exchanger; and a simple, high frequency, three phase motor drive. In Phase 1, a preliminary design of the system was performed. Analyses and trade studies were used to establish the thermodynamic performance of the system and the performance specifications for individual components. Key mechanical features for components were defined and

assembly layouts for the components and the system were prepared. Critical materials and processes were identified. Component and brassboard system level tests were conducted at cryogenic temperatures. The system met the cooling requirement of 5 W at 65 K. The system was also operated over a range of cooling loads from 0.5 W at 37 K to 10 W at 65 K. Input power to the system was higher than target values. The heat exchanger and inverter met or exceeded their respective performance targets. The compresssor/motor assembly was marginally below its performance target. The turboexpander met its aerodynamic efficiency target, but overall performance was below target because of excessive heat leak. The heat leak will be reduced to an acceptable value in the engineering model. The results of Phase 1 indicate that the 200 watt input power requirement can be met with state-of-the-art technology in a system which has very flexible integration requirements and negligible vibration levels. Author (revised)

N94-36807*# Thomson Research Projects, Inc., Lake Mills, WI.
MARS VERTICAL AXIS WIND MACHINES. THE DESIGN OF A DARREUS AND A GIROMILL FOR USE ON MARS Final Report
David Brach (Wisconsin Univ., Madison, WI.), John Dube (Wisconsin Univ., Madison, WI.), Jon Kelly (Wisconsin Univ., Madison, WI.), JoAnna Peterson (Wisconsin Univ., Madison, WI.), John Bollig (Wisconsin Univ., Madison, WI.), Lisa Gohr (Wisconsin Univ., Madison, WI.), Kamin Mahoney (Wisconsin Univ., Madison, WI.), and Dave Polidori (Wisconsin Univ., Madison, WI.) May 1992 219 p
(Contract NCC2-710)
(NASA-CR-196143; NAS 1.26:196143) Avail: CASI HC A10/MF A03

This report contains the design of both a Darrieus and a Giromill for use on Mars. The report has been organized so that the interested reader may read only about one machine without having to read the entire report. Where components for the two machines differ greatly, separate sections have been allotted for each machine. Each section is complete; therefore, no relevant information is missed by reading only the section for the machine of interest. Also, when components for both machines are similar, both machines have been combined into one section. This is done so that the reader interested in both machines need not read the same information twice. Derived from text

N94-36823*# Thomson Research Projects, Inc., Lake Mills, WI.
MARS VERTICAL AXIS WIND MACHINES: THE DESIGN OF A TORNADO VORTEX MACHINE FOR USE ON MARS
Daun Carlin (Wisconsin Univ., Madison, WI.), Amy Dyhr (Wisconsin Univ., Madison, WI.), Jon Kelly (Wisconsin Univ., Madison, WI.), J. Eric Schmirler (Wisconsin Univ., Madison, WI.), Mike Carlin (Wisconsin Univ., Madison, WI.), Won E. Hong (Wisconsin Univ., Madison, WI.), and Kamin Mahoney (Wisconsin Univ., Madison, WI.) Jun. 1994 53 p
(Contract NCC2-710)
(NASA-CR-196144; NAS 1.26:196144) Avail: CASI HC A04/MF A01

Ever since Viking 1 and 2 landed on the surface of Mars in the summer of 1976, man has yearned to go back. But before man steps foot upon the surface of Mars, unmanned missions such as the Martian Soft Lander and Martian Subsurface Penetrator will precede him. Alternative renewable power sources must be developed to supply the next generation of surface exploratory spacecraft, since RTG's, solar cells, and long-life batteries all have their significant drawbacks. One such alternative is to take advantage of the unique Martian atmospheric conditions by designing a small scale, Martian wind power generator, capable of surviving impact and fulfilling the long term (2-5 years), low-level power requirements (1-2 Watts) of an unmanned surface probe. After investigation of several wind machines, a tornado vortex generator was chosen based upon its capability of theoretically augmenting and increasing the available power that may be extracted from average Martian wind speeds of approximately 7.5 m/s. The Martian Tornado Vortex Wind Generator stands 1 meter high and has a diameter of 0.5 m. Martian winds enter the base and shroud of the Tornado Vortex Generator at 7.5 m/s and are increased to an exit velocity of 13.657 m/s due to the vortex that is created. This results in a rapid pressure drop of 4.56 kg/s(exp 2) m across the vortex core which aids in producing a net power output of 1.1765 Watts. The report contains the necessary analysis and requirements needed to feasibly operate a low-level powered, unmanned, Martian surface probe. Author (revised)

N94-37189# Sandia National Labs., Albuquerque, NM.
PROGRESS ON THE EMITTER WRAP-THROUGH SILICON SOLAR CELL
J. M. Gee, M. E. Buck, W. K. Schubert, and P. A. Basore 1993 11 p Presented at the 12th European Photovoltaic Solar Energy Conference and Exhibition, Amsterdam, Netherlands, 11-15 Apr. 1994
(Contract DE-AC04-94AL-85000)
(DE94-010382; SAND-93-1684C; CONF-940423-1) Avail: CASI HC A03/MF A01

The Emitter Wrap-Through (EWT) solar cell is a back-contacted solar cell with a carrier-collection junction (emitter) on the front surface. Elimination of grids from the front surface allows for higher performance by eliminating grid-obscuration losses and reducing series resistance, while keeping an emitter on the front surface maintains high collection efficiency in solar-grade materials with modest diffusion lengths. The EWT cell uses laser-drilled vias to wrap the emitter diffusion on the front surface to interdigitated contacts on the back surface. We report on progress towards demonstration of two concepts for the EWT cell. The first EWT concept uses a fabrication sequence based on heavily diffused grooves and plated metallizations, and the second EWT concept uses a single furnace step and screen-printed metallizations. We also report on demonstration of double-sided carrier collection in the EWT cell. DOE

N94-37381 Washington State Univ., Richland, WA.
INVESTIGATION OF POLYCRYSTALLINE THIN-FILM CuInSe2 SOLAR CELLS BASED ON ZnSe WINDOWS
L. C. Olsen May 1994 15 p Prepared for Midwest Research Inst., Golden, CO Limited Reproducibility: More than 20% of this document may be affected by microfiche quality
(Contract DE-AC02-83CH-10093)
(DE94-006936; NREL/TP-451-6469) Avail: CASI HC A03

Investigations of ZnSe/CIS solar cells are being carried out in an effort to improve the efficiencies CIS cells and to determine if ZnSe is a viable alternative to CdS as a window material. MOCVD growth of ZnSe is accomplished in a SPIRE 500XT reactor housed in the Electronic Materials Laboratory at WSU Tri-Cities by reacting a zinc adduct with H2Se. Conductive n-type ZnSe is grown by using iodine as a dopant. Ethyliodide was mixed with helium and installed on one of the gas lines to the system. ZnSe films have been grown on CIS substrates at 200 degrees C to 250 degrees C. ZnO is also being deposited by MOCVD by reacting tetrahydrofuran (THF) with a zinc adduct. ZnSe/CIS heterojunctions have been studied by growing n-ZnSe films onto 2 cm x 2 cm CIS substrates diced from materials supplied by Siemens and then depositing an array of aluminum circular areas 2.8.mm in diameter on top of the ZnSe to serve as contacts. Al films are deposited with a thickness of 80 to l00 angstroms so that light can pass through the film, thus allowing the illuminated characteristics of the ZnSe/CIS junction to be tested. Accounting for the 20 to 25 % transmittance through the Al film into the ZnSe/CIS structure, current devices have estimated, active-area AM1.5 efficiencies of 14%. Open circuit voltages greater than 500 mV are often attained. DOE

N94-37407# Midwest Research Inst., Golden, CO. National Renewable Energy Lab.
US MANUFACTURERS OF COMMERCIALLY AVAILABLE STAND-ALONE PHOTOVOLTAIC LIGHTING SYSTEMS
P. McNutt May 1994 16 p
(Contract DE-AC02-83CH-10093)
(DE94-006917; NREL/TP-411-6406) Avail: CASI HC A03/MF A01

This report introduces photovoltaic (PV) lighting systems, gives some specifications for ordering these systems, and provides a list of some of the manufacturers of these systems in the United States. These PV lighting systems are all commercially available. They are stand-alone systems because they are not tied to the electric utility power grid. DOE

N94-37418# Japan Solar Energy Society, Tokyo (Japan).
1993 JSES (JAPAN SOLAR ENERGY SOCIETY)/JWEA (JAPA N WIND ENERGY ASSOCIATION) JOINT CONFERENCE AND 1993 JAPAN-KOREA JOINT CONFERENCE ON SOLAR ENERGY
Dec. 1993 323 p In JAPANESE Conferences held in Tsukuba, Japan, 9-10 Dec. 1993
(DE94-767725; CONF-931269) Avail: CASI HC A14/MF A03

The 1993 JSES/JWEA Joint Conference was held on December 9 and

10, 1993. As for solar cells, reports are made on performance of a-Si photovoltaic modules, heightening efficiency of polycrystalline silicon solar cells, and solar cell/capacitor combined devices. As to solar concentration of solar cells, compound elliptic lens and characteristics of cone type concentrators are reported. With regard to the photovoltaic power generation system, described are results of solar house operation and eco energy house power generation. Relating to heat storage, mentioned are a design method of the seasonal thermal storage system using water as a medium and the optimal control of the ground thermal storage system. As to heat pumps, the paper states an analysis of an exothermic reactor on the solar chemical heat pump system, and a hybrid heat pump system using panels with photovoltaic modules as evaporator. In addition, a wind powered generation system for weather observation robot, and a floating wave power device are described. DOE

N94-37488# Fuel Cell Engineering Corp., Danbury, CT.
MCFC PRODUCT DEVELOPMENT TEST
A. K. Kush, A. J. Leo, and T. P. OShea 1993 10 p Presented at the Joint Contractors Meeting on Advanced Turbine Systems, Fuel Cells and Coal-Fired Heat, Morgantown, WV, 3-5 Aug. 1993
(Contract DE-FC21-92MC-29237)
(DE94-002005; DOE/MC-29237/94/C0248; CONF-930893-3) Avail: CASI HC A02/MF A01

The objective of the 2 MW Santa Clara Demonstration Project is the demonstration of the direct carbonate fuel cell technology at full scale. Specific objectives of the project include the demonstration of advantages of the carbonate fuel cell power plant, such as high efficiency, low emissions, reactive power capability, and high reliability and availability. The project will also provide a design basis for precommercial power plants. DOE

N94-37567# Energy Information Administration, Washington, DC. Office of Coal, Nuclear, Electric and Alternate Fuels.
ESTIMATES OF US BIOMASS ENERGY CONSUMPTION 1992
May 1994 46 p
(DE94-011458; DOE/EIA-0548(92)) Avail: CASI HC A03/MF A01

This report is the seventh in a series of publications developed by the Energy Information Administration (EIA) to quantify the biomass-derived primary energy used by the U.S. economy. It presents estimates of 1991 and 1992 consumption. The objective of this report is to provide updated estimates of biomass energy consumption for use by Congress, Federal and State agencies, biomass producers and end-use sectors, and the public at large. DOE

45 ENVIRONMENT POLLUTION

Includes atmospheric, noise, thermal, and water pollution.

N94-36470# Sandia National Labs., Albuquerque, NM.
PALEOCLIMATE VALIDATION OF A NUMERICAL CLIMATE MODEL
F. J. Schelling (Sandia National Labs., Las Vegas, NV.), H. W. Church, B. D. Zak, and S. L. Thompson 1994 4 p Presented at the International High-Level Radioactive Waste Management Conference, Las Vegas, NV, 22-26 May 1994
(Contract DE-AC04-94AL-85000)
(DE94-009287; SAND-93-4002C; CONF-940553-30) Avail: CASI HC A01/MF A01

An analysis planned to validate regional climate model results for a past climate state at Yucca Mountain, Nevada, against paleoclimate evidence for the period is described. This analysis, which will use the GENESIS model of global climate nested with the RegCM2 regional climate model, is part of a larger study for DOE's Yucca Mountain Site Characterization Project that is evaluating the impacts of long term future climate change on performance of the potential high level nuclear waste repository at Yucca Mountain. The planned analysis and anticipated results are presented. DOE

N94-36477# Pacific Northwest Lab., Richland, WA.
ARM: A CLIMATE PROCESS OBSERVATORY
G. M. Stokes and W. T. Pennell Jan. 1994 4 p Presented at the 5th Annual Symposium on Global Change Studies, Nashville, TN, 24-28 Jan. 1994
(Contract DE-AC06-76RL-01830)
(DE94-007473; PNL-SA-23162; CONF-940131-6) Avail: CASI HC A01/MF A01

In May 1992 the Department of Energy's Atmospheric Radiation Measurement (ARM) Program began deploying instrumentation and conducting measurements at its first field site near Lamont in North Central Oklahoma. ARM is a major program of atmospheric measurement and modeling intended to improve understanding of the processes and properties that affect atmospheric radiation. Particular emphasis is being placed on the role of clouds in radiative transport and on improving the representation of clouds and cloud radiative properties in climate models. In this paper we provide a brief overview of the ARM Program. We discuss the philosophy behind the ARM experiment design, describe the types of experiments underway and their objectives, and we portray how the suite of instrumentation and the observational strategy is expected to evolve as the process of experiment design, hypothesis testing, and learning plays out over the next decade. DOE

N94-36478# Pacific Northwest Lab., Richland, WA.
SHORT-TOWER SIGMA(THETA) MEASUREMENTS IN THE COLORADO PLATEAUS REGION
R. K. Hauser, C. D. Whiteman, and K. J. Allwine Jan. 1994 9 p Presented at the 74th American Meteorological Society Annual Meeting, Nashville, TN, 23-28 Jan. 1994
(Contract DE-AC06-76RL-01830)
(DE94-007478; PNL-SA-23105; CONF-940115-26) Avail: CASI HC A02/MF A01

The standard deviation of the wind direction, (sigma)(sub (theta)), is related to horizontal turbulent diffusion in the atmosphere and has been widely used in pollutant dispersion calculations. The elevation and exposure of sites in complex terrain is associated with the statistics of the distribution of hourly wind direction standard deviation. At ridge-top sites during the cool season, hourly (sigma)(sub (theta)) distributions have small standard deviations and positive kurtosis. Open-exposure sites that experience broad-channeled flows show the greatest positive skewness and kurtosis. Sheltered-exposure and basin locations exhibit large standard deviations, the smallest skewness, and negative kurtosis. The tendency for the product (sigma)(sub (theta))V(sub v) to yield a site-specific empirical constant is seen in hourly data in complex terrain, even when robust, relatively inexpensive wind sensors and datalogging equipment are used. The value of the constant exhibits dependence on elevation, the exposure, stability, and the strength of the overlying flow. It may be possible to build on these techniques and relationships to map the expected wind direction variability in complex terrain. DOE

N94-36533 National Physical Lab., Teddington (England).
UK METHANE EMISSIONS INVENTORY: A SCOPING STUDY ON THE USE OF AMBIENT MEASUREMENTS TO REDUCE UNCERTAINTIES
1994 87 p Prepared in cooperation with Warren Spring Lab., Stevenage, England and AEA Technology, London, England
(PB94-167855; NPL-DQM-98) Copyright Avail: Issuing Activity (National Technical Information Service (NTIS))

The UK already has a National Atmospheric Emissions Inventory (NAEI), produced by WSL under contract to the DOE (Air Quality Division), but it is known that there are uncertainties in the NAEI for various gases, including methane, which is the second most important in terms of its global warming potential. The report evaluates the present status of the UK emissions estimate for methane, and assess the practical benefits that could be realized by applying available measurement techniques to the most important emission sources. The report is in three parts. The first is a thorough re-working of the UK National Atmospheric Emissions Inventory for methane; the second part contains a review of techniques available for the measurement of atmospheric methane emissions, together with an evaluation of the benefits of applying them to the task of improving the estimate of specific contributions to the total estimate of UK methane emissions. The use of these techniques to verify the total value and to investigate the possibility of omissions from the inventory is also discussed. The report concludes with recommendations for the most cost-effective methods for improving the inventory. NTIS

N94-36552# Atmospheric and Environmental Research, Inc., Cambridge, MA.
ACCELERATED LINE-BY-LINE CALCULATIONS FOR THE RADIATIVE TRANSFER OF TRACE GASES RELATED TO CLIMATE STUDIES
S. A. Clough 15 Nov. 1993 11 p
(Contract DE-FG02-93ER-61549)
(DE94-004404; DOE/ER-61549/1) Avail: CASI HC A03/MF A01

In the present study we are studying the effects of including carbon dioxide, ozone, methane, and the halocarbons in addition to water vapor in the radiating atmosphere. The study has focused on two principal issues: the effect on the spectral fluxes and cooling rates of carbon dioxide, ozone and the halocarbons at 1990 concentration levels and the change in fluxes and cooling rates as a consequence of the anticipated ten year change in the profiles of these species. For the latter study the water vapor profiles have been taken as invariant in time. The radiative line-by-line calculations using LBLRTM (Line-By-Line Radiative Transfer Model) have been performed for tropical (TRP), mid-latitude winter (MLW) and mid-latitude summer (MLS) model atmospheres. The halocarbons considered in the present study are CCl4, CFC-11, CFC-12 and CFC-22. In addition to considering the radiative effects of carbon dioxide at 355 ppm, the assumed current level, we have also obtained results for doubled carbon dioxide at 710 ppm. An important focus of the current research effort is the effect of the ozone depletion profile on atmospheric radiative effects. DOE

N94-36973 Pacific-Sierra Research Corp., Santa Monica, CA.
CONTROLLED ATMOSPHERIC BREAKDOWN: APPLICATIONS AND RESEARCH OPPORTUNITIES
E. C. Field, Jr. 14 May 1993 54 p Limited Reproducibility: More than 20% of this document may be affected by microfiche quality
(Contract F19628-90-C-0100)
(AD-A278584; AD-E201846; PL-TR-93-2159; SR-2) Avail: Issuing Activity (Defense Technical Information Center (DTIC))

This document introduces applications and research opportunities associated with the controlled breakdown (i.e., ionization) of selected regions of the atmosphere. United States Air Force interest in this area originated in 1986 under Project Forecast 2, a far-reaching effort to exploit revolutionary technologies for enhancing the Air Force's Mission capabilities into the 21st Century. One such technology identified was the so-called Artificial Ionospheric Mirror (AIM), a concept to employ a ground-based, very high power, microwave transmitter to create localized patches of ionization ('mirrors') in the atmosphere, which could be used as reflectors of radar signal for over-the-horizon surveillance. In the course of research to assess the viability of the AIM concept, interactions with a variety of DoD and civilian agencies, as well as with scientists from various disciplines, have made the prospective benefits of such research clear. There is growing consensus that development of an experiment research facility to produce controlled breakdown of the atmosphere would provide many unique research opportunities and some potentially revolutionary applications. This short report summarizes some of these that key organizations and interested scientists have suggested. DTIC

N94-36987*# National Academy of Sciences - National Research Council, Washington, DC. Commission on Behavioral and Social Sciences and Education.
SCIENCE PRIORITIES FOR THE HUMAN DIMENSIONS OF GLOBAL CHANGE
1994 42 p Sponsored in part by NASA, Washington, NOAA, Dept. of Commerce, Geological Survey, Dept. of Interior, Dept. of Agriculture, Office of Naval Research, Dept. of Navy and DOE
(Grant NSF OCE-93-13563)
Avail: CASI HC A03/MF A01

The topics covered include the following: defining research needs; understanding land use change; improving policy analysis -- research on the decision-making process; designing policy instruments and institutions to address energy-related environmental problems; assessing impacts, vulnerability, and adaptation to global changes; and understanding population dynamics and global change. Derived from text

N94-36994 Integrated Environmental Services, Irvine, CA.
CALIFORNIA RESIDENTIAL INDOOR AIR QUALITY STUDY. VOLUME 1: METHODOLOGY AND DESCRIPTIVE STATISTICS Report, Sep. 1991 - Dec. 1992
A. L. Wilson, S. D. Colome, and Y. Tian May 1993 125 p Sponsored by Gas Research Inst. Limited Reproducibility: More than 20% of this document may be affected by microfiche quality
(Contract GRI-5091-251-2347)
(PB94-166048; GRI-93/0224.1-Vol-1) Avail: Issuing Activity (National Technical Information Service (NTIS))

Field and laboratory methods to measure the distribution of carbon monoxide and other pollutants, such as nitrogen dioxide, benzene, toluene, formaldehyde, radon, and methane, in residences were investigated. The data provides a basis for analyzing housing, weather, geographic, ventilation, and occupant-use factors that influence the concentration of several important contaminants found in residences. The study targeted approximately 100 homes in the service areas of three participating utilities. The report is intended to be the first in a series of reports that will explore the pilot study dataset and design further investigation. It presents the main aspects of the effort and provides descriptive statistics of the major parameters. NTIS

N94-36995 Integrated Environmental Services, Irvine, CA.
CALIFORNIA RESIDENTIAL INDOOR AIR QUALITY STUDY. VOLUME 1: METHODOLOGY AND DESCRIPTIVE STATISTICS. APPENDIX Report, Sep. 1991 - Dec. 1992
A. L. Wilson, S. D. Colome, and Y. Tian May 1993 344 p Limited Reproducibility: More than 20% of this document may be affected by microfiche quality
(Contract GRI-5091-251-2347)
(PB94-166055; GRI-93/0224.2-Vol-1-App) Avail: Issuing Activity (National Technical Information Service (NTIS))

The volume of appendixes accompanies a report of the investigation of field and laboratory methods to measure the distribution of carbon monoxide and other pollutants, such as nitrogen dioxide, benzene, toluene, formaldehyde, radon, and methane, in California residences. The appendixes include field forms and questionnaires, instruction materials for the customer service representatives conducting the surveys, home plots for the contaminants, passive sampler field blanks results, and a summary of the interference testings. NTIS

N94-37007# Kauppa-ja Teollisuusministerio, Helsinki, Uudenmaa (Finland). Energy Dept.
SIHTI: ENERGY AND ENVIRONMENTAL TECHNOLOGY Final Report, 1991 - 1992
A. Estlander (JP-Engineering Ltd., Helsinki, Uudenmaa, Finland.) and S. Pietilae (Ekono Environmental Technology, Espoo, Uudenmaa, Finland.) 1993 84 p
(ISSN 0788-8546)
(DE94-763290; KTM/E-B-171; ISBN-951-47-8004-3) Avail: CASI HC A05/MF A01

The research and development program SIHTI was carried out during 1991-1992, mainly concentrating on energy and environmental technology. SIHTI focused on examining emissions from various sources of energy in all stages of the production chain. The objective was to create new methods and equipment, with which the environmental drawbacks of energy production can be reduced. Also a development work aiming at reduced traffic emissions was included in the program. Totally the program included 53 projects, which were divided into the following subsections: energy production, traffic, fuel chains and other projects. In the energy production projects the main attention was paid to reduction of sulphur dioxide, nitrogen oxide and particulate emissions. Furthermore waste utilization and possibilities of reducing carbon dioxide emissions were studied. The traffic study was focused on developing of more environmental-friendly liquid fuels. The research of emissions at low ambient temperatures was developed to an international level. Further the use of gases and the rape seed oil ester as traffic fuel was studied in practical tests. In the fuel chain study the emissions from the most important fuel chains were examined all the way from the purchase of the primary energy to the final end product. Methods for further reduction of water discharges from peat production were developed. The other projects were concentrated on modelling development, environmental impact assessment and emission surveys. DOE

N94-37071# Sandia National Labs., Albuquerque, NM.
INTEGRATED ENVIRONMENTALLY COMPATIBLE SOLDERING TECHNOLOGIES Final Report

F. M. Hosking, D. R. Frear, R. L. Iman, D. M. Keicher, E. P. Lopez, H. C. Peebles, N. R. Sorensen, and P. T. Vianco May 1994 26 p
(Contract DE-AC04-94AL-85000)
(DE94-013456; SAND-93-4039) Avail: CASI HC A03/MF A01

Chemical fluxes are typically used during conventional electronic soldering to enhance solder wettability. Most fluxes contain very reactive, hazardous constituents that require special storage and handling. Corrosive flux residues that remain on soldered parts can severely degrade product reliability. The residues are removed with chlorofluorocarbon (CFC), hydrochlorofluorocarbon (HCFC), or other hazardous solvents that contribute to ozone depletion, release volatile organic compounds into the atmosphere, or add to the solvent waste stream. Alternative materials and processes that offer the potential for the reduction or elimination of cleaning are being developed to address these environmental issues. Timing of the effort is critical, since the targeted chemicals will soon be heavily taxed or banned. DOE's Office of Environmental Restoration and Waste Management (DOE/EM) has supported Sandia National Laboratories' Environmentally Conscious Manufacturing Integrated Demonstration (ECMID). Part of the ECM program involves the integration of several environmentally compatible soldering technologies for assembling electronics devices. Fluxless or 'low-residue/no clean' soldering technologies (conventional and ablative laser processing, controlled atmospheres, ultrasonic tinning, protective coatings, and environmentally compatible fluxes) have been demonstrated at Sandia (SNL/NM), the University of California at Berkeley, and Allied Signal Aerospace-Kansas City Division (AS-KCD). The university demonstrations were directed under the guidance of Sandia staff. Results of the FY93 Soldering ID are presented in this report. DOE

N94-37093# Westinghouse Savannah River Co., Aiken, SC.
LONG-RANGE MESOSCALE MODELING OF POLLUTANT TRANSPORT FOR THE EUROPEAN TRACER EXPERIMENT (ETEX)
J. D. Fast, D. P. Griggs, and R. P. Addis 15 Apr. 1994 6 p Presented at the 6th Conference on Mesoscale Processes, Portland, OR, 18-22 Jul. 1994
(Contract DE-AC09-89SR-18035)
(DE94-010820; WSRC-MS-94-0244; CONF-940769-1) Avail: CASI HC A02/MF A01

The European Tracer EXperiment (ETEX) program involves two tracer experiments each comprising from distinct elements: (a) long-range atmospheric tracer release, sampling, and analysis; (b) real-time model operation and evaluation; and (c) post-release model operation and evaluation. The experiments consist of the release of a non-buoyant tracer from a location in western Europe and sampling of the atmospheric concentration by a network of about 200 stations located in 17 countries. Twenty-three institutions from 19 countries are expected to participate in the real-time modeling program including the Savannah River Technology Center (SRTC) of the U.S. Department of Energy's Savannah River Site (SRS). Notification of the release will occur only after the initiation of the release. Participants will be required to provide 60-h concentration predictions as quickly a possible (within 6 h of being notified) and updated predictions every 12 h after the notification. In 1993 two 'dry runs' for the real-time modeling component of the program were conducted; the actual tracer release experiment is scheduled for the fall of 1994. This paper describes the modeling approach employed by SRTC and presents some of the results of the second ETEX real-time dry run. DOE

N94-37100# Argonne National Lab., IL.
THE POTENTIAL FOR CONTROL OF CARBON DIOXIDE EMISSIONS FROM INTEGRATED GASIFICATION/COMBINED-CYCLE SYSTEMS
C. D. Livengood, R. D. Doctor, J. C. Molburg, P. Thimmapuram, and G. F. Berry 1994 12 p Presented at the Annual Meeting and Exhibition of the Air and Waste Management Association, Cincinnati, OH, 19-24 Jun. 1994
(Contract W-31-109-eng-38)
(DE94-012646; ANL/ES/CP-80868; CONF-940632-16) Avail: CASI HC A03/MF A01

Initiatives to limit carbon dioxide emissions have drawn considerable interest to Integrated Gasification/Combined-Cycle (IGCC) power generation, a process that reduces CO2 production through efficient fuel used is amenable to CO2 capture. This paper presents a comparison of energy systems that encompass fuel supply, an IGCC system, CO2 recovery using commercial technologies CO2 transport by pipeline, and land-based sequestering in geological reservoirs. The intent is to evaluate the energy-efficiency impacts of controlling CO2 in such systems and to provide the CO2 budget, or an 'equivalent CO2' budget, associated with each of the individual energy-cycle steps. The value used for the 'equivalent CO2' budget is 1 kg/kWh CO2 . The base case for the comparison is a 457-MW IGCC system that uses an air-blown Kellogg-Rust-Westinghouse (KRW) agglomerating fluidized-bed gasifier, Illinois No. 6 bituminous coal, and in-bed sulfur removal. Mining, preparation, and transportation of the coal and limestone result in a net system electric power production of 454 MW with a 0.835 kg/kwh CO2 release rate. For comparison, the gasifier output is taken through a water-gas shift to convert CO to CO2 and then processed in a glycol-based absorber unit to recover CO2, prior to the combustion turbine. A 500-km pipeline then transports the CO2 for geological sequestering. The net electric power production for the system with CO2 recovery is 381 MW with a 0.156 kg/kwh CO2 release rate. DOE

N94-37154# Sandia National Labs., Albuquerque, NM.
UAV'S IN CLIMATE RESEARCH: THE ARM UNMANNED AEROSPACE VEHICLE PROGRAM
W. R. Bolton 1994 4 p Presented at the Association of Unmanned Vehicle Systems Conference, Detroit, MI, 25 May 1994
(Contract DE-AC04-76DR-00789)
(DE94-011753; SAND-94-8640C; CONF-9405146-1) Avail: CASI HC A01/MF A01

In the last year, a Department of Energy/Strategic Environmental Research and Development Program project known as 'ARM-UAV' has made important progress in developing and demonstrating the utility of unmanned aerospace vehicles as platforms for scientific measurements. Recent accomplishments include a series of flights using an atmospheric research payload carried by a General Atomics Gnat UAV at Edwards AFB, California, and over ground instruments located in north-central Oklahoma. This discussion provides background on the program and describes the recent flights. DOE

N94-37155# Lawrence Livermore National Lab., Livermore, CA.
PROJECT REPORT: AIRCRAFT
Donald J. Wuebbles, Steve Baughcum, Munir Metwally, and Robert Seals Apr. 1994 4 p Presented at the 4th International Workshop on Global Emissions Inventories, Boulder, CO, 30 Nov. - 2 Dec. 1993
(Contract W-7405-eng-48)
(DE94-011759; UCRL-JC-116530; CONF-9311208-1) Avail: CASI HC A01/MF A01

Analyses of scenarios of past and possible future emissions are an important aspect of assessing the potential environmental effects from aircraft, including the proposed high speed civil transport (HSCT). The development of a detailed three-dimensional database that accurately represents the integration of all aircraft emissions along realistic flight paths for such scenarios requires complex computational modeling capabilities. Such a detailed data set is required for the scenarios evaluated in this interim assessment. Within the NASA High-Speed Research Program, the Emissions Scenarios Committee provides a forum for identifying the required scenarios and evaluating the resulting database being developed with the advanced emissions modeling capabilities at the Boeing Company and McDonnell Douglas Corporation. DOE

N94-37187# Washington Univ., Seattle, WA.
ATMOSPHERIC GAS
R. Schudlich and S. Emerson 1993 14 p
(Contract DE-FG06-90ER-61037)
(DE94-007439; DOE/ER-61037/3) Avail: CASI HC A03/MF A01

This proposal requests support for a third year of funding to complete a modelling study of processes controlling the distribution and waters at an ocean location with detailed background measurements of biological physical properties. We determined concentrations of the gases O2, Ar, N2, and the stable isotope ratio (O-18/O-16) of molecular oxygen in surface waters at Station ALOHA in conjunction with the Global Ocean Flux Study (GOFS) Hawaiian Ocean Time-series project during the years 1989--90 and 1992--93, the latter currently being completed. Chemical tracers have been incorporated into an existing ocean mixed-layer model to simulate the physical processes controlling the distribution and seasonal cycle of dissolved gases in the upper ocean. The broad background of concurrent chemical, physical, and biological measurements at station ALOHA provides

enough redundancy of ground truth to assess the model's accuracy. Biological oxygen production estimated from modeled chemical tracers agrees with estimates based on measurements of carbon fluxes into the deep ocean and nitrate fluxes into the upper ocean during 1989--90, verifying for the first time the utility of chemical tracers for determining biological fluxes in the ocean. The results suggest that in the euphoric zone the net biological O2 production and CO2 consumption is 4.5 moles m(exp -2)yr(exp -1). We propose to continue this project an additional year to incorporate isotope data into the simulation and to analyze the 1992--93 data. DOE

N94-37208# Oak Ridge National Lab., TN. Environmental Sciences Div.
CATALOG OF DATA BASES AND REPORTS
Apr. 1994 186 p
(Contract DE-AC05-84OR-21400)
(DE94-012230; ORNL/CDIAC-34/R4; Publ-4244) Avail: CASI HC A09/MF A02

This document provides information about the many reports and other materials made available by the US Department of Energy (DOE) Global Change Research Program (GCRP). It is divided into nine sections plus author and title indexes. The reports in Section A provide information about the scope, activities, and direction of the GCRP; Sections B, C, D, and E contain information about research that has been sponsored by GCRP, including those produced by CDIAC. DOE

N94-37211# Pacific Northwest Lab., Richland, WA.
CLIMATE UNCERTAINTY AND THE REGIONAL ECONOMIC IMPACTS OF GLOBAL CLIMATE CHANGE
M. J. Scott, A. M. Liebetrau, and C. A. Lopresti Oct. 1993 24 p Presented at the Symposium on Regional Impacts of Global Climate Change: Assessing Change and Response at the Scales That Matter, Richland, WA, 19-21 Oct. 1993
(Contract DE-AC06-76RL-01830)
(DE94-012242; PNL-SA-23172; CONF-931085-1) Avail: CASI HC A03/MF A01

The US Department of Energy funded pioneering research analyzing the effects of climate change and CO2 fertilization at the regional level in the Missouri-Iowa-Nebraska-Kansas (MINK) region. That study used existing process models of the agricultural, water, energy, and forestry sectors and of the regional economy to conduct a wide-ranging, integrated analysis of the regional economic effects of climate change. Neither the full integration of the process models nor the full investigation of the uncertainties of climate and economic response to climate was accomplished because (1) the process models were time-consuming to run, and (2) the MINK study used a single rich historical climate analog, the 1930s 'dustbowl' period, to depict climate change. More analysis was required to develop ranges of climate influences over more extreme climate conditions. DOE

N94-37252*# McDonnell-Douglas Aerospace, Long Beach, CA. Transport Aircraft.
JET AIRCRAFT ENGINE EXHAUST EMISSIONS DATABASE DEVELOPMENT: YEAR 1990 AND 2015 SCENARIOS
Z. Harry Landau, Munir Metwally, Richard VanAlstyne, and Clay A. Ward Hampton, VA NASA. Langley Research Center Jul. 1994 80 p
(Contract NAS1-19345; RTOP 537-01-22-01)
(NASA-CR-4613; NAS 1.26:4613; CRAD-9103-TR-9248) Avail: CASI HC A05/MF A01

Studies relating to environmental emissions associated with the High Speed Civil Transport (HSCT) military jet and charter jet aircraft were conducted by McDonnell Douglas Aerospace Transport Aircraft. The report includes engine emission results for baseline 1990 charter and military scenario and the projected jet engine emissions results for a 2015 scenario for a Mach 1.6 HSCT charter and military fleet. Discussions of the methodology used in formulating these databases are provided.
Author (revised)

N94-37288# Wisconsin Univ., Madison, WI.
MODELING OF TRACE CONSTITUENT TRANSPORT WITH THE UNIVERSITY OF WISCONSIN GLOBAL ISENTROPIC-SIGMA MODEL
T. H. Zapotocny, D. R. Johnson, and F. M. Reames 1994 9 p Presented at the 74th American Meteorological Society Annual Meeting, Nashville, TN, 23-28 Jan. 1994
(Contract DE-FG02-92ER-61439)
(DE94-012729; CONF-940115-32) Avail: CASI HC A02/MF A01

The main goal of this report is to demonstrate the ability of the University of Wisconsin (UW) hybrid isentropic-sigma (theta-sigma) model for global NWP, especially the global distribution of precipitation and simulating the long-range transport of an inert trace constituent. Results from this prototype climate model are compared against the results of a nominally identical global sigma model in order to establish the relative advantages and disadvantages of each coordinate system for simulating long-range transport processes. The current work is an extension of works by Johnson et al. and Zapotocny et al. The first study used analytically specified initial conditions for theta-sigma and sigma coordinate channel models, the second study incorporated observed data into regional versions of both models, while the third study documented the first global results with the UW theta-sigma model. Section 2 of this report describes additions to the UW theta-sigma model since the Zapotocny et al. study. Section 3 evaluates a five day precipitation forecast produced by the UW theta-sigma model and presents a comparison of each model's ability to prognostically simulate and conserve an inert trace constituent. A summary is presented in Section 4. DOE

N94-37299# Los Alamos National Lab., NM.
MEXICO CITY AIR QUALITY RESEARCH INITIATIVE, VOLUME 4
A. Mauzy, ed. Apr. 1994 102 p
(Contract W-7405-eng-36)
(DE94-013201; LA-12699-Vol-4) Avail: CASI HC A06/MF A02

This volume describes the methods and the data gathered in an attempt to measure and characterize the meteorological factors and the concentration of different pollutants in the Mexico City Metropolitan Area. The main objective of this document was to provide input for the simulation models and to obtain information that could be used to test and improve the models' performance. Four field campaigns were conducted, as well as routine monitoring, in order to obtain a database of atmospheric dynamics and air pollution characteristics. Sections include Airborne measurements, Remote sensing measurements, and Traditional (in situ) measurements.
DOE

N94-37376 San Diego State Univ., CA.
RESPONSE OF PLANTS AND ECOSYSTEMS TO CO2 AND CLIMATE CHANGE
J. F. Reynolds 1993 19 p Limited Reproducibility: More than 20% of this document may be affected by microfiche quality
(Contract DE-FG03-86ER-60490)
(DE94-011583; DOE/ER-60490/T2) Avail: CASI HC A03

In recognition of the important role of vegetation in the bio-geosphere carbon cycle, the Carbon Dioxide Research Program of the US Department of Energy established the research program: Direct Effects of Increasing Carbon Dioxide on Vegetation. The ultimate goal is to develop a general ecosystem model to investigate, via hypothesis testing, the potential responses of different terrestrial ecosystems to changes in the global environment over the next century. The approach involves the parallel development of models at several hierarchical levels, from the leaf to the ecosystem. At the plant level, mechanism and the direct effects of CO2 in the development of a general plant growth model, GEPSI - GEneral Plant SImulator has been stressed. At the ecosystem level, we have stressed the translation of CO2 effects and other aspects of climate change throughout the ecosystem, including feedbacks and constraints to system response, in the development of a mechanistic, general ecosystem model SERECO - Simulation of Ecosystem Response to Elevated CO2 and Climate Change has been stressed. DOE

N94-37389# Los Alamos National Lab., NM.
SELECTED CASE STUDIES IN MODELING AND SIMULATION APPLIED TO ENVIRONMENTALLY CONSCIOUS DESIGN AND MANUFACTURING
T. W. Lyttle and D. M. Smith 1994 5 p Presented at the 5th International Symposium on Robotics and Manufacturing, Maui, HI, 14-18 Aug. 1994
(Contract W-7405-eng-36)
(DE94-007556; LA-UR-94-688; CONF-940859-4) Avail: CASI HC A01/MF A01

The Process Modeling System (ProMoS) is an object-oriented, mass balance-based, discrete-event manufacturing simulation framework. Analytical

capabilities within ProMoS include complete mass balance specifications and facility profiles for materials consumption, resource utilization and worker exposure. ProMoS software has been utilized in the design of several processing facilities including a Printed Wiring Board (PWB) Manufacturing plant and Department of Energy (DOE) nuclear material processing plants. ProMoS was employed to optimize facility design with respect to production/storage capacity, transportation/shipping constraints, waste generation, cost, worker safety and overall environmental consequences. In addition, ProMoS has been employed in the operational characterization of processing facilities at Los Alamos National Laboratory. The environments used to develop these assessment tools will be discussed in addition to a review of initial implementation results. DOE

N94-37405# Midwest Research Inst., Golden, CO. National Renewable Energy Lab.

BIBLIOGRAPHY OF WORK ON THE PHOTOCATALYTIC REMOVAL OF HAZARDOUS COMPOUNDS FROM WATER AND AIR

D. M. Blake May 1994 76 p

(Contract DE-AC02-83CH-10093)

(DE94-006906; NREL/TP-430-6084) Avail: CASI HC A05/MF A01

This is a bibliography of information in the open literature on work that has been done to date on the photocatalytic oxidation of compounds, principally organic compounds. The goal of the listing is removing hazardous compounds from water or air. It contains lists of substances and literature citations. The bibliography includes information obtained through the middle of 1993 and some selected references from the balance of that year. DOE

N94-37428# Lawrence Livermore National Lab., Livermore, CA.

GASEOUS EFFLUENT MONITORING AND IDENTIFICATION USING AN IMAGING FOURIER TRANSFORM SPECTROMETER

M. R. Carter, C. L. Bennett, D. J. Fields, and J. Hernandez Oct. 1993 13 p Presented at the International Symposium on Substance Identification Technologies, Innsbruck, Austria, 4-8 Oct. 1993

(Contract W-7405-eng-48)

(DE94-012627; UCRL-JC-114619; CONF-9310164-11) Avail: CASI HC A03/MF A01

We are developing an imaging Fourier transform spectrometer for chemical effluent monitoring. The system consists of a 2-D infrared imaging array in the focal plane of a Michelson interferometer. Individual images are coordinated with the positioning of a moving mirror in the Michelson interferometer. A three dimensional data cube with two spatial dimensions and one interferogram dimension is then Fourier transformed to produce a hyperspectral data cube with one spectral dimension and two spatial dimensions. The spectral range of the instrument is determined by the choice of optical components and the spectral range of the focal plane array. Measurements in the near UV, visible, near IR, and mid-IR ranges are possible with the existing instrument. Gaseous effluent monitoring and identification measurements will be primarily in the 'fingerprint' region of the spectrum, (lambda = 8 to 12 (mu)m). Initial measurements of effluent using this imaging interferometer in the mid-IR will be presented. DOE

N94-37429# Argonne National Lab., IL.

EVALUATION OF PARAMETERIZATIONS FOR POLLUTANT TRANSPORT AND DISPERSION IN AN URBAN STREET CANYON USING A THREE-DIMENSIONAL DYNAMIC FLOW MODEL

I. Y. Lee, J. D. Shannon, and H. M. Park 1994 13 p Presented at the Annual Meeting and Exhibition of the Air and Waste Management Association, Cincinnati, OH, 19-24 Jun. 1994

(Contract W-31-109-eng-38)

(DE94-012641; ANL/ER/CP-81934; CONF-940632-17) Avail: CASI HC A03/MF A01

Results produced from a 3-D, time-dependent flow model show that dispersion characteristics can be simulated and interpreted in terms of flow conditions and structural configurations. Our previously parameterized 2-D formulations for time constants are modified to include the effect of the orientation of the mean wind relative to the canyon. The parameterizations can be applied to urban air pollution models directly, because the independent parameters are readily available from mesoscale calculations. More numerical studies are planned to characterize turbulent flow in street canyons. The current version of the model will be coupled with an improved module to solve transport equations for turbulence kinetic energy and turbulence dissipation rate. A three-dimensional, time-dependent flow model has been applied to examine the processes by which pollutants emitted at street level are transported and diffused from street canyons, and to determine the exchange rates of pollutants between street canyons and the air above the canyon. DOE

N94-37440# Argonne National Lab., IL. Environmental Research Div.

MODELING ATMOSPHERIC CONCENTRATIONS AND DEPOSITION OF Hg

Jack D. Shannon 1994 7 p Presented at the Methylmercury and Human Health, Upton, NY, 22-23 Mar. 1994

(Contract W-31-109-eng-38)

(DE94-012633; ANL/ER/CP-82908; CONF-940371-1) Avail: CASI HC A02/MF A01

The deleterious effects on ecosystems of mercury pollution are well established and fish advisories are in effect for many lakes in North America. Because methylation and other transformation processes in ecosystems can alter the original speciation of deposited Hg, a decrease in atmospheric loading of Hg in all forms is highly desirable. The contribution to Hg deposition by emissions from current anthropogenic activities relative to the deposition contribution by emissions from natural processes must be estimated to establish what fraction of atmospheric loading to watersheds and ecosystems is at least potentially amenable to control actions. Additional modeling questions concern source-receptor relationships (SRR) for major point sources and for emissions aggregated over geopolitical regions or emission sectors, because of the usefulness of SRR in comparing effectiveness of alternate control strategies. Modeling of atmospheric Hg is less advanced than that of some other widespread air pollution problems such as acid deposition. Nonetheless, several promising studies have been made for northern Europe and North America. For this study of Hg deposition in eastern North America we extend modeling techniques used extensively and successfully during the last 15 years for concentrations and deposition of SO(x) and NO(x) over regional scales, with parameterization rates adjusted to suitable values for Hg transformation and removal. DOE

N94-37454# Department of Energy, Washington, DC. Environmental Sciences Div.

PROCEEDINGS OF THE THIRD ATMOSPHERIC RADIATION MEASUREMENT (ARM) SCIENCE TEAM MEETING

Mar. 1994 379 p Meeting held in Norman, OK, 1-5 Mar. 1993

(DE94-011194; CONF-9303122) Avail: CASI HC A17/MF A03

This document contains the summaries of papers presented at the 1993 Atmospheric Radiation Measurement (ARM) Science Team meeting held in Morman, Oklahoma. To put these papers in context, it is useful to consider the history and status of the ARM Program at the time of the meeting. DOE

N94-37492# AEA Technology, London (England).

ENVIRONMENTAL RISK MANAGEMENT

P. A. Parris (Department of Industry, London, England.) 1994 6 p Presented at the Seminar on Safety Certification and Environment, Doha, Qatar, 15-16 Jan. 1994

(DE94-620987; INIS-MF-13835; CONF-940168) Avail: CASI HC A02/MF A01 (US Sales Only)

A professional, auditable environmental approach is the only path a responsible government, institution or company can take. Such an approach can be applied to a small petrol station, an oil refinery or a multi-million dollar mining development. Environmental issues cannot be divorced from socio-economic criteria; each impacts on the other. Twenty years ago, financial criteria ruled decision making and the environment tagged along a poor third to social and safety issues. Today, financial issues are still dominant, but decision makers realized that environmental issues hold the same weight as socio-economic criteria and the three are inexorably intertwined. DOE

N94-37607*# Boeing Commercial Airplane Co., Seattle, WA.

STRATOSPHERIC EMISSIONS EFFECTS DATABASE DEVELOPMENT

Steven L. Baughcum, Stephen C. Henderson, Peter S. Hertel, Debra R. Maggiora, and Carlos A. Oncina Jul. 1994 165 p

(Contract NAS1-19360; RTOP 537-01-22-01)

(NASA-CR-4592; NAS 1.26:4592) Avail: CASI HC A08/MF A02

This report describes the development of a stratospheric emissions

effects database (SEED) of aircraft fuel burn and emissions from projected Year 2015 subsonic aircraft fleets and from projected fleets of high-speed civil transports (HSCT's). This report also describes the development of a similar database of emissions from Year 1990 scheduled commercial passenger airline and air cargo traffic. The objective of this work was to initiate, develop, and maintain an engineering database for use by atmospheric scientists conducting the Atmospheric Effects of Stratospheric Aircraft (AESA) modeling studies. Fuel burn and emissions of nitrogen oxides (NO(x) as NO2), carbon monoxide, and hydrocarbons (as CH4) have been calculated on a 1-degree latitude x 1-degree longitude x 1-kilometer altitude grid and delivered to NASA as electronic files. This report describes the assumptions and methodology for the calculations and summarizes the results of these calculations. Author (revised)

N94-37624# Pacific Northwest Lab., Richland, WA.
SURFACE-LAYER RESPONSE OVER SHRUB-STEPPE CANOPY DURING SPRINGTIME
J. M. Hubbe, R. R. Kirkham, J. L. Downs, and W. J. Shaw Mar. 1994 5 p Presented at the 21st American Meteorological Scoeity Conference on Agricultural and Forest Meteorology: 11th Biometeorology and Aerobiology Converence, San Diego, CA, 7-10 Mar. 1994
(Contract DE-AC06-76RL-01830)
(DE94-011235; PNL-SA-23484; CONF-940362-3; CONF-9403110-1) Avail: CASI HC A01/MF A01

The exchange of energy and trace gases between the atmosphere and heterogeneous surfaces is gaining increasing attention in the scientific community. An observational study of surface energetics and atmospheric response was undertaken in 1992 to provide data for model application to semi-arid climates and for the evaluation of various models. The objectives of this field study were to quantify surface-layer fluxes over a mixed canopy in a semi-arid climate, to quantify canopy and soil energetics during the transition from moist winter conditions to dry summer conditions and to investigate parameterization of surface exchange processes in a mixed canopy setting. DOE

N94-37631# Lawrence Livermore National Lab., Livermore, CA.
TROPOSPHERIC RADIATIVE FORCING OF CH4
A. S. Grossman and K. E. Grant Apr. 1994 12 p
(Contract W-7405-eng-48)
(DE94-011628; UCRL-ID-116533) Avail: CASI HC A03/MF A01

We have evaluated the tropospheric radiative forcing of CH4 in the 0-3000 cm(exp -1) wavenumber range and compared this with prior published calculations. The atmospheric test cases involved perturbed methane scenarios in both a McClatchey midlatitude summer, clear-sky-approximation model atmosphere, as well as a globally and seasonally averaged model atmosphere containing a representative cloud distribution. The scenarios involved pure CH4 radiative forcing and CH4 plus a mixture of H2O, CO2, O3, and N2O. The IR radiative forcing was calculated using a correlated k-distribution transmission model. The major purposes of this paper are: first, to use the correlated k-distribution model to calculate the tropospheric radiative forcing for CH4, as the only radiatively active gas and, in a mixture with H2O, CO2, O3, and N2O, for a McClatchey midlatitude summer, clear-sky model atmosphere, to compare the results to those obtained in the studies mentioned above. Second, we will calculate the tropospheric methane forcing in a globally and annually averaged atmosphere with and without a representative cloud distribution in order to validate the conjecture given in IPCC (1990) that the inclusion of clouds in the forcing calculations results in forcing values which are approximately 20 percent less than those obtained using clear sky approximations. DOE

N94-37731# Department of Energy, Washington, DC. Analytical Services Div.
THE INTEGRATED PERFORMANCE EVALUATION PROGRAM QUALITY ASSURANCE GUIDANCE IN SUPPORT OF EM ENVIRONMENTAL SAMPLING AND ANALYSIS ACTIVITIES
May 1994 29 p
(DE94-013043; DOE/EM-0160P) Avail: CASI HC A03/MF A01

EM's (DOE's Environmental Restoration and Waste Management) Integrated Performance Evaluation Program (IPEP) has the purpose of integrating information from existing PE programs with expanded QA activities to develop information about the quality of radiological, mixed waste, and hazardous environmental sample analyses provided by all laboratories supporting EM programs. The guidance addresses the goals of identifying specific PE sample programs and contacts, identifying specific requirements for participation in DOE's internal and external (regulatory) programs, identifying key issues relating to application and interpretation of PE materials for EM headquarters and field office managers, and providing technical guidance covering PE materials for site-specific activities. (PE) Performance Evaluation materials or samples are necessary for the quality assurance/control programs covering environmental data collection. DOE

N94-37740# Michigan Univ., Ann Arbor, MI. Dept. of Chemical Engineering.
BIOLOGICAL DETERMINANTS OF PHOTOBIOREACTOR DESIGN
B. O. Palsson and G. G. Brown 1994 18 p
(Contract DE-FG22-93PC-93212)
(DE94-011665; DOE/PC-93212/T2) Avail: CASI HC A03/MF A01

Microalgae is being considered for capture and sequestration of CO2 from power-plant flue-gases. High productivity of microalgae is necessary to make this process cost effective compared to the conventional methods used for reducing CO2 levels in the atmosphere. This obviates the need for large-scale cultivation technologies and proper photobioreactor technology. The physical factors that influence the performance of a photoautotrophic microalgal culture are the quality and composition of light, inlet carbon dioxide concentration, nutrients, and secondary metabolites at high cell densities. In developing photobioreactor technology, balancing of biological processes to the physical rate process becomes important. In this first quarterly report, the effect of various light compositions on the culture kinetics is studied. To determine the optimal composition, six wavelengths 470, 555, 560, 570, 580 and 605, each supplemented with 680 nm were used to cultivate cultures. Based on the results obtained it is concluded that a monochromatic red light of 680 nm is sufficient to obtain the maximum capacity. DOE

N94-37856 National Defence Research Establishment, Umea (Sweden). Huvudavdelning foer ABC-Skydd.
PROGRAM GAUSSPLYM: A TOOL IN WINDOWS ENVIRONMENT FOR STUDYING CONTINUOUS RELEASES [PROGRAMMET GAUSSPLYM: ETT VERKTYG I WINDOWS-MILJOE FOER STUDIER AV KONTINUERLIGA UTSLAEPP]
M. Thiessen Feb. 1994 34 p In SWEDISH Limited Reproducibility: More than 20% of this document may be affected by microfiche quality
(PB94-184603; FOA-C-40326-4.5) Avail: Issuing Activity (National Technical Information Service (NTIS))

The report provides documentation of a program that calculates concentrations of air pollutants arising from different types of atmospheric releases. NTIS

46 GEOPHYSICS

Includes aeronomy; upper and lower atmosphere studies; ionospheric and magnetospheric physics; and geomagnetism.

For space radiation see *93 Space Radiation.*

N94-36451# Alaska Univ., Fairbanks, AK.
VENT PROCESSES DURING THE 1912 ERUPTION AT NOVARUPTA, KATMAI NATIONAL PARK, ALASKA
T. Bates, J. Eichelberger, and S. Swanson 1 Jun. 1993 28 p
(Contract DE-FG06-92ER-14234)
(DE94-010740; DOE/ER-14234/2) Avail: CASI HC A03/MF A01

Blocks of welded fragmental material ejected at Novarupta during the great eruption of 1912 provide evidence of the contents and development of the vent. Because they appear to represent material held at magmatic temperature for hours to days and then quenched at depth and ejected, they provide unusual information on the timing of processes of degassing, welding, and magma mixing. Two breccia types are distinguished by proportions of the three magmatic components. Type 1 breccia (Hildreth's 'vitrophyre') is rhyolite- and andesite-rich ('volcanic inclusions' in the glassy matrix were found to be 1912 andesite), contains abundant lithics, and is found throughout deposits of the eruption's second and third days. It corresponds to magmatic proportions being erupted toward the end of the first day, or Episode 1. Type 2 is dacite-rich and poor in lithics, and occurs only at the surface. It corresponds to magmatic proportions erupted

during Episodes 2 and 3. A pyroclastic dike exposed in a bomb of Type 2 vent breccia is petrologically related to Novarupta lava. Water is strongly but not completely degassed from vent breccias (Type I breccia at 0.30 wt percent H2O and Type 2 breccia at 0.15 wt percent H2O even when bread crusted) and more thoroughly degassed from dome lava (rhyolite and andesite at less than 0.10 wt percent H2O), but the pyroclastic dike retains significant water (averages 0.90 wt percent H2O) and its host breccia likewise contains elevated water concentrations (0.30-0.40 wt percent H2O). The mafic component in Novarupta dome is derived from andesitic, rather than dacitic magma, and has crystallized substantially in response to mixing with its cooler host. DOE

N94-36738# Coleman Research Corp., Columbia, MD.
GEOPHYSICAL DATA FUSION FOR SUBSURFACE IMAGING
P. Hoekstra, J. Vandergraft, M. Blohm, and D. Porter Aug. 1993 46 p
(Contract DE-AC21-92MC-29106)
(DE94-000056; DOE/MC-29106/3531) Avail: CASI HC A03/MF A01

A geophysical data fusion methodology is under development to combine data from complementary geophysical sensors and incorporate geophysical understanding to obtain three dimensional images of the subsurface. The research reported here is the first phase of a three phase project. The project focuses on the characterization of thin clay lenses (aquitards) in a highly stratified sand and clay coastal geology to depths of up to 300 feet. The sensor suite used in this work includes time-domain electromagnetic induction (TDEM) and near surface seismic techniques. During this first phase of the project, enhancements to the acquisition and processing of TDEM data were studied, by use of simulated data, to assess improvements for the detection of thin clay layers. Secondly, studies were made of the use of compressional wave and shear wave seismic reflection data by using state-of-the-art high frequency vibrator technology. Finally, a newly developed processing technique, called 'data fusion' was implemented to process the geophysical data, and to incorporate a mathematical model of the subsurface strata. Examples are given of the results when applied to real seismic data collected at Hanford, WA, and for simulated data based on the geology of the Savannah River Site. DOE

N94-36758# Risk Engineering, Inc., Boulder, CO.
ANALYSIS SPECTRAL SHAPES FROM CALIFORNIA AND CENTRAL UNITED STATES GROUND MOTION
24 Jan. 1994 28 p Prepared for Oak Ridge Y-12 Plant, TN
(Contract DE-AC05-84OS-21400)
(DE94-010041; Y/EN-5087) Avail: CASI HC A03/MF A01

The objective of this study is to analyze the spectral shapes from earthquake records with magnitudes and distances comparable to those that dominate seismic hazard at Oak Ridge, in order to provide guidance for the selection of site-specific design-spectrum shapes for use in Oak Ridge. The authors rely heavily on California records because the number of relevant records from the central and eastern United States (CEUS) is not large enough for drawing statistically significant conclusions. They focus on the 0.5 to 10-Hz frequency range for two reasons: (1) this is the frequency range of most engineering interest, and (2) they avoid the effect of well-known differences in the high-frequency energy content between California and CEUS ground motions. DOE

N94-36949*# Southwest Research Inst., San Antonio, TX. Instrumentation and Space Research Div.
HIGH ALTITUDE PLASMA INSTRUMENT (HAPI) DATA ANALYSIS Final Report
J. L. Burch Jan. 1994 11 p
(Contract NAS5-33030; SwRI Proj. 15-3320; RTOP 602-00-00)
(NASA-CR-189360; NAS 1.26:189360) Avail: CASI HC A03/MF A01

The objectives of the Dynamics Explorer mission are to investigate the coupling of energy, mass, and momentum among the earth's magnetosphere, ionosphere, and upper atmosphere. At launch, on August 3, 1981, DE-1 was placed into an elliptical polar orbit having an apogee of 23,130 km to allow global auroral imaging and crossings of auroral field lines at altitudes of several thousand kilometers. At the same time DE-2 was placed into a polar orbit, coplanar with that of DE-1 but with a perigee altitude low enough (309 km) for neutral measurements and an apogee altitude of 1012 km. The DE-1 High Altitude Plasma Instrument (HAPI) provided data on low and medium energy electrons and ions from August 13, 1981 until December 1, 1981, when a high-voltage failure occured. Analysis of HAPI data for the time period of this contract has produced new results on the source mechanisms for electron conical distributions, particle acceleration phenomena in auroral acceleration regions, Birkeland currents throughout the nightside auroral regions, the source region for auroral kilometric radiation (AKR), and plasma injection phenomena in the polar cusp. CASI

N94-37016*# Rice Univ., Houston, TX. Dept. of Space Physics and Astronomy.
DYNAMICS EXPLORER DATA ANALYSIS Final Technical Report, 16 May 1986 - 30 Jun. 1993
Patricia H. Reiff 1993 8 p
(Grant NAG5-775)
(NASA-CR-196141; NAS 1.26:196141) Avail: CASI HC A02/MF A01

Work in the following areas is discussed: plasma physics of the auroral acceleration region; electrodynamic coupling as a function of substorm phase and interplanetary magnetic field (IMF) direction; and particle injection in the magnetospheric cusp. Derived from text

N94-37177# Ohio State Univ., Columbus. Research Foundation.
INVESTIGATION OF ULTRASONIC SURFACE WAVE INTERACTION WITH POROUS SATURATED ROCKS
1994 55 p
(Contract DE-FG02-87ER-13749)
(DE94-013378; DOE/ER-13749/T2) Avail: CASI HC A04/MF A01

Calculations showed that capillary forces can easily produce closed-pore boundary conditions at interface between nonwetting fluid (air) and a porous solid saturated by a wetting fluid (water). The direct excitation technique was used to measure surface wave velocity and attenuation on both wet and dry rocks. The strong correlation between the observed surface wave velocity change caused by water saturation and the formation permeability can be used for ultrasonic assessment of the dynamic permeability. The experimental system was improved further by introducing laser interferometric detection, which was adapted to surface wave inspection of fluid-saturated permeable materials. In a separate effort, the surface stiffness of different water-saturated porous solids was studied by a novel acoustical method. Areas for further study are described. DOE

N94-37215 Observatorio del Ebro, Roquetas (Spain).
EUROCAP PROGRAM: EBRE STATION Interim Report No. 3, Mar. - Aug. 1994
Luis F. Alberca Aug. 1994 34 p Limited Reproducibility: More than 20% of this document may be affected by microfiche quality
(Contract DAJA45-93-C-0041)
(AD-A280418; R/D-7131-EE-01) Avail: CASI HC A03

Hourly vertical incidence ionograms have been obtained regularly with the digisonde. The ARTIST output of the hourly ionograms have been sent to Fort Monmoth in floppy 5 1/4 HD diskettes as usual. The digisonde has been working without failures, so that only a small number of ionograms are lacking, due to power failures and other external causes. DTIC

N94-37314# Los Alamos National Lab., NM.
CHANNEL PROBE MEASUREMENTS FOR THE AMERICAN SECTOR CLUTTER EXPERIMENT, JANUARY 1994
T. J. Fitzgerald 20 May 1994 23 p
(Contract W-7405-eng-36)
(DE94-013086; LA-UR-94-1811) Avail: CASI HC A03/MF A01

The ionospheric phenomenon called Equatorial Spread F encompasses a variety of effects associated with plasma irregularities occurring in the post-sunset and nighttime ionosphere near the magnetic equator. These irregularities can seriously degrade the performance of systems which involve either of necessity or inadvertently radio propagation through the equatorial ionosphere. One such system is Over-the-Horizon (OTH) radars which operate in the high-frequency (hf) band and use ionospheric reflection for forward and backscatter propagation to ranges of thousands of kilometers. When such radars are directed towards the equator, Spread F irregularities can cause scintillation effects which may be aliased into the ranges of interest and have the effect of causing, excess clutter in which targets may be hidden. In January, 1994 Los Alamos participated in a campaign to measure Spread F effects on OTH propagation from the United States looking towards South America in conjunction with local diagnostics in Peru. During the campaign Los Alamos fielded a 1600 km bistatic path between Piura, Peru, and Arequipa, Peru, the one-hop reflection region for

this path was near the magnetic equator. We obtained four types of measurements: an oblique ionogram between Piura and Arequipa every three minutes; Doppler spread and spatial correlation for a single frequency cw path between Piura and Arequipa; Doppler spread, time-delay spread, and spatial coherence for a 10 kHz bandwidth path between Piura and Arequipa, and Doppler spread and time-delay spread for the one-way path between the AVA radar in New York and Arequipa, Peru. This report describes the diagnostic experiments that we carried out and gives a brief description of some of the data we obtained. DOE

N94-37470*# Iowa Univ., Iowa City, IA. Dept. of Physics and Astronomy.

ANALYSIS OF PLASMA MEASUREMENTS FOR THE GEOTAIL MISSION Semiannual Status Report, 1 Oct. 1993 - 31 Mar. 1994

Louis A. Frank 1994 7 p

(Grant NAG5-2371)

(NASA-CR-196274; NAS 1.26:196274) Avail: CASI HC A02/MF A01

The CPI plasma measurements from the Geotail spacecraft are currently used by a number of scientists in support of varied research projects. Measurements from the CPI hot plasma analyzer have been processed to compute one-minute averages of plasma densities, temperatures, and velocities for the period 1 Oct. 1992 - 31 July 1993. These parameters are used in a preliminary survey of the magnetotail for distances from earth of 10 to 210 earth radii. The cold plasmas within the magnetotail drift towards the midplane and are thought to be a principal source for the hot plasma sheet. A remarkable result from Geotail is the observation of cold ion beams coexisting as distinct components in the presence of hot plasma-sheet plasmas. The development and evolution of plasmoids is a topic of considerable interest in studies of the magnetotail and magnetospheric substorms. A number of possible plasmoids have been identified in the Geotail data set based upon reversals of the Z component of the magnetic field as observed with the MGF instrumentation. An intensive study of the electron and ion velocity distributions and the plasma parameters for several of these events reveals unexpected features. Collaborative work with several Geotail instrument teams and other researchers is also ongoing. CASI

N94-37489# Geological Survey, Denver, CO.

ANALYSIS OF DEEP SEISMIC REFLECTION AND OTHER DATA FROM THE SOUTHERN WASHINGTON CASCADES

W. D. Stanley, S. Y. Johnson, and V. F. Nuccio Dec. 1993 175 p

(Contract DE-AT21-92MC-29267)

(DE94-004075; DOE/MC-29267/3655) Avail: CASI HC A08/MF A02

This report describes results of a synthesis of geological, geophysical, and geochemical data from a largely volcanic rock covered region in southwestern Washington that has been identified as underlaid by thick marine sedimentary rocks. The work was funded by the Deep Source Gas projects at the Morgantown Energy Technology Center (METC). The subproject which resulted in this report is centered in the Branch of Geophysics, U.S. Geological Survey (USGS), in Denver. A lengthy period of cooperation between METC and the USGS has involved one task focused on the application of geophysical methods to the study of phenomena associated with fossil and active subduction zones and non-subduction suture zones that may have deeply emplaced sedimentary rocks. This report represents a summary synthesis of several geophysical and geological data sets. The Southern Washington Cascades Conductor (SWCC) has been examined using several types of data in addition to MT, seismic, magnetic, and gravity. Specific geological mapping tasks have been completed through funding by the Department of Energy and the USGS in the western part of the proposed basin near Morton, WA. Other regional geological studies using wells and outcrops done as part of the USGS Evolution of Sedimentary Basins programs have added information that constrain the possible nature of the SWCC rocks and their tectonic setting. Recently, evaluation of patterns of seismicity in the SWCC region has demonstrated the likelihood of several parallel and step-over strike-slip faults that may have produced the proposed basin or altered its geometry. In addition, the seismicity patterns trace the axis of key anticlinal structures and thrusts. DOE

N94-37527# Sandia National Labs., Albuquerque, NM.

A COMPUTATIONAL MODEL FOR THREE-DIMENSIONAL JOINTED MEDIA WITH A SINGLE JOINT SET

J. R. Koteras Feb. 1994 49 p

(Contract DE-AC04-94AL-85000)

(DE94-007582; SAND-92-2625) Avail: CASI HC A03/MF A01

This report describes a three-dimensional model for jointed rock or other media with a single set of joints. The joint set consists of evenly spaced joint planes. The normal joint response is nonlinear elastic and is based on a rational polynomial. Joint shear stress is treated as being linear elastic in the shear stress versus slip displacement before attaining a critical stress level governed by a Mohr-Coulomb faction criterion. The three-dimensional model represents an extension of a two-dimensional, multi-joint model that has been in use for several years. Although most of the concepts in the two-dimensional model translate in a straightforward manner to three dimensions, the concept of slip on the joint planes becomes more complex in three dimensions. While slip in two dimensions can be treated as a scalar quantity, it must be treated as a vector in the joint plane in three dimensions. For the three-dimensional model proposed here, the slip direction is assumed to be the direction of maximum principal strain in the joint plane. Five test problems are presented to verify the correctness of the computational implementation of the model. DOE

N94-37530# National Oceanic and Atmospheric Administration, Boulder, CO. Environmental Research Labs.

SOLAR-TERRESTRIAL PREDICTIONS, 4: PROCEEDINGS OF AWORKSHOP. VOLUME 3: GEOMAGNETIC PAPERS; IONOSPHERIC PAPERS

J. Hruska, M. A. Shea, D. F. Smart, and G. Heckman Sep. 1993 638 p Conference held in Ottawa, Canada on May 18-22, 1992 See also Volume 2, PB94-173184 Prepared in cooperation with Geological Survey of Canada, Ottawa, Ontario and Air Force Geophysics Lab., Hanscom AFB, MA

(PB94-173192) Avail: CASI HC A99/MF A06

This volume contains both invited and contributed papers on the geomagnetic field and the ionosphere. NTIS

N94-37581*# Harvard-Smithsonian Center for Astrophysics, Amado, AZ.

MEASUREMENT AND INTERPRETATION OF CRUSTAL DEFORMATION RATES ASSOCIATED WITH POSTGLACIAL REBOUND Semiannual Status Report No. 4, 15 Sep. 1993 - 14 Mar. 1994

James L. Davis Mar. 1994 98 p

(Grant NAG5-1930)

(NASA-CR-196300; NAS 1.26:196300) Copyright Avail: CASI HC A05/MF A02

This project involves obtaining GPS measurements in Scandinavia and using the measurements to estimate the viscosity profile of the earth's mantle and to correct tide-gauge measurements for the rebound effect. We report on several aspects of this project. The DSGS was not scheduled to be reoccupied with DOSE receivers during the report period. The permanent network set up by Onsala Space Observatory continues to operate, and the data are being evaluated. An important technical advance we intend for this project is to use the full three dimensional site velocity information for inferring geophysical parameters. During the report period, two papers have been been accepted for publication in the Journal of Geophysical Research and will be published in April. Reprints of these papers are contained in the Appendix. Derived from text

N94-37649 Phillips Lab., Hanscom AFB, MA.

ATMOSPHERIC STRUCTURE SIMULATION: AN ARMA MODEL FOR SMOOTH ISOTROPIC TWO-DIMENSIONAL GEOPHYSICAL POWER SPECTRA Interim Report

James H. Brown 5 Oct. 1993 72 p Limited Reproducibility: More than 20% of this document may be affected by microfiche quality

(AD-A280476; PL-TR-93-2224; ERP-1132) Avail: Issuing Activity (Defense Technical Information Center (DTIC))

Geophysical phenomena are often characterized by smooth continuous power spectral densities having a negative power law slope. Frequently, Fourier transform analysis has been employed to generate synthetic scenes from pseudorandom arrays by passing the stochastic data through a Fourier filter having the desired power spectral dependency. This report examines the possibility of producing two-dimensional synthetic structure by invoking autoregressive/moving average analysis, as contrasted with the Fourier method. Computations that apply multidimensional fast Fourier transforms to large data arrays consume enormous resources and time. An alternative

method is needed to reduce the computational burden, achieve circular symmetry, account for correlations in all directions, and lend itself to producing nonstationary scenes. Future editions of the Phillips Laboratory Strategic High Altitude Atmospheric Radiance Code (SHARC) will feature an ability to calculate structured radiance. The method explored herein provides a process to construct a nonstationary database for SHARC that accurately simulates symmetric two-dimensional geophysical power spectra and takes into account correlations along the line of sight that existing methods approximate. DTIC

N94-37669# Los Alamos National Lab., NM.
SUBSTORM STATISTICS: OCCURRENCES AND AMPLITUDES
J. E. Borovsky and R. J. Nemzek 1994 6 p Presented at the Substorms, Fairbanks, AK, 7-11 Mar. 1994
(Contract W-7405-eng-36)
(DE94-011694; LA-UR-94-1378; CONF-9403115-1) Avail: CASI HC A02/MF A01

The occurrences and amplitudes of substorms are statistically investigated with the use of three data sets: the AL index, the Los Alamos 3-satellite geosynchronous energetic-electron measurements, and the GOES-5 and -6 geosynchronous magnetic-field measurements. The investigation utilizes approximately 13,800 substorms in AL, approximately 1400 substorms in the energetic-electron flux, and approximately 100 substorms in the magnetic field. The rate of occurrence of substorms is determined as a function of the time of day, the time of year, the amount of magnetotail bending, the orientation of the geomagnetic dipole, the toward/away configuration of the IMF, and the parameters of the solar wind. The relative roles of dayside reconnection and viscous coupling in the production of substorms are assessed. Three amplitudes are defined for the substorms: the jump in the AL index, the peak of the greater than 30-keV integral electron flux at geosynchronous orbit near midnight, and the angle of rotation of the geosynchronous magnetic field near midnight. The substorm amplitudes are statistically analyzed, the amplitude measurements are cross correlated with each other, and the substorm amplitudes are determined as functions of the solar-wind parameters. Periodically occurring and randomly occurring substorms are analyzed separately. The energetic-particle-flux amplitudes are consistent with unloading and the AL amplitudes are consistent with direct driving plus unloading. DOE

N94-37701# Los Alamos National Lab., NM.
MAGNETOTAIL DYNAMICS: MHD SIMULATIONS OF DRIVEN AND SPONTANEOUS DYNAMIC CHANGES
J. Birn, K. Schindler, and M. Hesse 1994 14 p Presented at the ICS2 Conference, Fairbanks, AK, 7-11 Mar. 1994
(Contract W-7405-eng-36)
(DE94-011702; LA-UR-94-1455; CONF-9403116-1) Avail: CASI HC A03/MF A01

The dynamic evolution of the magnetotail during growth phase and expansion phase of a substorm is studied through three-dimensional time-dependent MHD simulations. To model growth phase effects, an external electric field with an equatorward inflow is applied at the boundaries over a finite time period. This leads to the formation of a thin current sheet with greatly enhanced current density in the near tail, embedded in the wider plasma/current sheet, which becomes diminished in strength. A faster, spontaneous current sheet formation occurs when entropy conservation is released in an isobaric model, while the ideal MHD constraint persists. This may be a suitable model for the late, explosive part of the growth phase. The transition to the substorm expansive phase is modeled by an increase in anomalous resistivity, using either uniform resistivity or a current density dependent resistivity which is turned on when the current density exceeds a certain threshold. In both cases the violation of ideal MHD leads to resistive instability and the formation of a near-Earth neutral line, fast flow, and plasmoid ejection, together with the dipolarization and current reduction in the region further earthward. The spontaneous increase in total region 1 type field-aligned currents associated with the disruptions of the thin current sheets is less significant than that found in earlier simulations of the disruption of a wider current sheet, whereas the driven increase in the region 1 type current is substantial. The results demonstrate that the same dynamic process which appears spontaneous in the behavior of some quantities might be interpreted as entirely driven from the observation of others. DOE

N94-37703*# Lockheed Missiles and Space Co., Palo Alto, CA. Research and Development.
ORIGINS OF ENERGETIC IONS IN THE EARTH'S MAGNETOSHEATH Final Report, 8 May 1991 - 7 Jun. 1994
Jun. 1994 11 p
(Contract NAS5-31213; RTOP 602-00-00)
(NASA-CR-189359; NAS 1.26:189359) Avail: CASI HC A03/MF A01

This final report describes activities under NASA contract NAS5-31213 to Lockheed Missiles and Space Company. The report covers the entire contract period from 8 May 1991 to 7 Jun. 1994. This is a contract under the NASA Guest Investigator Program for the analysis and interpretation of the combined scientific data from the Hot Plasma Composition Experiment (HPCE) and the Charge Energy Mass (CHEM) spectrometer on the AMPTE/Charge Composition Explorer (CCE) spacecraft. These combined data sets have been used to survey the energetic ion environment in the earth's magnetosheath to determine the origins and relative strengths of the energetic ion populations found there. Derived from text

N94-37780# National Oceanic and Atmospheric Administration, Boulder, CO. Environmental Research Lab.
SOLAR-TERRESTRIAL PREDICTIONS, 4: PROCEEDINGS OF A WORKSHOP. VOLUME 1: WORKSHOP OVERVIEW PAPERS; WORKING GROUP REPORTS; USER COMMUNITY REPORTS; REGIONAL WARNING CENTER REPORTS
J. Hruska, ed., M. A. Shea, ed., D. F. Smart, ed., and G. Heckman, ed. Sep. 1993 360 p Workshop held in Ottawa, Ontario, 18-22 May 1992 See also PB91-197079 and PB94-173184 Prepared in cooperation with Geological Survey of Canada, Ottawa, Ontario and Air Force Geophysics Lab., Hanscom AFB, MA
(PB94-173176) Avail: CASI HC A16/MF A03

The Proceedings of the Fourth Solar-Terrestrial Predictions Workshop contains manuscripts for 135 invited and contributed papers presented either orally or in poster format, at the Workshop held in Ottawa, Canada in May 1992. The first volume contains general papers related to the workshop and the working group reports. In addition this volume contains the invited and contributed papers from the user community and the reports from the Regional Warning Centers. NTIS

N94-37781# National Oceanic and Atmospheric Administration, Boulder, CO. Space Environmental Lab.
SOLAR-TERRESTRIAL PREDICTIONS, 4: PROCEEDINGS OF A WORKSHOP. VOLUME 2: SOLAR PAPERS; MAGNETOSPHERIC PAPERS
J. Hruska, ed., M. A. Shea, ed., D. F. Smart, ed., and G. Heckman, ed. Sep. 1993 759 p Conference held in Ottawa, Ontario, 18-22 May 1992 See also PB91-197087, PB94-173176 and PB94-173192 Prepared in cooperation with Geological Survey of Canada, Ottawa, Ontario and Air Force Geophysics Lab., Hanscom AFB, MA
(PB94-173184) Avail: CASI HC A99/MF A06

This volume contains both invited and contributed papers describing solar phenomena and the effects in the magnetosphere. NTIS

47 METEOROLOGY AND CLIMATOLOGY

Includes weather forecasting and modification.

N94-36479# Pacific Northwest Lab., Richland, WA.
TWO-CHANNEL MICROWAVE RADIOMETER FOR OBSERVATIONS OF TOTAL COLUMN PRECIPITABLE WATER VAPOR AND CLOUD LIQUID WATER PATH
J. C. Liljegren Jan. 1994 9 p Presented at the 5th Annual Symposium on Global Change Studies, Nashville, TN, 24-28 Jan. 1994
(Contract DE-AC06-76RL-01830)
(DE94-007480; PNL-SA-22773; CONF-940131-4) Avail: CASI HC A02/MF A01

The Atmospheric Radiation Measurement (ARM) Program is focused on improving the treatment of radiation transfer in models of the atmospheric general circulation, as well as on improving parameterizations of cloud properties and formation processes in these models. To help achieve these objectives, ARM is deploying several two-channel, microwave radiometers at the Cloud and Radiation Testbed (CART) site in Oklahoma for the

purpose of obtaining long time series observations of total precipitable water vapor (PWV) and cloud liquid water path (LWP). The performance of the WVR-1100 microwave radiometer deployed by ARM at the Oklahoma CART site central facility to provide time series measurements precipitable water vapor (PWV) and liquid water path (LWP) has been presented. The instrument has proven to be durable and reliable in continuous field operation since June, 1992. The accuracy of the PWV has been demonstrated to achieve the limiting accuracy of the statistical retrieval under clear sky conditions, degrading with increasing LWP. Improvements are planned to address moisture accumulation on the Teflon window, as well as to identify the presence of clouds with LWP at or below the retrieval uncertainty. DOE

N94-36739# Reynolds Electrical and Engineering Co., Inc., Las Vegas, NV.

A-TOUGH: A MULTIMEDIA FLUID-FLOW/ENERGY-TRANSPORT MODEL FOR FULLY-COUPLED ATMOSPHERIC-SUBSURFACE INTERACTIONS

P. Montazer (Multimedia Environmental Technology, Inc., Newport Beach, CA.), D. Hammermeister, and J. Ginanni 1994 4 p Presented at the International High-level Radioactive Waste Management Conference, Las Vegas, NV, 22-26 May 1994

(Contract DE-AC08-94NV-11432)

(DE94-004304; DOE/NV-11432/1; CONF-940553-4) Avail: CASI HC A01/MF A01

The long-term effect of changes in atmospheric climatological conditions on subsurface hydrological conditions in the unsaturated zone in and environments is an important factor in defining the performance of a high-level and low-level radioactive waste repositories in geological environment. Computer simulation coupled with paleohydrological studies can be used to understand and quantify the potential impact of future climatological conditions on repository performance. A Transport of Unsaturated Ground water and Heat (TOUGH) efficiently simulates (given current state-of-the-art technology) the physical processes involved in the near-surface atmosphere and its effect on subsurface conditions. This efficiency is due to the numerical techniques used in TOUGH and the efficient computational techniques used in the Vectorized-version (V-TOUGH) to solve non-linear thermodynamic equations that govern the flux of vapor and energy within subsurface porous and fractured media and between these media and the atmosphere. DOE

N94-36947# National Academy of Sciences - National Research Council, Washington, DC. Commission on Engineering and Technical Systems.

TOWARD A NEW NATIONAL WEATHER SERVICE: WEATHER FOR THOSE WHO FLY

Mar. 1994 110 p Sponsored in part by Dept. of Commerce and NOAA Avail: CASI HC A06/MF A02; 8 functional color pages

The National Weather Service Modernization Committee has examined present capabilities and practices for providing weather information to aviation and reviewed the plans of both the National Weather Service (NWS) and the Federal Aviation Administration (FAA) for taking advantage of new concepts and technologies in order to improve aviation weather information. Over the next decade, improvements will arise as a result of several factors: information content, presentation format, and availability. Three operational benefits will result from the improved and integrated NWS and FAA system. First, pilots, controllers, and traffic managers will have access to more accurate, higher-resolution analyses and forecasts, some of them tailored to be flight and route specific. Second, all involved will be using a common family of impact variables and decision aids. Third, controllers will be relieved of the duty of being weather information conduits; they and the pilots would have the same integrated information on their displays and each would know what the other was seing. The overall result of the NWS and FAA modernizations will be an aviation system with significantly improved safety, efficiency, and capacity. CASI

N94-37048# Pacific Northwest Lab., Richland, WA.

ON THE DEVELOPMENT OF BOUNDARY LAYER SECONDARY CIRCULATIONS RESULTING FROM HORIZONTALLY VARYING SURFACE HEAT FLUX

W. J. Shaw and J. C. Doran Mar. 1994 5 p Presented at the 21st American Meteorological Society Conference on Agricultural and Forest Meteorology, San Diego, CA, 7-10 Mar. 1994

(Contract DE-AC06-76RL-01830)

(DE94-011234; PNL-SA-23416; CONF-940362-5) Avail: CASI HC A01/MF A01

During the last decade there has been a surge in efforts to understand the processes at work in the inhomogeneous atmospheric boundary layer. Much of the interest in the problem has been driven by increasingly urgent needs to develop accurate assessments of man's contribution to climate change. It has been argued that subgrid-scale secondary circulations in the boundary layer can cause significant errors in parameterized turbulent surface fluxes. Such circulations, variously termed 'inland breezes,' 'lake breezes,' 'snow breezes,' or 'nonclassical mesoscale circulations,' are becoming widely discussed and modeled. Because surface fluxes are part of the lower boundary condition for global climate models, it is important to understand when these circulations occur and what their effects are on overall turbulent transfer. What are not yet clear are the combinations of the ambient wind and the horizontal scale and intensity of surface flux variability under which we may expect boundary layer secondary circulations to occur. Several authors have modeled the development of these circulations for ad hoc situations of alternating surface characteristics, and SA have developed one parameterization relating the scale of surface heat flux variability and the ambient wind to the evolution of NCMC's. In this paper we present observations, collected in a region of inhomogeneous surface fluxes, that suggest the development of a 'farm breeze,' and we develop an alternative scaling argument to that of SA that better represents our measurement conditions. DOE

N94-37115# Westinghouse Savannah River Co., Aiken, SC.

NUMERICAL SIMULATION OF NOCTURNAL DRAINAGE FLOWS IN AN IDEALIZED VALLEY-TRIBUTARY SYSTEM

Lance B. OSteen 1994 6 p Presented at the 6th Conference on Mesoscale Processes, Portland, OR, 18-22 Jul. 1994

(Contract DE-AC09-89SR-18035)

(DE94-011684; WSRC-MS-94-0251; CONF-940769-2) Avail: CASI HC A02/MF A01

During 1984 and 1988 a substantial amount of meteorological field data was collected in the Brush Creek valley area of western Colorado as a part of the Atmospheric Science in Complex Terrain (ASCOT) program. This field experiment was designed to investigate the characteristics of nocturnal drainage flows in valleys as well as valley tributaries and sidewalls. The data collected during the Brush Creek experiment has been used to study a variety of nocturnal flow phenomena including: velocity and thermal structure of slope and valley flows; mass, momentum, and energy balances in valleys and tributaries; and tracer transport and diffusion in valley drainage flows. In support of the Brush Creek experiments, several mesoscale modeling studies have been performed. The numerical studies dealt with various aspects of along-valley nocturnal drainage flow. However, a good deal of effort was expended studying tributary flows and their interaction with the along-valley wind system. These investigations generated considerable debate over the contribution of tributaries to the valley mass flux and the source of observed velocity oscillations in valley-tributary systems. In this study, results from simulations of nocturnal drainage in an idealized valley-tributary-plain system are presented. DOE

N94-37126 Massachusetts Inst. of Tech., Cambridge. Lincoln Lab.

AN AUTOMATED METHOD FOR LOW LEVEL WINDSHEAR ALERT SYSTEM (LLWAS) DATA QUALITY ANALYSIS

David A. Clark and F. W. Wilson 26 May 1994 59 p Limited Reproducibility: More than 20% of this document may be affected by microfiche quality

(Contract DTFA01-91-Z-02036)

(AD-A280313; ATC-207) Avail: Issuing Activity (Defense Technical Information Center (DTIC))

The Low Level Windshear Alert System (LLWAS) is an anemometer-based surface network used for detection of hazardous wind shear and acquisition of operational wind information in the airport terminal area. The quality of wind data provided by the LLWAS anemometers is important for the proper performance of the LLWAS wind shear detection algorithms. This report describes the development of an automated method for anemometer data quality analysis (DQA). This method identifies potential data quality problems through comparison of wind data from each sensor within a network to the mean wind speed and direction of the entire network. The design approach and implementation are described, and results

from testing using data from the demonstration Phase III LLWAS network in Orlando, FL are reported. Potential improvements to the automated DQA algorithm are presented based on experience gained during analysis of the Orlando data. These recommended improvements are provided to assist future development and refinement of the DQA methodology to be performed by the FAA Technical Center. DTIC

N94-37143 Federal Aviation Administration, Atlantic City, NJ.
AWOS DATA ACQUISITION SYSTEM (ADAS) OPERATIONAL TEST AND EVALUATION (OT/E) INTEGRATION AND OT/E OPERATIONAL TEST REPORT
Michael Greco, Eric Hoover, Jock Stratton, Pat Sweeney, and Ed Schlain May 1994 157 p Limited Reproducibility: More than 20% of this document may be affected by microfiche quality
(AD-A280492; ACW-200A; DOT/FAA/CT-TN93/48) Avail: Issuing Activity (Defense Technical Information Center (DTIC))

The Automated Weather Observation System (AWOS) Data Acquisition System (ADAS) is a planned element of the National Airspace System (NAS) modernization program. The objective of the ADAS is to provide collection, processing, archiving, and distribution of aviation-oriented weather observation data in support of the NAS. This report presents the results of the ADAS Operational Test and Evaluation (OT&E) Integration and OT and E Operational testing performed at the Federal Aviation Administration (FAA) Technical Center between December 1992, and July 1993. All ADAS interfaces have been thoroughly tested either through simulation or integrated with live NAS subsystems. During OT and E testing, the ADAS was interfaced with live AWOS's and Automated Surface Observation Systems (ASOS's), and also the National Airspace Data Interchange Network II (NADIN II), Weather Message Switching Center Replacement (WMSCR), Coded Time Source (CTS), and Maintenance Processor Subsystem (MPS). The MPS was executing testcom software in lieu of operational Interim Monitor Control Software (IMCS). The Real-Time Weather Processor (RWP), Data Link Processor (DLP), and Local Communications Network (LCN) interfaces were partially verified using the ADAS prime development contractors' Interactive Process Simulator (IPS). DTIC

N94-37180 Woods Hole Oceanographic Inst., MA.
EXPERIMENT ON RAPIDLY INTENSIFYING CYCLONES OVER THE ATLANTIC Final Report
Robert A. Weller 3 Jun. 1994 7 p Limited Reproducibility: More than 20% of this document may be affected by microfiche quality
(Contract N00014-90-J-1423)
(AD-A280365) Avail: Issuing Activity (Defense Technical Information Center (DTIC))

This is a Final Report on Contract N00014-90-J-1423, which was our participation in ERICA (the Experiment on Rapidly Intensifying Cyclones over the Atlantic). The goal of the Experiment on Rapidly Intensifying Cyclones over the Atlantic (ERICA) field study was to obtain new understanding of the physical mechanisms and processes that account for the wintertime phenomenon of explosively developing extratropical cyclones over the North Atlantic Ocean. The intensive field program ran from 1 December 1988 to 28 February 1989, focusing on a region north of Cape Hatteras to beyond New Foundland, east of Cape Cod, and south of Nova Scotia. DTIC

N94-37217 Phillips Lab., Hanscom AFB, MA.
THREE FLIGHTS INTO THUNDERSTORMS WITH THE REVISED ROCKET ELECTRIC FIELD SOUNDING (REFS) PAYLOAD
Instrumentation Papers, Oct. 1991 - Jul. 1993
J. C. Willett, D. C. Curtis, G. Y. Jumper, and W. F. Thorn 10 Aug. 1993 149 p Limited Reproducibility: More than 20% of this document may be affected by microfiche quality
(AD-A280424; PL-TR-93-2182; IP347) Avail: CASI HC A07

Three sounding rockets were launched into thunderstorms from the Langmuir Laboratory in New Mexico during July, 1992, to measure profiles of the ambient vector electrostatic field. The eight individual, shutter field mills on each of these rockets had a nominal full-scale range of +/- 900 kV/m and sensitivity of 225 V/m. The electric-field soundings passed several self-consistency tests and were corroborated by measurements from the surface and from both tethered and free balloons. Mill noise levels of less than 450 V/m, as well as other error sources, yielded a relative uncertainty of the measured ambient field components less than 1 kV/m flight. Absolute calibrations of both the longitudinal and the transverse field components (relative to the rocket axis of symmetry) were accurate to +/- 10% or better. Field magnitudes greater than 8OkV/m and electrostatic potential magnitudes over 120 MV were encountered inside the storms. The average field driving one natural cloud-to-ground lightning flash was estimated at 30 kV/m or less. Grounded triggering rockets were launched immediately after each sounding rocket, but no lightning was triggered, suggesting that ambient fields of 10 kV/m over the lowest 500 m were not sufficient to trigger lightning with the rocket-and-wire technique. DTIC

N94-37242# Lawrence Livermore National Lab., Livermore, CA.
THE INFLUENCE OF TRIBUTARIES ON NOCTURNAL VALLEY FLOWS
J. M. Leone, Jr. and H. Walker Apr. 1994 6 p Presented at the 6th Conference on Mesoscale Processes, Portland, OR, 18-22 Jul. 1994
(Contract W-7405-eng-48)
(DE94-011613; UCRL-JC-115860; CONF-940769-3) Avail: CASI HC A02/MF A01

While much is known about nocturnal drainage flow down a mountain valley, the factors that determine the structure of the valley flow are not completely understood. For example, there are a number of questions regarding the influence of tributaries on the valley flow. Does the presence of tributaries increase or decrease the mass flux out of the valley; does their presence alter the mass flux along the valley; how is the drainage jet structure modified by the presence of tributaries; or, is their presence insignificant? In this study, we investigate these questions via numerical experiments. DOE

N94-37294*# Purdue Univ., West Lafayette, IN. Dept. of Earth and Atmospheric Sciences.
THE LIFE CYCLES OF INTENSE CYCLONIC AND ANTICYCLONIC CIRCULATION SYSTEMS OBSERVED OVER OCEANS Semiannual Status Report, 1 Jan. - 30 Jun. 1994
Phillip J. Smith 1994 3 p
(Grant NAG8-915)
(NASA-CR-196271; NAS 1.26:196271) Avail: CASI HC A01/MF A01

The work over the past six months has focused on the October/November 1985 blocking case study noted in the last progress report. A summary of the results of this effort is contained in the attached preprint papers for the Symposium on the Life Cycles of Extratropical Cyclones. Using this case study as a model, Ph.D. student Anthony Lupo is now initiating the multiple-case diagnosis by first examining two more fall 1985 blocking episodes. In addition, two secondary efforts have been completed, as summarized in the attached M.S. thesis abstracts. Both studies, which were primarily funded by a fellowship and a teaching assistantship, complement the objectives of this study by providing diagnoses of additional cyclone cases to serve as a comparative base for the pre-blocking cyclones to be studied in the multiple-case blocking diagnosis. Author

N94-37371*# National Aeronautics and Space Administration. Goddard Inst. for Space Studies, New York, NY.
MEASUREMENTS AND MODELING OF THE EFFECT OF CONVECTIVE CLOUDS ON THE UPPER TROPOSPHERIC MOISTURE BUDGET
S. E. Bisson (Sandia National Labs., Livermore, CA.), J. E. M. Goldsmith (Sandia National Labs., Livermore, CA.), and A. D. DelGenio 1994 6 p Presented at the Atmospheric Radiation Measurement Science Team Meeting, Charleston, SC, 28 Feb. - 3 Mar. 1994
(Contract DE-AC04-76DR-00789)
(NASA-TM-109894; NAS 1.15:109894; DE94-012239; SAND-94-8595C; CONF-940277-3) Avail: CASI HC A02/MF A01

The goal of this study is to determine the upper tropospheric moisture budget associated with convective events, and in particular to extend process models to higher altitudes than have been achieved previously. Although upper tropospheric moisture concentrations are several orders of magnitude lower than those near the surface, upper tropospheric moisture exerts an important influence on climate. On a per-molecule basis, greenhouse absorption due to water vapor is about one hundred times more effective at high altitudes than at low altitudes. Several one-dimensional radiative convective models have been used to demonstrate the importance of upper tropospheric moisture on climate. These models show that for a given fractional increase in water vapor at a given altitude the response or change in surface temperature is qualitatively the same. At present,

considerable controversy exists over the nature of the vertical redistribution of water vapor in a changing climate, and particularly the distribution of water vapor in the upper troposphere. Lacking suitable data, this controversy is also reflected in the cumulus parameterization schemes that are currently used in models. Understanding upper tropospheric moistening processes are therefore of prime importance in addressing the water vapor feedback question. DOE

N94-37379 Pacific Northwest Lab., Richland, WA.
REPRESENTING THE INFLUENCE OF SUBGRID TOPOGRAPHY ON HYDROLOGY
L. R. Leung and S. J. Ghan Oct. 1993 31 p Presented at the 32nd Hanford Symposium on Health and the Environment, Richland, WA, 18-21 Oct. 1993 Limited Reproducibility: More than 20% of this document may be affected by microfiche quality
(Contract DE-AC06-76RL-01830)
(DE94-004595; PNL-SA-22546; CONF-9310135-4) Avail: CASI HC A03

Estimates of the impact of global climate change on land surface hydrology require climate information on scales far smaller than those explicitly resolved by global climate models of today and the foreseeable future. To bridge the gap between what is required and what is resolved, we propose a subgrid-scale parameterization of the influence of topography on clouds, precipitation, and land surface hydrology. The parameterization represents subgrid variations in surface elevation in terms of discrete elevation classes. Separate cloud and surface processes are calculated for each elevation class. The simulated surface temperature, precipitation, snowpack, and soil moisture for each elevation class can then be distributed according to the spatial distribution of surface elevation within each grid cell. The scheme is being applied to the Pacific Northwest Laboratory's climate version of the Penn State/NCAR Mesoscale Model. Validation is being addressed by driving the model with observed lateral boundary conditions for the Pacific Northwest and comparing with surface observations. Preliminary results from the simulation will be presented. DOE

N94-37394# Argonne National Lab., IL.
SITE SCIENTIFIC MISSION PLAN FOR THE SOUTHERN GREAT PLAINS CART SITE, JANUARY - JUNE 1994
J. M. Schneider (Oklahoma Univ., Norman, OK.), P. J. Lamb (Oklahoma Univ., Norman, OK.), and D. L. Sisterson Dec. 1993 80 p
(Contract W-31-109-eng-38)
(DE94-012114; ARM-94-001) Avail: CASI HC A05/MF A01

The Southern Great Plains (SGP) Cloud and Radiation Testbed (CART) site is designed to help satisfy the data needs of the Atmospheric Radiation Measurement (ARM) Program Science Team. This document defines the scientific priorities for site activities during the six months beginning on January 1, 1994, and also looks forward in lesser detail to subsequent six-month periods. The primary purpose of this Site Scientific Mission Plan is to provide guidance for the development of plans for site operations. It also provides information on current plans to the ARM Functional Teams (Management Team, Experiment Support Team, Operations Team, Data Management Team, Instrument Team, and Campaign Team), and it serves to disseminate the plans more generally within the ARM Program and among the Science Team. This document includes a description of the site's operational status and the primary envisaged site activities, together with information concerning approved and proposed Intensive Observation Periods. Amendments will be prepared and distributed whenever the content changes by more than 30 percent within a six-month period. The primary users of this document are the site operator, the site scientist, the Science Team through the ARM Program Science Director, the ARM Program Experiment Center, and the aforementioned ARM Program Functional Teams. This plan is a living document that will be updated and reissued every six months as the observational facilities are developed, tested, and augmented and as priorities are adjusted in response to developments in scientific planning and understanding. DOE

N94-37467# National Academy of Sciences - National Research Council, Washington, DC. Commission on Engineering and Technical Systems.
TOWARD A NEW NATIONAL WEATHER SERVICE: NATIONAL WEATHER SERVICE EMPLOYEE FEEDBACK
Mar. 1994 137 p Original contains color illustrations
Avail: CASI HC A07/MF A02

The United States has launched a program to modernize the National Weather Service (NWS), a component of the National Oceanic and Atmospheric Administration. The modernization involves new observational technology, powerful new information and forecast systems, and a new organizational structure. As the modernization process has proceeded, informal communications from about a dozen field employees to the NWS Modernization Committee and discussions with representatives of the NWS Employees Organization raised the committee's concern about the degree to which the NWS had prepared and involved its field personnel in anticipation of the forthcoming technological transition. Thus, the committee agreed to undertake a study of the matter to determine if recommendations were needed to NWS management regarding their handling of the NWS modernization and associated restructuring. The general objectives of this study were to determine the prevalence of concerns about modernization among NWS nonsupervisory employees in the field; determine the adequacy of communication about modernization between these employees and NWS local, regional, and national managers; and determine if subsets of employees (such as at certain offices, with certain backgrounds, etc.) report different concerns or have experienced different levels of communication.
Derived from text

N94-37565# Pacific Northwest Lab., Richland, WA.
AN EXPERIMENTAL AND NUMERICAL STUDY OF BOUNDARY LAYER STRUCTURE OVER AREAS OF INHOMOGENEOUS SENSIBLE HEAT FLUXES
S. Zhong and J. C. Doran Mar. 1994 5 p Presented at the 21st American Meteorological Society Conference on Agricultural and Forest Meteorology, San Diego, CA, 7-10 Mar. 1994
(Contract DE-AC06-76RL-01830)
(DE94-011441; PNL-SA-23405; CONF-940362-4) Avail: CASI HC A01/MF A01

In June of 1992 a boundary-layer experiment was carried out near Boardman, Oregon. The campaigns were part of a program of studies under the auspices of the U.S. Department of Energy's Atmospheric Radiation Measurement (ARM) program, whose goal is to improve the treatment of radiative transfer, particularly as affected by clouds, in general circulation models (GCM's) used for climate studies. One aspect of this program is concerned with the determination of appropriate lower boundary conditions for such models and the representation of subgrid-scale variability in regions where the surface conditions are not uniform. To study this problem, boundary-layer and surface properties were measured over a region of two sharply contrasting land types: a large, dry, sagebrush steppe area and irrigated farmland that formed the east, northeast, and western borders of the steppe. A combination of surface flux instrumentation, airsondes, sonars, and near-surface wind and temperature sensors was used. Measurements were carried out over the eastern portion of this region, which featured a well-defined boundary between the dry and irrigated areas. In this paper, the authors present some results from those observations and from a set of numerical simulations that address the effects of inhomogeneous surface fluxes on boundary-layer structure.
DOE

N94-37566# Pacific Northwest Lab., Richland, WA.
A STRATIFORM CLOUD PARAMETERIZATION FOR GENERAL CIRCULATION MODELS
S. J. Ghan, L. R. Leung, C. C. Chuang, J. E. Penner, and J. McCaa 1994 9 p Presented at the Atmospheric Radiation Measurement Science Team Meeting, Charleston, SC, 28 Feb. - 3 Mar. 1994
(Contract DE-AC06-76RL-01830)
(DE94-011442; PNL-SA-24063; CONF-940277-1) Avail: CASI HC A02/MF A01

The crude treatment of clouds in general circulation models (GCM's) is widely recognized as a major limitation in the application of these models to predictions of global climate change. The purpose of this project is to develop a parameterization for stratiform clouds in GCM's that expresses stratiform clouds in terms of bulk microphysical properties and their subgrid variability. In this parameterization, precipitating cloud species are distinguished from non-precipitating species, and the liquid phase is distinguished from the ice phase. The size of the non-precipitating cloud particles (which influences both the cloud radiative properties and the conversion of non-precipitating cloud species to precipitating species) is determined by predicting both the mass and number concentrations of each species. DOE

N94-37621# Lawrence Livermore National Lab., Livermore, CA.
FACTORS INFLUENCING THE PARAMETERIZATION OF ANVIL CLOUDS WITHIN GCMs
J. M. Leone, Jr. and H. N. S. Chin Dec. 1993 6 p Presented at the 3rd Atmospheric Radiation Measurement Science Team Meeting, Norman, OK, 1-5 Mar. 1993
(Contract W-7405-eng-48)
(DE94-010794; UCRL-JC-113583-Rev-1; CONF-9303122-5-Rev-1) Avail: CASI HC A02/MF A01

The overall goal of this project is to improve the representation of clouds and their effects within global climate models (GCMs). We have concentrated on a small portion of the overall goal: the evolution of convectively generated cirrus clouds and their effects on the large-scale environment. Because of the large range of time and length scales involved, we have been using a multi-scale attack. For the early time generation and development of the cirrus anvil, we are using a cloud-scale model with horizontal resolution of 1-2 kilometers; for the larger scale transport by the larger scale flow we are using a mesoscale model with a horizontal resolution of 20-60 kilometers. The eventual goal is to use the information obtained from these simulations, together with available observations, to derive improved cloud parameterizations for use in GCM's.This paper presents results from our cloud-scale studies and describes a new tool, a cirrus generator, that we have developed to aid in our mesoscale studies. DOE

N94-37790*# National Aeronautics and Space Administration. Goddard Space Flight Center, Greenbelt, MD.
NASA ER-2 DOPPLER RADAR REFLECTIVITY CALIBRATION FOR THE CAMEX PROJECT
I. J. Caylor (Science Systems and Applications, Inc., Lanham, MD.), G. M. Heymsfield, S. W. Bidwell, and S. Ameen Aug. 1994 19 p
(RTOP 460-28-16)
(NASA-TM-104611; Rept-94B00110; NAS 1.15:104611) Avail: CASI HC A03/MF A01

The NASA ER-2 Doppler radar (EDOP) was flown aboard the ER-2 high-altitude aircraft in September and October 1993 for the Convection and Moisture Experiment. During these flights, the first reliable reflectivity observations were performed with the EDOP instrument. This report details the procedure used to convert real-time engineering data into calibrated radar reflectivity. Application of the calibration results produces good agreement between the EDOP nadir pointing reflectivity and ground truth provided by a National Weather Service WSR-88D radar. The rms deviation between WSR-88D and EDOP is 6.9 dB, while measurements of the ocean surface backscatter coefficient are less than 3 dB from reported scatterometer coefficients. After an initial 30-minute period required for the instrument to reach thermal equilibrium, the radar is stable to better than 0.25 dB during flight. The range performance of EDOP shows excellent agreement with aircraft altimeter and meteorological sounding data. Author

48 OCEANOGRAPHY

Includes biological, dynamic, and physical oceanography; and marine resources.

For related information see also *43 Earth Resources and Remote Sensing.*

N94-36446 Martin Labs., Inc., Houston, TX.
MarChem 93, THE PROCEEDINGS, THE 1993 WORKSHOP ON MARINE CHEMISTRY INSTRUMENTATION Final Report
Stephen J. Martin, Louis A. Codispoti, F. E. DeBons, David H. Johnson, and Edward J. Green 1994 147 p Limited Reproducibility: More than 20% of this document may be affected by microfiche quality
(Contract N00014-93-1-0448)
(AD-A279035; ML-10448) Avail: Issuing Activity (Defense Technical Information Center (DTIC))

The MarChem93 workshop was held August 2-4, 1993. The purpose of the workshop was to bring together scientists from industry, universities, and government organizations and encourage them to improve ocean chemical instrumentation (OCI). The development of OCI is not progressing rapidly because: (1) Funding is limited to SBIR and STTR programs, (2) Market size is small and commercial applications are limited, and (3) Instrument developers are not organized to communicate effectively on a continuous basis. Recommendations are: (1) Establish MarChem as a virtual community on the Internet, (2) Continue to hold the MarChem workshop every two years, (3) Exploit large markets with applications for OCI such as environmental chemistry, and (4) The Executive Committee should have regular meetings to identify new members, new technology, and funding opportunities. The Executive Committee should identify research efforts in the field of chemical oceanographic instrumentation and recommend these opportunities to the appropriate funding agencies as suitable topics for Announcements of Opportunity, Broad Agency Announcements, or Request for Proposals. DTIC

N94-36761# Woods Hole Oceanographic Inst., MA. Dept. of Biology.
PHYTOPLANKTON BLOOMS AND COASTAL PHYSICAL PROCESSES Final Report
Donald M. Anderson 1993 5 p
(Contract N00014-89-J-1111)
(AD-A280646) Avail: CASI HC A01/MF A01

The overall goal of our study was to gain understanding of the modes by which the physics of coastal regions couple with biological processes to create mesoscale enhancements of phytoplankton production. We attempted to identify the influence of various types of circulation (e.g., wind-driven, buoyancy-driven, tidally-driven) on phytoplankton bloom dynamics and size structure in the southwestern Gulf of Maine. Specifically, we focused on the mechanisms regulating post spring-bloom production in the coastal boundary layer (around 10 km from the coast). This involved investigations of the scales of patchiness of individual phytoplankton populations in this region, with initial emphasis on dinoflagellates. DTIC

N94-36762# Washington Univ., Seattle, WA. Applied Physics Lab.
COOLING OF THE WEST SPITZBERGEN CURRENT: WINTERTIME OBSERVATIONS WEST OF SVALBARD
Timothy J. Boyd and Eric A. DAsaro 30 Aug. 1993 62 p
(Contracts N00014-87-K-0004; N00014-91-J-1405)
(AD-A280648) Avail: CASI HC A04/MF A01

The West Spitzbergen Current (WSC) is the major source of heat and salt for the Arctic Ocean and the areas of deep convection in the Greenland Sea. The WSC current cools dramatically downstream. Hydrographic and velocity data from a 3-week, midwinter cruise off Spitzbergen are used to investigate the heat budget of the WSC and the mechanisms of cooling. The downstream divergence of mean heat flux in the WSC produces a heat loss of at least 1000 + or - 400 Wm(exp -2) averaged over the width of the current. Approximately 350 Wm(exp -2) is lost to the atmosphere and 200 Wm(exp -2) lost to melting ice over a region somewhat wider than the current. Cooling of the WSC to the atmosphere converts the inflowing Atlantic Water (AW) to Lower Arctic Intermediate Water, which is sufficiently salty to convect. Cooling by ice converts the AW to much fresher Arctic Surface Water, which is too light to convect. The relative importance of these two conversions is primarily controlled by the rate at which the wind advects ice from the Barents Sea over the WSC. The warmest water of the WSC is often observed 100-200 m below the surface. Despite the lack of direct contact with the surface, this core cools at about 800 Wm(exp -2) in our observations. DTIC

N94-36958*# National Aeronautics and Space Administration. Goddard Space Flight Center, Greenbelt, MD.
SeaWiFS TECHNICAL REPORT SERIES. VOLUME 20: THE SeaWiFS BIO-OPTICAL ARCHIVE AND STORAGE SYSTEM (SeaBASS), PART 1
Stanford B. Hooker, ed., Charles R. McClain, James K. Firestone, Todd L. Westphal, Eueng-Nan Yeh, Yuntao Ge, and Elaine R. Firestone Jul. 1994 41 p
(NASA-TM-104566-Vol-20-Pt-1; NAS 1.15:104566-Vol-20-Pt-1; Rept-94B00104-Vol-20-Pt-1) Avail: CASI HC A03/MF A01

This document provides an overview of the Sea-viewing Wide Field-of-view Sensor (SeaWiFS) Bio-Optical Archive and Storage System (SeaBASS), which will serve as a repository for numerous data sets of interest to the SeaWiFS Science Team and other approved investigators in the oceanographic community. The data collected will be those data sets suitable for the development and evaluation of bio-optical algorithms which include results from SeaWiFS Intercalibration Round-Robin Experiments (SIRREXs), prelaunch characterization of the SeaWiFS

instrument by its manufacturer -- Hughes/Santa Barbara Research Center (SBRC), Marine Optical Characterization Experiment (MOCE) cruises, Marine Optical Buoy (MOBY) deployments and refurbishments, and field studies of other scientists outside of NASA. The primary goal of the data system is to provide a simple mechanism for querying the available archive and requesting specific items, while assuring that the data is made available only to authorized users. The design, construction, and maintenance of SeaBASS is the responsibility of the SeaWiFS Calibration and Validation Team (CVT). This report is concerned with documenting the execution of this task by the CVT and consists of a series of chapters detailing the various data sets involved. The topics presented are as follows: 1) overview of the SeaBASS file architecture, 2) the bio-optical data system, 3) the historical pigment database, 4) the SIRREX database, and 5) the SBRC database. Author

N94-36971 Naval Postgraduate School, Monterey, CA.
SIGNAL PROCESSING FOR THE 1992 BARENTS SEA TOMOGRAPHY EXPERIMENT M.S. Thesis
Philip G. McLaughlin Dec. 1993 59 p Limited Reproducibility: More than 20% of this document may be affected by microfiche quality
(AD-A278580) Avail: Issuing Activity (Defense Technical Information Center (DTIC))

In August 1992, an acoustic tomography experiment was conducted in the Barents Sea. The objective of this thesis is the development of space-time signal processing algorithms to extract the arrival times of rays and modes for that experiment. The temporal signal processing involves pulse compression of the phase-encoded signal. Spatial signal processing consists of plane wave and modal beamforming on data from a 16 element vertical line array. After signal processing an arrival detection, identification, and tracking algorithm is used to obtain travel time and travel time error estimates. After development and testing of these algorithms, 13 hours of acoustic data was processed for rays and eight hours of data was processed for modes. The resultant travel time information is then available for inversion to sound speed maps. DTIC

N94-36985 Naval Postgraduate School, Monterey, CA.
VARIABILITY OF THE CALIFORNIA CURRENT SYSTEM OFF POINT SUR, CALIFORNIA FROM APRIL 1988 TO DECEMBER 1990 M.S. Thesis
Frederick W. Rischmiller Dec. 1993 168 p Limited Reproducibility: More than 20% of this document may be affected by microfiche quality
(AD-A278579) Avail: Issuing Activity (Defense Technical Information Center (DTIC))

The Point Sur Transect was established in 1987 by the Department of Oceanography at the Naval Postgraduate School in order to further understand the nature of poleward flows in the California Current System (CCS). The POST extends offshore, perpendicular to bottom topography along 36 deg 20 min N to 123 deg 01.7 W where it meets and coincides with the California Cooperative Fisheries Investigation (CalCOFI) line 67. The sampling scheme along the transect consists of 22 CTD stations and is approximately 215 km in. length. POST was occupied 19 times from April 1988 to April 1991. Data from 15 of the 19 cruises were selected in order to determine the temporal and spatial variability of the CCS off Point Sur. PEGASUS data as well as hydrographic data and NOAA 11 AVHRR satellite imagery were utilized for comparison. The CUC was observed with speeds in excess of 20 cm/s throughout the year. DTIC

N94-37038 Colorado Univ., Boulder, CO.
TURBULENT TRANSFER IN THE MARINE PLANETARY BOUNDARY LAYER Final Report, 9 May 1984 - 30 Apr. 1994
Siri Jodha, S. Khalsa, and Howard P. Hanson 13 Jun. 1994 10 p Limited Reproducibility: More than 20% of this document may be affected by microfiche quality
(Contract N00014-84-K-0405)
(AD-A280549) Avail: CASI HC A02

Work under this contract focused on turbulent processes in the marine atmospheric boundary layer (MABL) and how they effect mixing between ocean and the free atmosphere. In particular, we investigated specific mechanisms of this turbulence within the MABL and how these mechanisms responded to varying boundary and internal forcing. By developing, from both observational and theoretical perspectives, a coherent picture of MABL turbulence in terms of the mechanics of turbulence, we gained new insight into the behavior of the MABL which will lead to improved predictability. DTIC

N94-37047 Woods Hole Oceanographic Inst., MA.
THE ROLE OF HORIZONTAL VARIABILITY IN AIR-SEA INTERACTION Final Report
Robert A. Weller 10 Jun. 1994 9 p Limited Reproducibility: More than 20% of this document may be affected by microfiche quality
(Contract N00014-90-J-1470)
(AD-A280561) Avail: CASI HC A02

The cooperative Frontal Air-Sea Interaction Experiment (FASINEX) was conducted in the subtropical convergence zone southwest of Bermuda from January to June 1986. The overall objective of the program was to investigate air-sea coupling in the vicinity of horizontal gradients associated with ocean fronts. The FASINEX field experiment was very successful and resulted in a rich and unique data set. The first goal of the analysis phase that followed the field work was a synthesis of results from all participants; this was accomplished by the preparation of a monograph consisting of multi-authored papers. The monograph was published in 1991. More highly focused scientific publication has continued since the monograph. The FASINEX data set is highly requested. DTIC

N94-37135 Coastal Engineering Research Center, Vicksburg, MS.
INDEX AND BULK PARAMETERS FOR FREQUENCY-DIRECTION SPECTRA MEASURED AT CERC FIELD RESEARCH FACILITY, SEPTEMBER 1992 TO AUGUST 1993 Final Report
Charles E. Long and Judy H. Roughton May 1994 118 p Limited Reproducibility: More than 20% of this document may be affected by microfiche quality
(AD-A280233; CERC-94-6) Avail: CASI HC A06

A multiyear series of wind wave frequency-direction spectral measurements has been undertaken at the Field Research Facility of the Coastal Engineering Research Center, U.S. Army Engineer Waterways Experiment Station. Cross-spectra of surface-corrected signals from a spatial array of 16 bottom-mounted pressure sensors have been used in conjunction with an iterative maximum likelihood algorithm to estimate frequency-direction spectra in about 8 m of water, approximately 900 m offshore. This report provides an index of and describes a means of access to 2,683 spectral observations obtained from September 1992 to August 1993. This period represents the seventh year of data collection. In addition to a list of data collection start times, bulk parameters are provided to characterize the observations. Included are characteristic wave height, spectral peak frequency and corresponding peak period, peak wave direction, directional spread, and reflection coefficient. Time series graphs of these parameters, as well as local winds and currents, illustrate some of the salient climatology. DTIC

N94-37216 Coastal Engineering Research Center, Vicksburg, MS.
INDEX AND BULK PARAMETERS FOR FREQUENCY-DIRECTION SPECTRA MEASURED AT CERC FIELD RESEARCH FACILITY, SEPTEMBER 1990 TO AUGUST 1991 Final Report
Charles E. Long and Juliana Atmadja May 1994 103 p Limited Reproducibility: More than 20% of this document may be affected by microfiche quality
(AD-A280423; CERC-94-5) Avail: CASI HC A06

A multiyear series of wind wave frequency-direction spectral measurements has been undertaken at the Field Research Facility of the Coastal Engineering Research Center, U.S. Army Engineer Waterways Experiment Station. Cross-spectra of surface-corrected signals from a spatial array of 15 bottom-mounted pressure sensors have been used in conjunction with an iterative maximum likelihood algorithm to estimate frequency-direction spectra in about 8 m of water, approximately 900 m offshore. This report provides an index of and describes a means of access to 1,973 spectral observations obtained from September 1990 to August 1991. This period represents the fifth year of data collection. In addition to a list of data collection start times, a set of bulk parameters is provided to characterize the observations. Included are characteristic wave height, spectral peak frequency and corresponding peak period, peak wave direction, directional spread, and reflection coefficient. Time series graphs of these parameters, as well as local winds and currents, illustrate some of the salient climatology.

Frequency-direction spectra, Wave database, Wave climate, Wind waves.
DTIC

N94-37229 Coastal Engineering Research Center, Vicksburg, MS.
INDEX AND BULK PARAMETERS FOR FREQUENCY-DIRECTION SPECTRA MEASURED AT CERC FIELD RESEARCH FACILITY, SEPTEMBER 1991 TO AUGUST 1992 Final Report
Charles E. Long and Janna L. Pemberton May 1994 115 p Limited Reproducibility: More than 20% of this document may be affected by microfiche quality
(AD-A280455; CERC-94-7) Avail: CASI HC A06

A multiyear series of wind wave frequency-direction spectral measurements has been undertaken at the Field Research Facility of the Coastal Engineering Research Center, U.S. Army Engineer Waterways Experiment Station. Cross-spectra of surface-corrected signals from a spatial array of 15 bottom-mounted pressure sensors have been used in conjunction with an iterative maximum likelihood algorithm to estimate frequency-direction spectra in about 8 m of water, approximately 900 m offshore. This report provides an index and describes a means of access to 2,779 spectral observations obtained from September 1991 to August 1992. This period represents the sixth year of data collection. In addition to a list of data collection start times, bulk parameters are provided to characterize the observations. Included are characteristic wave height, spectral peak frequency and corresponding peak period, peak wave direction, directional spread, and reflection coefficient. Time series graphs of these parameters, as well as local winds and currents, illustrate some of the salient climatology. Frequency-direction spectra, Wave database, Wave climate, Wind waves.
DTIC

N94-37397*# National Aeronautics and Space Administration. Goddard Space Flight Center, Greenbelt, MD.
AIRBORNE ROWS DATA REPORT FOR THE HIGH RESOLUTION EXPERIMENT, JUNE 1993
D. Vandemark, D. Hines, S. Bailey, and K. Stewart Jul. 1994 76 p
(Contract N0001494-MP-23031; RTOP 461-31-05-20)
(NASA-TM-104609; NAS 1.15:104609; Rept-94B00098) Avail: CASI HC A05/MF A01

Airborne radar ocean wave spectrometer (ROWS) data collected during the Office of Naval Research's High Resolution Remote Sensing Experiment of June 1993 are presented. This data summary covers six flights made using NASA's T-39 aircraft over a region of the North Atlantic off the coast of North Carolina and includes multiple crossings of the gulf stream. The Ku-band ROWS was operated in a configuration which continuously switched between an altimeter and a spectrometer channel. Data derived from the two channels include altimeter radar cross section, altimeter-derived sea surface mean square slope and wind speed, and directional and nondirectional longwave spectra. Discussion is provided for several events of particular interest. Author

N94-37494# Lawrence Livermore National Lab., Livermore, CA.
SIMPLE OCEAN CARBON CYCLE MODELS
K. Caldeira, M. I. Hoffert, and U. Siegenthaler Feb. 1994 38 p Presented at the Snowmass Global Change Institute Conference on the Global Carbon Cycle, Snowmass, CO, 19-30 Jul. 1993
(Contract W-7405-eng-48)
(DE94-011745; UCRL-JC-116517; CONF-9307181-1) Avail: CASI HC A03/MF A01

Simple ocean carbon cycle models can be used to calculate the rate at which the oceans are likely to absorb CO2 from the atmosphere. For problems involving steady-state ocean circulation, well calibrated ocean models produce results that are very similar to results obtained using general circulation models. Hence, simple ocean carbon cycle models may be appropriate for use in studies in which the time or expense of running large scale general circulation models would be prohibitive. Simple ocean models have the advantage of being based on a small number of explicit assumptions. The simplicity of these ocean models facilitates the understanding of model results. DOE

N94-37855 Helsinki Univ. of Technology, Espoo (Finland). Arctic Offshore Research Centre.
MEASURING THE UPPER PROFILE OF SEA ICE IN THE BAY OF BOTHNIA WITH A LASER PROFILOMETER
O. Salmela Nov. 1993 58 p See also AD-A256302 Limited Reproducibility: More than 20% of this document may be affected by microfiche quality
(PB94-184561; ISBN-951-22-1841-0) Avail: Issuing Activity (National Technical Information Service (NTIS))

Two laser profilometer measurements with a helicopter were carried out on 23rd and 24th of February 1993 on the Bay of Bothnia near Kemi. A description of ice conditions of each laser profilometer file is presented. The work was a co-operative project with Arctic Offshore Center (Helsinki University of Technology) and Finnish Institute of Marine Research. The results will be used for the validation and calibration work of ERS-1. The data were analyzed also by Lensu 1993 in the Finnish Institute of Marine Research, but the method and results were a little bit different. The laser profilometer used in the measurement described in this report was provided and the analysis program developed almost two years ago, and they have been successfully used for many measurements and analysis of sea ice. This report is the first public paper. NTIS

51 LIFE SCIENCES (GENERAL)

N94-36481# Argonne National Lab., IL.
FEMTOSECOND TRANSIENT ABSORPTION STUDIES OF THE LIGHT HARVESTING Chl a/b PROTEIN COMPLEX OF PHOTOSYSTEM 2 IN HIGHER PLANTS
T. Bittner, M. R. Wasielewski, and K. D. Irrgang 1994 4 p Presented at the 9th International Conference on Ultrafast Phenomena, Dana Point, CA, 1-5 May 1994
(Contract W-31-109-eng-38)
(DE94-009684; ANL/CHM/CP-81874; CONF-940593-6) Avail: CASI HC A01/MF A01

The first steps of the primary reactions in photosynthesis are the generation of electronically excited states (excitons) by light absorption within pigment protein complexes referred to as light harvesting antenna complexes and rapid exciton migration to the photoactive pigments embedded into the reaction center complex where the transformation into electrochemical free energy takes place. In green algae and higher plants the light harvesting Chl a/b complex associated with Photosystem 2 (LHC2) serves as the main antenna complex. In this communication we present intensity dependent transient absorption measurements with fs-time resolution in isolated LHC 2 preparations to address the problem of the interaction of ultrafast exciton migration and exciton-exciton annihilation.
DOE

N94-36522 Naval Research Lab., Bay Saint Louis, MS.
INDICATORS FOR SULFATE-REDUCING BACTERIA IN MICROBIOLOGICALLY INFLUENCED CORROSION Final Report
Brenda Little and Patricia Wagner Apr. 1994 21 p Limited Reproducibility: More than 20% of this document may be affected by microfiche quality
(NR Proj. 03103)
(AD-A278914; NRLD-BC-005-92-333) Avail: Issuing Activity (Defense Technical Information Center (DTIC))

Microbiologically influenced corrosion (MIC) is localized corrosion and results in pitting, crevice corrosion, selective dealloying, stress corrosion cracking, or under-deposit corrosion. Since MIC does not produce unique forms of corrosion, investigators have relied on the shape, color, smell, and morphology of surface deposits in association with numbers and types of organisms to indicate MIC. DTIC

N94-36554# Argonne National Lab., IL.
SOLVENT EFFECTS ON THE ENERGETICS AND DYNAMICS OF ULTRAFAST ELECTRON TRANSFER IN CHLOROPHYLL-PORPHYRIN-ACCEPTOR TRIADS
G. P. Wiederrecht, S. Watanabe, and M. R. Wasielewski 1994 4 p Presented at the 9th International Conference on Ultrafast Phenomena, Dana Point, CA, 1-5 May 1994
(Contract W-31-109-eng-38)
(DE94-009693; ANL/CHM/CP-81878; CONF-940593-9) Avail: CASI HC A01/MF A01

An understanding of the role of the medium that lies between electron

donors and acceptors is particularly important for the study of photosynthetic reaction centers where the medium is thought to have a large influence on the observed rates of electron transfer. In the bacterial photosynthetic reaction center a bacteriochlorophyll (BChl) molecule lies between the dimeric bacteriochlorophyll (BChl2) and the bacteriopheophytin (BPh) acceptor. Femtosecond transient absorption spectroscopy of native reaction centers has yielded evidence for both superexchange and two-step electron transfer mechanisms mediated by the bridging BChl. We have prepared molecules that mimic this structural arrangement to better understand the influence of solvation dynamics and the low-lying electron states of a bridging porphyrin molecule (ZP) on electron transfer rates within molecules that possess a chlorophyll donor (ZC) and either a napthoquinone (NQ) or a 3,4,9,10-perylenetetracarboxydiimide (PER) acceptor. DOE

N94-36555# Argonne National Lab., IL.
FEMTOSECOND TRANSIENT GRATING STUDIES OF ELECTRON TRANSFER IN PORPHYRIN AND CHLOROPHYLL DONOR-ACCEPTOR MOLECULES
G. P. Wiederrecht, W. A. Svec, and M. R. Wasielewski 1994 4 p Presented at the 9th International Conference on Ultrafast Phenomena, Dana Point, CA, 1-5 May 1994
(Contract W-31-109-eng-38)
(DE94-009694; ANL/CHM/CP-81875; CONF-940593-8) Avail: CASI HC A01/MF A01

Transient grating studies of electron transfer in artificial photosynthetic systems are described. These systems include simple donor-acceptor molecules where the donor, a chlorophyll or porphyrin, is rigidly attached to an easily reduced species such as napthoquinone or benzoquinone. We have previously synthesized acceptor molecules which have well defined absorption bands upon reduction and are well removed from the excited and cationic states of porphyrins and chlorophylls. They also possess large molar extinction coefficients that dominate the spectra and have well defined polarization characteristics. These traits are ideal for polarization sensitive transient grating experiments which enable accurate determination of the angle of the transition dipole between the initial excitation and the acceptor probe, dynamic solvation effects on the charge separated species, and any time dependent rotation of the chromophores relative to each other. An example of the type of molecule utilized for these experiments is a free base porphyrin (HP) donor and a pyromellitic diimide (PI) acceptor directly bonded to the porphyrin ring. DOE

N94-36720# Bio En-Gene-Er Associates, Inc., Wilmington, DE.
OPPORTUNITIES FOR INNOVATION: BIOTECHNOLOGY
R. M. Busche Sep. 1993 275 p
(Grant NANB2D1219)
(PB94-157831; NIST/GCR-93/633) Avail: CASI HC A12/MF A03

The purpose of this project is to help small businesses get on the fast track in biotechnology research and development leading to the spin off of viable commercial businesses, probably with the help of larger companies having the resources for commercialization that are lacking in a small enterprise. Such resources could include financing, and positions in marketing, manufacturing, regulatory affairs, and raw material supply, to name a few. In general, biotechnology can be expected to have a major impact on fundamental human needs engendered in the market segments of: health care, agriculture, forestry, food ingredients, industrial chemicals, plastics, energy, mining, pollution control, and bioelectronics. NTIS

N94-36751*# National Aeronautics and Space Administration. Lyndon B. Johnson Space Center, Houston, TX.
RECOMBINANT PROTEIN PRODUCTION AND INSECT CELL CULTURE AND PROCESS Patent Application
Glenn Spaulding, inventor (to NASA), Tacey Prewett, inventor (to NASA), Thomas Goodwin, inventor (to NASA), Karen Francis, inventor (to NASA), Angela Andrews, inventor (to NASA), and Kim OConnor, inventor (to NASA) 14 May 1993 26 p
(NASA-Case-MSC-22336-1; NAS 1.71:MSC-22336-1; US-Patent-Appl-SN-062856) Avail: CASI HC A03/MF A01

A process has been developed for recombinant production of selected polypeptides using transformed insect cells cultured in a horizontally rotating culture vessel modulated to create low shear conditions. A metabolically transformed insect cell line is produced using the culture procedure regardless of genetic transformation. The recombinant polypeptide can be produced by an alternative process using the cultured insect cells as host for a virus encoding the described polypeptide such as baculovirus. The insect cells can also be a host for viral production. NASA

N94-36765*# National Aeronautics and Space Administration. Lyndon B. Johnson Space Center, Houston, TX.
THREE DIMENSIONAL OPTIC TISSUE CULTURE AND PROCESS Patent Application
Glenn F. Spaulding, inventor (to NASA), Tacey L. Prewett, inventor (to NASA), Thomas J. Goodwin, inventor (to NASA), Karen M. Francis, inventor (to NASA), Delmar R. Cardwell, inventor (to NASA), Kim OConnor, inventor (to NASA), Wendy S. Fitzgerald, inventor (to NASA), and Laurie A. Aten, inventor (to NASA) 13 Mar. 1994 23 p
(NASA-Case-MSC-22368-1; NAS 1.71:MSC-22368-1; US-Patent-Appl-SN-242546) Avail: CASI HC A03/MF A01

A process for artificially producing three-dimensional optic tissue has been developed. The optic cells are cultured in a bioreactor at low shear conditions. The tissue forms normal, functional tissue organization and extracellular matrix. NASA

N94-36986*# San Jose State Univ., CA. Dept. of Biological Sciences.
[GROUND AND SPACE FLIGHT EXPERIMENTS OF THE EFFECTS OF LIGHT, SOUND AND/OR TEMPERATURE ON ANIMALS] Final Report
Daniel C. Holley, Vince Du, Jill Erikson, Jack Gott, Heather Hinchcliffe, Gary Mele, Karen Moeller, Tam Nguyen, Sarah Okumura, and Mark Robbins et al 3 Jun. 1994 293 p
(Contract NCC2-593)
(NASA-CR-196102; NAS 1.26:196102) Avail: CASI HC A13/MF A03

Papers on the following topics are presented: (1) rat long term habitability and breeding under low light intensity (5 lux); (2) effects of low light intensity on the rat circadian system; (3) effects of sound/noise on the circadian system of rats; (4) temperature related problems involving the animal enclosure modules (AEM) lighting system; and (5) NASA AEM filter test 92/93 (Rats). CASI

N94-36996*# Florida Inst. of Tech., Melbourne, FL. Dept. of Biological Sciences.
RAPID SUSCEPTIBILITY TESTING OF MYCOBACTERIUM AVIUM COMPLEX AND MYCOBACTERIUM TUBERCULOSIS ISOLATED FROM AIDS PATIENTS Final Progress Report, 1 Jun. 1992 - 31 May 1994
Arvind M. Dhople 1994 6 p
(Grant NAG10-0106)
(NASA-CR-196268; NAS 1.26:196268) Avail: CASI HC A02/MF A01

In ominous projections issued by both U.S. Public Health Service and the World Health Organization, the epidemic of HIV infection will continue to rise more rapidly worldwide than predicted earlier. The AIDS patients are susceptible to diseases called opportunistic infections of which tuberculosis and Mycobacterium avium complex (MAC) infection are most common. This has created an urgent need to uncover new drugs for the treatment of these infections. In the seventies, NASA scientists at Goddard Space Flight Center, Greenbelt, MD, had adopted a biochemical indicator, adenosine triphosphate (ATP), to detect presence of life in extraterrestrial space. We proposed to develop ATP assay technique to determine sensitivity of antibacterial compounds against MAC and M. tuberculosis.
Derived from text

N94-37045 Naval Aerospace Medical Research Lab., Pensacola, FL.
BEHAVIORAL PERFORMANCE IN MONKEYS EXPOSED TO TEMPO HIGH-PEAK-POWER MICROWAVE PULSES AT 3 GHz Interim Report, 1992-1993
J. A. DAndrea, B. L. Cobb, J. Knepton, and F. Bates Dec. 1993 22 p Limited Reproducibility: More than 20% of this document may be affected by microfiche quality
(Proj. MM3-3130)
(AD-A280551; NAMRL-1389) Avail: CASI HC A03/MF A01

The development of adequate safety standards for exposure to microwave radiation requires an extensive database which provides information on frequency, power, and modulation characteristics. This study was conducted to provide information on the behavioral effects of high-peak-power microwave pulses produced by an axially extracted virtual cathode oscillator. This pulsed microwave source, TEMPO (transformer energized megavolt pulsed output), was located at the Walter Reed Army

Institute of Research and for this study was configured to produce high-peak-power 3.0 GHz microwave pulses, 20-60 ns pulse duration with a 7.5 s interpulse interval. To investigate the behavioral effects of the high peak power pulses, four male rhesus monkeys (Macaca mulatto) were trained on a operant color discrimination task for food pellet reward. The task was twofold requiring monkeys to pull one plastic lever on a variable interval schedule (VI-25 s) and then respond to color signals and pull a second lever to obtain food. During the behavioral task, the monkeys were exposed to microwave pulses produced by TEMPO. Peak field power densities averaged 45.63 kW/sq cm, which produced a peak whole body specific absorption rate (SAR) of approximately 2.21 MW/kg (specific absorption (SA) per pulse was 1.3 J/kg). Average whole-body SAR, however, was low due to the short pulse duration and long interpulse interval. Behavioral performance on either component of the task was not altered significantly by the high-peak-power pulses. DTIC

N94-37156# California Univ., Berkeley. Lawrence Berkeley Lab, CA. Dept. of Biophysics.

HIGH RESOLUTION ELECTRON DIFFRACTION ANALYSIS OF STRUCTURAL CHANGES ASSOCIATED WITH THE PHOTOCYCLE OF BACTERIORHODOPSIN Ph.D. Thesis

Bong-Gyoon Han Apr. 1994 199 p

(Contract DE-AC03-76SF-00098)

(DE94-011800; LBL-35448) Avail: CASI HC A09/MF A03

Changes in protein structure that occur during the formation of the M photointermediate of bacteriorhodopsin can be directly visualized by electron diffraction techniques. Samples containing a high percentage of the M intermediate were trapped by rapidly cooling the crystals with liquid nitrogen following illumination with filtered green light at 240K and 260K respectively. Difference Fourier projection maps for M minus bR at two temperatures and for M(sub 260K) minus M(sub 240K) are presented. While it is likely that a unique M-substate is trapped when illuminated at 260K, the data indicate that the sample illuminated at 260 K produces a mixture of the M(sub 240K) substate and a second M-substate which may have a protein structure similar to the N-intermediate. The diffraction data clearly show that statistically significant structural changes occur upon formation of the M(sub 240K) specimen and then further upon formation of the second substate which is present in the mixture that is produced at 260K. A preliminary 3-D difference map, based on data collected with samples tilted up to 30 degrees, has been constructed at a resolution of 3.5 Angstrom parallel to the membrane plane and a resolution of 8.5 Angstrom perpendicular to the membrane. The data have been analyzed by a number of different criteria to ensure that the differences seen reflect real conformation changes at a level which is significantly above the noise in the map. Furthermore, a comparison of the positions of specific backbone and side-chain groups relative to significant difference peaks suggests that it will be necessary to further refine the atomic resolution model before it will be possible to interpret the changes in chemical structure that occur in the protein at this stage of the photocycle. DOE

N94-37248# Cornell Univ., Ithaca, NY. Dept. of Soil, Crop and Atmospheric Sciences.

EFFECTS OF FREEZING AND COLD ACCLIMATION ON THE PLASMA MEMBRANE OF ISOLATED PROTOPLASTS

P. L. Steponkus 1994 6 p

(Contract DE-FG02-84ER-13214)

(DE94-012487; DOE/ER-13214/8) Avail: CASI HC A02/MF A01

Our aim is to provide a mechanistic understanding of the cellular and molecular aspects of freezing injury and cold acclimation from a perspective of the structural and functional integrity of the plasma membrane - the primary site of freezing injury in winter cereals. We established that destabilization of the plasma membrane of winter rye, the most freezing-tolerant winter cereal, can result from several different lesions: expansion induced lysis, lamellar-to-hexagonal 2 phase transitions, and the fracture-jump lesion. The occurrence and incidence of these various lesions, depends on the freeze/thaw protocol and the stage of cold acclimation. In non-acclimated leaves and protoplasts, expansion-induced lysis is the predominant lesion at temperatures between -2 and -5 C, whereas freeze-induced formation of the H(sub II) phase is the predominant lesion at temperatures below -10 C. We investigated whether the difference in freezing tolerance and the threshold temperatures at which the lesions occur in rye and oats are a consequence of differences in the lipid composition of the plasma membrane. There are substantial differences between rye and oat cell membranes both before and after cold acclimation. The plasma membrane of oat contains greater proportions of acylated sterylglucosides and cerebrosides than that of rye, and there is little change in these two lipid classes during cold acclimation. The lyotropic phase behavior of lipid mixtures that resemble the plasma membrane of rye and oat was studied. The differences in lipid composition of rye and oats are of mechanistic significance because of their influence on the hydration characteristics of the plasma membrane, the propensity for dehydration-induced lipid-lipid demixing, and the intrinsic curvature of the lipid monolayers. These studies suggest that strategies for improving the freezing tolerance of winter cereals should include approaches to modify membrane lipid composition. DOE

N94-37355# Lawrence Livermore National Lab., Livermore, CA.

THE PROBLEMS OF THE MINIMAL SURFACE AND MINIMAL LINEAL MEASURE IN THREE DIMENSIONS

R. M. Christensen Feb. 1994 19 p

(Contract W-7405-eng-48)

(DE94-013002; UCRL-CR-116392) Avail: CASI HC A03/MF A01

A solution is given to the classical problem of the minimal surface in three dimensions formed from a repeating cell microstructure under isotropic conditions. The solution is found through a global/local minimization procedure and the resulting basic cell is composed of 14 faces. At the junctions where the intersections between faces meet at a point, half of the junctions involve 4 intersections and half involve 3 intersections. The same general solution also applies to the related minimal lineal measure problem where the measure is that of the length of the intersections connecting the junctions. Some implications and applications for materials science are given. DOE

N94-37434# Cornell Univ., Ithaca, NY.

CONVERSION OF ACETIC ACID TO METHANE BY THERMOPHILES

Stephen H. Zinder Feb. 1994 8 p

(Contract DE-FG02-85ER-13370)

(DE94-012478; DOE/ER-13370/T3) Avail: CASI HC A02/MF A01

Acetate is the precursor of approximately two-thirds of the methane produced by anaerobic bioreactors and many other methanogenic habitats. Besides their intrinsic interest, thermophilic acetotrophic methanogenic cultures usually grow at least twice as fast as their mesophilic counterparts, making them more amenable to study. In recent years, attention has been mainly focused on the thermophilic acetate utilizing methanogen Methanothrix strain CALS-1. Methanothrix, also called Methanosaeta, is one of only two methanogenic genera known to convert acetate to methane, the other being Methanosarcina. The faster-growing more versatile Methanosarcina has been better studied. However, when one examines anaerobic digestor contents, Methanothrix is often the dominant acetate-utilizing methanogen. As described in previous progress reports, the authors have achieved methanogenesis from acetate in cell-free extracts of Methanothrix strain CALS-1 grown in a pH auxostat. Using these cell extracts, specific activities for methanogenesis from acetate and ATP of 100-300 nmol/min were routinely obtained, levels comparable to the rate in whole cells, which is not usually the case in methanogenic extracts. Recently obtained results are given and discussed for the following: methanogenesis in crude extracts; role of the cell membrane in methanogenesis from acetate; carbon monoxide dehydrogenase; novel thermophilic cultures converting acetate to methane; and methanol-utilizing methanogen. DOE

N94-37535# China Nuclear Information Centre, Beijing (China).

STUDYING OF ION IMPLANTATION EFFECT ON THE BIOLOGY IN CHINA

eng-Liang Yu (Academia Sinica, Hefei, China.) Apr. 1993 12 p

(DE94-620692; CNIC-00746; ASIPP-0036) Avail: CASI HC A03/MF A01 (US Sales Only)

Since low energy ion effect on the biology was observed, the ion implantation as a new mutagenic source has been widely used in improving crops and modifying microbes in China. The basic phenomenon of ion implantation effect on the biology and analytical results are reported, and the examples of its application and its further development are shown. DOE

N94-37625# Pacific Northwest Lab., Richland, WA.
INVESTIGATION OF EXPOSURE TO EXTREMELY LOW FREQUENCY (ELF) MAGNETIC AND ELECTRIC FIELDS: ONGOING ANIMALS STUDIES
L. E. Anderson Mar. 1994 10 p Presented at the Electric Power Research Institute EMF Seminar on Focus on Research, Santa Clara, CA, 14-16 Mar. 1994
(Contract DE-AC06-76RL-01830)
(DE94-011239; PNL-SA-23995; CONF-9403111-1) Avail: CASI HC A02/MF A01

There is now convincing evidence from a large number of laboratories, that exposure to extremely low frequency (ELF) magnetic and electric fields produces biological responses in animals. Many of the observed effects appear to be directly or indirectly associated with the neural or neuroendocrine systems. Such effects include increased neuronal excitability, chemical and hormonal changes in the nervous system, altered behavioral responses (some of which are related to sensing the presence of the field) and changes in endogenous biological rhythms. Additional indices of general physiological status appear relatively unaffected by exposure, although effects have occasionally been described in bone growth and fracture repair, reproduction and development, and immune system function. A major current emphasis in laboratory research is to determine whether or not the reported epidemiological studies that suggest an association between EMF exposure and risk of cancer are supported in studies using animal models. Three major challenges exist for ongoing research: (1) knowledge about the mechanisms underlying observed bioeffects is incomplete; (2) researchers do not as yet understand what physical aspects of exposure produce biological responses; and (3) health consequences resulting from ELF exposure are unknown. Although no animal studies clearly demonstrate deleterious effects of ELF fields, several are suggestive of potential health impacts. From the perspective of laboratory animal studies, this paper discusses biological responses to ELF magnetic and/or electric field exposures. DOE

52 AEROSPACE MEDICINE

Includes physiological factors; biological effects of radiation; and effects of weightlessness on man and animals.

N94-36764# East Carolina Univ., Greenville, NC. School of Medicine.
EVALUATION OF DRIED STORAGE OF PLATELETS FOR TRANSFUSION: PHYSIOLOGIC INTEGRITY AND HEMOSTATIC FUNCTIONALITY Triannual Report No. 1, 1 Feb. - 31 May 1994
Arthur P. Bode 17 Jun. 1994 7 p
(Contract N00014-92-J-1244)
(AD-A280665) Avail: CASI HC A02/MF A01

Technical and administrative activities performed under this grant are briefly summarized. A subcontract summary is included addressing the hemostatic and thrombogenic effects of the rehydrated platelets and the characterization of the surface antigens of rehydrated platelets.
Derived from text

N94-36766*# National Aeronautics and Space Administration. Lyndon B. Johnson Space Center, Houston, TX.
METHOD AND APPARATUS FOR THE COLLECTION, STORAGE, AND REAL TIME ANALYSIS OF BLOOD AND OTHER BODILY FLUIDS Patent Application
Peggy A. Whitson, inventor (to NASA) and Vaughan L. Clift, inventor (to NASA) 19 May 1994 30 p
(NASA-Case-MSC-22463-1; NAS 1.71:MSC-22463-1; US-Patent-Appl-SN-247189) Avail: CASI HC A03/MF A01

The present invention provides a simple, portable, relatively inexpensive apparatus for accurately and efficiently collecting, separating, testing, and even storing between about 1-20 ml, preferably about 1-10 ml, of blood or other bodily fluid in situ. The apparatus includes a collection chamber bounded on its sides by an opening in a sheet of material, preferably clear plastic, abutting a filter card. The filter card is made of fibrous material, preferably less than about a millimeter thick, having an average pore size of less than about 3 microns. Preferably, the fibers are glass and the fibrous material has an average pore size of about 1 micron. The fibrous material is treated with a carbohydrate/protein mixture which contains between about 1-40 percent wt/vol carbohydrate and about 0.1-15 percent wt/vol nonspecific protein, preferably between about 10-20 percent carbohydrate and about 5-8 percent protein. A preferred carbohydrate/protein mixture comprises about 10 percent mannitol and about 6 percent albumin. The blood or other fluid moves through the filter card by capillary action aided by an absorbent matrix with a high Klemm factor which abuts the filter card. The absorbent matrix and/or filter card can be treated with a wide spectrum of test reagents. The speed, cleanliness, and efficiency of the separation process can be altered by: (a) changing the absolute concentration of the carbohydrate/protein mixture; (b) applying positive or negative pressure to one side of the filter; and/or (c) varying the relative density and pore size of the filter card and absorbent matrix. NASA

N94-37005*# Good Samaritan Hospital and Medical Center, Portland, OR. Neurological Sciences Inst. and Clinical Vestibular Lab.
RELATION OF MOTION SICKNESS SUSCEPTIBILITY TO VESTIBULAR AND BEHAVIORAL MEASURES OF ORIENTATION Annual Status Report
Robert J. Peterka Jul. 1994 29 p
(Grant NAGw-3782)
(NASA-CR-196121; NAS 1.26:196121) Avail: CASI HC A03/MF A01

The objective of this proposal is to determine the relationship of motion sickness susceptibility to vestibulo-ocular reflexes (VOR), motion perception, and behavioral utilization of sensory orientation cues for the control of postural equilibrium. The work is focused on reflexes and motion perception associated with pitch and roll movements that stimulate the vertical semicircular canals and otolith organs of the inner ear. This work is relevant to the space motion sickness problem since 0 g related sensory conflicts between vertical canal and otolith motion cues are a likely cause of space motion sickness. Results of experimentation are summarized and modifications to a two-axis rotation device are described. Abstracts of a number of papers generated during the reporting period are appended.
Derived from text

N94-37089 National Inst. of Standards and Technology, Gaithersburg, MD.
CHEMICAL AND STRUCTURAL CHARACTERIZATION OF NITROAROMATIC ADDUCTS WITH HEMOGLOBINS Final Report, 15 Jul. 1992 - 30 Sep. 1993
Walter J. Stevens 1 Feb. 1994 59 p Limited Reproducibility: More than 20% of this document may be affected by microfiche quality
(Contract MIPR-92MM2588)
(AD-A280533; USAMRDALC-01) Avail: CASI HC A04

The reactivity of dinitrobenzene (ortho-, para-, meta-DNB) with bovine he has been studied in vitro using spectroscopic and chromatographic methods. Deconvolution of time-dependent VIS/UV spectra of mixtures of hemoglobin with DNB show that DNB reacts readily with deoxyhemoglobin to form methemoglobin without the need for metabolic activation that has been inferred from previous in vivo studies. No reaction is observed with oxy- or carboxy-hemoglobin. Column and HPLC chromatographic separations of hemoglobin treated with C-14 radiolabelled DNB did not produce evidence for adduct formation. Similar analyses of hemoglobin from radiolabelled DNB- and TNB-treated rats also showed no direct evidence of strong adducts. DTIC

N94-37118 Edgerton, Germeshausen and Grier, Inc., Albuquerque, NM.
BLAST OVERPRESSURE STUDIES WITH ANIMALS AND MAN Final Report
Daniel L. Johnson 31 Oct. 1993 265 p Limited Reproducibility: More than 20% of this document may be affected by microfiche quality
(Contract DAMD17-88-C-8141; DA Proj. 3M1-62787-A-878)
(AD-A280240) Avail: CASI HC A12

The U.S. Army needs realistic safe limits for exposure to impulse noise produced by heavy weapons. Impulse noise limits, based on data from small arms, may be overly conservative. In order to define new limits for heavy weapons, this systematic 5-year study of the effects of high-intensity impulse noise on human volunteers was undertaken. The number of impulses, the peak pressure levels, and spectral distributions of energy of heavy weapon-like impulses were varied systematically. Five major groups of 273 volunteers were given a series of exposures to one of three impulse types and to three types of hearing protection. The impulse spectrum was varied by changing the distance between the volunteer

and an explosive detonation. The peak pressure level was varied in 3-dB steps by changing the weight of the explosive charge. The number of impulses per day was 6, 12, 25, 50, or 100. Volunteers wore hearing protection for all exposures. After each exposure, the amount of TTS, if any, was determined. Each volunteer started with an exposure of six impulses at the lowest intensity. If the TTS was less than 15 dB, the subject received six impulses at the next higher level the next day. DTIC

N94-37124 Krug Life Sciences, Inc., San Antonio, TX.
HYPOBARIC DECOMPRESSION SICKNESS MODEL DEVELOPMENT. PART 1: DIFFUSION OF INERT GAS FROM A VISCOELASTIC FLUID (BLOOD) INTO AN EXPANDING GAS PHASE Interim Report, 16 Mar. 1993 - 31 Jan. 1994
Lambros J. Petropoulos Apr. 1994 15 p Limited Reproducibility: More than 20% of this document may be affected by microfiche quality
(Contract F33615-92-C-0018)
(AD-A280298; AL/CF-TR-1994-0029-Pt-1) Avail: Issuing Activity (Defense Technical Information Center (DTIC))

Bubble growth within a volume of isothermal viscoelastic liquid containing uniformly distributed dissolved gas is considered. A nonlinear viscoelastic constitutive equation is used as a blood model. The problem of characterizing this growth-by-mass-transfer is being treated extensively, in order to better understand both the behavior of bubble growth due to supersaturation and its effects on altitude decompression sickness. DTIC

N94-37136 Army Research Inst. of Environmental Medicine, Natick, MA.
HOMEOSTATIC RESPONSES TO PROLONGED COLD EXPOSURE: HUMAN COLD ACCLIMATIZATION
Andrew J. Young May 1994 79 p Limited Reproducibility: More than 20% of this document may be affected by microfiche quality
(AD-A280234; USARIEM-TR-T94-11) Avail: CASI HC A05

This report reviews human physiological adjustments induced by chronic exposure to cold stress. Three broad types of adjustments are identified. The most commonly observed adjustment exhibited by humans chronically exposed to cold is a hypothermic habituation. Blunted shivering and vasoconstrictor responses to cold characterize this adjustment which enables maintenance of warmer skin during cold exposure. Metabolic acclimatization/acclimation has been observed in which shivering response to cold becomes exaggerated. Insulative acclimatization/acclimation has also been observed in which persons chronically exposed to cold vasoconstrict cutaneous vasculature more readily. The factors determining which pattern of adjustment occurs remain unidentified, although a theoretical explanation is presented which is based on the intensity of the cold stress experienced. DTIC

N94-37140# Texas A&M Univ., College Station, TX. Dept. of Biology.
MELATONIN, THE PINEAL GLAND, AND CIRCADIAN RHYTHMS Annual Report, 1 Mar. 1993 - 28 Feb. 1994
Vincent M. Cassone 28 Feb. 1994 6 p
(Grant AF-AFOSR-0244-90)
(AD-A280467; AFOSR-94-0358TR) Avail: CASI HC A02/MF A01

Pineal melatonin may effect the light sensitivity of rats such that, pineal ectomized rats perceive ambient intensity to be higher than sham-operated controls. We have tested this several ways. Essentially, we can find no evidence that pinealectomized rats are more sensitive to light than are pinealectomized rats. We have found that free-running circadian period lengthens in response to increasing light intensities at the same rate, but that pinealectomized rats become disrupted at lower intensities than do sham-operated animals. Further, our initial observation that enucleation of rats abolishes SCN iodomelatonin binding has proven incorrect when we corrected for circadian phase. Pineal melatonin influences circadian system coupling either at the level of coupling among circadian oscillators themselves or between these oscillators and their multiple outputs. DTIC

N94-37197# Lawrence Livermore National Lab., Livermore, CA.
DETECTION OF THE ELECTROCARDIOGRAM P-WAVE USING WAVELET ANALYSIS
Kanwaldip S. Anant, Garry H. Rodrigue, and Farid U. Dowla Jan. 1994 8 p Presented at the Society of Photo-Optical Instrumentation Engineers Conference on Intelligent Information Systems, Orlando, FL, 4-8 Apr. 1994
(Contract W-7405-eng-48)
(DE94-010791; UCRL-JC-115855; CONF-940449-7) Avail: CASI HC A02/MF A01

Since wavelet analysis is an effective tool for analyzing transient signals, we studied its feature extraction and representation properties for events in electrocardiogram (EKG) data. Significant features of the EKG include the P-wave, the QRS complex, and the T-wave. For this paper the feature that we chose to focus on was the P-wave. Wavelet analysis was used as a pre-processor for a backpropagation neural network with conjugate gradient learning. The inputs to the neural network were the wavelet transforms of EKG's at a particular scale. The desired output was the location of the P-wave. The results were compared to results obtained without using the wavelet transform as a pre-processor. DOE

N94-37224 Texas Univ., Houston, TX. Dept. of Anesthesiology.
CARDIAC PRESSURE CHANGES WITH VENOUS GAS EMBOLISM AND DECOMPRESSION Final Report, Nov. 1991 - Sep. 1993
Bruce D. Butler and George B. Kemper Apr. 1994 30 p Limited Reproducibility: More than 20% of this document may be affected by microfiche quality
(Contracts F33615-90-D-0606; F33615-90-D-0014)
(AD-A280412; AL/AO-TR-1993-0176) Avail: Issuing Activity (Defense Technical Information Center (DTIC))

Venous air embolism is reported with decompression to a decreased ambient pressure. With severe decompressions or in cases where an intracardiac septal defect (patent foramen ovale) exists, the venous bubbles can become arterialized and cause neurological decompression illness. Incidence rates of patent foramen ovale in the general population range from 25-34% and yet aviators, astronauts, and undersea divers who have decompression-induced venous bubbles do not demonstrate neurological symptoms at these high rates. This apparent disparity may be attributable to the normal pressure gradient across the atria of the heart that must be reversed for there to the be flow patency. We evaluated the effects of (1) venous air embolism (0.025, 0.05 and 0.15 ml*kg -1*min-1 for 180 min, (2) hyperbaric decompression, and (3) hypobaric decompression on the pressure gradient across the left and right atria. Left ventricular end-diastolic pressure was used as a measure of left atrial pressure. In a total of 92 experimental evaluations, there were no reported reversals in the mean pressure gradient across the atria, and a total of 3 transient reversals in the peak gradient pressures. This disparity may be due to insuffcent amounts of venous gas to cause a pressure and hence flow reversal across the atria. DTIC

N94-37282*# National Aeronautics and Space Administration. Langley Research Center, Hampton, VA.
ESTIMATES OF CELLULAR MUTAGENESIS FROM COSMIC RAYS
Francis A. Cucinotta and John W. Wilson Jul. 1994 13 p
(RTOP 199-45-16-11)
(NASA-TP-3453; L-17377; NAS 1.60:3453) Avail: CASI HC A03/MF A01

A parametric track structure model is used to estimate the cross section as a function of particle velocity and charge for mutations at the hypoxanthine guanine phosphoribosyl transferase (HGPRT) locus in human fibroblast cell cultures. Experiments that report the fraction of mutations per surviving cell for human lung and skin fibroblast cells indicate small differences in the mutation cross section for these two cell lines when differences in inactivation rates between these cell lines are considered. Using models of cosmic ray transport, the mutation rate at the HGPRT locus is estimated for cell cultures in space flight and rates of about 2 to 10 x 10(exp -6) per year are found for typical spacecraft shielding. A discussion of how model assumptions may alter the predictions is also presented.
Author (revised)

N94-37353 IIT Research Inst., Chicago, IL.
ELF COMMUNICATIONS SYSTEM ECOLOGICAL MONITORING PROGRAM: ELECTROMAGNETIC FIELD MEASUREMENTS AND ENGINEERING SUPPORT Final Report
D. P. Haradam, J. R. Gauger, and J. E. Zapotosky Apr. 1994 375 p Limited Reproducibility: More than 20% of this document may be affected by microfiche quality
(Contract N00039-93-C-0001)
(AD-A280489) Avail: Issuing Activity (Defense Technical Information Center (DTIC))

The ELF Communications System enables the U.S. Navy to communicate with submarines worldwide at operational depth and speed. The system consists of transmitting facilities in Wisconsin and Michigan that synchronously broadcast messages. Transmitters became fully operational in Wisconsin in 1985 and in Michigan in 1989. In situ studies to monitor for possible bioelectromagnetic effects from operation of both transmitters were initiated in 1982. The studies use a split-plot or blocked strategy to examine differences in space (treatment/control sites) or time (preoperational/operational). Physiological, developmental, behavioral, and ecological variables for dominant biota in upland, wetland, and riverine habitats near the ELF system have been examined in these studies. In Wisconsin, data collection for all studies was completed by the end of 1989; in Michigan, data collection continued through 1993. In support of this research, IIT Research Institute has annually documented the ambient ELF electromagnetic (EM) environment, including EM fields produced by both the ELF system and electric power distribution (60 Hz). This report documents ELF EM field intensities at all study sites active in 1993, and is comprehensive for the period 1983-1993. Other engineering activities performed during 1993 in support of the ecological studies are also described. DTIC

N94-37444# Brookhaven National Lab., Upton, NY.
ARTERIAL CROSS-SECTION MEASUREMENTS FROM DUAL ENERGY TRANSVENOUS CORONARY ANGIOGRAPHY IMAGES
D. Chapman and C. Schulze 1994 5 p Presented at the 1993 IEEE Nuclear Science Symposium and Medical Imaging Conference, San Francisco, CA, 2-5 Nov. 1993
(Contract DE-AC02-76CH-00016)
(DE94-011193; BNL-60385; CONF-931107-37) Avail: CASI HC A01/MF A01

The synchrotron based coronary angiography project at the National Synchrotron Light Source obtains images of coronary arteries using the digital subtraction technique after a distal venous injection of an iodine contrast agent. It allows two areal mass densities to be calculated from these images; one of the iodine and one of the water. Analysis procedures have been developed to arrive at these areal mass densities with corrections to the values being made for detector cross-talk and beam harmonics. From the iodine mass density distribution the relative arterial cross-section area is determined by a line integration across the arterial feature. Results will be given for an iodine tube phantom showing that the relative area of a feature whose lateral dimensions are smaller than the detector pixel resolution can be determined to a few percent. Also, results will be shown from a human image, showing the relative area of the right coronary artery mapped through a region of a previous stenosis subsequently treated by balloon angioplasty. Finally, limitation of the technique and plans to validate and improve the analysis will be discussed. DOE

N94-37445* National Aeronautics and Space Administration, Washington, DC.
AEROSPACE MEDICINE AND BIOLOGY: A CONTINUING BIBLIOGRAPHY WITH INDEXES (SUPPLEMENT 392)
Sep. 1994 45 p
(NASA-SP-7011(392); NAS 1.21:7011(392)) Avail: CASI HC A03

This bibliography lists 81 reports, articles and other documents introduced into the NASA Scientific and Technical Information System during Sep. 1994. Subject coverage includes: aerospace medicine and physiology, life support systems and man/system technology, protective clothing, exobiology and extraterrestrial life, planetary biology, and flight crew behavior and performance. Author

N94-37729# Joint Inst. for Nuclear Research, Dubna (USSR). Lab. of High Energy.
COMPARISON OF GASEOUS AND SEMICONDUCTOR DETECTORS FOR MEDICAL IMAGING
Yu. V. Zanevskij 1993 10 p
(DE94-621344; JINR-E-13-93-204) Avail: CASI HC A02/MF A01 (US Sales Only)

The basic types of gaseous and semiconductor detectors for medical imaging are considered. The goal of the present short review consists in comparing main parameters of these detectors and indicating novel development trends in this research area. DOE

N94-37263*# National Aeronautics and Space Administration. Lyndon B. Johnson Space Center, Houston, TX.
PROFILE ANALYSIS OF AFTER-EFFECTS EXPERIENCED DURING EXPOSURE TO SEVERAL VIRTUAL REALITY ENVIRONMENTS
Robert S. Kennedy (Essex Corp., Orlando, FL.), Marshall B. Jones (Hershey, Milton S. Medical Center, Hershey, PA.), Michael G. Lilienthal (Defense Logistics Agency, Alexandria, VA.), and Deborah L. Harm *In* AGARD, Virtual Interfaces: Research and Applications May 1994 9 p (For primary document see N94-37261 12-53)
Copyright Avail: CASI HC A02/MF A02

N94-37276# Naval Aerospace Medical Research Lab., Pensacola, FL. Acceleration Div.
ATTENUATING THE DISORIENTING EFFECTS OF HEAD MOVEMENT DURING WHOLE-BODY ROTATION USING A VISUAL REFERENCE: FURTHER TESTS OF A PREDICTIVE HYPOTHESIS
B. D. Lawson, F. E. Guedry, A. R. Rupert, and A. M. Anderson *In* AGARD, Virtual Interfaces: Research and Applications May 1994 14 p (For primary document see N94-37261 12-53)
(Contract N00014-90-J-1549)
Copyright Avail: CASI HC A03/MF A02

N94-37277# Army Personnel Research Establishment, Farnborough (England). Special Psychology Research Group.
SOME SIDE-EFFECTS OF IMMERSION VIRTUAL REALITY
E. C. Regan *In* AGARD, Virtual Interfaces: Research and Applications May 1994 8 p (For primary document see N94-37261 12-53)
Copyright Avail: CASI HC A02/MF A02

53 BEHAVIORAL SCIENCES

Includes psychological factors; individual and group behavior; crew training and evaluation; and psychiatric research.

N94-37233# Louisiana State Univ., Shreveport, LA.
CEREBRAL NEUROCHEMICAL MECHANISMS IN STRESS AND ANXIETY Annual Technical Report, 1 Feb. 1993 - 31 Jan. 1994
Adrian J. Dunn and Artur H. Swiergiel 28 Feb. 1994 44 p
(Contract F49620-93-1-0125)
(AD-A280473; AFOSR-94-0366TR) Avail: CASI HC A03/MF A01

Investigations are concerned with the cerebral mechanisms involved in stress. Current experiments focused on the locus coeruleus noradrenergic (LC-NE) system. In vivo microdialysis studies showed that both hemodynamic stress induced by nitroprusside, and electric footshock increased the apparent release of norepinephrine (NE) in the hypothalamus and prefrontal cortex. The potential role of corticotropin-releasing factor (CRF) in the activation of the LC-NE system was investigated. CRF infused into the LC, but not in surroyncring brain structures (such as the par nucleus), increased the apparent synaptic release of cortical NE. This effect was largely unilateral and involved CRF-receptors. We have performed preliminary studies using the new technique of In vivo voltammetry. These studies have confirmed the increased appearance of extracellular NE following nitroprusside infusion. The superior time resolution of this technique indicated that the NE response nitroprusside was short-lived. The classic benzodiazepine anxiolytic, chlorcgazepoxide (CDP), appeared to diminish the NE response to footshock and may also affect basal NE release. Behavioral studies indicated that activation of NE system with idazoxan almost completely inhibited stress-induced ultrasonic vocalization, with relatively small changes in stress-induced freezing. We failed to find any consistent effects of 6-hydroxydopamine-induced lesions of the dorsal noradrenergic bundle, although vocalization was slightly potentiated. DTIC

N94-37261# Advisory Group for Aerospace Research and Development, Neuilly-Sur-Seine (France). Aerospace Medical Panel.
VIRTUAL INTERFACES: RESEARCH AND APPLICATIONS [LES INTERFACES VIRTUELLES ENTRE RECHERCHE ET APPLICATIONS]
May 1994 186 p In ENGLISH and FRENCH Symposium held in Lisbon, Portugal, 18-22 Oct. 1993
(AGARD-CP-541; ISBN-92-835-0746-0) Copyright Avail: CASI HC A09/MF A02

Recent advances in technologies for information display and sensing of

human movements, combined with computer based models of natural and artificial environments, have led to the introduction of so-called virtual interfaces. Virtual interfaces offer increased flexibility and naturalness, so are considered for use in several domains including aviation, training, design, and simulation. Papers presented at this symposium considered issues of research and application in virtual interfaces broadly defined. Issues of technology integration for system development were considered separately from issues of movement monitoring or sensory display. Issues of human performance measurement were presented in the context of both research and application. For individual titles, see N94-37262 through N94-37281.

N94-37262# Syracuse Univ., NY. Center for Science and Technology.
TASK-SPECIFIC USABILITY REQUIREMENTS FOR VIRTUAL INFORMATION ENVIRONMENTS: INTERFACE DESIGN AND DATA REPRESENTATION FOR HUMAN OPERATORS OF COMPLEX MEDICAL SYSTEMS **c54**
Michael S. Nilan *In* AGARD, Virtual Interfaces: Research and Applications May 1994 8 p Sponsored in part by New York State Center for Advanced Technology in Computer Applications and Software Engineering; Alex Nason Foundation of New York City; and AFOSR (For primary document see N94-37261 12-53)
Copyright Avail: CASI HC A02/MF A02

The National Research Council has identified 'usability' as one of two major requirements for coherent development of computer and information systems over the next ten years. The use of multisensory virtual environment technology to display and provide access to system functions and data relevant to large-scale, complex, potentially volatile medical tasks (e.g., telepresence surgery) increases the (already critical) need for unobtrusive, transparent interface designs, and data representations. Unfortunately, the medical community must take responsibility for providing requirements specifications to the computer industry or else be forced to adapt to existing technical constraints. Recent research in interface design and data organization/representation for two dimensional computer applications indicates that dynamic representations of the specific task or problem that the human operator is performing is very effective. Employing a task-specific, 'user-based' methodology, steps in the task resolution are organized into a dynamic model of the task. Linked to this model are the functional system requirements and information/data need requirements divided into specific content requirements, display requirements (including spatial organization) and system help requirements. The resultant model is readily interpretable by system designers and in addition, provides them with specific task-related system evaluation criteria. Usability advantages of dynamic task representations include: minimal system/application training requirements for operators; and coherent, comprehensible, and uncluttered sensory field organization of system functions, relevant data, and help information. Because of its ability to provide specific task-related requirements to system designers, this methodological approach will insure maximum usability of high performance computing (including virtual reality technology) for critical medical applications. Author

N94-37263*# National Aeronautics and Space Administration. Lyndon B. Johnson Space Center, Houston, TX.
PROFILE ANALYSIS OF AFTER-EFFECTS EXPERIENCED DURING EXPOSURE TO SEVERAL VIRTUAL REALITY ENVIRONMENTS **c52**
Robert S. Kennedy (Essex Corp., Orlando, FL.), Marshall B. Jones (Hershey, Milton S. Medical Center, Hershey, PA.), Michael G. Lilienthal (Defense Logistics Agency, Alexandria, VA.), and Deborah L. Harm *In* AGARD, Virtual Interfaces: Research and Applications May 1994 9 p (For primary document see N94-37261 12-53)
Copyright Avail: CASI HC A02/MF A02

Motion sickness symptoms are an unwanted by-product of exposure to virtual environments. This problem is not new and was reported in the early flight simulators and experiments on ego motions and vection. The cardinal symptom of motion sickness is, of course, vomiting, but this symptom is ordinarily preceded by a variety of other symptoms. In his classic studies of motion sickness conducted before and during World War II, G. R. Wendt introduced a three point scale to score motion sickness beyond a vomit/no vomit dichotomy. Later, Navy scientists developed a Motion Sickness Questionnaire (MSQ), originally for use in a slowly rotating room. In the last 20 years the MSQ has been used in a series of studies of air, sea, and space sickness. Only recently, however, has it been appreciated that symptom patterns in the MSQ are not uniform but vary with the way sickness is induced. In seasickness, for example, nausea is the most prominent symptom. In Navy simulators, however, the most common symptom is eye strain, especially when cathode ray tubes are employed in the simulation. The latter result was obtained in a survey of over 1,500 pilot exposures. Using this database, Essex scientists conducted a factor analysis of the MSQ. We found that signs and symptoms of motion sickness fell mainly into three clusters: 1) oculomotor disturbance, 2) nausea and related neurovegetative problems, and 3) disorientation, ataxia, and vertigo. We have since rescored the MSQ results obtained in Navy simulators in terms of these three components. We have also compared these and other profiles obtained from three different vitual reality systems to profiles obtained in sea sickness, space sickness, and alcohol intoxication. We will show examples of these various profiles and point out simularities and differences among them which indicate aspects of what might be called 'virtual-reality sickness'. Author

N94-37264# Physics and Electronics Lab. TNO, The Hague (Netherlands). High Performance Computing.
ON THE FEASIBILITY OF VIRTUAL ENVIRONMENTS IN MEDICINE **c54**
A. C. M. Dumay and G. J. Jense *In* AGARD, Virtual Interfaces: Research and Applications May 1994 8 p (For primary document see N94-37261 12-53)
Copyright Avail: CASI HC A02/MF A02

Virtual Environments (VE) allow a human to interact with a (computer) system in such a way that a high level of presence in a computer-synthesized world is experienced. In principle, all human senses are involved with the interaction. Many applications may benefit from this type of human-machine interfacing, however, little have emerged so far for medicine. In this paper, we elaborate on some realistic potential applications of virtual environment technology in the field of medicine. These applications can be found in education/training, therapy, surgery, rehabilitation, diagnosis, telemedicine, and biomechanics. The value to be added to these applications by VE technology lies in the fact that patient data or patient models may be moderated to the physician in a more intuitive and natural manner. Despite these potentials, the short-term feasibility of these applications can be put into question for various reasons. Firstly, the current generation of display devices have a resolution that may show to be too low to achieve a sufficiently high degree of realism for medical applications. Secondly, there are no commercially-available actuators for tactile and force feedback which the physician desperately need for the simulation of the contact with the (virtual) patient. Thirdly, the enormous computing power required for these applications needs (yet) a considerable investment. With these limitations in mind, we believe that we are at the cradle of a whole new generation of VE applications in medicine. Author

N94-37265# Centre d'Etudes de la Navigation Aerienne, Toulouse (France).
ASSISTANCE IN INSTRUCTION AND TRAINING OF AIR TRAFFIC CONTROLLERS [AIDE A LA FORMATION ET L'ENTRAINEMENT DES CONTROLEURS DE TRAFIC AERIEN]
F. Marque, T. Labarrere, and F. Neel *In* AGARD, Virtual Interfaces: Research and Applications May 1994 9 p In FRENCH (For primary document see N94-37261 12-53)
Copyright Avail: CASI HC A02/MF A02

Under the control of the Center d'Etudes de la Navigation Aerienne (CENA: Air Navigation Study Center), the 'SPEECH' project utilizes the complementary input of industries (STERIA ENGINEERING AND TELECOM, SEXTANT AVIONIQUE and VECSYS) and of a research center (LIMSI) in the study and creation of a tool that would assist in the instruction and training of air traffic controllers. Based on the concomitant use of voice interface (synthesis and identification of speech) and of a supervisory system monitoring the dialogue, the prototype is able to rely completely on the audio channel. A validation from the operators of IHM vocal concepts, makes it possible today to consider operational usage of 'SPEECH' within the training process of air traffic controllers. The structure and the various elements of 'SPEECH' are introduced before attempting to evaluate its possible future applications. Details on the methodology used, based on the study of natural language, are also included. Author

N94-37266# Sextant Avionique, Saint Medard en Jalles (France).
INTERACTIVE LARGE SCREEN: A MULTI-MODE DIALOGUE TOOL FOR FUTURE COCKPITS [LE GRAND ECRAN INTERACTIF: UN OUTIL DE DIALOGUE MULTIMODAL POUR LES FUTURES CABINES DE PILOTAGE] **c54**
B. Barbier, E. Filiatre, and I. Irigaray *In* AGARD, Virtual Interfaces: Research and Applications May 1994 4 p In FRENCH (For primary document see N94-37261 12-53)
Copyright Avail: CASI HC A01/MF A02

The experimental make-up described here is constituted of a large size projection screen displaying an image on which an operator acts in real time, under control of a specific dialogue software, using several control devices (speech recognizer, numeric data glove, oculometer). Various human communication channels are then simultaneously used: vision and audition for the system-to-man flow; voice, gesture, and gaze for the man-to-system flow. Various ways of using and associating these communication channels allow to elaborate a multimodal dialogue. Author

N94-37267# Groningen Rijksuniv. (Netherlands). Traffic Research Centre.
IMMERSIVE VIRTUAL ENVIRONMENTS AS TRAINER: SYSTEM DESIGN FROM A COGNITIVE STANCE **c54**
M. Wierda, P. C. vanWolffelaar, and W. vanWinsum *In* AGARD, Virtual Interfaces: Research and Applications May 1994 6 p Sponsored by Ministry of Transport and Public Works (For primary document see N94-37261 12-53)
Copyright Avail: CASI HC A02/MF A02

Many of today's training-simulators for guiding, steering, or flying a vehicle are designed to have a safe, environmentally clean, flexible and cost effective educational environment. It is claimed that the training effectiveness can be increased significantly if the starting point of the design would be shifted from the 'enabling technology' position to a cognitive approach of the task to be learned in the simulator. An outline is given of this approach, encompassing a behavioral task-analysis, a cognitive process model, and an analysis of the educational goals in terms of cognitive and perceptual skills. It is concluded that knowledge in the domains of cognitive science and artificial intelligence is hardly used while this knowledge may bring about training simulators of a significantly other quality. Author

N94-37268# Aerospace Medical Research Labs., Wright-Patterson AFB, OH.
CREATION OF A VIRTUAL WORLD TO STUDY HUMAN SPATIAL PERCEPTION DURING SUSTAINED ACCELERATION
Tamara L. Chelette, Robert L. Esken, and Eric J. Martin *In* AGARD, Virtual Interfaces: Research and Applications May 1994 9 p (For primary document see N94-37261 12-53)
Copyright Avail: CASI HC A02/MF A02

The staff of the Combined Stress Branch has completed the integration of a system to allow quantitative measurement of perceived attitude while under sustained acceleration. Equipment involved included the computer control system of the Dynamic Environment simulator (DES), a computer generated graphics system, a virtual world helmet mounted display, and a tactile device for reporting attitude perception. The use of a new perceived attitude measurement system in this experiment required not only the technical achievement of the distributed system on the DES, but also required better parameter characterization and basic psychophysical performance studies. In addition, we recorded several confounds and issues concerning the use of a helmet mounted visual system for attitude information as well as head and neck support limitations of such a system. Experimental results include basic psychophysical accuracy and precision, evidence supporting the haptic system sensitivity to a G-excess illusion (even while the vestibular system is maintained at a constant position relative to the G vector), and modeling of pooled response that supports and quantifies the vestibular component of the G-excess illusion. Author

N94-37269# Defence Research Agency, Farnborough, Hampshire (England). Flight Systems Dept.
THE DRA VIRTUAL COCKPIT RESEARCH PROGRAM **c54**
Judith Ineson *In* AGARD, Virtual Interfaces: Research and Applications May 1994 12 p Sponsored by Ministry of Defence (For primary document see N94-37261 12-53)
Copyright Avail: CASI HC A03/MF A02

The aim of this paper is to describe work in progress at the Defence Research Agency (DRA) Farnborough on the Virtual Cockpit, with particular emphasis on format design and development. The paper reviews the reasons why the concept of the Virtual Cockpit is of interest, and the ways in which it differs from the common understanding of Virtual Reality. The potential advantages and disadvantages of such a man-machine interface are discussed. The overall aims of the DRA Virtual Cockpit research program are listed, together with a more detailed discussion of the areas of concern in the presentation of visual information. The current status of the research program is described. The hardware being used for this program comprises a head-coupled binocular helmet-mounted display (HMD) system in a skeletal cockpit rig with stereoscopic, computer generated graphics, and a set of demonstration formats showing examples of the type of imagery which might be employed in a Virtual Cockpit. This is followed by a description of APHIDS (Advanced Panoramic Helmet Interface Demonstrator System) - a more capable Virtual Cockpit research rig currently being built for DRA, and of its strengths and limitations. The paper concludes with an outline of how APHIDS will be employed in the next stage of the research program. Author

N94-37270# DIVISION Ltd., Almondsbury, Bristol (England).
VIRTUAL REALITY EVOLUTION OR REVOLUTION **c54**
Charles Grimsdale *In* AGARD, Virtual Interfaces: Research and Applications May 1994 4 p (For primary document see N94-37261 12-53)
Copyright Avail: CASI HC A01/MF A02

There is a growing body of research which can now lead us to a strong rationale for Virtual Reality as the next generation of Human Computer Interface. As an interface metaphor Virtual Reality clearly has great potential, throughout industry, commerce, and leisure. But how will it gain acceptance. It is my belief that this will be a process of evolution rather than revolution. Much has been written about the limitations of underlying computer systems, and 3D peripherals but there is a fundamental need for more powerful and flexible software upon which to build this new generation interface. Author

N94-37271# Aerospace Medical Research Labs., Wright-Patterson AFB, OH. Human Engineering Div.
MANUAL TRACKING PERFORMANCE USING A VIRTUAL HAND CONTROLLER: A COMPARISON STUDY **c54**
Robert G. Eggleston, William P. Janson, and Sridhar Adapalli *In* AGARD, Virtual Interfaces: Research and Applications May 1994 7 p (For primary document see N94-37261 12-53)
Copyright Avail: CASI HC A02/MF A02

This study compares a virtual hand controller (magnetic sensor attached to a glove) with a physical displacement stick in a single-axis manual control task. Three different control/display (C/D) ratios were used with each controller. Control performance was found to vary significantly with C/D ratio. When across-device comparisons were made at identical C/D ratios, a slight but significant performance advantage was found for the displacement stick at one C/D level. When between-device comparisons were made on the basis of a performance matching technique, the results were comparable for the virtual and physical hand controllers. The issue of how to best match test conditions to achieve an unbiased comparison of control devices is addressed. Arguments are advanced in favor of using the performance based matching technique. From this perspective, the data are interpreted to support the claim that comparable manual control performance can be achieved with a virtual hand controller. Author

N94-37272# Mooij and Associates, Oegstgeest (Netherlands).
A NON-INTRUSIVE WAY TO MEASURE POINT-OF-GAZE **c54**
G Zon, D. R., H. A. Mooij, and J. Bouwens *In* AGARD, Virtual Interfaces: Research and Applications May 1994 8 p (For primary document see N94-37261 12-53)
Copyright Avail: CASI HC A02/MF A02

OBSERVER is an instrument for obtaining data about where a subject is looking on fixed user specified surfaces. Since the processing of data takes place in real time, this instrument can be used to indicate areas of interest just by looking at them. In this paper, after an introduction on the application of point-of-gaze (POG) data, the OBSERVER system is described. Attention is given to subsystems as well as to calibration. As the first application of OBSERVER, that of a measuring instrument, an 'eye-witness quality experiment' is discussed. Author

N94-37273# SR Research, Toronto (Ontario).
OPERATOR GAZE POSITION CONTROL INTERFACES: INVESTIGATION OF PSYCHOPHYSICAL AND OPERATIONAL PARAMETERS **c54**
Dave M. Stampe, Eyal M. Reingold, and Julius J. Grodski *In* AGARD, Virtual Interfaces: Research and Applications May 1994 9 p (For primary document see N94-37261 12-53)
Copyright Avail: CASI HC A02/MF A02

Real-time monitoring of an operator's gaze position on a computer display of response options may form an important element of future computer interfaces and teleoperation control systems. In one implementation, the gaze position can serve as a pointer, and a critical length of gaze serves as selection, leaving the operator's hands free for other tasks. Control tasks such as multiple option selection, or looking for targets embedded within a picture are especially suited to selection by gaze position monitoring, since the search usually terminates on the object to be selected. More complex control functions can be implemented through multilevel 'menus' of choices. In the past, gaze monitoring systems restricted operator movement or required head restraints. The newest generation of gaze tracking systems allow free head movement and accurate gaze position monitoring over extended periods and are highly suited for control applications. Although gaze position control systems have been tried with moderate success in the past, little systematic investigation of the human parameters of gaze position control has been performed. In the present research program, important parameters of gaze selection such as fixation position accuracy, selection error rates, and the effects of real-time gaze position feedback were investigated. Experimental results will be used to suggest guidelines for creation and use of gaze position response in control interfaces. Author

N94-37274# Centre d'Essais en Vol, Bretigny-sur-Orge (France). Lab. de Medecine AeroSpatiale.
GAZE ORIENTATION UNDER G(z)-LOAD. METHODOLOGICAL ASPECTS: PRELIMINARY RESULTS [ORIENTATION DU REGARD SOUS FACTEUR DE CHARGE. ASPECTS METHODOLOGIQUES: RESULTATS PRELIMINAIRES] **c54**
Patrick B. Sandor, Isabelle Hortolland, Frederic Poux, and Alain Leger *In* AGARD, Virtual Interfaces: Research and Applications May 1994 7 p In FRENCH (For primary document see N94-37261 12-53)
Copyright Avail: CASI HC A02/MF A02

Gaze in head-free condition was computed under G(sub z)-load. Eye movements were measured with an oculometer using the pupil-to-corneal reflex method. Head movements were measured with an electro-optic system. The subject's head was at the center of a hemisphere (diameter 1.80 m). The internal face of this hemisphere was forming a screen on which a laser spot was to be projected. The subject's line-of-sight was computed, i.e. the direction of the eyeball in the head frame, which is mobile relative to the space. A procedure of correction of the parallax error allowed the determination of the point-of-gaze, which is the intersection point of the LDV with the screen. After static validation, two pilot experiments were performed under low G(sub z)-load. Results showed feasibility of the method in the experimental environment, and pursuit errors were quantified. Improvements are proposed. Author

N94-37275# British Aerospace Aircraft Group, Bristol (England). Human Factors Dept.
A COMPARISON OF TWO EXAMPLES OF MAGNETIC TRACKER SYSTEMS **c54**
M. Williams *In* AGARD, Virtual Interfaces: Research and Applications May 1994 19 p (For primary document see N94-37261 12-53)
Copyright Avail: CASI HC A03/MF A02

This paper is an account of an investigation of the performance of various position measuring devices which use low frequency AC or pulsed DC magnetic fields. They are used in many applications in computer graphics, and now for virtual reality, where it is necessary to estimate the observer's direction of gaze. As part of the Sowerby Research Center's program of eye movement research one such system is being integrated with a video based eye-tracker. There seems to be no independent, published assessment covering all aspects of all the systems which are of interest to this research program. This paper aims to fill that gap: it includes information relating to the static performance of two measuring systems: the 3-Space Polhemus Tracker and the Ascension Technologies' 'Bird'. The measurements relate to repeatability, noise, cross-talk, stability, range, and linearity. The influence of metal objects close to the transducers is also investigated. In most respects the 'Bird' sensor was found to be more appropriate for this application. Author

N94-37276# Naval Aerospace Medical Research Lab., Pensacola, FL. Acceleration Div.
ATTENUATING THE DISORIENTING EFFECTS OF HEAD MOVEMENT DURING WHOLE-BODY ROTATION USING A VISUAL REFERENCE: FURTHER TESTS OF A PREDICTIVE HYPOTHESIS **c52**
B. D. Lawson, F. E. Guedry, A. R. Rupert, and A. M. Anderson *In* AGARD, Virtual Interfaces: Research and Applications May 1994 14 p (For primary document see N94-37261 12-53)
(Contract N00014-90-J-1549)
Copyright Avail: CASI HC A03/MF A02

Research has shown that when subjects are seated upright and asked to perform an earthward head movement in the dark during whole-body rotation, they find the head movement disorienting if it is preceded by prolonged rotation of constant velocity, but not if it is made during the initial acceleratory phase of rotation. The disorienting effects of a head movement after prolonged constant velocity rotation can be attenuated by providing a visual reference to the Earth before the head movement. However, humans may not respond to vestibular or optokinetic simulation the same way for different planes of motion. We tested the disorienting effects of an earthward head movement during rotation about a vertical axis to see if the attenuating effect of a visual reference would be altered. Some subjects were tested while lying on their side and some while lying on their back. Subjective reports concerning head movements in the dark were similar to previous research, suggesting that an acceleratory stimulus in the plane of rotation will attenuate disorientation, regardless of the plane of rotation tested. Likewise, the visual reference attenuated the disorientation that is usually associated with a head movement following prolonged constant velocity rotation. However, the visual reference did not appear to exert as strong an attenuating effect as it had for subjects seated upright. The implication of this finding for the design of centrifuge-based flight simulators is discussed. Author

N94-37277# Army Personnel Research Establishment, Farnborough (England). Special Psychology Research Group.
SOME SIDE-EFFECTS OF IMMERSION VIRTUAL REALITY **c52**
E. C. Regan *In* AGARD, Virtual Interfaces: Research and Applications May 1994 8 p (For primary document see N94-37261 12-53)
Copyright Avail: CASI HC A02/MF A02

Virtual reality (VR) has become increasingly well-known over the last few years. However, little is known about the side-effects of prolonged immersion in VR. The main study described in this paper set out to investigate the frequency of occurrence and severity of side-effects of using an immersion VR system. Out of 150 subjects 61 percent reported symptoms of malaise at some point during a 20 minute immersion and 10 minute post-immersion period. These ranged from symptoms such as dizziness, stomach awareness, headaches, eyestrain, and lightheadedness to severe nausea. Some research which has been conducted which attempted to identify those factors that play a causative role in the side-effects of the VR system is discussed. Finally, some areas for future research are highlighted. Author

N94-37278# Army Aeromedical Research Lab., Fort Rucker, AL.
VISUAL ACCOMMODATION TO VIRTUAL IMAGE DISPLAYS WHEN KNOWLEDGE OF OBJECT DISTANCE CONFLICTS WITH OPTICAL DISTANCE
John C. Kotulak, Stephen E. Morse, and Roger W. Wiley *In* AGARD, Virtual Interfaces: Research and Applications May 1994 4 p (For primary document see N94-37261 12-53)
Copyright Avail: CASI HC A01/MF A02

In virtual image displays, the image is typically at or near optical infinity, while the object may be at any distance. This can create a conflict between the known distance of a target and its optical distance. If accommodation is drawn to the known distance of the object rather than the optical distance of its image, considerable retinal image blur can result. To determine whether this actually occurs, we measured the accommodation of seven young adult subjects with a dynamic infrared optometer. The subjects viewed a collimated virtual image of a target monocularly through third generation night vision goggles (ANVIS). Although the target itself

was positioned randomly at either 6.0, 1.0, 0.5, or 0.33 m from the observer, its image was maintained at infinity by compensatory adjustments of the ANVIS objective lens. The observer was aware fully of the actual distance of the target. A simulated clear starlight night sky condition was used in order to degrade image quality such that the accommodative feedback loop was semi-open, an intermediate state between the closed and open loop conditions of previous experiments. The results show that for some subjects, knowledge of object distance is a more powerful cue for accommodation that the image's optical distance; however, for the majority of subjects, this is not the case. The subjects who were susceptible to the knowledge of object distance cue reported severe blur when the object was nearby. We also found that these same subjects, i.e., the susceptible ones, tend to have a more proximal dark focus than those whose accommodation is not influenced by knowledge of object distance. The linkage between dark focus and susceptibility to proximal influences has not been previously demonstrated and needs to be explored further.

Author

N94-37279# SR Research, Toronto (Ontario).

LOW COST SOFTWARE-BASED RENDERING AND STEREOSCOPIC INTERFACES FOR TELEOPERATION AND VIRTUAL REALITY **c61**

Dave M. Stampe and Julius J. Grodski *In* AGARD, Virtual Interfaces: Research and Applications May 1994 6 p (For primary document see N94-37261 12-53)

Copyright Avail: CASI HC A02/MF A02

Many interface systems require generation of 3D graphics, whether as the entire display in virtual reality systems or as an overlay on live video in teleoperation. Costs must be kept low to make such systems practical, but real-time response speed must not be sacrificed. Described here is a very low-cost rendering and VR support package for 386 and 486 PC's, which requires no added hardware to achieve real-time drawing rates (20 to 60 frames per second). It includes integral support for generation and display of stereoscopic graphics in many formats, including field-alternate displays using LCD shutter glasses, and wide-angle head mounted displays. Many common PC interface devices are supported, including mouse, joystick, 6D pointing devices, and head trackers. Inexpensive PC multimedia cards allow output to be recorded on a VCR, or overlaid onto live video, including stereoscopic TV images from teleoperated remote cameras. Full source code is available, allowing the software to be customized for any application.

Author

N94-37280# Centre d'Etudes et de Recherches de Medecine Aerospatiale, Bretigny sur Orge (France).

3D SOUND EXPERIMENTAL APPROACH: METHODOLOGY AND PRELIMINARY RESULTS [APPROCHE EXPERIMENTALE DU SON 3D: METHODOLOGIE ET RESULTATS PRELIMINAIRES] **c71**

L. Pellieux, C. Gulli, P. Leroyer, B. Pledecocq, Alain Leger, and J. P. Menu *In* AGARD, Virtual Interfaces: Research and Applications May 1994 6 p In FRENCH (For primary document see N94-37261 12-53)

Copyright Avail: CASI HC A02/MF A02

The principle of 3D sound, its domain of application and the mechanisms used by man to locate sounds are reviewed. The work in progress is described. The goal is to measure human performance in locating a simulated sound source, using a stereophonic helmet. The study is made of two parts: individual measurements on the head's acoustic dispersion characteristics (head transfer functions) on four subjects, and performance testing on finding locations, the subjects listening to sounds issued from their own transfer functions. The subject must aim toward the perceived source as previously as possible, regardless of the length of time needed to respond. The sources are not materialized and the subject is kept in a dark environment. Results show that finding the angle of location is easy for the 4 subjects. On the other hand, finding the site is very difficult for 2 of the subjects. In the case of the best subject, there is an actual 6 degree error in the aim.

Author

N94-37281*# National Aeronautics and Space Administration. Lyndon B. Johnson Space Center, Houston, TX.

THE USE OF A TACTILE INTERFACE TO CONVEY POSITION AND MOTION PERCEPTIONS **c54**

A. H. Rupert (Naval Aerospace Medical Research Lab., Pensacola, FL.), F. E. Guedry (Naval Aerospace Medical Research Lab., Pensacola, FL.), and M. F. Reschke *In* AGARD, Virtual Interfaces: Research and Applications May 1994 7 p Sponsored by Naval Medical Research and Development Command (For primary document see N94-37261 12-53)

Copyright Avail: CASI HC A02/MF A02

Under normal terrestrial conditions, perception of position and motion is determined by central nervous system integration of concordant and redundant information from multiple sensory channels (somatosensory, vestibular, visual), which collectively yield vertical perceptions. In the acceleration environment experienced by the pilots, the somatosensory and vestibular sensors frequently present false information concerning the direction of gravity. When presented with conflicting sensory information, it is normal for pilots to experience episodes of disorientation. We have developed a tactile interface that obtains vertical roll and pitch information from a gyro-stabilized attitude indicator and maps this information in a one-to-one correspondence onto the torso of the body using a matrix of vibrotactors. This enables the pilot to continuously maintain an awareness of aircraft attitude without reference to visual cues, utilizing a sensory channel that normally operates at the subconscious level. Although initially developed to improve pilot spatial awareness, this device has obvious applications to 1) simulation and training, 2) nonvisual tracking of targets, which can reduce the need for pilots to make head movements in the high-G environment of aerial combat, and 3) orientation in environments with minimal somatosensory cues (e.g., underwater) or gravitational cues (e.g., space).

Author

54 MAN/SYSTEM TECHNOLOGY AND LIFE SUPPORT

Includes human engineering; biotechnology; and space suits and protective clothing.

For related information see also *16 Space Transportation.*

N94-36838*# National Aeronautics and Space Administration. Marshall Space Flight Center, Huntsville, AL.

SELECTIVELY LOCKABLE KNEE BRACE Patent Application

Neill Myers, inventor (to NASA), Mike Shadoan, inventor (to NASA), John Forbes, inventor (to NASA), and Kevin Baker, inventor (to NASA) 25 May 1994 17 p

(NASA-Case-MFS-28991-1; NAS 1.71:MFS-28991-1;

US-Patent-Appl-SN-252032) Avail: CASI HC A03/MF A01

A knee brace for aiding in rehabilitation of damaged leg muscles includes upper and lower housings, normally pivotable, one relative to the other about the knee joint axis of a patient. The upper housing is attachable to the thigh of the patient above the knee joint, while the lower housing is secured to a stirrup which extends downwardly along the patient's leg and is attached to the patient's shoe. An actuation rod is carried within the lower housing and is coupled to a cable. The upper and lower housings carry cooperative clutch/brake elements which normally are disengaged to permit relative movement between the upper and lower housings. When the cable is extended, the clutch/brake elements engage and lock the housings together. A heel strike mechanism fastened to the stirrup and the heel of the shoe is connected to the cable to selectively extend the cable and lock the brace in substantially any position when the patient places weight on the heel.

NASA

N94-36840*# National Aeronautics and Space Administration. Marshall Space Flight Center, Huntsville, AL.

CHANNEL IN HIP IMPLANT STEM Patent Application

Francisco Canabal, III, inventor (to NASA) 20 May 1994 11 p

(NASA-Case-MFS-28987-1; NAS 1.71:MFS-28987-1;

US-Patent-Appl-SN-252615) Avail: CASI HC A03/MF A01

A hip implant prosthesis has a femoral stem cemented into a cavity reamed in the femur bone of a person undergoing the transplant, the stem having an elongated central channel extending the entire length of the stem. During the implantation process the cavity is filled with bone-cement and as the stem is inserted the space between the stem and the cavity wall of the femur is closed, preferably by an elastomeric ring, so that the surplus cement is forced to flow out through the channel. Other channels may be formed in the stem from the outer end and opening onto the cavity at the enlarged portion of the stem. By restricting the flow of surplus cement in this manner, vortices and other undesirable

flow characteristics of the surplus cement exiting the cavity are eliminated or minimized so that structural faults in the solidified cement are minimized. NASA

N94-37347 Federal Aviation Administration, Cambridge, MA. National Transportation Systems Center.

HUMAN FACTORS FOR FLIGHT DECK CERTIFICATION PERSONNEL Final Report, Jun. 1989 - Sep. 1992

Kim M. Cardosi and M. S. Huntley Jul. 1993 418 p Limited Reproducibility: More than 20% of this document may be affected by microfiche quality

(AD-A280477; DOTVNTSC-FAA-93-4; DOT/FAA/RD-93/5) Avail: Issuing Activity (Defense Technical Information Center (DTIC))

This document is a compilation of proceedings and lecture material on human performance capabilities that was presented to FAA flight deck certification personnel. A five-day series of lectures was developed to provide certification specialists with information on fundamental characteristics of the human operator that are relevant to flight deck operations. The series was designed to proceed from the presentation of basic information on human sensory capabilities, through human cognition, to the application of this knowledge to the design of controls and displays in the automated cockpit. The initial lectures were prepared and presented by published academic researchers. The later ones were presented by senior human factors practitioners employed by major American airframe manufacturers. DTIC

N94-37458*# Tulane Univ., New Orleans, LA. Dept. of Mechanical Engineering.

METHODOLOGIES TO DETERMINE FORCES ON BONES AND MUSCLES OF BODY SEGMENTS DURING EXERCISE, EMPLOYING COMPACT SENSORS SUITABLE FOR USE IN CROWDED SPACE VEHICLES Semiannual Status Report

Fernando Figueroa 20 Jul. 1994 6 p

(Grant NAG9-720)

(NASA-CR-196272; NAS 1.26:196272) Avail: CASI HC A02/MF A01

A complete description of an instrumented ergometer system, including the sensors, the data acquisition system, and the methodologies to calculate the kinematic parameters were initially developed at Tulane University. This work was continued by the PI at NASA Johnson Space Center, where a flight ergometer was instrumented and tested during a KC-135 Zero-Gravity flight. The sensors that form part of the system include EMG probes and accelerometers mounted on the subject using the ergometer, load cells to measure pedal forces, and encoders to measure position and orientation of the pedal (foot). Currently, data from the flight test is being analyzed and processed to calculate the kinematic parameters of the individual. The formulation developed during the initial months of the grant will be used for this purpose. The system's components are compact (all sensors are very small). A salient feature of the system and associated methodology to determine the kinematics is that although it uses accelerometers, position is not determined by integration. Position is determined by determining the angle of two frames of reference for which acceleration at one point is known in coordinates of both frames. Author

N94-37741# Starmark Corp., Arlington, VA.

CIVIL USE OF NIGHT VISION DEVICES: EVALUATION PILOT'S GUIDE, PART 1 Final Report

David L. Green Jul. 1994 60 p Prepared for Systems Control Technology, Inc., Arlington, VA

(SCT-91RR-43; DOT/FAA/RD-94/18) Avail: CASI HC A04/MF A01

This document was developed to aid in the evaluation of the use of night vision goggles by civil helicopter pilots. This report was used to prepare pilots to participate in the flight test program. The principal task was to determine if there are any unresolved safety issues that would preclude pilot's use of NVG's during helicopter operations under Federal Aviation Regulations Parts 91 or 135. Certainly NVG's can enable a pilot to 'see better' at night and to accomplish certain flight objectives. However, the question is whether safety is degraded during any phase of the flight operation if pilots use these devices. Even if the use of NVG's dramatically improves operational effectiveness, current safety margins must be maintained or improved during all phases of flight. Author (revised)

N94-37742# Systems Control Technology, Inc., Arlington, VA.

NIGHT VISION GOGGLES IN EMERGENCY MEDICAL SERVICE (EMS) HELICOPTERS Final Report

William T. Sampson, Gary B. Simpson, and David L. Green Jul. 1994 90 p

(Contract DTFA01-87-C-00014)

(SCT-93RR-22; DOT/FAA/RD-94/21) Avail: CASI HC A05/MF A01

This document addresses the potential use of night vision goggles (NVG's) by the emergency medical service (EMS) industry. Key issues analyzed are the night environment, physiology of the eye, characteristics of night vision devices, maintenance of the NVG, and night operations. Pilots from the government and EMS industry participated in a flight program at the FAA Technical Center to assess the capabilities and utility of NVG's in EMS scenarios. The results of the tests are incorporated in the recommendations of this document. Information produced by other government agencies, with extensive experience with NVG's, was reviewed for use in this application and incorporated into the text. This investigation concludes that NVG's are a viable tool during en route and terminal operations during certain EMS scenarios. The NVG, when properly used, can increase safety, enhance situational awareness, and reduce pilot workload and stress normally associated with night operations. Author

N94-37743# Starmark Corp., Arlington, VA.

ASSESSMENT OF NIGHT VISION GOGGLE WORKLOAD: FLIGHT TEST ENGINEER'S GUIDE Final Report

David L. Green Jul. 1994 78 p Prepared for Systems Control Technology, Inc., Arlington, VA

(SCT-91RR-45; DOT/FAA/RD-94/20) Avail: CASI HC A05/MF A01

This document was developed to aid in the evaluation of the use of night vision goggles (NVG's) by civil helicopter pilots. This report was used to prepare pilots to participate in the flight test program. The principal task was to determine if there are any unresolved safety issues that would preclude pilot use of NVG's during helicopter operations under Federal Aviation Regulations Parts 91 or 135. Certainly NVG's can enable a pilot to 'see better' at night and to accomplish certain flight objectives. However, the question is whether safety is degraded during any phase of the flight operation if pilots use these devices. Even if the use of NVG's dramatically improves operational effectiveness, current safety margins must be maintained or improved during all phases of flight. Author (revised)

N94-37812 Centre National de la Recherche Scientifique, Marseilles (France).

POSTURAL STRATEGIES FOR THE CONTINUOUS CONTROL OF STATIC AND DYNAMIC BALANCE IN MAN Final Report [LES STRATEGIES POSTURALES DE CONTROLE CONTINU DE L'EQUILIBRE STATIQUE ET DYNAMIQUE CHEZ L'HOMME]

S. Mesure 1994 54 p In FRENCH Sponsored by Direction des Recherches, Etudes et Techniques and Centre de Documentation de l'Armement

(PB94-184678) Avail: Issuing Activity (National Technical Information Service (NTIS))

The authors tested the hypothesis that athletically trained subjects adjust their posture better to control balance than novices. Men and women of both groups were tested in a sharpened Romberg position, on either hard or soft surfaces with various types of lighting, or on seesaws with and without blindfolds. Acceleration meters measured body sway at the head, hips, and ankles. Frequency power spectrum analysis for both experiments showed that experts had better postural control. Cross-correlation functions (CCF's) were applied to simultaneous acceleration meter measurements to statistically determine the coordination of movements between two anatomical levels. CCF results showed that novices employ different relative body movements during static equilibrium, as shown by lateral head-hips significant CCF peaks. Quasi-dynamic results on the seesaws also showed better postural control in experts, but were tougher to analyze in terms of CCF's. The only significant difference in blindfolded performance was that novices fell more often. Results show clearly that the practice of a sport produces better postural balance. NTIS

N94-36623# Naval Air Warfare Center, Warminster, PA. Aircraft Div.

ADVANCED HELMET TRACKING TECHNOLOGY DEVELOPMENTS FOR NAVAL AVIATION

James H. Brindle *In* AGARD, Pointing and Tracking Systems May 1994 15 p (For primary document see N94-36616 12-18)
Copyright Avail: CASI HC A03/MF A02

N94-36624# General Electric Co. Ltd., Edinburgh (Scotland). Display Systems Group.
ADVANCES IN HELMET TRACKERS
W. M. Aspin *In* AGARD, Pointing and Tracking Systems May 1994 4 p (For primary document see N94-36616 12-18)
Copyright Avail: CASI HC A01/MF A02

N94-36632# Alenia Aeronautica, Turin (Italy). System Technology Dept.
STUDIES AND SIMULATIONS ON SENSOR FUSION AND CUEING FOR FIGHTER APPLICATION
M. Avalle *In* AGARD, Pointing and Tracking Systems May 1994 8 p (For primary document see N94-36616 12-18)
Copyright Avail: CASI HC A02/MF A02

N94-37262# Syracuse Univ., NY. Center for Science and Technology.
TASK-SPECIFIC USABILITY REQUIREMENTS FOR VIRTUAL INFORMATION ENVIRONMENTS: INTERFACE DESIGN AND DATA REPRESENTATION FOR HUMAN OPERATORS OF COMPLEX MEDICAL SYSTEMS
Michael S. Nilan *In* AGARD, Virtual Interfaces: Research and Applications May 1994 8 p Sponsored in part by New York State Center for Advanced Technology in Computer Applications and Software Engineering; Alex Nason Foundation of New York City; and AFOSR (For primary document see N94-37261 12-53)
Copyright Avail: CASI HC A02/MF A02

N94-37264# Physics and Electronics Lab. TNO, The Hague (Netherlands). High Performance Computing.
ON THE FEASIBILITY OF VIRTUAL ENVIRONMENTS IN MEDICINE
A. C. M. Dumay and G. J. Jense *In* AGARD, Virtual Interfaces: Research and Applications May 1994 8 p (For primary document see N94-37261 12-53)
Copyright Avail: CASI HC A02/MF A02

N94-37266# Sextant Avionique, Saint Medard en Jalles (France).
INTERACTIVE LARGE SCREEN: A MULTI-MODE DIALOGUE TOOL FOR FUTURE COCKPITS [LE GRAND ECRAN INTERACTIF: UN OUTIL DE DIALOGUE MULTIMODAL POUR LES FUTURES CABINES DE PILOTAGE]
B. Barbier, E. Filiatre, and I. Irigaray *In* AGARD, Virtual Interfaces: Research and Applications May 1994 4 p In FRENCH (For primary document see N94-37261 12-53)
Copyright Avail: CASI HC A01/MF A02

N94-37267# Groningen Rijksuniv. (Netherlands). Traffic Research Centre.
IMMERSIVE VIRTUAL ENVIRONMENTS AS TRAINER: SYSTEM DESIGN FROM A COGNITIVE STANCE
M. Wierda, P. C. vanWolffelaar, and W. vanWinsum *In* AGARD, Virtual Interfaces: Research and Applications May 1994 6 p Sponsored by Ministry of Transport and Public Works (For primary document see N94-37261 12-53)
Copyright Avail: CASI HC A02/MF A02

N94-37269# Defence Research Agency, Farnborough, Hampshire (England). Flight Systems Dept.
THE DRA VIRTUAL COCKPIT RESEARCH PROGRAM
Judith Ineson *In* AGARD, Virtual Interfaces: Research and Applications May 1994 12 p Sponsored by Ministry of Defence (For primary document see N94-37261 12-53)
Copyright Avail: CASI HC A03/MF A02

N94-37270# DIVISION Ltd., Almondsbury, Bristol (England).
VIRTUAL REALITY EVOLUTION OR REVOLUTION
Charles Grimsdale *In* AGARD, Virtual Interfaces: Research and Applications May 1994 4 p (For primary document see N94-37261 12-53)
Copyright Avail: CASI HC A01/MF A02

N94-37271# Aerospace Medical Research Labs., Wright-Patterson AFB, OH. Human Engineering Div.
MANUAL TRACKING PERFORMANCE USING A VIRTUAL HAND CONTROLLER: A COMPARISON STUDY
Robert G. Eggleston, William P. Janson, and Sridhar Adapalli *In* AGARD, Virtual Interfaces: Research and Applications May 1994 7 p (For primary document see N94-37261 12-53)
Copyright Avail: CASI HC A02/MF A02

N94-37272# Mooij and Associates, Oegstgeest (Netherlands).
A NON-INTRUSIVE WAY TO MEASURE POINT-OF-GAZE
G Zon, D. R., H. A. Mooij, and J. Bouwens *In* AGARD, Virtual Interfaces: Research and Applications May 1994 8 p (For primary document see N94-37261 12-53)
Copyright Avail: CASI HC A02/MF A02

N94-37273# SR Research, Toronto (Ontario).
OPERATOR GAZE POSITION CONTROL INTERFACES: INVESTIGATION OF PSYCHOPHYSICAL AND OPERATIONAL PARAMETERS
Dave M. Stampe, Eyal M. Reingold, and Julius J. Grodski *In* AGARD, Virtual Interfaces: Research and Applications May 1994 9 p (For primary document see N94-37261 12-53)
Copyright Avail: CASI HC A02/MF A02

N94-37274# Centre d'Essais en Vol, Bretigny-sur-Orge (France). Lab. de Medecine AeroSpatiale.
GAZE ORIENTATION UNDER G(z)-LOAD. METHODOLOGICAL ASPECTS: PRELIMINARY RESULTS [ORIENTATION DU REGARD SOUS FACTEUR DE CHARGE. ASPECTS METHODOLOGIQUES: RESULTATS PRELIMINAIRES]
Patrick B. Sandor, Isabelle Hortolland, Frederic Poux, and Alain Leger *In* AGARD, Virtual Interfaces: Research and Applications May 1994 7 p In FRENCH (For primary document see N94-37261 12-53)
Copyright Avail: CASI HC A02/MF A02

N94-37275# British Aerospace Aircraft Group, Bristol (England). Human Factors Dept.
A COMPARISON OF TWO EXAMPLES OF MAGNETIC TRACKER SYSTEMS
M. Williams *In* AGARD, Virtual Interfaces: Research and Applications May 1994 19 p (For primary document see N94-37261 12-53)
Copyright Avail: CASI HC A03/MF A02

N94-37281*# National Aeronautics and Space Administration. Lyndon B. Johnson Space Center, Houston, TX.
THE USE OF A TACTILE INTERFACE TO CONVEY POSITION AND MOTION PERCEPTIONS
A. H. Rupert (Naval Aerospace Medical Research Lab., Pensacola, FL.), F. E. Guedry (Naval Aerospace Medical Research Lab., Pensacola, FL.), and M. F. Reschke *In* AGARD, Virtual Interfaces: Research and Applications May 1994 7 p Sponsored by Naval Medical Research and Development Command (For primary document see N94-37261 12-53)
Copyright Avail: CASI HC A02/MF A02

55 SPACE BIOLOGY

Includes exobiology; planetary biology; and extraterrestrial life.

No abstracts in this category.

59 MATHEMATICAL AND COMPUTER SCIENCES (GENERAL)

No abstracts in this category.

60 COMPUTER OPERATIONS AND HARDWARE

Includes hardware for computer graphics, firmware, and data processing.

For components see *33 Electronics and Electrical Engineering.*

N94-36731# Texas A&M Univ., College Station, TX. Dept. of Electrical Engineering.

HARDWARE IMPLEMENTATION OF A DESKTOP SUPERCOMPUTER FOR HIGH PERFORMANCE IMAGE PROCESSING Technical Report, 1 Feb. - 1 May 1994

Jose PinedadeGyvez 1 May 1994 19 p

(Contract N00014-94-1-0516)

(AD-A280550; Rept-93549/1) Avail: CASI HC A03/MF A01

An efficient behavioral simulator for Cellular Neural Networks (CNN) is hereby reported. The simulator is capable of performing Single-Layer CNN simulations for any size of input image, thus a powerful tool for researchers investigating potential applications of CNN. This report presents an efficient algorithm exploiting the latency properties of Cellular Neural Networks along with numerical integration techniques; simulation results and comparisons are also presented. A novel approach to simulate the hardware of Cellular Neural Networks (CNN) is presented as well. The approach, time-multiplexing simulation, is prompted by the need to simulate hardware models and test hardware implementations of CNN. For practical size applications, due to hardware limitations, it is impossible to have a one-on-one mapping between the CNN hardware processors and all the pixels of the image. DTIC

61 COMPUTER PROGRAMMING AND SOFTWARE

Includes computer programs, routines, alogorithms, and specific applications, e.g., CAD/CAM.

N94-36480# Sandia National Labs., Albuquerque, NM.

SOFTWARE USE CONTROL

F. G. Trussell 1994 11 p Presented at the Nuclear Weapons Complex Software Quality Assurance Forum, Livermore, CA, 18-20 Apr. 1994

(Contract DE-AC04-94AL-85000)

(DE94-008429; SAND-94-0695C; CONF-9404113-1) Avail: CASI HC A03/MF A01

The topic of this technical presentation is Use Control Software. The nuclear weapon software design community is being subjected to many surety forces that are stretching the envelope of their designs. Given that software is a critical part of the use control system design, we must work to limit the errors of the software development process. The objective of this paper is to discuss a methodology that the author, as a member of the Security and Use Control Assessment Department, is working on. This is the first introduction of the proposed methodology. Software that is a part of any use control system, subsystem, device, or component is critical to the operation of that apparatus. The software is expected to meet the criteria of modern software quality. In a use control application, meeting the normal quality standards is short of the expectations in meeting the use control obligations. The NWC community expects the use control features of a nuclear weapon to provide assurance that the weapon is protected from unauthorized nuclear detonation. The methodology that the author is proposing will provide a focused scrutiny to software that is used in the hardware of use control systems, subsystems, devices, and components. The methodology proposes further scrutiny of the structure of the software, memory, variables, storage, and control features. DOE

N94-36484*# National Aeronautics and Space Administration. Goddard Space Flight Center, Greenbelt, MD.

PROCEEDINGS OF THE EIGHTEENTH ANNUAL SOFTWARE ENGINEERING WORKSHOP

Nov. 1993 489 p Workshop held in Greenbelt, MD, 1-2 Dec. 1993 Prepared in cooperation with Maryland Univ., College Park and Computer Sciences Corp., Greenbelt, MD

(RTOP 552-00-00)

(NASA-CR-189348; SEL-93-003; NAS 1.26:189348) Avail: CASI HC A21/MF A04

The workshop provided a forum for software practitioners from around the world to exchange information on the measurement, use, and evaluation of software methods, models, and tools. This year, approximately 450 people attended the workshop, which consisted of six sessions on the following topics: the Software Engineering Laboratory, measurement, technology assessment, advanced concepts, process, and software engineering issues in NASA. Three presentations were given in each of the topic areas. The content of those presentations and the research papers detailing the work reported are included in these proceedings. The workshop concluded with a tutorial session on how to start an Experience Factory. For individual titles, see N94-36485 through N94-36502.

N94-36485*# Maryland Univ., College Park, MD. Inst. for Advanced Computer Studies.

THE MATURING OF THE QUALITY IMPROVEMENT PARADIGM IN THE SEL

Victor R. Basili *In* NASA. Goddard Space Flight Center, Proceedings of the Eighteenth Annual Software Engineering Workshop Nov. 1993 p 39-59 (For primary document see N94-36484 12-61)

Avail: CASI HC A03/MF A04

The Software Engineering Laboratory uses a paradigm for improving the software process and product, called the quality improvement paradigm. This paradigm has evolved over the past 18 years, along with our software development processes and product. Since 1976, when we first began the SEL, we have learned a great deal about improving the software process and product, making a great many mistakes along the way. Quality improvement paradigm, as it is currently defined, can be broken up into six steps: characterize the current project and its environment with respect to the appropriate models and metrics; set the quantifiable goals for successful project performance and improvement; choose the appropriate process model and supporting methods and tools for this project; execute the processes, construct the products, and collect, validate, and analyze the data to provide real-time feedback for corrective action; analyze the data to evaluate the current practices, determine problems, record findings, and make recommendations for future project improvements; and package the experience gained in the form of updated and refined models and other forms of structured knowledge gained from this and prior projects and save it in an experience base to be reused on future projects.

Derived from text

N94-36486*# National Aeronautics and Space Administration. Goddard Space Flight Center, Greenbelt, MD.

PROCESS IMPROVEMENT AS AN INVESTMENT: MEASURING ITS WORTH

Frank McGarry and Kellyann Jeletic *In its* Proceedings of the Eighteenth Annual Software Engineering Workshop Nov. 1993 p 60-80 (For primary document see N94-36484 12-61)

Avail: CASI HC A03/MF A04

This paper discusses return on investment (ROI) generated from software process improvement programs. It details the steps needed to compute ROI and compares these steps from the perspective of two process improvement approaches: the widely known Software Engineering Institute's capability maturity model and the approach employed by NASA's Software Engineering Laboratory (SEL). The paper then describes the specific investments made in the SEL over the past 18 years and discusses the improvements gained from this investment by the production organization in the SEL. Author (revised)

N94-36487*# National Aeronautics and Space Administration. Goddard Space Flight Center, Greenbelt, MD.

RECENT SEL EXPERIMENTS AND STUDIES

Rose Pajerski and Donald Smith *In its* Proceedings of the Eighteenth Annual Software Engineering Workshop Nov. 1993 p 81-94 (For primary document see N94-36484 12-61)

Avail: CASI HC A03/MF A04

The studies discussed in this paper are all examples of activities that are performed as part of the Software Engineering Laboratory's (SEL's) process improvement model. Using this model, the SEL starts by understanding the product and process, then assesses the impact of new technologies, and finally packages what was learned. The preliminary examination of maintenance effort, error, and change profiles to establish a maintenance baseline exemplifies understanding-phase activities. The ongoing testing study that is examining the effects of various testing approaches on process and product measures is an example of typical assessing efforts. Finally, the derivation of cost and schedule estimation models from locally driven factors such as reuse level, application type, and language is an example of experience packaging. In the SEL, no study is ever really completed. Studies will be repeated and iterated upon in the future as part of the ongoing software improvement process.

Derived from text

N94-36488*# New South Wales Univ., Kensington (Australia). School of Information Systems.

SPECIFICATION-BASED SOFTWARE SIZING: AN EMPIRICAL INVESTIGATION OF FUNCTION METRICS

Ross Jeffery and John Stathis *In* NASA. Goddard Space Flight Center, Proceedings of the Eighteenth Annual Software Engineering Workshop Nov. 1993 p 97-115 (For primary document see N94-36484 12-61)

Avail: CASI HC A03/MF A04

For some time the software industry has espoused the need for improved specification-based software size metrics. This paper reports on a study of nineteen recently developed systems in a variety of application domains. The systems were developed by a single software services corporation using a variety of languages. The study investigated several metric characteristics. It shows that: earlier research into inter-item correlation within the overall function count is partially supported; a priori function counts, in themself, do not explain the majority of the effort variation in software development in the organization studied; documentation quality is critical to accurate function identification; and rater error is substantial in manual function counting. The implication of these findings for organizations using function based metrics are explored. Derived from text

N94-36489*# Jet Propulsion Lab., California Inst. of Tech., Pasadena, CA.

SOFTWARE FORECASTING AS IT IS REALLY DONE: A STUDY OF JPL SOFTWARE ENGINEERS

Martha Ann Griesel, Jairus M. Hihn, Kristin J. Bruno, Thomas J. Fouser, and Robert C. Tausworthe *In* NASA. Goddard Space Flight Center, Proceedings of the Eighteenth Annual Software Engineering Workshop Nov. 1993 p 116-143 (For primary document see N94-36484 12-61)

Avail: CASI HC A03/MF A04

This paper presents a summary of the results to date of a Jet Propulsion Laboratory internally funded research task to study the costing process and parameters used by internally recognized software cost estimating experts. Protocol Analysis and Markov process modeling were used to capture software engineer's forecasting mental models. While there is significant variation between the mental models that were studied, it was nevertheless possible to identify a core set of cost forecasting activities, and it was also found that the mental models cluster around three forecasting techniques. Further partitioning of the mental models revealed clustering of activities, that is very suggestive of a forecasting lifecycle. The different forecasting methods identified were based on the use of multiple-decomposition steps or multiple forecasting steps. The multiple forecasting steps involved either forecasting software size or an additional effort forecast. Virtually no subject used risk reduction steps in combination. The results of the analysis include: the identification of a core set of well defined costing activities, a proposed software forecasting life cycle, and the identification of several basic software forecasting mental models. The paper concludes with a discussion of the implications of the results for current individual and institutional practices. Author

N94-36490*# Colorado State Univ., Fort Collins, CO. Dept. of Computer Science.

ASSESSING EFFICIENCY OF SOFTWARE PRODUCTION FOR NASA-SEL DATA

Anneliese vonMayrhauser and Armin Roeseler *In* NASA. Goddard Space Flight Center, Proceedings of the Eighteenth Annual Software Engineering Workshop Nov. 1993 p 144-158 (For primary document see N94-36484 12-61)

Avail: CASI HC A03/MF A04

This paper uses production models to identify and quantify efficient allocation of resources and key drivers of software productivity for project data in the NASA-SEL database. While analysis allows identification of efficient projects, many of the metrics that could have provided a more detailed analysis are not at a level of measurement to allow production model analysis. Production models must be used with proper parameterization to be successful. This may mean a new look at which metrics are helpful for efficiency assessment. Author

N94-36491*# National Aeronautics and Space Administration. Goddard Space Flight Center, Greenbelt, MD.

THE (MIS)USE OF SUBJECTIVE PROCESS MEASURES IN SOFTWARE ENGINEERING

Jon D. Valett and Steven E. Condon *In its* Proceedings of the Eighteenth Annual Software Engineering Workshop Nov. 1993 p 161-175 (For primary document see N94-36484 12-61)

Avail: CASI HC A03/MF A04

A variety of measures are used in software engineering research to develop an understanding of the software process and product. These measures fall into three broad categories: quantitative, characteristics, and subjective. Quantitative measures are those to which a numerical value can be assigned, for example effort or lines of code (LOC). Characteristics describe the software process or product; they might include programming language or the type of application. While such factors do not provide a quantitative measurement of a process or product, they do help characterize them. Subjective measures (as defined in this study) are those that are based on the opinion or opinions of individuals; they are somewhat unique and difficult to quantify. Capturing of subjective measure data typically involves development of some type of scale. For example, 'team experience' is one of the subjective measures that were collected and studied by the Software Engineering Laboratory (SEL). Certainly, team experience could have an impact on the software process or product; actually measuring a team's experience, however, is not a strictly mathematical exercise. Simply adding up each team member's years of experience appears inadequate. In fact, most researchers would agree that 'years' do not directly translate into 'experience.' Team experience must be defined subjectively and then a scale must be developed e.g., high experience versus low experience; or high, medium, low experience; or a different or more granular scale. Using this type of scale, a particular team's overall experience can be compared with that of other teams in the development environment. Defining, collecting, and scaling subjective measures is difficult. First, precise definitions of the measures must be established. Next, choices must be made about whose opinions will be solicited to constitute the data. Finally, care must be given to defining the right scale and level of granularity for measurement. Derived from text

N94-36492*# Litton Data Systems, Agoura Hills, CA. Software Engineering Process Group.

ANALYSIS OF A SUCCESSFUL INSPECTION PROGRAM

Ray Madachy, Linda Little, and Sylvia Fan *In* NASA. Goddard Space Flight Center, Proceedings of the Eighteenth Annual Software Engineering Workshop Nov. 1993 p 176-198 (For primary document see N94-36484 12-61)

Avail: CASI HC A03/MF A04

Litton Data Systems has institutionalized the inspection process, and achieved dramatic results in terms of defect prevention and cost savings thus far. Additionally, several findings have been gleaned from an analysis to optimize the process. Over 300 inspections have been performed over the last two years on many types of documents, and this paper describes some quantitative results to-date from the initial 'champion' project.

Author

N94-36493*# IBM Federal Systems Div., Gaithersburg, MD. Software Technology for Adaptable, Reliable Systems Project.

LESSONS LEARNED APPLYING CASE METHODS/TOOLS TO Ada SOFTWARE DEVELOPMENT PROJECTS

Maurice H. Blumberg and Richard L. Randall *In* NASA. Goddard Space Flight Center, Proceedings of the Eighteenth Annual Software Engineering Workshop Nov. 1993 p 199-250 (For primary document see N94-36484 12-61)

Avail: CASI HC A04/MF A04

This paper describes the lessons learned from introducing CASE methods/tools into organizations and applying them to actual Ada software development projects. This paper will be useful to any organization planning to introduce a software engineering environment (SEE) or evolving an existing one. It contains management level lessons learned, as well as lessons learned in using specific SEE tools/methods. The experiences presented are from Alpha Test projects established under the STARS (Software Technology for Adaptable and Reliable Systems) project. They reflect the front end efforts by those projects to understand the tools/methods, initial experiences in their introduction and use, and later experiences in the use of specific tools/methods and the introduction of new ones. Author

N94-36494*# Unisys Corp., Paoli, PA. Engineering Center.

SOFTWARE ENGINEERING WITH APPLICATION-SPECIFIC LANGUAGES

David J. Campbell, Linda Barker, Deborah Mitchell, and Robert H. Pollack *In* NASA. Goddard Space Flight Center, Proceedings of the Eighteenth Annual Software Engineering Workshop Nov. 1993 p 253-273 (For primary document see N94-36484 12-61)

Avail: CASI HC A03/MF A04

Application-Specific Languages (ASL's) are small, special-purpose languages that are targeted to solve a specific class of problems. Using ASL's on software development projects can provide considerable cost savings, reduce risk, and enhance quality and reliability. ASL's provide a platform for reuse within a project or across many projects and enable less-experienced programmers to tap into the expertise of application-area experts. ASL's have been used on several software development projects for the Space Shuttle Program. On these projects, the use of ASL's resulted in considerable cost savings over conventional development techniques. Two of these projects are described. Author

N94-36495*# Jet Propulsion Lab., California Inst. of Tech., Pasadena, CA.

APPLYING FORMAL METHODS AND OBJECT-ORIENTED ANALYSIS TO EXISTING FLIGHT SOFTWARE

Betty H. C. Cheng (Michigan State Univ., East Lansing, MI.) and Brent Auernheimer (California State Univ., Fresno, CA.) *In* NASA. Goddard Space Flight Center, Proceedings of the Eighteenth Annual Software Engineering Workshop Nov. 1993 p 274-296 (For primary document see N94-36484 12-61)

(Grant NSF CCR-92-09873)

Avail: CASI HC A03/MF A04

Correctness is paramount for safety-critical software control systems. Critical software failures in medical radiation treatment, communications, and defense are familiar to the public. The significant quantity of software malfunctions regularly reported to the software engineering community, the laws concerning liability, and a recent NRC Aeronautics and Space Engineering Board report additionally motivate the use of error-reducing and defect detection software development techniques. The benefits of formal methods in requirements driven software development ('forward engineering') is well documented. One advantage of rigorously engineering software is that formal notations are precise, verifiable, and facilitate automated processing. This paper describes the application of formal methods to reverse engineering, where formal specifications are developed for a portion of the shuttle on-orbit digital autopilot (DAP). Three objectives of the project were to: demonstrate the use of formal methods on a shuttle application, facilitate the incorporation and validation of new requirements for the system, and verify the safety-critical properties to be exhibited by the software. Author

N94-36496*# TRW, Inc., Huntsville, AL. System Development Div.

INTEGRATING END-TO-END THREADS OF CONTROL INTO OBJECT-ORIENTED ANALYSIS AND DESIGN

Janet E. McCandlish, James R. MacDonald, and Sara J. Graves *In* NASA. Goddard Space Flight Center, Proceedings of the Eighteenth Annual Software Engineering Workshop Nov. 1993 p 297-320 (For primary document see N94-36484 12-61)

Avail: CASI HC A03/MF A04

Current object-oriented analysis and design methodologies fall short in their use of mechanisms for identifying threads of control for the system being developed. The scenarios which typically describe a system are more global than looking at the individual objects and representing their behavior. Unlike conventional methodologies that use data flow and process-dependency diagrams, object-oriented methodologies do not provide a model for representing these global threads end-to-end. Tracing through threads of control is key to ensuring that a system is complete and timing constraints are addressed. The existence of multiple threads of control in a system necessitates a partitioning of the system into processes. This paper describes the application and representation of end-to-end threads of control to the object-oriented analysis and design process using object-oriented constructs. The issue of representation is viewed as a grouping problem, that is, how to group classes/objects at a higher level of abstraction so that the system may be viewed as a whole with both classes/objects and their associated dynamic behavior. Existing object-oriented development methodology techniques are extended by adding design-level constructs termed logical composite classes and process composite classes. Logical composite classes are design-level classes which group classes/objects both logically and by thread of control information. Process composite classes further refine the logical composite class groupings by using process partitioning criteria to produce optimum concurrent execution results. The goal of these design-level constructs is to ultimately provide the basis for a mechanism that can support the creation of process composite classes in an automated way. Using an automated mechanism makes it easier to partition a system into concurrently executing elements that can be run in parallel on multiple processors. Author

N94-36497*# Softech, Inc., Alexandria, VA.

FUSING MODELING TECHNIQUES TO SUPPORT DOMAIN ANALYSIS FOR REUSE OPPORTUNITIES IDENTIFICATION

Susan Main Hall and Eileen McGuire *In* NASA. Goddard Space Flight Center, Proceedings of the Eighteenth Annual Software Engineering Workshop Nov. 1993 p 323-342 (For primary document see N94-36484 12-61)

Avail: CASI HC A03/MF A04

Functional modeling techniques or object-oriented graphical representations, which are more useful to someone trying to understand the general design or high level requirements of a system? For a recent domain analysis effort, the answer was a fusion of popular modeling techniques of both types. By using both functional and object-oriented techniques, the analysts involved were able to lean on their experience in function oriented software development, while taking advantage of the descriptive power available in object oriented models. In addition, a base of familiar modeling methods permitted the group of mostly new domain analysts to learn the details of the domain analysis process while producing a quality product. This paper describes the background of this project and then provides a high level definition of domain analysis. The majority of this paper focuses on the modeling method developed and utilized during this analysis effort. Author

N94-36498*# Reliable Software Technology Corp., Reston, VA.

AN EMPIRICAL COMPARISON OF A DYNAMIC SOFTWARE TESTABILITY METRIC TO STATIC CYCLOMATIC COMPLEXITY

Jeffrey M. Voas, Keith W. Miller, and Jeffrey E. Payne *In* NASA. Goddard Space Flight Center, Proceedings of the Eighteenth Annual Software Engineering Workshop Nov. 1993 p 343-365 (For primary document see N94-36484 12-61)

(Grant NAG1-884)

Avail: CASI HC A03/MF A04

This paper compares the dynamic testability prediction technique termed 'sensitivity analysis' to the static testability technique termed cyclomatic complexity. The application that we chose in this empirical study is a

CASE generated version of a B-737 autoland system. For the B-737 system we analyzed, we isolated those functions that we predict are more prone to hide errors during system/reliability testing. We also analyzed the code with several other well-known static metrics. This paper compares and contrasts the results of sensitivity analysis to the results of the static metrics. Author

N94-36499*# Martin Marietta Corp., Denver, CO. Astronautics Group.
SOFTWARE QUALITY: PROCESS OR PEOPLE
Regina Palmer and Modenna LaBaugh *In* NASA. Goddard Space Flight Center, Proceedings of the Eighteenth Annual Software Engineering Workshop Nov. 1993 p 366-397 (For primary document see N94-36484 12-61)
Avail: CASI HC A03/MF A04

This paper will present data related to software development processes and personnel involvement from the perspective of software quality assurance. We examine eight years of data collected from six projects. Data collected varied by project but usually included defect and fault density with limited use of code metrics, schedule adherence, and budget growth information. The data are a blend of AFSCP 800-14 and suggested productivity measures in Software Metrics: A Practioner's Guide to Improved Product Development. A software quality assurance database tool, SQUID, was used to store and tabulate the data. Derived from text

N94-36500*# National Aeronautics and Space Administration. Goddard Space Flight Center, Greenbelt, MD.
PROFILE OF NASA SOFTWARE ENGINEERING: LESSONS LEARNED FROM BUILDING THE BASELINE
Dana Hall (Science Applications International Corp., Washington, DC.) and Frank McGarry *In its* Proceedings of the Eighteenth Annual Software Engineering Workshop Nov. 1993 p 401-421 (For primary document see N94-36484 12-61)
Avail: CASI HC A03/MF A04

It is critically important in any improvement activity to first understand the organization's current status, strengths, and weaknesses and, only after that understanding is achieved, examine and implement promising improvements. This fundamental rule is certainly true for an organization seeking to further its software viability and effectiveness. This paper addresses the role of the organizational process baseline in a software improvement effort and the lessons we learned assembling such an understanding for NASA overall and for the NASA Goddard Space Flight Center in particular. We discuss important, core data that must be captured and contrast that with our experience in actually finding such information. Our baselining efforts have evolved into a set of data gathering, analysis, and crosschecking techniques and information presentation formats that may prove useful to others seeking to establish similar baselines for their organization. Author (revised)

N94-36501*# National Aeronautics and Space Administration. Goddard Space Flight Center, Greenbelt, MD.
IMPACT OF Ada IN THE FLIGHT DYNAMICS DIVISION: EXCITEMENT AND FRUSTRATION
John Bailey (Software Metrics, Inc., Haymarket, VA.), Sharon Waligora (Computer Sciences Corp., Lanham, MD.), and Mike Stark *In its* Proceedings of the Eighteenth Annual Software Engineering Workshop Nov. 1993 p 422-448 (For primary document see N94-36484 12-61)
Avail: CASI HC A03/MF A04

In 1985, NASA Goddard's Flight Dynamics Division (FDD) began investigating how the Ada language might apply to their software development projects. Although they began cautiously using Ada on only a few pilot projects, they expected that, if the Ada pilots showed promising results, they would fully transition their entire development organization from FORTRAN to Ada within 10 years. However, nearly 9 years later, the FDD still produces 80 percent of its software in FORTRAN, despite positive results on Ada projects. This paper reports preliminary results of an ongoing study, commissioned by the FDD, to quantify the impact of Ada in the FDD, to determine why Ada has not flourished, and to recommend future directions regarding Ada. Project trends in both languages are examined as are external factors and cultural issues that affected the infusion of this technology. This paper is the first public report on the Ada assessment study, which will conclude with a comprehensive final report in mid 1994. Author (revised)

N94-36502*# Maryland Univ., College Park, MD. Inst. for Advanced Computer Studies.
SOFTWARE ENGINEERING TECHNOLOGY TRANSFER: UNDERSTANDING THE PROCESS
Marvin V. Zelkowitz *In* NASA. Goddard Space Flight Center, Proceedings of the Eighteenth Annual Software Engineering Workshop Nov. 1993 p 450-468 (For primary document see N94-36484 12-61)
(Grant NsG-5123)
Avail: CASI HC A03/MF A04

Technology transfer is of crucial concern to both government and industry today. In this report, the mechanisms developed by NASA to transfer technology are explored and the actual mechanisms used to transfer software development technologies are investigated. Time, cost, and effectiveness of software engineering technology transfer is reported. Author (revised)

N94-36518* National Aeronautics and Space Administration. Langley Research Center, Hampton, VA.
EM-ANIMATE: A COMPUTER PROGRAM FOR DISPLAYING AND ANIMATING ELECTROMAGNETIC NEAR-FIELD AND SURFACE-CURRENT SOLUTIONS: VIDEO SUPPLEMENT TO NASA TECHNICAL MEMORANDUM 4539 (Videotape)
Kam W. Hom May 1994 See also X94-10367 Videotape: 6 min., color, sound, VHS
(RTOP 505-59-70-03)
(NASA-TM-4539-Video-Suppl; L-00993-168; NONP-NASA-VT-94-12970)
Avail: CASI VHS A01/BETA A22

In this video, several examples of electromagnetic field and surface-current animation sequences are shown to demonstrate the visualization capabilities of the EM-ANIMATE computer program. These examples show the animation of total and scattered electric near fields from test bodies of a flat plate, a corner reflector, and a sphere. These test cases show the electric-field behavior caused by different scattering mechanisms through the animation of electromagnetic data from the EM-ANIMATE routine. Author (revised)

N94-36546 Oxford Univ. (England). Programming Research Group.
DESIGN, IMPLEMENTAION AND EVALUATION OF A DECLARATIVE OBJECT-ORIENTED PROGRAMMING LANGUAGE
A. J. SocorroRamos Nov. 1993 228 p
(PB94-169208; PRG-113) Copyright Avail: Issuing Activity (National Technical Information Service (NTIS))

The thesis is a detailed study of FOOPS, a 'wide spectrum' object-oriented programming language. FOOPS supports all of the classical features of the object paradigm, including classes, overloading, polymorphism, and multiple class inheritance with overriding and dynamic binding. However, it goes beyond other object-oriented languages in its facilities for the specification, composition and reuse of modules. FOOPS is patterned after OBJ, a functional programming language, and from which it derives several of these facilities. The thesis considers the design of FOOPS, explaining all its features and examining their application to the design and development of object-oriented systems. Also, it describes a prototype implementation of FOOPS that was built using facilities given by the implementation of OBJ3, and which supports most features. Moreover, the thesis performs an in-depth evaluation of FOOPS that focuses on large-grain issues such as the distinction between classes and modules, module instantiation with views, vertical and horizontal structuring, and integrated support for specification and prototyping; comparisons with many other languages are given. Additionally, this thesis presents a detailed summary of current work towards a mathematical semantics for FOOPS. NTIS

N94-36698# IIT Research Inst., Bartlesville, OK.
NIPER Lab WARDEN: DESCRIPTION AND LabVIEW EXECUTABLE CODE OF A GENERAL-PURPOSE LABORATORY-AUTOMATION PROGRAM
S. M. Mahmood and D. K. Olsen Apr. 1994 121 p
(Contract DE-FC22-83FE-60149)
(DE94-000125; NIPER-689-Vol-1) Avail: CASI HC A06/MF A02

This report is Volume 1 (the description) of a two volume series that describes a general purpose, automation computer program developed by NIPER for data acquisition/control/analysis/presentation. This software was developed to provide interactive computer control of a variety of instruments

typically found in laboratories and pilot plants in order to improve efficiency in operation and safe handling of potentially hazardous operations. For example, it is easily adaptable for operating a laboratory that conducts experiments at extreme conditions of pressure and temperature, such as those found in a steamflooding laboratory. The software was developed in an object-oriented graphical language around National Instruments' LabVIEW which is the future trend in automation programming. DOE

N94-36699# IIT Research Inst., Bartlesville, OK.
NIPER Lab WARDEN: DESCRIPTIVE PANELS AND DIAGRAMS FOR NIPER Lab WARDEN SOFTWARE, VOLUME 2
S. M. Mahmood and D. K. Olsen Apr. 1994 236 p
(Contract DE-FC22-83FE-60149)
(DE94-000126; NIPER-689-Vol-2) Avail: CASI HC A11/MF A03

This report is the second volume of a two-volume series on the NIPER Lab WARDEN computer program, a modular laboratory or pilot plant automation software designed for data acquisition, control, analysis, and presentation. Volume 1 of the series is the User Manual that serves all users, whereas this volume is the Reference Manual intended for advanced users examining the structure or modifying the program. Volume 1 contains a brief introduction of LabVIEW and object-oriented programming, various features of the NIPER Lab WARDEN program, instructions on how to use these features, and several example problems and their step-by-step solutions. This volume (Volume 2) contains the complete program code needed to reproduce or modify the program. It includes the position in hierarchy, the connector pane, the front panel, and the block diagram for each of the virtual instruments (VI) in NIPER Lab WARDEN. The panels and block diagrams contained herein are generated from the computer program described in Volume 1 but are arranged to show and explain the structure and interrelationship between various elements of the program. DOE

N94-36818*# National Aeronautics and Space Administration. Langley Research Center, Hampton, VA.
EIGENSYSTEM REALIZATION ALGORITHM USER'S GUIDE FORVAX/VMS COMPUTERS: VERSION 931216
Richard S. Pappa May 1994 591 p
(RTOP 233-01-01-12)
(NASA-TM-109066; NAS 1.15:109066) Avail: CASI HC A25/MF A06

The eigensystem realization algorithm (ERA) is a multiple-input, multiple-output, time domain technique for structural modal identification and minimum-order system realization. Modal identification is the process of calculating structural eigenvalues and eigenvectors (natural vibration frequencies, damping, mode shapes, and modal masses) from experimental data. System realization is the process of constructing state-space dynamic models for modern control design. This user's guide documents VAX/VMS-based FORTRAN software developed by the author since 1984 in conjunction with many applications. It consists of a main ERA program and 66 pre- and post-processors. The software provides complete modal identification capabilities and most system realization capabilities. Author (revised)

N94-36914*# Computational Mechanics Co., Knoxville, TN.
AN ARBITRARY GRID CFD ALGORITHM FOR CONFIGURATION AERODYNAMICS ANALYSIS. VOLUME 1: THEORY AND VALIDATIONS Final Report
A. J. Baker, G. S. Iannelli, Paul D. Manhardt, and J. A. Orzechowski Dec. 1993 179 p
(Contract NAS2-12568; SBIR-02.07-5494)
(NASA-CR-195918; NAS 1.26:195918; CMC-TR2.1-94-Vol-1) Avail: CASI HC A09/MF A02

This report documents the user input and output data requirements for the FEMNAS finite element Navier-Stokes code for real-gas simulations of external aerodynamics flowfields. This code was developed for the configuration aerodynamics branch of NASA ARC, under SBIR Phase 2 contract NAS2-124568 by Computational Mechanics Corporation (COMCO). This report is in two volumes. Volume 1 contains the theory for the derived finite element algorithm and describes the test cases used to validate the computer program described in the Volume 2 user guide. Author (revised)

N94-36920*# Overset Methods, Inc., Vacaville, CA.
ON AUTOMATING DOMAIN CONNECTIVITY FOR OVERSET GRIDS
Ing-Tsau Chiu 30 Jun. 1994 12 p
(Grant NAG2-783)
(NASA-CR-196113; NAS 1.26:196113; OMI-04-92-2) Avail: CASI HC A03/MF A01

An alternative method for domain connectivity among systems of overset grids is presented. Reference uniform Cartesian systems of points are used to achieve highly efficient domain connectivity, and form the basis for a future fully automated system. The Cartesian systems are used to approximated body surfaces and to map the computational space of component grids. By exploiting the characteristics of Cartesian Systems, Chimera type hole-cutting and identification of donor elements for intergrid boundary points can be carried out very efficiently. The method is tested for a range of geometrically complex multiple-body overset grid systems. Author (revised)

N94-36922*# Computational Mechanics Co., Knoxville, TN.
AN ARBITRARY GRID CFD ALGORITHM FOR CONFIGURATION AERODYNAMICS ANALYSIS. VOLUME 2: FEMNAS USER GUIDE Final Report
Paul D. Manhardt, J. A. Orzechowski, and A. J. Baker Sep. 1992 63 p
(Contract NAS2-12568; SBIR-02.07-5494)
(NASA-CR-196135; NAS 1.26:196135; CMC-TR4.2-92-Vol-2) Avail: CASI HC A04/MF A01

This report documents the user input and output data requirements for the FEMNAS finite element Navier-Stokes code for real-gas simulations of external aerodynamics flowfields. This code was developed for the configuration aerodynamics branch of NASA ARC, under SBIR Phase 2 contract NAS2-124568 by Computational Mechanics Corporation (COMCO). This report is in two volumes. Volume 1 contains the theory for the derived finite element algorithm and describes the test cases used to validate the computer program described in the Volume 2 user guide. Author (revised)

N94-36974 Carnegie-Mellon Univ., Pittsburgh, PA. Software Engineering Inst.
A SURVEY OF COMMONLY APPLIED METHODS FOR SOFTWARE PROCESS IMPROVEMENT Final Report
Robert D. Austin and Daniel J. Paulish Feb. 1994 137 p Limited Reproducibility: More than 20% of this document may be affected by microfiche quality
(Contract F19628-90-C-0003)
(AD-A278595; CMU/SEI-93-TR-27; ESC-TR-93-201) Avail: Issuing Activity (Defense Technical Information Center (DTIC))

This report describes a number of commonly applied methods for improving the software development process. Each software process improvement method is described by surveying existing technical literature citations. Each method description contains background information concerning how the method works. Documented experience with the method is described. Suggestions are given for implementing the method, and a list of key references is given for further information. The methods are described in the context of the SEI Capability Maturity Model, and suggestions are given to assist organizations in selecting potential improvement methods based upon their current process maturity. DTIC

N94-37040 Naval Postgraduate School, Monterey, CA.
THE IMPLEMENTATION OF ELECTRONIC DATA INTERCHANGE (EDI) WITH DEFENSE TRANSPORTATION OPERATIONS M.S. Thesis
John G. Meier, III Mar. 1994 158 p Limited Reproducibility: More than 20% of this document may be affected by microfiche quality
(AD-A280568) Avail: CASI HC A08

Organizations have traditionally relied on paper to conduct business transactions. Although proven to be an effective and convenient medium for this purpose, paper may no longer be the most efficient. Advances in computers, communication, and electronic technology have provided alternatives to this traditional way of conducting business transactions. One such concept is electronic data interchange (EDI), which allows information to be processed faster, more accurately, and at a lower cost than similar manual, paper-based processing systems. This thesis examines the application of EDI to Defense transportation operations and includes a discussion of data format standards, hardware, software, and communications requirements. The Defense transportation EDI operating concepts involve the linking of carriers, MTMC, defense shipping activities, and DoD finance centers, which allows the electronic exchange of business

data such as Government bills of lading, freight rate tenders, and carrier payment information. EDI involves more than simply automating existing business documents and processes; when properly implemented, EDI is a catalyst for streamlining inefficient, redundant, and outdated business practices. DTIC

N94-37061*# Aerojet Electrosystems Co., Azusa, CA.
EARTH OBSERVING SYSTEM (EOS)/ADVANCED MICROWAVE SOUNDING UNIT A (AMSU-A) CONFIGURATION MANAGEMENT PLAN Final Report
J. Cavanaugh May 1994 35 p
(Contract NAS5-32314; RTOP 422-00-00)
(NASA-CR-189371; NAS 1.26:189371; Rept-9803-1; CDRL-005) Avail: CASI HC A03/MF A01

This plan describes methods and procedures Aerojet will follow in the implementation of configuration control for each established baseline. The plan is written in response to the GSFC EOS CM Plan 420-02-02, dated January 1990, and also meets he requirements specified in DOD-STD-480, DOD-D 1000B, MIL-STD-483A, and MIL-STD-490B. The plan establishes the configuration management process to be used for the deliverable hardware, software, and firmware of the EOS/AMSU-A during development, design, fabrication, test, and delivery. This revision includes minor updates to reflect Aerojet's CM policies. Author

N94-37119 Carnegie-Mellon Univ., Pittsburgh, PA. Dept. of Computer Science.
ADAPTABLE BINARY PROGRAMS
Robert Wahbe, Steven Lucco, and Susan L. Graham Apr. 1994 19 p Limited Reproducibility: More than 20% of this document may be affected by microfiche quality
(Contracts MDA972-92-J-1028; DABT63-92-C-0026; N00600-93-C-2481; NSF CDA-87-22788)
(AD-A280243; CMU-CS-94-137) Avail: Issuing Activity (Defense Technical Information Center (DTIC))

To accurately and comprehensively monitor a program's behavior, many performance measurement tools must transform the program's executable representation or binary. By instrumenting binary programs to monitor program events, tools can precisely analyze compiler optimization effectiveness, memory system performance, pipeline interlocking, and other dynamic program characteristics that are fully exposed only at this level. Binary transformation has also been used to support software-enforced fault isolation, debugging, machine re-targeting and machine-dependent optimization. At present, binary transformation applications face a difficult trade-off. Previous approaches to implementing robust transformations incur significant disk space and run-time overhead. To improve efficiency, some current systems sacrifice robustness, relying on heuristic assumptions about the program and recognition of complex, compiler-dependent code generation idioms. In this paper we present adaptable binaries, a technique for implementing robust, efficient, and compiler-independent binary transformations. We evaluated a prototype implementation of adaptable binaries under the Ultrix 4.2 operating system and the MIPS processor architecture. Using the C SPEC92 benchmarks, we assessed adaptable binaries in three ways. First, we demonstrated that the information necessary to build adaptable binaries can be compactly recorded, increasing space overhead by only 9% for the SPEC92 benchmarks. Second, we measured the run-time overhead of previous approaches to implementing robust binary transformations, and showed that adaptable binaries significantly reduce this overhead. Finally, we measured the run-time transformation overhead of two user applications, pixie and MemSpy. DTIC

N94-37120 Naval Postgraduate School, Monterey, CA. Dept. of Computer Science.
EFFICIENT CONTACT DETERMINATION BETWEEN GEOMETRIC MODELS Technical Report, Jan. - Dec. 1993
Ming C. Lin and Dinesh Manocha 8 Mar. 1994 36 p Limited Reproducibility: More than 20% of this document may be affected by microfiche quality
(AD-A280244; NPS-CS-94-007) Avail: Issuing Activity (Defense Technical Information Center (DTIC))

The problem of interference detection or contact determination between two or more objects in dynamic environment is fundamental in computer graphics, robotics, and virtual environments. Most of the earlier work is restricted to either polyhedral models or static environments. In this paper, we present efficient algorithms for contact determination and interference detection between geometric models undergoing rigid motion. The set of models include polyhedra and surfaces described by algebraic sets or piecewise algebraic functions. The algorithms make use of temporal and spatial coherence between successive instances and their running time is a function of the motion between successive instances. The main characteristics of these algorithms are their simplicity and efficiency. They have been implemented; their performance on many applications indicates their potential for real-time simulations. DTIC

N94-37123 International Software Systems, Inc., Austin, TX.
PROTO CODE GENERATION TECHNIQUES Final Report
Ramon D. Acosta May 1994 39 p Limited Reproducibility: More than 20% of this document may be affected by microfiche quality
(Contract F30602-91-C-0012)
(AD-A280275) Avail: Issuing Activity (Defense Technical Information Center (DTIC))

Proto is an integrated system for specifying, analyzing, and validating software requirements for concurrent systems. Proto supports codesign and analysis of high-level software and hardware architectures early in the system life cycle. The system comprises a comprehensive tool set for editing hierarchical dataflow specification, object-based data modeling, component reuse, resource modeling, user-interface prototyping, software/hardware allocation, interactive simulation, and code generation. This report contains a summary of Proto's functional capabilities, languages, tools, and methodology. DTIC

N94-37226 California Univ., San Diego, La Jolla, CA. Dept. of Mathematics.
H INFINITY CONTROL FOR NONLINEAR AND LINEAR SYSTEMS Final Technical Report, 1 Apr. 1991 - 31 Mar. 1994
J. W. Helton 31 Mar. 1994 17 p Limited Reproducibility: More than 20% of this document may be affected by microfiche quality
(Contract AF-AFOSR-0166-91)
(AD-A280450; AFOSR-94-0359TR) Avail: CASI HC A03

The design of a system or circuit in which stability is a key constraint frequently leads to an optimization problem over the space of functions analytic on the right half plane (R.H.P.). Mathematical techniques for solving such optimization problems for mean square error (L2 error) criteria have been widespread in engineering since the time of Wiener. Much of this research goes to developing techniques for handling worst case error (L infinity error) criteria. These occur naturally in design of control systems and amplifiers. Practically speaking there is evidence that frequency domain L infinity criteria control system designs have desirable robustness properties. The ultimate objective is to develop a new CAD approach to MIMO control design which has the flavor of classical control as well as a systematic approach to worst case frequency domain design as it occurs in many areas. The promise of this approach is sufficient to have attracted many investigators and it is currently the focus of much attention. This research addresses many aspects of the problem. They range from the development of computer algorithms of a radically different type to the discovery of theoretical methods for understanding computational design. Also considerable progress was made in extending existing H infinity control to nonlinear plants. Another major effort involves computer algebra for systems research. The objective is to treat (on a computer) systems formulas of the type an investigator would manipulate by hand. Considerable software was developed along these lines. DTIC

N94-37230 Naval Postgraduate School, Monterey, CA.
SACS: A CACHE SIMULATOR INCORPORATING TIMING ANALYSIS WITH BUFFER AND MEMORY MANAGEMENT M.S. Thesis
William G. Smith Mar. 1994 262 p Limited Reproducibility: More than 20% of this document may be affected by microfiche quality
(AD-A280472) Avail: Issuing Activity (Defense Technical Information Center (DTIC))

SACS is a cache simulator that provides the user with a wide range of timing information, in addition to providing typical information such as hit and miss rates. The SACS model includes read and write buffers, main memory, and cache memory. In addition, SACS supports a number of buffer and data forwarding policies, as well as the traditional block

replacement, write, and write miss policies. SACS also includes a self-testing mode which can be used to debug the program after source-code modification. DTIC

N94-37245# Los Alamos National Lab., NM.
INTERCHANGEABLE SPLINE REFERENCE GUIDE
R. M. Dolin May 1994 72 p
(Contract W-7405-eng-36)
(DE94-012368; LA-12746-M) Avail: CASI HC A04/MF A01

The WX-Division Integrated Software Tools (WIST) Team evolved from two previous committees, First was the W78 Solid Modeling Pilot Project's Spline Subcommittee, which later evolved into the Vv'X-Division Spline Committee. The mission of the WIST team is to investigate current CAE engineering processes relating to complex geometry and to develop methods for improving those processes. Specifically, the WIST team is developing technology that allows the Division to use multiple spline representations. We are also updating the contour system (CONSYS) data base to take full advantage of the Division's expanding electronic engineering process. Both of these efforts involve developing interfaces to commercial CAE systems and writing new software. The WIST team is comprised of members from V;X-11, -12 and 13. This 'cross-functional' approach to software development is somewhat new in the Division so an effort is being made to formalize our processes and assure quality at each phase of development. Chapter one represents a theory manual and is one phase of the formal process. The theory manual is followed by a software requirements document, specification document, software verification and validation documents. The purpose of this guide is to present the theory underlying the interchangeable spline technology and application. Verification and validation test results are also presented for proof of principle. DOE

N94-37430# Sandia National Labs., Albuquerque, NM.
POLICIES FOR IMPLEMENTING NETWORK FIREWALLS
C. D. Brown 1994 3 p Presented at the New Mexico High Tech Crime Investigation Association Conference, Albuquerque, NM, 28 Apr. 1994
(Contract DE-AC04-94AL-85000)
(DE94-011030; SAND-94-1213C; CONF-9404145-1) Avail: CASI HC A01/MF A01

Corporate networks are frequently protected by 'firewalls' or gateway systems that control access to/from other networks, e.g., the Internet, in order to reduce the network's vulnerability to hackers and other unauthorized access. Firewalls typically limit access to particular network nodes and application protocols, and they often perform special authentication and authorization functions. One of the difficult issues associated with network firewalls is determining which applications should be permitted through the firewall. For example, many networks permit the exchange of electronic mail with the outside but do not permit file access to be initiated by outside users, as this might allow outside users to access sensitive data or to surreptitiously modify data or programs (e.g., to install Trojan Horse software). However, if access through firewalls is severely restricted, legitimate network users may find it difficult or impossible to collaborate with outside users and to share data. Some of the most serious issues regarding firewalls involve setting policies for firewalls with the goal of achieving an acceptable balance between the need for greater functionality and the associated risks. Two common firewall implementation techniques, screening routers and application gateways, are discussed below, followed by some common policies implemented by network firewalls. DOE

N94-37453# Superconducting Super Collider Lab., Dallas, TX.
ZLIB++: OBJECT-ORIENTED NUMERICAL LIBRARY FOR DIFFERENTIAL ALGEBRA
N. Malitsky, A. Reshetov, and Y. Yan Jan. 1994 21 p
(Contract DE-AC35-89ER-40486)
(DE94-010839; SSCL-659) Avail: CASI HC A03/MF A01

New software engineering tools and object-oriented design have a great impact on the software development process. But in high energy physics all major packages were implemented in FORTRAN and porting of these codes to another language is rather complicated, primarily because of their huge size and heavy use of FORTRAN mathematical libraries. But some intrinsic accelerator concepts, such as nested structure of modern accelerators, look very pretty when implemented with the object-oriented approach. In this paper we present the object-oriented version of ZLIB, a numerical library for differential algebra, and show how the modern approaches can simplify the development and support of accelerator codes, decrease code size, and allow description of complex mathematical transformations by simple language. DOE

N94-37496# Sandia National Labs., Albuquerque, NM.
CHEMICAL RECOGNITION SOFTWARE
J. S. Wagner, M. W. Trahan, W. E. Nelson, P. H. Hargis, Jr., and G. C. Tisone 1994 14 p Presented at the 1994 Caliope Interim Technical Review, Oakland, CA, 26-28 Apr. 1994
(Contract DE-AC04-94AL-85000)
(DE94-012918; SAND-94-1435C; CONF-9404162-2) Avail: CASI HC A03/MF A01

We have developed a capability to make real time concentration measurements of individual chemicals in a complex mixture using a multispectral laser remote sensing system. Our chemical recognition and analysis software consists of three parts: (1) a rigorous multivariate analysis package for quantitative concentration and uncertainty estimates, (2) a genetic optimizer which customizes and tailors the multivariate algorithm for a particular application, and (3) an intelligent neural net chemical filter which pre-selects from the chemical database to find the appropriate candidate chemicals for quantitative analyses by the multivariate algorithms, as well as providing a quick-look concentration estimate and consistency check. Detailed simulations using both laboratory fluorescence data and computer synthesized spectra indicate that our software can make accurate concentration estimates from complex multicomponent mixtures, even when the mixture is noisy and contaminated with unknowns. DOE

N94-37509*# University of Southern California, Los Angeles, CA. Information Sciences Inst.
DISTRIBUTED VIRTUAL SYSTEM (DIVIRS) PROJECT Semiannual Progress Report No. 12, 1 Nov. 1993 - 30 Apr. 1994
Herbert Schorr and B. Clifford Neuman Jun. 1994 7 p
(Contract NCC2-539)
(NASA-CR-196262; NAS 1.26:196262) Avail: CASI HC A02/MF A01

As outlined in our continuation proposal 92-ISI-. OR (revised) on NASA cooperative agreement NCC2-539, we are (1) developing software, including a system manager and a job manager, that will manage available resources and that will enable programmers to develop and execute parallel applications in terms of a virtual configuration of processors, hiding the mapping to physical nodes; (2) developing communications routines that support the abstractions implemented in item one; (3) continuing the development of file and information systems based on the Virtual System Model; and (4) incorporating appropriate security measures to allow the mechanisms developed in items 1 through 3 to be used on an open network. The goal throughout our work is to provide a uniform model that can be applied to both parallel and distributed systems. We believe that multiprocessor systems should exist in the context of distributed systems, allowing them to be more easily shared by those that need them. Our work provides the mechanisms through which nodes on multiprocessors are allocated to jobs running within the distributed system and the mechanisms through which files needed by those jobs can be located and accessed. Author

N94-37539*# Institute for Computer Applications in Science and Engineering, Hampton, VA.
A SCALABLE PARALLEL ALGORITHM FOR MULTIPLE OBJECTIVE LINEAR PROGRAMS Final Report
Malgorzata M. Wiecek (Clemson Univ., SC.) and Hong Zhang (Clemson Univ., SC.) Jun. 1994 15 p Submitted for publication
(Contract NAS1-19480; RTOP 505-90-52-01; NSF DMS-93-08605)
(NASA-CR-194920; NAS 1.26:194920; ICASE-94-38) Avail: CASI HC A03/MF A01

This paper presents an ADBASE-based parallel algorithm for solving multiple objective linear programs (MOLP's). Job balance, speedup and scalability are of primary interest in evaluating efficiency of the new algorithm. Implementation results on Intel iPSC/2 and Paragon multiprocessors show that the algorithm significantly speeds up the process of solving MOLP's, which is understood as generating all or some efficient extreme points and unbounded efficient edges. The algorithm gives specially good results for large and very large problems. Motivation and justification for solving such large MOLP's are also included. Author

N94-37549# Argonne National Lab., IL.
UNSTABLE SOLITARY-WAVE SOLUTIONS OF THE GENERALIZED BENJAMIN-BONA-MAHONY EQUATION
W. R. McKinney (North Carolina State Univ., Raleigh, NC.), J. M. Restrepo, and J. L. Bona 1994 4 p Presented at the World Congress on Computational and Applied Mathematics, Atlanta, GA, 11-15 Jul. 1994
(Contract W-31-109-eng-38)
(DE94-013302; ANL/MCS/CP-82927; CONF-940719-4) Avail: CASI HC A01/MF A01

The evolution of solitary waves of the gBBM equation is investigated computationally. The experiments confirm previously derived theoretical stability estimates and, more importantly, yield insights into their behavior. For example, highly energetic unstable solitary waves when perturbed are shown to evolve into several stable solitary waves. DOE

N94-37551# Argonne National Lab., IL.
A COMPILATION SYSTEM THAT INTEGRATES HIGH PERFORMANCE FORTRAN AND FORTRAN M
I. Foster, Ming Xu, B. Avalani, and A. Choudhary 1994 9 p Presented at the Scalable High Performance Computing Conference, Knoxville, TN, 23 May 1994
(Contract W-31-109-eng-38)
(DE94-013308; ANL/MCS/CP-82973; CONF-9405100-5) Avail: CASI HC A02/MF A01

Task parallelism and data parallelism are often seen as mutually exclusive approaches to parallel programming. Yet there are important classes of application, for example in multidisciplinary simulation and command and control, that would benefit from an integration of the two approaches. In this paper, we describe a programming system that we are developing to explore this sort of integration. This system builds on previous work on task-parallel and data-parallel Fortran compilers to provide an environment in which the task-parallel language Fortran M can be used to coordinate data-parallel High Performance Fortran tasks. We use an image-processing problem to illustrate the issues that arise when building an integrated compilation system of this sort. DOE

N94-37556*# National Aeronautics and Space Administration. Marshall Space Flight Center, Huntsville, AL.
PORTABLE COLOR MULTIMEDIA TRAINING SYSTEMS BASED ON MONOCHROME LAPTOP COMPUTERS (CBT-IN-A-BRIEFCASE), WITH SPINOFF IMPLICATIONS FOR VIDEO UPLINK AND DOWNLINK IN SPACEFLIGHT OPERATIONS Final Report
D. W. Scott Aug. 1994 10 p
(Proj. 91-16)
(NASA-TM-108460; NAS 1.15:108460) Avail: CASI HC A02/MF A01

This report describes efforts to use digital motion video compression technology to develop a highly portable device that would convert 1990-91 era IBM-compatible and/or MacIntosh notebook computers into full-color, motion-video capable multimedia training systems. An architecture was conceived that would permit direct conversion of existing laser-disk-based multimedia courses with little or no reauthoring. The project did not physically demonstrate certain critical video keying techniques, but their implementation should be feasible. This investigation of digital motion video has spawned two significant spaceflight projects at MSFC: one to downlink multiple high-quality video signals from Spacelab, and the other to uplink videoconference-quality video in realtime and high quality video off-line, plus investigate interactive, multimedia-based techniques for enhancing onboard science operations. Other airborne or spaceborne spinoffs are possible. Author

N94-37656*# Research Inst. for Advanced Computer Science, Moffett Field, CA.
HIGH-ORDER CENTERED DIFFERENCE METHODS WITH SHARP SHOCK RESOLUTION
Bertil Gustafsson and Pelle Olsson Jul. 1994 27 p
(Contract NAS2-13721)
(NASA-CR-196374; NAS 1.26:196374; RIACS-TP-94-07) Avail: CASI HC A03/MF A01

In this paper we consider high-order centered finite difference approximations of hyperbolic conservation laws. We propose different ways of adding artificial viscosity to obtain sharp shock resolution. For the Riemann problem we give simple explicit formulas for obtaining stationary one and two-point shocks. This can be done for any order of accuracy. It is shown that the addition of artificial viscosity is equivalent to ensuring the Lax k-shock condition. We also show numerical experiments that verify the theoretical results. Author

N94-37673# Sandia National Labs., Albuquerque, NM.
USER'S MANUAL FOR SNL-SAND-2 CODE
P. J. Griffin, J. G. Kelly, and J. W. VanDenburg Apr. 1994 101 p
(Contract DE-AC04-94AL-85000)
(DE94-011744; SAND-93-3957) Avail: CASI HC A06/MF A02

Sandia National Laboratories, in the process of characterizing the neutron environments at its reactor facilities, has developed an enhanced version of W. McElroy's original SAND-II code. The enhanced input, output, and plotting interfaces make the code much easier to use. The basic physics and operation of the code remain unchanged. Important code enhancements include the interfaces to the latest ENDF/B-VI and IRDF-90 dosimetry-quality cross sections and the ability to use silicon displacement-sensitive devices as dosimetry sensors. DOE

N94-37739# Los Alamos National Lab., NM.
FUZZY LOGIC TO IMPROVE EFFICIENCY OF FINITE ELEMENT AND FINITE DIFFERENCE SCHEMES
M. D. Garcia and A. S. Heger 1994 6 p Presented at the 5th International Symposium on Robotics and Manufacturing, Maui, HI, 14-18 Aug. 1994
(Contract W-7405-eng-36)
(DE94-011718; LA-UR-94-1297; CONF-940859-18) Avail: CASI HC A02/MF A01

This paper explores possible applications of logic in the areas of finite element and finite difference methods applied to engineering design problems. The application of fuzzy logic to both front-end selection of computational options and within the numerical computation itself are proposed. Further, possible methods of overcoming these limitations through the application of methods are explored. Decision strategy is a fundamental limitation in performing finite element calculations, such as selecting the optimum coarseness of the grid, numerical integration algorithm, element type, implicit versus explicit schemes, and the like. This is particularly true of novice analysts who are confronted with a myriad of choices in performing a calculation. The advantage of having the myriad of options available to the analyst is, however, that it improves and optimizes the design process if the appropriate ones are selected. Unfortunately, the optimum choices are not always apparent and only through the process of elimination or prior extensive experience can the optimum choices or combination of choices be selected. The knowledge of expert analysts could be integrated into a fuzzy 'front-end' rule-based package to optimize the design process. The use of logic to capture the heuristic and human knowledge for selecting optimum solution strategies sets the framework for these proposed strategies. DOE

N94-37782# Los Alamos National Lab., NM.
OPEN ARCHITECTURE CONTROLLERS FOR ADVANCED MANUFACTURING
R. A. Gore 1994 4 p Presented at the 5th International Symposium on Robotics and Manufacturing, Maui, HI, 14-18 Aug. 1994
(Contract W-7405-eng-36)
(DE94-007572; LA-UR-94-586; CONF-940859-5) Avail: CASI HC A01/MF A01

The application of intelligent control systems to the real world of machining and manufacturing will benefit form the presence of open architecture control systems on the machines or the processes. The ability to modify the control system as the process or product changes can be essential to the success of the application of neural net or fuzzy logic controllers. The effort at Los Alamos to obtain a commercially available open architecture machine tool controller is described. DOE

N94-36626# Thomson-CSF, Bagneux (France). Div. Systemes Electronique.
HIGH ACCURACY CONTROL ALGORITHM APPLICATION TO A TRACKING TURRET
P. Nicodeme and P. Poulain *In* AGARD, Pointing and Tracking Systems May 1994 11 p (For primary document see N94-36616 12-18)
Copyright Avail: CASI HC A03/MF A02

N94-37279# SR Research, Toronto (Ontario).
LOW COST SOFTWARE-BASED RENDERING AND STEREOSCOPIC INTERFACES FOR TELEOPERATION AND VIRTUAL REALITY
Dave M. Stampe and Julius J. Grodski *In* AGARD, Virtual Interfaces: Research and Applications May 1994 6 p (For primary document see N94-37261 12-53)
Copyright Avail: CASI HC A02/MF A02

62 COMPUTER SYSTEMS

Includes computer networks and special application computer systems.

N94-36441# Argonne National Lab., IL.
USING GOPHER ON THE INTERNET
G. Davidoff 1994 38 p Presented at the Workshop at Suburban Library on Internet, Burr Ridge, IL, 26 Apr. 1994
(Contract W-31-109-eng-38)
(DE94-009736; ANL/IPD/CP-82431; CONF-9404138-1-Vugraphs) Avail: CASI HC A03/MF A01

This report is a compilation of viewgraphs with respect to the use of Gopher on Internet. There are viewgraphs on using Gopher at the University of California at Santa Cruz. Examples of other Internet Gopher servers around the world are given. Also discussed is the Library of Congress Gopher and JUGHEAD which is an acronym for Jonzy's Universal Gopher Hierarchy Excavation And Display. DOE

N94-36503*# Colorado Univ., Boulder, CO. Center for Space Structures and Controls.
A TRANSIENT FETI METHODOLOGY FOR LARGE-SCALE PARALLEL IMPLICIT COMPUTATIONS IN STRUCTURAL MECHANICS, PART 2
Charbel Farhat and Luis Crivelli Aug. 1993 23 p
(Grants NAG1-536427; NAG2-827; NSF ASC-87-17773)
(NASA-CR-194823; NAS 1.26:194823) Avail: CASI HC A03/MF A01

Explicit codes are often used to simulate the nonlinear dynamics of large-scale structural systems, even for low frequency response, because the storage and CPU requirements entailed by the repeated factorizations traditionally found in implicit codes rapidly overwhelm the available computing resources. With the advent of parallel processing, this trend is accelerating because explicit schemes are also easier to parallelize than implicit ones. However, the time step restriction imposed by the Courant stability condition on all explicit schemes cannot yet and perhaps will never be offset by the speed of parallel hardware. Therefore, it is essential to develop efficient and robust alternatives to direct methods that are also amenable to massively parallel processing because implicit codes using unconditionally stable time-integration algorithms are computationally more efficient than explicit codes when simulating low-frequency dynamics. Here we present a domain decomposition method for implicit schemes that requires significantly less storage than factorization algorithms, that is several times faster than other popular direct and iterative methods, that can be easily implemented on both shared and local memory parallel processors, and that is both computationally and communication-wise efficient. The proposed transient domain decomposition method is an extension of the method of Finite Element Tearing and Interconnecting (FETI) developed by Farhat and Roux for the solution of static problems. Serial and parallel performance results on the CRAY Y-MP/8 and the iPSC-860/128 systems are reported and analyzed for realistic structural dynamics problems. These results establish the superiority of the FETI method over both the serial/parallel conjugate gradient algorithm with diagonal scaling and the serial/parallel direct method, and contrast the computational power of the iPSC-860/128 parallel processor with that of the CRAY Y-MP/8 system. Author

N94-36547 Rutherford Appleton Lab., Chilton (England). Central Computing Dept.
PORTING INDUSTRIAL CODES AND DEVELOPING SPARSE LINEAR SOLVERS ON PARALLEL COMPUTERS
M. J. Dayde and I. S. Duff Mar. 1994 23 p Prepared in cooperation with Centre Europeen Recherche et de Formation Advanceen Calcul Scientific, Toulouse, France
(PB94-170503; RAL-94-019) Avail: Issuing Activity (National Technical Information Service (NTIS))

We address the main issues when porting existing codes from serial to parallel computers and when developing portable parallel software on MIMD multiprocessors (shared memory, virtual shared memory, and distributed memory multiprocessors, and networks of computers). We discuss the use of numerical libraries as a way of developing portable and efficient parallel code. We illustrate this by using examples from our experience in porting industrial codes and in designing parallel numerical libraries. We report in some detail on the parallelization of scientific applications coming from Centre National d'Etudes Spatiales and from Aerospatiale, and we illustrate how it is possible to develop portable and efficient numerical software by considering the parallel solution of sparse linear systems of equations. NTIS

N94-36932*# National Aeronautics and Space Administration. Langley Research Center, Hampton, VA.
A COMPARISON OF QUEUEING, CLUSTER AND DISTRIBUTED COMPUTING SYSTEMS
Joseph A. Kaplan and Michael L. Nelson Jun. 1994 51 p Revised
(RTOP 505-90-53-02)
(NASA-TM-109025; NAS 1.15:109025) Avail: CASI HC A04/MF A01

Using workstation clusters for distributed computing has become popular with the proliferation of inexpensive, powerful workstations. Workstation clusters offer both a cost effective alternative to batch processing and an easy entry into parallel computing. However, a number of workstations on a network does not constitute a cluster. Cluster management software is necessary to harness the collective computing power. We compare a variety of cluster management and queueing systems: Computing in Distributed Networked Environments (CODINE), Condor, CONNECT:Queue (formally NQS/Exec), Distributed Job Manager (DJM), Distributed Queueing System (DQS), Load Balancer, Load Leveler, Load Sharing Facility (LSF), NC TOOLSET, Network Queueing Environment (NQE), Portable Batch System (PBS), and Task Broker. The systems differ in their design philosophy and implementation. Based on published reports on the different systems and conversations with the developers and vendors, a comparison of the systems is made on the integral issues of clustered computing. Author (revised)

N94-36962*# Draper (Charles Stark) Lab., Inc., Cambridge, MA.
ADVANCED INFORMATION PROCESSING SYSTEM: THE ARMY FAULT-TOLERANT ARCHITECTURE DETAILED DESIGN OVERVIEW Final Report
Richard E. Harper, Carol A. Babikyan, Bryan P. Butler, Robert J. Clasen, Chris H. Harris, Jaynarayan H. Lala, Thomas K. Masotto, Gail A. Nagle, Mark J. Prizant, and Steven Treadwell Jun. 1994 138 p
(Contract NAS1-18565; RTOP 505-64-52-53)
(NASA-CR-194924; NAS 1.26:194924) Avail: CASI HC A07/MF A02

The Army Avionics Research and Development Activity (AVRADA) is pursuing programs that would enable effective and efficient management of large amounts of situational data that occurs during tactical rotorcraft missions. The Computer Aided Low Altitude Night Helicopter Flight Program has identified automated Terrain Following/Terrain Avoidance, Nap of the Earth (TF/TA, NOE) operation as key enabling technology for advanced tactical rotorcraft to enhance mission survivability and mission effectiveness. The processing of critical information at low altitudes with short reaction times is life-critical and mission-critical necessitating an ultra-reliable/high throughput computing platform for dependable service for flight control, fusion of sensor data, route planning, near-field/far-field navigation, and obstacle avoidance operations. To address these needs the Army Fault Tolerant Architecture (AFTA) is being designed and developed. This computer system is based upon the Fault Tolerant Parallel Processor (FTPP) developed by Charles Stark Draper Labs (CSDL). AFTA is hard real-time, Byzantine, fault-tolerant parallel processor which is programmed in the ADA language. This document describes the results of the Detailed Design (Phase 2 and 3 of a 3-year project) of the AFTA development. This document contains detailed descriptions of the program objectives, the TF/TA NOE application requirements, architecture, hardware design, operating systems design, systems performance measurements and analytical models. Author

N94-37411*# Institute for Computer Applications in Science and Engineering, Hampton, VA.
PARALLELIZED DIRECT EXECUTION SIMULATION OF MESSAGE-PASSING PARALLEL PROGRAMS Final Report

Phillip M. Dickens (IBM Watson Research Center, Yorktown Heights, NY.), Philip Heidelberger, and David M. Nicol Jun. 1994 28 p Submitted for publication
(Contract NAS1-19480; NSF-CCR-92-01195; RTOP 505-90-52-01)
(NASA-CR-194936; NAS 1.26:194936; ICASE-94-50) Avail: CASI HC A01/MF A01

As massively parallel computers proliferate, there is growing interest in findings ways by which performance of massively parallel codes can be efficiently predicted. This problem arises in diverse contexts such as parallelizing computers, parallel performance monitoring, and parallel algorithm development. In this paper we describe one solution where one directly executes the application code, but uses a discrete-event simulator to model details of the presumed parallel machine such as operating system and communication network behavior. Because this approach is computationally expensive, we are interested in its own parallelization specifically the parallelization of the discrete-event simulator. We describe methods suitable for parallelized direct execution simulation of message-passing parallel programs, and report on the performance of such a system, Large Application Parallel Simulation Environment (LAPSE), we have built on the Intel Paragon. On all codes measured to date, LAPSE predicts performance well typically within 10 percent relative error. Depending on the nature of the application code, we have observed low slowdowns (relative to natively executing code) and high relative speedups using up to 64 processors. Author

N94-37419# Oak Ridge National Lab., TN. Engineering Physics and Mathematics Div.
NEUTRON TRANSPORT METHODS ON SCALABLE SHARED MEMORY MULTIPROCESSORS
Y. Y. Azmy 1994 12 p Presented at the Topical Meeting on Advances in Reactor Physics, Knoxville, TN, 11-14 Apr. 1994
(Contract DE-AC05-84OR-21400)
(DE94-012324; CONF-940407-20) Avail: CASI HC A03/MF A01

We describe the parallel implementation of the source iterations traditionally used in solving the neutron transport equation on the highly-scalable shared memory, two-ringed Kendall Square, KSR1, with 64 cells. The program used in this work is the two-dimensional, Cartesian geometry, arbitrarily high order transport (AHOT) code which has a nodal and a characteristic method option. The parallel algorithm employs an angular domain decomposition in the mesh sweep stage and a spatial domain decomposition in the convergence test and iterate update stages, resulting in high speedup factors at parallel efficiencies in the 90% range. We construct a preliminary performance model for the parallel algorithm and validate it against measured execution times. DOE

N94-37487# Sandia National Labs., Albuquerque, NM.
EXPERIENCE WITH AUTOMATIC, DYNAMIC LOAD BALANCING AND ADAPTIVE FINITE ELEMENT COMPUTATION
S. R. Wheat, K. D. Devine, and A. B. Maccabe 1993 25 p Presented at the 27th Hawaii International Conference on System Sciences, Maui, HI, 4-7 Jan. 1994
(Contract DE-AC04-94AL-85000)
(DE94-001422; SAND-93-2172C; CONF-940136-2) Avail: CASI HC A03/MF A01

Distributed memory, massively parallel (MP), MIMD technology has enabled the development of applications requiring computational resources previously unobtainable. Structural mechanics and fluid dynamics applications, for example, are often solved by finite element methods (FEM's) requiring millions of degrees of freedom to accurately simulate physical phenomenon. Adaptive methods, which automatically refine or coarsen meshes and vary the order of accuracy of the numerical solution, offer greater robustness and computational efficiency than traditional FEM's by reducing the amount of computation required away from physical structures such as shock waves and boundary layers. On MP computers, FEM's frequently result in distributed processor load imbalances. To overcome load imbalance, many MP FEM's use static load balancing as a preprocessor to the finite element calculation. Adaptive methods complicate the load imbalance problem since the work per element is not uniform across the solution domain and changes as the computation proceeds. Therefore, dynamic load balancing is required to maintain global load balance. We describe a dynamic, fine-grained, element-based data migration system that maintains global load balance and is effective in the presence of changing work loads. Global load balance is achieved by overlapping neighborhoods of processors, where each neighborhood performs local load balancing. The method utilizes an automatic element management system library to which a programmer integrates the application's computational description. The library's flexibility supports a large class of finite element and finite difference based applications. DOE

N94-37500*# Draper (Charles Stark) Lab., Inc., Cambridge, MA.
ADVANCED INFORMATION PROCESSING SYSTEM: AUTHENTICATION PROTOCOLS FOR NETWORK COMMUNICATION Final Report
Richard E. Harper, Stuart J. Adams, Carol A. Babikyan, Bryan P. Butler, Anne L. Clark, and Jaynarayan H. Lala Jun. 1994 109 p
(Contract NAS1-18565; RTOP 505-64-52-53)
(NASA-CR-194923; NAS 1.26:194923) Avail: CASI HC A06/MF A02

In safety critical I/O and intercomputer communication networks, reliable message transmission is an important concern. Difficulties of communication and fault identification in networks arise primarily because the sender of a transmission cannot be identified with certainty, an intermediate node can corrupt a message without certainty of detection, and a babbling node cannot be identified and silenced without lengthy diagnosis and reconfiguration. Authentication protocols use digital signature techniques to verify the authenticity of messages with high probability. Such protocols appear to provide an efficient solution to many of these problems. The objective of this program is to develop, demonstrate, and evaluate intercomputer communication architectures which employ authentication. As a context for the evaluation, the authentication protocol-based communication concept was demonstrated under this program by hosting a real-time flight critical guidance, navigation and control algorithm on a distributed, heterogeneous, mixed redundancy system of workstations and embedded fault-tolerant computers. Author (revised)

N94-37519# Argonne National Lab., IL.
A SCALABLE HIGH-PERFORMANCE I/O SYSTEM
M. Henderson, B. Nickless, and R. Stevens 1994 7 p Presented at the Scalable High Performance Computing Conference, Knoxville, TN, 23 May 1994
(Contract W-31-109-eng-38)
(DE94-011513; ANL/MCS/CP-82804; CONF-9405100-3) Avail: CASI HC A02/MF A01

A significant weakness of many existing parallel supercomputers is their lack of high-performance parallel I/O. This weakness has prevented, in many cases, the full exploitation of the true potential of MPP systems. As part of a joint project with IBM, we have designed a parallel I/O system for an IBM SP system that can provide sustained I/O rates of greater than 160 MB/s from collections of compute nodes to archival disk and peak transfer rates that should exceed 400 MB/s from compute nodes to I/O servers. This testbed system is being used for a number of projects: first it will provide a high-performance experimental I/O system for traditional computational science applications; second it will be used as an I/O software and development environment for new parallel I/O algorithms and operating systems support; and third it will be used as the foundation for a number of new projects designed to develop enabling technology for the National Information Infrastructure. This report describes the system under development at Argonne National Laboratory, provides some preliminary performance results, and outlines future experiments and directions. DOE

N94-37568# Oak Ridge National Lab., TN.
PARALLEL SPECTRAL TRANSFORM SHALLOW WATER MODEL: A RUNTIME-TUNABLE PARALLEL BENCHMARK CODE
P. H. Worley and I. T. Foster 1994 9 p Presented at the Scalable High Performance Computing Conference, Knoxville, TN, 23 May 1994
(Contract DE-AC05-84OR-21400)
(DE94-011460; CONF-9405100-2) Avail: CASI HC A02/MF A01

Fairness is an important issue when benchmarking parallel computers using application codes. The best parallel algorithm on one platform may not be the best on another. While it is not feasible to reevaluate parallel algorithms and reimplement large codes whenever new machines become available, it is possible to embed algorithmic options into codes that allow them to be 'tuned' for a particular machine without requiring code modifications. In this paper, we describe a code in which such an approach was taken. PSTSWM was developed for evaluating parallel algorithms for the spectral transform method in atmospheric circulation models. Many

levels of runtime-selectable algorithmic options are supported. We discuss these options and our evaluation methodology. We also provide empirical results from a number of parallel machines, indicating the importance of tuning for each platform before making a comparison. DOE

N94-37583*# Draper (Charles Stark) Lab., Inc., Cambridge, MA.
ADVANCED INFORMATION PROCESSING SYSTEM: HOSTING OF ADVANCED GUIDANCE, NAVIGATION AND CONTROL ALGORITHMS ON AIPS USING ASTER Final Report
Richard Brenner, Jaynarayan H. Lala, Gail A. Nagle, Andrei Schor, and John Turkovich Aug. 1994 120 p
(Contract NAS1-18565; RTOP 506-59-61-03)
(NASA-CR-194960; NAS 1.26:194960) Avail: CASI HC A06/MF A02

This program demonstrated the integration of a number of technologies that can increase the availability and reliability of launch vehicles while lowering costs. Availability is increased with an advanced guidance algorithm that adapts trajectories in real-time. Reliability is increased with fault-tolerant computers and communication protocols. Costs are reduced by automatically generating code and documentation. This program was realized through the cooperative efforts of academia, industry, and government. The NASA-LaRC coordinated the effort, while Draper performed the integration. Georgia Institute of Technology supplied a weak Hamiltonian finite element method for optimal control problems. Martin Marietta used MATLAB to apply this method to a launch vehicle (FENOC). Draper supplied the fault-tolerant computing and software automation technology. The fault-tolerant technology includes sequential and parallel fault-tolerant processors (FTP & FTPP) and authentication protocols (AP) for communication. Fault-tolerant technology was incrementally incorporated. Development culminated with a heterogeneous network of workstations and fault-tolerant computers using AP. Draper's software automation system, ASTER, was used to specify a static guidance system based on FENOC, navigation, flight control (GN&C), models, and the interface to a user interface for mission control. ASTER generated Ada code for GN&C and C code for models. An algebraic transform engine (ATE) was developed to automatically translate MATLAB scripts into ASTER. Author (revised)

N94-37654*# Research Inst. for Advanced Computer Science, Moffett Field, CA.
IMPROVED LOAD DISTRIBUTION IN PARALLEL SPARSE CHOLESKY FACTORIZATION
Edward Rothberg (INTEL Corp., Beaverton, OR.) and Robert Schreiber Aug. 1994 12 p Submitted for publication
(Contract NAS2-13721)
(NASA-CR-196380; NAS 1.26:196380; RIACS-TP-94-13) Avail: CASI HC A03/MF A01

Compared to the customary column-oriented approaches, block-oriented, distributed-memory sparse Cholesky factorization benefits from an asymptotic reduction in interprocessor communication volume and an asymptotic increase in the amount of concurrency that is exposed in the problem. Unfortunately, block-oriented approaches (specifically, the block fan-out method) have suffered from poor balance of the computational load. As a result, achieved performance can be quite low. This paper investigates the reasons for this load imbalance and proposes simple block mapping heuristics that dramatically improve it. The result is a roughly 20% increase in realized parallel factorization performance, as demonstrated by performance results from an Intel Paragon system. We have achieved performance of nearly 3.2 billion floating point operations per second with this technique on a 196-node Paragon system. Author

N94-37760 Mitre Corp., Bedford, MA.
TECHNIQUES FOR REAL-TIME PARALLEL PROCESSING: SENSOR PROCESSING CASE STUDIES Final Technical Report
Richard A. Games, John D. Ramsdell, and Joseph J. Rushanan Apr. 1994 77 p Limited Reproducibility: More than 20% of this document may be affected by microfiche quality
(Contract F19628-94-C-0001)
(AD-A280633; MTR-93B0000186) Avail: CASI HC A05

The software development process for parallel processors is investigated with a focus on real-time sensor processing applications. Concepts that are relevant to real-time parallel processing are introduced including: a definition of scalable dataflow graphs motivated by the need to meet a fixed throughput constraint for varying problem sizes, an algorithm classification that makes explicit the impact that data dependencies have in real-time implementations, and a real-time implementation strategy that decomposes the most problematic algorithms into compositions of more predictable constituents and then uses scalable dataflow graphs and parallel processing to recover timing predictability by mapping data dependent timing uncertainties into the spatial dimension (processors). Two case studies apply these ideas: an implementation of the Modified Gram-Schmidt (MGS) algorithm on a MasPar MP1 and an implementation of the joint probabilistic data association (JPDA) algorithm on a Thinking Machines CM-2. The JPDA case study includes a SISAL implementation to illustrate the advantages of functional programming for these applications. DTIC

63 CYBERNETICS

Includes feedback and control theory, artificial intelligence, robotics and expert systems.

For related information see also *54 Man/System Technology and Life Support.*

N94-36535 ZIRST, Meylan (France).
ADAPTIVE MULTISENSOR FUSION FOR THE PERCEPTION AND INTERPRETATION OF OUTDOOR ROBOT SCENES [FUSION MULTI-SENSORIELLE ADAPTATIVE POUR LA PERCEPTION ET L'INTERPRETATION DE SCENES EXTERIEURES EN ROBOTIQUE]
Marie-France Collin May 1993 53 p In FRENCH Sponsored by Direction des Recherches, Etudes et Techniques and Centre de Documentation de l'Armement
(PB94-170719) Avail: Issuing Activity (National Technical Information Service (NTIS))

The author spent 18 months at the Johnson Space Center in Houston, studying and defining a new multisensor perception and fusion method to improve the autonomy and reliability of robot systems navigating independently on planetary surfaces. The first section on his report describes the organization of NASA and of the Johnson Space Center. The second sums up the scientific results of the research, which emphasized perception in all lighting conditions and extraction of surface roughness and dielectric constant (invariable parameters). Fuzzy logic was used to define a multisensor fusion method that takes into account the approximations of theoretical models and makes the system precise enough for use in navigation. Tests of synthesized multispectral images were developed, and the results of fusion and extraction were put into visual form. The third section of the report lists the economic and scientific repercussions of the research program. NTIS

N94-36722# Air Force Inst. of Tech., Wright-Patterson AFB, OH. School of Engineering.
SEARCHING FOR PLANS USING A HIERARCHY OF LEARNED MACROS AND SELECTIVE REUSE Ph.D. Thesis
Douglas E. Dyer Jun. 1994 117 p
(AD-A280594; AFIT/DS/ENG/94J-01) Avail: CASI HC A06/MF A02

This research presents a new approach to improving the performance of a macro planner: selective reuse. In macro planning, reuse can result in poorer performance than when planning with only primitive operators, a phenomenon that has been called the utility problem. The utility problem arises because the benefits of reuse are outweighed by the cost of retrieving a macro to reuse and the cost of searching through the larger search space caused by considering reuse candidates. Selective reuse contains the expansion of the search space by limiting the number of reuse candidates considered and limits the search required by considering only those reuse candidates that entail no additional work. Previously, performance improvement in a macro planner has been possible only by selective learning. Unlike selective learning, selective reuse never overlooks a learning opportunity that might have value in future problem solving. This research developed a polynomial-order retrieval method which reduces the cost of retrieving a reuse candidate likely to save search. A macro planner (HINGE) was implemented to explore selective reuse. To improve the probability of beneficial reuse, HINGE searches in a space of plans using a hierarchically-structured search method that provides multiple opportunities for reuse. DTIC

N94-36736# Air Force Inst. of Tech., Wright-Patterson AFB, OH. School of Engineering.

H2 OPTIMAL CONTROL WITH H-INFINITY, MU, AND L1 CONSTRAINTS Ph.D. Thesis

David E. Walker Jun. 1994 238 p

(AD-A280593; AFIT/DS/AA/94-2) Avail: CASI HC A11/MF A03

H2 optimization with convex constraints is considered. The optimal (order-free) solution is shown to be unique through convex analysis. H-inf constraints with feedforward terms and singular constraints are also allowed. The optimal fixed-order solution is shown to have the same characteristics as a mixed problem with regular H-inf constraints. Furthermore, these results are shown to hold for controller orders as low as the optimal H2 order. A numerical method is developed based on analytical gradients which results in sub- and super-optimal fixed-order controllers. The problem is extended to include an upper bound on a mu constraint through a modification of the D-K iteration method. Next, multiple H-inf constraints are developed. Fixed-order solutions to the multiple constraint problem are characterized and the numerical method is extended to include multiple constraints. Next, a continuous LI constraint is added. A numerical approach is proposed based on bounding the LI-norm by the 11-norm of an Euler approximating system. Finally, H2 optimization with a finite set of H-inf, mu, and LI constraints is characterized. SISO and MIMO numerical examples demonstrate the application of these methods. DTIC

N94-36924*# Institute for Computer Applications in Science and Engineering, Hampton, VA.

A PDE-BASED METHODOLOGY FOR MODELING, PARAMETER ESTIMATION AND FEEDBACK CONTROL IN STRUCTURAL AND STRUCTURAL ACOUSTIC SYSTEMS

H. T. Banks (North Carolina Univ., Raleigh, NC.), D. E. Brown (National Aeronautics and Space Administration. Langley Research Center, Hampton, VA.), Vern L. Metcalf (National Aeronautics and Space Administration. Langley Research Center, Hampton, VA.), R. J. Silcox (National Aeronautics and Space Administration. Langley Research Center, Hampton, VA.), Ralph C. Smith (Iowa State Univ. of Science and Technology, Ames, IA.), and Yun Wang (North Carolina Univ., Raleigh, NC.) May 1994 12 p

(Contracts NAS1-19480; NAS1-19000; F49620-93-1-0198; RTOP 505-90-52-01)

(NASA-CR-194928; NAS 1.26:194928; ICASE-94-43) Avail: CASI HC A03/MF A01

A problem of continued interest concerns the control of vibrations in a flexible structure and the related problem of reducing structure-borne noise in structural acoustic systems. In both cases, piezoceramic patches bonded to the structures have been successfully used as control actuators. Through the application of a controlling voltage, the patches can be used to reduce structural vibrations which in turn lead to methods for reducing structure-borne noise. A PDE-based methodology for modeling, estimating physical parameters, and implementing a feedback control scheme for problems of this type is discussed. While the illustrating example is a circular plate, the methodology is sufficiently general so as to be applicable in a variety of structural and structural acoustic systems. Author

N94-36928*# Institute for Computer Applications in Science and Engineering, Hampton, VA.

VIBRATION SUPPRESSION WITH APPROXIMATE FINITE DIMENSIONAL COMPENSATORS FOR DISTRIBUTED SYSTEMS: COMPUTATIONAL METHODS AND EXPERIMENTAL RESULTS Final Report

H. T. Banks (North Carolina Univ., Raleigh, NC.), Ralph C. Smith (Iowa State Univ. of Science and Technology, Ames, IA.), and Yun Wang (North Carolina Univ., Raleigh, NC.) May 1994 17 p Proceedings of the Second International Conference on Intelligent Materials held in Williamsburg, VA

(Contracts NAS1-19480; NAG1-1600; F49620-93-1-0198; RTOP 505-90-52-01)

(NASA-CR-194927; NAS 1.26:194927; ICASE-94-42) Avail: CASI HC A03/MF A01

Based on a distributed parameter model for vibrations, an approximate finite dimensional dynamic compensator is designed to suppress vibrations (multiple modes with a broad band of frequencies) of a circular plate with Kelvin-Voigt damping and clamped boundary conditions. The control is realized via piezoceramic patches bonded to the plate and is calculated from information available from several pointwise observed state variables. Examples from computational studies as well as use in laboratory experiments are presented to demonstrate the effectiveness of this design. Author

N94-37039 Naval Postgraduate School, Monterey, CA.

BEYOND INTELLIGENT VACUUM CLEANERS

Don Brutzman 1993 3 p Limited Reproducibility: More than 20% of this document may be affected by microfiche quality

(AD-A280565) Avail: CASI HC A01

Designing the ultimate autonomous vacuum cleaner is the quantifiable and clearly-defined goal of this symposium. It falls short of addressing the problems which most interest roboticists working in artificial intelligence. The painstaking progress and restricted performance of current mobile robots apparently necessitates such a low-level review. Overcoming such challenges and setbacks is essential if robots are to become capable of operating in more interesting regimes. Several questions are presented to help evaluate whether a robotics research program remains oriented towards meaningful long-term goals of autonomy, intelligence, and capable performance. DTIC

N94-37043 Air Force Inst. of Tech., Wright-Patterson AFB, OH.

SUBGROUPED REAL TIME RECURRENT LEARNING NEURAL NETWORKS M.S. Thesis

Jeffrey S. Dean May 1994 155 p Limited Reproducibility: More than 20% of this document may be affected by microfiche quality

(AD-A280618; AFIT/ENG/GE/94J-01) Avail: CASI HC A08

A subgrouped real time recurrent learning (RTRL) network was evaluated. The one layer net successfully learns the XOR problem and can be trained to perform time dependent functions. The net was tested as a predictor on the behavior of a signal, based on past behavior. While the net was not able to predict the signal's future behavior, it tracked the signal closely. The net was also tested as a classifier for time varying phenomena, for the differentiation of five classes of vehicle images based on features extracted from the visual information. The net achieved a 99.2% accuracy in recognizing the five vehicle classes. The behavior of the subgrouped RTRL net was compared to the RTRL network described in Capt R. Lindsey's AFIT Master's thesis. The subgrouped RTRL performance proved close to the RTRL network in accuracy while reducing the time required to train the network for multiple output (classification) problems. DTIC

N94-37058*# National Aeronautics and Space Administration. Langley Research Center, Hampton, VA.

ROBUST STABILIZATION OF MARGINALLY STABLE POSITIVE-REAL SYSTEMS

Suresh M. Joshi and Sandeep Gupta Jul. 1994 15 p

(RTOP 233-01-01-05)

(NASA-TM-109136; NAS 1.15:109136) Avail: CASI HC A03/MF A01

This paper investigates the stability of the negative feedback interconnection to two positive-real systems which have poles in the closed left-half of the complex plane. A new definition of marginally strict positive real systems is introduced, and sufficient conditions are obtained for the stability of the feedback interconnection of such systems, using the Lyapunov method. The conditions obtained have direct applications to dynamic dissipative controllers for flexible spacecraft and are the least restrictive ones published to date. Author

N94-37083# Oak Ridge National Lab., TN.

ADAPTIVE LEARNING OF MULTI-SENSOR INTEGRATION TECHNIQUES WITH GENETIC ALGORITHMS

J. E. Baker 1994 8 p Presented at the 5th International Symposium on Robotics and Manufacturing, Maui, HI, 14-18 Aug. 1994

(Contract DE-AC05-84OR-21400)

(DE94-012744; CONF-940859-21) Avail: CASI HC A02/MF A01

This research focuses on automating the time-consuming process of developing and optimizing multi-sensor integration techniques. Our approach is currently based on adaptively learning how to exploit low-level image detail. Although this system is specifically designed to be both sensor and application domain independent, an empirical validation with actual multi-modal sensor data is presented. DOE

N94-37425# Sandia National Labs., Albuquerque, NM.
BOOTSTRAP PLANNING: THEORY AND APPLICATION
P. C. Chen 1994 13 p Presented at the 12th National Conference on Artificial Intelligence, Seattle, WA, 1 Aug. 1994
(Contract DE-AC04-94AL-85000)
(DE94-006466; SAND-94-0296C; CONF-940860-1) Avail: CASI HC A03/MF A01

We identify a general framework for weak planning called bootstrap planning, which is defined as global planning using only a local planner along with some memory for learning intermediate subgoals. We present a family of algorithms for bootstrap planning, and provide some initial theory on their performance. In our theoretical analysis, we develop a random digraph problem model and use it to make some performance predictions and comparisons of these algorithms. We also use it to provide some techniques for approximating the optimal resource bound on the local planner to achieve the best global planner. We validate our theoretical results with empirical demonstration on the 15-puzzle. We show how to reduce the planning cost of a global planner by 2 orders of magnitude using bootstrap planning. We also demonstrate a natural but not widely recognized connection between search costs and the lognormal distribution. DOE

N94-37526 Air Force Inst. of Tech., Wright-Patterson AFB, OH. School of Engineering.
FEATURE AND MODEL SELECTION IN FEEDFORWARD NEURAL NETWORKS Ph.D. Thesis
Jean M. Steppe Jun. 1994 227 p Limited Reproducibility: More than 20% of this document may be affected by microfiche quality
(AD-A280709; AFIT/DS/ENS/94-1) Avail: CASI HC A11

This research advances feature and model selection for feedforward neural networks. Feature selection involves determining a good feature subset given a set of candidate features. Model selection involves determining an appropriate architecture (number of middle nodes) for the neural network. Specific advances are made in neural network feature saliency metrics used for evaluating or ranking features, statistical identification of irrelevant/noisy features, and statistical investigation of reduced neural network architectures and reduced feature subsets. New feature saliency metrics are presented which provide a more succinct quantitative measure of a feature's importance than other similar metrics. A catalogue of feature saliency metric definitions and interrelationships is also developed which consolidates the set of available metrics for the neural network practitioner. The statistical screening procedure developed for identifying noisy features involves statistically comparing the saliency of candidate features with the saliency of a known noisy feature. The neural network selection algorithms are developed by posing the neural network model as a nonlinear regression statistical model, and using the likelihood ratio test statistic within a backwards sequential procedure to search for a parsimonious model with equivalent prediction accuracy. Additionally, a comprehensive statistically-based methodology is developed for identifying both a good feature set and an appropriate neural network architecture for a specific situation. DTIC

N94-37529# Sandia National Labs., Albuquerque, NM.
ROBOT TRAJECTORY PLANNING VIA DYNAMIC PROGRAMMING
C. R. Dohrmann and R. D. Robinett 1994 7 p Presented at the 5th International Symposium on Robotics and Manufacturing, Maui, HI, 14-18 Aug. 1994
(Contract DE-AC04-94AL-85000)
(DE94-008424; SAND-94-0623C; CONF-940859-6) Avail: CASI HC A02/MF A01

The method of dynamic programming is applied to three example problems dealing with robot trajectory planning. The first two examples involve end-effector tracking of a straight line with rest-to-rest motions of planar two-link and three-link rigid robots. These examples illustrate the usefulness of the method for producing smooth trajectories either in the presence or absence of joint redundancies. The last example demonstrates the use of the method for rest-to-rest maneuvers of a single-link manipulator with a flexible payload. Simulation results for this example display interesting symmetries that are characteristic of such maneuvers. Details concerning the implementation and computational aspects of the method are discussed. DOE

N94-37589*# National Aeronautics and Space Administration. Langley Research Center, Hampton, VA.
TECHNOLOGY DEMONSTRATION OF SPACE INTRAVEHICULAR AUTOMATION AND ROBOTICS
A. Terry Morris and L. Keith Barker Jul. 1994 30 p
(RTOP 233-03-03-02)
(NASA-TM-109138; NAS 1.15:109138) Avail: CASI HC A03/MF A01

Automation and robotic technologies are being developed and capabilities demonstrated which would increase the productivity of microgravity science and materials processing in the space station laboratory module, especially when the crew is not present. The Automation Technology Branch at NASA Langley has been working in the area of intravehicular automation and robotics (IVAR) to provide a user-friendly development facility, to determine customer requirements for automated laboratory systems, and to improve the quality and efficiency of commercial production and scientific experimentation in space. This paper will describe the IVAR facility and present the results of a demonstration using a simulated protein crystal growth experiment inside a full-scale mockup of the space station laboratory module using a unique seven-degree-of-freedom robot. Author (revised)

N94-37590*# Georgia Inst. of Tech., Atlanta, GA. School of Aerospace Engineering
ROBUST STABILITY OF SECOND-ORDER SYSTEMS Progress Report, 24 Aug. 1993 - 24 Aug. 1994
C.-H. Chuang 19 Aug. 1994 23 p
(Grant NAG1-1397)
(NASA-CR-196384; NAS 1.26:196384) Avail: CASI HC A03/MF A01

This progress report gives current progress of the research in nonlinear robust control using positive real concept. The progress is documented in a draft paper. In the paper, the manipulator dynamics is reformulated differently from the existing equations of motion for free base robots. This new formulation gives a compact form of the dynamic equations for easy computation. The nonlinear terms are now considered. The results show that for an additional nonlinear friction term, the feedback controller designed using passivity concept works quite well. Although design of such a controller requires simulation of the dynamics for the example shown in the following draft, this design procedure is feasible. Author (revised)

N94-37735# Oak Ridge National Lab., TN.
A NEW TECHNIQUE FOR DYNAMIC LOAD DISTRIBUTION WHEN TWO MANIPULATORS MUTUALLY LIFT A RIGID OBJECT, PART 2
M. A. Unseren 1994 7 p Presented at the 5th International Symposium on Robotics and Manufacturing, Maui, HI, 14-18 Aug. 1994
(Contract DE-AC05-84OR-21400)
(DE94-010126; CONF-940859-16-Pt-2) Avail: CASI HC A02/MF A01

A rigid body model for the entire system which accounts for the load distribution scheme proposed in Part 1 as well as for the dynamics of the manipulators and the kinematic constraints is derived in the joint space. A technique is presented for expressing the object dynamics in terms of the joint variables of both manipulators which leads to a positive definite and symmetric inertia matrix. The model is then transformed to obtain reduced order equations of motion and a separate set of equations which govern the behavior of the internal contact forces. The control architecture is applied to the model which results in the explicit decoupling of the position and internal contact force-controlled degrees of freedom (DOF). DOE

N94-37783# Sandia National Labs., Albuquerque, NM.
WHAT IS AN OPEN ARCHITECTURE ROBOT CONTROLLER?
W. E. Ford 14 Feb. 1994 7 p Presented at the 9th Institute of Electrical and Electronics Engineers (IEEE) International Symposium on Intelligent Control, Columbus, OH, 16-18 Aug. 1994
(Contract DE-AC04-94AL-85000)
(DE94-007854; SAND-94-0513C; CONF-940869-1) Avail: CASI HC A02/MF A01

This paper addresses the issue of what is an open architecture robot controller. Three different classifications are defined along with the various advantages and shortcomings of each approach. Knowledge from past research and new technology has been included in this analysis. The conclusions recommend a communication-based hybrid approach with well defined interfaces between modules. DOE

N94-37784# Sandia National Labs., Albuquerque, NM.
INTERACTIVE COLLABORATIVE ENVIRONMENTS (ICE): PLATFORM INDEPENDENT X APPLICATION SHARING AND MULTI-MEDIA OVER WIDE AREA NETWORKS
M. R. Ashby and H. W. Lin 1994 6 p Presented at the 5th International Symposium on Robotics and Manufacturing, Maui, HI, 14-18 Aug. 1994
(Contract DE-AC04-94AL-85000)
(DE94-008868; SAND-94-0734C; CONF-940859-9) Avail: CASI HC A02/MF A01

Platform-independent Interaction Collaborative Environments (ICE) technologies include support for simultaneous display and control of unmodified X application software by two or more people, at separate locations, using different workstation hardware. Audio and video provide remote collaborators with the ability to discuss what they are all simultaneously seeing on their workstations. Remote pointing and marking capabilities are also provided independent of the application. The authors briefly describe their X application sharing work, and requirements for supporting tools, including multi-media. Finally they review some of the pilot project network applications of their work to robotics and manufacturing environments. DOE

N94-37785# Sandia National Labs., Albuquerque, NM.
REMOTE USE OF DISTRIBUTED ROBOTICS RESOURCES TO ENHANCE TECHNOLOGY DEVELOPMENT AND INSERTION
R. W. Harrigan, M. J. McDonald, and B. R. Davies 1994 9 p Presented at the 5th International Symposium on Robotics and Manufacturing, Maui, HI, 14-18 Aug. 1994
(Contract DE-AC04-94AL-85000)
(DE94-009285; SAND-94-0596C; CONF-940859-14) Avail: CASI HC A02/MF A01

This paper describes Virtual Collaborative Environments (VCE's), an information architecture that enables remote sharing of mechatronic (intelligent electrochemical devices) resources. This architecture will leverage the proposed National Information Infrastructure (NII) or information highway to share valuable resources and reduce product-to-market cycles. Benefits of sharing mechatronic resources with VCE's are explored. An existing prototype VCE is described and experimental and illustrative results from using the prototype VCE system are discussed. DOE

N94-36628# Universitaet der Bundeswehr Muenchen, Neubiberg (Germany). Fakultaet fuer Luft-und Raumfahrttechnik.
TWO-AXIS CAMERA PLATFORM FOR MACHINE VISION
J. Schiehlen and E. D. Dickmanns *In* AGARD, Pointing and Tracking Systems May 1994 6 p (For primary document see N94-36616 12-18)
Copyright Avail: CASI HC A02/MF A02

64 NUMERICAL ANALYSIS

Includes iteration, difference equations, and numerical approximation.

N94-36455# Bettis Atomic Power Lab., Pittsburgh, PA.
A COARSE-MESH NODAL METHOD-DIFFUSIVE-MESH FINITE DIFFERENCE METHOD
H. Joo and W. R. Nichols 1994 7 p Presented at the 35th Annual Meeting of the American Nuclear Society, New Orleans, LA, 11-16 Jun. 1994
(Contract DE-AC11-93PN-38195)
(DE94-010809; WAPD-T-3030; CONF-940602-8) Avail: CASI HC A02/MF A01

Modern nodal methods have been successfully used for conventional light water reactor core analyses where the homogenized, node average cross sections (XSs) and the flux discontinuity factors (DFs) based on equivalence theory can reliably predict core behavior. For other types of cores and other geometries characterized by tightly-coupled, heterogeneous core configurations, the intranodal flux shapes obtained from a homogenized nodal problem may not accurately portray steep flux gradients near fuel assembly interfaces or various reactivity control elements. This may require extreme values of DFs (either very large, very small, or even negative) to achieve a desired solution accuracy. Extreme values of DFs, however, can disrupt the convergence of the iterative methods used to solve for the node average fluxes, and can lead to a difficulty in interpolating adjacent DF values. Several attempts to remedy the problem have been made, but nothing has been satisfactory. A new coarse-mesh nodal scheme called the Diffusive-Mesh Finite Difference (DMFD) technique, as contrasted with the coarse-mesh finite difference (CMFD) technique, has been developed to resolve this problem. This new technique and the development of a few-group, multidimensional kinetics computer program are described in this paper. DOE

N94-36562*# Institute for Computer Applications in Science and Engineering, Hampton, VA.
A NOTE ON THE REGULARITY OF SOLUTIONS OF INFINITE DIMENSIONAL RICCATI EQUATIONS Final Report
John A. Burns and Belinda B. King Mar. 1994 19 p Submitted for publication
(Contract NAS1-19480; RTOP 505-90-52-01)
(NASA-CR-194898; NAS 1.26:194898; ICASE-94-20; AD-A280357) Avail: CASI HC A03/MF A01

This note is concerned with the regularity of solutions of algebraic Riccati equations arising from infinite dimensional LQR and LQG control problems. We show that distributed parameter systems described by certain parabolic partial differential equations often have a special structure that smoothes solutions of the corresponding Riccati equation. This analysis is motivated by the need to find specific representations for Riccati operators that can be used in the development of computational schemes for problems where the input and output operators are not Hilbert-Schmidt. This situation occurs in many boundary control problems and in certain distributed control problems associated with optimal sensor/actuator placement. Author

N94-36647*# National Aeronautics and Space Administration. Lewis Research Center, Cleveland, OH.
PRECONDITIONED IMPLICIT SOLVERS FOR THE NAVIER-STOKES EQUATIONS ON DISTRIBUTED-MEMORY MACHINES
Kumud Ajmani, Meng-Sing Liou, and Rodger W. Dyson Jan. 1994 12 p Presented at the 32nd Aerospace Sciences Meeting and Exhibit, Reno, NV, 10-13 Jan. 1994; sponsored by AIAA
(Contract NCC3-233; RTOP 505-90-5K)
(NASA-TM-106449; E-8302; ICOMP-93-49; NAS 1.15:106449; AIAA Paper 94-0408) Avail: CASI HC A03/MF A01

The GMRES method is parallelized, and combined with local preconditioning to construct an implicit parallel solver to obtain steady-state solutions for the Navier-Stokes equations of fluid flow on distributed-memory machines. The new implicit parallel solver is designed to preserve the convergence rate of the equivalent 'serial' solver. A static domain-decomposition is used to partition the computational domain amongst the available processing nodes of the parallel machine. The SPMD (Single-Program Multiple-Data) programming model is combined with message-passing tools to develop the parallel code on a 32-node Intel Hypercube and a 512-node Intel Delta machine. The implicit parallel solver is validated for internal and external flow problems, and is found to compare identically with flow solutions obtained on a Cray Y-MP/8. A peak computational speed of 2300 MFlops/sec has been achieved on 512 nodes of the Intel Delta machine,k for a problem size of 1024 K equations (256 K grid points). Author

N94-36685# Los Alamos National Lab., NM.
NONLINEARITY WITH DISORDER: SPATIO-TEMPORAL COMPLEX BEHAVIOR ARISING FROM LENGTH SCALES COMPETITION
A. Sanchez and A. R. Bishop 20 Sep. 1993 18 p Presented at the Fluctuations and Order: The New Synthesis Workshop, Los Alamos, NM, 9-12 Sep. 1993
(Contract W-7405-eng-36)
(DE94-000675; LA-UR-93-3496; CONF-9309185-3) Avail: CASI HC A03/MF A01

One of the many mechanisms underlying complex behavior in physical systems is competition between different length or time scales, which may arise naturally in the considered system or may be imposed by external influences. The purpose of this paper is the following. By means of three examples the authors will illustrate how identification of relevant length scales can lead to a separation of the system behavior in two regimes.

Far from the competition region, it can be described in very simple ways, usually involving a few degrees of freedom. On the contrary, when relevant scales are in conflict, the behavior of the system turns out to be complex, typically chaotic. Therefore, the success of this approach is that it goes straightforwardly to the deep reasons for complex behavior, making amenable to analytical studies all other regimes. DOE

N94-36723# Air Force Inst. of Tech., Wright-Patterson AFB, OH. School of Engineering.

MULTIRATE TIME-FREQUENCY DISTRIBUTIONS Ph.D. Thesis

John R. OHair May 1994 41 p

(AD-A280595; AFIT/DS/ENG/94-03) Avail: CASI HC A03/MF A01

Multirate systems, which find application in the design and analysis of filter banks, are demonstrated to also be useful as a computational paradigm. It is shown that any problem which can be expressed a set of vector-vector, matrix-vector or matrix-matrix operations can be recast using multirate. This means all of numerical linear algebra can be recast using multirate as the underlying computational paradigm. As a non-trivial example, the multirate computational paradigm is applied to the problem of Generalized Discrete Time-Frequency Distributions (GDTFD) to create a new family of fast algorithms. The first of this new class of distributions is called the Decimated GDTFD (D-GDTFD). These distributions trade bandwidth for speed. For a decimation factor of m, there is an in fold increase in throughput. The D-GDTFD requires significantly less storage than the GDTFD, only 1/m2 of the storage of the GDTFD. By combining several D-GDTFD's, it is possible to reconstruct a GDTFD. This reconstruction of DGDTFD's is the Multirate Time-Frequency Distribution (MRTFD). If the individual D-GDTFD's can also be implemented in parallel, improvement in throughput on the order of m 2 or more results. DTIC

N94-36923*# Institute for Computer Applications in Science and Engineering, Hampton, VA.

A GALERKIN METHOD FOR LINEAR PDE SYSTEMS IN CIRCULAR GEOMETRIES WITH STRUCTURAL ACOUSTIC APPLICATIONS Final Report

Ralph C. Smith (Iowa State Univ. of Science and Technology, Ames, IA.) May 1994 34 p Submitted for publication

(Contract NAS1-19480; NAG1-1600; RTOP 505-90-52-01)

(NASA-CR-194925; NAS 1.26:194925; ICASE-94-40) Avail: CASI HC A03/MF A01

A Galerkin method for systems of PDE's in circular geometries is presented with motivating problems being drawn from structural, acoustic, and structural acoustic applications. Depending upon the application under consideration, piecewise splines or Legendre polynomials are used when approximating the system dynamics with modifications included to incorporate the analytic solution decay near the coordinate singularity. This provides an efficient method which retains its accuracy throughout the circular domain without degradation at singularity. Because the problems under consideration are linear or weakly nonlinear with constant or piecewise constant coefficients, transform methods for the problems are not investigated. While the specific method is developed for the two dimensional wave equations on a circular domain and the equation of transverse motion for a thin circular plate, examples demonstrating the extension of the techniques to a fully coupled structural acoustic system are used to illustrate the flexibility of the method when approximating the dynamics of more complex systems. Author (revised)

N94-36991*# Institute for Computer Applications in Science and Engineering, Hampton, VA.

PARAMETER ESTIMATION IN A STRUCTURAL ACOUSTIC SYSTEM WITH FULLY NONLINEAR COUPLING CONDITIONS Final Report

H. T. Banks (North Carolina Univ., Raleigh, NC.) and Ralph C. Smith (Iowa State Univ. of Science and Technology, Ames, IA.) May 1994 42 p Submitted for publication

(Contracts NAS1-19480; F49620-93-1-0198; AF-AFOSR-0091-90; RTOP 505-90-52-01)

(NASA-CR-194926; NAS 1.26:194926; ICASE-94-41) Avail: CASI HC A03/MF A01

A methodology for estimating physical parameters in a class of structural acoustic systems is presented. The general model under consideration consists of an interior cavity which is separated from an exterior noise source by an enclosing elastic structure. Piezoceramic patches are bonded to or embedded in the structure; these can be used both as actuators and sensors in applications ranging from the control of interior noise levels to the determination of structural flaws through nondestructive evaluation techniques. The presence and excitation of patches, however, changes the geometry and material properties of the structure as well as involves unknown patch parameters, thus necessitating the development of parameter estimation techniques which are applicable in this coupled setting. In developing a framework for approximation, parameter estimation and implementation, strong consideration is given to the fact that the input operator is unbonded due to the discrete nature of the patches. Moreover, the model is weakly nonlinear. As a result of the coupling mechanism between the structural vibrations and the interior acoustic dynamics. Within this context, an illustrating model is given, well-posedness and approximations results are discussed and an applicable parameter estimation methodology is presented. The scheme is then illustrated through several numerical examples with simulations modeling a variety of commonly used structural acoustic techniques for systems excitations and data collection. Author

N94-37073# Oak Ridge National Lab., TN.

A METHOD FOR OBTAINING A LEAST SQUARES FIT OF A HYPERPLANE TO UNCERTAIN DATA

D. B. Reister and M. D. Morris May 1994 16 p

(Contract DE-AC05-84OR-21400)

(DE94-012498; ORNL/TM-12686) Avail: CASI HC A03/MF A01

For many least squares problems, the uncertainty is in one of the variables, for example, $y = f(x)$ or $z = f(x,y)$. However, for some problems, the uncertainty is in the geometric transformation from measured data to Cartesian coordinates and all of the calculated variables are uncertain. When we seek the best least squares fit of a hyperplane to the data, we obtain an over determined system (we have $n + 1$ equations to determine n unknowns). By neglecting one of the equations at a time, we can obtain $n + 1$ different solutions for the unknown parameters. However, we cannot average the $n + 1$ hyperplanes to obtain a single best estimate. To obtain a solution without neglecting any of the equations, we solve an eigenvalue problem and use the eigenvector associated with the smallest eigenvalue to determine the unknown parameters. We have performed numerical experiments that compare our eigenvalue method to the approach of neglecting one equation at a time. DOE

N94-37098 Joint Inst. for Nuclear Research, Dubna (USSR). Lab. of Computing Techniques and Automation.

COST-EFFECTIVE COMPUTATIONS WITH BOUNDARY INTERFACE OPERATORS IN ELLIPTIC PROBLEMS

B. N. Khoromskij, G. E. Mazurkevich, and E. G. Nikonov 1993 23 p Limited Reproducibility: More than 20% of this document may be affected by microfiche quality

(DE94-621506; JINR-E-11-93-163) Avail: CASI HC A03 (US Sales Only)

The numerical algorithm for fast computations with interface operators associated with the elliptic boundary value problems (BVP) defined on step-type domains is presented. The algorithm is based on the asymptotically almost optimal technique developed for treatment of the discrete Poincare-Steklov (PS) operators associated with the finite-difference Laplacian on rectangles when using the uniform grid with a 'displacement by h/2'. The approach can be regarded as an extension of the method proposed for the partial solution of the finite-difference Laplace equation to the case of displaced grids and mixed boundary conditions. It is shown that the action of the PS operator for the Dirichlet problem and mixed BVP can be computed with expenses of the order of O(Nlog(sup 2)N) both for arithmetical operations and computer memory needs, where N is the number of unknowns on the rectangle boundary. The single domain algorithm is applied to solving the multidomain elliptic interface problems with piecewise constant coefficients. The numerical experiments presented confirm almost linear growth of the computational costs and memory needs with respect to the dimension of the discrete interface problem. DOE

N94-37146 California Univ., Santa Barbara, CA. Dept. of Electrical and Computer Engineering.

SOLVING ILL-CONDITIONED MATRIX EQUATIONS IN CONTROL Final Technical Report, 15 Jun. 1991 - 14 Oct. 1993

Marc Q. Jacobs May 1994 10 p Limited Reproducibility: More than

20% of this document may be affected by microfiche quality
(Grant AF-AFOSR-0240-91)
(AD-A280502; UCSB-TR-1; AFOSR-94-0360TR) Avail: CASI HC A02

The primary objective of this grant has been the study of algorithms for solving ill-conditioned matrix equations arising in control, filtering, and system theory. Much of our work has concentrated on matrix Riccati and Lyapunov equations which are absolutely fundamental to the field. We have made significant advances on a number of fronts in the numerical solution of large-scale and ill-conditioned Lyapunov, Sylvester, and Riccati equations. Substantial progress has been made in other areas as well, including a new family of algorithms based on matrix interpolation for frequency response and related problems, a number of key advances in numerical linear algebra, algorithms for infinite-dimensional systems, a new theory of small sample statistical condition estimation, and software implementations of many of our algorithms. Our results have been reported in over thirty scholarly articles. DTIC

N94-37170# Academy of Sciences (USSR), Novosibirsk (USSR). Inst. Yadernoj Fiziki.
WICK-CUTKOVSKY MODEL: AN INTRODUCTION [MODEL' VIKA-KATKOVSKOGO: VVEDENIE]
Z. K. Silagadze 1992 74 p In RUSSIAN
(DE94-618365; IYaF-92-33) Avail: CASI HC A04/MF A01 (US Sales Only)

Introduction in the Wick-Cutkovsky (WC) quantum model for a two-particle bound state is considered. The model corresponds to the interaction of two scalar particles through the scalar massless quantum exchange in the ladder approximation. The Bethe-Salpeter equation in the nonrelativistic theory and the Fock method for a two-dimensional hydrogen atom are considered. Problems of the stereographic projection in a general form and in the WC model are discussed. It is noted that the WC model has the SO(4) hidden symmetry for equal and unequal masses. DOE

N94-37174# Joint Inst. for Nuclear Research, Dubna (USSR). Lab. of Theoretical Physics.
SOLVING THE TWO-DIMENSIONAL SCHROEDINGER EQUATION IN SELF-CONSISTENT BASIS [RESHENIE DVUMERNOGO URAVNENIYA SHREDINGERA V SAMOSOGLASOVANNOM BAZISE]
S. I. Vinitskij, E. V. Inopin, and N. A. Chekanov 1993 11 p In RUSSIAN Presented at the 1993 Laser Physics International Conference, Moscow, Russia, Jun. - Jul. 1993
(DE94-621535; JINR-R-4-93-150) Avail: CASI HC A03/MF A01 (US Sales Only)

New approach for numerical calculations of energy spectra and wave functions of two-dimensional Schroedinger equation is presented. This approach is more preferable for the Hamiltonians with the complicated potential energy surface in comparison with direct diagonalization method. The formulation of the approach is given for the example of the C3(nu) symmetric Hamiltonian. DOE

N94-37175# Joint Inst. for Nuclear Research, Dubna (USSR). Lab. of Computing Techniques and Automation.
NUMERICAL SOLUTION TO THE BOUNDARY-VALUE PROBLEM FOR THE BETHE-SALPETER EQUATION WITH QUADRATICALLY RISING POTENTIAL [CHISLENNOE RESHENIE KRAEVOJ ZADACHI DIYA URAVNENIYA BETE-SOLPITERS S KVADRATICHNO RASTUSHCHIM POTENTSIALOM]
I. V. Amirkhanov, T. Z. Nasirov, and N. A. Sarikov 1993 16 p In RUSSIAN
(DE94-621606; JINR-R-11-93-173) Avail: CASI HC A03/MF A01 (US Sales Only)

An algorithm for the numerical solving of the boundary value problem for bound states of two quarks described by the Bethe-Salpeter equation with oscillator potential is proposed. In the algorithm the iterative scheme of the continuous analog of the Newton's method is realized. The initial approximation was found by the method of 'contrary' progonka. Numerical values of the masses of the basic and excited states for pseudoscalar, scalar-vector and axially-vector mesons are obtained. DOE

N94-37246# Argonne National Lab., IL. Mathematics and Computer Science Div.
THE IMPACT OF HPF DATA LAYOUT ON THE DESIGN OF EFFICIENT AND MAINTAINABLE PARALLEL LINEAR ALGEBRA LIBRARIES
Technical Memorandum No. 184
C. H. Bischof, S. Huss-Lederman, E. M. Jacobson, Xiaobai Sun, and A. Tsao Mar. 1994 8 p
(Contract W-31-109-eng-38)
(DE94-012382; ANL/MCS-TM-184) Avail: CASI HC A02/MF A01

In this document, the authors are concerned with the effects of data layouts for nonsquare processor meshes on the implementation of common dense linear algebra kernels such as matrix-matrix multiplication, LU factorizations, or eigenvalue solvers. In particular, they address ease of programming and tunability of the resulting software. They introduce a generalization of the torus wrap data layout that results in a decoupling of 'local' and 'global' data layout view. As a result, it allows for intuitive programming of linear algebra algorithms and for tuning of the algorithm for a particular mesh aspect ratio or machine characteristics. This layout is as simple as the proposed HPF layout but, in the authors opinion, enhances ease of programming as well as case of performance tuning. They emphasize that they do not advocate that all users need be concerned with these issues. They do, however, believe, that for the foreseeable future 'assembler coding' (as message-passing code is likely to be viewed from an HPF programmers' perspective) will be needed to deliver high performance for computationally intensive kernels. As a result, they believe that the adoption of this approach not only would accelerate the generation of efficient linear algebra software libraries but also would accelerate the adoption of HPF as a result. They point out, however, that the adoption of this new layout would necessitate that an HPF compiler ensure that data objects are operated in a consistent fashion across subroutine and function calls. DOE

N94-37247# Argonne National Lab., IL.
AUTOMATIC, SELF-ADAPTIVE CONTROL OF UNFOLD TRANSFORMATIONS
James M. Boyle 1994 26 p Presented at the International Federation for Information Processing Conference on Programming Concepts, Methods and Calculi, San Miniato, Italy, 6-10 Jun. 1994
(Contract W-31-109-eng-38)
(DE94-012455; ANL/MCS/CP-82092; CONF-9406170-1) Avail: CASI HC A03/MF A01

I describe an automated approach to partial evaluation based on elementary simplifications and implemented by program transformations. The approach emphasizes program algebra and relies on canonical forms and distributive laws to expose instances to which the elementary simplifications apply. I discuss some of the considerations that led to the design of this approach. This design discussion should be useful both in understanding the structure of the partial evaluation transformations themselves, and as an example of how to approach the design of automated program transformations in general. This approach to partial evaluation has been applied to a number of practical examples of moderate complexity, including eliminating a data structure from a specification of practical interest, a partial-differential-equation solver. This approach has the virtues of being implemented, automated, and able to partially evaluate specifications of practical interest. DOE

N94-37375 Gosudarstvennyi Komitet po Ispolzovaniyu Atomnoi Energii, Serpukhov (USSR). Inst. Fiziki Vysokikh Ehnergij.
THE CANONICAL SYMMETRY FOR INTEGRAL SYSTEMS
A. N. Lesnov and A. V. Rasumov 1992 20 p Submitted for publication Limited Reproducibility: More than 20% of this document may be affected by microfiche quality
(DE94-618486; IHEP-OTF-92-146) Avail: CASI HC A03 (US Sales Only)

The properties of discrete nonlinear symmetries of integral equations are investigated. These symmetries are shown to be canonical transformations. On the basis of the considered examples, it is concluded, that the densities of the conservation laws are changed under these transformations by spatial divergencies. DOE

N94-37449*# MCAT Inst., San Jose, CA.
DEVELOPMENT OF ADVANCED NAVIER-STOKES SOLVER
Seokkwan Yoon Jun. 1994 20 p

(Contract NCC2-505)
(NASA-CR-195094; NAS 1.26:195094; MCAT-94-004) Avail: CASI HC A03/MF A01

The objective of research was to develop and validate new computational algorithms for solving the steady and unsteady Euler and Navier-Stokes equations. The end-products are new three-dimensional Euler and Navier-Stokes codes that are faster, more reliable, more accurate, and easier to use. The three-dimensional Euler and full/thin-layer Reynolds-averaged Navier-Stokes equations for compressible/incompressible flows are solved on structured hexahedral grids. The Baldwin-Lomax algebraic turbulence model is used for closure. The space discretization is based on a cell-centered finite-volume method augmented by a variety of numerical dissipation models with optional total variation diminishing limiters. The governing equations are integrated in time by an implicit method based on lower-upper factorization and symmetric Gauss-Seidel relaxation. The algorithm is vectorized on diagonal planes of sweep using two-dimensional indices in three dimensions. Convergence rates and the robustness of the codes are enhanced by the use of an implicit full approximation storage multigrid method. Derived from text

N94-37483 Academy of Sciences (USSR), Kiev (USSR). Inst. for Theoretical Physics.
REPRESENTATIONS OF THE q-DEFORMED ALGEBRAS U(q) (so(2,1)) AND U(q) (so(3,1)
O. M. Gavrilik and A. U. Klimyk 1993 23 p Submitted for publication
Limited Reproducibility: More than 20% of this document may be affected by microfiche quality
(DE94-616619; ITP-93-29E) Avail: CASI HC A03 (US Sales Only)

Representations of algebra U(sub q) (so(sub 2,1)) are studied. This algebra is a q-deformation of the universal enveloping algebra U(so(sub 2,1)) of the Lie algebra of the group SO(sub 0)(2,1) and differs from the quantum algebra U(sub q)(SU(sub 1,1)). Classifications of irreducible representations and of infinitesimally irreducible representations of U(sub q)(SU(sub 1,1)). The sets of irreducible representations and of infinitesimally unitary irreducible representations of the algebra U(sub q)(so(sub 3,1)) are given. We also consider representations of U(sub q)(so(sub n,1)) which are of class 1 with respect to subalgebra U(sub q)(so(sub n)). DOE

N94-37497# Lawrence Livermore National Lab., Livermore, CA.
MULTIQUADRIC COLLOCATION METHODS IN THE NUMERICAL SOLUTION OF VOLTERRA INTEGRAL EQUATIONS WITH WEAKLY SINGULAR KERNELS
A. Makroglou (Manchester Univ., England.) and E. J. Kansa Dec. 1993 5 p
(Contract W-7405-eng-48)
(DE94-013000; UCRL-CR-116109-Summ) Avail: CASI HC A01/MF A01

Nonlinear Volterra integral equation with weakly singular kernels are considered and are solved by applying piecewise collocation methods based on multiquadric approximations combined with Gauss quadrature rules. DOE

N94-37518# Argonne National Lab., IL.
PARALLEL TRIDIAGNOALIZATION THROUGH TWO-STEP BAND REDUCTION
C. Bischof, X. Sun, and B. Lang 1994 5 p Presented at the Scalable High Performance Computing Conference, Knoxville, TN, 23 May 1994
(Contract W-31-109-eng-38)
(DE94-011512; ANL/MCS/CP-82803; CONF-9405100-4) Avail: CASI HC A01/MF A01

We present a two-step variant of the 'successive band reduction' paradigm for the tridiagonalization of symmetric matrices. Here we reduce a full matrix first to narrow-banded form and then to tridiagonal form. The first step allows easy exploitation of block orthogonal transformations. In the second step, we employ a new blocked version of a banded matrix tridiagonalization algorithm by Lang. In particular, we are able to express the update of the orthogonal transformation matrix in terms of block transformations. This expression leads to an algorithm that is almost entirely based on BLAS-3 kernels and has greatly improved data movement and communication characteristics. We also present some performance results on the Intel Touchstone DELTA and the IBM SP1. DOE

N94-37540*# Institute for Computer Applications in Science and Engineering, Hampton, VA.
FINITE ELEMENT APPROXIMATION OF AN OPTIMAL CONTROL PROBLEM FOR THE VON KARMAN EQUATIONS Final Report
L. Steven Hou (York Univ., Ontario.) and James C. Turner (Ohio State Univ., Columbus.) Jul. 1994 18 p Submitted for publication
(Contracts NAS1-19480; RTOP 505-90-52-01; DAAL03-91-G-0237; NSERC-OGP-0137436)
(NASA-CR-194955; NAS 1.26:194955; ICASE-94-63) Avail: CASI HC A03/MF A01

This paper is concerned with optimal control problems for the von Karman equations with distributed controls. We first show that optimal solutions exist. We then show that Lagrange multipliers may be used to enforce the constraints and derive an optimality system from which optimal states and controls may be deduced. Finally we define finite element approximations of solutions for the optimality system and derive error estimates for the approximations. Author

N94-37620# Sandia National Labs., Albuquerque, NM.
LINEAR-SIZE NONOBTUSE TRIANGULATION OF POLYGONS
M. Bern (Xerox Palo Alto Research Center, CA.), S. Mitchell, and J. Ruppert 1994 10 p Presented at the 10th Annual Symposium on Computational Geometry, Stony Brook, NY, 6-8 Jun. 1994
(Contract DE-AC04-94AL-85000)
(DE94-010746; SAND-94-1045C; CONF-9406162-1) Avail: CASI HC A02/MF A01

We give an algorithm for triangulating n-vertex polygonal regions (with holes) so that no angle in the final triangulation measures more than pi/2. The number of triangles in the triangulation is only 0(n), improving a previous bound of 0(n(sup 2)), and the worst-case running time is 0(n log(sup 2)n). The basic technique used in the algorithm, recursive subdivision by disks, is new and may have wider application in mesh generation. We also report on an implementation of our algorithm. DOE

N94-37655*# Research Inst. for Advanced Computer Science, Moffett Field, CA.
TENSOR-GMRES METHOD FOR LARGE SPARSE SYSTEMS OF NONLINEAR EQUATIONS
Dan Feng and Thomas H. Pulliam Jul. 1994 41 p
(Contract NAS2-13721)
(NASA-CR-196379; NAS 1.26:196379; RIACS-TP-94-12) Avail: CASI HC A03/MF A01

This paper introduces a tensor-Krylov method, the tensor-GMRES method, for large sparse systems of nonlinear equations. This method is a coupling of tensor model formation and solution techniques for nonlinear equations with Krylov subspace projection techniques for unsymmetric systems of linear equations. Traditional tensor methods for nonlinear equations are based on a quadratic model of the nonlinear function, a standard linear model augmented by a simple second order term. These methods are shown to be significantly more efficient than standard methods both on nonsingular problems and on problems where the Jacobian matrix at the solution is singular. A major disadvantage of the traditional tensor methods is that the solution of the tensor model requires the factorization of the Jacobian matrix, which may not be suitable for problems where the Jacobian matrix is large and has a 'bad' sparsity structure for an efficient factorization. We overcome this difficulty by forming and solving the tensor model using an extension of a Newton-GMRES scheme. Like traditional tensor methods, we show that the new tensor method has significant computational advantages over the analogous Newton counterpart. Consistent with Krylov subspace based methods, the new tensor method does not depend on the factorization of the Jacobian matrix. As a matter of fact, the Jacobian matrix is never needed explicitly. Author

N94-37675 Brookhaven National Lab., Upton, NY.
SYMPLECTIC TRACKING USING POINT MAGNETS AND A REFERENCE ORBIT MADE OF CIRCULAR ARCS AND STRAIGHT LINES
G. Parzen 1994 3 p Presented at the 4th European Particle Accelerator Conference, London, England, 27 Jun. - 1 Jul. 1994 Limited Reproducibility: More than 20% of this document may be affected by microfiche quality
(Contract DE-AC02-76CH-00016)
(DE94-011919; BNL-49799; CONF-940618-1) Avail: CASI HC A03

Symplectic tracking with point magnets is achieved using a reference orbit made up of circular arcs and straight lines. For this choice of the reference orbit, results are given for the transfer functions, transfer matrices and the transit times of the magnets. DOE

N94-37718# California Univ., Berkeley. Lawrence Berkeley Lab, CA.
A LAGRANGIAN-EULERIAN FINITE ELEMENT METHOD WITH ADAPTIVE GRIDDING FOR ADVECTION-DISPERSION PROBLEMS
Y. Ijiri and K. Karasaki Feb. 1994 15 p Presented at the Computational Methods in Water Resources, Heidelberg, Germany, 19-22 Jul. 1994
(Contract DE-AC03-76SF-00098)
(DE94-011372; LBL-35224; CONF-940742-5) Avail: CASI HC A03/MF A01

In the present paper, a Lagrangian-Eulerian finite element method with adaptive gridding for solving advection-dispersion equations is described. The code creates new grid points in the vicinity of sharp fronts at every time step in order to reduce numerical dispersion. The code yields quite accurate solutions for a wide range of mesh Peclet numbers and for mesh Courant numbers well in excess of 1. DOE

N94-37719# California Univ., Berkeley. Lawrence Berkeley Lab, CA.
A NOTE ON ANALYTIC RECOVERY OF TRANSITION PROBABILITIES IN THREE DIMENSIONAL DIFFUSE TOMOGRAPHY
S. K. Patch Feb. 1994 13 p Presented at the Society of Photo-Optical Instrumentation Engineers Conference on Intelligent Information Systems, Orlando, FL, 4-8 Apr. 1994 r. 1994
(Contract DE-AC03-76SF-00098)
(DE94-011378; LBL-35281; CONF-940449-8) Avail: CASI HC A03/MF A01

The word 'tomography' refers to imaging an object by slices. X rays, for example, have high energy and travel straight through the body. Data analysis is linear and yields a scalar valued function. The oxymoron diffuse tomography refers to low energy imaging in which the paths of the radiant energy are not necessarily straight and are unknown. Data analysis in diffuse tomography is highly nonlinear and yields a vector valued function. Problems in diffuse tomography are highly nonlinear because low energy is used. Clinical applications such as neonatal imaging and annual mammograms are not amenable to high energy techniques which might overexpose the patient to harmful radiation. Experimentalists in the medical arena are presently working with near infrared radiation; mathematicians have done preliminary mathematical analysis of diffuse tomographic methods. An analytic algorithm for recovering Markov transition probabilities from boundary value data for the smallest nontrivial problem in three dimensions is outlined in this paper. DOE

N94-37833# Helsinki Univ. of Technology, Espoo (Finland). Inst. of Mathematics.
NOTE ON CERTAIN RIGID SUBSHIFTS
K. Eloranta Nov. 1993 12 p
(PB94-179058; ISBN-951-22-1833-X) Avail: CASI HC A03/MF A01

We study the subshifts of finite type on (0, 1)(sup Z(sup 2)) having the property that in every 3 X 3 square there is a fixed number of ones. In particular, we investigate shift-deformations of allowed configurations and show the topological non-transitivity of the shift-action. The last property is also shown to hold for all two-dimensional subshifts of the same generalized type. NTIS

N94-37852 Institut des Hautes Etudes Scientifiques, Bures-sur-Yvette (France).
LOCALIZATION OF TOPOLOGICAL PONTRYAGIN CLASSES BY PROPAGATION WITH FINITE SPEED
H. Moscovici and F. Wu Aug. 1993 30 p Limited Reproducibility: More than 20% of this document may be affected by microfiche quality
(PB94-180866; IHES/M/93/44) Avail: CASI HC A03

The amount of twisting needed to build a smooth manifold M from local charts is encoded at the fine, geometric level in certain globally defined closed forms, manufactured out of local curvature matrices, and at the topological level in their classes modulo exact forms, which constitute the Pontryagin classes of M. Curvatures, and hence the Pontryagin forms, involve two derivatives. However, the (rational) Pontryagin classes make perfect sense when M is only a topological manifold. Reconstructing the topological Pontryagin classes from local data has been a longstanding problem. The authors announced in a 1993 paper, a local construction of the real Pontryagin classes of topological manifolds based on a 1990 paper by Connes and Moscovici, which however employs unbounded realizations for the K-orientation class, given by the Lipschitz signature operators constructed in a 1983 paper by Teleman. It is the purpose of the paper to supply complete proofs for the results claimed in the authors' 1993 paper. NTIS

N94-37853 Institut des Hautes Etudes Scientifiques, Bures-sur-Yvette (France).
EIGENFUNCTION BOUNDS FOR COMPACT MANIFOLDS WITH INTEGRABLE GEODESIC FLOW
J. Bourgain Sep. 1993 9 p Limited Reproducibility: More than 20% of this document may be affected by microfiche quality
(PB94-180874; IHES/M/93/49) Avail: CASI HC A02

In this note the authors investigate the size of eigenfunctions of the Laplace-Beltrami operator on a compact smooth manifold X without boundary. NTIS

65 STATISTICS AND PROBABILITY

Includes data sampling and smoothing; Monte Carlo method; and stochastic processes.

N94-36449# Los Alamos National Lab., NM.
MCNP: MULTIGROUP/ADJOINT CAPABILITIES
J. C. Wagner, E. L. Redmond, II, S. P. Palmtag, and J. S. Hendricks Apr. 1994 119 p
(Contract W-7405-eng-36)
(DE94-010682; LA-12704) Avail: CASI HC A06/MF A02

This report discusses various aspects related to the use and validity of the general purpose Monte Carlo code MCNP for multigroup/adjoint calculations. The increased desire to perform comparisons between Monte Carlo and deterministic codes, along with the ever-present desire to increase the efficiency of large MCNP calculations has produced a greater user demand for the multigroup/adjoint capabilities. To more fully utilize these capabilities, we review the applications of the Monte Carlo multigroup/adjoint method, describe how to generate multigroup cross sections for MCNP with the auxiliary CRSRD code, describe how to use the multigroup/adjoint capability in MCNP, and provide examples and results indicating the effectiveness and validity of the MCNP multigroup/adjoint treatment. This information should assist users in taking advantage of the MCNP multigroup/adjoint capabilities. DOE

N94-36728# Educational Testing Service, Princeton, NJ.
DEALING WITH UNCERTAINTY ABOUT ITEM PARAMETERS: EXPECTED RESPONSE FUNCTIONS Final Report
Robert J. Mislevy, Marilyn S. Wingersky, and Kathleen M. Sheehan Apr. 1994 49 p
(Contract N00014-88-K-0304; NR Proj. RR0-4204)
(AD-A280610; ETS-RR-94-28-ONR) Avail: CASI HC A03/MF A01

It is a common practice in item response theory (IRT) to treat estimates of item parameters, say B, as if they were the known, true quantities, B. However, ignoring the uncertainty associated with item parameters can lead to biases and over-confidence in subsequent inferences such as ability estimation, especially when item-calibration samples are small. This paper demonstrates how to incorporate uncertainty about B with Lewis's expected response functions (ERF's), pointwise expected values of item response conditional on examinee proficiency averaged over posterior distributions of item parameters. This paper presents ERF's, outlines procedures for computing them and using them in practical work, and gives an illustration with data from the National Assessment of Educational Progress. Advantages of approximating ERF's response curves with members of familiar parametric families of IRT curves are noted. DTIC

N94-36732# Educational Testing Service, Princeton, NJ.
PROBABILITY-BASED INFERENCE IN COGNITIVE DIAGNOSIS Final Report
Robert J. Mislevy Feb. 1994 58 p
(Contract N00014-88-K-0304; NR Proj. RR0-4204)
(AD-A280553; ETS-RR-94-3-ONR) Avail: CASI HC A04/MF A01

Recent developments in cognitive psychology suggest models for knowledge and learning that often fall outside the realm of standard test theory. This paper concerns probability-based inference in terms of such models. An approach utilizing Bayesian inference networks is outlined. Basic ideas of structure and computation in inference networks are discussed, and illustrated with an example from the domain of mixed-number subtraction. DTIC

N94-37046 Educational Testing Service, Princeton, NJ.
VIRTUAL REPRESENTATION OF IID OBSERVATIONS IN BAYESIAN BELIEF NETWORKS Final Report
Robert J. Mislevy Apr. 1994 20 p Limited Reproducibility: More than 20% of this document may be affected by microfiche quality
(Contract N00014-88-K-0304; Proj. RR0-4204)
(AD-A280552; ETS-RM-94-13-ONR) Avail: Issuing Activity (Defense Technical Information Center (DTIC))

Local computation for updating Bayesian belief networks proceeds in the context of a 'join tree,' consisting of subsets of interrelated variables (cliques) joined by their intersection sets in a singly-connected graphical structure. When multiple independent and identically-distributed (IID) observations of a variable can be made, identically structured cliques corresponding to each potential observation appear as terminal nodes in the join tree. This note shows how it is possible to absorb information from an indefinite number of observations of this type without preconstructing and manipulating cliques for all potential observations. An update and replace strategy carries the necessary information with only two nodes for a family of IID observations of a variable at any point in time. DTIC

N94-37062# Gosudarstvennyi Komitet po Ispolzovaniyu Atomnoi Energii, Serpukhov (USSR). Inst. of High Energy Physics.
VARIATIONAL DISCRETE SYMMETRIES
A. N. Lesnov, A. B. Shabat, and R. I. Yamilov 1992 10 p
(DE94-618485; IHEP-OTF-92-143) Avail: CASI HC A02/MF A01 (US Sales Only)

The invertible differential substitutions that conserve the standard Poisson brackets and act on Hamiltonians in an appropriate way are considered. These canonical auto-Baecklund transformations proved to be a very simple and efficient tool in the theory of solitons. In particular, these allow one to prove a general involutivity theorem and to build up simple formulae for soliton-like solutions of (2+1)-dimensional Hamiltonian systems as well as in (1+1)-dimensional case. DOE

N94-37564# Sandia National Labs., Albuquerque, NM.
ON THE USE OF FUZZY LOGIC ASSESSMENT FOR HIGH CONSEQUENCE IMPLEMENTATION RISK ANALYSIS
S. Spray, A. Cooper, and R. Bennett 1994 8 p Presented at the National Aeronautics and Space Administration (NASA) Symposium on Neural Fuzzy Logic, San Diego, CA, 9-10 Jun. 1994
(Contract DE-AC04-94AL-85000)
(DE94-011417; SAND-94-1347C; CONF-9406160-1) Avail: CASI HC A02/MF A01

'High consequence' operations are systems, structures, and/or strategies for which it is crucial to provide assured protection against some potential catastrophe or catastrophes. The word 'catastrophe' implies a significant loss of a resource (e.g., money, lives, health, environment, national security, etc.). The implementation of operations that are to be as catastrophe-free as possible must incorporate a very high level of protection. Unfortunately, real world limitations on available resources, mainly money and time, preclude absolute protection. For this reason, conventional 'risk analysis' focuses on cost-effective protection, demonstrating through analysis that the benefits of any protective measures chosen outweigh their cost. This is a 'crisp' one-parameter (usually monetary) comparison. A major problem with this approach, especially for high consequence operations, is that it may not be possible to accurately determine quantitative 'costs,' and furthermore, the costs may not be accurately quantifiable. Similarly, it may not be possible to accurately determine or to quantify the benefits of protection in high consequence operations. These weaknesses are addressed in this paper by introducing multiple parameters instead of a single monetary measure both for costs of implementing protective measures and their benefits. In addition, a fuzzy-algebra comparison based on fuzzy number theory is introduced as a tool in providing cost/benefit tradeoff depiction, with the incorporation of measures of the uncertainty that necessarily exists in the input information. The result allows a more informative comparison to be made through use of fuzzy results, especially at the extreme bounds of the uncertainty. DOE

N94-37327# Pratt and Whitney Aircraft, West Palm Beach, FL.
STATISTICAL CHARACTERIZATION OF RARE EVENTS
Charles Annis and Sharon Vukelich *In* AGARD, Impact of Materials Defects on Engine Structures Integrity Apr. 1993 10 p (For primary document see N94-37321 12-38)
Copyright Avail: CASI HC A02/MF A02

66 SYSTEMS ANALYSIS

Includes mathematical modeling; network analysis; and operations research.

N94-36970 Air Force Inst. of Tech., Wright-Patterson AFB, OH. School of Engineering.
A MEAN VALUE ANALYSIS HEURISTIC FOR ANALYSIS OF AIRCRAFT SORTIE GENERATION M.S. Thesis
Richard C. Jenkins Mar. 1994 91 p Limited Reproducibility: More than 20% of this document may be affected by microfiche quality
(AD-A278578; AFIT/GOR/ENS/94M-07) Avail: CASI HC A05

The primary objective of this study was to develop an analytical methodology based on the Mean Value Analysis algorithm that approximates the performance characteristics of a queueing network model (QNM) containing a fork-join queue with probabilistic branching. These performance characteristics are response time, throughput and queue length at each station. The QNM solved contains the essential features of the aircraft sortie generation process. The sensitivity of the method's accuracy to increases in server utilization was determined. The comparisons of the results of the MVA heuristic to the outputs of the Logistics Composite Model (LCOM) simulation indicate that the heuristic's accuracy decreased as server utilization increases. When server utilization was kept in realistic ranges, the results of the heuristic for a single fork-join queue were very accurate. For non-maintenance stations, results were within 1 to 2 percent of the LCOM simulation output. For stations on the fork-join queue paths, heuristic results were within 5 percent of the LCOM simulation's output for that portion of the network. DTIC

N94-36633# British Aerospace Defence Ltd., Preston (England). Military Aircraft Div.
SENSOR DATA FUSION FOR AIR TO AIR SITUATION AWARENESS BEYOND VISUAL RANGE
C. A. Noonan, M. E. Everett, and R. C. Freeman *In* AGARD, Pointing and Tracking Systems May 1994 8 p (For primary document see N94-36616 12-18)
Copyright Avail: CASI HC A02/MF A02

67 THEORETICAL MATHEMATICS

Includes topology and number theory.

N94-37028 Maryland Univ., College Park, MD.
THEORETICAL INVESTIGATIONS OF CHAOTIC DYNAMICS Final Report, 1 Nov. 1991 - 31 Oct. 1993
James Yorke 31 Oct. 1993 12 p Limited Reproducibility: More than 20% of this document may be affected by microfiche quality
(Contract F49620-92-J-0033)
(AD-A280325; AFOSR-04-0348TR) Avail: Issuing Activity (Defense Technical Information Center (DTIC))

An important component of the work for AFOSR was the discovery and investigation of 'riddled basins.' A riddled basin for a chaotic attractor's basin is arbitrarily close to points in another attractor's basin (the first basin is riddled with holes). When an attractor has a riddled basin there is an extreme end-state sensitivity to initial conditions in the sense that for any initial condition in the riddled basin an arbitrarily small error in computation can result in the erroneous prediction of which attractor the initial condition is eventually attracted to. This contrasts with the more

usual situation of a chaotic attractor with a nonriddled basin where any error in computation propagates exponentially but one can reliably say which attractor the initial condition is attracted to. Since the researchers' discovery of the phenomenon of riddled basins, physical examples have been found in scattering, statistical mechanical, and ecological models. As can be seen from the bibliography, they have also done extensive work in other areas of dynamics, including the properties of indecomposable continua occurring in models of turbulent fluid flow. DTIC

N94-37130 Air Force Inst. of Tech., Wright-Patterson AFB, OH. School of Engineering.
EMBEDDED CHAOTIC TIME SERIES: APPLICATIONS IN PREDICTION AND SPATIO-TEMPORAL CLASSIFICATION Ph.D. Thesis
James R. Stright Jun. 1994 147 p Limited Reproducibility: More than 20% of this document may be affected by microfiche quality
(AD-A280690; AFIT/DS/ENG/94J-04) Avail: Issuing Activity (Defense Technical Information Center (DTIC))

The Deterministic Versus Stochastic algorithm developed by Martin Casdagli is modified to produce two new methodologies, each of which selectively uses embedding space nearest neighbors. Neighbors which are considered prediction relevant are retained for local linear prediction, while those which are considered likely to represent noise are ignored. For many time series, it is shown possible to improve on local linear prediction with both of the new algorithms. Furthermore, the theory of embedology is applied to determine a length of test sequence sufficient for accurate classification of moving objects. Sequentially recorded feature vectors of a moving object form a training trajectory in feature space. Each of the sequences of feature vector components is a time series, and under certain conditions, each of these time series has approximately the same fractal dimension. The embedding theorem is applied to this fractal dimension to establish a number of observations sufficient to determine the feature space trajectory of the object. It is argued that this number is a reasonable test sequence length for use in object classification. Experiments with data corresponding to five military vehicles (observed following a projected Lorenz trajectory on a viewing sphere) show that this number is indeed adequate. DTIC

70 PHYSICS (GENERAL)

For precision time and time interval (PTTI) see *35 Instrumentation and Photography;* for geophysics, astrophysics or solar physics see *46 Geophysics, 90 Astrophysics,* or *92 Solar Physics.*

N94-36556# Los Alamos National Lab., NM.
DESIGN AND ANALYSIS OF HIGH-FIELD QUASI-CONTINUOUS MAGNETS
H. J. Boenig, L. J. Campbell, D. G. Rickel, J. D. Rogers, J. B. Schillig, J. R. Sims, P. Pernambuco-Wise, H. J. Schneider-Muntau, and L. VanBockstal 1993 5 p Presented at the 13th International Conference on Magnet Technology, Victoria, Ontario, 20-24 Sep. 1993
(Contract W-7405-eng-36)
(DE94-000762; LA-UR-93-3390; CONF-930926-2) Avail: CASI HC A01/MF A01

Pulsed magnets of 60 tesla or more with a flat-top of 100 ms (quasi-continuous) are among the user facilities to be provided by the NHMFL. The design of such magnets is constrained by available materials and thermal recycle time. The design path discussed here tailors materials and current densities or independent concentric coils. The progressive design steps are illustrated by a specific example of an eight-coil, 60T magnet. In the preliminary design stage closed form calculations of magnetic, structural, thermal, and electrical circuit behavior are used to achieve a practical design that meets initial requirements. Design refinement incorporates finite element analyses and test results on materials, fabrication and prototypes. Higher fields are possible without large changes. DOE

N94-36560# California Univ., Berkeley. Lawrence Berkeley Lab, CA.
QUANTUM HARMONIC BROWNIAN MOTION IN A GENERAL ENVIRONMENT: A MODIFIED PHASE-SPACE APPROACH Ph.D. Thesis
L. Yeh 23 Jun. 1993 128 p
(Contract DE-AC03-76SF-00098)
(DE94-003249; LBL-33448; UCB-PTH-93/01) Avail: CASI HC A07/MF A02

After extensive investigations over three decades, the linear-coupling model and its equivalents have become the standard microscopic models for quantum harmonic Brownian motion, in which a harmonically bound Brownian particle is coupled to a quantum dissipative heat bath of general type modeled by infinitely many harmonic oscillators. The dynamics of these models have been studied by many authors using the quantum Langevin equation, the path-integral approach, quasi-probability distribution functions (e.g., the Wigner function), etc. However, the quantum Langevin equation is only applicable to some special problems, while other approaches all involve complicated calculations due to the inevitable reduction (i.e., contraction) operation for ignoring/eliminating the degrees of freedom of the heat bath. In this dissertation, the author proposes an improved methodology via a modified phase-space approach which employs the characteristic function (the symplectic Fourier transform of the Wigner function) as the representative of the density operator. This representative is claimed to be the most natural one for performing the reduction, not only because of its simplicity but also because of its manifestation of geometric meaning. Accordingly, it is particularly convenient for studying the time evolution of the Brownian particle with an arbitrary initial state. The power of this characteristic function is illuminated through a detailed study of several physically interesting problems, including the environment-induced damping of quantum interference, the exact quantum Fokker-Planck equations, and the relaxation of non-factorizable initial states. All derivations and calculations are shown to be much simplified in comparison with other approaches. In addition to dynamical problems, a novel derivation of the fluctuation-dissipation theorem which is valid for all quantum linear systems is presented. DOE

N94-36643*# Sverdrup Technology, Inc., Brook Park, OH.
LASER-SATURATED FLUORESCENCE MEASUREMENTS IN LAMINAR SOOTING DIFFUSION FLAMES Final Report
Changlie Wey May 1993 18 p
(Contract NAS3-24105; RTOP 505-62-52)
(NASA-CR-191025; E-7771; NAS 1.26:191025) Avail: CASI HC A03/MF A01

The hydroxyl radical is known to be one of the most important intermediate species in the combustion processes. The hydroxyl radical has also been considered a dominant oxidizer of soot particles in flames. In this investigation the hydroxyl concentration profiles in sooting diffusion flames were measured by the laser-saturated fluorescence (LSF) method. The temperature distributions in the flames were measured by the two-line LSF technique and by thermocouple. In the sooting region the OH fluorescence was too weak to make accurate temperature measurements. The hydroxyl fluorescence profiles for all four flames presented herein show that the OH fluorescence intensities peaked near the flame front. The OH fluorescence intensity dropped sharply toward the dark region of the flame and continued declining to the sooting region. The OH fluorescence profiles also indicate that the OH fluorescence decreased with increasing height in the flames for all flames investigated. Varying the oxidizer composition resulted in a corresponding variation in the maximum OH concentration and the flame temperature. Furthermore, it appears that the maximum OH concentration for each flame increased with increasing flame temperature. Author (revised)

N94-36718 National Inst. of Standards and Technology, Gaithersburg, MD.
DETERMINATION OF DENSITY OF MASS STANDARDS: REQUIREMENT AND METHOD
R. M. Schoonover, M.-S. Hwang, and R. Nater Feb. 1994 22 p See also PB91-112854 Limited Reproducibility: More than 20% of this document may be affected by microfiche quality
(PB94-163078; NISTIR-5378) Avail: CASI HC A03

The usual method of a mass assignment to an artifact is by comparing the forces exerted on a balance pan. The observed difference between the standard mass and the unknown object is then expressed as the solution of the two force equations which includes terms for their respective displacement volumes, i.e., densities. With the advent of commercially available balances with precision near the 1 ppb level, the user must pay particular attention to the artifact density and its associated error if the available precision is to be meaningful. Described here are the need and

a method to determine the artifact density, and an error analysis that leads to the selection of the appropriate equipment. Measurements of a 200-g silicon crystal of known density were performed to demonstrate the accuracy of the method. NTIS

N94-36782*# National Aeronautics and Space Administration. Marshall Space Flight Center, Huntsville, AL.
VARIABLE STIFFNESS TORSION SPRINGS Patent Application
Dean C. Alhorn, inventor (to NASA) and Michael E. Polites, inventor (to NASA) 20 May 1994 26 p
(NASA-Case-MFS-28930-1; NAS 1.71:MFS-28930-1; US-Patent-Appl-SN-246460) Avail: CASI HC A03/MF A01

In a torsion spring the spring action is a result of the relationships between the torque applied in twisting the spring, the angle through which the torsion spring twists, and the modulus of elasticity of the spring material in shear. Torsion springs employed industrially have been strips, rods, or bars, generally termed shafts, capabable of being flexed by twisting their axes. They rely on the variations in shearing forces to furnish an internal restoring torque. In the torsion springs herein the restoring torque is external and therefore independent of the shearing modulus of elasticity of the torsion spring shaft. Also provided herein is a variable stiffness torsion spring. This torsion spring can be so adjusted as to have a given spring constant. Such variable stiffness torsion springs are extremely usefui in gimballed payloads such as sensors, telescopes, and electronic devices on such platforms as a space shuttle or a space station. NASA

N94-36948 National Academy of Sciences - National Research Council, Washington, DC. Commission on Physical Sciences, Mathematics, and Applications.
BEGINNING A DIALOGUE ON THE CHANGING ENVIRONMENT FOR THE PHYSICAL AND MATHEMATICAL SCIENCES
1994 59 p
Copyright Avail: Issuing Activity (National Academy of Sciences - National Research Council, Washington, DC)

Although it was our purpose to outline the issues and to improve the focus of our concerns rather than to develop solutions, we did agree that an era of important change is upon us and we should continue to meet to improve our focus on the mathematical and physical sciences, to develop a better set of data, and to think through some responses that address areas where the interests and activities of the universities, government, and industry overlap. It was generally believed that the current dynamic of the research enterprise cannot be sustained. Important changes are already under way in industrial laboratories, the U.S. administration is considering a new approach to science policy and new roles for government laboratories, and universities are experiencing considerable distress in trying to maintain quality and vitality in carrying out their responsibilities within the overall research system. In this rapidly changing environment, new ideas and flexibilities are required, but the greatest need is a better understanding of how our national innovation system, which was greatly changed and vastly expanded after World War 2, needs to be reshaped to meet the civic responsibilities of the science enterprise in the next decade.
Derived from text

N94-37006# Joint Publications Research Service, Arlington, VA.
JPRS REPORT: SCIENCE AND TECHNOLOGY. CENTRAL EURASIA
23 Jun. 1994 91 p Transl. into ENGLISH from Russian articles
(JPRS-UST-94-013) Avail: CASI HC A05/MF A01

Translated articles cover the following topics: power laser with compound beam aperture, phase conjugation mirrors, and pulse compressors; forming informational signals with two-frequency YAG:Nd+++ lasers for communication and ranging; gain limitation effect in electric-discharge CO2-lasers; pattern recognition and data processing in remote laser sounding of earth surface and geosystems; NH3-CO2 9-13 micron lidar for sounding the atmosphere; efficient operating mode of frequency-tunable liquid laser; feasibility of electric-discharge excimer laser with condensed noble gas as active medium; pumping wide-aperture excimer laser 'GARPUN' with counterpropagating electron beams; coherent doppler wind lidar with TEA CO2-laser; free-electron x-ray laser operating in quantum mode; propagation of ultrashort light pulses through nonlinear medium; resonator for technological YAG:Nd laser; instruments for remote sensing of earth in optical wavelength range; environment signatures and simulation of inputs to optoelectronic remote observation systems; evaluating probability of resolution of test objects by ensemble of aerospace IR instruments in surface tests; use of holographic diffraction patterns for inspection of multiple-aperture optical telescopic system phasing; constructing equation systems to control aircraft with nonlinear aerodynamics based on principle of step-by-step adaptive control; measurement of carrier frequency of phase manipulated signal using fast fourier transform; scattering of sound and radio waves by turbulent structures in the stratosphere; experimental study of optical pulse propagation through clouds; and unique characteristics of radiation scattering by nonspherical particles of atmospheric aerosol.
CASI

N94-37078# Academy of Sciences (USSR), Novosibirsk (USSR). Inst. Yadernoj Fiziki.
RELAXATION OF THE DENSITY MATRIX FOR AN ARBITRARY SPIN IN RANDOM EXTERNAL FIELDS
I. B. Khriplovich 1992 12 p
(DE94-618457; BUDKERINP-92-83) Avail: CASI HC A03/MF A01 (US Sales Only)

The relaxation of the density matrix for an arbitrary spin S under magnetic noise is independent of S under the assumption that the g-factor is S-independent. However, the decrements of polarization moments increase with the multipolarity l as l(l+1). For isotropic noise created by external fields of arbitrary multipolarities the relaxation is also S-independent in the classical limit S approaches infinity under the analogous assumption. In the case of anisotropic noise of the multipolarity higher than unity the relaxation of a pure state is described in the limit S much greater than l much greater than 1 by the heat equation. Here under the same assumption the relaxation falls off at S approaches infinity as 1/S(exp 2). If no such assumption on the S-dependence of the interaction parameters is made, the relaxation under magnetic noise and arbitrary isotropic one may depend on S, but this dependence remains smooth in the limit S approaches infinity. DOE

N94-37301# Helsinki Univ. of Technology, Espoo (Finland). Lab. of Physics.
[ACTIVITIES OF THE LABORATORY OF PHYSICS, HELSINKI UNIVERSITY OF TECHNOLOGY] Report, 1992
1994 38 p See also PB89-212633
(PB94-175247) Avail: CASI HC A03/MF A01

Helsinki University of Technology is the major university for engineering education and research in Finland. The university comprises six faculties and several separate institutes. The faculties are divided into departments with approximately 70 laboratories in total. The student enrollment is around 9,300, of which 1,300 are graduate students. The Laboratory of Physics is one of the four laboratories in the Department of Technical Physics. As one of the largest laboratories in the university, it takes care of the basic physics teaching for all of the engineering students. In addition, the laboratory offers a wide selection of advanced and graduate courses for those majoring in the physical sciences and their applications. The Laboratory of Physics has a strong commitment in basic and applied physics, with an emphasis on condensed matter and materials physics. The main areas of current activity include surface physics, positron annihilation, defects in semiconductors and metals, theoretical and computational physics, ion-atom collisions, and biophysics. NTIS

N94-37517# Argonne National Lab., IL.
MAGNETIC AND STRUCTURAL INSTABILITIES OF FERROMAGNETIC AND ANTIFERROMAGNETIC Fe/Cu(100)
Dong-Qi Li, J. Pearson, Z. Q. Qiu, S. D. Bader, and M. Freitag Apr. 1994 12 p Presented at the 6th Joint Conference on Magnetism and Magnetic Materials, Albuquerque, NM, 20-23 Jun. 1994
(Contract W-31-109-eng-38)
(DE94-011504; ANL/MSD/CP-82160; CONF-940629-3) Avail: CASI HC A03/MF A01

Fe wedges epitaxially grown on Cu(100) have been employed to investigate the interplay between magnetic and structural instabilities. Two to four monolayers (ML) clean Fe films grown at room temperature are ferromagnetic with perpendicular easy axes. Bcc Fe films greater than 11 ML thick are ferromagnetic with in-plane easy axes. Most importantly, 6-11 ML fcc Fe films are antiferromagnetic and have a ferromagnetic surface. Films grown below 200 K and annealed to room temperature do not exhibit the antiferromagnetic phase, but remain ferromagnetic and undergo

a spin-reorientation transition from perpendicular to in-plane at approximately 6 ML. A new phase diagram for Fe/Cu(100) is proposed as a function of thickness and growth temperature. In addition, an impurity-stabilized layer-by-layer growth that persists to 30-40 ML Fe is also reported. DOE

N94-37536# Lawrence Livermore National Lab., Livermore, CA.
EFFECT OF THE STIMULATED BRILLOUIN BACKSCATTERING ON SELF-FOCUSING THRESHOLD
A. M. Rubenchik, E. G. Shapiro, and S. K. Turitsyn Mar. 1994 3 p Presented at the European Quantum Electronics Conference 1994, Amsterdam, Netherlands, 28 Aug. - 2 Sep. 1994
(Contract W-7405-eng-48)
(DE94-008678; UCRL-JC-116818; CONF-940871-1) Avail: CASI HC A01/MF A01

In many physical problems Stimulated Brillouin Scattering (SBS) and self-focusing are manifested simultaneously. We consider the effect of the SBS on self-focusing of laser radiation in plasmas. It was found that the self-focusing may be suppressed substantially by the SBS effect. DOE

71 ACOUSTICS

Includes sound generation, transmission and attenuation. For noise pollution see *45 Environmental Pollution*.

N94-36551# Colorado School of Mines, Golden, CO. Center for Wave Phenomena.
ELIMINATION OF NUMERICAL DISPERSION IN FINITE-DIFFERENCE MODELING AND MIGRATION BY FLUX-CORRECTED TRANSPORT
Tong Fei and K. Larner Nov. 1993 38 p
(Contract DE-FG02-89ER-14079)
(DE94-004159; CWP-142P; DOE/ER-14079/30) Avail: CASI HC A03/MF A01

Finite-difference acoustic-wave modeling and reverse-time depth migration based on the full wave equation are general approaches that can take into account arbitrary variations in velocity and density, and can handle turning waves well. However, conventional finite-difference methods for solving the acoustic wave equation suffer from numerical dispersion when too few samples per wavelength are used. Here, we present two flux-corrected transport (FCT) algorithms, one based on the second-order equation and the other based on first-order wave equations derived from the second-order one. Combining the FCT technique with conventional finite-difference modeling or reverse-time wave extrapolation can ensure finite-difference solutions without numerical dispersion even for shock waves and impulsive sources. Computed two-dimensional migration images show accurate positioning of reflectors with greater than 90-degree dip. Moreover, application to real data shows no indication of numerical dispersion. The FCT correction, which can be applied to finite-difference approximations of any order in space and time, is an efficient alternative to use of approximations of increasing order. DOE

N94-37308*# National Aeronautics and Space Administration. Lewis Research Center, Cleveland, OH.
SCATTERING CROSS SECTION OF SOUND WAVES BY THE MODAL ELEMENT METHOD
Kenneth J. Baumeister and Kevin L. Kreider Jul. 1994 7 p Prpoosed for presentation at the Winter Annual Meeting, Chicago, IL, 16-18 Nov. 1994; sponsored by ASME
(RTOP 505-62-52)
(NASA-TM-106667; E-8989; NAS 1.15:106667) Avail: CASI HC A02/MF A01

#he modal element method has been employed to determine the scattered field from a plane acoustic wave impinging on a two dimensional body. In the modal element method, the scattering body is represented by finite elements, which are coupled to an eigenfunction expansion representing the acoustic pressure in the infinite computational domain surrounding the body. The present paper extends the previous work by developing the algorithm necessary to calculate the acoustics scattering cross section by the modal element method. The scattering cross section is the acoustical equivalent to the Radar Cross Section (RCS) in electromagnetic theory. Since the scattering cross section is evaluated at infinite distance from the body, an asymptotic approximation is used in conjunction with the standard modal element method. For validation, the scattering cross section of the rigid circular cylinder is computed for the frequency range 0.1 is less than or equal to ka is less than or equal to 100. Results show excellent agreement with the analytic solution. Author

N94-37632# Helsinki Univ. of Technology, Espoo (Finland). Radio Lab.
STUDY ON THE MEASUREMENT UNCERTAINTY OF NOISE PROPERTIES OF A MILLIMETER WAVE AMPLIFIER
J. Mallat, R. Leppaenen, and A. Raeisaenen Dec. 1993 32 p
(ISSN 0355-5712)
(PB94-170917; ISBN-951-22-1930-1; Rept-S-200) Avail: CASI HC A03/MF A01

A study was carried out on the performance of a simple, low-cost noise temperature measurement system for measuring the noise properties of an LNA at 60 GHz. A construction of a noise measurement system for noise measurement of an HEMT amplifier at the frequency range of 59 to 61 GHz is presented. The uncertainty of the noise measurement is discussed. A noise temperature of 764 K for a system consisting of an amplifier (DUT) and the test receiver was measured at room temperature with an uncertainty of + or - 14 K. The uncertainty in determining the noise temperature of about 627 K (equivalent to a noise figure of 5 dB) of a DUT was estimated to be + or - 25 K. Because the noise properties of the DUT have to be measured in the temperature region from -10 to 50 C, a temperature chamber must be used. This with the associated extra waveguides increases the uncertainty to + or - 52 K. The effects of the temperature distribution along the waveguides are also considered. NTIS

N94-37280# Centre d'Etudes et de Recherches de Medecine Aerospatiale, Bretigny sur Orge (France).
3D SOUND EXPERIMENTAL APPROACH: METHODOLOGY AND PRELIMINARY RESULTS [APPROCHE EXPERIMENTALE DU SON 3D: METHODOLOGIE ET RESULTATS PRELIMINAIRES]
L. Pellieux, C. Gulli, P. Leroyer, B. Pledecocq, Alain Leger, and J. P. Menu *In* AGARD, Virtual Interfaces: Research and Applications May 1994 6 p In FRENCH (For primary document see N94-37261 12-53)
Copyright Avail: CASI HC A02/MF A02

72 ATOMIC AND MOLECULAR PHYSICS

Includes atomic structure, electron properties, and molecular spectra.

N94-36442# Brookhaven National Lab., Upton, NY.
THE E2/M1 MIXING RATIO IN THE EXCITATION OF THE DELTA FROM POLARIZED PHOTO-REACTIONS
1993 9 p Presented at the 14th European Conference on Few-Body Problems in Physics, Amsterdam, Netherlands, 22-27 Aug. 1993
(Contract DE-AC02-76CH-00016)
(DE94-004235; BNL-49593; CONF-9308164-7) Avail: CASI HC A02/MF A01

In constituent quark models, a tensor interaction, mixing quark spins with their relative motion, is introduced to reproduce the observed baryon spectrum. This has a consequence completely analogous to the nuclear tensor force between the n and p in deuterium. A D-state component is mixed into what would otherwise be a purely S-wave object. The D-wave component breaks spherical symmetry, resulting in a nonvanishing matrix element for the nucleon and a static quadrupole moment and deformation for its first excited state, the Delta resonance, at approximately 325 MeV. The magnitude and sign of this D-state component are quite sensitive to the internal structure of the proton and have been of great interest in recent years. The intrinsic deformation of the spin 1/2 nucleon cannot be observed directly; it must be inferred from transition amplitudes such as N yields Delta. In a spherical bag model, the Delta is viewed as a pure quark-spin-flip transition proceeding only through M1 excitation. If there are D-state admixtures in the ground state of the nucleon and/or Delta, quadrupole excitation, in addition to spin-flip M1, is also allowed. The problem is to evaluate the relative magnitude of this E2 excitation in the presence of the dominant M1 transition. A variety of models predict this mixing ratio to be quite small, anywhere from -0.9% to -6%, so that a high degree of precision is demanded of experiment. DOE

N94-36457# Los Alamos National Lab., NM.
OLDER MUONS ARE WISER: USING TIME INFORMATION IN (MU)LCR SPECTROSCOPY
M. Leon 19 May 1993 8 p Presented at the 6th International Conference on Muon Spin Rotation/Relaxation/Resonance, Maui, HI, 7-11 Jun. 1993
(Contract W-7405-eng-36)
(DE93-018556; LA-UR-93-2556; CONF-9306228-1) Avail: CASI HC A02/MF A01

For (mu)LCR with slow polarization transfer, the weak resonance signals can be strengthened by delaying the positron observation period, for pulsed and chopped muon beams. Furthermore, the sensitivity to drifts can be reduced or eliminated by using the ratios of late to early e(+) counts. These possibilities for using time information are discussed quantitatively. DOE

N94-36459# Fermi National Accelerator Lab., Batavia, IL.
TOP QUARK SEARCH AT CDF
J. M. Benlloch (Massachusetts Inst. of Tech., Cambridge.) Nov. 1993 8 p Presented at the 16th Kazimierz Meeting on Elementary Particle Physics: New Physics with New Experiments, Kazimierz, Poland, 24-28 May 1993
(Contract DE-AC02-76CH-03000)
(DE94-003643; FNAL/C-93-329-E; CONF-9305311-1) Avail: CASI HC A02/MF A01

The current status of the top quark search at CDF is presented. A lower limit on the top mass of 113 GeV has been established using the dilepton channel with the data collected during the 1988-1989 and 1992-1993 runs at square root of s = 1.8 TeV. Prospects for top quark discovery during the 1993-1994 run are also outlined. DOE

N94-36460# Brookhaven National Lab., Upton, NY.
HIGH BARYON DENSITY FROM RELATIVISTIC HEAVY ION COLLISIONS
Y. Pang, S. H. Kahana, and T. J. Schlagel Oct. 1993 38 p Presented at the Particle Physics at the Fermi Scale Workshop, Beijing, China, 27 May - 4 Jun. 1993
(Contracts DE-AC02-76CH-00016; DE-FG02-93ER-40768)
(DE94-003894; BNL-49626; CONF-9305282-2) Avail: CASI HC A03/MF A01

A quantitative model, based on hadronic physics, is developed and applied to heavy ion collisions at BNL-AGS energies. This model is in excellent agreement with observed particle spectra in heavy ion collisions using Si beams, where baryon densities of three and four times the normal nuclear matter density (rho(sub 0)) are reached. For Au on Au collisions, the authors predict the formation of matter at very high densities (up to 10 rho(sub 0)). DOE

N94-36463# Fermi National Accelerator Lab., Batavia, IL.
MEASUREMENT OF THE ELASTIC, TOTAL AND DIFFRACTION CROSS SECTIONS AT TEVATRON ENERGIES
S. Belforte Nov. 1993 3 p Presented at the International Europhysics Conference on High-Energy Physics, Marseille, France, 22-28 Jul. 1993
(Contract DE-AC02-76CH-03000)
(DE94-004659; FNAL/C-93/358-E; CONF-930761-5) Avail: CASI HC A01/MF A01

The CDF collaboration has measured the differential elastic cross section d-sigma(sub el)/dt, the single diffraction dissociation double differential cross section d(sup 2)-sigma(sub sd)/dM(sup 2)dt and the total inelastic cross section for antiproton-proton collisions at center of mass energies radical s = 546 and 1800 GeV. Data for this measurement have been collected in short dedicated runs during the 1988-1989 data taking period of CDF. The elastic scattering slope is 15.28 +/- 0.58 (16.98 +/- 0.25) GeV(exp -2) at square root of s = 546 (1800) GeV. Using the luminosity independent method (1 + rho(exp 2)) sigma(sub T) is measured to be 62.64 +/- 0.95 (81.83 +/ 2.29) mb at square root of s = 546 (1800) GeV. Assuming rho = 0.15 the elastic, total, and single diffraction cross sections are sigma(sub el) = 12.87 +/- 0.30, sigma(sub T) = 61.26 +/- 0.93, and sigma(sub sd) = 7.89 +/- 0.33 mb (sigma(sub el) = 19.70 +/- 0.85, sigma(sub T) = 80.03 +/- 2.24, and sigma(sub sd) = 9.46 +/- 0.44 mb) at square root of s = 546 (1800) GeV. DOE

N94-36483# Argonne National Lab., IL.
DEEP INELASTIC SCATTERING RESULTS FROM THE FIRST YEAR OF HERA OPERATION
S. R. Magill 1993 16 p Presented at the Workshop on Physics at Current Accelerators and the Supercollider, Argonne, IL, 2-5 Jun. 1993
(Contract W-31-109-eng-38)
(DE94-004578; ANL-HEP-CP-93-99; CONF-9306176-19) Avail: CASI HC A03/MF A01

The first year of operation of the HERA electron-proton collider has resulted in deep inelastic scattering (DIS) physics results from both the H1 and ZEUS experiments. Reported here are the H1 and ZEUS measurements of the proton structure function F(sub 2) at higher Q(sup 2) and lower x than previously reported from fixed target experiments. Also included are the results of QCD studies on hadronic final states and jets and the observation of high Q(sup 2) charged current events from both experiments. Finally, the observation of events with large rapidity gaps by the ZEUS collaboration is also reported. DOE

N94-36504# Gosudarstvennyi Komitet po Ispolzovaniyu Atomnoi Energii, Serpukhov (USSR).
ANGULAR DEPENDENCE OF PARTON-PARTON SCATTERING EXTRACTED FROM HADRON PAIR PRODUCTION IN pp COLLISIONS AT RADICALS EQUAL TO 11.5 GeV
A. A. Volkov, A. V. Kostritskij, V. V. Abramov, B. Yu. Baldin, A. F. Buzulutskov, V. V. Churakov, V. Yu. Glebov, P. I. Goncharov, A. N. Gurzhiev, and Dyshkant. A. S. 1992 6 p
(DE94-611174; IHEP-OMMS-92-52) Avail: CASI HC A02/MF A01 (US Sales Only)

The angular dependence of symmetrical hadron pair production cross section with effective mass in the range of 2.95-4.7 GeV/c(exp 2) is measured with a GCD-based calculations double arm spectrometer. The results are compared to calculations based on QCD. DOE

N94-36506# Fermi National Accelerator Lab., Batavia, IL.
A SEARCH FOR FIRST GENERATION SCALAR LEPTOQUARKS AT RADICAL s EQUAL TO 1.8 TeV WITH THE D0 DETECTOR Ph.D. Thesis
D. M. Norman 1993 162 p
(Contract DE-AC02-76CH-03000)
(DE94-008846; DOE/CH-03000/T20) Avail: CASI HC A08/MF A02

A search for first generation scalar leptoquarks was done at the D0 detector at Fermi National Accelerator Laboratory from 15 pb(exp -1) of data taken during the 1992-1993 colder run. At Fermilab's p(bar p) collider with a center-of-mass energy of 1.8 TeV, leptoquarks are produced mostly by the strong force in pairs. Leptoquarks carry fractional charge, color, and also lepton and baryon quantum numbers. First generation leptoquarks couple exclusively to the electron, electron neutrino, and the u and d quarks; such a leptoquark would decay into, for example, an electron plus a quark. Signatures for leptoquarks at p(bar p) colliders that have been investigated at D0 are two electrons plus two jets and one electron plus missing energy (from an electron neutrino) plus two jets. DOE

N94-36512# Argonne National Lab., IL.
CP VIOLATION OUTSIDE THE STANDARD MODEL PHENOMENOLOGY FOR PEDESTRIANS
H. J. Lipkin (Weizmann Inst. of Science, Rehovoth, Israel.) 23 Sep. 1993 8 p Presented at the Workshop on B Physics at Hadron Accelerators, Snowmass, CO, 21 Jun. - 2 Jul. 1993
(Contract W-31-109-eng-38)
(DE94-002216; ANL-HEP-CP-93-77; CONF-9306258-4) Avail: CASI HC A02/MF A01

So far the only experimental evidence for CP violation is the 1964 discovery of K(sub L)(yields)2(pi) where the two mass eigenstates produced by neutral meson mixing both decay into the same CP eigenstate. This result is described by two parameters (epsilon) and (epsilon)(prime). Today (epsilon) (approx) its 1964 value, (epsilon)(prime) data are still inconclusive and there is no new evidence for CP violation. One might expect to observe similar phenomena in other systems and also direct CP violation as charge asymmetries between decays of charge conjugate hadrons H(sup (+-)) (yields) f(sup (+-)). Why is it so hard to find CP violation? How can B Physics help? Does CP lead beyond the standard model? The author presents a pedestrian symmetry approach which exhibits the difficulties

and future possibilities of these two types of CP-violation experiments, neutral meson mixing and direct charge asymmetry: what may work, what doesn't work and why. DOE

N94-36513# Argonne National Lab., IL.
PHYSICS DIVISION ANNUAL REVIEW, 1 APRIL 1992 - 31 MARCH 1993
K. J. Thayer, ed. Aug. 1993 226 p
(Contract W-31-109-eng-38)
(DE94-002497; ANL-93/12) Avail: CASI HC A11/MF A03

Work on the ATLAS device is covered, as well as work on a number of others in the lab, as well as collaborative projects. Heavy ion nuclear physics research looked at quasi-elastic, and deep-inelastic reactions, cluster states, superdeformed nuclei, and nuclear shape effects. There were programs on accelerator mass spectroscopy, and accelerator and linac development. There were efforts in medium energy nuclear physics, weak interactions, theoretical nuclear and atomic physics, and experimental atomic and molecular physics based on accelerators and synchrotron radiation. DOE

N94-36515# Los Alamos National Lab., NM.
GENERALIZED SQUEEZED STATES FROM GENERALIZED COHERENT STATES
M. M. Nieto 1993 12 p Presented at the Coherent States: Past Present and Future, Oak Ridge, TN, 14-17 Jun. 1993
(Contract W-7405-eng-36)
(DE94-002689; LA-UR-93-3731; CONF-9306140-1) Avail: CASI HC A03/MF A01

Both the coherent states and also the squeezed states of the harmonic oscillator have long been understood from the three classical points of view: the (1) displacement operator, (2) annihilation- (or ladder-) operator, and (3) minimum-uncertainty methods. For general systems, there is the same understanding except for ladder-operator and displacement-operator squeezed states. After reviewing the known concepts, the author proposes a method for obtaining generalized minimum-uncertainty squeezed states, gives examples, and relates it to known concepts. He comments on the remaining concept, that of general displacement-operator squeezed states. DOE

N94-36516# Lawrence Livermore National Lab., Livermore, CA.
LOW-ENERGY ELECTRON COLLISIONS WITH METAL CLUSTERS: ELECTRON CAPTURE AND CLUSTER FRAGMENTATION
V. V. Kresin, A. Scheidemann, and W. D. Knight 24 Aug. 1993 13 p Presented at the ICPEAC: Satellite Meeting on Electron Collision with Molecules, Clusters and Surfaces, London, England, 29-30 Jul. 1993
(Contract W-7405-eng-48)
(DE94-003623; UCRL-JC-114743; CONF-930717-2) Avail: CASI HC A03/MF A01

The authors have carried out the first measurement of absolute cross sections for the interaction between electrons and size-resolved free metal clusters. Integral inelastic scattering cross sections have been determined for electron-Na(sub n) cluster collisions in the energy range from 0.1 eV to 30 eV. At energies less than 1 eV, cross sections increase with decreasing impact energies, while at higher energies they remain essentially constant. The dominant processes are electron attachment in the low-energy range, and collision-induced fragmentation at higher energies. The magnitude of electron capture cross sections can be quantitatively explained by the effect of the strong polarization field induced in the cluster by the incident electron. The cross sections are very large, reaching values of hundreds of angstrom(sup 2); this is due to the highly polarizable nature of metal clusters. The inelastic interaction range for fragmentation collisions is also found to considerably exceed the cluster radius, again reflecting the long-range character of electron-cluster interactions. The important role played by the polarization interaction represents a bridge between the study of collision processes and the extensive research on cluster response properties. Furthermore, insight into the mechanisms of electron scattering is important for understanding production and detection of cluster ions in mass spectrometry and related processes. DOE

N94-36521 Utah Univ., Salt Lake City, UT. Dept. of Chemistry.
ISOLATED SO4-2 AND PO4-3 ANIONS DO NOT EXIST
Alexander I. Boldyrev and Jack Simons 22 Apr. 1994 13 p Limited Reproducibility: More than 20% of this document may be affected by microfiche quality
(Contract N00014-89-J-1497)
(AD-A278831; TR-42) Avail: CASI HC A03

Ab initio theoretical methods that incorporate effects of orbital relaxation and electron correlation are used to examine the possibility that doubly or triply charged oxy-anions of the class SO4-2, SeO4-2, TeO4-2, or PO4-3, AsO4-3, SbO4-3 are stable relative to electron detachment in the absence of any surrounding medium. In all of these cases, our findings indicate quite clearly that these multiply charged oxy-anions are not stable. DTIC

N94-36523 Joint Inst. for Nuclear Research, Dubna (USSR). Lab. of Nuclear Problems.
MEASUREMENT AND PROCESSING OF GAMMAS ACCOMPANYING MUON PAIRS IN THE REACTION PI(-)C YIELDS MU(+)MU(-) + GAMMA + X AT 38 GeV
A. V. Bannikov, G. A. Chelkov, Z. V. Krumshtejn, V. I. Petrukhin, L. S. Vertogradov, J. Bohm, K. Piska, A. K. Javrishvili, T. A. Lomtadze, and E. G. Tskhadadze 1992 11 p Submitted for publication Limited Reproducibility: More than 20% of this document may be affected by microfiche quality
(DE94-617044; JINR-E-1-92-372) Avail: CASI HC A03 (US Sales Only)

A set of carbon targets and lead glass converters were placed in the sensitive volume of a streamer chamber of the magnetic spectrometer RISK in the experiment SERP-151 on the study of exclusive processes of production of muon pairs and J/Psi-particles in (pi)C interactions at 38 GeV. DOE

N94-36524# Argonne National Lab., IL.
PICOSECOND LASER INDUCED ELECTRIC FIELD MODULATION OF CAROTENOID ABSORPTION BANDS
D. Gosztola, Hiroko Yamada, and M. R. Wasielewski 1994 3 p Presented at the 9th International Conference on Ultrafast Phenomena, Dana Point, CA, 1-5 May 1994
(Contract W-31-109-eng-38)
(DE94-009692; ANL/CHM/CP-81873; CONF-940593-10) Avail: CASI HC A01/MF A01

We present a new and unique way of forming an intense electric field near a molecule in order to induce electrochromism. We have done this by creating an electron-hole pair within close proximity to, but electronically isolated from, a polarizable molecule. The molecular system that we have utilized consists of a zinc porphyrin-pyromellitic diimide light induced charge transfer complex held rigidly proximate to a (beta)-carotene using a calix(4)arene linkage. The formation of the charge separated state of the porphyrin-diimide results in a dipole formed by the 8.4 Angstrom separation of the electron-hole pair. The electric field from this dipole was found to induce electrochromism in the carotene. DOE

N94-36526# Brookhaven National Lab., Upton, NY.
THE t(ANTI t)(GAMMA) BACKGROUND TO pp (YIELDS) W(GAMMA) + X AT THE SSC
U. Baur (Florida State Univ., Tallahassee, FL) and A. Stange Sep. 1993 8 p Presented at the Workshop on Physics at Current Accelerators and the Supercollider, Argonne, IL, 2-5 Jun. 1993
(Contracts DE-AC02-76CH-00016; DE-FG05-87ER-40319)
(DE94-001386; BNL-49462; FSU-HEP-930830; CONF-9306176-9) Avail: CASI HC A02/MF A01

The authors calculate the pp (yields) t(anti t)(gamma) + X (yields) W(gamma) + X cross section at SSC energies. Approximately 40 percent of the total cross section originates from photon bremsstrahlung off the final state jet in t(anti t)j production. Without cuts restricting the hadronic activity, the t(anti t)(gamma) rate is a factor 10 (2) larger than the tree level W(gamma) cross section for a top quark mass of 110 GeV (200 GeV). Imposing a jet veto cut, the t(anti t)(gamma) rate can be suppressed to a level well below the W(gamma) + 0 jet signal cross section. DOE

N94-36527# Argonne National Lab., IL.
SUMMARY OF THE EXTENSIONS OF THE STANDARD MODEL WORKING GROUP
S. Godfrey (Carleton Univ., Ottawa, Ontario.) and T. G. Rizzo Sep. 1993 7 p Presented at the Workshop on Physics at Current Accelerators and the Supercollider, Argonne, IL, 2-5 Jun. 1993

(Contract W-31-109-eng-38)
(DE94-002217; ANL-HEP-CP-93-60; CONF-9306176-11) Avail: CASI HC A02/MF A01

The authors summarize the results of the extended gauge group working group of the Madison-Argonne Workshop on Present and Future Colliders. Contributions are described on the previously unexamined two photon fusion production of heavy leptons, new studies of Z(prime) couplings to (nu)(anti (nu)) and q(anti q), and previously unexplored vector leptoquark production. More detailed accounts of these studies can be found in individual contributions. DOE

N94-36528# Fermi National Accelerator Lab., Batavia, IL.
B-LIFETIME MEASUREMENTS AT THE TEVATRON
H. Wenzel Nov. 1993 14 p Presented at the Advanced Study Conference on Heavy Flavours, Pavia, Italy, 3-7 Sep. 1993
(Contract DE-AC02-76CH-03000)
(DE94-003617; FNAL/C-93/319-E; CONF-9309292-1) Avail: CASI HC A03/MF A01

During the run period from May 1992 to the beginning of June 1993 the Collider Detector at Fermilab (CDF) has recorded approx.= 21.4 pb(exp -1) of p(anti p) collider data at (radical)s = 1.8 TeV. For this run the detector had been upgraded which significantly enhanced its b-physics capabilities. The upgrades include a high precision Silicon VerteX detector (SVX) which enables CDF to reconstruct the decay vertex and decay length of b-hadrons. In this article the author reports on several measurements of the lifetime of b-flavored hadrons. The determination of the average b-lifetime using inclusive J/(psi)'s, the measurement of the B(+/-) and B(0) lifetimes by reconstructing exclusive final states including a J/(psi) or (psi)(2S) and a measurement of the B(sub s)(exp 0) meson lifetime exploiting the decay: B(sub s) (yields) l(nu)D(sub s)(+) (yields) l(nu)(phi)(pi)(+) (yields) l(nu)K(+)K(-)(pi)(+). DOE

N94-36538# Argonne National Lab., IL.
THE POMERON AND QUANTUM CHROMODYNAMICS (QCD) WITH MANY LIGHT QUARKS
A. R. White 26 Aug. 1993 9 p Presented at the 19th International Conference on Elastic and Diffractive Scattering (5th Blois Workshop), Providence, RI, 8-12 Jun. 1993
(Contract W-31-109-eng-38)
(DE94-001351; ANL-HEP-CP-93-70; CONF-9306221-8) Avail: CASI HC A02/MF A01

An outline is given of the physics relating the Pomeron phase transition to the anomaly in Quantum Chromodynamics (QCD) with many massless quarks. Implications for the existence of a further quark sector and its relation to dynamical electroweak symmetry breaking are described. DOE

N94-36539# Brookhaven National Lab., Upton, NY.
EFFECTIVE LAGRANGIAN FOR GLUONS AND HIGGS PSEUDOSCALARS
R. P. Kauffman and W. Schaffer Aug. 1993 8 p Presented at the Workshop on Physics at Current Accelerators and the Supercollider, Argonne, IL, 2-5 Jun. 1993
(Contract DE-AC02-76CH-00016)
(DE94-001381; BNL-49448; CONF-9306176-10) Avail: CASI HC A02/MF A01

Models of electroweak symmetry breaking with more than a single doublet of Higgs scalars contain a neutral pseudoscalar boson. The production of such a pseudoscalar in hadron collisions proceeds primarily via gluon fusion through a top-quark loop (except for those models in which the pseudoscalar coupling to bottom quarks is strongly enhanced). The authors compute the QCD corrections to this process in the heavy-quark limit, using an effective Lagrangian derived from the axial anomaly. DOE

N94-36549 Rutherford Appleton Lab., Chilton (England).
DIRECT PHOTOPRODUCTION OF JETS IN THE k(T)-FACTORISATION PRESCRIPTION
J. R. Forshaw and R. G. Roberts Mar. 1994 18 p
(PB94-171139; RAL-94-028) Avail: Issuing Activity (National Technical Information Service (NTIS))

We study the cross section for dijet production via direct photons, as seen at the HERA collider. Rather than assuming the standard factorization formula for the cross section (where the incoming partons are assumed to be on-shell), we use the kT-factorization formula. This formalism ought to be more appropriate for jet production in regions where the cross section is sensitive to the small-x parton distribution functions. We study the rapidity distribution and the azimuthal angular distribution of the jets and compare with the traditional approach. Our calculations reveal a breakdown of the traditional approach as one moves into the regime of small x. NTIS

N94-36558# Fermi National Accelerator Lab., Batavia, IL.
BLOIS 5: EXPERIMENTAL SUMMARY
M. G. Albrow Sep. 1993 21 p Presented at the 19th International Conference on Elastic and Diffractive Scattering (5th Blois Workshop), Providence, RI, 8-12 Jun. 1993
(Contract DE-AC02-76CH-03000)
(DE94-001219; FNAL/C-93/266; CONF-9306221-6) Avail: CASI HC A03/MF A01

The author gives a summary talk of the best experimental data given at the 5th Blois Workshop on Elastic and Diffractive Scattering. He addresses the following eight areas in his talk: total and elastic cross sections; single diffractive excitation; electron-proton scattering; di-jets and rapidity gaps; areas of future study; spins and asymmetries; high-transverse momentum and masses at the Tevatron; and disoriented chiral condensates and cosmic radiation. DOE

N94-36695# California Univ., Berkeley. Lawrence Berkeley Lab, CA.
ELECTROWEAK PHYSICS AT THE TEVATRON COLLIDER
H. Aihara Aug. 1993 19 p Presented at the Conference on Physics in Collision, Heidelberg, Germany, 16-18 Jun. 1993
(Contract DE-AC03-76SF-00098)
(DE93-040927; LBL-34572; CONF-9306251-1) Avail: CASI HC A03/MF A01

Preliminary results on electroweak physics from the 1992--1993 run with the CDF and D0 detectors at the Tevatron collider are presented. New measurements of the ratio of the W and Z production cross sections times the branching fractions for subsequent decay into leptons are shown. The W width, (Gamma)(W), and a limit on the top-quark mass independent of decay mode are extracted. The status of a measurement of the charge asymmetry of electrons from W decay is given. Also shown are a study of diboson (W(gamma), Z(gamma) and WZ) production and a search for a new neutral gauge boson (Z(prime)). DOE

N94-36696# Argonne National Lab., IL.
FORWARD SCATTERING OF NEUTRONS FROM POLYMERIC AND MAGNETIC MULTILAYERS
G. P. Felcher Aug. 1993 11 p Presented at the 3rd International Conference on Surface X-Ray and Neutron Scattering, Dubna, Russia, 24-29 Jun. 1993
(Contract W-31-109-eng-38)
(DE93-041158; ANL/MSD/CP-79818; CONF-9306248-2) Avail: CASI HC A03/MF A01

Grazing incidence neutrons are not only reflected and refracted from imperfect layers, but also partially scattered by lateral dishomogeneities. In general, scattering may take place both in the reflection plane ('forward scattering') and out of it. The forward scattering from multilayers is highly structured in ridges, whose maxima can be indexed in terms of the multilayer spacings. In experiments on diverse diblock copolymers, two kind of ridges were found, either at constant-k(sub z) loci or else at constant-q(sub z) loci. The relative intensity of the ridges appears to be related to the type and size of imperfections of the lamellar structure. Constant-q(sub z) streaks of magnetic nature were also found in the forward scattering of metallic superlattices (Fe/Cr, Co/Ru, Fe/Nb) in the antiferromagnetic state. Here the diffuse scattering appears around the antiferromagnetic peaks while absent from the structural peaks, as if the crystalline superlattice were to partition into antiferromagnetic domains of limited lateral extension and columnar character. DOE

N94-36697# Lawrence Livermore National Lab., Livermore, CA.
QUANTUM AND QUASI-CLASSICAL ANALYSES OF HIGH ORDER EMISSION PROCESSES
K. J. Schafer and K. C. Kulander Jun. 1993 6 p Presented at the 5th Short Wavelength: Physics with Intense Laser Pulses, San Diego, CA, 29-31 Mar. 1993

(Contract W-7405-eng-48)
(DE93-041348; UCRL-JC-113294; CONF-9303119-5) Avail: CASI HC A02/MF A01

High-order harmonic generation from atoms and ions cuts off in accord with the simple rule: E(sub c) approximately = I(sub p) + 3U(sub p). This cutoff rule as well as the lack of a cutoff in high-order electron energy spectra can be understood via a simple extension of existing two step quasi-classical models. DOE

N94-36700# Fermi National Accelerator Lab., Batavia, IL.
B QUARK PRODUCTION CROSS SECTIONS AND THE B- (BAR B) CORRELATED PRODUCTION CROSS SECTION AT CDF
B. T. Huffman (Pittsburgh Univ., Pittsburgh, PA.) Sep. 1993 8 p Presented at the 5th International Symposium on Heavy Flavor Physics, Montreal, Ontario, 6-10 Jul. 1993
(Contract DE-AC02-76CH-03000)
(DE94-000620; FNAL/C-93/274-E; CONF-9307143-1) Avail: CASI HC A02/MF A01

Recent results on b quark and B meson production cross sections have been obtained at (radical)s = 1.8 TeV proton-antiproton collisions using the Collider Detector Facility (CDF) at Fermilab, using the exclusive decay modes B(sup (+-)) yields J/(Psi) K(sup (+-)) and B(sup 0) yields J/(Psi) K*. Another measurement made using data from the 1988--89 run on the correlated b + (bar b) cross section is also presented. DOE

N94-36747# Academy of Sciences (USSR), Novosibirsk (USSR). Inst. Yadernoj Fiziki.
PRODUCTION OF A POSITRON AND A BOUND ELECTRON BY HIGH-ENERGY PHOTON IN A STRONG COULOMB FIELD
A. I. Milshtejn and V. M. Strakhovenko 1992 14 p
(DE94-618501; BUDKERINP-92-89) Avail: CASI HC A03/MF A01 (US Sales Only)

The cross section of e(+)e(-) pair creation by a high-energy photon with capture of the produced e(-) in arbitrary bound state of arising hydrogen-like atom is found using the quasiclassical approach with exact regard for a Coulomb field. Formulae are essentially simplified for large quantum numbers of the bound state. That permits the authors to find the total cross section of the process. DOE

N94-36749# Academy of Sciences (USSR), Novosibirsk (USSR). Inst. Yadernoj Fiziki.
INTRODUCTION TO THE HEAVY QUARK EFFECTIVE THEORY, PART 1
A. G. Grozin 1992 42 p
(DE94-618512; BUDKERINP-92-97-Pt-1) Avail: CASI HC A03/MF A01 (US Sales Only)

Heavy Quark Effective Theory (HQET) is a new approach to QCD problems involving a heavy quark. In the leading approximation, the heavy quark is considered as a static source of the gluon field; 1/m corrections can be systematically included in the perturbation theory. HQET also simplifies lattice simulation and sum rules analysis of heavy hadrons. DOE

N94-36964*# Hawaii Univ., Manoa, HI. Dept. of Physics and Astronomy.
STUDIES OF THE THERMAL AND OPTICAL RESPONSES OF H ATOMS IN SOLID H2 Final Technical Report
James R. Gaines and Chester A. Vause, III [1990] 23 p Sponsored by NASA. Lewis Research Center
(NASA-CR-196114; NAS 1.26:196114) Avail: CASI HC A03/MF A01

It was the goal of this reserch project to model both the storage of energy in solid hydrogen in the form of atoms and the conversion of this stored energy into other forms of useful energy. The basic ideas of rocket propulsion originate in classical physics and they remain unchanged. To escape a strong gravitational field, the 'burn time' must be minimized but in negligible force fields, the burn time is unimportant and only the relative masses of rocket to fuel determine a specific exhaust velocity. It is in this latter case that low mass fuels such as hydrogen become very important. The burning of hydrogen in oxygen is a 'benchmark' fuel today providing a specific impulse of 400 seconds or better. More exotic fuels will be needed for many of the interesting explorations of the future but they still must have large energy releases per unit mass. It is in this context that propulsion based on hydrogen atom recombination receives attention and these studies will serve as engineering guides. Author (revised)

N94-37034# California Univ., Santa Barbara, CA. Dept. of Physics.
COMBINED ATOMIC FORCE AND SCANNING REFLECTION INTERFERENCE CONTRAST MICROSCOPY Technical Report No. 12, 1 Jan. - 31 Dec. 1994
P. E. Hillner, M. Radmacher, and P. K. Hansma Sep. 1994 15 p
(Contract N00014-92-J-1260)
(AD-A280341) Avail: CASI HC A03/MF A01

A sphere attached to a cantilever is used simultaneously as an atomic force microscope (AFM) tip and as a curved reflective surface for producing scanning reflection interference contrast microscope (RICM) images of fluorescent beads dried onto a glass slide. The AFM and RICM images are acquired in direct registration which enables the identification of individually excited beads in the AFM images. The addition of a sharp, electron beam-deposited tip to the sphere gives nanometer resolution AFM images without loss of optical contrast. DTIC

N94-37041 Colorado Univ., Boulder, CO.
SPONTANEOUS FORCE OPTICAL TRAPS Final Progress Report, 1 Oct. 1990 - 30 Sep. 1993
Carl Wieman 30 Sep. 1993 13 p Limited Reproducibility: More than 20% of this document may be affected by microfiche quality
(Contract N00014-91-J-1006)
(AD-A280574) Avail: CASI HC A03

During the past grant period (10/90 - present) we have made advances in laser trapping and cooling on several fronts. These efforts cover a spectrum which goes from developing new technology which has immediate application in the construction of better atomic clocks at one end, to developing basic physics ideas on how to achieve a Bose condensed vapor at the other. This latter subject is one where it is likely to be many years before the full implications of this proposed new state of matter and its possible applications are fully realized. DTIC

N94-37063# Instituto de Fisica Teorica, Sao Paulo (Brazil).
RELATIVISTIC DI-QUARK MODEL OF p p-BAR YIELDS K(+)K(-) REACTION
T. Frederico, J. Dey, and L. Tomio Sep. 1993 16 p
(DE94-618519; IFT-P-056-93) Avail: CASI HC A03/MF A01 (US Sales Only)

The newly available experimental data (LEAP 92) on K K-bar production is compared with a model calculation. It is believed that the simplicity of the model makes it a useful tool for studying charm and beauty baryon production, for which also experimental data will soon be profuse. DOE

N94-37064# Joint Inst. for Nuclear Research, Dubna (USSR).
SIMPLE AND EFFICIENT METHOD OF SECONDARY VERTEX SEARCHING
V. V. Ivanov and D. B. Pontekorvo 1993 14 p
(DE94-618542; JINR-R-10-93-271) Avail: CASI HC A03/MF A01 (US Sales Only)

New variables permitting effective selection of events containing a secondary vertex are proposed. Reconstruction of an event and searching for the primary and secondary vertices are not required for this purpose. If a neural network is utilized for classification of events in the space of these variables, then the identification of signal and background events will partially be totally unambiguous. DOE

N94-37065# Moscow State Univ. (Russia). Inst. of Nuclear Physics.
SUM RULES FOR 1/m CORRECTIONS TO THE FORM FACTORS OF SEMILEPTONIC B DECAYS
V. N. Bajer and A. G. Grozin 1992 16 p
(DE94-618548; BUDKERINP-92-80) Avail: CASI HC A03/MF A01 (US Sales Only)

Semileptonic B decays are described by the Isgur-Wise form factor to the leading order in 1/m; four new functions appear in the first order. Values of these functions are crucial for the applicability of the whole approach to processes involving c quark. The sum rules for three subleading B yields D(sup (*)) form factors from the QCD sum rules with finite masses

by expanding to the first order in 1/m are obtained. The results respect the pattern of the first 1/m corrections established in heavy quark effective theory, and obey the Luke theorem. DOE

N94-37066# Joint Inst. for Nuclear Research, Dubna (USSR). Lab. of Theoretical Physics.

RADIATIVE AND RARE MU AND PI DECAYS

A. B. Arbuzov, E. A. Kuraev, N. V. Makhaldiani, and N. P. Merenkov 1993 14 p

(DE94-618549; JINR-E-4-93-196) Avail: CASI HC A03/MF A01 (US Sales Only)

The width of the radiative decay of polarized muon has been calculated. The distribution in the hard part of the final electron spectra is presented. Also the integrated width for some electron energy cuts has been estimated. The radiative corrections to the pion beta-decay are considered, as well as some background processes. DOE

N94-37067# Fermi National Accelerator Lab., Batavia, IL.

MASS IDENTIFIED PARTICLE PRODUCTION AND BOSE EINSTEIN CORRELATIONS AT 1800 GeV

T. Alexopoulos May 1994 6 p Presented at the 2nd International Conference on Physics and Astrophysics of Quark-Gluon Plasma, Calcutta, India, 19-23 Jan. 1993

(Contract DE-AC02-76CH-03000)

(DE94-013418; FNAL/C-94/124-E; CONF-9301109-5) Avail: CASI HC A02/MF A01

Results were shown on transverse momentum distributions of pi, k, and p from Fermilab experiment E735. This experiment, related to the search for quark gluon plasma, was run at the Fermilab Tevatron collider with (bar p)p collisions at square root of s = 1800 GeV. Dependence of particle ratios on transverse momentum and center of mass energies was shown. Results were also shown on Bose Einstein correlations between pairs of identical pions and a measure of size and lifetime of the source. DOE

N94-37075# Joint Inst. for Nuclear Research, Dubna (USSR). Lab. of Nuclear Problems.

WIDE APERTURE SCINTILLATION HODOSCOPE WITH FEU-143 PHOTOMULTIPLIERS

L. G. Afanasev, M. A. Ivanov, V. V. Karpukhin, V. I. Komarov, A. V. Kulikov, and V. V. Yazkov 1993 14 p Submitted for publication

(DE94-618211; JINR-E-13-93-234) Avail: CASI HC A03/MF A01 (US Sales Only)

Scintillation hodoscopes with FEU-143 photomultipliers are described. Every of two hodoscopes consists of 8 elements each of length 1400 mm and cross section 56x56 mm. The time and amplitude characteristics were obtained in real conditions of the physical experiment at the Protvino U-70 accelerator. A resolution on time difference between hits of two hodoscopes is 224 ps. A separation of pions and protons by their ionization losses is also provided at momenta less than 1000 MeV/c. DOE

N94-37076# Joint Inst. for Nuclear Research, Dubna (USSR). Lab. of Nuclear Problems.

NEW METHOD FOR MINIMIZING REGULAR FUNCTIONS WITH CONSTRAINTS ON PARAMETER REGION

V. S. Kurbatov and I. N. Silin 1993 7 p

(DE94-618340; JINR-E-1-93-253) Avail: CASI HC A02/MF A01 (US Sales Only)

The new method of function minimization is developed. Its main features are considered. It is possible minimization of regular function with the arbitrary structure. For chi(exp 2)-like function the usage of simplified second derivatives is possible with the control of correctness. The constraints of arbitrary structure can be used. The means for fast movement along multidimensional valleys are used. The method is tested on real data of K(exp (pi)2) decay of the experiment on rare K(sup -)-decays. DOE

N94-37077# Joint Inst. for Nuclear Research, Dubna (USSR).

THE MATHEMATICAL SIMULATION OF PHYSICAL PROCESSES IN ECR MULTICHARGED IONS SOURCES [MATEMATICHESKOE MODELIROVANIE FIZICHESKIKH PROTSESSOV V ECR-ISTOCHNIKAKH MNOGOZARYADNYKH IONOV]

N. A. Tokareva and G. D. Shirkov 1993 10 p In RUSSIAN

(DE94-618343; JINR-R-9-93-240) Avail: CASI HC A02/MF A01 (US Sales Only)

The article presents a new model of the highly charged ion production in ECR sources which takes into account the violation of plasma charged neutrality condition. Mathematical methods have been analyzed to calculate the multicharged ion extraction in the RF pulse mode. The proposed calculation method has been chosen on the basis of the performed numerical experiments to solve the considered task. DOE

N94-37084# Stanford Research Inst., Menlo Park, CA.

HARD DIFFRACTION AND DEEP INELASTIC SCATTERING

J. D. Bjorken Apr. 1994 17 p Presented at the International Workshop on Deep Inelastic Scattering and Related Subjects, Eilat, Israel, 6-11 Feb. 1994

(Contract DE-AC03-76SF-00515)

(DE94-013353; SLAC-PUB-6477; CONF-940233-1) Avail: CASI HC A03/MF A01

Since the advent of hard-collision physics, the study of diffractive processes - shadow physics - has been less prominent than before. However, there is now a renewed interest in the subject, especially in that aspect which synthesizes the short-distance, hard-collision phenomena with the classical physics of large rapidity-gaps. This is especially stimulated by the recent data on deep-inelastic scattering from HERA, as well as the theoretical work which relates to it. The word diffraction is sometimes used by high-energy physicists in a loose way. The author defines this term to mean: A diffractive process occurs if and only if there is a large rapidity gap in the produced-particle phase space which is not exponentially suppressed. Here a rapidity gap means essentially no hadrons produced into the rapidity gap (which operates in the 'lego' phase-space of pseudo-rapidity and azimuthal angle). And non-exponential suppression implies that the cross-section for creating a gap with width delta(eta) does not have a power-law decrease with increasing subenergy s = e(exp delta(eta)), but behaves at most like some power of pseudorapidity delta(eta) approximately = log(s). The term hard diffraction shall simply refer to those diffractive process which have jets in the final-state phase-space. DOE

N94-37085# Stanford Research Inst., Menlo Park, CA.

PRECISE DETERMINATION OF THE WEAK MIXING ANGLE FROM A MEASUREMENT OF ALR IN e(+)e(-) YIELDS Z0

M. Woods May 1994 5 p Presented at the 29th Moriond Meeting on Quantum Chromodynamics and High Energy Hadronic Interactions, Les Arcs, France, 19-26 Mar. 1994

(Contract DE-AC03-76SF-00515)

(DE94-013355; SLAC-PUB-6493; CONF-940327-2) Avail: CASI HC A01/MF A01

In the 1993 SLC/SLD run, the SLD recorded 50,000 Z events produced by the collision of longitudinally polarized electrons on unpolarized positrons at a center-of-mass energy of 91.26 GeV. The luminosity-weighted average polarization of the SLC electron beam was (63.0(+-)1.1)%. The authors measure the left-right cross-section asymmetry in Z boson production, A(sub LR), to be 0.1628 +/- 0.0071 (stat.) +/- 0.0028 (syst.) which determines the effective weak mixing angle to be sin(exp 2)theta(sup eff)(sub W) = 0.2292 +/- 0.0009 (stat.) +/- 0.0004 (syst.). DOE

N94-37086# Stanford Research Inst., Menlo Park, CA.

THE FORM FACTORS OF THE NUCLEONS

F. Schlumpf May 1994 5 p Presented at the 14th International Conference on Few Body Problems in Physics, Williamsburg, VA, 26-31 May 1994

(Contract DE-AC03-76SF-00515)

(DE94-013357; SLAC-PUB-6502; CONF-9405132-4) Avail: CASI HC A01/MF A01

The author demonstrates that a relativistic constituent quark model can give nucleon form factors that agree well with recent, accurate measurements. The relativistic features of the model and the specific form of the wave function are essential for the result. DOE

N94-37087# Stanford Research Inst., Menlo Park, CA.

A STUDY OF JET HANDEDNESS IN HADRONIC Z0 DECAYS

D. Muller May 1994 8 p Presented at the 29th Moriond Meeting on

Quantum Chromodynamics and High Energy Hadronic Interactions, Les Arcs, France, 19-26 Mar. 1994
(Contract DE-AC03-76SF-00515)
(DE94-013358; SLAC-PUB-6511; CONF-940327-1) Avail: CASI HC A02/MF A01

The authors have searched for inclusive signatures of polarization in hadronic jets from Z(sup 0) yields q(bar q) decays using the 'jet handedness' method. They exploited the large polar angle asymmetry induced by the high SLC electron beam polarization to select samples of quark jets and antiquark jets, expected to be left- and right-polarized respectively. They find no evidence for jet handedness in their global sample and set a preliminary upper limit of 7% at 95% C.L. on the magnitude of the analyzing power of this technique. They have used the SLD vertex detector to exclude events containing heavy (b, c) quarks, in which the handedness is expected to be small due to the dominance of decays of spinless mesons. They find no evidence for jet handedness in this high-purity sample of light (u, d, and s) quark jets, and set a preliminary upper limit of 11% on the magnitude of the analyzing power in this case. They have investigated several alternative definitions of jet handedness in an attempt to optimize the analyzing power. They find no evidence of jet handedness by any method. DOE

N94-37096 Academy of Sciences (USSR), Novosibirsk (USSR). Inst. Yadernoj Fiziki.
DETERMINATION OF THE UPSILON(1s) LEPTONIC WIDTH
S. E. Baru, A. E. Blinov, and V. E. Blinov et al 1992 23 p Limited Reproducibility: More than 20% of this document may be affected by microfiche quality
(DE94-618534; BUDKERINP-92-46) Avail: CASI HC A03 (US Sales Only)

The data recorded with the MD-1 detector operated at the VEPP-4 storage ring were analyzed and the Upsilon(1s) resonance leptonic partial width and mass are determined. Gamma(sub ee) = 1.29+-0.03+-0.03 keV, M = 9460.59+-0.09+-0.05 MeV/c(exp 2) are find. This new value of the Upsilon(1s) mass should superside the previously published value. DOE

N94-37097 Joint Inst. for Nuclear Research, Dubna (USSR). Lab. of Theoretical Physics.
DIRECT PHOTOIONIZATION OF EXCITED HELIUM [PRYAMAYA FOTOIONIZATSIYA VOZBUZHDENNOGO GELIYA]
S. Danzan, B. Zhadamba, O. Lkhagva, S. I. Strakhova, and Ts. Sukhbaatar 1993 22 p In RUSSIAN Limited Reproducibility: More than 20% of this document may be affected by microfiche quality
(DE94-618732; JINR-R-4-93-198) Avail: CASI HC A03 (US Sales Only)

The sensitivity of direct photoionization characteristics of the excited helium to the inclusion of the closed channels and to the choice of the structure models of the continuum and initial states in an energy region below the resonances converging to the second threshold is investigated. DOE

N94-37099# Joint Inst. for Nuclear Research, Dubna (USSR). Lab. of Theoretical Physics.
FIVE-LEPTON DECAY MODES OF MUON AND TAU MESONS
A. B. Arbuzov, E. A. Kuraev, N. V. Makhaldiani, and N. P. Merenkov 1993 18 p Submitted for publication
(DE94-621636; JINR-E-4-93-87) Avail: CASI HC A03/MF A01 (US Sales Only)

For the decays mu, tau yields 3l2(nu) the widths differential on energy reactions of charged leptons were calculated. The case of 'soft pair' production was also taken into account. An analysis of one-particle distributions is presented. Phones for a search for a neutrinoless decay mu yields 3e and for a muonium-antimuonium transition mu(+)e(-) yields mu(-)(+) are estimated. On the ground of the results obtained, the estimation of the spectra in the logarithmic approximation of five-lepton (tau) lepton decays are presented. DOE

N94-37109 Missouri Univ., Columbia, MO. Dept. of Physics.
MICROSCOPIC THEORY OF THE DIELECTRIC RESPONSE OF HIGHLY DISPERSIVE BIOLOGICAL MEDIA Final Report, 1 May 1991 - 31 Jan. 1994
Giovanni Vignale 31 Jan. 1994 5 p Limited Reproducibility: More than 20% of this document may be affected by microfiche quality
(Grant AF-AFOSR-0203-91)
(AD-A280516; AFOSR-94-0349TR) Avail: CASI HC A01

The researchers formulated a theory to describe and calculate the dynamical dielectric response of classical interacting molecular liquids in terms of their corresponding static response functions. There are two basic ideas in this approach. One idea is to use a local effective field to tale into account the long range coherent effects of the molecular interactions. These local fields are derived from the static structural properties of the liquid. The other idea to calculate the self-part of the Van Hove correlation function from the solution of a Boltzmann transport equation in phase space in a number conserving relaxation time approximation. This smoothly interpolates between the hydrodynamic and free particle regimes. Thus they obtained an important generalization of previous theories of molecular liquids, which only treated the self-part of the van Hove correlation function in the hydrodynamic limit, that is w=o and q-0. DTIC

N94-37113# State Univ. of New York, Stony Brook, NY.
ATOMIC AND ELECTRONIC STRUCTURE OF METALS AND ALLOYS: RARE EARTHS, ULTRATHIN FILMS AND SURFACE ALLOYS
1993 7 p
(Contract DE-FG02-86ER-45239)
(DE94-011581; DOE/ER-45239/9) Avail: CASI HC A02/MF A01

The project has been productive: 47 refereed publications in about 5 years. While confined to the area of surfaces and thin films, the project has covered a wide range of physical properties and different materials: rare earths, bulk and surface alloys, metal surfaces, magnetism, and especially atomic and electronic structure of ultrathin films. Notable achievements include quantitative studies of atomic structure of clean rare-earth surfaces: Tb(0001), Tb(112'0), Gd(0001), and Gd(112'0). Surface alloys studied included Cu/001/c(2 x 2)-Au and Cu/001/c(2 x 2)-Pd. The most important achievement of the project lies in the application of quantitative low-energy electron diffraction to ultrathin films, particularly magnetic metals on nonmagnetic substrates. DOE

N94-37152# Brookhaven National Lab., Upton, NY.
PRODUCTION OF PHI MESONS IN CENTRAL Si+Au COLLISIONS AT 14.6 A GeV/c
Yufeng Wang (Columbia Univ., New York, NY.) 1993 10 p Presented at the Workshop on Heavy Ion Physics at the Alternating Gradient Synchrotron, Cambridge, MA, 14-17 Jan. 1993
(Contract DE-AC02-76CH-00016)
(DE94-011726; BNL-60245; CONF-930173-14) Avail: CASI HC A02/MF A01

The production of phi mesons from central Si+Au collisions has been measured by E859 at the BNL-AGS by selecting events with identified K(+) K(-) pairs. The values for the mass and width of the phi obtained from the invariant mass of the kaon pairs are consistent with those of the Particle Data Book. Preliminary results for the invariant 1/(2 pi m(sub T)) d(sup 2)n/dm(sub T)dy distribution and dn/dy are presented. The inverse slope parameter for an exponential m(sub T) fit to the m(sub T) spectrum is 171 +/- 18 MeV. An analysis of the ratio of the phi signal to the combinatoric background in the K(+) K(-) invariant mass distribution provides a rough estimate of the size of the reaction region, which is found to be consistent with the E859 interferometry measurements. DOE

N94-37158# Brookhaven National Lab., Upton, NY.
KAON CORRELATION SYSTEMATICS IN E859
Ole E. Vossnack (Columbia Univ., Irvington, NY.) 1993 11 p Presented at the Workshop on Heavy Ion Physics at the Alternating Gradient Synchrotron, Cambridge, MA, 14-17 Jan. 1993
(Contract DE-AC02-76CH-00016)
(DE94-011927; BNL-60249; CONF-930173-20) Avail: CASI HC A03/MF A01

Bose-Einstein correlations between K(+)'s and between pi(+)'s produced in collisions of 14.6 A GeV/c Si-28 ions and Au-197 nuclei have been measured using the E859 spectrometer. Parameters obtained from fits to correlation functions in relative momentum describe a K(+) source that is slightly smaller than the pi(+) source and comparable in size to the Si-28 projectile. Correlation functions were also formed for pi K(+) and p K(+) pairs extracted from the data set. Bose-Einstein correlations are expected to be absent here. The observed correlations can be

understood as being the result primarily of the two-particle Coulomb interaction. For the p K(+) pairs, an adequate description is obtained only when taking into account the finite sizes of the p and K(+) sources. The space-time coordinate distributions of pions and kaons produced by the event generator ARC for the 14.6 A GeV/c Si-28 on Au-197 collision yield source sizes that are larger than those observed in the experiment. Much closer agreement is seen when viewing the distributions through a simulated version of the detector. DOE

N94-37171# Academy of Sciences (USSR), Novosibirsk (USSR). Inst. Yadernoj Fiziki.

XAFS-LIKE STRUCTURE OF RESONANT RAMAN SCATTERING

V. A. Chernov, S. V. Mytnichenko, and S. G. Nikitenko 1992 11 p

(DE94-618410; BUDKERINP-92-88) Avail: CASI HC A03/MF A01 (US Sales Only)

The KM-shell resonant Raman scattering from a nickel sample has been measured at an energy of incident x-ray photons of about 120 eV below the K-edge. XAFS-like oscillations have been observed in the scattered spectrum for the first time. The observed spectrum is compared with the XAFS spectrum. The basic differences between these two methods are discussed. DOE

N94-37173# Joint Inst. for Nuclear Research, Dubna (USSR). Lab. of Theoretical Physics.

RESONANCE PHOTOIONIZATION OF THE EXCITED HELIUM

S. Danzan, B. Zhadamba, Ts. Sukhbaatar, O. Lkhagva, and S. I. Strakhova 1993 22 p

(DE94-618733; JINR-R-4-93-199) Avail: CASI HC A03/MF A01 (US Sales Only)

The influence of the closed channel on the structure formation of the autoionization resonance in the photoionization of the excited He is investigated. DOE

N94-37209# Lawrence Livermore National Lab., Livermore, CA.

A REJECTION METHOD FOR SELECTION OF SCATTERED STATES

William S. Lawson May 1994 6 p Presented at the 3d International Workshop on Computational Electronics, Portland, OR, 18-20 May 1994

(Contract W-7405-eng-48)

(DE94-012232; UCRL-JC-116299; CONF-9405147-1) Avail: CASI HC A02/MF A01

A rejection method is presented that sidesteps much of the labor necessary in the usual techniques for choosing a scattered state after an electron-phonon collision with full band structure. The phonon wave number is chosen randomly, then tested to see if the resultant collision will satisfy energy conservation to within some accuracy. If not, the collision is rejected, and if so, then the wave number is adjusted in order to enforce energy conservation more precisely. The price one pays is in a high rejection rate. If the cost of a rejection is small, however, this rejection rate can be tolerated. This method will not compete with analytical models (near valley minima), but may outperform the more usual techniques. Accuracies of a few percent are practical. Simulations were preformed with the first conduction band of gallium arsenide. DOE

N94-37210# Sandia National Labs., Albuquerque, NM.

DENSITY AND COMPOSITION ANALYSIS USING FOCUSED MEV ION MICROBEAM TECHNIQUES

A. J. Antolak, A. E. Pontau, D. H. Morse, G. S. Bench, D. W. Heikkinen, and D. L. Weirup 1994 12 p Presented at the 8th Symposium on Radiation Measurements and Applications, Ann Arbor, MI, 16-19 May 1994

(Contracts DE-AC04-94AL-85000; W-7405-eng-48)

(DE94-012241; SAND-94-8625C; CONF-940524-5) Avail: CASI HC A03/MF A01

Nuclear microscopy uses focused MeV ion microbeams to nondestructively characterize materials and components with micron scale spatial resolution. Although a number of accelerator-based microbeam methods are available for materials analysis, this paper centers on the techniques of ion microtomography (IMT) and particle-induced x-ray emission (PIXE). IMT provides quantitative three-dimensional density information with micron-scale spatial resolution and 1% density variation sensitivity. Recently, IMT has become more versatile because greater emphasis has been placed on understanding the effects of reconstruction artifacts, beam spatial broadening, and limited projection data sets. PIXE provides quantitative elemental information with detection sensitivities to 1 micro-g/g or below in some instances. By scanning the beam, two-dimensional maps of elemental concentration can also be recorded. However, since x-rays are produced along the entire path of the ion beam as it penetrates the sample, these measurements only give depth-averaged information in general. PIXE tomography (PIXET) is the natural extension from conventional PIXE analysis to the full three-dimensional measurement and forms the bridge linking the complementary techniques of PIXE and IMT. This paper presents recent developments and applications of these ion beam techniques in a diverse range of fields including characterizing metal-matrix composites, biological specimens, and inertial confinement fusion targets. DOE

N94-37238# Oak Ridge National Lab., TN.

DETERMINATION OF INTERFACE STRUCTURE AND BONDING AT ATOMIC RESOLUTION IN THE STEM

S. J. Pennycook, A. J. McGibbon, M. M. McGibbon, N. D. Browning, M. F. Chisholm, and D. E. Jesson Mar. 1994 6 p Presented at the 13th International Congress on Electron Microscopy, Paris, France, 17-22 Jul. 1994

(Contract DE-AC05-84OR-21400)

(DE94-011466; CONF-940766-1) Avail: CASI HC A02/MF A01

The scanning transmission electron microscope now routinely produces probes of atomic dimensions, 2.2 A at 100 kV and 1.3 A at 300 kV. This capability opens up a new strategy for determining the structure and bonding of materials at the atomic scale, which is particularly advantageous for complex interfaces such as grain boundaries. The Z-contrast image allows the high-Z column locations to be determined by direct inspection, and quantified through maximum entropy methods to a positional accuracy of currently approximately 0.2 A. With the same electron probe, located to sub-Angstrom precision with reference to the Z-contrast image, parallel detection EELS can determine light element coordination from core edge fine structure, in principle around a single atomic column. There are several attractive features to combining Z-contrast imaging with EELS. First, the incoherent nature of Z-contrast imaging provides higher resolution, compared with 0.66 for phase contrast imaging, freedom from contrast reversals and a highly local image. This allows a greatly extended regime of intuitive image interpretation. For example, the presence of dumbbells, with a spacing of 1.36 A, in a Si group of zone axes (110) image is seen directly at 2.2 A resolution from the elongation of the image features. For microanalysis, the Z-contrast image facilitates the accurate placement of the probe over selected atomic columns, either a single atomic column or using a line scan to reduce the effects of beam damage. Column-by-column analysis by EELS is possible, without beam broadening, through the columnar channeling effect that occurs when a highly convergent coherent probe is incident along a low order crystal zone axis. DOE

N94-37249# Argonne National Lab., IL.

TIME-OF-FLIGHT PULSED ION BEAM SURFACE ANALYSIS AS A MEANS OF IN SITU, REAL-TIME CHARACTERIZATION OF THE GROWTH OF FERRO-ELECTRIC AND CONDUCTIVE OXIDE HETEROSTRUCTURES

A. R. Krauss, D. M. Gruen, O. Auciello, Y. Lin, and R. P. H. Chang Apr. 1994 13 p Presented at the 6th International Symposium on Integrated Ferroelectrics, Monterey, CA, 14-16 Mar. 1994

(Contracts W-31-109-eng-38; N00014-93-1-0591)

(DE94-012628; ANL/CHM/CP-81275; CONF-9403120-1) Avail: CASI HC A03/MF A01

Pulsed beam Time-of-Flight Ion Scattering and Recoil Spectroscopy (TOF-ISARS) surface analysis methods have been developed which permit real-time, in situ characterization of the growth layer of multi-component oxide thin films. Results are presented from a study of the deposition of Pb, Zr, Ti and Ru using a sequential layer-by-layer deposition method under ambient oxygen pressure conditions appropriate to the growth of PZT films, revealing layer-by-layer as well as 2D and 3D island growth processes during deposition. Thermodynamic stability conditions result in modification of the layered structure, during deposition, in some cases altering the layer ordering of the growth region. Calculations using the Miedema model for surface segregation are in accord with experimental results that reveal an exchange between deposited Zr and Ti atoms and an underlying Pb layer. In addition, the room temperature studies revealed that Pb grows layer-by-layer, nucleating as 2D islands, while Zr tends to form three-dimensional islands. At room temperature, the Zr surface

concentration is strongly enhanced by the presence of oxygen, but at high temperatures, surface Pb is found to be stabilized by the presence of an oxygen ambient, illustrating the importance of real-time, in situ analysis of the growth layer as opposed to more conventional surface analytical methods which require interruption of the deposition process in order to characterize the film surface. DOE

N94-37298# Fermi National Accelerator Lab., Batavia, IL.
PROSPECTS FOR MEASURING B(s) MIXING AT CDF
J. E. Skarha (Johns Hopkins Univ., Baltimore, MD.) and A. B. Wicklund (Argonne National Lab., IL.) Oct. 1993 8 p Presented at the Workshop on B Physics at Hadron Accelerators, Snowmass, CO, 21 Jun. - 2 Jul. 1993
(Contract DE-AC02-76CH-03000)
(DE94-013147; FNAL/C-93/301-E; CONF-9306258-15) Avail: CASI HC A02/MF A01

The original design of the Collider Detector at Fermilab (CDF) was optimized for high p(sub T) physics measurements associated with W and Z boson, top quark, and QCD jet production. This choice resulted in an emphasis on the central pseudorapidity region (/eta/ less than 1.0) for detector coverage. Thus, CDF has excellent tracking, good calorimetry, and a suitable muon system in the central region. Even with this limited coverage, the large (bar-p)p yields bX cross section of nearly 100 (mu)barns for /eta/ less than 1.0 has allowed the CDF experiment to make many B physics measurements. In audition, with the successful operation of the CDF silicon vertex detector (SVX), the capability for making time-dependent B(s) mixing measurements becomes a reality. Upgrade plans, which include extending the tracking and lepton identification into the forward region and the implementation of a high-rate DAQ system, make a time-dependent B(s) mixing measurement an attractive goal during the anticipated high-luminosity Main Injector collider runs. We discuss here the feasibility and potential of making a B(s) mixing measurement based on extrapolations of the current CDF detector performance using colliding beam data and the expected upgrade plans. DOE

N94-37305# EG and G Energy Measurements, Inc., Santa Barbara, CA. Special Technologies Lab.
DATA SIMULATION FOR THE ASSOCIATED PARTICLE IMAGING SYSTEM
L. N. Tunnell 1994 6 p Presented at the Nondestructive Assay and Nondestructive Examination Waste Characterization Conference, Pocatello, ID, 14-16 Feb. 1994
(Contract DE-AC08-93NV-11265)
(DE94-012664; EGG-11265-3007; CONF-940216-2) Avail: CASI HC A02/MF A01

A data simulation procedure for the Associated Particle Imaging (API) system has been developed by postprocessing output from the Monte Carlo Neutron Photon (MCNP) code. This paper compares the simulated results to our experimental data. DOE

N94-37312# Fermi National Accelerator Lab., Batavia, IL.
PARTICLE PHYSICS
D. Green May 1994 27 p
(Contract DE-AC02-76CH-03000)
(DE94-012944; FNAL-TM-1887) Avail: CASI HC A03/MF A01

This report discusses the following topics: The standard model - synthesis and overview; accelerators and other facilities; mapping the SM constituents onto the detectors; a model pp/(bar p)p collider detector; and other experimental techniques. DOE

N94-37313# Vanderbilt Univ., Nashville, TN.
MCHF CALCULATIONS OF ISOTOPE SHIFTS. 1: PROGRAM IMPLEMENTATION AND TEST RUNS. 2: LARGE-SCALE ACTIVE SPACE CALCULATIONS
P. Joensson (Lund Inst. of Tech., Sweden.) and C. F. Fischer 30 Mar. 1994 27 p
(Contract DE-FG05-88ER-13867)
(DE94-013036; DOE/ER-13867/14) Avail: CASI HC A03/MF A01

A new isotope shift program, part of the MCHF atomic structure package, has been written and tested. The program calculates the isotope shift of an atomic level from MCHF or CI wave functions. The program is specially designed to be used with very large CI expansions, for which angular data cannot be stored on disk. To explore the capacity of the program, large-scale isotope shift calculations have been performed for a number of low lying levels in B I and B II. From the isotope shifts of these levels the transition isotope shift has been calculated for the resonance transitions in B I and B II. The calculated transition isotope shifts in B I are in very good agreement with experimental shifts, and compare favorably with shifts obtained from a many-body perturbation calculation. DOE

N94-37360# National Lab. for High Energy Physics, Ibaraki (Japan).
PROCEEDINGS OF THE WORKSHOP ON NEGATIVE ION FORMATION AND BEAM HANDLING
A. Takagi, ed. and Y. Mori, ed. Jan. 1993 182 p Workshop held in Tsukuba, Japan, 27-28 Jul. 1992
(DE94-748683; KEK-PROC-92-17; CONF-9207233) Avail: CASI HC A09/MF A02

The Workshop on Negative Ion Formation and Beam Handling was held at National Laboratory for High Energy Physics (KEK) on July 27 and 28. More than 40 participants attended the workshop. Negative ions and beams are becoming very useful and attractive in many fields of science, in particular in accelerator science and nuclear fusion and various types of negative ion sources have been developed so far. However, the fundamental mechanisms of negative ion generation in the ion sources and of beam formation are still not clear. This workshop aimed to discuss the problems on these points in detail. DOE

N94-37364# Brookhaven National Lab., Upton, NY.
COMPARISON OF OXYGEN AND SILICON INDUCED REACTIONS AT 14.6 A(GeV/C)
D. S. Zachary (Massachusetts Inst. of Tech., Cambridge.) 1993 4 p Presented at the HIPAGS 1993: Workshop on Heavy Ion Physics at the Alternating Gradient Synchrotron, Cambridge, MA, 14-17 Jan. 1993
(Contracts DE-AC02-76CH-00016; DE-AC03-76SF-00098; W-7405-eng-48; W-31-109-eng-38)
(DE94-011922; BNL-60251; CONF-930173-19) Avail: CASI HC A01/MF A01

Oxygen induced reactions have been studied with minimum bias as well as with central triggers. A recent comparison of pion production for Au-197 + Au and Si-28 + Au central collisions has shown a possible A(sup 2/3) dependence for the projectile and an A(sup 1/3) dependence with the target nucleon number. We find for central (O-16 + Au) collisions that the pion yield dose similarly scale. The K/(pi) ratio for central O-16 + Au reactions is .16 +/- .01, very similar to the central K/(pi) ratio for the Si-28 + Au reaction. DOE

N94-37383# Oak Ridge National Lab., TN.
EFFECT OF TEMPERATURE ON THE ELECTRON ATTACHMENT AND DETACHMENT PROPERTIES OF c-C4F6
P. G. Datskos, L. G. Christophorou, and J. G. Carter 1994 8 p Presented at the 7th International Symposium on Gaseous Dielectrics, Knoxville, TN, 24-28 Apr. 1994
(Contract DE-AC05-84OR-21400)
(DE94-012750; CONF-940414-1) Avail: CASI HC A02/MF A01

The temperature dependence of the low-energy electron attachment and autodetachment processes for c-C4F6 in a N2 buffer gas has been studied in the temperature, T, range of 300 to 600 K and the mean electron energy, (epsilon), range from 0.19 to 1.0 eV. The low-energy electron attachment rate constant for c-C4F6 shows only a slight dependence on gas temperature. In contrast, the autodetachment frequency increases by more than four orders of magnitude when T is increased from 300 to 600 K. This increase in autodetachment is due to the increase in the internal energy content of the c-C4,F6(-) anion with increasing T. The autodetachment process under consideration is a heat-activated process and has an activation energy E* of 0.24 eV. Significance of these results to gaseous dielectrics is indicated. DOE

N94-37387# Japan Atomic Energy Research Inst., Tokyo (Japan).
STOPPING POWER OF CHARGED PARTICLES FROM 10 eV/amu TO 10 GeV/amu
Yoshihiro Nakane, Shun-Ichi Tanaka, Shiori Furihata, and Satoshi Iwai Aug. 1993 183 p
(DE94-719024; JAERI-M-93-152) Avail: CASI HC A09/MF A02

Electric collision, nuclear collision and total stopping powers in 10 kinds

of elements: H2, He, Be, C, Al, Fe, Cu, W, Pb and U, and 4 kinds of materials: water, phantom, LiF-TLD, and SSNTD (solid state neutron track detector) have been calculated for 10 kinds of charged particles from 10 eV/amu to 10 GeV/amu with STOPPING, SPAR, and RSTAN/RSHEV codes, in which the charged particles are important projectiles for evaluating the dose and detector responses of radiations, and for accelerator shielding calculations. Calculated data are presented. DOE

N94-37414# Joint Inst. for Nuclear Research, Dubna (USSR). Lab. of Computing Techniques and Automation.
ABOUT EXISTENCE OF A BARYON WITH THE 3.52 GeV/c2 MASS [OSUSHCHESTVOVANII BARIONA S MASSOJ 3.52 GEHV/S2]
V. M. Karnaukhov, V. I. Moroz, K. Koka, and A. Mihul 1993 15 p In RUSSIAN Submitted for publication
(DE94-621641; JINR-R-1-93-121) Avail: CASI HC A03/MF A01 (US Sales Only)

A study of 16 GeV/c pi(-)(rho) interactions shows a narrow peak in the effective mass spectrum of the system K(sub s)(sup 0)K(+) (rho)(pi(-) pi(-). A kinematical analysis finds an angular distributions peculiarity of the particles indicated system for the peak region. It is possible that this peculiarity is connected with the production and decay mechanism of a neutral baryon. A possible baryon with the (3521(+-)3) MeV/c(sup 2) mass and the (6(sub -6)(sup +21)) MeV/c(sup 2) width is produced in the central region of pi(-)(rho) interactions with the (15(+-)3) (mu)b cross section. DOE

N94-37417# Tokyo Univ., Tanashi (Japan). Inst. for Nuclear Study.
FIRST OBSERVATION OF LASER-INDUCED RESONANT ANNIHILATION IN METASTABLE ANTIPROTONIC HELIUM ATOMS
N. Morita (Institute for Molecular Science, Okazaki, Japan.), M. Kumakura (Institute for Molecular Science, Okazaki, Japan.), and T. Yamazaki et al Nov. 1993 13 p
(DE94-748668; INS-1014) Avail: CASI HC A03/MF A01 (US Sales Only)

We have observed the first laser-induced resonant transitions in antiprotonic helium atoms. These occur between metastable states and Auger dominated short lived states, and show that the anomalous longevity of antiprotons previously observed in helium media results from the formation of high-n high-l atomic states of p-barHe(+). The observed transition with vacuum wavelength 597.259 (+/-) 0.002 nm and lower-state lifetime 15 (+/-) 1 ns is tentatively assigned to (n,l) = (39,35) yields (38,34). DOE

N94-37528# Joint Inst. for Nuclear Research, Dubna (USSR). Lab. of Theoretical Physics.
THE ANGULAR AND ENERGY DISTRIBUTIONS OF EJECTED ELECTRONS IN ELECTRON-IMPACT IONIZATION OF HELIUM [UGLOVOE I EHNERGETICHESKOE RASPREDELENIYA EHZHEKTIRUEMYKH EHLEKTRONOV PRI IONIZATSII ATOMA GELIYA EHLEKTRONNYM UDAROM]
O. Lkhagva and L. Khehnmehdehkh 1993 19 p In RUSSIAN
(DE94-618748; JINR-R-4-93-200) Avail: CASI HC A03/MF A01 (US Sales Only)

The angular and energy distributions of ejected electrons in the direct He(e,2e)He(+) reaction are studied. It is shown that the first Born approximation is applicable for the description of ejected electrons for incident electron energies E(sub 0) greater than or = 500 eV at arbitrary ejection angles. Furthermore, it is shown that the anisotropy of ejected electrons and the predominance of higher order multipole terms give rise to differences in the angular distributions of double differential cross sections for different kinematic conditions. DOE

N94-37550# Argonne National Lab., IL.
ELECTRON-TRANSFER REACTIONS INVOLVING TWO HARMONIC POTENTIALS WITH A DIFFERENT FORCE CONSTANT: THE ZUSMAN APPROACH VERSUS THE SPIN-BOSON MODEL
J. Tang 1994 36 p
(Contract W-31-109-eng-38)
(DE94-013306; ANL/CHM/PP-81877) Avail: CASI HC A03/MF A01

Two approaches: (a generalized spin-boson model with a nonlinear spin-boson coupling and the Zusman's stochastic Liouville formalism) are employed to analyze the electron-transfer reactions involving two harmonic potentials with a different force constant. An analytical rate formula, expressed as a convoluted integral of the individual rate kernel for each mode, is derived with full consideration of quantum tunneling effects. For a dominant solvent mode at low frequency, the formula can be reduced to the results of the Zusman's theory, showing asymmetry of the Marcus rate plot between the normal and the inverted regions. DOE

N94-37553# Stanford Linear Accelerator Center, CA.
A PHOTOEMISSION STUDY OF Au, Ge, AND O2 DEPOSITION ON NH4F ETCHED Si(111)
J. Terry, R. Cao, C. Wigren, and P. Pianetta Mar. 1994 15 p Presented at the 40th National Symposium of the American Vacuum Society (AVS), Orlando, FL, 15-19 Nov. 1993
(Contract DE-AC03-76SF-00515)
(DE94-013352; SU-SLAC-PUB-6466; SU-SLAC/SSRL-0072; CONF-9311104-22) Avail: CASI HC A03/MF A01

We have studied the interaction of a metal, Au, a semiconductor, Ge, and a non-metal, O2, with the NH4F etched Si(111) surface with photoemission spectroscopy. Two components were present in Si 2p core level spectra from the H-terminated surface. We observed the flat band condition from the as-etched, n-type, Si(111) surface. We performed stepwise depositions of Au and measured the band bending with photoemission spectroscopy. The Fermi level pinned near mid-gap as Au was deposited onto the as-etched surface. After the deposition of 1 ML of Au, a Au-silicide layer formed. This interfacial component indicated that the passivating H layer was compromised. As the Au coverage was increased, layers of pure Au formed between the bulk silicon and the Au-silicide layer. The observed behavior was nearly identical to that of Au deposition on the Si(111) 7 x 7 surface. Next, we tested the ability of the monohydride layer to sustain surfactant assisted growth of Ge. Ge islanding was observed at 400 deg. C indicating that good surfactant growth was not obtained. Although the monohydride layer was not a good surfactant for the Si(111) surface at this temperature. Further study at different temperatures is needed to determine the ability of the ideal monohydride layer to act as a surfactant. Finally, we observed no oxidation of the as-etched surface at room temperature upon exposure to molecular oxygen. DOE

N94-37558 California Univ., Berkeley. Lawrence Berkeley Lab, CA.
STRANGENESS AND THE QUARK-GLUON PLASMA: AN EXPERIMENTER'S PERSPECTIVE
G. Odyniec Feb. 1994 31 p Presented at the 3rd Workshop on Relativistic Aspects of Nuclear Physics, Rio de Janeiro, Brazil, 25-27 Aug. 1993 Limited Reproducibility: More than 20% of this document may be affected by microfiche quality
(Contract DE-AC03-76SF-00098)
(DE94-011377; LBL-35128; CONF-9308210-2) Avail: CASI HC A03

Current status of experimental results on strange particle production in relativistic nucleus-nucleus collisions is reviewed. Emphasis is placed on the relevance to the hypothetical quark-gluon plasma formation and the origin of the Universe. DOE

N94-37651# Joint Inst. for Nuclear Research, Dubna (USSR). Lab. of Nuclear Reactions.
ON THE SHAPE OF X RAY SPECTRA EXCITED BY HEAVY IONS [O FORME RENTGENOVSKIKH SPEKTROV, VOZBUZHDENNYKH TYAZHELYMI IONAMI]
V. A. Altynov 1993 15 p In RUSSIAN
(DE94-618747; JINR-R-14-93-247) Avail: CASI HC A03/MF A01 (US Sales Only)

Some physical factors determining the shape of x-ray spectra excited in collisions with heavy ions are considered. It is concluded that (1) the substantial broadening of multiple ionization satellites at the increase of the emitter atomic number is caused by the Doppler effect and complication of their multiple structure; (2) the presence of velocity in the target atom as well as the incident ions field do not influence the position of the satellites' center of gravity; and (3) for correct interpretation of experimental data one has to take into account a possible overlapping of components of neighboring satellites. DOE

N94-37652# Instituto de Pesquisas Energeticas e Nucleares, Sao Paulo (Brazil).
THE DYNAMICS OF HYDROGEN ATOMS DISSOLVED IN Zr Cr2 ALLOY M.S. Thesis [A DINAMICA DOS ATOMAS DE HIDROGENIO DISSOLVIDOS NA LIGA ZR CR2]
J. I. deMoura 1992 94 p In PORTUGESE
(DE94-618756; INIS-BR-3257) Avail: CASI HC A05/MF A01 (US Sales Only)

The localized vibration modes of hydrogen in the ZrCr2H(x) compound were studied for three hydrogen concentrations, namely x = 0.45, 2, and 3, by inelastic neutron scattering with the beryllium filter-time of flight facility installed at the IEA-R1 research reactor at IPEN-CNEN/SP. Four frequencies of localized hydrogen vibrations were observed, three of which with 28 MeV full width at a half maximum (FWHM) at neutron energy transfers of 184, 151, and 134 MeV with no perceptible changes as a function of hydrogen concentration. The fourth mode is observed at neutron energy transfer of 106 MeV for x=0.45 and x=2 whereas it decreases to 98 MeV for x=3. DOE

N94-37671 Los Alamos National Lab., NM.
NEUTRINO-NUCLEON SCATTERING
G. T. Garvey 1994 16 p Presented at the CERN SMC Meeting on Internal Spin Structure of the Nucleon, New Haven, CT, 5-6 Jan. 1994 Limited Reproducibility: More than 20% of this document may be affected by microfiche quality
(Contract W-7405-eng-36)
(DE94-011720; LA-UR-94-1300; CONF-940173-3) Avail: CASI HC A03

In the following, the author tries to summarize the current status of neutrino-nucleon scattering as it bears on contemporary issues regarding the spin structure of the nucleon. It is straightforward to express the electroweak current of a hadron in terms of its underlying electroweak partonic currents. The matrix elements of these currents are, of course, presently incalculable but may be characterized by form factors extracted from experiment. When neutrinos are used as probes, there are several problems associated with carrying out the required cross section measurements. Active neutrino detectors of necessity contain nuclei more complex than hydrogen. These nuclei create additional backgrounds and create complications of interpretation that make these experiments challenging. However, given the continued demonstrated difficulty of measuring and extracting the spin structure functions, it appears that there are no easy measurements to investigate the nucleon spin structure save the earlier experiments that fixed the axial vector form factors of well-known baryon decays (neutron, lambda, etc.). With the emergence of the provocative results from the EMC group on the spin structure function of the proton, there has been renewed interest in the information contained in the cross sections for neutral current neutrino-nucleon scattering. The theoretical background for describing this process has been worked out in detail. It is presented in briefest outline to define the terms needed to describe experimental results. DOE

N94-37672# Brookhaven National Lab., Upton, NY.
SEARCH FOR THE H DIBARYON BY Xi(-) CAPTURE ON THE DEUTERON
Toru Iijima (Kyoto Univ., Japan.) 1993 7 p Presented at the 13th International Conference on Particles and Nuclei, Perugia, Italy, 27 Jun. - 3 Jul. 1993
(Contract DE-AC02-76CH-00016)
(DE94-011733; BNL-60355; CONF-930637-15) Avail: CASI HC A02/MF A01

The present status of the H-dibaryon search experiment at Brookhaven (E813) using the formation reaction through Xi(-) atomic capture on the deuteron, (Xi(-), d)(sub atom) yields H n, is reported with emphasis placed on the analysis of the data collected with the 1992 slow extracted proton beam run. DOE

N94-37674# Chicago Univ., Chicago, IL.
CDF RESULTS ON ELECTROWEAK PHYSICS
H. J. Frisch (Chicago Univ., Chicago, IL.) Nov. 1993 21 p Presented at the 19th International Conference on Elastic and Diffractive Scattering (Fifth Blois Workshop), Providence, RI, 8-12 Jun. 1993
(Contract DE-AC02-76CH-03000)
(DE94-011750; FNAL/C-93/337-E; CONF-9306221-10) Avail: CASI HC A03/MF A01

The second major run of the (bar p)p Fermilab Tevatron collider has just ended on June 1. The CDF detector has accumulated almost five times the data sample of its previous 1988-1989 run. We present new results on the ratio of W to Z boson production cross-sections and on the charge asymmetry in W decay. We give a progress report on the measurement of the W mass. New results from the 1988-1989 data on Drell-Yan production and on W (gamma) production are also presented. DOE

N94-37715# California Univ., Berkeley. Lawrence Berkeley Lab, CA.
HADRON PRODUCTION IN S+NUCLEUS COLLISIONS AT 200 GeV/NUCLEON
S. Margetis Mar. 1994 8 p Presented at the 10th Winter Workshop on Nuclear Dynamics, Snowbird, UT, 15-21 Jan. 1994
(Contract DE-AC03-76SF-00098)
(DE94-011344; LBL-35295; CONF-940169-4) Avail: CASI HC A02/MF A01

Central collisions between nuclei at relativistic energies form a hot and dense hadronic system over a large volume. Phenomenological models, as well as QCD calculations on the lattice, predict a phase transition in nuclear matter leading to deconfinement, a state of matter in which quarks and gluons are free to move inside the entire volume of the deconfined region. This new state was given the name of Quark Gluon Plasma (QGP). Based on the conjecture that collisions of heavy nuclei at high energies can create the necessary condition of a high energy density thermalized system, a series of experiments were built to search for possible signals of QGP creation. The NA35 collaboration uses a wide acceptance apparatus at the CERN SPS which detects the majority of charged hadrons (h(+-)), and neutral strange particles produced in reactions of p, O-16 and S-32 projectiles at 60 and 200 GeV/nucleon lab momentum on different targets. It consists of two major tracking devices which provide the momentum measurement of the charged particles: a 2 m long streamer chamber (SC) which is placed inside a 1.5 T vertex magnet, viewed by three cameras, and a 2.5x1.5x1.0 m(sup 3) Time Projection Chamber (TPC). A set of calorimeters was used as the basic trigger device of the experiment, to select central (small impact parameter) collisions. In the data presented here, a calorimeter placed in the beam path selects near head-on collisions, i.e. events where only a small amount of energy (mostly spectator nucleon energy) was detected in an angular acceptance of less than 0.3 degrees around the beam axis. The data sample consists of three systems: S+S, S+Ag and S+Au at 200 GeV/c with trigger cross section of 3, 3.2 and 6% of the total inelastic cross section, respectively. DOE

N94-37716# California Univ., Berkeley. Lawrence Berkeley Lab, CA.
PRE-EQUILIBRIUM PARTON DYNAMICS: PROCEEDINGS
Xin-Nian Wang, ed. 1993 361 p Proceedings of the Pre-Equilibrium Parton Dynamics held in Berkeley, CA, 23 Aug. - 3 Sep. 1993
(Contract DE-AC03-76SF-00098)
(DE94-011347; LBL-34831; CONF-9308181) Avail: CASI HC A16/MF A03

This report contains papers on the following topics: parton production and evolution; QCD transport theory; interference in the medium; QCD and phase transition; and future heavy ion experiments. DOE

N94-37717# California Univ., Berkeley. Lawrence Berkeley Lab, CA.
THE SPIN OBSERVABLES OF ELECTRON-NUCLEON SCATTERING FROM THE FORMALISM OF NUCLEON-NUCLEON SCATTERING
H. E. Conzett Mar. 1994 4 p Presented at the 14th International Conference on Few Body Problems in Physics, Williamsburg, VA, 26-31 May 1994
(Contract DE-AC03-76SF-00098)
(DE94-011368; LBL-35316; CONF-9405132-3) Avail: CASI HC A01/MF A01

The eN scattering spin observables are derived from the long established NN scattering formalism. Some conditions on the eN observables emerge more transparently than from the specific eN calculations themselves. DOE

N94-37720# California Univ., Berkeley. Lawrence Berkeley Lab, CA.
FAST BEAM STUDIES OF FREE RADICAL PHOTODISSOCIATION Ph.D. Thesis
D. R. Cyr Nov. 1993 459 p
(Contract DE-AC03-76SF-00098)
(DE94-011380; LBL-34924) Avail: CASI HC A20/MF A04

The photodissociation of free radicals is studied in order to characterize the spectroscopy and dissociation dynamics of the dissociative electronic states in these species. To accomplish this, a novel method of radical production, based on the photodetachment of the corresponding negative ion, has been combined with a highly complementary form of photofragment translational spectroscopy. The optical spectroscopy of transitions to dissociative states is determined by monitoring the total photofragment yield as a function of dissociation photon energy. Branching ratios to various product channels, internal energy distributions of the fragments, bond dissociation energies, and the translational energy-dependent photofragment recoil angular distributions are then determined at selected excitation energies. A detailed picture of the dissociation dynamics can then be formulated, allowing insight concerning the interactions of potential energy surfaces involved in the dissociation. After an introduction to the concepts and techniques mentioned above, the experimental apparatus used in these experiments is described in detail. The basis and methods used in the treatment of data, especially in the dissociation dynamics experiments, are then put forward. DOE

N94-37721# Pittsburgh Univ., Pittsburgh, PA. Dept. of Physics and Astronomy.
EXPERIMENTAL PARTICLE PHYSICS AT THE UNIVERSITY OF PITTSBURGH
E. Engels, Jr., P. F. Shepard, and J. A. Thompson May 1994 151 p
(Contract DE-FG02-91ER-40646)
(DE94-011636; DOE/ER-40646/4) Avail: CASI HC A08/MF A02

Task A involves the study of kaon decays. The overall physics focus of the current work is rare and semi-rare decays of the phi and the short-lived kaon, with an emphasis on those aspects needed in preparation for the proposed. Phi-factory measurements of CPT violation. Another aspect of the rare kaon decay work is E865 at BNL, a search for K(+) yields pi(+)mu(+)e(-), a lepton number violating process. Pittsburgh's E865 responsibilities are the design and construction of the Cerenkov counters. The major goals of task B are as follows: (1) the analysis of the E706 (direct photon production) data taken during the 1987--1988 and 1990--1991 target runs at Fermilab and (2) the continuation of work within SVXII group of the CDF collaboration. The CDF program involves a dedicated effort towards the design of the silicon vertex detector upgrade, SVXII. DOE

73 NUCLEAR AND HIGH-ENERGY PHYSICS

Includes elementary and nuclear particles; and reactor theory. For space radiation see *93 Space Radiation*.

N94-36545 Science Research Council, Chilton (England).
PARTICLE PHYSICS EXPERIMENTS REPORT, 1993
1994 254 p See also PB93-187110 Prepared in cooperation with Rutherford Appleton Lab., Chilton, England
(PB94-169109; RAL-94-009) Copyright Avail: Issuing Activity (National Technical Information Service (NTIS))

This report describes work carried out in 1993 on experiments approved by the Particle Physics Experiments Selection Panel. The contents consist of unedited contributions from each experiment. NTIS

N94-36694# Argonne National Lab., IL.
HIGH ENERGY PHYSICS DIVISION OF RESEARCH ACTIVITIES Semiannual Report, 1 Jul. - 30 Dec. 1992
P. Schoessow, ed., P. Moonier, ed., R. Talaga, ed., and R. Wagner, ed. Jul. 1993 102 p
(Contract W-31-109-eng-38)
(DE93-019681; ANL-HEP-TR-93-22) Avail: CASI HC A06/MF A02

This report describes the research conducted in the High Energy Physics Division of Argonne National Laboratory during the period of July 1, 1992--December 30, 1992. Topics covered here include experimental and theoretical particle physics, advanced accelerator physics, detector development, and experimental facilities research. Lists of division publications and colloquia are included. DOE

N94-36748# Academy of Sciences (USSR), Novosibirsk (USSR). Inst. Yadernoj Fiziki.
METHODS OF CALCULATION OF HIGHER POWER CORRECTIONS IN QCD
A. G. Grozin 1992 24 p
(DE94-618511; BUDKERINP-92-11) Avail: CASI HC A03/MF A01 (US Sales Only)

The algorithms of calculation of higher power corrections in QCD sum rules based on the fixed-point gauge are reviewed. The systematic classification of vacuum condensates is divided heavy quark condensates and correlators and light quark ones are discussed. DOE

N94-37194# Argonne National Lab., IL. Reactor Analysis Div.
AN OVERVIEW OF THE CURRENT STATUS OF RESONANCE THEORY IN REACTOR PHYSICS APPLICATIONS
R. N. Hwang 1993 50 p Presented at the 10th International School of Nuclear Physics, Neutron Physics, and Nuclear Energy, Varner, Bulgaria, 3-11 Oct. 1993
(Contract W-31109-eng-38)
(DE94-010465; ANL/RA/CP-80550; CONF-9310313-1) Avail: CASI HC A03/MF A01

The neutron resonance phenomena constitute one of the most fundamental subjects in nuclear physics as well as in reactor physics. It is the area where the concepts of nuclear interaction and the treatment of the neutronic balance in reactor lattices become intertwined. The later requires the detailed knowledge of resonance structures of many nuclide of practical interest to the development of nuclear energy. The key issue of the resonance treatment in reactor applications is directly associated with the use of the microscopic cross sections in the macroscopic reactor cells with a wide range of composition, temperature,and geometric configurations. It gives rise to the so called self-shielding effect. The accurate estimations of such an effect are essential not only in the calculation of the criticality of a reactor but also from the point of view of safety considerations. The latter manefests through the Doppler effect particularly crucial to the fast reactor development. The task of accurate treatment of the self-shielding effect, however, is by no means simple. In fact, it is perhaps the most complicated problem in neutron physics which, strictly speaking, requires the dependence of many physical variables. Two important elements of particular interest are: (1) a concise description of the resonance cross sections as a function of energy and temperature; (2) accurate estimation of the corresponding neutron flux where appropriate. These topics will be discussed from both the historical as well as the state-of-art perspectives. DOE

N94-37200# California Univ., Berkeley. Lawrence Berkeley Lab, CA.
SUPPRESSION OF BEAM-BREAK-UP IN A STANDING WAVE FREE ELECTRON LASER TWO-BEAM ACCELERATOR
H. Li and J. S. Kim Mar. 1994 8 p Presented at the Conference on Optics, Electro-Optics, and Laser Applications in Science and Engineering, Los Angeles, CA, 22-29 Jan. 1994 Prepared in cooperation with LLNL, Livermore, CA
(Contracts DE-AC03-76SF-00098; W-7405-eng-48)
(DE94-011348; LBL-35324; CBP-72; CONF-940142-38) Avail: CASI HC A02/MF A01

Various schemes are examined in this study on the suppression of beam break-up (BBU) in a standing wave free electron laser two-beam accelerator (SWFEL/TBA). Two schemes are found to be not only able to effectively suppress the BBU but at the same time have minimum effect on the microwave generation process inside the SWFEL cavities. One is making the cavity-iris junction sufficiently gradual and the other is stagger-tuning the cavities. DOE

N94-37220# Oak Ridge National Lab., TN.
TESTING NEW TECHNOLOGY FOR THE HEAVY ION EXPERIMENT AT CERN
C. L. Britton, Jr., M. L. Simpson, J. W. Walker, and A. L. Wintenberg 17 Dec. 1993 10 p

(Contract DE-AC05-84OR-21400)
(DE94-004747; ORNL/FTR-4875) Avail: CASI HC A02/MF A01 (US Sales Only)

The travelers spent two weeks at the European Organization for Nuclear Research (CERN) working with G. R. Young of the Oak Ridge National Laboratory Physics Division to install and test prototype electronics developed for the lead-glass calorimeter of the WA98 experiment at CERN. These tests were generally successful, and information needed to finalize the design was obtained. Discussions involving both the ORNL personnel and other WA98 collaborators were also held to finalize the design of the electronics, production plans, production schedule, and installation schedule. DOE

N94-37234# National Lab. for High Energy Physics, Ibaraki (Japan).
PHYSICS WITH PRIMARY BEAMS OF THE KEK-PS
Kazuhiro Tanaka, ed. and Masahito Yoshii, ed. Aug. 1993 124 p
(DE94-748635; KEK-93-8) Avail: CASI HC A06/MF A02

The 12-GeV Proton Synchrotron (PS) at the National Laboratory for High Energy Physics (KEK) has provided great opportunities to high-energy-physics and related communities as a unique high-energy hadron machine, since its operation in 1976. Activities of the KEK-PS are indispensable for the rapid development in the field. Six experimental subjects are proposed in this report: (1) media effects in (phi) meson decay, (2) multifragmentation in high-energy reactions, (3) mechanism of high-energy reactions by means of radio-chemical methods, (4) physics with polarized high-energy neutrons, (5) physics with polarized high-energy deuterons, and (6) hypernucleus with high-energy heavy-ion beams. As a summary, new facilities (a new injector, a new beamline and a new experimental area) and physics programs with primary beams, proposed in this report are themselves unique and valuable. Moreover, technical developments and physics outcomes stimulated with those new facilities are indispensable for future plans of the KEK-PS. DOE

N94-37236# National Lab. for High Energy Physics, Ibaraki (Japan).
[ACTIVITIES OF THE PHOTON FACTORY] Report, 1992
1993 642 p
(DE94-748682; KEK-PR-93-1) Avail: CASI HC A99/MF A06

This issue is the annual report of the Photon Factory, National laboratory of High Energy Physics. First, the outline of the Photon Factory is presented. Injector linac, light source, beamlines and instrumentation, the Tristan synchrotron radiation facility at the accumulation ring, and the Tristan super light facility are described in detail. The facility is open to researchers. The user's reports are collected as well. (J.P.N. DOE

N94-37237# Tsukuba Univ., Ibaraki (Japan). Accelerator Center.
[ACTIVITIES OF THE TANDEM ACCELERATOR CENTER, UNIVERSITY OF TSUKUBA] Annual Report
Oct. 1993 136 p
(DE94-748687; UTTAC-60) Avail: CASI HC A07/MF A02

This annual report includes the research activities and the technical developments carried out at the Tandem Accelerator Center in University of Tsukuba for the period from April 1992 to March 1993. New experimental investigations were made on (1) nuclear spectroscopy was initiated by a new (gamma) ray spectrometer; (2) polarization phenomena in nuclear reactions; (3) the application of energetic heavy ions to solid state physics; (4) the behavior of self interstitial atoms and its migration mechanism in Mo metal; (5) the studies on electronic conduction of metal oxides and bronzes by NMR; (6) Moessbauer studies on Fe-Cr alloy and the RBS analysis of YBCO superconductor films; and (7) a new field was challenged on the micro cluster physics. Nuclear collective motion and the relativistic mean-field theory is also included in this report. DOE

N94-37303# Acceleration Consultants, Albuquerque, NM.
BMAP DIPOLE MAGNETIC FIELD ANALYSIS AND ORBIT TRACKING/CALCULATIONS OF ENERGY DEPOSITION IN GaAs WHEBY DETECTORS
S. Humphries, Jr., R. M. Baltrusaitis, C. Ekdahl, C. Young, and C. Warn 1994 20 p Presented at the 1993 Computational Accelerator Physics Conference, Pleasanton, CA, 22-26 Feb. 1993 Prepared for Los Alamos National Lab., NM
(Contract W-7405-eng-36)
(DE94-012080; LA-SUB-94-74; CONF-930269-26) Avail: CASI HC A03/MF A01

This report contains two separate papers. The first paper discusses BMAP which is a versatile program for field analysis and orbit tracking in dipole magnets. The program was created to aid the design of charged-particle magnetic spectrometers. BMAP is written in Pascal and runs on any IBM-PC computer or compatible. The second paper covers a study on energy deposition in GaAS WHEBY detectors. The study was done for two purposes: (1) to set up a three-dimensional electron-photon transport problem using the ACCEPT computer code; and (2) to calculate energy deposition in GaAs detectors in the WHEBY for a given flux of electrons. DOE

N94-37310# Los Alamos National Lab., NM.
NON-EQUILIBRIUM EVOLUTION OF THE DISORIENTED CHIRAL CONDENSATE IN HEAVY-ION COLLISIONS
Y. Kluger 1994 25 p Presented at the Theoretical Physics Institute on Continuous Advances in Quantum Chromodynamics Conference, Minneapolis, MN, 17-20 Feb. 1994
(Contract W-7405-eng-36)
(DE94-012897; LA-UR-94-1566; CONF-940280-1) Avail: CASI HC A03/MF A01

We study the dynamics of the chiral phase transition expected during the expansion of the quark-qluon plasma produced in a high energy hadron or heavy ion collision in the O(4) linear sigma model to leading order in a large N expansion for strong coupling constants. Starting from an approximate equilibrium configuration at an initial proper time tau in the disordered phase, we study the transition to the ordered broken symmetry phase as the system expands and cools. We give results for the proper time evolution of the effective pion mass, the order parameter (sigma) as well as for the pion two point correlation function expressed in terms of a time dependent phase space number density and pair correlation density. We investigate the possibility of disoriented chiral condensate being formed during the expansion. In order to create large domains of disoriented chiral condensates low-momentum instabilities have to last for long enough periods of time. Our simulations show that instabilities that are formed during the initial stages of the expansion survive for proper times that are at most 3 fm/c. DOE

N94-37463# Japan Atomic Energy Research Inst., Tokyo (Japan).
PRODUCTION OF HIGH CURRENT H(-) BEAMS IN A CESIUM SEEDED VOLUME NEGATIVE ION SOURCE EQUIPPED WITH PG FILTER
Masanobu Tanaka (Japan Atomic Energy Research Inst., Naka, Japan.), Masaya Hanada (Japan Atomic Energy Research Inst., Naka, Japan.), Takashi Inoue (Japan Atomic Energy Research Inst., Naka, Japan.), and Yoshikazu Okumura (Japan Atomic Energy Research Inst., Naka, Japan.) Jul. 1993 30 p In JAPANESE
(DE94-718962; JAERI-M-93-132) Avail: CASI HC A03/MF A01

For neutral beam injectors of fusion reactors, it is required to produce uniform high current H(-) beams with large cross section. To realize this requirement, we have developed a large volume-production type negative ion source equipped with a uniform electromagnetic filter called PG filter, where a transverse magnetic field is generated by the current flowing in a plasma grid (PG). In this experiment, we tested PG filter with cesium for the first time and obtained maximum H(-) beam current of 7A (26 mA/sq cm) at an arc power of 35 kV (70 V, 500 A). This efficiency of H(-) production is better than that of external filter and other type of filters. At a very low filling pressure (0.3 Pa) in the negative ion generator, H(-) beam of 4.4 A (16 mA/sq cm) was produced. It satisfies the design value of the negative ion source for JT-60U. Investigated were the optimum magnetic filter strength in a cesium seeded condition, the extracted electron current that gives electrodes heat load and the beam bending angle by the magnetic filter field, which are useful for the design of future large negative ion sources. DOE

N94-37508*# Old Dominion Univ., Norfolk, VA. Dept. of Mathematics and Statisitics.
THEORETICAL STUDIES OF A MOLECULAR BEAM GENERATOR Progress Report, 15 May 1994
John H. Heinbockel Jul. 1994 18 p
(Grant NAG1-1424)
(NASA-CR-196306; NAS 1.26:196306) Avail: CASI HC A03/MF A01

We consider the problem of modeling a high temperature diatomic gas N2 flowing through a converging-diverging high expansion nozzle. The problem is modeled in two ways. The first model uses a single temperature with variable specific heats as functions of this temperature. For the second model we assume that the various degrees of freedom all have a Boltzmann population distribution which means that each degree of freedom has its own temperature and consequently each system state can be characterized by these temperatures. This suggests the formulation of a second model with a vibrational degree of freedom as having its own temperature along with a rotational-translational degree of freedom with its own temperature. Initially the vibrational degree of freedom is excited by heating the gas to a high temperature. As the high temperature gas expands through the nozzle throat there is a sudden drop in the rotational-translational temperature along with a finite relaxation time for the vibrational degree of freedom to achieve equilibrium with the rotational-translational degree of freedom. That is, the temperature change that occurs when the N2 gas passes through the nozzle throat is so great that the changes in the vibrational degree of freedom lags behind the rotational-translational energy changes. The resulting relaxation time is finite. It is in this context that the term nonequilibrium is used. That is, the term nonequilibrium denotes the fact that the energy content of the various degrees of freedom are characterized by two temperatures. We neglect any chemical reactions resulting from the high temperatures which could also add nonequilibrium effects. We develop the basic equations for the two models in various forms in order to check the derivations with other sources. The final form which is solved numerically consists of the scaled equations in a conservative dimensionless form. Derived from text

N94-37547# Fermi National Accelerator Lab., Batavia, IL.
FERMILAB'S DART DA SYSTEM
R. Pordes, J. Anderson, D. Berg, D. Black, R. Forster, J. Franzen, S. Kent, R. Kwarciany, J. Meadows, and C. Moore et al Apr. 1994 7 p Presented at the Meeting on Computing in High-Energy Physics, San Francisco, CA, 21-27 Apr. 1994
(Contract DE-AC02-76CH-03000)
(DE94-013240; FNAL/C-94/103; CONF-940492-3) Avail: CASI HC A02/MF A01

DART is the new data acquisition system designed and implemented for six Fermilab experiments by the Fermilab Computing Division and the experiments themselves. The complexity of the experiments varies greatly. Their data taking throughput and event filtering requirements range from a few (2-5) to tens (80) of CAMAC, FASTBUS and home built front end crates; from a few 100 KByte/sec to 160 MByte/sec front end data collection rates; and from 0-3000 Mips of level 3 processing. The authors report on the architecture and implementation of DART to this date, and the hardware and software components which are being developed and supported. DOE

N94-37619# Argonne National Lab., IL.
LASER COOLING OF 24Mg+ IN THE ASTRID STORAGE RING
J. S. Nielsen, J. S. Hangst, O. Poulsen, P. Shi, and J. P. Schiffer 1994 4 p Presented at the CERN Workshop on Beam Cooling and Related Topics, Geneva, Switzerland, 4-8 Oct. 1993
(Contract W-31-109-eng-38)
(DE94-010445; ANL/PHY/CP-82605; CONF-9310193-11) Avail: CASI HC A01/MF A01

Laser cooling of Mg-24(+) has now begun at the ASTRID storage ring. In contrast to Li-7(+), which has been used up to now, it is now possible for the laser to interact with all of the beam. In this paper, some of the results from the first beam time with Mg-24(+) are described. By frequency chirping a single laser, laser cooling has been performed on a coasting beam, and first evidence of sympathetic transverse cooling has been observed. DOE

N94-37629# Los Alamos National Lab., NM.
THE EFFECTS OF PROTON-BEAM QUALITY ON THE PRODUCTION OF GAMMA RAYS FOR NUCLEAR RESONANCE ABSORPTION IN NITROGEN
R. Graybill, ed. May 1994 13 p
(Contract W-7405-eng-36)
(DE94-011609; LA-12777-MS) Avail: CASI HC A03/MF A01

The authors describe a method for performing nuclear-resonance absorption with the proton beam from a radio-frequency quadrupole (RFQ) linear accelerator. The objective was to assess the suitability of the pulsed beam from an RFQ to image nitrogen compared to electrostatic accelerators. This choice of accelerator results in trade-offs in performance and complexity, in return for the prospect of higher average current. In spite of a reduced resonance attenuation coefficient in nitrogen, they successfully produced three-dimensional tomographic images of real explosives in luggage the first time the unoptimized system was operated. The results and assessments of the initial laboratory measurements are reported. DOE

N94-37727# National Lab. for High Energy Physics, Tsukuba (Japan).
PROCEEDINGS OF THE WORKSHOP ON TRISTAN PHYSICS AT HIGH LUMINOSITIES
Masanori Yamauchi, ed. Apr. 1993 310 p Workshop held in Tsukuba, Japan, 15-16 Dec. 1992
(DE94-737969; KEK-Proc-93-2; CONF-9212108) Avail: CASI HC A14/MF A03

This publication is a collection of the papers presented at the title meeting. DOE

74 OPTICS

Includes light phenomena; and optical devices.
For lasers see *36 Lasers and Masers.*

N94-36468 International Society for Optical Engineering, Bellingham, WA.
PROCEEDINGS OF SPIE: THE INTERNATIONAL SOCIETY FOR OPTICAL ENGINEERING, COMPUTATIONAL VISION BASED ON NEUROBIOLOGY, VOLUME 2054
Teri B. Lawton 9 Jul. 1993 254 p Meeting held in Pacific Grove, CA, 6-9 Jul. 1993 Limited Reproducibility: More than 20% of this document may be affected by microfiche quality
(AD-A278731) Avail: Issuing Activity (Defense Technical Information Center (DTIC))

Modulation of cortical firing rate is a major factor in defining cortical filter properties. Active response suppression (inhibition) is seen whenever cortical cells are exposed to grating stimuli that are non-optical, in either the domain of orientation or spatial frequency. Responses are also reduced by pre-exposure to gratings of high contrast. The first phenomenon is termed spatially-dependent inhibition, the second contrast gain control. We have explored the physiological basis for these two phenomena in striate cortical cells of anesthetized cat. Sequences of spikes in responses show bursts characterized by interspike intervals of 8 msec or less. Both burst frequency and burst length depend on average firing rate, but at a given firing rate burst length is lower for non-optimal orientations. Burst length is also shortened by local injection of GABA. Burst length modulation is not seen in the case of contrast gain control. These results support the existence of two independent mechanisms for modulating cortical responsiveness. A GABA-ergic mechanism that shortens spike bursts is invoked by presentation of spatially non-optimal stimuli. Response normalization after presentation of high contrasts does not affect burst length and is not affected by GABA. DTIC

N94-36693# Lawrence Livermore National Lab., Livermore, CA.
DETERMINING THE REFRACTIVE INDEX OF A LAMBDA/4 THIN FILM ON A THICK SUBSTRATE FROM A TRANSMITTANCE MEASUREMENT
R. Chow, G. E. Loomis, and P. Biltoft Jun. 1993 12 p
(Contract W-7405-eng-48)
(DE93-019584; UCRL-ID-114560) Avail: CASI HC A03/MF A01

The refractive index is a key optical constant required by optical thin film designers. The coater-designer team must constantly verify the refractive indices of the non-absorbing optical thin films since the refractive index of a deposited material can vary by switching coating systems or operators as well as expected changes during the course of a coating run. A transmittance measurement on a spectrophotometer is an easy and accurate (usually to within (+-)0.5% spread) method of determining the refractive index. In one technique, the refractive index is obtained from visually curve-fitting a calculated (using a thin film design program and selecting the refractive index) transmittance spectrum to the measured transmittance spectrum. There are two other techniques which are discussed in this report: A quick, approximate method vs. the exact derivation. What the

authors have not been able to find in the literature is the exact transmittance dependence as a function of the refractive indices (layers) through which the light passes and which accounts for the substrate back reflections. There are undocumented approximation methods as well as one in the literature by Cheremukhin and Rozhnox. Otherwise, most texts either derive the transmittances through optical multilayers or just the effect of back reflections on the transmittance for thick substrates. Without correcting for substrate back reflections, the derived refractive indices from the measured transmittances are in error by as much as 10%. In this work, the authors have utilized both an exact and an approximate method of determining the refractive index of the film. It is found that both the exact and approximate methods of determining the refractive index of thin optical coatings are within the measurement errors of commercially available spectrophotometers. DOE

N94-37110 California Univ., Santa Barbara, CA. Dept. of Physics.
A NEW, OPTICAL-LEVER BASED ATOMIC FORCE MICROSCOPE Technical Report No. 11, 1 Jan. - 31 Dec. 1994
P. K. Hansma, B. Drake, D. Grigg, C. B. Prater, F. Yashar, G. Gurley, V. Elings, S. Feinstein, and R. Lal 1994 9 p Submitted for publication Limited Reproducibility: More than 20% of this document may be affected by microfiche quality
(Contract N00014-92-J-1260)
(AD-A280524) Avail: CASI HC A02

A new optical-lever based atomic force microscope is described in which the cantilever scans and is accurately tracked by a scanning focused spot. It can operate at forces below one nanoNewton over image areas greater than 100 microns x 100 microns. It can be combined with optical microscopes of high numerical aperture and operated with the sample and cantilever in fluids. As examples of its applications, images of living cells in Petri dishes and a 6 in. (15.24 mm) silicon wafer are included. Author (DTIC)

N94-37112# Lawrence Livermore National Lab., Livermore, CA.
U-TURN ALTERNATIVE TO THE LARGE APERTURE SWITCH
Charles S. Vann Mar. 1994 8 p
(Contract W-7405-eng-48)
(DE94-011541; UCRL-ID-116758) Avail: CASI HC A02/MF A01

The primary alternative laser architecture is the U-turn design. The U-turn has significantly different cost and performance risks than the full-aperture switch, which makes it a highly desirable alternative. The U-turn was conceived at LLNL in 1992. A similar concept, the L-turn, had already been discovered by the French at CEL-V. Both concepts are based on the multipass glass amplifier design, but the full-aperture Pockels cell and polarizer are replaced with smaller and less expensive optics. Eliminating the large switch and polarizer not only reduces component costs, it also provides options for shortening the laser which, in turn, could reduce the size and cost of the laser building. Efficient use of the amplifier aperture (small vignetting allowance) requires that the U-turn have a long transport spatial filter; however, this is not a disadvantage if a long spatial filter is already required for image relaying to the frequency converter. Given a long spatial filter, the U-turn is potentially more efficient because losses in the switch and polarizer are avoided. DOE

N94-37142 Air Force Inst. of Tech., Wright-Patterson AFB, OH.
A DIFFRACTION-BASED MODEL OF ANISOPLANATISM EFFECTS IN ADAPTIVE OPTIC SYSTEMS Ph.D. Thesis
Steven E. Troxel Jun. 1994 136 p Limited Reproducibility: More than 20% of this document may be affected by microfiche quality
(AD-A280491; AFIT/DS/ENG/94J-05) Avail: Issuing Activity (Defense Technical Information Center (DTIC))

This dissertation presents a new method for computing the angle dependent performance measures of an adaptive-optics system. New theory is presented that uses the diffraction-based propagation model to yield optical transfer function (OTF) expressions that are more accurate as compared to current theory that neglects diffraction. Author (revised)

N94-37149 Northwestern Univ., Evanston, IL. Dept. of Electrical Engineering and Computer Science.
InTlSb FOR LONG-WAVELENGTH INFRARED PHOTODETECTORS AND ARRAYS
Manijeh Razeghi 1994 14 p Limited Reproducibility: More than 20% of this document may be affected by microfiche quality
(Contract N00014-92-J-1951)
(AD-A280207) Avail: CASI HC A03

The objective of this research program is to grow InTlSb alloys for long-wavelength infrared detectors by low-pressure metalorganic chemical vapor deposition and to investigate their physical properties. As the start towards this goal, optimum growth conditions for high quality InSb epitaxial films on InSb, GaAs, and Si have been determined. InSb films grown under these conditions exhibited one of the best structural and electrical properties reported so far. Growth of InTlSb was then carried out using cyclopentadienylthallium as the source for thallium. This has led to the first successful growth of InTlSb having an extended infrared response. By changing the thallium flow, thallium content was varied and the resulting absorption edge varied from 5.5 micrometers to 9.0 micrometers. For conditions yielding a 9.0 micrometer absorption edge, a thick sample was grown which resulted in a photoconductor having a specific detectivity of D(*) = 10(exp 9) cmHz(sup 1/2)/W(sup -1) at 77K and 7 micrometers. These results demonstrate InTlSb as feasible material system for infrared detection. DTIC

N94-37157# Brookhaven National Lab., Upton, NY.
TUNE MODULATION DUE TO GRADIENT RIPPLE AND THE DYNAMIC APERTURE
G. Parzen 1994 3 p Presented at the 4th European Particle Accelerator Conference, London, England, 27 Jun. - 1 Jul. 1994
(Contract DE-AC02-76CH-00016)
(DE94-011922; BNL-49801; CONF-940618-3) Avail: CASI HC A01/MF A01

A tracking study was done of the effects of a tune modulation, due to a gradient ripple in the quadrupoles, on the dynamic aperture. The tracking runs were for about 1 x 10(exp 6) turns. The dependence of the dynamic aperture on the frequency of the gradient ripple was also studied. DOE

N94-37165# California Univ., Berkeley. Lawrence Berkeley Lab, CA.
RECOVERING DEPTH FROM FOCUS USING ITERATIVE IMAGE ESTIMATION TECHNIQUES
J. Vitria and J. Llacer Sep. 1993 53 p
(Contract DE-AC03-76SF-00098)
(DE94-010994; LBL-35158) Avail: CASI HC A04/MF A01

We examine the possibility of using linear and nonlinear image estimation techniques to build a depth map of a three dimensional scene from a sequence of partially focused images. In particular, the techniques proposed to solve the problem of construction of a depth map are: (1) linear methods based on regularization procedures and (2) nonlinear methods based on statistical modeling. In the first case, we have implemented a matrix-oriented method to recover the point spread function (PSF) of a sequence of partially defocused images. In the second case, the chosen method has been a procedure based on image estimation by means of the EM algorithm, a well known technique in image reconstruction in medical applications. This method has been generalized to deal with optically defocused image sequences. DOE

N94-37191# Lawrence Livermore National Lab., Livermore, CA.
FINAL REPORT ON SPECTRAL BROADENING BY CROSS-PHASE MODULATION IN LINEARLY BIREFRINGENT OPTICAL FIBERS
C.-J. Chen (Maryland Univ., Baltimore, MD.), P. K. A. Wai (Maryland Univ., Baltimore, MD.), and C. R. Menyuk (Maryland Univ., Baltimore, MD.) Dec. 1993 44 p
(Contract W-7405-eng-48)
(DE94-010406; UCRL-CR-115942) Avail: CASI HC A03/MF A01

Spectral widening by using the cross-phase modulation in a linearly birefringent optical fiber is investigated numerically. The coupled nonlinear Schroedinger equation that describes the wave propagation of each polarization in a birefringent optical fiber is discussed. Based on this equation, we generated computer simulations for different values of birefringence and dispersion. We found that a smooth output signal with intensity fluctuations of less than 10% and a spectral width of more than 50 Angstroms is possible with low dispersion and low birefringence, e.g., D = -10 psec/nm-km and (delta)n 2 x 10(exp -5). We also found that the Raman effect does not play a significant role. DOE

N94-37258# Brookhaven National Lab., Upton, NY.
GUIDING HARD X RAYS WITH GLASS POLYCAPILLARY FIBER
Q.-F. Xiao (X-Ray Optical Systems, Inc., Albany, NY.), I. Y. Ponomarev (X-Ray Optical Systems, Inc., Albany, NY.), A. I. Kolomitsev (X-Ray Optical Systems, Inc., Albany, NY.), D. M. Gibson (X-Ray Optical Systems, Inc., Albany, NY.), F. A. Dilmanian, and E. Nachaliel 1993 10 p Presented at the Synchrotron Radiation Instrumentation, Gaithersburg, MD, 23-26 Aug. 1993
(Contracts DE-AC02-76CH-00016; DE-FG02-91ER-81221)
(DE94-004949; BNL-49773; CONF-930824-31) Avail: CASI HC A02/MF A01

X rays can be guided through a polycapillary fiber by multiple total reflections from the smooth channel walls of the fiber. Using monochromatic Synchrotron Radiation at energies of 22 and 44 keV, we measured the efficiency of transmission of x rays through polycapillary fibers with channel diameters of about 13 (mu)m. Efficiencies of 57.3 percent and 54.5 percent for 22 keV and 44 keV x rays, respectively, were obtained with a 120-mm-long straight polycapillary fiber aligned with the incident beam. These values are close to the open fraction of the fiber, which is about 60 percent. In addition, transmission efficiency was measured as a function of the tilt angle between the incident beam and the axis of the fiber. We also measured the transmission efficiency as a function of the deflection angle for a 114-mm-long curved polycapillary fiber. The measurements are compared with a ray-tracing simulation. DOE

N94-37350 Phillips Lab., Kirtland AFB, NM.
THREE-STAGE ATTENUATION USING GLAN-THOMPSON PRISMS Final Report, Oct. 1991 - Dec. 1992
Doris A. Bruner, William T. Kemp, Robert J. Champetier, and Mark M. Altamirano May 1994 42 p Limited Reproducibility: More than 20% of this document may be affected by microfiche quality
(AD-A280481; PL-TR-93-1041) Avail: CASI HC A03

Conventional three-polarizer attenuators were developed in the 1960's and had accuracies limited to 0.001 transmittance unit. In 1971, Mielenz and Eckerle determined that at least ten times more accuracy could be obtained using two new types of attenuators which employed either a half-wave or a quarter-wave retardation plate, in conjunction with two sheet polarizers. The purpose of the current effort was to test the same concept using extremely high quality optical Glan-Thompson prisms, extremely precise automated stages, and an experimental setup designed to provide accurate measurement for high extinction ratios, to determine the feasibility of using a three-stage polarizer attenuator with laser beams in the 350- to 2500-nm range. This device would be used to calibrate experimental signals and/or the transmittance of neutral density filters. The experimental results indicated that this attenuator could only provide uncertainties of 1 to 2 percent. The photometric accuracy was not tested with natural sources. However, this attenuator was useful in providing practical accuracies of a few percent over a wide dynamic range with a simple technique. It can be used to calibrate neutral density filters over a wavelength range from 350 to 2500 nm and an optical density range of nine orders of magnitude. DTIC

N94-37374# Oak Ridge National Lab., TN.
MEASUREMENT OF SCANNING ELECTRON MICROSCOPE RESOLUTION
J. Bentley, E. A. Kenik, and N. D. Evans 1994 2 p Presented at the Microscopy Society of America and Microbeam Analysis Society Joint Meeting, New Orleans, LA, 31 Jul. - 5 Aug. 1994
(Contract DE-AC05-84OR-21400)
(DE94-012661; CONF-940753-6) Avail: CASI HC A01/MF A01

Resolution is traditionally determined with specimens such as gold islands on bulk C supports; however this is subjective. By substituting a thin C support for the traditional bulk C, while retaining the gold islands, the essential features of the traditional SEM resolution test specimen remain unchanged, but an independent and reliable measurement of particle sizes and spacings becomes possible using TEM. A test specimen consisting of latex spheres supported on a thin, holey C film, obliquely shadowed with gold, can be used for resolution tests at the sub-2nm level; the latex sphere arrangement, shadows in the gold coverage, and holes in the C film enable the same area to be found rapidly in TEM and SEM instruments. The area used for assessing SEM performance is also imaged by TEM, either before or after the SEM work; advantages of each sequence are discussed. DOE

N94-37486# Lawrence Livermore National Lab., Livermore, CA.
COHERENT MULTIPLE-FOIL X-RAY TRANSITION RADIATION
M. J. Moran, B. Chang, and M. B. Schneider 25 Aug. 1993 12 p Presented at the International Symposium on Radiation of Relativistic Electrons in Periodical Structures, Tomsk, Russia, 6-10 Sep. 1993
(Contract W-7405-eng-48)
(DE93-040831; UCRL-JC-114239; CONF-9309233-1) Avail: CASI HC A03/MF A01

Intense x-ray transition radiation can be generated when relativistic electrons pass through a multiple-foil target. When the foil spacing is periodic, the transition radiation can be spatially coherent with respect to the target period. The spatial coherence can be evident in the spectra and angular distributions of transition radiation from such targets. A series of experiments has measured coherent transition radiation distributions from multiple-foil targets (up to six foils) with spacings of 50 and 100 microns. The electron energy was about 75 MeV and the photon energies were about 200 eV. Agreement between calculation and experimental data is excellent. DOE

N94-37532# Michigan Univ., Ann Arbor, MI.
SUBMICROMETER FIBER-OPTIC CHEMICAL SENSORS: MEASURING pH INSIDE SINGLE CELLS
R. Kopelman 1993 51 p
(Contract DE-FG02-90ER-61085)
(DE94-004160; DOE/ER-61085/3) Avail: CASI HC A04/MF A01

Starting from scratch, we went in two and a half years to 0.04 micron optical microscopy resolution. We have demonstrated the application of near-field scanning optical microscopy to DNA samples and opened the new fields of near-field scanning spectroscopy and submicron opto-chemical sensors. All of these developments have been important steps towards in-situ DNA imaging and characterization on the nanoscale. Our first goal was to make NSOM (near-field scanning optical microscopy) a working enterprise, capable of 'zooming-in' towards a sample and imaging with a resolution exceeding that of traditional microscopy by a factor of ten. This has been achieved. Not only do we have a resolution of about 40 nm but we can image a 1 x 1 micron object in less than 10 seconds. Furthermore, the NSOM is a practical instrument. The tips survive for days or weeks of scanning and new methods of force feedback will soon protect the most fragile samples. Reproducible images of metal gratings, gold particles, dye balls (for calibration) and of several DNA samples have been made, proving the practicality of our approach. We also give highly resolved Force/NSOM images of human blood cells. Our second goal has been to form molecular optics (e.g., exciton donor) tips with a resolution of 2-10 nm for molecular excitation microscopy (MEM). We have produced such tips, and scanned with them, but only with a resolution comparable to that of our standard NSOM tips. However, we have demonstrated their potential for high resolution imaging capabilities: (1) An energy transfer (tip to sample) based feedback capability. (2) A Kasha (external heavy atom) effect based feedback. In addition, a novel and practical opto-chemical sensor that is a billion times smaller than the best ones available has been developed as well. Finally, we have also performed spatially resolved fluorescence spectroscopy. DOE

N94-37579*# Tennessee Technological Univ., Cookeville, TN. Center for Manufacturing Research and Technology Utilization.
DESIGN OF A COMPOSITE FILTER REALIZABLE ON PRACTICAL SPATIAL LIGHT MODULATORS Final Report
P. K. Rajan and Ramachandran Ramakrishnan Jul. 1994 164 p
(Grant NAG9-710)
(NASA-CR-196297; NAS 1.26:196297; MCTR-0794-01) Avail: CASI HC A08/MF A02

Hybrid optical correlator systems use two spatial light modulators (SLM's), one at the input plane and the other at the filter plane. Currently available SLM's such as the deformable mirror device (DMD) and liquid crystal television (LCTV) SLM's exhibit arbitrarily constrained operating characteristics. The pattern recognition filters designed with the assumption that the SLM's have ideal operating characteristic may not behave as expected when implemented on the DMD or LCTV SLM's. Therefore it is necessary to incorporate the SLM constraints in the design of the filters. In this report, an iterative method is developed for the design of an unconstrained minimum average correlation energy (MACE) filter. Then using this algorithm a new approach for the design of a SLM constrained distortion

invariant filter in the presence of input SLM is developed. Two different optimization algorithms are used to maximize the objective function during filter synthesis, one based on the simplex method and the other based on the Hooke and Jeeves method. Also, the simulated annealing based filter design algorithm proposed by Khan and Rajan is refined and improved. The performance of the filter is evaluated in terms of its recognition/discrimination capabilities using computer simulations and the results are compared with a simulated annealing optimization based MACE filter. The filters are designed for different LCTV SLM's operating characteristics and the correlation responses are compared. The distortion tolerance and the false class image discrimination qualities of the filter are comparable to those of the simulated annealing based filter but the new filter design takes about 1/6 of the computer time taken by the simulated annealing filter design. Author (revised)

N94-37657*# Christopher Newport Coll., Newport News, VA. Dept. of Physics and Computer Science.
PROSPECTIVE COMMUNICATIONS RESEARCH TO SUPPORT FLY BY LIGHT/POWER BY WIRE Final Report, 18 Jul. - 26 Dec. 1991
David Game 13 Jul. 1994 18 p
(Grant NAG1-1309)
(NASA-CR-196369; NAS 1.26:196369) Avail: CASI HC A03/MF A01

A NASA Research Grant NAG-1-1309, Distributed Fiber Optic Systems for Commercial Aircraft, was awarded during July 1991. This report primarily constitutes a summary of findings of the original background research done at that time. NASA is embarking on a research project to design the next generation of commercial aircraft, fly by light/power by wire. The objectives of this effort are to improve commercial aircraft design by (1) reducing the weight of the aircraft to improve efficiency and (2) improving the fault tolerance and safety of the aircraft by enhancing current systems with new technologies or introducing new systems into the aircraft. Derived from text

N94-37774 Department of the Navy, Washington, DC.
METHOD OF FORMING WAVEGUIDES WITH ION EXCHANGE OF HALOGEN IONS Patent
Jasbinder S. Sanghera, inventor (to Navy), Pablo C. Pureza, inventor (to Navy), and Ishwar D. Aggarwal, inventor (to Navy) 15 Mar. 1994 7 p
Filed 1 Sep. 1992 Supersedes AD-D015564
(AD-D016304; US-Patent-5,294,240; US-Patent-Appl-SN-937765; US-Patent-Class-65-3.14) Avail: US Patent and Trademark Office

This invention pertains to optical waveguides which includes waveguides of all shapes and sizes, preforms, and optical fibers made from the preforms, and to a method for making waveguides devoid of a physical interface. The method includes preparation of a waveguide from a halide-containing glass, heating the waveguide to a temperature below crystallization temperature of the glass so that it is still solid, providing a gaseous reactive medium containing halide ions of higher electronegativity than halide ions in the waveguide, exposing the waveguide to said reactive medium for a sufficient duration for the halide ions of higher electronegativity in the reactive medium to replace at least a portion of the halide ions of lower electronegativity in the waveguide, and cooling the waveguide whereby a lower refractive index is formed on the side of the waveguide exposed to the reactive medium than the refractive index internally of the waveguide so that light can travel through the portion of the waveguide having the higher refractive index. DTIC

N94-36622# GEC-Marconi Avionics Ltd., Basilon, Essex (England).
INFRARED SEARCH AND TRACK DEMONSTRATOR PROGRAMME
W. D. McGinn, C. J. Tucker, and S. Nallanthighal *In* AGARD, Pointing and Tracking Systems May 1994 10 p (For primary document see N94-36616 12-18)
Copyright Avail: CASI HC A02/MF A02

N94-36625# Draper (Charles Stark) Lab., Inc., Cambridge, MA.
INERTIAL PSEUDO STAR REFERENCE UNIT
Michael F. Luniewicz, Dale T. Woodbury, Jerold P. Gilmore, and Tze T. Chien *In* AGARD, Pointing and Tracking Systems May 1994 14 p
(For primary document see N94-36616 12-18)
Copyright Avail: CASI HC A03/MF A02

75 PLASMA PHYSICS

Includes magnetohydrodynamics and plasma fusion.
For ionospheric plasmas see *46 Geophysics*. For space plasmas see *90 Astrophysics*.

N94-36448# Sandia National Labs., Albuquerque, NM.
D-D FUSION EXPERIMENTS USING FAST z-PINCHES
R. B. Spielman, G. T. Baldwin, and G. Cooper et al 1994 11 p
Presented at the International Conference on Progress and Applications of Plasma Focus Research, Hoboken, NJ, 27 May 1994
(Contract DE-AC04-94AL-85000)
(DE94-010090; SAND-94-0934C; CONF-9405128-1) Avail: CASI HC A03/MF A01

The development of high current (I greater than 10 MA) drivers provides us with a new tool for the study of neutron-producing plasmas in the thermal regime. The imploded deuterium mass (or collisionality) increases as I(exp 2) and the ability of the driver to heat the plasma to relevant fusion temperatures improves as the power of the driver increases. Additionally, fast (less than 100 ns) implosions are more stable to the usual MHD instabilities that plagued the traditional slower implosions. We describe experiments in which deuterium gas puffs or CD2 fiber arrays were imploded in a fast z-pinch configuration on Sandia's Saturn facility generating up to 3 x 10(exp 12) D-D neutrons. These experiments were designed to explore the physics of neutron-generating plasmas in a z-pinch geometry. Specifically, we intended to produce neutrons from a nearly thermal plasma where the electrons and ions have a nearly Maxwellian distribution. This is to be clearly differentiated from the more usual D-D beam-target neutrons generated in many dense plasma focus (DPF) devices. DOE

N94-36472# National Inst. for Fusion Science, Nagoya (Japan).
Q-PROFILE FLATTENING DUE TO NONLINEAR DEVELOPMENT OF RESISTIVE KINK MODE AND ENSUING FAST CRASH IN SAWTOOTH OSCILLATIONS
K. Watanabe, T. Sato, and Y. Nakayama Jul. 1993 34 p
(DE94-727625; AD-B17920; NIFS-238) Avail: CASI HC A03/MF A01

Presented is a new full-torus, compressible, resistive MHD simulation model that can adequately explain the mechanism of the fast crash in the sawtooth oscillation. The simulation results reveal that the q value, which at first decreases in accordance with current peaking subject to ohmic heating, starts increasing in the q less than 1 region due to strong excitation of nonlinear resistive kink modes and tends to be bottom-flattened. When the q profile is largely flattened in the q less than 1 region, the dynamic pressure of the m=1 kink mode pushes the hot core plasma in the main flow direction and the hot core deviates from the magnetic axis. Then, a strong plasma compression occurs at the stagnation point of the directed plasma flow which is coincident with the m=1 rational surface. Consequently, the poloidal magnetic field lines are driven to reconnect rapidly with each other across the q=1 surface, and the deviated hot core is pushed out towards the wall to destroy its confinement. The driven magnetic reconnection leading to the crash is found to occur as a result of the q-profile flattening, in contrast to Kadomtsev's model where the q-profile becomes flattened as a result of reconnection exchanging the magnetic flux. The crash is governed by the MHD time scale, about 100 poloidal Alfven transit times, which is much faster than the Kadomtsev reconnection time. The resistive kink mode and its nonlinear behavior control the whole process of the sawtooth oscillation. Especially, the m=1 plasma flow induced by the resistive kink instability, neither the magnetic force nor the pressure force, plays a decisive role in triggering the crash. DOE

N94-36536# Texas State Univ., Austin, TX. Inst. for Fusion Studies.
ON THE INTERPRETATION OF DIAMAGNETIC LOOP MEASUREMENTS FOR A CURRENT-CARRYING PLASMA COLUMN IN A CONDUCTING CHAMBER
A. N. Aleynikov (Academy of Sciences, USSR, Novosibirsk, USSR.), V. S. Cherkassky (Academy of Sciences, USSR, Novosibirsk, USSR.), B. A. Knyazev (Academy of Sciences, USSR, Novosibirsk, USSR.), and B. N. Breizman Oct. 1993 18 p
(Contract DE-FG05-80ET-53088)
(DE94-007107; DOE/ET-53088/628; IFSR-628) Avail: CASI HC A03/MF A01

A general expression is derived for the signal of a magnetic loop encircling a plasma column inside a conducting chamber with nonuniform current distribution over the plasma cross-section. The ratio of the paramagnetic component to the diamagnetic component of the signal is shown to be independent of the loop radius. Both components increases the loop radius decreases from the chamber radius to the plasma radius. From the derived expressions, the paramagnetic component of the signal is calculated numerically for several current distributions including those of interest for the experiments. At a given total current, the paramagnetic component of the signal may vary considerably, which generally has to be taken into account in interpreting experimental data. The results of the calculations are used to process the data obtained in the experiments on the SPIN plasma device. DOE

N94-36566# International Atomic Energy Agency, Vienna (Austria).
MICROWAVE REFLECTOMETRY FOR FUSION PLASMA DIAGNOSTICS
1992 264 p Presented at the IAEA Technical Committee Meeting on Microwave Reflectometry for Fusion Plasma Diagnostics, Abingdon, England, 4-6 Mar. 1992
(DE94-620118; INIS-MF-13810; CONF-9203297) Avail: CASI HC A12/MF A03 (US Sales Only)

This document contains a collection of 26 papers on 'Microwave Reflectometry for Fusion Plasma Diagnostics', presented at the IAEA Technical Committee Meeting of the same name held at the JET Joint Undertaking, Abingdon, United Kingdom, March 4-6, 1992. It contains five papers on the measurement of plasma density profiles, six papers on theory and simulations in support of the development and application of this type of plasma diagnostics, eight papers on the measurement of density transients and fluctuations, and seven on new approaches to reflectometry-based plasma diagnostics. DOE

N94-37072# Sandia National Labs., Albuquerque, NM.
PRERADIATION STUDIES FOR NON-THERMAL Z-PINCH WIRE LOAD EXPERIMENTS ON SATURN
T. W. L. Sanford, D. R. Humphreys, J. W. Poukey, B. M. Marder, J. A. Halbleib, J. T. Crow, R. B. Spielman, and R. C. Mock Jun. 1994 58 p
(Contract DE-AC04-94AL-85000)
(DE94-013459; SAND-94-0694) Avail: CASI HC A04/MF A01

The implosion dynamics of compact wire arrays on Saturn are explored as a function of wire mass m, wire length l, wire radii R, and radial power-flow feed geometry using the ZORK code. Electron losses and the likelihood of arcing in the radial feed adjacent the wire load are analyzed using the TWOQUICK and CYLTRAN codes. The physical characteristics of the implosion and subsequent thermal radiation production are estimated using the LASNEX code in one dimension. These analyses show that compact tungsten wire arrays with parameters suggested by D. Mosher and with a 21-nH vacuum feed geometry satisfy the empirical scaling criterion I/(M/l) approximately 2 MA/(mg/cm) of Mosher for optimizing nonthermal radiation from z pinches, generate low electron losses in the radial feeds, and generate electric fields at the insulator stack below the Charlie Martin flashover limit thereby permitting full power to be delivered to the load. Under such conditions, peak currents of approximately 5 MA can be delivered to wire loads approximately 20 ns before the driving voltage reverses at the insulator stack, potentially allowing the m = 0 instability to develop with the subsequent emission of nonthermal radiation as predicted by the Mosher model. DOE

N94-37081# Lawrence Livermore National Lab., Livermore, CA.
DESIGN OF THE DIVERTOR THOMSON SCATTERING SYSTEM ON D3-D
T. N. Carlstrom (General Atomics Technologies Corp., San Diego, CA.), J. H. Foote, D. G. Nilson, and B. W. Rice May 1994 15 p Presented at the 10th Topical Conference on High-Temperature Plasma Diagnostics, Rochester, NY, 8-12 May 1994
(Contracts W-7405-eng-48; DE-AC03-89ER-51114)
(DE94-012672; UCRL-JC-116270; CONF-940552-7) Avail: CASI HC A03/MF A01

Local measurements of n(sub e) and T(sub e) in the divertor region are necessary for a more complete understanding of divertor physics. We have designed an extension to the existing multipulse Thomson scattering system to measure n(sub e) in the range 5 x 10(exp 18) to 5 x 10(exp 20) m(exp -3) and T(sub e) 5--500 eV, with 1 cm resolution from 1--21 cm above the floor of the DIII-D vessel, in the region of the X-point for lower single-null diverted plasmas. One of the existing 8, 20 Hz, ND:YAG lasers will be redirected to a separate vertical port, and viewed radially with a specially designed, f/6.8 lens. Fiber optics carry the light to additional polychromators whose interference filters have been optimized for low T(sub e) measurements. Other aspects of the system, including the beam path to the vessel, polychromator design, real time data acquisition, laser control, calibration facility, and DIII-D timing, and the data acquisition interface will be shared with the existing multipulse Thomson system. An in-situ laser alignment monitor will provide alignment information for each laser pulse. DOE

N94-37082# Lawrence Livermore National Lab., Livermore, CA.
THE ROLE OF HEATING AND CURRENT DRIVE IN ITER
W. M. Nevins and S. Haney 18 Oct. 1993 26 p Presented at the International Thermonuclear Experimental Reactor Radio Frequency Technical Meeting, Garching, Germany, 21-27 Oct. 1993
(Contract W-7405-eng-48)
(DE94-012679; UCRL-JC-115423; CONF-9310322-1) Avail: CASI HC A03/MF A01

This report discusses and summarizes the role of heating and non-inductive current drive in ITER as: (1) ITER must have heating power sufficient for ignition. (2) The heating system must be capable of current drive. (3) Steady-state operation is an ultimate goal. It is recognized that additional heating and current drive power (beyond what is initially installed on ITER) may be required. (4) The ultimate goal of steady-state operation means steady-state with Q(sub CD) greater than or = 5. Unlike the terms of reference for the ITER CDA, the ITER Technical Objectives and Approaches for the EDA sets no goal for the neutron wall load during steady-state operation. (5) In addition to bulk current drive, the ITER heating and current drive system should be used for current profile control and for burn control. DOE

N94-37101# Los Alamos National Lab., NM.
CONCEPTUAL DESIGN FOR A FAST NEUTRON IONIZATION CHAMBER FOR FUSION REACTOR PLASMA DIAGNOSTICS
W. C. Sailor and C. W. Barnes 1994 5 p Presented at the 11th Topical Meeting on the Technology of Fusion Energy, New Orleans, LA, 19-24 Jun. 1994
(Contract W-7405-eng-36)
(DE94-013396; LA-UR-94-1832; CONF-940630-9) Avail: CASI HC A01/MF A01

A conceptual design for a radiation-hard 'pointing' fast neutron ionization chamber that is capable of delivering a 1 MHz count rate of T(D,n) events at ITER is given. The detector will use an approximately 1 cc volume of CO2 fill gas at 0.1 bar pressure in a 500 V/cm electric field. The pulse widths will be approximately 10 ns, enabling it to operate in a flux of approximately 6 times 10(exp 13) DT n/sq cm/sec. A special collimator design is used, giving an estimated angular resolution of 4.5 deg HWHM. DOE

N94-37139# Wisconsin Univ., Madison, WI. Dept. of Electrical and Computer Engineering.
BASIC STUDIES IN PLASMA WAVE INTERACTIONS Final Report, 1 May 1989 - 30 Apr. 1994
J. E. Scharer May 1994 40 p
(Grant AF-AFOSR-0353-89)
(AD-A280465; AFOSR-94-0368TR) Avail: CASI HC A03/MF A01

Research on microwave propagation, reflection, absorption and backscatter in XUV excimer laser (193 run) and microwave (2.45 GHz) produced plasmas has been carried out. Our research on high density, low temperature (n(e) = 5 x 10(exp 13)/cu cm, 1 eV) laser-created plasma and broadband (1-3 GHz) microwave transmission, absorption and backscatter between two antennas in a plasma are described. Research on the creation of a laser produced sheet beam plasma for either a low loss, rapidly scanable agile microwave mirror reflector (10 GHz) or a diffuse, lossy absorber is being carried out. Measurements and theoretical analysis of these topics are described. We also discuss our collaborations with other research groups and our theoretical and computational research to support and interpret the experimental observations. DTIC

N94-37167# California Univ., Davis, CA.
INITIAL STUDIES OF REFLECTOMETER FOR ITER
N. C. Luhmann, Jr. Dec. 1993 5 p
(Contract DE-FG03-92ER-54185)
(DE94-012476; DOE/ER-54185/T1) Avail: CASI HC A01/MF A01

ITER-related activities taking place over the last year were concentrated primarily on the area of advanced reflectometry systems. In particular, we have concentrated on reflectometer systems for density profile and density fluctuation studies on ITER. This interest has led us to spend much of our time investigating the pulsed radar time-of-flight reflectometer approaches (i.e. moderate pulse and ultrashort pulse). Pulsed radar systems offer the ability to make detailed profile measurements using fixed frequency sources, avoiding the need for highly stable sweepable sources as required by the more traditional FM radar systems. DOE

N94-37182 Naval Research Lab., Washington, DC.
PROPAGATION OF RADIUS-TAILORED LASER PULSES OVER EXTENDED DISTANCES IN A UNIFORM PLASMA Interim Report
J. Krall, E. Esarey, P. Sprangle, and G. Joyce 16 May 1994 26 p
Limited Reproducibility: More than 20% of this document may be affected by microfiche quality
(AD-A280405; NRL/MR/6790-94-7465) Avail: Issuing Activity (Defense Technical Information Center (DTIC))

A Maxwell-fluid model is described, which allows simulation of laser pulses over extended distances (multiple diffraction lengths) in an underdense plasma. This model is used to simulate radius-tailored laser pulses, which can propagate over such distances with minimal distortion in a uniform plasma. Theoretical model equations governing the choice of radius tailoring are also given. A radius-tailored pulse has constant power approximately equal to the critical power for relativistic guiding over the length of the pulse and a spot size at focus that varies over the length of the pulse. A laser pulse configuration of this type can be constructed from a series of ultra-short Gaussian pulses. DTIC

N94-37207# Lawrence Livermore National Lab., Livermore, CA.
TIME-STEP STABILITY FOR SELF-CONSISTENT MONTE CARLO DEVICE SIMULATION
P. W. Rambo and J. Denavit May 1994 6 p Presented at the 3d International Workshop on Computational Electronics, Portland, OR, 18-20 May 1994
(Contract W-7405-eng-48)
(DE94-012145; UCRL-JC-116300; CONF-9405147-3) Avail: CASI HC A02/MF A01

An important numerical constraint on self consistent Monte Carlo device simulation is the stability limit on the time step imposed by plasma oscillations. The widely quoted stability limit for the time step between Poisson field solutions, Delta t less than 2/omega(sub p) where omega(sub p) is the plasma frequency, is specific to the leapfrog particle advance used in collisionless plasma simulation and does not apply to typical particle advance schemes used for device simulation. The authors present a stability criterion applicable to several algorithms in use for solid state modeling; this criterion is verified with numerical simulation. This work clarifies the time step limitation due to plasma oscillations and provides a useful guide for the efficient choice of time step size in Monte Carlo simulation. Because frequent solution of the Poisson equation can be a sizable computational burden, methods for allowing larger time step are desirable. The use of advanced time levels to allow stability with omega(sub p) Delta t much greater than 1 is well known in the simulation of collisionless plasmas; they have adapted these implicit methods to semiconductor modeling and demonstrated stable simulation or time steps larger than the explicit limit. DOE

N94-37231# National Inst. for Fusion Science, Nagoya (Japan).
CONFINEMENT IMPROVEMENT IN H-MODE-LIKE PLASMAS IN HELICAL SYSTEMS
K. Itoh, H. Sanuki, S. Itoh, A. Fukuyama, and M. Yagi Jun. 1993 23 p
(DE94-727619; NIFS-232) Avail: CASI HC A03/MF A01

The reduction of the anomalous transport due to the inhomogeneous radial electric field is theoretically studied for toroidal helical plasmas. The self-sustained interchange-mode turbulence is analyzed for the system with magnetic shear and magnetic hill. For the system with magnetic well like conventional stellarators, the ballooning mode turbulence is studied. Influence of the radial electric field inhomogeneity on the transport coefficients and fluctuations are quantitatively shown. Unified theory of the transport coefficients in the L-mode and H-mode-like plasmas are presented. DOE

N94-37235# Japan Atomic Energy Research Inst., Tokyo (Japan).
TOWARDS NUCLEAR FUSION REACTORS
Nov. 1993 115 p
(DE94-748680; INIS-JP-017) Avail: CASI HC A06/MF A02

The results of nuclear fusion researches in JAERI are summarized. In this report, the following themes are collected: the concept of fusion reactor (including ITER), fusion reactor safety, plasma confinement, fusion reactor equipment, and so on. DOE

N94-37292# Los Alamos National Lab., NM.
STARTUP AND SHUTDOWN OF THE PULSAR TOKAMAK REACTOR
K. A. Werley and C. G. Bathke 1994 7 p Presented at the 11th Topical Meeting on the Technology of Fusion Energy, New Orleans, LA, 19-24 Jun. 1994
(Contract W-7405-eng-36)
(DE94-013128; LA-UR-94-1823; CONF-940630-8) Avail: CASI HC A02/MF A01

Start-up conditions are examined for a pulsed tokamak reactor that uses only inductive plasma current drive for startup, burn and shutdown. A zero-dimensional (profile-averaged) model that describes plasma power and particle balance equations is used to study several aspects of plasma startup and shutdown, including optimization of the startup pathway tradeoff of auxiliary startup heating power versus startup time, volt-second consumption, thermal stability and partial-power operations. DOE

N94-37297# Lawrence Livermore National Lab., Livermore, CA.
MOTIONAL STARK EFFECT UPGRADES ON D3-D
B. W. Rice, D. G. Nilson, and D. Wroblewski Apr. 1994 9 p Presented at the 10th Topical Conference on High-Temperature Plasma Diagnostics, Rochester, NY, 8-12 May 1994
(Contracts W-7405-eng-48; DE-AC03-84ER-51044)
(DE94-013146; UCRL-JC-116269; CONF-940552-8) Avail: CASI HC A02/MF A01

The measurement and control of the plasma current density profile (or q profile) is critical to the advanced tokamak program on DIII-D. A complete understanding of the stability and transport properties of advanced operating regimes requires detail poloidal field measurements over the entire plasma radius from the core to the edge. In support of this effort, the authors have recently completed an upgrade of the existing MSE diagnostic, increasing the number of channels from 8 to 16. A new viewing geometry has been added to the outer edge of the plasma which improves the radial resolution in this region from 10 cm to less than 4 cm. This view requires the use of a reflector that has been designed to minimize polarization amplitude and phase effects. Vacuum-compatible polarizers have also been added to the instrument for in-situ calibration. Future use of the MSE diagnostic for feedback control of the q profile will also be discussed. DOE

N94-37307# Lawrence Livermore National Lab., Livermore, CA.
THE LOGIC BEHIND THICK, LIQUID-WALLED, FUSION CONCEPTS
R. W. Moir 15 Apr. 1994 20 p Presented at the 3rd International Symposium on Fusion Nuclear Technology, Los Angeles, CA, 27 Jun. - 1 Jul. 1994
(Contract W-7405-eng-48)
(DE94-012678; UCRL-JC-115748; CONF-940664-2) Avail: CASI HC A03/MF A01

It may be possible to surround the region where fusion reactions are taking place with a neutronically thick liquid blanket which has penetrations that allow only a few tenths of a percent of the neutrons to leak out. Even these neutrons can be attenuated by adding an accurately placed liquid or solid near the target to shadow-shield the beam ports from line-of-sight neutrons. The logic of such designs are discussed and their evolution is described with examples applied to both magnetic and inertial fusion (HYLIFE-II). These designs with liquid protection are self healing when exposed to pulsed loading and have a number of advantages-over the usual designs with solid first walls. For example, the liquid-protected solid components will last the life of the plant, and therefore the capacity factor is estimated to be approximately 10% higher than for the

non-liquid-walled blankets, because no blanket replacement shutdowns are required. The component replacement, operations, and maintenance costs might be half the usual value because no blanket change-out costs or accompanying facilities are required. These combined savings might lower the cost of electricity by 20%. Nuclear-grade construction should not be needed, largely because the liquid attenuates neutrons and results in less activation of materials. Upon decommissioning, the reactor materials should qualify for disposal by shallow burial even when constructed of ordinary 304 stainless steel. The need for a high-intensity 14-MeV neutron test facility to develop first-wall materials is avoided or greatly reduced, saving billions of development dollars. Flowing molten Li, the molten salt Flibe (Li2BeF4), and molten Lil7Pb83 have been considered. An advantage of molten salt is that it will not burn and has a low tritium solubility and therefore low tritium inventory. DOE

N94-37309# Texas Univ., Austin, TX. Inst. for Fusion Studies.
MARFE'S IN TOKAMAK EDGE PLASMA: PATTERN FORMATION UNDER NONLOCAL CONSTRAINTS
B. Meerson (Hebrew Univ., Jerusalem, Israel.), N. Petviashvili (Texas Univ., Austin, TX.), and T. Tajima (Texas Univ., Austin, TX.) Apr. 1994 14 p
(Contract DE-FG05-80ET-53088)
(DE94-012766; DOE/ET-53088/658; IFSR-658) Avail: CASI HC A03/MF A01

A simplified two-dimensional nonlinear fluid model is developed to elucidate the basic mechanism of the formation of multifaceted asymmetric radiation from the edge of tokamak plasmas (MARFE). In the framework of a mixed Eulerian-Lagrangian description, the problem is reduced to reaction-diffusion-type equation with nonlocality, which obeys the constraints of length constancy and mass conservation along the magnetic field. With a simple cooling function, this model predicts formation of stationary MARFE-like structures. DOE

N94-37316# Los Alamos National Lab., NM.
INERTIAL ELECTROSTATIC CONFINEMENT (IEC) DEVICES
R. A. Nebel, L. Turner, T. N. Tiouririne, D. C. Barnes, W. D. Nystrom, R. W. Bussard, G. H. Miley, J. Javedani, and Y. Yamamoto 1994 11 p Presented at the Nondestructive Assay and Nondestructive Examination Waste Characterization Conference, Pocatello, ID, 14-16 Feb. 1994
(Contract W-7405-eng-36)
(DE94-013114; LA-UR-94-1739; CONF-940216-4) Avail: CASI HC A03/MF A01

Inertial Electrostatic Confinement (IEC) is one of the earliest plasma confinement concepts, having first been suggested by P. T. Farnsworth in the 1950's. The concept involves a simple apparatus of concentric spherical electrostatic grids or a combination of grids and magnetic fields. An electrostatic structure is formed from the confluence of electron or ion beams. Gridded IEC systems have demonstrated neutron yields as high as 2 x 10(exp 10) neutrons/sec. These systems have considerable potential as small, inexpensive, portable neutron sources for assaying applications. Neutron tomography is also a potential application. Atomic physics effects strongly influence the performance of all of these systems. Important atomic effects include elastic scattering, ionization, excitation, and charge exchange. This paper discusses how an IEC system is influenced by these effects and how to design around them. Theoretical modeling and experimental results are presented. DOE

N94-37354# Wisconsin Univ., Madison, WI.
A FAST SPECTROSCOPIC DIAGNOSTIC FOR THE MEASUREMENT OF PLASMA IMPURITY ION DYNAMICS
D. J. DenHartog and R. J. Fonck Apr. 1994 15 p
(Contract DE-FG02-85ER-53198)
(DE94-012985; DOE/ER-53198/238) Avail: CASI HC A03/MF A01

A high-resolution spectrometer has been developed and used to measure simultaneously impurity ion temperature and flow velocities in high temperature plasmas with 10 micro-s temporal resolution (limited by digitization rate). This device is actually a duo-spectrometer: measurements from two different chordal views of the plasma can be made simultaneously via two separate quartz input fiber optic bundles coupled to the entrance slits which are tilted to compensate for line curvature. The dispersed spectra on the exit plane of the duo-spectrometer are coupled via quartz fiber optics to two arrays of 16 photomultiplier tubes each. Measurement made by recording the Doppler broadened and shifted 227.091 nm emission from the CV impurity ions in the MST reversed-field pinch (RFP) plasma have achieved precisions of less than 6 eV for temperatures of 150 Ev and less than 0.7 km/s for flow velocities of 6 km/s. Representative results from the MST RFP indicate that the toroidal flow velocity drops and ion temperature increases during saw tooth events in MST. DOE

N94-37358# National Inst. for Fusion Science, Nagoya (Japan).
ELMy-H MODE AS LIMIT CYCLE AND TRANSIENT RESPONSES OF H-MODES IN TOKAMAKS
Sanae Itoh (Kyushu Univ., Fukuoka, Japan.), Kimitaka Itoh, and Atsushi Fukuyama May 1993 56 p
(DE94-727510; NIFS-221) Avail: CASI HC A04/MF A01

A model of edge localized modes (ELM's) in tokamaks is presented. The model of the L/H transition is extended to include the temporal evolution and the spatial structure. The existence of the electric field bifurcation infers a hysteresis curve between the plasma gradient and the loss flux (flow). The time-dependent Ginzburg-Landau equation is formulated for the electric field development. The self-generated oscillation of edge density appears, associated with periodic bursts of the loss, under the condition of constant particle flux from the core. This is attributed to the small and frequent ELMy activity in H-mode. Periodic decay and reestablishment of the transport barrier occur. This oscillation appears near the L/H transition boundary in the parameter space. It is found that in H and ELMy-H states, the edge region forms an intermediate radial structure of diffusion coefficient (mesophase) between H-phase and L-phase. The diffusion Prandtl number, the ratio of the viscosity to the diffusivity, is found to determine the thickness of the barrier. Phase diagram of L, ELMy-H, H, and L/H bistable-states is obtained on plasma parameter space. To consider other types of ELM's, transient responses to the perturbations of the flux from the core are studied in each phase. In low collisionality plasma a sudden decrease of the flux can cause the transient bursting of a few ELM's before the L to H transition is completed. Large scale pulse from the core causes the transient return to L-phase and a giant burst occurs in high collisionality plasma. In ELMy-H state, external oscillations cause the mode-locking and other complicated dynamics. The perturbation in the flux widens the parameter regime of the occurrence of burstings. DOE

N94-37359# National Inst. for Fusion Science, Nagoya (Japan).
ANOMALOUS CROSS FIELD FLUX IN CHS
T. Yamagishi (Fukui Inst. of Tech., Japan.) May 1993 22 p
(DE94-727547; NIFS-227) Avail: CASI HC A03/MF A01

Anomalous quasi-linear fluxes induced by the curvature drift resonance and transit resonance are evaluated in a rotating helical plasma. The radial electric field makes the Doppler shift, but does not contribute to the anomalous fluxes. The curvature drift resonance induces the new curvature term in the quasi-linear fluxes. The effect of helical magnetic field is through this curvature of magnetic field lines, and contributes to the inward transport. The ion heat diffusivity due to the curvature drift resonance is obtained in the form modified gyro-Bohm coefficient and is compared with experimentally observed one in CHS Heliotron. DOE

N94-37361 Texas Univ., Austin, TX. Inst. for Fusion Studies.
ISOTOPE SCALING AND ETA(i) MODE WITH IMPURITIES IN TOKAMAK PLASMAS
J. Q. Dong, W. Horton, and W. D. Dorland Apr. 1994 19 p Limited Reproducibility: More than 20% of this document may be affected by microfiche quality
(Contract DE-FG05-80ET-53088)
(DE94-012763; DOE/ET-53088/654; IFSR-654) Avail: CASI HC A03

The ion temperature gradient driven instability, or eta(sub i) mode, is studied for discharges with hydrogen, deuterium, or tritium in a toroidal magnetic configuration. Impurity effects on the mode and the instability which is driven by the presence of impurity ions (impurity modes) are studied as well. It is found that the maximum growth rate of the eta(sub i) mode scales as M(exp -1/2) for pure hydrogen, deuterium, or tritium discharges, where M is the mass of the working gas ion. With the inclusion of impurity ions the growth rates of eta(sub i) mode decrease in all three kinds of plasmas with a hydrogen plasma still having the highest maximum growth rate, tritium the lowest, and deuterium in between. However, the isotope effects are weaker and scale as M(sub eff)(exp -1/2) with the presence of impurity ions, where the effective mass M(sub eff) is a

combination of A(sub i) and A(sub z), the mass number of hydrogenic and impurity ions. For the impurity mode the situation is similar to that of the eta(sub i) mode without impurity ions. Experimental database shows that the plasma energy confinement time scales as tau(sub E) approximately A(sub i)(sup 1/2) in clean plasmas. The correlation of the theoretical results with the experimental confinement scaling is discussed. DOE

N94-37384# National Inst. for Fusion Science, Nagoya (Japan).
A ROLE OF NEUTRAL HYDROGEN IN CHS PLASMAS WITH REHEAT AND COLLAPSE AND COMPARISON WITH JIPPT-IIU TOKAMAK PLASMAS
S. Morita, H. Yamada, H. Iguchi, K. Adati, R. Akiyama, H. Arimoto, M. Fujiwara, Y. Hamada, K. Ida, and H. Idei et al Sep. 1992 16 p Presented at the 14th International Conference on Plasma Physics and Controlled Nuclear Fusion Research, Wuerzburg, Germany, 30 Sep. - 7 Oct. 1992
(DE94-718985; NIFS-186; CONF-9209396; IAEA-CN-56/C-2-5) Avail: CASI HC A03/MF A01

Results are described on NBI plasmas of the Compact Helical System (CHS). An increase in the stored energy, which is called plasma 'reheat', is observed with density peaking when gas puffing is turned off in the high density region. A plasma collapse with large increase in radiation loss occurs even in discharges whose Z(sub eff) values (typically, less than 2-3) do not show any increase when the gas puffing is continued. Both phenomena are basically explained by the edge electron temperature due to the difference in the amount of edge hydrogen neutrals. After turning off the gas puffing, the central electron density n(sub e0) shows an increase of 80% and the density peaking factor (n(sub e0)/n-bar(sub e)) changes from 1.0 to 2.0, in typical cases, and a high inward velocity of the impurities appears (v = 20 m/s). The accumulation is studied in relation to the poloidal rotation and the edge temperature. These results are compared with results from plasmas with IOC- and H-modes in the JIPPT-IIU tokamak. DOE

N94-37392# Lawrence Livermore National Lab., Livermore, CA.
TIME-RESOLVED PROBING OF ELECTRON THERMAL TRANSPORT IN PLASMA PRODUCED BY FEMTOSECOND LASER PULSES
B. T. V. Vu, A. Szoke, O. L. Landen, and R. W. Lee 20 Apr. 1994 6 p Presented at the Topical Meeting on High Field Interactions and Short Wavelength Generation, Saint Malo, France, 22-24 Aug. 1994
(Contract W-7405-eng-48)
(DE94-012061; UCRL-JC-115947-Rev-1; CONF-940889-2-Rev-1) Avail: CASI HC A02/MF A01

We present the first direct observation of a supersonic ionization front supported by electron thermal transport in a hot solid density plasma produced by 100 ft/sec-laser-pulse irradiation of a transparent fused quartz target. DOE

N94-37415# Japan Atomic Energy Research Inst., Tokyo (Japan).
MATERIAL AND DESIGN CONSIDERATIONS FOR THE CARBON ARMORED ITER DIVERTOR
I. Smid (Japan Atomic Energy Research Inst., Naka, Japan.), Masato Akiba (Japan Atomic Energy Research Inst., Naka, Japan.), Masanori Araki (Japan Atomic Energy Research Inst., Naka, Japan.), Satoshi Suzuki (Japan Atomic Energy Research Inst., Naka, Japan.), and Kazuyoshi Satoh (Japan Atomic Energy Research Inst., Naka, Japan.) Jul. 1993 208 p
(DE94-737854; JAERI-M-93-149) Avail: CASI HC A10/MF A03 (US Sales Only)

The properties of materials for the carbon armored ITER divertor were evaluated from literature and manufacturers' documentation. Most of these data, however, have been not known or not published yet. We have evaluated an optimum data set of the candidate materials of the ITER divertor, which were needed for finite element analyses (FEM). The materials evaluated are as follows; MFC-1, CX2002U, SEP-N112, P-130, IG-430U for the carbon based materials, and Oxygen Free Copper (OFCu), Dispersion Strengthened Copper (DSCu), TZM, W5Re and W-Cu as a heat sink material. It should be noted that W-Cu is first proposed for a heat sink application of the ITER divertor plate. The finite element analyses were performed for the residual stress induced by brazing, thermal response and thermal stresses under a uniform heat flux of 15 MW/sq m to the plasma facing surface. The stress free temperature of 750 C is assumed for the residual stress by brazing. Ten different geometries of the divertor were considered in the analyses including possible material combinations. The FEM results show that the material combinations of MFC-1 and W-30Cu or DSUc in the flat-plate geometry satisfy the presently accepted ITER requirements. The combinations of CX2002U and TZM or W5Re is considered a good choice in terms of residual and thermal stresses, whereas the surface temperature exceeds the ITER requirements. DOE

N94-37436# General Atomic Co., San Diego, CA.
RECENT DIII-D HIGH POWER HEATING AND CURRENT DRIVE EXPERIMENTS
T. C. Simonen, G. L. Jackson, M. A. Mahdavi, T. W. Petrie, P. A. Politzer, T. S. Taylor, and E. A. Lazarus et al Feb. 1994 27 p Presented at the 5th International Toki Conference on Plasma Physics and Controlled Nuclear Fusion: Physics and Technology of Plasma Heating and Current Drive, Toki, Japan, 16-19 Nov. 1993 Submitted for publication
(Contracts DE-AC03-89ER-51114; W-7405-eng-48; DE-AC05-84OR-21400; DE-FC03-86ER-52126; GA Proj. 3466)
(DE94-012509; GA-A-21603; CONF-931178-2) Avail: CASI HC A03/MF A01

This paper describes recent DIII-D high power heating and current drive experiments. Described are experiments with improved wall conditioning, divertor particle pumping, radiative divertor experiments, studies of plasma shape and high poloidal beta. DOE

N94-37437# Lawrence Livermore National Lab., Livermore, CA.
IONIZATION BALANCE AND GAIN CALCULATIONS FOR NEON-LIKE SELENIUM X-RAY LASER PLASMAS
A. L. Osterheld, R. S. Walling, B. K. F. Young, W. H. Goldstein, G. Shimkaveg, B. J. MacGowan, L. DaSilva, R. London, D. Matthews, and R. E. Stewart 21 Jan. 1994 25 p Presented at the Radiative Properties of Hot Dense Matter Conference, Santa Barbara, CA, 2-6 Nov. 1992
(Contract W-7405-eng-48)
(DE94-012590; UCRL-JC-116042; CONF-9211211-6) Avail: CASI HC A03/MF A01

The authors have developed compact collisional-radiative models to describe the ionization balance and excitation mechanisms in neon-like selenium x-ray laser plasmas. These models can be used for calculations of the ionization dynamics, detailed emission spectra, and gain coefficients. Careful attention has been paid to indirect processes such as dielectronic recombination, excitation-autoionization, and resonant excitation. They discuss the importance of different atomic processes and model approximations in the ionization balance and gain calculations. These results will be compared to experimental measurements and to previous calculations. DOE

N94-37441# Argonne National Lab., IL. Energy Technology Div.
TRANSIENT THERMAL AND DYNAMIC STRESSES IN STRONGBACK-DESIGN BLANKETS
Saurin Majumdar 1994 24 p Presented at the 3rd International Symposium on Fusion Nuclear Technology, Los Angeles, CA, 27 Jun. - 1 Jul. 1994
(Contract W-31-109-eng-38)
(DE94-012639; ANL/ET/CP-81391; CONF-940664-5) Avail: CASI HC A03/MF A01

Transient thermal stresses of the first wall are compared for strongback-design blankets that contain stainless steel, ferritic steel, or a vanadium alloy as structural materials. Transient dynamics stresses due to plasma disruptions are computed on a parametric basis. Disruption loading characteristics, for which transient effects are important, are identified. Also explored are the relative merits of supporting the blanket at the top versus the bottom from the standpoint of dynamic stresses. DOE

N94-37464# Japan Atomic Energy Research Inst., Tokyo (Japan).
TWO-DIMENSIONAL OVER-ALL NEUTRONICS ANALYSIS OF THE ITER DEVICE
S. Zimin (Japan Atomic Energy Research Inst., Naka, Japan.), Hideyuki Takatsu (Japan Atomic Energy Research Inst., Naka, Japan.), Seiji Mori (Japan Atomic Energy Research Inst., Naka, Japan.), Yasushi Seki (Japan Atomic Energy Research Inst., Naka, Japan.), Satoshi Satoh (Japan Atomic Energy Research Inst., Naka, Japan.), Eisuke Tada (Japan Atomic Energy Research Inst., Naka, Japan.), and Koichi Maki Jul. 1993 83 p
(DE94-718963; JAERI-M-93-141) Avail: CASI HC A05/MF A01

The present work attempts to carry out a comprehensive neutronics analysis of the International Thermonuclear Experimental Reactor (ITER) developed during the Conceptual Design Activities (CDA). The two-dimensional cylindrical over-all calculational models of ITER CDA device including the first wall, blanket, shield, vacuum vessel, magnets, cryostat and support structures were developed for this purpose with a help of the DOGII code. Two dimensional DOT 3.5 code with the FUSION-40 nuclear data library was employed for transport calculations of neutron and gamma ray fluxes, tritium breeding ratio (TBR), and nuclear heating in reactor components. The induced activity calculational code CINAC was employed for the calculations of exposure dose rate after reactor shutdown around the ITER CDA device. The two-dimensional over-all calculational model includes the design specifics such as the pebble bed Li2O/Be layered blanket, the thin double wall vacuum vessel, the concrete cryostat integrated with the over-all ITER design, the top maintenance shield plug, the additional ring biological shield placed under the top cryostat lid around the above-mentioned top maintenance shield plug etc. All the above-mentioned design specifics were included in the employed calculational models. Some alternative design options, such as the water-rich shielding blanket instead of lithium-bearing one, the additional biological shield plug at the top zone between the poloidal field (PF) coil No. 5, and the maintenance shield plug, were calculated as well. Much efforts have been focused on analyses of obtained results. These analyses aimed to obtain necessary recommendations on improving the ITER CDA design. DOE

N94-37466# National Inst. for Fusion Science, Nagoya (Japan).
BOUNCE RESONANCE HEATING AND TRANSPORT IN A MAGNETIC MIRROR
Hitoshi Hojo (Tsukuba Univ., Ibaraki, Japan.) and Tadatsugu Hatori May 1993 16 p Submitted for publication
(DE94-727545; NIFS-225; JP9311132) Avail: CASI HC A03/MF A01

Bounce resonance heating and associated radial transport in a magnetic mirror are studied. A general expression for the absorbed power and radial particle flux due to bounce resonance is obtained by use of a gyrokinetic equation with the eikonal representation for waves. It is shown that the power absorption yields the outward (inward) particle flux with positive (negative) azimuthal mode number of RF wave fields and the power emission meaning instabilities yields the reverse particle flux with the same mode number for the ion. The particle flux for the electron is opposite to that for the ion. DOE

N94-37484# Japan Atomic Energy Research Inst., Tokyo (Japan).
IMPROVEMENT STUDY OF THE DIVERTOR CONFIGURATION OF THE STEADY STATE TOKAMAK REACTOR (SSTR)
Kouki Moriyama (Japan Atomic Energy Research Inst., Naka, Japan.), Yasushi Seki (Japan Atomic Energy Research Inst., Naka, Japan.), Toru Nishino, and Seiichirou Yamazaki Jul. 1993 77 p In JAPANESE
(DE94-718961; JAERI-M-93-130) Avail: CASI HC A05/MF A01

The divertor configuration improvement of the Steady State Tokamak Reactor (SSTR) was studied. In the study, lower temperature and higher density divertor plasma was aimed at to reduce the peak heat flux to the divertor plate, by adding baffle plates near the divertor plasma, or by providing slots to the divertor plates. The divertor plasmas were simulated for the conventional divertor configuration employed in the SSTR design, the one with baffle plates added, the one with exhaust duct in the bottom direction called the private side pumping, and gas target in slot divertor configuration. The divertor plasma characteristics were analyzed and evaluated using the numerical simulation code, UEDA. As the result, the divertor configuration with baffle plates is found to be superior in lowering the temperature, increasing the particle density of the divertor plasma and in reducing the peak heat flux. On the other hand, the gas divertor in the slot configuration and private side pumping divertor configuration are both found to have major difficulties. DOE

N94-37485# National Inst. for Fusion Science, Nagoya (Japan).
THEORY OF ANOMALOUS TRANSPORT IN H-MODE PLASMAS
S. I. Itoh (Kyushu Univ., Fukuoka, Japan.), K. Itoh, A. Fukuyama, and M. Yagi May 1993 22 p Submitted for publication
(DE94-727546; NIFS-226; JP9311133) Avail: CASI HC A03/MF A01

Theory of the anomalous transport is developed, and the unified formula for the L- and H-mode plasmas is presented. The self-sustained ballooning-mode turbulence is solved in the presence of the inhomogeneous radial electric field, E(sub r). Reductions in transport coefficients and the amplitude and decorrelation length of fluctuations due to E(sub r)' are quantitatively analyzed. Combined with the E(sub r)-bifurcation model, the thickness of the transport barrier is simultaneously determined. DOE

N94-37493# International Atomic Energy Agency, Vienna (Austria).
RESEARCH USING SMALL TOKAMAKS
1993 244 p Presented at the IAEA Technical Committee Meeting on Research Using Small Tokamaks, Wuerzburg, Germany, 28-29 Sep. 1992
(DE94-621827; INIS-MF-13779; CONF-9209420) Avail: CASI HC A11/MF A03 (US Sales Only)

This document consists of a collection of papers presented at the IAEA Technical Committee Meeting on Research Using Small Tokamaks. It contains 22 papers on a wide variety of research aspects, including diagnostics, design, transport, equilibrium, stability, and confinement. DOE

N94-37626# Sandia National Labs., Albuquerque, NM.
INITIAL REPORT ON CALORIMETRY FOR THE TORE SUPRA OUTBOARD PUMP LIMITER
R. E. Nygren, T. J. Lutz, and J. D. Miller Jan. 1994 69 p
(Contract DE-AC04-94AL-85000)
(DE94-011244; SAND-93-1922) Avail: CASI HC A04/MF A01

This report describes the instrumentation locations of the Tore Supra Phase 3 Outboard Limiter, including the locations and signal names of the flowmeters and thermocouples. Shot 11044 was evaluated in some detail. The heat loads in the fourteen cooling tubes that form the limiter head were calculated from the data and the results compared with the heat loads predicted using a 3-D model heat transfer calculation that calculates the distribution of power on the limiter based upon the power scrape-off length, the mag magnetic configuration, and the shape of the limiter. DOE

N94-37728# Academy of Sciences (USSR), Novosibirsk (USSR). Inst. Yadernoj Fiziki.
LANGMUIR WAVES IN THE ELECTRON-POSITRON PLASMA
N. S. Buchelnikova and E. P. Matochkin 1992 41 p
(DE94-618779; IYaF-92-36) Avail: CASI HC A03/MF A01 (US Sales Only)

The numerical experiments (PIC-method) were made to study the evolution of the travelling Langmuir waves in the electron-positron plasma. In the case of small amplitudes the modulational instability leads to the formation of the Langmuir solitons, in the case of large amplitudes to the collapse. The electron-positron plasma can be considered to be a model of the equal mass negative and positive ion plasma. DOE

N94-37730# Wisconsin Univ., Madison, WI.
FAST ELECTRON GENERATION AND TRANSPORT IN A TURBULENT, MAGNETIZED PLASMA Ph.D. Thesis
W. R. Stoneking May 1994 88 p
(Contract DE-FG02-85ER-53198)
(DE94-012986; DOE/ER-53198/239) Avail: CASI HC A05/MF A01

The nature of fast electron generation and transport in the Madison Symmetric Torus (MST) Reversed Field Pinch (RFP) is investigated using two Electron Energy Analyzer (EEA) probes and a thermocouple calorimeter. The parallel velocity distribution of the fast electron population is well fit by a drifted Maxwellian distribution with temperature of about 100 eV and drift velocity of about 2 (times) 10(exp 6) m/s. Cross-calibration of the EEA with the calorimeter provides a measurement of the fast electron perpendicular temperature of 30 eV, much lower than the parallel temperature, and is evidence that the kinetic dynamo mechanism (KDT) is not operative in MST. The fast electron current is found to match to the parallel current at the edge, and the fast electron density is about 4 (times) 10(exp 11) cm(exp -3) independent of the ratio of the applied toroidal electric field to the critical electric field for runaways. First time measurements of magnetic fluctuation induced particle transport are reported. By correlating electron current fluctuations with radial magnetic fluctuations the transported flux of electrons is found to be negligible outside r/a(approximately)0.9, but rises the level of the expected total particle losses inside r/a(approximately)0.85. A comparison of the measured diffusion coefficient is made with the ausilinear stochastic diffusion coefficient. Evidence exists that the reduction of the transport is due to the presence of a radial ambipolar electric field of magnitude 500 V/m, that acts to

equilibrate the ion and electron transport rates. The convective energy transport associated with the measured particle transport is large enough to account for the observed magnetic fluctuation induced energy transport in MST. DOE

N94-37732# Lawrence Livermore National Lab., Livermore, CA.
THREE-DIMENSIONAL GYROKINETIC PARTICLE-IN-CELL SIMULATION OF PLASMAS ON A MASSIVELY PARALLEL COMPUTER: LDRD CORE COMPETENCY PROJECT Final Report, 1991 - 1993
J. A. Byers, T. J. Williams, B. I. Cohen, and A. M. Dimits 27 Apr. 1994 6 p
(Contract W-7405-eng-48)
(DE94-013367; UCRL-ID-117214) Avail: CASI HC A02/MF A01

One of the programs of the Magnetic fusion Energy (MFE) Theory and Computations Program is studying the anomalous transport of thermal energy across the field lines in the core of a tokamak. We use the method of gyrokinetic particle-in-cell simulation in this study. For this LDRD project we employed massively parallel processing, new algorithms, and new algorithms, and new formal techniques to improve this research. Specifically, we sought to take steps toward: researching experimentally-relevant parameters in our simulations, learning parallel computing to have as a resource for our group, and achieving a 100 (times) speedup over our starting-point Cray2 simulation code's performance. DOE

N94-37734# National Inst. for Fusion Science, Nagoya (Japan).
SELF-SUSTAINED TURBULENCE AND L-MODE CONFINEMENT IN TOROIDAL PLASMAS
K. Itoh, S. Itoh, A. Fukuyama, M. Yagi, and M. Azumi Apr. 1993 114 p
(DE94-748497; NIFS-219) Avail: CASI HC A06/MF A02

Theory of the L-mode confinement in toroidal plasmas is developed. The quantitative effect of the anomalous transport, which is caused by microscopic fluctuations, on the pressure-gradient-driven modes is analyzed. The ExB nonlinearity is renormalized in a form of the transport coefficient such as the thermal diffusivity, the ion viscosity and the current diffusivity. The destabilization by the current-diffusivity and the stabilization by the thermal transport and ion viscosity are analyzed. By use of the mean-field approximations, the nonlinear dispersion relation is solved. Growth rate and stability condition are expressed in terms of the renormalized transport coefficients. The transport coefficients in the steady state are obtained by the marginal stability condition for the least stable mode. This method is applied to the microscopic ballooning mode for the toroidal plasma with the magnetic well (such as tokamak). The comparison with experimental observations are made. A good agreement is found in various aspects of the L-mode plasmas. The typical wavenumber and level of the fluctuations for the self-sustained turbulence is also obtained. The analysis is also made for the plasma with magnetic hill and shear (such as torsatron/heliotron devices). This method is applied to the interchange modes. Formula of the anomalous transport is obtained. Also investigated is the case of the magnetic well and low magnetic shear (conventional stellarator). The roles of the pressure gradient and the collisionless skin depth in determining the anomalous transport are found to be generic in toroidal plasmas. The difference in the magnetic configuration affects the transport coefficient. These formula explain major experimental observations. DOE

76 SOLID-STATE PHYSICS

Includes superconductivity.

For related information, see also *33 Electronics and Electrical Engineering* and *36 Lasers and Masers.*

N94-36454# Rice Univ., Houston, TX.
SUPERSONIC BARE METAL CLUSTER BEAMS Progress Report
R. E. Smalley 1994 4 p
(Contract DE-FG05-85ER-13429)
(DE94-010790; DOE/ER-13429/8) Avail: CASI HC A01/MF A01

This progress report describes work in the Rice group on fullerene research projects. Seven papers have gone out in this period, including two patent applications. Work includes one publication which describes a new method for the production of fullerenes using direct solar vaporization of a carbon feedstock. DOE

N94-36540# Sandia National Labs., Albuquerque, NM.
CORRELATION OF HOT-CARRIER STRESS AND IONIZATION INDUCED DEGRADATION IN BIPOLAR TRANSISTORS
R. L. Pease (RLP Research, Inc., Albuquerque, NM.), S. L. Kosier (Arizona Univ., Tucson, AZ.), R. D. Schrimpf (Arizona Univ., Tucson, AZ.), and W. E. Combs (Naval Surface Warfare Center, Crane, IN.) 1994 5 p Presented at the 31st Annual International Nuclear and Space Radiation Effects Conference, Tucson, AZ, 18-22 Jul. 1994
(Contract DE-AC04-94AL-85000)
(DE94-007289; SAND-94-0459C; CONF-940726-2) Avail: CASI HC A01/MF A01

The correlation of hot carrier stress and ionization induced gain degradation in npn BJT's was studied to determine if hot-carrier stress could be used as a hardness assurance tool for total dose. The correlation was measured at the wafer level and for several hardening variations for a single process technology. Additional experiments are planned and will be presented in the full paper. Based on a detailed physical analysis of the mechanisms for hot-carrier stress and ionization no correlation was expected. The results demonstrated the lack of correlation and indicate that hot-carrier stress degradation is not a predictor of total dose response. DOE

N94-36542# Atomic Energy of Canada Ltd., Chalk River (Ontario). Nuclear Labs.
PHASE TRANSITIONS IN CRYSTALLINE SOLIDS 1
J. R. Walker and L. L. Boyle Sep. 1993 41 p
(DE94-619029; AECL-10882) Avail: CASI HC A03/MF A01 (US Sales Only)

Many crystalline materials of interest to the Canadian Nuclear Program have the potential to undergo phase transitions in their range of application. During such phase transitions, a representation of the space group of the higher symmetry polymorph softens to induce the transition. This report is the first in a series of reports concerned with the group-theoretic properties of phase transitions in crystalline materials. The object of the research is to identify all spectroscopically-active soft modes for the 230 three-dimensional space groups. Identification of these soft modes will enable a detailed examination of phase transitions in materials of interest to the Canadian Nuclear Program and aid in the optimization of material properties. In this report, the group-theoretic properties of crystal structures and phase transitions are reviewed. It is demonstrated that the problem of extending a group reduces to that of determining its automorphisms. The automorphism groups of the crystallographic and icosahedral point groups are derived using a consistent presentation. DOE

N94-36548 Rutherford Appleton Lab., Chilton (England). ISIS Pulsed Neutron Facility.
COLLABORATION IN CRYSTALLOGRAPHY: PROCEEDINGS OF THE 1ST JOINT SEMINAR OF THE ISIS-INCR COLLABORATION IN CRYSTALLOGRAPHY
C. C. Wilson and V. I. Simonov Mar. 1993 168 p Conference held in Abingdon, England, 22-26 Mar. 1993 See also PB89-166185 Prepared in cooperation with Academy of Sciences (USSR), Moscow, USSR
(PB94-171097) Avail: Issuing Activity (National Technical Information Service (NTIS))

Contents: Summary of the First Joint Seminar; Crystal structure and its correlation with physical properties; Refinement of atomic models of Tl-phases of high temperature superconductors; The crystal structures of Li(sub 4-3x)(Ga,Al)(sub x)SiO4 and Li(3.7)Al(0.1)GeO(4) solid solutions; Structure and phase transitions in ferroelectric Rb(1+) and NH4(1+) selenates; Ionic conducting cerate perovskites; Structural phase transitions and modulated state in the superionic Na4TiP2O9; Determination of novel zeolite structures; Structural studies of alkali-metal loaded zeolites; High resolution electron microscopy of epitaxial structures; Disorder in silver halides; New multicomponent materials based on metal fluorides and prospects for their practical applications; Preparation of single and polycrystalline multi-component materials using crystallization from melts; Neutron scattering studies of the fluorite structured fast-ion conductors; Algorithm and techniques of refinement of crystal structures of twins; Organic structures from high resolution neutron powder diffraction; Single crystal structure determination by time-of-flight Laue diffraction. NTIS

N94-36727# Massachusetts Inst. of Tech., Cambridge. Dept. of Chemical Engineering.
DIAMOND DEPOSITION AND DEFECT CHEMISTRY STUDIED VIA SOLID STATE NMR Final Report, 1 Jun. 1990 - 30 Jun. 1994
Karen K. Gleason 30 Jun. 1994 119 p
(Contract N00014-90-J-1901)
(AD-A280609; MIT-9181AL) Avail: CASI HC A06/MF A02

Diamond defects were quantified by nuclear magnetic resonance (NMR). While maintaining the macroscopic integrity of the films, concentrations between 0.001 and 1.0 at.% H were measured, among the lowest ever reported by solid-state 1H NMR. These concentrations were correlated to infrared absorption in the 8 to 10 micron region and to thermal conductivity. Despite the low concentrations, Multiple Quantum NMR reveals a high degree of hydrogen clustering consistent with grain boundary passivation. Most hydrogen is rigidly held, but some, probably in -OCH3 and -NCH3 defects, undergoes rotation at room temperature. Similar results were obtained for hot-filament, microwave-plasma and DC arc-jet films, suggesting a common surface chemistry, but no hydrogen was detected in an as-deposited combustion film. 13C NMR provided the first quantitative determination of non-diamond bonded carbon defects, providing a benchmark for Raman spectroscopy, the primary characterization method for diamond. Selective 13C labeling demonstrated heterogeneous reactions involving carbon occur at the hot-filament. With high-speed magic-angle-spinning 19F NMR, CFx (x=1-3) functionalities were resolved on the surface of plasma-treated diamond powder. Understanding these defects impacts the understanding of film growth mechanisms and structure-property relationships for CVD diamond. DTIC

N94-36734# Massachusetts Inst. of Tech., Lexington. Lincoln Lab.
SOLID STATE RESEARCH Quarterly Technical Report, 1 Aug. - 31 Oct. 1993
31 Oct. 1993 64 p
(Contract F19628-90-C-0002)
(AD-A280573; Rept-1993:4; ESC-TR-94-084; XC-ESC/MA) Avail: CASI HC A04/MF A01

This report covers in detail the research work of the Solid State Division at Lincoln Laboratory for the period 1 August through 31 October 1993. The topics covered are Electrooptical Devices, Quantum Electronics, Materials Research, Submicrometer Technology, High Speed Electronics, Microelectronics, and Analog Device Technology. Funding is provided primarily by the Air Force, with additional support provided by the Army, ARPA, Navy, BMDO, and NASA. DTIC

N94-36742# California Univ., Berkeley, CA. Dept. of Physics.
JOSEPHSON ACOUSTIC RADIATION IN SUPERFLUID HELIUM Progress Report
May 1994 2 p
(Contract N00014-94-I-0043)
(AD-A280208) Avail: CASI HC A01/MF A01

The project to observe and measure Josephson acoustic radiation has begun. The most significant accomplishments in these first months are the following: A prototype cell has been designed and constructed. Various aspects of the cell have been tested. The apparatus have been designed in a modular form so that individual components can be optimized separately. We have developed a displacement liquid Helium pump to force superfluid through a submicron apertures for times on the order of 100 seconds. The pump consists of a flexible plastic membrane which is metal coated on one side. Application of a voltage between the membrane and a nearby fixed electrode forces the membrane to move, thus pushing superfluid through the aperture. DTIC

N94-36744# Boeing Co., Seattle, WA.
NEW PLASMA SOURCE OF HYDRIDES FOR EPITAXIAL GROWTH
B. J. Stanbery May 1994 21 p Prepared for Midwest Research Inst., Golden, CO
(Contract DE-AC02-83CH-10093)
(DE94-006918; NREL/TP-451-6400) Avail: CASI HC A03/MF A01

This report describes a novel plasma-activated selenium source that was developed during the course of this subcontract and which is significantly different than any other heretofore reported in the scientific literature. It involves microwave excited, magnetically confined plasma sources that are intended to operate under electron cyclotron resonance (ECR) conditions at 2.455 GHz. This source is designed to excite and dissociate the molecular vapor evaporating or subliming from a heated solid or liquid reservoir. It can combine an effusion cell vapor flux with a stream of hydrogen or helium gas, enabling the in-situ generation of hydrides for use in low-pressure growth techniques where long mean free paths are desirable. Experiments were conducted to demonstrate a stable discharge within the source, and measures were identified to improve its operational characteristics. Application of this novel source is anticipated to enable a low-temperature, safe process for the growth of high-quality epitaxial compound semiconductor films. This reduction of epitaxial growth temperatures may enable the fabrication of novel photovoltaic devices that have heretofore been impossible due to the deleterious effects of interdiffusion at heterointerfaces resulting from the high temperatures required to grow adequate quality material using conventional processes. DOE

N94-36745# Colorado School of Mines, Golden, CO.
SMALL-ANGLE X RAY SCATTERING STUDIES OF MICROVOIDS IN AMORPHOUS-SILICON-BASED SEMICONDUCTORS
D. L. Williamson, S. J. Jones, and Y. Chen May 1994 50 p Prepared for Midwest Research Inst., Golden, CO
(Contract DE-AC02-83CH-10093)
(DE94-006931; NREL/TP-451-6395) Avail: CASI HC A03/MF A01

Our general objectives are to provide new details of the microstructure for the size scale from about 1 to 30 nm in high-quality a-Si:H and related alloys prepared by current state-of-the-art deposition methods as well as by new and emerging deposition technologies and thereby help determine the role of microvoids and other density fluctuations in controlling the opto-electronic properties. More specifically, the objectives are to determine whether the presence of microstructure as detected by small-angle x-ray scattering (SAXS) (1) limits the photovoltaic properties of device-quality a-Si:H, (2) plays a role in determining the photo-stability of a-Si:H, and (3) is responsible for degradation of the photovoltaic properties due to alloying with Ge, C and other constituents. The approach involves collaboration with several groups that can supply relevant systematic sets of samples and the associated opto-electronic data to help address these issues. Since the SAXS technique has not been a standard characterization technique for thin-film materials, and was recently set up at CSM with support by NREL, the project involves considerable development of the method with regard to standardizing the procedures, minimizing substrate influences and implementing improved data reduction and modeling methodology. Precise, highly reproducible, and accurate results are being sought in order to allow useful, reliable, and sensitive comparisons of materials deposited under different conditions, by different methods, and by different systems that represent the same nominal method. DOE

N94-36746# Fermi National Accelerator Lab., Batavia, IL.
ASSESS PROGRESS BEING MADE FOR THE KTeV ELECTROMAGNETIC CALORIMETER CRYSTAL ORDER IN FRANCE
S. R. Childress 27 Aug. 1993 9 p
(Contract DE-AC02-76CH-03000)
(DE94-009396; DOE/FTR-94009396) Avail: CASI HC A02/MF A01 (US Sales Only)

This report contains a record of our activities at the Quartz & Silice facility during this visit. Significant progress was achieved in illustrating the importance and practical application of particular measurements in characterizing crystal quality, and in understanding problems with crystal polishing techniques currently being used. Detailed discussions with Quartz & Silice personnel on these issues were held, as were discussions on current production and furnace growth cycle options which may significantly increase ingot production rates. DOE

N94-36755 Martin Marietta Labs., Syracuse, NY.
LOW TEMPERATURE MATERIALS Final Technical Report, Jun. 1991 - Jan. 1994
J. M. Ballingall, P. Ho, J. Mazurowski, L. Lester, and K. C. Hwang Mar. 1994 59 p Limited Reproducibility: More than 20% of this document may be affected by microfiche quality
(Contract F49620-91-C-0044)
(AD-A278703; AFOSR-94-0231TR) Avail: Issuing Activity (Defense Technical Information Center (DTIC))

In(x)Ga(l-x)As (x=025-0.35) grown at low temperature on GaAs by molecular beam epitaxy is characterized by Hall effect, transmission electron

microscopy, and ultrafast optical testing. As with low temperature (LT) GaAs, the resistivity is generally higher after a brief anneal at 600 C. High-resolution transmission electron micrography shows all the as-grown epilayers grown directly on GaAs to be heavily dislocated due to the large lattice mismatch (2-3%). Annealed layers also show precipitate formation, in addition to the dislocations. Like LT GaAs, In(x)Ga(1-x)As lifetimes shorten as growth temperatures are reduced; and LT In(x)Ga(l-x)As lifetimes are generally shorter in as-grown samples than in annealed samples. The metal-semiconductor-metal photodetectors we fabricated on the material exhibit response times of 1-3 picoseconds, comparable to results reported on GaAs grown at low temperature, and the fastest ever reported in the wavelength range of 1.0-1.3 microns. To improve the crystalline quality and to distinguish detector speed and responsivity limitations due to dislocations versus defects induced by LT growth, we have grown 3 microns-thick graded layers of In(x)Al(l-x)As between the GaAs substrates and In(0.35)Ga(0.65)As films. The In(x)Al(l-x)As layers are heavily dislocated, with the dislocation density increasing with distance from the GaAs substrate, and abruptly terminating at or below the In(0.35)Ga(0.65)As layer. DTIC

N94-37027 Science Applications International Corp., McLean, VA. Applied Physics Operation.
SOLID STATE FLUOROMETER: PROTOTYPE DEVELOPMENT Final Report, 22 Sep. 1992 - 31 May 1993
Joseph Czarnaski, Karen Foster, John Hardgrove, Richard Oprison, and James Hickman Mar. 1994 56 p Limited Reproducibility: More than 20% of this document may be affected by microfiche quality
(Contract F33615-91-D-0652)
(AD-A280321; SAIC-01-0262-01-1222; AL/OE-TR-1993-0162) Avail: Issuing Activity (Defense Technical Information Center (DTIC))

The development of new detectors for chemical and biological warfare agents is of interest to the DOD. One way to detect these agents is by fluorescent labeling of one of the species involved in a binding event. The U.S. Air Force has developed a system that combines a biological assay with a fluorescent molecule tag. The binding event is quantified by measuring the ratio of red to green fluorescence. With a solid state fluorometer fast binding detection is possible in a small, lightweight package that could easily be interfaced to a microprocessor with readout. We have begun the development of a solid state microfluorometer. The development has been divided into three phases: (1) prototype development, (2) device operational parameter investigation, and (3) design and construction. This report details the construction of the prototype device. The prototype has a 488-nm laser for excitation, and red and green detectors for fluorescent emission. The calibration of the detectors and the computer interface construction is described. It can be used as a fluorescent imaging system as well. DTIC

N94-37036# Conductus, Inc., Sunnyvale, CA.
SUBMILLIMETER QUASIOPTICAL JOSEPHSON JUNCTION OSCILLATOR WITH INTEGRATED TUNING ELEMENTS Final Report, 1 Jul. 1993 - 28 Feb. 1994
Aleksandar Pance and Andrew Barfknecht 30 Apr. 1994 27 p
(Contract F49620-93-C-0037)
(AD-A280380; Rept-94003-SBIR-2-F; AFOSR-94-0347TR) Avail: CASI HC A03/MF A01

The goal of this program was to demonstrate a quasioptical Josephson oscillator with integrated tuning elements using standard Conductus niobium technology. This device is based on a novel approach that incorporates integrated tuning and impedance-matching structures at every Josephson junction/antenna pair. The device has been designed, fabricated, and successfully tested. A new unit cell has been devised, incorporating a subarray of 1 to 16 Josephson junctions. Microstrip transformers are used locally between each subarray and its antenna. The oscillator with 110 Josephson junctions and bow-tie antennas was found to radiate close to its maximum available power at 115 GHz. The on-chip SIS radiation detector has detected 2.64 nW of power. The oscillator was tuned across 19 GHz, or 16% of fractional bandwidth, in reasonable agreement with the predicted value of 19%. This is the first demonstration of a distributed array Josephson oscillator, where each junction feeds its own antenna and phase-locks to the radiation of other junctions. It is also the first demonstration of using integrated microstrip tuning and impedance matching elements at every Josephson junction of an oscillator. Finally, this is the first distributed Josephson oscillator reported to date that appears to radiate close to its maximum available power. DTIC

N94-37054# Argonne National Lab., IL.
QUADRUPOLAR EFFECTS IN PrCu2Si2
R. Osborn and E. A. Goremychkin 1994 10 p Presented at the 6th Joint Conference on Magnetism and Magnetic Materials, Albuquerque, NM, 20-23 Jun. 1994
(Contract W-31-109-eng-38)
(DE94-011509; ANL/MSD/CP-82754; CONF-940629-4) Avail: CASI HC A02/MF A01

As part of a systematic study of the crystal field (CF) potential in RCu2Si2 compounds (R = Ce, Pr, Nd, Tb, Ho, Er) using inelastic neutron scattering, we have determined the CF level scheme and potential in the antiferromagnet PrCu2Si2 both above and below T(sub N). There have been recent speculations that the quadrupole moment of PrCu2Si2 has been quenched by the quadrupolar Kondo effect. Using the CF potential derived from our results, we have calculated the quadrupole moment Q(sub 2) of PrCu2Si2 and compared it to the other members of the RCu2Si2 series. The temperature dependence of the quadrupole moment of PrCu2Si2 is significantly weaker than all the other compounds, e.g. it is approximately five times smaller than HoCu2Si2. Therefore, it is the CF potential which is responsible for quenching Q(sub 2) at low temperature rather than a quadrupolar Kondo effect. Furthermore, the CF Schottky contribution to C/T nu T(exp 2) is approximately linear above T(sub N) and explains the anomalously high linear term in the specific heat. However, the evolution of the CF potential across the rare earth series provides evidence of an enhanced hybridization contribution to the CF potential of PrCu2Si2, intermediate between the heavy fermion CeCu2Si2 and the other rare earth compounds. DOE

N94-37057# Los Alamos National Lab., NM.
CONSEQUENCES OF COMPETING HYBRIDIZATION FOR MAGNETIC ORDERING IN CORRELATED-ELECTRON LATTICES
C. Sanchez-Castro (West Virginia Univ., Morgantown, VA.), B. R. Cooper (West Virginia Univ., Morgantown, VA.), and K. S. Bedell 1994 10 p Presented at the 6th Joint Conference on Magnetism and Magnetic Materials, Albuquerque, NM, 20-23 Jun. 1994
(Contract W-7405-eng-36)
(DE94-011648; LA-UR-94-1164; CONF-940629-5) Avail: CASI HC A02/MF A01

We present a method for calculating the f - f ion interaction in systems where a transition metal species also hybridizes with the same Fermi sea. For the physical systems of interest, typically species f is a light rare earth (e.g. Ce or Pr) or a light actinide (U) involving a partially filled f-shell and species d is a d-shell transition metal ion; there may be experimental evidence of competition between magnetic ordering of the f and d electron systems (e.g. when f is U and d is Mn). The method treats first the strong hybridization between the d and the conduction electrons to obtain a new ground state with delocalized d electrons. Then it calculates the f - f ion interaction by perturbation theory. We identify the mechanisms by which the d electrons modify the f - f ion interaction. DOE

N94-37069# Argonne National Lab., IL.
COMPARISON OF THE CRYSTAL STRUCTURE AND MOLECULAR MODELS OF N,N-DIISOBUTYL-2- (OCTYLPHENYLPHOSPHINYL) ACETAMIDE (CMPO)
R. D. Rogers, A. N. Rollins, R. C. Gatrone, and E. P. Horwitz 1994 41 p
(Contract W-31-109-eng-38)
(DE94-013434; ANL/CHM/PP-81023) Avail: CASI HC A03/MF A01

The compound crystallizes in the space group P2(sub 1)/c with a=13.446(6), b=22.280(7), c=17.217(7) Angstrom, b=92.07(4) degrees, and D(sub calc)=1.05 g/cu cm for Z=8 (at 20 C). Molecular mechanics, molecular dynamics, and MNDO calculations were also performed on CMPO utilizing the SYBYL suite of programs. Results from these calculations are compared to the crystal structure and to similar calculations performed on CMPO using ALCHEMY. The calculations agree fairly well with the crystal structure. DOE

N94-37103*# Clemson Univ., SC. Dept. of Ceramic Engineering.
DEVELOPMENT OF HIGH Tc (GREATER THAN 100 K) Bi, Tl AND Y-BASED MATERIALS AS SUPERCONDUCTING CIRCUIT ELEMENTS Final Report, Mar. 1990 - Jul. 1994
Gene Haertling, Gregory Grabert, and Phillip Gilmour 15 Jul. 1994

195 p
(Grant NAG1-1108)
(NASA-CR-196276; NAS 1.26:196276) Avail: CASI HC A09/MF A03

Experimental work on this project over the last four years has resulted in establishing processing and characterization techniques for producing both the Bi-based and Tl-based superconductors in their high temperature (2223) forms. In the bulk, dry pressed form, maximum critical temperatures (Tc) of 108.2 K and 117.8 K, respectively, were measured. Results have further shown that the Bi and Tl-based superconducting materials in bulk form are noticeably different from the Y-based 123 material in that superconductivity is considerably harder to achieve, maintain, and reproduce. This is due primarily to the difficulty in obtaining the higher Tc phase in pure form since it commonly co-exists with other undesirable, lower Tc phases. In particular, it has been found that long processing times for calcining and firing (20 - 200 hrs.) and close control of temperatures which are very near the melting point are required in order to obtain higher proportions of the desirable, high Tc (2223) phase. Thus far, the BSCCO bulk materials has been prepared in uniaxially pressed, hot pressed, and tapecast form. The uniaxially pressed material has been synthesized by the mixed oxide, coprecipitation, and melt quenching processes. The tapecast and hot pressed materials have been prepared via the mixed oxide process. In addition, thick films of BSCCO (2223 phase) have been prepared by screen printing on to yttria and magnesia stabilized zirconia with only moderate success; i.e., superconductivity was achieved in these thick films, but the highest Tc obtained in these films was 89.0 K. The Tc's of the bulk hot pressed, tapecast, and screen printed thick film materials were found to be 108.2, 102.4, and 89.0 K, respectively.

Derived from text

N94-37129 Air Force Inst. of Tech., Wright-Patterson AFB, OH. School of Engineering.
THE EXCITATION MECHANISM OF PRASEODYMIUM-DOPED SEMICONDUCTORS Ph.D. Thesis
Paul L. Thee Jun. 1994 171 p Limited Reproducibility: More than 20% of this document may be affected by microfiche quality
(AD-A280687; AFIT/DS/ENP/94-01) Avail: Issuing Activity (Defense Technical Information Center (DTIC))

This study on praseodymium (Pr) luminescence in Al(x)Ga(1-x)As was conducted to enhance the understanding of the excitation mechanism. Pr was implanted at 390 keV with doses from 5 x 10(exp 12) to 5 x 10(exp 13)/sq cm into Al(x)Ga(1-x)As (x=0.0 to 0.50) wafers which were annealed using the rapid thermal annealing (RTA) method. Low temperature photoluminescence (PL) was conducted using an Ar-ion laser and Ge detector. PL emissions of Pr from all hosts include peaks near 1.3 and 1.6 micrometers which are assigned to the intra-4f transitions of 1G4 yielding 3H5 and 3F3 yielding 3H4, respectively. The intensity of PL emissions depends strongly on the Al mole fraction. Selective excitation luminescence experiments revealed that the Pr-related PL intensity is quenched when the excitation laser energy is decreased below the host free exciton energy. Temperature dependent PL studies revealed activation energies corresponding to bound exciton dissociation from the Pr ions. Coimplantation of Pr with Er, B, C, N, 0, and F all proved to quench the Pr luminescence. An excitation model proposes that Pr luminescence can occur when the Pr forms bound excitons and absorbs the recombination energy. DTIC

N94-37166# Iowa State Univ. of Science and Technology, Ames, IA. Dept. of Physics and Astronomy.
CRITICAL-STATE FLUX-DENSITY PROFILES IN TYPE-2 SUPERCONDUCTING THIN-FILM STRIPS AND DISKS
J. R. Clem 1994 4 p Presented at the 7th IWCC International Workshop on Critical Currents in Superconductors, Alpbach, Austria, 24-27 Jan. 1994
(Contract W-7405-eng-82)
(DE94-011199; IS-M-780; CONF-940122-4) Avail: CASI HC A01/MF A01

When a weak magnetic field is applied to a superconducting strip or disk of thickness d (of the order of the penetration depth (lambda)) much less than its width or radius, induced super-currents flow so as to prevent magnetic flux from penetrating the superconductor (except within (lambda) of the edge). A stronger field causes vortices to enter, and the profiles of the macroscopic flux density B are determined by critical-state equations describing bulk pinning. Near the sample edge, where the vortices are, the magnitude of the current density J is J(sub c). In vortex-free regions of the sample, the magnitude of J is less than J(sub c) but is not zero. The profiles of B can be calculated analytically by assuming that J, averaged over the film thickness, is given by the difference between the values of the tangential component of B at the top and bottom surfaces of the film. This paper examines the basis for this assumption, which is equivalent to assuming that the current density is determined solely by the curvature of H, rather than by the gradient of its magnitude. It is shown that this is a good approximation for thin-film strips and disks. DOE

N94-37192# Argonne National Lab., IL. Materials Science Div.
SUBSTRATE EFFECTS ON THE STRUCTURE AND OPTICAL PROPERTIES OF EPITAXIAL PbTiO3 THIN FILMS PREPARED BY METAL-ORGANIC CHEMICAL VAPOR DEPOSITION
C. M. Foster, Z. Li, G. R. Bai, H. You, D. Guo, and H. L.M. Chang Apr. 1994 8 p Presented at the Spring Meeting of the Materials Research Society, San Francisco, CA, 4-8 Apr. 1994
(Contract W-31109-eng-38)
(DE94-010432; ANL/MSD/CP-81222; CONF-940411-11) Avail: CASI HC A02/MF A01

Epitaxial PbTiO3 films were prepared by metal-organic chemical vapor deposition (MOCVD) on MgO(001), SrTiO3(001), and LaAlO3(001) surfaces. Four-circle x-ray diffraction and optical waveguiding experiments were performed to characterize the deposited films. The films on all three substrates were single-crystal; however, the domain structure of the films was strongly dependent on the substrate material. Films on MgO and LaAlO3 substrates showed a large amount of 90 degree domain structures, whereas, the degree of twinning was greatly suppressed for films on SrTiO3. The refractive indices and optical birefringence of the films were measured as a function of wavelength using the film-prism coupling method. The authors found that for films on LaAlO3(001), the ordinary index and for films on MgO(001) both the ordinary and extraordinary refractive indices were higher than those of bulk single-crystal PbTiO3. For films grown on SrTiO3(001), the ordinary refractive index was very close to that of single crystal PbTiO3. They correlate the increased refractive index and the reduced birefringence to the degree of epitaxial strain and twinning in the samples, respectively. DOE

N94-37193# Argonne National Lab., IL.
SUPERCONDUCTING TlCa2Ba2Cu3O9 THICK FILMS Final Report
1994 9 p Prepared in cooperation with GE Co., Schenectady, NY
(Contract W-31109-eng-38)
(DE94-010436; ANL/ITD/RP-82647) Avail: CASI HC A02/MF A01

GE Corporate Research and Development's (GE-CRD) program to develop the two-zone silver addition (TZSA) process for fabricating superconducting films of TlCa2Ba2Cu3O9 has activities in the areas of (1) precursor preparation, (2) the thallium oxide vapor process, (3) the effects of post-synthesis annealing ambient and temperature on superconducting properties, (4) the influence of film stoichiometry and composition on superconducting properties, (5) microstructure and film growth mechanism, (6) the preparation of thicker films, (7) the fabrication of films on flexible substrates, and (8) process scale-up. As part of its effort under the ANL Pilot Center Agreement, GE-CRD has supplied to ANL a complete two-zone furnace, has provided consultation on its use and on the planning of experiments, has processed ANL samples in GE's furnaces to help define optimum process conditions, and has provided precursor and finished films as requested. These contributions are described more fully in the descriptions of the work performed at ANL presented elsewhere in this report. Under the Pilot Center Agreement work at GE-CRD has been directed toward the optimization of the TZSA process with emphasis on (A) process improvement, (B) effects of silver content on film properties, (C) the relationship between microstructure and J(sub c), and (D) toward the assessment of the compatibility of silver substrates with the process chemistry. DOE

N94-37212# Oak Ridge National Lab., TN.
PAIR CORRELATIONS IN CRYSTALLINE SOLID SOLUTIONS
G. E. Ice, C. J. Sparks, L. Shaffer, and P. Zschack 1994 10 p Presented at the Fall Meeting of the Minerals, Metals and Materials Society: Physical Metallurgy and Materials, Pittsburgh, PA, 17-21 Oct. 1993
(Contract DE-AC05-84OR-21400)
(DE94-012319; CONF-931009-25) Avail: CASI HC A02/MF A01

Recent measurements of pair correlations in metallic solid solutions

challenge simple models of atomic size in alloy structure. These measurements take advantage of intense and tunable synchrotron X radiation to control the x-ray scattering contrast between atoms in a solid solution. For binary alloys with elements nearby in the periodic table it is possible to tune the x-ray energy near the K edge so that the scattering contrast varies from near zero to +/- 5 electron units. Even larger contrast variation is possible near L edges or with complementary x-ray and neutron diffraction data sets. With adjusted scattering contrast it is possible to measure short range order (SRO), even in alloys with elements nearby in the periodic table. It is also possible to detect chemically-specific static displacements of +/- 0.001 Angstrom or less and with fewer assumptions than with previous experimental methods. We compare the measured chemically-specific static displacements in Fe22.5Ni77.5 and Cr47Fe53 with previous models and with the results of other experiments. DOE

N94-37228 Naval Postgraduate School, Monterey, CA.
X-RAY DIFFRACTION STUDIES OF EVAPORATED GOLD THIN FILMS DEPOSITED ON ALUMINUM NITRIDE SUBSTATES M.S. Thesis
Clifford B. Munns 24 Mar. 1994 71 p Limited Reproducibility: More than 20% of this document may be affected by microfiche quality
(AD-A280454) Avail: CASI HC A04

X-ray diffraction was utilized to determine the root mean square (r.m.s.) strains and average particle sizes in evaporated gold thin films on aluminum nitride substrates as a function of substrate surface condition prior to deposition. The substrate treatments evaluated were surface roughness, use of titanium and chromium inter-layers, presence of an oxide layer on the substrate surface, and vacuum conditions used during deposition. The Warren-Averbach method was utilized to obtain the r.m.s. strains and particle sizes from peak breadth data, using both cosine and modulus methods. It was concluded that the highest strain deviations; therefore, the largest film plastic deformation occurred when the substrate surface was rough, when chromium was used as an inter-layer, and when ultra high vacuum conditions were used during deposition. It is proposed that for a fixed film-substrate system, the r.m.s. strain, which is indicative of the level of plastic deformation in the film induced due to differential contraction following deposition, may serve as an indirect measure of the interfacial adhesion. DTIC

N94-37285# Purdue Univ., West Lafayette, IN.
MIDWEST SUPERCONDUCTIVITY CONSORTIUM
Jan. 1994 86 p
(Contract DE-FG02-90ER-45427)
(DE94-012716; DOE/ER-45427/4) Avail: CASI HC A05/MF A01

The Midwest Superconductivity Consortium, MISCON, in the fourth year of operations further strengthened its mission to advance the science and understanding of high T(sub c) superconductivity. The goals of the organization and the individual projects continue to reflect the current needs for new knowledge in the field and the unique capabilities of the institutions involved. Group efforts and cooperative laboratory interactions to achieve the greatest possible synergy under the Consortium continue to be emphasized. Industrial affiliations coupled with technology transfer initiatives were expanded. Activities of the participants during the past year achieved an interactive and high level of performance. The number of notable achievements in the field contributed by Consortium investigators increased. The programmatic research continues to focus upon key materials-related problems in two areas. The first area has a focus upon 'Synthesis and Processing' while the second is centered around 'Limiting Features in Transport Properties of High T(sub c) Materials'. DOE

N94-37287# Sandia National Labs., Albuquerque, NM.
THEORETICAL AND EXPERIMENTAL INVESTIGATIONS OF FULLERENE DERIVATIVES: C60H2, C60H4, C70H2 AND C60CH22
S. J. Jacobs, K. T. Gillen, P. A. Cahill, C. C. Henderson, and C. M. Rohlfing 1993 6 p Presented at the Spring Meeting of the Materials Research Society, San Francisco, CA, 4-8 Apr. 1994
(Contract DE-AC04-94AL-85000)
(DE94-012727; SAND-93-2581C; CONF-940411-22) Avail: CASI HC A02/MF A01

Hydroboration of C70 in toluene yields a 2:1 mixture of 1,9-C70H2 and 7,8-C70H2. Equilibration of these two isomers in the presence of a Pt catalyst reveals a free energy difference of 1.4 plus/minus 0.2 kcal/mol. Whereas semiempirical calculations have been found to predict the energy ordering of many fullerene derivatives incorrectly, ab initio Hartree-Fock (HF) calculations have been found to yield quantitative predictions of experiment. The HF/6-31G* level energy separation of 1,9-C70H2 and 7,8-C70H2 of 1.3 kcal/mol is in excellent agreement with experiment. Relative stabilities of isomers of bis(methano)fullerenes were found to parallel those of analogous C60H4 isomers. Density functional theory (DFT) methods have been tested and are equivalent in accuracy to HF methods if similar basis sets are used. C60H2 and C60H4 can be efficiently produced on larger (greater than 50 mg) scales with diimide generated from potassium azodicarboxylate and acetic acid in o-dichlorobenzene. DOE

N94-37290# Los Alamos National Lab., NM.
QUANTUM CONFINEMENT IN GaP NANOCLUSTERS
B. K. Laurich, D. C. Smith, and M. D. Healy 1994 7 p Presented at the Spring Meeting of the Materials Research Society, San Francisco, CA, 4-8 Apr. 1994
(Contract W-7405-eng-36)
(DE94-013119; LA-UR-94-1715; CONF-940411-23) Avail: CASI HC A02/MF A01

We have prepared GaP and GaAs nanoclusters from organometallic condensation reactions of E(Si(ChH3)3)3 (E = P, As) and GaCl3. The size of the as synthesized clusters is 10 Angstrom to 15 Angstrom. Larger clusters of 20 Angstrom to 30 Angstrom size were obtained by thermal annealing of the as grown material. X-ray diffraction and transmission electron microscopy confirm the high crystalline quality. A lattice contraction of 6.7% could be seen for 10 (Angstrom) sized GaAs clusters. The clusters are nearly spherical in shape. Optical absorption spectra show a distinct line which can be assigned to the fundamental transition of the quantum confined electronic state. The measured blue shift, with respect to the GaP bulk absorption edge is 0.53 eV. As the cluster is smaller than the exciton radius, we can calculate the cluster size from this blue shift and obtain 20.2 Angstrom, consistent with the results from X-ray diffraction of 19.5 Angstrom for the same sample. DOE

N94-37291# Los Alamos National Lab., NM.
STRUCTURAL GROUND-STATE OF La2CuO4 IN THE LTO PHASE: EVIDENCE OF LOCAL DISORDER
S. J. L. Billinge, G. H. Kwei, and H. Takagi 1994 2 p Presented at the Meeting on Materials and Mechanisms of Superconductivity: High Temperature Superconductors, Grenoble, France, 4-9 Jul. 1994
(Contract W-7405-eng-36)
(DE94-013126; LA-UR-94-1657; CONF-940701-2) Avail: CASI HC A01/MF A01

We present neutron scattering data which indicate that the local structure of La2CuO4 in the LTO phase is disordered. Data from two different diffractometers are compared and systematic differences between the pair distribution functions (PDF) of the LTO model and the data are reproduced in both cases. DOE

N94-37311# South Carolina State Coll., Orangeburg, SC. Dept. of Natural Sciences.
APPLICATIONS OF HIGH TRANSITION TEMPERATURE SUPERCONDUCTORS AT THE SAVANNAH RIVER SITE
J. E. Payne and L. L. Payne Apr. 1994 11 p
(Contract DE-FG09-92SR-18273)
(DE94-012938; DOE/SR-18273/2) Avail: CASI HC A03/MF A01

The second year of the research program has involved further evaluation of the applications of high transition temperature superconducting devices at the Savannah River Site and the fabrication of magnetic shields from high T(sub c) materials that might be of use in programs at the site. In cooperation with AVX Corporation, a satisfactory magnetic shield has been developed and the results of tests on it are included in this report. In addition, results have been reported by undergraduate students. The improved version of a nitrogen temperature SQUID for applications such as those that might be encountered at the site has suffered setbacks in development. It has been possible to begin the initial studies with a high (Tc) device but some of the more detailed analysis has been restricted. The new device was received this month and will have an important impact on the outcome of the project by allowing for a more complete evaluation of a device that can be used in an industrial situation. DOE

N94-37356# Sandia National Labs., Albuquerque, NM.
FIRST-PRINCIPLES DETERMINATION OF THE POLARIZABILITIES OF CARBON TUBULES AS A FUNCTION OF LENGTH
A. A. Quong and M. R. Pederson 1994 4 p Presented at the Spring Meeting of the Materials Research Society, San Francisco, CA, 4-8 Apr. 1994
(Contract DE-AC04-76DP-00789)
(DE94-013015; SAND-94-8641C; CONF-940411-20) Avail: CASI HC A01/MF A01

We use the local density approximation to the density functional theory to determine the axial polarizabilities of fullerene tubules as a function of length and winding topologies. Specifically, we present linear polarizabilities for tubules of composition C12H24, C36H24, C40H20, and C60H24. The size-dependent variation in the dipole-coupled gaps between pairs of occupied and unoccupied levels leads to enhancements in the polarizability per valence electron as the length of the tubule increases. The results are compared to recent density-functional based calculations of the linear and nonlinear polarizabilities for fullerene and benzene molecules. DOE

N94-37369# Oak Ridge National Lab., TN.
IONIC PROPERTIES OF HYDROGENATED AND FLUORINATED FULLERENES
R. Compton, R. Hettich, Chang-Ming Jin, A. Tuinman, and B. Dunlap 1994 2 p Presented at the Spring Meeting of the Materials Research Society, San Francisco, CA, 4-8 Apr. 1994
(Contract DE-AC05-84OR-21400)
(DE94-012110; CONF-940411-17) Avail: CASI HC A01/MF A01

Using mass spectrometry, the ionization potentials (IP) of C(60)H(n) for even-numbered n=2-12 were determined to be 6.75-7.5 eV, and for odd-numbered n were below 6.75 eV (for C(60), IP is 7.65 eV). Electron affinities (EA) of these species rapidly decrease with increasing n. IP's and EA's for C(60)F(x), on the other hand, both increase dramatically upon fluorination. A second electron can be added to gaseous C(60)F(48)(-); the resulting doubly charged anion is more stable with respect to loss of one of the excess electrons. DOE

N94-37377 Argonne National Lab., IL.
MELT-PROCESSING OF Y-Ba-Cu-O SUPERCONDUCTORS FOR IMPROVED LEVITATION
U. Balachandran, W. Zhong, J. E. Emerson, and R. L. McDaniel Apr. 1994 2 p Presented at the International Workshop on Superconductivity: Critical Current of High-Temperature Superconductors and Related Topics, Kyoto, Japan, 6-9 Jun. 1994 Limited Reproducibility: More than 20% of this document may be affected by microfiche quality
(Contract W-31-109-eng-38)
(DE94-011503; ANL/ET/CP-81946; CONF-940651-4) Avail: CASI HC A01

Melt processed bulk YBa2Cu3O(7-delta) (YBCO) superconductors are of considerable interest in the application of low-friction, superconducting permanent magnet bearings and flywheel-energy-storage devices. The mechanisms of enhanced flux pinning in the melt processed samples has been the subject of many investigations. Fine precipitates of Y(2)BaCuO(5) (211) are considered potential flux-pinning sites by many investigators. Several groups have reported the refinement of 211 precipitates through Pt additions. In this paper, the authors describe the melt processing of YBCO with additives such as 211, Pt, and Ag. Large single domain regions are obtained using small SmBa2Cu3O(7-delta) (Sm-123) single crystal seeds. The microstructure and levitation forces are measured and reported here. DOE

N94-37382# Oak Ridge National Lab., TN.
MICROSTRUCTURE AND CHEMISTRY OF MgO- AND CoO-DOPED NICKEL-TITANATE SPINELS
I. M. Anderson, J. Bentley, and C. B. Carter 1994 3 p Presented at the Microscopy Society of America and Microbeam Analysis Society Joint Meeting, New Orleans, LA, 31 Jul. - 5 Aug. 1994
(Contract DE-AC05-84OR-21400)
(DE94-012741; CONF-940753-7) Avail: CASI HC A01/MF A01

Four specimens Me(x)Ni(1-x)O - 14.2 mol% TiO2 (Me=Mg, Co, and x = 0.1 or 0.2) were prepared by cold pressing and firing. After heating and quenching, slices were examined in a TEM and x-ray spectrometry carried out. Dark-field images were recorded near the (001)-pole of the two cubic phases with spinel (220) reflection. The spinel-structured phase appears bright, the periclase-structured phase dark. In the 20% CoO doped specimen, the spinel and periclase phases form a continuously interpenetrating network (scale 40 nm); examination of the site distributions with ALCHEMI indicates that the Ti cations occupy mostly the octahedral site (tetrahedral site in undoped material). The spinel MgNiTiO4 is unstable. The arrangements of some of the faceted particles in groups suggest that a large periclase-structured particle may have subdivided. DOE

N94-37400# Oak Ridge National Lab., TN.
ALCHEMI FORMULATED FOR DELOCALIZATION AND ANTI-SITE DEFECTS
I. M. Anderson and J. Bentley 1994 2 p Presented at the 13th International Congress on Electron Microscopy, Paris, France, 17-22 Jul. 1994
(Contract DE-AC05-84OR-21400)
(DE94-012740; CONF-940766-6) Avail: CASI HC A01/MF A01

ALCHEMI (atom location by channeling enhanced microanalysis) provides a useful method for determining the site distributions of impurity atoms in crystals with multiple sublattices. Delocalization of low energy excitations and the dubious statistical confidence level of the technique are problems; a recent formulation of ALCHEMI analysis (Walls, 1992) addresses both problems. This paper extends this analysis for the distribution of atoms over two sublattices; expressions are derived for the fit parameters that are exact given the assumptions of the model, which allows for arbitrary localization constants, and for the possibility of anti-site defects. DOE

N94-37435# Cornell Univ., Ithaca, NY. Materials Science and Engineering Div.
STUDIES OF THE III-V COMPOUNDS IN THE MEGABAR REGIME
Arhtur L. Ruoff 1994 9 p
(Contract DE-FG02-87ER-45320)
(DE94-012488; DOE/ER-45320/6) Avail: CASI HC A02/MF A01

In this project the authors develop techniques for making high pressure measurements (x-ray diffraction and optical measurements) on samples in the multimegabar regime and they make systematic studies of the crystal structure of III-V compounds and other materials as a function of pressure with the broad objective of providing experimental data over a broad range of coordination number and interatomic spacing which can play a leading role in the testing and development of theoretical models of binding. They also create new materials. It was shown that all the compounds AlN, GaN, and InN transform to the C1-type structure with AlN remaining as 100% rocksalt structure on release of pressure. Various parameters in the equation of state (EOS) were measured. The EOS of BP was measured to 110 GPa but no phase transitions were seen. AlAs was shown to transform from the initial zincblende phase to the nickel arsenide phase, the first case of this in the IV-V compounds. The first experiments on CdTe were carried to 51 GPa and are now being analyzed. DOE

N94-37498# Brookhaven National Lab., Upton, NY.
PRELIMINARY SOFT X RAY STUDIES OF BETA-SiC
M. L. Shek, K. E. Miyano, D. L. Ederer, Q. Y. Dong, and T. A. Callcott 1994 24 p Presented at the 40th National Symposium of the American Vacuum Society (AVS), Orlando, FL, 15-19 Nov. 1993
(Contract DE-AC02-76CH-00016)
(DE94-013023; BNL-60381; CONF-9311104-21) Avail: CASI HC A03/MF A01

We have looked at beta-SiC with soft x-ray emission and photoemission spectroscopy. From the Si L(sub 23) and C K emissions, the Si s+d-like and C p partial density of states in the bulk valence band are identified, and compared with valence band photoemission. In addition to bulk electronic structural features, photoemission from a (3 (times) 2) Si-rich surface shows two surface-derived valence features at (approximately)(minus)2.6 and (approximately)(minus)1.6 eV relative to the Fermi level. The intensities of these valence features vary as those of surface Si 2p core level components shifted by (minus)0.5 eV and (minus)1.4 eV from the bulk-like SiC Si 2p core level. We have also used the Si L(sub 23) absorption edge as a probe of the unfilled states near the conduction band minimum. DOE

N94-37499# Brookhaven National Lab., Upton, NY.
POSITRON IMPLANTATION IN SOLIDS
V. J. Ghosh, K. G. Lynn, and D. O. Welch 1993 54 p Presented at

the International School of Physics on Enrico Fermi on Positron Spectroscopy of Solids, Varenna, Italy, 6-30 Jul. 1993
(Contract DE-AC02-76CH-00016)
(DE94-013029; BNL-60186; CONF-9307155-3) Avail: CASI HC A04/MF A01

The Monte Carlo technique for modeling positron prior to annihilation and electron implantation in semi-infinite metals is described. Particle implantation is modelled as a multistep process, a series of collisions with the atoms of the host material. In elastic collisions with neutral atoms there is no transfer of energy. The particle loses energy by several different channels, excitation of the electron gas, ionization of the ion cores, or, at low energies, by phonon excitation. These competing scattering mechanisms have been incorporated into the Monte Carlo framework and several different models are being used. Brief descriptions of these Monte Carlo schemes, as well as an analytic model for positron implantation are included. Results of the Monte Carlo simulations are presented and compared with experimental data. Problems associated with modeling positron implantation are discussed and the need for more experimental data on energy-loss in different materials is stressed. Positron implantation in multilayers of different metals is briefly described and extensions of this work to include a study of multilayers and heterostructures is suggested. DOE

N94-37545# Oak Ridge National Lab., TN.
ATOMIC RESOLUTION CHARACTERIZATION OF A SrTiO3 GRAIN BOUNDARY IN THE STEM
M. M. McGibbon, N. D. Browning, M. F. Chisholm, A. J. McGibbon, S. J. Pennycook, V. Ravikumar, and V. P. Dravid Mar. 1994 3 p Presented at the Microscopy Society of America and Microbeam Analysis Society Joint Meeting, New Orleans, LA, 31 Jul. - 5 Aug. 1994
(Contracts DE-AC05-84OR-21400; DE-AC05-76OR-00033; DE-FG02-92ER-45475)
(DE94-011469; CONF-940753-5) Avail: CASI HC A01/MF A01

This paper uses the complementary techniques of high resolution Z-contrast imaging and PEELS (parallel detection electron energy loss spectroscopy) to investigate the atomic structure and chemistry of a 25 degree symmetric tilt boundary in a bicrystal of the electroceramic SrTiO3. The grain boundary is composed of two different boundary structural units which occur in about equal numbers: one which contains Ti-O columns and the other does not. DOE

N94-37569# Oak Ridge National Lab., TN.
EFFECT OF THERMAL ANNEALING ON GRAIN BOUNDARY CHEMISTRY OF POLYCRYSTALLINE TlBa2Ca2Cu3O(y) FILMS
Z. L. Wang (National Inst. of Standards and Technology, Gaithersburg, MD.), A. Goyal, D. M. Kroeger, and E. D. Specht 1994 3 p Presented at the Microscopy Society of America and Microbeam Analysis Society Joint Meeting, New Orleans, LA, 31 Jul. - 5 Aug. 1994
(Contract DE-AC05-84OR-21400)
(DE94-011464; CONF-940753-4) Avail: CASI HC A01/MF A01

This short communication discusses the effect of heat treatment (annealing at 600 C in oxygen) on the grain boundary chemistry of Tl(x)Ba2Ca2Cu3O(y) films. It was found that the enhancement of critical current density (J sub c) in this material does not result from improvement of the properties of twist grain boundary. CASI

N94-37570# Oak Ridge National Lab., TN.
THE MBE GROWTH AND OPTICAL QUALITY OF BaTiO3 AND SrTiO3 THIN FILMS ON MgO
R. A. McKee, E. D. Specht, K. B. Alexander, and F. J. Walker 1994 7 p Presented at the Spring Meeting of the Materials Research Society, San Francisco, CA, 4-8 Apr. 1994
(Contract DE-AC05-84OR-21400)
(DE94-011468; CONF-940411-16) Avail: CASI HC A02/MF A01

High quality epitaxial BaTiO3 and SrTiO3 have been grown on MgO; stabilized at a one unit cell height; and grown to film thicknesses of 0.5-0.7 (mu)m. These relatively thick films remain adherent when thermally cycled between growth temperatures and room temperature, are crack free with high optical quality, and have both in-plane and out-of-plane X-ray rocking curves of 0.3-0.5 degrees. These films have been grown using molecular beam epitaxy (MBE) methods starting with the TiO2 layer of the perovskite structure. The TiO2-layer/MgO interface uniquely satisfies electrostatic requirements for perovskite heteroepitaxy and provides the template structure that leads to the high quality films that are obtained. Wavelength dependence of optical loss has been characterized between 475 nm and 705 nm with loss coefficients less than I dB/cm being obtained at the He-Ne wavelength. DOE

N94-37676# Georgia Univ., Athens. Dept. of Physics and Astronomy.
OPTICAL STUDIES OF DYNAMICAL PROCESSES IN DISORDERED SYSTEMS
W. M. Yen 1994 8 p
(Contract DE-FG09-87ER-45291)
(DE94-011945; DOE/ER-45291/7) Avail: CASI HC A02/MF A01

We present a brief summary of the progress we have attained in the course of the second year of the present three year rant. The focus of our research continues to be on studies of those dynamical processes such as relaxation and energy diffusion which affect the structure and the optical properties of disordered and amorphous materials. We have been particularly concerned with some new glass compositions which are luminescent in the near infrared (NIR) and on the factors which determine the efficiencies of these materials. In addition, we have begun to investigate the nature and the dynamics of the elementary excitations characteristic of amorphous materials. DOE

N94-37677# Purdue Univ., West Lafayette, IN.
CRYSTALLOGRAPHIC STUDIES OF NITROGENASE AND HYDROGENASE
J. T. Bolin 1994 4 p
(Contract DE-FG02-92ER-20070)
(DE94-011972; DOE/ER-20070/1) Avail: CASI HC A01/MF A01

The long term goal of this project is to obtain detailed knowledge of the structure and function of nitrogenase and hydrogenase through the analysis of physical, chemical, and biological data with reference to three-dimensional, atomic resolution crystal structures of components of the enzyme and/or complexes of the components. The current objectives to determine the crystal structure of wild-type Av1, the nitrogenase MoFe protein from Azotobacter vinelandii; to refine this structure at high resolution; and to initiate studies of mutant MoFe proteins that express altered chemical and physical properties. Further we seek to determine the crystal structure of the bi-directional all-Fe hydrogenase from C. pasteurianum, Cp-hydrI, and to initiate studies of the uptake hydrogenase from the same organism, Cp-hydrii. DOE

N94-37770 Department of the Navy, Washington, DC.
IMPLANTING IMPURITIES IN SEMICONDUCTORS AND SEMICONDUCTOR IMPLANTED WITH IMPURITIES Patent
Frederick G. Moore, inventor (to Navy) and Harry B. Dietrich, inventor (to Navy) 15 Mar. 1994 12 p Filed 26 Aug. 1991 Supersedes AD-D015196
(AD-D016298; US-Patent-5,294,557; US-Patent-Appl-SN-749825; US-Patent-Class-437-22) Avail: US Patent and Trademark Office

A method for ion-implanting a dopant species in semiconductors includes the steps of implanting a dopant species in a semiconductor material at a predetermined rate, the predetermined rate being based on a rate corresponding to a maximum in a characteristic graph of percent activation as a function of dopant species implantation rate; and annealing the dopant implanted semiconductor. DTIC

N94-37776 Department of the Navy, Washington, DC.
HIGH T(SUB c) COPPER-OXIDE SUPERCONDUCTORS COMPRISING Tl-Sr-Ca-Cu-O Patent
William L. Lechter, inventor (to Navy), Michael S. Osofsky, inventor (to Navy), Earl F. Skelton, inventor (to Navy), and Louis E. Toth, inventor (to Navy) 29 Mar. 1994 5 p Filed 31 Mar. 1992
(AD-D016307; US-Patent-5,298,484; US-Patent-Appl-SN-860721; US-Patent-Class-505-1) Avail: US Patent and Trademark Office

High T(sub c) superconducting compounds are made by forming a reaction mixture of the oxides of Sr, Cu, Ca and Tl, compressing these into a hardened body, and placing the hardened body into a container. The container is then evacuated and sealed. The hardened body is heated under pressure until the oxides of Sr, Ca, Cu, and Tl react to form a superconducting compound. DTIC

77 THERMODYNAMICS AND STATISTICAL PHYSICS

Includes quantum mechanics; theoretical physics; and Bose and Fermi statistics.

For related information see also *25 Inorganic and Physical Chemistry* and *34 Fluid Mechanics and Heat Transfer.*

N94-36507# Texas Univ., Austin, TX.
COHERENCE AND CHAOS
E. C. G. Sudarshan 1993 12 p Presented at the Coherent States: Past Present and Future, Oak Ridge, TN, 14-17 Jun. 1993
(Contract DE-FG03-93ER-40757)
(DE94-008529; DOE/ER-40757/015; CONF-9306140-3) Avail: CASI HC A03/MF A01

The annihilation operator for harmonic oscillator is a weighted shift operator and can be realized on a family of over complete coherent states. Shift operators arise in dynamical maps of systems exhibiting deterministic chaos. Generalized coherent states, called harmonious states, realize these maps in a simple manner. By analytic continuation the spectral family can be altered, thus furnishing an alternative perspective on resonant scattering. Singular distributions are necessary to reproduce the rich structure of chaotic and scattering systems. DOE

N94-36508# Texas Univ., Austin, TX.
SCATTERING THEORY FOR THE QUANTUM ENVELOPE OF A CLASSICAL SYSTEM
E. C. G. Sudarshan 1993 12 p
(Contract DE-FG03-93ER-40757)
(DE94-008530; DOE/ER-40757/29) Avail: CASI HC A03/MF A01

Classical dynamics, reformulated in terms of its quantum envelope is studied for the stationary states of the interacting system. The dynamical variable of 'elapsed time' plays a crucial role in this study. It is shown that the perturbation series for the elapsed time can be summed in various simple cases even when standard perturbation series diverge. For the special class of systems where the interactions fall off sufficiently fast at infinity one could define 'in' and 'out' states; and consequently the wave matrices and scattering matrices. The scattering phase shifts bear a simple relation to the time delay in scattering. DOE

N94-36725# Naval Postgraduate School, Monterey, CA.
THE INFLUENCE OF FIN HEIGHT AND WALL CONDUCTIVITY ON INTEGRAL-FIN TUBES DURING STEAM CONDENSATION M.S. Thesis
David W. Meyer Mar. 1994 162 p
(AD-A280597) Avail: CASI HC A08/MF A02

Heat transfer performance of horizontal, integral-fin tubes made of copper, aluminum, copper-nickel, and stainless steel was evaluated using a boiler and steam condenser assembly. Testing was done at vacuum and atmospheric pressure conditions. The tubes tested had an inner diameter of 12.7mm, a root diameter of 13.88mm, and fin heights ranging from 0.5mm to 1.5mm, in 0.25mm increments. The outside heat transfer coefficient was determined first by finding the overall heat transfer coefficient, U(o), then by using the Modified Wilson Plot Technique. The results indicated that the performance of a finned tube is very dependent on fin height and tube material. Moreover, the results were compared with the predictive models of Beatty and Katz, Rose, Adamek and Webb, and Honda et al., with a modified version of the Rose model demonstrating the best predictive capabilities. DTIC

N94-37079# Academy of Sciences of the Ukraine, Kiev. Inst. Teoreticheskoj Fiziki.
THE ASYMPTOTICS OF MATRIX ELEMENTS OF GAUSSIAN POTENTIAL BETWEEN THE BASIS FUNCTIONS OF THREE-DIMENSIONAL HARMONIC OSCILLATOR
G. F. Filippov, A. G. Kosinov, and I. P. Okhrimenko 1993 13 p
(DE94-618467; ITP-93-22E) Avail: CASI HC A03/MF A01 (US Sales Only)

The asymptotic expression may be used to calculate matrix elements of the Gaussian potential between the basis functions of three-dimensional harmonic oscillator (n l absolute value of (V(sub 0) exp(-r(exp 2)/mu(exp 2)) tilde-n l), starting with some values of quantum numbers n and tilde-n. The asymptotic expression is found, and its behavior is investigated for different values of quantum numbers n, tilde-n, l, and ratio mu/r(sub 0). DOE

N94-37094# Princeton Univ., NJ.
THERMODYNAMICS OF MINERALS STABLE NEAR THE EARTH'S SURFACE
A. Navrotsky 1994 6 p
(Contract DE-FG02-85ER-13437)
(DE94-012479; DOE/ER-13437/T3) Avail: CASI HC A02/MF A01

The following are studied/discussed: high-temperature oxide melt calorimetry using molten 2PbO * B2O3; final state of H2O and CO2 on dissolution of crystalline volatile-bearing phase; enthalpy of interaction of water with lead borate; thermochemistry of amphiboles, micas, zeolites, and carbonates in the (Mg,Fe,Ca)CO3 system; radiation damage in minerals (zircons); and crystalline silicas. DOE

N94-37172# Joint Inst. for Nuclear Research, Dubna (USSR). Lab. of Theoretical Physics.
IS IT POSSIBLE TO ASSIGN PHYSICAL MEANING TO FIELD THEORY WITH HIGHER DERIVATIVES?
A. M. Chervyakov and V. V. Nesterenko 1993 20 p
(DE94-618468; JINR-E-2-93-193) Avail: CASI HC A03/MF A01 (US Sales Only)

To overcome the difficulties with the energy indefiniteness in field theories with higher derivatives, it is supposed to use the mechanical analogy, the Timoshenko theory of the transverse flexural vibrations of beams or rods well known in mechanical engineering. It enables one to introduce the notion of a 'mechanical' energy in such field models that is wittingly positive definite. This approach can be applied at least to the higher derivative models which effectively describe the extended localized solutions in usual first order field theories (vortex solutions in Higgs models and so on). Any problems with a negative norm ghost states and unitarity violation do not arise here. DOE

N94-37366# Stanford Linear Accelerator Center, CA.
TESTING VIOLATION OF CPT AND QUANTUM MECHANICS IN THE K(0) - BAR-K(0) SYSTEM
P. Huet May 1994 7 p Presented at the 1st International Conference on Phenomenology of Unification from Present to Future, Rome, Italy, 23-26 Mar. 1994
(Contract DE-AC03-76SF-00515)
(DE94-012057; SU-SLAC-PUB-6491; CONF-9403118-1) Avail: CASI HC A02/MF A01

I report a recent study made in collaboration with M.E. Peskin, on the time dependence of a kaon beam propagating according to a generalization of quantum mechanics due to Ellis, Hagelin, Nanopoulos and Srednicki, in which CP- and CPT-violating signatures arise from the evolution of pure states to mixed states. Constraints on the magnitude of its parameters are established on the basis of existing experimental data. New facilities such as phi factories are shown to be particularly adequate to study this generalization from quantum mechanics and to disentangle its parameters from other CPT violating perturbations of the kaon system. DOE

N94-37543# Stanford Research Inst., Menlo Park, CA.
POLARIZATION PHENOMENA IN QUANTUM CHROMODYNAMICS
S. J. Brodsky Mar. 1994 47 p Presented at the 21st Annual SLAC Summer Institute on Particle Physics: Spin Structure in High-Energy Processes, Stanford, CA, 26 Jul. - 6 Aug. 1993
(Contract DE-AC03-76SF-00515)
(DE94-010663; SLAC-PUB-6450; CONF-930767-8) Avail: CASI HC A03/MF A01

The author discusses a number of interrelated hadronic spin effects which test fundamental features of perturbative and non-perturbative QCD. For example, the anomalous magnetic moment of the proton and the axial coupling g(sub A) on the nucleon are shown to be related to each other for fixed proton radius, independent of the form of the underlying three-quark relativistic quark wavefunction. The renormalization scale and scheme ambiguities for the radiative corrections to the Bjorken sum rule for the polarized structure functions can be eliminated by using commensurate scale relations with other observables. Other examples include (a) new constraints on the shape and normalization of the polarized quark and

gluon structure functions of the proton at large and small x(sub bj); (b) consequences of the principle of hadron helicity retention in high x(sub F) inclusive reactions; (c) applications of hadron helicity conservation to high momentum transfer exclusive reactions; and (d) the dependence of nuclear structure functions and shadowing on virtual photon polarization. He also discusses the implications of a number of measurements which are in striking conflict with leading-twist perturbative QCD predictions, such as the extraordinarily large spin correlation A(sub NN) observed in large angle proton-proton scattering, the anomalously large (rho)(pi) branching ratio of the J/(psi), and the rapidly changing polarization dependence of both J/(psi) and continuum lepton pair hadronp roduction observed at large x(sub F). The azimuthal angular dependence of the Drell-Yan process is shown to be highly sensitive to the projectile distribution amplitude, the fundamental valence light-cone wavefunction of the hadron. DOE

80 SOCIAL SCIENCES (GENERAL)

Includes educational matters.

N94-37092# Sandia National Labs., Albuquerque, NM.
MATH AND SCIENCE ILLITERACY: SOCIAL AND ECONOMIC IMPACTS
J. L. Williams 1994 5 p Presented at the Society of Women Engineers National Convention and Student Conference, Pittsburgh, PA, 22-24 Jun. 1994
(Contract DE-AC04-94AL-85000)
(DE94-010801; SAND-94-1155C; CONF-940646-2) Avail: CASI HC A01/MF A01

Today's highly competitive global economy is being driven by increasingly rapid technological development. This paper explores the problems of math and science illiteracy in the United States and the potential impact on our economic survival in this environment during the next century. Established educational methods that reward task performance, emphasize passive lecture, and fail to demonstrate relevance to real life are partly to blame. Social norms, stereotypes, and race and gender bias also have an impact. To address this crisis, we need to question the philosophy of an educational system that values task over concept. Many schools have already initiated programs at all grade levels to make math and science learning more relevant, stimulating, and fun. Teaching methods that integrate math and science learning with teamwork, social context, and other academic subjects promote the development of higher-order thinking skills and help students see math and science as necessary skills. DOE

81 ADMINISTRATION AND MANAGEMENT

Includes management planning and research.

N94-37447# Advisory Group for Aerospace Research and Development, Neuilly-Sur-Seine (France). Technical Information Panel.
A GUIDE TO TENDERS AND CONTRACTS ALERTING SERVICES [GUIDE DES SERVICES D'ANNONCES D'APPELS D'OFFRES ET DES MARCHES]
Mar. 1993 27 p
(AGARD-R-799; ISBN-92-835-0704-5) Copyright Avail: CASI HC A03/MF A01

This documents lists, for each of the NATO nations, the main services available for alerting potential bidders and others to government and defense tenders and contracts. This information was compiled by members of the Technical Information Panel of AGARD and the publication was sponsored by the panel. Author

82 DOCUMENTATION AND INFORMATION SCIENCE

Includes information management; information storage and retrieval technology; technical writing; graphic arts; and micrography.

For computer documentation see *61 Computer Programming and Software.*

N94-36750*# National Aeronautics and Space Administration, Washington, DC.
NASA ACCESS MECHANISM: LESSONS LEARNED DOCUMENT
Lisa Burdick, Rick Dunbar, Denise Duncan, Curtis Generous, Judy Hunter, John Lycas, and Ardeth Taber-Dudas Jul. 1994 42 p
(NASA-TM-109924; NAS 1.15:109924) Avail: CASI HC A03/MF A01

The six-month beta test of the NASA Access Mechanism (NAM) prototype was completed on June 30, 1993. This report documents the lessons learned from the use of this Graphical User Interface to NASA databases such as the NASA STI Database, outside databases, Internet resources, and peers in the NASA R&D community. Design decisions, such as the use of XWindows software, a client-server distributed architecture, and use of the NASA Science Internet, are explained. Users' reactions to the interface and suggestions for design changes are reported, as are the changes made by the software developers based on new technology for information discovery and retrieval. The lessons learned section also reports reactions from the public, both at demonstrations and in response to articles in the trade press and journals. Recommendations are included for future versions, such as a World Wide Web (WWW) and Mosaic based interface to heterogeneous databases, and NAM-Lite, a version which allows customization to include utilities provided locally at NASA Centers. Author

N94-36841*# National Aeronautics and Space Administration, Washington, DC.
NASA STI PROGRAM COORDINATING COUNCIL ELEVENTH MEETING: NASA STI MODERNIZATION PLAN
Dec. 1993 150 p Meeting held in Washington, DC, 9 Sep. 1993
(NASA-TM-109415; NAS 1.15:109415) Avail: CASI HC A07/MF A02

The theme of this NASA Scientific and Technical Information Program Coordinating Council Meeting was the modernization of the STI Program. Topics covered included the activities of the Engineering Review Board in the creation of the Infrastructure Upgrade Plan, the progress of the RECON Replacement Project, the use and status of Electronic SCAN (Selected Current Aerospace Notices), the Machine Translation Project, multimedia, electronic document interchange, the NASA Access Mechanism, computer network upgrades, and standards in the architectural effort. For individual titles, see N94-36842 through N94-36852.

N94-36842*# National Aeronautics and Space Administration, Washington, DC.
NASA STI MODERNIZATION PLAN
Karen Kaye *In its* NASA STI Program Coordinating Council Eleventh Meeting: NASA STI Modernization Plan Dec. 1993 p 1-16 (For primary document see N94-36841 12-82)
Avail: CASI HC A03/MF A02

The NASA Scientific and Technical Information (STI) modernization plan is described as a phased approach to a shared network environment. The plan is based on end user needs articulated in continuing user studies in addition to technical requirements. The modernization phases are outlined in a chronology covering the 1993-1997 time frame. Various challenges and constraints are discussed. Emphasis is placed on sustaining user involvement and meeting user needs in measurable ways as the development of the system architecture proceeds. CASI

N94-36843*# National Aeronautics and Space Administration, Washington, DC.
THE ENGINEERING REVIEW BOARD
Judy Hunter *In its* NASA STI Program Coordinating Council Eleventh Meeting: NASA STI Modernization Plan Dec. 1993 p 17-26 (For primary document see N94-36841 12-82)
Avail: CASI HC A02/MF A02

The NASA Engineering Review Board (ERB) is a permanent panel established to create an information infrastructure upgrade plan to support modernization efforts. The ERB looks at concepts and proposals from a

system-wide perspective and identifies critical review milestones in the modernization plan. The background, role, and future directions of the ERB are described. CASI

N94-36844*# National Aeronautics and Space Administration, Washington, DC.
RECON REPLACEMENT PROJECT
Linda Hill *In its* NASA STI Program Coordinating Council Eleventh Meeting: NASA STI Modernization Plan Dec. 1993 p 27-33 (For primary document see N94-36841 12-82)
Avail: CASI HC A02/MF A02

The background, project components, and interface requirements of the RECON/STIMS Replacement Project are described. A requirements document was developed outlining the desired functions, architecture, and capabilities to be covered in the procurement process and a Request for Proposal (RFP) was disseminated. The data structure of the existing bibliographic records and files were examined and an inventory of all existing data elements in RECON records was performed. The goal is a standards based, open architecture system. CASI

N94-36845*# National Aeronautics and Space Administration, Washington, DC.
ELECTRONIC SCAN (SELECTED CURRENT AEROSPACE NOTICES)
Rick Dunbar *In its* NASA STI Program Coordinating Council Eleventh Meeting: NASA STI Modernization Plan Dec. 1993 p 35-54 (For primary document see N94-36841 12-82)
Avail: CASI HC A03/MF A02

The on-line version of the NASA Selected Current Aerospace Notices (SCAN) is described and the three methods for electronic access on the Internet are listed. These are (1) File Transfer Protocol (FTP), (2) Gopher, and (3) LISTSERV. An electronic address and a brief description is given for each of them. CASI

N94-36846*# National Aeronautics and Space Administration, Washington, DC.
MACHINE TRANSLATION PROJECT
Katie Bajis *In its* NASA STI Program Coordinating Council Eleventh Meeting: NASA STI Modernization Plan Dec. 1993 p 55-63 (For primary document see N94-36841 12-82)
Avail: CASI HC A02/MF A02

The characteristics and capabilities of existing machine translation systems were examined and procurement recommendations were developed. Four systems, SYSTRAN, GLOBALINK, PC TRANSLATOR, and STYLUS, were determined to meet the NASA requirements for a machine translation system. Initially, four language pairs were selected for implementation. These are Russian-English, French-English, German-English, and Japanese-English. CASI

N94-36847*# National Aeronautics and Space Administration, Washington, DC.
MULTIMEDIA
Karen Kaye *In its* NASA STI Program Coordinating Council Eleventh Meeting: NASA STI Modernization Plan Dec. 1993 p 65-78 (For primary document see N94-36841 12-82)
Avail: CASI HC A03/MF A02

Multimedia initiative objectives for the NASA Scientific and Technical Information (STI) program are described. A multimedia classification scheme was developed and the types of non-print media currently in use are inventoried. The NASA STI Program multimedia initiative is driven by a changing user population and technical requirements in the areas of publications, dissemination, and user and management support. CASI

N94-36848*# National Aeronautics and Space Administration, Washington, DC.
ELECTRONIC DOCUMENT INTERCHANGE
Dick Tuey *In its* NASA STI Program Coordinating Council Eleventh Meeting: NASA STI Modernization Plan Dec. 1993 p 79-88 (For primary document see N94-36841 12-82)
Avail: CASI HC A02/MF A02

Evaluation and implementation tasks for the NASA-wide electronic publishing system known as networked DOCUTECH are examined and the system configuration is graphically depicted. DOCUTECH provides the capability to print on demand electronically stored documents. Use of the electronic publishing system in several applications has generated productivity gains ranging from 33 to 88 percent at geographically dispersed NASA centers. CASI

N94-36849*# National Aeronautics and Space Administration, Washington, DC.
ELECTRONIC DOCUMENT INTERCHANGE
Jim Erwin *In its* NASA STI Program Coordinating Council Eleventh Meeting: NASA STI Modernization Plan Dec. 1993 p 89-91 (For primary document see N94-36841 12-82)
Avail: CASI HC A01/MF A02

The operational impact of various storage formats related to electronic publishing of documents in the NASA Scientific and Technical Information (STI) Program is discussed. Questions are raised about the development of full text, surrogate, and hybrid storage formats. It appears that the eventual configuration will contain a mix of storage formats based on user demand. CASI

N94-36850*# National Aeronautics and Space Administration, Washington, DC.
NASA ACCESS MECHANISM (NAM)
Judy Hunter *In its* NASA STI Program Coordinating Council Eleventh Meeting: NASA STI Modernization Plan Dec. 1993 p 93-109 (For primary document see N94-36841 12-82)
Avail: CASI HC A03/MF A02

A 1991 user survey indicated that NASA users want (1) access to diverse sources of information; (2) an intuitive approach to system use; (3) avoidance of system query languages; (4) access to peers and other informal sources of information; and (5) simplified and enhanced presentation of search results. Based on these requirements and the use of an intelligent gateway processor, the NASA Access Mechanism (NAM) is being developed to provide the users with the semblance of a one stop shopping environment for information management. CASI

N94-36851*# National Aeronautics and Space Administration, Washington, DC.
NETWORK UPGRADES
Roland Ridgeway *In its* NASA STI Program Coordinating Council Eleventh Meeting: NASA STI Modernization Plan Dec. 1993 p 111-12 (For primary document see N94-36841 12-82)
Avail: CASI HC A02/MF A02

The NASA Scientific and Technical Information (STI) Project modernization plan covers both software and hardware upgrades. On the hardware side, replacing terminals with PC's will enhance office automation functions, provide mainframe and computer network systems access, and facilitate client/server functions. The modernization plan upgrades will involve commercial off-the-shelf software, user interface and client development tools, and the redesign and integration of application systems and software. CASI

N94-36852*# Mitre Corp., Washington, DC.
STANDARDS IN THE ARCHITECTURAL EFFORT
Howard Markham *In* National Aeronautics and Space Administration, NASA STI Program Coordinating Council Eleventh Meeting: NASA STI Modernization Plan Dec. 1993 p 121-147 (For primary document see N94-36841 12-82)
Avail: CASI HC A03/MF A02

The NASA Scientific and Technical Information (STI) Project Architecture Group was established to build a framework for modernization, provide guidance and direction for standardization and integration efforts, and to develop a set of concepts, interfaces, and entities to specifiy standards. The STI data processing architecture is a set of diagrams and descriptions that characterize the principal functions and services as well as hardware and software components. The use of standards promotes scalability and interchangeability. CASI

N94-36853*# National Aeronautics and Space Administration, Washington, DC.
NASA STI PROGRAM COORDINATING COUNCIL TWELFTH MEETING: STANDARDS

Aug. 1994 218 p Meeting was held in Washington, DC, 13 Apr. 1994
(NASA-TM-109925; NAS 1.15:109925) Avail: CASI HC A10/MF A03

The theme of this NASA Scientific and Technical Information Program Coordinating Council Meeting was standards and their formation and application. Topics covered included scientific and technical information architecture, the Open Systems Interconnection Transmission Control Protocol/Internet Protocol, Machine-Readable Cataloging (MARC) open system environment procurement, and the Government Information Locator Service. For individual titles, see N94-36854 through N94-36860.

N94-36854*# National Aeronautics and Space Administration, Washington, DC.

STI ARCHITECTURAL FRAMEWORK WORKING GROUP

Karen Kaye *In its* NASA STI Program Coordinating Council Twelfth Meeting: Standards Aug. 1994 p 1-10 (For primary document see N94-36853 12-82)

Avail: CASI HC A02/MF A03

A general overview of the architecture developed for the NASA scientific and technical information (STI) modernization plan is presented. The value of standardization as a technique to reduce life cycle costs, to facilitate interoperability and scalability and to simplify the management process is explained. Definitions for both de facto and de jure standards follow with emphasis on government and industrial standards. The methodology applied in developing the STI architecture is described. CASI

N94-36855*# National Aeronautics and Space Administration, Washington, DC.

OSI AND TCP/IP

Lynwood P. Randolph *In its* NASA STI Program Coordinating Council Twelfth Meeting: Standards Aug. 1994 p 11-52 (For primary document see N94-36853 12-82)

Avail: CASI HC A03/MF A03

The Open Systems Interconnection Transmission Control Protocol/ Internet Protocol (OSI TCP/IP) and the Government Open Systems Interconnection Profile (GOSIP) are compared and described in terms of Federal internetworking. The organization and functions of the Federal Internetworking Requirements Panel (FIRP) are discussed and the panel's conclusions and recommendations with respect to the standards and implementation of the National Information Infrastructure (NII) are presented. Author

N94-36856*# Library of Congress, Washington, DC.

A CONCISE INTRODUCTION TO MARC

Randall K. Barry *In* National Aeronautics and Space Administration, NASA STI Program Coordinating Council Twelfth Meeting: Standards Aug. 1994 p 53-83 (For primary document see N94-36853 12-82)

Avail: CASI HC A03/MF A03

The record structure, content designation and data content that make up a MAchine-Readable Cataloging (MARC) record are described. Distinguishing characteristics of the MARC record structure are identified and content designations are defined. The use of MARC as both an American national standard (ANSI Z39.2) and an international standard (ISO 2709) is noted. The relational between MARC and the Standardized General Markup Language (SGML) is explored and areas of overlap are identified. CASI

N94-36857*# National Inst. of Standards and Technology, Gaithersburg, MD.

OPEN SYSTEM ENVIRONMENTS

Fritz Schulz *In* National Aeronautics and Space Administration, NASA STI Program Coordinating Council Twelfth Meeting: Standards Aug. 1994 p 85-115 (For primary document see N94-36853 12-82)

Avail: CASI HC A03/MF A03

An open system is defined as a system that implements open specifications for interfaces, services, and supporting formats to enable properly engineered applications software to be ported with minimal changes across a wide range of systems; and to interact with users in a style which facilitates user portability. Based on that definition, a reference model for an open system environment is presented. CASI

N94-36858*# National Inst. of Standards and Technology, Gaithersburg, MD.

OPEN SYSTEM ENVIRONMENT PROCUREMENT

Gary Fisher *In* National Aeronautics and Space Administration, NASA STI Program Coordinating Council Twelfth Meeting: Standards Aug. 1994 p 116-158 (For primary document see N94-36853 12-82)

Avail: CASI HC A03/MF A03

Relationships between the request for procurement (RFP) process and open system environment (OSE) standards are described. A guide was prepared to help Federal agency personnel overcome problems in writing an adequate statement of work and developing realistic evaluation criteria when transitioning to an OSE. The guide contains appropriate decision points and transition strategies for developing applications that are affordable, scalable and interoperable across a broad range of computing environments. While useful, the guide does not eliminate the requirement that agencies posses in-depth expertise in software development, communications, and database technology in order to evaluate open systems. CASI

N94-36859*# Geological Survey, Washington, DC.

Z39.50 AND GILS MODEL

Eliot Christian *In* National Aeronautics and Space Administration, NASA STI Program Coordinating Council Twelfth Meeting: Standards Aug. 1994 p 161-185 (For primary document see N94-36853 12-82)

Avail: CASI HC A03/MF A03

The Government Information Locator System (GILS) is a component of the National Information Infrastructure (NII) which provides electronic access to sources of publicly accessible information maintained throughout the Federal Government. GILS is an internetworking information resource that identifies other information resources, describes the information available in the referenced resources, and provides assistance in how to obtain the information either directly or through intermediaries. The GILS core content which references each Federal information system holding publicly accessible data or information is described in terms of mandatory and optional core elements. CASI

N94-36860*# National Aeronautics and Space Administration, Washington, DC.

GOVERNMENT INFORMATION LOCATOR SERVICE (GILS). DRAFT REPORT TO THE INFORMATION INFRASTRUCTURE TASK FORCE

In its NASA STI Program Coordinating Council Twelfth Meeting: Standards Aug. 1994 p 187-212 (For primary document see N94-36853 12-82)

Avail: CASI HC A03/MF A03

This is a draft report on the Government Information Locator Service (GILS) to the National Information Infrastructure (NII) task force. GILS is designed to take advantage of internetworking technology known as client-server architecture which allows information to be distributed among multiple independent information servers. Two appendices are provided -- (1) A glossary of related terminology and (2) extracts from a draft GILS profile for the use of the American National Standard Information Retrieval Application Service Definition and Protocol Specification for Library Applications. CASI

N94-37008*# Jet Propulsion Lab., California Inst. of Tech., Pasadena, CA.

PUBLICATIONS OF THE JET PROPULSION LABORATORY, 1992

15 Jun. 1994 36 p
(NASA-CR-196125; NAS 1.26:196125; JPL-Bibl-39-33) Avail: CASI HC A03/MF A01

JPL Bibliography 39-33 describes and indexes by primary author the externally distributed technical reporting, released during calendar year 1992, that resulted from scientific and engineering work performed or managed by the Jet Propulsion Laboratory. Three classes of publications are included: (1) JPL Publication (92-series) in which the information is complete for a specific accomplishment; (2) articles from the quarterly Telecommunications and Data Acquisition (TDA) Progress Report (42-series) (each collection of articles in this class of publication presents a periodic survey of current accomplishments by the Deep Space Network as well as other developments in Earth-based radio technology); and (3) articles published in the open literature. Derived from text

N94-37042 Air Force Inst. of Tech., Wright-Patterson AFB, OH.
GLOBAL PICTURE ARCHIVING AND COMMUNICATION SYSTEMS (GPACS): AN OVERVIEW Final Report
Russell C. Ellis Apr. 1994 176 p Limited Reproducibility: More than 20% of this document may be affected by microfiche quality
(AD-A280617; AFIT/GCS/ENG/94J-02) Avail: CASI HC A09

The world is currently experiencing a computer revolution. With the expansion and development of new computer technology, the age of video is upon us. The medical world is also currently undergoing a dramatic change. With the development and perfection of noninvasive techniques of probing the body, large amounts of computer data is collected and much of it is used to generate images. The organization and management of these images is the topic of this thesis. The discussion of storage schemes, databases, communications and data compression techniques gives the reader a background and some insight to the current state of the art in picture archiving and communication systems (PACS) and how this schema will some day be expanded to a global scale called Global PACS (GPACS). DTIC

N94-37333# Advisory Group for Aerospace Research and Development, Neuilly-Sur-Seine (France). Technical Information Panel.
INTERNATIONAL HIGH SPEED NETWORKS FOR SCIENTIFIC AND TECHNICAL INFORMATION [LES RESEAUX INTERNATIONAUX RAPIDES D'ECHANGE D'INFORMATION SCIENTIFIQUE ET TECHNIQUE]
Feb. 1994 99 p In ENGLISH and FRENCH Meeting held in Ottawa, Ontario, 6-7 Oct. 1993
(AGARD-CP-544; ISBN-92-835-0736-3) Copyright Avail: CASI HC A05/MF A02

Contains the papers presented at the Technical Information Panel's Specialists' Meeting held in Ottawa, Canada, 6-7 Oct. 1993. Subjects covered include description of Internet and other global information networks, the virtual library, the supply of documents, electronic journals, bulletin boards, electronic mail and conferencing, information systems for unstructured files, standards, training, and a view of the future. For individual titles, see N94-37334 through N94-37346.

N94-37334# National Library of Canada, Ottawa (Ontario).
AN INTRODUCTION TO THE INTERNET AND ITS SERVICES
Gary Cleveland *In* AGARD, International High Speed Networks for Scientific and Technical Information Feb. 1994 4 p (For primary document see N94-37333 12-82)
Copyright Avail: CASI HC A01/MF A02

The emergence of research networks, computer networks that serve academic and educational communities, offer libraries throughout the world the opportunity to enhance library resource sharing and information access. The best known example of this structure are the networks collectively known as the Internet. The Internet is actually a conglomeration of thousands of networks found in North America, Europe, and every other continent. It is a 'metanetwork' that: 1) physically interconnects TCP/IP-based networks, many of which have hundreds of component networks; and 2) provides gateways to other types of networks, such as BITNET, an electronic mail network that supports computer communications through 32 countries. This paper provides a nontechnical, high-level overview of the Internet and its services. Specific topics include a description of the Internet, how it began, and its current size; its overall structure; the types of international networks it interconnects; the network services that are available; and how these network services are used by libraries. Author (revised)

N94-37335# European Space Agency. ESRIN, Frascati (Italy). Projects and Engineering Dept.
GLOBAL INFORMATION NETWORKS: HOW THEY WORK
Angelo Bodini *In* AGARD, International High Speed Networks for Scientific and Technical Information Feb. 1994 11 p (For primary document see N94-37333 12-82)
Copyright Avail: CASI HC A03/MF A02

'Network' is a word largely used today in many different contexts, and its meaning is highly dependent on the context. This paper focuses on telecommunications networks. A first distinction is introduced between networks structures, services provided by networks, and services provided by hosts connected to networks. Information services belong normally to the last category. Connectivity is highlighted as a basic network service, to support interactive communications, end-to-end file transfers, and data dissemination. Higher level network functions, such as electronic mail, conferences, bulletin boards, and directories make use of lower level connectivity functions but provided services of a different nature, referred to as value added services (VAS). Examples of this classification, which is mapped along the OSI reference model, are taken from Packet Switched Networks, Internet, Decnet, EARN/Bitnet and the protocols mostly used are outlined. A similar classification is to be made also for the gateways, i.e. devices and systems which interconnect different heterogeneous networks. The importance of gateways is invaluable, being the key to multiplying the connectivity of individual network implementations and fundamental steps towards the creation of a global virtual network for information services. Author (revised)

N94-37336# Industry and Science Canada, Ottawa (Ontario). Information Technologies.
THE CANADIAN NETWORK FOR THE ADVANCEMENT OF RESEARCH, INDUSTRY AND EDUCATION (CANARIE)
W. J. Padden *In* AGARD, International High Speed Networks for Scientific and Technical Information Feb. 1994 2 p (For primary document see N94-37333 12-82)
Copyright Avail: CASI HC A01/MF A02

The extension of voice communications to include the simultaneous telecommunication of data, text, and imagery in combined multimedia formats provides researchers with a radically new means of engaging in collaborative research and development with one another. Being able to simultaneously share and manipulate the same images and data on a given topic appearing on their computer screens, at any distance from one another, while at the same time being able to converse on that topic, promises more innovative, more efficient, and less time-consuming ways of conducting research and development. Whereas the speed of computers has risen exponentially over the past two decades, the capacity of telephone lines to carry the data that computers are capable of generating has not kept pace, albeit for very justifiable reasons associated with the traditional environment of the telephone industry. Consequently, governments around the world are fostering the development of very high speed transmission facilities and international telecommunications protocols, as exemplified by the Open Systems Interconnection (OSI) models, in order to exploit the social and economic benefits of multimedia networking in business, research, and education. CANARIE is a proposed, national, high-speed backbone network which, when fully implemented in a multimedia format, will enable engineers and research scientists in any field, and in laboratories anywhere in Canada, to collaborate with one another and with their international colleagues on research and development projects of common interest, without the inhibitions presently imposed by the lack of proximity to one another. It may be anticipated that this 'shortening of economic distance' among them will lead to an increase in research and development activity and improvements in their productivity. It will also tend to accelerate the diffusion of technology from the laboratories into marketable products, and serve as a model for improving performance, hence competitiveness, in every sector of the economy. Derived from text

N94-37337# Knowledge Exchange Technologies Ltd., Strassen (Luxembourg).
STANDARDS FOR DATA AND DOCUMENT INTERCHANGE
Geoffrey A. Stephenson *In* AGARD, International High Speed Networks for Scientific and Technical Information Feb. 1994 9 p (For primary document see N94-37333 12-82)
Copyright Avail: CASI HC A02/MF A02

In this paper I have tried to give an overview of the importance of standards for document interchange and an idea of where we are at present. There is a growing demand for documents in an electronic form to be interchanged between different platforms and software environments. Standards exist to enable most information to be interchanged in an application neutral way. The main barrier to such interchange is lack of awareness of the methods available and a lack of communication between users and vendors as to the priority of improving interchange. Users have to make their priorities clear to vendors if they are to be offered the facilities they require in the application packages they want to use.
Author

N94-37338*# National Aeronautics and Space Administration, Washington, DC.

THE VIRTUAL LIBRARY: COMING OF AGE

Judy F. Hunter and Gladys A. Cotter *In* AGARD, International High Speed Networks for Scientific and Technical Information Feb. 1994 6 p (For primary document see N94-37333 12-82)

Copyright Avail: CASI HC A02/MF A02

With the high speed networking capabilities, multiple media options, and massive amounts of information that exist in electronic format today, the concept of a 'virtual' library or 'library without walls' is becoming viable. In virtual library environment, the information processed goes beyond the traditional definition of documents to include the results of scientific and technical research and development (reports, software, data) recorded in any format or media: electronic, audio, video, or scanned images. Network access to information must include tools to help locate information sources and navigate the networks to connect to the sources, as well as methods to extract the relevant information. Graphical User Interfaces (GUI's) that are intuitive and navigational tools such as Intelligent Gateway Processors (IGP) will provide users with seamless and transparent use of high speed networks to access, organize, and manage information. Traditional libraries will become points of electronic access to information on multiple medias. The emphasis will be towards unique collections of information at each library rather than entire collections at every library. It is no longer a question of whether there is enough information available; it is more a question of how to manage the vast volumes of information. The future equation will involve being able to organize knowledge, manage information, and provide access at the point of origin. Author

N94-37339# Tsentralni Aerogidrodinamicheskii Inst., Moscow (USSR).

PROBLEMS OF INTERNATIONAL EXCHANGE OF SCIENTIFIC AND TECHNICAL INFORMATION FOR A RUSSIAN AEROSPACE RESEARCH INSTITUTE

Victor M. Tyurin *In* AGARD, International High Speed Networks for Scientific and Technical Information Feb. 1994 5 p (For primary document see N94-37333 12-82)

Copyright Avail: CASI HC A01/MF A02

The problems of international exchange of scientific and technical information for an aerospace research institute in Russia arise from this research area being classified; publications were strictly limited. This resulted in absence of specialized data bases; there is very little amount of information prepared properly for utilization in electronic networks. The other problem is underdevelopment of domestic networks for information exchange; there are not channels for connection with international networks. Changes in Russian policy and economics necessitate settling these problems for increasing efficiency of the organizations. There exists a plan to develop multibranch high-speed information-exchange networks, each having a coordination/control center connected with international networks. Author

N94-37340# Canada Inst. for Scientific and Technical Information, Ottawa (Ontario).

ELECTRONIC DOCUMENT DELIVERY: TOWARDS THE VIRTUAL LIBRARY

M. Brandreth and C. MacKeigan *In* AGARD, International High Speed Networks for Scientific and Technical Information Feb. 1994 4 p (For primary document see N94-37333 12-82)

Copyright Avail: CASI HC A01/MF A02

Reduced funding, global competition and technological change are forcing libraries and information centers to turn to new methods of providing services. Publishers of scientific and technical information expect printed journals to remain their primary product for several more years, despite the advent of electronic journals. Library collections will continue to be largely paper-based, but clients will demand much faster document delivery services from them. Many libraries must also maximize the investment in their collections by expanding their clientele. Electronic scanning of documents coupled with transmission over high speed, high capacity networks offers a potential solution to these problems. For more than a year, CISTI has been using proprietary imaging workstations to supply documents to one of its Branches. Much more flexibility is needed to reach the disparate receiving equipment used by a varied Canadian and international clientele. The paper describes experience with the Ariel Workstation, able to transmit to a variety of receivers including identical scanning workstations, other workstations, facsimile machines, and microcomputers with facsimile boards. Ability to rationalize library collections is seen as an important consequence. Author

N94-37341# Institute for Scientific and Technical Information, Vandoeuvre-les-Nancy (France).

PROVIDING ELECTRONIC DOCUMENTS IN EUROPE: EXPERIENCE OF INIST [LA FOURNITURE DE DOCUMENTS ELECTRONIQUES EN EUROPE: L'EXPERIENCE DE L'INIST]

Christian Lupovici *In* AGARD, International High Speed Networks for Scientific and Technical Information Feb. 1994 5 p In FRENCH (For primary document see N94-37333 12-82)

Copyright Avail: CASI HC A01/MF A02

The creation of the Institute for Scientific and Technical Information (INIST - Institut de l' Information Scientifique et Technique) in France in 1988, was the result of a decision from the Ministry on Research to develop a multidisciplinary department in charge of creating a data base in documentation center, for the diffusion of scientific and technical information, for French, European, and international researchers. The most modern technologies were adopted. For each step of acquisition of data, a specific technology was adapted and integrated in the general information system, from the time the documents were acquired to the creation of the data base and the production of primary documents: PASCAL for Science, Technology, and Medicine, FRANCIS for Social and Human Sciences. There are 5 steps in the INIST chain of production: management and classification of documents, using a GEAC 9000 system; analytical indexing of articles in periodicals and creation of abstracts (This work being done on computers and subcontracted to a private firm); numerical classification; storage of document on optical systems; and management of the system created to order and receive documents. The main technological challenges of the Hermes program are perfecting the thermal protection systems, developing fuel batteries, and designing the aerodynamics of the vehicle. This article presents what methods and means have been adopted to define the shapes which will satisfy the objectives of atmospheric travel. Author

N94-37342# Loughborough Univ. of Technology (England). HUSAT Research Inst.

ELECTRONIC JOURNALS

Cliff McKnight *In* AGARD, International High Speed Networks for Scientific and Technical Information Feb. 1994 6 p (For primary document see N94-37333 12-82)

Copyright Avail: CASI HC A02/MF A02

In 1981 a Royal Society study of the scientific information system in the UK described the electronic journal as 'perhaps the most radical innovation in prospect for the primary literature'. Twelve years and as many projects later, has the electronic journal gone any way towards realizing its potential? In order to answer this question, it is necessary to consider what the electronic journal has to offer. Or, to put it another way, what is wrong with the paper journal? The common criticisms of the paper journal are that they are often not on the shelf (mis-shelved, gone for binding, being used by someone else); they are hard to search through; they take up too much space; and there are too many of them to keep up with. In contrast, electronic journals are always there (assuming the network hasn't crashed); easy to search (but can flood you with hits unless you are careful in the way you conduct your search); and occupy much less space. In addition, various electronic 'filters' can be used to ensure that users receive notification of relevant journals - the 'selective dissemination of information' or SDI. These are the commonly attributed general advantages of electronic journals. However, they do not seem yet to have been sufficient to establish the electronic journal firmly in the scholarly communication chain. In order to see why this is the case, some of the electronic journal experiments are considered. Finally, suggestions are made regarding problems remaining to be tackled. Derived from text

N94-37343# Consejo Superior de Investigaciones Cientificas, Madrid (Spain). Centro Tecnico de Informatica.

BULLETIN BOARDS, ELECTRONIC MAIL, CONFERENCING, CURRENT USE BY SCIENTISTS AND ENGINEERS: EFFECTS ON LIBRARIES AND INFORMATION CENTRES: DO THEY HAVE A ROLE?

Victor Castelo *In* AGARD, International High Speed Networks for Scientific and Technical Information Feb. 1994 5 p (For primary document

see N94-37333 12-82)
Copyright Avail: CASI HC A01/MF A02

This paper introduces the present scenario of networking the different systems of exchanging information person to person, the way to access the information and to know where the information is. A summary of the more utilized applications is made, some of them have appeared in the last years as the result of a normal evolution: bulletin boards, Gopher, WAIS, World-Wide Web, e-mail, conferencing, directory service, etc. All these applications represent an added value to networking allowing the user (scientist, engineer, librarian, etc.) to communicate with others on their same area of interest. Additionally the user can obtain information about how to connect to servers and get items, programs, data, etc., and to follow conferences or make questions in a forum. As an example of an important application of distributed directory the Paradise project is discussed, it yields some tools in order to look for information on institutions, people and other objects. Taking all these considerations into account, it is intended to make an analysis about the current use of these tools by engineers and scientists. The role that the libraries and information centers should play in this context is also discussed. Author (revised)

N94-37344# CAE Electronics Ltd., Saint Laurent (Quebec).
TRAINING AND OPERATIONS SUPPORT SYSTEM (TOPS)
Guy Langlois and Ian Gordon *In* AGARD, International High Speed Networks for Scientific and Technical Information Feb. 1994 3 p (For primary document see N94-37333 12-82)
Copyright Avail: CASI HC A01/MF A02

This paper describes a potential training and operations support system and discusses the enabling technologies that make it possible - high speed global networks, powerful computers, and an object oriented data base management system (OODBMS). It illustrates a real world example of the system using a scenario involving an aircraft maintenance technician. Author

N94-37345# WAIS, Inc., Menlo Park, CA.
WIDE AREA INFORMATION SERVERS: AN EXECUTIVE INFORMATION SYSTEM FOR UNSTRUCTURED FILES
Brewster Kahle and Harry Morris *In* AGARD, International High Speed Networks for Scientific and Technical Information Feb. 1994 9 p (For primary document see N94-37333 12-82)
Copyright Avail: CASI HC A02/MF A02

In this paper we present a corporation information system for untrained users to search gigabytes of unformatted data using quasi-natural language and relevance feedback queries. The data can reside on distributed servers anywhere on a wide area network giving the users access to personal, corporate, and published information from a single interface. Effective queries can be turned into profiles, allowing the system to automatically alert the user when new data is available. The system was tested by twenty executive users located in 6 cities. Our primary goal in building the system was to determine if the technology and infrastructure existed to make end-user searching of unstructered information profitable. We found that effective search and user interface technologies for end-users are available, but network technologies are still a limiting cost factor. As a result of the experiment we are continuing the development of the system. This paper describes the overall system architecture, the implemented subset, and the lessons learned. Author

N94-37346# France Telecom North America, New York, NY.
INFORMATION RETRIEVAL SERVICES ON WIDE AREA NETWORKS: A VISION OF THE FUTURE
J. LeMezec *In* AGARD, International High Speed Networks for Scientific and Technical Information Feb. 1994 7 p (For primary document see N94-37333 12-82)
Copyright Avail: CASI HC A02/MF A02

This paper refers to some existing systems and to R&D work, especially in France Telecom, in order to help define a vision of future systems and services that store and retrieve information on wide area networks. Special reference is made to the Minitel network, a videotex network involving 6 million terminals and 20,000 services; JPEG 'Minitel Photo' and the first Fast Speed Teletel services were developed in 1992. Other services prepared for short-term experimentation, include multimedia videotex on ISDN. Two main contributions to a future broadband multimedia network are then discussed: standardization of multimedia and the deployment of ATM (Asynchronous Transfer Mode). Finally, a vision of a multi-purpose worldwide network of networks is proposed and the challenges posed by its construction are presented. Author (revised)

N94-37348# Pacific Northwest Lab., Richland, WA.
INTERACTIVE CALCULATOR FOR USE WITH MULTI-DIMENSIONAL netCDF FILES
D. W. Denbo (Pacific Northwest Lab., Sequim, WA.) Jan. 1994 4 p Presented at the 74th American Meteorological Society Annual Meeting, Nashville, TN, 23-28 Jan. 1994
(Contract DE-AC06-76RL-01830)
(DE94-007477; PNL-SA-23046; CONF-940115-27) Avail: CASI HC A01/MF A01

The interactive exploration of numerical results and observations has become increasingly difficult as the size of these data sets becomes larger. The scientist needs to be able to easily extract subsets of very large data sets and use these subsets in algebraic expressions to test hypotheses about the relationships between variables. The netCDF calculator (nccalc) satisfies many of these needs by providing several built-in functions and a framework that helps the scientist manipulate four dimensional data sets written using the netCDF data format. DOE

N94-37563# Sandia National Labs., Albuquerque, NM.
INTEGRATED ENGINEERING INFORMATION TECHNOLOGY, FY 1993 ACCOMPLISHMENTS
R. N. Harris, D. K. Miller, G. L. Neugebauer, J. R. Orona, R. A. Partridge, and J. D. Herman Mar. 1994 209 p
(Contract DE-AC04-94AL-85000)
(DE94-011406; SAND-93-3897) Avail: CASI HC A10/MF A03

The Integrated Engineering Information Technology (IEIT) project is providing a comprehensive, easy-to-use computer network solution for communicating with coworkers both inside and outside Sandia National Laboratories. IEIT capabilities include computer networking, electronic mail, mechanical design, and data management. These network-based tools have one fundamental purpose: to help create a concurrent engineering environment that will enable Sandia organizations to excel in today's increasingly competitive business environment. DOE

N94-37757# Loral Systems, Inc., Orlando, FL. Advanced Distributed Simulation Technology Program Office.
ADVANCED DISTRIBUTED SIMULATION TECHNOLOGY. SIMWORLD DATA BASE
Brett Butler, Tony Valle, and Jim Watson 18 Apr. 1994 41 p
(Contract N61339-91-D-0001)
(AD-A280262; ADST-94-W003283) Avail: CASI HC A03/MF A01

This document describes the status of a prototype implementation of the SIMWORLD Data Base (SWDB). The SIMWORLD Data Base is the major component of the Common Data Base (CDB), which is a key element of the BDS-D Architecture concept (Version 1.0). The document concerns the establishment of an ORACLE relational data base with an initial complement of DIS entities and assets structured in compliance with a proposed Common Data Base Standard. The development of the data base structure and evaluation of an interface to a DIS SAF simulator (ModSAF) are described. Recommendations for substantive modifications to the proposed CDB Standard are made. Aspects of the next incremental extension of the CDB concept toward supporting an exercise planning capability are also discussed. DTIC

83 ECONOMICS AND COST ANALYSIS

Includes cost effectiveness studies.

No abstracts in this category.

84 LAW, POLITICAL SCIENCE AND SPACE POLICY

Includes NASA appropriation hearings; aviation law; space law and policy; international law; international cooperation; and patent policy.

No abstracts in this category.

85 URBAN TECHNOLOGY AND TRANSPORTATION

Includes applications of space technology to urban problems; technology transfer; technology assessment; and surface and mass transportation.

For related information see also *03 Air Transportation and Safety, 16 Space Transportation,* and *44 Energy Production and Conversion.*

N94-37765*# National Aeronautics and Space Administration, Washington, DC.
NASA COMMERCIAL TECHNOLOGY. AGENDA FOR CHANGE
18 Jul. 1994 18 p
(NASA-TM-109898; NASA-CU-28159; NAS 1.15:109898) Avail: CASI HC A03/MF A01

The essence of NASA's new way of doing business to support the agency's commercial technology mission objectives is described. A summary description of the various changes needed to successfully perform this mission is provided. Derived from text

88 SPACE SCIENCES (GENERAL)

No abstracts in this category.

89 ASTRONOMY

Includes radio, gamma-ray, and infrared astronomy, and astrometry.

N94-36642*# E-Systems, Inc., Greenville, TX.
SOFIA: AIRCRAFT SYSTEM, AFT TELESCOPE CAVITY CONFIGURATION, PHASE 2. VOLUME 1: EXECUTIVE SUMMARY Final Report
Feb. 1994 6 p
(Contract NAS2-13599)
(NASA-CR-196362; NAS 1.26:196362; G5189.01.26-Vol-1) Avail: CASI HC A02/MF A01

This volume summarizes the tasks performed by E-Systems during Phase 2 of a study evaluating the structural modifications required to install the Stratospheric Observatory for Infrared Astronomy, SOFIA in the Boeing 747 airplane. An optimal structural modification concept for installation of the Infrared telescope is identified, and the concept is validated by analysis of the static and dynamic characteristics of the modified structure. Derived from text

N94-36688*# Smithsonian Astrophysical Observatory, Cambridge, MA.
THE BL LAC PHENOMENON: X-RAY OBSERVATIONS OF TRANSITION OBJECTS AND DETERMINATION OF THE X-RAY SPECTRUM OF A COMPLETE SAMPLE OF FLAT-SPECTRUM RADIO SOURCES Semiannual Report No. 4, 15 Aug. 1993 - 14 Feb. 1994
Diana M. Worrall Apr. 1994 45 p
(Grants NAG5-1724; NAG5-1882)
(NASA-CR-195951; NAS 1.26:195951) Avail: CASI HC A03/MF A01

This report summarizes the activities related to two ROSAT investigations: (1) x-ray properties of radio galaxies thought to contain BL Lac type nuclei; and (2) x-ray spectra of a complete sample of flat-spectrum radio sources. The following papers describing the research are provided as attachments: Multiple X-ray Emission Components in Low Power Radio Galaxies; New X-ray Results on Radio Galaxies; Analysis Techniques for a Multiwavelength Study of Radio Galaxies; Separation of X-ray Emission Components in Radio Galaxies; X-ray Emission in Powerful Radio Galaxies and Quasars; Extended and Compact X-ray Emission in Powerful Radio Galaxies; and X-ray Spectra of a Complete Sample of Extragalactic Core-dominated Radio Sources. CASI

N94-36690*# Arizona Univ., Tucson, AZ.
ULTRAVIOLET SPECTROPOLARIMETRY OF HIGH REDSHIFT QUASARS WITH THE HUBBLE SPACE TELESCOPE Final Report, 1 Jan. 1992 - 30 Sep. 1993
Chris D. Impey, Matthew A. Malkan, Wayne Webb, and C. E. Petry 1993 42 p
(Contract NAS5-26555)
(NASA-CR-196014; NAS 1.26:196014) Avail: CASI HC A03/MF A01

Ultraviolet spectropolarimetry of three bright high-redshift low polarization quasars (LPQ's) was obtained with the Faint Object Spectrograph of the Hubble Space Telescope. Two of the quasars, PG 1634+706 and PG 2302+029, had polarizations of rho is approximately equal to 0.5-1.0 percent throughout the ultraviolet, and showed no significant variation of polarization amplitude or position angle with wavelength. PG 2302+029 was also marginally (2.4 sigma) circularly polarized in the optical continuum. For the highest redshift quasar, PG 1222+228 (Ton 1530), the polarization was measured down to rest wavelengths below 800 A. Although the continuum of PG 1222+228 was weakened by Lyman limit absorption from an intergalactic gas cloud, the polarization increased sharply from 1 percent to about 4.5 percent, a change of 4 sigma significance. This abrupt rise in polarization does not appear attributable to any known instrumental artifact. These UV polarizations were only slightly less than those previously observed for these same objects in the optical. The polarization spectra were flat with a typical slope of the polarized flux pF(sub upsilon) varies as upsilon(exp -0.8 plus or minus 0.5). Unlike the polarization spectra of several high luminosity Seyfert 1 nuclei studied previously, such a flat wavelength dependence of polarization cannot be explained by scattering from dust grains. The hypotheses that the polarization in these quasars is produced by transmission through aligned interstellar grains (in the Milky Way or the host galaxy), or by a synchrotron power law component, also appear to be ruled out. These observed spectra are consistent with a wavelength-independent polarization proportional to the total nonstellar light or, possibly, to the contribution of the blue thermal component. Author

N94-36794*# Space Telescope Science Inst., Baltimore, MD.
HUBBLE SPACE TELESCOPE FAINT OBJECT SPECTROGRAPH INSTRUMENT HANDBOOK, VERSION 5.0
A. L. Kinney, ed. May 1994 86 p
(Contract NAS5-26555; RTOP 633-00-00)
(NASA-CR-189367; NAS 1.26:189367) Avail: CASI HC A05/MF A01

This version of the FOS Instrument Handbook is for the refurbished telescope, which is affected by an increase in throughput, especially for the smaller apertures, a decrease in efficiency due to the extra reflections of the COSTAR optics, and a change in focal length. The improved PSF affects all exposure time calculations due to better aperture throughputs and increases the spectral resolution. The extra reflections of COSTAR decrease the efficiency by 10-20 percent. The change in focal length affects the aperture sizes as projected on the sky. The aperture designations that are already in use both in the exposure logsheets and in the project data base (PDB) have not been changed. Apertures are referred to here by their size, followed by the designation used on the exposure logsheet. Author (revised)

N94-36795*# Space Telescope Science Inst., Baltimore, MD.
HUBBLE SPACE TELESCOPE FAINT OBJECT CAMERA INSTRUMENT HANDBOOK (POST-COSTAR), VERSION 5.0
A. Nota, ed., R. Jedrzejewski, ed., P. Greenfield, ed., and W. Hack, ed.

May 1994 104 p
(Contract NAS5-26555; RTOP 633-00-00)
(NASA-CR-189365; NAS 1.26:189365) Avail: CASI HC A06/MF A02

The faint object camera (FOC) is a long-focal-ratio, photon-counting device capable of taking high-resolution two-dimensional images of the sky up to 14 by 14 arc seconds squared in size with pixel dimensions as small as 0.014 by 0.014 arc seconds squared in the 1150 to 6500 A wavelength range. Its performance approaches that of an ideal imaging system at low light levels. The FOC is the only instrument on board the Hubble Space Telescope (HST) to fully use the spatial resolution capabilities of the optical telescope assembly (OTA) and is one of the European Space Agency's contributions to the HST program. Derived from text

N94-36918*# Space Telescope Science Inst., Baltimore, MD.
HUBBLE SPACE TELESCOPE WIDE FIELD AND PLANETARY CAMERA 2 INSTRUMENT HANDBOOK, VERSION 2.0
C. J. Burrows, ed. May 1994 93 p
(Contract NAS5-26555; RTOP 633-00-00)
(NASA-CR-189368; NAS 1.26:189368) Avail: CASI HC A05/MF A01

This document provides the capabilities of the Wide Field and Planetary Camera 2 Instrument. Author

N94-36963*# Space Telescope Science Inst., Baltimore, MD.
HUBBLE SPACE TELESCOPE CYCLE 5. PHASE 1: PROPOSAL INSTRUCTIONS, VERSION 4.0
Piero Madau, ed. Jun. 1994 101 p
(Contract NAS5-26555; RTOP 633-00-00)
(NASA-CR-189364; NAS 1.26:189364) Avail: CASI HC A06/MF A02

This document has the following purposes: it describes the information that must be submitted to the Space Telescope Science Institute by Phase 1 proposers, both electronically and on paper, and describes how to submit it; it describes how to fill out the proposal LATEX templates; it describes how to estimate the number of spacecraft orbits that the proposed observations will require; it provides detailed information about the parameters that are used in the forms to describe the requested observations; and it provides information about the preparation and electronic submission of proposal files. Examples of completed proposal forms are included. Author (revised)

N94-37037*# California Univ., La Jolla, CA.
GUARANTEED TIME OBSERVATIONS SUPPORT FOR FAINT OBJECT SPECTROGRAPH (FOS) ON HST Technical Progress Report, 1 Nov. 1993 - 30 Apr. 1994
Richard Harms 1994 105 p
(Grant NAG5-1630)
(NASA-CR-196305; NAS 1.26:196305) Copyright Avail: CASI HC A06/MF A02

The goals of the GTO effort are for investigations defined in previous years by the IDT to be carried out as HST observations and for the results to be communicated to the scientific community and to the public. The search for possible black holes in the nuclei of both normal and active nucleus galaxies has had to be delayed to the post-servicing era. FOS spectropolarimetric observations of the nuclear region of the peculiar Seyfert galaxy Mrk 231 reveal that the continuum polarization peaks at 18% in the near UV and then declines rapidly toward shorter wavelengths. The papers on the absorption line analysis for our galactic halo address the spatial distribution of high and intermediate level ions in the halo and illustrate the patchy and heterogeneous nature of the halo. The papers on the scattering characteristics of the HST/FOS have provided us with data that shows that the HST mirror surfaces are quite smooth, even at the UV wavelengths. WF-PC and FOC images of the halo PN K648 have been fully analyzed. CASI

N94-37555# Fermi National Accelerator Lab., Batavia, IL.
THE DISTRIBUTED DEVELOPMENT ENVIRONMENT FOR SDSS SOFTWARE
E. Berman, V. Gurbani, B. Mackinnon, H. Newberg, D. Petravick, R. Pordes, G. Sergey, C. Stoughton, R. Lupton, and T. Nicinski Apr. 1994 6 p Presented at the Meeting on Computing in High-Energy Physics, San Francisco, CA, 21-27 Apr. 1994
(Contract DE-AC02-76CH-03000)
(DE94-013238; FNAL/C-94/093; CONF-940492-2) Avail: CASI HC A02/MF A01

The authors present an integrated science software development environment, code maintenance and support system for the Sloan Digital Sky Survey (SDSS) now being actively used throughout the collaboration. DOE

N94-37667# Fermi National Accelerator Lab., Batavia, IL.
SLOAN DIGITAL SKY SURVEY
S. M. Kent, C. Stoughton, H. Newberg, J. Loveday, D. Petravick, V. Gurbani, E. Berman, G. Sergey, and R. Lupton Apr. 1994 10 p Presented at the 3rd Annual Conference on Astronomical Data Analysius Software and Systems, Victoria, Ontario, 13-15 Oct. 1993
(Contract DE-AC02-76CH-03000)
(DE94-011749; FNAL/C-94/084; CONF-9310239-2) Avail: CASI HC A02/MF A01

The Sloan Digital Sky Survey will produce a detailed digital photometric map of half the northern sky to about 23 magnitude using a special purpose wide field 2.5 meter telescope. From this map we will select approximately 10(sup 6) galaxies and 10(sup 5) quasars, and obtain high resolution spectra using the same telescope. The imaging catalog will contain 10(sup 8) galaxies, a similar number of stars, and 10(sup 6) quasar candidates. DOE

N94-37702*# Alabama Univ., Huntsville, AL. Dept. of Physics.
GAMMA RAY ASTRONOMY Final Report, 27 Jul. 1993 - 27 Mar. 1994
William S. Paciesas Mar. 1994 43 p
(Contract NAS8-38609)
(NASA-CR-193970; NAS 1.26:193970) Avail: CASI HC A03/MF A01

The Burst and Transient Source Experiment (BATSE) is one of four instruments on the Compton observatory which was launched by the space shuttle Atlantis on April 5, 1991. As of mid-March, 1994, BATSE detected more than 925 cosmic gamma-ray bursts and more than 725 solar flares. Pulsed gamma rays have been detected from at least 16 sources and emission from at least 28 sources (including most of the pulsed sources) has been detected by the earth occultation technique. UAH participation in BATSE is extensive but can be divided into two main areas, operations and data analysis. The daily BATSE operations tasks represent a substantial level of effort and involve a large team composed of MSFC personnel as well as contractors such as UAH. The scientific data reduction and analysis of BATSE data is also a substantial level of effort in which UAH personnel have made significant contributions. Derived from text

N94-37825*# Texas Univ., Austin, TX. Dept. of Astronomy.
FAR-INFRARED EMISSION LINE SPECTROSCOPY OF PLANETARY NEBULAE FROM THE KAO Final Technical Report, 1 Oct. 1985 - 30 Sep. 1993
Harriet L. Dinerstein 15 Jul. 1994 7 p
(Grant NAG2-372)
(NASA-CR-196289; NAS 1.26:196289) Avail: CASI HC A02/MF A01

The main focus of the overall project was to study the properties of planetary nebulae using far-infrared emission lines. The observations were conducted with the 'cooled grating spectrometer' or CGS, a moderate-resolution echelle spectrometer designed and built at the Ames Research Center. During the first few years of the program, the emphasis was on emission lines of doubly-ionized oxygen and nitrogen ((O III) 52 and 88 microns, (N III) 57 microns), which arise in the ionized regions of the nebulae. Starting around 1989, our emphasis shifted to observing fine-structure lines of neutral oxygen and singly-ionized carbon ((O I) 63 and 145 microns, (C II) 157 microns), which arise from predominantly neutral material outside the ionized regions. This program was typically assigned one or two observing flights per year. Because these studies required obtaining a substantial sample of objects in order to reach meaningful conclusions, publication of comprehensive papers summarizing all of the results is still pending. However, numerous interim reports based on the airborne results as well as on closely-related supporting observations have been published during the grant period. The bibliographic information for these reports is given in the publications section. An overall summary of the planetary nebula results was presented at the Airborne Astronomy Symposium (20th Anniversary of the KAO) on 8 July 1994; reprints will be provided when available. In parallel with the planetary nebula study, we

also observed the (O III) and (N III) lines in several H II regions, and attempted (unsuccessfully) to detect these lines in several old nova remnants and the supernova remnant Cassiopeia A. Derived from text

N94-37834# Helsinki Univ. of Technology, Kylmaelae (Finland). Metsaehovi Radio Research Station.
CORRELATED RADIO AND OPTICAL VARIATIONS IN A SAMPLE OF AGN. A SIMULTANEOUS RADIO-OPTICAL FLARE IN BL LACERTAE
M. Tornikoski, E. Valtaoja, H. Teraesranta, A. G. Smith, and A. D. Nair 1993 33 p
(PB94-179181) Avail: CASI HC A03/MF A01

The document contains 2 papers. In the first paper, the authors have studied flux variations in the optical and at radio wavelengths of a sample of extragalactic sources. Even though similar analyses have been done earlier, this is the first extensive study of connections between long-term optical and high radio frequency (from 22 GHz up to 230 GHz) variability in a large sample (22 sources) of AGN. In 10 out of the 22 sources, the authors found a clear radio-optical correlation, and in as many as 6 sources the optical and high frequency radio variability was simultaneous. In the second paper, an outburst of BL Lacertae was observed in the optical and at 22 and 37 GHz. The flare peaked at all frequencies within one week. Previous correlation analyses have demonstrated that radio variations in BL Lacertae are time delayed by as much as a few years. It is suggested that this, the first clear case of a truly simultaneous radio-optical flare, indicates the existence of at least two kinds of optical events. NTIS

90 ASTROPHYSICS

Includes cosmology; celestial mechanics; space plasmas; and interstellar and interplanetary gases and dust.

For related information see also *75 Plasma Physics*.

N94-36759# Argonne National Lab., IL. Chemical Technology Div.
A POSSIBLE ORIGIN OF EL6 CHONDRITES FROM A HIGH TEMPERATURE-HIGH PRESSURE SOLAR GAS
M. Blander, L. Unger, A. Pelton, and G. Eriksson 1994 13 p
(Contract W-31-109-eng-38)
(DE94-010467; ANL/CMT/PP-73161) Avail: CASI HC A03/MF A01

Condensates from a gas of 'solar' composition were calculated to investigate the origins of EL6 chondrites using a free energy minimization program with a data base for the thermodynamic properties of multicomponent molten silicates as well as for other liquid soliids, solid solutions and gaseous species. Because of high volatility of silicon and silica, the high silicon content of metal (2.6 mole percent) can only be produced at pressures 10(exp -2) atm at temperatures above 1475 K. At 100-500 atm, a liquid silicate phase crystallizes at a temperature where the silicon content of the metal, ferrosilite content of the enstatite and albite concentration in the plagioclase are close to measured values. In pyrometallurgy, liquid silicates are catalysts for reactions in which Si-O-Si bridging bonds are broken or formed. Thus, one attractive mode for freezing in the compositions of these three phases is disappearance of fluxing liquid. If the plagioclase can continue to react with the nebula without a liquid phase, lower pressures of 10(exp -1) to 1 atm might be possible. Even if the nebula is more reducing than a solar gas, the measured properties of EL6 chondrites might be reconciled with only slightly lower pressures (less than 3 times lower). The temperatures would be about the same as indicated in our calculations since the product of the silicon content of the metal and the square of the ferrosilite content of the enstatite constitute a cosmothermometer for the mineral assemblage in EL6 chondrites. DOE

N94-37004*# Tennessee Univ., Knoxville, TN. Dept. of Geological Sciences.
LIGHT STABLE ISOTOPE ANALYSIS OF METEORITES BY ION MICROPROBE Final Report, 1 Feb. 1992 - 31 Jul. 1994
Harry Y. McSween, Jr. 7 Jul. 1994 19 p
(Contract NAGw-2800; DE-AC05-85OR-21400)
(NASA-CR-196096; NAS 1.26:196096) Avail: CASI HC A03/MF A01

The main goal was to develop the necessary secondary ion mass spectrometer (SIMS) techniques to use a Cameca ims-4f ion microprobe to measure light stable isotope ratios (H, C, O and S) in situ and in non-conducting mineral phases. The intended application of these techniques was the analysis of meteorite samples, although the techniques that have been developed are equally applicable to the investigation of terrestrial samples. The first year established techniques for the analysis of O isotope ratios (delta O-18 and delta O-17) in conducting mineral phases and the measurement of S isotope ratios (delta S-34) in a variety of sulphide phases. In addition, a technique was developed to measure delta S-34 values in sulphates, which are insulators. Other research undertaken in the first year resulted in SIMS techniques for the measurement of wide variety of trace elements in carbonate minerals, with the aim of understanding the nature of alteration fluids in carbonaceous chondrites. In the second year we developed techniques for analyzing O isotope ratios in nonconducting mineral phases. These methods are potentially applicable to the measurement of other light stable isotopes such as H, C and S in insulators. Also, we have further explored the analytical techniques used for the analysis of S isotopes in sulphides by analyzing troilite in a number of L and H ordinary chondrites. This was done to see if there was any systematic differences with petrological type. Author

N94-37049# California Univ., Berkeley. Lawrence Berkeley Lab, CA.
ABSOLUTE LIMIT ON ROTATION OF GRAVITATIONALLY BOUND STARS
N. K. Glendenning Mar. 1994 7 p Presented at the Aspen Winter Conference on Astrophysics: Millisecond Pulsars, a Decade of Surprises, Aspen, CO, 3-7 Jan. 1994
(Contract DE-AC03-76SF-00098)
(DE94-011367; LBL-35277; CONF-940182-1) Avail: CASI HC A02/MF A01

The authors seek an absolute limit on the rotational period for a neutron star as a function of its mass, based on the minimal constraints imposed by Einstein's theory of relativity, Le Chatelier's principle, causality, and a low-density equation of state, uncertainties which can be evaluated as to their effect on the result. This establishes a limiting curve in the mass-period plane below which no pulsar that is a neutron star can lie. For example, the minimum possible Kepler period, which is an absolute limit on rotation below which mass-shedding would occur, is 0.33 ms for a M = 1.442 solar mass neutron star (the mass of PSR1913+16). If the limit were found to be broken by any pulsar, it would signal that the confined hadronic phase of ordinary nucleons and nuclei is only metastable. DOE

N94-37164# Lawrence Livermore National Lab., Livermore, CA.
THE WINDS OF CATACLYSMIC VARIABLES
C. W. Mauche and J. C. Raymond 16 Feb. 1994 21 p Presented at the Cosmic Winds and the Heliosphere Conference, Tucson, AZ, 18-22 Oct. 1993
(Contract W-7405-eng-48)
(DE94-010897; UCRL-JC-116941; CONF-9310316-1) Avail: CASI HC A03/MF A01

The authors present an observational and theoretical review of the winds of cataclysmic variables (CV's). Specifically, they consider the related problems of the geometry and mass-loss rate of the winds of CV's, their ionization state and variability, and the results from studies of eclipsing CV's. Finally, they consider the properties of accretion disk wind models. Some of these models predict substantial angular momentum loss, which could affect both disk structure and binary evolution. DOE

N94-37557 California Univ., Berkeley. Lawrence Berkeley Lab, CA.
THE MESOZOIC ERA OF RELATIVISTIC HEAVY ION PHYSICS AND BEYOND
J. W. Harris Mar. 1994 13 p Presented at the NATO Advanced Study Institute on Hot and Dense Nuclear Matter, Bodrum, Turkey, 26 Sep. - 9 Oct. 1993 Limited Reproducibility: More than 20% of this document may be affected by microfiche quality
(Contract DE-AC03-76SF-00098)
(DE94-011341; LBL-35330; CONF-930999-10) Avail: CASI HC A03

In order to understand how matter 15 billion years ago in the form of quarks, gluons and leptons at a temperature of 2 x 10(exp 12) degrees K evolved to become today's Universe, the goal of relativistic and ultra-relativistic heavy ion physics is to understand the equation of state of nuclear, hadronic and partonic matter. This quest is of cross-disciplinary interest. The phase transition from partonic matter to hadronic matter tens of micro-seconds after the beginning of the universe is of interest to

cosmology. Fluctuations during this phase transition would influence nucleosynthesis and the understanding of baryonic inhomogeneities in the universe. The nuclear matter equation of state, which describes the incompressibility of nuclear matter, governs neutron star stability. It determines the possible existence of strange quark matter stars and the dynamics of supernova expansion in astrophysics. The existence of collective nuclear phenomena in nuclear physics is also determined by the nuclear equation of state. In relativistic heavy ion collisions collective nuclear flow has been observed and is being studied extensively to obtain a better understanding of the incompressibility of nuclear matter. In high energy nuclear and particle physics, production and excitations of hadronic final states have been studied in detail and are important to an overall understanding of the equation of state of nuclear matter at finite temperature. The possibility in ultra-relativistic heavy ion collisions to create and study highly excited hadronic and partonic degrees of freedom provides a unique opportunity for understanding the behavior of nuclear, hadronic and partonic matter. Study of the QCD vacuum, of particular interest in particle physics, would provide a better understanding of symmetry-breaking mechanisms and the origins of the masses of the various quarks and particles. DOE

91 LUNAR AND PLANETARY EXPLORATION

Includes planetology; and manned and unmanned flights.

For spacecraft design or space stations see *18 Spacecraft Design, Testing and Performance.*

N94-36961*# Pennsylvania State Univ., Erie, PA. Div. of Science.
INFRARED SPECTROSCOPY OF JUPITER AND SATURN Final Technical Report
Roger F. Knacke 1993 17 p
(Grant NAGw-2796)
(NASA-CR-196294; NAS 1.26:196294) Copyright Avail: CASI HC A03/MF A01

Infrared spectroscopy provides unique insights into the chemistry and dynamics of the atmospheres of Jupiter, Saturn, and Titan. In 1991 we obtained data at J, H, K, and M and made repeated observations of Titan's albedo as the satellite orbited Saturn. The J albedo is 12% +/- 3% greater than the albedo measured in 1979; the H and K albedos are the same. There was no evidence for variations at any wavelength over the eastern half of Titan's orbit. We also obtained low resolution (R=50) spectra of Titan between 3.1 and 5.1 microns. The spectra contain evidence for CO and CH3D absorptions. Spectra of Callisto and Ganymede in the 4.5 micron spectral region are featureless and give albedos of 0.08 and 0.04 respectively. If Titan's atmosphere is transparent near 5 microns, its surface albedo there is similar to Callisto's. In 1992 and 1993 we obtained further spectroscopic data of Titan with the UKIRT CGS4 spectrometer. We discovered two unexpected and unexplained spectral features in the 3-4 micron spectrum of Titan. An apparent emission feature near the 3 micron (nu sub 3) band of methane indicated temperatures higher than known to be present in Titan's upper stratosphere and may be caused by unexpected non-LTE emission. An absorption feature near 3.47 microns may be caused by absorption in solid grains or aerosols in Titan's clouds. The feature is similar but not identical to organics in the interstellar matter and in comets. Derived from text

92 SOLAR PHYSICS

Includes solar activity, solar flares, solar radiation and sunspots.

For related information see *93 Space Radiation.*

N94-36469*# Alabama Univ., Huntsville, AL. Dept. of Mechanical and Aerospace Engineering.
A STUDY OF PHYSICAL MECHANISMS FOR FILAMENT ERUPTION AND CORONAL MASS EJECTION VIA NUMERICAL SIMULATION Final Report, 1 Oct. 1979 - 31 Mar. 1994
S. T. Wu Jun. 1994 246 p
(Grant NAGw-9)
(NASA-CR-196087; NAS 1.26:196087) Copyright Avail: CASI HC A11/MF A03

Papers covering the following topics are presented: flare physics; coronal dynamics; interplanetary dynamics; and numerical methods. CASI

N94-37012*# California Univ., Los Angeles, CA.
AN INVESTIGATION OF SOLAR WIND EFFECTS ON THE EVOLUTION OF THE MARTIAN ATMOSPHERE Final Report, 1 Dec. 1990 - 31 May 1994
Janet G. Luhmann 1994 4 p
(Grant NAGw-2295)
(NASA-CR-193424; NAS 1.26:193424) Avail: CASI HC A01/MF A01

This investigation concentrated on the question of how atmosphere escape, related to both photochemistry and the Mars solar wind interaction, may have affected the evolution of Mars' atmosphere over time. The principal investigator and postdoctoral researcher adopted the premise that contemporary escape processes have dominated the losses to space over the past 3.5 billion years, but that the associated loss rates have been modified by solar evolution. A model was constructed for the contemporary escape scenario based on knowledge gained from both Venus in-situ measurements from Pioneer Venus Orbiter and Mars measurements from Phobos-2. Venus provided a valuable second example of a weakly magnetized planet having a similar solar wind interaction where we have more knowledge from observations. The model included photochemical losses from recombining ionospheric molecular ions, scavenging Martian upper atmosphere ('pickup') ions by the solar wind, and sputtering of the atmosphere by reentering pickup ions. The existence of the latter mechanism was realized during the course of the supported investigation, and is now thought by Jakosky and Pepin to explain some of the Martian noble gas isotope ratios. Derived from text

N94-37668# Los Alamos National Lab., NM.
RANDOM AND PERIODIC SUBSTORMS AND THEIR ORIGINS IN THE SOLAR WIND
J. E. Borovsky, R. D. Belian, R. J. Nemzek, and C. W. Smith 1994 7 p
Presented at the Substorms, Fairbanks, AK, 7-11 Mar. 1994
(Contract W-7405-eng-36)
(DE94-011693; LA-UR-94-1379; CONF-9403115-2) Avail: CASI HC A02/MF A01

Substorms occur (recur) in two fashions: periodically with time or randomly in time. A statistical analysis of the time intervals (Delta)t between subsequent substorm onsets clearly shows these two types of substorms. When substorms are recurring periodically, the period is 3.1 plus/minus 1.2 hours, and the distribution of periods is gaussian. When substorms are occurring randomly, the time intervals (Delta)t between successive substorm onsets are distributed according to the exponential distribution exp(-(Delta)t//5 hours), with a 5-hour mean interval between random onsets. With the use of the Los Alamos geosynchronous energetic-particle dam and the OMNI solar-wind data, it is shown that periodic substorms are associated with time intervals when the average value of the IMF is southward for extended periods of time and it is shown that randomly occurring substorms are statistically correlated with randomly occurring northward-to-southward reversals of the 1-hour-averaged values of the IMF B(sub z). DOE

93 SPACE RADIATION

Includes cosmic radiation; and inner and outer earth's radiation belts.

For biological effects of radiation see *52 Aerospace Medicine.* For theory see *73 Nuclear and High-Energy Physics.*

N94-36689*# Wisconsin Univ., Madison, WI. Space Science and Engineering Center.
SCIENTIFIC AND TECHNICAL SUPPORT FOR THE GALILEO NET FLUX RADIOMETER EXPERIMENT Final Report, 1 Jan. 1990 - 30 Nov. 1993
Lawrence A. Sromovsky 8 Jun. 1994 21 p
(Contract NCC2-679)
(NASA-CR-196009; NAS 1.26:196009) Avail: CASI HC A03/MF A01

This report describes work supported by a post-launch grant (NCC 2-679) that originally covered the period from 1 January 1990 through 31 December 1992. This was extended an additional nine months at no cost until 30 September 1993, and once more until to 30 November 93. A final

report on the effort from 1 January 1990 through 30 November 1993 (anticipated) is provided following the background discussion. Tasks required during the post launch period are briefly as follows: (1) attend PSG (Project Science Group) meetings; (2) support in-flight checkouts; maintain and keep safe the spare instrument and GSE (Ground Support Equipment); (3) organize and maintain documentation; (4) finish calibration measurements, documentation, and analysis; (5) characterize and diagnose instrument anomalies; (6) develop descent data analysis tools; and (7) science data analysis and publication. The following sections provide background information on the NFR instrument followed by the complete progress report. CASI

N94-36921*# National Academy of Sciences - National Research Council, Washington, DC. Board on Physics and Astronomy.
COSMIC RAYS: PHYSICS AND ASTROPHYSICS. A RESEARCH BRIEFING
1994 23 p
(Grant NAGw-3557)
(NASA-CR-196118; NAS 1.26:196118) Avail: CASI HC A03/MF A01

Some recent results in cosmic-ray physics are summarized, and how they raise new questions of interest for both physics and astrophysics is described. An important technical advance, the recently demonstrated capability of long-duration balloon flights of heavy payloads, will offer a great advantage for achieving some of these goals. Derived from text

N94-37251*# Iowa Univ., Iowa City, IA. Dept. of Physics and Astronomy
PLASMA AND RADIO WAVES FROM NEPTUNE: SOURCE MECHAMISMS AND PROPAGATION Final Report, 15 Jul. 1992 - 14 Jul. 1994
J. Douglas Menietti 15 Jul. 1994 5 p
(Grant NAGw-3143)
(NASA-CR-196284; NAS 1.26:196284) Avail: CASI HC A01/MF A01

The purpose of this project was to conduct a comprehensive investigation of the radio wave emission observed by the planetary radio astronomy (PRA) instrument on board Voyager 2 as it flew by Neptune. The study has included data analysis, theoretical and numerical calculations, and ray tracing to determine the possible source mechanisms and locations of the radiation, including the narrowband bursty and smooth components of the Neptune radio emission. Derived from text

N94-37293# Los Alamos National Lab., NM.
A HIGH PRECISION GAMMA RAY SPECTROMETER FOR THE MARS 1994 MISSION
I. G. Mitrofanov (Academy of Sciences, USSR, Moscow, USSR.), D. S. Anfimov (Academy of Sciences, USSR, Moscow, USSR.), and A. M. Chernenko (Academy of Sciences, USSR, Moscow, USSR.) 1994 9 p Presented at the Low Cost Planetary Missions Meeting, Laurel, MD, 12-15 Apr. 1994
(Contract W-7405-eng-36)
(DE94-013133; LA-UR-94-1862; CONF-9404169-1) Avail: CASI HC A02/MF A01

The high precision gamma-ray spectrometer (PGS) is scheduled to be launched on the Mars-94 mission in October 1994, and to go into an elliptical polar orbit around Mars. The PGS consists of two high-purity germanium (Ge) detectors, associated electronics, and a passive cooler and will be mounted on one of the solar panels. The PGS will measure nuclear gamma-ray emissions from the martian surface, cosmic gamma-ray bursts, and the high-energy component of solar flares in the broad energy range from 50 KeV to 8 MeV using 4096 energy channels. DOE

99 GENERAL

N94-36975 Research and Development Labs., Culver City, CA.
UNITED STATES AIR FORCE SUMMER RESEARCH PROGRAM, 1993. VOLUME 7: ARMSTRONG LABORATORY Final Report
Dec. 1993 521 p Limited Reproducibility: More than 20% of this document may be affected by microfiche quality
(AD-A278655) Avail: Issuing Activity (Defense Technical Information Center (DTIC))

The topics covered include the following: (1) detection of Ureaplasma urealyticum in clinical samples by polymerase chain reaction DNA amplification; and (2) determination of the sequency of the amplicon of Ureaplasma diversum generated by polymerase chain reaction with universla bacterial 16s rRNA primers. DTIC

N94-36976 Research and Development Labs., Culver City, CA.
UNITED STATES AIR FORCE SUMMER RESEARCH PROGRAM, 1993. VOLUME 14: ROME LABORATORY Final Report
Dec. 1993 167 p Limited Reproducibility: More than 20% of this document may be affected by microfiche quality
(AD-A278656) Avail: Issuing Activity (Defense Technical Information Center (DTIC))

Topics covered include the following: Rome Labs video bulletin board; object-oriented parallel programming in DERIC; object-oriented systems; radar noise elimination utilizing neural networks; multimedia; study of C programming; infrared measurements of electromagnetic fields; triangulation using FM stations; a study of array antennas and neural networks for future applications in direction finding; the effects of wet and dry silicon dioxide passivation etchants on aluminum metallizations for integrated circuits; how to establish and configure a local area network; computer simulation of radio receivers; noise reduction improvement testing -- comparing old and new INTEL; validating the FPASP4 software development environment; and real time 12 bit analog to digital computer interface. DTIC

N94-36977 Research and Development Labs., Culver City, CA.
UNITED STATES AIR FORCE SUMMER RESEARCH PROGRAM, 1993. VOLUME 13: PHILLIPS LABORATORY Final Report
Dec. 1993 193 p Limited Reproducibility: More than 20% of this document may be affected by microfiche quality
(AD-A278657) Avail: Issuing Activity (Defense Technical Information Center (DTIC))

The topics covered include the following: the presence of sulfuric acid in the stratosphere and its effect on high altitude aircraft; the auroras and the defense meteorological satellite program; a study of ionosphere; a verification of the NGM- and LFM-MOS forcasting models' cloud amounts forecasts; hyperspectral imaging -- field experiments; general optics; experiments in the nonlinear optics branch of the Phillips Laboratory; emission spectroscopy of a 30 kW ammonia arcjet run at 16 kW; computer aided design of 21st century HEDM materials; reduction and analysis of extended x-ray absorption fine structure (EXAFS) data; development and testing of liquid crystal polymer solid rocket motors; Sun Microsystems computer workstations; data organization and analysis using Microsoft EXEL and Word; and database processing and secondary electrons. DTIC

N94-36978 Research and Development Labs., Culver City, CA.
UNITED STATES AIR FORCE SUMMER RESEARCH PROGRAM, 1993. VOLUME 16: ARNOLD ENGINEERING DEVELOPMENT CENTER, FRANK J. SEILER RESEARCH LABORATORY AND WILFORD HALL MEDICAL CENTER Final Report
Dec. 1993 149 p Limited Reproducibility: More than 20% of this document may be affected by microfiche quality
(AD-A278658) Avail: Issuing Activity (Defense Technical Information Center (DTIC))

Papers on the following topics are presented: the possible time reduction of CFD solutions resulting from grid sequencing; the modification of a facility display and recording system; J6 large rocket test facility -- steam system math model validation; store-separation graphical analysis package (SGAP); balance checkout procdure program for pitch, roll, and yaw; infrared borescope evaluation; bilinear second-order recursive notch filters; the angular rotation matrix expansion table calculator; tool kit program; and comparison of atomic absorption and ICP atomic emission spectrometers. CASI

N94-36979 Research and Development Labs., Culver City, CA.
UNITED STATES AIR FORCE SUMMER RESEARCH PROGRAM, 1993. VOLUME 3: PHILLIPS LABORATORY Final Report
1993 702 p Limited Reproducibility: More than 20% of this document

may be affected by microfiche quality
(AD-A278694) Avail: Issuing Activity (Defense Technical Information Center (DTIC))

Papers on the following topics are presented: ion-molecule reactions at high temperatures; optical and atmospheric turbulence; generation of ELF and VLF waves in the HF heater-modulated polar electrojet by two heater-modulation schemes; inc.dence rate estimate of elevated pediatric blood lead at two air force bases; large-scale coronal magnetic fields -- noise storms, soft x-rays and inversion of radio polarization; the effects of anisoplanatism on shear coherent interferometric photography; large stable second-harmonic coefficients in corona-poled polymeric thin films; lidar and atmospheric monitoring; mode beating in iodine lasers; estimation of the squared modulus of the complex coherence factor from amplitude or intensity measurements at high light levels; phase retrieval via sensor fusion in interferometric aperture synthesis; the impact of condensing water vapor in chemical oxygen iodine lasers; specimen size effects on fracture parameters for solid propellant materials; computer-aided polymer and high-energy density material design; synthesis of polymers for gelation of liquid salt systems; spray measurements using microwave beam; research in emerging technologies at Phillips Laboratory; a preliminary investigation into the nature of the graded propellant/insulation interface in solid rocket motors; conceptual design study of a solar concentrator/support structure -- a 3-D finite element model; on the maximization of the simi-major axis a of a maneuverable satellite moving initially in a circular orbit above the earth; nonlinear bending vibration of flexible sounding rockets -- an opportunity for nonlinear identification; analysis of a detector test station and the performance of a visible light photon counter; calibration techniques for Bremsstrahlung x-ray sources with end-point energies of 60-160 KEv; system support for the SPPD parallel system architecture; a feasibility study of a 70-K periodic sorption cryocooler and thermal management of sodium sulfur battery module; spin evolution of the LAGEOS satellite; preliminary design of a dual source for simulating the AM0 spectrum; and design of an active vibration control system for isolation of an optical bench. CASI

N94-36980 Research and Development Labs., Culver City, CA.
UNITED STATES AIR FORCE SUMMER RESEARCH PROGRAM, 1993. VOLUME 4: ROME LABORATORY Final Report
Dec. 1993 428 p Limited Reproducibility: More than 20% of this document may be affected by microfiche quality
(AD-A278695) Avail: Issuing Activity (Defense Technical Information Center (DTIC))

Research projects are presented that cover the following topics: computer networks; computerized simulation; distributed data processing; input/output models; knowledge based systems; file transfer protocol; object-oriented data bases; and internetted data bases. CASI

N94-36981 Research and Development Labs., Culver City, CA.
UNITED STATES AIR FORCE SUMMER RESEARCH PROGRAM, 1993. VOLUME 5A: WRIGHT LABORATORY Final Report
Dec. 1993 615 p Limited Reproducibility: More than 20% of this document may be affected by microfiche quality
(AD-A278696) Avail: Issuing Activity (Defense Technical Information Center (DTIC))

Research projects covering the following topics are presented: molecular structure; molecular vibration; thermal expansion; elastic properties; probability distribution functions; and computer aided diagnosis. CASI

N94-36982 Research and Development Labs., Culver City, CA.
UNITED STATES AIR FORCE SUMMER RESEARCH PROGRAM, 1993. VOLUME 6: ARNOLD ENGINEERING DEVELOPMENT CENTER, FRANK J. SEILER RESEARCH LABORATORY AND WILFORD HALL MEDICAL CENTER Final Report
Dec. 1993 179 p Limited Reproducibility: More than 20% of this document may be affected by microfiche quality
(AD-A278697) Avail: Issuing Activity (Defense Technical Information Center (DTIC))

Research projects covering the following topics are presented: viscosity; polymers; blood plasma; chemical concentration; solutions; differential thermal analysis; solvation; erythrocytes; and water chemistry. CASI

N94-36983 Research and Development Labs., Culver City, CA.
UNITED STATES AIR FORCE SUMMER RESEARCH PROGRAM, 1993. VOLUME 8: PHILLIPS LABORATORY Final Report
Dec. 1993 360 p Limited Reproducibility: More than 20% of this document may be affected by microfiche quality
(AD-A278698) Avail: Issuing Activity (Defense Technical Information Center (DTIC))

Research projects covering the following topics are presented: soil dynamics; radar dynamics; radar cross sections; backscattering; electromagnetic scattering; moisture content; dielectric properties; numerical analysis; and waveforms. CASI

N94-36984 Research and Development Labs., Culver City, CA.
UNITED STATES AIR FORCE SUMMER RESEARCH PROGRAM, 1993. VOLUME 9: ROME LABORATORY Final Report
Dec. 1993 234 p Limited Reproducibility: More than 20% of this document may be affected by microfiche quality
(AD-A278699) Avail: Issuing Activity (Defense Technical Information Center (DTIC))

Research projects covering the following topics are presented: computerized simulation; computer networks; distributed data processing; computer program reliability; systems analysis; and internetted data bases. CASI

Typical Subject Index Listing

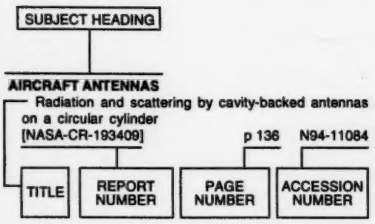

The subject heading is a key to the subject content of the document. Titles, report numbers, and accession numbers of pertinent documents are provided under each subject heading. When the title is insufficiently descriptive of the document content, a title extension is added, separated from the title by three hyphens. The report number helps to indicate the type of document cited (e.g., NASA report, NASA translation, NASA contractor report). The accession number is the number by which the document abstracts are arranged in this journal and by which the document is sold or requested. The page number helps you locate the citation in the abstract section. The titles, with title extensions if present, are arranged under each subject heading in ascending accession number order. The subject headings have been selected from the latest revision of the *NASA Thesaurus*.

A

ABLATIVE MATERIALS
Modeling of outgassing and matrix decomposition in carbon-phenolic composites
[NASA-CR-196319] p 4405 N94-37471

ABORT TRAJECTORIES
Optimal control theory determination of feasible return-to-launch-site aborts for the HL-20 Personnel Launch System vehicle
[NASA-TP-3449] p 4396 N94-37260

ABORTED MISSIONS
Optimal control theory determination of feasible return-to-launch-site aborts for the HL-20 Personnel Launch System vehicle
[NASA-TP-3449] p 4396 N94-37260

ABSORBENTS
Method and apparatus for the collection, storage, and real time analysis of blood and other bodily fluids
[NASA-CASE-MSC-22463-1] p 4480 N94-36766

ABSORPTION
The potential for control of carbon dioxide emissions from integrated gasification/combined-cycle systems
[DE94-012646] p 4465 N94-37100

ABSORPTION SPECTRA
Picosecond laser induced electric field modulation of carotenoid absorption bands
[DE94-009692] p 4512 N94-36524
Femtosecond transient grating studies of electron transfer in porphyrin and chlorophyll donor-acceptor molecules
[DE94-009694] p 4478 N94-36555
Poly(p-phenylene) derivatives new high performance nonlinear optical polymers
[AD-A280248] p 4422 N94-37121
XAFS-like structure of resonant Raman scattering
[DE94-618410] p 4517 N94-37171
Optical spectroscopy of a nitrogen-hydrogen complex in ZnSe
[DE94-011622] p 4413 N94-37630

ABSORPTION SPECTROSCOPY
Femtosecond transient absorption studies of the light harvesting Chl a/b protein complex of Photosystem 2 in higher plants
[DE94-009684] p 4477 N94-36481
Solvent effects on the energetics and dynamics of ultrafast electron transfer in chlorophyll-porphyrin-acceptor triads
[DE94-009693] p 4477 N94-36554
XAFS-like structure of resonant Raman scattering
[DE94-618410] p 4517 N94-37171
Optical spectroscopy of a nitrogen-hydrogen complex in ZnSe
[DE94-011622] p 4413 N94-37630

ACCELERATION (PHYSICS)
JPRS report: Central Eurasia. Aviation and cosmonautics, No. 4, April 1993
[JPRS-UAC-94-003] p 4391 N94-36999

ACCEPTOR MATERIALS
Solvent effects on the energetics and dynamics of ultrafast electron transfer in chlorophyll-porphyrin-acceptor triads
[DE94-009693] p 4477 N94-36554
Femtosecond transient grating studies of electron transfer in porphyrin and chlorophyll donor-acceptor molecules
[DE94-009694] p 4478 N94-36555
Organometallic NLO polymers. 4: Organometallic main-chain, side-chain, and guest-host polymers: A study of their orientation and relaxation using second harmonic generation
[AD-A280347] p 4423 N94-37179
Optical spectroscopy of a nitrogen-hydrogen complex in ZnSe
[DE94-011622] p 4413 N94-37630

ACCLIMATIZATION
Effects of freezing and cold acclimation on the plasma membrane of isolated protoplasts
[DE94-012487] p 4479 N94-37248

ACCRETION DISKS
The winds of cataclysmic variables
[DE94-010897] p 4548 N94-37164

ACCURACY
Determination of density of mass standards: Requirement and method
[PB94-163078] p 4508 N94-36718

ACETIC ACID
Conversion of acetic acid to methane by thermophiles
[DE94-012478] p 4479 N94-37434

ACIDITY
Thermodynamic and kinetic aspects of surface acidity
[DE94-012351] p 4411 N94-37372

ACOUSTIC COUPLING
Parameter estimation in a structural acoustic system with fully nonlinear coupling conditions
[NASA-CR-194926] p 4503 N94-36991

ACOUSTIC EXCITATION
Parameter estimation in a structural acoustic system with fully nonlinear coupling conditions
[NASA-CR-194926] p 4503 N94-36991

ACOUSTIC MEASUREMENT
Study on the measurement uncertainty of noise properties of a millimeter wave amplifier
[PB94-170917] p 4510 N94-37632

ACOUSTIC PROPERTIES
Variability of the California Current System off Point Sur, California from April 1988 to December 1990
[AD-A278579] p 4476 N94-36985

ACOUSTIC VELOCITY
Signal processing for the 1992 Barents Sea tomography experiment
[AD-A278580] p 4476 N94-36971

ACOUSTICS
Josephson acoustic radiation in superfluid helium
[AD-A280208] p 4533 N94-36742
A Galerkin method for linear PDE systems in circular geometries with structural acoustic applications
[NASA-CR-194925] p 4503 N94-36923
Segment-based acoustic models for continuous speech recognition
[AD-A280332] p 4434 N94-37032
Fundamentals studies of radial wave thermoacoustic engines
[AD-A280534] p 4431 N94-37090
3D sound experimental approach: Methodology and preliminary results p 4486 N94-37280
Scattering cross section of sound waves by the modal element method
[NASA-TM-106667] p 4510 N94-37308

ACQUIRED IMMUNODEFICIENCY SYNDROME
Rapid susceptibility testing of Mycobacterium avium complex and Mycobacterium tuberculosis isolated from AIDS patients
[NASA-CR-196268] p 4478 N94-36996

ACRYLATES
Organic NLO polymers. 2: Main-chain and guest-host Chi(2)NLO polymers: NLO-phore structure versus poling
[AD-A280230] p 4423 N94-37133
Solution characterization of poly(isobornyl methacrylate) in tetrahydrofuran
[AD-A280497] p 4409 N94-37145
Organometallic NLO polymers. 4: Organometallic main-chain, side-chain, and guest-host polymers: A study of their orientation and relaxation using second harmonic generation
[AD-A280347] p 4423 N94-37179
Thermal cis-trans isomerization rates of azobenzenes bound in the side chain of some copolymers and blends
[AD-A280451] p 4424 N94-37227

ACRYLIC RESINS
Highly fluorinated polymers
[NASA-CR-196270] p 4422 N94-37025
Basic solutions to carbon/carbon oxidation: Science and technology
[AD-A280447] p 4404 N94-37232

ACRYLONITRILES
Basic solutions to carbon/carbon oxidation: Science and technology
[AD-A280447] p 4404 N94-37232

ACTINIDE SERIES
Consequences of competing hybridization for magnetic ordering in correlated-electron lattices
[DE94-011648] p 4534 N94-37057
Development of immobilized ligands for actinide separations
[DE94-012714] p 4410 N94-37284

ACTIVATED CARBON
The development of short, high surface area activated carbon fibers
[AD-A280509] p 4404 N94-37105

ACTIVATION ENERGY
Thermomechanical studies of tungsten heavy alloys
[AD-A280250] p 4417 N94-37122
Finite-rate chemistry and transient effects in Direct Numerical Simulations of turbulent non-premixed flames
[DE94-005250] p 4410 N94-37222
Flux creep: Its dependence on current denisty and relation to critical current densities from transport and magnetic measurements
[DE94-011701] p 4440 N94-37738

ACTIVE CONTROL
Neural network for positioning Space Station solar arrays
[NASA-TM-106656] p 4431 N94-36943
Multirate flutter suppression system design for the Benchmark Active Controls Technology Wing
[NASA-CR-196112] p 4388 N94-36965
Modeling and control of intelligent flexible structures
[AD-A280478] p 4396 N94-37349

ACTIVE GALACTIC NUCLEI
Correlated radio and optical variations in a sample of AGN. A simultaneous radio-optical flare in BL lacertae
[PB94-179181] p 4548 N94-37834

ACTUATORS
A dynamic model of a linear actuator based on polymer hydrogel
[DE94-010800] p 4408 N94-37091

ADA (PROGRAMMING LANGUAGE)
Lessons learned applying CASE methods/tools to Ada software development projects p 4491 N94-36493

Impact of Ada in the Flight Dynamics Division: Excitement and frustration p 4492 N94-36501

ADAPTIVE OPTICS

Pointing and tracking concept for a high energy laser weapon application p 4393 N94-36619

Adaptive optics for laser beamforming in the atmosphere p 4393 N94-36621

A diffraction-based model of anisoplanatism effects in adaptive optic systems [AD-A280491] p 4524 N94-37142

ADDITIVES

Combustion characterization of methylal in reciprocating engines [DE94-006949] p 4411 N94-37409

Mechanical behavior and phase stability of NiAl-based shape memory alloys [DE94-012336] p 4419 N94-37420

ADDUCTS

Chemical and structural characterization of nitroaromatic adducts with hemoglobins [AD-A280533] p 4480 N94-37089

ADENOSINE TRIPHOSPHATE

Rapid susceptibility testing of Mycobacterium avium complex and Mycobacterium tuberculosis isolated from AIDS patients [NASA-CR-196268] p 4478 N94-36996

ADHESION

Compilation of diamond-like carbon properties for barriers and hard coatings [DE94-012139] p 4427 N94-37725

Surface modification of polymers with self-assembled monolayers that promote adhesion, outgrowth and differentiation of biological cells [AD-D016321] p 4427 N94-37829

ADHESIVE BONDING

The cyclic fatigue behaviour of adhesive joints [AD-A280453] p 4456 N94-37186

ADHESIVE JOINTS

Channel in hip implant stem [NASA-CASE-MFS-28987-1] p 4466 N94-36840

ADIABATIC EQUATIONS

Bond selective chemistry beyond the adiabatic approximation [DE94-012486] p 4408 N94-37095

ADSORPTION

Dipole forbidden vibrational modes for NO and CO on Cu observed in the far IR [DE94-003199] p 4408 N94-36559

Nonlinear optical spectroscopy for surface studies [DE94-011623] p 4406 N94-37056

Laser probing of interfaces [DE94-011300] p 4449 N94-37628

Morphological aspects of surface reactions [DE94-011208] p 4413 N94-37713

ADVANCED VERY HIGH RESOLUTION RADIOMETER

Variability of the California Current System off Point Sur, California from April 1988 to December 1990 [AD-A278579] p 4476 N94-36985

ADVECTION

A flux splitting scheme with high-resolution and robustness for discontinuities [NASA-TM-106452] p 4441 N94-36646

A Lagrangian-Eulerian finite element method with adaptive gridding for advection-dispersion problems [DE94-011372] p 4506 N94-37718

AEROACOUSTICS

Mixing and noise benefit versus thrust penalty in supersonic jets using impingement tones [NASA-TM-106583] p 4382 N94-36686

AERODYNAMIC CHARACTERISTICS

An aerodynamic and static-stability analysis of the Hypersonic Applied Research Technology (HART) missile [AD-A280631] p 4382 N94-36729

Unsteady flow field of large-amplitude pitching airfoils [AD-A280444] p 4383 N94-37219

Subsonic aerodynamic characteristic of semispan commercial transport model with wing-mounted advanced ducted propeller operating in reverse thrust --- conducted in the Langley 14 by 22 foot subsonic wind tunnel [NASA-TP-3427] p 4384 N94-37505

Aerodynamic characteristics of the National Launch System (NLS) 1 1/2 stage launch vehicle [NASA-TP-3488] p 4384 N94-37577

AERODYNAMIC CONFIGURATIONS

An arbitrary grid CFD algorithm for configuration aerodynamics analysis. Volume 1: Theory and validations [NASA-CR-195918] p 4493 N94-36914

An arbitrary grid CFD algorithm for configuration aerodynamics analysis. Volume 2: FEMNAS user guide [NASA-CR-196135] p 4493 N94-36922

AERODYNAMIC HEATING

Active cooling from the sixties to NASP [NASA-TM-109079] p 4456 N94-37541

AERODYNAMIC STABILITY

Unsteady flow field of large-amplitude pitching airfoils [AD-A280444] p 4383 N94-37219

AERODYNAMIC STALLING

Unsteady flow field of large-amplitude pitching airfoils [AD-A280444] p 4383 N94-37219

AERODYNAMICS

Impact of Ada in the Flight Dynamics Division: Excitement and frustration p 4492 N94-36501

Aeronautical engineering: A continuing bibliography with indexes (supplement 307) [NASA-SP-7037(307)] p 4381 N94-37117

AEROEMBOLISM

Cardiac pressure changes with venous gas embolism and decompression [AD-A280412] p 4481 N94-37224

AERONAUTICAL ENGINEERING

Aeronautical engineering: A continuing bibliography with indexes (supplement 307) [NASA-SP-7037(307)] p 4381 N94-37117

AERONAUTICS

JPRS report: Central Eurasia. Aviation and cosmonautics, No. 4, April 1993 [JPRS-UAC-94-003] p 4391 N94-36999

JPRS report: Central Eurasia. Aviation and cosmonautics, No. 5, May 1993 [JPRS-UAC-94-004] p 4391 N94-37000

JPRS report: Central Eurasia. Aviation and cosmonautics, No. 6, June 1993 [JPRS-UAC-94-005] p 4391 N94-37001

AEROSERVOELASTICITY

Aeroservoelastic stabilization considerations for pointing and tracking systems p 4394 N94-36627

AEROSPACE ENGINEERING

Possibilities and pitfalls in aerospace applications of titanium matrix composites p 4400 N94-36650

JPRS report: Science and technology. Central Eurasia: Space [JPRS-USP-94-004] p 4391 N94-37002

JPRS report: Science and technology. Central Eurasia: Space p 4391 N94-37003

Publications of the Jet Propulsion Laboratory, 1992 [NASA-CR-196125] p 4542 N94-37008

JPRS report: Science and technology. Central Eurasia: Engineering and equipment [JPRS-UEQ-93-007] p 4431 N94-37523

JPRS report: Science and technology. Central Eurasia: Engineering and equipment [JPRS-UEQ-93-008] p 4432 N94-37524

JPRS report: Science and technology. Central Eurasia: Engineering and equipment [JPRS-UEQ-93-005] p 4432 N94-37538

AEROSPACE ENVIRONMENTS

Properties of perfluoropolyethers for space applications [NASA-TM-106616] p 4426 N94-37520

AEROSPACE MEDICINE

Relation of motion sickness susceptibility to vestibular and behavioral measures of orientation [NASA-CR-196121] p 4480 N94-37005

Cardiac pressure changes with venous gas embolism and decompression [AD-A280412] p 4481 N94-37224

Aerospace medicine and biology: A continuing bibliography with indexes (supplement 392) [NASA-SP-7011(392)] p 4482 N94-37445

AEROSPACE PLANES

Hot dynamic test rig for measuring hypersonic engine seal flow and durability [NASA-TM-106507] p 4450 N94-36645

AEROSPACE SAFETY

Space Shuttle: Incomplete data and funding approach increase cost risk for upgrade program. Report to Congressional Requesters [GAO/NSIAD-94-23] p 4392 N94-37026

AEROSPACE SCIENCES

JPRS report: Science and technology. Central Eurasia: Space [JPRS-USP-94-004] p 4391 N94-37002

JPRS report: Science and technology. Central Eurasia: Space p 4391 N94-37003

Publications of the Jet Propulsion Laboratory, 1992 [NASA-CR-196125] p 4542 N94-37008

Problems of international exchange of scientific and technical information for a Russian aerospace research institute p 4544 N94-37339

AEROSPACE SYSTEMS

Operational environments for electrical power wiring on NASA space systems [NASA-TM-106655] p 4398 N94-36951

AEROSPACE TECHNOLOGY TRANSFER

Problems of international exchange of scientific and technical information for a Russian aerospace research institute p 4544 N94-37339

NASA commercial technology. Agenda for change [NASA-TM-109898] p 4546 N94-37765

AEROSPACE VEHICLES

Possibilities and pitfalls in aerospace applications of titanium matrix composites p 4400 N94-36650

AEROTHERMOCHEMISTRY

Hypersonic, nonequilibrium flow over the FIRE 2 forebody at 1634 sec [NASA-TM-109141] p 4444 N94-37455

AEROTHERMODYNAMICS

A shadowgraph study of Space Transportation System (STS): The Space Shuttle Launch Vehicle (SSLV) [NASA-RP-1341] p 4382 N94-36741

Computational chemistry research [NASA-CR-196120] p 4408 N94-36989

AGRICULTURE

Opportunities for innovation: Biotechnology [PB94-157831] p 4478 N94-36720

Climate uncertainty and the regional economic impacts of global climate change [DE94-012242] p 4466 N94-37211

AIR

Influences of flame-vortex interactions on formation of oxides of nitrogen in curved methane-air diffusion flamelets [DE94-005105] p 4409 N94-37221

Finite-rate chemistry and transient effects in Direct Numerical Simulations of turbulent non-premixed flames [DE94-005250] p 4410 N94-37222

AIR CONDITIONING

Refrigeration and Air-Conditioning Technology Workshop [DE94-010813] p 4431 N94-37452

AIR DATA SYSTEMS

Measurement uncertainty and feasibility study of a flush airdata system for a hypersonic flight experiment [NASA-TM-4627] p 4383 N94-37378

AIR LAND INTERACTIONS

On the development of boundary layer secondary circulations resulting from horizontally varying surface heat flux [DE94-011234] p 4472 N94-37048

Representing the influence of subgrid topography on hydrology [DE94-004595] p 4474 N94-37379

An experimental and numerical study of boundary layer structure over areas of inhomogeneous sensible heat fluxes [DE94-011441] p 4474 N94-37565

AIR NAVIGATION

Landing of an unmanned helicopter on a moving platform. High accuracy navigation and tracking p 4387 N94-36618

Assistance in instruction and training of air traffic controllers p 4483 N94-37265

System for broadcasting marker beacon signals and processing responses from seeking entities [AD-D016313] p 4385 N94-37839

AIR POLLUTION

UK methane emissions inventory: A scoping study on the use of ambient measurements to reduce uncertainties [PB94-167855] p 4463 N94-36533

SIHTI: Energy and environmental technology [DE94-763290] p 4464 N94-37007

Long-range mesoscale modeling of pollutant transport for the European Tracer EXperiment (ETEX) [DE94-010820] p 4465 N94-37093

Evaluation of flame-sprayed polymer coatings for civil works navigation structures [AD-A280507] p 4422 N94-37104

Project report: Aircraft --- atmospheric effects of stratospheric aircraft [DE94-011759] p 4465 N94-37155

Jet aircraft engine exhaust emissions database development: Year 1990 and 2015 scenarios [NASA-CR-4613] p 4466 N94-37252

Mexico City air quality research initiative, volume 4 [DE94-013201] p 4466 N94-37299

Evaluation of parameterizations for pollutant transport and dispersion in an urban street canyon using a three-dimensional dynamic flow model [DE94-012641] p 4467 N94-37429

Modeling atmospheric concentrations and deposition of Hg [DE94-012633] p 4467 N94-37440

Stratospheric emissions effects database development [NASA-CR-4592] p 4467 N94-37607

Biological determinants of photobioreactor design [DE94-011665] p 4468 N94-37740

Program GAUSSPLYM: A tool in Windows environment for studying continuous releases [PB94-184603] p 4468 N94-37856

AIR QUALITY
UK methane emissions inventory: A scoping study on the use of ambient measurements to reduce uncertainties
[PB94-167855] p 4463 N94-36533
California residential indoor air quality study. Volume 1: Methodology and descriptive statistics
[PB94-166048] p 4464 N94-36994
California residential indoor air quality study. Volume 1: Methodology and descriptive statistics. Appendix
[PB94-166055] p 4464 N94-36995
Mexico City air quality research initiative, volume 4
[DE94-013201] p 4466 N94-37299
Comparative alternative/clean fuels provisions of the Clean Air Act Amendments of 1990 and the Energy Policy Act of 1992
[DE94-006887] p 4429 N94-37426

AIR SAMPLING
Long-range mesoscale modeling of pollutant transport for the European Tracer EXperiment (ETEX)
[DE94-010820] p 4465 N94-37093

AIR TRAFFIC
Project report: Aircraft --- atmospheric effects of stratospheric aircraft
[DE94-011759] p 4465 N94-37155
Stratospheric emissions effects database development
[NASA-CR-4592] p 4467 N94-37607

AIR TRAFFIC CONTROL
An error-resistant linguistic protocol for air traffic control
[NASA-CR-196098] p 4385 N94-37013

AIR TRAFFIC CONTROLLERS (PERSONNEL)
Assistance in instruction and training of air traffic controllers p 4483 N94-37265

AIR TRANSPORTATION
Accomplishments under the Airport Improvement Program
[AD-A280661] p 4389 N94-36763
Analysis of vertiport studies funded by the Airport Improvement Program (AIP)
[SCT-93RR-21] p 4390 N94-37424

AIR WATER INTERACTIONS
Turbulent transfer in the marine planetary boundary layer
[AD-A280549] p 4476 N94-37038
The role of horizontal variability in air-sea interaction
[AD-A280561] p 4476 N94-37047
Index and bulk parameters for frequency-direction spectra measured at CERC Field Research Facility, September 1992 to August 1993
[AD-A280233] p 4476 N94-37135
Experiment on rapidly intensifying cyclones over the Atlantic
[AD-A280365] p 4473 N94-37180
Atmospheric gas
[DE94-007439] p 4465 N94-37187
Index and bulk parameters for frequency-direction spectra measured at CERC Field Research Facility, September 1990 to August 1991
[AD-A280423] p 4476 N94-37216
Index and bulk parameters for frequency-direction spectra measured at CERC Field Research Facility, September 1991 to August 1992
[AD-A280455] p 4477 N94-37229

AIRBORNE EQUIPMENT
Imaging targets embedded in a lossy half space with Synthetic Aperture Radar
[DE94-010807] p 4435 N94-37391

AIRBORNE RADAR
Airborne ROWS data report for the high resolution experiment, June 1993
[NASA-TM-104609] p 4477 N94-37397
NASA ER-2 Doppler radar reflectivity calibration for the CAMEX project
[NASA-TM-104611] p 4475 N94-37790

AIRBORNE/SPACEBORNE COMPUTERS
Space Generic Open Avionics Architecture (SGOAA) standard specification
[NASA-CR-188290] p 4387 N94-36933
Advanced information processing system: The Army Fault-Tolerant Architecture detailed design overview
[NASA-CR-194924] p 4497 N94-36962

AIRCRAFT ACCIDENT INVESTIGATION
JPRS report: Central Eurasia. Aviation and cosmonautics, No. 5, May 1993
[JPRS-UAC-94-004] p 4391 N94-37000

AIRCRAFT ACCIDENTS
JPRS report: Central Eurasia. Aviation and cosmonautics, No. 5, May 1993
[JPRS-UAC-94-004] p 4391 N94-37000
Composite helicopter accident profiles: Deficient crew/aircraft performance
[SCT-90RR-46] p 4385 N94-37604

AIRCRAFT COMMUNICATION
An error-resistant linguistic protocol for air traffic control
[NASA-CR-196098] p 4385 N94-37013

AIRCRAFT CONFIGURATIONS
Automatic procedures for computing complete configuration geometry from individual component descriptions
[NASA-TM-4607] p 4382 N94-36942

AIRCRAFT CONSTRUCTION MATERIALS
Characterisation of Fibre Reinforced Titanium Matrix Composites
[AD-A2775206] p 4400 N94-36649
Possibilities and pitfalls in aerospace applications of titanium matrix composites p 4400 N94-36650
Applications of Titanium Matrix Composite to large airframe structure p 4400 N94-36651
SCS-6 (tm) fiber reinforced titanium p 4400 N94-36652
Composites based on titanium with external and internal reinforcement p 4401 N94-36654
Manufacture and properties of sigma fibre reinforced titanium p 4401 N94-36655
Properties of TMC processed by fibre coating and hiping p 4401 N94-36656
Fibre-matrix interface properties in Ti-matrix composites: Chemical compatibility and micromechanical behaviour p 4401 N94-36657
Oxidation behavior of titanium aluminide matrix materials p 4401 N94-36658
Methodologies for thermal and mechanical testing of TMC materials p 4401 N94-36659
NASA-UVA Light Aerospace Alloy and Structures Technology Program (LA2ST)
[NASA-CR-196290] p 4415 N94-36809
JPRS report: Science and technology. Central Eurasia: Materials science
[JPRS-UMS-93-008] p 4404 N94-37010
Defects and their effects on the integrity of nickel based aeroengine discs p 4421 N94-37328
Substantiating powder metal life methodologies for engines p 4455 N94-37330
Predicting defect behaviour p 4455 N94-37331
A comparison of graphite/epoxy tape laminates and 2-D braided composites mechanical properties
[NASA-CR-4610] p 4420 N94-37582

AIRCRAFT CONTROL
An empirical comparison of a dynamic software testability metric to static cyclomatic complexity p 4491 N94-36498
Aeroservoelastic stabilization considerations for pointing and tracking systems p 4394 N94-36627
Design and evaluation of a Stochastic Optimal Feed-forward and Feedback Technology (SOFFT) flight control architecture
[NASA-TP-3419] p 4388 N94-37014
Predicting the effects of unmodeled dynamics on an aircraft flight control system design using eigenspace assignment
[NASA-TM-4548] p 4388 N94-37059
A non-intrusive way to measure point-of-gaze p 4484 N94-37272
Prospective communications research to support fly by light/power by wire
[NASA-CR-196369] p 4526 N94-37657

AIRCRAFT DESIGN
Prospective communications research to support fly by light/power by wire
[NASA-CR-196369] p 4526 N94-37657

AIRCRAFT ENGINES
Characterisation of Fibre Reinforced Titanium Matrix Composites
[AD-A2775206] p 4400 N94-36649
Manufacture and properties of sigma fibre reinforced titanium p 4401 N94-36655
Impact of Materials Defects on Engine Structures Integrity
[AGARD-R-790] p 4453 N94-37321
History and prognosis of material discontinuity effects on engine components structural integrity p 4453 N94-37322
Alternate melting and refining routes p 4421 N94-37323
Defects and their effects on the integrity of nickel based aeroengine discs p 4421 N94-37328
Turbine disks: Lifing against defects and materials development p 4454 N94-37329
Substantiating powder metal life methodologies for engines p 4455 N94-37330
Predicting defect behaviour p 4455 N94-37331
Fiber optic (flight quality) sensors for advanced aircraft propulsion
[NASA-CR-191195] p 4387 N94-37401

AIRCRAFT EQUIPMENT
Laser designation pods optimized concept for day/night operations p 4393 N94-36620
Infrared search and track demonstrator programme p 4393 N94-36622

AIRCRAFT FUELS
Advanced thermally stable, coal-derived, jet fuels development program. Experiment system and model development
[AD-A278968] p 4428 N94-36505

AIRCRAFT GUIDANCE
Advanced information processing system: The Army Fault-Tolerant Architecture detailed design overview
[NASA-CR-194924] p 4497 N94-36962

AIRCRAFT LANDING
An empirical comparison of a dynamic software testability metric to static cyclomatic complexity p 4491 N94-36498
Landing of an unmanned helicopter on a moving platform. High accuracy navigation and tracking p 4387 N94-36618
Two-axis camera platform for machine vision p 4394 N94-36628
Synthetic vision display evaluation studies
[NASA-CR-194963] p 4387 N94-37658

AIRCRAFT MAINTENANCE
Aircraft battle damage repair for the 1990's and beyond
[AD-A278635] p 4386 N94-36465
A mean value analysis heuristic for analysis of aircraft sortie generation
[AD-A278578] p 4507 N94-36970
Training and operations support system (TOPS) p 4545 N94-37344
Planning German Army helicopter maintenance and mission assignment
[AD-A280483] p 4381 N94-37352

AIRCRAFT MODELS
A mean value analysis heuristic for analysis of aircraft sortie generation
[AD-A278578] p 4507 N94-36970
Stability analysis of an F/A-18 E/F cable mount m odel
[NASA-TM-108989] p 4386 N94-37636
Design of scaled down structural models p 4457 N94-37797

AIRCRAFT RELIABILITY
Possibilities and pitfalls in aerospace applications of titanium matrix composites p 4400 N94-36650
Prospective communications research to support fly by light/power by wire
[NASA-CR-196369] p 4526 N94-37657

AIRCRAFT SAFETY
Rotorwash analysis handbook. Volume 1: Development and analysis
[SCT-93RR-17-VOL-1] p 4381 N94-36466
Rotorwash analysis handbook. Volume 2: Appendixes
[SCT-93RR-17-VOL-2] p 4382 N94-36467
Aircraft command in emergency situations prototype development users manual
[DOT/FAA/CT-94/24] p 4385 N94-37706

AIRCRAFT STRUCTURES
Correlation of analytical and experimental hot structure vibration results
[NASA-TM-104269] p 4386 N94-36644
Applications of Titanium Matrix Composite to large airframe structure p 4400 N94-36651
Literature review and preliminary studies of fretting and fretting fatigue including special applications to aircraft joints
[AD-A280310] p 4456 N94-37125
Active cooling from the sixties to NASP
[NASA-TM-109079] p 4456 N94-37541

AIRFOILS
Unsteady flow field of large-amplitude pitching airfoils
[AD-A280444] p 4383 N94-37219
Prediction of film cooling on gas turbine airfoils
[NASA-TM-106653] p 4387 N94-37448

AIRFRAMES
Characterisation of Fibre Reinforced Titanium Matrix Composites
[AD-A2775206] p 4400 N94-36649
Applications of Titanium Matrix Composite to large airframe structure p 4400 N94-36651
SCS-6 (tm) fiber reinforced titanium p 4400 N94-36652

AIRGLOW
UK methane emissions inventory: A scoping study on the use of ambient measurements to reduce uncertainties
[PB94-167855] p 4463 N94-36533

AIRPORT PLANNING
Rotorwash analysis handbook. Volume 1: Development and analysis
[SCT-93RR-17-VOL-1] p 4381 N94-36466
Rotorwash analysis handbook. Volume 2: Appendixes
[SCT-93RR-17-VOL-2] p 4382 N94-36467

Analysis of vertiport studies funded by the Airport Improvement Program (AIP)
[SCT-93RR-21] p 4390 N94-37424

AIRPORTS
Accomplishments under the Airport Improvement Program
[AD-A280661] p 4389 N94-36763

ALBEDO
Infrared spectroscopy of Jupiter and Saturn
[NASA-CR-196294] p 4549 N94-36961

ALCOHOLS
Combustion characterization of methylal in reciprocating engines
[DE94-006949] p 4411 N94-37409
Estimates of US biomass energy consumption 1992
[DE94-011458] p 4463 N94-37567

ALGAE
Femtosecond transient absorption studies of the light harvesting Chl a/b protein complex of Photosystem 2 in higher plants
[DE94-009684] p 4477 N94-36481
Biological determinants of photobioreactor design
[DE94-011665] p 4468 N94-37740

ALGEBRA
Multirate time-frequency distributions
[AD-A280595] p 4503 N94-36723
The impact of HPF data layout on the design of efficient and maintainable parallel linear algebra libraries
[DE94-012382] p 4504 N94-37246
Automatic, self-adaptive control of unfold transformations
[DE94-012455] p 4504 N94-37247

ALGORITHMS
First results from a prototype level-1 calorimeter trigger system for LHC, RD 27 (UK) collaboration
[PB94-167475] p 4436 N94-36532
Elimination of numerical dispersion in finite-difference modeling and migration by flux-corrected transport
[DE94-004159] p 4510 N94-36551
A coupled/uncoupled deformation and fatigue damage algorithm utilizing the finite element method
[NASA-TM-106526] p 4455 N94-36561
High accuracy control algorithm application to a tracking turret p 4394 N94-36626
Multitarget track initiation using a modified Hough transform p 4395 N94-36630
Radar tracking in multipath: Techniques for improved performance p 4395 N94-36631
Multirate time-frequency distributions
[AD-A280595] p 4503 N94-36723
Methods of calculation of higher power corrections in QCD
[DE94-618511] p 4521 N94-36748
A model-based approach for detection of runways and other objects in image sequences acquired using an on-board camera
[NASA-CR-196424] p 4446 N94-36812
An algorithm for the automatic control of boundary layer flow
[ISVR-TR-233] p 4442 N94-36817
An arbitrary grid CFD algorithm for configuration aerodynamics analysis. Volume 1: Theory and validations
[NASA-CR-195918] p 4493 N94-36914
An arbitrary grid CFD algorithm for configuration aerodynamics analysis. Volume 2: FEMNAS user guide
[NASA-CR-196135] p 4493 N94-36922
Solving ill-conditioned matrix equations in control
[AD-A280502] p 4503 N94-37146
Numerical solution to the boundary-value problem for the Bethe-Salpeter equation with quadratically rising potential
[DE94-621606] p 4504 N94-37175
The impact of HPF data layout on the design of efficient and maintainable parallel linear algebra libraries
[DE94-012382] p 4504 N94-37246
Progress in navigation filter estimate fusion and its application to spacecraft rendezvous
[NASA-TM-104794] p 4392 N94-37386
Development of advanced Navier-Stokes solver
[NASA-CR-195094] p 4504 N94-37449
A scalable parallel algorithm for multiple objective linear programs
[NASA-CR-194920] p 4495 N94-37539
Parallel Spectral Transform Shallow Water Model: A runtime-tunable parallel benchmark code
[DE94-011460] p 4498 N94-37568
Tensor-GMRES method for large sparse systems of nonlinear equations
[NASA-CR-196379] p 4505 N94-37655
Techniques for real-time parallel processing: Sensor processing case studies
[AD-A280633] p 4499 N94-37760

ALIPHATIC HYDROCARBONS
Bond selective chemistry beyond the adiabatic approximation
[DE94-012486] p 4408 N94-37095

ALKANES
Methyl chloride via oxyhydrochlorination of methane
[DE94-010691] p 4406 N94-36450
Tert-butylalumoxanes: Synthetic analogs for methylalumoxane (MAO) and new catalytic routes to polyolefins and polyketones
[AD-A280511] p 4399 N94-37106

ALKENES
Diosmacycloalkanes as models for the formation of hydrocarbons from surface methylenes
[DE94-011211] p 4413 N94-37754

ALLOYING
Small-angle x ray scattering studies of microvoids in amorphous-silicon-based semiconductors
[DE94-006931] p 4533 N94-36745
JPRS report: Science and technology. Central Eurasia: Materials science
[JPRS-UMS-93-008] p 4404 N94-37010
Using nonequilibrium alloying techniques for corrosion inhibition in Gr/Al and Gr/Mg metal matrix composites
[AD-A280529] p 4404 N94-37088
Mechanical behavior and phase stability of NiAl-based shape memory alloys
[DE94-012336] p 4419 N94-37420
Physical and mechanical metallurgy of NiAl
[NASA-TP-3398] p 4419 N94-37503

ALLOYS
Using nonequilibrium alloying techniques for corrosion inhibition in Gr/Al and Gr/Mg metal matrix composites
[AD-A280529] p 4404 N94-37088
Atomic and electronic structure of metals and alloys: Rare earths, ultrathin films and surface alloys
[DE94-011581] p 4516 N94-37113

ALTERNATING CURRENT
A comparison of two examples of magnetic tracker systems p 4485 N94-37275

ALTIMETRY
Airborne ROWS data report for the high resolution experiment, June 1993
[NASA-TM-104609] p 4477 N94-37397

ALTITUDE SICKNESS
Hypobaric decompression sickness model development. Part 1: Diffusion of inert gas from a viscoelastic fluid (blood) into an expanding gas phase
[AD-A280298] p 4481 N94-37124

ALUMINIDES
Fibre-matrix interface properties in Ti-matrix composites: Chemical compatibility and micromechanical behaviour p 4401 N94-36657
Oxidation behavior of titanium aluminide matrix materials p 4401 N94-36658
Process simulation and modeling for advanced intermetallic alloys
[AD-A280327] p 4416 N94-37030
Feasibility of (IMC)(sub d)-reinforced metal matrix composites
[AD-A280626] p 4404 N94-37044
Mechanical behavior and phase stability of NiAl-based shape memory alloys
[DE94-012336] p 4419 N94-37420
Physical and mechanical metallurgy of NiAl
[NASA-TP-3398] p 4419 N94-37503

ALUMINUM
Production of amorphous metal layers using ion implantation and investigation of the related modification of some surface properties
[DE94-617509] p 4414 N94-36541
Validation and implementation of optical diagnostics for particle sizing in rocket motors
[AD-A278581] p 4428 N94-36972
LET spectra of fragmented 600-MeV/A iron beam on aluminum and polyethylene: A preliminary analysis
[NASA-TP-3436] p 4416 N94-36993
Using nonequilibrium alloying techniques for corrosion inhibition in Gr/Al and Gr/Mg metal matrix composites
[AD-A280529] p 4404 N94-37088
Numerical simulation of dynamic fracture and failure in solids
[DE94-010379] p 4457 N94-37705

ALUMINUM ALLOYS
Oxidation behavior of titanium aluminide matrix materials p 4401 N94-36658
NiAl-base composite containing high volume fraction of AlN for advanced engines
[NASA-CASE-LEW-15818-1] p 4403 N94-36752
NASA-UVA Light Aerospace Alloy and Structures Technology Program (LA2ST)
[NASA-CR-196290] p 4415 N94-36809
Processing and mechanical properties of NiAl-based in-situ composites
[NASA-CR-195333] p 4416 N94-36954
The cyclic fatigue behaviour of adhesive joints
[AD-A280453] p 4456 N94-37186
Atomic level characterization of defects in microalloyed NiAl: An atom probe investigation
[DE94-012732] p 4418 N94-37396
The effect of reactive elements on the segregation behavior and microstructure of alpha-Al2O3 scales on beta-NiAl
[DE94-012739] p 4418 N94-37399
Characterization of mechanical properties degradation using small punch testing technique
[DE94-011202] p 4418 N94-37410
The corrosion protection of several aluminum alloys by chromic acid and sulfuric acid anodizing
[NASA-TP-3490] p 4420 N94-37578

ALUMINUM ARSENIDES
Studies of the III-V compounds in the megabar regime
[DE94-012488] p 4537 N94-37435

ALUMINUM COMPOUNDS
Tert-butylalumoxanes: Synthetic analogs for methylalumoxane (MAO) and new catalytic routes to polyolefins and polyketones
[AD-A280511] p 4399 N94-37106

ALUMINUM GALLIUM ARSENIDES
The excitation mechanism of praseodymium-doped semiconductors
[AD-A280687] p 4535 N94-37129

ALUMINUM NITRIDES
X-ray diffraction studies of evaporated gold thin films deposited on aluminum nitride substates
[AD-A280454] p 4536 N94-37228
Studies of the III-V compounds in the megabar regime
[DE94-012488] p 4537 N94-37435

ALUMINUM OXIDES
Validation and implementation of optical diagnostics for particle sizing in rocket motors
[AD-A278581] p 4428 N94-36972
Development of low dielectric constant alumina-based ceramics for microelectronic substrates
[DE94-011360] p 4439 N94-37302
The effect of reactive elements on the segregation behavior and microstructure of alpha-Al2O3 scales on beta-NiAl
[DE94-012739] p 4418 N94-37399

AMBIENT TEMPERATURE
Site Scientific Mission Plan for the Southern Great Plains CART site, January - June 1994
[DE94-012114] p 4474 N94-37394

AMERICIUM
Study on extraction behavior of TRPO with different composition
[DE94-620287] p 4412 N94-37534

AMINES
Thermodynamic and kinetic aspects of surface acidity
[DE94-012351] p 4411 N94-37372

AMMONIUM COMPOUNDS
A photoemission study of Au, Ge, and O2 deposition on NH4F etched Si(111)
[DE94-013352] p 4519 N94-37553

AMORPHOUS MATERIALS
Production of amorphous metal layers using ion implantation and investigation of the related modification of some surface properties
[DE94-617509] p 4414 N94-36541
Optically induced high efficiency gratings in azo polymer films
[AD-A280505] p 4423 N94-37147
An amorphous fluoropolymer: Next generation optical coating candidate
[DE94-012386] p 4425 N94-37422
Residual stress and Raman spectra of laser deposited highly-tetrahedral-coordinated-amorphous-carbon films
[DE94-012067] p 4426 N94-37537
Optical studies of dynamical processes in disordered systems
[DE94-011945] p 4538 N94-37676
Compilation of diamond-like carbon properties for barriers and hard coatings
[DE94-012139] p 4427 N94-37725

AMORPHOUS SILICON
Amorphous silicon photovoltaic manufacturing technology, phase 2A
[DE94-006895] p 4461 N94-36476

AMPHIBOLES
Thermodynamics of minerals stable near the Earth's surface
[DE94-012479] p 4539 N94-37094

AMPLIFICATION
Experimental characterisation of gas microstrip detectors. Part 1: Gain characteristics
[PB94-167087] p 4445 N94-36531
Time-gated imaging through defense-scattering materials using stimulated Raman amplification
[AD-D016305] p 4440 N94-37775

AMPLIFIER DESIGN
U-turn alternative to the large aperture switch
[DE94-011541] p 4524 N94-37112
Single event mirroring and sense amplifier designs for enhanced SE tolerance of DRAMs
[DE94-010397] p 4438 N94-37190
AMPLIFIERS
Field emitter array RF amplifier development project. Cathode technology development. Phase 1
[AD-A280515] p 4437 N94-37108
AMPOULES
Ampoule failure sensor time response testing: Experiments 2 and 3
[NASA-TM-108458] p 4446 N94-36822
ANALOG DATA
Crosspoint analog data selector
[AD-D016326] p 4440 N94-37832
ANALOG TO DIGITAL CONVERTERS
KONRAD: Wide band digital HF receiver
[PB94-184686] p 4435 N94-37813
ANALOGIES
Is it possible to assign physical meaning to field theory with higher derivatives?
[DE94-618468] p 4539 N94-37172
ANALYSIS OF VARIANCE
Rescaled box counting for the topological analysis of spatial data
[DE94-009820] p 4461 N94-36464
ANALYTIC FUNCTIONS
Coherence and chaos
[DE94-008529] p 4539 N94-36507
ANDESITE
Vent processes during the 1912 eruption at Novarupta, Katmai National Park, Alaska
[DE94-010740] p 4468 N94-36451
ANELASTICITY
Analysis of anelastic flow and numerical treatment via finite elements
[DE94-012141] p 4445 N94-37726
ANEMOMETERS
An automated method for Low Level Windshear Alert System (LLWAS) data quality analysis
[AD-A280313] p 4472 N94-37126
ANGIOGRAPHY
Arterial cross-section measurements from dual energy transvenous coronary angiography images
[DE94-011193] p 4482 N94-37444
ANGLE OF ATTACK
A shadowgraph study of Space Transportation System (STS): The Space Shuttle Launch Vehicle (SSLV)
[NASA-RP-1341] p 4382 N94-36741
Controlling forebody asymmetries in flight: Experience with boundary layer transition strips
[NASA-TM-4595] p 4383 N94-36844
Unsteady flow field of large-amplitude pitching airfoils
[AD-A280444] p 4383 N94-37219
ANGULAR DISTRIBUTION
Angular dependence of parton-parton scattering extracted from hadron pair production in pp collisions at radicals equal to 11.5 GeV
[DE94-611174] p 4511 N94-36504
Coherent multiple-foil x-ray transition radiation
[DE93-040831] p 4525 N94-37486
The angular and energy distributions of ejected electrons in electron-impact ionization of helium
[DE94-618748] p 4519 N94-37528
ANGULAR MOMENTUM
The asymptotics of matrix elements of Gaussian potential between the basis functions of three-dimensional harmonic oscillator
[DE94-618467] p 4539 N94-37079
The winds of cataclysmic variables
[DE94-010897] p 4548 N94-37164
ANHYDRIDES
Synthesis of phthalonitrile resins containing ether and imide linkages with aromatic diamine curing agent
[AD-D016309] p 4427 N94-37778
ANIMALS
Blast overpressure studies with animals and man
[AD-A280240] p 4480 N94-37118
Investigation of exposure to Extremely Low Frequency (ELF) magnetic and electric fields: Ongoing animals studies
[DE94-011239] p 4480 N94-37625
ANIMATION
EM-ANIMATE: A computer program for displaying and animating electromagnetic near-field and surface-current solutions: Video supplement to NASA Technical Memorandum 4539
[NASA-TM-4539-VIDEO-SUPPL] p 4492 N94-36518
ANIONS
Isolated SO4-2 and PO4-3 anions do not exist
[AD-A278831] p 4512 N94-36521
Ionic properties of hydrogenated and fluorinated fullerenes
[DE94-012110] p 4537 N94-37369
ANNEALING
The effect of reactive elements on the segregation behavior and microstructure of alpha-Al2O3 scales on beta-NiAl
[DE94-012739] p 4418 N94-37399
Effect of thermal annealing on grain boundary chemistry of polycrystalline TlBa2Ca2Cu3O(y) films
[DE94-011464] p 4538 N94-37569
ANNIHILATION REACTIONS
Measurement of the elastic, total and diffraction cross sections at tevatron energies
[DE94-004659] p 4511 N94-36483
A search for first generation scalar leptoquarks at radical s equal to 1.8 TeV with the D0 detector
[DE94-008846] p 4511 N94-36506
Coherence and chaos
[DE94-008529] p 4539 N94-36507
Relativistic di-quark model of p p-bar yields K(+)K(-) reaction
[DE94-618519] p 4514 N94-37063
Mass identified particle production and Bose Einstein correlations at 1800 GeV
[DE94-013418] p 4515 N94-37067
First observation of laser-induced resonant annihilation in metastable antiprotonic helium atoms
[DE94-748668] p 4519 N94-37417
ANNUAL VARIATIONS
Substorm statistics: Occurrences and amplitudes
[DE94-011694] p 4471 N94-37669
ANNULAR SUSPENSION AND POINTING SYSTEM
Large angle magnetic suspension test fixture
[NASA-CR-196138] p 4390 N94-37450
ANODES
Field emitter array RF amplifier development project. Phase 1, option 1
[AD-A280513] p 4437 N94-37107
ANODIC COATINGS
The corrosion protection of several aluminum alloys by chromic acid and sulfuric acid anodizing
[NASA-TP-3490] p 4420 N94-37578
ANODIZING
The corrosion protection of several aluminum alloys by chromic acid and sulfuric acid anodizing
[NASA-TP-3490] p 4420 N94-37578
ANOMALIES
Scientific and technical support for the Galileo net flux radiometer experiment
[NASA-CR-196009] p 4549 N94-36689
ANTENNA ARRAYS
Processing, packaging, and characterization of electroceramic materials for phased array antennas
[AD-A280251] p 4432 N94-36743
Submillimeter quasioptical Josephson junction oscillator with integrated tuning elements
[AD-A280380] p 4534 N94-37036
Baseline antenna design for space exploration initiative
[NASA-CR-196298] p 4435 N94-37255
ANTENNA COMPONENTS
Design and analysis of a mode B and mode JD satellite Earth station
[AD-A280417] p 4391 N94-37225
ANTENNA DESIGN
Submillimeter quasioptical Josephson junction oscillator with integrated tuning elements
[AD-A280380] p 4534 N94-37036
Baseline antenna design for space exploration initiative
[NASA-CR-196298] p 4435 N94-37255
ANTICYCLONES
The life cycles of intense cyclonic and anticyclonic circulation systems observed over oceans
[NASA-CR-196271] p 4473 N94-37294
ANTIFERROMAGNETISM
Forward scattering of neutrons from polymeric and magnetic multilayers
[DE93-041158] p 4513 N94-36696
Magnetic and structural instabilities of ferromagnetic and antiferromagnetic Fe/Cu(100)
[DE94-011504] p 4509 N94-37517
ANTIINFECTIVES AND ANTIBACTERIALS
Rapid susceptibility testing of Mycobacterium avium complex and Mycobacterium tuberculosis isolated from AIDS patients
[NASA-CR-196268] p 4478 N94-36996
ANTIMONIDES
InTlSb for long-wavelength infrared photodetectors and arrays
[AD-A280207] p 4524 N94-37149
ANTIPROTONS
First observation of laser-induced resonant annihilation in metastable antiprotonic helium atoms
[DE94-748668] p 4519 N94-37417
ANTIREFLECTION COATINGS
An amorphous fluoropolymer: Next generation optical coating candidate
[DE94-012386] p 4425 N94-37422
ANVIL CLOUDS
Factors influencing the parameterization of anvil clouds within GCMs
[DE94-010794] p 4475 N94-37621
ANXIETY
Cerebral neurochemical mechanisms in stress and anxiety
[AD-A280473] p 4482 N94-37233
APERTURES
Wide aperture scintillation hodoscope with FEU-143 photomultipliers
[DE94-618211] p 4515 N94-37075
A new, optical-lever based atomic force microscope
[AD-A280524] p 4524 N94-37110
Tune modulation due to gradient ripple and the dynamic aperture
[DE94-011922] p 4524 N94-37157
APPLICATION SPECIFIC INTEGRATED CIRCUITS
First results from a prototype level-1 calorimeter trigger system for LHC, RD 27 (UK) collaboration
[PB94-167475] p 4436 N94-36532
APPLICATIONS PROGRAMS (COMPUTERS)
Applying formal methods and object-oriented analysis to existing flight software p 4491 N94-36495
EM-ANIMATE: A computer program for displaying and animating electromagnetic near-field and surface-current solutions: Video supplement to NASA Technical Memorandum 4539
[NASA-TM-4539-VIDEO-SUPPL] p 4492 N94-36518
Multiphase flow with interphase exchanges (MFIX) documentation theory guide
[DE94-000087] p 4441 N94-36550
Earth Observing System/Advanced Microwave Sounding Unit-A (EOS/AMSU-A) software management plan
[NASA-CR-189362] p 4461 N94-36919
Large-scale three-dimensional geothermal reservoir simulation on PC's
[DE94-011374] p 4443 N94-37050
Strength evaluation of socket joints
[NASA-CR-4608] p 4389 N94-37259
CHEETAH: A fast thermochemical code for detonation
[DE94-012586] p 4429 N94-37427
Parallel Spectral Transform Shallow Water Model: A runtime-tunable parallel benchmark code
[DE94-011460] p 4498 N94-37568
Interactive Collaborative Environments (ICE): Platform independent X application sharing and multi-media over wide area networks
[DE94-008868] p 4502 N94-37784
Program GAUSSPLYM: A tool in Windows environment for studying continuous releases
[PB94-184603] p 4468 N94-37856
APPROXIMATION
Approximate analysis for repeated eigenvalue problems with applications to controls-structure integrated design
[NASA-TP-3439] p 4397 N94-37502
ARC MELTING
The influence of VAR processes and parameters on white spot formation in Alloy 718
[DE94-012071] p 4417 N94-37367
ARCHITECTURE (COMPUTERS)
NASA Access Mechanism: Lessons learned document
[NASA-TM-109924] p 4540 N94-36750
NASA STI Program Coordinating Council Eleventh Meeting: NASA STI Modernization Plan
[NASA-TM-109415] p 4540 N94-36841
NASA STI modernization plan p 4540 N94-36842
RECON Replacement Project p 4541 N94-36844
Standards in the architectural effort
p 4541 N94-36852
STI Architectural Framework Working Group
p 4542 N94-36854
Advanced information processing system: The Army Fault-Tolerant Architecture detailed design overview
[NASA-CR-194924] p 4497 N94-36962
Proto code generation techniques
[AD-A280275] p 4494 N94-37123
SACS: A cache simulator incorporating timing analysis with buffer and memory management
[AD-A280472] p 4494 N94-37230
Fermilab's DART DA system
[DE94-013240] p 4523 N94-37547
Open architecture controllers for advanced manufacturing
[DE94-007572] p 4496 N94-37782
What is an open architecture robot controller?
[DE94-007854] p 4501 N94-37783
Remote use of distributed robotics resources to enhance technology development and insertion
[DE94-009285] p 4502 N94-37785

ARCTIC OCEAN
Cooling of the West Spitzbergen Current: Wintertime observations west of Svalbard
[AD-A280648] p 4475 N94-36762
ARCTIC REGIONS
Measuring the upper profile of sea ice in the Bay of Bothnia with a laser profilometer
[PB94-184561] p 4477 N94-37855
ARGON PLASMA
Turning soot into diamonds with microwaves
[DE94-013426] p 4422 N94-37068
ARID LANDS
Surface-layer response over shrub-steppe canopy during springtime
[DE94-011235] p 4468 N94-37624
ARMED FORCES (FOREIGN)
A guide to tenders and contracts alerting services
[AGARD-R-799] p 4540 N94-37447
ARMED FORCES (UNITED STATES)
A guide to tenders and contracts alerting services
[AGARD-R-799] p 4540 N94-37447
ARPA COMPUTER NETWORK
Field emitter array RF amplifier development project. Phase 1, option 1
[AD-A280513] p 4437 N94-37107
ARRAYS
Diode array alternative to paint removal solid-state cw laser
[DE94-011482] p 4448 N94-37203
ARTERIES
Arterial cross-section measurements from dual energy transvenous coronary angiography images
[DE94-011193] p 4482 N94-37444
ARTIFICIAL INTELLIGENCE
Searching for plans using a hierarchy of learned macros and selective reuse
[AD-A280594] p 4499 N94-36722
Beyond intelligent vacuum cleaners
[AD-A280565] p 4500 N94-37039
Bootstrap planning: Theory and application
[DE94-006466] p 4501 N94-37425
Open architecture controllers for advanced manufacturing
[DE94-007572] p 4496 N94-37782
What is an open architecture robot controller?
[DE94-007854] p 4501 N94-37783
ARTIFICIAL SATELLITES
UVPI imaging from the LACE satellite: The Low Cost Launch Vehicle (LCLV) rocket plume
[AD-A278785] p 4398 N94-36445
ARTS
Atomic oxygen treatment for non-contact removal of organic protective coatings from painting surfaces
[NASA-TM-106650] p 4421 N94-36952
ASCENT
Aerodynamic characteristics of the National Launch System (NLS) 1 1/2 stage launch vehicle
[NASA-TP-3488] p 4384 N94-37577
ASIA
JPRS report: Science and technology. Central Eurasia: Space
[JPRS-USP-94-004] p 4391 N94-37002
ASSAYING
Rapid susceptibility testing of Mycobacterium avium complex and Mycobacterium tuberculosis isolated from AIDS patients
[NASA-CR-196268] p 4476 N94-36996
ASTRONAUTICS
JPRS report: Central Eurasia. Aviation and cosmonautics, No. 4, April 1993
[JPRS-UAC-94-003] p 4391 N94-36999
JPRS report: Central Eurasia. Aviation and cosmonautics, No. 5, May 1993
[JPRS-UAC-94-004] p 4391 N94-37000
JPRS report: Central Eurasia. Aviation and cosmonautics, No. 6, June 1993
[JPRS-UAC-94-005] p 4391 N94-37001
ASTRONOMICAL CATALOGS
Sloan Digital Sky Survey
[DE94-011749] p 4547 N94-37667
ASTRONOMICAL MODELS
The winds of cataclysmic variables
[DE94-010897] p 4548 N94-37164
Gamma ray astronomy
[NASA-CR-193970] p 4547 N94-37702
ASTRONOMICAL PHOTOGRAPHY
Hubble Space Telescope faint object camera instrument handbook (Post-COSTAR), version 5.0
[NASA-CR-189365] p 4546 N94-36795
ASTRONOMICAL PHOTOMETRY
Infrared spectroscopy of Jupiter and Saturn
[NASA-CR-196294] p 4549 N94-36961
Guaranteed time observations support for Faint Object Spectrograph (FOS) on HST
[NASA-CR-196305] p 4547 N94-37037
Sloan Digital Sky Survey
[DE94-011749] p 4547 N94-37667
ASTRONOMICAL POLARIMETRY
Ultraviolet spectropolarimetry of high redshift quasars with the Hubble Space Telescope
[NASA-CR-196014] p 4546 N94-36690
Guaranteed time observations support for Faint Object Spectrograph (FOS) on HST
[NASA-CR-196305] p 4547 N94-37037
ASTRONOMICAL SPECTROSCOPY
Ultraviolet spectropolarimetry of high redshift quasars with the Hubble Space Telescope
[NASA-CR-196014] p 4546 N94-36690
Infrared spectroscopy of Jupiter and Saturn
[NASA-CR-196294] p 4549 N94-36961
Guaranteed time observations support for Faint Object Spectrograph (FOS) on HST
[NASA-CR-196305] p 4547 N94-37037
Far-infrared emission line spectroscopy of planetary nebulae from the KAO
[NASA-CR-196289] p 4547 N94-37825
ASTROPHYSICS
Intensity of waves diffracted from symmetrical profile lamellar gratings
[DE94-011101] p 4433 N94-36753
Cosmic rays: Physics and astrophysics. A research briefing
[NASA-CR-196118] p 4550 N94-36921
ASYMMETRY
CP violation outside the standard model phenomenology for pedestrians
[DE94-002216] p 4511 N94-36512
Dipole forbidden vibrational modes for NO and CO on Cu observed in the far IR
[DE94-003199] p 4408 N94-36559
ASYMPTOTIC METHODS
Scattering cross section of sound waves by the modal element method
[NASA-TM-106667] p 4510 N94-37308
ATHLETES
Postural strategies for the continuous control of static and dynamic balance in man
[PB94-184678] p 4487 N94-37812
ATLANTIC OCEAN
The role of horizontal variability in air-sea interaction
[AD-A280561] p 4476 N94-37047
Experiment on rapidly intensifying cyclones over the Atlantic
[AD-A280365] p 4473 N94-37180
ATMOSPHERIC BOUNDARY LAYER
Turbulent transfer in the marine planetary boundary layer
[AD-A280549] p 4476 N94-37038
On the development of boundary layer secondary circulations resulting from horizontally varying surface heat flux
[DE94-011234] p 4472 N94-37048
ATMOSPHERIC CHEMISTRY
Atmospheric gas
[DE94-007439] p 4465 N94-37187
Modeling atmospheric concentrations and deposition of Hg
[DE94-012633] p 4467 N94-37440
ATMOSPHERIC CIRCULATION
On the development of boundary layer secondary circulations resulting from horizontally varying surface heat flux
[DE94-011234] p 4472 N94-37048
Site Scientific Mission Plan for the Southern Great Plains CART site, January - June 1994
[DE94-012114] p 4474 N94-37394
ATMOSPHERIC COMPOSITION
Accelerated line-by-line calculations for the radiative transfer of trace gases related to climate studies
[DE94-004404] p 4464 N94-36552
Long-range mesoscale modeling of pollutant transport for the European Tracer EXperiment (ETEX)
[DE94-010820] p 4465 N94-37093
Atmospheric gas
[DE94-007439] p 4465 N94-37187
Modeling of trace constituent transport with the University of Wisconsin global isentropic-sigma model
[DE94-012729] p 4466 N94-37288
Surface-layer response over shrub-steppe canopy during springtime
[DE94-011235] p 4468 N94-37624
Tropospheric radiative forcing of CH4
[DE94-011628] p 4468 N94-37631
ATMOSPHERIC CORRECTION
Adaptive optics for laser beamforming in the atmosphere p 4393 N94-36621
ATMOSPHERIC EFFECTS
Project report: Aircraft — atmospheric effects of stratospheric aircraft
[DE94-011759] p 4465 N94-37155
Jet aircraft engine exhaust emissions database development: Year 1990 and 2015 scenarios
[NASA-CR-4613] p 4466 N94-37252
Stratospheric emissions effects database development
[NASA-CR-4592] p 4467 N94-37607
ATMOSPHERIC GENERAL CIRCULATION MODELS
Measurements and modeling of the effect of convective clouds on the upper tropospheric moisture budget
[NASA-TM-109894] p 4473 N94-37371
Proceedings of the Third Atmospheric Radiation Measurement (ARM) Science Team Meeting
[DE94-011194] p 4467 N94-37454
Simple ocean carbon cycle models
[DE94-011745] p 4477 N94-37494
A stratiform cloud parameterization for general circulation models
[DE94-011442] p 4474 N94-37566
ATMOSPHERIC IONIZATION
Controlled atmospheric breakdown: Applications and research opportunities
[AD-A278584] p 4464 N94-36973
ATMOSPHERIC MODELS
Paleoclimate validation of a numerical climate model
[DE94-009287] p 4463 N94-36470
Accelerated line-by-line calculations for the radiative transfer of trace gases related to climate studies
[DE94-004404] p 4464 N94-36552
Long-range mesoscale modeling of pollutant transport for the European Tracer EXperiment (ETEX)
[DE94-010820] p 4465 N94-37093
Modeling of trace constituent transport with the University of Wisconsin global isentropic-sigma model
[DE94-012729] p 4466 N94-37288
Representing the influence of subgrid topography on hydrology
[DE94-004595] p 4474 N94-37379
Modeling atmospheric concentrations and deposition of Hg
[DE94-012633] p 4467 N94-37440
Factors influencing the parameterization of anvil clouds within GCMs
[DE94-010794] p 4475 N94-37621
Surface-layer response over shrub-steppe canopy during springtime
[DE94-011235] p 4468 N94-37624
Tropospheric radiative forcing of CH4
[DE94-011628] p 4468 N94-37631
Atmospheric structure simulation: An ARMA model for smooth isotropic two-dimensional geophysical power spectra
[AD-A280476] p 4470 N94-37649
ATMOSPHERIC MOISTURE
Accelerated line-by-line calculations for the radiative transfer of trace gases related to climate studies
[DE94-004404] p 4464 N94-36552
Measurements and modeling of the effect of convective clouds on the upper tropospheric moisture budget
[NASA-TM-109894] p 4473 N94-37371
Tropospheric radiative forcing of CH4
[DE94-011628] p 4468 N94-37631
ATMOSPHERIC PHYSICS
High Altitude Plasma Instrument (HAPI) data analysis
[NASA-CR-189360] p 4469 N94-36949
Atmospheric structure simulation: An ARMA model for smooth isotropic two-dimensional geophysical power spectra
[AD-A280476] p 4470 N94-37649
ATMOSPHERIC RADIATION
ARM: A climate process observatory
[DE94-007473] p 4463 N94-36477
Two-channel microwave radiometer for observations of total column precipitable water vapor and cloud liquid water path
[DE94-007480] p 4471 N94-36479
Site Scientific Mission Plan for the Southern Great Plains CART site, January - June 1994
[DE94-012114] p 4474 N94-37394
Proceedings of the Third Atmospheric Radiation Measurement (ARM) Science Team Meeting
[DE94-011194] p 4467 N94-37454
An experimental and numerical study of boundary layer structure over areas of inhomogeneous sensible heat fluxes
[DE94-011441] p 4474 N94-37565
Tropospheric radiative forcing of CH4
[DE94-011628] p 4468 N94-37631
ATMOSPHERIC SOUNDING
UAV's in climate research: The ARM Unmanned Aerospace Vehicle Program
[DE94-011753] p 4465 N94-37154
ATMOSPHERIC TEMPERATURE
Accelerated line-by-line calculations for the radiative transfer of trace gases related to climate studies
[DE94-004404] p 4464 N94-36552

ATMOSPHERIC TURBULENCE
Turbulent transfer in the marine planetary boundary layer
[AD-A280549] p 4476 N94-37038
ATOMIC CLOCKS
Spontaneous force optical traps
[AD-A280574] p 4514 N94-37041
ATOMIC CLUSTERS
Low-energy electron collisions with metal clusters: Electron capture and cluster fragmentation
[DE94-003623] p 4512 N94-36516
ATOMIC COLLISIONS
Computational chemistry research
[NASA-CR-196120] p 4406 N94-36989
ATOMIC ENERGY LEVELS
MCHF calculations of isotope shifts. 1: Program implementation and test runs. 2: Large-scale active space calculations
[DE94-013036] p 4518 N94-37313
ATOMIC EXCITATIONS
Ionization balance and gain calculations for neon-like selenium x-ray laser plasmas
[DE94-012590] p 4530 N94-37437
ATOMIC FORCE MICROSCOPY
Combined atomic force and scanning reflection interference contrast microscopy
[AD-A280341] p 4514 N94-37034
A new, optical-lever based atomic force microscope
[AD-A280524] p 4524 N94-37110
ATOMIC PHYSICS
Physics Division annual review, 1 April 1992 - 31 March 1993
[DE94-002497] p 4512 N94-36513
Direct photoionization of excited helium
[DE94-618732] p 4516 N94-37097
Ionization balance and gain calculations for neon-like selenium x-ray laser plasmas
[DE94-012590] p 4530 N94-37437
ATOMIC RECOMBINATION
Studies of the thermal and optical responses of H atoms in solid H2
[NASA-CR-196114] p 4514 N94-36964
ATOMIC STRUCTURE
Atomic and electronic structure of metals and alloys: Rare earths, ultrathin films and surface alloys
[DE94-011581] p 4516 N94-37113
Pair correlations in crystalline solid solutions
[DE94-012319] p 4535 N94-37212
Modelling of surfaces. Part 1: Monatomic metallic surfaces using equivalent crystal theory
[NASA-TM-106680] p 4419 N94-37459
Theoretical studies of the transport properties in compound semiconductors
[NASA-CR-196109] p 4439 N94-37501
Atomic resolution characterization of a SrTiO3 grain boundary in the STEM
[DE94-011469] p 4538 N94-37545
ATTENUATION
Attenuating the disorienting effects of head movement during whole-body rotation using a visual reference: Further tests of a predictive hypothesis p 4482 N94-37276
ATTENUATORS
Three-stage attenuation using Glan-Thompson prisms
[AD-A280481] p 4525 N94-37350
ATTITUDE (INCLINATION)
Optical position measurement for a large gap magnetic suspension system: Design and performance analysis
[NASA-TP-3438] p 4447 N94-36946
Creation of a virtual world to study human spatial perception during sustained acceleration
p 4484 N94-37268
ATTITUDE CONTROL
Inertial pseudo star reference unit
p 4394 N94-36625
Creation of a virtual world to study human spatial perception during sustained acceleration
p 4484 N94-37268
ATTITUDE INDICATORS
The use of a tactile interface to convey position and motion perceptions p 4486 N94-37281
AUDITORY DEFECTS
Blast overpressure studies with animals and man
[AD-A280240] p 4480 N94-37118
AUDITORY PERCEPTION
3D sound experimental approach: Methodology and preliminary results p 4486 N94-37280
Human factors for flight deck certification personnel
[AD-A280477] p 4487 N94-37347
AUDITORY SIGNALS
Segment-based acoustic models for continuous speech recognition
[AD-A280332] p 4434 N94-37032
AUGER SPECTROSCOPY
AEM and AES of radiation-induced segregation in proton-irradiated stainless steels
[DE94-012734] p 4418 N94-37398
AURORAL ARCS
Dynamics explorer data analysis
[NASA-CR-196141] p 4469 N94-37016
AURORAL ZONES
High Altitude Plasma Instrument (HAPI) data analysis
[NASA-CR-189360] p 4469 N94-36949
Dynamics explorer data analysis
[NASA-CR-196141] p 4469 N94-37016
AURORAS
High Altitude Plasma Instrument (HAPI) data analysis
[NASA-CR-189360] p 4469 N94-36949
AUSTENITE
Mechanical performance of austempered ductile iron
[AD-A280452] p 4420 N94-37758
AUSTENITIC STAINLESS STEELS
Elemental mapping of segregation in stainless steels with an imaging filter
[DE94-012659] p 4417 N94-37304
Transient thermal and dynamic stresses in strongback-design blankets
[DE94-012639] p 4530 N94-37441
Residual stresses in a multi-pass weld in an austenitic stainless steel plate before and after thermal stress relief
[DE94-013278] p 4420 N94-37548
AUTOMATIC CONTROL
An empirical comparison of a dynamic software testability metric to static cyclomatic complexity
p 4491 N94-36498
An algorithm for the automatic control of boundary layer flow
[ISVR-TR-233] p 4442 N94-36817
Automatic, self-adaptive control of unfold transformations
[DE94-012455] p 4504 N94-37247
Technology demonstration of space intravehicular automation and robotics
[NASA-TM-109138] p 4501 N94-37589
AUTOMATIC WEATHER STATIONS
AWOS Data Acquisition System (ADAS) Operational Test and Evaluation (OT/E) integration and OT/E operational test report
[AD-A280492] p 4473 N94-37143
AUTOMATION
NIPER Lab WARDEN: Description and LabVIEW executable code of a general-purpose laboratory-automation program
[DE94-000125] p 4492 N94-36698
AUTOMOBILE ENGINES
Potential benefits of oxygen-enriched intake air in a vehicle powered by a spark-ignition engine
[DE94-013452] p 4451 N94-37070
Technical evaluation and assessment of CNG/LPG bi-fuel and flex-fuel vehicle viability
[DE94-006925] p 4451 N94-37408
Advanced Turbine Technology Applications Project (ATTAP)
[NASA-CR-195367] p 4452 N94-37763
AUTOMOBILE FUELS
Alternative fuel information: Facts about CNG and LPG conversion
[DE94-006888] p 4429 N94-37402
Alternative fuel information: Glossary
[DE94-006889] p 4429 N94-37403
Alternative fuel information: State alternative fuel laws and incentives
[DE94-006892] p 4429 N94-37404
Technical evaluation and assessment of CNG/LPG bi-fuel and flex-fuel vehicle viability
[DE94-006925] p 4451 N94-37408
Comparative alternative/clean fuels provisions of the Clean Air Act Amendments of 1990 and the Energy Policy Act of 1992
[DE94-006887] p 4429 N94-37426
Advanced Turbine Technology Applications Project (ATTAP)
[NASA-CR-195367] p 4452 N94-37763
AUTOMORPHISMS
Phase transitions in crystalline solids 1
[DE94-619029] p 4532 N94-36542
AUTONOMOUS NAVIGATION
Adaptive multisensor fusion for the perception and interpretation of outdoor robot scenes
[PB94-170719] p 4499 N94-36535
Two-axis camera platform for machine vision
p 4394 N94-36628
Global Positioning System Synchronized Active Light Autonomous Docking System
[NASA-CASE-MFS-28853-1] p 4395 N94-36825
AVIATION METEOROLOGY
Toward a new National Weather Service: Weather for those who fly p 4472 N94-36947
AVIONICS
ICAAS piloted simulation results p 4393 N94-36617
Preload release mechanism
[NASA-CASE-MSC-22327-1] p 4450 N94-36839
Space Generic Open Avionics Architecture (SGOAA) standard specification
[NASA-CR-188290] p 4387 N94-36933
Advanced information processing system: The Army Fault-Tolerant Architecture detailed design overview
[NASA-CR-194924] p 4497 N94-36962
AXIAL LOADS
Sub-ply level scaling approach investigated for graphite-epoxy composite beam columns
p 4458 N94-37798
AZO COMPOUNDS
Optically induced high efficiency gratings in azo polymer films
[AD-A280505] p 4423 N94-37147
Azobenzene-containing polymers: Some optoelectronic properties
[AD-A280448] p 4424 N94-37185
Thermal cis-trans isomerization rates of azobenzenes bound in the side chain of some copolymers and blends
[AD-A280451] p 4424 N94-37227

B

B-50 AIRCRAFT
Replacement of silicone polymer A with silicone polymer B and the subsequent characterization of the new cellular silicone materials
[DE94-010105] p 4421 N94-36474
BACKGROUND RADIATION
Magnetic Earth Ionosphere Resonant Frequencies (NASA-MEIRF Project)
[NASA-CR-196303] p 4435 N94-37461
BACKSCATTERING
Basic studies in plasma wave interactions
[AD-A280465] p 4527 N94-37139
Effect of the stimulated Brillouin backscattering on self-focusing threshold
[DE94-008678] p 4510 N94-37536
BACTERIA
Indicators for sulfate-reducing bacteria in microbiologically influenced corrosion
[AD-A278914] p 4477 N94-36522
United States Air Force Summer Research Program, 1993. Volume 7: Armstrong Laboratory
[AD-A278655] p 4550 N94-36975
BACTERIAL DISEASES
Rapid susceptibility testing of Mycobacterium avium complex and Mycobacterium tuberculosis isolated from AIDS patients
[NASA-CR-196268] p 4478 N94-36996
BACTERIOLOGY
United States Air Force Summer Research Program, 1993. Volume 7: Armstrong Laboratory
[AD-A278655] p 4550 N94-36975
BALANCE
Determination of density of mass standards: Requirement and method
[PB94-163078] p 4508 N94-36718
Electronic balance and some gravimetric applications (the density of solids and liquids, pycnometry and mass)
[PB94-163052] p 4446 N94-36719
BALANCING
Postural strategies for the continuous control of static and dynamic balance in man
[PB94-184678] p 4487 N94-37812
BALLOONING MODES
Confinement improvement in H-mode-like plasmas in helical systems
[DE94-727619] p 4528 N94-37231
Theory of anomalous transport in H-mode plasmas
[DE94-727546] p 4531 N94-37485
Self-sustained turbulence and L-mode confinement in toroidal plasmas
[DE94-748497] p 4532 N94-37734
BAND STRUCTURE OF SOLIDS
A rejection method for selection of scattered states
[DE94-012232] p 4517 N94-37209
BANDPASS FILTERS
Phase shifter for directly sampled bandpass signals
[AD-D016320] p 4440 N94-37840
BANDWIDTH
Raman scattering of variable bandwidth KrF radiation in long air paths
[DE94-012912] p 4449 N94-37495
BARENTS SEA
Signal processing for the 1992 Barents Sea tomography experiment
[AD-A278580] p 4476 N94-36971
BARIUM COMPOUNDS
Effect of thermal annealing on grain boundary chemistry of polycrystalline TlBa2Ca2Cu3O(y) films
[DE94-011464] p 4538 N94-37569

BARIUM TITANATES
The MBE growth and optical quality of BaTiO3 and SrTiO3 thin films on MgO
[DE94-011468] p 4538 N94-37570

BARYONS
High baryon density from relativistic heavy ion collisions
[DE94-003894] p 4511 N94-36460
Relativistic di-quark model of p p-bar yields K(+)K(-) reaction
[DE94-618519] p 4514 N94-37063
About existence of a baryon with the 3.52 GeV/c2 mass
[DE94-621641] p 4519 N94-37414
Search for the H dibaryon by Xi(-) capture on the deuteron
[DE94-011733] p 4520 N94-37672
Hadron production in S+nucleus collisions at 200 GeV/nucleon
[DE94-011344] p 4520 N94-37715

BAYES THEOREM
Dealing with uncertainty about item parameters: Expected response functions
[AD-A280610] p 4506 N94-36728
Probability-based inference in cognitive diagnosis
[AD-A280553] p 4506 N94-36732
Virtual representation of IID observations in Bayesian belief networks
[AD-A280552] p 4507 N94-37046

BAYS (TOPOGRAPHIC FEATURES)
Measuring the upper profile of sea ice in the Bay of Bothnia with a laser profilometer
[PB94-184561] p 4477 N94-37855

BEAM CURRENTS
Production of high current H(-) beams in a cesium seeded volume negative ion source equipped with PG filter
[DE94-718962] p 4522 N94-37463

BEAM INTERACTIONS
Suppression of beam-break-up in a standing wave free electron laser two-beam accelerator
[DE94-011348] p 4521 N94-37200

BEAMFORMING
Adaptive optics for laser beamforming in the atmosphere p 4393 N94-36621
Signal processing for the 1992 Barents Sea tomography experiment
[AD-A278580] p 4476 N94-36971
Proceedings of the Workshop on Negative Ion Formation and Beam Handling
[DE94-746683] p 4518 N94-37360

BEAMS (RADIATION)
United States Air Force Summer Research Program, 1993. Volume 13: Phillips Laboratory
[AD-A278657] p 4550 N94-36977

BEAMS (SUPPORTS)
Detection of delaminations in composite beams using piezoelectric sensors
[NASA-TM-106611] p 4403 N94-36956
Sub-ply level scaling approach investigated for graphite-epoxy composite beam columns
p 4458 N94-37798

BENDING MOMENTS
Strength evaluation of socket joints
[NASA-CR-4608] p 4389 N94-37259

BENZENE
California residential indoor air quality study. Volume 1: Methodology and descriptive statistics
[PB94-166048] p 4464 N94-36994

BETATRONS
Tune modulation due to gradient ripple and the dynamic aperture
[DE94-011922] p 4524 N94-37157
Suppression of beam-break-up in a standing wave free electron laser two-beam accelerator
[DE94-011348] p 4521 N94-37200

BETHE-SALPETER EQUATION
Wick-Cutkovsky model: An introduction
[DE94-618365] p 4504 N94-37170
Numerical solution to the boundary-value problem for the Bethe-Salpeter equation with quadratically rising potential
[DE94-621606] p 4504 N94-37175

BIBLIOGRAPHIES
Publications of the Jet Propulsion Laboratory, 1992
[NASA-CR-196125] p 4542 N94-37008
Aeronautical engineering: A continuing bibliography with indexes (supplement 307)
[NASA-SP-7037(307)] p 4381 N94-37117
Catalog of data bases and reports
[DE94-012230] p 4466 N94-37208
Bibliography of work on the photocatalytic removal of hazardous compounds from water and air
[DE94-006906] p 4467 N94-37405

BICRYSTALS
Atomic resolution characterization of a SrTiO3 grain boundary in the STEM
[DE94-011469] p 4538 N94-37545

BIMETALS
Photodissociation and spectroscopy of gas phase bimetallic clusters
[DE94-012607] p 4419 N94-37438

BINARY ALLOYS
Use of rotation to suppress thermosolutal convection in directionally solidified binary alloys
[NASA-CR-196372] p 4415 N94-36811
Pair correlations in crystalline solid solutions
[DE94-012319] p 4535 N94-37212
Scanning x-ray diffraction: A technique with high compositional resolution for studying phase formation in co-deposited thin films
[DE94-011496] p 4420 N94-37516

BINARY DATA
Adaptable binary programs
[AD-A280243] p 4494 N94-37119

BINARY MIXTURES
Stability and dynamics of spatio-temporal structures
[DE94-013035] p 4412 N94-37491

BINARY STARS
The winds of cataclysmic variables
[DE94-010897] p 4548 N94-37164

BINARY SYSTEMS (MATERIALS)
Metal-carbon nanostructures
[DE94-009177] p 4400 N94-36509

BIOASSAY
Solid state fluorometer: Prototype development
[AD-A280321] p 4534 N94-37027

BIOASTRONAUTICS
Estimates of cellular mutagenesis from cosmic rays
[NASA-TP-3453] p 4481 N94-37282

BIOCHEMISTRY
Indicators for sulfate-reducing bacteria in microbiologically influenced corrosion
[AD-A278914] p 4477 N94-36522
Rapid susceptibility testing of Mycobacterium avium complex and Mycobacterium tuberculosis isolated from AIDS patients
[NASA-CR-196268] p 4478 N94-36996

BIODEGRADATION
Indicators for sulfate-reducing bacteria in microbiologically influenced corrosion
[AD-A278914] p 4477 N94-36522
Biological determinants of photobioreactor design
[DE94-011665] p 4468 N94-37740

BIODYNAMICS
On nature's scaling effects p 4459 N94-37803
Postural strategies for the continuous control of static and dynamic balance in man
[PB94-184678] p 4487 N94-37812

BIOINSTRUMENTATION
Methodologies to determine forces on bones and muscles of body segments during exercise, employing compact sensors suitable for use in crowded space vehicles
[NASA-CR-196272] p 4487 N94-37458

BIOLOGICAL EFFECTS
Behavioral performance in monkeys exposed to TEMPO high-peak-power microwave pulses at 3 GHz
[AD-A280551] p 4478 N94-37045
ELF Communications System ecological monitoring program: Electromagnetic field measurements and engineering support
[AD-A280489] p 4481 N94-37353
Aerospace medicine and biology: A continuing bibliography with indexes (supplement 392)
[NASA-SP-7011(392)] p 4482 N94-37445
Studying of ion implantation effect on the biology in China
[DE94-620692] p 4479 N94-37535
Investigation of exposure to Extremely Low Frequency (ELF) magnetic and electric fields: Ongoing animals studies
[DE94-011239] p 4480 N94-37625

BIOMASS
Integrated gasification combined cycle and steam injection gas turbine powered by biomass joint-venture evaluation
[DE94-006905] p 4461 N94-36740

BIOMASS ENERGY PRODUCTION
Estimates of US biomass energy consumption 1992
[DE94-011458] p 4463 N94-37567

BIONICS
Opportunities for innovation: Biotechnology
[PB94-157831] p 4478 N94-36720

BIOREACTORS
Biological determinants of photobioreactor design
[DE94-011665] p 4468 N94-37740

BIOSYNTHESIS
Conversion of acetic acid to methane by thermophiles
[DE94-012478] p 4479 N94-37434

BIOTECHNOLOGY
Opportunities for innovation: Biotechnology
[PB94-157831] p 4478 N94-36720
Three dimensional optic tissue culture and process
[NASA-CASE-MSC-22368-1] p 4478 N94-36765
Status review and accomplishments of the Materials Research Center at the University of Pittsburgh
[AD-A280422] p 4399 N94-37214

BIPOLAR TRANSISTORS
Correlation of hot-carrier stress and ionization induced degradation in bipolar transistors
[DE94-007289] p 4532 N94-36540

BIREFRINGENCE
High average power pulsed phase conjugate laser with birefringence correction
[DE94-012062] p 4447 N94-37160
Final report on spectral broadening by cross-phase modulation in linearly birefringent optical fibers
[DE94-010406] p 4524 N94-37191

BIRKELAND CURRENTS
High Altitude Plasma Instrument (HAPI) data analysis
[NASA-CR-189360] p 4469 N94-36949

BISMUTH OXIDES
Development of high Tc (greater than 100 K) Bi, Tl and Y-based materials as superconducting circuit elements
[NASA-CR-196276] p 4534 N94-37103

BL LACERTAE OBJECTS
The BL LAC phenomenon: X-ray observations of transition objects and determination of the x-ray spectrum of a complete sample of flat-spectrum radio sources
[NASA-CR-195951] p 4546 N94-36688
Correlated radio and optical variations in a sample of AGN. A simultaneous radio-optical flare in BL lacertae
[PB94-179181] p 4548 N94-37834

BLADE SLAP NOISE
Forward sweep, low noise rotor blade
[NASA-CASE-LAR-14569-1] p 4386 N94-36767

BLADE TIPS
Experimental measurements and analytical analysis related to gas turbine heat transfer. Part 1: Time-averaged heat-flux and surface-pressure measurements on the vanes and blades of the SSME fuel-side turbine and comparison with prediction. Part 2: Phase-resolved surface-pressure and heat-flux measurements on the first blade of the SSME fuel-side turbine
[NASA-CR-196296] p 4442 N94-36969

BLADE-VORTEX INTERACTION
Forward sweep, low noise rotor blade
[NASA-CASE-LAR-14569-1] p 4386 N94-36767

BLANKETS (FUSION REACTORS)
The logic behind thick, liquid-walled, fusion concepts
[DE94-012678] p 4528 N94-37307
Transient thermal and dynamic stresses in strongback-design blankets
[DE94-012639] p 4530 N94-37441
Two-dimensional over-all neutronics analysis of the ITER device
[DE94-718963] p 4530 N94-37464
Characterization of nuclear transmutations in materials irradiated test facilities
[DE94-013309] p 4420 N94-37552

BLANKS
California residential indoor air quality study. Volume 1: Methodology and descriptive statistics. Appendix
[PB94-166055] p 4464 N94-36995

BLOCK DIAGRAMS
NIPER Lab WARDEN: Descriptive panels and diagrams for NIPER Lab WARDEN software, volume 2
[DE94-000126] p 4493 N94-36699

BLOCKING
The life cycles of intense cyclonic and anticyclonic circulation systems observed over oceans
[NASA-CR-196271] p 4473 N94-37294

BLOOD
Evaluation of dried storage of platelets for transfusion: Physiologic integrity and hemostatic functionality
[AD-A280665] p 4480 N94-36764
Method and apparatus for the collection, storage, and real time analysis of blood and other bodily fluids
[NASA-CASE-MSC-22463-1] p 4480 N94-36766
Hypobaric decompression sickness model development. Part 1: Diffusion of inert gas from a viscoelastic fluid (blood) into an expanding gas phase
[AD-A280298] p 4481 N94-37124

BLOOD PLASMA
United States Air Force Summer Research Program, 1993. Volume 6: Arnold Engineering Development Center, Frank J. Seiler Research Laboratory and Wilford Hall Medical Center
[AD-A278697] p 4551 N94-36982

BODY CENTERED CUBIC LATTICES
Modelling of surfaces. Part 1: Monatomic metallic surfaces using equivalent crystal theory
[NASA-TM-106680] p 4419 N94-37459

BODY FLUIDS
Method and apparatus for the collection, storage, and real time analysis of blood and other bodily fluids
[NASA-CASE-MSC-22463-1] p 4480 N94-36766
BODY-WING CONFIGURATIONS
Automatic computation of Euler-marching and subsonic grids for wing-fuselage configurations
[NASA-TM-4573] p 4383 N94-36950
BOEING 737 AIRCRAFT
An empirical comparison of a dynamic software testability metric to static cyclomatic complexity
p 4491 N94-36498
BOILERS
The influence of fin height and wall conductivity on integral-fin tubes during steam condensation
[AD-A280597] p 4539 N94-36725
Robotic weld overlay coatings for erosion control
[DE94-013477] p 4417 N94-37116
BOLTED JOINTS
Experimental observations of scale effects on bonded and bolted joints in composite structures
p 4458 N94-37801
BOLTZMANN TRANSPORT EQUATION
Microscopic theory of the dielectric response of highly dispersive biological media
[AD-A280516] p 4516 N94-37109
BONDED JOINTS
The cyclic fatigue behaviour of adhesive joints
[AD-A280453] p 4456 N94-37186
Experimental observations of scale effects on bonded and bolted joints in composite structures
p 4458 N94-37801
BONDING
Determination of interface structure and bonding at atomic resolution in the stem
[DE94-011466] p 4517 N94-37238
BONES
Methodologies to determine forces on bones and muscles of body segments during exercise, employing compact sensors suitable for use in crowded space vehicles
[NASA-CR-196272] p 4487 N94-37458
BORN APPROXIMATION
The angular and energy distributions of ejected electrons in electron-impact ionization of helium
[DE94-618748] p 4519 N94-37528
BORON
Production of amorphous metal layers using ion implantation and investigation of the related modification of some surface properties
[DE94-617509] p 4414 N94-36541
Mechanical behavior and phase stability of NiAl-based shape memory alloys
[DE94-012336] p 4419 N94-37420
BOSONS
Precise determination of the weak mixing angle from a measurement of ALR in e(+)e(-) yields Z0
[DE94-013355] p 4515 N94-37085
CDF results on electroweak physics
[DE94-011750] p 4520 N94-37674
Proceedings of the Workshop on TRISTAN Physics at High Luminosities
[DE94-737969] p 4523 N94-37727
BOUNDARY CONDITIONS
Cost-effective computations with boundary interface operators in elliptic problems
[DE94-621506] p 4503 N94-37098
Solving the two-dimensional Schroedinger equation in self-consistent basis
[DE94-621535] p 4504 N94-37174
Investigation of ultrasonic surface wave interaction with porous saturated rocks
[DE94-013378] p 4469 N94-37177
An experimental and numerical study of boundary layer structure over areas of inhomogeneous sensible heat fluxes
[DE94-011441] p 4474 N94-37565
BOUNDARY LAYER CONTROL
An algorithm for the automatic control of boundary layer flow
[ISVR-TR-233] p 4442 N94-36817
Controlling forebody asymmetries in flight: Experience with boundary layer transition strips
[NASA-TM-4595] p 4383 N94-36944
Supersonic laminar flow control research
[NASA-CR-196260] p 4384 N94-37511
BOUNDARY LAYER FLOW
An algorithm for the automatic control of boundary layer flow
[ISVR-TR-233] p 4442 N94-36817
Unsteady flow field of large-amplitude pitching airfoils
[AD-A280444] p 4383 N94-37219
Evolution of turbulent fields in explosions
[DE94-010405] p 4444 N94-37390
BOUNDARY LAYER SEPARATION
Unsteady flow field of large-amplitude pitching airfoils
[AD-A280444] p 4383 N94-37219
BOUNDARY LAYER STABILITY
Supersonic laminar flow control research
[NASA-CR-196260] p 4384 N94-37511
BOUNDARY LAYER TRANSITION
Preliminary analysis for a Mach 8 crossflow transition experiment on the Pegasus (R) space booster
[NASA-TM-104272] p 4381 N94-36648
Holt film wall shear instrumentation for boundary layer transition research
[NASA-CR-196040] p 4443 N94-37060
Supersonic laminar flow control research
[NASA-CR-196260] p 4384 N94-37511
BOUNDARY LAYERS
Evolution of turbulent fields in explosions
[DE94-010405] p 4444 N94-37390
An experimental and numerical study of boundary layer structure over areas of inhomogeneous sensible heat fluxes
[DE94-011441] p 4474 N94-37565
BOUNDARY VALUE PROBLEMS
Theoretical investigations of chaotic dynamics
[AD-A280325] p 4507 N94-37028
Cost-effective computations with boundary interface operators in elliptic problems
[DE94-621506] p 4503 N94-37098
Numerical solution to the boundary-value problem for the Bethe-Salpeter equation with quadratically rising potential
[DE94-621606] p 4504 N94-37175
BRAIDED COMPOSITES
A comparison of graphite/epoxy tape laminates and 2-D braided composites mechanical properties
[NASA-CR-4610] p 4420 N94-37582
BRAYTON CYCLE
Preliminary design for a reverse Brayton cycle cryogenic cooler
[NASA-CR-189341] p 4461 N94-36805
BREAKING
Canopy breaking device
[AD-D016294] p 4385 N94-37767
BRECCIA
Vent processes during the 1912 eruption at Novarupta, Katmai National Park, Alaska
[DE94-010740] p 4468 N94-36451
BREEDING (REPRODUCTION)
Ground and space flight experiments of the effects of light, sound and/or temperature on animals
[NASA-CR-196102] p 4478 N94-36986
BREMSSTRAHLUNG
The t(anti t)(gamma) background to pp (yields) W(gamma) + X at the SSC
[DE94-001386] p 4512 N94-36526
BRILLOUIN EFFECT
Effect of the stimulated Brillouin backscattering on self-focusing threshold
[DE94-008678] p 4510 N94-37536
BRILLOUIN ZONES
A rejection method for selection of scattered states
[DE94-012232] p 4517 N94-37209
BROADBAND
Raman scattering of variable bandwidth KrF radiation in long air paths
[DE94-012912] p 4449 N94-37495
BROADCASTING
System for broadcasting marker beacon signals and processing responses from seeking entities
[AD-D016313] p 4385 N94-37839
BROKEN SYMMETRY
Non-equilibrium evolution of the disoriented chiral condensate in heavy-ion collisions
[DE94-012897] p 4522 N94-37310
Testing violation of CPT and quantum mechanics in the K(0) - bar-K(0) system
[DE94-012057] p 4539 N94-37366
BRONZES
Activities of the Tandem Accelerator Center, University of Tsukuba
[DE94-748687] p 4522 N94-37237
BROWNIAN MOVEMENTS
Quantum harmonic Brownian motion in a general environment: A modified phase-space approach
[DE94-003249] p 4508 N94-36560
BSCCO SUPERCONDUCTORS
Development of high Tc (greater than 100 K) Bi, Tl and Y-based materials as superconducting circuit elements
[NASA-CR-196276] p 4534 N94-37103
Fabrication and properties of Ag-clad Bi-2223 conductors and magnets
[DE94-011502] p 4438 N94-37111
BUBBLE CHAMBERS
A freon-filled, holographic bubble chamber as a high energy photon burst spectrometer
[DE94-011645] p 4446 N94-37723
BUBBLES
Determination of the dispersion constant in a constrained vapor bubble thermosyphon
[NASA-CR-196124] p 4442 N94-36992
Hypobaric decompression sickness model development. Part 1: Diffusion of inert gas from a viscoelastic fluid (blood) into an expanding gas phase
[AD-A280298] p 4481 N94-37124
Flow visualization for Lagrangian particle methods
[DE94-010757] p 4443 N94-37195
A freon-filled, holographic bubble chamber as a high energy photon burst spectrometer
[DE94-011645] p 4446 N94-37723
BUFFER STORAGE
SACS: A cache simulator incorporating timing analysis with buffer and memory management
[AD-A280472] p 4494 N94-37230
BUMPERS
Permanent superconducting magnets for space applications
[NASA-CR-196293] p 4439 N94-37634
BUOYANCY
A combined experiment/computational study of flow in turbine blade cooling passage
[NASA-CR-4584] p 4442 N94-36957
Coupled Marangoni-Benard/Rayleigh-Benard instability with temperature dependent viscosity
[NASA-TM-106646] p 4444 N94-37507
BURAN SPACE SHUTTLE
JPRS report: Central Eurasia. Aviation and cosmonautics, No. 4, April 1993
[JPRS-UAC-94-003] p 4391 N94-36999
BURN-IN
Role of burn-in during qualification testing
[DE94-007864] p 4439 N94-37513
BURNING RATE
Rich methane/air flames: Burning velocities, extinction limits, and flammability limit
[DE94-004340] p 4407 N94-36462
Rich flammability limits in CH3OH/CO/diluent mixtures
[DE94-004341] p 4407 N94-36482
BURST TESTS
Mitigation of harmful effects of welds in zirconium alloy components
[DE94-619033] p 4414 N94-36543
BUTANES
The hydrogenolysis and isomerization of light hydrocarbons over Pt catalysts
[DE94-013142] p 4410 N94-37296
BUTT JOINTS
Tensile strength of simulated and welded butt joints in W-Cu composite sheet
[NASA-TM-4584] p 4405 N94-37460

C

CABLES (ROPES)
Stability analysis of an F/A-18 E/F cable mount model
[NASA-TM-108989] p 4386 N94-37636
CALCIUM
Mineralogy and metallurgical properties of iron ore sinter based on magnetite fines
[DE94-763309] p 4414 N94-36525
CALCIUM COMPOUNDS
Effect of thermal annealing on grain boundary chemistry of polycrystalline TlBa2Ca2Cu3O(y) films
[DE94-011464] p 4538 N94-37569
High T(sub c) copper-oxide superconductors comprising Tl-Sr-Ca-Cu-O
[AD-D016307] p 4538 N94-37776
CALCULATORS
Interactive calculator for use with multi-dimensional netCDF files
[DE94-007477] p 4545 N94-37348
CALIBRATING
SeaWiFS technical report series. Volume 20: The SeaWiFS bio-optical archive and storage system (SeaBASS), part 1
[NASA-TM-104566-VOL-20-PT-1] p 4475 N94-36958
NOAA polar satellite calibration: A system description
[NOAA-TR-NESDIS-77] p 4396 N94-37009
Array element gain and phase estimation in the presence of interference
[AD-A280381] p 4434 N94-37162
Calibration and initial testing of a new hydraulic simulator
[AD-A280632] p 4390 N94-37163
NASA ER-2 Doppler radar reflectivity calibration for the CAMEX project
[NASA-TM-104611] p 4475 N94-37790
CALORIMETERS
First results from a prototype level-1 calorimeter trigger system for LHC, RD 27 (UK) collaboration
[PB94-167475] p 4436 N94-36532

Assess progress being made for the KTeV electromagnetic calorimeter crystal order in France
[DE94-009396] p 4533 N94-36746
Testing new technology for the heavy ion experiment at CERN
[DE94-004747] p 4521 N94-37220

CAMERAS
Two-axis camera platform for machine vision
p 4394 N94-36628
Hubble Space Telescope Wide Field and Planetary Camera 2 Instrument handbook, version 2.0
[NASA-CR-189368] p 4547 N94-36918

CANOPIES
Canopy breaking device
[AD-D016294] p 4385 N94-37767

CANOPIES (VEGETATION)
Surface-layer response over shrub-steppe canopy during springtime
[DE94-011235] p 4468 N94-37624

CANTILEVER BEAMS
The cyclic fatigue behaviour of adhesive joints
[AD-A280453] p 4456 N94-37186

CAPACITORS
A charge distribution analysis instrument for catalysis and material science applications
[DE94-011587] p 4438 N94-37241

CARBIDES
Metal-carbon nanostructures
[DE94-009177] p 4400 N94-36509
Novel carbon-ion fuel cells
[DE94-010716] p 4461 N94-36511

CARBON
Supersonic bare metal cluster beams
[DE94-010790] p 4532 N94-36454
Material and design considerations for the carbon armored ITER divertor
[DE94-737854] p 4530 N94-37415
Residual stress and Raman spectra of laser deposited highly-tetrahedral-coordinated-amorphous-carbon films
[DE94-012067] p 4426 N94-37537
Compilation of diamond-like carbon properties for barriers and hard coatings
[DE94-012139] p 4427 N94-37725

CARBON CYCLE
Response of plants and ecosystems to CO2 and climate change
[DE94-011583] p 4466 N94-37376
Simple ocean carbon cycle models
[DE94-011745] p 4477 N94-37494

CARBON DIOXIDE
Sintering of dioxide pellets in an oxidizing atmosphere (CO2)
[DE94-613046] p 4414 N94-36517
Accelerated line-by-line calculations for the radiative transfer of trace gases related to climate studies
[DE94-004404] p 4464 N94-36552
SIHTI: Energy and environmental technology
[DE94-763290] p 4464 N94-37007
The potential for control of carbon dioxide emissions from integrated gasification/combined-cycle systems
[DE94-012646] p 4465 N94-37100
Response of plants and ecosystems to CO2 and climate change
[DE94-011583] p 4466 N94-37376
Simple ocean carbon cycle models
[DE94-011745] p 4477 N94-37494
Tropospheric radiative forcing of CH4
[DE94-011628] p 4468 N94-37631

CARBON DIOXIDE CONCENTRATION
Climate uncertainty and the regional economic impacts of global climate change
[DE94-012242] p 4466 N94-37211
Biological determinants of photobioreactor design
[DE94-011665] p 4468 N94-37740

CARBON FIBERS
The development of short, high surface area activated carbon fibers
[AD-A280509] p 4404 N94-37105

CARBON MONOXIDE
Rich flammability limits in CH3OH/CO/diluent mixtures
[DE94-004341] p 4407 N94-36482
California residential indoor air quality study. Volume 1: Methodology and descriptive statistics
[PB94-166048] p 4464 N94-36994
Stratospheric emissions effects database development
[NASA-CR-4592] p 4467 N94-37607

CARBON TETRACHLORIDE
Accelerated line-by-line calculations for the radiative transfer of trace gases related to climate studies
[DE94-004404] p 4464 N94-36552

CARBON 12
Measurement and processing of gammas accompanying muon pairs in the reaction pi(-)C yields mu(+)mu(-) + gamma + X at 38 GeV
[DE94-617044] p 4512 N94-36523

CARBON-CARBON COMPOSITES
Basic solutions to carbon/carbon oxidation: Science and technology
[AD-A280447] p 4404 N94-37232
Carbon-carbon heat pipe testing and evaluation
[NASA-TM-106630] p 4405 N94-37318

CARBON-PHENOLIC COMPOSITES
Modeling of outgassing and matrix decomposition in carbon-phenolic composites
[NASA-CR-196319] p 4405 N94-37471

CARBONIZATION
The development of short, high surface area activated carbon fibers
[AD-A280509] p 4404 N94-37105

CARBORANE
Carborane-siloxane or silane-unsaturated hydrocarbon based polymers
[AD-D016220] p 4425 N94-37482
Carborane-(silane or siloxane)-unsaturated hydrocarbon based thermosetting polymers
[AD-D016311] p 4427 N94-37818

CARBOXYHEMOGLOBIN
Chemical and structural characterization of nitroaromatic adducts with hemoglobins
[AD-A280533] p 4480 N94-37089

CARIBBEAN REGION
NRL HF propagation measurements between Guadeloupe and Providenciales during the CRRES exercises
[DE94-012078] p 4435 N94-37393

CAROTENE
Picosecond laser induced electric field modulation of carotenoid absorption bands
[DE94-009692] p 4512 N94-36524

CARTESIAN COORDINATES
On automating domain connectivity for overset grids
[NASA-CR-196113] p 4493 N94-36920

CARTRIDGES
Ampoule failure sensor time response testing: Experiments 2 and 3
[NASA-TM-108458] p 4446 N94-36822

CASCADE RANGE (CA-OR-WA)
Analysis of deep seismic reflection and other data from the Southern Washington Cascades
[DE94-004075] p 4470 N94-37489

CASES (CONTAINERS)
Marker beacon case
[AD-D016322] p 4385 N94-37830

CASTING
Evaluating plastic assembly processes for high reliability applications using HAST and Assembly Test Chips
[DE94-010750] p 4439 N94-37363

CATACLYSMIC VARIABLES
The winds of cataclysmic variables
[DE94-010897] p 4548 N94-37164

CATALOGS (PUBLICATIONS)
Catalog of data bases and reports
[DE94-012230] p 4466 N94-37208
Engineering directorate technical facilities catalog
[NASA-TM-109895] p 4390 N94-37443

CATALYSIS
Tert-butylalumoxanes: Synthetic analogs for methylalumoxane (MAO) and new catalytic routes to polyolefins and polyketones
[AD-A280511] p 4399 N94-37106
An investigation of molybdenum and molybdenum oxide catalyzed hydrocarbon formation reactions
[DE94-013700] p 4409 N94-37132
Status review and accomplishments of the Materials Research Center at the University of Pittsburgh
[AD-A280422] p 4399 N94-37214
A charge distribution analysis instrument for catalysis and material science applications
[DE94-011587] p 4438 N94-37241
Superacid catalysis of light hydrocarbon conversion
[DE94-011132] p 4411 N94-37431
Tert-butylalumoxanes: Synthetic analogs for methylalumoxane (MAO) and new catalytic routes to polyolefins and polyketones
[AD-A280532] p 4399 N94-37650

CATALYSTS
Methyl chloride via oxyhydrochlorination of methane
[DE94-010691] p 4406 N94-36450
Direct catalytic decomposition of nitric oxide
[DE94-005025] p 4407 N94-36475
Scoping economics for the commercial manufacture of metallocene catalysts
[DE94-011526] p 4422 N94-37055
Tert-butylalumoxanes: Synthetic analogs for methylalumoxane (MAO) and new catalytic routes to polyolefins and polyketones
[AD-A280511] p 4399 N94-37106
An investigation of molybdenum and molybdenum oxide catalyzed hydrocarbon formation reactions
[DE94-013700] p 4409 N94-37132
The hydrogenolysis and isomerization of light hydrocarbons over Pt catalysts
[DE94-013142] p 4410 N94-37296
Thermodynamic and kinetic aspects of surface acidity
[DE94-012351] p 4411 N94-37372
Bibliography of work on the photocatalytic removal of hazardous compounds from water and air
[DE94-006906] p 4467 N94-37405
Development of durable high-temperature catalysts for natural gas combustion: Catalytic materials (CATMAT (trade name)) properties database
[PB94-171824] p 4412 N94-37462
Iron hydrous titanium oxide catalysts for the dehydrogenation of ethylbenzene to styrene
[DE94-010381] p 4412 N94-37542

CATALYTIC ACTIVITY
Iron hydrous titanium oxide catalysts for the dehydrogenation of ethylbenzene to styrene
[DE94-010381] p 4412 N94-37542

CATHODES
Sodium/nickel-chloride battery development
[DE94-011481] p 4437 N94-37053
Field emitter array RF amplifier development project. Cathode technology development. Phase 1
[AD-A280515] p 4437 N94-37108

CATIONS
Direct catalytic decomposition of nitric oxide
[DE94-005025] p 4407 N94-36475
Photochemistry without protons. Radical cation chemistry in zeolites
[DE94-012631] p 4412 N94-37439
Laser cooling of 24Mg+ in the ASTRID storage ring
[DE94-010445] p 4523 N94-37619

CAUCHY PROBLEM
A flux splitting scheme with high-resolution and robustness for discontinuities
[NASA-TM-106452] p 4441 N94-36646
The mathematical simulation of physical processes in ECR multicharged ions sources
[DE94-618343] p 4515 N94-37077
High-order centered difference methods with sharp shock resolution
[NASA-CR-196374] p 4496 N94-37656

CAVITIES
SOFIA: Aircraft system, aft telescope cavity configuration, phase 2. Volume 1: Executive summary
[NASA-CR-196362] p 4546 N94-36642

CELLS (BIOLOGY)
Recombinant protein production and insect cell culture and process
[NASA-CASE-MSC-22336-1] p 4478 N94-36751
A new, optical-lever based atomic force microscope
[AD-A280524] p 4524 N94-37110
Submicrometer fiber-optic chemical sensors: Measuring pH inside single cells
[DE94-004160] p 4525 N94-37532
Surface modification of polymers with self-assembled monolayers that promote adhesion, outgrowth and differentiation of biological cells
[AD-D016321] p 4427 N94-37829

CEMENTATION
Studies of the effect of microstructure on the dynamic behavior of granular and particulate media
[AD-A279012] p 4455 N94-36520

CENTRAL NERVOUS SYSTEM
The use of a tactile interface to convey position and motion perceptions p 4486 N94-37281

CERAMIC COATINGS
Development of intermetallic coatings for fusion power applications
[DE94-012647] p 4419 N94-37442

CERAMIC MATRIX COMPOSITES
Some considerations for modeling the creep behavior of composite materials
[DE94-012112] p 4404 N94-37205
Status review and accomplishments of the Materials Research Center at the University of Pittsburgh
[AD-A280422] p 4399 N94-37214
Modeling of forced CVI for tube fabrication
[DE94-012718] p 4410 N94-37286
Mechanical behavior of MoSi2 and MoSi2 composites
[DE94-013116] p 4405 N94-37289
Methodologies for the thermomechanical characterization of continuous-fiber ceramic matrix composites: A review of test methods
[DE94-012111] p 4405 N94-37370
Development of nondestructive evaluation methods and prediction of effects of flaws on the fracture behavior of structural ceramics
[DE94-012466] p 4425 N94-37423

CERAMICS
Modeling of thermal barrier coatings
[NASA-CR-195365] p 4421 N94-36837
Processing, packaging, and characterization of electroceramic materials for phased array antennas
[AD-A280251] p 4432 N94-36743

Interaction effects of cracks, flaws and damage in ceramic
[AD-A280368] p 4423 N94-37181
Defect initiation/growth and energy dissipation induced by deformation and fracture
[AD-A280411] p 4424 N94-37184
Status review and accomplishments of the Materials Research Center at the University of Pittsburgh
[AD-A280422] p 4399 N94-37214
Mechanical behavior of MoSi2 and MoSi2 composites
[DE94-013116] p 4405 N94-37289
Development of low dielectric constant alumina-based ceramics for microelectronic substrates
[DE94-011360] p 4439 N94-37302
Copper-containing ceramic precursor synthesis: Solid-state transformations and materials technology
[NASA-TM-106556] p 4399 N94-37315
Development of processing techniques for advanced thermal protection materials
[NASA-CR-196261] p 4426 N94-37510
Atomic resolution characterization of a SrTiO3 grain boundary in the STEM
[DE94-011469] p 4538 N94-37545
Advanced Turbine Technology Applications Project (ATTAP)
[NASA-CR-195367] p 4452 N94-37763

CEREBRUM
Cerebral neurochemical mechanisms in stress and anxiety
[AD-A280473] p 4482 N94-37233

CERENKOV COUNTERS
Experimental particle physics at the University of Pittsburgh
[DE94-011636] p 4521 N94-37721

CESIUM
TFE verification program
[DE94-009870] p 4398 N94-37514

CESIUM VAPOR
Spontaneous force optical traps
[AD-A280574] p 4514 N94-37041

CHANNEL FLOW
A combined experiment/computational study of flow in turbine blade cooling passage
[NASA-CR-4584] p 4442 N94-36957

CHAOS
Coherence and chaos
[DE94-008529] p 4539 N94-36507
Theoretical investigations of chaotic dynamics
[AD-A280325] p 4507 N94-37028
Embedded chaotic time series: Applications in prediction and spatio-temporal classification
[AD-A280690] p 4508 N94-37130

CHARGE CARRIERS
Quantum confinement in GaP nanoclusters
[DE94-013119] p 4536 N94-37290

CHARGE DISTRIBUTION
A charge distribution analysis instrument for catalysis and material science applications
[DE94-011587] p 4438 N94-37241

CHARGED PARTICLES
Isolated SO4-2 and PO4-3 anions do not exist
[AD-A278831] p 4512 N94-36521
Confinement improvement in H-mode-like plasmas in helical systems
[DE94-727619] p 4528 N94-37231
Stopping power of charged particles from 10 eV/amu to 10 GeV/amu
[DE94-719024] p 4518 N94-37387
Research using small tokamaks
[DE94-621827] p 4531 N94-37493

CHARPY IMPACT TEST
Data compatibility for various Charpy-tests
[DE94-617534] p 4416 N94-37074

CHEMICAL ANALYSIS
MarChem 93, the proceedings, the 1993 workshop on marine chemistry instrumentation
[AD-A279035] p 4475 N94-36446
Molecular beam surface analysis
[DE94-010773] p 4406 N94-36453
Indicators for sulfate-reducing bacteria in microbiologically influenced corrosion
[AD-A278914] p 4477 N94-36522
Mineralogy and metallurgical properties of iron ore sinter based on magnetite fines
[DE94-763309] p 4414 N94-36525
New materials and multidimensional cluster analysis for SAW chemical sensor arrays
[DE94-012066] p 4409 N94-37161
ALCHEMI formulated for delocalization and anti-site defects
[DE94-012740] p 4537 N94-37400
Chemical recognition software
[DE94-012918] p 4495 N94-37496
The integrated performance evaluation program quality assurance guidance in support of EM environmental sampling and analysis activities
[DE94-013043] p 4468 N94-37731

CHEMICAL BONDS
Comparison of the crystal structure and molecular models of N,N-diisobutyl-2- (octylphenylphosphinyl) acetamide (CMPO)
[DE94-013434] p 4534 N94-37069
Bond selective chemistry beyond the adiabatic approximation
[DE94-012486] p 4408 N94-37095

CHEMICAL CLEANING
Atomic oxygen treatment for non-contact removal of organic protective coatings from painting surfaces
[NASA-TM-106650] p 4421 N94-36952
Integrated environmentally compatible soldering technologies
[DE94-013456] p 4464 N94-37071

CHEMICAL COMPOSITION
A possible origin of EL6 chondrites from a high temperature-high pressure solar gas
[DE94-010467] p 4548 N94-36759
Information on alternative refrigerants and lubricants: The ARTI refrigerant database
[DE94-009997] p 4426 N94-37490

CHEMICAL ENERGY
Photochemistry without protons. Radical cation chemistry in zeolites
[DE94-012631] p 4412 N94-37439

CHEMICAL ENGINEERING
JPRS report: Science and technology. Central Eurasia
[JPRS-UST-94-013] p 4509 N94-37006
Scoping economics for the commercial manufacture of metallocene catalysts
[DE94-011526] p 4422 N94-37055
Activities of the Chemical Technology Division
[DE94-013050] p 4410 N94-37357

CHEMICAL EXPLOSIONS
The effects of proton-beam quality on the production of gamma rays for nuclear resonance absorption in nitrogen
[DE94-011609] p 4523 N94-37629

CHEMICAL PROPERTIES
Chemical and structural characterization of nitroaromatic adducts with hemoglobins
[AD-A280533] p 4480 N94-37089
Development of durable high-temperature catalysts for natural gas combustion: Catalytic materials (CATMAT (trade name)) properties database
[PB94-171824] p 4412 N94-37462

CHEMICAL REACTIONS
Bond selective chemistry beyond the adiabatic approximation
[DE94-012486] p 4408 N94-37095
An investigation of molybdenum and molybdenum oxide catalyzed hydrocarbon formation reactions
[DE94-013700] p 4409 N94-37132
Finite-rate chemistry and transient effects in Direct Numerical Simulations of turbulent non-premixed flames
[DE94-005250] p 4410 N94-37222
Hydrogen storage for vehicular applications: Technology status and key development areas
[DE94-011626] p 4428 N94-37243
Copper-containing ceramic precursor synthesis: Solid-state transformations and materials technology
[NASA-TM-106556] p 4399 N94-37315
Thermal decomposition reactions of HMX and RDX and their importance in predicting cookoff hazards
[DE94-011430] p 4429 N94-37413
Electron-transfer reactions involving two harmonic potentials with a different force constant: The Zusman approach versus the spin-boson model
[DE94-013306] p 4519 N94-37550

CHEMICAL TESTS
Sealed tube comparisons of the compatibility of desiccants with refrigerants and lubricants
[DE94-012371] p 4425 N94-37421

CHEMICAL VAPOR INFILTRATION
Modeling of forced CVI for tube fabrication
[DE94-012718] p 4410 N94-37286

CHEMICAL WARFARE
Solid state fluorometer: Prototype development
[AD-A280321] p 4534 N94-37027

CHEMILUMINESCENCE
Chemiluminescent microemulsions
[AD-D016292] p 4413 N94-37761

CHEMISORPTION
Diosmacycloalkanes as models for the formation of hydrocarbons from surface methylenes
[DE94-011211] p 4413 N94-37754

CHIPS (ELECTRONICS)
Development of low dielectric constant alumina-based ceramics for microelectronic substrates
[DE94-011360] p 4439 N94-37302
Evaluating plastic assembly processes for high reliability applications using HAST and Assembly Test Chips
[DE94-010750] p 4439 N94-37363

CHIRAL DYNAMICS
Non-equilibrium evolution of the disoriented chiral condensate in heavy-ion collisions
[DE94-012897] p 4522 N94-37310

CHLORINATION
Methyl chloride via oxyhydrochlorination of methane
[DE94-010691] p 4406 N94-36450

CHLOROPHYLLS
Solvent effects on the energetics and dynamics of ultrafast electron transfer in chlorophyll-porphyrin-acceptor triads
[DE94-009693] p 4477 N94-36554
Femtosecond transient grating studies of electron transfer in porphyrin and chlorophyll donor-acceptor molecules
[DE94-009694] p 4478 N94-36555

CHOLESKY FACTORIZATION
Improved load distribution in parallel sparse Cholesky factorization
[NASA-CR-196380] p 4499 N94-37654

CHONDRITES
A possible origin of EL6 chondrites from a high temperature-high pressure solar gas
[DE94-010467] p 4548 N94-36759

CHROMIC ACID
The corrosion protection of several aluminum alloys by chromic acid and sulfuric acid anodizing
[NASA-TP-3490] p 4420 N94-37578

CHROMIUM ALLOYS
Characterization and processing of sintered products from nano-crystalline powders generated by the RTDS method
[DE94-004765] p 4415 N94-36553
Chromium/molybdenum alloy plating. Part 1: The electrodeposition of low contraction chromium/molybdenum alloys using unipolar (on/off) pulse plating
[AD-A280236] p 4417 N94-37138
Examination of weldability of Ni-Cr-W superalloys
[DE94-719014] p 4418 N94-37385
The dynamics of hydrogen atoms dissolved in Zr Cr2 alloy
[DE94-618756] p 4520 N94-37652

CHROMOPHORES
Poly(p-phenylene) derivatives new high performance nonlinear optical polymers
[AD-A280248] p 4422 N94-37121
Holographic grating relaxation studies of probe diffusion in amorphous polymers
[AD-A280496] p 4423 N94-37144

CIRCADIAN RHYTHMS
Ground and space flight experiments of the effects of light, sound and/or temperature on animals
[NASA-CR-196102] p 4478 N94-36986
Melatonin, the pineal gland, and circadian rhythms
[AD-A280467] p 4481 N94-37140

CIRCUIT BOARDS
Integrated environmentally compatible soldering technologies
[DE94-013456] p 4464 N94-37071

CIRCUITS
Single event mirroring and sense amplifier designs for enhanced SE tolerance of DRAMs
[DE94-010397] p 4438 N94-37190
H infinity control for nonlinear and linear systems
[AD-A280450] p 4494 N94-37226

CIRCULAR CYLINDERS
Pressure-sensing performance of upright cylinders in a Mach 10 boundary-layer
[NASA-TM-4633] p 4383 N94-37395

CIRCULAR PLATES
A Galerkin method for linear PDE systems in circular geometries with structural acoustic applications
[NASA-CR-194925] p 4503 N94-36923

CIRRUS CLOUDS
Factors influencing the parameterization of anvil clouds within GCMs
[DE94-010794] p 4475 N94-37621

CITIES
Mexico City air quality research initiative, volume 4
[DE94-013201] p 4466 N94-37299
Evaluation of parameterizations for pollutant transport and dispersion in an urban street canyon using a three-dimensional dynamic flow model
[DE94-012641] p 4467 N94-37429

CIVIL AVIATION
Criminal Acts Against Civil Aviation, 1993
[AD-A280694] p 4384 N94-37131
Civil use of night vision devices: Evaluation pilot's guide, part 1
[SCT-91RR-43] p 4487 N94-37741

Assessment of night vision goggle workload: Flight test engineer's guide
[SCT-91RR-45] p 4487 N94-37743

CLASSIFYING
Embedded chaotic time series: Applications in prediction and spatio-temporal classification
[AD-A280690] p 4508 N94-37130

CLAYS
Geophysical data fusion for subsurface imaging
[DE94-000056] p 4469 N94-36738

CLEAN ENERGY
Comparative alternative/clean fuels provisions of the Clean Air Act Amendments of 1990 and the Energy Policy Act of 1992
[DE94-006887] p 4429 N94-37426

CLEAN ROOMS
Real-time SAW measurements of NVR in cleanroom and in microenvironment
[DE94-011937] p 4389 N94-37159
Development of high sensitivity techniques for characterizing outgassing of polymeric construction materials for microenvironments
[DE94-012066] p 4424 N94-37204

CLEANING
Real-time SAW measurements of NVR in cleanroom and in microenvironment
[DE94-011937] p 4389 N94-37159

CLIMATE
ARM: A climate process observatory
[DE94-007473] p 4463 N94-36477
Representing the influence of subgrid topography on hydrology
[DE94-004595] p 4474 N94-37379
Factors influencing the parameterization of anvil clouds within GCMs
[DE94-010794] p 4475 N94-37621
Surface-layer response over shrub-steppe canopy during springtime
[DE94-011235] p 4468 N94-37624

CLIMATE CHANGE
Paleoclimate validation of a numerical climate model
[DE94-009287] p 4463 N94-36470
Modeling the Earth system in the Mission to Planet Earth era
[NASA-TM-109892] p 4461 N94-36827
Science priorities for the human dimensions of global change p 4464 N94-36987
UAV's in climate research: The ARM Unmanned Aerospace Vehicle Program
[DE94-011753] p 4465 N94-37154
Catalog of data bases and reports
[DE94-012230] p 4466 N94-37208
Climate uncertainty and the regional economic impacts of global climate change
[DE94-012242] p 4466 N94-37211
Response of plants and ecosystems to CO2 and climate change
[DE94-011583] p 4466 N94-37376

CLIMATOLOGY
Paleoclimate validation of a numerical climate model
[DE94-009287] p 4463 N94-36470
Modeling the Earth system in the Mission to Planet Earth era
[NASA-TM-109892] p 4461 N94-36827
Index and bulk parameters for frequency-direction spectra measured at CERC Field Research Facility, September 1990 to August 1991
[AD-A280423] p 4476 N94-37216
Index and bulk parameters for frequency-direction spectra measured at CERC Field Research Facility, September 1991 to August 1992
[AD-A280455] p 4477 N94-37229
Proceedings of the Third Atmospheric Radiation Measurement (ARM) Science Team Meeting
[DE94-011194] p 4467 N94-37454
Factors influencing the parameterization of anvil clouds within GCMs
[DE94-010794] p 4475 N94-37621

CLOUD COVER
Proceedings of the Third Atmospheric Radiation Measurement (ARM) Science Team Meeting
[DE94-011194] p 4467 N94-37454

CLOUD PHYSICS
ARM: A climate process observatory
[DE94-007473] p 4463 N94-36477
Two-channel microwave radiometer for observations of total column precipitable water vapor and cloud liquid water path
[DE94-007480] p 4471 N94-36479
A stratiform cloud parameterization for general circulation models
[DE94-011442] p 4474 N94-37566

CLOUDS (METEOROLOGY)
Measurements and modeling of the effect of convective clouds on the upper tropospheric moisture budget
[NASA-TM-109894] p 4473 N94-37371
Representing the influence of subgrid topography on hydrology
[DE94-004595] p 4474 N94-37379

CLUSTER ANALYSIS
New materials and multidimensional cluster analysis for SAW chemical sensor arrays
[DE94-012066] p 4409 N94-37161

CLUTTER
Channel probe measurements for the American Sector Clutter Experiment, January 1994
[DE94-013086] p 4469 N94-37314

CMOS
Single event mirroring and sense amplifier designs for enhanced SE tolerance of DRAMs
[DE94-010397] p 4438 N94-37190

COAL
Advanced thermally stable, coal-derived, jet fuels development program. Experiment system and model development
[AD-A278968] p 4428 N94-36505
Coal-fueled diesel technology development: Fuel injection equipment for coal-fueled diesel engines
[DE94-004088] p 4452 N94-37512

COAL DERIVED LIQUIDS
Advanced thermally stable, coal-derived, jet fuels development program. Experiment system and model development
[AD-A278968] p 4428 N94-36505

COAL GASIFICATION
The potential for control of carbon dioxide emissions from integrated gasification/combined-cycle systems
[DE94-012646] p 4465 N94-37100

COASTAL CURRENTS
Variability of the California Current System off Point Sur, California from April 1988 to December 1990
[AD-A278579] p 4476 N94-36985

COASTAL ECOLOGY
Phytoplankton blooms and coastal physical processes
[AD-A280646] p 4475 N94-36761

COASTAL WATER
Phytoplankton blooms and coastal physical processes
[AD-A280646] p 4475 N94-36761
Index and bulk parameters for frequency-direction spectra measured at CERC Field Research Facility, September 1990 to August 1991
[AD-A280423] p 4476 N94-37216
Index and bulk parameters for frequency-direction spectra measured at CERC Field Research Facility, September 1991 to August 1992
[AD-A280455] p 4477 N94-37229

COATING
Strategic choices in surface treatments
[PB94-170669] p 4414 N94-36534
Properties of TMC processed by fibre coating and hiping p 4401 N94-36656
Fibre-matrix interface properties in Ti-matrix composites: Chemical compatibility and micromechanical behaviour p 4401 N94-36657
Determining the refractive index of a lambda/4 thin film on a thick substrate from a transmittance measurement
[DE93-019584] p 4523 N94-36693

COATINGS
Strategic choices in surface treatments
[PB94-170669] p 4414 N94-36534

COBALT OXIDES
Microstructure and chemistry of MgO- and CoO-doped nickel-titanate spinels
[DE94-012741] p 4537 N94-37382

COCKPITS
Interactive large screen: A multi-mode dialogue tool for future cockpits p 4484 N94-37266
The DRA Virtual Cockpit Research Program p 4484 N94-37269
Human factors for flight deck certification personnel
[AD-A280477] p 4487 N94-37347

CODERS
Error control techniques for satellite and space communications
[NASA-CR-196302] p 4433 N94-36931

COGNITIVE PSYCHOLOGY
Probability-based inference in cognitive diagnosis
[AD-A280553] p 4506 N94-36732
Immersive virtual environments as trainer: System design from a cognitive stance p 4484 N94-37267

COHERENCE
Coherence and chaos
[DE94-008529] p 4539 N94-36507

COHERENT RADIATION
Coherent multiple-foil x-ray transition radiation
[DE93-040831] p 4525 N94-37486

COLD ACCLIMATIZATION
Homeostatic responses to prolonged cold exposure: Human cold acclimatization
[AD-A280234] p 4481 N94-37136

COLD CATHODE TUBES
Field emitter array RF amplifier development project. Phase 1, option 1
[AD-A280377] p 4437 N94-37035
Field emitter array RF amplifier development project. Phase 1, option 1
[AD-A280513] p 4437 N94-37107

COLD PLASMAS
Effects of freezing and cold acclimation on the plasma membrane of isolated protoplasts
[DE94-012487] p 4479 N94-37248
Analysis of plasma measurements for the Geotail mission
[NASA-CR-196274] p 4470 N94-37470

COLD PRESSING
Microstructure and chemistry of MgO- and CoO-doped nickel-titanate spinels
[DE94-012741] p 4537 N94-37382

COLD TOLERANCE
Homeostatic responses to prolonged cold exposure: Human cold acclimatization
[AD-A280234] p 4481 N94-37136

COLLIMATORS
Method of N-15 analysis by mass-spectroscopy on ion implanter MPB-200
[DE94-618203] p 4407 N94-36529
Conceptual design for a fast neutron ionization chamber for fusion reactor plasma diagnostics
[DE94-013396] p 4527 N94-37101

COLLISION AVOIDANCE
Composite helicopter accident profiles: Deficient crew/aircraft performance
[SCT-90RR-46] p 4385 N94-37604

COLLISIONS
Positron implantation in solids
[DE94-013029] p 4537 N94-37499

COLLOCATION
Multiquadric collocation methods in the numerical solution of Volterra integral equations with weakly singular kernels
[DE94-013000] p 4505 N94-37497

COLOR VISION
Human factors for flight deck certification personnel
[AD-A280477] p 4487 N94-37347

COLUMNS (SUPPORTS)
Sub-ply level scaling approach investigated for graphite-epoxy composite beam columns p 4458 N94-37798

COMBAT
Aircraft battle damage repair for the 1990's and beyond
[AD-A278635] p 4386 N94-36465

COMBINED STRESS
Creation of a virtual world to study human spatial perception during sustained acceleration p 4484 N94-37268

COMBUSTIBLE FLOW
Effects of two-phase flow on the deflagration of porous energetic materials
[DE94-011423] p 4411 N94-37412

COMBUSTION
LNG vehicle technology, economics, and safety assessment
[PB94-165487] p 4450 N94-36721
Design and development of experimental facilities for short duration, low-gravity combustion and fire experiments
[NASA-CR-196107] p 4389 N94-36967
SIHTI: Energy and environmental technology
[DE94-763290] p 4464 N94-37007
Infrared spectroscopy of organic free radicals related to combustion processes
[DE94-012481] p 4409 N94-37168
Finite-rate chemistry and transient effects in Direct Numerical Simulations of turbulent non-premixed flames
[DE94-005250] p 4410 N94-37222
Coal-fueled diesel technology development: Fuel injection equipment for coal-fueled diesel engines
[DE94-004088] p 4452 N94-37512
Probing flame chemistry with MBMS, theory, and modeling
[DE94-011224] p 4413 N94-37623

COMBUSTION CHAMBERS
Development of durable high-temperature catalysts for natural gas combustion: Catalytic materials (CATMAT (trade name)) properties database
[PB94-171824] p 4412 N94-37462

COMBUSTION CHEMISTRY
Rich methane/air flames: Burning velocities, extinction limits, and flammability limit
[DE94-004340] p 4407 N94-36462
Rich flammability limits in CH3OH/CO/diluent mixtures
[DE94-004341] p 4407 N94-36482
A fully coupled thermal, chemical, mechanical cookoff model
[DE94-011432] p 4428 N94-37201

CHEETAH: A fast thermochemical code for detonation
[DE94-012586] p 4429 N94-37427
Probing flame chemistry with MBMS, theory, and modeling
[DE94-011224] p 4413 N94-37623

COMBUSTION EFFICIENCY
Combustion characterization of methylal in reciprocating engines
[DE94-006949] p 4411 N94-37409

COMBUSTION PHYSICS
Laser-saturated fluorescence measurements in laminar scoting diffusion flames
[NASA-CR-191025] p 4508 N94-36643
Bond selective chemistry beyond the adiabatic approximation
[DE94-012486] p 4408 N94-37095
Infrared spectroscopy of organic free radicals related to combustion processes
[DE94-012481] p 4409 N94-37168
Some effects of heat release in premixed flames
[DE94-011346] p 4409 N94-37199
Spray combustion model improvement study, 1
[NASA-CR-196122] p 4410 N94-37250
Effects of two-phase flow on the deflagration of porous energetic materials
[DE94-011423] p 4411 N94-37412
CHEETAH: A fast thermochemical code for detonation
[DE94-012586] p 4429 N94-37427
Probing flame chemistry with MBMS, theory, and modeling
[DE94-011224] p 4413 N94-37623

COMBUSTION PRODUCTS
Potential benefits of oxygen-enriched intake air in a vehicle powered by a spark-ignition engine
[DE94-013452] p 4451 N94-37070
Influences of flame-vortex interactions on formation of oxides of nitrogen in curved methane-air diffusion flamelets
[DE94-005105] p 4409 N94-37221
Effects of molecular transport on turbulence-chemistry interactions in a hydrogen-argon-air jet diffusion flame
[DE94-005107] p 4413 N94-37711
Advanced Turbine Technology Applications Project (ATTAP)
[NASA-CR-195367] p 4452 N94-37763

COMMAND AND CONTROL
Analysis of end-to-end encryption and traffic flow confidentiality options
[AD-A278612] p 4433 N94-36754

COMMAND GUIDANCE
Evaluation of GPS position and attitude determination for automated rendezvous and docking missions
[NASA-CR-4614] p 4397 N94-37506

COMMERCE
Opportunities for innovation: Biotechnology
[PB94-157831] p 4478 N94-36720
NASA commercial technology. Agenda for change
[NASA-TM-109898] p 4546 N94-37765

COMMERCIAL AIRCRAFT
World jet airplane inventory at year-end 1993
[PB94-164993] p 4384 N94-36530
Prospective communications research to support fly by light/power by wire
[NASA-CR-196369] p 4526 N94-37657

COMMERCIAL SPACECRAFT
Design and analysis of a mode B and mode JD satellite Earth station
[AD-A280417] p 4391 N94-37225

COMMUNICATING
Toward a new National Weather Service: National Weather Service employee feedback
p 4474 N94-37467

COMMUNICATION EQUIPMENT
Error control techniques for satellite and space communications
[NASA-CR-196302] p 4433 N94-36931

COMMUNICATION NETWORKS
Analysis of end-to-end encryption and traffic flow confidentiality options
[AD-A278612] p 4433 N94-36754
Network survivability performance
[AD-A278745] p 4433 N94-36756
Network survivability performance (computer diskette)
[AD-M000332] p 4433 N94-36757
Controlled atmospheric breakdown: Applications and research opportunities
[AD-A278584] p 4464 N94-36973
A two-level formal specification of a defense communications system
[DE94-012117] p 4434 N94-37206
International High Speed Networks for Scientific and Technical Information
[AGARD-CP-544] p 4543 N94-37333
Global information networks: How they work
p 4543 N94-37335
The Canadian network for the advancement of research, industry and education (CANARIE) p 4543 N94-37336
The virtual library: Coming of age
p 4544 N94-37338
Problems of international exchange of scientific and technical information for a Russian aerospace research institute p 4544 N94-37339
Electronic document delivery: Towards the virtual library p 4544 N94-37340
Bulletin boards, electronic mail, conferencing, current use by scientists and engineers: Effects on libraries and information centres: Do they have a role?
p 4544 N94-37343
Integrated Engineering Information Technology, FY 1993 accomplishments
[DE94-011406] p 4545 N94-37563
Interactive Collaborative Environments (ICE): Platform independent X application sharing and multi-media over wide area networks
[DE94-008868] p 4502 N94-37784

COMMUNICATION SATELLITES
Preliminary PANSAT ground station software design and use of an expert system to analyze telemetry
[AD-A280600] p 4392 N94-36726
Error control techniques for satellite and space communications
[NASA-CR-196302] p 4433 N94-36931

COMPATIBILITY
Fibre-matrix interface properties in Ti-matrix composites: Chemical compatibility and micromechanical behaviour
p 4401 N94-36657
Data compatibility for various Charpy-tests
[DE94-617534] p 4416 N94-37074
Materials Compatibility and Lubricant Research on CFC-refrigerant substitutes
[DE94-012352] p 4425 N94-37373
Sealed tube comparisons of the compatibility of desiccants with refrigerants and lubricants
[DE94-012371] p 4425 N94-37421

COMPENSATORS
Vibration suppression with approximate finite dimensional compensators for distributed systems: Computational methods and experimental results
[NASA-CR-194927] p 4500 N94-36928
Multirate flutter suppression system design for the Benchmark Active Controls Technology Wing
[NASA-CR-196112] p 4388 N94-36965

COMPILERS
Adaptable binary programs
[AD-A280243] p 4494 N94-37119
A compilation system that integrates high performance FORTRAN and FORTRAN M
[DE94-013308] p 4496 N94-37551

COMPLEX SYSTEMS
Nonlinearity with disorder: Spatio-temporal complex behavior arising from length scales competition
[DE94-000675] p 4502 N94-36685
On automating domain connectivity for overset grids
[NASA-CR-196113] p 4493 N94-36920
Task-specific usability requirements for virtual information environments: Interface design and data representation for human operators of complex medical systems p 4483 N94-37262
Ordering design tasks based on coupling strengths
[NASA-TM-109137] p 4387 N94-37762

COMPOSITE MATERIALS
JPRS report: Science and technology. Central Eurasia: Materials science
[JPRS-UMS-93-008] p 4404 N94-37010
Poly(p-phenylene) derivatives new high performance nonlinear optical polymers
[AD-A280248] p 4422 N94-37121
Tensile strength of simulated and welded butt joints in W-Cu composite sheet
[NASA-TM-4584] p 4405 N94-37460
Workshop on Scaling Effects in Composite Materials and Structures
[NASA-CP-3271] p 4457 N94-37796
The effects of specimen scale on the compression strength of composite materials p 4459 N94-37802
Size effect in composite materials and structures: Basic concepts and design considerations
p 4460 N94-37808

COMPOSITE STRUCTURES
Applications of Titanium Matrix Composite to large airframe structure p 4400 N94-36651
Detection of delaminations in composite beams using piezoelectric sensors
[NASA-TM-106611] p 4403 N94-36956
Advanced manufacturing technology for polymer composite structures in Japan p 4422 N94-36968
Modeling of forced CVI for tube fabrication
[DE94-012718] p 4410 N94-37286
Probability techniques for reliability analysis of composite materials
[NASA-CR-195294] p 4406 N94-37633
Workshop on Scaling Effects in Composite Materials and Structures
[NASA-CP-3271] p 4457 N94-37796
Effects of scale in predicting global structural response p 4458 N94-37799
On nature's scaling effects p 4459 N94-37803
Size effect in composite materials and structures: Basic concepts and design considerations
p 4460 N94-37808
Scaling of impact damage in fiber composites
p 4460 N94-37810

COMPRESSED GAS
A possible origin of EL6 chondrites from a high temperature-high pressure solar gas
[DE94-010467] p 4548 N94-36759
Technical evaluation and assessment of CNG/LPG bi-fuel and flex-fuel vehicle viability
[DE94-006925] p 4451 N94-37408

COMPRESSIBILITY EFFECTS
The stabilizing effect of compressibility in turbulent shear flow
[NASA-CR-194932] p 4444 N94-37605

COMPRESSIBLE FLOW
A flux splitting scheme with high-resolution and robustness for discontinuities
[NASA-TM-106452] p 4441 N94-36646
Development of advanced Navier-Stokes solver
[NASA-CR-195094] p 4504 N94-37449
The stabilizing effect of compressibility in turbulent shear flow
[NASA-CR-194932] p 4444 N94-37605

COMPRESSION LOADS
Fluids at high shock pressures and temperatures and some thoughts about future possibilities
[DE94-003625] p 4407 N94-36458
On nature's scaling effects p 4459 N94-37803

COMPRESSION TESTS
Methodologies for the thermomechanical characterization of continuous-fiber ceramic matrix composites: A review of test methods
[DE94-012111] p 4405 N94-37370
The effects of specimen scale on the compression strength of composite materials p 4459 N94-37802

COMPRESSIVE STRENGTH
A comparison of graphite/epoxy tape laminates and 2-D braided composites mechanical properties
[NASA-CR-4610] p 4420 N94-37582
The effects of specimen scale on the compression strength of composite materials p 4459 N94-37802

COMPRESSOR ROTORS
Development of mechanical testing methods for titanium matrix composites (traction-ogligo-cyclic fatigue)
p 4403 N94-36669

COMPTON EFFECT
A freon-filled, holographic bubble chamber as a high energy photon burst spectrometer
[DE94-011645] p 4446 N94-37723

COMPUTATION
Multirate time-frequency distributions
[AD-A280595] p 4503 N94-36723

COMPUTATIONAL ASTROPHYSICS
A study of physical mechanisms for filament eruption and coronal mass ejection via numerical simulation
[NASA-CR-196087] p 4549 N94-36489

COMPUTATIONAL CHEMISTRY
Computational chemistry research
[NASA-CR-196120] p 4408 N94-36989

COMPUTATIONAL FLUID DYNAMICS
Preconditioned implicit solvers for the Navier-Stokes equations on distributed-memory machines
[NASA-TM-106449] p 4502 N94-36647
Experimental investigation of nozzle/plume aerodynamics at hypersonic speeds
[NASA-CR-195829] p 4382 N94-36687
Computational investigation of an improved cowl concept for hypersonic propulsive nozzles
[AD-A280596] p 4441 N94-36724
An aerodynamic and static-stability analysis of the Hypersonic Applied Research Technology (HART) missile
[AD-A280631] p 4382 N94-36729
Turbulence modeling of free shear layers for high performance aircraft
[NASA-CR-196137] p 4442 N94-36808
An arbitrary grid CFD algorithm for configuration aerodynamics analysis. Volume 1: Theory and validations
[NASA-CR-195918] p 4493 N94-36914
An arbitrary grid CFD algorithm for configuration aerodynamics analysis. Volume 2: FEMNAS user guide
[NASA-CR-196135] p 4493 N94-36922
Automatic computation of Euler-marching and subsonic grids for wing-fuselage configurations
[NASA-TM-4573] p 4383 N94-36950

Navier-Stokes and potential theory solutions for ahelicopter fuselage and comparison with experiment
[NASA-TM-4566] p 4383 N94-36966
Computational chemistry research
[NASA-CR-196120] p 4408 N94-36989
Large-scale three-dimensional geothermal reservoir simulation on PC's
[DE94-011374] p 4443 N94-37050
A fundamental study of hypersonic unstarts
[AD-A280506] p 4443 N94-37128
Simulation of three-dimensional multi-phase flow characteristics in the deswirl section of the CDIF MHD power train
[DE94-012644] p 4443 N94-37176
A method for flow simulation about complex geometries using both structured and unstructured grids
[NASA-TM-106633] p 4383 N94-37283
Development of advanced Navier-Stokes solver
[NASA-CR-195094] p 4504 N94-37449
Unstructured grid methods for the simulation of 3D transient flows
[NASA-CR-196139] p 4444 N94-37525
Numerical study of the flow of granular materials down an inclined plane
[DE94-010729] p 4444 N94-37544
The stabilizing effect of compressibility in turbulent shear flow
[NASA-CR-194932] p 4444 N94-37605

COMPUTATIONAL GEOMETRY
Automatic procedures for computing complete configuration geometry from individual component descriptions
[NASA-TM-4607] p 4382 N94-36942

COMPUTATIONAL GRIDS
Preconditioned implicit solvers for the Navier-Stokes equations on distributed-memory machines
[NASA-TM-106449] p 4502 N94-36647
On automating domain connectivity for overset grids
[NASA-CR-196113] p 4493 N94-36920
Automatic procedures for computing complete configuration geometry from individual component descriptions
[NASA-TM-4607] p 4382 N94-36942
Automatic computation of Euler-marching and subsonic grids for wing-fuselage configurations
[NASA-TM-4573] p 4383 N94-36950
Large-scale three-dimensional geothermal reservoir simulation on PC's
[DE94-011374] p 4443 N94-37050
Cost-effective computations with boundary interface operators in elliptic problems
[DE94-621506] p 4503 N94-37098
The impact of HPF data layout on the design of efficient and maintainable parallel linear algebra libraries
[DE94-012382] p 4504 N94-37246
A method for flow simulation about complex geometries using both structured and unstructured grids
[NASA-TM-106633] p 4383 N94-37283
Evolution of turbulent fields in explosions
[DE94-010405] p 4444 N94-37390
Unstructured grid methods for the simulation of 3D transient flows
[NASA-CR-196139] p 4444 N94-37525
A Lagrangian-Eulerian finite element method with adaptive gridding for advection-dispersion problems
[DE94-011372] p 4506 N94-37718

COMPUTER AIDED DESIGN
An empirical comparison of a dynamic software testability metric to static cyclomatic complexity
p 4491 N94-36498
A survey of commonly applied methods for software process improvement
[AD-A278595] p 4493 N94-36974
H infinity control for nonlinear and linear systems
[AD-A280450] p 4494 N94-37226
Interchangeable spline reference guide
[DE94-012368] p 4495 N94-37245
Fuzzy logic to improve efficiency of finite element and finite difference schemes
[DE94-011718] p 4496 N94-37739

COMPUTER AIDED MANUFACTURING
Open architecture controllers for advanced manufacturing
[DE94-007572] p 4496 N94-37782
Interactive Collaborative Environments (ICE): Platform independent X application sharing and multi-media over wide area networks
[DE94-008868] p 4502 N94-37784

COMPUTER ASSISTED INSTRUCTION
Evaluation of a tool for producing and presenting interactive videodisc job aids
[AD-A278599] p 4432 N94-36473
Portable color multimedia training systems based on monochrome laptop computers (CBT-in-a-briefcase), with spinoff implications for video uplink and downlink in spaceflight operations
[NASA-TM-108460] p 4496 N94-37556

COMPUTER COMPONENTS
Design and analysis of a mode B and mode JD satellite Earth station
[AD-A280417] p 4391 N94-37225

COMPUTER CONFERENCING
Bulletin boards, electronic mail, conferencing, current use by scientists and engineers: Effects on libraries and information centres: Do they have a role?
p 4544 N94-37343

COMPUTER GRAPHICS
EM-ANIMATE: A computer program for displaying and animating electromagnetic near-field and surface-current solutions: Video supplement to NASA Technical Memorandum 4539
[NASA-TM-4539-VIDEO-SUPPL] p 4492 N94-36518
Nonlinearity with disorder: Spatio-temporal complex behavior arising from length scales competition
[DE94-000675] p 4502 N94-36685
Efficient contact determination between geometric models
[AD-A280244] p 4494 N94-37120
Low cost software-based rendering and stereoscopic interfaces for teleoperation and virtual reality
p 4486 N94-37279
Synthetic vision display evaluation studies
[NASA-CR-194963] p 4387 N94-37658

COMPUTER INFORMATION SECURITY
Analysis of end-to-end encryption and traffic flow confidentiality options
[AD-A278612] p 4433 N94-36754
Advanced information processing system: Authentication protocols for network communication
[NASA-CR-194923] p 4498 N94-37500
Distributed VIRtual System (DIVIRS) project
[NASA-CR-196262] p 4495 N94-37509

COMPUTER NETWORKS
NASA STI Program Coordinating Council Eleventh Meeting: NASA STI Modernization Plan
[NASA-TM-109415] p 4540 N94-36841
NASA STI modernization plan p 4540 N94-36842
Electronic document interchange
p 4541 N94-36848
Open system environments p 4542 N94-36857
Open system environment procurement
p 4542 N94-36858
A comparison of queueing, cluster and distributed computing systems
[NASA-TM-109025] p 4497 N94-36932
United States Air Force Summer Research Program, 1993. Volume 14: Rome Laboratory
[AD-A278656] p 4550 N94-36976
United States Air Force Summer Research Program, 1993. Volume 9: Rome Laboratory
[AD-A278699] p 4551 N94-36984
A two-level formal specification of a defense communications system
[DE94-012117] p 4434 N94-37206
The virtual library: Coming of age
p 4544 N94-37338
Electronic document delivery: Towards the virtual library p 4544 N94-37340
Policies for implementing network firewalls
[DE94-011030] p 4495 N94-37430
Advanced information processing system: Authentication protocols for network communication
[NASA-CR-194923] p 4498 N94-37500
Integrated Engineering Information Technology, FY 1993 accomplishments
[DE94-011406] p 4545 N94-37563
Open architecture controllers for advanced manufacturing
[DE94-007572] p 4496 N94-37782
Remote use of distributed robotics resources to enhance technology development and insertion
[DE94-009285] p 4502 N94-37785

COMPUTER PROGRAMMING
Software use control
[DE94-008429] p 4489 N94-36480
Proceedings of the Eighteenth Annual Software Engineering Workshop
[NASA-CR-189348] p 4489 N94-36484
Specification-based software sizing: An empirical investigation of function metrics p 4490 N94-36488
Assessing efficiency of software production for NASA-SEL data p 4490 N94-36490
Software quality: Process or people
p 4492 N94-36499
Profile of NASA software engineering: Lessons learned from building the baseline p 4492 N94-36500
NIPER Lab WARDEN: Descriptive panels and diagrams for NIPER Lab WARDEN software, volume 2
[DE94-000126] p 4493 N94-36699
A survey of commonly applied methods for software process improvement
[AD-A278595] p 4493 N94-36974
United States Air Force Summer Research Program, 1993. Volume 14: Rome Laboratory
[AD-A278656] p 4550 N94-36976
Proto code generation techniques
[AD-A280275] p 4494 N94-37123
Automatic, self-adaptive control of unfold transformations
[DE94-012455] p 4504 N94-37247
The distributed development environment for SDSS software
[DE94-013238] p 4547 N94-37555
Parallel Spectral Transform Shallow Water Model: A runtime-tunable parallel benchmark code
[DE94-011460] p 4498 N94-37568
Advanced distributed simulation technology advanced rotary wing aircraft. Software programmer's manual visual system module
[AD-A280260] p 4390 N94-37755
Techniques for real-time parallel processing: Sensor processing case studies
[AD-A280633] p 4499 N94-37760

COMPUTER PROGRAMS
MCNP: Multigroup/adjoint capabilities
[DE94-010682] p 4506 N94-36449
Software forecasting as it is really done: A study of JPL software engineers p 4490 N94-36489
Porting industrial codes and developing sparse linear solvers on parallel computers
[PB94-170503] p 4497 N94-36547
NIPER Lab WARDEN: Description and LabVIEW executable code of a general-purpose laboratory-automation program
[DE94-000125] p 4492 N94-36698
NIPER Lab WARDEN: Descriptive panels and diagrams for NIPER Lab WARDEN software, volume 2
[DE94-000126] p 4493 N94-36699
Preliminary PANSAT ground station software design and use of an expert system to analyze telemetry
[AD-A280600] p 4392 N94-36726
A-TOUGH: A multimedia fluid-flow/energy-transport model for fully-coupled atmospheric-subsurface interactions
[DE94-004304] p 4472 N94-36739
Network upgrades p 4541 N94-36851
Standards in the architectural effort
p 4541 N94-36852
An arbitrary grid CFD algorithm for configuration aerodynamics analysis. Volume 1: Theory and validations
[NASA-CR-195918] p 4493 N94-36914
An arbitrary grid CFD algorithm for configuration aerodynamics analysis. Volume 2: FEMNAS user guide
[NASA-CR-196135] p 4493 N94-36922
A survey of commonly applied methods for software process improvement
[AD-A278595] p 4493 N94-36974
Fracture mechanics life analytical methods verification testing
[NASA-CR-4602] p 4455 N94-37015
Fundamentals studies of radial wave thermoacoustic engines
[AD-A280534] p 4431 N94-37090
Proto code generation techniques
[AD-A280275] p 4494 N94-37123
A fully coupled thermal, chemical, mechanical cookoff model
[DE94-011432] p 4428 N94-37201
Interchangeable spline reference guide
[DE94-012368] p 4495 N94-37245
Low cost software-based rendering and stereoscopic interfaces for teleoperation and virtual reality
p 4486 N94-37279
User's manual for SNL-SAND-2 code
[DE94-011744] p 4496 N94-37673
Interactive Collaborative Environments (ICE): Platform independent X application sharing and multi-media over wide area networks
[DE94-008868] p 4502 N94-37784

COMPUTER SYSTEMS DESIGN
Fusing modeling techniques to support domain analysis for reuse opportunities identification
p 4491 N94-36497
Advanced information processing system: The Army Fault-Tolerant Architecture detailed design overview
[NASA-CR-194924] p 4497 N94-36962
Fault tolerance in opto-electronic computing
[AD-A280219] p 4453 N94-37150
Fermilab's DART DA system
[DE94-013240] p 4523 N94-37547

COMPUTER SYSTEMS PERFORMANCE
A comparison of queueing, cluster and distributed computing systems
[NASA-TM-109025] p 4497 N94-36932
Fault tolerance in opto-electronic computing
[AD-A280219] p 4453 N94-37150
Parallelized direct execution simulation of message-passing parallel programs
[NASA-CR-194936] p 4497 N94-37411
Improved load distribution in parallel sparse Cholesky factorization
[NASA-CR-196380] p 4499 N94-37654
COMPUTER SYSTEMS PROGRAMS
A comparison of queueing, cluster and distributed computing systems
[NASA-TM-109025] p 4497 N94-36932
Distributed VIRtual System (DIVIRS) project
[NASA-CR-196262] p 4495 N94-37509
COMPUTER SYSTEMS SIMULATION
Hardware implementation of a desktop supercomputer for high performance image processing
[AD-A280550] p 4489 N94-36731
Parallelized direct execution simulation of message-passing parallel programs
[NASA-CR-194936] p 4497 N94-37411
COMPUTER TECHNIQUES
World jet airplane inventory at year-end 1993
[PB94-164993] p 4384 N94-36530
NIPER Lab WARDEN: Description and LabVIEW executable code of a general-purpose laboratory-automation program
[DE94-000125] p 4492 N94-36698
United States Air Force Summer Research Program, 1993. Volume 5A: Wright Laboratory
[AD-A278696] p 4551 N94-36981
The implementation of Electronic Data Interchange (EDI) with defense transportation operations
[AD-A280568] p 4493 N94-37040
Global Picture Archiving and Communication Systems (GPACS): An overview
[AD-A280617] p 4543 N94-37042
Task-specific usability requirements for virtual information environments: Interface design and data representation for human operators of complex medical systems p 4483 N94-37262
COMPUTER VISION
Proceedings of SPIE: The International Society for Optical Engineering, Computational Vision Based on Neurobiology, volume 2054
[AD-A278731] p 4523 N94-36468
Adaptive multisensor fusion for the perception and interpretation of outdoor robot scenes
[PB94-170719] p 4499 N94-36535
Two-axis camera platform for machine vision p 4394 N94-36628
A model-based approach for detection of runways and other objects in image sequences acquired using an on-board camera
[NASA-CR-196424] p 4446 N94-36812
COMPUTERIZED SIMULATION
Rotorwash analysis handbook. Volume 2: Appendixes
[SCT-93RR-17-VOL-2] p 4382 N94-36467
A study of physical mechanisms for filament eruption and coronal mass ejection via numerical simulation
[NASA-CR-196087] p 4549 N94-36469
Applying formal methods and object-oriented analysis to existing flight software p 4491 N94-36495
A transient FETI methodology for large-scale parallel implicit computations in structural mechanics, part 2
[NASA-CR-194823] p 4497 N94-36503
EM-ANIMATE: A computer program for displaying and animating electromagnetic near-field and surface-current solutions: Video supplement to NASA Technical Memorandum 4539
[NASA-TM-4539-VIDEO-SUPPL] p 4492 N94-36518
Multiphase flow with interphase exchanges (MFIX) documentation theory guide
[DE94-000087] p 4441 N94-36550
Hardware implementation of a desktop supercomputer for high performance image processing
[AD-A280550] p 4489 N94-36731
A-TOUGH: A multimedia fluid-flow/energy-transport model for fully-coupled atmospheric-subsurface interactions
[DE94-004304] p 4472 N94-36739
An arbitrary grid CFD algorithm for configuration aerodynamics analysis. Volume 1: Theory and validations
[NASA-CR-195918] p 4493 N94-36914
An arbitrary grid CFD algorithm for configuration aerodynamics analysis. Volume 2: FEMNAS user guide
[NASA-CR-196135] p 4493 N94-36922
United States Air Force Summer Research Program, 1993. Volume 3: Phillips Laboratory
[AD-A278694] p 4550 N94-36979
Large-scale three-dimensional geothermal reservoir simulation on PC's
[DE94-011374] p 4443 N94-37050
Efficient contact determination between geometric models
[AD-A280244] p 4494 N94-37120
Proto code generation techniques
[AD-A280275] p 4494 N94-37123
Array element gain and phase estimation in the presence of interference
[AD-A280381] p 4434 N94-37162
Time-step stability for self-consistent Monte Carlo device simulation
[DE94-012145] p 4528 N94-37207
SACS: A cache simulator incorporating timing analysis with buffer and memory management
[AD-A280472] p 4494 N94-37230
The influence of tributaries on nocturnal valley flows
[DE94-011613] p 4473 N94-37242
Virtual Interfaces: Research and Applications
[AGARD-CP-541] p 4482 N94-37261
Modeling of forced CVI for tube fabrication
[DE94-012718] p 4410 N94-37286
Selected case studies in modeling and simulation applied to environmentally conscious design and manufacturing
[DE94-007556] p 4466 N94-37389
Neutron transport methods on scalable shared memory multiprocessors
[DE94-012324] p 4498 N94-37419
Improvement study of the divertor configuration of the Steady State Tokamak Reactor (SSTR)
[DE94-718961] p 4531 N94-37484
Chemical recognition software
[DE94-012918] p 4495 N94-37496
Numerical simulation of dynamic fracture and failure in solids
[DE94-010379] p 4457 N94-37705
Advanced distributed simulation technology. SIMWORLD data base
[AD-A280262] p 4545 N94-37757
COMPUTERS
Understanding and managing power system harmonics
[AD-A280627] p 4440 N94-37759
CONCENTRATION (COMPOSITION)
Atmospheric gas
[DE94-007439] p 4465 N94-37187
Chemical recognition software
[DE94-012918] p 4495 N94-37496
CONCRETES
Numerical simulation of dynamic fracture and failure in solids
[DE94-010379] p 4457 N94-37705
CONDENSATES
Methods of calculation of higher power corrections in QCD
[DE94-618511] p 4521 N94-36748
CONDENSED MATTER PHYSICS
Activities of the Laboratory of Physics, Helsinki University of Technology
[PB94-175247] p 4509 N94-37301
CONDENSERS (LIQUEFIERS)
The influence of fin height and wall conductivity on integral-fin tubes during steam condensation
[AD-A280597] p 4539 N94-36725
CONDUCTING POLYMERS
Pressure dependence of the conductivity and magnetoconductance in oriented iodine-doped polyacetylene
[PB94-184488] p 4427 N94-37854
CONDUCTION BANDS
A rejection method for selection of scattered states
[DE94-012232] p 4517 N94-37209
CONFERENCES
MarChem 93, the proceedings, the 1993 workshop on marine chemistry instrumentation
[AD-A279035] p 4475 N94-36446
Proceedings of SPIE: The International Society for Optical Engineering, Computational Vision Based on Neurobiology, volume 2054
[AD-A278731] p 4523 N94-36468
Proceedings of the Eighteenth Annual Software Engineering Workshop
[NASA-CR-189348] p 4489 N94-36484
Strategic choices in surface treatments
[PB94-170669] p 4414 N94-36534
Collaboration in Crystallography: Proceedings of the 1st Joint Seminar of the ISIS-INCR Collaboration in Crystallography
[PB94-171097] p 4532 N94-36548
Pointing and Tracking Systems
[AGARD-CP-539] p 4392 N94-36616
Characterisation of Fibre Reinforced Titanium Matrix Composites
[AD-A2775206] p 4400 N94-36649
Gas-Phase and Surface Chemistry in Electronic Materials Processing. Materials Research Society Symposium proceedings, volume 334
[AD-A280586] p 4408 N94-36735
NASA STI Program Coordinating Council Eleventh Meeting: NASA STI Modernization Plan
[NASA-TM-109415] p 4540 N94-36841
Abstracts of 2nd International Conference on Lasers and their Applications
[DE94-617409] p 4448 N94-37169
Virtual Interfaces: Research and Applications
[AGARD-CP-541] p 4482 N94-37261
The life cycles of intense cyclonic and anticyclonic circulation systems observed over oceans
[NASA-CR-196271] p 4473 N94-37294
Proceedings of the Workshop on Negative Ion Formation and Beam Handling
[DE94-748663] p 4518 N94-37360
1993 JSES (Japan Solar Energy Society)/JWEA (Japan Wind Energy Association) Joint Conference and 1993 Japan-Korea Joint Conference on Solar Energy
[DE94-767725] p 4462 N94-37418
Proceedings of the Third Atmospheric Radiation Measurement (ARM) Science Team Meeting
[DE94-011194] p 4467 N94-37454
Solar-Terrestrial Predictions, 4: Proceedings of aworkshop. Volume 3: Geomagnetic papers; ionospheric papers
[PB94-173192] p 4470 N94-37530
The 1st International Symposium on Organic Photochromism: Molecules and Systems
[PB94-179488] p 4399 N94-37531
Pre-equilibrium parton dynamics: Proceedings
[DE94-011347] p 4520 N94-37716
Proceedings of the Workshop on TRISTAN Physics at High Luminosities
[DE94-737969] p 4523 N94-37727
Solar-Terrestrial Predictions, 4: Proceedings of a workshop. Volume 1: Workshop overview papers; working group reports; User community reports; Regional Warning Center Reports
[PB94-173176] p 4471 N94-37780
Solar-Terrestrial Predictions, 4: Proceedings of a workshop. Volume 2: Solar papers; magnetospheric papers
[PB94-173184] p 4471 N94-37781
CONFIGURATION INTERACTION
MCHF calculations of isotope shifts. 1: Program implementation and test runs. 2: Large-scale active space calculations
[DE94-013036] p 4518 N94-37313
CONFIGURATION MANAGEMENT
Earth Observing System (EOS)/Advanced Microwave Sounding Unit A (AMSU-A) configuration management plan
[NASA-CR-189371] p 4494 N94-37061
CONFINEMENT
Self-sustained turbulence and L-mode confinement in toroidal plasmas
[DE94-748497] p 4532 N94-37734
CONGRESSIONAL REPORTS
Accomplishments under the Airport Improvement Program
[AD-A280661] p 4389 N94-36763
Space Station: Impact of the expanded Russian role on funding and research. Report to the Ranking Minority Member, Subcommittee on Oversight of Government Management, Committee on Governmental Affairs, US Senate
[GAO/NSIAD-94-220] p 4396 N94-37257
CONJUGATE GRADIENT METHOD
Detection of the electrocardiogram P-wave using wavelet analysis
[DE94-010791] p 4481 N94-37197
CONNECTORS
Jumper connector analysis
[DE94-010373] p 4451 N94-37188
CONSERVATION
Microscopic theory of the dielectric response of highly dispersive biological media
[AD-A280516] p 4516 N94-37109
CONSERVATION LAWS
The canonical symmetry for integral systems
[DE94-618488] p 4504 N94-37375
Evolution of turbulent fields in explosions
[DE94-010405] p 4444 N94-37390
High-order centered difference methods with sharp shock resolution
[NASA-CR-196374] p 4496 N94-37656
A nonconservative scheme for isentropic gas dynamics
[DE94-011488] p 4445 N94-37724
CONSTITUTIVE EQUATIONS
Modelling and testing fibre reinforced titanium for design purposes p 4403 N94-36670

Some considerations for modeling the creep behavior of composite materials
[DE94-012112] p 4404 N94-37205

CONTACT LOADS
Strength evaluation of socket joints
[NASA-CR-4608] p 4389 N94-37259

CONTAINMENT
A dynamic model of a linear actuator based on polymer hydrogel
[DE94-010800] p 4408 N94-37091

CONTAMINANTS
Short-tower sigma(theta) measurements in the Colorado Plateaus region
[DE94-007478] p 4463 N94-36478
California residential indoor air quality study. Volume 1: Methodology and descriptive statistics
[PB94-166048] p 4464 N94-36994
California residential indoor air quality study. Volume 1: Methodology and descriptive statistics. Appendix
[PB94-166055] p 4464 N94-36995
Mexico City air quality research initiative, volume 4
[DE94-013201] p 4466 N94-37299
Evaluation of parameterizations for pollutant transport and dispersion in an urban street canyon using a three-dimensional dynamic flow model
[DE94-012641] p 4467 N94-37429

CONTAMINATION
Real-time SAW measurements of NVR in cleanroom and in microenvironment
[DE94-011937] p 4389 N94-37159
Development of high sensitivity techniques for characterizing outgassing of polymeric construction materials for microenvironments
[DE94-012068] p 4424 N94-37204

CONTINUITY (MATHEMATICS)
Coherence and chaos
[DE94-008529] p 4539 N94-36507

CONTINUOUS RADIATION
Molecular beam surface analysis
[DE94-010773] p 4406 N94-36453
Field emitter array RF amplifier development project. Phase 1, option 1
[AD-A280513] p 4437 N94-37107

CONTINUOUS WAVE LASERS
Diode array alternative to paint removal solid-state cw laser
[DE94-011482] p 4448 N94-37203
Two-micron modelocked laser system
[AD-D016219] p 4448 N94-37481
Diode-pumped, continuously tunable, 2.3 micron CW laser specification
[AD-D016312] p 4450 N94-37838

CONTINUUM MECHANICS
A methodology to predict damage initiation, damage growth and residual strength in titanium matrix composites
[NASA-TM-109135] p 4405 N94-37320
Experimental and finite-element simulation results for a plane-strain punch-test using isotropic and anisotropic materials
[DE94-011711] p 4457 N94-37670

CONTINUUM MODELING
A coupled/uncoupled deformation and fatigue damage algorithm utilizing the finite element method
[NASA-TM-106526] p 4455 N94-36561
Numerical study of the flow of granular materials down an inclined plane
[DE94-010729] p 4444 N94-37544

CONTRACTS
A guide to tenders and contracts alerting services
[AGARD-R-799] p 4540 N94-37447

CONTROL EQUIPMENT
Interactive large screen: A multi-mode dialogue tool for future cockpits p 4484 N94-37266
A non-intrusive way to measure point-of-gaze p 4484 N94-37272

CONTROL STABILITY
Robust stabilization of marginally stable positive-real systems
[NASA-TM-109136] p 4500 N94-37058
H infinity control for nonlinear and linear systems
[AD-A280450] p 4494 N94-37226
Robust stability of second-order systems
[NASA-CR-196384] p 4501 N94-37590

CONTROL SYSTEMS DESIGN
Software use control
[DE94-008429] p 4489 N94-36480
High accuracy control algorithm application to a tracking turret p 4394 N94-36626
Aeroservoelastic stabilization considerations for pointing and tracking systems p 4394 N94-36627
Mixed H2/H-infinity optimization with multiple H infinity constraints
[AD-A280572] p 4388 N94-36733
Eigensystem realization algorithm user's guide forVAX/VMS computers: Version 931216
[NASA-TM-109066] p 4493 N94-36818
Gain weighted eigenspace assignment
[NASA-TM-109130] p 4388 N94-36820
Error control techniques for satellite and space communications
[NASA-CR-196302] p 4433 N94-36931
Multirate flutter suppression system design for the Benchmark Active Controls Technology Wing
[NASA-CR-196112] p 4388 N94-36965
Design and evaluation of a Stochastic Optimal Feed-forward and Feedback Technology (SOFFT) flight control architecture
[NASA-TP-3419] p 4388 N94-37014
Predicting the effects of unmodeled dynamics on an aircraft flight control system design using eigenspace assignment
[NASA-TM-4548] p 4388 N94-37059
H infinity control for nonlinear and linear systems
[AD-A280450] p 4494 N94-37226
Virtual Interfaces: Research and Applications
[AGARD-CP-541] p 4482 N94-37261
Interactive large screen: A multi-mode dialogue tool for future cockpits p 4484 N94-37266
Approximate analysis for repeated eigenvalue problems with applications to controls-structure integrated design
[NASA-TP-3439] p 4397 N94-37502
Robust stability of second-order systems
[NASA-CR-196384] p 4501 N94-37590
Open architecture controllers for advanced manufacturing
[DE94-007572] p 4496 N94-37782
What is an open architecture robot controller?
[DE94-007854] p 4501 N94-37783

CONTROL THEORY
H2 optimal control with H-infinity, mu, and L1 constraints
[AD-A280593] p 4500 N94-36736
Robust stabilization of marginally stable positive-real systems
[NASA-TM-109136] p 4500 N94-37058
Predicting the effects of unmodeled dynamics on an aircraft flight control system design using eigenspace assignment
[NASA-TM-4548] p 4388 N94-37059
Solving ill-conditioned matrix equations in control
[AD-A280502] p 4503 N94-37146
Modeling and control of intelligent flexible structures
[AD-A280478] p 4396 N94-37349
Finite element approximation of an optimal control problem for the von Karman equations
[NASA-CR-194955] p 4505 N94-37540

CONTROLLED ATMOSPHERES
Real-time SAW measurements of NVR in cleanroom and in microenvironment
[DE94-011937] p 4389 N94-37159

CONTROLLED FUSION
D-D fusion experiments using fast z-pinches
[DE94-010090] p 4526 N94-36448

CONTROLLERS
High accuracy control algorithm application to a tracking turret p 4394 N94-36626
Two-axis camera platform for machine vision p 4394 N94-36628
H2 optimal control with H-infinity, mu, and L1 constraints
[AD-A280593] p 4500 N94-36736
Design and evaluation of a Stochastic Optimal Feed-forward and Feedback Technology (SOFFT) flight control architecture
[NASA-TP-3419] p 4388 N94-37014
Robust stabilization of marginally stable positive-real systems
[NASA-TM-109136] p 4500 N94-37058
Manual tracking performance using a virtual hand controller: A comparison study p 4484 N94-37271
Open architecture controllers for advanced manufacturing
[DE94-007572] p 4496 N94-37782
What is an open architecture robot controller?
[DE94-007854] p 4501 N94-37783
Neurocontrol of a broadband (ATM) Clos' switching network
[PB94-179389] p 4441 N94-37851

CONVECTION
Measurements and modeling of the effect of convective clouds on the upper tropospheric moisture budget
[NASA-TM-109894] p 4473 N94-37371
Stability and dynamics of spatio-temporal structures
[DE94-013035] p 4412 N94-37491

CONVECTIVE HEAT TRANSFER
A combined experiment/computational study of flow in turbine blade cooling passage
[NASA-CR-4584] p 4442 N94-36957
Hypersonic, nonequilibrium flow over the FIRE 2 forebody at 1634 sec
[NASA-TM-109141] p 4444 N94-37455
Active cooling from the sixties to NASP
[NASA-TM-109079] p 4456 N94-37541

CONVERGENCE
A coarse-mesh nodal method-diffusive-mesh finite difference method
[DE94-010809] p 4502 N94-36455
New method for minimizing regular functions with constraints on parameter region
[DE94-618340] p 4515 N94-37076
A nonconservative scheme for isentropic gas dynamics
[DE94-011488] p 4445 N94-37724

CONVERGENT-DIVERGENT NOZZLES
Mixing and noise benefit versus thrust penalty in supersonic jets using impingement tones
[NASA-TM-106583] p 4382 N94-36686
Theoretical studies of a molecular beam generator
[NASA-CR-196306] p 4522 N94-37508

CONVERSION
Superacid catalysis of light hydrocarbon conversion
[DE94-011132] p 4411 N94-37431

COOLING
Cooling of the West Spitzbergen Current: Wintertime observations west of Svalbard
[AD-A280648] p 4475 N94-36762
A combined experiment/computational study of flow in turbine blade cooling passage
[NASA-CR-4584] p 4442 N94-36957
Miniature thermoacoustic refrigerator
[AD-A280326] p 4431 N94-37029
Refrigeration and Air-Conditioning Technology Workshop
[DE94-010813] p 4431 N94-37452
Laser cooling of 24Mg+ in the ASTRID storage ring
[DE94-010445] p 4523 N94-37619
Initial report on calorimetry for the Tore Supra Outboard pump Limiter
[DE94-011244] p 4531 N94-37626

COOLING SYSTEMS
Preliminary design for a reverse Brayton cycle cryogenic cooler
[NASA-CR-189341] p 4461 N94-36805
Miniature thermoacoustic refrigerator
[AD-A280326] p 4431 N94-37029
Diode array alternative to paint removal solid-state cw laser
[DE94-011482] p 4448 N94-37203
Development of intermetallic coatings for fusion power applications
[DE94-012647] p 4419 N94-37442
Active cooling from the sixties to NASP
[NASA-TM-109079] p 4456 N94-37541

COPOLYMERS
Replacement of silicone polymer A with silicone polymer B and the subsequent characterization of the new cellular silicone materials
[DE94-010105] p 4421 N94-36474
Forward scattering of neutrons from polymeric and magnetic multilayers
[DE93-041158] p 4513 N94-36896
Thermal cis-trans isomerization rates of azobenzenes bound in the side chain of some copolymers and blends
[AD-A280451] p 4424 N94-37227

COPPER
Determination of copper in tap water using solid-phase spectrophotometry
[NASA-TM-106480] p 4408 N94-36537
Dipole forbidden vibrational modes for NO and CO on Cu observed in the far IR
[DE94-003199] p 4408 N94-36559
An externally heated copper vapour laser
[DE94-619484] p 4447 N94-36565
Frequency doubling of copper lasers using temperature-tuned ADP
[DE94-011542] p 4448 N94-37240
New hollow-cathode electrode for high-power copper lasers
[DE94-011637] p 4448 N94-37244
Copper-containing ceramic precursor synthesis: Solid-state transformations and materials technology
[NASA-TM-106556] p 4399 N94-37315

COPPER ALLOYS
Characterization of nuclear transmutations in materials irradiated test facilities
[DE94-013309] p 4420 N94-37552

COPPER COMPOUNDS
Quadrupolar effects in PrCu2Si2
[DE94-011509] p 4534 N94-37054
Structural ground-state of La2CuO4 in the LTO phase: Evidence of local disorder
[DE94-013126] p 4536 N94-37291

COPPER OXIDES
Effect of thermal annealing on grain boundary chemistry of polycrystalline TlBa2Ca2Cu3O(y) films
[DE94-011464] p 4538 N94-37569
High T(sub c) copper-oxide superconductors comprising Tl-Sr-Ca-Cu-O
[AD-D016307] p 4538 N94-37776
COPPER SELENIDES
Investigation of polycrystalline thin-film CuInSe2 solar cells based on ZnSe windows
[DE94-006936] p 4482 N94-37381
COPPER SULFIDES
Copper-containing ceramic precursor synthesis: Solid-state transformations and materials technology
[NASA-TM-106556] p 4399 N94-37315
CORNEA
Three dimensional optic tissue culture and process
[NASA-CASE-MSC-22368-1] p 4478 N94-36765
CORONARY CIRCULATION
Arterial cross-section measurements from dual energy transvenous coronary angiography images
[DE94-011193] p 4482 N94-37444
CORRECTION
Methods of calculation of higher power corrections in QCD
[DE94-618511] p 4521 N94-36748
Introduction to the heavy quark effective theory, part 1
[DE94-618512] p 4514 N94-36749
CORRELATION
Correlation of hot-carrier stress and ionization induced degradation in bipolar transistors
[DE94-007289] p 4532 N94-36540
Correlation of analytical and experimental hot structure vibration results
[NASA-TM-104269] p 4386 N94-36644
Microscopic theory of the dielectric response of highly dispersive biological media
[AD-A280516] p 4516 N94-37109
CORROSION
Indicators for sulfate-reducing bacteria in microbiologically influenced corrosion
[AD-A278914] p 4477 N94-36522
NASA-UVA Light Aerospace Alloy and Structures Technology Program (LA2ST)
[NASA-CR-196290] p 4415 N94-36809
Evaluation of flame-sprayed polymer coatings for civil works navigation structures
[AD-A280507] p 4422 N94-37104
Evaluating plastic assembly processes for high reliability applications using HAST and Assembly Test Chips
[DE94-010750] p 4439 N94-37363
CORROSION PREVENTION
Using nonequilibrium alloying techniques for corrosion inhibition in Gr/Al and Gr/Mg metal matrix composites
[AD-A280529] p 4404 N94-37088
The corrosion protection of several aluminum alloys by chromic acid and sulfuric acid anodizing
[NASA-TP-3490] p 4420 N94-37578
CORROSION RESISTANCE
Production of amorphous metal layers using ion implantation and investigation of the related modification of some surface properties
[DE94-617509] p 4414 N94-36541
Using nonequilibrium alloying techniques for corrosion inhibition in Gr/Al and Gr/Mg metal matrix composites
[AD-A280529] p 4404 N94-37088
Interfaces of high-protection performance polyaryls-coated zinc phosphated steels
[DE94-011732] p 4417 N94-37153
Evaluating plastic assembly processes for high reliability applications using HAST and Assembly Test Chips
[DE94-010750] p 4439 N94-37363
The effect of reactive elements on the segregation behavior and microstructure of alpha-Al2O3 scales on beta-NiAl
[DE94-012739] p 4418 N94-37399
Development of intermetallic coatings for fusion power applications
[DE94-012647] p 4419 N94-37442
CORROSION TESTS
Interfaces of high-protection performance polyaryls-coated zinc phosphated steels
[DE94-011732] p 4417 N94-37153
COSMIC RAYS
Cosmic rays: Physics and astrophysics. A research briefing
[NASA-CR-196118] p 4550 N94-36921
COSMOLOGY
The Mesozoic Era of relativistic heavy ion physics and beyond
[DE94-011341] p 4548 N94-37557
COST ANALYSIS
Operations and support cost modeling of conceptual space vehicles
[NASA-CR-196299] p 4397 N94-37580
COST EFFECTIVENESS
Process improvement as an investment: Measuring its worth p 4489 N94-36486
UK methane emissions inventory: A scoping study on the use of ambient measurements to reduce uncertainties
[PB94-167855] p 4463 N94-36533
Cost-effective computations with boundary interface operators in elliptic problems
[DE94-621506] p 4503 N94-37098
COST ESTIMATES
Recent SEL experiments and studies p 4490 N94-36487
Software forecasting as it is really done: A study of JPL software engineers p 4490 N94-36489
Scoping economics for the commercial manufacture of metallocene catalysts
[DE94-011526] p 4422 N94-37055
Operations and support cost modeling of conceptual space vehicles
[NASA-CR-196299] p 4397 N94-37580
COST REDUCTION
MODIL cryocooler producibility demonstration project results
[DE93-019213] p 4430 N94-36444
COSTS
On the use of fuzzy logic assessment for high consequence implementation risk analysis
[DE94-011417] p 4507 N94-37564
COUPLINGS
Summary of the extensions of the Standard Model working group
[DE94-002217] p 4512 N94-36527
COVARIANCE
A method for obtaining a least squares fit of a hyperplane to uncertain data
[DE94-012498] p 4503 N94-37073
COWLINGS
Computational investigation of an improved cowl concept for hypersonic propulsive nozzles
[AD-A280596] p 4441 N94-36724
CRACK ARREST
Crack growth under cycle loading in fibre reinforced titanium metal matrix composites p 4402 N94-36665
CRACK INITIATION
Defect initiation/growth and energy dissipation induced by deformation and fracture
[AD-A280411] p 4424 N94-37184
A methodology to predict damage initiation, damage growth and residual strength in titanium matrix composites
[NASA-TM-109135] p 4405 N94-37320
CRACK PROPAGATION
Residual strength and life prediction techniques for Ti MMC p 4402 N94-36662
Crack growth under cycle loading in fibre reinforced titanium metal matrix composites p 4402 N94-36665
Pre-standardisation work on fatigue and fracture testing of titanium matrix composites p 4402 N94-36667
Fracture mechanics life analytical methods verification testing
[NASA-CR-4602] p 4455 N94-37015
Literature review and preliminary studies of fretting and fretting fatigue including special applications to aircraft joints
[AD-A280310] p 4456 N94-37125
Interaction effects of cracks, flaws and damage in ceramic
[AD-A280368] p 4423 N94-37181
Defect initiation/growth and energy dissipation induced by deformation and fracture
[AD-A280411] p 4424 N94-37184
The cyclic fatigue behaviour of adhesive joints
[AD-A280453] p 4456 N94-37186
A methodology to predict damage initiation, damage growth and residual strength in titanium matrix composites
[NASA-TM-109135] p 4405 N94-37320
Defects and their effects on the integrity of nickel based aeroengine discs p 4421 N94-37328
Predicting defect behaviour p 4455 N94-37331
Fatigue case study and loading spectra for wind turbines
[DE94-010798] p 4457 N94-37622
Strength characteristics and crack growth behavior of a composite with well aligned fibers p 4459 N94-37804
CRACK TIPS
Strength characteristics and crack growth behavior of a composite with well aligned fibers p 4459 N94-37804
CRACKING (CHEMICAL ENGINEERING)
Thermodynamic and kinetic aspects of surface acidity
[DE94-012351] p 4411 N94-37372
CRACKING (FRACTURING)
Mitigation of harmful effects of welds in zirconium alloy components
[DE94-619033] p 4414 N94-36543
Interaction effects of cracks, flaws and damage in ceramic
[AD-A280368] p 4423 N94-37181
Exploratory study on H13 steel dies
[DE94-012118] p 4420 N94-37678
Damage and strength of composite materials: Trends, predictions, and challenges p 4459 N94-37805
CRACKS
Literature review and preliminary studies of fretting and fretting fatigue including special applications to aircraft joints
[AD-A280310] p 4456 N94-37125
Interaction effects of cracks, flaws and damage in ceramic
[AD-A280368] p 4423 N94-37181
CRASHES
Composite helicopter accident profiles: Deficient crew/aircraft performance
[SCT-90RR-46] p 4385 N94-37604
CRAY COMPUTERS
Preconditioned implicit solvers for the Navier-Stokes equations on distributed-memory machines
[NASA-TM-106449] p 4502 N94-36647
CREEP PROPERTIES
Modelling irradiation creep of zirconium alloys
[DE94-619055] p 4414 N94-36544
Modeling of thermal barrier coatings
[NASA-CR-195365] p 4421 N94-36637
Metal matrix composites: Analysis of simple specimens and model components under creep and fatigue loading p 4402 N94-36661
Irradiation assisted stress corrosion cracking of HTH Alloy X-750 and Alloy 625
[DE94-012667] p 4416 N94-37080
Ability of the total strain version of strainrange partitioning to characterize thermomechanical fatigue behavior
[NASA-TM-4556] p 4455 N94-37102
Some considerations for modeling the creep behavior of composite materials
[DE94-012112] p 4404 N94-37205
Creep-fatigue interaction property of a nickel-base heat-resistant alloy Hastelloy XR in simulated HTGR helium gas environment
[DE94-737934] p 4418 N94-37416
Creep properties with short period excessive loadings on a nickel-base heat-resistant alloy Hastelloy XR
[DE94-718965] p 4419 N94-37465
Physical and mechanical metallurgy of NiAl
[NASA-TP-3398] p 4419 N94-37503
Flux creep: Its dependence on current denisty and relation to critical current densities from transport and magnetic measurements
[DE94-011701] p 4440 N94-37738
Statistical scaling relationships and size effects in the strength and creep rupture of fibrous composites p 4460 N94-37809
CREEP RUPTURE STRENGTH
Statistical scaling relationships and size effects in the strength and creep rupture of fibrous composites p 4460 N94-37809
CREEP STRENGTH
Substantiating powder metal life methodologies for engines p 4455 N94-37330
CREEP TESTS
Metal matrix composites: Analysis of simple specimens and model components under creep and fatigue loading p 4402 N94-36661
Creep properties with short period excessive loadings on a nickel-base heat-resistant alloy Hastelloy XR
[DE94-718965] p 4419 N94-37465
CREW WORKSTATIONS
Advanced helmet tracking technology developments for Naval aviation p 4393 N94-36623
CRIME
Criminal Acts Against Civil Aviation, 1993
[AD-A280694] p 4384 N94-37131
CROSS FLOW
Preliminary analysis for a Mach 8 crossflow transition experiment on the Pegasus (R) space booster
[NASA-TM-104272] p 4381 N94-36648
CROSSTALK
A comparison of two examples of magnetic tracker systems p 4485 N94-37275
CRRES (SATELLITE)
NRL HF propagation measurements between Guadeloupe and Providenciales during the CRRES exercises
[DE94-012078] p 4435 N94-37393

CRYOGENIC COOLING
Preliminary design for a reverse Brayton cycle cryogenic cooler
[NASA-CR-189341] p 4461 N94-36805
CRYOGENIC EQUIPMENT
Electrically conductive, thermally insulating cryogenic current leads
[NASA-CASE-LAR-14964-1-CU] p 4437 N94-36781
CRYOGENIC FLUID STORAGE
Cryogenic fluid management technologies for space transportation. Zero G thermodynamic vent system
[NASA-CR-193981] p 4430 N94-36806
CRYOGENICS
MODIL cryocooler producibility demonstration project results
[DE93-019213] p 4430 N94-36444
NiAl-base composite containing high volume fraction of AlN for advanced engines
[NASA-CASE-LEW-15818-1] p 4403 N94-36752
CRYOSTATS
Pulsed field magnets at the United States National High Magnetic Field Laboratory
[DE94-002624] p 4436 N94-36514
CRYPTOGRAPHY
Analysis of end-to-end encryption and traffic flow confidentiality options
[AD-A278612] p 4433 N94-36754
CRYSTAL DEFECTS
Forward scattering of neutrons from polymeric and magnetic multilayers
[DE93-041158] p 4513 N94-36696
Diamond deposition and defect chemistry studied via solid state NMR
[AD-A280609] p 4533 N94-36727
ALCHEMI formulated for delocalization and anti-site defects
[DE94-012740] p 4537 N94-37400
CRYSTAL DISLOCATIONS
Low temperature materials — indium gallium arsenides
[AD-A278703] p 4533 N94-36755
CRYSTAL FIELD THEORY
Quadrupolar effects in PrCu2Si2
[DE94-011509] p 4534 N94-37054
Modelling of surfaces. Part 1: Monatomic metallic surfaces using equivalent crystal theory
[NASA-TM-106680] p 4419 N94-37459
CRYSTAL GROWTH
Ampoule failure sensor time response testing: Experiments 2 and 3
[NASA-TM-108458] p 4446 N94-36822
Turning soot into diamonds with microwaves
[DE94-013426] p 4422 N94-37068
CRYSTAL LATTICES
Phase transitions in crystalline solids 1
[DE94-619029] p 4532 N94-36542
Consequences of competing hybridization for magnetic ordering in correlated-electron lattices
[DE94-011648] p 4534 N94-37057
High resolution electron diffraction analysis of structural changes associated with the photocycle of bacteriorhodopsin
[DE94-011800] p 4479 N94-37156
Pair correlations in crystalline solid solutions
[DE94-012319] p 4535 N94-37212
ALCHEMI formulated for delocalization and anti-site defects
[DE94-012740] p 4537 N94-37400
The application of maximum entropy to Z-contrast imaging in a stem
[DE94-011470] p 4412 N94-37546
CRYSTAL STRUCTURE
Collaboration in Crystallography: Proceedings of the 1st Joint Seminar of the ISIS-INCR Collaboration in Crystallography
[PB94-171097] p 4532 N94-36548
Forward scattering of neutrons from polymeric and magnetic multilayers
[DE93-041158] p 4513 N94-36696
Comparison of the crystal structure and molecular models of N,N-diisobutyl-2- (octylphenylphosphinyl) acetamide (CMPO)
[DE94-013434] p 4534 N94-37069
Studies of the III-V compounds in the megabar regime
[DE94-012488] p 4537 N94-37435
Crystallographic studies of nitrogenase and hydrogenase
[DE94-011972] p 4538 N94-37677
CRYSTALLOGRAPHY
Collaboration in Crystallography: Proceedings of the 1st Joint Seminar of the ISIS-INCR Collaboration in Crystallography
[PB94-171097] p 4532 N94-36548
High resolution electron diffraction analysis of structural changes associated with the photocycle of bacteriorhodopsin
[DE94-011800] p 4479 N94-37156
Pair correlations in crystalline solid solutions
[DE94-012319] p 4535 N94-37212
Scanning x-ray diffraction: A technique with high compositional resolution for studying phase formation in co-deposited thin films
[DE94-011496] p 4420 N94-37516
Crystallographic studies of nitrogenase and hydrogenase
[DE94-011972] p 4538 N94-37677
CRYSTALS
Assess progress being made for the KTeV electromagnetic calorimeter crystal order in France
[DE94-009396] p 4533 N94-36746
CULTIVATION
Biological determinants of photobioreactor design
[DE94-011665] p 4468 N94-37740
CULTURE TECHNIQUES
Recombinant protein production and insect cell culture and process
[NASA-CASE-MSC-22336-1] p 4478 N94-36751
Three dimensional optic tissue culture and process
[NASA-CASE-MSC-22368-1] p 4478 N94-36765
CUMULATIVE DAMAGE
Fatigue case study and loading spectra for wind turbines
[DE94-010798] p 4457 N94-37622
CURING
Double network elastomers and method of making same
[AD-D016323] p 4427 N94-37831
CURRENT DENSITY
Design and analysis of high-field quasi-continuous magnets
[DE94-000762] p 4508 N94-36556
Field emitter array RF amplifier development project. Cathode technology development. Phase 1
[AD-A280515] p 4437 N94-37108
Critical-state flux-density profiles in type-2 superconducting thin-film strips and disks
[DE94-011199] p 4535 N94-37166
Motional Stark effect upgrades on D3-D
[DE94-013146] p 4528 N94-37297
Flux creep: Its dependence on current denisty and relation to critical current densities from transport and magnetic measurements
[DE94-011701] p 4440 N94-37738
CURRENT SHEETS
Magnetotail dynamics: MHD simulations of driven and spontaneous dynamic changes
[DE94-011702] p 4471 N94-37701
CYANO COMPOUNDS
Organic NLO polymers. 2: Main-chain and guest-host Chi(2)NLO polymers: NLO-phore structure versus poling
[AD-A280230] p 4423 N94-37133
CYCLIC COMPOUNDS
Cyclization of bis-urethanes as a new method for the synthesis of 5-substituted, 6-membered cyclic ureas
[AD-A280232] p 4399 N94-37134
CYCLIC LOADS
Crack growth under cycle loading in fibre reinforced titanium metal matrix composites p 4402 N94-36665
Prediction of thermal and mechanical stress-strain responses of TMC's subjected to complex TMF histories p 4402 N94-36666
The cyclic fatigue behaviour of adhesive joints
[AD-A280453] p 4456 N94-37186
CYCLOGENESIS
Experiment on rapidly intensifying cyclones over the Atlantic
[AD-A280365] p 4473 N94-37180
CYCLONES
Experiment on rapidly intensifying cyclones over the Atlantic
[AD-A280365] p 4473 N94-37180
The life cycles of intense cyclonic and anticyclonic circulation systems observed over oceans
[NASA-CR-196271] p 4473 N94-37294
CYCLOTRON RADIATION
New plasma source of hydrides for epitaxial growth
[DE94-006918] p 4533 N94-36744
CYCLOTRON RESONANCE
New plasma source of hydrides for epitaxial growth
[DE94-006918] p 4533 N94-36744
The mathematical simulation of physical processes in ECR multicharged ions sources
[DE94-618343] p 4515 N94-37077
CYLINDRICAL SHELLS
Laminated thin shell structures subjected to free vibration in a hygrothermal environment
[NASA-TM-106600] p 4456 N94-37456

D

DAMAGE
A coupled/uncoupled deformation and fatigue damage algorithm utilizing the finite element method
[NASA-TM-106526] p 4455 N94-36561
Vibration signature analysis of a faulted gear transmission system
[NASA-TM-106623] p 4450 N94-36953
Turbine disks: Lifing against defects and materials development p 4454 N94-37329
Damage and strength of composite materials: Trends, predictions, and challenges p 4459 N94-37805
DAMAGE ASSESSMENT
Interaction effects of cracks, flaws and damage in ceramic
[AD-A280368] p 4423 N94-37181
DATA ACQUISITION
The (mis)use of subjective process measures in software engineering p 4490 N94-36491
Geophysical data fusion for subsurface imaging
[DE94-000056] p 4469 N94-36738
Experimental uncertainty and drag measurements in the national transonic facility
[NASA-CR-4600] p 4389 N94-36945
Data compatibility for various Charpy-tests
[DE94-617534] p 4416 N94-37074
Design of the divertor Thomson scattering system on D3-D
[DE94-012672] p 4527 N94-37081
AWOS Data Acquisition System (ADAS) Operational Test and Evaluation (OT/E) integration and OT/E operational test report
[AD-A280492] p 4473 N94-37143
UAV's in climate research: The ARM Unmanned Aerospace Vehicle Program
[DE94-011753] p 4465 N94-37154
Index and bulk parameters for frequency-direction spectra measured at CERC Field Research Facility, September 1990 to August 1991
[AD-A280423] p 4476 N94-37216
Index and bulk parameters for frequency-direction spectra measured at CERC Field Research Facility, September 1991 to August 1992
[AD-A280455] p 4477 N94-37229
A non-intrusive way to measure point-of-gaze p 4484 N94-37272
Providing electronic documents in Europe: Experience of INIST p 4544 N94-37341
Fermilab's DART DA system
[DE94-013240] p 4523 N94-37547
Crosspoint analog data selector
[AD-D016326] p 4440 N94-37832
DATA BASE MANAGEMENT SYSTEMS
RECON Replacement Project p 4541 N94-36844
NASA Access Mechanism (NAM) p 4541 N94-36850
Standards in the architectural effort p 4541 N94-36852
TRENDS: A flight test relational database user's guide and reference manual
[NASA-TM-108806] p 4381 N94-37332
DATA BASES
Software quality: Process or people p 4492 N94-36499
Hypersonic shock/boundary-layer interaction database: New and corrected data
[NASA-CR-177638] p 4441 N94-36519
NASA Access Mechanism: Lessons learned document
[NASA-TM-109924] p 4540 N94-36750
NASA STI Program Coordinating Council Eleventh Meeting: NASA STI Modernization Plan
[NASA-TM-109415] p 4540 N94-36841
NASA STI modernization plan p 4540 N94-36842
The Engineering Review Board p 4540 N94-36843
RECON Replacement Project p 4541 N94-36844
NASA Access Mechanism (NAM) p 4541 N94-36850
Network upgrades p 4541 N94-36851
SeaWiFS technical report series. Volume 20: The SeaWiFS bio-optical archive and storage system (SeaBASS), part 1
[NASA-TM-104566-VOL-20-PT-1] p 4475 N94-36958
United States Air Force Summer Research Program, 1993. Volume 9: Rome Laboratory
[AD-A278699] p 4551 N94-36984
Global Picture Archiving and Communication Systems (GPACS): An overview
[AD-A280617] p 4543 N94-37042
Data compatibility for various Charpy-tests
[DE94-617534] p 4416 N94-37074
Interchangeable spline reference guide
[DE94-012368] p 4495 N94-37245
Providing electronic documents in Europe: Experience of INIST p 4544 N94-37341

Development of durable high-temperature catalysts for natural gas combustion: Catalytic materials (CATMAT (trade name)) properties database
[PB94-171824] p 4412 N94-37462
Information on alternative refrigerants and lubricants: The ARTI refrigerant database
[DE94-009997] p 4426 N94-37490
Stratospheric emissions effects database development
[NASA-CR-4592] p 4467 N94-37607
Advanced distributed simulation technology. SIMWORLD data base
[AD-A280262] p 4545 N94-37757

DATA COMPRESSION
Global Picture Archiving and Communication Systems (GPACS): An overview
[AD-A280617] p 4543 N94-37042

DATA CORRELATION
The (mis)use of subjective process measures in software engineering p 4490 N94-36491

DATA FLOW ANALYSIS
Integrating end-to-end threads of control into object-oriented analysis and design
p 4491 N94-36496

DATA INTEGRATION
Studies and simulations on sensor fusion and cueing for fighter application p 4395 N94-36632
Sensor data fusion for air to air situation awareness beyond visual range p 4395 N94-36633
Contact level fusion of radar and IRST contacts on almost electromagnetically silent platform
p 4395 N94-36634
Geophysical data fusion for subsurface imaging
[DE94-000056] p 4469 N94-36738
Distributed detection theory and data fusion
[AD-A280410] p 4434 N94-37183

DATA MANAGEMENT
Global Picture Archiving and Communication Systems (GPACS): An overview
[AD-A280617] p 4543 N94-37042

DATA PROCESSING
Standards in the architectural effort
p 4541 N94-36852
Advanced information processing system: Hosting of advanced guidance, navigation and control algorithms on AIPS using ASTER
[NASA-CR-194960] p 4499 N94-37583

DATA PROCESSING EQUIPMENT
The impact of HPF data layout on the design of efficient and maintainable parallel linear algebra libraries
[DE94-012382] p 4504 N94-37246

DATA REDUCTION
A more exact analysis of Sandia Laser Tracker data
[DE94-011411] p 4447 N94-37051
Gamma ray astronomy
[NASA-CR-193970] p 4547 N94-37702

DATA RETRIEVAL
TRENDS: A flight test relational database user's guide and reference manual
[NASA-TM-108806] p 4381 N94-37332

DATA SIMULATION
Data simulation for the Associated Particle Imaging system
[DE94-012664] p 4518 N94-37305

DATA STRUCTURES
RECON Replacement Project p 4541 N94-36844

DATA SYSTEMS
SeaWiFS technical report series. Volume 20: The SeaWiFS bio-optical archive and storage system (SeaBASS), part 1
[NASA-TM-104566-VOL-20-PT-1] p 4475 N94-36958
Global Picture Archiving and Communication Systems (GPACS): An overview
[AD-A280617] p 4543 N94-37042
A non-intrusive way to measure point-of-gaze
p 4484 N94-37272

DATA TRANSFER (COMPUTERS)
Standards for data and document interchange
p 4543 N94-37337
A scalable high-performance I/O system
[DE94-011513] p 4498 N94-37519

DATA TRANSMISSION
Standards for data and document interchange
p 4543 N94-37337
Electronic document delivery: Towards the virtual library p 4544 N94-37340
Progress in navigation filter estimate fusion and its application to spacecraft rendezvous
[NASA-TM-104794] p 4392 N94-37386
Interactive Collaborative Environments (ICE): Platform independent X application sharing and multi-media over wide area networks
[DE94-008868] p 4502 N94-37784
Remote use of distributed robotics resources to enhance technology development and insertion
[DE94-009285] p 4502 N94-37785

DEBONDING (MATERIALS)
Fibre-matrix interface properties in Ti-matrix composites: Chemical compatibility and micromechanical behaviour
p 4401 N94-36657
Micromechanical modeling of damage growth in titanium based metal-matrix composites p 4402 N94-36664

DECISION MAKING
Science priorities for the human dimensions of global change p 4464 N94-36987
Human factors for flight deck certification personnel
[AD-A280477] p 4487 N94-37347
Environmental risk management
[DE94-620987] p 4467 N94-37492

DECODING
Studies on image compression and image reconstruction
[NASA-CR-196304] p 4433 N94-36810

DECOMPOSITION
Molecular beam surface analysis
[DE94-010773] p 4406 N94-36453
Direct catalytic decomposition of nitric oxide
[DE94-005025] p 4407 N94-36475
Modeling of outgassing and matrix decomposition in carbon-phenolic composites
[NASA-CR-196319] p 4405 N94-37471
Perfluorodiethoxymethane on nickel and nickel oxide surfaces
[DE94-011200] p 4426 N94-37712
Ordering design tasks based on coupling strengths
[NASA-TM-109137] p 4387 N94-37762

DECOMPRESSION SICKNESS
Hypobaric decompression sickness model development. Part 1: Diffusion of inert gas from a viscoelastic fluid (blood) into an expanding gas phase
[AD-A280298] p 4481 N94-37124
Cardiac pressure changes with venous gas embolism and decompression
[AD-A280412] p 4481 N94-37224

DEFECTS
Impact of Materials Defects on Engine Structures Integrity
[AGARD-R-790] p 4453 N94-37321
History and prognosis of material discontinuity effects on engine components structural integrity
p 4453 N94-37322
Alternate melting and refining routes
p 4421 N94-37323
Process enhancements of superalloy material
p 4421 N94-37324
Defects and their effects on the integrity of nickel based aeroengine discs p 4421 N94-37328
Turbine disks: Lifing against defects and materials development p 4454 N94-37329
Predicting defect behaviour p 4455 N94-37331
The influence of VAR processes and parameters on white spot formation in Alloy 718
[DE94-012071] p 4417 N94-37367
Atomic level characterization of defects in microalloyed NiAl: An atom probe investigation
[DE94-012732] p 4418 N94-37396
Scaling effects of defects in fiber-reinforced composites p 4459 N94-37807

DEFENSE COMMUNICATIONS SYSTEM (DCS)
A two-level formal specification of a defense communications system
[DE94-012117] p 4434 N94-37206

DEFENSE PROGRAM
United States Air Force Summer Research Program, 1993. Volume 7: Armstrong Laboratory
[AD-A278655] p 4550 N94-36975
United States Air Force Summer Research Program, 1993. Volume 14: Rome Laboratory
[AD-A278656] p 4550 N94-36976
United States Air Force Summer Research Program, 1993. Volume 13: Phillips Laboratory
[AD-A278657] p 4550 N94-36977
United States Air Force Summer Research Program, 1993. Volume 16: Arnold Engineering Development Center, Frank J. Seiler Research Laboratory and Wilford Hall Medical Center
[AD-A278658] p 4550 N94-36978
United States Air Force Summer Research Program, 1993. Volume 3: Phillips Laboratory
[AD-A278694] p 4550 N94-36979
United States Air Force Summer Research Program, 1993. Volume 4: Rome Laboratory
[AD-A278695] p 4551 N94-36980
United States Air Force Summer Research Program, 1993. Volume 5A: Wright Laboratory
[AD-A278696] p 4551 N94-36981
United States Air Force Summer Research Program, 1993. Volume 6: Arnold Engineering Development Center, Frank J. Seiler Research Laboratory and Wilford Hall Medical Center
[AD-A278697] p 4551 N94-36982
United States Air Force Summer Research Program, 1993. Volume 8: Phillips Laboratory
[AD-A278698] p 4551 N94-36983
United States Air Force Summer Research Program, 1993. Volume 9: Rome Laboratory
[AD-A278699] p 4551 N94-36984
The implementation of Electronic Data Interchange (EDI) with defense transportation operations
[AD-A280568] p 4493 N94-37040

DEFLAGRATION
Effects of two-phase flow on the deflagration of porous energetic materials
[DE94-011423] p 4411 N94-37412

DEFLECTION
Replacement of silicone polymer A with silicone polymer B and the subsequent characterization of the new cellular silicone materials
[DE94-010105] p 4421 N94-36474

DEFOCUSING
Recovering depth from focus using iterative image estimation techniques
[DE94-010994] p 4524 N94-37165

DEFORMATION
A coupled/uncoupled deformation and fatigue damage algorithm utilizing the finite element method
[NASA-TM-106526] p 4455 N94-36561
Measurement and interpretation of crustal deformation rates associated with postglacial rebound
[NASA-CR-196300] p 4470 N94-37581

DEGRADATION
Correlation of hot-carrier stress and ionization induced degradation in bipolar transistors
[DE94-007289] p 4532 N94-36540

DEGREES OF FREEDOM
Quantum harmonic Brownian motion in a general environment: A modified phase-space approach
[DE94-003249] p 4508 N94-36560
Issues concerning the updating of finite-element models from experimental data
[NASA-TM-109116] p 4456 N94-37253
A new technique for dynamic load distribution when two manipulators mutually lift a rigid object, part 2
[DE94-010126] p 4501 N94-37735

DEHYDROGENATION
Iron hydrous titanium oxide catalysts for the dehydrogenation of ethylbenzene to styrene
[DE94-010381] p 4412 N94-37542

DELAMINATING
Detection of delaminations in composite beams using piezoelectric sensors
[NASA-TM-106611] p 4403 N94-36956
Damage and strength of composite materials: Trends, predictions, and challenges p 4459 N94-37805
Scaling of impact damage in fiber composites
p 4460 N94-37810

DENSIFICATION
Characterization and processing of sintered products from nano-crystalline powders generated by the RTDS method
[DE94-004765] p 4415 N94-36553

DENSITY (MASS/VOLUME)
Determination of density of mass standards: Requirement and method
[PB94-163078] p 4508 N94-36718
Electronic balance and some gravimetric applications (the density of solids and liquids, pycnometry and mass)
[PB94-163052] p 4446 N94-36719

DENSITY MEASUREMENT
Microwave reflectometry for fusion plasma diagnostics
[DE94-620118] p 4527 N94-36566

DEOXYRIBONUCLEIC ACID
United States Air Force Summer Research Program, 1993. Volume 7: Armstrong Laboratory
[AD-A278655] p 4550 N94-36975
Chemical and structural characterization of nitroaromatic adducts with hemoglobins
[AD-A280533] p 4480 N94-37089

DEPOSITION
Gas-Phase and Surface Chemistry in Electronic Materials Processing. Materials Research Society Symposium proceedings, volume 334
[AD-A280586] p 4408 N94-36735
X-ray diffraction studies of evaporated gold thin films deposited on aluminum nitride substates
[AD-A280454] p 4536 N94-37228
Modeling atmospheric concentrations and deposition of Hg
[DE94-012633] p 4467 N94-37440
A photoemission study of Au, Ge, and O2 deposition on NH4F etched Si(111)
[DE94-013352] p 4519 N94-37553

DEPOSITS
Vent processes during the 1912 eruption at Novarupta, Katmai National Park, Alaska
[DE94-010740] p 4468 N94-36451

Interferometric JFTOT tube deposit measuring device
[AD-D016295] p 4430 N94-37768

DEPTH
Recovering depth from focus using iterative image estimation techniques
[DE94-010994] p 4524 N94-37165

DESICCANTS
Sealed tube comparisons of the compatibility of desiccants with refrigerants and lubricants
[DE94-012371] p 4425 N94-37421

DESIGN ANALYSIS
Fusing modeling techniques to support domain analysis for reuse opportunities identification
p 4491 N94-36497
Modelling and testing fibre reinforced titanium for design purposes p 4403 N94-36670
A dynamic model of a linear actuator based on polymer hydrogel
[DE94-010800] p 4408 N94-37091
NASA Lewis wind tunnel model systems criteria
[NASA-TM-106565] p 4390 N94-37522
Fuzzy logic to improve efficiency of finite element and finite difference schemes
[DE94-011718] p 4496 N94-37739
Ordering design tasks based on coupling strengths
[NASA-TM-109137] p 4387 N94-37762

DESORPTION
Laser probing of interfaces
[DE94-011300] p 4449 N94-37628

DESTABILIZATION
Effects of freezing and cold acclimation on the plasma membrane of isolated protoplasts
[DE94-012487] p 4479 N94-37248
Self-sustained turbulence and L-mode confinement in toroidal plasmas
[DE94-748497] p 4532 N94-37734

DETACHMENT
Effect of temperature on the electron attachment and detachment properties of c-C4F6
[DE94-012750] p 4518 N94-37383

DETECTION
Detection of delaminations in composite beams using piezoelectric sensors
[NASA-TM-106611] p 4403 N94-36956
Distributed detection theory and data fusion
[AD-A280410] p 4434 N94-37183
Time-gated imaging through defense-scattering materials using stimulated Raman amplification
[AD-D016305] p 4440 N94-37775

DETECTORS
Prospects for measuring B(s) mixing at CDF
[DE94-013147] p 4518 N94-37298

DETERMINANTS
Biological determinants of photobioreactor design
[DE94-011665] p 4468 N94-37740

DETONATION
CHEETAH: A fast thermochemical code for detonation
[DE94-012586] p 4429 N94-37427

DETONATION WAVES
A fully coupled thermal, chemical, mechanical cookoff model
[DE94-011432] p 4428 N94-37201

DEUTERIUM
D-D fusion experiments using fast z-pinches
[DE94-010090] p 4526 N94-36448

DEUTERIUM FLUORIDES
A coarse-mesh nodal method-diffusive-mesh finite difference method
[DE94-010809] p 4502 N94-36455

DEUTERONS
Physics with primary beams of the KEK-PS
[DE94-748635] p 4522 N94-37234
Search for the H dibaryon by Xi(-) capture on the deuteron
[DE94-011733] p 4520 N94-37672

DIAGNOSIS
On the feasibility of virtual environments in medicine
p 4483 N94-37264

DIAMAGNETISM
On the interpretation of diamagnetic loop measurements for a current-carrying plasma column in a conducting chamber
[DE94-007107] p 4526 N94-36536

DIAMOND FILMS
Diamond deposition and defect chemistry studied via solid state NMR
[AD-A280609] p 4533 N94-36727
Turning soot into diamonds with microwaves
[DE94-013426] p 4422 N94-37068

DIAMONDS
Compilation of diamond-like carbon properties for barriers and hard coatings
[DE94-012139] p 4427 N94-37725

DICHOTOMIES
Profile analysis of after-effects experienced during exposure to several virtual reality environments
p 4482 N94-37263

DICTIONARIES
Alternative fuel information: Glossary
[DE94-006889] p 4429 N94-37403

DIELECTRICS
Microscopic theory of the dielectric response of highly dispersive biological media
[AD-A280516] p 4516 N94-37109
Effect of temperature on the electron attachment and detachment properties of c-C4F6
[DE94-012750] p 4518 N94-37383
Fluorinated resins with low dielectric constant
[AD-D016303] p 4427 N94-37773

DIES
Exploratory study on H13 steel dies
[DE94-012118] p 4420 N94-37678

DIESEL ENGINES
Coal-fueled diesel technology development: Fuel injection equipment for coal-fueled diesel engines
[DE94-004088] p 4452 N94-37512

DIESEL FUELS
Combustion characterization of methylal in reciprocating engines
[DE94-006949] p 4411 N94-37409

DIFFERENTIAL CALCULUS
ZLIB++: Object-oriented numerical library for differential algebra
[DE94-010839] p 4495 N94-37453

DIFFERENTIAL EQUATIONS
Theoretical investigations of chaotic dynamics
[AD-A280325] p 4507 N94-37028

DIFFERENTIAL GEOMETRY
A method for thermal analysis of spiral bevel gears
[NASA-TM-106612] p 4451 N94-37451

DIFFERENTIATION (BIOLOGY)
Surface modification of polymers with self-assembled monolayers that promote adhesion, outgrowth and differentiation of biological cells
[AD-D016321] p 4427 N94-37829

DIFFRACTION
Four beam interferometer manual: Operating instructions for the INEL diffraction Moire interferometer
[DE94-010772] p 4453 N94-36452
Measurement of the elastic, total and diffraction cross sections at tevatron energies
[DE94-004659] p 4511 N94-36463
Blois 5: Experimental summary
[DE94-001219] p 4513 N94-36558
Hard diffraction and deep inelastic scattering
[DE94-013353] p 4515 N94-37084
A diffraction-based model of anisoplanatism effects in adaptive optic systems
[AD-A280491] p 4524 N94-37142

DIFFUSE RADIATION
A note on analytic recovery of transition probabilities in three dimensional diffuse tomography
[DE94-011378] p 4506 N94-37719

DIFFUSION
A-TOUGH: A multimedia fluid-flow/energy-transport model for fully-coupled atmospheric-subsurface interactions
[DE94-004304] p 4472 N94-36739
Hypobaric decompression sickness model development. Part 1: Diffusion of inert gas from a viscoelastic fluid (blood) into an expanding gas phase
[AD-A280298] p 4481 N94-37124
Influences of flame-vortex interactions on formation of oxides of nitrogen in curved methane-air diffusion flamelets
[DE94-005105] p 4409 N94-37221

DIFFUSION COEFFICIENT
Holographic grating relaxation studies of probe diffusion in amorphous polymers
[AD-A280496] p 4423 N94-37144

DIFFUSION FLAMES
Laser-saturated fluorescence measurements in laminar sooting diffusion flames
[NASA-CR-191025] p 4508 N94-36643
Influences of flame-vortex interactions on formation of oxides of nitrogen in curved methane-air diffusion flamelets
[DE94-005105] p 4409 N94-37221
Finite-rate chemistry and transient effects in Direct Numerical Simulations of turbulent non-premixed flames
[DE94-005250] p 4410 N94-37222
Effects of molecular transport on turbulence-chemistry interactions in a hydrogen-argon-air jet diffusion flame
[DE94-005107] p 4413 N94-37711

DIFLUORO COMPOUNDS
Highly fluorinated polymers
[NASA-CR-196270] p 4422 N94-37025

DIGITAL DATA
Sloan Digital Sky Survey
[DE94-011749] p 4547 N94-37667

DIGITAL ELECTRONICS
High temperature superconducting digital circuits and subsystems
[DE94-001207] p 4436 N94-36557

DIGITAL FILTERS
KONRAD: Wide band digital HF receiver
[PB94-184686] p 4435 N94-37813
Phase shifter for directly sampled bandpass signals
[AD-D016320] p 4440 N94-37840

DIGITAL SPACECRAFT TELEVISION
Portable color multimedia training systems based on monochrome laptop computers (CBT-in-a-briefcase), with spinoff implications for video uplink and downlink in spaceflight operations
[NASA-TM-108460] p 4496 N94-37556

DIGITAL SYSTEMS
Comparison of gaseous and semiconductor detectors for medical imaging
[DE94-621344] p 4482 N94-37729

DILUTION
Pulsed field magnets at the United States National High Magnetic Field Laboratory
[DE94-002624] p 4436 N94-36514

DIODES
Diode array alternative to paint removal solid-state cw laser
[DE94-011482] p 4448 N94-37203

DIOXIDES
Sintering of dioxide pellets in an oxidizing atmosphere (CO2)
[DE94-613046] p 4414 N94-36517

DIRECT CURRENT
Field emitter array RF amplifier development project. Phase 1, option 1
[AD-A280513] p 4437 N94-37107
A comparison of two examples of magnetic tracker systems p 4485 N94-37275

DIRECTIONAL SOLIDIFICATION (CRYSTALS)
Use of rotation to suppress thermosolutal convection in directionally solidified binary alloys
[NASA-CR-196372] p 4415 N94-36811
Processing and mechanical properties of NiAl-based in-situ composites
[NASA-CR-195333] p 4416 N94-36954
Process enhancements of superalloy material
p 4421 N94-37324

DIRICHLET PROBLEM
Cost-effective computations with boundary interface operators in elliptic problems
[DE94-621506] p 4503 N94-37098

DISCONTINUITY
A coarse-mesh nodal method-diffusive-mesh finite difference method
[DE94-010809] p 4502 N94-36455
A flux splitting scheme with high-resolution and robustness for discontinuities
[NASA-TM-106452] p 4441 N94-36646

DISKS
Defects and their effects on the integrity of nickel based aeroengine discs p 4421 N94-37328
Turbine disks: Lifing against defects and materials development p 4454 N94-37329

DISORIENTATION
Attenuating the disorienting effects of head movement during whole-body rotation using a visual reference: Further tests of a predictive hypothesis p 4482 N94-37276
The use of a tactile interface to convey position and motion perceptions p 4486 N94-37281

DISPERSING
Microscopic theory of the dielectric response of highly dispersive biological media
[AD-A280516] p 4516 N94-37109

DISPERSION
Determination of the dispersion constant in a constrained vapor bubble thermosyphon
[NASA-CR-196124] p 4442 N94-36992
A Lagrangian-Eulerian finite element method with adaptive gridding for advection-dispersion problems
[DE94-011372] p 4506 N94-37718

DISPLACEMENT
Generalized squeezed states from generalized coherent states
[DE94-002689] p 4512 N94-36515
Determination of density of mass standards: Requirement and method
[PB94-163078] p 4508 N94-36718

DISPLAY DEVICES
Terminal Doppler Weather Radar (TDWR) build 5 Test and Evaluation Master Plan (TEMP)
[AD-A280426] p 4434 N94-37218
Virtual Interfaces: Research and Applications
[AGARD-CP-541] p 4482 N94-37261

Creation of a virtual world to study human spatial perception during sustained acceleration
p 4484 N94-37268
The DRA Virtual Cockpit Research Program
p 4484 N94-37269
Visual accommodation to virtual image displays when knowledge of object distance conflicts with optical distance
p 4485 N94-37278
Low cost software-based rendering and stereoscopic interfaces for teleoperation and virtual reality
p 4486 N94-37279
Human factors for flight deck certification personnel
[AD-A280477] p 4487 N94-37347
Synthetic vision display evaluation studies
[NASA-CR-194963] p 4387 N94-37658

DISSIPATION
Quantum harmonic Brownian motion in a general environment: A modified phase-space approach
[DE94-003249] p 4508 N94-36560

DISSOLVED GASES
Hypobaric decompression sickness model development. Part 1: Diffusion of inert gas from a viscoelastic fluid (blood) into an expanding gas phase
[AD-A280298] p 4481 N94-37124
Atmospheric gas
[DE94-007439] p 4465 N94-37187

DISTORTION
Four beam interferometer manual: Operating instructions for the INEL diffraction Moire interferometer
[DE94-010772] p 4453 N94-36452

DISTRIBUTED PARAMETER SYSTEMS
A note on the regularity of solutions of infinite dimensional Riccati equations
[NASA-CR-194898] p 4502 N94-36562
Vibration suppression with approximate finite dimensional compensators for distributed systems: Computational methods and experimental results
[NASA-CR-194927] p 4500 N94-36928

DISTRIBUTED PROCESSING
Open system environments p 4542 N94-36857
A comparison of queueing, cluster and distributed computing systems
[NASA-TM-109025] p 4497 N94-36932
Distributed VIRtual System (DIVIRS) project
[NASA-CR-196262] p 4495 N94-37509

DISTRIBUTION FUNCTIONS
Quantum harmonic Brownian motion in a general environment: A modified phase-space approach
[DE94-003249] p 4508 N94-36560
Flow visualization for Lagrangian particle methods
[DE94-010757] p 4443 N94-37195

DIURNAL VARIATIONS
Substorm statistics: Occurrences and amplitudes
[DE94-011694] p 4471 N94-37669

DIVERTERS
Design of the divertor Thomson scattering system on D3-D
[DE94-012672] p 4527 N94-37081
The role of heating and current drive in ITER
[DE94-012679] p 4527 N94-37082
Material and design considerations for the carbon armored ITER divertor
[DE94-737854] p 4530 N94-37415
Improvement study of the divertor configuration of the Steady State Tokamak Reactor (SSTR)
[DE94-718961] p 4531 N94-37484

DIVING (UNDERWATER)
Cardiac pressure changes with venous gas embolism and decompression
[AD-A280412] p 4481 N94-37224

DOCUMENT STORAGE
Electronic document interchange
p 4541 N94-36848
Electronic document interchange
p 4541 N94-36849

DOCUMENTS
Electronic document interchange
p 4541 N94-36848
Electronic document delivery: Towards the virtual library
p 4544 N94-37340

DONOR MATERIALS
Solvent effects on the energetics and dynamics of ultrafast electron transfer in chlorophyll-porphyrin-acceptor triads
[DE94-009693] p 4477 N94-36554

DOPED CRYSTALS
Microstructure and chemistry of MgO- and CoO-doped nickel-titanate spinels
[DE94-012741] p 4537 N94-37382
Atomic level characterization of defects in microalloyed NiAl: An atom probe investigation
[DE94-012732] p 4418 N94-37396
The effect of reactive elements on the segregation behavior and microstructure of alpha-Al2O3 scales on beta-NiAl
[DE94-012739] p 4418 N94-37399

DOPPLER RADAR
Terminal Doppler Weather Radar (TDWR) build 5 Test and Evaluation Master Plan (TEMP)
[AD-A280426] p 4434 N94-37218
NASA ER-2 Doppler radar reflectivity calibration for the CAMEX project
[NASA-TM-104611] p 4475 N94-37790

DOSIMETERS
User's manual for SNL-SAND-2 code
[DE94-011744] p 4496 N94-37673

DOWNTIME
Aircraft battle damage repair for the 1990's and beyond
[AD-A278635] p 4386 N94-36465

DOWNWASH
Rotorwash analysis handbook. Volume 1: Development and analysis
[SCT-93RR-17-VOL-1] p 4381 N94-36466
Rotorwash analysis handbook. Volume 2: Appendixes
[SCT-93RR-17-VOL-2] p 4382 N94-36467

DRAINAGE
Numerical simulation of nocturnal drainage flows in an idealized valley-tributary system
[DE94-011684] p 4472 N94-37115
The influence of tributaries on nocturnal valley flows
[DE94-011613] p 4473 N94-37242

DRAINAGE PATTERNS
Numerical simulation of nocturnal drainage flows in an idealized valley-tributary system
[DE94-011684] p 4472 N94-37115

DRIFT RATE
Laboratory evaluation of the Standard Elektrik Lorenz (SEL) fibre-optic rate gyroscope
[AD-A280191] p 4446 N94-36760
Fast electron generation and transport in a turbulent, magnetized plasma
[DE94-012986] p 4531 N94-37730

DRONE VEHICLES
Landing of an unmanned helicopter on a moving platform. High accuracy navigation and tracking
p 4387 N94-36618

DROP TESTS
Internally damped, self-arresting vertical drop-weight apparatus
[NASA-CASE-LAR-15003-1] p 4389 N94-36826

DUCTILE-BRITTLE TRANSITION
Characterization of mechanical properties degradation using small punch testing technique
[DE94-011202] p 4418 N94-37410

DUCTILITY
Mechanical behavior and phase stability of NiAl-based shape memory alloys
[DE94-012336] p 4419 N94-37420
Mechanical performance of austempered ductile iron
[AD-A280452] p 4420 N94-37758

DYNAMIC CHARACTERISTICS
Studies of the effect of microstructure on the dynamic behavior of granular and particulate media
[AD-A279012] p 4455 N94-36520

DYNAMIC LOADS
Studies of the effect of microstructure on the dynamic behavior of granular and particulate media
[AD-A279012] p 4455 N94-36520
Transient thermal and dynamic stresses in strongback-design blankets
[DE94-012639] p 4530 N94-37441
A new technique for dynamic load distribution when two manipulators mutually lift a rigid object, part 2
[DE94-010126] p 4501 N94-37735

DYNAMIC MODELS
Eigensystem realization algorithm user's guide forVAX/VMS computers: Version 931216
[NASA-TM-109066] p 4493 N94-36818
Predicting the effects of unmodeled dynamics on an aircraft flight control system design using eigenspace assignment
[NASA-TM-4548] p 4388 N94-37059
A dynamic model of a linear actuator based on polymer hydrogel
[DE94-010800] p 4408 N94-37091
Issues concerning the updating of finite-element models from experimental data
[NASA-TM-109116] p 4456 N94-37253
Configurational evolution dynamics and stability during in-situ development of large orbiting spacecraft
[AD-A280482] p 4397 N94-37351
Dynamics of a split torque helicopter transmission
[NASA-TM-106410] p 4452 N94-37457
Study of Japanese electrodynamic-suspension maglev systems
[DE94-011486] p 4452 N94-37515

DYNAMIC PROGRAMMING
Robot trajectory planning via dynamic programming
[DE94-008424] p 4501 N94-37529

DYNAMIC RANGE
KONRAD: Wide band digital HF receiver
[PB94-184686] p 4435 N94-37813

DYNAMIC RESPONSE
A transient FETI methodology for large-scale parallel implicit computations in structural mechanics, part 2
[NASA-CR-194823] p 4497 N94-36503
Microscopic theory of the dielectric response of highly dispersive biological media
[AD-A280516] p 4516 N94-37109
Micromechanical modeling of advanced materials
[DE94-011249] p 4405 N94-37627

DYNAMIC STABILITY
Aeroservoelastic stabilization considerations for pointing and tracking systems p 4394 N94-36627
Correlation of analytical and experimental hot structure vibration results
[NASA-TM-104269] p 4386 N94-36644
Configurational evolution dynamics and stability during in-situ development of large orbiting spacecraft
[AD-A280482] p 4397 N94-37351
Stability analysis of an F/A-18 E/F cable mount m odel
[NASA-TM-108989] p 4386 N94-37636

DYNAMIC STRUCTURAL ANALYSIS
A transient FETI methodology for large-scale parallel implicit computations in structural mechanics, part 2
[NASA-CR-194823] p 4497 N94-36503
Eigensystem realization algorithm user's guide forVAX/VMS computers: Version 931216
[NASA-TM-109066] p 4493 N94-36818
Issues concerning the updating of finite-element models from experimental data
[NASA-TM-109116] p 4456 N94-37253
Stability and dynamics of spatio-temporal structures
[DE94-013035] p 4412 N94-37491

DYNAMIC TESTS
Hot dynamic test rig for measuring hypersonic engine seal flow and durability
[NASA-TM-106507] p 4450 N94-36645

DYNAMICAL SYSTEMS
Coherence and chaos
[DE94-008529] p 4539 N94-36507

DYNAMICS EXPLORER SATELLITES
Dynamics explorer data analysis
[NASA-CR-196141] p 4469 N94-37016

E

E REGION
Design of the divertor Thomson scattering system on D3-D
[DE94-012672] p 4527 N94-37081

EARTH ATMOSPHERE
Controlled atmospheric breakdown: Applications and research opportunities
[AD-A278584] p 4464 N94-36973

EARTH CRUST
Measurement and interpretation of crustal deformation rates associated with postglacial rebound
[NASA-CR-196300] p 4470 N94-37581

EARTH GRAVITATION
The use of a tactile interface to convey position and motion perceptions p 4486 N94-37281

EARTH IONOSPHERE
Dynamics explorer data analysis
[NASA-CR-196141] p 4469 N94-37016
Magnetic Earth Ionosphere Resonant Frequencies (NASA-MEIRF Project)
[NASA-CR-196303] p 4435 N94-37461
Solar-Terrestrial Predictions, 4: Proceedings of aworkshop. Volume 3: Geomagnetic papers; ionospheric papers
[PB94-173192] p 4470 N94-37530

EARTH MAGNETOSPHERE
Dynamics explorer data analysis
[NASA-CR-196141] p 4469 N94-37016
Solar-Terrestrial Predictions, 4: Proceedings of aworkshop. Volume 3: Geomagnetic papers; ionospheric papers
[PB94-173192] p 4470 N94-37530
Random and periodic substorms and their origins in the solar wind
[DE94-011693] p 4549 N94-37668
Substorm statistics: Occurrences and amplitudes
[DE94-011694] p 4471 N94-37669
Solar-Terrestrial Predictions, 4: Proceedings of a workshop. Volume 1: Workshop overview papers; working group reports; User community reports; Regional Warning Center Reports
[PB94-173176] p 4471 N94-37780
Solar-Terrestrial Predictions, 4: Proceedings of a workshop. Volume 2: Solar papers; magnetospheric papers
[PB94-173184] p 4471 N94-37781

EARTH MOVEMENTS
Analysis spectral shapes from California and central United States ground motion
[DE94-010041] p 4469 N94-36758
Measurement and interpretation of crustal deformation rates associated with postglacial rebound
[NASA-CR-196300] p 4470 N94-37581
EARTH OBSERVING SYSTEM (EOS)
Earth Observing System/Advanced Microwave Sounding Unit-A (EOS/AMSU-A) software management plan
[NASA-CR-189362] p 4461 N94-36919
Earth Observing System (EOS)/Advanced Microwave Sounding Unit A (AMSU-A) configuration management plan
[NASA-CR-189371] p 4494 N94-37061
EARTH ORBITAL ENVIRONMENTS
Operational environments for electrical power wiring on NASA space systems
[NASA-TM-106655] p 4398 N94-36951
Evaluation of seals and lubricants used on the Long Duration Exposure Facility
[NASA-CR-4604] p 4399 N94-37614
EARTH ORBITAL RENDEZVOUS
Neural network for positioning Space Station solar arrays
[NASA-TM-106656] p 4431 N94-36943
EARTH SCIENCES
JPRS report: Science and technology. Central Eurasia
[JPRS-UST-94-013] p 4509 N94-37006
EARTHQUAKES
Analysis spectral shapes from California and central United States ground motion
[DE94-010041] p 4469 N94-36758
ECOLOGY
ELF Communications System ecological monitoring program: Electromagnetic field measurements and engineering support
[AD-A280489] p 4481 N94-37353
ECONOMIC ANALYSIS
Structural composite construction materials manufactured from municipal solid waste
[AD-A280635] p 4403 N94-36730
Integrated gasification combined cycle and steam injection gas turbine powered by biomass joint-venture evaluation
[DE94-006905] p 4461 N94-36740
Scoping economics for the commercial manufacture of metallocene catalysts
[DE94-011526] p 4422 N94-37055
Climate uncertainty and the regional economic impacts of global climate change
[DE94-012242] p 4466 N94-37211
ECONOMIC IMPACT
Math and science illiteracy: Social and economic impacts
[DE94-010801] p 4540 N94-37092
Climate uncertainty and the regional economic impacts of global climate change
[DE94-012242] p 4466 N94-37211
ECOSYSTEMS
Response of plants and ecosystems to CO2 and climate change
[DE94-011583] p 4466 N94-37376
EDUCATION
Design and development of experimental facilities for short duration, low-gravity combustion and fire experiments
[NASA-CR-196107] p 4389 N94-36967
United States Air Force Summer Research Program, 1993. Volume 7: Armstrong Laboratory
[AD-A278655] p 4550 N94-36975
United States Air Force Summer Research Program, 1993. Volume 14: Rome Laboratory
[AD-A278656] p 4550 N94-36976
United States Air Force Summer Research Program, 1993. Volume 16: Arnold Engineering Development Center, Frank J. Seiler Research Laboratory and Wilford Hall Medical Center
[AD-A278658] p 4550 N94-36978
United States Air Force Summer Research Program, 1993. Volume 4: Rome Laboratory
[AD-A278695] p 4551 N94-36980
United States Air Force Summer Research Program, 1993. Volume 5A: Wright Laboratory
[AD-A278696] p 4551 N94-36981
United States Air Force Summer Research Program, 1993. Volume 6: Arnold Engineering Development Center, Frank J. Seiler Research Laboratory and Wilford Hall Medical Center
[AD-A278697] p 4551 N94-36982
United States Air Force Summer Research Program, 1993. Volume 8: Phillips Laboratory
[AD-A278698] p 4551 N94-36983
United States Air Force Summer Research Program, 1993. Volume 9: Rome Laboratory
[AD-A278699] p 4551 N94-36984
California residential indoor air quality study. Volume 1: Methodology and descriptive statistics. Appendix
[PB94-166055] p 4464 N94-36995
Math and science illiteracy: Social and economic impacts
[DE94-010801] p 4540 N94-37092
Assistance in instruction and training of air traffic controllers p 4483 N94-37265
Training and operations support system (TOPS) p 4545 N94-37344
EDUCATIONAL TELEVISION
Evaluation of a tool for producing and presenting interactive videodisc job aids
[AD-A278599] p 4432 N94-36473
EFFICIENCY
The 250 watt average power electro-quality Q-switched diode pumped power oscillator
[DE94-011644] p 4449 N94-37737
EFFLUENTS
Gaseous effluent monitoring and identification using an imaging Fourier transform spectrometer
[DE94-012627] p 4467 N94-37428
EIGENVALUES
Eigensystem realization algorithm user's guide forVAX/VMS computers: Version 931216
[NASA-TM-109066] p 4493 N94-36818
Gain weighted eigenspace assignment
[NASA-TM-109130] p 4388 N94-36820
Approximate analysis for repeated eigenvalue problems with applications to controls-structure integrated design
[NASA-TP-3439] p 4397 N94-37502
EIGENVECTORS
CP violation outside the standard model phenomenology for pedestrians
[DE94-002216] p 4511 N94-36512
Quantum harmonic Brownian motion in a general environment: A modified phase-space approach
[DE94-003249] p 4508 N94-36560
Eigensystem realization algorithm user's guide forVAX/VMS computers: Version 931216
[NASA-TM-109066] p 4493 N94-36818
Gain weighted eigenspace assignment
[NASA-TM-109130] p 4388 N94-36820
Eigenfunction bounds for compact manifolds with integrable geodesic flow
[PB94-180874] p 4506 N94-37853
EJECTION
Calibration and initial testing of a new hydraulic simulator
[AD-A280632] p 4390 N94-37163
EJECTION SEATS
Canopy breaking device
[AD-D016284] p 4385 N94-37767
ELASTIC PROPERTIES
Scaling, elasticity, and CLPT p 4458 N94-37800
ELASTIC SCATTERING
Measurement of the elastic, total and diffraction cross sections at tevatron energies
[DE94-004659] p 4511 N94-36463
Blois 5: Experimental summary
[DE94-001219] p 4513 N94-36558
Positron implantation in solids
[DE94-013029] p 4537 N94-37499
Neutrino-nucleon scattering
[DE94-011720] p 4520 N94-37671
ELASTOMERS
Double network elastomers and method of making same
[AD-D016323] p 4427 N94-37831
ELASTOPLASTICITY
Experimental and finite-element simulation results for a plane-strain punch-test using isotropic and anisotropic materials
[DE94-011711] p 4457 N94-37670
ELECTRIC AUTOMOBILES
Fuel savings and emissions reductions from light duty fuel cell vehicles
[DE94-006909] p 4451 N94-37406
ELECTRIC BATTERIES
Activities of the Chemical Technology Division
[DE94-013050] p 4410 N94-37357
ELECTRIC CONDUCTORS
Electrically conductive, thermally insulating cryogenic current leads
[NASA-CASE-LAR-14964-1-CU] p 4437 N94-36781
United States Air Force Summer Research Program, 1993. Volume 13: Phillips Laboratory
[AD-A278657] p 4550 N94-36977
ELECTRIC CONNECTORS
Preload release mechanism
[NASA-CASE-MSC-22327-1] p 4450 N94-36839
ELECTRIC FIELDS
Picosecond laser induced electric field modulation of carotenoid absorption bands
[DE94-009692] p 4512 N94-36524
Conceptual design for a fast neutron ionization chamber for fusion reactor plasma diagnostics
[DE94-013396] p 4527 N94-37101
Three flights into thunderstorms with the revised Rocket Electric Field Sounding (REFS) payload
[AD-A280424] p 4473 N94-37217
A comparison of two examples of magnetic tracker systems p 4485 N94-37275
ELMy-H mode as limit cycle and transient responses of H-modes in tokamaks
[DE94-727510] p 4529 N94-37358
Investigation of exposure to Extremely Low Frequency (ELF) magnetic and electric fields: Ongoing animals studies
[DE94-011239] p 4480 N94-37825
ELECTRIC FILTERS
Single event mirroring and sense amplifier designs for enhanced SE tolerance of DRAMs
[DE94-010397] p 4438 N94-37190
ELECTRIC GENERATORS
Mars vertical axis wind machines. The design of a Darreus and a Giromill for use on Mars
[NASA-CR-196143] p 4462 N94-36807
Mars vertical axis wind machines: The design of a tornado vortex machine for use on Mars
[NASA-CR-196144] p 4462 N94-36823
ELECTRIC MOTOR VEHICLES
Sodium/nickel-chloride battery development
[DE94-011481] p 4437 N94-37053
Fuel savings and emissions reductions from light duty fuel cell vehicles
[DE94-006909] p 4451 N94-37406
ELECTRIC POWER SUPPLIES
ORNL superconducting technology program for electric power systems
[DE94-011471] p 4438 N94-37239
ELECTRIC PROPULSION
Characteristics of ions emitted from high-current hollow cathodes
[NASA-CR-195372] p 4398 N94-37764
ELECTRIC WIRE
Operational environments for electrical power wiring on NASA space systems
[NASA-TM-106655] p 4398 N94-36951
Preradiation studies for non-thermal Z-pinch wire load experiments on Saturn
[DE94-013459] p 4527 N94-37072
ELECTRICAL ENGINEERING
JPRS report: Science and technology. Central Eurasia
[JPRS-UST-94-013] p 4509 N94-37006
MCFC product development test
[DE94-002005] p 4463 N94-37488
ELECTRICAL IMPEDANCE
Sodium-23 NMR and complex impedance studies of gel electrolytes based on poly(acrylonitrile)
[AD-A280330] p 4408 N94-37031
ELECTRICAL INSULATION
Operational environments for electrical power wiring on NASA space systems
[NASA-TM-106655] p 4398 N94-36951
Development of intermetallic coatings for fusion power applications
[DE94-012647] p 4419 N94-37442
ELECTRICAL PROPERTIES
Small-angle x ray scattering studies of microvoids in amorphous-silicon-based semiconductors
[DE94-006931] p 4533 N94-36745
Low temperature materials --- indium gallium arsenides
[AD-A278703] p 4533 N94-36755
Azobenzene-containing polymers: Some optoelectronic properties
[AD-A280448] p 4424 N94-37185
ELECTRICAL RESISTIVITY
Fluids at high shock pressures and temperatures and some thoughts about future possibilities
[DE94-003625] p 4407 N94-36458
Sodium-23 NMR and complex impedance studies of gel electrolytes based on poly(acrylonitrile)
[AD-A280330] p 4408 N94-37031
Pressure dependence of the conductivity and magnetoconductance in oriented iodine-doped polyacetylene
[PB94-184488] p 4427 N94-37854
ELECTRO-OPTICS
Multiple target track-while-scan in the airborne EO environment p 4394 N94-36629
Fault tolerance in opto-electronic computing
[AD-A280219] p 4453 N94-37150
Azobenzene-containing polymers: Some optoelectronic properties
[AD-A280448] p 4424 N94-37185

Suppression of beam-break-up in a standing wave free electron laser two-beam accelerator
[DE94-011348] p 4521 N94-37200
Status review and accomplishments of the Materials Research Center at the University of Pittsburgh
[AD-A280422] p 4399 N94-37214
Gaze orientation under G(z)-load. Methodological aspects: Preliminary results p 4485 N94-37274
Fiber optic (flight quality) sensors for advanced aircraft propulsion
[NASA-CR-191195] p 4387 N94-37401

ELECTROACOUSTICS
Miniature thermoacoustic refrigerator
[AD-A280326] p 4431 N94-37029

ELECTROCARDIOGRAPHY
Detection of the electrocardiogram P-wave using wavelet analysis
[DE94-010791] p 4481 N94-37197

ELECTROCHEMICAL CORROSION
Production of amorphous metal layers using ion implantation and investigation of the related modification of some surface properties
[DE94-617509] p 4414 N94-36541

ELECTROCHEMISTRY
Remote use of distributed robotics resources to enhance technology development and insertion
[DE94-009285] p 4502 N94-37785

ELECTROCHROMISM
Picosecond laser induced electric field modulation of carotenoid absorption bands
[DE94-009692] p 4512 N94-36524

ELECTRODE MATERIALS
Processing, packaging, and characterization of electroceramic materials for phased array antennas
[AD-A280251] p 4432 N94-36743
Sodium/nickel-chloride battery development
[DE94-011481] p 4437 N94-37053

ELECTRODEPOSITION
Chromium/molybdenum alloy plating. Part 1: The electrodeposition of low contraction chromium/molybdenum alloys using unipolar (on/off) pulse plating
[AD-A280236] p 4417 N94-37138

ELECTRODES
A charge distribution analysis instrument for catalysis and material science applications
[DE94-011587] p 4438 N94-37241
New hollow-cathode electrode for high-power copper lasers
[DE94-011637] p 4448 N94-37244

ELECTROJETS
United States Air Force Summer Research Program, 1993. Volume 3: Phillips Laboratory
[AD-A278694] p 4550 N94-36979

ELECTROLYTES
Sodium-23 NMR and complex impedance studies of gel electrolytes based on poly(acrylonitrile)
[AD-A280330] p 4408 N94-37031

ELECTROMAGNETIC ABSORPTION
Femtosecond transient absorption studies of the light harvesting Chl a/b protein complex of Photosystem 2 in higher plants
[DE94-009684] p 4477 N94-36481

ELECTROMAGNETIC FIELDS
EM-ANIMATE: A computer program for displaying and animating electromagnetic near-field and surface-current solutions: Video supplement to NASA Technical Memorandum 4539
[NASA-TM-4539-VIDEO-SUPPL] p 4492 N94-36518
ELF Communications System ecological monitoring program: Electromagnetic field measurements and engineering support
[AD-A280489] p 4481 N94-37353

ELECTROMAGNETIC INTERFERENCE
MTI compatible coherent sidelobe canceller
[AD-D016300] p 4435 N94-37771

ELECTROMAGNETIC PULSES
Behavioral performance in monkeys exposed to TEMPO high-peak-power microwave pulses at 3 GHz
[AD-A280551] p 4478 N94-37045

ELECTROMAGNETIC RADIATION
United States Air Force Summer Research Program, 1993. Volume 13: Phillips Laboratory
[AD-A278657] p 4550 N94-36977

ELECTROMAGNETIC SCATTERING
EM-ANIMATE: A computer program for displaying and animating electromagnetic near-field and surface-current solutions: Video supplement to NASA Technical Memorandum 4539
[NASA-TM-4539-VIDEO-SUPPL] p 4492 N94-36518
Raman scattering of variable bandwidth KrF radiation in long air paths
[DE94-012912] p 4449 N94-37495

ELECTROMYOGRAPHY
Methodologies to determine forces on bones and muscles of body segments during exercise, employing compact sensors suitable for use in crowded space vehicles
[NASA-CR-196272] p 4487 N94-37458

ELECTRON ACCELERATORS
Preradiation studies for non-thermal Z-pinch wire load experiments on Saturn
[DE94-013459] p 4527 N94-37072

ELECTRON AFFINITY
Ionic properties of hydrogenated and fluorinated fullerenes
[DE94-012110] p 4537 N94-37369

ELECTRON ATTACHMENT
Low-energy electron collisions with metal clusters: Electron capture and cluster fragmentation
[DE94-003623] p 4512 N94-36516
Effect of temperature on the electron attachment and detachment properties of c-C4F6
[DE94-012750] p 4518 N94-37383

ELECTRON BEAMS
Precise determination of the weak mixing angle from a measurement of ALR in e(+)e(-) yields Z0
[DE94-013355] p 4515 N94-37085
A study of jet handedness in hadronic Z0 decays
[DE94-013358] p 4515 N94-37087
A new, optical-lever based atomic force microscope
[AD-A280524] p 4524 N94-37110
Suppression of beam-break-up in a standing wave free electron laser two-beam accelerator
[DE94-011348] p 4521 N94-37200

ELECTRON CAPTURE
Low-energy electron collisions with metal clusters: Electron capture and cluster fragmentation
[DE94-003623] p 4512 N94-36516

ELECTRON CYCLOTRON HEATING
Microwave generation for magnetic fusion energy applications
[DE94-012107] p 4448 N94-37368

ELECTRON DENSITY (CONCENTRATION)
Fast electron generation and transport in a turbulent, magnetized plasma
[DE94-012986] p 4531 N94-37730

ELECTRON DIFFRACTION
High resolution electron diffraction analysis of structural changes associated with the photocycle of bacteriorhodopsin
[DE94-011800] p 4479 N94-37156

ELECTRON DISTRIBUTION
High Altitude Plasma Instrument (HAPI) data analysis
[NASA-CR-189360] p 4469 N94-36949

ELECTRON ENERGY
Quantum and quasi-classical analyses of high order emission processes
[DE93-041348] p 4513 N94-36697
Effect of temperature on the electron attachment and detachment properties of c-C4F6
[DE94-012750] p 4518 N94-37383
The angular and energy distributions of ejected electrons in electron-impact ionization of helium
[DE94-618748] p 4519 N94-37528

ELECTRON IMPACT
The angular and energy distributions of ejected electrons in electron-impact ionization of helium
[DE94-618748] p 4519 N94-37528

ELECTRON MICROSCOPES
Measurement of scanning electron microscope resolution
[DE94-012661] p 4525 N94-37374

ELECTRON MICROSCOPY
Elemental mapping of segregation in stainless steels with an imaging filter
[DE94-012659] p 4417 N94-37304
AEM and AES of radiation-induced segregation in proton-irradiated stainless steels
[DE94-012734] p 4418 N94-37398

ELECTRON PROBES
Determination of interface structure and bonding at atomic resolution in the stem
[DE94-011466] p 4517 N94-37238

ELECTRON SCATTERING
Low-energy electron collisions with metal clusters: Electron capture and cluster fragmentation
[DE94-003623] p 4512 N94-36516
Blois 5: Experimental summary
[DE94-001219] p 4513 N94-36558
The spin observables of electron-nucleon scattering from the formalism of nucleon-nucleon scattering
[DE94-011368] p 4520 N94-37717
A freon-filled, holographic bubble chamber as a high energy photon burst spectrometer
[DE94-011645] p 4446 N94-37723

ELECTRON SPECTROSCOPY
AEM and AES of radiation-induced segregation in proton-irradiated stainless steels
[DE94-012734] p 4418 N94-37398

ELECTRON STATES
Consequences of competing hybridization for magnetic ordering in correlated-electron lattices
[DE94-011648] p 4534 N94-37057

ELECTRON TRANSFER
Solvent effects on the energetics and dynamics of ultrafast electron transfer in chlorophyll-porphyrin-acceptor triads
[DE94-009693] p 4477 N94-36554
Femtosecond transient grating studies of electron transfer in porphyrin and chlorophyll donor-acceptor molecules
[DE94-009694] p 4478 N94-36555
Time-resolved probing of electron thermal transport in plasma produced by femtosecond laser pulses
[DE94-012061] p 4530 N94-37392
Electron-transfer reactions involving two harmonic potentials with a different force constant: The Zusman approach versus the spin-boson model
[DE94-013306] p 4519 N94-37550
Fast electron generation and transport in a turbulent, magnetized plasma
[DE94-012986] p 4531 N94-37730

ELECTRON-POSITRON PAIRS
Precise determination of the weak mixing angle from a measurement of ALR in e(+)e(-) yields Z0
[DE94-013355] p 4515 N94-37085

ELECTRON-POSITRON PLASMAS
Langmuir waves in the electron-positron plasma
[DE94-618779] p 4531 N94-37728

ELECTRONIC BULLETIN BOARDS
Bulletin boards, electronic mail, conferencing, current use by scientists and engineers: Effects on libraries and information centres: Do they have a role?
p 4544 N94-37343

ELECTRONIC COUNTERMEASURES
VHF adaptive antenna development task
[AD-A280320] p 4434 N94-37127

ELECTRONIC EQUIPMENT
Testing new technology for the heavy ion experiment at CERN
[DE94-004747] p 4521 N94-37220

ELECTRONIC MAIL
Electronic SCAN (Selected Current Aerospace Notices) p 4541 N94-36845
Electronic document interchange
p 4541 N94-36849
NASA Access Mechanism (NAM)
p 4541 N94-36850
Network upgrades p 4541 N94-36851
The implementation of Electronic Data Interchange (EDI) with defense transportation operations
[AD-A280568] p 4493 N94-37040
An introduction to the Internet and its services
p 4543 N94-37334
Bulletin boards, electronic mail, conferencing, current use by scientists and engineers: Effects on libraries and information centres: Do they have a role?
p 4544 N94-37343
Policies for implementing network firewalls
[DE94-011030] p 4495 N94-37430

ELECTRONIC PACKAGING
Evaluating plastic assembly processes for high reliability applications using HAST and Assembly Test Chips
[DE94-010750] p 4439 N94-37363

ELECTRONS
Production of a positron and a bound electron by high-energy photon in a strong Coulomb field
[DE94-618501] p 4514 N94-36747
Precise determination of the weak mixing angle from a measurement of ALR in e(+)e(-) yields Z0
[DE94-013355] p 4515 N94-37085

ELECTROPLATING
Chromium/molybdenum alloy plating. Part 1: The electrodeposition of low contraction chromium/molybdenum alloys using unipolar (on/off) pulse plating
[AD-A280236] p 4417 N94-37138

ELECTROSTATICS
A charge distribution analysis instrument for catalysis and material science applications
[DE94-011587] p 4438 N94-37241

ELECTROWEAK INTERACTIONS (FIELD THEORY)
The Pomeron and Quantum Chromodynamics (QCD) with many light quarks
[DE94-001351] p 4513 N94-36538
Effective Lagrangian for gluons and Higgs pseudoscalars
[DE94-001381] p 4513 N94-36539
Electroweak physics at the Tevatron collider
[DE93-040927] p 4513 N94-36695

CDF results on electroweak physics
[DE94-011750] p 4520 N94-37674

ELECTROWEAK MODEL
Electroweak physics at the Tevatron collider
[DE93-040927] p 4513 N94-36695

ELEMENTARY PARTICLE INTERACTIONS
Deep inelastic scattering results from the first year of HERA operation
[DE94-004578] p 4511 N94-36483
Particle physics experiments report, 1993
[PB94-169109] p 4521 N94-36545
B quark production cross sections and the b- (bar b) correlated production cross section at CDF
[DE94-000620] p 4514 N94-36700
Direct photoionization of excited helium
[DE94-618732] p 4516 N94-37097
Wick-Cutkovsky model: An introduction
[DE94-618365] p 4504 N94-37170

ELEMENTARY PARTICLES
Particle physics experiments report, 1993
[PB94-169109] p 4521 N94-36545

ELLIPSOMETERS
Microscopic image processing systems for measuring nonuniform film thickness profiles
[DE94-005336] p 4424 N94-37223

ELLIPTIC DIFFERENTIAL EQUATIONS
Cost-effective computations with boundary interface operators in elliptic problems
[DE94-621506] p 4503 N94-37096

ELONGATION
Mechanical performance of austempered ductile iron
[AD-A280452] p 4420 N94-37758

EMBRITTLEMENT
Characterization of mechanical properties degradation using small punch testing technique
[DE94-011202] p 4418 N94-37410

EMERGENCIES
Aircraft command in emergency situations prototype development users manual
[DOT/FAA/CT-94/24] p 4385 N94-37706

EMISSION
SIHTI: Energy and environmental technology
[DE94-763290] p 4464 N94-37007

EMISSION SPECTRA
Quantum and quasi-classical analyses of high order emission processes
[DE93-041348] p 4513 N94-36697
Far-infrared emission line spectroscopy of planetary nebulae from the KAO
[NASA-CR-196289] p 4547 N94-37825

EMITTERS
Field emitter array RF amplifier development project phase one, cathode technology development
[AD-A280334] p 4437 N94-37033
Field emitter array RF amplifier development project. Phase 1, option 1
[AD-A280377] p 4437 N94-37035
Field emitter array RF amplifier development project. Phase 1, option 1
[AD-A280513] p 4437 N94-37107
Field emitter array RF amplifier development project. Cathode technology development. Phase 1
[AD-A280515] p 4437 N94-37108
Progress on the emitter wrap-through silicon solar cell
[DE94-010382] p 4462 N94-37189
Status review and accomplishments of the Materials Research Center at the University of Pittsburgh
[AD-A280422] p 4399 N94-37214

EMPLOYEE RELATIONS
Toward a new National Weather Service: National Weather Service employee feedback
p 4474 N94-37467

EMULSIONS
Chemiluminescent microemulsions
[AD-D016292] p 4413 N94-37761

ENCAPSULATED MICROCIRCUITS
Evaluating plastic assembly processes for high reliability applications using HAST and Assembly Test Chips
[DE94-010750] p 4439 N94-37363

ENCAPSULATING
Amorphous silicon photovoltaic manufacturing technology, phase 2A
[DE94-006895] p 4461 N94-36476

ENERGY CONSERVATION
The potential for control of carbon dioxide emissions from integrated gasification/combined-cycle systems
[DE94-012646] p 4465 N94-37100
ORNL superconducting technology program for electric power systems
[DE94-011471] p 4438 N94-37239

ENERGY CONSUMPTION
Estimates of US biomass energy consumption 1992
[DE94-011458] p 4463 N94-37567

ENERGY CONVERSION
Mars vertical axis wind machines. The design of a Darreus and a Giromill for use on Mars
[NASA-CR-196143] p 4462 N94-36807

ENERGY DISSIPATION
Defect initiation/growth and energy dissipation induced by deformation and fracture
[AD-A280411] p 4424 N94-37184

ENERGY DISTRIBUTION
The angular and energy distributions of ejected electrons in electron-impact ionization of helium
[DE94-618748] p 4519 N94-37528

ENERGY LEVELS
Theory of metal insulator transition in strongly correlated electron systems
[DE94-013135] p 4438 N94-37295

ENERGY POLICY
Alternative fuel information: State alternative fuel laws and incentives
[DE94-006892] p 4429 N94-37404

ENERGY SPECTRA
Quantum and quasi-classical analyses of high order emission processes
[DE93-041348] p 4513 N94-36697
Solving the two-dimensional Schroedinger equation in self-consistent basis
[DE94-621535] p 4504 N94-37174

ENERGY STORAGE
Photochemistry without protons. Radical cation chemistry in zeolites
[DE94-012631] p 4412 N94-37439
Advanced laser driver for soft x-ray projection lithography
[DE94-011643] p 4449 N94-37722

ENERGY TECHNOLOGY
Advanced thermally stable, coal-derived, jet fuels development program. Experiment system and model development
[AD-A278968] p 4428 N94-36505
Advanced manufacturing technology for polymer composite structures in Japan p 4422 N94-36968
SIHTI: Energy and environmental technology
[DE94-763290] p 4464 N94-37007
Activities of the Chemical Technology Division
[DE94-013050] p 4410 N94-37357
MCFC product development test
[DE94-002005] p 4463 N94-37488
JPRS report: Science and technology. Central Eurasia: Engineering and equipment
[JPRS-UEQ-93-007] p 4431 N94-37523
JPRS report: Science and technology. Central Eurasia: Engineering and equipment
[JPRS-UEQ-93-008] p 4432 N94-37524
JPRS report: Science and technology. Central Eurasia: Engineering and equipment
[JPRS-UEQ-93-005] p 4432 N94-37538

ENERGY TRANSFER
A-TOUGH: A multimedia fluid-flow/energy-transport model for fully-coupled atmospheric-subsurface interactions
[DE94-004304] p 4472 N94-36739
Momentum-energy transport from turbulence driven by parallel flow shear
[DE94-012765] p 4443 N94-37362
Analysis of anelastic flow and numerical treatment via finite elements
[DE94-012141] p 4445 N94-37726

ENGINE CONTROL
Technical evaluation and assessment of CNG/LPG bi-fuel and flex-fuel vehicle viability
[DE94-006925] p 4451 N94-37408

ENGINE DESIGN
Hot dynamic test rig for measuring hypersonic engine seal flow and durability
[NASA-TM-106507] p 4450 N94-36645
Technical evaluation and assessment of CNG/LPG bi-fuel and flex-fuel vehicle viability
[DE94-006925] p 4451 N94-37408
Advanced Turbine Technology Applications Project (ATTAP)
[NASA-CR-195367] p 4452 N94-37763

ENGINE INLETS
A fundamental study of hypersonic unstarts
[AD-A280506] p 4443 N94-37128

ENGINE MONITORING INSTRUMENTS
Fiber optic (flight quality) sensors for advanced aircraft propulsion
[NASA-CR-191195] p 4387 N94-37401

ENGINE NOISE
Mixing and noise benefit versus thrust penalty in supersonic jets using impingement tones
[NASA-TM-106583] p 4382 N94-36686

ENGINE PARTS
A coupled/uncoupled deformation and fatigue damage algorithm utilizing the finite element method
[NASA-TM-106526] p 4455 N94-36561
SCS-6 (tm) fiber reinforced titanium
p 4400 N94-36652
Impact of Materials Defects on Engine Structures Integrity
[AGARD-R-790] p 4453 N94-37321
History and prognosis of material discontinuity effects on engine components structural integrity
p 4453 N94-37322
Alternate melting and refining routes
p 4421 N94-37323
Process enhancements of superalloy material
p 4421 N94-37324
The control of cleanness in powder metallurgy materials for turbine disks p 4421 N94-37325
Maintaining constant standards during the forging process p 4421 N94-37326
Defects and their effects on the integrity of nickel based aeroengine discs p 4421 N94-37328
Turbine disks: Lifing against defects and materials development p 4454 N94-37329
Substantiating powder metal life methodologies for engines p 4455 N94-37330
Predicting defect behaviour p 4455 N94-37331

ENGINE TESTS
Hot dynamic test rig for measuring hypersonic engine seal flow and durability
[NASA-TM-106507] p 4450 N94-36645
Potential benefits of oxygen-enriched intake air in a vehicle powered by a spark-ignition engine
[DE94-013452] p 4451 N94-37070
NASA reload program
[NASA-CR-193972] p 4429 N94-37446
Advanced Turbine Technology Applications Project (ATTAP)
[NASA-CR-195367] p 4452 N94-37763

ENGINEERING
JPRS report: Science and technology. Central Eurasia: Engineering and equipment
[JPRS-UEQ-93-007] p 4431 N94-37523
JPRS report: Science and technology. Central Eurasia: Engineering and equipment
[JPRS-UEQ-93-008] p 4432 N94-37524
JPRS report: Science and technology. Central Eurasia: Engineering and equipment
[JPRS-UEQ-93-005] p 4432 N94-37538

ENGINEERING MANAGEMENT
Ordering design tasks based on coupling strengths
[NASA-TM-109137] p 4387 N94-37762

ENTRAINMENT
Effects of molecular transport on turbulence-chemistry interactions in a hydrogen-argon-air jet diffusion flame
[DE94-005107] p 4413 N94-37711

ENTROPY
A nonconservative scheme for isentropic gas dynamics
[DE94-011488] p 4445 N94-37724

ENVIRONMENT EFFECTS
Science priorities for the human dimensions of global change p 4464 N94-36987
Project report: Aircraft — atmospheric effects of stratospheric aircraft
[DE94-011759] p 4465 N94-37155
Jet aircraft engine exhaust emissions database development: Year 1990 and 2015 scenarios
[NASA-CR-4613] p 4466 N94-37252
ELF Communications System ecological monitoring program: Electromagnetic field measurements and engineering support
[AD-A280489] p 4481 N94-37353
Factors influencing the parameterization of anvil clouds within GCMs
[DE94-010794] p 4475 N94-37621
Tropospheric radiative forcing of CH4
[DE94-011628] p 4468 N94-37631

ENVIRONMENT MANAGEMENT
Science priorities for the human dimensions of global change p 4464 N94-36987
Environmental risk management
[DE94-620987] p 4467 N94-37492
The integrated performance evaluation program quality assurance guidance in support of EM environmental sampling and analysis activities
[DE94-013043] p 4468 N94-37731

ENVIRONMENT MODELS
Modeling the Earth system in the Mission to Planet Earth era
[NASA-TM-109892] p 4461 N94-36827
Climate uncertainty and the regional economic impacts of global climate change
[DE94-012242] p 4466 N94-37211
Response of plants and ecosystems to CO2 and climate change
[DE94-011583] p 4466 N94-37376
Modeling atmospheric concentrations and deposition of Hg
[DE94-012633] p 4467 N94-37440

Surface-layer response over shrub-steppe canopy during springtime
[DE94-011235] p 4468 N94-37624

ENVIRONMENT PROTECTION

Science priorities for the human dimensions of global change p 4464 N94-36987

Alternative fuel information: Glossary
[DE94-006889] p 4429 N94-37403

Alternative fuel information: State alternative fuel laws and incentives
[DE94-006892] p 4429 N94-37404

Comparative alternative/clean fuels provisions of the Clean Air Act Amendments of 1990 and the Energy Policy Act of 1992
[DE94-006887] p 4429 N94-37426

ENVIRONMENT SIMULATION

Atmospheric structure simulation: An ARMA model for smooth isotropic two-dimensional geophysical power spectra
[AD-A280476] p 4470 N94-37649

ENVIRONMENT SIMULATORS

Creation of a virtual world to study human spatial perception during sustained acceleration p 4484 N94-37268

ENVIRONMENTAL MONITORING

Modeling the Earth system in the Mission to Planet Earth era
[NASA-TM-109892] p 4461 N94-36827

United States Air Force Summer Research Program, 1993. Volume 3: Phillips Laboratory
[AD-A278694] p 4550 N94-36979

ENVIRONMENTAL SURVEYS

Receiver design, performance analysis, and evaluation for space-borne laser altimeters and space-to-space laser ranging systems
[NASA-CR-194747] p 4397 N94-36988

ENZYMES

Crystallographic studies of nitrogenase and hydrogenase
[DE94-011972] p 4538 N94-37677

EPIDEMIOLOGY

Investigation of exposure to Extremely Low Frequency (ELF) magnetic and electric fields: Ongoing animals studies
[DE94-011239] p 4480 N94-37625

EPITAXY

Gas-Phase and Surface Chemistry in Electronic Materials Processing. Materials Research Society Symposium proceedings, volume 334
[AD-A280586] p 4408 N94-36735

New plasma source of hydrides for epitaxial growth
[DE94-006918] p 4533 N94-36744

Substrate effects on the structure and optical properties of epitaxial PbTiO3 thin films prepared by metal-organic chemical vapor deposition
[DE94-010432] p 4535 N94-37192

EPOXY RESINS

Evaluating plastic assembly processes for high reliability applications using HAST and Assembly Test Chips
[DE94-010750] p 4439 N94-37363

EQUATIONS OF MOTION

Analysis of anelastic flow and numerical treatment via finite elements
[DE94-012141] p 4445 N94-37726

EQUATIONS OF STATE

Studies of the III-V compounds in the megabar regime
[DE94-012488] p 4537 N94-37435

EQUIPMENT SPECIFICATIONS

Space Generic Open Avionics Architecture (SGOAA) standard specification
[NASA-CR-188290] p 4387 N94-36933

EQUIVALENCE

A coarse-mesh nodal method-diffusive-mesh finite difference method
[DE94-010809] p 4502 N94-36455

ERGOMETERS

Methodologies to determine forces on bones and muscles of body segments during exercise, employing compact sensors suitable for use in crowded space vehicles
[NASA-CR-196272] p 4487 N94-37458

EROSION

Robotic weld overlay coatings for erosion control
[DE94-013477] p 4417 N94-37116

Numerical simulation of dynamic fracture and failure in solids
[DE94-010379] p 4457 N94-37705

ERROR ANALYSIS

Determination of density of mass standards: Requirement and method
[PB94-163078] p 4508 N94-36718

Error control techniques for satellite and space communications
[NASA-CR-196302] p 4433 N94-36931

Experimental uncertainty and drag measurements in the national transonic facility
[NASA-CR-4600] p 4389 N94-36945

A more exact analysis of Sandia Laser Tracker data
[DE94-011411] p 4447 N94-37051

Measurement uncertainty and feasibility study of a flush airdata system for a hypersonic flight experiment
[NASA-TM-4627] p 4383 N94-37378

Study on the measurement uncertainty of noise properties of a millimeter wave amplifier
[PB94-170917] p 4510 N94-37632

ERRORS

Measurement uncertainty and feasibility study of a flush airdata system for a hypersonic flight experiment
[NASA-TM-4627] p 4383 N94-37378

Angle interferometer cross axis errors
[DE94-006190] p 4446 N94-37388

ERYTHROCYTES

United States Air Force Summer Research Program, 1993. Volume 6: Arnold Engineering Development Center, Frank J. Seiler Research Laboratory and Wilford Hall Medical Center
[AD-A278697] p 4551 N94-36982

ESTIMATING

Dealing with uncertainty about item parameters: Expected response functions
[AD-A280610] p 4506 N94-36728

Recovering depth from focus using iterative image estimation techniques
[DE94-010994] p 4524 N94-37165

ETCHANTS

A photoemission study of Au, Ge, and O2 deposition on NH4F etched Si(111)
[DE94-013352] p 4519 N94-37553

ETHERS

Synthesis of phthalonitrile resins containing ether and imide linkages with aromatic diamine curing agent
[AD-D016309] p 4427 N94-37778

EULER EQUATIONS OF MOTION

A fundamental study of hypersonic unstarts
[AD-A280506] p 4443 N94-37128

Development of advanced Navier-Stokes solver
[NASA-CR-195094] p 4504 N94-37449

EULER-LAGRANGE EQUATION

A Lagrangian-Eulerian finite element method with adaptive gridding for advection-dispersion problems
[DE94-011372] p 4506 N94-37718

EUROPE

JPRS report: Science and technology. Central Eurasia: Space
[JPRS-USP-94-004] p 4391 N94-37002

EUTECTIC ALLOYS

Processing and mechanical properties of NiAl-based in-situ composites
[NASA-CR-195333] p 4416 N94-36954

EXCIMER LASERS

Frequency doubling of copper lasers using temperature-tuned ADP
[DE94-011542] p 4448 N94-37240

EXCITATION

Blois 5: Experimental summary
[DE94-001219] p 4513 N94-36558

The excitation mechanism of praseodymium-doped semiconductors
[AD-A280687] p 4535 N94-37129

EXCITONS

Femtosecond transient absorption studies of the light harvesting Chl a/b protein complex of Photosystem 2 in higher plants
[DE94-009684] p 4477 N94-36481

EXERCISE PHYSIOLOGY

Postural strategies for the continuous control of static and dynamic balance in man
[PB94-184678] p 4487 N94-37812

EXHAUST EMISSION

Potential benefits of oxygen-enriched intake air in a vehicle powered by a spark-ignition engine
[DE94-013452] p 4451 N94-37070

Project report: Aircraft — atmospheric effects of stratospheric aircraft
[DE94-011759] p 4465 N94-37155

Jet aircraft engine exhaust emissions database development: Year 1990 and 2015 scenarios
[NASA-CR-4613] p 4466 N94-37252

Alternative fuel information: Facts about CNG and LPG conversion
[DE94-006888] p 4429 N94-37402

Fuel savings and emissions reductions from light duty fuel cell vehicles
[DE94-006909] p 4451 N94-37406

Combustion characterization of methylal in reciprocating engines
[DE94-006949] p 4411 N94-37409

Stratospheric emissions effects database development
[NASA-CR-4592] p 4467 N94-37607

EXHAUST GASES

Jet aircraft engine exhaust emissions database development: Year 1990 and 2015 scenarios
[NASA-CR-4613] p 4466 N94-37252

Evaluation of parameterizations for pollutant transport and dispersion in an urban street canyon using a three-dimensional dynamic flow model
[DE94-012641] p 4467 N94-37429

EXHAUST NOZZLES

Probabilistic assessment of space nuclear propulsion system nozzle
[NASA-TM-106539] p 4457 N94-37704

EXOBIOLOGY

Aerospace medicine and biology: A continuing bibliography with indexes (supplement 392)
[NASA-SP-7011(392)] p 4482 N94-37445

EXPERT SYSTEMS

Preliminary PANSAT ground station software design and use of an expert system to analyze telemetry
[AD-A280600] p 4392 N94-36726

Virtual representation of IID observations in Bayesian belief networks
[AD-A280552] p 4507 N94-37046

Distributed detection theory and data fusion
[AD-A280410] p 4434 N94-37183

Reference manual for the Thermal Analyst's Help Desk Expert System
[NASA-CR-194941] p 4397 N94-37504

EXPLOSIONS

Evolution of turbulent fields in explosions
[DE94-010405] p 4444 N94-37390

EXPLOSIVES

Molecular beam surface analysis
[DE94-010773] p 4406 N94-36453

DDT modeling and shock compression experiments of porous or damaged energetic materials
[DE94-011419] p 4428 N94-37052

The effects of proton-beam quality on the production of gamma rays for nuclear resonance absorption in nitrogen
[DE94-011609] p 4523 N94-37629

EXPOSURE

Blast overpressure studies with animals and man
[AD-A280240] p 4480 N94-37118

Homeostatic responses to prolonged cold exposure: Human cold acclimatization
[AD-A280234] p 4481 N94-37136

Profile analysis of after-effects experienced during exposure to several virtual reality environments p 4482 N94-37263

Investigation of exposure to Extremely Low Frequency (ELF) magnetic and electric fields: Ongoing animals studies
[DE94-011239] p 4480 N94-37625

EXTINCTION

Rich methane/air flames: Burning velocities, extinction limits, and flammability limit
[DE94-004340] p 4407 N94-36462

Rich flammability limits in CH3OH/CO/diluent mixtures
[DE94-004341] p 4407 N94-36482

EXTRACTION

The determination of hydrogen in sodium by vacuum extraction
[DE94-620278] p 4412 N94-37533

EXTRAGALACTIC RADIO SOURCES

The BL LAC phenomenon: X-ray observations of transition objects and determination of the x-ray spectrum of a complete sample of flat-spectrum radio sources
[NASA-CR-195951] p 4546 N94-36688

EXTRAPOLATION

Elimination of numerical dispersion in finite-difference modeling and migration by flux-corrected transport
[DE94-004159] p 4510 N94-36551

EXTREMELY LOW FREQUENCIES

ELF Communications System ecological monitoring program: Electromagnetic field measurements and engineering support
[AD-A280489] p 4481 N94-37353

Magnetic Earth Ionosphere Resonant Frequencies (NASA-MEIRF Project)
[NASA-CR-196303] p 4435 N94-37461

Investigation of exposure to Extremely Low Frequency (ELF) magnetic and electric fields: Ongoing animals studies
[DE94-011239] p 4480 N94-37625

EXTREMELY LOW RADIO FREQUENCIES

Investigation of exposure to Extremely Low Frequency (ELF) magnetic and electric fields: Ongoing animals studies
[DE94-011239] p 4480 N94-37625

EXTRUDING

Feasibility of (IMC)(sub d)-reinforced metal matrix composites
[AD-A280626] p 4404 N94-37044

EYE MOVEMENTS
Gaze orientation under G(z)-load. Methodological aspects: Preliminary results p 4485 N94-37274
A comparison of two examples of magnetic tracker systems p 4485 N94-37275

F

F-18 AIRCRAFT
Controlling forebody asymmetries in flight: Experience with boundary layer transition strips
[NASA-TM-4595] p 4383 N94-36944
Fiber optic (flight quality) sensors for advanced aircraft propulsion
[NASA-CR-191195] p 4387 N94-37401
Stability analysis of an F/A-18 E/F cable mount m odel
[NASA-TM-108969] p 4386 N94-37636
FABRICATION
Development of high Tc (greater than 100 K) Bi, Tl and Y-based materials as superconducting circuit elements
[NASA-CR-196276] p 4534 N94-37103
Fabrication and properties of Ag-clad Bi-2223 conductors and magnets
[DE94-011502] p 4438 N94-37111
Laser drilling of printed wiring boards: Sandia LDRD program
[DE94-011004] p 4448 N94-37198
Modeling of forced CVI for tube fabrication
[DE94-012718] p 4410 N94-37286
Method of forming waveguides with ion exchange of halogen ions
[AD-D016304] p 4526 N94-37774
FACE CENTERED CUBIC LATTICES
Modelling of surfaces. Part 1: Monatomic metallic surfaces using equivalent crystal theory
[NASA-TM-106680] p 4419 N94-37459
FACTORIZATION
Direct photoproduction of jets in the k(T)-factorisation prescription
[PB94-171139] p 4513 N94-36549
FAILURE
Ampoule failure sensor time response testing: Experiments 2 and 3
[NASA-TM-108458] p 4446 N94-36822
FAILURE ANALYSIS
Vibration signature analysis of a faulted gear transmission system
[NASA-TM-106623] p 4450 N94-36953
Ability of the total strain version of strainrange partitioning to characterize thermomechanical fatigue behavior
[NASA-TM-4556] p 4455 N94-37102
Statistical characterization of rare events p 4454 N94-37327
Probability techniques for reliability analysis of composite materials
[NASA-CR-195294] p 4406 N94-37633
Numerical simulation of dynamic fracture and failure in solids
[DE94-010379] p 4457 N94-37705
Effects of scale in predicting global structural response p 4458 N94-37799
FAILURE MODES
Numerical simulation of dynamic fracture and failure in solids
[DE94-010379] p 4457 N94-37705
Effects of scale in predicting global structural response p 4458 N94-37799
FAINT OBJECT CAMERA
Hubble Space Telescope faint object camera instrument handbook (Post-COSTAR), version 5.0
[NASA-CR-189365] p 4546 N94-36795
FAR INFRARED RADIATION
Dipole forbidden vibrational modes for NO and CO on Cu observed in the far IR
[DE94-003199] p 4408 N94-36559
Far-infrared emission line spectroscopy of planetary nebulae from the KAO
[NASA-CR-196289] p 4547 N94-37825
FARM CROPS
Studying of ion implantation effect on the biology in China
[DE94-620692] p 4479 N94-37535
FARMLANDS
An experimental and numerical study of boundary layer structure over areas of inhomogeneous serisible heat fluxes
[DE94-011441] p 4474 N94-37565
FAST NEUTRONS
Conceptual design for a fast neutron ionization chamber for fusion reactor plasma diagnostics
[DE94-013396] p 4527 N94-37101
FATIGUE (MATERIALS)
Metal matrix composites: Analysis of simple specimens and model components under creep and fatigue loading p 4402 N94-36661
Residual strength and life prediction techniques for Ti MMC p 4402 N94-36662
Pre-standardisation work on fatigue and fracture testing of titanium matrix composites p 4402 N94-36667
FATIGUE LIFE
A coupled/uncoupled deformation and fatigue damage algorithm utilizing the finite element method
[NASA-TM-106526] p 4455 N94-36561
Process/composite concurrent tailoring of SiC/Ti composites p 4402 N94-36663
Development of mechanical testing methods for titanium matrix composites (traction-ogligo-cyclic fatigue) p 4403 N94-36669
NASA-UVA Light Aerospace Alloy and Structures Technology Program (LA2ST)
[NASA-CR-196290] p 4415 N94-36809
Fracture mechanics life analytical methods verification testing
[NASA-CR-4602] p 4455 N94-37015
Ability of the total strain version of strainrange partitioning to characterize thermomechanical fatigue behavior
[NASA-TM-4556] p 4455 N94-37102
Literature review and preliminary studies of fretting and fretting fatigue including special applications to aircraft joints
[AD-A280310] p 4456 N94-37125
Evaluation of the EHL film thickness and extreme pressure additives on gear surface fatigue life
[NASA-TM-106663] p 4451 N94-37319
Defects and their effects on the integrity of nickel based aeroengine discs p 4421 N94-37328
Substantiating powder metal life methodologies for engines p 4455 N94-37330
Predicting defect behaviour p 4455 N94-37331
Creep-fatigue interaction property of a nickel-base heat-resistant alloy Hastelloy XR in simulated HTGR helium gas environment
[DE94-737934] p 4418 N94-37416
Fatigue case study and loading spectra for wind turbines
[DE94-010798] p 4457 N94-37622
FATIGUE TESTS
Metal matrix composites: Analysis of simple specimens and model components under creep and fatigue loading p 4402 N94-36661
Residual strength and life prediction techniques for Ti MMC p 4402 N94-36662
Prediction of thermal and mechanical stress-strain responses of TMC's subjected to complex TMF histories p 4402 N94-36666
Pre-standardisation work on fatigue and fracture testing of titanium matrix composites p 4402 N94-36667
ASTM and VAMAS activities in titanium matrix composites test methods development p 4403 N94-36668
Development of mechanical testing methods for titanium matrix composites (traction-ogligo-cyclic fatigue) p 4403 N94-36669
Interfaces of high-protection performance polyaryls-coated zinc phosphated steels
[DE94-011732] p 4417 N94-37153
The cyclic fatigue behaviour of adhesive joints
[AD-A280453] p 4456 N94-37186
Evaluation of the EHL film thickness and extreme pressure additives on gear surface fatigue life
[NASA-TM-106663] p 4451 N94-37319
Creep-fatigue interaction property of a nickel-base heat-resistant alloy Hastelloy XR in simulated HTGR helium gas environment
[DE94-737934] p 4418 N94-37416
An enhancement to the NA4 gear vibration diagnostic parameter
[NASA-TM-106553] p 4452 N94-37521
Experimental observations of scale effects on bonded and bolted joints in composite structures p 4458 N94-37801
FAULT DETECTION
An enhancement to the NA4 gear vibration diagnostic parameter
[NASA-TM-106553] p 4452 N94-37521
FAULT TOLERANCE
Advanced information processing system: The Army Fault-Tolerant Architecture detailed design overview
[NASA-CR-194924] p 4497 N94-36962
Fault tolerance in opto-electronic computing
[AD-A280219] p 4453 N94-37150
Advanced information processing system: Authentication protocols for network communication
[NASA-CR-194923] p 4498 N94-37500
Advanced information processing system: Hosting of advanced guidance, navigation and control algorithms on AIPS using ASTER
[NASA-CR-194960] p 4499 N94-37583
FAYALITE
Mineralogy and metallurgical properties of iron ore sinter based on magnetite fines
[DE94-763309] p 4414 N94-36525
FEASIBILITY ANALYSIS
On the feasibility of virtual environments in medicine p 4483 N94-37264
Measurement uncertainty and feasibility study of a flush airdata system for a hypersonic flight experiment
[NASA-TM-4627] p 4383 N94-37378
FEDERAL BUDGETS
Space Station: Impact of the expanded Russian role on funding and research. Report to the Ranking Minority Member, Subcommittee on Oversight of Government Management, Committee on Governmental Affairs, US Senate
[GAO/NSIAD-94-220] p 4396 N94-37257
FEEDBACK CONTROL
MODIL cryocooler producibility demonstration project results
[DE93-019213] p 4430 N94-36444
A note on the regularity of solutions of infinite dimensional Riccati equations
[NASA-CR-194898] p 4502 N94-36562
Gain weighted eigenspace assignment
[NASA-TM-109130] p 4388 N94-36820
A PDE-based methodology for modeling, parameter estimation and feedback control in structural and structural acoustic systems
[NASA-CR-194928] p 4500 N94-36924
Vibration suppression with approximate finite dimensional compensators for distributed systems: Computational methods and experimental results
[NASA-CR-194927] p 4500 N94-36928
Design and evaluation of a Stochastic Optimal Feed-forward and Feedback Technology (SOFFT) flight control architecture
[NASA-TP-3419] p 4388 N94-37014
Robust stabilization of marginally stable positive-real systems
[NASA-TM-109136] p 4500 N94-37058
Predicting the effects of unmodeled dynamics on an aircraft flight control system design using eigenspace assignment
[NASA-TM-4548] p 4388 N94-37059
Visual accommodation to virtual image displays when knowledge of object distance conflicts with optical distance p 4485 N94-37278
Robust stability of second-order systems
[NASA-CR-196384] p 4501 N94-37590
FEEDFORWARD CONTROL
Design and evaluation of a Stochastic Optimal Feed-forward and Feedback Technology (SOFFT) flight control architecture
[NASA-TP-3419] p 4388 N94-37014
FEET (ANATOMY)
Methodologies to determine forces on bones and muscles of body segments during exercise, employing compact sensors suitable for use in crowded space vehicles
[NASA-CR-196272] p 4487 N94-37458
FEMUR
Channel in hip implant stem
[NASA-CASE-MFS-28987-1] p 4486 N94-36840
FERRITES
Mineralogy and metallurgical properties of iron ore sinter based on magnetite fines
[DE94-763309] p 4414 N94-36525
FERRITIC STAINLESS STEELS
Transient thermal and dynamic stresses in strongback-design blankets
[DE94-012639] p 4530 N94-37441
FERROCENES
Organometallic NLO polymers. 4: Organometallic main-chain, side-chain, and guest-host polymers: A study of their orientation and relaxation using second harmonic generation
[AD-A280347] p 4423 N94-37179
FERROMAGNETIC FILMS
Magnetic and structural instabilities of ferromagnetic and antiferromagnetic Fe/Cu(100)
[DE94-011504] p 4509 N94-37517
FERROMAGNETISM
Magnetic and structural instabilities of ferromagnetic and antiferromagnetic Fe/Cu(100)
[DE94-011504] p 4509 N94-37517
FEYNMAN DIAGRAMS
Five-lepton decay modes of muon and tau mesons
[DE94-621636] p 4516 N94-37099
FIBER COMPOSITES
Flame resistant fibrous structures development
[NASA-CR-185700] p 4421 N94-36641

Characterisation of Fibre Reinforced Titanium Matrix Composites
[AD-A2775206] p 4400 N94-36649
SCS-6 (tm) fiber reinforced titanium
p 4400 N94-36652
Manufacture and properties of sigma fibre reinforced titanium p 4401 N94-36655
Properties of TMC processed by fibre coating and hiping p 4401 N94-36656
Fibre-matrix interface properties in Ti-matrix composites: Chemical compatibility and micromechanical behaviour
p 4401 N94-36657
Micromechanical modeling of damage growth in titanium based metal-matrix composites p 4402 N94-36664
Crack growth under cycle loading in fibre reinforced titanium metal matrix composites p 4402 N94-36665
Prediction of thermal and mechanical stress-strain responses of TMC's subjected to complex TMF histories
p 4402 N94-36666
Pre-standardisation work on fatigue and fracture testing of titanium matrix composites p 4402 N94-36667
ASTM and VAMAS activities in titanium matrix composites test methods development
p 4403 N94-36668
Development of mechanical testing methods for titanium matrix composites (traction-ogligo-cyclic fatigue)
p 4403 N94-36669
Modelling and testing fibre reinforced titanium for design purposes p 4403 N94-36670
Structural composite construction materials manufactured from municipal solid waste
[AD-A280635] p 4403 N94-36730
A methodology to predict damage initiation, damage growth and residual strength in titanium matrix composites
[NASA-TM-109135] p 4405 N94-37320
Methodologies for the thermomechanical characterization of continuous-fiber ceramic matrix composites: A review of test methods
[DE94-012111] p 4405 N94-37370
Laminated thin shell structures subjected to free vibration in a hygrothermal environment
[NASA-TM-106600] p 4456 N94-37456
Probability techniques for reliability analysis of composite materials
[NASA-CR-195294] p 4406 N94-37633
A simple evaluation of thermally-induced streses in the vicinity of the stitch in a through-thickness reinforced cross-ply laminate
[NASA-CR-196317] p 4406 N94-37653
Strength characteristics and crack growth behavior of a composite with well aligned fibers
p 4459 N94-37804
Scaling effects of defects in fiber-reinforced composites p 4459 N94-37807
Statistical scaling relationships and size effects in the strength and creep rupture of fibrous composites
p 4460 N94-37809
Scaling of impact damage in fiber composites
p 4460 N94-37810

FIBER OPTICS
Laboratory evaluation of the Standard Elektrik Lorenz (SEL) fibre-optic rate gyroscope
[AD-A280191] p 4446 N94-36760
Design of the divertor Thomson scattering system on D3-D
[DE94-012672] p 4527 N94-37081
Guiding hard x rays with glass polycapillary fiber
[DE94-004949] p 4525 N94-37258
Fiber optic (flight quality) sensors for advanced aircraft propulsion
[NASA-CR-191195] p 4387 N94-37401
Submicrometer fiber-optic chemical sensors: Measuring pH inside single cells
[DE94-004160] p 4525 N94-37532
Prospective communications research to support fly by light/power by wire
[NASA-CR-196369] p 4526 N94-37657

FIBER ORIENTATION
Development of nondestructive evaluation methods and prediction of effects of flaws on the fracture behavior of structural ceramics
[DE94-012466] p 4425 N94-37423
Laminated thin shell structures subjected to free vibration in a hygrothermal environment
[NASA-TM-106600] p 4456 N94-37456

FIBER STRENGTH
The development of short, high surface area activated carbon fibers
[AD-A280509] p 4404 N94-37105

FIBER VOLUME FRACTION
Laminated thin shell structures subjected to free vibration in a hygrothermal environment
[NASA-TM-106600] p 4456 N94-37456

FIBROBLASTS
Estimates of cellular mutagenesis from cosmic rays
[NASA-TP-3453] p 4481 N94-37282

FIELD ALIGNED CURRENTS
Magnetotail dynamics: MHD simulations of driven and spontaneous dynamic changes
[DE94-011702] p 4471 N94-37701

FIELD EMISSION
Field emitter array RF amplifier development project phase one, cathode technology development
[AD-A280334] p 4437 N94-37033
Field emitter array RF amplifier development project. Phase 1, option 1
[AD-A280377] p 4437 N94-37035
Field emitter array RF amplifier development project. Phase 1, option 1
[AD-A280513] p 4437 N94-37107
Field emitter array RF amplifier development project. Cathode technology development. Phase 1
[AD-A280515] p 4437 N94-37108

FIELD THEORY (PHYSICS)
Generalized squeezed states from generalized coherent states
[DE94-002689] p 4512 N94-36515
Wick-Cutkovsky model: An introduction
[DE94-618365] p 4504 N94-37170
Is it possible to assign physical meaning to field theory with higher derivatives?
[DE94-618468] p 4539 N94-37172

FIGHTER AIRCRAFT
ICAAS piloted simulation results p 4393 N94-36617
Aeroservoelastic stabilization considerations for pointing and tracking systems p 4394 N94-36627
Studies and simulations on sensor fusion and cueing for fighter application p 4395 N94-36632
Sensor data fusion for air to air situation awareness beyond visual range p 4395 N94-36633

FILAMENT WINDING
Manufacture and properties of sigma fibre reinforced titanium p 4401 N94-36655
Advanced manufacturing technology for polymer composite structures in Japan p 4422 N94-36968

FILE MAINTENANCE (COMPUTERS)
Recent SEL experiments and studies
p 4490 N94-36487

FILM COOLING
Prediction of film cooling on gas turbine airfoils
[NASA-TM-106653] p 4387 N94-37448

FILM THICKNESS
Microscopic image processing systems for measuring nonuniform film thickness profiles
[DE94-005336] p 4424 N94-37223
Evaluation of the EHL film thickness and extreme pressure additives on gear surface fatigue life
[NASA-TM-106663] p 4451 N94-37319

FILTRATION
Method and apparatus for the collection, storage, and real time analysis of blood and other bodily fluids
[NASA-CASE-MSC-22463-1] p 4480 N94-36766

FINANCIAL MANAGEMENT
The implementation of Electronic Data Interchange (EDI) with defense transportation operations
[AD-A280568] p 4493 N94-37040

FINE STRUCTURE
XAFS-like structure of resonant Raman scattering
[DE94-618410] p 4517 N94-37171
Determination of interface structure and bonding at atomic resolution in the stem
[DE94-011466] p 4517 N94-37238

FINITE DIFFERENCE THEORY
A coarse-mesh nodal method-diffusive-mesh finite difference method
[DE94-010809] p 4502 N94-36455
Elimination of numerical dispersion in finite-difference modeling and migration by flux-corrected transport
[DE94-004159] p 4510 N94-36551
Cost-effective computations with boundary interface operators in elliptic problems
[DE94-621506] p 4503 N94-37098
Modeling of outgassing and matrix decomposition in carbon-phenolic composites
[NASA-CR-196319] p 4405 N94-37471
High-order centered difference methods with sharp shock resolution
[NASA-CR-196374] p 4496 N94-37656
Fuzzy logic to improve efficiency of finite element and finite difference schemes
[DE94-011718] p 4496 N94-37739

FINITE ELEMENT METHOD
A transient FETI methodology for large-scale parallel implicit computations in structural mechanics, part 2
[NASA-CR-194823] p 4497 N94-36503
A coupled/uncoupled deformation and fatigue damage algorithm utilizing the finite element method
[NASA-TM-106526] p 4455 N94-36561
Modeling of thermal barrier coatings
[NASA-CR-195365] p 4421 N94-36637
Correlation of analytical and experimental hot structure vibration results
[NASA-TM-104269] p 4386 N94-36644
An arbitrary grid CFD algorithm for configuration aerodynamics analysis. Volume 1: Theory and validations
[NASA-CR-195918] p 4493 N94-36914
An arbitrary grid CFD algorithm for configuration aerodynamics analysis. Volume 2: FEMNAS user guide
[NASA-CR-196135] p 4493 N94-36922
Interaction effects of cracks, flaws and damage in ceramic
[AD-A280368] p 4423 N94-37181
Jumper connector analysis
[DE94-010373] p 4451 N94-37188
Processing solid propellants for recycling
[DE94-011433] p 4428 N94-37202
Issues concerning the updating of finite-element models from experimental data
[NASA-TM-109116] p 4456 N94-37253
Scattering cross section of sound waves by the modal element method
[NASA-TM-106667] p 4510 N94-37308
A method for thermal analysis of spiral bevel gears
[NASA-TM-106612] p 4451 N94-37451
Experience with automatic, dynamic load balancing and adaptive finite element computation
[DE94-001422] p 4498 N94-37487
Finite element approximation of an optimal control problem for the von Karman equations
[NASA-CR-194955] p 4505 N94-37540
Linear-size nonobtuse triangulation of polygons
[DE94-010746] p 4505 N94-37620
Experimental and finite-element simulation results for a plane-strain punch-test using isotropic and anisotropic materials
[DE94-011711] p 4457 N94-37670
Numerical simulation of dynamic fracture and failure in solids
[DE94-010379] p 4457 N94-37705
A Lagrangian-Eulerian finite element method with adaptive gridding for advection-dispersion problems
[DE94-011372] p 4506 N94-37718
Analysis of anelastic flow and numerical treatment via finite elements
[DE94-012141] p 4445 N94-37726
Fuzzy logic to improve efficiency of finite element and finite difference schemes
[DE94-011718] p 4496 N94-37739

FINNED BODIES
The influence of fin height and wall conductivity on integral-fin tubes during steam condensation
[AD-A280597] p 4539 N94-36725

FINS
An aerodynamic and static-stability analysis of the Hypersonic Applied Research Technology (HART) missile
[AD-A280631] p 4382 N94-36729

FIRE CONTROL
ICAAS piloted simulation results p 4393 N94-36617
Aeroservoelastic stabilization considerations for pointing and tracking systems p 4394 N94-36627

FIRE PREVENTION
Flame resistant fibrous structures development
[NASA-CR-185700] p 4421 N94-36641
Aircraft command in emergency situations prototype development users manual
[DOT/FAA/CT-94/24] p 4385 N94-37706

FIRES
Design and development of experimental facilities for short duration, low-gravity combustion and fire experiments
[NASA-CR-196107] p 4389 N94-36967

FIRING (IGNITING)
A fully coupled thermal, chemical, mechanical cookoff model
[DE94-011432] p 4428 N94-37201

FITTINGS
Jumper connector analysis
[DE94-010373] p 4451 N94-37188

FIXTURES
Large angle magnetic suspension test fixture
[NASA-CR-196138] p 4390 N94-37450

FLAME PROPAGATION
Laser-saturated fluorescence measurements in laminar sooting diffusion flames
[NASA-CR-191025] p 4508 N94-36643
Some effects of heat release in premixed flames
[DE94-011346] p 4409 N94-37199
Probing flame chemistry with MBMS, theory, and modeling
[DE94-011224] p 4413 N94-37623

FLAME TEMPERATURE
Laser-saturated fluorescence measurements in laminar sooting diffusion flames
[NASA-CR-191025] p 4508 N94-36643
FLAMES
Influences of flame-vortex interactions on formation of oxides of nitrogen in curved methane-air diffusion flamelets
[DE94-005105] p 4409 N94-37221
Stability and dynamics of spatio-temporal structures
[DE94-013035] p 4412 N94-37491
FLAMMABILITY
Rich methane/air flames: Burning velocities, extinction limits, and flammability limit
[DE94-004340] p 4407 N94-36462
Rich flammability limits in CH3OH/CO/diluent mixtures
[DE94-004341] p 4407 N94-36482
Flame resistant fibrous structures development
[NASA-CR-185700] p 4421 N94-36641
FLASHOVER
Preradiation studies for non-thermal Z-pinch wire load experiments on Saturn
[DE94-013459] p 4527 N94-37072
FLATNESS
Angle interferometer cross axis errors
[DE94-006190] p 4446 N94-37388
FLATTENING
Q-profile flattening due to nonlinear development of resistive kink mode and ensuing fast crash in sawtooth oscillations
[DE94-727625] p 4526 N94-36472
FLEXIBLE BODIES
Modeling and control of intelligent flexible structures
[AD-A280478] p 4396 N94-37349
FLEXIBLE SPACECRAFT
Configurational evolution dynamics and stability during in-situ development of large orbiting spacecraft
[AD-A280482] p 4397 N94-37351
Approximate analysis for repeated eigenvalue problems with applications to controls-structure integrated design
[NASA-TP-3439] p 4397 N94-37502
FLIGHT CHARACTERISTICS
Controlling forebody asymmetries in flight: Experience with boundary layer transition strips
[NASA-TM-4595] p 4383 N94-36944
FLIGHT CONDITIONS
Toward a new National Weather Service: Weather for those who fly p 4472 N94-36947
FLIGHT CONTROL
ICAAS piloted simulation results p 4393 N94-36617
Advanced information processing system: The Army Fault-Tolerant Architecture detailed design overview
[NASA-CR-194924] p 4497 N94-36962
Design and evaluation of a Stochastic Optimal Feed-forward and Feedback Technology (SOFFT) flight control architecture
[NASA-TP-3419] p 4388 N94-37014
Predicting the effects of unmodeled dynamics on an aircraft flight control system design using eigenspace assignment
[NASA-TM-4548] p 4388 N94-37059
FLIGHT HAZARDS
An automated method for Low Level Windshear Alert System (LLWAS) data quality analysis
[AD-A280313] p 4472 N94-37126
FLIGHT OPERATIONS
Composite helicopter accident profiles: Deficient crew/aircraft performance
[SCT-90RR-46] p 4385 N94-37604
Night vision goggles in Emergency Medical Service (EMS) helicopters
[SCT-93RR-22] p 4487 N94-37742
FLIGHT SAFETY
An automated method for Low Level Windshear Alert System (LLWAS) data quality analysis
[AD-A280313] p 4472 N94-37126
Composite helicopter accident profiles: Deficient crew/aircraft performance
[SCT-90RR-46] p 4385 N94-37604
Night vision goggles in Emergency Medical Service (EMS) helicopters
[SCT-93RR-22] p 4487 N94-37742
FLIGHT SIMULATION
Applying formal methods and object-oriented analysis to existing flight software p 4491 N94-36495
ICAAS piloted simulation results p 4393 N94-36617
Attenuating the disorienting effects of head movement during whole-body rotation using a visual reference: Further tests of a predictive hypothesis p 4482 N94-37276
Advanced distributed simulation technology advanced rotary wing aircraft. Software programmer's manual visual system module
[AD-A280260] p 4390 N94-37755
Advanced distributed simulation technology advanced rotary wing aircraft. System/segment specification. Volume 4: Simulation system module RAH-66 Kit
[AD-A280261] p 4391 N94-37756
FLIGHT SIMULATORS
Virtual Interfaces: Research and Applications
[AGARD-CP-541] p 4482 N94-37261
Profile analysis of after-effects experienced during exposure to several virtual reality environments p 4482 N94-37263
Immersive virtual environments as trainer: System design from a cognitive stance p 4484 N94-37267
Attenuating the disorienting effects of head movement during whole-body rotation using a visual reference: Further tests of a predictive hypothesis p 4482 N94-37276
Some side-effects of immersion virtual reality p 4482 N94-37277
Visual accommodation to virtual image displays when knowledge of object distance conflicts with optical distance p 4485 N94-37278
Advanced distributed simulation technology advanced rotary wing aircraft. System/segment specification. Volume 4: Simulation system module RAH-66 Kit
[AD-A280261] p 4391 N94-37756
FLIGHT TESTS
Controlling forebody asymmetries in flight: Experience with boundary layer transition strips
[NASA-TM-4595] p 4383 N94-36944
TRENDS: A flight test relational database user's guide and reference manual
[NASA-TM-108806] p 4381 N94-37332
Civil use of night vision devices: Evaluation pilot's guide, part 1
[SCT-91RR-43] p 4487 N94-37741
Assessment of night vision goggle workload: Flight test engineer's guide
[SCT-91RR-45] p 4487 N94-37743
FLOATING POINT ARITHMETIC
Improved load distribution in parallel sparse Cholesky factorization
[NASA-CR-196380] p 4499 N94-37654
FLOW CHARACTERISTICS
An aerodynamic and static-stability analysis of the Hypersonic Applied Research Technology (HART) missile
[AD-A280631] p 4382 N94-36729
Navier-Stokes and potential theory solutions for ahelicopter fuselage and comparison with experiment
[NASA-TM-4566] p 4383 N94-36966
Simulation of three-dimensional multi-phase flow characteristics in the deswirl section of the CDIF MHD power train
[DE94-012644] p 4443 N94-37176
Prediction of film cooling on gas turbine airfoils
[NASA-TM-106653] p 4387 N94-37448
FLOW DEFLECTION
Computational investigation of an improved cowl concept for hypersonic propulsive nozzles
[AD-A280596] p 4441 N94-36724
FLOW DISTRIBUTION
A shadowgraph study of Space Transportation System (STS): The Space Shuttle Launch Vehicle (SSLV)
[NASA-RP-1341] p 4382 N94-36741
An arbitrary grid CFD algorithm for configuration aerodynamics analysis. Volume 1: Theory and validations
[NASA-CR-195918] p 4493 N94-36914
On automating domain connectivity for overset grids
[NASA-CR-196113] p 4493 N94-36920
An arbitrary grid CFD algorithm for configuration aerodynamics analysis. Volume 2: FEMNAS user guide
[NASA-CR-196135] p 4493 N94-36922
A combined experiment/computational study of flow in turbine blade cooling passage
[NASA-CR-4584] p 4442 N94-36957
Calibration and initial testing of a new hydraulic simulator
[AD-A280632] p 4390 N94-37163
Some effects of heat release in premixed flames
[DE94-011346] p 4409 N94-37199
Unsteady flow field of large-amplitude pitching airfoils
[AD-A280444] p 4383 N94-37219
FLOW EQUATIONS
A flux splitting scheme with high-resolution and robustness for discontinuities
[NASA-TM-106452] p 4441 N94-36646
The alternative faces of turbulent flow
[TM-5-94] p 4442 N94-36934
FLOW MEASUREMENT
Experimental uncertainty and drag measurements in the national transonic facility
[NASA-CR-4600] p 4389 N94-36945
Holt film wall shear instrumentation for boundary layer transition research
[NASA-CR-196040] p 4443 N94-37060
FLOW STABILITY
Coupled Marangoni-Benard/Rayleigh-Benard instability with temperature dependent viscosity
[NASA-TM-106646] p 4444 N94-37507
The stabilizing effect of compressibility in turbulent shear flow
[NASA-CR-194932] p 4444 N94-37605
Towards enhancing and delaying disturbances in free shear flows
[NASA-CR-194945] p 4445 N94-37606
FLOW VELOCITY
An algorithm for the automatic control of boundary layer flow
[ISVR-TR-233] p 4442 N94-36817
A combined experiment/computational study of flow in turbine blade cooling passage
[NASA-CR-4584] p 4442 N94-36957
A fast spectroscopic diagnostic for the measurement of plasma impurity ion dynamics
[DE94-012985] p 4529 N94-37354
FLOW VISUALIZATION
A shadowgraph study of Space Transportation System (STS): The Space Shuttle Launch Vehicle (SSLV)
[NASA-RP-1341] p 4382 N94-36741
Flow visualization for Lagrangian particle methods
[DE94-010757] p 4443 N94-37195
FLOWMETERS
Initial report on calorimetry for the Tore Supra Outboard pump Limiter
[DE94-011244] p 4531 N94-37626
FLUE GASES
Biological determinants of photobioreactor design
[DE94-011665] p 4468 N94-37740
FLUENCE
Irradiation assisted stress corrosion cracking of HTH Alloy X-750 and Alloy 625
[DE94-012667] p 4416 N94-37080
FLUID DYNAMICS
On automating domain connectivity for overset grids
[NASA-CR-196113] p 4493 N94-36920
Flow visualization for Lagrangian particle methods
[DE94-010757] p 4443 N94-37195
Project JOVE --- microgravity experiments and applications
[NASA-CR-196292] p 4445 N94-37635
FLUID FILMS
Microscopic image processing systems for measuring nonuniform film thickness profiles
[DE94-005336] p 4424 N94-37223
FLUID FILTERS
Method and apparatus for the collection, storage, and real time analysis of blood and other bodily fluids
[NASA-CASE-MSC-22463-1] p 4480 N94-36766
FLUID FLOW
Analysis of anelastic flow and numerical treatment via finite elements
[DE94-012141] p 4445 N94-37726
FLUID MANAGEMENT
Cryogenic fluid management technologies for space transportation. Zero G thermodynamic vent system
[NASA-CR-193981] p 4430 N94-36806
FLUIDICS
A dynamic model of a linear actuator based on polymer hydrogel
[DE94-010800] p 4408 N94-37091
FLUIDIZED BED PROCESSORS
Robotic weld overlay coatings for erosion control
[DE94-013477] p 4417 N94-37116
FLUORESCENCE
Laser-saturated fluorescence measurements in laminar sooting diffusion flames
[NASA-CR-191025] p 4508 N94-36643
Combined atomic force and scanning reflection interference contrast microscopy
[AD-A280341] p 4514 N94-37034
Understanding and managing power system harmonics
[AD-A280627] p 4440 N94-37759
FLUORIDES
A photoemission study of Au, Ge, and O2 deposition on NH4F etched Si(111)
[DE94-013352] p 4519 N94-37553
FLUORINE ORGANIC COMPOUNDS
Highly fluorinated polymers
[NASA-CR-196270] p 4422 N94-37025
Effect of temperature on the electron attachment and detachment properties of c-C4F6
[DE94-012750] p 4518 N94-37383
FLUOROHYDROCARBONS
Fluorinated resins with low dielectric constant
[AD-D016303] p 4427 N94-37773
FLUTTER
Multirate flutter suppression system design for the Benchmark Active Controls Technology Wing
[NASA-CR-196112] p 4388 N94-36965

FLUX (RATE)
Anomalous cross field flux in CHS
[DE94-727547] p 4529 N94-37359
FLUX DENSITY
LNG vehicle technology, economics, and safety assessment
[PB94-165487] p 4450 N94-36721
Critical-state flux-density profiles in type-2 superconducting thin-film strips and disks
[DE94-011199] p 4535 N94-37166
FLUX VECTOR SPLITTING
A flux splitting scheme with high-resolution and robustness for discontinuities
[NASA-TM-106452] p 4441 N94-36646
FLUXES
Integrated environmentally compatible soldering technologies
[DE94-013456] p 4464 N94-37071
FLY BY LIGHT CONTROL
Prospective communications research to support fly by light/power by wire
[NASA-CR-196369] p 4526 N94-37657
FOAMS
The problems of the minimal surface and minimal lineal measure in three dimensions
[DE94-013002] p 4479 N94-37355
FORCE DISTRIBUTION
Electronic balance and some gravimetric applications (the density of solids and liquids, pycnometry and mass)
[PB94-163052] p 4446 N94-36719
FOREBODIES
Controlling forebody asymmetries in flight: Experience with boundary layer transition strips
[NASA-TM-4595] p 4383 N94-36944
Hypersonic, nonequilibrium flow over the FIRE 2 forebody at 1634 sec
[NASA-TM-109141] p 4444 N94-37455
FORECASTING
Software forecasting as it is really done: A study of JPL software engineers p 4490 N94-36489
FOREST MANAGEMENT
Opportunities for innovation: Biotechnology
[PB94-157831] p 4478 N94-36720
FORGING
Maintaining constant standards during the forging process p 4421 N94-37326
FORM FACTORS
Sum rules for 1/m corrections to the form factors of semileptonic B decays
[DE94-618548] p 4514 N94-37065
The form factors of the nucleons
[DE94-013357] p 4515 N94-37086
FORMALDEHYDE
California residential indoor air quality study. Volume 1: Methodology and descriptive statistics
[PB94-166048] p 4464 N94-36994
FORMALISM
Applying formal methods and object-oriented analysis to existing flight software p 4491 N94-36495
FORMS (PAPER)
Hubble Space Telescope cycle 5. Phase 1: Proposal instructions, version 4.0
[NASA-CR-189364] p 4547 N94-36963
FORTRAN
A compilation system that integrates high performance FORTRAN and FORTRAN M
[DE94-013308] p 4496 N94-37551
FORWARD SCATTERING
Forward scattering of neutrons from polymeric and magnetic multilayers
[DE93-041158] p 4513 N94-36696
FOSSIL FUELS
Coal-fueled diesel technology development: Fuel injection equipment for coal-fueled diesel engines
[DE94-004088] p 4452 N94-37512
FOULING
Indicators for sulfate-reducing bacteria in microbiologically influenced corrosion
[AD-A278914] p 4477 N94-36522
FOURIER ANALYSIS
Noise reduction for speech enhancement using non-linear wavelet processing
[AD-A280469] p 4434 N94-37141
FOURIER TRANSFORMATION
Metal-carbon nanostructures
[DE94-009177] p 4400 N94-36509
Quantum harmonic Brownian motion in a general environment: A modified phase-space approach
[DE94-003249] p 4508 N94-36560
FRACTURE MECHANICS
Crack growth under cycle loading in fibre reinforced titanium metal matrix composites p 4402 N94-36665
Fracture mechanics life analytical methods verification testing
[NASA-CR-4602] p 4455 N94-37015
Interaction effects of cracks, flaws and damage in ceramic
[AD-A280368] p 4423 N94-37181
The cyclic fatigue behaviour of adhesive joints
[AD-A280453] p 4456 N94-37186
A methodology to predict damage initiation, damage growth and residual strength in titanium matrix composites
[NASA-TM-109135] p 4405 N94-37320
Defects and their effects on the integrity of nickel based aeroengine discs p 4421 N94-37328
Predicting defect behaviour p 4455 N94-37331
Development of nondestructive evaluation methods and prediction of effects of flaws on the fracture behavior of structural ceramics
[DE94-012466] p 4425 N94-37423
Fatigue case study and loading spectra for wind turbines
[DE94-010798] p 4457 N94-37622
Numerical simulation of dynamic fracture and failure in solids
[DE94-010379] p 4457 N94-37705
Strength characteristics and crack growth behavior of a composite with well aligned fibers p 4459 N94-37804
Damage and strength of composite materials: Trends, predictions, and challenges p 4459 N94-37805
Scaling effects of defects in fiber-reinforced composites p 4459 N94-37807
Scaling of impact damage in fiber composites p 4460 N94-37810
FRACTURE STRENGTH
Residual strength and life prediction techniques for Ti MMC p 4402 N94-36662
Pre-standardisation work on fatigue and fracture testing of titanium matrix composites p 4402 N94-36667
NASA-UVA Light Aerospace Alloy and Structures Technology Program (LA2ST)
[NASA-CR-196290] p 4415 N94-36809
Substantiating powder metal life methodologies for engines p 4455 N94-37330
Characterization of mechanical properties degradation using small punch testing technique
[DE94-011202] p 4418 N94-37410
Physical and mechanical metallurgy of NiAl
[NASA-TP-3398] p 4419 N94-37503
Damage and strength of composite materials: Trends, predictions, and challenges p 4459 N94-37805
FRACTURES (MATERIALS)
A computational model for three-dimensional jointed media with a single joint set
[DE94-007582] p 4470 N94-37527
FRACTURING
Interaction effects of cracks, flaws and damage in ceramic
[AD-A280368] p 4423 N94-37181
Defect initiation/growth and energy dissipation induced by deformation and fracture
[AD-A280411] p 4424 N94-37184
FRAGMENTATION
Low-energy electron collisions with metal clusters: Electron capture and cluster fragmentation
[DE94-003623] p 4512 N94-36516
FRANCE
Information retrieval services on wide area networks: A vision of the future p 4545 N94-37346
FRANCK-CONDON PRINCIPLE
Bond selective chemistry beyond the adiabatic approximation
[DE94-012486] p 4408 N94-37095
FREE CONVECTION
Use of rotation to suppress thermosolutal convection in directionally solidified binary alloys
[NASA-CR-196372] p 4415 N94-36811
FREE ELECTRON LASERS
Suppression of beam-break-up in a standing wave free electron laser two-beam accelerator
[DE94-011348] p 4521 N94-37200
Microwave generation for magnetic fusion energy applications
[DE94-012107] p 4448 N94-37368
Recent progress of the Los Alamos advanced free electron laser
[DE94-011654] p 4449 N94-37733
FREE ENERGY
A possible origin of EL6 chondrites from a high temperature-high pressure solar gas
[DE94-010467] p 4548 N94-36759
FREE FLOW
Towards enhancing and delaying disturbances in free shear flows
[NASA-CR-194945] p 4445 N94-37606
FREE RADICALS
Infrared spectroscopy of organic free radicals related to combustion processes
[DE94-012481] p 4409 N94-37168
Fast beam studies of free radical photodissociation
[DE94-011380] p 4521 N94-37720
FREE VIBRATION
Laminated thin shell structures subjected to free vibration in a hygrothermal environment
[NASA-TM-106600] p 4456 N94-37456
FREEZING
Effects of freezing and cold acclimation on the plasma membrane of isolated protoplasts
[DE94-012487] p 4479 N94-37248
FREON
A freon-filled, holographic bubble chamber as a high energy photon burst spectrometer
[DE94-011645] p 4446 N94-37723
FREQUENCIES
Proceedings of SPIE: The International Society for Optical Engineering, Computational Vision Based on Neurobiology, volume 2054
[AD-A278731] p 4523 N94-36468
FREQUENCY DISTRIBUTION
Multirate time-frequency distributions
[AD-A280595] p 4503 N94-36723
FREQUENCY MODULATION
A high power microwave frequency modulated KrF laser
[DE94-009303] p 4447 N94-36510
Frequency doubling of copper lasers using temperature-tuned ADP
[DE94-011542] p 4448 N94-37240
FREQUENCY RESPONSE
Holt film wall shear instrumentation for boundary layer transition research
[NASA-CR-196040] p 4443 N94-37060
FRESH WATER
Evaluation of flame-sprayed polymer coatings for civil works navigation structures
[AD-A280507] p 4422 N94-37104
FRETTING
Literature review and preliminary studies of fretting and fretting fatigue including special applications to aircraft joints
[AD-A280310] p 4456 N94-37125
FRICTION
Dynamics of a split torque helicopter transmission
[NASA-TM-106410] p 4452 N94-37457
Robust stability of second-order systems
[NASA-CR-196384] p 4501 N94-37590
FRONTS (METEOROLOGY)
The role of horizontal variability in air-sea interaction
[AD-A280561] p 4476 N94-37047
FUEL CELL POWER PLANTS
MCFC product development test
[DE94-002005] p 4463 N94-37488
FUEL CELLS
Novel carbon-ion fuel cells
[DE94-010716] p 4461 N94-36511
Activities of the Chemical Technology Division
[DE94-013050] p 4410 N94-37357
Fuel savings and emissions reductions from light duty fuel cell vehicles
[DE94-006909] p 4451 N94-37406
MCFC product development test
[DE94-002005] p 4463 N94-37488
FUEL COMBUSTION
Bond selective chemistry beyond the adiabatic approximation
[DE94-012486] p 4408 N94-37095
Spray combustion model improvement study, 1
[NASA-CR-196122] p 4410 N94-37250
Combustion characterization of methylal in reciprocating engines
[DE94-006949] p 4411 N94-37409
Advanced Turbine Technology Applications Project (ATTAP)
[NASA-CR-195367] p 4452 N94-37763
FUEL CONSUMPTION
Fuel savings and emissions reductions from light duty fuel cell vehicles
[DE94-006909] p 4451 N94-37406
FUEL INJECTION
Coal-fueled diesel technology development: Fuel injection equipment for coal-fueled diesel engines
[DE94-004088] p 4452 N94-37512
FUEL PUMPS
Coal-fueled diesel technology development: Fuel injection equipment for coal-fueled diesel engines
[DE94-004088] p 4452 N94-37512
FUEL SPRAYS
Spray combustion model improvement study, 1
[NASA-CR-196122] p 4410 N94-37250
FUEL SYSTEMS
Coal-fueled diesel technology development: Fuel injection equipment for coal-fueled diesel engines
[DE94-004088] p 4452 N94-37512

FUEL TESTS
Combustion characterization of methylal in reciprocating engines
[DE94-006949] p 4411 N94-37409
Interferometric JFTOT tube deposit measuring device
[AD-D016295] p 4430 N94-37768
FUELS
Estimates of US biomass energy consumption 1992
[DE94-011458] p 4463 N94-37567
FULLERENES
Supersonic bare metal cluster beams
[DE94-010790] p 4532 N94-36454
Turning soot into diamonds with microwaves
[DE94-013426] p 4422 N94-37068
Theoretical and experimental investigations of fullerene derivatives: C60H2, C60H4, C70H2 and C60CH22
[DE94-012727] p 4536 N94-37287
First-principles determination of the polarizabilities of carbon tubules as a function of length
[DE94-013015] p 4537 N94-37356
Ionic properties of hydrogenated and fluorinated fullerenes
[DE94-012110] p 4537 N94-37369
FUNCTIONAL DESIGN SPECIFICATIONS
A two-level formal specification of a defense communications system
[DE94-012117] p 4434 N94-37206
FUNCTIONALS
New method for minimizing regular functions with constraints on parameter region
[DE94-618340] p 4515 N94-37076
FURNACES
Assess progress being made for the KTeV electromagnetic calorimeter crystal order in France
[DE94-009396] p 4533 N94-36746
The development of short, high surface area activated carbon fibers
[AD-A280509] p 4404 N94-37105
FUSELAGES
Navier-Stokes and potential theory solutions for ahelicopter fuselage and comparison with experiment
[NASA-TM-4568] p 4383 N94-36966
FUSION REACTORS
Conceptual design for a fast neutron ionization chamber for fusion reactor plasma diagnostics
[DE94-013396] p 4527 N94-37101
Towards nuclear fusion reactors
[DE94-748680] p 4528 N94-37235
Development of intermetallic coatings for fusion power applications
[DE94-012647] p 4419 N94-37442
Two-dimensional over-all neutronics analysis of the ITER device
[DE94-718963] p 4530 N94-37464
FUZZY SETS
On the use of fuzzy logic assessment for high consequence implementation risk analysis
[DE94-011417] p 4507 N94-37564
FUZZY SYSTEMS
Fuzzy logic to improve efficiency of finite element and finite difference schemes
[DE94-011718] p 4496 N94-37739
Open architecture controllers for advanced manufacturing
[DE94-007572] p 4496 N94-37782

G

GALACTIC COSMIC RAYS
Estimates of cellular mutagenesis from cosmic rays
[NASA-TP-3453] p 4481 N94-37282
GALACTIC HALOS
Guaranteed time observations support for Faint Object Spectrograph (FOS) on HST
[NASA-CR-196305] p 4547 N94-37037
GALERKIN METHOD
A Galerkin method for linear PDE systems in circular geometries with structural acoustic applications
[NASA-CR-194925] p 4503 N94-36923
GALILEO SPACECRAFT
Scientific and technical support for the Galileo net flux radiometer experiment
[NASA-CR-196009] p 4549 N94-36669
GALLIUM ARSENIDES
Ampoule failure sensor time response testing: Experiments 2 and 3
[NASA-TM-108458] p 4446 N94-36822
Quantum confinement in GaP nanoclusters
[DE94-013119] p 4536 N94-37290
BMAP dipole magnetic field analysis and orbit tracking/calculations of energy deposition in GaAs WHEBY detectors
[DE94-012080] p 4522 N94-37303
GALLIUM NITRIDES
Studies of the III-V compounds in the megabar regime
[DE94-012488] p 4537 N94-37435
GALLIUM PHOSPHIDES
Quantum confinement in GaP nanoclusters
[DE94-013119] p 4536 N94-37290
GAMMA RAY ABSORPTION
The effects of proton-beam quality on the production of gamma rays for nuclear resonance absorption in nitrogen
[DE94-011609] p 4523 N94-37629
GAMMA RAY ASTRONOMY
Gamma ray astronomy
[NASA-CR-193970] p 4547 N94-37702
GAMMA RAY BURSTS
Gamma ray astronomy
[NASA-CR-193970] p 4547 N94-37702
GAMMA RAY SPECTRA
Gamma ray astronomy
[NASA-CR-193970] p 4547 N94-37702
GAMMA RAY SPECTROMETERS
Activities of the Tandem Accelerator Center, University of Tsukuba
[DE94-748687] p 4522 N94-37237
A high precision gamma ray spectrometer for the Mars 1994 mission
[DE94-013133] p 4550 N94-37293
GAMMA RAYS
The t(anti t)(gamma) background to pp (yields) W(gamma) + X at the SSC
[DE94-001386] p 4512 N94-36526
Studying of ion implantation effect on the biology in China
[DE94-620692] p 4479 N94-37535
GAS ANALYSIS
SAW chemical sensor arrays using new thin-film materials
[DE94-011940] p 4411 N94-37365
GAS COMPOSITION
Atmospheric gas
[DE94-007439] p 4465 N94-37187
GAS DETECTORS
Experimental characterisation of gas microstrip detectors. Part 1: Gain characteristics
[PB94-167087] p 4445 N94-36531
Comparison of gaseous and semiconductor detectors for medical imaging
[DE94-621344] p 4482 N94-37729
GAS DISSOCIATION
Direct catalytic decomposition of nitric oxide
[DE94-005025] p 4407 N94-36475
GAS DYNAMICS
Theoretical studies of a molecular beam generator
[NASA-CR-196306] p 4522 N94-37508
A nonconservative scheme for isentropic gas dynamics
[DE94-011488] p 4445 N94-37724
GAS GENERATORS
Computational investigation of an improved cowl concept for hypersonic propulsive nozzles
[AD-A280596] p 4441 N94-36724
GAS IONIZATION
The angular and energy distributions of ejected electrons in electron-impact ionization of helium
[DE94-618748] p 4519 N94-37528
GAS TEMPERATURE
Effect of temperature on the electron attachment and detachment properties of c-C4F6
[DE94-012750] p 4518 N94-37383
GAS TRANSPORT
The potential for control of carbon dioxide emissions from integrated gasification/combined-cycle systems
[DE94-012646] p 4465 N94-37100
GAS TURBINE ENGINES
Defects and their effects on the integrity of nickel based aeroengine discs p 4421 N94-37328
Turbine disks: Lifing against defects and materials development p 4454 N94-37329
Substantiating powder metal life methodologies for engines p 4455 N94-37330
Advanced Turbine Technology Applications Project (ATTAP)
[NASA-CR-195367] p 4452 N94-37763
GAS TURBINES
Integrated gasification combined cycle and steam injection gas turbine powered by biomass joint-venture evaluation
[DE94-006905] p 4461 N94-36740
Experimental measurements and analytical analysis related to gas turbine heat transfer. Part 1: Time-averaged heat-flux and surface-pressure measurements on the vanes and blades of the SSME fuel-side turbine and comparison with prediction. Part 2: Phase-resolved surface-pressure and heat-flux measurements on the first blade of the SSME fuel-side turbine
[NASA-CR-196296] p 4442 N94-36969
Prediction of film cooling on gas turbine airfoils
[NASA-TM-106653] p 4387 N94-37448
GASIFICATION
Integrated gasification combined cycle and steam injection gas turbine powered by biomass joint-venture evaluation
[DE94-006905] p 4461 N94-36740
GEAR TEETH
Vibration signature analysis of a faulted gear transmission system
[NASA-TM-106623] p 4450 N94-36953
Dynamics of a split torque helicopter transmission
[NASA-TM-106410] p 4452 N94-37457
An enhancement to the NA4 gear vibration diagnostic parameter
[NASA-TM-106553] p 4452 N94-37521
GEARS
Evaluation of the EHL film thickness and extreme pressure additives on gear surface fatigue life
[NASA-TM-106663] p 4451 N94-37319
A method for thermal analysis of spiral bevel gears
[NASA-TM-106612] p 4451 N94-37451
Dynamics of a split torque helicopter transmission
[NASA-TM-106410] p 4452 N94-37457
An enhancement to the NA4 gear vibration diagnostic parameter
[NASA-TM-106553] p 4452 N94-37521
GELS
Sodium-23 NMR and complex impedance studies of gel electrolytes based on poly(acrylonitrile)
[AD-A280330] p 4408 N94-37031
A dynamic model of a linear actuator based on polymer hydrogel
[DE94-010800] p 4408 N94-37091
GENERAL OVERVIEWS
Physical and mechanical metallurgy of NiAl
[NASA-TP-3398] p 4419 N94-37503
GENETIC ALGORITHMS
Adaptive learning of multi-sensor integration techniques with genetic algorithms
[DE94-012744] p 4500 N94-37083
GENETIC CODE
Recombinant protein production and insect cell culture and process
[NASA-CASE-MSC-22336-1] p 4478 N94-36751
GENETIC ENGINEERING
Recombinant protein production and insect cell culture and process
[NASA-CASE-MSC-22336-1] p 4478 N94-36751
GENETICS
United States Air Force Summer Research Program, 1993. Volume 7: Armstrong Laboratory
[AD-A278655] p 4550 N94-36975
Estimates of cellular mutagenesis from cosmic rays
[NASA-TP-3453] p 4481 N94-37282
GEOCHEMISTRY
Thermodynamics of minerals stable near the Earth's surface
[DE94-012479] p 4539 N94-37094
Analysis of deep seismic reflection and other data from the Southern Washington Cascades
[DE94-004075] p 4470 N94-37489
GEODYNAMICS
Measurement and interpretation of crustal deformation rates associated with postglacial rebound
[NASA-CR-196300] p 4470 N94-37581
GEOLOGICAL FAULTS
A computational model for three-dimensional jointed media with a single joint set
[DE94-007582] p 4470 N94-37527
GEOLOGICAL SURVEYS
Analysis of deep seismic reflection and other data from the Southern Washington Cascades
[DE94-004075] p 4470 N94-37489
GEOLOGY
Geophysical data fusion for subsurface imaging
[DE94-000056] p 4469 N94-36738
The potential for control of carbon dioxide emissions from integrated gasification/combined-cycle systems
[DE94-012646] p 4465 N94-37100
GEOMAGNETIC TAIL
Analysis of plasma measurements for the Geotail mission
[NASA-CR-196274] p 4470 N94-37470
Magnetotail dynamics: MHD simulations of driven and spontaneous dynamic changes
[DE94-011702] p 4471 N94-37701
GEOMAGNETISM
Solar-Terrestrial Predictions, 4: Proceedings of aworkshop. Volume 3: Geomagnetic papers; ionospheric papers
[PB94-173192] p 4470 N94-37530
Substorm statistics: Occurrences and amplitudes
[DE94-011694] p 4471 N94-37669

Solar-Terrestrial Predictions, 4: Proceedings of a workshop. Volume 1: Workshop overview papers; working group reports; User community reports; Regional Warning Center Reports
[PB94-173176] p 4471 N94-37780
Solar-Terrestrial Predictions, 4: Proceedings of a workshop. Volume 2: Solar papers; magnetospheric papers
[PB94-173184] p 4471 N94-37781

GEOPHYSICS
Geophysical data fusion for subsurface imaging
[DE94-000056] p 4469 N94-36738
Analysis of deep seismic reflection and other data from the Southern Washington Cascades
[DE94-004075] p 4470 N94-37489
Measurement and interpretation of crustal deformation rates associated with postglacial rebound
[NASA-CR-196300] p 4470 N94-37581

GEOTHERMAL RESOURCES
Large-scale three-dimensional geothermal reservoir simulation on PC's
[DE94-011374] p 4443 N94-37050

GERMANIUM
A photoemission study of Au, Ge, and O2 deposition on NH4F etched Si(111)
[DE94-013352] p 4519 N94-37553

GLACIERS
Measurement and interpretation of crustal deformation rates associated with postglacial rebound
[NASA-CR-196300] p 4470 N94-37581

GLASS
Analytical electron microscopy examination of solid reaction products in long-term test of SRL 200 waste glasses
[DE94-000482] p 4411 N94-37380
Optical studies of dynamical processes in disordered systems
[DE94-011945] p 4538 N94-37676

GLASS FIBER REINFORCED PLASTICS
Micromechanical modeling of advanced materials
[DE94-011249] p 4405 N94-37627

GLASS FIBERS
Guiding hard x rays with glass polycapillary fiber
[DE94-004949] p 4525 N94-37258

GLOBAL POSITIONING SYSTEM
Global Positioning System Synchronized Active Light Autonomous Docking System
[NASA-CASE-MFS-28853-1] p 4395 N94-36825
Eurocap program: Ebre Station
[AD-A280418] p 4469 N94-37215
Evaluation of GPS position and attitude determination for automated rendezvous and docking missions
[NASA-CR-4614] p 4397 N94-37506

GLOBAL WARMING
UK methane emissions inventory: A scoping study on the use of ambient measurements to reduce uncertainties
[PB94-167855] p 4463 N94-36533
Refrigeration and Air-Conditioning Technology Workshop
[DE94-010813] p 4431 N94-37452

GLOVES
Interactive large screen: A multi-mode dialogue tool for future cockpits p 4484 N94-37266
Manual tracking performance using a virtual hand controller: A comparison study p 4484 N94-37271

GLOW DISCHARGES
New hollow-cathode electrode for high-power copper lasers
[DE94-011637] p 4448 N94-37244

GLUONS
Effective Lagrangian for gluons and Higgs pseudoscalars
[DE94-001381] p 4513 N94-36539
Strangeness and the quark-gluon plasma: An experimenter's perspective
[DE94-011377] p 4519 N94-37558

GOGGLES
Visual accommodation to virtual image displays when knowledge of object distance conflicts with optical distance p 4485 N94-37278
Civil use of night vision devices: Evaluation pilot's guide, part 1
[SCT-91RR-43] p 4487 N94-37741
Night vision goggles in Emergency Medical Service (EMS) helicopters
[SCT-93RR-22] p 4487 N94-37742
Assessment of night vision goggle workload: Flight test engineer's guide
[SCT-91RR-45] p 4487 N94-37743

GOLD
X-ray diffraction studies of evaporated gold thin films deposited on aluminum nitride substates
[AD-A280454] p 4536 N94-37228
A photoemission study of Au, Ge, and O2 deposition on NH4F etched Si(111)
[DE94-013352] p 4519 N94-37553

GOLD ISOTOPES
Production of phi mesons in central Si+Au collisions at 14.6 A GeV/c
[DE94-011726] p 4516 N94-37152

GOVERNMENT PROCUREMENT
Open system environment procurement p 4542 N94-36858

GOVERNMENT/INDUSTRY RELATIONS
Beginning a dialogue on the changing environment for the physical and mathematical sciences p 4509 N94-36948

GRAIN BOUNDARIES
Characterization and processing of sintered products from nano-crystalline powders generated by the RTDS method
[DE94-004765] p 4415 N94-36553
Interaction effects of cracks, flaws and damage in ceramic
[AD-A280368] p 4423 N94-37181
Determination of interface structure and bonding at atomic resolution in the stem
[DE94-011466] p 4517 N94-37238
Atomic level characterization of defects in microalloyed NiAl: An atom probe investigation
[DE94-012732] p 4418 N94-37396
AEM and AES of radiation-induced segregation in proton-irradiated stainless steels
[DE94-012734] p 4418 N94-37398
The effect of reactive elements on the segregation behavior and microstructure of alpha-Al2O3 scales on beta-NiAl
[DE94-012739] p 4418 N94-37399
Atomic resolution characterization of a SrTiO3 grain boundary in the STEM
[DE94-011469] p 4538 N94-37545
Effect of thermal annealing on grain boundary chemistry of polycrystalline TlBa2Ca2Cu3O(y) films
[DE94-011464] p 4538 N94-37569

GRAMMARS
An error-resistant linguistic protocol for air traffic control
[NASA-CR-196098] p 4385 N94-37013

GRANULAR MATERIALS
Studies of the effect of microstructure on the dynamic behavior of granular and particulate media
[AD-A279012] p 4455 N94-36520
Numerical study of the flow of granular materials down an inclined plane
[DE94-010729] p 4444 N94-37544

GRAPHICAL USER INTERFACE
NASA Access Mechanism: Lessons learned document
[NASA-TM-109924] p 4540 N94-36750

GRAPHITE
Using nonequilibrium alloying techniques for corrosion inhibition in Gr/Al and Gr/Mg metal matrix composites
[AD-A280529] p 4404 N94-37088
Mechanical performance of austempered ductile iron
[AD-A280452] p 4420 N94-37758

GRAPHITE-EPOXY COMPOSITES
A comparison of graphite/epoxy tape laminates and 2-D braided composites mechanical properties
[NASA-CR-4610] p 4420 N94-37582
A simple evaluation of thermally-induced stresses in the vicinity of the stitch in a through-thickness reinforced cross-ply laminate
[NASA-CR-196317] p 4406 N94-37653
Sub-ply level scaling approach investigated for graphite-epoxy composite beam columns p 4458 N94-37798
Effects of ply thickness on thermal cycle induced damage and thermal strain p 4459 N94-37806
Statistical scaling relationships and size effects in the strength and creep rupture of fibrous composites p 4460 N94-37809
Scaling of impact damage in fiber composites p 4460 N94-37810

GRAPHS (CHARTS)
A graphic view of Geometric Dimensioning and Tolerancing
[DE94-011478] p 4435 N94-37736

GRATINGS (SPECTRA)
Four beam interferometer manual: Operating instructions for the INEL diffraction Moire interferometer
[DE94-010772] p 4453 N94-36452
Intensity of waves diffracted from symmetrical profile lamellar gratings
[DE94-611101] p 4433 N94-36753
Optically induced high efficiency gratings in azo polymer films
[AD-A280505] p 4423 N94-37147

GRAVIMETRY
Electronic balance and some gravimetric applications (the density of solids and liquids, pycnometry and mass)
[PB94-163052] p 4446 N94-36719

GRAZING INCIDENCE
Forward scattering of neutrons from polymeric and magnetic multilayers
[DE93-041158] p 4513 N94-36696

GREEN'S FUNCTIONS
Nonlinearity with disorder: Spatio-temporal complex behavior arising from length scales competition
[DE94-000675] p 4502 N94-36685

GREENHOUSE EFFECT
Factors influencing the parameterization of anvil clouds within GCMs
[DE94-010794] p 4475 N94-37621
Tropospheric radiative forcing of CH4
[DE94-011628] p 4468 N94-37631

GRID GENERATION (MATHEMATICS)
Automatic procedures for computing complete configuration geometry from individual component descriptions
[NASA-TM-4607] p 4382 N94-36942
Automatic computation of Euler-marching and subsonic grids for wing-fuselage configurations
[NASA-TM-4573] p 4383 N94-36950
A method for flow simulation about complex geometries using both structured and unstructured grids
[NASA-TM-106633] p 4383 N94-37283
Evolution of turbulent fields in explosions
[DE94-010405] p 4444 N94-37390
Linear-size nonobtuse triangulation of polygons
[DE94-010746] p 4505 N94-37620

GROUND EFFECT (AERODYNAMICS)
Rotorwash analysis handbook. Volume 1: Development and analysis
[SCT-93RR-17-VOL-1] p 4381 N94-36466
Rotorwash analysis handbook. Volume 2: Appendixes
[SCT-93RR-17-VOL-2] p 4382 N94-36467
Subsonic aerodynamic characteristic of semispan commercial transport model with wing-mounted advanced ducted propeller operating in reverse thrust — conducted in the Langley 14 by 22 foot subsonic wind tunnel
[NASA-TP-3427] p 4384 N94-37505

GROUND STATE
Consequences of competing hybridization for magnetic ordering in correlated-electron lattices
[DE94-011648] p 4534 N94-37057
Structural ground-state of La2CuO4 in the LTO phase: Evidence of local disorder
[DE94-013126] p 4536 N94-37291

GROUND STATIONS
Preliminary PANSAT ground station software design and use of an expert system to analyze telemetry
[AD-A280600] p 4392 N94-36726
Design and analysis of a mode B and mode JD satellite Earth station
[AD-A280417] p 4391 N94-37225

GROUND SUPPORT SYSTEMS
Planning German Army helicopter maintenance and mission assignment
[AD-A280483] p 4381 N94-37352

GROUND TRUTH
NASA ER-2 Doppler radar reflectivity calibration for the CAMEX project
[NASA-TM-104611] p 4475 N94-37790

GROUND WIND
On the development of boundary layer secondary circulations resulting from horizontally varying surface heat flux
[DE94-011234] p 4472 N94-37048

GROUP THEORY
Representations of the q-deformed algebras U(q) (so(2,1)) and U(q) (so(3,1)
[DE94-616619] p 4505 N94-37483

GROWTH
Surface modification of polymers with self-assembled monolayers that promote adhesion, outgrowth and differentiation of biological cells
[AD-D016321] p 4427 N94-37829

GUIDANCE SENSORS
Global Positioning System Synchronized Active Light Autonomous Docking System
[NASA-CASE-MFS-28853-1] p 4395 N94-36825

GYROSCOPES
Laboratory evaluation of the Standard Elektrik Lorenz (SEL) fibre-optic rate gyroscope
[AD-A280191] p 4446 N94-36760

GYROSTABILIZERS
The use of a tactile interface to convey position and motion perceptions p 4486 N94-37281

H

H-INFINITY CONTROL
Mixed H2/H-infinity optimization with multiple H infinity constraints
[AD-A280572] p 4388 N94-36733
H2 optimal control with H-infinity, mu, and L1 constraints
[AD-A280593] p 4500 N94-36736
HABITATS
Ground and space flight experiments of the effects of light, sound and/or temperature on animals
[NASA-CR-196102] p 4478 N94-36986
HADRONS
Deep inelastic scattering results from the first year of HERA operation
[DE94-004578] p 4511 N94-36483
Angular dependence of parton-parton scattering extracted from hadron pair production in pp collisions at radicals equal to 11.5 GeV
[DE94-611174] p 4511 N94-36504
CP violation outside the standard model phenomenology for pedestrians
[DE94-002216] p 4511 N94-36512
The t(anti t)(gamma) background to pp (yields) W(gamma) + X at the SSC
[DE94-001386] p 4512 N94-36526
B-lifetime measurements at the tevatron
[DE94-003617] p 4513 N94-36528
First results from a prototype level-1 calorimeter trigger system for LHC, RD 27 (UK) collaboration
[PB94-167475] p 4436 N94-36532
New method for minimizing regular functions with constraints on parameter region
[DE94-618340] p 4515 N94-37076
Hard diffraction and deep inelastic scattering
[DE94-013353] p 4515 N94-37084
A study of jet handedness in hadronic Z0 decays
[DE94-013358] p 4515 N94-37087
Physics with primary beams of the KEK-PS
[DE94-748635] p 4522 N94-37234
First observation of laser-induced resonant annihilation in metastable antiprotonic helium atoms
[DE94-748668] p 4519 N94-37417
Polarization phenomena in quantum chromodynamics
[DE94-010663] p 4539 N94-37543
Hadron production in S+nucleus collisions at 200 GeV/nucleon
[DE94-011344] p 4520 N94-37715
Experimental particle physics at the University of Pittsburgh
[DE94-011636] p 4521 N94-37721
HALF PLANES
H infinity control for nonlinear and linear systems
[AD-A280450] p 4494 N94-37226
HALF SPACES
Imaging targets embedded in a lossy half space with Synthetic Aperture Radar
[DE94-010807] p 4435 N94-37391
HALOCARBONS
Accelerated line-by-line calculations for the radiative transfer of trace gases related to climate studies
[DE94-004404] p 4464 N94-36552
HALOGENS
Method of forming waveguides with ion exchange of halogen ions
[AD-D016304] p 4526 N94-37774
HAMILTONIAN FUNCTIONS
Variational discrete symmetries
[DE94-618485] p 4507 N94-37062
Solving the two-dimensional Schroedinger equation in self-consistent basis
[DE94-621535] p 4504 N94-37174
HANDBOOKS
Rotorwash analysis handbook. Volume 1: Development and analysis
[SCT-93RR-17-VOL-1] p 4381 N94-36466
Rotorwash analysis handbook. Volume 2: Appendixes
[SCT-93RR-17-VOL-2] p 4382 N94-36467
Hubble Space Telescope faint object spectrograph instrument handbook, version 5.0
[NASA-CR-189367] p 4546 N94-36794
Hubble Space Telescope faint object camera instrument handbook (Post-COSTAR), version 5.0
[NASA-CR-189365] p 4546 N94-36795
Hubble Space Telescope Wide Field and Planetary Camera 2 Instrument handbook, version 2.0
[NASA-CR-189368] p 4547 N94-36918
HANDEDNESS
A study of jet handedness in hadronic Z0 decays
[DE94-013358] p 4515 N94-37087
HARDNESS TESTS
Robotic weld overlay coatings for erosion control
[DE94-013477] p 4417 N94-37116
HARMONIC GENERATIONS
Quantum and quasi-classical analyses of high order emission processes
[DE93-041348] p 4513 N94-36697
Organometallic NLO polymers. 4: Organometallic main-chain, side-chain, and guest-host polymers: A study of their orientation and relaxation using second harmonic generation
[AD-A280347] p 4423 N94-37179
Laser probing of interfaces
[DE94-011300] p 4449 N94-37628
HARMONIC MOTION
Quantum harmonic Brownian motion in a general environment: A modified phase-space approach
[DE94-003249] p 4508 N94-36560
HARMONIC OSCILLATORS
Coherence and chaos
[DE94-008529] p 4539 N94-36507
Generalized squeezed states from generalized coherent states
[DE94-002689] p 4512 N94-36515
Quantum harmonic Brownian motion in a general environment: A modified phase-space approach
[DE94-003249] p 4508 N94-36560
The asymptotics of matrix elements of Gaussian potential between the basis functions of three-dimensional harmonic oscillator
[DE94-618467] p 4539 N94-37079
HARMONICS
Understanding and managing power system harmonics
[AD-A280627] p 4440 N94-37759
HASTELLOY (TRADEMARK)
Creep-fatigue interaction property of a nickel-base heat-resistant alloy Hastelloy XR in simulated HTGR helium gas environment
[DE94-737934] p 4418 N94-37416
Creep properties with short period excessive loadings on a nickel-base heat-resistant alloy Hastelloy XR
[DE94-718965] p 4419 N94-37465
HAZARDS
Thermal decomposition reactions of HMX and RDX and their importance in predicting cookoff hazards
[DE94-011430] p 4429 N94-37413
HEAD MOVEMENT
Advances in helmet trackers p 4394 N94-36624
Operator gaze position control interfaces: Investigation of psychophysical and operational parameters p 4485 N94-37273
Gaze orientation under G(z)-load. Methodological aspects: Preliminary results p 4485 N94-37274
Attenuating the disorienting effects of head movement during whole-body rotation using a visual reference: Further tests of a predictive hypothesis p 4482 N94-37276
HEADACHE
Some side-effects of immersion virtual reality p 4482 N94-37277
HEALTH
Opportunities for innovation: Biotechnology
[PB94-157831] p 4478 N94-36720
HEARING
Blast overpressure studies with animals and man
[AD-A280240] p 4480 N94-37118
HEART
Cardiac pressure changes with venous gas embolism and decompression
[AD-A280412] p 4481 N94-37224
HEAT AFFECTED ZONE
Mitigation of harmful effects of welds in zirconium alloy components
[DE94-619033] p 4414 N94-36543
HEAT BALANCE
Reference manual for the Thermal Analyst's Help Desk Expert System
[NASA-CR-194941] p 4397 N94-37504
HEAT EXCHANGERS
Review of advanced radiator technologies for spacecraft power systems and space thermal control
[NASA-TM-4555] p 4398 N94-36821
HEAT FLUX
Experimental measurements and analytical analysis related to gas turbine heat transfer. Part 1: Time-averaged heat-flux and surface-pressure measurements on the vanes and blades of the SSME fuel-side turbine and comparison with prediction. Part 2: Phase-resolved surface-pressure and heat-flux measurements on the first blade of the SSME fuel-side turbine
[NASA-CR-196296] p 4442 N94-36969
On the development of boundary layer secondary circulations resulting from horizontally varying surface heat flux
[DE94-011234] p 4472 N94-37048
Improvement study of the divertor configuration of the Steady State Tokamak Reactor (SSTR)
[DE94-718961] p 4531 N94-37484
An experimental and numerical study of boundary layer structure over areas of inhomogeneous sensible heat fluxes
[DE94-011441] p 4474 N94-37565
HEAT MEASUREMENT
Methodologies for thermal and mechanical testing of TMC materials p 4401 N94-36659
Thermodynamics of minerals stable near the Earth's surface
[DE94-012479] p 4539 N94-37094
Initial report on calorimetry for the Tore Supra Outboard pump Limiter
[DE94-011244] p 4531 N94-37626
HEAT PIPES
Carbon-carbon heat pipe testing and evaluation
[NASA-TM-106630] p 4405 N94-37318
HEAT RESISTANT ALLOYS
Modeling of thermal barrier coatings
[NASA-CR-195365] p 4421 N94-36637
Ability of the total strain version of strainrange partitioning to characterize thermomechanical fatigue behavior
[NASA-TM-4556] p 4455 N94-37102
Alternate melting and refining routes p 4421 N94-37323
Process enhancements of superalloy material p 4421 N94-37324
Maintaining constant standards during the forging process p 4421 N94-37326
Substantiating powder metal life methodologies for engines p 4455 N94-37330
The influence of VAR processes and parameters on white spot formation in Alloy 718
[DE94-012071] p 4417 N94-37367
Examination of weldability of Ni-Cr-W superalloys
[DE94-719014] p 4418 N94-37385
The effect of reactive elements on the segregation behavior and microstructure of alpha-Al2O3 scales on beta-NiAl
[DE94-012739] p 4418 N94-37399
Creep properties with short period excessive loadings on a nickel-base heat-resistant alloy Hastelloy XR
[DE94-718965] p 4419 N94-37465
HEAT STORAGE
1993 JSES (Japan Solar Energy Society)/JWEA (Japan Wind Energy Association) Joint Conference and 1993 Japan-Korea Joint Conference on Solar Energy
[DE94-767725] p 4462 N94-37418
HEAT TRANSFER
Multiphase flow with interphase exchanges (MFIX) documentation theory guide
[DE94-000087] p 4441 N94-36550
Preliminary analysis for a Mach 8 crossflow transition experiment on the Pegasus (R) space booster
[NASA-TM-104272] p 4381 N94-36648
The influence of fin height and wall conductivity on integral-fin tubes during steam condensation
[AD-A280597] p 4539 N94-36725
Experimental measurements and analytical analysis related to gas turbine heat transfer. Part 1: Time-averaged heat-flux and surface-pressure measurements on the vanes and blades of the SSME fuel-side turbine and comparison with prediction. Part 2: Phase-resolved surface-pressure and heat-flux measurements on the first blade of the SSME fuel-side turbine
[NASA-CR-196296] p 4442 N94-36969
Some effects of heat release in premixed flames
[DE94-011346] p 4409 N94-37199
Finite-rate chemistry and transient effects in Direct Numerical Simulations of turbulent non-premixed flames
[DE94-005250] p 4410 N94-37222
Frequency doubling of copper lasers using temperature-tuned ADP
[DE94-011542] p 4448 N94-37240
Prediction of film cooling on gas turbine airfoils
[NASA-TM-106653] p 4387 N94-37448
A method for thermal analysis of spiral bevel gears
[NASA-TM-106612] p 4451 N94-37451
Improvement study of the divertor configuration of the Steady State Tokamak Reactor (SSTR)
[DE94-718961] p 4531 N94-37484
Initial report on calorimetry for the Tore Supra Outboard pump Limiter
[DE94-011244] p 4531 N94-37626
Analysis of anelastic flow and numerical treatment via finite elements
[DE94-012141] p 4445 N94-37726
HEAT TREATMENT
Mitigation of harmful effects of welds in zirconium alloy components
[DE94-619033] p 4414 N94-36543
HEATING
Q-profile flattening due to nonlinear development of resistive kink mode and ensuing fast crash in sawtooth oscillations
[DE94-727625] p 4526 N94-36472

Microstructure and chemistry of MgO- and CoO-doped nickel-titanate spinels
[DE94-012741] p 4537 N94-37382

HEAVY IONS
High baryon density from relativistic heavy ion collisions
[DE94-003894] p 4511 N94-36460
Physics Division annual review, 1 April 1992 - 31 March 1993
[DE94-002497] p 4512 N94-36513
LET spectra of fragmented 600-MeV/A iron beam on aluminum and polyethylene: A preliminary analysis
[NASA-TP-3436] p 4416 N94-36993
Testing new technology for the heavy ion experiment at CERN
[DE94-004747] p 4521 N94-37220
Physics with primary beams of the KEK-PS
[DE94-748635] p 4522 N94-37234
Activities of the Tandem Accelerator Center, University of Tsukuba
[DE94-748687] p 4522 N94-37237
Non-equilibrium evolution of the disoriented chiral condensate in heavy-ion collisions
[DE94-012897] p 4522 N94-37310
Comparison of oxygen and silicon induced reactions at 14.6 A(GeV/C)
[DE94-011923] p 4518 N94-37364
The Mesozoic Era of relativistic heavy ion physics and beyond
[DE94-011341] p 4548 N94-37557
On the shape of x ray spectra excited by heavy ions
[DE94-618747] p 4519 N94-37651

HEAVY NUCLEI
Hadron production in S+nucleus collisions at 200 GeV/nucleon
[DE94-011344] p 4520 N94-37715

HELICOPTER CONTROL
Landing of an unmanned helicopter on a moving platform. High accuracy navigation and tracking
p 4387 N94-36618

HELICOPTER PROPELLER DRIVE
Dynamics of a split torque helicopter transmission
[NASA-TM-106410] p 4452 N94-37457

HELICOPTER WAKES
Rotorwash analysis handbook. Volume 1: Development and analysis
[SCT-93RR-17-VOL-1] p 4381 N94-36466
Rotorwash analysis handbook. Volume 2: Appendixes
[SCT-93RR-17-VOL-2] p 4382 N94-36467

HELICOPTERS
Navier-Stokes and potential theory solutions for ahelicopter fuselage and comparison with experiment
[NASA-TM-4566] p 4383 N94-36966
Composite helicopter accident profiles: Deficient crew/aircraft performance
[SCT-90RR-46] p 4385 N94-37604
Civil use of night vision devices: Evaluation pilot's guide, part 1
[SCT-91RR-43] p 4487 N94-37741
Night vision goggles in Emergency Medical Service (EMS) helicopters
[SCT-93RR-22] p 4487 N94-37742
Assessment of night vision goggle workload: Flight test engineer's guide
[SCT-91RR-45] p 4487 N94-37743

HELIOTRONS
Confinement improvement in H-mode-like plasmas in helical systems
[DE94-727619] p 4528 N94-37231
Anomalous cross field flux in CHS
[DE94-727547] p 4529 N94-37359
Research using small tokamaks
[DE94-621827] p 4531 N94-37493

HELIPORTS
Rotorwash analysis handbook. Volume 1: Development and analysis
[SCT-93RR-17-VOL-1] p 4381 N94-36466
Rotorwash analysis handbook. Volume 2: Appendixes
[SCT-93RR-17-VOL-2] p 4382 N94-36467
Analysis of vertiport studies funded by the Airport Improvement Program (AIP)
[SCT-93RR-21] p 4390 N94-37424

HELIUM
Direct photoionization of excited helium
[DE94-618732] p 4516 N94-37097
Resonance photoionization of the excited helium
[DE94-618733] p 4517 N94-37173
The angular and energy distributions of ejected electrons in electron-impact ionization of helium
[DE94-618748] p 4519 N94-37528

HELIUM ATOMS
First observation of laser-induced resonant annihilation in metastable antiprotonic helium atoms
[DE94-748668] p 4519 N94-37417

HELIUM IONS
The angular and energy distributions of ejected electrons in electron-impact ionization of helium
[DE94-618748] p 4519 N94-37528

HELIUM ISOTOPES
Pulsed field magnets at the United States National High Magnetic Field Laboratory
[DE94-002624] p 4436 N94-36514

HELMET MOUNTED DISPLAYS
Advanced helmet tracking technology developments for Naval aviation p 4393 N94-36623
Advances in helmet trackers p 4394 N94-36624
Creation of a virtual world to study human spatial perception during sustained acceleration
p 4484 N94-37268
The DRA Virtual Cockpit Research Program
p 4484 N94-37269
Some side-effects of immersion virtual reality
p 4482 N94-37277
Low cost software-based rendering and stereoscopic interfaces for teleoperation and virtual reality
p 4486 N94-37279

HELMETS
3D sound experimental approach: Methodology and preliminary results p 4486 N94-37280

HEMATITE
Mineralogy and metallurgical properties of iron ore sinter based on magnetite fines
[DE94-763309] p 4414 N94-36525

HEMODYNAMIC RESPONSES
Cerebral neurochemical mechanisms in stress and anxiety
[AD-A280473] p 4482 N94-37233

HEMOGLOBIN
Chemical and structural characterization of nitroaromatic adducts with hemoglobins
[AD-A280533] p 4480 N94-37089

HETEROCYCLIC COMPOUNDS
Organic NLO polymers. 5: Homopolymerization of indole based NLO-phore: A heterocycle Chi(2)NLO main-chain polymer
[AD-A280229] p 4423 N94-37151

HETEROGENEITY
A coarse-mesh nodal method-diffusive-mesh finite difference method
[DE94-010609] p 4502 N94-36455

HETEROJUNCTION DEVICES
Investigation of polycrystalline thin-film CuInSe2 solar cells based on ZnSe windows
[DE94-006936] p 4462 N94-37381

HETEROJUNCTIONS
Theoretical studies of the transport properties in compound semiconductors
[NASA-CR-196109] p 4439 N94-37501

HEURISTIC METHODS
A mean value analysis heuristic for analysis of aircraft sortie generation
[AD-A278578] p 4507 N94-36970
Improved load distribution in parallel sparse Cholesky factorization
[NASA-CR-196380] p 4499 N94-37654

HIGGS BOSONS
Effective Lagrangian for gluons and Higgs pseudoscalars
[DE94-001381] p 4513 N94-36539
High Energy Physics Division of research activities
[DE93-019681] p 4521 N94-36694

HIGH CURRENT
Production of high current H(-) beams in a cesium seeded volume negative ion source equipped with PG filter
[DE94-718962] p 4522 N94-37463
Characteristics of ions emitted from high-current hollow cathodes
[NASA-CR-195372] p 4398 N94-37764

HIGH ELECTRON MOBILITY TRANSISTORS
Study on the measurement uncertainty of noise properties of a millimeter wave amplifier
[PB94-170917] p 4510 N94-37632

HIGH ENERGY INTERACTIONS
High Energy Physics Division of research activities
[DE93-019681] p 4521 N94-36694
Physics with primary beams of the KEK-PS
[DE94-748635] p 4522 N94-37234
Activities of the Photon Factory
[DE94-748682] p 4522 N94-37236
Particle physics
[DE94-012944] p 4518 N94-37312
Experimental particle physics at the University of Pittsburgh
[DE94-011636] p 4521 N94-37721
Proceedings of the Workshop on TRISTAN Physics at High Luminosities
[DE94-737969] p 4523 N94-37727

HIGH FIELD MAGNETS
Design and analysis of high-field quasi-continuous magnets
[DE94-000762] p 4508 N94-36556

HIGH FREQUENCIES
NRL HF propagation measurements between Guadeloupe and Providenciales during the CRRES exercises
[DE94-012078] p 4435 N94-37393
KONRAD: Wide band digital HF receiver
[PB94-184686] p 4435 N94-37813

HIGH POWER LASERS
A high power microwave frequency modulated KrF laser
[DE94-009303] p 4447 N94-36510
Pointing and tracking concept for a high energy laser weapon application p 4393 N94-36619
U-turn alternative to the large aperture switch
[DE94-011541] p 4524 N94-37112
New hollow-cathode electrode for high-power copper lasers
[DE94-011637] p 4448 N94-37244

HIGH PRESSURE
Studies of the III-V compounds in the megabar regime
[DE94-012488] p 4537 N94-37435

HIGH RESOLUTION
A flux splitting scheme with high-resolution and robustness for discontinuities
[NASA-TM-106452] p 4441 N94-36646

HIGH STRENGTH ALLOYS
Substantiating powder metal life methodologies for engines p 4455 N94-37330

HIGH TEMPERATURE
Four beam interferometer manual: Operating instructions for the INEL diffraction Moire interferometer
[DE94-010772] p 4453 N94-36452
High temperature superconducting digital circuits and subsystems
[DE94-001207] p 4436 N94-36557
Correlation of analytical and experimental hot structure vibration results
[NASA-TM-104269] p 4386 N94-36644
Hot dynamic test rig for measuring hypersonic engine seal flow and durability
[NASA-TM-106507] p 4450 N94-36645
Thermodynamics of minerals stable near the Earth's surface
[DE94-012479] p 4539 N94-37094

HIGH TEMPERATURE AIR
Computational chemistry research
[NASA-CR-196120] p 4408 N94-36989

HIGH TEMPERATURE FLUIDS
Fluids at high shock pressures and temperatures and some thoughts about future possibilities
[DE94-003625] p 4407 N94-36458

HIGH TEMPERATURE GAS COOLED REACTORS
Examination of weldability of Ni-Cr-W superalloys
[DE94-719014] p 4418 N94-37385

HIGH TEMPERATURE GASES
Theoretical studies of a molecular beam generator
[NASA-CR-196306] p 4522 N94-37508

HIGH TEMPERATURE PLASMAS
Q-profile flattening due to nonlinear development of resistive kink mode and ensuing fast crash in sawtooth oscillations
[DE94-727625] p 4526 N94-36472
A fast spectroscopic diagnostic for the measurement of plasma impurity ion dynamics
[DE94-012985] p 4529 N94-37354
Analysis of plasma measurements for the Geotail mission
[NASA-CR-196274] p 4470 N94-37470
Origins of energetic ions in the Earth's magnetosheath
[NASA-CR-189359] p 4471 N94-37703

HIGH TEMPERATURE SUPERCONDUCTORS
Development of high Tc (greater than 100 K) Bi, Tl and Y-based materials as superconducting circuit elements
[NASA-CR-196276] p 4534 N94-37103
Superconducting TlCa2Ba2Cu3O9 thick films
[DE94-010436] p 4535 N94-37193
ORNL superconducting technology program for electric power systems
[DE94-011471] p 4438 N94-37239
Midwest Superconductivity Consortium
[DE94-012716] p 4536 N94-37285
Applications of high transition temperature superconductors at the Savannah River Site
[DE94-012938] p 4536 N94-37311
Effect of thermal annealing on grain boundary chemistry of polycrystalline TlBa2Ca2Cu3O(y) films
[DE94-011464] p 4538 N94-37569
Flux creep: Its dependence on current denisty and relation to critical current densities from transport and magnetic measurements
[DE94-011701] p 4440 N94-37738

High T(sub c) copper-oxide superconductors comprising Tl-Sr-Ca-Cu-O
[AD-D016307] p 4536 N94-37776
HIGH TEMPERATURE TESTS
Metal matrix composites: Analysis of simple specimens and model components under creep and fatigue loading
p 4402 N94-36661
Creep properties with short period excessive loadings on a nickel-base heat-resistant alloy Hastelloy XR
[DE94-718965] p 4419 N94-37465
Development of processing techniques for advanced thermal protection materials
[NASA-CR-196251] p 4426 N94-37510
HMX
Thermal decomposition reactions of HMX and RDX and their importance in predicting cookoff hazards
[DE94-011430] p 4429 N94-37413
HODOSCOPES
Wide aperture scintillation hodoscope with FEU-143 photomultipliers
[DE94-618211] p 4515 N94-37075
HOLES (ELECTRON DEFICIENCIES)
Picosecond laser induced electric field modulation of carotenoid absorption bands
[DE94-009692] p 4512 N94-36524
HOLLOW CATHODES
Characteristics of ions emitted from high-current hollow cathodes
[NASA-CR-195372] p 4398 N94-37764
HOLMIUM
Holmium quasi-two level laser
[AD-D016302] p 4449 N94-37772
Intracavity-pumped 2.1 micrometer Ho(3+):YAGl aser
[AD-D016308] p 4449 N94-37777
HOLOGRAPHY
Holographic grating relaxation studies of probe diffusion in amorphous polymers
[AD-A280496] p 4423 N94-37144
A freon-filled, holographic bubble chamber as a high energy photon burst spectrometer
[DE94-011645] p 4446 N94-37723
HOMOGENEOUS TURBULENCE
Finite-rate chemistry and transient effects in Direct Numerical Simulations of turbulent non-premixed flames
[DE94-005250] p 4410 N94-37222
HORIZONTAL DISTRIBUTION
The role of horizontal variability in air-sea interaction
[AD-A280561] p 4476 N94-37047
HORMONES
Melatonin, the pineal gland, and circadian rhythms
[AD-A280467] p 4481 N94-37140
HOT ISOSTATIC PRESSING
Manufacture and properties of sigma fibre reinforced titanium p 4401 N94-36655
Properties of TMC processed by fibre coating and hiping p 4401 N94-36656
HUBBLE SPACE TELESCOPE
Hubble Space Telescope faint object spectrograph instrument handbook, version 5.0
[NASA-CR-189367] p 4546 N94-36794
Hubble Space Telescope faint object camera instrument handbook (Post-COSTAR), version 5.0
[NASA-CR-189365] p 4546 N94-36795
Hubble Space Telescope Wide Field and Planetary Camera 2 instrument handbook, version 2.0
[NASA-CR-189368] p 4547 N94-36918
Hubble Space Telescope cycle 5. Phase 1: Proposal instructions, version 4.0
[NASA-CR-189364] p 4547 N94-36963
HUMAN BEINGS
Blast overpressure studies with animals and man
[AD-A280240] p 4480 N94-37118
HUMAN CENTRIFUGES
Attenuating the disorienting effects of head movement during whole-body rotation using a visual reference: Further tests of a predictive hypothesis p 4482 N94-37276
HUMAN FACTORS ENGINEERING
Virtual Interfaces: Research and Applications
[AGARD-CP-541] p 4482 N94-37261
Task-specific usability requirements for virtual information environments: Interface design and data representation for human operators of complex medical systems p 4483 N94-37262
Human factors for flight deck certification personnel
[AD-A280477] p 4487 N94-37347
Synthetic vision display evaluation studies
[NASA-CR-194963] p 4387 N94-37658
HUMAN PERFORMANCE
Math and science illiteracy: Social and economic impacts
[DE94-010801] p 4540 N94-37092
Virtual Interfaces: Research and Applications
[AGARD-CP-541] p 4482 N94-37261
3D sound experimental approach: Methodology and preliminary results p 4486 N94-37280
HUMAN-COMPUTER INTERFACE
Virtual Interfaces: Research and Applications
[AGARD-CP-541] p 4482 N94-37261
Task-specific usability requirements for virtual information environments: Interface design and data representation for human operators of complex medical systems p 4483 N94-37262
On the feasibility of virtual environments in medicine p 4483 N94-37264
Interactive large screen: A multi-mode dialogue tool for future cockpits p 4484 N94-37266
Virtual reality evolution or revolution p 4484 N94-37270
A non-intrusive way to measure point-of-gaze p 4484 N94-37272
Operator gaze position control interfaces: Investigation of psychophysical and operational parameters p 4485 N94-37273
Visual accommodation to virtual image displays when knowledge of object distance conflicts with optical distance p 4485 N94-37278
Low cost software-based rendering and stereoscopic interfaces for teleoperation and virtual reality p 4486 N94-37279
HYDRATION
Evaluation of dried storage of platelets for transfusion: Physiologic integrity and hemostatic functionality
[AD-A280665] p 4480 N94-36764
HYDRIDES
New plasma source of hydrides for epitaxial growth
[DE94-006918] p 4533 N94-36744
Hydrogen storage for vehicular applications: Technology status and key development areas
[DE94-011626] p 4428 N94-37243
HYDROBORATION
Theoretical and experimental investigations of fullerene derivatives: C60H2, C60H4, C70H2 and C60CH22
[DE94-012727] p 4536 N94-37287
HYDROCARBON COMBUSTION
Rich methane/air flames: Burning velocities, extinction limits, and flammability limit
[DE94-004340] p 4407 N94-36462
Rich flammability limits in CH3OH/CO/diluent mixtures
[DE94-004341] p 4407 N94-36482
HYDROCARBONS
Some effects of heat release in premixed flames
[DE94-011346] p 4409 N94-37199
The hydrogenolysis and isomerization of light hydrocarbons over Pt catalysts
[DE94-013142] p 4410 N94-37296
Superacid catalysis of light hydrocarbon conversion
[DE94-011132] p 4411 N94-37431
Carborane-siloxane or silane-unsaturated hydrocarbon based polymers
[AD-D016220] p 4425 N94-37482
Stratospheric emissions effects database development
[NASA-CR-4592] p 4467 N94-37607
Probing flame chemistry with MBMS, theory, and modeling
[DE94-011224] p 4413 N94-37623
Morphological aspects of surface reactions
[DE94-011208] p 4413 N94-37713
Diosmacycloalkanes as models for the formation of hydrocarbons from surface methylenes
[DE94-011211] p 4413 N94-37754
Carborane-(silane or siloxane)-unsaturated hydrocarbon based thermosetting polymers
[AD-D016311] p 4427 N94-37818
HYDRODYNAMICS
Multiphase flow with interphase exchanges (MFIX) documentation theory guide
[DE94-000087] p 4441 N94-36550
Microscopic theory of the dielectric response of highly dispersive biological media
[AD-A280516] p 4516 N94-37109
Solution characterization of poly(isobornyl methacrylate) in tetrahydrofuran
[AD-A280497] p 4409 N94-37145
Some effects of heat release in premixed flames
[DE94-011346] p 4409 N94-37199
HYDROGEN
Diamond deposition and defect chemistry studied via solid state NMR
[AD-A280609] p 4533 N94-36727
Studies of the thermal and optical responses of H atoms in solid H2
[NASA-CR-196114] p 4514 N94-36964
Hydrogen storage for vehicular applications: Technology status and key development areas
[DE94-011626] p 4428 N94-37243
Thermal-oxidative pretreatment and evaluation of poly (hexafluoropropene oxide) fluids
[NASA-TM-106659] p 4424 N94-37300
A role of neutral hydrogen in CHS plasmas with reheat and collapse and comparison with JIPPT-IIU tokamak plasmas
[DE94-718985] p 4530 N94-37384
The determination of hydrogen in sodium by vacuum extraction
[DE94-620278] p 4412 N94-37533
Optical spectroscopy of a nitrogen-hydrogen complex in ZnSe
[DE94-011622] p 4413 N94-37630
HYDROGEN ATOMS
Production of a positron and a bound electron by high-energy photon in a strong Coulomb field
[DE94-618501] p 4514 N94-36747
Studies of the thermal and optical responses of H atoms in solid H2
[NASA-CR-196114] p 4514 N94-36964
Wick-Cutkovsky model: An introduction
[DE94-618365] p 4504 N94-37170
The dynamics of hydrogen atoms dissolved in Zr Cr2 alloy
[DE94-618756] p 4520 N94-37652
HYDROGEN EMBRITTLEMENT
Mitigation of harmful effects of welds in zirconium alloy components
[DE94-619033] p 4414 N94-36543
NASA-UVA Light Aerospace Alloy and Structures Technology Program (LA2ST)
[NASA-CR-196290] p 4415 N94-36809
HYDROGEN IONS
Production of high current H(-) beams in a cesium seeded volume negative ion source equipped with PG filter
[DE94-718962] p 4522 N94-37463
HYDROGEN PLASMA
Isotope scaling and eta(i) mode with impurities in tokamak plasmas
[DE94-012763] p 4529 N94-37361
HYDROGENATION
Theoretical and experimental investigations of fullerene derivatives: C60H2, C60H4, C70H2 and C60CH22
[DE94-012727] p 4536 N94-37287
HYDROGENOLYSIS
The hydrogenolysis and isomerization of light hydrocarbons over Pt catalysts
[DE94-013142] p 4410 N94-37296
HYDROGEOLOGY
Numerical simulation of nocturnal drainage flows in an idealized valley-tributary system
[DE94-011684] p 4472 N94-37115
HYDROGRAPHY
Variability of the California Current System off Point Sur, California from April 1988 to December 1990
[AD-A278579] p 4476 N94-36985
HYDROLOGY
Representing the influence of subgrid topography on hydrology
[DE94-004595] p 4474 N94-37379
HYDROLOGY MODELS
Numerical simulation of nocturnal drainage flows in an idealized valley-tributary system
[DE94-011684] p 4472 N94-37115
HYDROLYSIS
Tert-butylalumoxanes: Synthetic analogs for methylalumoxane (MAO) and new catalytic routes to polyolefins and polyketones
[AD-A280511] p 4399 N94-37106
Tert-butylalumoxanes: Synthetic analogs for methylalumoxane (MAO) and new catalytic routes to polyolefins and polyketones
[AD-A280532] p 4399 N94-37650
HYDROSTATIC PRESSURE
Microscopic theory of the dielectric response of highly dispersive biological media
[AD-A280516] p 4516 N94-37109
HYDROXYL RADICALS
Laser-saturated fluorescence measurements in laminar sooting diffusion flames
[NASA-CR-191025] p 4508 N94-36643
HYGRAL PROPERTIES
Laminated thin shell structures subjected to free vibration in a hygrothermal environment
[NASA-TM-106600] p 4456 N94-37456
HYPERBOLIC DIFFERENTIAL EQUATIONS
High-order centered difference methods with sharp shock resolution
[NASA-CR-196374] p 4496 N94-37656
HYPERCUBE MULTIPROCESSORS
Preconditioned implicit solvers for the Navier-Stokes equations on distributed-memory machines
[NASA-TM-106449] p 4502 N94-36647
HYPERPLANES
A method for obtaining a least squares fit of a hyperplane to uncertain data
[DE94-012498] p 4503 N94-37073

HYPERSONIC BOUNDARY LAYER
Pressure-sensing performance of upright cylinders in a Mach 10 boundary-layer
[NASA-TM-4633] p 4383 N94-37395
HYPERSONIC FLIGHT
Measurement uncertainty and feasibility study of a flush airdata system for a hypersonic flight experiment
[NASA-TM-4627] p 4383 N94-37378
HYPERSONIC FLOW
Hot dynamic test rig for measuring hypersonic engine seal flow and durability
[NASA-TM-106507] p 4450 N94-36645
A fundamental study of hypersonic unstarts
[AD-A280506] p 4443 N94-37128
Hypersonic, nonequilibrium flow over the FIRE 2 forebody at 1634 sec
[NASA-TM-109141] p 4444 N94-37455
HYPERSONIC HEAT TRANSFER
Hypersonic, nonequilibrium flow over the FIRE 2 forebody at 1634 sec
[NASA-TM-109141] p 4444 N94-37455
Active cooling from the sixties to NASP
[NASA-TM-109079] p 4456 N94-37541
HYPERSONIC INLETS
A fundamental study of hypersonic unstarts
[AD-A280506] p 4443 N94-37128
HYPERSONIC NOZZLES
Computational investigation of an improved cowl concept for hypersonic propulsive nozzles
[AD-A280596] p 4441 N94-36724
HYPERSONIC SHOCK
Hypersonic shock/boundary-layer interaction database: New and corrected data
[NASA-CR-177638] p 4441 N94-36519
HYPERSONIC SPEED
Preliminary analysis for a Mach 8 crossflow transition experiment on the Pegasus (R) space booster
[NASA-TM-104272] p 4381 N94-36648
An aerodynamic and static-stability analysis of the Hypersonic Applied Research Technology (HART) missile
[AD-A280631] p 4382 N94-36729
Pressure-sensing performance of upright cylinders in a Mach 10 boundary-layer
[NASA-TM-4633] p 4383 N94-37395
HYPERSONIC VEHICLES
Applications of Titanium Matrix Composite to large airframe structure p 4400 N94-36651
Methodologies for thermal and mechanical testing of TMC materials p 4401 N94-36659
Active cooling from the sixties to NASP
[NASA-TM-109079] p 4456 N94-37541
HYPERSONICS
Hot dynamic test rig for measuring hypersonic engine seal flow and durability
[NASA-TM-106507] p 4450 N94-36645
Experimental investigation of nozzle/plume aerodynamics at hypersonic speeds
[NASA-CR-195829] p 4382 N94-36687
HYPOBARIC ATMOSPHERES
Hypobaric decompression sickness model development. Part 1: Diffusion of inert gas from a viscoelastic fluid (blood) into an expanding gas phase
[AD-A280298] p 4481 N94-37124
HYPOTHALAMUS
Cerebral neurochemical mechanisms in stress and anxiety
[AD-A280473] p 4482 N94-37233
HYPOTHESES
ARM: A climate process observatory
[DE94-007473] p 4463 N94-36477

I

IGNITION
Thermal decomposition reactions of HMX and RDX and their importance in predicting cookoff hazards
[DE94-011430] p 4429 N94-37413
ILL-CONDITIONED PROBLEMS (MATHEMATICS)
Solving ill-conditioned matrix equations in control
[AD-A280502] p 4503 N94-37146
ILLUMINATING
US manufacturers of commercially available stand-alone photovoltaic lighting systems
[DE94-006917] p 4462 N94-37407
IMAGE ANALYSIS
A model-based approach for detection of runways and other objects in image sequences acquired using an on-board camera
[NASA-CR-196424] p 4446 N94-36812
IMAGE CLASSIFICATION
Subgrouped real time recurrent learning neural networks
[AD-A280618] p 4500 N94-37043
IMAGE FILTERS
Elemental mapping of segregation in stainless steels with an imaging filter
[DE94-012659] p 4417 N94-37304
IMAGE PROCESSING
Proceedings of SPIE: The International Society for Optical Engineering, Computational Vision Based on Neurobiology, volume 2054
[AD-A278731] p 4523 N94-36468
Hardware implementation of a desktop supercomputer for high performance image processing
[AD-A280550] p 4489 N94-36731
Studies on image compression and image reconstruction
[NASA-CR-196304] p 4433 N94-36810
Global Picture Archiving and Communication Systems (GPACS): An overview
[AD-A280617] p 4543 N94-37042
Adaptive learning of multi-sensor integration techniques with genetic algorithms
[DE94-012744] p 4500 N94-37083
Efficient contact determination between geometric models
[AD-A280244] p 4494 N94-37120
Recovering depth from focus using iterative image estimation techniques
[DE94-010994] p 4524 N94-37165
Microscopic image processing systems for measuring nonuniform film thickness profiles
[DE94-005336] p 4424 N94-37223
On the feasibility of virtual environments in medicine p 4483 N94-37264
The application of maximum entropy to Z-contrast imaging in a stem
[DE94-011470] p 4412 N94-37546
A note on analytic recovery of transition probabilities in three dimensional diffuse tomography
[DE94-011378] p 4506 N94-37719
IMAGE RECONSTRUCTION
Studies on image compression and image reconstruction
[NASA-CR-196304] p 4433 N94-36810
Recovering depth from focus using iterative image estimation techniques
[DE94-010994] p 4524 N94-37165
IMAGE RESOLUTION
Visual accommodation to virtual image displays when knowledge of object distance conflicts with optical distance p 4485 N94-37278
IMAGING SPECTROMETERS
Gaseous effluent monitoring and identification using an imaging Fourier transform spectrometer
[DE94-012627] p 4467 N94-37428
IMAGING TECHNIQUES
UVPI imaging from the LACE satellite: The Low Cost Launch Vehicle (LCLV) rocket plume
[AD-A278785] p 4398 N94-36445
Geophysical data fusion for subsurface imaging
[DE94-000056] p 4469 N94-36738
Combined atomic force and scanning reflection interference contrast microscopy
[AD-A280341] p 4514 N94-37034
Microscopic image processing systems for measuring nonuniform film thickness profiles
[DE94-005336] p 4424 N94-37223
Determination of interface structure and bonding at atomic resolution in the stem
[DE94-011466] p 4517 N94-37238
Elemental mapping of segregation in stainless steels with an imaging filter
[DE94-012659] p 4417 N94-37304
Data simulation for the Associated Particle Imaging system
[DE94-012664] p 4518 N94-37305
Electronic document delivery: Towards the virtual library p 4544 N94-37340
Imaging targets embedded in a lossy half space with Synthetic Aperture Radar
[DE94-010807] p 4435 N94-37391
Submicrometer fiber-optic chemical sensors: Measuring pH inside single cells
[DE94-004160] p 4525 N94-37532
Comparison of gaseous and semiconductor detectors for medical imaging
[DE94-621344] p 4482 N94-37729
Time-gated imaging through defense-scattering materials using stimulated Raman amplification
[AD-D016305] p 4440 N94-37775
IMIDES
Synthesis of phthalonitrile resins containing ether and imide linkages with aromatic diamine curing agent
[AD-D016309] p 4427 N94-37778
IMPACT DAMAGE
Scaling of impact damage in fiber composites p 4460 N94-37810
Impact force as a scaling parameter p 4460 N94-37811
IMPACT LOADS
Impact force as a scaling parameter p 4460 N94-37811
IMPACT TESTS
Internally damped, self-arresting vertical drop-weight apparatus
[NASA-CASE-LAR-15003-1] p 4389 N94-36826
Scaling of impact damage in fiber composites p 4460 N94-37810
IMPACT TOLERANCES
Impact force as a scaling parameter p 4460 N94-37811
IMPELLERS
NiAl-base composite containing high volume fraction of AlN for advanced engines
[NASA-CASE-LEW-15818-1] p 4403 N94-36752
IMPLANTATION
Channel in hip implant stem
[NASA-CASE-MFS-28987-1] p 4486 N94-36840
Positron implantation in solids
[DE94-013029] p 4537 N94-37499
IMPLOSIONS
Preradiation studies for non-thermal Z-pinch wire load experiments on Saturn
[DE94-013459] p 4527 N94-37072
IMPULSES
Blast overpressure studies with animals and man
[AD-A280240] p 4480 N94-37118
IMPURITIES
Implanting impurities in semiconductors and semiconductor implanted with impurities
[AD-D016298] p 4538 N94-37770
INCENTIVES
Alternative fuel information: State alternative fuel laws and incentives
[DE94-006892] p 4429 N94-37404
Comparative alternative/clean fuels provisions of the Clean Air Act Amendments of 1990 and the Energy Policy Act of 1992
[DE94-006887] p 4429 N94-37426
INCLUSIONS
Vent processes during the 1912 eruption at Novarupta, Katmai National Park, Alaska
[DE94-010740] p 4468 N94-36451
The control of cleanness in powder metallurgy materials for turbine disks p 4421 N94-37325
INCOMPRESSIBLE FLUIDS
Towards enhancing and delaying disturbances in free shear flows
[NASA-CR-194945] p 4445 N94-37606
INCONEL (TRADEMARK)
Irradiation assisted stress corrosion cracking of HTH Alloy X-750 and Alloy 625
[DE94-012667] p 4416 N94-37080
The influence of VAR processes and parameters on white spot formation in Alloy 718
[DE94-012071] p 4417 N94-37367
INDEPENDENT VARIABLES
A mixture model for shock compression of porous multi-component reactive materials
[DE93-017638] p 4400 N94-36456
INDEXES (DOCUMENTATION)
Aeronautical engineering: A continuing bibliography with indexes (supplement 307)
[NASA-SP-7037(307)] p 4381 N94-37117
Catalog of data bases and reports
[DE94-012230] p 4466 N94-37208
INDIUM COMPOUNDS
InTlSb for long-wavelength infrared photodetectors and arrays
[AD-A280207] p 4524 N94-37149
Investigation of polycrystalline thin-film CuInSe2 solar cells based on ZnSe windows
[DE94-006936] p 4462 N94-37381
Studies of the III-V compounds in the megabar regime
[DE94-012488] p 4537 N94-37435
INDIUM GALLIUM ARSENIDES
Low temperature materials --- indium gallium arsenides
[AD-A278703] p 4533 N94-36755
INDOLES
Organic NLO polymers. 5: Homopolymerization of indole based NLO-phore: A heterocycle Chi(2)NLO main-chain polymer
[AD-A280229] p 4423 N94-37151
INDOOR AIR POLLUTION
California residential indoor air quality study. Volume 1: Methodology and descriptive statistics
[PB94-166048] p 4464 N94-36994
California residential indoor air quality study. Volume 1: Methodology and descriptive statistics. Appendix
[PB94-166055] p 4464 N94-36995

INDUSTRIAL ENERGY
Opportunities for innovation: Biotechnology
[PB94-157831] p 4478 N94-36720
INDUSTRIES
Abstracts of 2nd International Conference on Lasers and their Applications
[DE94-617409] p 4448 N94-37169
INELASTIC SCATTERING
Measurement of the elastic, total and diffraction cross sections at tevatron energies
[DE94-004659] p 4511 N94-36463
Deep inelastic scattering results from the first year of HERA operation
[DE94-004578] p 4511 N94-36483
Low-energy electron collisions with metal clusters: Electron capture and cluster fragmentation
[DE94-003623] p 4512 N94-36516
Hard diffraction and deep inelastic scattering
[DE94-013353] p 4515 N94-37084
The dynamics of hydrogen atoms dissolved in Zr Cr2 alloy
[DE94-618756] p 4520 N94-37652
INERTIAL CONFINEMENT FUSION
A freon-filled, holographic bubble chamber as a high energy photon burst spectrometer
[DE94-011645] p 4446 N94-37723
INERTIAL NAVIGATION
Landing of an unmanned helicopter on a moving platform. High accuracy navigation and tracking
p 4387 N94-36618
Laboratory evaluation of the Standard Elektrik Lorenz (SEL) fibre-optic rate gyroscope
[AD-A280191] p 4446 N94-36760
INERTIAL PLATFORMS
Inertial pseudo star reference unit
p 4394 N94-36625
INERTIAL REFERENCE SYSTEMS
Inertial pseudo star reference unit
p 4394 N94-36625
INFERENCE
Probability-based inference in cognitive diagnosis
[AD-A280553] p 4506 N94-36732
Virtual representation of IID observations in Bayesian belief networks
[AD-A280552] p 4507 N94-37046
INFORMATION DISSEMINATION
Electronic SCAN (Selected Current Aerospace Notices) p 4541 N94-36845
Multimedia p 4541 N94-36847
Electronic document interchange
p 4541 N94-36848
Electronic document interchange
p 4541 N94-36849
International High Speed Networks for Scientific and Technical information
[AGARD-CP-544] p 4543 N94-37333
Problems of international exchange of scientific and technical information for a Russian aerospace research institute p 4544 N94-37339
Providing electronic documents in Europe: Experience of INIST p 4544 N94-37341
Electronic journals p 4544 N94-37342
INFORMATION FLOW
Analysis of end-to-end encryption and traffic flow confidentiality options
[AD-A278612] p 4433 N94-36754
INFORMATION MANAGEMENT
NASA Access Mechanism (NAM)
p 4541 N94-36850
NASA STI Program Coordinating Council Twelfth Meeting: Standards
[NASA-TM-109925] p 4541 N94-36853
A concise introduction to MARC p 4542 N94-36856
INFORMATION RETRIEVAL
Using Gopher on the Internet
[DE94-009736] p 4497 N94-36441
NASA Access Mechanism: Lessons learned document
[NASA-TM-109924] p 4540 N94-36750
Electronic document interchange
p 4541 N94-36848
Z39.50 and GILS model — Government Information Locator Service p 4542 N94-36859
Government Information Locator Service (GILS). Draft report to the Information Infrastructure Task Force
p 4542 N94-36860
Wide area information servers: An executive information system for unstructured files p 4545 N94-37345
Information retrieval services on wide area networks: A vision of the future p 4545 N94-37346
INFORMATION SYSTEMS
Using Gopher on the Internet
[DE94-009736] p 4497 N94-36441
NASA Access Mechanism: Lessons learned document
[NASA-TM-109924] p 4540 N94-36750
NASA STI Program Coordinating Council Eleventh Meeting: NASA STI Modernization Plan
[NASA-TM-109415] p 4540 N94-36841
NASA STI modernization plan p 4540 N94-36842
The Engineering Review Board p 4540 N94-36843
RECON Replacement Project p 4541 N94-36844
Electronic SCAN (Selected Current Aerospace Notices) p 4541 N94-36845
Multimedia p 4541 N94-36847
Electronic document interchange
p 4541 N94-36848
Electronic document interchange
p 4541 N94-36849
NASA Access Mechanism (NAM)
p 4541 N94-36850
Network upgrades p 4541 N94-36851
Standards in the architectural effort
p 4541 N94-36852
NASA STI Program Coordinating Council Twelfth Meeting: Standards
[NASA-TM-109925] p 4541 N94-36853
STI Architectural Framework Working Group
p 4542 N94-36854
OSI and TCP/IP p 4542 N94-36855
Open system environments p 4542 N94-36857
Open system environment procurement
p 4542 N94-36858
Z39.50 and GILS model — Government Information Locator Service p 4542 N94-36859
Government Information Locator Service (GILS). Draft report to the Information Infrastructure Task Force
p 4542 N94-36860
Toward a new National Weather Service: Weather for those who fly p 4472 N94-36947
SeaWiFS technical report series. Volume 20: The SeaWiFS bio-optical archive and storage system (SeaBASS), part 1
[NASA-TM-104566-VOL-20-PT-1] p 4475 N94-36958
Advanced information processing system: The Army Fault-Tolerant Architecture detailed design overview
[NASA-CR-194924] p 4497 N94-36962
Virtual Interfaces: Research and Applications
[AGARD-CP-541] p 4482 N94-37261
Task-specific usability requirements for virtual information environments: Interface design and data representation for human operators of complex medical systems p 4483 N94-37262
International High Speed Networks for Scientific and Technical Information
[AGARD-CP-544] p 4543 N94-37333
An introduction to the Internet and its services
p 4543 N94-37334
Global information networks: How they work
p 4543 N94-37335
The virtual library: Coming of age
p 4544 N94-37338
Providing electronic documents in Europe: Experience of INIST p 4544 N94-37341
Training and operations support system (TOPS)
p 4545 N94-37344
Wide area information servers: An executive information system for unstructured files p 4545 N94-37345
Interactive calculator for use with multi-dimensional netCDF files
[DE94-007477] p 4545 N94-37348
Information on alternative refrigerants and lubricants: The ARTI refrigerant database
[DE94-009997] p 4426 N94-37490
Integrated Engineering Information Technology, FY 1993 accomplishments
[DE94-011406] p 4545 N94-37563
A graphic view of Geometric Dimensioning and Tolerancing
[DE94-011478] p 4435 N94-37736
INFORMATION TRANSFER
Global information networks: How they work
p 4543 N94-37335
Standards for data and document interchange
p 4543 N94-37337
Problems of international exchange of scientific and technical information for a Russian aerospace research institute p 4544 N94-37339
Electronic document delivery: Towards the virtual library p 4544 N94-37340
Providing electronic documents in Europe: Experience of INIST p 4544 N94-37341
Bulletin boards, electronic mail, conferencing, current use by scientists and engineers: Effects on libraries and information centres: Do they have a role?
p 4544 N94-37343
INFRARED ASTRONOMY
Far-infrared emission line spectroscopy of planetary nebulae from the KAO
[NASA-CR-196289] p 4547 N94-37825
INFRARED DETECTORS
MODIL cryocooler producibility demonstration project results
[DE93-019213] p 4430 N94-36444
InTlSb for long-wavelength infrared photodetectors and arrays
[AD-A280207] p 4524 N94-37149
Status review and accomplishments of the Materials Research Center at the University of Pittsburgh
[AD-A280422] p 4399 N94-37214
Microwave detection of a superconducting infrared sensor
[AD-D016297] p 4440 N94-37769
INFRARED IMAGERY
Infrared search and track demonstrator programme
p 4393 N94-36622
INFRARED LASERS
Holmium quasi-two level laser
[AD-D016302] p 4449 N94-37772
INFRARED PHOTOMETRY
Infrared spectroscopy of Jupiter and Saturn
[NASA-CR-196294] p 4549 N94-36961
INFRARED SPECTRA
Infrared spectroscopy of Jupiter and Saturn
[NASA-CR-196294] p 4549 N94-36961
Optical spectroscopy of a nitrogen-hydrogen complex in ZnSe
[DE94-011622] p 4413 N94-37630
Far-infrared emission line spectroscopy of planetary nebulae from the KAO
[NASA-CR-196289] p 4547 N94-37825
INFRARED SPECTROSCOPY
Infrared spectroscopy of Jupiter and Saturn
[NASA-CR-196294] p 4549 N94-36961
Infrared spectroscopy of organic free radicals related to combustion processes
[DE94-012481] p 4409 N94-37168
Gaseous effluent monitoring and identification using an imaging Fourier transform spectrometer
[DE94-012627] p 4467 N94-37428
Optical spectroscopy of a nitrogen-hydrogen complex in ZnSe
[DE94-011622] p 4413 N94-37630
Far-infrared emission line spectroscopy of planetary nebulae from the KAO
[NASA-CR-196289] p 4547 N94-37825
INFRARED TELESCOPES
SOFIA: Aircraft system, aft telescope cavity configuration, phase 2. Volume 1: Executive summary
[NASA-CR-196362] p 4546 N94-36642
INFRARED TRACKING
Pointing and Tracking Systems
[AGARD-CP-539] p 4392 N94-36616
Pointing and tracking concept for a high energy laser weapon application p 4393 N94-36619
Infrared search and track demonstrator programme
p 4393 N94-36622
Contact level fusion of radar and IRST contacts on almost electromagnetically silent platform
p 4395 N94-36634
INGOTS
Assess progress being made for the KTeV electromagnetic calorimeter crystal order in France
[DE94-009396] p 4533 N94-36746
INJECTION
Proceedings of SPIE: The International Society for Optical Engineering, Computational Vision Based on Neurobiology, volume 2054
[AD-A278731] p 4523 N94-36468
INJECTORS
Physics with primary beams of the KEK-PS
[DE94-748635] p 4522 N94-37234
INPUT/OUTPUT ROUTINES
A scalable high-performance I/O system
[DE94-011513] p 4498 N94-37519
INSECTS
Recombinant protein production and insect cell culture and process
[NASA-CASE-MSC-22336-1] p 4478 N94-36751
INSERTION LOSS
Processing, packaging, and characterization of electroceramic materials for phased array antennas
[AD-A280251] p 4432 N94-36743
INSPECTION
Analysis of a successful inspection program
p 4490 N94-36492
INSULATORS
Theory of metal insulator transition in strongly correlated electron systems
[DE94-013135] p 4438 N94-37295
INTEGRAL EQUATIONS
The canonical symmetry for integral systems
[DE94-618486] p 4504 N94-37375

Multiquadric collocation methods in the numerical solution of Volterra integral equations with weakly singular kernels
[DE94-013000] p 4505 N94-37497

INTEGRATED CIRCUITS
A proposed SEU tolerant DRAM cell
[DE94-010758] p 4438 N94-37196
Role of burn-in during qualification testing
[DE94-007864] p 4439 N94-37513

INTEGRATED OPTICS
Fault tolerance in opto-electronic computing
[AD-A280219] p 4453 N94-37150

INTERFACES
Laser probing of interfaces
[DE94-011300] p 4449 N94-37628

INTERFACIAL TENSION
Coupled Marangoni-Benard/Rayleigh-Benard instability with temperature dependent viscosity
[NASA-TM-106646] p 4444 N94-37507

INTERFEROMETERS
Four beam interferometer manual: Operating instructions for the INEL diffraction Moire interferometer
[DE94-010772] p 4453 N94-36452
Microscopic image processing systems for measuring nonuniform film thickness profiles
[DE94-005336] p 4424 N94-37223
Angle interferometer cross axis errors
[DE94-006190] p 4446 N94-37388

INTERFEROMETRY
Four beam interferometer manual: Operating instructions for the INEL diffraction Moire interferometer
[DE94-010772] p 4453 N94-36452
Angle interferometer cross axis errors
[DE94-006190] p 4446 N94-37388
Interferometric JFTOT tube deposit measuring device
[AD-D016295] p 4430 N94-37768

INTERMETALLICS
Process/composite concurrent tailoring of SiC/Ti composites p 4402 N94-36663
Processing and mechanical properties of NiAl-based in-situ composites
[NASA-CR-195333] p 4416 N94-36954
Process simulation and modeling for advanced intermetallic alloys
[AD-A280327] p 4416 N94-37030
Feasibility of (IMC)(sub d)-reinforced metal matrix composites
[AD-A280626] p 4404 N94-37044
Atomic level characterization of defects in microalloyed NiAl: An atom probe investigation
[DE94-012732] p 4418 N94-37396
Development of intermetallic coatings for fusion power applications
[DE94-012647] p 4419 N94-37442

INTERMOLECULAR FORCES
Microscopic image processing systems for measuring nonuniform film thickness profiles
[DE94-005336] p 4424 N94-37223

INTERNAL COMBUSTION ENGINES
Potential benefits of oxygen-enriched intake air in a vehicle powered by a spark-ignition engine
[DE94-013452] p 4451 N94-37070

INTERNATIONAL COOPERATION
Space Station: Impact of the expanded Russian role on funding and research. Report to the Ranking Minority Member, Subcommittee on Oversight of Government Management, Committee on Governmental Affairs, US Senate
[GAO/NSIAD-94-220] p 4396 N94-37257
Problems of international exchange of scientific and technical information for a Russian aerospace research institute p 4544 N94-37339

INTERNETS
Using Gopher on the Internet
[DE94-009736] p 4497 N94-36441
MarChem 93, the proceedings, the 1993 workshop on marine chemistry instrumentation
[AD-A279035] p 4475 N94-36446
Analysis of end-to-end encryption and traffic flow confidentiality options
[AD-A278612] p 4433 N94-36754
Electronic SCAN (Selected Current Aerospace Notices) p 4541 N94-36845
NASA Access Mechanism (NAM) p 4541 N94-36850
OSI and TCP/IP p 4542 N94-36855
Open system environments p 4542 N94-36857
Z39.50 and GILS model — Government Information Locator Service p 4542 N94-36859
Government Information Locator Service (GILS). Draft report to the Information Infrastructure Task Force p 4542 N94-36860
An introduction to the Internet and its services p 4543 N94-37334
Bulletin boards, electronic mail, conferencing, current use by scientists and engineers: Effects on libraries and information centres: Do they have a role? p 4544 N94-37343
Wide area information servers: An executive information system for unstructured files p 4545 N94-37345
Information retrieval services on wide area networks: A vision of the future p 4545 N94-37346
Policies for implementing network firewalls
[DE94-011030] p 4495 N94-37430

INTERPLANETARY MAGNETIC FIELDS
Dynamics explorer data analysis
[NASA-CR-196141] p 4469 N94-37016

INTERPOLATION
A coarse-mesh nodal method-diffusive-mesh finite difference method
[DE94-010809] p 4502 N94-36455

INTERPROCESSOR COMMUNICATION
Experience with automatic, dynamic load balancing and adaptive finite element computation
[DE94-001422] p 4498 N94-37487
Advanced information processing system: Authentication protocols for network communication
[NASA-CR-194923] p 4498 N94-37500
A scalable high-performance I/O system
[DE94-011513] p 4498 N94-37519

INVENTORIES
World jet airplane inventory at year-end 1993
[PB94-164993] p 4384 N94-36530
UK methane emissions inventory: A scoping study on the use of ambient measurements to reduce uncertainties
[PB94-167855] p 4463 N94-36533

INVESTMENT CASTING
Advances in rapid prototyping
[DE94-010075] p 4430 N94-36447

INVISCID FLOW
Unstructured grid methods for the simulation of 3D transient flows
[NASA-CR-196139] p 4444 N94-37525
Towards enhancing and delaying disturbances in free shear flows
[NASA-CR-194945] p 4445 N94-37606

ION ATOM INTERACTIONS
Consequences of competing hybridization for magnetic ordering in correlated-electron lattices
[DE94-011648] p 4534 N94-37057

ION BEAMS
LET spectra of fragmented 600-MeV/A iron beam on aluminum and polyethylene: A preliminary analysis
[NASA-TP-3436] p 4416 N94-36993
Density and composition analysis using focused MeV ion microbeam techniques
[DE94-012241] p 4517 N94-37210
Physics with primary beams of the KEK-PS
[DE94-748635] p 4522 N94-37234
Time-of-flight pulsed ion beam surface analysis as a means of in situ, real-time characterization of the growth of ferro-electric and conductive oxide heterostructures
[DE94-012628] p 4517 N94-37249
Proceedings of the Workshop on Negative Ion Formation and Beam Handling
[DE94-748683] p 4518 N94-37360

ION CYCLOTRON RADIATION
Bounce resonance heating and transport in a magnetic mirror
[DE94-727545] p 4531 N94-37466

ION ENGINES
Conceptual design: TFE verification program
[DE94-012469] p 4398 N94-37433
Characteristics of ions emitted from high-current hollow cathodes
[NASA-CR-195372] p 4398 N94-37764

ION EXCHANGE RESINS
Determination of copper in tap water using solid-phase spectrophotometry
[NASA-TM-106480] p 4408 N94-36537

ION EXCHANGING
Method of forming waveguides with ion exchange of halogen ions
[AD-D016304] p 4526 N94-37774

ION EXTRACTION
The mathematical simulation of physical processes in ECR multicharged ions sources
[DE94-618343] p 4515 N94-37077

ION IMPLANTATION
First results from the Los Alamos plasma source ion implantation experiment
[DE94-003931] p 4414 N94-36461
Production of amorphous metal layers using ion implantation and investigation of the related modification of some surface properties
[DE94-617509] p 4414 N94-36541
Irradiation effects in Fe-30 percent Ni alloy during Ar ion implantation
[DE94-619057] p 4415 N94-36564
Studying of ion implantation effect on the biology in China
[DE94-620692] p 4479 N94-37535
Implanting impurities in semiconductors and semiconductor implanted with impurities
[AD-D016298] p 4538 N94-37770

ION IRRADIATION
Irradiation effects in Fe-30 percent Ni alloy during Ar ion implantation
[DE94-619057] p 4415 N94-36564

ION MICROSCOPES
Density and composition analysis using focused MeV ion microbeam techniques
[DE94-012241] p 4517 N94-37210
Atomic level characterization of defects in microalloyed NiAl: An atom probe investigation
[DE94-012732] p 4418 N94-37396

ION PLATING
Processing of titanium matrix composites p 4401 N94-36653

ION PROBES
Light stable isotope analysis of meteorites by ion microprobe
[NASA-CR-196096] p 4548 N94-37004

ION SCATTERING
Time-of-flight pulsed ion beam surface analysis as a means of in situ, real-time characterization of the growth of ferro-electric and conductive oxide heterostructures
[DE94-012628] p 4517 N94-37249

ION SOURCES
Proceedings of the Workshop on Negative Ion Formation and Beam Handling
[DE94-748683] p 4518 N94-37360
Production of high current H(-) beams in a cesium seeded volume negative ion source equipped with PG filter
[DE94-718962] p 4522 N94-37463

ION TEMPERATURE
A fast spectroscopic diagnostic for the measurement of plasma impurity ion dynamics
[DE94-012985] p 4529 N94-37354
Isotope scaling and eta(i) mode with impurities in tokamak plasmas
[DE94-012763] p 4529 N94-37361

IONIC COLLISIONS
High baryon density from relativistic heavy ion collisions
[DE94-003894] p 4511 N94-36460
Production of phi mesons in central Si+Au collisions at 14.6 A GeV/c
[DE94-011726] p 4516 N94-37152
Kaon correlation systematics in E859
[DE94-011927] p 4516 N94-37158
Non-equilibrium evolution of the disoriented chiral condensate in heavy-ion collisions
[DE94-012897] p 4522 N94-37310
Comparison of oxygen and silicon induced reactions at 14.6 A(GeV/C)
[DE94-011923] p 4518 N94-37364
On the shape of x ray spectra excited by heavy ions
[DE94-618747] p 4519 N94-37651

IONIZATION
Correlation of hot-carrier stress and ionization induced degradation in bipolar transistors
[DE94-007289] p 4532 N94-36540
The winds of cataclysmic variables
[DE94-010897] p 4548 N94-37164
Time-resolved probing of electron thermal transport in plasma produced by femtosecond laser pulses
[DE94-012061] p 4530 N94-37392
Ionization balance and gain calculations for neon-like selenium x-ray laser plasmas
[DE94-012590] p 4530 N94-37437
On the shape of x ray spectra excited by heavy ions
[DE94-618747] p 4519 N94-37651

IONIZATION CHAMBERS
Conceptual design for a fast neutron ionization chamber for fusion reactor plasma diagnostics
[DE94-013396] p 4527 N94-37101

IONIZATION POTENTIALS
Ionic properties of hydrogenated and fluorinated fullerenes
[DE94-012110] p 4537 N94-37369

IONOGRAMS
Eurocap program: Ebre Station
[AD-A280418] p 4469 N94-37215

IONOSPHERIC DISTURBANCES
Channel probe measurements for the American Sector Clutter Experiment, January 1994
[DE94-013086] p 4469 N94-37314

IONOSPHERIC PROPAGATION
TIPC user manual
[DE94-004470] p 4432 N94-36443
Channel probe measurements for the American Sector Clutter Experiment, January 1994
[DE94-013086] p 4469 N94-37314

IONS
The mathematical simulation of physical processes in ECR multicharged ions sources
[DE94-618343] p 4515 N94-37077
Origins of energetic ions in the Earth's magnetosheath
[NASA-CR-189359] p 4471 N94-37703
Characteristics of ions emitted from high-current hollow cathodes
[NASA-CR-195372] p 4398 N94-37764
IRAN
Abstracts of 2nd International Conference on Lasers and their Applications
[DE94-617409] p 4448 N94-37169
IRON
LET spectra of fragmented 600-MeV/A iron beam on aluminum and polyethylene: A preliminary analysis
[NASA-TP-3436] p 4416 N94-36993
Mechanical behavior and phase stability of NiAl-based shape memory alloys
[DE94-012336] p 4419 N94-37420
Superacid catalysis of light hydrocarbon conversion
[DE94-011132] p 4411 N94-37431
Magnetic and structural instabilities of ferromagnetic and antiferromagnetic Fe/Cu(100)
[DE94-011504] p 4509 N94-37517
Mechanical performance of austempered ductile iron
[AD-A280452] p 4420 N94-37758
IRON ALLOYS
Irradiation effects in Fe-30 percent Ni alloy during Ar ion implantation
[DE94-619057] p 4415 N94-36564
Characterization of mechanical properties degradation using small punch testing technique
[DE94-011202] p 4418 N94-37410
IRON ORES
Mineralogy and metallurgical properties of iron ore sinter based on magnetite fines
[DE94-763309] p 4414 N94-36525
IRON OXIDES
Iron hydrous titanium oxide catalysts for the dehydrogenation of ethylbenzene to styrene
[DE94-010381] p 4412 N94-37542
IRRADIATION
Precipitation in Zr-2.5 Nb enhanced by proton irradiation
[DE94-619056] p 4415 N94-36563
Data compatibility for various Charpy-tests
[DE94-617534] p 4416 N94-37074
AEM and AES of radiation-induced segregation in proton-irradiated stainless steels
[DE94-012734] p 4418 N94-37398
Role of burn-in during qualification testing
[DE94-007864] p 4439 N94-37513
IRRIGATION
A dynamic model of a linear actuator based on polymer hydrogel
[DE94-010800] p 4408 N94-37091
ISOMERIZATION
Thermal cis-trans isomerization rates of azobenzenes bound in the side chain of some copolymers and blends
[AD-A280451] p 4424 N94-37227
The hydrogenolysis and isomerization of light hydrocarbons over Pt catalysts
[DE94-013142] p 4410 N94-37296
ISOMERS
Thermal cis-trans isomerization rates of azobenzenes bound in the side chain of some copolymers and blends
[AD-A280451] p 4424 N94-37227
ISOTOPE EFFECT
MCHF calculations of isotope shifts. 1: Program implementation and test runs. 2: Large-scale active space calculations
[DE94-013036] p 4518 N94-37313
ISOTOPES
Light stable isotope analysis of meteorites by ion microprobe
[NASA-CR-196096] p 4548 N94-37004
Atmospheric gas
[DE94-007439] p 4465 N94-37187
ITERATIVE SOLUTION
A coarse-mesh nodal method-diffusive-mesh finite difference method
[DE94-010809] p 4502 N94-36455
Recovering depth from focus using iterative image estimation techniques
[DE94-010994] p 4524 N94-37165
Neutron transport methods on scalable shared memory multiprocessors
[DE94-012324] p 4498 N94-37419
Hierarchically parallelized constrained nonlinear solvers with automated substructuring
[NASA-CR-194474] p 4456 N94-37554
Ordering design tasks based on coupling strengths
[NASA-TM-109137] p 4387 N94-37762

J

JACOBI MATRIX METHOD
Tensor-GMRES method for large sparse systems of nonlinear equations
[NASA-CR-196379] p 4505 N94-37655
JAMMERS
VHF adaptive antenna development task
[AD-A280320] p 4434 N94-37127
JAMMING
VHF adaptive antenna development task
[AD-A280320] p 4434 N94-37127
JAPAN
Advanced manufacturing technology for polymer composite structures in Japan p 4422 N94-36968
JET AIRCRAFT
World jet airplane inventory at year-end 1993
[PB94-164993] p 4384 N94-36530
Jet aircraft engine exhaust emissions database development: Year 1990 and 2015 scenarios
[NASA-CR-4613] p 4466 N94-37252
JET ENGINE FUELS
Advanced thermally stable, coal-derived, jet fuels development program. Experiment system and model development
[AD-A278968] p 4428 N94-36505
Interferometric JFTOT tube deposit measuring device
[AD-D016295] p 4430 N94-37768
JET ENGINES
Impact of Materials Defects on Engine Structures Integrity
[AGARD-R-790] p 4453 N94-37321
History and prognosis of material discontinuity effects on engine components structural integrity
p 4453 N94-37322
JET FLOW
Towards enhancing and delaying disturbances in free shear flows
[NASA-CR-194945] p 4445 N94-37606
Effects of molecular transport on turbulence-chemistry interactions in a hydrogen-argon-air jet diffusion flame
[DE94-005107] p 4413 N94-37711
JET IMPINGEMENT
Mixing and noise benefit versus thrust penalty in supersonic jets using impingement tones
[NASA-TM-106583] p 4382 N94-36686
Turbulence modeling of free shear layers for high performance aircraft
[NASA-CR-196137] p 4442 N94-36808
Neural network for positioning Space Station solar arrays
[NASA-TM-106656] p 4431 N94-36943
Numerical analysis of an impinging jet reactor for the CVD and gas-phase nucleation of titania
[NASA-TM-106619] p 4431 N94-37254
JET MIXING FLOW
Mixing and noise benefit versus thrust penalty in supersonic jets using impingement tones
[NASA-TM-106583] p 4382 N94-36686
JET THRUST
Mixing and noise benefit versus thrust penalty in supersonic jets using impingement tones
[NASA-TM-106583] p 4382 N94-36686
JETS
Direct photoproduction of jets in the k(T)-factorisation prescription
[PB94-171139] p 4513 N94-36549
JOINTS (ANATOMY)
Selectively lockable knee brace
[NASA-CASE-MFS-28991-1] p 4486 N94-36838
Channel in hip implant stem
[NASA-CASE-MFS-28967-1] p 4486 N94-36840
JOINTS (JUNCTIONS)
Literature review and preliminary studies of fretting and fretting fatigue including special applications to aircraft joints
[AD-A280310] p 4456 N94-37125
Strength evaluation of socket joints
[NASA-CR-4608] p 4389 N94-37259
JOSEPHSON JUNCTIONS
Josephson acoustic radiation in superfluid helium
[AD-A280208] p 4533 N94-36742
Submillimeter quasioptical Josephson junction oscillator with integrated tuning elements
[AD-A280380] p 4534 N94-37036
JUMPERS
Jumper connector analysis
[DE94-010373] p 4451 N94-37188

K

K-EPSILON TURBULENCE MODEL
Turbulence modeling of free shear layers for high performance aircraft
[NASA-CR-196137] p 4442 N94-36808
KALMAN FILTERS
Contact level fusion of radar and IRST contacts on almost electromagnetically silent platform
p 4395 N94-36634
Progress in navigation filter estimate fusion and its application to spacecraft rendezvous
[NASA-TM-104794] p 4392 N94-37386
KAON PRODUCTION
Relativistic di-quark model of p p-bar yields K(+)K(-) reaction
[DE94-618519] p 4514 N94-37063
KAONS
Angular dependence of parton-parton scattering extracted from hadron pair production in pp collisions at radicals equal to 11.5 GeV
[DE94-611174] p 4511 N94-36504
B-lifetime measurements at the tevatron
[DE94-003617] p 4513 N94-36528
Relativistic di-quark model of p p-bar yields K(+)K(-) reaction
[DE94-618519] p 4514 N94-37063
New method for minimizing regular functions with constraints on parameter region
[DE94-618340] p 4515 N94-37076
Kaon correlation systematics in E859
[DE94-011927] p 4516 N94-37158
Testing violation of CPT and quantum mechanics in the K(0) - bar-K(0) system
[DE94-012057] p 4539 N94-37366
Experimental particle physics at the University of Pittsburgh
[DE94-011636] p 4521 N94-37721
KETONES
Tert-butylalumoxanes: Synthetic analogs for methylalumoxane (MAO) and new catalytic routes to polyolefins and polyketones
[AD-A280511] p 4399 N94-37106
Tert-butylalumoxanes: Synthetic analogs for methylalumoxane (MAO) and new catalytic routes to polyolefins and polyketones
[AD-A280532] p 4399 N94-37650
KEVLAR (TRADEMARK)
The development of short, high surface area activated carbon fibers
[AD-A280509] p 4404 N94-37105
KINEMATICS
A mixture model for shock compression of porous multi-component reactive materials
[DE93-017638] p 4400 N94-36456
Methodologies to determine forces on bones and muscles of body segments during exercise, employing compact sensors suitable for use in crowded space vehicles
[NASA-CR-196272] p 4487 N94-37458
A new technique for dynamic load distribution when two manipulators mutually lift a rigid object, part 2
[DE94-010126] p 4501 N94-37735
KNEE (ANATOMY)
Selectively lockable knee brace
[NASA-CASE-MFS-28991-1] p 4486 N94-36838
KNOOP HARDNESS
First results from the Los Alamos plasma source ion implantation experiment
[DE94-003931] p 4414 N94-36461
KNOWLEDGE BASED SYSTEMS
Ordering design tasks based on coupling strengths
[NASA-TM-109137] p 4387 N94-37762
KONDO EFFECT
Quadrupolar effects in PrCu2Si2
[DE94-011509] p 4534 N94-37054
KRYPTON FLUORIDE LASERS
A high power microwave frequency modulated KrF laser
[DE94-009303] p 4447 N94-36510

L

LABORATORY EQUIPMENT
NIPER Lab WARDEN: Description and LabVIEW executable code of a general-purpose laboratory-automation program
[DE94-000125] p 4492 N94-36698
NIPER Lab WARDEN: Descriptive panels and diagrams for NIPER Lab WARDEN software, volume 2
[DE94-000126] p 4493 N94-36699
Technology demonstration of space intravehicular automation and robotics
[NASA-TM-109138] p 4501 N94-37589

LACQUERS
Atomic oxygen treatment for non-contact removal of organic protective coatings from painting surfaces
[NASA-TM-106650] p 4421 N94-36952
LAGRANGIAN FUNCTION
Effective Lagrangian for gluons and Higgs pseudoscalars
[DE94-001381] p 4513 N94-36539
Flow visualization for Lagrangian particle methods
[DE94-010757] p 4443 N94-37195
LAMINAR BOUNDARY LAYER
An algorithm for the automatic control of boundary layer flow
[ISVR-TR-233] p 4442 N94-36817
Supersonic laminar flow control research
[NASA-CR-196260] p 4384 N94-37511
LAMINAR FLOW
Laser-saturated fluorescence measurements in laminar sooting diffusion flames
[NASA-CR-191025] p 4508 N94-36643
Finite-rate chemistry and transient effects in Direct Numerical Simulations of turbulent non-premixed flames
[DE94-005250] p 4410 N94-37222
Supersonic laminar flow control research
[NASA-CR-196260] p 4384 N94-37511
LAMINATES
Flame resistant fibrous structures development
[NASA-CR-185700] p 4421 N94-36641
Applications of Titanium Matrix Composite to large airframe structure p 4400 N94-36651
Residual strength and life prediction techniques for Ti MMC p 4402 N94-36662
Prediction of thermal and mechanical stress-strain responses of TMC's subjected to complex TMF histories p 4402 N94-36666
Pre-standardisation work on fatigue and fracture testing of titanium matrix composites p 4402 N94-36667
ASTM and VAMAS activities in titanium matrix composites test methods development p 4403 N94-36668
Detection of delaminations in composite beams using piezoelectric sensors
[NASA-TM-106611] p 4403 N94-36956
Advanced manufacturing technology for polymer composite structures in Japan p 4422 N94-36968
Development of nondestructive evaluation methods and prediction of effects of flaws on the fracture behavior of structural ceramics
[DE94-012466] p 4425 N94-37423
Laminated thin shell structures subjected to free vibration in a hygrothermal environment
[NASA-TM-106600] p 4456 N94-37456
A comparison of graphite/epoxy tape laminates and 2-D braided composites mechanical properties
[NASA-CR-4610] p 4420 N94-37582
Probability techniques for reliability analysis of composite materials
[NASA-CR-195294] p 4406 N94-37633
A simple evaluation of thermally-induced streses in the vicinity of the stitch in a through-thickness reinforced cross-ply laminate
[NASA-CR-196317] p 4406 N94-37653
Sub-ply level scaling approach investigated for graphite-epoxy composite beam columns p 4458 N94-37798
Scaling, elasticity, and CLPT p 4458 N94-37800
Experimental observations of scale effects on bonded and bolted joints in composite structures p 4458 N94-37801
The effects of specimen scale on the compression strength of composite materials p 4459 N94-37802
Damage and strength of composite materials: Trends, predictions, and challenges p 4459 N94-37805
Effects of ply thickness on thermal cycle induced damage and thermal strain p 4459 N94-37806
LAND SURFACE TEMPERATURE
Representing the influence of subgrid topography on hydrology
[DE94-004595] p 4474 N94-37379
LAND USE
Science priorities for the human dimensions of global change p 4464 N94-36987
LANDING AIDS
An empirical comparison of a dynamic software testability metric to static cyclomatic complexity p 4491 N94-36498
LANDING SIMULATION
Synthetic vision display evaluation studies
[NASA-CR-194963] p 4387 N94-37658
LANGEVIN FORMULA
Quantum harmonic Brownian motion in a general environment: A modified phase-space approach
[DE94-003249] p 4508 N94-36560
LANTHANUM COMPOUNDS
Structural ground-state of La2CuO4 in the LTO phase: Evidence of local disorder
[DE94-013126] p 4536 N94-37291
LAPLACE EQUATION
Cost-effective computations with boundary interface operators in elliptic problems
[DE94-621506] p 4503 N94-37098
LARGE SPACE STRUCTURES
Configurational evolution dynamics and stability during in-situ development of large orbiting spacecraft
[AD-A280482] p 4397 N94-37351
LASER ALTIMETERS
Receiver design, performance analysis, and evaluation for space-borne laser altimeters and space-to-space laser ranging systems
[NASA-CR-194747] p 4397 N94-36988
Measuring the upper profile of sea ice in the Bay of Bothnia with a laser profilometer
[PB94-184561] p 4477 N94-37855
LASER APPLICATIONS
Advances in rapid prototyping
[DE94-010075] p 4430 N94-36447
Laser-saturated fluorescence measurements in laminar sooting diffusion flames
[NASA-CR-191025] p 4508 N94-36643
Design and development of experimental facilities for short duration, low-gravity combustion and fire experiments
[NASA-CR-196107] p 4389 N94-36967
Spontaneous force optical traps
[AD-A280574] p 4514 N94-37041
Abstracts of 2nd International Conference on Lasers and their Applications
[DE94-617409] p 4448 N94-37169
Laser cooling of 24Mg+ in the ASTRID storage ring
[DE94-010445] p 4523 N94-37619
Laser probing of interfaces
[DE94-011300] p 4449 N94-37628
Recent progress of the Los Alamos advanced free electron laser
[DE94-011654] p 4449 N94-37733
LASER ARRAYS
Advanced laser driver for soft x-ray projection lithography
[DE94-011643] p 4449 N94-37722
LASER BEAMS
Pointing and tracking concept for a high energy laser weapon application p 4393 N94-36619
Adaptive optics for laser beamforming in the atmosphere p 4393 N94-36621
Quantum and quasi-classical analyses of high order emission processes
[DE93-041348] p 4513 N94-36697
Ionization balance and gain calculations for neon-like selenium x-ray laser plasmas
[DE94-012590] p 4530 N94-37437
Effect of the stimulated Brillouin backscattering on self-focusing threshold
[DE94-008678] p 4510 N94-37536
LASER CAVITIES
U-turn alternative to the large aperture switch
[DE94-011541] p 4524 N94-37112
Greater than 100 watt average power at 0.53 micron with 25 ns, 2.5 kHz repetition rate pulses from a single power oscillator
[DE94-011641] p 4447 N94-37114
Two-micron modelocked laser system
[AD-D016219] p 4448 N94-37481
Advanced laser driver for soft x-ray projection lithography
[DE94-011643] p 4449 N94-37722
LASER DRILLING
Laser drilling of printed wiring boards: Sandia LDRD program
[DE94-011004] p 4448 N94-37198
LASER GUIDANCE
Laser designation pods optimized concept for day/night operations p 4393 N94-36620
LASER HEATING
First observation of laser-induced resonant annihilation in metastable antiprotonic helium atoms
[DE94-748668] p 4519 N94-37417
LASER INDUCED FLUORESCENCE
Solid state fluorometer: Prototype development
[AD-A280321] p 4534 N94-37027
LASER MATERIALS
Diode array alternative to paint removal solid-state cw laser
[DE94-011482] p 4448 N94-37203
Holmium quasi-two level laser
[AD-D016302] p 4449 N94-37772
LASER MODE LOCKING
Two-micron modelocked laser system
[AD-D016219] p 4448 N94-37481
LASER OUTPUTS
An externally heated copper vapour laser
[DE94-619484] p 4447 N94-36565
Greater than 100 watt average power at 0.53 micron with 25 ns, 2.5 kHz repetition rate pulses from a single power oscillator
[DE94-011641] p 4447 N94-37114
High average power pulsed phase conjugate laser with birefringence correction
[DE94-012062] p 4447 N94-37160
Two-micron modelocked laser system
[AD-D016219] p 4448 N94-37481
Intracavity-pumped 2.1 micrometer Ho(3+):YAGl aser
[AD-D016308] p 4449 N94-37777
LASER PLASMA INTERACTIONS
Basic studies in plasma wave interactions
[AD-A280465] p 4527 N94-37139
LASER PLASMAS
Basic studies in plasma wave interactions
[AD-A280465] p 4527 N94-37139
Ionization balance and gain calculations for neon-like selenium x-ray laser plasmas
[DE94-012590] p 4530 N94-37437
LASER PUMPING
Advanced laser driver for soft x-ray projection lithography
[DE94-011643] p 4449 N94-37722
Holmium quasi-two level laser
[AD-D016302] p 4449 N94-37772
Intracavity-pumped 2.1 micrometer Ho(3+):YAGl aser
[AD-D016308] p 4449 N94-37777
LASER RANGE FINDERS
Receiver design, performance analysis, and evaluation for space-borne laser altimeters and space-to-space laser ranging systems
[NASA-CR-194747] p 4397 N94-36988
Measuring the upper profile of sea ice in the Bay of Bothnia with a laser profilometer
[PB94-184561] p 4477 N94-37855
LASER RANGER/TRACKER
Landing of an unmanned helicopter on a moving platform. High accuracy navigation and tracking p 4387 N94-36618
A more exact analysis of Sandia Laser Tracker data
[DE94-011411] p 4447 N94-37051
LASER SPECTROSCOPY
Nonlinear optical spectroscopy for surface studies
[DE94-011623] p 4408 N94-37056
Abstracts of 2nd International Conference on Lasers and their Applications
[DE94-617409] p 4448 N94-37169
LASER TARGET DESIGNATORS
Laser designation pods optimized concept for day/night operations p 4393 N94-36620
LASER WEAPONS
Pointing and tracking concept for a high energy laser weapon application p 4393 N94-36619
LASERS
Picosecond laser induced electric field modulation of carotenoid absorption bands
[DE94-009692] p 4512 N94-36524
JPRS report: Science and technology. Central Eurasia
[JPRS-UST-94-013] p 4509 N94-37006
Design of the divertor Thomson scattering system on D3-D
[DE94-012672] p 4527 N94-37081
Abstracts of 2nd International Conference on Lasers and their Applications
[DE94-617409] p 4448 N94-37169
Frequency doubling of copper lasers using temperature-tuned ADP
[DE94-011542] p 4448 N94-37240
Advanced laser driver for soft x-ray projection lithography
[DE94-011643] p 4449 N94-37722
LAUNCH VEHICLES
UVPI imaging from the LACE satellite: The Low Cost Launch Vehicle (LCLV) rocket plume
[AD-A278785] p 4398 N94-36445
Aerodynamic characteristics of the National Launch System (NLS) 1 1/2 stage launch vehicle
[NASA-TP-3488] p 4384 N94-37577
Advanced information processing system: Hosting of advanced guidance, navigation and control algorithms on AIPS using ASTER
[NASA-CR-194960] p 4499 N94-37583
LAUNCHING
Scientific and technical support for the Galileo net flux radiometer experiment
[NASA-CR-196009] p 4549 N94-36689
Marker beacon case
[AD-D016322] p 4385 N94-37830
LAVA
Vent processes during the 1912 eruption at Novarupta, Katmai National Park, Alaska
[DE94-010740] p 4468 N94-36451

LAY-UP
Manufacture and properties of sigma fibre reinforced titanium p 4401 N94-36655
Development of nondestructive evaluation methods and prediction of effects of flaws on the fracture behavior of structural ceramics
[DE94-012466] p 4425 N94-37423

LAYOUTS
The impact of HPF data layout on the design of efficient and maintainable parallel linear algebra libraries
[DE94-012382] p 4504 N94-37246

LEACHING
Analytical electron microscopy examination of solid reaction products in long-term test of SRL 200 waste glasses
[DE94-005482] p 4411 N94-37380

LEAD ALLOYS
Use of rotation to suppress thermosolutal convection in directionally solidified binary alloys
[NASA-CR-196372] p 4415 N94-36811

LEAD OXIDES
Substrate effects on the structure and optical properties of epitaxial PbTiO3 thin films prepared by metal-organic chemical vapor deposition
[DE94-010432] p 4535 N94-37192

LEAKAGE
Hot dynamic test rig for measuring hypersonic engine seal flow and durability
[NASA-TM-106507] p 4450 N94-36645

LEAST SQUARES METHOD
A method for obtaining a least squares fit of a hyperplane to uncertain data
[DE94-012498] p 4503 N94-37073

LEG (ANATOMY)
Methodologies to determine forces on bones and muscles of body segments during exercise, employing compact sensors suitable for use in crowded space vehicles
[NASA-CR-196272] p 4487 N94-37458

LENSES
Design of the divertor Thomson scattering system on D3-D
[DE94-012672] p 4527 N94-37081

LEPTONS
A search for first generation scalar leptoquarks at radical s equal to 1.8 TeV with the D0 detector
[DE94-006846] p 4511 N94-36506
Summary of the extensions of the Standard Model working group
[DE94-002217] p 4512 N94-36527
Determination of the upsilon(1s) leptonic width
[DE94-618534] p 4516 N94-37096
Five-lepton decay modes of muon and tau mesons
[DE94-621636] p 4516 N94-37099
Experimental particle physics at the University of Pittsburgh
[DE94-011636] p 4521 N94-37721

LEVITATION
Melt-processing of Y-Ba-Cu-O superconductors for improved levitation
[DE94-011503] p 4537 N94-37377

LIBRARIES
The impact of HPF data layout on the design of efficient and maintainable parallel linear algebra libraries
[DE94-012382] p 4504 N94-37246
International High Speed Networks for Scientific and Technical Information
[AGARD-CP-544] p 4543 N94-37333
An introduction to the Internet and its services
p 4543 N94-37334
The virtual library: Coming of age
p 4544 N94-37336
Electronic document delivery: Towards the virtual library p 4544 N94-37340
Bulletin boards, electronic mail, conferencing, current use by scientists and engineers: Effects on libraries and information centres: Do they have a role?
p 4544 N94-37343

LIE GROUPS
Representations of the q-deformed algebras U(q) (so(2,1)) and U(q) (so(3,1)
[DE94-616619] p 4505 N94-37483

LIFE (DURABILITY)
Characterisation of Fibre Reinforced Titanium Matrix Composites
[AD-A2775206] p 4400 N94-36649
The life cycles of intense cyclonic and anticyclonic circulation systems observed over oceans
[NASA-CR-196271] p 4473 N94-37294

LIFE CYCLE COSTS
LNG vehicle technology, economics, and safety assessment
[PB94-165487] p 4450 N94-36721
Space Shuttle: Incomplete data and funding approach increase cost risk for upgrade program. Report to Congressional Requesters
[GAO/NSIAD-94-23] p 4392 N94-37026
Operations and support cost modeling of conceptual space vehicles
[NASA-CR-196299] p 4397 N94-37580

LIFE SCIENCES
JPRS report: Science and technology. Central Eurasia
[JPRS-UST-94-013] p 4509 N94-37006
Aerospace medicine and biology: A continuing bibliography with indexes (supplement 392)
[NASA-SP-7011(392)] p 4482 N94-37445

LIFE SUPPORT SYSTEMS
Aerospace medicine and biology: A continuing bibliography with indexes (supplement 392)
[NASA-SP-7011(392)] p 4482 N94-37445

LIFTING BODIES
Optimal control theory determination of feasible return-to-launch-site aborts for the HL-20 Personnel Launch System vehicle
[NASA-TP-3449] p 4396 N94-37260

LIGANDS
Development of immobilized ligands for actinide separations
[DE94-012714] p 4410 N94-37284

LIGHT (VISIBLE RADIATION)
Ground and space flight experiments of the effects of light, sound and/or temperature on animals
[NASA-CR-196102] p 4478 N94-36986

LIGHT AMPLIFIERS
U-turn alternative to the large aperture switch
[DE94-011541] p 4524 N94-37112
Sensitivity and signal to noise ratio improvement of a one micron ladar system incorporating a neodymium doped optical fiber preamplifier. Laser radar testbed
[AD-A280235] p 4447 N94-37137

LIGHT ELEMENTS
Determination of interface structure and bonding at atomic resolution in the stem
[DE94-011466] p 4517 N94-37238

LIGHT GAS GUNS
Experimental investigation of nozzle/plume aerodynamics at hypersonic speeds
[NASA-CR-195829] p 4382 N94-36687

LIGHT HELICOPTERS
Planning German Army helicopter maintenance and mission assignment
[AD-A280483] p 4381 N94-37352

LIGHT MODULATION
Two-micron modelocked laser system
[AD-D016219] p 4448 N94-37481
Design of a composite filter realizable on practical spatial light modulators
[NASA-CR-196297] p 4525 N94-37579

LIGHT SCATTERING
United States Air Force Summer Research Program, 1993. Volume 13: Phillips Laboratory
[AD-A278657] p 4550 N94-36977
Time-gated imaging through defense-scattering materials using stimulated Raman amplification
[AD-D016305] p 4440 N94-37775

LIGHT SOURCES
Time-gated imaging through defense-scattering materials using stimulated Raman amplification
[AD-D016305] p 4440 N94-37775

LIGHT TRANSMISSION
Guiding hard x rays with glass polycapillary fiber
[DE94-004949] p 4525 N94-37258

LIGHT WATER REACTORS
A coarse-mesh nodal method-diffusive-mesh finite difference method
[DE94-010809] p 4502 N94-36455

LIGHTING EQUIPMENT
US manufacturers of commercially available stand-alone photovoltaic lighting systems
[DE94-006917] p 4462 N94-37407

LIGHTNING
Three flights into thunderstorms with the revised Rocket Electric Field Sounding (REFS) payload
[AD-A280424] p 4473 N94-37217

LIMITERS (FUSION REACTORS)
Initial report on calorimetry for the Tore Supra Outboard pump Limiter
[DE94-011244] p 4531 N94-37626

LINE OF SIGHT
Gaze orientation under G(z)-load. Methodological aspects: Preliminary results p 4485 N94-37274

LINE SPECTRA
Far-infrared emission line spectroscopy of planetary nebulae from the KAO
[NASA-CR-196289] p 4547 N94-37825

LINEAR ACCELERATORS
High Energy Physics Division of research activities
[DE93-019681] p 4521 N94-36694
Activities of the Photon Factory
[DE94-748682] p 4522 N94-37236
Recent progress of the Los Alamos advanced free electron laser
[DE94-011654] p 4449 N94-37733

LINEAR ENERGY TRANSFER (LET)
LET spectra of fragmented 600-MeV/A iron beam on aluminum and polyethylene: A preliminary analysis
[NASA-TP-3436] p 4416 N94-36993

LINEAR FILTERS
Contact level fusion of radar and IRST contacts on almost electromagnetically silent platform
p 4395 N94-36634

LINEAR PROGRAMMING
A scalable parallel algorithm for multiple objective linear programs
[NASA-CR-194920] p 4495 N94-37539

LINEAR QUADRATIC GAUSSIAN CONTROL
A note on the regularity of solutions of infinite dimensional Riccati equations
[NASA-CR-194898] p 4502 N94-36562

LINEAR QUADRATIC REGULATOR
A note on the regularity of solutions of infinite dimensional Riccati equations
[NASA-CR-194898] p 4502 N94-36562

LINEAR SYSTEMS
A Galerkin method for linear PDE systems in circular geometries with structural acoustic applications
[NASA-CR-194925] p 4503 N94-36923
Robust stabilization of marginally stable positive-real systems
[NASA-TM-109136] p 4500 N94-37058

LINGUISTICS
An error-resistant linguistic protocol for air traffic control
[NASA-CR-196098] p 4385 N94-37013

LIQUEFIED GASES
Alternative fuel information: Facts about CNG and LPG conversion
[DE94-006688] p 4429 N94-37402
Technical evaluation and assessment of CNG/LPG bi-fuel and flex-fuel vehicle viability
[DE94-006925] p 4451 N94-37408

LIQUEFIED NATURAL GAS
LNG vehicle technology, economics, and safety assessment
[PB94-165487] p 4450 N94-36721

LIQUID ATOMIZATION
Spray combustion model improvement study, 1
[NASA-CR-196122] p 4410 N94-37250

LIQUID CHROMATOGRAPHY
Chemical and structural characterization of nitroaromatic adducts with hemoglobins
[AD-A280533] p 4480 N94-37089

LIQUID COOLING
Active cooling from the sixties to NASP
[NASA-TM-109079] p 4456 N94-37541

LIQUID HELIUM
Josephson acoustic radiation in superfluid helium
[AD-A280208] p 4533 N94-36742

LIQUID HELIUM 2
Josephson acoustic radiation in superfluid helium
[AD-A280208] p 4533 N94-36742

LIQUID HYDROGEN
Fluids at high shock pressures and temperatures and some thoughts about future possibilities
[DE94-003625] p 4407 N94-36458
Cryogenic fluid management technologies for space transportation. Zero G thermodynamic vent system
[NASA-CR-193981] p 4430 N94-36806

LIQUID LITHIUM
Development of intermetallic coatings for fusion power applications
[DE94-012647] p 4419 N94-37442

LIQUID METAL FAST BREEDER REACTORS
An overview of the current status of resonance theory in reactor physics applications
[DE94-010465] p 4521 N94-37194

LIQUID METALS
The logic behind thick, liquid-walled, fusion concepts
[DE94-012678] p 4528 N94-37307

LIQUID NITROGEN
Fluids at high shock pressures and temperatures and some thoughts about future possibilities
[DE94-003625] p 4407 N94-36458

LIQUID PHASES
Mineralogy and metallurgical properties of iron ore sinter based on magnetite fines
[DE94-763309] p 4414 N94-36525

LIQUID SURFACES
Hydrogen storage for vehicular applications: Technology status and key development areas
[DE94-011626] p 4428 N94-37243

LIQUID-SOLID INTERFACES
Determination of the dispersion constant in a constrained vapor bubble thermosyphon
[NASA-CR-196124] p 4442 N94-36992
Nonlinear optical spectroscopy for surface studies
[DE94-011623] p 4408 N94-37056
LIQUID-VAPOR INTERFACES
Determination of the dispersion constant in a constrained vapor bubble thermosyphon
[NASA-CR-196124] p 4442 N94-36992
Nonlinear optical spectroscopy for surface studies
[DE94-011623] p 4408 N94-37056
LIQUIDS
Electronic balance and some gravimetric applications (the density of solids and liquids, pycnometry and mass)
[PB94-163052] p 4446 N94-36719
Microscopic theory of the dielectric response of highly dispersive biological media
[AD-A280516] p 4516 N94-37109
LITHOGRAPHY
Advanced laser driver for soft x-ray projection lithography
[DE94-011643] p 4449 N94-37722
LOAD TESTING MACHINES
Internally damped, self-arresting vertical drop-weight apparatus
[NASA-CASE-LAR-15003-1] p 4389 N94-36826
Characterization of mechanical properties degradation using small punch testing technique
[DE94-011202] p 4418 N94-37410
LOAD TESTS
Internally damped, self-arresting vertical drop-weight apparatus
[NASA-CASE-LAR-15003-1] p 4389 N94-36826
Methodologies for the thermomechanical characterization of continuous-fiber ceramic matrix composites: A review of test methods
[DE94-012111] p 4405 N94-37370
Characterization of mechanical properties degradation using small punch testing technique
[DE94-011202] p 4418 N94-37410
LOADS (FORCES)
Replacement of silicone polymer A with silicone polymer B and the subsequent characterization of the new cellular silicone materials
[DE94-010105] p 4421 N94-36474
Predicting defect behaviour p 4455 N94-37331
A method for thermal analysis of spiral bevel gears
[NASA-TM-106612] p 4451 N94-37451
Dynamics of a split torque helicopter transmission
[NASA-TM-106410] p 4452 N94-37457
Fatigue case study and loading spectra for wind turbines
[DE94-010798] p 4457 N94-37622
Understanding and managing power system harmonics
[AD-A280627] p 4440 N94-37759
LOCAL AREA NETWORKS
Network upgrades p 4541 N94-36851
LOCKING
Adaptable binary programs
[AD-A280243] p 4494 N94-37119
LOGIC CIRCUITS
High temperature superconducting digital circuits and subsystems
[DE94-001207] p 4436 N94-36557
LOGISTICS
A mean value analysis heuristic for analysis of aircraft sortie generation
[AD-A278578] p 4507 N94-36970
LOGISTICS MANAGEMENT
The implementation of Electronic Data Interchange (EDI) with defense transportation operations
[AD-A280568] p 4493 N94-37040
LONG DURATION EXPOSURE FACILITY
Evaluation of seals and lubricants used on the Long Duration Exposure Facility
[NASA-CR-4604] p 4399 N94-37614
LONGITUDINAL WAVES
Fundamentals studies of radial wave thermoacoustic engines
[AD-A280534] p 4431 N94-37090
LOSSY MEDIA
Imaging targets embedded in a lossy half space with Synthetic Aperture Radar
[DE94-010807] p 4435 N94-37391
LOW FREQUENCIES
A comparison of two examples of magnetic tracker systems p 4485 N94-37275
LOW TEMPERATURE PHYSICS
Quadrupolar effects in PrCu2Si2
[DE94-011509] p 4534 N94-37054
LUBRICANTS
Evaluation of the EHL film thickness and extreme pressure additives on gear surface fatigue life
[NASA-TM-106663] p 4451 N94-37319
Materials Compatibility and Lubricant Research on CFC-refrigerant substitutes
[DE94-012352] p 4425 N94-37373
Sealed tube comparisons of the compatibility of desiccants with refrigerants and lubricants
[DE94-012371] p 4425 N94-37421
Information on alternative refrigerants and lubricants: The ARTI refrigerant database
[DE94-009997] p 4426 N94-37490
Properties of perfluoropolyethers for space applications
[NASA-TM-106616] p 4426 N94-37520
Evaluation of seals and lubricants used on the Long Duration Exposure Facility
[NASA-CR-4604] p 4399 N94-37614
Perfluorodiethoxymethane on nickel and nickel oxide surfaces
[DE94-011200] p 4426 N94-37712
LUBRICATION
Evaluation of the EHL film thickness and extreme pressure additives on gear surface fatigue life
[NASA-TM-106663] p 4451 N94-37319
LUMINESCENCE
Optical studies of dynamical processes in disordered systems
[DE94-011945] p 4538 N94-37676
LUMINOSITY
Proceedings of the Workshop on TRISTAN Physics at High Luminosities
[DE94-737969] p 4523 N94-37727
LUNAR ENVIRONMENT
Operational environments for electrical power wiring on NASA space systems
[NASA-TM-106655] p 4398 N94-36951

M

MACH NUMBER
A shadowgraph study of Space Transportation System (STS): The Space Shuttle Launch Vehicle (SSLV)
[NASA-RP-1341] p 4382 N94-36741
Subsonic aerodynamic characteristic of semispan commercial transport model with wing-mounted advanced ducted propeller operating in reverse thrust --- conducted in the Langley 14 by 22 foot subsonic wind tunnel
[NASA-TP-3427] p 4384 N94-37505
MACHINE LEARNING
Subgrouped real time recurrent learning neural networks
[AD-A280618] p 4500 N94-37043
Adaptive learning of multi-sensor integration techniques with genetic algorithms
[DE94-012744] p 4500 N94-37083
Bootstrap planning: Theory and application
[DE94-006466] p 4501 N94-37425
MACHINE TOOLS
Open architecture controllers for advanced manufacturing
[DE94-007572] p 4496 N94-37782
MACHINE TRANSLATION
Machine Translation Project p 4541 N94-36846
MAGMA
Vent processes during the 1912 eruption at Novarupta, Katmai National Park, Alaska
[DE94-010740] p 4468 N94-36451
MAGNESIUM
Using nonequilibrium alloying techniques for corrosion inhibition in Gr/Al and Gr/Mg metal matrix composites
[AD-A280529] p 4404 N94-37088
MAGNESIUM ISOTOPES
Laser cooling of 24Mg+ in the ASTRID storage ring
[DE94-010445] p 4523 N94-37619
MAGNESIUM OXIDES
Substrate effects on the structure and optical properties of epitaxial PbTiO3 thin films prepared by metal-organic chemical vapor deposition
[DE94-010432] p 4535 N94-37192
Microstructure and chemistry of MgO- and CoO-doped nickel-titanate spinels
[DE94-012741] p 4537 N94-37382
The MBE growth and optical quality of BaTiO3 and SrTiO3 thin films on MgO
[DE94-011468] p 4538 N94-37570
MAGNETIC BEARINGS
Large angle magnetic suspension test fixture
[NASA-CR-196138] p 4390 N94-37450
MAGNETIC DISTURBANCES
Solar-Terrestrial Predictions, 4: Proceedings of a workshop. Volume 1: Workshop overview papers; working group reports; User community reports; Regional Warning Center Reports
[PB94-173176] p 4471 N94-37780
MAGNETIC FIELDS
Q-profile flattening due to nonlinear development of resistive kink mode and ensuing fast crash in sawtooth oscillations
[DE94-727625] p 4526 N94-36472
Pulsed field magnets at the United States National High Magnetic Field Laboratory
[DE94-002624] p 4436 N94-36514
Method of N-15 analysis by mass-spectroscopy on ion implanter MPB-200
[DE94-618203] p 4407 N94-36529
Design and analysis of high-field quasi-continuous magnets
[DE94-000762] p 4508 N94-36556
Relaxation of the density matrix for an arbitrary spin in random external fields
[DE94-618457] p 4509 N94-37078
Critical-state flux-density profiles in type-2 superconducting thin-film strips and disks
[DE94-011199] p 4535 N94-37166
A comparison of two examples of magnetic tracker systems p 4485 N94-37275
BMAP dipole magnetic field analysis and orbit tracking/calculations of energy deposition in GaAs WHEBY detectors
[DE94-012080] p 4522 N94-37303
Investigation of exposure to Extremely Low Frequency (ELF) magnetic and electric fields: Ongoing animals studies
[DE94-011239] p 4480 N94-37625
Symplectic tracking using point magnets and a reference orbit made of circular arcs and straight lines
[DE94-011919] p 4505 N94-37675
A freon-filled, holographic bubble chamber as a high energy photon burst spectrometer
[DE94-011645] p 4446 N94-37723
MAGNETIC FLUX
Critical-state flux-density profiles in type-2 superconducting thin-film strips and disks
[DE94-011199] p 4535 N94-37166
MAGNETIC LEVITATION VEHICLES
Study of Japanese electrodynamic-suspension maglev systems
[DE94-011486] p 4452 N94-37515
MAGNETIC MEASUREMENT
Flux creep: Its dependence on current denisty and relation to critical current densities from transport and magnetic measurements
[DE94-011701] p 4440 N94-37738
MAGNETIC MIRRORS
Bounce resonance heating and transport in a magnetic mirror
[DE94-727545] p 4531 N94-37486
MAGNETIC SHIELDING
Applications of high transition temperature superconductors at the Savannah River Site
[DE94-012938] p 4536 N94-37311
MAGNETIC STORMS
Analysis of plasma measurements for the Geotail mission
[NASA-CR-196274] p 4470 N94-37470
Random and periodic substorms and their origins in the solar wind
[DE94-011693] p 4549 N94-37668
Substorm statistics: Occurrences and amplitudes
[DE94-011694] p 4471 N94-37669
MAGNETIC SUSPENSION
Optical position measurement for a large gap magnetic suspension system: Design and performance analysis
[NASA-TP-3438] p 4447 N94-36946
Melt-processing of Y-Ba-Cu-O superconductors for improved levitation
[DE94-011503] p 4537 N94-37377
Large angle magnetic suspension test fixture
[NASA-CR-196138] p 4390 N94-37450
Study of Japanese electrodynamic-suspension maglev systems
[DE94-011486] p 4452 N94-37515
MAGNETITE
Mineralogy and metallurgical properties of iron ore sinter based on magnetite fines
[DE94-763309] p 4414 N94-36525
MAGNETIZATION
Consequences of competing hybridization for magnetic ordering in correlated-electron lattices
[DE94-011648] p 4534 N94-37057
MAGNETOHYDRODYNAMIC FLOW
Q-profile flattening due to nonlinear development of resistive kink mode and ensuing fast crash in sawtooth oscillations
[DE94-727625] p 4526 N94-36472
Momentum-energy transport from turbulence driven by parallel flow shear
[DE94-012765] p 4443 N94-37362

MAGNETOHYDRODYNAMIC STABILITY
Initial studies of reflectometer for ITER
[DE94-012476] p 4526 N94-37167
Confinement improvement in H-mode-like plasmas in helical systems
[DE94-727619] p 4528 N94-37231
Anomalous cross field flux in CHS
[DE94-727547] p 4529 N94-37359
Isotope scaling and eta(i) mode with impurities in tokamak plasmas
[DE94-012763] p 4529 N94-37361
Recent DIII-D high power heating and current drive experiments
[DE94-012509] p 4530 N94-37436
Theory of anomalous transport in H-mode plasmas
[DE94-727546] p 4531 N94-37485
Langmuir waves in the electron-positron plasma
[DE94-616779] p 4531 N94-37728
MAGNETOHYDRODYNAMIC WAVES
Q-profile flattening due to nonlinear development of resistive kink mode and ensuing fast crash in sawtooth oscillations
[DE94-727625] p 4526 N94-36472
MAGNETOHYDRODYNAMICS
A study of physical mechanisms for filament eruption and coronal mass ejection via numerical simulation
[NASA-CR-196087] p 4549 N94-36469
Simulation of three-dimensional multi-phase flow characteristics in the deswirl section of the CDIF MHD power train
[DE94-012644] p 4443 N94-37176
Momentum-energy transport from turbulence driven by parallel flow shear
[DE94-012765] p 4443 N94-37362
Project JOVE — microgravity experiments and applications
[NASA-CR-196292] p 4445 N94-37635
Magnetotail dynamics: MHD simulations of driven and spontaneous dynamic changes
[DE94-011702] p 4471 N94-37701
MAGNETOPAUSE
Origins of energetic ions in the Earth's magnetosheath
[NASA-CR-189359] p 4471 N94-37703
MAGNETORESISTIVITY
Pressure dependence of the conductivity and magnetoconductance in oriented iodine-doped polyacetylene
[PB94-184488] p 4427 N94-37854
MAGNETOSHEATH
Origins of energetic ions in the Earth's magnetosheath
[NASA-CR-189359] p 4471 N94-37703
MAGNETOSPHERIC INSTABILITY
Analysis of plasma measurements for the Geotail mission
[NASA-CR-196274] p 4470 N94-37470
Substorm statistics: Occurrences and amplitudes
[DE94-011694] p 4471 N94-37669
MAGNETS
Design and analysis of high-field quasi-continuous magnets
[DE94-000762] p 4508 N94-36556
BMAP dipole magnetic field analysis and orbit tracking/calculations of energy deposition in GaAs WHEBY detectors
[DE94-012080] p 4522 N94-37303
MAINTENANCE TRAINING
Evaluation of a tool for producing and presenting interactive videodisc job aids
[AD-A278599] p 4432 N94-36473
MAN ENVIRONMENT INTERACTIONS
Science priorities for the human dimensions of global change p 4464 N94-36987
MAN MACHINE SYSTEMS
Virtual Interfaces: Research and Applications
[AGARD-CP-541] p 4482 N94-37261
Task-specific usability requirements for virtual information environments: Interface design and data representation for human operators of complex medical systems p 4483 N94-37262
On the feasibility of virtual environments in medicine p 4483 N94-37264
Interactive large screen: A multi-mode dialogue tool for future cockpits p 4484 N94-37266
The DRA Virtual Cockpit Research Program p 4484 N94-37269
Virtual reality evolution or revolution p 4484 N94-37270
A non-intrusive way to measure point-of-gaze p 4484 N94-37272
Operator gaze position control interfaces: Investigation of psychophysical and operational parameters p 4485 N94-37273
Visual accommodation to virtual image displays when knowledge of object distance conflicts with optical distance p 4485 N94-37278
Aerospace medicine and biology: A continuing bibliography with indexes (supplement 392)
[NASA-SP-7011(392)] p 4482 N94-37445
MANAGEMENT PLANNING
Earth Observing System/Advanced Microwave Sounding Unit-A (EOS/AMSU-A) software management plan
[NASA-CR-189362] p 4461 N94-36919
Earth Observing System (EOS)/Advanced Microwave Sounding Unit A (AMSU-A) configuration management plan
[NASA-CR-189371] p 4494 N94-37061
Toward a new National Weather Service: National Weather Service employee feedback p 4474 N94-37467
MANGANESE
Mechanical behavior and phase stability of NiAl-based shape memory alloys
[DE94-012336] p 4419 N94-37420
Superacid catalysis of light hydrocarbon conversion
[DE94-011132] p 4411 N94-37431
MANIFOLDS (MATHEMATICS)
Localization of topological Pontryagin classes by propagation with finite speed
[PB94-180866] p 4506 N94-37852
Eigenfunction bounds for compact manifolds with integrable geodesic flow
[PB94-180874] p 4506 N94-37853
MANIPULATORS
Technology demonstration of space intravehicular automation and robotics
[NASA-TM-109138] p 4501 N94-37589
Robust stability of second-order systems
[NASA-CR-196384] p 4501 N94-37590
A new technique for dynamic load distribution when two manipulators mutually lift a rigid object, part 2
[DE94-010126] p 4501 N94-37735
MANUAL CONTROL
Manual tracking performance using a virtual hand controller: A comparison study p 4484 N94-37271
MANUFACTURING
MODIL cryocooler producibility demonstration project results
[DE93-019213] p 4430 N94-36444
Amorphous silicon photovoltaic manufacturing technology, phase 2A
[DE94-006895] p 4461 N94-36476
Manufacture and properties of sigma fibre reinforced titanium p 4401 N94-36655
Opportunities for innovation: Biotechnology
[PB94-157831] p 4478 N94-36720
Advanced manufacturing technology for polymer composite structures in Japan p 4422 N94-36968
Scoping economics for the commercial manufacture of metallocene catalysts
[DE94-011526] p 4422 N94-37055
Using nonequilibrium alloying techniques for corrosion inhibition in Gr/Al and Gr/Mg metal matrix composites
[AD-A280529] p 4404 N94-37088
The control of cleanness in powder metallurgy materials for turbine disks p 4421 N94-37325
Maintaining constant standards during the forging process p 4421 N94-37326
Selected case studies in modeling and simulation applied to environmentally conscious design and manufacturing
[DE94-007556] p 4466 N94-37389
A graphic view of Geometric Dimensioning and Tolerancing
[DE94-011478] p 4435 N94-37736
MAPPING
Eurocap program: Ebre Station
[AD-A280418] p 4469 N94-37215
MARANGONI CONVECTION
Coupled Marangoni-Benard/Rayleigh-Benard instability with temperature dependent viscosity
[NASA-TM-106646] p 4444 N94-37507
MARINE CHEMISTRY
MarChem 93, the proceedings, the 1993 workshop on marine chemistry instrumentation
[AD-A279035] p 4475 N94-36446
MARINE METEOROLOGY
Turbulent transfer in the marine planetary boundary layer
[AD-A280549] p 4476 N94-37038
The role of horizontal variability in air-sea interaction
[AD-A280561] p 4476 N94-37047
Experiment on rapidly intensifying cyclones over the Atlantic
[AD-A280365] p 4473 N94-37180
MARKET RESEARCH
Structural composite construction materials manufactured from municipal solid waste
[AD-A280635] p 4403 N94-36730
MARKETING
World jet airplane inventory at year-end 1993
[PB94-164993] p 4384 N94-36530
Opportunities for innovation: Biotechnology
[PB94-157831] p 4478 N94-36720
MARKOV PROCESSES
A note on analytic recovery of transition probabilities in three dimensional diffuse tomography
[DE94-011378] p 4506 N94-37719
MARS ATMOSPHERE
Mars vertical axis wind machines. The design of a Darreus and a Giromill for use on Mars
[NASA-CR-196143] p 4462 N94-36807
Mars vertical axis wind machines: The design of a tornado vortex machine for use on Mars
[NASA-CR-196144] p 4462 N94-36823
An investigation of solar wind effects on the evolution of the Martian atmosphere
[NASA-CR-193424] p 4549 N94-37012
MARS ENVIRONMENT
Operational environments for electrical power wiring on NASA space systems
[NASA-TM-106655] p 4398 N94-36951
Receiver design, performance analysis, and evaluation for space-borne laser altimeters and space-to-space laser ranging systems
[NASA-CR-194747] p 4397 N94-36988
MARS PROBES
Receiver design, performance analysis, and evaluation for space-borne laser altimeters and space-to-space laser ranging systems
[NASA-CR-194747] p 4397 N94-36988
Baseline antenna design for space exploration initiative
[NASA-CR-196298] p 4435 N94-37255
MARTENSITE
Mechanical performance of austempered ductile iron
[AD-A280452] p 4420 N94-37758
MARTENSITIC STAINLESS STEELS
Characterization of nuclear transmutations in materials irradiated test facilities
[DE94-013309] p 4420 N94-37552
MASS DISTRIBUTION
Selected case studies in modeling and simulation applied to environmentally conscious design and manufacturing
[DE94-007556] p 4466 N94-37389
MASS SPECTRA
Production of phi mesons in central Si+Au collisions at 14.6 A GeV/c
[DE94-011726] p 4516 N94-37152
MASS SPECTROMETERS
Method of N-15 analysis by mass-spectroscopy on ion implanter MPB-200
[DE94-618203] p 4407 N94-36529
A fast spectroscopic diagnostic for the measurement of plasma impurity ion dynamics
[DE94-012985] p 4529 N94-37354
MASS SPECTROSCOPY
Metal-carbon nanostructures
[DE94-009177] p 4400 N94-36509
Physics Division annual review, 1 April 1992 - 31 March 1993
[DE94-002497] p 4512 N94-36513
United States Air Force Summer Research Program, 1993. Volume 16: Arnold Engineering Development Center, Frank J. Seiler Research Laboratory and Wilford Hall Medical Center
[AD-A278658] p 4550 N94-36978
Light stable isotope analysis of meteorites by ion microprobe
[NASA-CR-196096] p 4548 N94-37004
Probing flame chemistry with MBMS, theory, and modeling
[DE94-011224] p 4413 N94-37623
MASS TRANSFER
A Lagrangian-Eulerian finite element method with adaptive gridding for advection-dispersion problems
[DE94-011372] p 4506 N94-37718
MASSIVELY PARALLEL PROCESSORS
Turbulence modeling of free shear layers for high performance aircraft
[NASA-CR-196137] p 4442 N94-36808
Parallelized direct execution simulation of message-passing parallel programs
[NASA-CR-194936] p 4497 N94-37411
A scalable high-performance I/O system
[DE94-011513] p 4498 N94-37519
Three-dimensional gyrokinetic particle-in-cell simulation of plasmas on a massively parallel computer: LDRD Core Competency Project
[DE94-013367] p 4532 N94-37732
MATERIALS SCIENCE
JPRS report: Science and technology. Central Eurasia: Materials science
[JPRS-UMS-93-008] p 4404 N94-37010
JPRS report: Science and technology. Central Eurasia: Engineering and equipment
[JPRS-UEQ-93-007] p 4431 N94-37523

MATERIALS TESTS
Methodologies for thermal and mechanical testing of TMC materials p 4401 N94-36659
Experimental and finite-element simulation results for a plane-strain punch-test using isotropic and anisotropic materials
[DE94-011711] p 4457 N94-37670
MATHEMATICAL MODELS
A mixture model for shock compression of porous multi-component reactive materials
[DE93-017638] p 4400 N94-36456
Modelling irradiation creep of zirconium alloys
[DE94-619055] p 4414 N94-36544
Elimination of numerical dispersion in finite-difference modeling and migration by flux-corrected transport
[DE94-004159] p 4510 N94-36551
Accelerated line-by-line calculations for the radiative transfer of trace gases related to climate studies
[DE94-004404] p 4464 N94-36552
Quantum and quasi-classical analyses of high order emission processes
[DE93-041348] p 4513 N94-36697
Modeling the Earth system in the Mission to Planet Earth era
[NASA-TM-109892] p 4461 N94-36827
A PDE-based methodology for modeling, parameter estimation and feedback control in structural and structural acoustic systems
[NASA-CR-194928] p 4500 N94-36924
JPRS report: Central Eurasia. Aviation and cosmonautics, No. 5, May 1993
[JPRS-UAC-94-004] p 4391 N94-37000
DDT modeling and shock compression experiments of porous or damaged energetic materials
[DE94-011419] p 4428 N94-37052
Propagation of radius-tailored laser pulses over extended distances in a uniform plasma
[AD-A280405] p 4528 N94-37182
Some effects of heat release in premixed flames
[DE94-011346] p 4409 N94-37199
Some considerations for modeling the creep behavior of composite materials
[DE94-012112] p 4404 N94-37205
Time-dependent simulations of filament propagation in photoconducting switches
[DE94-012146] p 4438 N94-37213
Spray combustion model improvement study, 1
[NASA-CR-196122] p 4410 N94-37250
Issues concerning the updating of finite-element models from experimental data
[NASA-TM-109116] p 4456 N94-37253
MARFE's in tokamak edge plasma: Pattern formation under nonlocal constraints
[DE94-012766] p 4529 N94-37309
Predicting defect behaviour p 4455 N94-37331
Selected case studies in modeling and simulation applied to environmentally conscious design and manufacturing
[DE94-007556] p 4466 N94-37389
Ionization balance and gain calculations for neon-like selenium x-ray laser plasmas
[DE94-012590] p 4530 N94-37437
Dynamics of a split torque helicopter transmission
[NASA-TM-106410] p 4452 N94-37457
Simple ocean carbon cycle models
[DE94-011745] p 4477 N94-37494
Theoretical studies of a molecular beam generator
[NASA-CR-196306] p 4522 N94-37508
Study of Japanese electrodynamic-suspension maglev systems
[DE94-011486] p 4452 N94-37515
A computational model for three-dimensional jointed media with a single joint set
[DE94-007582] p 4470 N94-37527
Operations and support cost modeling of conceptual space vehicles
[NASA-CR-196299] p 4397 N94-37580
MATHEMATICS
Beginning a dialogue on the changing environment for the physical and mathematical sciences p 4509 N94-36948
MATRICES (MATHEMATICS)
Solving ill-conditioned matrix equations in control
[AD-A280502] p 4503 N94-37146
Parallel tridiagnoalization through two-step band reduction
[DE94-011512] p 4505 N94-37518
A new technique for dynamic load distribution when two manipulators mutually lift a rigid object, part 2
[DE94-010126] p 4501 N94-37735
MATRIX MATERIALS
Properties of TMC processed by fibre coating and hiping p 4401 N94-36656
Oxidation behavior of titanium aluminide matrix materials p 4401 N94-36658
Modeling of outgassing and matrix decomposition in carbon-phenolic composites
[NASA-CR-196319] p 4405 N94-37471
MATTER (PHYSICS)
The Mesozoic Era of relativistic heavy ion physics and beyond
[DE94-011341] p 4548 N94-37557
MAXIMUM ENTROPY METHOD
Determination of interface structure and bonding at atomic resolution in the stem
[DE94-011466] p 4517 N94-37238
The application of maximum entropy to Z-contrast imaging in a stem
[DE94-011470] p 4412 N94-37546
MAXIMUM LIKELIHOOD ESTIMATES
Radar tracking in multipath: Techniques for improved performance p 4395 N94-36631
Index and bulk parameters for frequency-direction spectra measured at CERC Field Research Facility, September 1990 to August 1991
[AD-A280423] p 4476 N94-37216
Index and bulk parameters for frequency-direction spectra measured at CERC Field Research Facility, September 1991 to August 1992
[AD-A280455] p 4477 N94-37229
MAXWELL FLUIDS
Propagation of radius-tailored laser pulses over extended distances in a uniform plasma
[AD-A280405] p 4528 N94-37182
MAXWELL-BOLTZMANN DENSITY FUNCTION
Fast electron generation and transport in a turbulent, magnetized plasma
[DE94-012986] p 4531 N94-37730
MEAN SQUARE VALUES
H infinity control for nonlinear and linear systems
[AD-A280450] p 4494 N94-37226
X-ray diffraction studies of evaporated gold thin films deposited on aluminum nitride substates
[AD-A280454] p 4536 N94-37228
MEASURING INSTRUMENTS
Summary of the extensions of the Standard Model working group
[DE94-002217] p 4512 N94-36527
Methods of calculation of higher power corrections in QCD
[DE94-618511] p 4521 N94-36748
United States Air Force Summer Research Program, 1993. Volume 16: Arnold Engineering Development Center, Frank J. Seiler Research Laboratory and Wilford Hall Medical Center
[AD-A278658] p 4550 N94-36978
A non-intrusive way to measure point-of-gaze p 4484 N94-37272
MECHANICAL DEVICES
Preload release mechanism
[NASA-CASE-MSC-22327-1] p 4450 N94-36839
MECHANICAL ENGINEERING
Integrated Engineering Information Technology, FY 1993 accomplishments
[DE94-011406] p 4545 N94-37563
Advanced Turbine Technology Applications Project (ATTAP)
[NASA-CR-195367] p 4452 N94-37763
MECHANICAL PROPERTIES
Flame resistant fibrous structures development
[NASA-CR-185700] p 4421 N94-36641
Characterisation of Fibre Reinforced Titanium Matrix Composites
[AD-A2775206] p 4400 N94-36649
Possibilities and pitfalls in aerospace applications of titanium matrix composites p 4400 N94-36650
Manufacture and properties of sigma fibre reinforced titanium p 4401 N94-36655
Fibre-matrix interface properties in Ti-matrix composites: Chemical compatibility and micromechanical behaviour p 4401 N94-36657
Methodologies for thermal and mechanical testing of TMC materials p 4401 N94-36659
Processing and mechanical properties of NiAl-based in-situ composites
[NASA-CR-195333] p 4416 N94-36954
Data compatibility for various Charpy-tests
[DE94-617534] p 4416 N94-37074
Chromium/molybdenum alloy plating. Part 1: The electrodeposition of low contraction chromium/molybdenum alloys using unipolar (on/off) pulse plating
[AD-A280236] p 4417 N94-37138
Defect initiation/growth and energy dissipation induced by deformation and fracture
[AD-A280411] p 4424 N94-37184
A fully coupled thermal, chemical, mechanical cookoff model
[DE94-011432] p 4428 N94-37201
Status review and accomplishments of the Materials Research Center at the University of Pittsburgh
[AD-A280422] p 4399 N94-37214
Mechanical behavior of MoSi2 and MoSi2 composites
[DE94-013116] p 4405 N94-37289
Atomic level characterization of defects in microalloyed NiAl: An atom probe investigation
[DE94-012732] p 4418 N94-37396
Characterization of mechanical properties degradation using small punch testing technique
[DE94-011202] p 4418 N94-37410
Development of durable high-temperature catalysts for natural gas combustion: Catalytic materials (CATMAT (trade name)) properties database
[PB94-171824] p 4412 N94-37462
Micromechanical modeling of advanced materials
[DE94-011249] p 4405 N94-37627
Double network elastomers and method of making same
[AD-D016323] p 4427 N94-37831
MEDICAL ELECTRONICS
On the feasibility of virtual environments in medicine p 4483 N94-37264
MEDICAL EQUIPMENT
On the feasibility of virtual environments in medicine p 4483 N94-37264
MEDICAL SCIENCE
Task-specific usability requirements for virtual information environments: Interface design and data representation for human operators of complex medical systems p 4483 N94-37262
MEDICAL SERVICES
Global Picture Archiving and Communication Systems (GPACS): An overview
[AD-A280617] p 4543 N94-37042
Night vision goggles in Emergency Medical Service (EMS) helicopters
[SCT-93RR-22] p 4487 N94-37742
MELTING
Alternate melting and refining routes p 4421 N94-37323
Process enhancements of superalloy material p 4421 N94-37324
MEMBRANES
Effects of freezing and cold acclimation on the plasma membrane of isolated protoplasts
[DE94-012487] p 4479 N94-37248
MEMORY (COMPUTERS)
Software use control
[DE94-008429] p 4489 N94-36480
Cost-effective computations with boundary interface operators in elliptic problems
[DE94-621506] p 4503 N94-37098
Adaptable binary programs
[AD-A280243] p 4494 N94-37119
SACS: A cache simulator incorporating timing analysis with buffer and memory management
[AD-A280472] p 4494 N94-37230
MENISCI
Determination of the dispersion constant in a constrained vapor bubble thermosyphon
[NASA-CR-196124] p 4442 N94-36992
MENTAL PERFORMANCE
Immersive virtual environments as trainer: System design from a cognitive stance p 4484 N94-37267
MERCURY (METAL)
Modeling atmospheric concentrations and deposition of Hg
[DE94-012633] p 4467 N94-37440
MERCURY CADMIUM TELLURIDES
Use of rotation to suppress thermosolutal convection in directionally solidified binary alloys
[NASA-CR-196372] p 4415 N94-36811
MESON-NUCLEON INTERACTIONS
Search for the H dibaryon by Xi(-) capture on the deuteron
[DE94-011733] p 4520 N94-37672
MESONS
B-lifetime measurements at the tevatron
[DE94-003617] p 4513 N94-36528
B quark production cross sections and the b- (bar b) correlated production cross section at CDF
[DE94-000620] p 4514 N94-36700
Sum rules for 1/m corrections to the form factors of semileptonic B decays
[DE94-618548] p 4514 N94-37065
Mass identified particle production and Bose Einstein correlations at 1800 GeV
[DE94-013418] p 4515 N94-37067
A study of jet handedness in hadronic Z0 decays
[DE94-013358] p 4515 N94-37087
Five-lepton decay modes of muon and tau mesons
[DE94-621636] p 4516 N94-37099
Production of phi mesons in central Si+Au collisions at 14.6 A GeV/c
[DE94-011726] p 4516 N94-37152

Physics with primary beams of the KEK-PS
[DE94-748635] p 4522 N94-37234
Prospects for measuring B(s) mixing at CDF
[DE94-013147] p 4518 N94-37298

MESOSCALE PHENOMENA
Variability of the California Current System off Point Sur, California from April 1988 to December 1990
[AD-A276579] p 4476 N94-36985
On the development of boundary layer secondary circulations resulting from horizontally varying surface heat flux
[DE94-011234] p 4472 N94-37048
Long-range mesoscale modeling of pollutant transport for the European Tracer EXperiment (ETEX)
[DE94-010820] p 4465 N94-37093
Factors influencing the parameterization of anvil clouds within GCMs
[DE94-010794] p 4475 N94-37621

METABOLISM
Chemical and structural characterization of nitroaromatic adducts with hemoglobins
[AD-A280533] p 4480 N94-37089

METABOLITES
Biological determinants of photobioreactor design
[DE94-011665] p 4468 N94-37740

METAL CLUSTERS
Supersonic bare metal cluster beams
[DE94-010790] p 4532 N94-36454
Metal-carbon nanostructures
[DE94-009177] p 4400 N94-36509
Low-energy electron collisions with metal clusters: Electron capture and cluster fragmentation
[DE94-003623] p 4512 N94-36516
Photodissociation and spectroscopy of gas phase bimetallic clusters
[DE94-012607] p 4419 N94-37438

METAL COATINGS
Field emitter array RF amplifier development project. Cathode technology development. Phase 1
[AD-A280515] p 4437 N94-37108
Chromium/molybdenum alloy plating. Part 1: The electrodeposition of low contraction chromium/molybdenum alloys using unipolar (on/off) pulse plating
[AD-A280236] p 4417 N94-37138
Development of intermetallic coatings for fusion power applications
[DE94-012647] p 4419 N94-37442

METAL FATIGUE
Ability of the total strain version of strainrange partitioning to characterize thermomechanical fatigue behavior
[NASA-TM-4556] p 4455 N94-37102
Physical and mechanical metallurgy of NiAl
[NASA-TP-3398] p 4419 N94-37503

METAL FILMS
Irradiation effects in Fe-30 percent Ni alloy during Ar ion implantation
[DE94-619057] p 4415 N94-36564
X-ray diffraction studies of evaporated gold thin films deposited on aluminum nitride substates
[AD-A280454] p 4536 N94-37228
Scanning x-ray diffraction: A technique with high compositional resolution for studying phase formation in co-deposited thin films
[DE94-011496] p 4420 N94-37516

METAL IONS
Direct catalytic decomposition of nitric oxide
[DE94-005025] p 4407 N94-36475
Determination of copper in tap water using solid-phase spectrophotometry
[NASA-TM-106480] p 4408 N94-36537
Consequences of competing hybridization for magnetic ordering in correlated-electron lattices
[DE94-011648] p 4534 N94-37057
Photodissociation and spectroscopy of gas phase bimetallic clusters
[DE94-012607] p 4419 N94-37438

METAL MATRIX COMPOSITES
A coupled/uncoupled deformation and fatigue damage algorithm utilizing the finite element method
[NASA-TM-106526] p 4455 N94-36561
Characterisation of Fibre Reinforced Titanium Matrix Composites
[AD-A2775206] p 4400 N94-36649
Possibilities and pitfalls in aerospace applications of titanium matrix composites p 4400 N94-36650
Applications of Titanium Matrix Composite to large airframe structure p 4400 N94-36651
SCS-6 (tm) fiber reinforced titanium p 4400 N94-36652
Processing of titanium matrix composites p 4401 N94-36653
Composites based on titanium with external and internal reinforcement p 4401 N94-36654
Manufacture and properties of sigma fibre reinforced titanium p 4401 N94-36655
Properties of TMC processed by fibre coating and hiping p 4401 N94-36656
Oxidation behavior of titanium aluminide matrix materials p 4401 N94-36658
Methodologies for thermal and mechanical testing of TMC materials p 4401 N94-36659
Ultrasonic nondestructive characterization methods for the development and life prediction of titanium matrix composites p 4401 N94-36660
Metal matrix composites: Analysis of simple specimens and model components under creep and fatigue loading p 4402 N94-36661
Residual strength and life prediction techniques for Ti MMC p 4402 N94-36662
Process/composite concurrent tailoring of SiC/Ti composites p 4402 N94-36663
Micromechanical modeling of damage growth in titanium based metal-matrix composites p 4402 N94-36664
Crack growth under cycle loading in fibre reinforced titanium metal matrix composites p 4402 N94-36665
Prediction of thermal and mechanical stress-strain responses of TMC's subjected to complex TMF histories p 4402 N94-36666
Pre-standardisation work on fatigue and fracture testing of titanium matrix composites p 4402 N94-36667
ASTM and VAMAS activities in titanium matrix composites test methods development p 4403 N94-36668
Development of mechanical testing methods for titanium matrix composites (traction-ogligo-cyclic fatigue) p 4403 N94-36669
Modelling and testing fibre reinforced titanium for design purposes p 4403 N94-36670
NiAl-base composite containing high volume fraction of AlN for advanced engines
[NASA-CASE-LEW-15818-1] p 4403 N94-36752
Feasibility of (IMC)(sub d)-reinforced metal matrix composites
[AD-A280626] p 4404 N94-37044
Using nonequilibrium alloying techniques for corrosion inhibition in Gr/Al and Gr/Mg metal matrix composites
[AD-A280529] p 4404 N94-37088
Status review and accomplishments of the Materials Research Center at the University of Pittsburgh
[AD-A280422] p 4399 N94-37214
A methodology to predict damage initiation, damage growth and residual strength in titanium matrix composites
[NASA-TM-109135] p 4405 N94-37320
Physical and mechanical metallurgy of NiAl
[NASA-TP-3398] p 4419 N94-37503

METAL OXIDES
Activities of the Tandem Accelerator Center, University of Tsukuba
[DE94-748687] p 4522 N94-37237

METAL PARTICLES
Validation and implementation of optical diagnostics for particle sizing in rocket motors
[AD-A278581] p 4428 N94-36972

METAL PLATES
Residual stresses in a multi-pass weld in an austenitic stainless steel plate before and after thermal stress relief
[DE94-013278] p 4420 N94-37548

METAL POWDER
NiAl-base composite containing high volume fraction of AlN for advanced engines
[NASA-CASE-LEW-15818-1] p 4403 N94-36752
Substantiating powder metal life methodologies for engines p 4455 N94-37330

METAL PROPELLANTS
Validation and implementation of optical diagnostics for particle sizing in rocket motors
[AD-A278581] p 4428 N94-36972

METAL SURFACES
First results from the Los Alamos plasma source ion implantation experiment
[DE94-003931] p 4414 N94-36461
Atomic and electronic structure of metals and alloys: Rare earths, ultrathin films and surface alloys
[DE94-011581] p 4516 N94-37113
Modelling of surfaces. Part 1: Monatomic metallic surfaces using equivalent crystal theory
[NASA-TM-106680] p 4419 N94-37459
Perfluorodiethoxymethane on nickel and nickel oxide surfaces
[DE94-011200] p 4426 N94-37712
Morphological aspects of surface reactions
[DE94-011208] p 4413 N94-37713

METAL VAPOR LASERS
An externally heated copper vapour laser
[DE94-619484] p 4447 N94-36565
New hollow-cathode electrode for high-power copper lasers
[DE94-011637] p 4448 N94-37244

METAL-GAS SYSTEMS
Metal-carbon nanostructures
[DE94-009177] p 4400 N94-36509

METAL-WATER REACTIONS
Interfaces of high-protection performance polyaryls-coated zinc phosphated steels
[DE94-011732] p 4417 N94-37153

METALLIC GLASSES
Production of amorphous metal layers using ion implantation and investigation of the related modification of some surface properties
[DE94-617509] p 4414 N94-36541

METALORGANIC CHEMICAL VAPOR DEPOSITION
InTlSb for long-wavelength infrared photodetectors and arrays
[AD-A280207] p 4524 N94-37149
Substrate effects on the structure and optical properties of epitaxial PbTiO3 thin films prepared by metal-organic chemical vapor deposition
[DE94-010432] p 4535 N94-37192
Investigation of polycrystalline thin-film CuInSe2 solar cells based on ZnSe windows
[DE94-006936] p 4462 N94-37381

METALS
Data compatibility for various Charpy-tests
[DE94-617534] p 4416 N94-37074
Atomic and electronic structure of metals and alloys: Rare earths, ultrathin films and surface alloys
[DE94-011581] p 4516 N94-37113
Defect initiation/growth and energy dissipation induced by deformation and fracture
[AD-A280411] p 4424 N94-37184
Theory of metal insulator transition in strongly correlated electron systems
[DE94-013135] p 4438 N94-37295
Positron implantation in solids
[DE94-013029] p 4537 N94-37499

METASTABLE ATOMS
First observation of laser-induced resonant annihilation in metastable antiprotonic helium atoms
[DE94-748668] p 4519 N94-37417

METEORITIC COMPOSITION
Light stable isotope analysis of meteorites by ion microprobe
[NASA-CR-196096] p 4548 N94-37004

METEOROLOGICAL PARAMETERS
Chilbolton Advanced Meteorological Radar: A tool for multi-disciplinary atmospheric research
[PB94-167467] p 4432 N94-36567
Terminal Doppler Weather Radar (TDWR) build 5 Test and Evaluation Master Plan (TEMP)
[AD-A280426] p 4434 N94-37218

METEOROLOGICAL RADAR
Chilbolton Advanced Meteorological Radar: A tool for multi-disciplinary atmospheric research
[PB94-167467] p 4432 N94-36567
Terminal Doppler Weather Radar (TDWR) build 5 Test and Evaluation Master Plan (TEMP)
[AD-A280426] p 4434 N94-37218
NASA ER-2 Doppler radar reflectivity calibration for the CAMEX project
[NASA-TM-104611] p 4475 N94-37790

METEOROLOGICAL SERVICES
Toward a new National Weather Service: Weather for those who fly p 4472 N94-36947
Toward a new National Weather Service: National Weather Service employee feedback p 4474 N94-37467

METHANATION
Conversion of acetic acid to methane by thermophiles
[DE94-012478] p 4479 N94-37434

METHANE
Methyl chloride via oxyhydrochlorination of methane
[DE94-010691] p 4406 N94-36450
Rich methane/air flames: Burning velocities, extinction limits, and flammability limit
[DE94-004340] p 4407 N94-36462
UK methane emissions inventory: A scoping study on the use of ambient measurements to reduce uncertainties
[PB94-167855] p 4463 N94-36533
Accelerated line-by-line calculations for the radiative transfer of trace gases related to climate studies
[DE94-004404] p 4464 N94-36552
California residential indoor air quality study. Volume 1: Methodology and descriptive statistics
[PB94-166048] p 4464 N94-36994
Influences of flame-vortex interactions on formation of oxides of nitrogen in curved methane-air diffusion flamelets
[DE94-005105] p 4409 N94-37221

Finite-rate chemistry and transient effects in Direct Numerical Simulations of turbulent non-premixed flames [DE94-005250] p 4410 N94-37222
Conversion of acetic acid to methane by thermophiles [DE94-012478] p 4479 N94-37434
Tropospheric radiative forcing of CH4 [DE94-011628] p 4468 N94-37631

METHYL ALCOHOL
Rich flammability limits in CH3OH/CO/diluent mixtures [DE94-004341] p 4407 N94-36482

METHYL CHLORIDE
Methyl chloride via oxyhydrochlorination of methane [DE94-010691] p 4406 N94-36450

METHYL COMPOUNDS
Infrared spectroscopy of organic free radicals related to combustion processes [DE94-012481] p 4409 N94-37168
Thermal cis-trans isomerization rates of azobenzenes bound in the side chain of some copolymers and blends [AD-A280451] p 4424 N94-37227
Thermodynamic and kinetic aspects of surface acidity [DE94-012351] p 4411 N94-37372

METHYLENE
Diosmacycloalkanes as models for the formation of hydrocarbons from surface methylenes [DE94-011211] p 4413 N94-37754

METRIC SPACE
Note on certain rigid subshifts [PB94-179058] p 4506 N94-37833

MICA
Thermodynamics of minerals stable near the Earth's surface [DE94-012479] p 4539 N94-37094

MICHELSON INTERFEROMETERS
Gaseous effluent monitoring and identification using an imaging Fourier transform spectrometer [DE94-012627] p 4467 N94-37428

MICROANALYSIS
Density and composition analysis using focused MeV ion microbeam techniques [DE94-012241] p 4517 N94-37210
Elemental mapping of segregation in stainless steels with an imaging filter [DE94-012659] p 4417 N94-37304
AEM and AES of radiation-induced segregation in proton-irradiated stainless steels [DE94-012734] p 4418 N94-37398
ALCHEMI formulated for delocalization and anti-site defects [DE94-012740] p 4537 N94-37400
Scanning x-ray diffraction: A technique with high compositional resolution for studying phase formation in co-deposited thin films [DE94-011496] p 4420 N94-37516

MICROBEAMS
Density and composition analysis using focused MeV ion microbeam techniques [DE94-012241] p 4517 N94-37210

MICROCLIMATOLOGY
Surface-layer response over shrub-steppe canopy during springtime [DE94-011235] p 4468 N94-37624

MICROCRACKS
Defect initiation/growth and energy dissipation induced by deformation and fracture [AD-A280411] p 4424 N94-37184
A simple evaluation of thermally-induced streses in the vicinity of the stitch in a through-thickness reinforced cross-ply laminate [NASA-CR-196317] p 4406 N94-37653
Effects of ply thickness on thermal cycle induced damage and thermal strain p 4459 N94-37806

MICROELECTRONICS
Single event mirroring and sense amplifier designs for enhanced SE tolerance of DRAMs [DE94-010397] p 4438 N94-37190
Development of low dielectric constant alumina-based ceramics for microelectronic substrates [DE94-011360] p 4439 N94-37302

MICROGRAVITY
Design and development of experimental facilities for short duration, low-gravity combustion and fire experiments [NASA-CR-196107] p 4389 N94-36967
Methodologies to determine forces on bones and muscles of body segments during exercise, employing compact sensors suitable for use in crowded space vehicles [NASA-CR-196272] p 4487 N94-37458
Project JOVE — microgravity experiments and applications [NASA-CR-196292] p 4445 N94-37635

MICROGRAVITY APPLICATIONS
Project JOVE — microgravity experiments and applications [NASA-CR-196292] p 4445 N94-37635

MICROHARDNESS
First results from the Los Alamos plasma source ion implantation experiment [DE94-003931] p 4414 N94-36461

MICROMECHANICS
Fibre-matrix interface properties in Ti-matrix composites: Chemical compatibility and micromechanical behaviour p 4401 N94-36657
Metal matrix composites: Analysis of simple specimens and model components under creep and fatigue loading p 4402 N94-36661
Micromechanical modeling of damage growth in titanium based metal-matrix composites p 4402 N94-36664
Modelling and testing fibre reinforced titanium for design purposes p 4403 N94-36670
A fully coupled thermal, chemical, mechanical cookoff model [DE94-011432] p 4428 N94-37201
A methodology to predict damage initiation, damage growth and residual strength in titanium matrix composites [NASA-TM-109135] p 4405 N94-37320
Micromechanical modeling of advanced materials [DE94-011249] p 4405 N94-37627
Strength characteristics and crack growth behavior of a composite with well aligned fibers p 4459 N94-37804
Statistical scaling relationships and size effects in the strength and creep rupture of fibrous composites p 4460 N94-37809

MICROORGANISMS
Studying of ion implantation effect on the biology in China [DE94-620692] p 4479 N94-37535
Biological determinants of photobioreactor design [DE94-011665] p 4468 N94-37740

MICROPOROSITY
Mechanical performance of austempered ductile iron [AD-A280452] p 4420 N94-37758

MICROSCOPY
Density and composition analysis using focused MeV ion microbeam techniques [DE94-012241] p 4517 N94-37210
Submicrometer fiber-optic chemical sensors: Measuring pH inside single cells [DE94-004160] p 4525 N94-37532

MICROSTRIP DEVICES
Submillimeter quasioptical Josephson junction oscillator with integrated tuning elements [AD-A280380] p 4534 N94-37036

MICROSTRIP TRANSMISSION LINES
Microwave detection of a superconducting infrared sensor [AD-D016297] p 4440 N94-37769

MICROSTRUCTURE
Studies of the effect of microstructure on the dynamic behavior of granular and particulate media [AD-A279012] p 4455 N94-36520
Characterization and processing of sintered products from nano-crystalline powders generated by the RTDS method [DE94-004765] p 4415 N94-36553
Properties of TMC processed by fibre coating and hiping p 4401 N94-36656
Small-angle x ray scattering studies of microvoids in amorphous-silicon-based semiconductors [DE94-006931] p 4533 N94-36745
Low temperature materials — indium gallium arsenides [AD-A278703] p 4533 N94-36755
Feasibility of (IMC)(sub d)-reinforced metal matrix composites [AD-A280626] p 4404 N94-37044
Chromium/molybdenum alloy plating. Part 1: The electrodeposition of low contraction chromium/molybdenum alloys using unipolar (on/off) pulse plating [AD-A280236] p 4417 N94-37138
Interaction effects of cracks, flaws and damage in ceramic [AD-A280368] p 4423 N94-37181
Microstructure and chemistry of MgO- and CoO-doped nickel-titanate spinels [DE94-012741] p 4537 N94-37382
Atomic level characterization of defects in microalloyed NiAl: An atom probe investigation [DE94-012732] p 4418 N94-37396
The effect of reactive elements on the segregation behavior and microstructure of alpha-Al2O3 scales on beta-NiAl [DE94-012739] p 4418 N94-37399
Micromechanical modeling of advanced materials [DE94-011249] p 4405 N94-37627
Strength characteristics and crack growth behavior of a composite with well aligned fibers p 4459 N94-37804
Scaling effects of defects in fiber-reinforced composites p 4459 N94-37807

MICROWAVE ABSORPTION
Basic studies in plasma wave interactions [AD-A280465] p 4527 N94-37139

MICROWAVE AMPLIFIERS
Field emitter array RF amplifier development project phase one, cathode technology development [AD-A280334] p 4437 N94-37033
Field emitter array RF amplifier development project. Phase 1, option 1 [AD-A280377] p 4437 N94-37035
Microwave generation for magnetic fusion energy applications [DE94-012107] p 4448 N94-37368
Study on the measurement uncertainty of noise properties of a millimeter wave amplifier [PB94-170917] p 4510 N94-37632

MICROWAVE ANTENNAS
Submillimeter quasioptical Josephson junction oscillator with integrated tuning elements [AD-A280380] p 4534 N94-37036

MICROWAVE ATTENUATION
Chilbolton Advanced Meteorological Radar: A tool for multi-disciplinary atmospheric research [PB94-167467] p 4432 N94-36567

MICROWAVE CIRCUITS
Radially combined 30 W, 14-16 GHz amplifier [DE94-010078] p 4432 N94-36471
A novel transition between rectangular waveguide and layered ridge dielectric waveguide [NASA-TM-106661] p 4433 N94-36955
Microwave detection of a superconducting infrared sensor [AD-D016297] p 4440 N94-37769

MICROWAVE EQUIPMENT
Earth Observing System/Advanced Microwave Sounding Unit-A (EOS/AMSU-A) software management plan [NASA-CR-189362] p 4461 N94-36919

MICROWAVE FREQUENCIES
A high power microwave frequency modulated KrF laser [DE94-009303] p 4447 N94-36510
Study on the measurement uncertainty of noise properties of a millimeter wave amplifier [PB94-170917] p 4510 N94-37632

MICROWAVE IMAGERY
A model-based approach for detection of runways and other objects in image sequences acquired using an on-board camera [NASA-CR-196424] p 4446 N94-36812

MICROWAVE LANDING SYSTEMS
A model-based approach for detection of runways and other objects in image sequences acquired using an on-board camera [NASA-CR-196424] p 4446 N94-36812

MICROWAVE OSCILLATORS
Submillimeter quasioptical Josephson junction oscillator with integrated tuning elements [AD-A280380] p 4534 N94-37036

MICROWAVE RADIOMETERS
Two-channel microwave radiometer for observations of total column precipitable water vapor and cloud liquid water path [DE94-007480] p 4471 N94-36479

MICROWAVE REFLECTOMETERS
Microwave reflectometry for fusion plasma diagnostics [DE94-620118] p 4527 N94-36566

MICROWAVE SOUNDING
Earth Observing System/Advanced Microwave Sounding Unit-A (EOS/AMSU-A) software management plan [NASA-CR-189362] p 4461 N94-36919
Earth Observing System (EOS)/Advanced Microwave Sounding Unit A (AMSU-A) configuration management plan [NASA-CR-189371] p 4494 N94-37061

MICROWAVE TUBES
Evaluation of some slow-wave vane structures for aminiature traveling-wave tube at 30 GHz [NASA-TM-106654] p 4437 N94-36819

MICROWAVES
A high power microwave frequency modulated KrF laser [DE94-009303] p 4447 N94-36510
New plasma source of hydrides for epitaxial growth [DE94-006918] p 4533 N94-36744
Behavioral performance in monkeys exposed to TEMPO high-peak-power microwave pulses at 3 GHz [AD-A280551] p 4478 N94-37045
Turning soot into diamonds with microwaves [DE94-013426] p 4422 N94-37068
Suppression of beam-break-up in a standing wave free electron laser two-beam accelerator [DE94-011348] p 4521 N94-37200

MIDCOURSE GUIDANCE
Evaluation of GPS position and attitude determination for automated rendezvous and docking missions
[NASA-CR-4614] p 4397 N94-37506
MILITARY AIRCRAFT
Aircraft battle damage repair for the 1990's and beyond
[AD-A278635] p 4386 N94-36465
MILITARY HELICOPTERS
Planning German Army helicopter maintenance and mission assignment
[AD-A280483] p 4381 N94-37352
MILITARY TECHNOLOGY
Controlled atmospheric breakdown: Applications and research opportunities
[AD-A278584] p 4464 N94-36973
United States Air Force Summer Research Program, 1993. Volume 13: Phillips Laboratory
[AD-A278657] p 4550 N94-36977
United States Air Force Summer Research Program, 1993. Volume 16: Arnold Engineering Development Center, Frank J. Seiler Research Laboratory and Wilford Hall Medical Center
[AD-A278658] p 4550 N94-36978
United States Air Force Summer Research Program, 1993. Volume 3: Phillips Laboratory
[AD-A278694] p 4550 N94-36979
United States Air Force Summer Research Program, 1993. Volume 4: Rome Laboratory
[AD-A278695] p 4551 N94-36980
United States Air Force Summer Research Program, 1993. Volume 8: Phillips Laboratory
[AD-A278698] p 4551 N94-36983
United States Air Force Summer Research Program, 1993. Volume 9: Rome Laboratory
[AD-A278699] p 4551 N94-36984
MILLIMETER WAVES
Intensity of waves diffracted from symmetrical profile lamellar gratings
[DE94-611101] p 4433 N94-36753
A novel transition between rectangular waveguide and layered ridge dielectric waveguide
[NASA-TM-106661] p 4433 N94-36955
Microwave generation for magnetic fusion energy applications
[DE94-012107] p 4448 N94-37368
Study on the measurement uncertainty of noise properties of a millimeter wave amplifier
[PB94-170917] p 4510 N94-37632
MILLING
NiAl-base composite containing high volume fraction of AlN for advanced engines
[NASA-CASE-LEW-15818-1] p 4403 N94-36752
MIMD (COMPUTERS)
Porting industrial codes and developing sparse linear solvers on parallel computers
[PB94-170503] p 4497 N94-36547
MIMO (CONTROL SYSTEMS)
Mixed H2/H-infinity optimization with multiple H infinity constraints
[AD-A280572] p 4388 N94-36733
Eigensystem realization algorithm user's guide forVAX/VMS computers: Version 931216
[NASA-TM-109066] p 4493 N94-36818
H infinity control for nonlinear and linear systems
[AD-A280450] p 4494 N94-37226
MINERALOGY
Mineralogy and metallurgical properties of iron ore sinter based on magnetite fines
[DE94-763309] p 4414 N94-36525
Light stable isotope analysis of meteorites by ion microprobe
[NASA-CR-196096] p 4548 N94-37004
Thermodynamics of minerals stable near the Earth's surface
[DE94-012479] p 4539 N94-37094
MINERALS
Thermodynamics of minerals stable near the Earth's surface
[DE94-012479] p 4539 N94-37094
MINIATURIZATION
Evaluation of some slow-wave vane structures for aminiature traveling-wave tube at 30 GHz
[NASA-TM-106654] p 4437 N94-36819
MINIMAL SURFACES
The problems of the minimal surface and minimal lineal measure in three dimensions
[DE94-013002] p 4479 N94-37355
MINING
Opportunities for innovation: Biotechnology
[PB94-157831] p 4478 N94-36720
MIRRORS
Adaptive optics for laser beamforming in the atmosphere p 4393 N94-36621
MISSILE CONFIGURATIONS
An aerodynamic and static-stability analysis of the Hypersonic Applied Research Technology (HART) missile
[AD-A280631] p 4382 N94-36729
MISSILE DETECTION
UVPI imaging from the LACE satellite: The Low Cost Launch Vehicle (LCLV) rocket plume
[AD-A278785] p 4398 N94-36445
MISSILE TRACKING
UVPI imaging from the LACE satellite: The Low Cost Launch Vehicle (LCLV) rocket plume
[AD-A278785] p 4398 N94-36445
MISSILES
An aerodynamic and static-stability analysis of the Hypersonic Applied Research Technology (HART) missile
[AD-A280631] p 4382 N94-36729
MISSION PLANNING
Planning German Army helicopter maintenance and mission assignment
[AD-A280483] p 4381 N94-37352
MIXING LAYERS (FLUIDS)
The stabilizing effect of compressibility in turbulent shear flow
[NASA-CR-194932] p 4444 N94-37605
Towards enhancing and delaying disturbances in free shear flows
[NASA-CR-194945] p 4445 N94-37606
MIXING RATIOS
The E2/M1 mixing ratio in the excitation of the Delta from polarized photo-reactions
[DE94-004235] p 4510 N94-36442
MIXTURES
Thermal cis-trans isomerization rates of azobenzenes bound in the side chain of some copolymers and blends
[AD-A280451] p 4424 N94-37227
MODULATION
Picosecond laser induced electric field modulation of carotenoid absorption bands
[DE94-009692] p 4512 N94-36524
MODULATORS
Design of a composite filter realizable on practical spatial light modulators
[NASA-CR-196297] p 4525 N94-37579
MODULES
Amorphous silicon photovoltaic manufacturing technology, phase 2A
[DE94-006895] p 4461 N94-36476
MOIRE INTERFEROMETRY
Four beam interferometer manual: Operating instructions for the INEL diffraction Moire interferometer
[DE94-010772] p 4453 N94-36452
MOISTURE
Evaluating plastic assembly processes for high reliability applications using HAST and Assembly Test Chips
[DE94-010750] p 4439 N94-37363
MOLDS
Advanced manufacturing technology for polymer composite structures in Japan p 4422 N94-36968
MOLECULAR BEAM EPITAXY
Low temperature materials — indium gallium arsenides
[AD-A278703] p 4533 N94-36755
The MBE growth and optical quality of BaTiO3 and SrTiO3 thin films on MgO
[DE94-011468] p 4538 N94-37570
MOLECULAR BEAMS
Molecular beam surface analysis
[DE94-010773] p 4406 N94-36453
Theoretical studies of a molecular beam generator
[NASA-CR-196306] p 4522 N94-37508
MOLECULAR BIOLOGY
High resolution electron diffraction analysis of structural changes associated with the photocycle of bacteriorhodopsin
[DE94-011800] p 4479 N94-37156
MOLECULAR CLUSTERS
Status review and accomplishments of the Materials Research Center at the University of Pittsburgh
[AD-A280422] p 4399 N94-37214
Quantum confinement in GaP nanoclusters
[DE94-013119] p 4536 N94-37290
Photodissociation and spectroscopy of gas phase bimetallic clusters
[DE94-012607] p 4419 N94-37438
MOLECULAR DYNAMICS
United States Air Force Summer Research Program, 1993. Volume 5A: Wright Laboratory
[AD-A278696] p 4551 N94-36981
MOLECULAR INTERACTIONS
Microscopic theory of the dielectric response of highly dispersive biological media
[AD-A280516] p 4516 N94-37109
Effects of molecular transport on turbulence-chemistry interactions in a hydrogen-argon-air jet diffusion flame
[DE94-005107] p 4413 N94-37711
MOLECULAR STRUCTURE
United States Air Force Summer Research Program, 1993. Volume 5A: Wright Laboratory
[AD-A278696] p 4551 N94-36981
Comparison of the crystal structure and molecular models of N,N-diisobutyl-2- (octylphenylphosphinyl) acetamide (CMPO)
[DE94-013434] p 4534 N94-37069
High resolution electron diffraction analysis of structural changes associated with the photocycle of bacteriorhodopsin
[DE94-011800] p 4479 N94-37156
Organometallic NLO polymers. 4: Organometallic main-chain, side-chain, and guest-host polymers: A study of their orientation and relaxation using second harmonic generation
[AD-A280347] p 4423 N94-37179
Copper-containing ceramic precursor synthesis: Solid-state transformations and materials technology
[NASA-TM-106556] p 4399 N94-37315
First-principles determination of the polarizabilities of carbon tubules as a function of length
[DE94-013015] p 4537 N94-37356
Tert-butylalumoxanes: Synthetic analogs for methylalumoxane (MAO) and new catalytic routes to polyolefins and polyketones
[AD-A280532] p 4399 N94-37650
MOLECULAR WEIGHT
Probing flame chemistry with MBMS, theory, and modeling
[DE94-011224] p 4413 N94-37623
MOLECULES
The 1st International Symposium on Organic Photochromism: Molecules and Systems
[PB94-179488] p 4399 N94-37531
MOLTEN SALTS
The logic behind thick, liquid-walled, fusion concepts
[DE94-012678] p 4528 N94-37307
MOLYBDENUM
An investigation of molybdenum and molybdenum oxide catalyzed hydrocarbon formation reactions
[DE94-013700] p 4409 N94-37132
MOLYBDENUM ALLOYS
Chromium/molybdenum alloy plating. Part 1: The electrodeposition of low contraction chromium/molybdenum alloys using unipolar (on/off) pulse plating
[AD-A280236] p 4417 N94-37138
MOLYBDENUM COMPOUNDS
Mechanical behavior of MoSi2 and MoSi2 composites
[DE94-013116] p 4405 N94-37289
MOLYBDENUM OXIDES
An investigation of molybdenum and molybdenum oxide catalyzed hydrocarbon formation reactions
[DE94-013700] p 4409 N94-37132
MONOMERS
Thermal cis-trans isomerization rates of azobenzenes bound in the side chain of some copolymers and blends
[AD-A280451] p 4424 N94-37227
Basic solutions to carbon/carbon oxidation: Science and technology
[AD-A280447] p 4404 N94-37232
Synthesis of phthalonitrile resins containing ether and imide linkages with aromatic diamine curing agent
[AD-D016309] p 4427 N94-37778
MONOMOLECULAR FILMS
SAW chemical sensor arrays using new thin-film materials
[DE94-011940] p 4411 N94-37365
Magnetic and structural instabilities of ferromagnetic and antiferromagnetic Fe/Cu(100)
[DE94-011504] p 4509 N94-37517
MONTE CARLO METHOD
MCNP: Multigroup/adjoint capabilities
[DE94-010682] p 4506 N94-36449
Time-step stability for self-consistent Monte Carlo device simulation
[DE94-012145] p 4528 N94-37207
Statistical characterization of rare events p 4454 N94-37327
Positron implantation in solids
[DE94-013029] p 4537 N94-37499
Probability techniques for reliability analysis of composite materials
[NASA-CR-195294] p 4408 N94-37633
MORPHOLOGY
Morphological aspects of surface reactions
[DE94-011208] p 4413 N94-37713
MOTION PERCEPTION
Relation of motion sickness susceptibility to vestibular and behavioral measures of orientation
[NASA-CR-196121] p 4480 N94-37005

The use of a tactile interface to convey position and motion perceptions p 4486 N94-37281

MOTION SICKNESS

Relation of motion sickness susceptibility to vestibular and behavioral measures of orientation [NASA-CR-196121] p 4480 N94-37005

Profile analysis of after-effects experienced during exposure to several virtual reality environments p 4482 N94-37263

MOUNTAINS

Paleoclimate validation of a numerical climate model [DE94-009287] p 4463 N94-36470

MOVING TARGET INDICATORS

MTI compatible coherent sidelobe canceller [AD-D016300] p 4435 N94-37771

MSM (SEMICONDUCTORS)

Low temperature materials — indium gallium arsenides [AD-A278703] p 4533 N94-36755

MULTIGRID METHODS

A method for flow simulation about complex geometries using both structured and unstructured grids [NASA-TM-106633] p 4383 N94-37283

Prediction of film cooling on gas turbine airfoils [NASA-TM-106653] p 4387 N94-37448

Unstructured grid methods for the simulation of 3D transient flows [NASA-CR-196139] p 4444 N94-37525

MULTIMEDIA

Evaluation of a tool for producing and presenting interactive videodisc job aids [AD-A278599] p 4432 N94-36473

Multimedia p 4541 N94-36847

Low cost software-based rendering and stereoscopic interfaces for teleoperation and virtual reality p 4486 N94-37279

The Canadian network for the advancement of research, industry and education (CANARIE) p 4543 N94-37336

Portable color multimedia training systems based on monochrome laptop computers (CBT-in-a-briefcase), with spinoff implications for video uplink and downlink in spaceflight operations [NASA-TM-108460] p 4496 N94-37556

Interactive Collaborative Environments (ICE): Platform independent X application sharing and multi-media over wide area networks [DE94-008868] p 4502 N94-37784

MULTIPATH TRANSMISSION

Radar tracking in multipath: Techniques for improved performance p 4395 N94-36631

Array element gain and phase estimation in the presence of interference [AD-A280381] p 4434 N94-37162

MULTIPHASE FLOW

Multiphase flow with interphase exchanges (MFIX) documentation theory guide [DE94-000087] p 4441 N94-36550

Simulation of three-dimensional multi-phase flow characteristics in the deswirl section of the CDIF MHD power train [DE94-012644] p 4443 N94-37176

MULTIPLE TARGET TRACKING

Multiple target track-while-scan in the airborne EO environment p 4394 N94-36629

Multitarget track initiation using a modified Hough transform p 4395 N94-36630

MULTIPROCESSING (COMPUTERS)

Porting industrial codes and developing sparse linear solvers on parallel computers [PB94-170503] p 4497 N94-36547

MULTISENSOR APPLICATIONS

Adaptive multisensor fusion for the perception and interpretation of outdoor robot scenes [PB94-170719] p 4499 N94-36535

Studies and simulations on sensor fusion and cueing for fighter application p 4395 N94-36632

Sensor data fusion for air to air situation awareness beyond visual range p 4395 N94-36633

Contact level fusion of radar and IRST contacts on almost electromagnetically silent platform p 4395 N94-36634

Adaptive learning of multi-sensor integration techniques with genetic algorithms [DE94-012744] p 4500 N94-37083

MULTISTAGE ROCKET VEHICLES

Aerodynamic characteristics of the National Launch System (NLS) 1 1/2 stage launch vehicle [NASA-TP-3488] p 4384 N94-37577

MULTIVARIATE STATISTICAL ANALYSIS

Chemical recognition software [DE94-012918] p 4495 N94-37496

MUONIUM

Five-lepton decay modes of muon and tau mesons [DE94-621636] p 4516 N94-37099

MUONS

Older muons are wiser: Using time information in (mu)LCR spectroscopy [DE93-018556] p 4511 N94-36457

Measurement and processing of gammas accompanying muon pairs in the reaction pi(-)C yields mu(+)mu(-) + gamma + X at 38 GeV [DE94-617044] p 4512 N94-36523

Radiative and rare mu and pi decays [DE94-618549] p 4515 N94-37066

Five-lepton decay modes of muon and tau mesons [DE94-621636] p 4516 N94-37099

The 24/36/48 Cathode Strip Chamber layout for SSC GEM detector muon subsystem [DE94-012676] p 4439 N94-37306

MUSCLES

Methodologies to determine forces on bones and muscles of body segments during exercise, employing compact sensors suitable for use in crowded space vehicles [NASA-CR-196272] p 4487 N94-37458

MUTAGENS

Studying of ion implantation effect on the biology in China [DE94-620692] p 4479 N94-37535

MUTATIONS

Estimates of cellular mutagenesis from cosmic rays [NASA-TP-3453] p 4481 N94-37282

Studying of ion implantation effect on the biology in China [DE94-620692] p 4479 N94-37535

N

NAP-OF-THE-EARTH NAVIGATION

Advanced information processing system: The Army Fault-Tolerant Architecture detailed design overview [NASA-CR-194924] p 4497 N94-36962

NASA PROGRAMS

Profile of NASA software engineering: Lessons learned from building the baseline p 4492 N94-36500

Impact of Ada in the Flight Dynamics Division: Excitement and frustration p 4492 N94-36501

Software engineering technology transfer: Understanding the process p 4492 N94-36502

NASA STI Program Coordinating Council Eleventh Meeting: NASA STI Modernization Plan [NASA-TM-109415] p 4540 N94-36841

NASA STI modernization plan p 4540 N94-36842

The Engineering Review Board p 4540 N94-36843

RECON Replacement Project p 4541 N94-36844

Electronic SCAN (Selected Current Aerospace Notices) p 4541 N94-36845

Machine Translation Project p 4541 N94-36846

Multimedia p 4541 N94-36847

Electronic document interchange p 4541 N94-36848

Electronic document interchange p 4541 N94-36849

NASA Access Mechanism (NAM) p 4541 N94-36850

Network upgrades p 4541 N94-36851

Standards in the architectural effort p 4541 N94-36852

NASA STI Program Coordinating Council Twelfth Meeting: Standards [NASA-TM-109925] p 4541 N94-36853

STI Architectural Framework Working Group p 4542 N94-36854

Design and development of experimental facilities for short duration, low-gravity combustion and fire experiments [NASA-CR-196107] p 4389 N94-36967

Engineering directorate technical facilities catalog [NASA-TM-109895] p 4390 N94-37443

NASA reload program [NASA-CR-193972] p 4429 N94-37446

NASA commercial technology. Agenda for change [NASA-TM-109898] p 4546 N94-37765

NATIONAL AIRSPACE SYSTEM

AWOS Data Acquisition System (ADAS) Operational Test and Evaluation (OT/E) integration and OT/E operational test report [AD-A280492] p 4473 N94-37143

NATIONAL LAUNCH VEHICLE PROGRAM

Aerodynamic characteristics of the National Launch System (NLS) 1 1/2 stage launch vehicle [NASA-TP-3488] p 4384 N94-37577

NATIONAL PARKS

Vent processes during the 1912 eruption at Novarupta, Katmai National Park, Alaska [DE94-010740] p 4468 N94-36451

NATURAL GAS

Alternative fuel information: Facts about CNG and LPG conversion [DE94-006888] p 4429 N94-37402

Technical evaluation and assessment of CNG/LPG bi-fuel and flex-fuel vehicle viability [DE94-006925] p 4451 N94-37408

NATURAL GAS EXPLORATION

Analysis of deep seismic reflection and other data from the Southern Washington Cascades [DE94-004075] p 4470 N94-37489

NATURAL LANGUAGE PROCESSING

An error-resistant linguistic protocol for air traffic control [NASA-CR-196098] p 4385 N94-37013

NAUSEA

Profile analysis of after-effects experienced during exposure to several virtual reality environments p 4482 N94-37263

Some side-effects of immersion virtual reality p 4482 N94-37277

NAVIER-STOKES EQUATION

Preconditioned implicit solvers for the Navier-Stokes equations on distributed-memory machines [NASA-TM-106449] p 4502 N94-36647

An aerodynamic and static-stability analysis of the Hypersonic Applied Research Technology (HART) missile [AD-A280631] p 4382 N94-36729

An arbitrary grid CFD algorithm for configuration aerodynamics analysis. Volume 1: Theory and validations [NASA-CR-195918] p 4493 N94-36914

An arbitrary grid CFD algorithm for configuration aerodynamics analysis. Volume 2: FEMNAS user guide [NASA-CR-196135] p 4493 N94-36922

Navier-Stokes and potential theory solutions for ahelicopter fuselage and comparison with experiment [NASA-TM-4566] p 4383 N94-36966

A fundamental study of hypersonic unstarts [AD-A280506] p 4443 N94-37128

Flow visualization for Lagrangian particle methods [DE94-010757] p 4443 N94-37195

Prediction of film cooling on gas turbine airfoils [NASA-TM-106653] p 4387 N94-37448

Development of advanced Navier-Stokes solver [NASA-CR-195094] p 4504 N94-37449

NAVIGATION

Evaluation of flame-sprayed polymer coatings for civil works navigation structures [AD-A280507] p 4422 N94-37104

Progress in navigation filter estimate fusion and its application to spacecraft rendezvous [NASA-TM-104794] p 4392 N94-37386

NAVIGATION INSTRUMENTS

Evaluation of flame-sprayed polymer coatings for civil works navigation structures [AD-A280507] p 4422 N94-37104

NEAR FIELDS

EM-ANIMATE: A computer program for displaying and animating electromagnetic near-field and surface-current solutions: Video supplement to NASA Technical Memorandum 4539 [NASA-TM-4539-VIDEO-SUPPL] p 4492 N94-36518

NEAR INFRARED RADIATION

Intensity of waves diffracted from symmetrical profile lamellar gratings [DE94-611101] p 4433 N94-36753

Holmium quasi-two level laser [AD-D016302] p 4449 N94-37772

NEGATIVE FEEDBACK

Robust stabilization of marginally stable positive-real systems [NASA-TM-109136] p 4500 N94-37058

NEGATIVE IONS

Proceedings of the Workshop on Negative Ion Formation and Beam Handling [DE94-748683] p 4518 N94-37360

Production of high current H(-) beams in a cesium seeded volume negative ion source equipped with PG filter [DE94-718962] p 4522 N94-37463

NEODYMIUM

Sensitivity and signal to noise ratio improvement of a one micron ladar system incorporating a neodymium doped optical fiber preamplifier. Laser radar testbed [AD-A280235] p 4447 N94-37137

NEODYMIUM LASERS

Greater than 100 watt average power at 0.53 micron with 25 ns, 2.5 kHz repetition rate pulses from a single power oscillator [DE94-011641] p 4447 N94-37114

High average power pulsed phase conjugate laser with birefringence correction [DE94-012062] p 4447 N94-37160

Advanced laser driver for soft x-ray projection lithography
[DE94-011643] p 4449 N94-37722

NEPTUNE (PLANET)
Plasma and radio waves from Neptune: Source mechanisms and propagation
[NASA-CR-196284] p 4550 N94-37251

NETWORK CONTROL
A comparison of queueing, cluster and distributed computing systems
[NASA-TM-109025] p 4497 N94-36932

NEURAL NETS
Hardware implementation of a desktop supercomputer for high performance image processing
[AD-A280550] p 4489 N94-36731
Neural network for positioning Space Station solar arrays
[NASA-TM-106656] p 4431 N94-36943
Subgrouped real time recurrent learning neural networks
[AD-A280618] p 4500 N94-37043
Simple and efficient method of secondary vertex searching
[DE94-618542] p 4514 N94-37064
Feature and model selection in feedforward neural networks
[AD-A280709] p 4501 N94-37526
Open architecture controllers for advanced manufacturing
[DE94-007572] p 4496 N94-37782
Neurocontrol of a broadband (ATM) Clos' switching network
[PB94-179389] p 4441 N94-37851

NEUROLOGY
Cardiac pressure changes with venous gas embolism and decompression
[AD-A280412] p 4481 N94-37224

NEUROPHYSIOLOGY
Proceedings of SPIE: The International Society for Optical Engineering, Computational Vision Based on Neurobiology, volume 2054
[AD-A278731] p 4523 N94-36468
Cerebral neurochemical mechanisms in stress and anxiety
[AD-A280473] p 4482 N94-37233
Investigation of exposure to Extremely Low Frequency (ELF) magnetic and electric fields: Ongoing animals studies
[DE94-011239] p 4480 N94-37625

NEUROTRANSMITTERS
Cerebral neurochemical mechanisms in stress and anxiety
[AD-A280473] p 4482 N94-37233

NEUTRAL GASES
A role of neutral hydrogen in CHS plasmas with reheat and collapse and comparison with JIPPT-IIU tokamak plasmas
[DE94-718985] p 4530 N94-37384

NEUTRAL PARTICLES
About existence of a baryon with the 3.52 GeV/c2 mass
[DE94-621641] p 4519 N94-37414

NEUTRINOS
Five-lepton decay modes of muon and tau mesons
[DE94-621636] p 4516 N94-37099
Neutrino-nucleon scattering
[DE94-011720] p 4520 N94-37671

NEUTRON BEAMS
Physics with primary beams of the KEK-PS
[DE94-748635] p 4522 N94-37234

NEUTRON COUNTERS
Stopping power of charged particles from 10 eV/amu to 10 GeV/amu
[DE94-719024] p 4518 N94-37387

NEUTRON DIFFRACTION
Structural ground-state of La2CuO4 in the LTO phase: Evidence of local disorder
[DE94-013126] p 4536 N94-37291

NEUTRON DISTRIBUTION
Two-dimensional over-all neutronics analysis of the ITER device
[DE94-718963] p 4530 N94-37464

NEUTRON EMISSION
D-D fusion experiments using fast z-pinches
[DE94-010090] p 4526 N94-36448

NEUTRON IRRADIATION
Modelling irradiation creep of zirconium alloys
[DE94-619055] p 4414 N94-36544
Irradiation assisted stress corrosion cracking of HTH Alloy X-750 and Alloy 625
[DE94-012667] p 4416 N94-37080
Characterization of mechanical properties degradation using small punch testing technique
[DE94-011202] p 4418 N94-37410
Characterization of nuclear transmutations in materials irradiated test facilities
[DE94-013309] p 4420 N94-37552

NEUTRON PHYSICS
An overview of the current status of resonance theory in reactor physics applications
[DE94-010465] p 4521 N94-37194

NEUTRON SCATTERING
The dynamics of hydrogen atoms dissolved in Zr Cr2 alloy
[DE94-618756] p 4520 N94-37652

NEUTRON SOURCES
D-D fusion experiments using fast z-pinches
[DE94-010090] p 4526 N94-36448
Inertial Electrostatic Confinement (IEC) devices
[DE94-013114] p 4529 N94-37316

NEUTRON SPECTRA
User's manual for SNL-SAND-2 code
[DE94-011744] p 4496 N94-37673

NEUTRON STARS
Absolute limit on rotation of gravitationally bound stars
[DE94-011367] p 4548 N94-37049

NEUTRONS
MCNP: Multigroup/adjoint capabilities
[DE94-010682] p 4506 N94-36449
Forward scattering of neutrons from polymeric and magnetic multilayers
[DE93-041158] p 4513 N94-36696
An overview of the current status of resonance theory in reactor physics applications
[DE94-010465] p 4521 N94-37194
Physics with primary beams of the KEK-PS
[DE94-748635] p 4522 N94-37234
Data simulation for the Associated Particle Imaging system
[DE94-012664] p 4518 N94-37305
The logic behind thick, liquid-walled, fusion concepts
[DE94-012678] p 4528 N94-37307
Neutron transport methods on scalable shared memory multiprocessors
[DE94-012324] p 4498 N94-37419

NEWTON-RAPHSON METHOD
Hierarchically parallelized constrained nonlinear solvers with automated substructuring
[NASA-CR-194474] p 4456 N94-37554

NICKEL
Sodium/nickel-chloride battery development
[DE94-011481] p 4437 N94-37053
XAFS-like structure of resonant Raman scattering
[DE94-618410] p 4517 N94-37171
Perfluorodiethoxymethane on nickel and nickel oxide surfaces
[DE94-011200] p 4426 N94-37712

NICKEL ALLOYS
Characterization and processing of sintered products from nano-crystalline powders generated by the RTDS method
[DE94-004765] p 4415 N94-36553
Irradiation effects in Fe-30 percent Ni alloy during Ar ion implantation
[DE94-619057] p 4415 N94-36564
NiAl-base composite containing high volume fraction of AlN for advanced engines
[NASA-CASE-LEW-15818-1] p 4403 N94-36752
Processing and mechanical properties of NiAl-based in-situ composites
[NASA-CR-195333] p 4416 N94-36954
Process enhancements of superalloy material p 4421 N94-37324
Maintaining constant standards during the forging process p 4421 N94-37326
Defects and their effects on the integrity of nickel based aeroengine discs p 4421 N94-37328
Substantiating powder metal life methodologies for engines p 4455 N94-37330
Examination of weldability of Ni-Cr-W superalloys
[DE94-719014] p 4418 N94-37385
Atomic level characterization of defects in microalloyed NiAl: An atom probe investigation
[DE94-012732] p 4418 N94-37396
The effect of reactive elements on the segregation behavior and microstructure of alpha-Al2O3 scales on beta-NiAl
[DE94-012739] p 4418 N94-37399
Mechanical behavior and phase stability of NiAl-based shape memory alloys
[DE94-012336] p 4419 N94-37420
Physical and mechanical metallurgy of NiAl
[NASA-TP-3398] p 4419 N94-37503

NICKEL OXIDES
Perfluorodiethoxymethane on nickel and nickel oxide surfaces
[DE94-011200] p 4426 N94-37712

NIGHT
Laser designation pods optimized concept for day/night operations p 4393 N94-36620

NIGHT FLIGHTS (AIRCRAFT)
Civil use of night vision devices: Evaluation pilot's guide, part 1
[SCT-91RR-43] p 4487 N94-37741
Night vision goggles in Emergency Medical Service (EMS) helicopters
[SCT-93RR-22] p 4487 N94-37742
Assessment of night vision goggle workload: Flight test engineer's guide
[SCT-91RR-45] p 4487 N94-37743

NIGHT VISION
Visual accommodation to virtual image displays when knowledge of object distance conflicts with optical distance p 4485 N94-37278
Civil use of night vision devices: Evaluation pilot's guide, part 1
[SCT-91RR-43] p 4487 N94-37741
Night vision goggles in Emergency Medical Service (EMS) helicopters
[SCT-93RR-22] p 4487 N94-37742
Assessment of night vision goggle workload: Flight test engineer's guide
[SCT-91RR-45] p 4487 N94-37743

NIOBIUM ALLOYS
Precipitation in Zr-2.5 Nb enhanced by proton irradiation
[DE94-619056] p 4415 N94-36563

NITRIC OXIDE
Direct catalytic decomposition of nitric oxide
[DE94-005025] p 4407 N94-36475

NITRIDES
NiAl-base composite containing high volume fraction of AlN for advanced engines
[NASA-CASE-LEW-15818-1] p 4403 N94-36752

NITRILES
Synthesis of phthalonitrile resins containing ether and imide linkages with aromatic diamine curing agent
[AD-D016309] p 4427 N94-37778

NITROBENZENES
Chemical and structural characterization of nitroaromatic adducts with hemoglobins
[AD-A280533] p 4480 N94-37089

NITROGEN
Direct catalytic decomposition of nitric oxide
[DE94-005025] p 4407 N94-36475
Theoretical studies of a molecular beam generator
[NASA-CR-196306] p 4522 N94-37508
Optical spectroscopy of a nitrogen-hydrogen complex in ZnSe
[DE94-011622] p 4413 N94-37630

NITROGEN DIOXIDE
California residential indoor air quality study. Volume 1: Methodology and descriptive statistics
[PB94-166048] p 4464 N94-36994

NITROGEN OXIDES
Dipole forbidden vibrational modes for NO and CO on Cu observed in the far IR
[DE94-003199] p 4408 N94-36559
SIHTI: Energy and environmental technology
[DE94-763290] p 4464 N94-37007
Influences of flame-vortex interactions on formation of oxides of nitrogen in curved methane-air diffusion flamelets
[DE94-005105] p 4409 N94-37221
Stratospheric emissions effects database development
[NASA-CR-4592] p 4467 N94-37607

NITROGEN PLASMA
First results from the Los Alamos plasma source ion implantation experiment
[DE94-003931] p 4414 N94-36461

NITROGEN POLYMERS
Basic solutions to carbon/carbon oxidation: Science and technology
[AD-A280447] p 4404 N94-37232

NITROGEN 15
Method of N-15 analysis by mass-spectroscopy on ion implanter MPB-200
[DE94-618203] p 4407 N94-36529

NITROGLYCERIN
Processing solid propellants for recycling
[DE94-011433] p 4428 N94-37202

NITROUS OXIDES
Influences of flame-vortex interactions on formation of oxides of nitrogen in curved methane-air diffusion flamelets
[DE94-005105] p 4409 N94-37221
Tropospheric radiative forcing of CH4
[DE94-011628] p 4468 N94-37631

NOAA SATELLITES
Variability of the California Current System off Point Sur, California from April 1988 to December 1990
[AD-A278579] p 4476 N94-36985
NOAA polar satellite calibration: A system description
[NOAA-TR-NESDIS-77] p 4396 N94-37009

NOISE (SOUND)
Ground and space flight experiments of the effects of light, sound and/or temperature on animals
[NASA-CR-196102] p 4478 N94-36986
NOISE GENERATORS
Study on the measurement uncertainty of noise properties of a millimeter wave amplifier
[PB94-170917] p 4510 N94-37632
NOISE INTENSITY
Three flights into thunderstorms with the revised Rocket Electric Field Sounding (REFS) payload
[AD-A280424] p 4473 N94-37217
NOISE MEASUREMENT
Study on the measurement uncertainty of noise properties of a millimeter wave amplifier
[PB94-170917] p 4510 N94-37632
NOISE REDUCTION
Forward sweep, low noise rotor blade
[NASA-CASE-LAR-14569-1] p 4386 N94-36767
A PDE-based methodology for modeling, parameter estimation and feedback control in structural and structural acoustic systems
[NASA-CR-194928] p 4500 N94-36924
Noise reduction for speech enhancement using non-linear wavelet processing
[AD-A280469] p 4434 N94-37141
NOISE SPECTRA
Blast overpressure studies with animals and man
[AD-A280240] p 4480 N94-37118
NOISE TEMPERATURE
Study on the measurement uncertainty of noise properties of a millimeter wave amplifier
[PB94-170917] p 4510 N94-37632
NONDESTRUCTIVE TESTS
Characterisation of Fibre Reinforced Titanium Matrix Composites
[AD-A2775206] p 4400 N94-36649
Ultrasonic nondestructive characterization methods for the development and life prediction of titanium matrix composites p 4401 N94-36660
Detection of delaminations in composite beams using piezoelectric sensors
[NASA-TM-106611] p 4403 N94-36956
Density and composition analysis using focused MeV ion microbeam techniques
[DE94-012241] p 4517 N94-37210
Process enhancements of superalloy material p 4421 N94-37324
Development of nondestructive evaluation methods and prediction of effects of flaws on the fracture behavior of structural ceramics
[DE94-012466] p 4425 N94-37423
NONEQUILIBRIUM CONDITIONS
Using nonequilibrium alloying techniques for corrosion inhibition in Gr/Al and Gr/Mg metal matrix composites
[AD-A280529] p 4404 N94-37088
NONEQUILIBRIUM FLOW
A flux splitting scheme with high-resolution and robustness for discontinuities
[NASA-TM-106452] p 4441 N94-36646
Experimental investigation of nozzle/plume aerodynamics at hypersonic speeds
[NASA-CR-195829] p 4382 N94-36687
Hypersonic, nonequilibrium flow over the FIRE 2 forebody at 1634 sec
[NASA-TM-109141] p 4444 N94-37455
Theoretical studies of a molecular beam generator
[NASA-CR-196306] p 4522 N94-37508
NONINTRUSIVE MEASUREMENT
A non-intrusive way to measure point-of-gaze p 4484 N94-37272
NONLINEAR EQUATIONS
Multiquadric collocation methods in the numerical solution of Volterra integral equations with weakly singular kernels
[DE94-013000] p 4505 N94-37497
Hierarchically parallelized constrained nonlinear solvers with automated substructuring
[NASA-CR-194474] p 4456 N94-37554
Tensor-GMRES method for large sparse systems of nonlinear equations
[NASA-CR-196379] p 4505 N94-37655
NONLINEAR OPTICS
Nonlinear optical spectroscopy for surface studies
[DE94-011623] p 4408 N94-37056
Poly(p-phenylene) derivatives new high performance nonlinear optical polymers
[AD-A280248] p 4422 N94-37121
Organic NLO polymers. 2: Main-chain and guest-host Chi(2)NLO polymers: NLO-phore structure versus poling
[AD-A280230] p 4423 N94-37133
Organic nonlinear optical (NLO) polymers. 4: Thermally stable NLO polymers
[AD-A280196] p 4423 N94-37148
Organic NLO polymers. 5: Homopolymerization of indole based NLO-phore: A heterocycle Chi(2)NLO main-chain polymer
[AD-A280229] p 4423 N94-37151
Abstracts of 2nd International Conference on Lasers and their Applications
[DE94-617409] p 4448 N94-37169
Organometallic NLO polymers. 4: Organometallic main-chain, side-chain, and guest-host polymers: A study of their orientation and relaxation using second harmonic generation
[AD-A280347] p 4423 N94-37179
Laser probing of interfaces
[DE94-011300] p 4449 N94-37628
NONLINEAR SYSTEMS
Nonlinearity with disorder: Spatio-temporal complex behavior arising from length scales competition
[DE94-000675] p 4502 N94-36685
Parameter estimation in a structural acoustic system with fully nonlinear coupling conditions
[NASA-CR-194926] p 4503 N94-36991
Theoretical investigations of chaotic dynamics
[AD-A280325] p 4507 N94-37028
H infinity control for nonlinear and linear systems
[AD-A280450] p 4494 N94-37226
The canonical symmetry for integral systems
[DE94-618486] p 4504 N94-37375
NONLINEARITY
Recovering depth from focus using iterative image estimation techniques
[DE94-010994] p 4524 N94-37165
Understanding and managing power system harmonics
[AD-A280627] p 4440 N94-37759
NOREPINEPHRINE
Cerebral neurochemical mechanisms in stress and anxiety
[AD-A280473] p 4482 N94-37233
NORTHERN SKY
Sloan Digital Sky Survey
[DE94-011749] p 4547 N94-37667
NOSE TIPS
An aerodynamic and static-stability analysis of the Hypersonic Applied Research Technology (HART) missile
[AD-A280631] p 4382 N94-36729
NOZZLE DESIGN
NASA reload program
[NASA-CR-193972] p 4429 N94-37446
NOZZLE FLOW
Experimental investigation of nozzle/plume aerodynamics at hypersonic speeds
[NASA-CR-195829] p 4382 N94-36687
Computational investigation of an improved cowl concept for hypersonic propulsive nozzles
[AD-A280596] p 4441 N94-36724
Theoretical studies of a molecular beam generator
[NASA-CR-196306] p 4522 N94-37508
NOZZLE GEOMETRY
Probabilistic assessment of space nuclear propulsion system nozzle
[NASA-TM-106539] p 4457 N94-37704
NOZZLE INSERTS
Mixing and noise benefit versus thrust penalty in supersonic jets using impingement tones
[NASA-TM-106583] p 4382 N94-36686
NUCLEAR EXPLOSION EFFECT
Controlled atmospheric breakdown: Applications and research opportunities
[AD-A278584] p 4464 N94-36973
NUCLEAR EXPLOSIONS
Controlled atmospheric breakdown: Applications and research opportunities
[AD-A278584] p 4464 N94-36973
NUCLEAR FUEL ELEMENTS
TFE verification program
[DE94-009870] p 4398 N94-37514
NUCLEAR FUSION
Towards nuclear fusion reactors
[DE94-748680] p 4528 N94-37235
Three-dimensional gyrokinetic particle-in-cell simulation of plasmas on a massively parallel computer: LDRD Core Competency Project
[DE94-013367] p 4532 N94-37732
NUCLEAR INTERACTIONS
High baryon density from relativistic heavy ion collisions
[DE94-003894] p 4511 N94-36460
An overview of the current status of resonance theory in reactor physics applications
[DE94-010465] p 4521 N94-37194
Strangeness and the quark-gluon plasma: An experimenter's perspective
[DE94-011377] p 4519 N94-37558
NUCLEAR MAGNETIC RESONANCE
Diamond deposition and defect chemistry studied via solid state NMR
[AD-A280609] p 4533 N94-36727
Sodium-23 NMR and complex impedance studies of gel electrolytes based on poly(acrylonitrile)
[AD-A280330] p 4408 N94-37031
Activities of the Tandem Accelerator Center, University of Tsukuba
[DE94-748687] p 4522 N94-37237
Thermal-oxidative pretreatment and evaluation of poly (hexafluoropropene oxide) fluids
[NASA-TM-106659] p 4424 N94-37300
The effects of proton-beam quality on the production of gamma rays for nuclear resonance absorption in nitrogen
[DE94-011609] p 4523 N94-37629
NUCLEAR PHYSICS
Physics Division annual review, 1 April 1992 - 31 March 1993
[DE94-002497] p 4512 N94-36513
NUCLEAR PROPULSION
Probabilistic assessment of space nuclear propulsion system nozzle
[NASA-TM-106539] p 4457 N94-37704
NUCLEAR REACTIONS
Activities of the Tandem Accelerator Center, University of Tsukuba
[DE94-748687] p 4522 N94-37237
NUCLEAR REACTORS
Activities of the Chemical Technology Division
[DE94-013050] p 4410 N94-37357
NUCLEAR RESEARCH
Testing new technology for the heavy ion experiment at CERN
[DE94-004747] p 4521 N94-37220
NUCLEAR ROCKET ENGINES
Conceptual design: TFE verification program
[DE94-012469] p 4398 N94-37433
NUCLEAR WEAPONS
Software use control
[DE94-008429] p 4489 N94-36480
NUCLEATION
Literature review and preliminary studies of fretting and fretting fatigue including special applications to aircraft joints
[AD-A280310] p 4456 N94-37125
Numerical analysis of an impinging jet reactor for the CVD and gas-phase nucleation of titania
[NASA-TM-106619] p 4431 N94-37254
NUCLEON-NUCLEON INTERACTIONS
Hadron production in S+nucleus collisions at 200 GeV/nucleon
[DE94-011344] p 4520 N94-37715
NUCLEON-NUCLEON SCATTERING
The spin observables of electron-nucleon scattering from the formalism of nucleon-nucleon scattering
[DE94-011368] p 4520 N94-37717
NUCLEONS
The form factors of the nucleons
[DE94-013357] p 4515 N94-37086
Neutrino-nucleon scattering
[DE94-011720] p 4520 N94-37671
The spin observables of electron-nucleon scattering from the formalism of nucleon-nucleon scattering
[DE94-011368] p 4520 N94-37717
NUCLIDES
An overview of the current status of resonance theory in reactor physics applications
[DE94-010465] p 4521 N94-37194
NUMERICAL ANALYSIS
Numerical analysis of an impinging jet reactor for the CVD and gas-phase nucleation of titania
[NASA-TM-106619] p 4431 N94-37254
Two-dimensional over-all neutronics analysis of the ITER device
[DE94-718963] p 4530 N94-37464
Langmuir waves in the electron-positron plasma
[DE94-618779] p 4531 N94-37728
NUMERICAL CONTROL
NIPER Lab WARDEN: Description and LabVIEW executable code of a general-purpose laboratory-automation program
[DE94-000125] p 4492 N94-36698
Creation of a virtual world to study human spatial perception during sustained acceleration p 4484 N94-37268
Operator gaze position control interfaces: Investigation of psychophysical and operational parameters p 4485 N94-37273
Advanced information processing system: Hosting of advanced guidance, navigation and control algorithms on AIPS using ASTER
[NASA-CR-194960] p 4499 N94-37583

Open architecture controllers for advanced manufacturing
[DE94-007572] p 4496 N94-37782
What is an open architecture robot controller?
[DE94-007854] p 4501 N94-37783
NUMERICAL DATA BASES
SeaWiFS technical report series. Volume 20: The SeaWiFS bio-optical archive and storage system (SeaBASS), part 1
[NASA-TM-104566-VOL-20-PT-1] p 4475 N94-36958
NUMERICAL STABILITY
Time-step stability for self-consistent Monte Carlo device simulation
[DE94-012145] p 4528 N94-37207

O

OBJECT-ORIENTED PROGRAMMING
Integrating end-to-end threads of control into object-oriented analysis and design
p 4491 N94-36496
Fusing modeling techniques to support domain analysis for reuse opportunities identification
p 4491 N94-36497
Impact of Ada in the Flight Dynamics Division: Excitement and frustration p 4492 N94-36501
Design, implementaion and evaluation of a declarative object-oriented programming language
[PB94-169208] p 4492 N94-36546
ZLIB++: Object-oriented numerical library for differential algebra
[DE94-010839] p 4495 N94-37453
OBSERVATORIES
ARM: A climate process observatory
[DE94-007473] p 4463 N94-36477
OCEAN BOTTOM
Variability of the California Current System off Point Sur, California from April 1988 to December 1990
[AD-A278579] p 4476 N94-36985
OCEAN CURRENTS
Cooling of the West Spitzbergen Current: Wintertime observations west of Svalbard
[AD-A280648] p 4475 N94-36762
Simple ocean carbon cycle models
[DE94-011745] p 4477 N94-37494
OCEAN MODELS
Atmospheric gas
[DE94-007439] p 4465 N94-37187
OCEAN SURFACE
Index and bulk parameters for frequency-direction spectra measured at CERC Field Research Facility, September 1992 to August 1993
[AD-A280233] p 4476 N94-37135
Experiment on rapidly intensifying cyclones over the Atlantic
[AD-A280365] p 4473 N94-37180
Airborne ROWS data report for the high resolution experiment, June 1993
[NASA-TM-104609] p 4477 N94-37397
OCEAN TEMPERATURE
Cooling of the West Spitzbergen Current: Wintertime observations west of Svalbard
[AD-A280648] p 4475 N94-36762
OCEANOGRAPHIC PARAMETERS
SeaWiFS technical report series. Volume 20: The SeaWiFS bio-optical archive and storage system (SeaBASS), part 1
[NASA-TM-104566-VOL-20-PT-1] p 4475 N94-36958
Variability of the California Current System off Point Sur, California from April 1988 to December 1990
[AD-A278579] p 4476 N94-36985
Atmospheric gas
[DE94-007439] p 4465 N94-37187
OCEANOGRAPHY
Variability of the California Current System off Point Sur, California from April 1988 to December 1990
[AD-A278579] p 4476 N94-36985
The role of horizontal variability in air-sea interaction
[AD-A280561] p 4476 N94-37047
OCEANS
The life cycles of intense cyclonic and anticyclonic circulation systems observed over oceans
[NASA-CR-196271] p 4473 N94-37294
OCULOMETERS
Interactive large screen: A multi-mode dialogue tool for future cockpits p 4484 N94-37266
Gaze orientation under G(z)-load. Methodological aspects: Preliminary results p 4485 N94-37274
OFFICE AUTOMATION
Network upgrades p 4541 N94-36851
OILS
Environmental risk management
[DE94-620987] p 4467 N94-37492
OLIGOMERS
Substituted silyl-terminated compounds and polymers thereof
[AD-D016310] p 4427 N94-37779
ON-LINE SYSTEMS
NASA Access Mechanism: Lessons learned document
[NASA-TM-109924] p 4540 N94-36750
Electronic SCAN (Selected Current Aerospace Notices) p 4541 N94-36845
Network upgrades p 4541 N94-36851
Data compatibility for various Charpy-tests
[DE94-617534] p 4416 N94-37074
Wide aperture scintillation hodoscope with FEU-143 photomultipliers
[DE94-618211] p 4515 N94-37075
ONBOARD DATA PROCESSING
Space Generic Open Avionics Architecture (SGOAA) standard specification
[NASA-CR-188290] p 4387 N94-36933
OPERATIONAL HAZARDS
Rotorwash analysis handbook. Volume 1: Development and analysis
[SCT-93RR-17-VOL-1] p 4381 N94-36466
Rotorwash analysis handbook. Volume 2: Appendixes
[SCT-93RR-17-VOL-2] p 4382 N94-36467
OPTICAL COMMUNICATION
The Canadian network for the advancement of research, industry and education (CANARIE) p 4543 N94-37336
OPTICAL COMPUTERS
Fault tolerance in opto-electronic computing
[AD-A280219] p 4453 N94-37150
OPTICAL CORRELATORS
Design of a composite filter realizable on practical spatial light modulators
[NASA-CR-196297] p 4525 N94-37579
OPTICAL COUNTERMEASURES
Time-gated imaging through defense-scattering materials using stimulated Raman amplification
[AD-D016305] p 4440 N94-37775
OPTICAL EQUIPMENT
A new, optical-lever based atomic force microscope
[AD-A280524] p 4524 N94-37110
OPTICAL FIBERS
Sensitivity and signal to noise ratio improvement of a one micron ladar system incorporating a neodymium doped optical fiber preamplifier. Laser radar testbed
[AD-A280235] p 4447 N94-37137
Final report on spectral broadening by cross-phase modulation in linearly birefringent optical fibers
[DE94-010406] p 4524 N94-37191
Guiding hard x rays with glass polycapillary fiber
[DE94-004949] p 4525 N94-37258
Method of forming waveguides with ion exchange of halogen ions
[AD-D016304] p 4526 N94-37774
OPTICAL FILTERS
Design of a composite filter realizable on practical spatial light modulators
[NASA-CR-196297] p 4525 N94-37579
OPTICAL MATERIALS
Determining the refractive index of a lambda/4 thin film on a thick substrate from a transmittance measurement
[DE93-019584] p 4523 N94-36693
Organic NLO polymers. 2: Main-chain and guest-host Chi(2)NLO polymers: NLO-phore structure versus poling
[AD-A280230] p 4423 N94-37133
Organic nonlinear optical (NLO) polymers. 4: Thermally stable NLO polymers
[AD-A280196] p 4423 N94-37148
Organic NLO polymers. 5: Homopolymerization of indole based NLO-phore: A heterocycle Chi(2)NLO main-chain polymer
[AD-A280229] p 4423 N94-37151
Substrate effects on the structure and optical properties of epitaxial PbTiO3 thin films prepared by metal-organic chemical vapor deposition
[DE94-010432] p 4535 N94-37192
Investigation of polycrystalline thin-film CuInSe2 solar cells based on ZnSe windows
[DE94-006936] p 4462 N94-37381
An amorphous fluoropolymer: Next generation optical coating candidate
[DE94-012386] p 4425 N94-37422
OPTICAL MEASUREMENT
Microwave reflectometry for fusion plasma diagnostics
[DE94-620118] p 4527 N94-36566
Initial studies of reflectometer for ITER
[DE94-012476] p 4528 N94-37167
OPTICAL MEASURING INSTRUMENTS
Optical position measurement for a large gap magnetic suspension system: Design and performance analysis
[NASA-TP-3438] p 4447 N94-36946
OPTICAL MICROSCOPES
Combined atomic force and scanning reflection interference contrast microscopy
[AD-A280341] p 4514 N94-37034
A new, optical-lever based atomic force microscope
[AD-A280524] p 4524 N94-37110
OPTICAL PROPERTIES
Azobenzene-containing polymers: Some optoelectronic properties
[AD-A280448] p 4424 N94-37185
Substrate effects on the structure and optical properties of epitaxial PbTiO3 thin films prepared by metal-organic chemical vapor deposition
[DE94-010432] p 4535 N94-37192
The MBE growth and optical quality of BaTiO3 and SrTiO3 thin films on MgO
[DE94-011468] p 4538 N94-37570
Optical studies of dynamical processes in disordered systems
[DE94-011945] p 4538 N94-37676
OPTICAL PUMPING
Advanced laser driver for soft x-ray projection lithography
[DE94-011643] p 4449 N94-37722
OPTICAL RADAR
Receiver design, performance analysis, and evaluation for space-borne laser altimeters and space-to-space laser ranging systems
[NASA-CR-194747] p 4397 N94-36988
Sensitivity and signal to noise ratio improvement of a one micron ladar system incorporating a neodymium doped optical fiber preamplifier. Laser radar testbed
[AD-A280235] p 4447 N94-37137
OPTICAL SWITCHING
Time-dependent simulations of filament propagation in photoconducting switches
[DE94-012146] p 4438 N94-37213
OPTICAL TRACKING
Pointing and Tracking Systems
[AGARD-CP-539] p 4392 N94-36616
Pointing and tracking concept for a high energy laser weapon application p 4393 N94-36619
Global Positioning System Synchronized Active Light Autonomous Docking System
[NASA-CASE-MFS-28853-1] p 4395 N94-36825
Optical position measurement for a large gap magnetic suspension system: Design and performance analysis
[NASA-TP-3438] p 4447 N94-36946
United States Air Force Summer Research Program, 1993. Volume 13: Phillips Laboratory
[AD-A278657] p 4550 N94-36977
A more exact analysis of Sandia Laser Tracker data
[DE94-011411] p 4447 N94-37051
OPTICAL TRANSFER FUNCTION
A diffraction-based model of anisoplanatism effects in adaptive optic systems
[AD-A280491] p 4524 N94-37142
OPTICAL WAVEGUIDES
Method of forming waveguides with ion exchange of halogen ions
[AD-D016304] p 4526 N94-37774
OPTIMAL CONTROL
Mixed H2/H-infinity optimization with multiple H infinity constraints
[AD-A280572] p 4388 N94-36733
H2 optimal control with H-infinity, mu, and L1 constraints
[AD-A280593] p 4500 N94-36736
Optimal control theory determination of feasible return-to-launch-site aborts for the HL-20 Personnel Launch System vehicle
[NASA-TP-3449] p 4396 N94-37260
Finite element approximation of an optimal control problem for the von Karman equations
[NASA-CR-194955] p 4505 N94-37540
OPTIMIZATION
New method for minimizing regular functions with constraints on parameter region
[DE94-618340] p 4515 N94-37076
Optimization for minimum sensitivity to uncertain parameters
[NASA-TM-109139] p 4386 N94-37256
OPTOELECTRONIC DEVICES
Design of a composite filter realizable on practical spatial light modulators
[NASA-CR-196297] p 4525 N94-37579
ORBITAL MECHANICS
Configurational evolution dynamics and stability during in-situ development of large orbiting spacecraft
[AD-A280482] p 4397 N94-37351
ORBITAL RENDEZVOUS
Evaluation of GPS position and attitude determination for automated rendezvous and docking missions
[NASA-CR-4614] p 4397 N94-37506
ORGANIC COMPOUNDS
Real-time SAW measurements of NVR in cleanroom and in microenvironment
[DE94-011937] p 4389 N94-37159

SAW chemical sensor arrays using new thin-film materials
[DE94-011940] p 4411 N94-37365
The 1st International Symposium on Organic Photochromism: Molecules and Systems
[PB94-179488] p 4399 N94-37531

ORGANIC PHOSPHORUS COMPOUNDS
Study on extraction behavior of TRPO with different composition
[DE94-620287] p 4412 N94-37534

ORGANOMETALLIC COMPOUNDS
Tert-butylalumoxanes: Synthetic analogs for methylalumoxane (MAO) and new catalytic routes to polyolefins and polyketones
[AD-A280511] p 4399 N94-37106
Tert-butylalumoxanes: Synthetic analogs for methylalumoxane (MAO) and new catalytic routes to polyolefins and polyketones
[AD-A280532] p 4399 N94-37650

ORGANOMETALLIC POLYMERS
Organometallic NLO polymers. 4: Organometallic main-chain, side-chain, and guest-host polymers: A study of their orientation and relaxation using second harmonic generation
[AD-A280347] p 4423 N94-37179

OSCILLATING FLOW
A flux splitting scheme with high-resolution and robustness for discontinuities
[NASA-TM-106452] p 4441 N94-36646

OSCILLATIONS
Q-profile flattening due to nonlinear development of resistive kink mode and ensuing fast crash in sawtooth oscillations
[DE94-727625] p 4526 N94-36472
Suppression of beam-break-up in a standing wave free electron laser two-beam accelerator
[DE94-011348] p 4521 N94-37200

OSCILLATORS
The 250 watt average power electro-quality Q-switched diode pumped power oscillator
[DE94-011644] p 4449 N94-37737

OUTGASSING
Development of high sensitivity techniques for characterizing outgassing of polymeric construction materials for microenvironments
[DE94-012068] p 4424 N94-37204
Modeling of outgassing and matrix decomposition in carbon-phenolic composites
[NASA-CR-196319] p 4405 N94-37471

OVER-THE-HORIZON RADAR
Channel probe measurements for the American Sector Clutter Experiment, January 1994
[DE94-013086] p 4469 N94-37314

OVERPRESSURE
Blast overpressure studies with animals and man
[AD-A280240] p 4480 N94-37118

OXIDATION
Sintering of dioxide pellets in an oxidizing atmosphere (CO2)
[DE94-613046] p 4414 N94-36517
Oxidation behavior of titanium aluminide matrix materials p 4401 N94-36658
Basic solutions to carbon/carbon oxidation: Science and technology
[AD-A280447] p 4404 N94-37232
The effect of reactive elements on the segregation behavior and microstructure of alpha-Al2O3 scales on beta-NiAl
[DE94-012739] p 4418 N94-37399
Bibliography of work on the photocatalytic removal of hazardous compounds from water and air
[DE94-006906] p 4467 N94-37405

OXIDATION RESISTANCE
The effect of reactive elements on the segregation behavior and microstructure of alpha-Al2O3 scales on beta-NiAl
[DE94-012739] p 4418 N94-37399
Physical and mechanical metallurgy of NiAl
[NASA-TP-3398] p 4419 N94-37503

OXIDE FILMS
Substrate effects on the structure and optical properties of epitaxial PbTiO3 thin films prepared by metal-organic chemical vapor deposition
[DE94-010432] p 4535 N94-37192
Time-of-flight pulsed ion beam surface analysis as a means of in situ, real-time characterization of the growth of ferro-electric and conductive oxide heterostructures
[DE94-012628] p 4517 N94-37249
Low temperature atmospheric pressure chemical vapor deposition of group 14 oxide films
[DE94-013115] p 4425 N94-37317

OXIDES
Processing, packaging, and characterization of electroceramic materials for phased array antennas
[AD-A280251] p 4432 N94-36743
Thermodynamics of minerals stable near the Earth's surface
[DE94-012479] p 4539 N94-37094
Time-of-flight pulsed ion beam surface analysis as a means of in situ, real-time characterization of the growth of ferro-electric and conductive oxide heterostructures
[DE94-012628] p 4517 N94-37249
Thermal-oxidative pretreatment and evaluation of poly (hexafluoropropene oxide) fluids
[NASA-TM-106659] p 4424 N94-37300
Study on extraction behavior of TRPO with different composition
[DE94-620287] p 4412 N94-37534

OXIDIZERS
Laser-saturated fluorescence measurements in laminar sooting diffusion flames
[NASA-CR-191025] p 4508 N94-36643

OXYGEN
Atmospheric gas
[DE94-007439] p 4465 N94-37187
Comparison of oxygen and silicon induced reactions at 14.6 A(GeV/C)
[DE94-011923] p 4518 N94-37364

OXYGEN PLASMA
Atomic oxygen treatment for non-contact removal of organic protective coatings from painting surfaces
[NASA-TM-106650] p 4421 N94-36952

OXYGENATION
Potential benefits of oxygen-enriched intake air in a vehicle powered by a spark-ignition engine
[DE94-013452] p 4451 N94-37070

OZONE
Tropospheric radiative forcing of CH4
[DE94-011628] p 4468 N94-37631

P

P WAVES
Detection of the electrocardiogram P-wave using wavelet analysis
[DE94-010791] p 4481 N94-37197

PACKAGING
Processing, packaging, and characterization of electroceramic materials for phased array antennas
[AD-A280251] p 4432 N94-36743

PACKET SWITCHING
Neurocontrol of a broadband (ATM) Clos' switching network
[PB94-179389] p 4441 N94-37851

PAINTS
Atomic oxygen treatment for non-contact removal of organic protective coatings from painting surfaces
[NASA-TM-106650] p 4421 N94-36952
Evaluation of flame-sprayed polymer coatings for civil works navigation structures
[AD-A280507] p 4422 N94-37104
Diode array alternative to paint removal solid-state cw laser
[DE94-011482] p 4448 N94-37203

PAIR PRODUCTION
Angular dependence of parton-parton scattering extracted from hadron pair production in pp collisions at radicals equal to 11.5 GeV
[DE94-611174] p 4511 N94-36504
Measurement and processing of gammas accompanying muon pairs in the reaction pi(-)C yields mu(+)mu(-) + gamma + X at 38 GeV
[DE94-617044] p 4512 N94-36523
Five-lepton decay modes of muon and tau mesons
[DE94-621636] p 4516 N94-37099
A freon-filled, holographic bubble chamber as a high energy photon burst spectrometer
[DE94-011645] p 4446 N94-37723

PANEL METHOD (FLUID DYNAMICS)
Navier-Stokes and potential theory solutions for ahelicopter fuselage and comparison with experiment
[NASA-TM-4566] p 4383 N94-36966

PAPER (MATERIAL)
Structural composite construction materials manufactured from municipal solid waste
[AD-A280635] p 4403 N94-36730

PARABOLIC REFLECTORS
A new, optical-lever based atomic force microscope
[AD-A280524] p 4524 N94-37110

PARALLAX
Gaze orientation under G(z)-load. Methodological aspects: Preliminary results p 4485 N94-37274

PARALLEL COMPUTERS
Advanced information processing system: The Army Fault-Tolerant Architecture detailed design overview
[NASA-CR-194924] p 4497 N94-36962
Parallelized direct execution simulation of message-passing parallel programs
[NASA-CR-194936] p 4497 N94-37411
Three-dimensional gyrokinetic particle-in-cell simulation of plasmas on a massively parallel computer: LDRD Core Competency Project
[DE94-013367] p 4532 N94-37732

PARALLEL FLOW
The alternative faces of turbulent flow
[TM-5-94] p 4442 N94-36934
Momentum-energy transport from turbulence driven by parallel flow shear
[DE94-012765] p 4443 N94-37362

PARALLEL PROCESSING (COMPUTERS)
A transient FETI methodology for large-scale parallel implicit computations in structural mechanics, part 2
[NASA-CR-194823] p 4497 N94-36503
Porting industrial codes and developing sparse linear solvers on parallel computers
[PB94-170503] p 4497 N94-36547
Preconditioned implicit solvers for the Navier-Stokes equations on distributed-memory machines
[NASA-TM-106449] p 4502 N94-36647
Turbulence modeling of free shear layers for high performance aircraft
[NASA-CR-196137] p 4442 N94-36808
Research in parallel computing
[NASA-CR-196267] p 4442 N94-36960
The impact of HPF data layout on the design of efficient and maintainable parallel linear algebra libraries
[DE94-012382] p 4504 N94-37246
Parallelized direct execution simulation of message-passing parallel programs
[NASA-CR-194936] p 4497 N94-37411
Neutron transport methods on scalable shared memory multiprocessors
[DE94-012324] p 4498 N94-37419
Experience with automatic, dynamic load balancing and adaptive finite element computation
[DE94-001422] p 4498 N94-37487
Distributed VIRtual System (DIVIRS) project
[NASA-CR-196262] p 4495 N94-37509
Parallel tridiagnoalization through two-step band reduction
[DE94-011512] p 4505 N94-37518
A scalable parallel algorithm for multiple objective linear programs
[NASA-CR-194920] p 4495 N94-37539
Hierarchically parallelized constrained nonlinear solvers with automated substructuring
[NASA-CR-194474] p 4456 N94-37554
Parallel Spectral Transform Shallow Water Model: A runtime-tunable parallel benchmark code
[DE94-011460] p 4498 N94-37568
Improved load distribution in parallel sparse Cholesky factorization
[NASA-CR-196380] p 4499 N94-37654
Three-dimensional gyrokinetic particle-in-cell simulation of plasmas on a massively parallel computer: LDRD Core Competency Project
[DE94-013367] p 4532 N94-37732
Techniques for real-time parallel processing: Sensor processing case studies
[AD-A280633] p 4499 N94-37760

PARALLEL PROGRAMMING
Porting industrial codes and developing sparse linear solvers on parallel computers
[PB94-170503] p 4497 N94-36547
A compilation system that integrates high performance FORTRAN and FORTRAN M
[DE94-013308] p 4496 N94-37551

PARAMETER IDENTIFICATION
A PDE-based methodology for modeling, parameter estimation and feedback control in structural and structural acoustic systems
[NASA-CR-194928] p 4500 N94-36924
Parameter estimation in a structural acoustic system with fully nonlinear coupling conditions
[NASA-CR-194926] p 4503 N94-36991

PARAMETERIZATION
Two-channel microwave radiometer for observations of total column precipitable water vapor and cloud liquid water path
[DE94-007480] p 4471 N94-36479
Assessing efficiency of software production for NASA-SEL data p 4490 N94-36490
Representing the influence of subgrid topography on hydrology
[DE94-004595] p 4474 N94-37379
Evaluation of parameterizations for pollutant transport and dispersion in an urban street canyon using a three-dimensional dynamic flow model
[DE94-012641] p 4467 N94-37429
A stratiform cloud parameterization for general circulation models
[DE94-011442] p 4474 N94-37566
Factors influencing the parameterization of anvil clouds within GCMs
[DE94-010794] p 4475 N94-37621

PARTIAL DIFFERENTIAL EQUATIONS
A Galerkin method for linear PDE systems in circular geometries with structural acoustic applications
[NASA-CR-194925] p 4503 N94-36923
PARTICLE ACCELERATION
Cosmic rays: Physics and astrophysics. A research briefing
[NASA-CR-196118] p 4550 N94-36921
High Altitude Plasma Instrument (HAPI) data analysis
[NASA-CR-189360] p 4469 N94-36949
PARTICLE ACCELERATOR TARGETS
Coherent multiple-foil x-ray transition radiation
[DE93-040831] p 4525 N94-37486
Experimental particle physics at the University of Pittsburgh
[DE94-011636] p 4521 N94-37721
PARTICLE ACCELERATORS
High Energy Physics Division of research activities
[DE93-019681] p 4521 N94-36694
Propagation of radius-tailored laser pulses over extended distances in a uniform plasma
[AD-A280405] p 4528 N94-37182
Activities of the Tandem Accelerator Center, University of Tsukuba
[DE94-748687] p 4522 N94-37237
Particle physics
[DE94-012944] p 4518 N94-37312
Experimental particle physics at the University of Pittsburgh
[DE94-011636] p 4521 N94-37721
PARTICLE BEAMS
Symplectic tracking using point magnets and a reference orbit made of circular arcs and straight lines
[DE94-011919] p 4505 N94-37675
PARTICLE COLLISIONS
B quark production cross sections and the b- (bar b) correlated production cross section at CDF
[DE94-000620] p 4514 N94-36700
Hard diffraction and deep inelastic scattering
[DE94-013353] p 4515 N94-37084
Precise determination of the weak mixing angle from a measurement of ALR in e(+)e(-) yields Z0
[DE94-013355] p 4515 N94-37085
Direct photoionization of excited helium
[DE94-618732] p 4516 N94-37097
A rejection method for selection of scattered states
[DE94-012232] p 4517 N94-37209
Stopping power of charged particles from 10 eV/amu to 10 GeV/amu
[DE94-719024] p 4518 N94-37387
The angular and energy distributions of ejected electrons in electron-impact ionization of helium
[DE94-618748] p 4519 N94-37528
Hadron production in S+nucleus collisions at 200 GeV/nucleon
[DE94-011344] p 4520 N94-37715
PARTICLE DECAY
Top quark search at CDF
[DE94-003643] p 4511 N94-36459
A search for first generation scalar leptoquarks at radical s equal to 1.8 TeV with the D0 detector
[DE94-008846] p 4511 N94-36506
B-lifetime measurements at the tevatron
[DE94-003617] p 4513 N94-36528
High Energy Physics Division of research activities
[DE93-019681] p 4521 N94-36694
Sum rules for 1/m corrections to the form factors of semileptonic B decays
[DE94-618548] p 4514 N94-37065
Radiative and rare mu and pi decays
[DE94-618549] p 4515 N94-37066
New method for minimizing regular functions with constraints on parameter region
[DE94-618340] p 4515 N94-37076
A study of jet handedness in hadronic Z0 decays
[DE94-013358] p 4515 N94-37087
Five-lepton decay modes of muon and tau mesons
[DE94-621636] p 4516 N94-37099
Physics with primary beams of the KEK-PS
[DE94-748635] p 4522 N94-37234
Prospects for measuring B(s) mixing at CDF
[DE94-013147] p 4518 N94-37298
CDF results on electroweak physics
[DE94-011750] p 4520 N94-37674
Experimental particle physics at the University of Pittsburgh
[DE94-011636] p 4521 N94-37721
PARTICLE DENSITY (CONCENTRATION)
High baryon density from relativistic heavy ion collisions
[DE94-003894] p 4511 N94-36460
PARTICLE DIFFUSION
Neutron transport methods on scalable shared memory multiprocessors
[DE94-012324] p 4498 N94-37419
PARTICLE ENERGY
Fundamentals studies of radial wave thermoacoustic engines
[AD-A280534] p 4431 N94-37090
Positron implantation in solids
[DE94-013029] p 4537 N94-37499
PARTICLE INTERACTIONS
Measurement and processing of gammas accompanying muon pairs in the reaction pi(-)C yields mu(+)mu(-) + gamma + X at 38 GeV
[DE94-617044] p 4512 N94-36523
Blois 5: Experimental summary
[DE94-001219] p 4513 N94-36558
High Energy Physics Division of research activities
[DE93-019681] p 4521 N94-36694
PARTICLE MASS
Top quark search at CDF
[DE94-003643] p 4511 N94-36459
About existence of a baryon with the 3.52 GeV/c2 mass
[DE94-621641] p 4519 N94-37414
PARTICLE PRODUCTION
High baryon density from relativistic heavy ion collisions
[DE94-003894] p 4511 N94-36460
High Energy Physics Division of research activities
[DE93-019681] p 4521 N94-36694
Electroweak physics at the Tevatron collider
[DE93-040927] p 4513 N94-36695
B quark production cross sections and the b- (bar b) correlated production cross section at CDF
[DE94-000620] p 4514 N94-36700
Mass identified particle production and Bose Einstein correlations at 1800 GeV
[DE94-013418] p 4515 N94-37067
The mathematical simulation of physical processes in ECR multicharged ions sources
[DE94-618343] p 4515 N94-37077
Hard diffraction and deep inelastic scattering
[DE94-013353] p 4515 N94-37084
Precise determination of the weak mixing angle from a measurement of ALR in e(+)e(-) yields Z0
[DE94-013355] p 4515 N94-37085
Production of phi mesons in central Si+Au collisions at 14.6 A GeV/c
[DE94-011726] p 4516 N94-37152
Kaon correlation systematics in E859
[DE94-011927] p 4516 N94-37158
Comparison of oxygen and silicon induced reactions at 14.6 A(GeV/C)
[DE94-011923] p 4518 N94-37364
About existence of a baryon with the 3.52 GeV/c2 mass
[DE94-621641] p 4519 N94-37414
Strangeness and the quark-gluon plasma: An experimenter's perspective
[DE94-011377] p 4519 N94-37558
CDF results on electroweak physics
[DE94-011750] p 4520 N94-37674
Hadron production in S+nucleus collisions at 200 GeV/nucleon
[DE94-011344] p 4520 N94-37715
Pre-equilibrium parton dynamics: Proceedings
[DE94-011347] p 4520 N94-37716
PARTICLE SPIN
The E2/M1 mixing ratio in the excitation of the Delta from polarized photo-reactions
[DE94-004235] p 4510 N94-36442
Relaxation of the density matrix for an arbitrary spin in random external fields
[DE94-618457] p 4509 N94-37078
Polarization phenomena in quantum chromodynamics
[DE94-010663] p 4539 N94-37543
Neutrino-nucleon scattering
[DE94-011720] p 4520 N94-37671
The spin observables of electron-nucleon scattering from the formalism of nucleon-nucleon scattering
[DE94-011368] p 4520 N94-37717
PARTICLE THEORY
The E2/M1 mixing ratio in the excitation of the Delta from polarized photo-reactions
[DE94-004235] p 4510 N94-36442
High baryon density from relativistic heavy ion collisions
[DE94-003894] p 4511 N94-36460
Radiative and rare mu and pi decays
[DE94-618549] p 4515 N94-37066
Particle physics
[DE94-012944] p 4518 N94-37312
PARTICLE TRACKS
Simple and efficient method of secondary vertex searching
[DE94-618542] p 4514 N94-37064
PARTICLE TRAJECTORIES
Simple and efficient method of secondary vertex searching
[DE94-618542] p 4514 N94-37064
Symplectic tracking using point magnets and a reference orbit made of circular arcs and straight lines
[DE94-011919] p 4505 N94-37675
PARTICULATE REINFORCED COMPOSITES
NiAl-base composite containing high volume fraction of AlN for advanced engines
[NASA-CASE-LEW-15818-1] p 4403 N94-36752
PARTICULATES
Studies of the effect of microstructure on the dynamic behavior of granular and particulate media
[AD-A279012] p 4455 N94-36520
PARTITIONS (MATHEMATICS)
Ability of the total strain version of strainrange partitioning to characterize thermomechanical fatigue behavior
[NASA-TM-4556] p 4455 N94-37102
PARTONS
Angular dependence of parton-parton scattering extracted from hadron pair production in pp collisions at radicals equal to 11.5 GeV
[DE94-611174] p 4511 N94-36504
The Mesozoic Era of relativistic heavy ion physics and beyond
[DE94-011341] p 4548 N94-37557
Pre-equilibrium parton dynamics: Proceedings
[DE94-011347] p 4520 N94-37716
PATENT APPLICATIONS
Supersonic bare metal cluster beams
[DE94-010790] p 4532 N94-36454
PATTERN RECOGNITION
A model-based approach for detection of runways and other objects in image sequences acquired using an on-board camera
[NASA-CR-196424] p 4446 N94-36812
Subgrouped real time recurrent learning neural networks
[AD-A280618] p 4500 N94-37043
Simple and efficient method of secondary vertex searching
[DE94-618542] p 4514 N94-37064
Detection of the electrocardiogram P-wave using wavelet analysis
[DE94-010791] p 4481 N94-37197
Design of a composite filter realizable on practical spatial light modulators
[NASA-CR-196297] p 4525 N94-37579
PECULIAR GALAXIES
Guaranteed time observations support for Faint Object Spectrograph (FOS) on HST
[NASA-CR-196305] p 4547 N94-37037
PEEK
Interfaces of high-protection performance polyaryls-coated zinc phosphated steels
[DE94-011732] p 4417 N94-37153
PEGASUS AIR-LAUNCHED BOOSTER
Preliminary analysis for a Mach 8 crossflow transition experiment on the Pegasus (R) space booster
[NASA-TM-104272] p 4381 N94-36648
PELLETS
Sintering of dioxide pellets in an oxidizing atmosphere (CO2)
[DE94-613046] p 4414 N94-36517
PERFLUORO COMPOUNDS
Perfluorodiethoxymethane on nickel and nickel oxide surfaces
[DE94-011200] p 4426 N94-37712
PERFORMANCE TESTS
Receiver design, performance analysis, and evaluation for space-borne laser altimeters and space-to-space laser ranging systems
[NASA-CR-194747] p 4397 N94-36988
Long-range mesoscale modeling of pollutant transport for the European Tracer EXperiment (ETEX)
[DE94-010820] p 4465 N94-37093
Role of burn-in during qualification testing
[DE94-007864] p 4439 N94-37513
The integrated performance evaluation program quality assurance guidance in support of EM environmental sampling and analysis activities
[DE94-013043] p 4468 N94-37731
Civil use of night vision devices: Evaluation pilot's guide, part 1
[SCT-91RR-43] p 4487 N94-37741
Assessment of night vision goggle workload: Flight test engineer's guide
[SCT-91RR-45] p 4487 N94-37743
Advanced Turbine Technology Applications Project (ATTAP)
[NASA-CR-195367] p 4452 N94-37763

PERICLASE
Microstructure and chemistry of MgO- and CoO-doped nickel-titanate spinels
[DE94-012741] p 4537 N94-37382
PERIODICALS
Electronic journals p 4544 N94-37342
PERMANENT MAGNETS
Permanent superconducting magnets for space applications
[NASA-CR-196293] p 4439 N94-37634
Recent progress of the Los Alamos advanced free electron laser
[DE94-011654] p 4449 N94-37733
PERMITTIVITY
Development of low dielectric constant alumina-based ceramics for microelectronic substrates
[DE94-011360] p 4439 N94-37302
Fluorinated resins with low dielectric constant
[AD-D016303] p 4427 N94-37773
PERSONAL COMPUTERS
Portable color multimedia training systems based on monochrome laptop computers (CBT-in-a-briefcase), with spinoff implications for video uplink and downlink in spaceflight operations
[NASA-TM-108460] p 4496 N94-37556
PERSONNEL MANAGEMENT
Toward a new National Weather Service: National Weather Service employee feedback
p 4474 N94-37467
PERTURBATION
Scattering theory for the quantum envelope of a classical system
[DE94-008530] p 4539 N94-36508
PERTURBATION THEORY
Nonlinearity with disorder: Spatio-temporal complex behavior arising from length scales competition
[DE94-000675] p 4502 N94-36685
PH
A dynamic model of a linear actuator based on polymer hydrogel
[DE94-010800] p 4408 N94-37091
Submicrometer fiber-optic chemical sensors: Measuring pH inside single cells
[DE94-004160] p 4525 N94-37532
PHASE DIAGRAMS
Magnetic and structural instabilities of ferromagnetic and antiferromagnetic Fe/Cu(100)
[DE94-011504] p 4509 N94-37517
PHASE MATCHING
Frequency doubling of copper lasers using temperature-tuned ADP
[DE94-011542] p 4448 N94-37240
PHASE MODULATION
Final report on spectral broadening by cross-phase modulation in linearly birefringent optical fibers
[DE94-010406] p 4524 N94-37191
PHASE SHIFT
Phase shifter for directly sampled bandpass signals
[AD-D016320] p 4440 N94-37840
PHASE STABILITY (MATERIALS)
Process simulation and modeling for advanced intermetallic alloys
[AD-A280327] p 4416 N94-37030
Mechanical behavior and phase stability of NiAl-based shape memory alloys
[DE94-012336] p 4419 N94-37420
PHASE TRANSFORMATIONS
Phase transitions in crystalline solids 1
[DE94-619029] p 4532 N94-36542
Theory of metal insulator transition in strongly correlated electron systems
[DE94-013135] p 4438 N94-37295
Non-equilibrium evolution of the disoriented chiral condensate in heavy-ion collisions
[DE94-012897] p 4522 N94-37310
Analytical electron microscopy examination of solid reaction products in long-term test of SRL 200 waste glasses
[DE94-005482] p 4411 N94-37380
Studies of the III-V compounds in the megaber regime
[DE94-012488] p 4537 N94-37435
Laser probing of interfaces
[DE94-011300] p 4449 N94-37628
PHASED ARRAYS
Processing, packaging, and characterization of electroceramic materials for phased array antennas
[AD-A280251] p 4432 N94-36743
Baseline antenna design for space exploration initiative
[NASA-CR-196298] p 4435 N94-37255
PHENOMENOLOGY
CP violation outside the standard model phenomenology for pedestrians
[DE94-002216] p 4511 N94-36512
PHONEMICS
Segment-based acoustic models for continuous speech recognition
[AD-A280332] p 4434 N94-37032
PHONONS
A rejection method for selection of scattered states
[DE94-012232] p 4517 N94-37209
PHOSPHATES
Isolated SO4-2 and PO4-3 anions do not exist
[AD-A278831] p 4512 N94-36521
PHOSPHINES
Study on extraction behavior of TRPO with different composition
[DE94-620287] p 4412 N94-37534
PHOSPHONIUM COMPOUNDS
Development of immobilized ligands for actinide separations
[DE94-012714] p 4410 N94-37284
PHOSPHORUS COMPOUNDS
Highly fluorinated polymers
[NASA-CR-196270] p 4422 N94-37025
PHOTOCHEMICAL REACTIONS
An investigation of solar wind effects on the evolution of the Martian atmosphere
[NASA-CR-193424] p 4549 N94-37012
Photochemistry without protons. Radical cation chemistry in zeolites
[DE94-012631] p 4412 N94-37439
The 1st International Symposium on Organic Photochromism: Molecules and Systems
[PB94-179488] p 4399 N94-37531
PHOTOCHROMISM
The 1st International Symposium on Organic Photochromism: Molecules and Systems
[PB94-179488] p 4399 N94-37531
PHOTOCONDUCTIVITY
Low temperature materials — indium gallium arsenides
[AD-A278703] p 4533 N94-36755
PHOTOCONDUCTORS
InTlSb for long-wavelength infrared photodetectors and arrays
[AD-A280207] p 4524 N94-37149
Time-dependent simulations of filament propagation in photoconducting switches
[DE94-012146] p 4438 N94-37213
PHOTODETACHMENT
Fast beam studies of free radical photodissociation
[DE94-011380] p 4521 N94-37720
PHOTODISSOCIATION
Photodissociation and spectroscopy of gas phase bimetallic clusters
[DE94-012607] p 4419 N94-37438
Fast beam studies of free radical photodissociation
[DE94-011380] p 4521 N94-37720
PHOTOELASTICITY
Studies of the effect of microstructure on the dynamic behavior of granular and particulate media
[AD-A279012] p 4455 N94-36520
PHOTOELECTRIC EMISSION
Preliminary soft x ray studies of beta-SiC
[DE94-013023] p 4537 N94-37498
A photoemission study of Au, Ge, and O2 deposition on NH4F etched Si(111)
[DE94-013352] p 4519 N94-37553
PHOTOEXCITATION
The E2/M1 mixing ratio in the excitation of the Delta from polarized photo-reactions
[DE94-004235] p 4510 N94-36442
PHOTOIONIZATION
Direct photoionization of excited helium
[DE94-618732] p 4516 N94-37097
Infrared spectroscopy of organic free radicals related to combustion processes
[DE94-012481] p 4409 N94-37168
Resonance photoionization of the excited helium
[DE94-618733] p 4517 N94-37173
PHOTOLUMINESCENCE
The excitation mechanism of praseodymium-doped semiconductors
[AD-A280687] p 4535 N94-37129
PHOTOLYSIS
Metal-carbon nanostructures
[DE94-009177] p 4400 N94-36509
Bond selective chemistry beyond the adiabatic approximation
[DE94-012486] p 4408 N94-37095
PHOTOMETERS
InTlSb for long-wavelength infrared photodetectors and arrays
[AD-A280207] p 4524 N94-37149
PHOTOMETRY
Three-stage attenuation using Glan-Thompson prisms
[AD-A280481] p 4525 N94-37350
PHOTOMULTIPLIER TUBES
Wide aperture scintillation hodoscope with FEU-143 photomultipliers
[DE94-618211] p 4515 N94-37075
PHOTON-ELECTRON INTERACTION
XAFS-like structure of resonant Raman scattering
[DE94-618410] p 4517 N94-37171
PHOTONICS
Poly(p-phenylene) derivatives new high performance nonlinear optical polymers
[AD-A280248] p 4422 N94-37121
PHOTONS
MCNP: Multigroup/adjoint capabilities
[DE94-010682] p 4506 N94-36449
The t(anti t)(gamma) background to pp (yields) W(gamma) + X at the SSC
[DE94-001386] p 4512 N94-36526
Summary of the extensions of the Standard Model working group
[DE94-002217] p 4512 N94-36527
Production of a positron and a bound electron by high-energy photon in a strong Coulomb field
[DE94-618501] p 4514 N94-36747
Direct photoionization of excited helium
[DE94-618732] p 4516 N94-37097
Activities of the Photon Factory
[DE94-748682] p 4522 N94-37236
Experimental particle physics at the University of Pittsburgh
[DE94-011636] p 4521 N94-37721
A freon-filled, holographic bubble chamber as a high energy photon burst spectrometer
[DE94-011645] p 4448 N94-37723
PHOTOPRODUCTION
The E2/M1 mixing ratio in the excitation of the Delta from polarized photo-reactions
[DE94-004235] p 4510 N94-36442
Direct photoproduction of jets in the k(T)-factorisation prescription
[PB94-171139] p 4513 N94-36549
PHOTOSYNTHESIS
Femtosecond transient absorption studies of the light harvesting Chl a/b protein complex of Photosystem 2 in higher plants
[DE94-009684] p 4477 N94-36481
Solvent effects on the energetics and dynamics of ultrafast electron transfer in chlorophyll-porphyrin-acceptor triads
[DE94-009693] p 4477 N94-36554
Femtosecond transient grating studies of electron transfer in porphyrin and chlorophyll donor-acceptor molecules
[DE94-009694] p 4478 N94-36555
High resolution electron diffraction analysis of structural changes associated with the photocycle of bacteriorhodopsin
[DE94-011800] p 4479 N94-37156
PHOTOTRANSISTORS
Time-dependent simulations of filament propagation in photoconducting switches
[DE94-012146] p 4438 N94-37213
PHOTOVOLTAIC EFFECT
Small-angle x ray scattering studies of microvoids in amorphous-silicon-based semiconductors
[DE94-006931] p 4533 N94-36745
PHYSICAL CHEMISTRY
Activities of the Chemical Technology Division
[DE94-013050] p 4410 N94-37357
PHYSICAL EXERCISE
Methodologies to determine forces on bones and muscles of body segments during exercise, employing compact sensors suitable for use in crowded space vehicles
[NASA-CR-196272] p 4487 N94-37458
PHYSICAL FACTORS
On the shape of x ray spectra excited by heavy ions
[DE94-618747] p 4519 N94-37651
PHYSICS
Cosmic rays: Physics and astrophysics. A research briefing
[NASA-CR-196118] p 4550 N94-36921
Beginning a dialogue on the changing environment for the physical and mathematical sciences
p 4509 N94-36948
PHYSIOLOGICAL EFFECTS
Ground and space flight experiments of the effects of light, sound and/or temperature on animals
[NASA-CR-196102] p 4478 N94-36936
Behavioral performance in monkeys exposed to TEMPO high-peak-power microwave pulses at 3 GHz
[AD-A280551] p 4478 N94-37045
Blast overpressure studies with animals and man
[AD-A280240] p 4480 N94-37118
Homeostatic responses to prolonged cold exposure: Human cold acclimatization
[AD-A280234] p 4481 N94-37136

Melatonin, the pineal gland, and circadian rhythms
[AD-A280467] p 4481 N94-37140
Cerebral neurochemical mechanisms in stress and anxiety
[AD-A280473] p 4482 N94-37233

PHYSIOLOGICAL RESPONSES
Investigation of exposure to Extremely Low Frequency (ELF) magnetic and electric fields: Ongoing animals studies
[DE94-011239] p 4480 N94-37625

PHYSIOLOGICAL TESTS
Behavioral performance in monkeys exposed to TEMPO high-peak-power microwave pulses at 3 GHz
[AD-A280551] p 4478 N94-37045
Postural strategies for the continuous control of static and dynamic balance in man
[PB94-184678] p 4487 N94-37812

PHYTOPLANKTON
Phytoplankton blooms and coastal physical processes
[AD-A280646] p 4475 N94-36761

PIEZOELECTRIC TRANSDUCERS
Detection of delaminations in composite beams using piezoelectric sensors
[NASA-TM-106611] p 4403 N94-36956

PILOT PERFORMANCE
The use of a tactile interface to convey position and motion perceptions p 4486 N94-37281
Human factors for flight deck certification personnel
[AD-A280477] p 4487 N94-37347
Composite helicopter accident profiles: Deficient crew/aircraft performance
[SCT-90RR-46] p 4385 N94-37604
Synthetic vision display evaluation studies
[NASA-CR-194963] p 4387 N94-37658

PILOT PLANTS
NIPER Lab WARDEN: Descriptive panels and diagrams for NIPER Lab WARDEN software, volume 2
[DE94-000126] p 4493 N94-36689

PILOTLESS AIRCRAFT
UAV's in climate research: The ARM Unmanned Aerospace Vehicle Program
[DE94-011753] p 4485 N94-37154

PINEAL GLAND
Melatonin, the pineal gland, and circadian rhythms
[AD-A280467] p 4481 N94-37140

PINNING
Critical-state flux-density profiles in type-2 superconducting thin-film strips and disks
[DE94-011199] p 4535 N94-37166

PIONS
Angular dependence of parton-parton scattering extracted from hadron pair production in pp collisions at radicals equal to 11.5 GeV
[DE94-611174] p 4511 N94-36504
Measurement and processing of gammas accompanying muon pairs in the reaction pi(-)C yields mu(+)mu(-) + gamma + X at 38 GeV
[DE94-617044] p 4512 N94-36523
Radiative and rare mu and pi decays
[DE94-618549] p 4515 N94-37066
Mass identified particle production and Bose Einstein correlations at 1800 GeV
[DE94-013418] p 4515 N94-37067
Kaon correlation systematics in E859
[DE94-011927] p 4516 N94-37158
Comparison of oxygen and silicon induced reactions at 14.6 A(GeV/C)
[DE94-011923] p 4518 N94-37364

PIPELINES
First results from a prototype level-1 calorimeter trigger system for LHC, RD 27 (UK) collaboration
[PB94-167475] p 4436 N94-36532
The potential for control of carbon dioxide emissions from integrated gasification/combined-cycle systems
[DE94-012646] p 4465 N94-37100
Jumper connector analysis
[DE94-010373] p 4451 N94-37188

PIPELINING (COMPUTERS)
Adaptable binary programs
[AD-A280243] p 4494 N94-37119

PIPES (TUBES)
Mitigation of harmful effects of welds in zirconium alloy components
[DE94-619033] p 4414 N94-36543
Jumper connector analysis
[DE94-010373] p 4451 N94-37188

PLANE STRAIN
Experimental and finite-element simulation results for a plane-strain punch-test using isotropic and anisotropic materials
[DE94-011711] p 4457 N94-37670

PLANE WAVES
Signal processing for the 1992 Barents Sea tomography experiment
[AD-A278580] p 4476 N94-36971
Scattering cross section of sound waves by the modal element method
[NASA-TM-106667] p 4510 N94-37308

PLANETARY BOUNDARY LAYER
Turbulent transfer in the marine planetary boundary layer
[AD-A280549] p 4476 N94-37038

PLANETARY EVOLUTION
An investigation of solar wind effects on the evolution of the Martian atmosphere
[NASA-CR-193424] p 4549 N94-37012

PLANETARY NEBULAE
Far-infrared emission line spectroscopy of planetary nebulae from the KAO
[NASA-CR-196289] p 4547 N94-37825

PLANETARY RADIATION
Plasma and radio waves from Neptune: Source mechanisms and propagation
[NASA-CR-196284] p 4550 N94-37251

PLANNING
Bootstrap planning: Theory and application
[DE94-006466] p 4501 N94-37425

PLANTS (BOTANY)
Response of plants and ecosystems to CO2 and climate change
[DE94-011583] p 4466 N94-37376
Surface-layer response over shrub-steppe canopy during springtime
[DE94-011235] p 4468 N94-37624

PLASMA COMPOSITION
A role of neutral hydrogen in CHS plasmas with reheat and collapse and comparison with JIPPT-IIU tokamak plasmas
[DE94-718985] p 4530 N94-37384

PLASMA COMPRESSION
Q-profile flattening due to nonlinear development of resistive kink mode and ensuing fast crash in sawtooth oscillations
[DE94-727625] p 4526 N94-36472

PLASMA CONTROL
The role of heating and current drive in ITER
[DE94-012679] p 4527 N94-37082
Confinement improvement in H-mode-like plasmas in helical systems
[DE94-727619] p 4528 N94-37231
Towards nuclear fusion reactors
[DE94-748680] p 4528 N94-37235
Inertial Electrostatic Confinement (IEC) devices
[DE94-013114] p 4529 N94-37316
ELMy-H mode as limit cycle and transient responses of H-modes in tokamaks
[DE94-727510] p 4529 N94-37358
Isotope scaling and eta(i) mode with impurities in tokamak plasmas
[DE94-012763] p 4529 N94-37361
A role of neutral hydrogen in CHS plasmas with reheat and collapse and comparison with JIPPT-IIU tokamak plasmas
[DE94-718985] p 4530 N94-37384
Recent DIII-D high power heating and current drive experiments
[DE94-012509] p 4530 N94-37436
Theory of anomalous transport in H-mode plasmas
[DE94-727546] p 4531 N94-37485

PLASMA CURRENTS
On the interpretation of diamagnetic loop measurements for a current-carrying plasma column in a conducting chamber
[DE94-007107] p 4526 N94-36536
Motional Stark effect upgrades on D3-D
[DE94-013146] p 4528 N94-37297

PLASMA DENSITY
D-D fusion experiments using fast z-pinches
[DE94-010090] p 4526 N94-36448
Microwave reflectometry for fusion plasma diagnostics
[DE94-620118] p 4527 N94-36566
ELMy-H mode as limit cycle and transient responses of H-modes in tokamaks
[DE94-727510] p 4529 N94-37358

PLASMA DIAGNOSTICS
On the interpretation of diamagnetic loop measurements for a current-carrying plasma column in a conducting chamber
[DE94-007107] p 4526 N94-36536
Microwave reflectometry for fusion plasma diagnostics
[DE94-620118] p 4527 N94-36566
Conceptual design for a fast neutron ionization chamber for fusion reactor plasma diagnostics
[DE94-013396] p 4527 N94-37101
Initial studies of reflectometer for ITER
[DE94-012476] p 4528 N94-37167
Motional Stark effect upgrades on D3-D
[DE94-013146] p 4528 N94-37297
A fast spectroscopic diagnostic for the measurement of plasma impurity ion dynamics
[DE94-012985] p 4529 N94-37354
Research using small tokamaks
[DE94-621827] p 4531 N94-37493
A freon-filled, holographic bubble chamber as a high energy photon burst spectrometer
[DE94-011645] p 4446 N94-37723

PLASMA DIFFUSION
Theory of anomalous transport in H-mode plasmas
[DE94-727546] p 4531 N94-37485

PLASMA DRIFT
Anomalous cross field flux in CHS
[DE94-727547] p 4529 N94-37359

PLASMA DYNAMICS
Non-equilibrium evolution of the disoriented chiral condensate in heavy-ion collisions
[DE94-012897] p 4522 N94-37310
ELMy-H mode as limit cycle and transient responses of H-modes in tokamaks
[DE94-727510] p 4529 N94-37358
Bounce resonance heating and transport in a magnetic mirror
[DE94-727545] p 4531 N94-37466

PLASMA HEATING
The role of heating and current drive in ITER
[DE94-012679] p 4527 N94-37082
A role of neutral hydrogen in CHS plasmas with reheat and collapse and comparison with JIPPT-IIU tokamak plasmas
[DE94-718985] p 4530 N94-37384
Recent DIII-D high power heating and current drive experiments
[DE94-012509] p 4530 N94-37436

PLASMA LAYERS
A role of neutral hydrogen in CHS plasmas with reheat and collapse and comparison with JIPPT-IIU tokamak plasmas
[DE94-718985] p 4530 N94-37384
Origins of energetic ions in the Earth's magnetosheath
[NASA-CR-189359] p 4471 N94-37703

PLASMA LOSS
ELMy-H mode as limit cycle and transient responses of H-modes in tokamaks
[DE94-727510] p 4529 N94-37358

PLASMA OSCILLATIONS
Time-step stability for self-consistent Monte Carlo device simulation
[DE94-012145] p 4528 N94-37207
ELMy-H mode as limit cycle and transient responses of H-modes in tokamaks
[DE94-727510] p 4529 N94-37358

PLASMA PHYSICS
D-D fusion experiments using fast z-pinches
[DE94-010090] p 4526 N94-36448
High Altitude Plasma Instrument (HAPI) data analysis
[NASA-CR-189360] p 4469 N94-36949
Dynamics explorer data analysis
[NASA-CR-196141] p 4469 N94-37016
Propagation of radius-tailored laser pulses over extended distances in a uniform plasma
[AD-A280405] p 4528 N94-37182
Towards nuclear fusion reactors
[DE94-748680] p 4528 N94-37235
MARFE's in tokamak edge plasma: Pattern formation under nonlocal constraints
[DE94-012766] p 4529 N94-37309
A role of neutral hydrogen in CHS plasmas with reheat and collapse and comparison with JIPPT-IIU tokamak plasmas
[DE94-718985] p 4530 N94-37384

PLASMA RADIATION
MARFE's in tokamak edge plasma: Pattern formation under nonlocal constraints
[DE94-012766] p 4529 N94-37309

PLASMA TEMPERATURE
On the interpretation of diamagnetic loop measurements for a current-carrying plasma column in a conducting chamber
[DE94-007107] p 4526 N94-36536

PLASMA TURBULENCE
Confinement improvement in H-mode-like plasmas in helical systems
[DE94-727619] p 4528 N94-37231
Momentum-energy transport from turbulence driven by parallel flow shear
[DE94-012765] p 4443 N94-37362
Theory of anomalous transport in H-mode plasmas
[DE94-727546] p 4531 N94-37485

PLASMA WAVES
Basic studies in plasma wave interactions
[AD-A280465] p 4527 N94-37139
Time-step stability for self-consistent Monte Carlo device simulation
[DE94-012145] p 4528 N94-37207
Plasma and radio waves from Neptune: Source mechanisms and propagation
[NASA-CR-196284] p 4550 N94-37251

Langmuir waves in the electron-positron plasma
[DE94-618779] p 4531 N94-37728

PLASMA-ELECTROMAGNETIC INTERACTION
Basic studies in plasma wave interactions
[AD-A280465] p 4527 N94-37139

PLASMAS (PHYSICS)
New plasma source of hydrides for epitaxial growth
[DE94-006918] p 4533 N94-36744
The mathematical simulation of physical processes in ECR multicharged ions sources
[DE94-618343] p 4515 N94-37077
Design of the divertor Thomson scattering system on D3-D
[DE94-012672] p 4527 N94-37081
Improvement study of the divertor configuration of the Steady State Tokamak Reactor (SSTR)
[DE94-718961] p 4531 N94-37484
Langmuir waves in the electron-positron plasma
[DE94-618779] p 4531 N94-37728
Fast electron generation and transport in a turbulent, magnetized plasma
[DE94-012986] p 4531 N94-37730
Three-dimensional gyrokinetic particle-in-cell simulation of plasmas on a massively parallel computer: LDRD Core Competency Project
[DE94-013367] p 4532 N94-37732
Characteristics of ions emitted from high-current hollow cathodes
[NASA-CR-195372] p 4398 N94-37764

PLASTIC COATINGS
Evaluation of flame-sprayed polymer coatings for civil works navigation structures
[AD-A280507] p 4422 N94-37104

PLASTIC DEFORMATION
Literature review and preliminary studies of fretting and fretting fatigue including special applications to aircraft joints
[AD-A280310] p 4456 N94-37125
Defect initiation/growth and energy dissipation induced by deformation and fracture
[AD-A280411] p 4424 N94-37184

PLASTIC PROPERTIES
Ability of the total strain version of strainrange partitioning to characterize thermomechanical fatigue behavior
[NASA-TM-4556] p 4455 N94-37102

PLASTICS
Opportunities for innovation: Biotechnology
[PB94-157831] p 4478 N94-36720
Structural composite construction materials manufactured from municipal solid waste
[AD-A280635] p 4403 N94-36730
Gas microstrip detectors on resistive plastic substrates
[DE94-011336] p 4426 N94-37714
Fluorinated resins with low dielectric constant
[AD-D016303] p 4427 N94-37773

PLATE THEORY
Scaling, elasticity, and CLPT p 4458 N94-37800

PLATEAUS
Short-tower sigma(theta) measurements in the Colorado Plateaus region
[DE94-007478] p 4463 N94-36478

PLATELETS
Evaluation of dried storage of platelets for transfusion: Physiologic integrity and hemostatic functionality
[AD-A280665] p 4480 N94-36764

PLATES (STRUCTURAL MEMBERS)
Angle interferometer cross axis errors
[DE94-006190] p 4446 N94-37388

PLATINUM
The hydrogenolysis and isomerization of light hydrocarbons over Pt catalysts
[DE94-013142] p 4410 N94-37296

PLUMES
UVPI imaging from the LACE satellite: The Low Cost Launch Vehicle (LCLV) rocket plume
[AD-A278785] p 4398 N94-36445
Experimental investigation of nozzle/plume aerodynamics at hypersonic speeds
[NASA-CR-195829] p 4382 N94-36687
NASA reload program
[NASA-CR-193972] p 4429 N94-37446
Program GAUSSPLYM: A tool in Windows environment for studying continuous releases
[PB94-184603] p 4468 N94-37856

POINTING CONTROL SYSTEMS
Pointing and Tracking Systems
[AGARD-CP-539] p 4392 N94-36616
Pointing and tracking concept for a high energy laser weapon application p 4393 N94-36619
Inertial pseudo star reference unit p 4394 N94-36625
Aeroservoelastic stabilization considerations for pointing and tracking systems p 4394 N94-36627
Neural network for positioning Space Station solar arrays
[NASA-TM-106656] p 4431 N94-36943
Large angle magnetic suspension test fixture
[NASA-CR-196138] p 4390 N94-37450

POLAR REGIONS
High Altitude Plasma Instrument (HAPI) data analysis
[NASA-CR-189360] p 4469 N94-36949

POLARIZATION (SPIN ALIGNMENT)
Relaxation of the density matrix for an arbitrary spin in random external fields
[DE94-618457] p 4509 N94-37078
Polarization phenomena in quantum chromodynamics
[DE94-010663] p 4539 N94-37543

POLARIZATION (WAVES)
Chilbolton Advanced Meteorological Radar: A tool for multi-disciplinary atmospheric research
[PB94-167467] p 4432 N94-36567

POLARIZATION CHARACTERISTICS
First-principles determination of the polarizabilities of carbon tubules as a function of length
[DE94-013015] p 4537 N94-37356

POLARIZERS
Three-stage attenuation using Glan-Thompson prisms
[AD-A280481] p 4525 N94-37350

POLICIES
Science priorities for the human dimensions of global change p 4464 N94-36987
JPRS report: Science and technology. Central Eurasia: Space
[JPRS-USP-94-004] p 4391 N94-37002
Comparative alternative/clean fuels provisions of the Clean Air Act Amendments of 1990 and the Energy Policy Act of 1992
[DE94-006887] p 4429 N94-37426

POLLUTION CONTROL
Opportunities for innovation: Biotechnology
[PB94-157831] p 4478 N94-36720
Potential benefits of oxygen-enriched intake air in a vehicle powered by a spark-ignition engine
[DE94-013452] p 4451 N94-37070
Evaluation of flame-sprayed polymer coatings for civil works navigation structures
[AD-A280507] p 4422 N94-37104
Processing solid propellants for recycling
[DE94-011433] p 4428 N94-37202
Bibliography of work on the photocatalytic removal of hazardous compounds from water and air
[DE94-006906] p 4467 N94-37405
Comparative alternative/clean fuels provisions of the Clean Air Act Amendments of 1990 and the Energy Policy Act of 1992
[DE94-006887] p 4429 N94-37426
Biological determinants of photobioreactor design
[DE94-011665] p 4468 N94-37740

POLLUTION MONITORING
UK methane emissions inventory: A scoping study on the use of ambient measurements to reduce uncertainties
[PB94-167855] p 4463 N94-36533
Mexico City air quality research initiative, volume 4
[DE94-013201] p 4466 N94-37299
Gaseous effluent monitoring and identification using an imaging Fourier transform spectrometer
[DE94-012627] p 4467 N94-37428
Program GAUSSPLYM: A tool in Windows environment for studying continuous releases
[PB94-184603] p 4468 N94-37856

POLLUTION TRANSPORT
Long-range mesoscale modeling of pollutant transport for the European Tracer EXperiment (ETEX)
[DE94-010820] p 4465 N94-37093
Modeling of trace constituent transport with the University of Wisconsin global isentropic-sigma model
[DE94-012729] p 4466 N94-37288
Evaluation of parameterizations for pollutant transport and dispersion in an urban street canyon using a three-dimensional dynamic flow model
[DE94-012641] p 4467 N94-37429
Modeling atmospheric concentrations and deposition of Hg
[DE94-012633] p 4467 N94-37440
Program GAUSSPLYM: A tool in Windows environment for studying continuous releases
[PB94-184603] p 4468 N94-37856

POLYACETYLENE
Pressure dependence of the conductivity and magnetoconductance in oriented iodine-doped polyacetylene
[PB94-184488] p 4427 N94-37854

POLYACRYLONITRILE
Sodium-23 NMR and complex impedance studies of gel electrolytes based on poly(acrylonitrile)
[AD-A280330] p 4408 N94-37031
The development of short, high surface area activated carbon fibers
[AD-A280509] p 4404 N94-37105
Basic solutions to carbon/carbon oxidation: Science and technology
[AD-A280447] p 4404 N94-37232

POLYBUTADIENE
Basic solutions to carbon/carbon oxidation: Science and technology
[AD-A280447] p 4404 N94-37232

POLYCARBONATES
Advances in rapid prototyping
[DE94-010075] p 4430 N94-36447
Development of high sensitivity techniques for characterizing outgassing of polymeric construction materials for microenvironments
[DE94-012068] p 4424 N94-37204

POLYCRYSTALS
Modelling irradiation creep of zirconium alloys
[DE94-619055] p 4414 N94-36544
Diamond deposition and defect chemistry studied via solid state NMR
[AD-A280609] p 4533 N94-36727
Effect of thermal annealing on grain boundary chemistry of polycrystalline TlBa2Ca2Cu3O(y) films
[DE94-011464] p 4538 N94-37569

POLYESTERS
Highly fluorinated polymers
[NASA-CR-196270] p 4422 N94-37025

POLYETHER RESINS
Properties of perfluoropolyethers for space applications
[NASA-TM-106616] p 4426 N94-37520

POLYETHYLENES
LET spectra of fragmented 600-MeV/A iron beam on aluminum and polyethylene: A preliminary analysis
[NASA-TP-3436] p 4416 N94-36993

POLYHEDRONS
Efficient contact determination between geometric models
[AD-A280244] p 4494 N94-37120

POLYMER BLENDS
Thermal cis-trans isomerization rates of azobenzenes bound in the side chain of some copolymers and blends
[AD-A280451] p 4424 N94-37227

POLYMER CHEMISTRY
Highly fluorinated polymers
[NASA-CR-196270] p 4422 N94-37025
Tert-butylalumoxanes: Synthetic analogs for methylalumoxane (MAO) and new catalytic routes to polyolefins and polyketones
[AD-A280532] p 4399 N94-37650

POLYMER MATRIX COMPOSITES
Advanced manufacturing technology for polymer composite structures in Japan p 4422 N94-36968

POLYMERIZATION
Highly fluorinated polymers
[NASA-CR-196270] p 4422 N94-37025
Scoping economics for the commercial manufacture of metallocene catalysts
[DE94-011526] p 4422 N94-37055
Tert-butylalumoxanes: Synthetic analogs for methylalumoxane (MAO) and new catalytic routes to polyolefins and polyketones
[AD-A280511] p 4399 N94-37106
Organic NLO polymers. 2: Main-chain and guest-host Chi(2)NLO polymers: NLO-phore structure versus poling
[AD-A280230] p 4423 N94-37133
Organic NLO polymers. 5: Homopolymerization of indole based NLO-phore: A heterocycle Chi(2)NLO main-chain polymer
[AD-A280229] p 4423 N94-37151
Organometallic NLO polymers. 4: Organometallic main-chain, side-chain, and guest-host polymers: A study of their orientation and relaxation using second harmonic generation
[AD-A280347] p 4423 N94-37179
Carborane-siloxane or silane-unsaturated hydrocarbon based polymers
[AD-D016220] p 4425 N94-37482
Fluorinated resins with low dielectric constant
[AD-D016303] p 4427 N94-37773
Synthesis of phthalonitrile resins containing ether and imide linkages with aromatic diamine curing agent
[AD-D016309] p 4427 N94-37778

POLYMERS
Replacement of silicone polymer A with silicone polymer B and the subsequent characterization of the new cellular silicone materials
[DE94-010105] p 4421 N94-36474
Flame resistant fibrous structures development
[NASA-CR-185700] p 4421 N94-36641
Highly fluorinated polymers
[NASA-CR-196270] p 4422 N94-37025

Poly(p-phenylene) derivatives new high performance nonlinear optical polymers
[AD-A280248] p 4422 N94-37121
Organic NLO polymers. 2: Main-chain and guest-host Chi(2)NLO polymers: NLO-phore structure versus poling
[AD-A280230] p 4423 N94-37133
Holographic grating relaxation studies of probe diffusion in amorphous polymers
[AD-A280496] p 4423 N94-37144
Solution characterization of poly(isobornyl methacrylate) in tetrahydrofuran
[AD-A280497] p 4409 N94-37145
Optically induced high efficiency gratings in azo polymer films
[AD-A280505] p 4423 N94-37147
Organic nonlinear optical (NLO) polymers. 4: Thermally stable NLO polymers
[AD-A280196] p 4423 N94-37148
Organic NLO polymers. 5: Homopolymerization of indole based NLO-phore: A heterocycle Chi(2)NLO main-chain polymer
[AD-A280229] p 4423 N94-37151
Azobenzene-containing polymers: Some optoelectronic properties
[AD-A280448] p 4424 N94-37185
Substituted silyl-terminated compounds and polymers thereof
[AD-D016310] p 4427 N94-37779

POLYPEPTIDES
Recombinant protein production and insect cell culture and process
[NASA-CASE-MSC-22336-1] p 4478 N94-36751

POLYPHENYLS
Organic nonlinear optical (NLO) polymers. 4: Thermally stable NLO polymers
[AD-A280196] p 4423 N94-37148

POLYPROPYLENE
Scoping economics for the commercial manufacture of metallocene catalysts
[DE94-011526] p 4422 N94-37055

POLYSILANES
Carborane-(silane or siloxane)-unsaturated hydrocarbon based thermosetting polymers
[AD-D016311] p 4427 N94-37818

POLYSILOXANES
Carborane-(silane or siloxane)-unsaturated hydrocarbon based thermosetting polymers
[AD-D016311] p 4427 N94-37818

POMERONS
The Pomeron and Quantum Chromodynamics (QCD) with many light quarks
[DE94-001351] p 4513 N94-36538

PONDEROMOTIVE FORCES
Quantum and quasi-classical analyses of high order emission processes
[DE93-041348] p 4513 N94-36697

POROSITY
A mixture model for shock compression of porous multi-component reactive materials
[DE93-017638] p 4400 N94-36456
Investigation of ultrasonic surface wave interaction with porous saturated rocks
[DE94-013378] p 4469 N94-37177

POROUS MATERIALS
A mixture model for shock compression of porous multi-component reactive materials
[DE93-017638] p 4400 N94-36456
DDT modeling and shock compression experiments of porous or damaged energetic materials
[DE94-011419] p 4428 N94-37052
The problems of the minimal surface and minimal lineal measure in three dimensions
[DE94-013002] p 4479 N94-37355
Effects of two-phase flow on the deflagration of porous energetic materials
[DE94-011423] p 4411 N94-37412

PORPHYRINS
Solvent effects on the energetics and dynamics of ultrafast electron transfer in chlorophyll-porphyrin-acceptor triads
[DE94-009693] p 4477 N94-36554
Femtosecond transient grating studies of electron transfer in porphyrin and chlorophyll donor-acceptor molecules
[DE94-009694] p 4478 N94-36555

PORTABLE EQUIPMENT
Portable color multimedia training systems based on monochrome laptop computers (CBT-in-a-briefcase), with spinoff implications for video uplink and downlink in spaceflight operations
[NASA-TM-108460] p 4496 N94-37556

POSITION (LOCATION)
Short-tower sigma(theta) measurements in the Colorado Plateaus region
[DE94-007478] p 4463 N94-36478

POSITION ERRORS
A more exact analysis of Sandia Laser Tracker data
[DE94-011411] p 4447 N94-37051
Operator gaze position control interfaces: Investigation of psychophysical and operational parameters
p 4485 N94-37273

POSITION INDICATORS
A comparison of two examples of magnetic tracker systems p 4485 N94-37275

POSITION SENSING
Optical position measurement for a large gap magnetic suspension system: Design and performance analysis
[NASA-TP-3438] p 4447 N94-36946

POSITRON ANNIHILATION
Positron implantation in solids
[DE94-013029] p 4537 N94-37499

POSITRONS
Older muons are wiser: Using time information in (mu)LCR spectroscopy
[DE93-018556] p 4511 N94-36457
Production of a positron and a bound electron by high-energy photon in a strong Coulomb field
[DE94-618501] p 4514 N94-36747
Precise determination of the weak mixing angle from a measurement of ALR in e(+)e(-) yields Z0
[DE94-013355] p 4515 N94-37085
Five-lepton decay modes of muon and tau mesons
[DE94-621636] p 4516 N94-37099
A freon-filled, holographic bubble chamber as a high energy photon burst spectrometer
[DE94-011645] p 4446 N94-37723

POSTURE
Postural strategies for the continuous control of static and dynamic balance in man
[PB94-184678] p 4487 N94-37812

POTABLE WATER
Determination of copper in tap water using solid-phase spectrophotometry
[NASA-TM-106480] p 4408 N94-36537

POTENTIAL ENERGY
The asymptotics of matrix elements of Gaussian potential between the basis functions of three-dimensional harmonic oscillator
[DE94-618467] p 4539 N94-37079
Solving the two-dimensional Schroedinger equation in self-consistent basis
[DE94-621535] p 4504 N94-37174

POTENTIAL THEORY
Navier-Stokes and potential theory solutions for ahelicopter fuselage and comparison with experiment
[NASA-TM-4566] p 4383 N94-36966

POWDER (PARTICLES)
A mixture model for shock compression of porous multi-component reactive materials
[DE93-017638] p 4400 N94-36456
Characterization and processing of sintered products from nano-crystalline powders generated by the RTDS method
[DE94-004765] p 4415 N94-36553

POWDER METALLURGY
NiAl-base composite containing high volume fraction of AlN for advanced engines
[NASA-CASE-LEW-15818-1] p 4403 N94-36752
The control of cleanness in powder metallurgy materials for turbine disks p 4421 N94-37325
Defects and their effects on the integrity of nickel based aeroengine discs p 4421 N94-37328
Substantiating powder metal life methodologies for engines p 4455 N94-37330

POWER AMPLIFIERS
Radially combined 30 W, 14-16 GHz amplifier
[DE94-010078] p 4432 N94-36471
Field emitter array RF amplifier development project phase one, cathode technology development
[AD-A280334] p 4437 N94-37033
Field emitter array RF amplifier development project. Phase 1, option 1
[AD-A280377] p 4437 N94-37035
High average power pulsed phase conjugate laser with birefringence correction
[DE94-012062] p 4447 N94-37160
Single event mirroring and sense amplifier designs for enhanced SE tolerance of DRAMs
[DE94-010397] p 4438 N94-37190

POWER SPECTRA
Atmospheric structure simulation: An ARMA model for smooth isotropic two-dimensional geophysical power spectra
[AD-A280476] p 4470 N94-37649

PRASEODYMIUM
The excitation mechanism of praseodymium-doped semiconductors
[AD-A280687] p 4535 N94-37129

PRASEODYMIUM COMPOUNDS
Quadrupolar effects in PrCu2Si2
[DE94-011509] p 4534 N94-37054

PREAMPLIFIERS
Sensitivity and signal to noise ratio improvement of a one micron ladar system incorporating a neodymium doped optical fiber preamplifier. Laser radar testbed
[AD-A280235] p 4447 N94-37137

PRECIPITATES
Precipitation in Zr-2.5 Nb enhanced by proton irradiation
[DE94-619056] p 4415 N94-36563

PRECIPITATION (METEOROLOGY)
Modeling of trace constituent transport with the University of Wisconsin global isentropic-sigma model
[DE94-012729] p 4466 N94-37288
NASA ER-2 Doppler radar reflectivity calibration for the CAMEX project
[NASA-TM-104611] p 4475 N94-37790

PRECIPITATION HARDENING
Substantiating powder metal life methodologies for engines p 4455 N94-37330

PRECONDITIONING
Preconditioned implicit solvers for the Navier-Stokes equations on distributed-memory machines
[NASA-TM-106449] p 4502 N94-36647
Research in parallel computing
[NASA-CR-196267] p 4442 N94-36960

PREDICTION ANALYSIS TECHNIQUES
An empirical comparison of a dynamic software testability metric to static cyclomatic complexity
p 4491 N94-36498
Characterisation of Fibre Reinforced Titanium Matrix Composites
[AD-A2775206] p 4400 N94-36649
Vibration signature analysis of a faulted gear transmission system
[NASA-TM-106623] p 4450 N94-36953
United States Air Force Summer Research Program, 1993. Volume 3: Phillips Laboratory
[AD-A278694] p 4550 N94-36979
Bond selective chemistry beyond the adiabatic approximation
[DE94-012486] p 4408 N94-37095
Ability of the total strain version of strainrange partitioning to characterize thermomechanical fatigue behavior
[NASA-TM-4556] p 4455 N94-37102
Embedded chaotic time series: Applications in prediction and spatio-temporal classification
[AD-A280690] p 4508 N94-37130
Substantiating powder metal life methodologies for engines p 4455 N94-37330
Predicting defect behaviour p 4455 N94-37331
Fatigue case study and loading spectra for wind turbines
[DE94-010798] p 4457 N94-37622

PREDICTIONS
Process/composite concurrent tailoring of SiC/Ti composites p 4402 N94-36663

PREFORMS
SCS-6 (tm) fiber reinforced titanium
p 4400 N94-36652

PREMIXED FLAMES
Rich methane/air flames: Burning velocities, extinction limits, and flammability limit
[DE94-004340] p 4407 N94-36462
Rich flammability limits in CH3OH/CO/diluent mixtures
[DE94-004341] p 4407 N94-36482
Some effects of heat release in premixed flames
[DE94-011346] p 4409 N94-37199

PREPROCESSING
Experience with automatic, dynamic load balancing and adaptive finite element computation
[DE94-001422] p 4498 N94-37487

PRESSURE
Experimental measurements and analytical analysis related to gas turbine heat transfer. Part 1: Time-averaged heat-flux and surface-pressure measurements on the vanes and blades of the SSME fuel-side turbine and comparison with prediction. Part 2: Phase-resolved surface-pressure and heat-flux measurements on the first blade of the SSME fuel-side turbine
[NASA-CR-196296] p 4442 N94-36969

PRESSURE DEPENDENCE
Pressure dependence of the conductivity and magnetoconductance in oriented iodine-doped polyacetylene
[PB94-184488] p 4427 N94-37854

PRESSURE DISTRIBUTION
Controlling forebody asymmetries in flight: Experience with boundary layer transition strips
[NASA-TM-4595] p 4383 N94-36944
Pressure-sensing performance of upright cylinders in a Mach 10 boundary-layer
[NASA-TM-4633] p 4383 N94-37395
Aerodynamic characteristics of the National Launch System (NLS) 1 1/2 stage launch vehicle
[NASA-TP-3488] p 4384 N94-37577

PRESSURE MEASUREMENT
Experimental measurements and analytical analysis related to gas turbine heat transfer. Part 1: Time-averaged heat-flux and surface-pressure measurements on the vanes and blades of the SSME fuel-side turbine and comparison with prediction. Part 2: Phase-resolved surface-pressure and heat-flux measurements on the first blade of the SSME fuel-side turbine
[NASA-CR-196296] p 4442 N94-36969
Measurement uncertainty and feasibility study of a flush airdata system for a hypersonic flight experiment
[NASA-TM-4627] p 4383 N94-37378
Pressure-sensing performance of upright cylinders in a Mach 10 boundary-layer
[NASA-TM-4633] p 4383 N94-37395
PRESSURE REDUCTION
Cardiac pressure changes with venous gas embolism and decompression
[AD-A280412] p 4481 N94-37224
PRESSURE REGULATORS
Dual valve plate two-way pressure relief valve
[AD-D016293] p 4452 N94-37766
PRESSURE VESSELS
Data compatibility for various Charpy-tests
[DE94-617534] p 4416 N94-37074
PRESTRESSING
Jumper connector analysis
[DE94-010373] p 4451 N94-37188
PRETREATMENT
Thermal-oxidative pretreatment and evaluation of poly (hexafluoropropene oxide) fluids
[NASA-TM-106659] p 4424 N94-37300
PRINTED CIRCUITS
Laser drilling of printed wiring boards: Sandia LDRD program
[DE94-011004] p 4448 N94-37198
Selected case studies in modeling and simulation applied to environmentally conscious design and manufacturing
[DE94-007556] p 4466 N94-37389
PRINTING
Electronic document interchange
p 4541 N94-36848
PRIORITIES
Science priorities for the human dimensions of global change p 4464 N94-36987
Standards for data and document interchange
p 4543 N94-37337
PRISMS
Three-stage attenuation using Glan-Thompson prisms
[AD-A280481] p 4525 N94-37350
PROBABILITY THEORY
Probability-based inference in cognitive diagnosis
[AD-A280553] p 4506 N94-36732
Virtual representation of IID observations in Bayesian belief networks
[AD-A280552] p 4507 N94-37046
Statistical characterization of rare events
p 4454 N94-37327
Probability techniques for reliability analysis of composite materials
[NASA-CR-195294] p 4406 N94-37633
Probabilistic assessment of space nuclear propulsion system nozzle
[NASA-TM-106539] p 4457 N94-37704
PROBES
Laser probing of interfaces
[DE94-011300] p 4449 N94-37628
PROBLEM SOLVING
Searching for plans using a hierarchy of learned macros and selective reuse
[AD-A280594] p 4499 N94-36722
A scalable parallel algorithm for multiple objective linear programs
[NASA-CR-194920] p 4495 N94-37539
PROCEDURES
A graphic view of Geometric Dimensioning and Tolerancing
[DE94-011478] p 4435 N94-37736
PROCESS CONTROL (INDUSTRY)
Maintaining constant standards during the forging process p 4421 N94-37326
PROCUREMENT
Machine Translation Project p 4541 N94-36846
A guide to tenders and contracts alerting services
[AGARD-R-799] p 4540 N94-37447
PRODUCT DEVELOPMENT
Proceedings of the Eighteenth Annual Software Engineering Workshop
[NASA-CR-189348] p 4489 N94-36484
The maturing of the quality improvement paradigm in the SEL p 4489 N94-36485
Process improvement as an investment: Measuring its worth p 4489 N94-36486
Software quality: Process or people
p 4492 N94-36499
MCFC product development test
[DE94-002005] p 4463 N94-37488
PRODUCTION MANAGEMENT
Assessing efficiency of software production for NASA-SEL data p 4490 N94-36490
PROFILOMETERS
Measuring the upper profile of sea ice in the Bay of Bothnia with a laser profilometer
[PB94-184561] p 4477 N94-37855
PROGRAM VERIFICATION (COMPUTERS)
Analysis of a successful inspection program
p 4490 N94-36492
Software quality: Process or people
p 4492 N94-36499
An arbitrary grid CFD algorithm for configuration aerodynamics analysis. Volume 1: Theory and validations
[NASA-CR-195918] p 4493 N94-36914
A survey of commonly applied methods for software process improvement
[AD-A278595] p 4493 N94-36974
Adaptable binary programs
[AD-A280243] p 4494 N94-37119
Proto code generation techniques
[AD-A280275] p 4494 N94-37123
SACS: A cache simulator incorporating timing analysis with buffer and memory management
[AD-A280472] p 4494 N94-37230
PROGRAMMING ENVIRONMENTS
Lessons learned applying CASE methods/tools to Ada software development projects p 4491 N94-36493
Standards for data and document interchange
p 4543 N94-37337
The distributed development environment for SDSS software
[DE94-013238] p 4547 N94-37555
PROGRAMMING LANGUAGES
Software engineering with application-specific languages p 4491 N94-36494
Design, implementaion and evaluation of a declarative object-oriented programming language
[PB94-169208] p 4492 N94-36546
PROJECT MANAGEMENT
The maturing of the quality improvement paradigm in the SEL p 4489 N94-36485
The Engineering Review Board p 4540 N94-36843
JPRS report: Science and technology. Central Eurasia: Space
[JPRS-USP-94-004] p 4391 N94-37002
PROJECT PLANNING
NASA STI Program Coordinating Council Eleventh Meeting: NASA STI Modernization Plan
[NASA-TM-109415] p 4540 N94-36841
NASA STI modernization plan p 4540 N94-36842
The Engineering Review Board p 4540 N94-36843
Network upgrades p 4541 N94-36851
PROPANE
Alternative fuel information: Facts about CNG and LPG conversion
[DE94-006888] p 4429 N94-37402
Probing flame chemistry with MBMS, theory, and modeling
[DE94-011224] p 4413 N94-37623
PROPELLANT CHEMISTRY
NASA reload program
[NASA-CR-193972] p 4429 N94-37446
PROPELLANT COMBUSTION
Validation and implementation of optical diagnostics for particle sizing in rocket motors
[AD-A278581] p 4428 N94-36972
A fully coupled thermal, chemical, mechanical cookoff model
[DE94-011432] p 4428 N94-37201
PROPELLANT STORAGE
Cryogenic fluid management technologies for space transportation. Zero G thermodynamic vent system
[NASA-CR-193981] p 4430 N94-36806
PROPOSALS
Hubble Space Telescope cycle 5. Phase 1: Proposal instructions, version 4.0
[NASA-CR-189364] p 4547 N94-36963
PROPULSION SYSTEM PERFORMANCE
Hot dynamic test rig for measuring hypersonic engine seal flow and durability
[NASA-TM-106507] p 4450 N94-36645
Possibilities and pitfalls in aerospace applications of titanium matrix composites p 4400 N94-36650
Characteristics of ions emitted from high-current hollow cathodes
[NASA-CR-195372] p 4398 N94-37764
PROPYLENE
An investigation of molybdenum and molybdenum oxide catalyzed hydrocarbon formation reactions
[DE94-013700] p 4409 N94-37132
PROSTHETIC DEVICES
Selectively lockable knee brace
[NASA-CASE-MFS-28991-1] p 4486 N94-36838
Channel in hip implant stem
[NASA-CASE-MFS-28987-1] p 4486 N94-36840
PROTECTION
Blast overpressure studies with animals and man
[AD-A280240] p 4480 N94-37118
PROTECTIVE CLOTHING
Aerospace medicine and biology: A continuing bibliography with indexes (supplement 392)
[NASA-SP-7011(392)] p 4482 N94-37445
PROTECTIVE COATINGS
Atomic oxygen treatment for non-contact removal of organic protective coatings from painting surfaces
[NASA-TM-106650] p 4421 N94-36952
Robotic weld overlay coatings for erosion control
[DE94-013477] p 4417 N94-37116
Interfaces of high-protection performance polyaryls-coated zinc phosphated steels
[DE94-011732] p 4417 N94-37153
Compilation of diamond-like carbon properties for barriers and hard coatings
[DE94-012139] p 4427 N94-37725
PROTEINS
Femtosecond transient absorption studies of the light harvesting Chl a/b protein complex of Photosystem 2 in higher plants
[DE94-009684] p 4477 N94-36481
Recombinant protein production and insect cell culture and process
[NASA-CASE-MSC-22336-1] p 4478 N94-36751
Chemical and structural characterization of nitroaromatic adducts with hemoglobins
[AD-A280533] p 4480 N94-37089
High resolution electron diffraction analysis of structural changes associated with the photocycle of bacteriorhodopsin
[DE94-011800] p 4479 N94-37156
Status review and accomplishments of the Materials Research Center at the University of Pittsburgh
[AD-A280422] p 4399 N94-37214
Crystallographic studies of nitrogenase and hydrogenase
[DE94-011972] p 4538 N94-37677
PROTOCOL (COMPUTERS)
Analysis of end-to-end encryption and traffic flow confidentiality options
[AD-A278612] p 4433 N94-36754
OSI and TCP/IP p 4542 N94-36855
Research in parallel computing
[NASA-CR-196267] p 4442 N94-36960
An error-resistant linguistic protocol for air traffic control
[NASA-CR-196098] p 4385 N94-37013
Global information networks: How they work
p 4543 N94-37335
Policies for implementing network firewalls
[DE94-011030] p 4495 N94-37430
Advanced information processing system: Authentication protocols for network communication
[NASA-CR-194923] p 4498 N94-37500
PROTON BEAMS
The effects of proton-beam quality on the production of gamma rays for nuclear resonance absorption in nitrogen
[DE94-011609] p 4523 N94-37629
PROTON IRRADIATION
Precipitation in Zr-2.5 Nb enhanced by proton irradiation
[DE94-619056] p 4415 N94-36563
PROTONS
The E2/M1 mixing ratio in the excitation of the Delta from polarized photo-reactions
[DE94-004235] p 4510 N94-36442
Deep inelastic scattering results from the first year of HERA operation
[DE94-004578] p 4511 N94-36483
Angular dependence of parton-parton scattering extracted from hadron pair production in pp collisions at radicals equal to 11.5 GeV
[DE94-611174] p 4511 N94-36504
Mass identified particle production and Bose Einstein correlations at 1800 GeV
[DE94-013418] p 4515 N94-37067
Physics with primary beams of the KEK-PS
[DE94-748635] p 4522 N94-37234
AEM and AES of radiation-induced segregation in proton-irradiated stainless steels
[DE94-012734] p 4418 N94-37398
PROTOPLASTS
Effects of freezing and cold acclimation on the plasma membrane of isolated protoplasts
[DE94-012487] p 4479 N94-37248

PROTOTYPES
Advances in rapid prototyping
[DE94-010075] p 4430 N94-36447
First results from a prototype level-1 calorimeter trigger system for LHC, RD 27 (UK) collaboration
[PB94-167475] p 4436 N94-36532
Solid state fluorometer: Prototype development
[AD-A280321] p 4534 N94-37027
PSYCHOMETRICS
Dealing with uncertainty about item parameters: Expected response functions
[AD-A280610] p 4506 N94-36728
PUBLIC LAW
Alternative fuel information: State alternative fuel laws and incentives
[DE94-006892] p 4429 N94-37404
Comparative alternative/clean fuels provisions of the Clean Air Act Amendments of 1990 and the Energy Policy Act of 1992
[DE94-006887] p 4429 N94-37426
PULSARS
Absolute limit on rotation of gravitationally bound stars
[DE94-011367] p 4548 N94-37049
PULSE COMPRESSION
Signal processing for the 1992 Barents Sea tomography experiment
[AD-A278580] p 4476 N94-36971
PULSE DURATION
Advanced laser driver for soft x-ray projection lithography
[DE94-011643] p 4449 N94-37722
PULSE MODULATION
Propagation of radius-tailored laser pulses over extended distances in a uniform plasma
[AD-A280405] p 4528 N94-37182
PULSE RADAR
Initial studies of reflectometer for ITER
[DE94-012476] p 4528 N94-37167
PULSED LASER DEPOSITION
Residual stress and Raman spectra of laser deposited highly-tetrahedral-coordinated-amorphous-carbon films
[DE94-012067] p 4426 N94-37537
PULSED LASERS
An externally heated copper vapour laser
[DE94-619484] p 4447 N94-36565
High average power pulsed phase conjugate laser with birefringence correction
[DE94-012062] p 4447 N94-37160
Propagation of radius-tailored laser pulses over extended distances in a uniform plasma
[AD-A280405] p 4528 N94-37182
Time-resolved probing of electron thermal transport in plasma produced by femtosecond laser pulses
[DE94-012061] p 4530 N94-37392
PULTRUSION
Advanced manufacturing technology for polymer composite structures in Japan p 4422 N94-36968
PURSUIT TRACKING
Two-axis camera platform for machine vision
p 4394 N94-36628
PYROLYSIS
Basic solutions to carbon/carbon oxidation: Science and technology
[AD-A280447] p 4404 N94-37232

Q

Q SWITCHED LASERS
Greater than 100 watt average power at 0.53 micron with 25 ns, 2.5 kHz repetition rate pulses from a single power oscillator
[DE94-011641] p 4447 N94-37114
The 250 watt average power electro-quality Q-switched diode pumped power oscillator
[DE94-011644] p 4449 N94-37737
Q VALUES
Q-profile flattening due to nonlinear development of resistive kink mode and ensuing fast crash in sawtooth oscillations
[DE94-727625] p 4526 N94-36472
QUADRATURES
Multiquadric collocation methods in the numerical solution of Volterra integral equations with weakly singular kernels
[DE94-013000] p 4505 N94-37497
QUADRUPOLES
Method of N-15 analysis by mass-spectroscopy on ion implanter MPB-200
[DE94-618203] p 4407 N94-36529
Quadrupolar effects in PrCu2Si2
[DE94-011509] p 4534 N94-37054
Tune modulation due to gradient ripple and the dynamic aperture
[DE94-011922] p 4524 N94-37157
QUALITATIVE ANALYSIS
United States Air Force Summer Research Program, 1993. Volume 16: Arnold Engineering Development Center, Frank J. Seiler Research Laboratory and Wilford Hall Medical Center
[AD-A278658] p 4550 N94-36978
SAW chemical sensor arrays using new thin-film materials
[DE94-011940] p 4411 N94-37365
QUALITY CONTROL
The maturing of the quality improvement paradigm in the SEL p 4489 N94-36485
Process improvement as an investment: Measuring its worth p 4489 N94-36486
Recent SEL experiments and studies
p 4490 N94-36487
Software quality: Process or people
p 4492 N94-36499
Impact of Materials Defects on Engine Structures Integrity
[AGARD-R-790] p 4453 N94-37321
The control of cleanness in powder metallurgy materials for turbine disks p 4421 N94-37325
Maintaining constant standards during the forging process p 4421 N94-37326
NASA Lewis wind tunnel model systems criteria
[NASA-TM-106565] p 4390 N94-37522
The integrated performance evaluation program quality assurance guidance in support of EM environmental sampling and analysis activities
[DE94-013043] p 4468 N94-37731
QUANTITATIVE ANALYSIS
Method of N-15 analysis by mass-spectroscopy on ion implanter MPB-200
[DE94-618203] p 4407 N94-36529
Development of high sensitivity techniques for characterizing outgassing of polymeric construction materials for microenvironments
[DE94-012068] p 4424 N94-37204
QUANTUM CHEMISTRY
Isolated SO4-2 and PO4-3 anions do not exist
[AD-A278831] p 4512 N94-36521
QUANTUM CHROMODYNAMICS
Angular dependence of parton-parton scattering extracted from hadron pair production in pp collisions at radicals equal to 11.5 GeV
[DE94-611174] p 4511 N94-36504
The Pomeron and Quantum Chromodynamics (QCD) with many light quarks
[DE94-001351] p 4513 N94-36538
Effective Lagrangian for gluons and Higgs pseudoscalars
[DE94-001381] p 4513 N94-36539
High Energy Physics Division of research activities
[DE93-019681] p 4521 N94-36694
Methods of calculation of higher power corrections in QCD
[DE94-618511] p 4521 N94-36748
Introduction to the heavy quark effective theory, part 1
[DE94-618512] p 4514 N94-36749
Relativistic di-quark model of p p-bar yields K(+)K(-) reaction
[DE94-618519] p 4514 N94-37063
Sum rules for 1/m corrections to the form factors of semileptonic B decays
[DE94-618548] p 4514 N94-37065
A study of jet handedness in hadronic Z0 decays
[DE94-013358] p 4515 N94-37087
Polarization phenomena in quantum chromodynamics
[DE94-010663] p 4539 N94-37543
Strangeness and the quark-gluon plasma: An experimenter's perspective
[DE94-011377] p 4519 N94-37558
Pre-equilibrium parton dynamics: Proceedings
[DE94-011347] p 4520 N94-37716
QUANTUM MECHANICS
Scattering theory for the quantum envelope of a classical system
[DE94-008530] p 4539 N94-36508
Testing violation of CPT and quantum mechanics in the K(0) - bar-K(0) system
[DE94-012057] p 4539 N94-37366
The angular and energy distributions of ejected electrons in electron-impact ionization of helium
[DE94-618748] p 4519 N94-37528
QUANTUM NUMBERS
The asymptotics of matrix elements of Gaussian potential between the basis functions of three-dimensional harmonic oscillator
[DE94-618467] p 4539 N94-37079
QUANTUM STATISTICS
Mass identified particle production and Bose Einstein correlations at 1800 GeV
[DE94-013418] p 4515 N94-37067
Kaon correlation systematics in E859
[DE94-011927] p 4516 N94-37158
QUANTUM THEORY
Wick-Cutkovsky model: An introduction
[DE94-618365] p 4504 N94-37170
QUARK MODELS
The E2/M1 mixing ratio in the excitation of the Delta from polarized photo-reactions
[DE94-004235] p 4510 N94-36442
Relativistic di-quark model of p p-bar yields K(+)K(-) reaction
[DE94-618519] p 4514 N94-37063
Sum rules for 1/m corrections to the form factors of semileptonic B decays
[DE94-618548] p 4514 N94-37065
The form factors of the nucleons
[DE94-013357] p 4515 N94-37086
QUARKS
Top quark search at CDF
[DE94-003643] p 4511 N94-36459
A search for first generation scalar leptoquarks at radical s equal to 1.8 TeV with the D0 detector
[DE94-008846] p 4511 N94-36506
The t(anti t)(gamma) background to pp (yields) W(gamma) + X at the SSC
[DE94-001386] p 4512 N94-36526
Summary of the extensions of the Standard Model working group
[DE94-002217] p 4512 N94-36527
The Pomeron and Quantum Chromodynamics (QCD) with many light quarks
[DE94-001351] p 4513 N94-36538
B quark production cross sections and the b- (bar b) correlated production cross section at CDF
[DE94-000620] p 4514 N94-36700
Methods of calculation of higher power corrections in QCD
[DE94-618511] p 4521 N94-36748
Introduction to the heavy quark effective theory, part 1
[DE94-618512] p 4514 N94-36749
A study of jet handedness in hadronic Z0 decays
[DE94-013358] p 4515 N94-37087
Numerical solution to the boundary-value problem for the Bethe-Salpeter equation with quadratically rising potential
[DE94-621606] p 4504 N94-37175
Non-equilibrium evolution of the disoriented chiral condensate in heavy-ion collisions
[DE94-012897] p 4522 N94-37310
The Mesozoic Era of relativistic heavy ion physics and beyond
[DE94-011341] p 4548 N94-37557
Strangeness and the quark-gluon plasma: An experimenter's perspective
[DE94-011377] p 4519 N94-37558
Pre-equilibrium parton dynamics: Proceedings
[DE94-011347] p 4520 N94-37716
QUARTZ
Assess progress being made for the KTeV electromagnetic calorimeter crystal order in France
[DE94-009396] p 4533 N94-36746
QUASARS
The BL LAC phenomenon: X-ray observations of transition objects and determination of the x-ray spectrum of a complete sample of flat-spectrum radio sources
[NASA-CR-195951] p 4546 N94-36688
Ultraviolet spectropolarimetry of high redshift quasars with the Hubble Space Telescope
[NASA-CR-196014] p 4546 N94-36690
Correlated radio and optical variations in a sample of AGN. A simultaneous radio-optical flare in BL lacertae
[PB94-179181] p 4548 N94-37834
QUEUEING THEORY
A mean value analysis heuristic for analysis of aircraft sortie generation
[AD-A278578] p 4507 N94-36970
QUINONES
Femtosecond transient grating studies of electron transfer in porphyrin and chlorophyll donor-acceptor molecules
[DE94-009694] p 4478 N94-36555

R

RADAR TARGETS
Imaging targets embedded in a lossy half space with Synthetic Aperture Radar
[DE94-010807] p 4435 N94-37391
RADAR TRACKING
Pointing and Tracking Systems
[AGARD-CP-539] p 4392 N94-36616
Multitarget track initiation using a modified Hough transform p 4395 N94-36630
Radar tracking in multipath: Techniques for improved performance p 4395 N94-36631

Contact level fusion of radar and IRST contacts on almost electromagnetically silent platform
p 4395 N94-36634

RADAR TRANSMISSION
Channel probe measurements for the American Sector Clutter Experiment, January 1994
[DE94-013086] p 4469 N94-37314
MTI compatible coherent sidelobe canceller
[AD-D016300] p 4435 N94-37771

RADIANT FLUX DENSITY
UVPI imaging from the LACE satellite: The Low Cost Launch Vehicle (LCLV) rocket plume
[AD-A278785] p 4398 N94-36445

RADIATION ABSORPTION
The effects of proton-beam quality on the production of gamma rays for nuclear resonance absorption in nitrogen
[DE94-011609] p 4523 N94-37629

RADIATION CHEMISTRY
Physics with primary beams of the KEK-PS
[DE94-748635] p 4522 N94-37234

RADIATION COUNTERS
Testing new technology for the heavy ion experiment at CERN
[DE94-004747] p 4521 N94-37220
Particle physics
[DE94-012944] p 4518 N94-37312
Experimental particle physics at the University of Pittsburgh
[DE94-011636] p 4521 N94-37721

RADIATION DAMAGE
Irradiation assisted stress corrosion cracking of HTH Alloy X-750 and Alloy 625
[DE94-012667] p 4416 N94-37080
Thermodynamics of minerals stable near the Earth's surface
[DE94-012479] p 4539 N94-37094
Estimates of cellular mutagenesis from cosmic rays
[NASA-TP-3453] p 4481 N94-37282

RADIATION DETECTORS
High Energy Physics Division of research activities
[DE93-019681] p 4521 N94-36694
LET spectra of fragmented 600-MeV/A iron beam on aluminum and polyethylene: A preliminary analysis
[NASA-TP-3436] p 4416 N94-36993
BMAP dipole magnetic field analysis and orbit tracking/calculations of energy deposition in GaAs WHEBY detectors
[DE94-012080] p 4522 N94-37303
The 24/36/48 Cathode Strip Chamber layout for SSC GEM detector muon subsystem
[DE94-012676] p 4439 N94-37306
Gas microstrip detectors on resistive plastic substrates
[DE94-011336] p 4426 N94-37714

RADIATION DISTRIBUTION
Coherent multiple-foil x-ray transition radiation
[DE93-040831] p 4525 N94-37486

RADIATION DOSAGE
Stopping power of charged particles from 10 eV/amu to 10 GeV/amu
[DE94-719024] p 4518 N94-37387
Two-dimensional over-all neutronics analysis of the ITER device
[DE94-718963] p 4530 N94-37464

RADIATION EFFECTS
Correlation of hot-carrier stress and ionization induced degradation in bipolar transistors
[DE94-007289] p 4532 N94-36540
Modelling irradiation creep of zirconium alloys
[DE94-619055] p 4414 N94-36544
Precipitation in Zr-2.5 Nb enhanced by proton irradiation
[DE94-619056] p 4415 N94-36563
Irradiation effects in Fe-30 percent Ni alloy during Ar ion implantation
[DE94-619057] p 4415 N94-36564
Ground and space flight experiments of the effects of light, sound and/or temperature on animals
[NASA-CR-196102] p 4478 N94-36986
Behavioral performance in monkeys exposed to TEMPO high-peak-power microwave pulses at 3 GHz
[AD-A280551] p 4478 N94-37045
Data compatibility for various Charpy-tests
[DE94-617534] p 4416 N94-37074
Irradiation assisted stress corrosion cracking of HTH Alloy X-750 and Alloy 625
[DE94-012667] p 4416 N94-37080
AEM and AES of radiation-induced segregation in proton-irradiated stainless steels
[DE94-012734] p 4418 N94-37398
Characterization of mechanical properties degradation using small punch testing technique
[DE94-011202] p 4418 N94-37410
Role of burn-in during qualification testing
[DE94-007864] p 4439 N94-37513
Studying of ion implantation effect on the biology in China
[DE94-620692] p 4479 N94-37535
Characterization of nuclear transmutations in materials irradiated test facilities
[DE94-013309] p 4420 N94-37552
Investigation of exposure to Extremely Low Frequency (ELF) magnetic and electric fields: Ongoing animals studies
[DE94-011239] p 4480 N94-37625

RADIATION HARDENING
Single event mirroring and sense amplifier designs for enhanced SE tolerance of DRAMs
[DE94-010397] p 4438 N94-37190
A proposed SEU tolerant DRAM cell
[DE94-010758] p 4438 N94-37196
Role of burn-in during qualification testing
[DE94-007864] p 4439 N94-37513

RADIATION MEASUREMENT
ARM: A climate process observatory
[DE94-007473] p 4463 N94-36477
Two-channel microwave radiometer for observations of total column precipitable water vapor and cloud liquid water path
[DE94-007480] p 4471 N94-36479
Site Scientific Mission Plan for the Southern Great Plains CART site, January - June 1994
[DE94-012114] p 4474 N94-37394
Proceedings of the Third Atmospheric Radiation Measurement (ARM) Science Team Meeting
[DE94-011194] p 4467 N94-37454

RADIATION SHIELDING
Estimates of cellular mutagenesis from cosmic rays
[NASA-TP-3453] p 4481 N94-37282
The logic behind thick, liquid-walled, fusion concepts
[DE94-012678] p 4528 N94-37307
Stopping power of charged particles from 10 eV/amu to 10 GeV/amu
[DE94-719024] p 4518 N94-37387
Two-dimensional over-all neutronics analysis of the ITER device
[DE94-718963] p 4530 N94-37464

RADIATION TRANSPORT
Data simulation for the Associated Particle Imaging system
[DE94-012664] p 4518 N94-37305
User's manual for SNL-SAND-2 code
[DE94-011744] p 4496 N94-37673

RADIATIVE HEAT TRANSFER
Hypersonic, nonequilibrium flow over the FIRE 2 forebody at 1634 sec
[NASA-TM-109141] p 4444 N94-37455
Factors influencing the parameterization of anvil clouds within GCMs
[DE94-010794] p 4475 N94-37621

RADIATIVE TRANSFER
Two-channel microwave radiometer for observations of total column precipitable water vapor and cloud liquid water path
[DE94-007480] p 4471 N94-36479
Accelerated line-by-line calculations for the radiative transfer of trace gases related to climate studies
[DE94-004404] p 4464 N94-36552
Proceedings of the Third Atmospheric Radiation Measurement (ARM) Science Team Meeting
[DE94-011194] p 4467 N94-37454
Tropospheric radiative forcing of CH4
[DE94-011628] p 4468 N94-37631

RADIO ASTRONOMY
Plasma and radio waves from Neptune: Source mechanisms and propagation
[NASA-CR-196284] p 4550 N94-37251
Correlated radio and optical variations in a sample of AGN. A simultaneous radio-optical flare in BL lacertae
[PB94-179181] p 4548 N94-37834

RADIO BEACONS
Marker beacon case
[AD-D016322] p 4385 N94-37830
System for broadcasting marker beacon signals and processing responses from seeking entities
[AD-D016313] p 4385 N94-37839

RADIO COMMUNICATION
VHF adaptive antenna development task
[AD-A280320] p 4434 N94-37127
ELF Communications System ecological monitoring program: Electromagnetic field measurements and engineering support
[AD-A280489] p 4481 N94-37353

RADIO EMISSION
Plasma and radio waves from Neptune: Source mechanisms and propagation
[NASA-CR-196284] p 4550 N94-37251

RADIO EQUIPMENT
VHF adaptive antenna development task
[AD-A280320] p 4434 N94-37127
Design and analysis of a mode B and mode JD satellite Earth station
[AD-A280417] p 4391 N94-37225

RADIO FILTERS
KONRAD: Wide band digital HF receiver
[PB94-184666] p 4435 N94-37813

RADIO FREQUENCIES
The mathematical simulation of physical processes in ECR multicharged ions sources
[DE94-618343] p 4515 N94-37077
Field emitter array RF amplifier development project. Phase 1, option 1
[AD-A280513] p 4437 N94-37107
Field emitter array RF amplifier development project. Cathode technology development. Phase 1
[AD-A280515] p 4437 N94-37108

RADIO FREQUENCY HEATING
Bounce resonance heating and transport in a magnetic mirror
[DE94-727545] p 4531 N94-37466

RADIO FREQUENCY INTERFERENCE
VHF adaptive antenna development task
[AD-A280320] p 4434 N94-37127

RADIO GALAXIES
The BL LAC phenomenon: X-ray observations of transition objects and determination of the x-ray spectrum of a complete sample of flat-spectrum radio sources
[NASA-CR-195951] p 4546 N94-36688

RADIO RECEIVERS
KONRAD: Wide band digital HF receiver
[PB94-184666] p 4435 N94-37813

RADIO SIGNALS
VHF adaptive antenna development task
[AD-A280320] p 4434 N94-37127
Wavefront simulator for evaluating RF communication array signal processors
[AD-D016281] p 4436 N94-37835

RADIO SOURCES (ASTRONOMY)
Correlated radio and optical variations in a sample of AGN. A simultaneous radio-optical flare in BL lacertae
[PB94-179181] p 4548 N94-37834

RADIO TRANSMISSION
Wavefront simulator for evaluating RF communication array signal processors
[AD-D016281] p 4436 N94-37835

RADIO TRANSMITTERS
ELF Communications System ecological monitoring program: Electromagnetic field measurements and engineering support
[AD-A280489] p 4481 N94-37353
NRL HF propagation measurements between Guadeloupe and Providenciales during the CRRES exercises
[DE94-012078] p 4435 N94-37393

RADIO WAVES
Intensity of waves diffracted from symmetrical profile lamellar gratings
[DE94-611101] p 4433 N94-36753

RADIOACTIVE DECAY
Determination of the upsilon(1s) leptonic width
[DE94-618534] p 4516 N94-37096
Five-lepton decay modes of muon and tau mesons
[DE94-621636] p 4516 N94-37099

RADIOACTIVE WASTES
Paleoclimate validation of a numerical climate model
[DE94-009287] p 4463 N94-36470
Activities of the Chemical Technology Division
[DE94-013050] p 4410 N94-37357
Analytical electron microscopy examination of solid reaction products in long-term test of SRL 200 waste glasses
[DE94-005482] p 4411 N94-37380

RADIOLOGY
The integrated performance evaluation program quality assurance guidance in support of EMI environmental sampling and analysis activities
[DE94-013043] p 4468 N94-37731

RADIOMETERS
Scientific and technical support for the Galileo net flux radiometer experiment
[NASA-CR-196009] p 4549 N94-36689
NOAA polar satellite calibration: A system description
[NOAA-TR-NESDIS-77] p 4396 N94-37009

RADON
California residential indoor air quality study. Volume 1: Methodology and descriptive statistics
[PB94-166048] p 4464 N94-36994

RAIL TRANSPORTATION
Study of Japanese electrodynamic-suspension maglev systems
[DE94-011486] p 4452 N94-37515

RAMAN SPECTRA
XAFS-like structure of resonant Raman scattering
[DE94-618410] p 4517 N94-37171

Final report on spectral broadening by cross-phase modulation in linearly birefringent optical fibers
[DE94-010406] p 4524 N94-37191
Raman scattering of variable bandwidth KrF radiation in long air paths
[DE94-012912] p 4449 N94-37495
Residual stress and Raman spectra of laser deposited highly-tetrahedral-coordinated-amorphous-carbon films
[DE94-012067] p 4426 N94-37537
Optical spectroscopy of a nitrogen-hydrogen complex in ZnSe
[DE94-011622] p 4413 N94-37630

RAMAN SPECTROSCOPY
Raman scattering of variable bandwidth KrF radiation in long air paths
[DE94-012912] p 4449 N94-37495
Optical spectroscopy of a nitrogen-hydrogen complex in ZnSe
[DE94-011622] p 4413 N94-37630

RANDOM ACCESS MEMORY
A proposed SEU tolerant DRAM cell
[DE94-010758] p 4438 N94-37196

RANDOM NOISE
Relaxation of the density matrix for an arbitrary spin in random external fields
[DE94-618457] p 4509 N94-37078

RANGEFINDING
A more exact analysis of Sandia Laser Tracker data
[DE94-011411] p 4447 N94-37051

RARE EARTH ELEMENTS
Consequences of competing hybridization for magnetic ordering in correlated-electron lattices
[DE94-011648] p 4534 N94-37057

RARE GASES
Hypobaric decompression sickness model development. Part 1: Diffusion of inert gas from a viscoelastic fluid (blood) into an expanding gas phase
[AD-A280298] p 4481 N94-37124

RATS
Ground and space flight experiments of the effects of light, sound and/or temperature on animals
[NASA-CR-196102] p 4478 N94-36986

RAYLEIGH-BENARD CONVECTION
Coupled Marangoni-Benard/Rayleigh-Benard instability with temperature dependent viscosity
[NASA-TM-106646] p 4444 N94-37507

RAYON
The development of short, high surface area activated carbon fibers
[AD-A280509] p 4404 N94-37105

RDX
A fully coupled thermal, chemical, mechanical cookoff model
[DE94-011432] p 4428 N94-37201
Thermal decomposition reactions of HMX and RDX and their importance in predicting cookoff hazards
[DE94-011430] p 4429 N94-37413

REACTING FLOW
A flux splitting scheme with high-resolution and robustness for discontinuities
[NASA-TM-106452] p 4441 N94-36646

REACTION KINETICS
Rich methane/air flames: Burning velocities, extinction limits, and flammability limit
[DE94-004340] p 4407 N94-36462
Bond selective chemistry beyond the adiabatic approximation
[DE94-012486] p 4408 N94-37095
Thermomechanical studies of tungsten heavy alloys
[AD-A280250] p 4417 N94-37122
A fully coupled thermal, chemical, mechanical cookoff model
[DE94-011432] p 4428 N94-37201
Influences of flame-vortex interactions on formation of oxides of nitrogen in curved methane-air diffusion flamelets
[DE94-005105] p 4409 N94-37221
Thermodynamic and kinetic aspects of surface acidity
[DE94-012351] p 4411 N94-37372
Effect of temperature on the electron attachment and detachment properties of c-C4F8
[DE94-012750] p 4518 N94-37383
Electron-transfer reactions involving two harmonic potentials with a different force constant: The Zusman approach versus the spin-boson model
[DE94-013306] p 4519 N94-37550
Probing flame chemistry with MBMS, theory, and modeling
[DE94-011224] p 4413 N94-37623
Effects of molecular transport on turbulence-chemistry interactions in a hydrogen-argon-air jet diffusion flame
[DE94-005107] p 4413 N94-37711

REACTION PRODUCTS
Analytical electron microscopy examination of solid reaction products in long-term test of SRL 200 waste glasses
[DE94-005482] p 4411 N94-37380

REACTIVITY
A coarse-mesh nodal method-diffusive-mesh finite difference method
[DE94-010809] p 4502 N94-36455
A mixture model for shock compression of porous multi-component reactive materials
[DE93-017638] p 4400 N94-36456
DDT modeling and shock compression experiments of porous or damaged energetic materials
[DE94-011419] p 4428 N94-37052
Chemical and structural characterization of nitroaromatic adducts with hemoglobins
[AD-A280533] p 4480 N94-37089
The effect of reactive elements on the segregation behavior and microstructure of alpha-Al2O3 scales on beta-NiAl
[DE94-012739] p 4418 N94-37399

REACTOR CORES
A coarse-mesh nodal method-diffusive-mesh finite difference method
[DE94-010809] p 4502 N94-36455

REACTOR DESIGN
Conceptual design: TFE verification program
[DE94-012469] p 4398 N94-37433
Two-dimensional over-all neutronics analysis of the ITER device
[DE94-718963] p 4530 N94-37464
TFE verification program
[DE94-009870] p 4398 N94-37514

REACTOR MATERIALS
Towards nuclear fusion reactors
[DE94-748680] p 4528 N94-37235
Examination of weldability of Ni-Cr-W superalloys
[DE94-719014] p 4418 N94-37385
Material and design considerations for the carbon armored ITER divertor
[DE94-737854] p 4530 N94-37415
Creep-fatigue interaction property of a nickel-base heat-resistant alloy Hastelloy XR in simulated HTGR helium gas environment
[DE94-737934] p 4418 N94-37416
Transient thermal and dynamic stresses in strongback-design blankets
[DE94-012639] p 4530 N94-37441
Development of intermetallic coatings for fusion power applications
[DE94-012647] p 4419 N94-37442
Creep properties with short period excessive loadings on a nickel-base heat-resistant alloy Hastelloy XR
[DE94-718965] p 4419 N94-37465
Characterization of nuclear transmutations in materials irradiated test facilities
[DE94-013309] p 4420 N94-37552

REACTOR PHYSICS
An overview of the current status of resonance theory in reactor physics applications
[DE94-010465] p 4521 N94-37194

REACTOR SAFETY
An overview of the current status of resonance theory in reactor physics applications
[DE94-010465] p 4521 N94-37194
Towards nuclear fusion reactors
[DE94-748680] p 4528 N94-37235

REAL TIME OPERATION
Subgrouped real time recurrent learning neural networks
[AD-A280618] p 4500 N94-37043
Design of the divertor Thomson scattering system on D3-D
[DE94-012672] p 4527 N94-37081
Long-range mesoscale modeling of pollutant transport for the European Tracer EXperiment (ETEX)
[DE94-010820] p 4465 N94-37093
Efficient contact determination between geometric models
[AD-A280244] p 4494 N94-37120
VHF adaptive antenna development task
[AD-A280320] p 4434 N94-37127
Interaction effects of cracks, flaws and damage in ceramic
[AD-A280368] p 4423 N94-37181
Time-of-flight pulsed ion beam surface analysis as a means of in situ, real-time characterization of the growth of ferro-electric and conductive oxide heterostructures
[DE94-012628] p 4517 N94-37249
Interactive large screen: A multi-mode dialogue tool for future cockpits p 4484 N94-37266
A non-intrusive way to measure point-of-gaze p 4484 N94-37272
Operator gaze position control interfaces: Investigation of psychophysical and operational parameters p 4485 N94-37273
Low cost software-based rendering and stereoscopic interfaces for teleoperation and virtual reality p 4486 N94-37279
Chemical recognition software
[DE94-012918] p 4495 N94-37496
Advanced information processing system: Authentication protocols for network communication
[NASA-CR-194923] p 4498 N94-37500
Techniques for real-time parallel processing: Sensor processing case studies
[AD-A280633] p 4499 N94-37760

RECEIVERS
Receiver design, performance analysis, and evaluation for space-borne laser altimeters and space-to-space laser ranging systems
[NASA-CR-194747] p 4397 N94-36988
NRL HF propagation measurements between Guadeloupe and Providenciales during the CRRES exercises
[DE94-012078] p 4435 N94-37393
Study on the measurement uncertainty of noise properties of a millimeter wave amplifier
[PB94-170917] p 4510 N94-37632

RECORDS
A concise introduction to MARC p 4542 N94-36856

RECRYSTALLIZATION
Thermomechanical studies of tungsten heavy alloys
[AD-A280250] p 4417 N94-37122

RECTANGLES
Cost-effective computations with boundary interface operators in elliptic problems
[DE94-621506] p 4503 N94-37098

RECTANGULAR WAVEGUIDES
A novel transition between rectangular waveguide and layered ridge dielectric waveguide
[NASA-TM-106661] p 4433 N94-36955

RECYCLING
Structural composite construction materials manufactured from municipal solid waste
[AD-A280635] p 4403 N94-36730
Processing solid propellants for recycling
[DE94-011433] p 4428 N94-37202

REFINING
Alternate melting and refining routes p 4421 N94-37323

REFLECTANCE
NASA ER-2 Doppler radar reflectivity calibration for the CAMEX project
[NASA-TM-104611] p 4475 N94-37790

REFLECTOMETERS
Initial studies of reflectometer for ITER
[DE94-012476] p 4528 N94-37167

REFLECTOR ANTENNAS
Baseline antenna design for space exploration initiative
[NASA-CR-196298] p 4435 N94-37255

REFLECTORS
An amorphous fluoropolymer: Next generation optical coating candidate
[DE94-012386] p 4425 N94-37422

REFLEXES
Relation of motion sickness susceptibility to vestibular and behavioral measures of orientation
[NASA-CR-196121] p 4480 N94-37005
Gaze orientation under G(z)-load. Methodological aspects: Preliminary results p 4485 N94-37274

REFRACTIVITY
Determining the refractive index of a lambda/4 thin film on a thick substrate from a transmittance measurement
[DE93-019584] p 4523 N94-36693
An amorphous fluoropolymer: Next generation optical coating candidate
[DE94-012386] p 4425 N94-37422

REFRACTORY MATERIALS
Possibilities and pitfalls in aerospace applications of titanium matrix composites p 4400 N94-36650
Mechanical behavior of MoSi2 and MoSi2 composites
[DE94-013116] p 4405 N94-37289
Development of durable high-temperature catalysts for natural gas combustion: Catalytic materials (CATMAT (trade name)) properties database
[PB94-171824] p 4412 N94-37462
Development of processing techniques for advanced thermal protection materials
[NASA-CR-196261] p 4426 N94-37510
Substituted silyl-terminated compounds and polymers thereof
[AD-D016310] p 4427 N94-37779

REFRIGERANTS
Materials Compatibility and Lubricant Research on CFC-refrigerant substitutes
[DE94-012352] p 4425 N94-37373

Sealed tube comparisons of the compatibility of desiccants with refrigerants and lubricants
[DE94-012371] p 4425 N94-37421
Information on alternative refrigerants and lubricants: The ARTI refrigerant database
[DE94-009997] p 4426 N94-37490

REFRIGERATING
Miniature thermoacoustic refrigerator
[AD-A280326] p 4431 N94-37029
Refrigeration and Air-Conditioning Technology Workshop
[DE94-010813] p 4431 N94-37452

REFRIGERATORS
MODIL cryocooler producibility demonstration project results
[DE93-019213] p 4430 N94-36444
Miniature thermoacoustic refrigerator
[AD-A280326] p 4431 N94-37029
Fundamentals studies of radial wave thermoacoustic engines
[AD-A280534] p 4431 N94-37090

REFUELING
LNG vehicle technology, economics, and safety assessment
[PB94-165487] p 4450 N94-36721

REGENERATIVE COOLING
Active cooling from the sixties to NASP
[NASA-TM-109079] p 4456 N94-37541

REGRESSION ANALYSIS
United States Air Force Summer Research Program, 1993. Volume 3: Phillips Laboratory
[AD-A278694] p 4550 N94-36979
Feature and model selection in feedforward neural networks
[AD-A280709] p 4501 N94-37526
Atmospheric structure simulation: An ARMA model for smooth isotropic two-dimensional geophysical power spectra
[AD-A280476] p 4470 N94-37649

REINFORCING FIBERS
SCS-6 (tm) fiber reinforced titanium
p 4400 N94-36652
Properties of TMC processed by fibre coating and hiping p 4401 N94-36656
A simple evaluation of thermally-induced stresses in the vicinity of the stitch in a through-thickness reinforced cross-ply laminate
[NASA-CR-196317] p 4406 N94-37653

REINFORCING MATERIALS
Using nonequilibrium alloying techniques for corrosion inhibition in Gr/Al and Gr/Mg metal matrix composites
[AD-A280529] p 4404 N94-37088

RELATIVISTIC ELECTRON BEAMS
Coherent multiple-foil x-ray transition radiation
[DE93-040831] p 4525 N94-37486

RELATIVISTIC PARTICLES
High baryon density from relativistic heavy ion collisions
[DE94-003894] p 4511 N94-36460
The Mesozoic Era of relativistic heavy ion physics and beyond
[DE94-011341] p 4548 N94-37557
Strangeness and the quark-gluon plasma: An experimenter's perspective
[DE94-011377] p 4519 N94-37558

RELATIVISTIC THEORY
The form factors of the nucleons
[DE94-013357] p 4515 N94-37086
Activities of the Tandem Accelerator Center, University of Tsukuba
[DE94-748687] p 4522 N94-37237

RELIABILITY ANALYSIS
Possibilities and pitfalls in aerospace applications of titanium matrix composites p 4400 N94-36650
Network survivability performance
[AD-A278746] p 4433 N94-36756
Network survivability performance (computer diskette)
[AD-M000332] p 4433 N94-36757
Evaluating plastic assembly processes for high reliability applications using HAST and Assembly Test Chips
[DE94-010750] p 4439 N94-37363
Probability techniques for reliability analysis of composite materials
[NASA-CR-195294] p 4406 N94-37633
Probabilistic assessment of space nuclear propulsion system nozzle
[NASA-TM-106539] p 4457 N94-37704

RELIABILITY ENGINEERING
On the use of fuzzy logic assessment for high consequence implementation risk analysis
[DE94-011417] p 4507 N94-37564

RELIEF VALVES
Dual valve plate two-way pressure relief valve
[AD-D016293] p 4452 N94-37766

REMOTE CONTROL
Remote use of distributed robotics resources to enhance technology development and insertion
[DE94-009285] p 4502 N94-37785

REMOTE SENSING
SeaWiFS technical report series. Volume 20: The SeaWiFS bio-optical archive and storage system (SeaBASS), part 1
[NASA-TM-104566-VOL-20-PT-1] p 4475 N94-36958
Airborne ROWS data report for the high resolution experiment, June 1993
[NASA-TM-104609] p 4477 N94-37397
Gaseous effluent monitoring and identification using an imaging Fourier transform spectrometer
[DE94-012627] p 4467 N94-37428
Chemical recognition software
[DE94-012918] p 4495 N94-37496
Laser probing of interfaces
[DE94-011300] p 4449 N94-37628
Measuring the upper profile of sea ice in the Bay of Bothnia with a laser profilometer
[PB94-184561] p 4477 N94-37855

REMOTE SENSORS
Gaseous effluent monitoring and identification using an imaging Fourier transform spectrometer
[DE94-012627] p 4467 N94-37428

REMOVAL
Atomic oxygen treatment for non-contact removal of organic protective coatings from painting surfaces
[NASA-TM-106650] p 4421 N94-36952

RENDEZVOUS GUIDANCE
Global Positioning System Synchronized Active Light Autonomous Docking System
[NASA-CASE-MFS-28853-1] p 4395 N94-36825
Evaluation of GPS position and attitude determination for automated rendezvous and docking missions
[NASA-CR-4614] p 4397 N94-37506

RESEARCH
Beginning a dialogue on the changing environment for the physical and mathematical sciences
p 4509 N94-36948
UAV's in climate research: The ARM Unmanned Aerospace Vehicle Program
[DE94-011753] p 4465 N94-37154
Catalog of data bases and reports
[DE94-012230] p 4466 N94-37208
Activities of the Laboratory of Physics, Helsinki University of Technology
[PB94-175247] p 4509 N94-37301

RESEARCH AIRCRAFT
Predicting the effects of unmodeled dynamics on an aircraft flight control system design using eigenspace assignment
[NASA-TM-4548] p 4388 N94-37059

RESEARCH AND DEVELOPMENT
Solid state research
[AD-A280573] p 4533 N94-36734
NASA-UVA Light Aerospace Alloy and Structures Technology Program (LA2ST)
[NASA-CR-196290] p 4415 N94-36809
United States Air Force Summer Research Program, 1993. Volume 13: Phillips Laboratory
[AD-A278657] p 4550 N94-36977
United States Air Force Summer Research Program, 1993. Volume 16: Arnold Engineering Development Center, Frank J. Seiler Research Laboratory and Wilford Hall Medical Center
[AD-A278658] p 4550 N94-36978
United States Air Force Summer Research Program, 1993. Volume 3: Phillips Laboratory
[AD-A278694] p 4550 N94-36979
United States Air Force Summer Research Program, 1993. Volume 4: Rome Laboratory
[AD-A278695] p 4551 N94-36980
United States Air Force Summer Research Program, 1993. Volume 5A: Wright Laboratory
[AD-A278696] p 4551 N94-36981
United States Air Force Summer Research Program, 1993. Volume 6: Arnold Engineering Development Center, Frank J. Seiler Research Laboratory and Wilford Hall Medical Center
[AD-A278697] p 4551 N94-36982
United States Air Force Summer Research Program, 1993. Volume 8: Phillips Laboratory
[AD-A278698] p 4551 N94-36983
United States Air Force Summer Research Program, 1993. Volume 9: Rome Laboratory
[AD-A278699] p 4551 N94-36984
JPRS report: Science and technology. Central Eurasia: Space
[JPRS-USP-94-004] p 4391 N94-37002
JPRS report: Science and technology. Central Eurasia: Space p 4391 N94-37003
JPRS report: Science and technology. Central Eurasia
[JPRS-UST-94-013] p 4509 N94-37006
JPRS report: Science and technology. Central Eurasia: Materials science
[JPRS-UMS-93-008] p 4404 N94-37010
ORNL superconducting technology program for electric power systems
[DE94-011471] p 4438 N94-37239
Hydrogen storage for vehicular applications: Technology status and key development areas
[DE94-011626] p 4428 N94-37243
The Canadian network for the advancement of research, industry and education (CANARIE) p 4543 N94-37336
Materials Compatibility and Lubricant Research on CFC-refrigerant substitutes
[DE94-012352] p 4425 N94-37373
JPRS report: Science and technology. Central Eurasia: Engineering and equipment
[JPRS-UEQ-93-007] p 4431 N94-37523
JPRS report: Science and technology. Central Eurasia: Engineering and equipment
[JPRS-UEQ-93-008] p 4432 N94-37524
JPRS report: Science and technology. Central Eurasia: Engineering and equipment
[JPRS-UEQ-93-005] p 4432 N94-37538
NASA commercial technology. Agenda for change
[NASA-TM-109898] p 4546 N94-37765

RESEARCH FACILITIES
High Energy Physics Division of research activities
[DE93-019681] p 4521 N94-36694
Design and development of experimental facilities for short duration, low-gravity combustion and fire experiments
[NASA-CR-196107] p 4389 N94-36967
Engineering directorate technical facilities catalog
[NASA-TM-109895] p 4390 N94-37443

RESEARCH PROJECTS
United States Air Force Summer Research Program, 1993. Volume 6: Arnold Engineering Development Center, Frank J. Seiler Research Laboratory and Wilford Hall Medical Center
[AD-A278697] p 4551 N94-36982

RESIDUAL STRENGTH
A methodology to predict damage initiation, damage growth and residual strength in titanium matrix composites
[NASA-TM-109135] p 4405 N94-37320
Impact force as a scaling parameter
p 4460 N94-37811

RESIDUAL STRESS
Mitigation of harmful effects of welds in zirconium alloy components
[DE94-619033] p 4414 N94-36543
Micromechanical modeling of damage growth in titanium based metal-matrix composites p 4402 N94-36664
Material and design considerations for the carbon armored ITER divertor
[DE94-737854] p 4530 N94-37415
Residual stress and Raman spectra of laser deposited highly-tetrahedral-coordinated-amorphous-carbon films
[DE94-012067] p 4426 N94-37537
Residual stresses in a multi-pass weld in an austenitic stainless steel plate before and after thermal stress relief
[DE94-013278] p 4420 N94-37548

RESIDUES
Interferometric JFTOT tube deposit measuring device
[AD-D016295] p 4430 N94-37768

RESIN MATRIX COMPOSITES
Structural composite construction materials manufactured from municipal solid waste
[AD-A280635] p 4403 N94-36730

RESINS
Fluorinated resins with low dielectric constant
[AD-D016303] p 4427 N94-37773

RESOLUTION
Measurement of scanning electron microscope resolution
[DE94-012661] p 4525 N94-37374

RESONANCE
Older muons are wiser: Using time information in (mu)LCR spectroscopy
[DE93-018556] p 4511 N94-36457
Determination of the upsilon(1s) leptonic width
[DE94-618534] p 4516 N94-37096
Resonance photoionization of the excited helium
[DE94-618733] p 4517 N94-37173
An overview of the current status of resonance theory in reactor physics applications
[DE94-010465] p 4521 N94-37194

RESONANT FREQUENCIES
Laminated thin shell structures subjected to free vibration in a hygrothermal environment
[NASA-TM-106600] p 4456 N94-37456
Magnetic Earth Ionosphere Resonant Frequencies (NASA-MEIRF Project)
[NASA-CR-196303] p 4435 N94-37461

RESONATORS
Fundamentals studies of radial wave thermoacoustic engines
[AD-A280534] p 4431 N94-37090
RESTORATION
The integrated performance evaluation program quality assurance guidance in support of EM environmental sampling and analysis activities
[DE94-013043] p 4468 N94-37731
RETINAL IMAGES
Visual accommodation to virtual image displays when knowledge of object distance conflicts with optical distance p 4485 N94-37278
REVERSE ENGINEERING
Applying formal methods and object-oriented analysis to existing flight software p 4491 N94-36495
REYNOLDS EQUATION
Development of advanced Navier-Stokes solver
[NASA-CR-195094] p 4504 N94-37449
REYNOLDS NUMBER
Subsonic aerodynamic characteristic of semispan commercial transport model with wing-mounted advanced ducted propeller operating in reverse thrust — conducted in the Langley 14 by 22 foot subsonic wind tunnel
[NASA-TP-3427] p 4384 N94-37505
REYNOLDS STRESS
The alternative faces of turbulent flow
[TM-5-94] p 4442 N94-36934
Momentum-energy transport from turbulence driven by parallel flow shear
[DE94-012765] p 4443 N94-37362
RHODIUM
Morphological aspects of surface reactions
[DE94-011208] p 4413 N94-37713
RICCATI EQUATION
A note on the regularity of solutions of infinite dimensional Riccati equations
[NASA-CR-194898] p 4502 N94-36562
RIGID STRUCTURES
Predicting the effects of unmodeled dynamics on an aircraft flight control system design using eigenspace assignment
[NASA-TM-4548] p 4388 N94-37059
A new technique for dynamic load distribution when two manipulators mutually lift a rigid object, part 2
[DE94-010126] p 4501 N94-37735
RIPPLES
Tune modulation due to gradient ripple and the dynamic aperture
[DE94-011922] p 4524 N94-37157
RISK
Analysis spectral shapes from California and central United States ground motion
[DE94-010041] p 4469 N94-36758
Environmental risk management
[DE94-620987] p 4467 N94-37492
On the use of fuzzy logic assessment for high consequence implementation risk analysis
[DE94-011417] p 4507 N94-37564
ROBOT ARMS
Technology demonstration of space intravehicular automation and robotics
[NASA-TM-109138] p 4501 N94-37589
ROBOT CONTROL
Robust stability of second-order systems
[NASA-CR-196384] p 4501 N94-37590
What is an open architecture robot controller?
[DE94-007854] p 4501 N94-37783
ROBOT DYNAMICS
Robot trajectory planning via dynamic programming
[DE94-008424] p 4501 N94-37529
Robust stability of second-order systems
[NASA-CR-196384] p 4501 N94-37590
ROBOT SENSORS
Adaptive multisensor fusion for the perception and interpretation of outdoor robot scenes
[PB94-170719] p 4499 N94-36535
ROBOTICS
Beyond intelligent vacuum cleaners
[AD-A280565] p 4500 N94-37039
Efficient contact determination between geometric models
[AD-A280244] p 4494 N94-37120
Bootstrap planning: Theory and application
[DE94-006466] p 4501 N94-37425
Technology demonstration of space intravehicular automation and robotics
[NASA-TM-109138] p 4501 N94-37589
Interactive Collaborative Environments (ICE): Platform independent X application sharing and multi-media over wide area networks
[DE94-008668] p 4502 N94-37784
Remote use of distributed robotics resources to enhance technology development and insertion
[DE94-009285] p 4502 N94-37785
ROBOTS
Adaptive multisensor fusion for the perception and interpretation of outdoor robot scenes
[PB94-170719] p 4499 N94-36535
Beyond intelligent vacuum cleaners
[AD-A280565] p 4500 N94-37039
Adaptive learning of multi-sensor integration techniques with genetic algorithms
[DE94-012744] p 4500 N94-37083
Robot trajectory planning via dynamic programming
[DE94-008424] p 4501 N94-37529
Remote use of distributed robotics resources to enhance technology development and insertion
[DE94-009285] p 4502 N94-37785
ROBUSTNESS (MATHEMATICS)
A flux splitting scheme with high-resolution and robustness for discontinuities
[NASA-TM-106452] p 4441 N94-36646
H infinity control for nonlinear and linear systems
[AD-A280450] p 4494 N94-37226
Optimization for minimum sensitivity to uncertain parameters
[NASA-TM-109139] p 4386 N94-37256
ROCK INTRUSIONS
Vent processes during the 1912 eruption at Novarupta, Katmai National Park, Alaska
[DE94-010740] p 4468 N94-36451
ROCKET ENGINES
UVPI imaging from the LACE satellite: The Low Cost Launch Vehicle (LCLV) rocket plume
[AD-A278785] p 4398 N94-36445
Validation and implementation of optical diagnostics for particle sizing in rocket motors
[AD-A278581] p 4428 N94-36972
ROCKET NOZZLES
NASA reload program
[NASA-CR-193972] p 4429 N94-37446
ROCKET SOUNDING
Three flights into thunderstorms with the revised Rocket Electric Field Sounding (REFS) payload
[AD-A280424] p 4473 N94-37217
ROCKS
Investigation of ultrasonic surface wave interaction with porous saturated rocks
[DE94-013378] p 4469 N94-37177
A computational model for three-dimensional jointed media with a single joint set
[DE94-007582] p 4470 N94-37527
ROTARY WING AIRCRAFT
Rotorwash analysis handbook. Volume 1: Development and analysis
[SCT-93RR-17-VOL-1] p 4381 N94-36466
Rotorwash analysis handbook. Volume 2: Appendixes
[SCT-93RR-17-VOL-2] p 4382 N94-36467
TRENDS: A flight test relational database user's guide and reference manual
[NASA-TM-108806] p 4381 N94-37332
Advanced distributed simulation technology advanced rotary wing aircraft. Software programmer's manual visual system module
[AD-A280260] p 4390 N94-37755
Advanced distributed simulation technology advanced rotary wing aircraft. System/segment specification. Volume 4: Simulation system module RAH-66 Kit
[AD-A280261] p 4391 N94-37756
ROTARY WINGS
Forward sweep, low noise rotor blade
[NASA-CASE-LAR-14569-1] p 4386 N94-36767
ROTATING BODIES
Attenuating the disorienting effects of head movement during whole-body rotation using a visual reference: Further tests of a predictive hypothesis p 4482 N94-37276
ROTATING LIQUIDS
Use of rotation to suppress thermosolutal convection in directionally solidified binary alloys
[NASA-CR-196372] p 4415 N94-36811
ROTATING PLASMAS
Anomalous cross field flux in CHS
[DE94-727547] p 4529 N94-37359
RUN TIME (COMPUTERS)
Parallel Spectral Transform Shallow Water Model: A runtime-tunable parallel benchmark code
[DE94-011460] p 4498 N94-37568
RUNWAYS
A model-based approach for detection of runways and other objects in image sequences acquired using an on-board camera
[NASA-CR-196424] p 4446 N94-36812
RUSSIAN FEDERATION
JPRS report: Central Eurasia. Aviation and cosmonautics, No. 4, April 1993
[JPRS-UAC-94-003] p 4391 N94-36999
JPRS report: Science and technology. Central Eurasia: Space
[JPRS-USP-94-004] p 4391 N94-37002
JPRS report: Science and technology. Central Eurasia: Space p 4391 N94-37003
JPRS report: Science and technology. Central Eurasia
[JPRS-UST-94-013] p 4509 N94-37006
JPRS report: Science and technology. Central Eurasia: Materials science
[JPRS-UMS-93-008] p 4404 N94-37010
Space Station: Impact of the expanded Russian role on funding and research. Report to the Ranking Minority Member, Subcommittee on Oversight of Government Management, Committee on Governmental Affairs, US Senate
[GAO/NSIAD-94-220] p 4396 N94-37257
Problems of international exchange of scientific and technical information for a Russian aerospace research institute p 4544 N94-37339

S

S-N DIAGRAMS
Pre-standardisation work on fatigue and fracture testing of titanium matrix composites p 4402 N94-36667
SAFETY
Information on alternative refrigerants and lubricants: The ARTI refrigerant database
[DE94-009997] p 4426 N94-37490
SAFETY DEVICES
Aircraft command in emergency situations prototype development users manual
[DOT/FAA/CT-94/24] p 4385 N94-37706
SAFETY MANAGEMENT
Space Shuttle: Incomplete data and funding approach increase cost risk for upgrade program. Report to Congressional Requesters
[GAO/NSIAD-94-23] p 4392 N94-37026
NASA Lewis wind tunnel model systems criteria
[NASA-TM-106565] p 4390 N94-37522
SAMPLERS
California residential indoor air quality study. Volume 1: Methodology and descriptive statistics. Appendix
[PB94-166055] p 4464 N94-36995
SANDS
Geophysical data fusion for subsurface imaging
[DE94-000056] p 4469 N94-36738
SATELLITE ATMOSPHERES
Infrared spectroscopy of Jupiter and Saturn
[NASA-CR-196294] p 4549 N94-36961
SATELLITE COMMUNICATION
Preliminary PANSAT ground station software design and use of an expert system to analyze telemetry
[AD-A280600] p 4392 N94-36726
Error control techniques for satellite and space communications
[NASA-CR-196302] p 4433 N94-36931
SATELLITE IMAGERY
Variability of the California Current System off Point Sur, California from April 1988 to December 1990
[AD-A278579] p 4476 N94-36985
SATELLITE OBSERVATION
SeaWiFS technical report series. Volume 20: The SeaWiFS bio-optical archive and storage system (SeaBASS), part 1
[NASA-TM-104566-VOL-20-PT-1] p 4475 N94-36958
SATELLITE TRACKING
Design and analysis of a mode B and mode JD satellite Earth station
[AD-A280417] p 4391 N94-37225
SATELLITE-BORNE INSTRUMENTS
Characterization of spacecraft and environmental disturbances on a SmallSat
[NASA-CR-194915] p 4396 N94-36990
NOAA polar satellite calibration: A system description
[NOAA-TR-NESDIS-77] p 4396 N94-37009
SCALARS
Effective Lagrangian for gluons and Higgs pseudoscalars
[DE94-001381] p 4513 N94-36539
SCALE EFFECT
Workshop on Scaling Effects in Composite Materials and Structures
[NASA-CP-3271] p 4457 N94-37796
Experimental observations of scale effects on bonded and bolted joints in composite structures p 4458 N94-37801
The effects of specimen scale on the compression strength of composite materials p 4459 N94-37802
On nature's scaling effects p 4459 N94-37803
Damage and strength of composite materials: Trends, predictions, and challenges p 4459 N94-37805
Scaling effects of defects in fiber-reinforced composites p 4459 N94-37807
Size effect in composite materials and structures: Basic concepts and design considerations p 4460 N94-37808

Statistical scaling relationships and size effects in the strength and creep rupture of fibrous composites
p 4460 N94-37809

SCALE MODELS
Design of scaled down structural models
p 4457 N94-37797
Sub-ply level scaling approach investigated for graphite-epoxy composite beam columns
p 4458 N94-37796
Effects of scale in predicting global structural response
p 4458 N94-37799

SCALING LAWS
Nonlinearity with disorder: Spatio-temporal complex behavior arising from length scales competition
[DE94-000675] p 4502 N94-36685
The role of heating and current drive in ITER
[DE94-012679] p 4527 N94-37082
Isotope scaling and eta(i) mode with impurities in tokamak plasmas
[DE94-012783] p 4529 N94-37361
Workshop on Scaling Effects in Composite Materials and Structures
[NASA-CP-3271] p 4457 N94-37796
Design of scaled down structural models
p 4457 N94-37797
Scaling, elasticity, and CLPT
p 4458 N94-37800
Statistical scaling relationships and size effects in the strength and creep rupture of fibrous composites
p 4460 N94-37809
Scaling of impact damage in fiber composites
p 4460 N94-37810
Impact force as a scaling parameter
p 4460 N94-37811

SCANNERS
A new, optical-lever based atomic force microscope
[AD-A280524] p 4524 N94-37110
Poly(p-phenylene) derivatives new high performance nonlinear optical polymers
[AD-A280248] p 4422 N94-37121

SCANNING ELECTRON MICROSCOPY
Processing, packaging, and characterization of electroceramic materials for phased array antennas
[AD-A280251] p 4432 N94-36743
Determination of interface structure and bonding at atomic resolution in the stem
[DE94-011466] p 4517 N94-37238
Measurement of scanning electron microscope resolution
[DE94-012661] p 4525 N94-37374
Atomic resolution characterization of a SrTiO3 grain boundary in the STEM
[DE94-011469] p 4538 N94-37545
The application of maximum entropy to Z-contrast imaging in a stem
[DE94-011470] p 4412 N94-37546

SCATTERING
Scattering theory for the quantum envelope of a classical system
[DE94-008530] p 4539 N94-36508
Dipole forbidden vibrational modes for NO and CO on Cu observed in the far IR
[DE94-003199] p 4408 N94-36559
A rejection method for selection of scattered states
[DE94-012232] p 4517 N94-37209

SCATTERING CROSS SECTIONS
Measurement of the elastic, total and diffraction cross sections at tevatron energies
[DE94-004659] p 4511 N94-36463
Scattering cross section of sound waves by the modal element method
[NASA-TM-106667] p 4510 N94-37308
Neutrino-nucleon scattering
[DE94-011720] p 4520 N94-37671

SCENE ANALYSIS
Adaptive multisensor fusion for the perception and interpretation of outdoor robot scenes
[PB94-170719] p 4499 N94-36535

SCHEDULES
Recent SEL experiments and studies
p 4490 N94-36487

SCHEDULING
Planning German Army helicopter maintenance and mission assignment
[AD-A280483] p 4381 N94-37352

SCHROEDINGER EQUATION
Nonlinearity with disorder: Spatio-temporal complex behavior arising from length scales competition
[DE94-000675] p 4502 N94-36685
Solving the two-dimensional Schroedinger equation in self-consistent basis
[DE94-621535] p 4504 N94-37174
Final report on spectral broadening by cross-phase modulation in linearly birefringent optical fibers
[DE94-010406] p 4524 N94-37191
The angular and energy distributions of ejected electrons in electron-impact ionization of helium
[DE94-618748] p 4519 N94-37528

SCIENTIFIC VISUALIZATION
EM-ANIMATE: A computer program for displaying and animating electromagnetic near-field and surface-current solutions: Video supplement to NASA Technical Memorandum 4539
[NASA-TM-4539-VIDEO-SUPPL] p 4492 N94-36518

SCINTILLATION
Wide aperture scintillation hodoscope with FEU-143 photomultipliers
[DE94-618211] p 4515 N94-37075

SCINTILLATION COUNTERS
High Energy Physics Division of research activities
[DE93-019681] p 4521 N94-36694
Simple and efficient method of secondary vertex searching
[DE94-618542] p 4514 N94-37064
Wide aperture scintillation hodoscope with FEU-143 photomultipliers
[DE94-618211] p 4515 N94-37075

SEA ICE
Measuring the upper profile of sea ice in the Bay of Bothnia with a laser profilometer
[PB94-184561] p 4477 N94-37855

SEA STATES
Airborne ROWS data report for the high resolution experiment, June 1993
[NASA-TM-104609] p 4477 N94-37397

SEA WATER
Cooling of the West Spitzbergen Current: Wintertime observations west of Svalbard
[AD-A280648] p 4475 N94-36762

SEALS (STOPPERS)
Hot dynamic test rig for measuring hypersonic engine seal flow and durability
[NASA-TM-106507] p 4450 N94-36645
Evaluation of seals and lubricants used on the Long Duration Exposure Facility
[NASA-CR-4604] p 4399 N94-37614

SEARCHING
Searching for plans using a hierarchy of learned macros and selective reuse
[AD-A280594] p 4499 N94-36722
Simple and efficient method of secondary vertex searching
[DE94-618542] p 4514 N94-37064

SEAS
Cooling of the West Spitzbergen Current: Wintertime observations west of Svalbard
[AD-A280648] p 4475 N94-36762

SECONDARY FLOW
Unsteady flow field of large-amplitude pitching airfoils
[AD-A280444] p 4383 N94-37219

SECURITY
Software use control
[DE94-008429] p 4489 N94-36480
Criminal Acts Against Civil Aviation, 1993
[AD-A280694] p 4384 N94-37131
The effects of proton-beam quality on the production of gamma rays for nuclear resonance absorption in nitrogen
[DE94-011609] p 4523 N94-37629

SEDIMENTARY ROCKS
Analysis of deep seismic reflection and other data from the Southern Washington Cascades
[DE94-004075] p 4470 N94-37489

SEISMOGRAMS
Analysis of deep seismic reflection and other data from the Southern Washington Cascades
[DE94-004075] p 4470 N94-37489

SEISMOLOGY
Analysis spectral shapes from California and central United States ground motion
[DE94-010041] p 4469 N94-36758

SELECTORS
Crosspoint analog data selector
[AD-D016326] p 4440 N94-37832

SELENIUM
New plasma source of hydrides for epitaxial growth
[DE94-006918] p 4533 N94-36744
Ionization balance and gain calculations for neon-like selenium x-ray laser plasmas
[DE94-012590] p 4530 N94-37437

SELF ADAPTIVE CONTROL SYSTEMS
Automatic, self-adaptive control of unfold transformations
[DE94-012455] p 4504 N94-37247

SELF FOCUSING
Effect of the stimulated Brillouin backscattering on self-focusing threshold
[DE94-008678] p 4510 N94-37536

SEMICONDUCTOR DEVICES
A proposed SEU tolerant DRAM cell
[DE94-010758] p 4438 N94-37196
Time-step stability for self-consistent Monte Carlo device simulation
[DE94-012145] p 4528 N94-37207

SEMICONDUCTOR LASERS
Diode array alternative to paint removal solid-state cw laser
[DE94-011482] p 4448 N94-37203
Advanced laser driver for soft x-ray projection lithography
[DE94-011643] p 4449 N94-37722

SEMICONDUCTORS (MATERIALS)
Gas-Phase and Surface Chemistry in Electronic Materials Processing. Materials Research Society Symposium proceedings, volume 334
[AD-A280586] p 4408 N94-36735
Small-angle x ray scattering studies of microvoids in amorphous-silicon-based semiconductors
[DE94-006931] p 4533 N94-36745
Ampoule failure sensor time response testing: Experiments 2 and 3
[NASA-TM-108458] p 4446 N94-36822
The excitation mechanism of praseodymium-doped semiconductors
[AD-A280687] p 4535 N94-37129
Preliminary soft x ray studies of beta-SiC
[DE94-013023] p 4537 N94-37498
Theoretical studies of the transport properties in compound semiconductors
[NASA-CR-196109] p 4439 N94-37501
The application of maximum entropy to Z-contrast imaging in a stem
[DE94-011470] p 4412 N94-37546
Experimental particle physics at the University of Pittsburgh
[DE94-011636] p 4521 N94-37721
Comparison of gaseous and semiconductor detectors for medical imaging
[DE94-621344] p 4482 N94-37729
Implanting impurities in semiconductors and semiconductor implanted with impurities
[AD-D016298] p 4538 N94-37770

SENSITIVITY
Molecular beam surface analysis
[DE94-010773] p 4406 N94-36453
Older muons are wiser: Using time information in (mu)LCR spectroscopy
[DE93-018556] p 4511 N94-36457
Optimization for minimum sensitivity to uncertain parameters
[NASA-TM-109139] p 4386 N94-37256

SENSORS
Ampoule failure sensor time response testing: Experiments 2 and 3
[NASA-TM-108458] p 4446 N94-36822
Detection of delaminations in composite beams using piezoelectric sensors
[NASA-TM-106611] p 4403 N94-36956

SENSORY PERCEPTION
On the feasibility of virtual environments in medicine
p 4483 N94-37264
The use of a tactile interface to convey position and motion perceptions
p 4486 N94-37281

SEPARATED FLOW
Unsteady flow field of large-amplitude pitching airfoils
[AD-A280444] p 4383 N94-37219

SEPARATION
Development of immobilized ligands for actinide separations
[DE94-012714] p 4410 N94-37284

SERVICE LIFE
Space Shuttle: Incomplete data and funding approach increase cost risk for upgrade program. Report to Congressional Requesters
[GAO/NSIAD-94-23] p 4392 N94-37026
Impact of Materials Defects on Engine Structures Integrity
[AGARD-R-790] p 4453 N94-37321
Alternate melting and refining routes
p 4421 N94-37323

SERVICES
Information retrieval services on wide area networks: A vision of the future
p 4545 N94-37346

SERVOMECHANISMS
High accuracy control algorithm application to a tracking turret
p 4394 N94-36626
A dynamic model of a linear actuator based on polymer hydrogel
[DE94-010800] p 4408 N94-37091

SET THEORY
Interactive calculator for use with multi-dimensional netCDF files
[DE94-007477] p 4545 N94-37348

SEYFERT GALAXIES
Guaranteed time observations support for Faint Object Spectrograph (FOS) on HST
[NASA-CR-196305] p 4547 N94-37037

SHADOWGRAPH PHOTOGRAPHY
A shadowgraph study of Space Transportation System (STS): The Space Shuttle Launch Vehicle (SSLV)
[NASA-RP-1341] p 4382 N94-36741
SHAPE MEMORY ALLOYS
Mechanical behavior and phase stability of NiAl-based shape memory alloys
[DE94-012336] p 4419 N94-37420
SHEAR FLOW
Momentum-energy transport from turbulence driven by parallel flow shear
[DE94-012765] p 4443 N94-37362
The stabilizing effect of compressibility in turbulent shear flow
[NASA-CR-194932] p 4444 N94-37605
Towards enhancing and delaying disturbances in free shear flows
[NASA-CR-194945] p 4445 N94-37606
SHEAR LAYERS
Turbulence modeling of free shear layers for high performance aircraft
[NASA-CR-196137] p 4442 N94-36808
Holt film wall shear instrumentation for boundary layer transition research
[NASA-CR-196040] p 4443 N94-37060
SHEAR STRENGTH
A comparison of graphite/epoxy tape laminates and 2-D braided composites mechanical properties
[NASA-CR-4610] p 4420 N94-37582
SHEAR STRESS
Fibre-matrix interface properties in Ti-matrix composites: Chemical compatibility and micromechanical behaviour p 4401 N94-36657
SHIELDING
Method of N-15 analysis by mass-spectroscopy on ion implanter MPB-200
[DE94-618203] p 4407 N94-36529
SHIPS
Landing of an unmanned helicopter on a moving platform. High accuracy navigation and tracking p 4387 N94-36618
SHIVERING
Homeostatic responses to prolonged cold exposure: Human cold acclimatization
[AD-A280234] p 4481 N94-37136
SHOCK LOADS
A mixture model for shock compression of porous multi-component reactive materials
[DE93-017636] p 4400 N94-36456
Fluids at high shock pressures and temperatures and some thoughts about future possibilities
[DE94-003625] p 4407 N94-36458
DDT modeling and shock compression experiments of porous or damaged energetic materials
[DE94-011419] p 4428 N94-37052
SHOCK TESTS
Fluids at high shock pressures and temperatures and some thoughts about future possibilities
[DE94-003625] p 4407 N94-36458
SHOCK TUBES
Experimental investigation of nozzle/plume aerodynamics at hypersonic speeds
[NASA-CR-195829] p 4382 N94-36687
SHOCK TUNNELS
Experimental investigation of nozzle/plume aerodynamics at hypersonic speeds
[NASA-CR-195829] p 4382 N94-36687
SHOCK WAVE INTERACTION
Hypersonic shock/boundary-layer interaction database: New and corrected data
[NASA-CR-177638] p 4441 N94-36519
SHOCK WAVES
High-order centered difference methods with sharp shock resolution
[NASA-CR-196374] p 4496 N94-37656
A nonconservative scheme for isentropic gas dynamics
[DE94-011488] p 4445 N94-37724
SHOT PEENING
Literature review and preliminary studies of fretting and fretting fatigue including special applications to aircraft joints
[AD-A280310] p 4456 N94-37125
SHROUDED PROPELLERS
Subsonic aerodynamic characteristic of semispan commercial transport model with wing-mounted advanced ducted propeller operating in reverse thrust — conducted in the Langley 14 by 22 foot subsonic wind tunnel
[NASA-TP-3427] p 4384 N94-37505
SHUTDOWNS
Startup and shutdown of the PULSAR Tokamak Reactor
[DE94-013128] p 4526 N94-37292
SIDELOBE REDUCTION
MTI compatible coherent sidelobe canceller
[AD-D016300] p 4435 N94-37771
SIGNAL DETECTION
Distributed detection theory and data fusion
[AD-A280410] p 4434 N94-37183
SIGNAL ENCODING
Studies on image compression and image reconstruction
[NASA-CR-196304] p 4433 N94-36810
SIGNAL PROCESSING
Chilbolton Advanced Meteorological Radar: A tool for multi-disciplinary atmospheric research
[PB94-167467] p 4432 N94-36567
Radar tracking in multipath: Techniques for improved performance p 4395 N94-36631
Multirate time-frequency distributions
[AD-A280595] p 4503 N94-36723
Signal processing for the 1992 Barents Sea tomography experiment
[AD-A278580] p 4476 N94-36971
VHF adaptive antenna development task
[AD-A280320] p 4434 N94-37127
Detection of the electrocardiogram P-wave using wavelet analysis
[DE94-010791] p 4481 N94-37197
KONRAD: Wide band digital HF receiver
[PB94-184686] p 4435 N94-37813
Wavefront simulator for evaluating RF communication array signal processors
[AD-D016281] p 4436 N94-37835
Phase shifter for directly sampled bandpass signals
[AD-D016320] p 4440 N94-37840
SIGNAL TO NOISE RATIOS
Sensitivity and signal to noise ratio improvement of a one micron lidar system incorporating a neodymium doped optical fiber preamplifier. Laser radar testbed
[AD-A280235] p 4447 N94-37137
SIGNAL TRANSMISSION
Signal processing for the 1992 Barents Sea tomography experiment
[AD-A278580] p 4476 N94-36971
SIGNATURE ANALYSIS
Vibration signature analysis of a faulted gear transmission system
[NASA-TM-106623] p 4450 N94-36953
NASA reload program
[NASA-CR-193972] p 4429 N94-37446
SIGNS AND SYMPTOMS
Cardiac pressure changes with venous gas embolism and decompression
[AD-A280412] p 4481 N94-37224
Profile analysis of after-effects experienced during exposure to several virtual reality environments p 4482 N94-37263
Some side-effects of immersion virtual reality p 4482 N94-37277
SILANES
Carborane-siloxane or silane-unsaturated hydrocarbon based polymers
[AD-D016220] p 4425 N94-37482
Carborane-(silane or siloxane)-unsaturated hydrocarbon based thermosetting polymers
[AD-D016311] p 4427 N94-37818
SILICATES
A possible origin of EL6 chondrites from a high temperature-high pressure solar gas
[DE94-010467] p 4548 N94-36759
SILICIDES
Quadrupolar effects in PrCu2Si2
[DE94-011509] p 4534 N94-37054
Mechanical behavior of MoSi2 and MoSi2 composites
[DE94-013116] p 4405 N94-37289
SILICON
B-lifetime measurements at the tevatron
[DE94-003617] p 4513 N94-36528
A possible origin of EL6 chondrites from a high temperature-high pressure solar gas
[DE94-010467] p 4548 N94-36759
Field emitter array RF amplifier development project. Cathode technology development. Phase 1
[AD-A280515] p 4437 N94-37108
Progress on the emitter wrap-through silicon solar cell
[DE94-010382] p 4462 N94-37189
Comparison of oxygen and silicon induced reactions at 14.6 A(GeV/C)
[DE94-011923] p 4518 N94-37364
A photoemission study of Au, Ge, and O2 deposition on NH4F etched Si(111)
[DE94-013352] p 4519 N94-37553
SILICON CARBIDES
Properties of TMC processed by fibre coating and hiping p 4401 N94-36656
Fibre-matrix interface properties in Ti-matrix composites: Chemical compatibility and micromechanical behaviour p 4401 N94-36657
Prediction of thermal and mechanical stress-strain responses of TMC's subjected to complex TMF histories p 4402 N94-36666
Development of mechanical testing methods for titanium matrix composites (traction-ogligo-cyclic fatigue) p 4403 N94-36669
Development of nondestructive evaluation methods and prediction of effects of flaws on the fracture behavior of structural ceramics
[DE94-012466] p 4425 N94-37423
Theoretical studies of the transport properties in compound semiconductors
[NASA-CR-196109] p 4439 N94-37501
SILICON COMPOUNDS
Substituted silyl-terminated compounds and polymers thereof
[AD-D016310] p 4427 N94-37779
SILICON DIOXIDE
Mineralogy and metallurgical properties of iron ore sinter based on magnetite fines
[DE94-763309] p 4414 N94-36525
Low temperature atmospheric pressure chemical vapor deposition of group 14 oxide films
[DE94-013115] p 4425 N94-37317
SILICON ISOTOPES
Production of phi mesons in central Si+Au collisions at 14.6 A GeV/c
[DE94-011726] p 4516 N94-37152
SILICONES
Replacement of silicone polymer A with silicone polymer B and the subsequent characterization of the new cellular silicone materials
[DE94-010105] p 4421 N94-36474
SILOXANES
Carborane-siloxane or silane-unsaturated hydrocarbon based polymers
[AD-D016220] p 4425 N94-37482
SIMILARITY NUMBERS
Design of scaled down structural models p 4457 N94-37797
SIMILITUDE LAW
Workshop on Scaling Effects in Composite Materials and Structures
[NASA-CP-3271] p 4457 N94-37796
Design of scaled down structural models p 4457 N94-37797
On nature's scaling effects p 4459 N94-37803
SIMULATION
Introduction to the heavy quark effective theory, part 1
[DE94-618512] p 4514 N94-36749
Controlled atmospheric breakdown: Applications and research opportunities
[AD-A278584] p 4464 N94-36973
VHF adaptive antenna development task
[AD-A280320] p 4434 N94-37127
Simulation of three-dimensional multi-phase flow characteristics in the deswirl section of the CDIF MHD power train
[DE94-012644] p 4443 N94-37176
SIMULATORS
Calibration and initial testing of a new hydraulic simulator
[AD-A280632] p 4390 N94-37163
SACS: A cache simulator incorporating timing analysis with buffer and memory management
[AD-A280472] p 4494 N94-37230
Immersive virtual environments as trainer: System design from a cognitive stance p 4484 N94-37267
Wavefront simulator for evaluating RF communication array signal processors
[AD-D016281] p 4436 N94-37835
SINGLE CRYSTALS
Substrate effects on the structure and optical properties of epitaxial PbTiO3 thin films prepared by metal-organic chemical vapor deposition
[DE94-010432] p 4535 N94-37192
Applications of high transition temperature superconductors at the Savannah River Site
[DE94-012938] p 4536 N94-37311
Perfluorodiethoxymethane on nickel and nickel oxide surfaces
[DE94-011200] p 4426 N94-37712
SINGLE EVENT UPSETS
Single event mirroring and sense amplifier designs for enhanced SE tolerance of DRAMs
[DE94-010397] p 4438 N94-37190
A proposed SEU tolerant DRAM cell
[DE94-010758] p 4438 N94-37196
SINTERING
Advances in rapid prototyping
[DE94-010075] p 4430 N94-36447
Sintering of dioxide pellets in an oxidizing atmosphere (CO2)
[DE94-613046] p 4414 N94-36517
Mineralogy and metallurgical properties of iron ore sinter based on magnetite fines
[DE94-763309] p 4414 N94-36525

Characterization and processing of sintered products from nano-crystalline powders generated by the RTDS method
[DE94-004765] p 4415 N94-36553

SISO (CONTROL SYSTEMS)
Mixed H2/H-infinity optimization with multiple H infinity constraints
[AD-A280572] p 4388 N94-36733

SIZE DISTRIBUTION
Validation and implementation of optical diagnostics for particle sizing in rocket motors
[AD-A278581] p 4428 N94-36972

SKEWNESS
Short-tower sigma(theta) measurements in the Colorado Plateaus region
[DE94-007478] p 4463 N94-36478

SKY SURVEYS (ASTRONOMY)
The distributed development environment for SDSS software
[DE94-013238] p 4547 N94-37555
Sloan Digital Sky Survey
[DE94-011749] p 4547 N94-37667

SLABS
The 250 watt average power electro-quality Q-switched diode pumped power oscillator
[DE94-011644] p 4449 N94-37737

SLAGS
Mineralogy and metallurgical properties of iron ore sinter based on magnetite fines
[DE94-763309] p 4414 N94-36525

SLEWING
Modeling and control of intelligent flexible structures
[AD-A280478] p 4396 N94-37349

SMALL SCIENTIFIC SATELLITES
Characterization of spacecraft and environmental disturbances on a SmallSat
[NASA-CR-194915] p 4396 N94-36990

SMART STRUCTURES
A PDE-based methodology for modeling, parameter estimation and feedback control in structural and structural acoustic systems
[NASA-CR-194928] p 4500 N94-36924
Vibration suppression with approximate finite dimensional compensators for distributed systems: Computational methods and experimental results
[NASA-CR-194927] p 4500 N94-36928
Modeling and control of intelligent flexible structures
[AD-A280478] p 4396 N94-37349

SMOKE DETECTORS
Design and development of experimental facilities for short duration, low-gravity combustion and fire experiments
[NASA-CR-196107] p 4389 N94-36867
Aircraft command in emergency situations prototype development users manual
[DOT/FAA/CT-94/24] p 4385 N94-37706

SOCIAL FACTORS
Math and science illiteracy: Social and economic impacts
[DE94-010801] p 4540 N94-37092

SODIUM
The determination of hydrogen in sodium by vacuum extraction
[DE94-620278] p 4412 N94-37533

SODIUM ISOTOPES
Sodium-23 NMR and complex impedance studies of gel electrolytes based on poly(acrylonitrile)
[AD-A280330] p 4408 N94-37031

SOFIA (AIRBORNE OBSERVATORY)
SOFIA: Aircraft system, aft telescope cavity configuration, phase 2. Volume 1: Executive summary
[NASA-CR-196362] p 4546 N94-36642

SOFTWARE ENGINEERING
Software use control
[DE94-008429] p 4489 N94-36480
Proceedings of the Eighteenth Annual Software Engineering Workshop
[NASA-CR-189348] p 4489 N94-36484
The maturing of the quality improvement paradigm in the SEL p 4489 N94-36485
Process improvement as an investment: Measuring its worth p 4489 N94-36486
Recent SEL experiments and studies p 4490 N94-36487
Specification-based software sizing: An empirical investigation of function metrics p 4490 N94-36488
Software forecasting as it is really done: A study of JPL software engineers p 4490 N94-36489
Assessing efficiency of software production for NASA-SEL data p 4490 N94-36490
The (mis)use of subjective process measures in software engineering p 4490 N94-36491
Lessons learned applying CASE methods/tools to Ada software development projects p 4491 N94-36493
Software engineering with application-specific languages p 4491 N94-36494
Integrating end-to-end threads of control into object-oriented analysis and design p 4491 N94-36496
Fusing modeling techniques to support domain analysis for reuse opportunities identification p 4491 N94-36497
An empirical comparison of a dynamic software testability metric to static cyclomatic complexity p 4491 N94-36498
Software quality: Process or people p 4492 N94-36499
Profile of NASA software engineering: Lessons learned from building the baseline p 4492 N94-36500
Impact of Ada in the Flight Dynamics Division: Excitement and frustration p 4492 N94-36501
Software engineering technology transfer: Understanding the process p 4492 N94-36502
Earth Observing System/Advanced Microwave Sounding Unit-A (EOS/AMSU-A) software management plan
[NASA-CR-189362] p 4461 N94-36919
A survey of commonly applied methods for software process improvement
[AD-A278595] p 4493 N94-36974
Proto code generation techniques
[AD-A280275] p 4494 N94-37123
Advanced information processing system: Hosting of advanced guidance, navigation and control algorithms on AIPS using ASTER
[NASA-CR-194960] p 4499 N94-37583
Techniques for real-time parallel processing: Sensor processing case studies
[AD-A280633] p 4499 N94-37780

SOFTWARE RELIABILITY
Analysis of a successful inspection program p 4490 N94-36492
Applying formal methods and object-oriented analysis to existing flight software p 4491 N94-36495
Software quality: Process or people p 4492 N94-36499
Impact of Ada in the Flight Dynamics Division: Excitement and frustration p 4492 N94-36501
United States Air Force Summer Research Program, 1993. Volume 9: Rome Laboratory
[AD-A278699] p 4551 N94-36984

SOFTWARE REUSE
Fusing modeling techniques to support domain analysis for reuse opportunities identification p 4491 N94-36497
Porting industrial codes and developing sparse linear solvers on parallel computers
[PB94-170503] p 4497 N94-36547

SOFTWARE TOOLS
Software quality: Process or people p 4492 N94-36499
Interchangeable spline reference guide
[DE94-012368] p 4495 N94-37245

SOLAR ACTIVITY
United States Air Force Summer Research Program, 1993. Volume 3: Phillips Laboratory
[AD-A278694] p 4550 N94-36979

SOLAR ACTIVITY EFFECTS
Solar-Terrestrial Predictions, 4: Proceedings of a workshop. Volume 1: Workshop overview papers; working group reports; User community reports; Regional Warning Center Reports
[PB94-173176] p 4471 N94-37780
Solar-Terrestrial Predictions, 4: Proceedings of a workshop. Volume 2: Solar papers; magnetospheric papers
[PB94-173184] p 4471 N94-37781

SOLAR ARRAYS
Neural network for positioning Space Station solar arrays
[NASA-TM-106656] p 4431 N94-36943

SOLAR CELLS
Progress on the emitter wrap-through silicon solar cell
[DE94-010362] p 4462 N94-37189
Investigation of polycrystalline thin-film CuInSe2 solar cells based on ZnSe windows
[DE94-006936] p 4462 N94-37381
1993 JSES (Japan Solar Energy Society)/JWEA (Japan Wind Energy Association) Joint Conference and 1993 Japan-Korea Joint Conference on Solar Energy
[DE94-767725] p 4462 N94-37418

SOLAR COLLECTORS
1993 JSES (Japan Solar Energy Society)/JWEA (Japan Wind Energy Association) Joint Conference and 1993 Japan-Korea Joint Conference on Solar Energy
[DE94-767725] p 4462 N94-37418

SOLAR CORONA
A study of physical mechanisms for filament eruption and coronal mass ejection via numerical simulation
[NASA-CR-196087] p 4549 N94-36469
United States Air Force Summer Research Program, 1993. Volume 3: Phillips Laboratory
[AD-A278694] p 4550 N94-36979

SOLAR ENERGY
1993 JSES (Japan Solar Energy Society)/JWEA (Japan Wind Energy Association) Joint Conference and 1993 Japan-Korea Joint Conference on Solar Energy
[DE94-767725] p 4462 N94-37418

SOLAR ENERGY CONVERSION
1993 JSES (Japan Solar Energy Society)/JWEA (Japan Wind Energy Association) Joint Conference and 1993 Japan-Korea Joint Conference on Solar Energy
[DE94-767725] p 4462 N94-37418

SOLAR FLARES
A study of physical mechanisms for filament eruption and coronal mass ejection via numerical simulation
[NASA-CR-196087] p 4549 N94-36469

SOLAR PHYSICS
A study of physical mechanisms for filament eruption and coronal mass ejection via numerical simulation
[NASA-CR-196087] p 4549 N94-36469

SOLAR PLANETARY INTERACTIONS
An investigation of solar wind effects on the evolution of the Martian atmosphere
[NASA-CR-193424] p 4549 N94-37012

SOLAR PROMINENCES
A study of physical mechanisms for filament eruption and coronal mass ejection via numerical simulation
[NASA-CR-196087] p 4549 N94-36469

SOLAR TERRESTRIAL INTERACTIONS
A study of physical mechanisms for filament eruption and coronal mass ejection via numerical simulation
[NASA-CR-196087] p 4549 N94-36469
Analysis of plasma measurements for the Geotail mission
[NASA-CR-196274] p 4470 N94-37470
Solar-Terrestrial Predictions, 4: Proceedings of a workshop. Volume 3: Geomagnetic papers; ionospheric papers
[PB94-173192] p 4470 N94-37530
Random and periodic substorms and their origins in the solar wind
[DE94-011693] p 4549 N94-37668
Solar-Terrestrial Predictions, 4: Proceedings of a workshop. Volume 1: Workshop overview papers; working group reports; User community reports; Regional Warning Center Reports
[PB94-173176] p 4471 N94-37780
Solar-Terrestrial Predictions, 4: Proceedings of a workshop. Volume 2: Solar papers; magnetospheric papers
[PB94-173184] p 4471 N94-37781

SOLAR WIND
An investigation of solar wind effects on the evolution of the Martian atmosphere
[NASA-CR-193424] p 4549 N94-37012
Analysis of plasma measurements for the Geotail mission
[NASA-CR-196274] p 4470 N94-37470
Random and periodic substorms and their origins in the solar wind
[DE94-011693] p 4549 N94-37668

SOLDERING
Integrated environmentally compatible soldering technologies
[DE94-013456] p 4464 N94-37071

SOLID CRYOGENS
Studies of the thermal and optical responses of H atoms in solid H2
[NASA-CR-196114] p 4514 N94-36964

SOLID PROPELLANT COMBUSTION
Processing solid propellants for recycling
[DE94-011433] p 4428 N94-37202
Effects of two-phase flow on the deflagration of porous energetic materials
[DE94-011423] p 4411 N94-37412

SOLID PROPELLANT ROCKET ENGINES
Validation and implementation of optical diagnostics for particle sizing in rocket motors
[AD-A278581] p 4428 N94-36972
Processing solid propellants for recycling
[DE94-011433] p 4428 N94-37202
NASA reload program
[NASA-CR-193972] p 4429 N94-37446

SOLID PROPELLANTS
DDT modeling and shock compression experiments of porous or damaged energetic materials
[DE94-011419] p 4428 N94-37052
Processing solid propellants for recycling
[DE94-011433] p 4428 N94-37202

SOLID ROCKET PROPELLANTS
Validation and implementation of optical diagnostics for particle sizing in rocket motors
[AD-A278581] p 4428 N94-36972
NASA reload program
[NASA-CR-193972] p 4429 N94-37446

SOLID SOLUTIONS
Pair correlations in crystalline solid solutions
[DE94-012319] p 4535 N94-37212
SOLID STATE
Solid state research
[AD-A280573] p 4533 N94-36734
SOLID STATE DEVICES
Solid state research
[AD-A280573] p 4533 N94-36734
Solid state fluorometer: Prototype development
[AD-A280321] p 4534 N94-37027
Stopping power of charged particles from 10 eV/amu to 10 GeV/amu
[DE94-719024] p 4518 N94-37387
SOLID STATE LASERS
Diode array alternative to paint removal solid-state cw laser
[DE94-011482] p 4448 N94-37203
Diode-pumped, continuously tunable, 2.3 micron CW laser specification
[AD-D016312] p 4450 N94-37838
SOLID STATE PHYSICS
Activities of the Laboratory of Physics, Helsinki University of Technology
[PB94-175247] p 4509 N94-37301
SOLID WASTES
Structural composite construction materials manufactured from municipal solid waste
[AD-A280635] p 4403 N94-36730
Estimates of US biomass energy consumption 1992
[DE94-011458] p 4463 N94-37567
SOLIDIFIED GASES
Studies of the thermal and optical responses of H atoms in solid H2
[NASA-CR-196114] p 4514 N94-36964
SOLIDS
Determination of density of mass standards: Requirement and method
[PB94-163078] p 4508 N94-36718
Electronic balance and some gravimetric applications (the density of solids and liquids, pycnometry and mass)
[PB94-163052] p 4446 N94-36719
SOLIDS FLOW
Numerical study of the flow of granular materials down an inclined plane
[DE94-010729] p 4444 N94-37544
SOLITARY WAVES
Nonlinearity with disorder: Spatio-temporal complex behavior arising from length scales competition
[DE94-000675] p 4502 N94-36685
Variational discrete symmetries
[DE94-618485] p 4507 N94-37062
Unstable solitary-wave solutions of the generalized Benjamin-Bona-Mahony equation
[DE94-013302] p 4496 N94-37549
Langmuir waves in the electron-positron plasma
[DE94-618779] p 4531 N94-37728
SOLUBILITY
Methyl chloride via oxyhydrochlorination of methane
[DE94-010691] p 4406 N94-36450
SOLUTES
Elemental mapping of segregation in stainless steels with an imaging filter
[DE94-012659] p 4417 N94-37304
SOLVATION
United States Air Force Summer Research Program, 1993. Volume 6: Arnold Engineering Development Center, Frank J. Seiler Research Laboratory and Wilford Hall Medical Center
[AD-A278697] p 4551 N94-36982
SOLVENT EXTRACTION
Study on extraction behavior of TRPO with different composition
[DE94-620287] p 4412 N94-37534
SOLVENTS
Solvent effects on the energetics and dynamics of ultrafast electron transfer in chlorophyll-porphyrin-acceptor triads
[DE94-009693] p 4477 N94-36554
Integrated environmentally compatible soldering technologies
[DE94-013456] p 4464 N94-37071
SOOT
Laser-saturated fluorescence measurements in laminar sooting diffusion flames
[NASA-CR-191025] p 4508 N94-36643
SORPTION
New materials and multidimensional cluster analysis for SAW chemical sensor arrays
[DE94-012066] p 4409 N94-37161
SOUND DETECTING AND RANGING
Real-time SAW measurements of NVR in cleanroom and in microenvironment
[DE94-011937] p 4389 N94-37159
SOUND GENERATORS
Miniature thermoacoustic refrigerator
[AD-A280326] p 4431 N94-37029
SOUND LOCALIZATION
3D sound experimental approach: Methodology and preliminary results p 4486 N94-37280
SOUND PRESSURE
Scattering cross section of sound waves by the modal element method
[NASA-TM-106667] p 4510 N94-37308
SOUND WAVES
Elimination of numerical dispersion in finite-difference modeling and migration by flux-corrected transport
[DE94-004159] p 4510 N94-36551
Josephson acoustic radiation in superfluid helium
[AD-A280206] p 4533 N94-36742
Signal processing for the 1992 Barents Sea tomography experiment
[AD-A278580] p 4476 N94-36971
Scattering cross section of sound waves by the modal element method
[NASA-TM-106667] p 4510 N94-37308
SOUNDING ROCKETS
Three flights into thunderstorms with the revised Rocket Electric Field Sounding (REFS) payload
[AD-A280424] p 4473 N94-37217
SPACE ADAPTATION SYNDROME
Relation of motion sickness susceptibility to vestibular and behavioral measures of orientation
[NASA-CR-196121] p 4480 N94-37005
Profile analysis of after-effects experienced during exposure to several virtual reality environments p 4482 N94-37263
SPACE COMMUNICATION
Error control techniques for satellite and space communications
[NASA-CR-196302] p 4433 N94-36931
Baseline antenna design for space exploration initiative
[NASA-CR-196298] p 4435 N94-37255
SPACE ERECTABLE STRUCTURES
Configurational evolution dynamics and stability during in-situ development of large orbiting spacecraft
[AD-A280482] p 4397 N94-37351
SPACE EXPLORATION
Baseline antenna design for space exploration initiative
[NASA-CR-196298] p 4435 N94-37255
SPACE LABORATORIES
Design and development of experimental facilities for short duration, low-gravity combustion and fire experiments
[NASA-CR-196107] p 4389 N94-36967
Technology demonstration of space intravehicular automation and robotics
[NASA-TM-109138] p 4501 N94-37589
SPACE LAW
JPRS report: Science and technology. Central Eurasia: Space p 4391 N94-37003
SPACE NAVIGATION
Evaluation of GPS position and attitude determination for automated rendezvous and docking missions
[NASA-CR-4614] p 4397 N94-37506
SPACE PERCEPTION
Human factors for flight deck certification personnel
[AD-A280477] p 4487 N94-37347
Synthetic vision display evaluation studies
[NASA-CR-194963] p 4387 N94-37658
SPACE PLASMAS
Origins of energetic ions in the Earth's magnetosheath
[NASA-CR-189359] p 4471 N94-37703
SPACE POWER REACTORS
Conceptual design: TFE verification program
[DE94-012469] p 4398 N94-37433
TFE verification program
[DE94-009870] p 4398 N94-37514
SPACE PROCESSING
Ampoule failure sensor time response testing: Experiments 2 and 3
[NASA-TM-108458] p 4446 N94-36822
Technology demonstration of space intravehicular automation and robotics
[NASA-TM-109138] p 4501 N94-37589
Project JOVE --- microgravity experiments and applications
[NASA-CR-196292] p 4445 N94-37635
SPACE PROGRAMS
JPRS report: Central Eurasia. Aviation and cosmonautics, No. 4, April 1993
[JPRS-UAC-94-003] p 4391 N94-36999
Space Station: Impact of the expanded Russian role on funding and research. Report to the Ranking Minority Member, Subcommittee on Oversight of Government Management, Committee on Governmental Affairs, US Senate
[GAO/NSIAD-94-220] p 4396 N94-37257
SPACE RENDEZVOUS
Progress in navigation filter estimate fusion and its application to spacecraft rendezvous
[NASA-TM-104794] p 4392 N94-37386
SPACE SHUTTLE MAIN ENGINE
Experimental measurements and analytical analysis related to gas turbine heat transfer. Part 1: Time-averaged heat-flux and surface-pressure measurements on the vanes and blades of the SSME fuel-side turbine and comparison with prediction. Part 2: Phase-resolved surface-pressure and heat-flux measurements on the first blade of the SSME fuel-side turbine
[NASA-CR-196296] p 4442 N94-36969
SPACE SHUTTLES
A shadowgraph study of Space Transportation System (STS): The Space Shuttle Launch Vehicle (SSLV)
[NASA-RP-1341] p 4382 N94-36741
JPRS report: Central Eurasia. Aviation and cosmonautics, No. 4, April 1993
[JPRS-UAC-94-003] p 4391 N94-36999
Space Shuttle: Incomplete data and funding approach increase cost risk for upgrade program. Report to Congressional Requesters
[GAO/NSIAD-94-23] p 4392 N94-37026
Optimal control theory determination of feasible return-to-launch-site aborts for the HL-20 Personnel Launch System vehicle
[NASA-TP-3449] p 4396 N94-37260
SPACE STATION POWER SUPPLIES
Neural network for positioning Space Station solar arrays
[NASA-TM-106656] p 4431 N94-36943
SPACE STATIONS
Space Station: Impact of the expanded Russian role on funding and research. Report to the Ranking Minority Member, Subcommittee on Oversight of Government Management, Committee on Governmental Affairs, US Senate
[GAO/NSIAD-94-220] p 4396 N94-37257
SPACE STORAGE
Cryogenic fluid management technologies for space transportation. Zero G thermodynamic vent system
[NASA-CR-193981] p 4430 N94-36806
SPACE TRANSPORTATION SYSTEM
A shadowgraph study of Space Transportation System (STS): The Space Shuttle Launch Vehicle (SSLV)
[NASA-RP-1341] p 4382 N94-36741
Operations and support cost modeling of conceptual space vehicles
[NASA-CR-196299] p 4397 N94-37580
SPACEBORNE ASTRONOMY
Hubble Space Telescope faint object spectrograph instrument handbook, version 5.0
[NASA-CR-189367] p 4546 N94-36794
Hubble Space Telescope cycle 5. Phase 1: Proposal instructions, version 4.0
[NASA-CR-189364] p 4547 N94-36963
SPACEBORNE EXPERIMENTS
Design and development of experimental facilities for short duration, low-gravity combustion and fire experiments
[NASA-CR-196107] p 4389 N94-36967
Ground and space flight experiments of the effects of light, sound and/or temperature on animals
[NASA-CR-196102] p 4478 N94-36986
SPACEBORNE LASERS
Receiver design, performance analysis, and evaluation for space-borne laser altimeters and space-to-space laser ranging systems
[NASA-CR-194747] p 4397 N94-36988
SPACEBORNE PHOTOGRAPHY
Hubble Space Telescope faint object camera instrument handbook (Post-COSTAR), version 5.0
[NASA-CR-189365] p 4546 N94-36795
SPACECRAFT ANTENNAS
Baseline antenna design for space exploration initiative
[NASA-CR-196298] p 4435 N94-37255
SPACECRAFT CONFIGURATIONS
Configurational evolution dynamics and stability during in-situ development of large orbiting spacecraft
[AD-A280482] p 4397 N94-37351
SPACECRAFT CONSTRUCTION MATERIALS
Flame resistant fibrous structures development
[NASA-CR-185700] p 4421 N94-36641
Possibilities and pitfalls in aerospace applications of titanium matrix composites p 4400 N94-36650
Applications of Titanium Matrix Composite to large airframe structure p 4400 N94-36651
Composites based on titanium with external and internal reinforcement p 4401 N94-36654
Methodologies for thermal and mechanical testing of TMC materials p 4401 N94-36659
NASA-UVA Light Aerospace Alloy and Structures Technology Program (LA2ST)
[NASA-CR-196290] p 4415 N94-36809

JPRS report: Science and technology. Central Eurasia: Materials science
[JPRS-UMS-93-008] p 4404 N94-37010
Development of processing techniques for advanced thermal protection materials
[NASA-CR-196261] p 4426 N94-37510
Evaluation of seals and lubricants used on the Long Duration Exposure Facility
[NASA-CR-4604] p 4399 N94-37614
Effects of ply thickness on thermal cycle induced damage and thermal strain p 4459 N94-37806

SPACECRAFT CONTROL
Neural network for positioning Space Station solar arrays
[NASA-TM-106656] p 4431 N94-36943

SPACECRAFT DESIGN
Approximate analysis for repeated eigenvalue problems with applications to controls-structure integrated design
[NASA-TP-3439] p 4397 N94-37502

SPACECRAFT DOCKING
Global Positioning System Synchronized Active Light Autonomous Docking System
[NASA-CASE-MFS-28853-1] p 4395 N94-36825
Evaluation of GPS position and attitude determination for automated rendezvous and docking missions
[NASA-CR-4614] p 4397 N94-37506
Permanent superconducting magnets for space applications
[NASA-CR-196293] p 4439 N94-37634

SPACECRAFT ELECTRONIC EQUIPMENT
Space Generic Open Avionics Architecture (SGOAA) standard specification
[NASA-CR-188290] p 4387 N94-36933

SPACECRAFT ENVIRONMENTS
Characterization of spacecraft and environmental disturbances on a SmallSat
[NASA-CR-194915] p 4396 N94-36990

SPACECRAFT EQUIPMENT
Preliminary design for a reverse Brayton cycle cryogenic cooler
[NASA-CR-189341] p 4461 N94-36805

SPACECRAFT GUIDANCE
Global Positioning System Synchronized Active Light Autonomous Docking System
[NASA-CASE-MFS-28853-1] p 4395 N94-36825
Progress in navigation filter estimate fusion and its application to spacecraft rendezvous
[NASA-TM-104794] p 4392 N94-37386
Evaluation of GPS position and attitude determination for automated rendezvous and docking missions
[NASA-CR-4614] p 4397 N94-37506
Advanced information processing system: Hosting of advanced guidance, navigation and control algorithms on AIPS using ASTER
[NASA-CR-194960] p 4499 N94-37583

SPACECRAFT INSTRUMENTS
Hubble Space Telescope faint object spectrograph instrument handbook, version 5.0
[NASA-CR-189367] p 4546 N94-36794
Hubble Space Telescope faint object camera instrument handbook (Post-COSTAR), version 5.0
[NASA-CR-189365] p 4546 N94-36795
A high precision gamma ray spectrometer for the Mars 1994 mission
[DE94-013133] p 4550 N94-37293

SPACECRAFT LAUNCHING
A shadowgraph study of Space Transportation System (STS): The Space Shuttle Launch Vehicle (SSLV)
[NASA-RP-1341] p 4382 N94-36741
Optimal control theory determination of feasible return-to-launch-site aborts for the HL-20 Personnel Launch System vehicle
[NASA-TP-3449] p 4396 N94-37260

SPACECRAFT LUBRICATION
Properties of perfluoropolyethers for space applications
[NASA-TM-106616] p 4426 N94-37520
Evaluation of seals and lubricants used on the Long Duration Exposure Facility
[NASA-CR-4604] p 4399 N94-37614

SPACECRAFT MAINTENANCE
Space Shuttle: Incomplete data and funding approach increase cost risk for upgrade program. Report to Congressional Requesters
[GAO/NSIAD-94-23] p 4392 N94-37026
Operations and support cost modeling of conceptual space vehicles
[NASA-CR-196299] p 4397 N94-37580

SPACECRAFT MODELS
Configurational evolution dynamics and stability during in-situ development of large orbiting spacecraft
[AD-A280482] p 4397 N94-37351

SPACECRAFT MODULES
Calibration and initial testing of a new hydraulic simulator
[AD-A280632] p 4390 N94-37163

SPACECRAFT POWER SUPPLIES
Mars vertical axis wind machines: The design of a tornado vortex machine for use on Mars
[NASA-CR-196144] p 4462 N94-36823
Conceptual design: TFE verification program
[DE94-012469] p 4398 N94-37433

SPACECRAFT PROPULSION
Possibilities and pitfalls in aerospace applications of titanium matrix composites p 4400 N94-36650
Characteristics of ions emitted from high-current hollow cathodes
[NASA-CR-195372] p 4398 N94-37764

SPACECRAFT RADIATORS
Review of advanced radiator technologies for spacecraft power systems and space thermal control
[NASA-TM-4555] p 4398 N94-36821
Carbon-carbon heat pipe testing and evaluation
[NASA-TM-106630] p 4405 N94-37318
Reference manual for the Thermal Analyst's Help Desk Expert System
[NASA-CR-194941] p 4397 N94-37504

SPACECRAFT RELIABILITY
Possibilities and pitfalls in aerospace applications of titanium matrix composites p 4400 N94-36650
Probabilistic assessment of space nuclear propulsion system nozzle
[NASA-TM-106539] p 4457 N94-37704

SPACECRAFT SHIELDING
Estimates of cellular mutagenesis from cosmic rays
[NASA-TP-3453] p 4481 N94-37282

SPACECRAFT STRUCTURES
Approximate analysis for repeated eigenvalue problems with applications to controls-structure integrated design
[NASA-TP-3439] p 4397 N94-37502

SPACECRAFT TEMPERATURE
Reference manual for the Thermal Analyst's Help Desk Expert System
[NASA-CR-194941] p 4397 N94-37504

SPARK IGNITION
Potential benefits of oxygen-enriched intake air in a vehicle powered by a spark-ignition engine
[DE94-013452] p 4451 N94-37070

SPATIAL DISTRIBUTION
Rescaled box counting for the topological analysis of spatial data
[DE94-009820] p 4461 N94-36464

SPATIAL RESOLUTION
Submicrometer fiber-optic chemical sensors: Measuring pH inside single cells
[DE94-004160] p 4525 N94-37532
Comparison of gaseous and semiconductor detectors for medical imaging
[DE94-621344] p 4482 N94-37729

SPECIFIC IMPULSE
Characteristics of ions emitted from high-current hollow cathodes
[NASA-CR-195372] p 4398 N94-37764

SPECIFICATIONS
Specification-based software sizing: An empirical investigation of function metrics p 4490 N94-36488
Software engineering with application-specific languages p 4491 N94-36494
Advanced distributed simulation technology advanced rotary wing aircraft. System/segment specification. Volume 4: Simulation system module RAH-66 Kit
[AD-A280261] p 4391 N94-37756

SPECTRA
Analysis spectral shapes from California and central United States ground motion
[DE94-010041] p 4469 N94-36758

SPECTRAL LINE WIDTH
Final report on spectral broadening by cross-phase modulation in linearly birefringent optical fibers
[DE94-010406] p 4524 N94-37191

SPECTROGRAPHS
Hubble Space Telescope faint object spectrograph instrument handbook, version 5.0
[NASA-CR-189367] p 4546 N94-36794
Guaranteed time observations support for Faint Object Spectrograph (FOS) on HST
[NASA-CR-196305] p 4547 N94-37037

SPECTROMETERS
Airborne ROWS data report for the high resolution experiment, June 1993
[NASA-TM-104609] p 4477 N94-37397

SPECTROPHOTOMETERS
Determining the refractive index of a lambda/4 thin film on a thick substrate from a transmittance measurement
[DE93-019584] p 4523 N94-36693
Hubble Space Telescope Wide Field and Planetary Camera 2 Instrument handbook, version 2.0
[NASA-CR-189368] p 4547 N94-36918

SPECTROPHOTOMETRY
Determination of copper in tap water using solid-phase spectrophotometry
[NASA-TM-106480] p 4408 N94-36537
Guaranteed time observations support for Faint Object Spectrograph (FOS) on HST
[NASA-CR-196305] p 4547 N94-37037

SPECTROSCOPIC ANALYSIS
Chemical and structural characterization of nitroaromatic adducts with hemoglobins
[AD-A280533] p 4480 N94-37089

SPECTROSCOPY
Older muons are wiser: Using time information in (mu)LCR spectroscopy
[DE93-018556] p 4511 N94-36457
Activities of the Tandem Accelerator Center, University of Tsukuba
[DE94-748687] p 4522 N94-37237
Time-of-flight pulsed ion beam surface analysis as a means of in situ, real-time characterization of the growth of ferro-electric and conductive oxide heterostructures
[DE94-012628] p 4517 N94-37249
A high precision gamma ray spectrometer for the Mars 1994 mission
[DE94-013133] p 4550 N94-37293
A fast spectroscopic diagnostic for the measurement of plasma impurity ion dynamics
[DE94-012985] p 4529 N94-37354

SPECTRUM ANALYSIS
Index and bulk parameters for frequency-direction spectra measured at CERC Field Research Facility, September 1992 to August 1993
[AD-A280233] p 4476 N94-37135
Index and bulk parameters for frequency-direction spectra measured at CERC Field Research Facility, September 1990 to August 1991
[AD-A280423] p 4476 N94-37216
Index and bulk parameters for frequency-direction spectra measured at CERC Field Research Facility, September 1991 to August 1992
[AD-A280455] p 4477 N94-37229
Fatigue case study and loading spectra for wind turbines
[DE94-010798] p 4457 N94-37622

SPEECH RECOGNITION
Segment-based acoustic models for continuous speech recognition
[AD-A280332] p 4434 N94-37032
Noise reduction for speech enhancement using non-linear wavelet processing
[AD-A280469] p 4434 N94-37141

SPHERICAL COORDINATES
Contact level fusion of radar and IRST contacts on almost electromagnetically silent platform p 4395 N94-36634

SPIN-LATTICE RELAXATION
Relaxation of the density matrix for an arbitrary spin in random external fields
[DE94-618457] p 4509 N94-37078

SPINEL
Microstructure and chemistry of MgO- and CoO-doped nickel-titanate spinels
[DE94-012741] p 4537 N94-37382

SPLINES
Interchangeable spline reference guide
[DE94-012368] p 4495 N94-37245

SPLITTING
A flux splitting scheme with high-resolution and robustness for discontinuities
[NASA-TM-106452] p 4441 N94-36846

SPORTS MEDICINE
Postural strategies for the continuous control of static and dynamic balance in man
[PB94-184678] p 4487 N94-37812

SPOT (FRENCH SATELLITE)
JPRS report: Central Eurasia. Aviation and cosmonautics, No. 6, June 1993
[JPRS-UAC-94-005] p 4391 N94-37001

SPREAD F
Channel probe measurements for the American Sector Clutter Experiment, January 1994
[DE94-013086] p 4469 N94-37314

SPREAD REFLECTION
Index and bulk parameters for frequency-direction spectra measured at CERC Field Research Facility, September 1990 to August 1991
[AD-A280423] p 4476 N94-37216
Index and bulk parameters for frequency-direction spectra measured at CERC Field Research Facility, September 1991 to August 1992
[AD-A280455] p 4477 N94-37229

SPRING (SEASON)
Surface-layer response over shrub-steppe canopy during springtime
[DE94-011235] p 4468 N94-37624

SPRINGS (ELASTIC)
Variable stiffness torsion springs
[NASA-CASE-MFS-28930-1] p 4509 N94-36782

SPUTTERING
Processing of titanium matrix composites
p 4401 N94-36653
SQUEEZED STATES (QUANTUM THEORY)
Generalized squeezed states from generalized coherent states
[DE94-002689] p 4512 N94-36515
SQUID (DETECTORS)
Applications of high transition temperature superconductors at the Savannah River Site
[DE94-012938] p 4536 N94-37311
SR-71 AIRCRAFT
JPRS report: Central Eurasia. Aviation and cosmonautics, No. 6, June 1993
[JPRS-UAC-94-005] p 4391 N94-37001
STABILITY
Methyl chloride via oxyhydrochlorination of methane
[DE94-010691] p 4406 N94-36450
Experimental characterisation of gas microstrip detectors. Part 1: Gain characteristics
[PB94-167087] p 4445 N94-36531
New hollow-cathode electrode for high-power copper lasers
[DE94-011637] p 4448 N94-37244
Stability and dynamics of spatio-temporal structures
[DE94-013035] p 4412 N94-37491
STABILITY TESTS
Stability analysis of an F/A-18 E/F cable mount m odel
[NASA-TM-108989] p 4386 N94-37636
STABILIZED PLATFORMS
Inertial pseudo star reference unit
p 4394 N94-36625
STAINLESS STEELS
Ability of the total strain version of strainrange partitioning to characterize thermomechanical fatigue behavior
[NASA-TM-4556] p 4455 N94-37102
AEM and AES of radiation-induced segregation in proton-irradiated stainless steels
[DE94-012734] p 4418 N94-37398
STANDARD DEVIATION
Short-tower sigma(theta) measurements in the Colorado Plateaus region
[DE94-007478] p 4463 N94-36478
STANDARD MODEL (PARTICLE PHYSICS)
Top quark search at CDF
[DE94-003643] p 4511 N94-36459
Radiative and rare mu and pi decays
[DE94-618549] p 4515 N94-37066
Particle physics
[DE94-012944] p 4518 N94-37312
STANDARDIZATION
Standards in the architectural effort
p 4541 N94-36852
Standards for data and document interchange
p 4543 N94-37337
STANDARDS
NASA STI Program Coordinating Council Eleventh Meeting: NASA STI Modernization Plan
[NASA-TM-109415] p 4540 N94-36841
Standards in the architectural effort
p 4541 N94-36852
NASA STI Program Coordinating Council Twelfth Meeting: Standards
[NASA-TM-109925] p 4541 N94-36853
STI Architectural Framework Working Group
p 4542 N94-36854
OSI and TCP/IP p 4542 N94-36855
A concise introduction to MARC p 4542 N94-36856
Open system environments p 4542 N94-36857
Open system environment procurement
p 4542 N94-36858
Z39.50 and GILS model — Government Information Locator Service p 4542 N94-36859
Government Information Locator Service (GILS). Draft report to the Information Infrastructure Task Force
p 4542 N94-36860
Space Generic Open Avionics Architecture (SGOAA) standard specification
[NASA-CR-188290] p 4387 N94-36933
Standards for data and document interchange
p 4543 N94-37337
Advanced distributed simulation technology. SIMWORLD data base
[AD-A280262] p 4545 N94-37757
STANDING WAVES
Fundamentals studies of radial wave thermoacoustic engines
[AD-A280534] p 4431 N94-37090
Suppression of beam-break-up in a standing wave free electron laser two-beam accelerator
[DE94-011348] p 4521 N94-37200
STANTON NUMBER
Experimental measurements and analytical analysis related to gas turbine heat transfer. Part 1: Time-averaged heat-flux and surface-pressure measurements on the vanes and blades of the SSME fuel-side turbine and comparison with prediction. Part 2: Phase-resolved surface-pressure and heat-flux measurements on the first blade of the SSME fuel-side turbine
[NASA-CR-196296] p 4442 N94-36969
STARK EFFECT
Motional Stark effect upgrades on D3-D
[DE94-013146] p 4528 N94-37297
STARTING
Startup and shutdown of the PULSAR Tokamak Reactor
[DE94-013128] p 4528 N94-37292
STATE VECTORS
Contact level fusion of radar and IRST contacts on almost electromagnetically silent platform
p 4395 N94-36634
Progress in navigation filter estimate fusion and its application to spacecraft rendezvous
[NASA-TM-104794] p 4392 N94-37386
STATIC STABILITY
An aerodynamic and static-stability analysis of the Hypersonic Applied Research Technology (HART) missile
[AD-A280631] p 4382 N94-36729
Aerodynamic characteristics of the National Launch System (NLS) 1 1/2 stage launch vehicle
[NASA-TP-3488] p 4384 N94-37577
STATIC TESTS
Residual strength and life prediction techniques for Ti MMC p 4402 N94-36662
STATISTICAL ANALYSIS
Recovering depth from focus using iterative image estimation techniques
[DE94-010994] p 4524 N94-37165
Statistical characterization of rare events
p 4454 N94-37327
Predicting defect behaviour p 4455 N94-37331
Fatigue case study and loading spectra for wind turbines
[DE94-010798] p 4457 N94-37622
STATISTICAL DISTRIBUTIONS
Statistical characterization of rare events
p 4454 N94-37327
STEADY STATE
Preconditioned implicit solvers for the Navier-Stokes equations on distributed-memory machines
[NASA-TM-106449] p 4502 N94-36647
STEADY STATE CREEP
Modeling of thermal barrier coatings
[NASA-CR-195365] p 4421 N94-36637
STEAM TURBINES
The influence of fin height and wall conductivity on integral-fin tubes during steam condensation
[AD-A280597] p 4539 N94-36725
Integrated gasification combined cycle and steam injection gas turbine powered by biomass joint-venture evaluation
[DE94-006905] p 4461 N94-36740
STEELS
Evaluation of flame-sprayed polymer coatings for civil works navigation structures
[AD-A280507] p 4422 N94-37104
The development of short, high surface area activated carbon fibers
[AD-A280509] p 4404 N94-37105
Interfaces of high-protection performance polyaryls-coated zinc phosphated steels
[DE94-011732] p 4417 N94-37153
Alternate melting and refining routes
p 4421 N94-37323
Exploratory study on H13 steel dies
[DE94-012118] p 4420 N94-37678
Numerical simulation of dynamic fracture and failure in solids
[DE94-010379] p 4457 N94-37705
STEERING
Immersive virtual environments as trainer: System design from a cognitive stance p 4484 N94-37267
STELLAR MASS
Absolute limit on rotation of gravitationally bound stars
[DE94-011367] p 4548 N94-37049
STELLAR MASS EJECTION
A study of physical mechanisms for filament eruption and coronal mass ejection via numerical simulation
[NASA-CR-196087] p 4549 N94-36469
The winds of cataclysmic variables
[DE94-010897] p 4548 N94-37164
STELLAR PHYSICS
Absolute limit on rotation of gravitationally bound stars
[DE94-011367] p 4548 N94-37049
STELLAR ROTATION
Absolute limit on rotation of gravitationally bound stars
[DE94-011367] p 4548 N94-37049
STELLAR SPECTRA
Ultraviolet spectropolarimetry of high redshift quasars with the Hubble Space Telescope
[NASA-CR-196014] p 4546 N94-36690
STELLAR WINDS
The winds of cataclysmic variables
[DE94-010897] p 4548 N94-37164
STELLARATORS
Confinement improvement in H-mode-like plasmas in helical systems
[DE94-727619] p 4528 N94-37231
STEPPES
An experimental and numerical study of boundary layer structure over areas of inhomogeneous sensible heat fluxes
[DE94-011441] p 4474 N94-37565
Surface-layer response over shrub-steppe canopy during springtime
[DE94-011235] p 4468 N94-37624
STEREOPHONICS
3D sound experimental approach: Methodology and preliminary results p 4486 N94-37280
STEREOSCOPIC VISION
Low cost software-based rendering and stereoscopic interfaces for teleoperation and virtual reality
p 4486 N94-37279
STIFFNESS
Variable stiffness torsion springs
[NASA-CASE-MFS-28930-1] p 4509 N94-36782
STOCHASTIC PROCESSES
Design and evaluation of a Stochastic Optimal Feed-forward and Feedback Technology (SOFFT) flight control architecture
[NASA-TP-3419] p 4388 N94-37014
Segment-based acoustic models for continuous speech recognition
[AD-A280332] p 4434 N94-37032
STOCKPILING
Replacement of silicone polymer A with silicone polymer B and the subsequent characterization of the new cellular silicone materials
[DE94-010105] p 4421 N94-36474
STOPPING POWER
Stopping power of charged particles from 10 eV/amu to 10 GeV/amu
[DE94-719024] p 4518 N94-37387
STORAGE BATTERIES
Sodium/nickel-chloride battery development
[DE94-011481] p 4437 N94-37053
STORAGE RINGS (PARTICLE ACCELERATORS)
Direct photoproduction of jets in the k(T)-factorisation prescription
[PB94-171139] p 4513 N94-36549
High Energy Physics Division of research activities
[DE93-019681] p 4521 N94-36694
Determination of the upsilon(1s) leptonic width
[DE94-618534] p 4516 N94-37096
Activities of the Photon Factory
[DE94-748682] p 4522 N94-37236
Laser cooling of 24Mg+ in the ASTRID storage ring
[DE94-010445] p 4523 N94-37619
STORMS
Three flights into thunderstorms with the revised Rocket Electric Field Sounding (REFS) payload
[AD-A280424] p 4473 N94-37217
STRAIN HARDENING
Experimental and finite-element simulation results for a plane-strain punch-test using isotropic and anisotropic materials
[DE94-011711] p 4457 N94-37670
Mechanical performance of austempered ductile iron
[AD-A280452] p 4420 N94-37758
STRAIN RATE
Ability of the total strain version of strainrange partitioning to characterize thermomechanical fatigue behavior
[NASA-TM-4556] p 4455 N94-37102
Experimental and finite-element simulation results for a plane-strain punch-test using isotropic and anisotropic materials
[DE94-011711] p 4457 N94-37670
STRANGE ATTRACTORS
Theoretical investigations of chaotic dynamics
[AD-A280325] p 4507 N94-37028
STRANGENESS
Strangeness and the quark-gluon plasma: An experimenter's perspective
[DE94-011377] p 4519 N94-37558
Hadron production in S+nucleus collisions at 200 GeV/nucleon
[DE94-011344] p 4520 N94-37715

STRATOSPHERE
Project report: Aircraft — atmospheric effects of stratospheric aircraft
[DE94-011759] p 4465 N94-37155
Jet aircraft engine exhaust emissions database development: Year 1990 and 2015 scenarios
[NASA-CR-4613] p 4466 N94-37252
Stratospheric emissions effects database development
[NASA-CR-4592] p 4467 N94-37607

STRATUS CLOUDS
A stratiform cloud parameterization for general circulation models
[DE94-011442] p 4474 N94-37566

STRESS (PHYSIOLOGY)
Cardiac pressure changes with venous gas embolism and decompression
[AD-A280412] p 4481 N94-37224
Cerebral neurochemical mechanisms in stress and anxiety
[AD-A280473] p 4482 N94-37233

STRESS (PSYCHOLOGY)
Cerebral neurochemical mechanisms in stress and anxiety
[AD-A280473] p 4482 N94-37233

STRESS ANALYSIS
Metal matrix composites: Analysis of simple specimens and model components under creep and fatigue loading
p 4402 N94-36661
Jumper connector analysis
[DE94-010373] p 4451 N94-37188
Some considerations for modeling the creep behavior of composite materials
[DE94-012112] p 4404 N94-37205
Strength evaluation of socket joints
[NASA-CR-4608] p 4389 N94-37259
Transient thermal and dynamic stresses in strongback-design blankets
[DE94-012639] p 4530 N94-37441
Fatigue case study and loading spectra for wind turbines
[DE94-010798] p 4457 N94-37622
A simple evaluation of thermally-induced streses in the vicinity of the stitch in a through-thickness reinforced cross-ply laminate
[NASA-CR-196317] p 4406 N94-37653
Scaling, elasticity, and CLPT p 4458 N94-37800

STRESS CONCENTRATION
Modeling of thermal barrier coatings
[NASA-CR-195365] p 4421 N94-36637

STRESS CORROSION CRACKING
Irradiation assisted stress corrosion cracking of HTH Alloy X-750 and Alloy 625
[DE94-012667] p 4416 N94-37080

STRESS DISTRIBUTION
Studies of the effect of microstructure on the dynamic behavior of granular and particulate media
[AD-A279012] p 4455 N94-36520
Size effect in composite materials and structures: Basic concepts and design considerations
p 4460 N94-37808

STRESS INTENSITY FACTORS
Irradiation assisted stress corrosion cracking of HTH Alloy X-750 and Alloy 625
[DE94-012667] p 4416 N94-37080
A methodology to predict damage initiation, damage growth and residual strength in titanium matrix composites
[NASA-TM-109135] p 4405 N94-37320
Defects and their effects on the integrity of nickel based aeroengine discs p 4421 N94-37328
Strength characteristics and crack growth behavior of a composite with well aligned fibers
p 4459 N94-37804

STRESS RELAXATION
Replacement of silicone polymer A with silicone polymer B and the subsequent characterization of the new cellular silicone materials
[DE94-010105] p 4421 N94-36474
Residual stresses in a multi-pass weld in an austenitic stainless steel plate before and after thermal stress relief
[DE94-013278] p 4420 N94-37548

STRESS-STRAIN RELATIONSHIPS
Micromechanical modeling of damage growth in titanium based metal-matrix composites p 4402 N94-36664
Prediction of thermal and mechanical stress-strain responses of TMC's subjected to complex TMF histories
p 4402 N94-36666
A fully coupled thermal, chemical, mechanical cookoff model
[DE94-011432] p 4428 N94-37201
A comparison of graphite/epoxy tape laminates and 2-D braided composites mechanical properties
[NASA-CR-4610] p 4420 N94-37582

STRING THEORY
Is it possible to assign physical meaning to field theory with higher derivatives?
[DE94-618468] p 4539 N94-37172

STRONTIUM COMPOUNDS
High T(sub c) copper-oxide superconductors comprising Tl-Sr-Ca-Cu-O
[AD-D016307] p 4538 N94-37776

STRONTIUM OXIDES
Determination of interface structure and bonding at atomic resolution in the stem
[DE94-011466] p 4517 N94-37238

STRONTIUM TITANATES
Atomic resolution characterization of a SrTiO3 grain boundary in the STEM
[DE94-011489] p 4538 N94-37545
The MBE growth and optical quality of BaTiO3 and SrTiO3 thin films on MgO
[DE94-011468] p 4538 N94-37570

STRUCTURAL ANALYSIS
ALCHEMI formulated for delocalization and anti-site defects
[DE94-012740] p 4537 N94-37400
JPRS report: Science and technology. Central Eurasia: Engineering and equipment
[JPRS-UEQ-93-005] p 4432 N94-37538
Hierarchically parallelized constrained nonlinear solvers with automated substructuring
[NASA-CR-194474] p 4456 N94-37554
Probabilistic assessment of space nuclear propulsion system nozzle
[NASA-TM-106539] p 4457 N94-37704
Workshop on Scaling Effects in Composite Materials and Structures
[NASA-CP-3271] p 4457 N94-37796
Effects of scale in predicting global structural response p 4458 N94-37799

STRUCTURAL BASINS
Analysis of deep seismic reflection and other data from the Southern Washington Cascades
[DE94-004075] p 4470 N94-37489

STRUCTURAL DESIGN
Applications of Titanium Matrix Composite to large airframe structure p 4400 N94-36651
Optimization for minimum sensitivity to uncertain parameters
[NASA-TM-109139] p 4386 N94-37256
Statistical characterization of rare events
p 4454 N94-37327
Examination of weldability of Ni-Cr-W superalloys
[DE94-719014] p 4418 N94-37385
Approximate analysis for repeated eigenvalue problems with applications to controls-structure integrated design
[NASA-TP-3439] p 4397 N94-37502

STRUCTURAL FAILURE
History and prognosis of material discontinuity effects on engine components structural integrity
p 4453 N94-37322
Turbine disks: Lifing against defects and materials development p 4454 N94-37329

STRUCTURAL RELIABILITY
Probability techniques for reliability analysis of composite materials
[NASA-CR-195294] p 4406 N94-37633

STRUCTURAL STABILITY
Correlation of analytical and experimental hot structure vibration results
[NASA-TM-104269] p 4386 N94-36644

STRUCTURAL VIBRATION
Correlation of analytical and experimental hot structure vibration results
[NASA-TM-104269] p 4386 N94-36644
A Galerkin method for linear PDE systems in circular geometries with structural acoustic applications
[NASA-CR-194925] p 4503 N94-36923
A PDE-based methodology for modeling, parameter estimation and feedback control in structural and structural acoustic systems
[NASA-CR-194928] p 4500 N94-36924
Vibration suppression with approximate finite dimensional compensators for distributed systems: Computational methods and experimental results
[NASA-CR-194927] p 4500 N94-36928
Parameter estimation in a structural acoustic system with fully nonlinear coupling conditions
[NASA-CR-194926] p 4503 N94-36991
Laminated thin shell structures subjected to free vibration in a hygrothermal environment
[NASA-TM-106600] p 4456 N94-37456

STYRENES
Iron hydrous titanium oxide catalysts for the dehydrogenation of ethylbenzene to styrene
[DE94-010381] p 4412 N94-37542

SUBASSEMBLIES
MODIL cryocooler producibility demonstration project results
[DE93-019213] p 4430 N94-36444

SUBMILLIMETER WAVES
Submillimeter quasioptical Josephson junction oscillator with integrated tuning elements
[AD-A280380] p 4534 N94-37036

SUBROUTINE LIBRARIES (COMPUTERS)
ZLIB++: Object-oriented numerical library for differential algebra
[DE94-010839] p 4495 N94-37453

SUBSONIC FLOW
Automatic computation of Euler-marching and subsonic grids for wing-fuselage configurations
[NASA-TM-4573] p 4383 N94-36950

SUBSONIC SPEED
Subsonic aerodynamic characteristic of semispan commercial transport model with wing-mounted advanced ducted propeller operating in reverse thrust — conducted in the Langley 14 by 22 foot subsonic wind tunnel
[NASA-TP-3427] p 4384 N94-37505

SUBSTITUTES
Materials Compatibility and Lubricant Research on CFC-refrigerant substitutes
[DE94-012352] p 4425 N94-37373

SUBSTRATES
Determining the refractive index of a lambda/4 thin film on a thick substrate from a transmittance measurement
[DE93-019584] p 4523 N94-36693
Substrate effects on the structure and optical properties of epitaxial PbTiO3 thin films prepared by metal-organic chemical vapor deposition
[DE94-010432] p 4535 N94-37192
X-ray diffraction studies of evaporated gold thin films deposited on aluminum nitride substates
[AD-A280454] p 4536 N94-37228
Development of low dielectric constant alumina-based ceramics for microelectronic substrates
[DE94-011360] p 4439 N94-37302
Morphological aspects of surface reactions
[DE94-011208] p 4413 N94-37713
Gas microstrip detectors on resistive plastic substrates
[DE94-011336] p 4426 N94-37714

SUCTION
An algorithm for the automatic control of boundary layer flow
[ISVR-TR-233] p 4442 N94-36817
Experimental measurements and analytical analysis related to gas turbine heat transfer. Part 1: Time-averaged heat-flux and surface-pressure measurements on the vanes and blades of the SSME fuel-side turbine and comparison with prediction. Part 2: Phase-resolved surface-pressure and heat-flux measurements on the first blade of the SSME fuel-side turbine
[NASA-CR-196296] p 4442 N94-36969
Unsteady flow field of large-amplitude pitching airfoils
[AD-A280444] p 4383 N94-37219

SULFATES
Isolated SO4-2 and PO4-3 anions do not exist
[AD-A278831] p 4512 N94-36521
Indicators for sulfate-reducing bacteria in microbiologically influenced corrosion
[AD-A278914] p 4477 N94-36522

SULFATION
Superacid catalysis of light hydrocarbon conversion
[DE94-011132] p 4411 N94-37431

SULFUR DIOXIDES
SIHTI: Energy and environmental technology
[DE94-763290] p 4464 N94-37007

SULFURIC ACID
The corrosion protection of several aluminum alloys by chromic acid and sulfuric acid anodizing
[NASA-TP-3490] p 4420 N94-37578

SUM RULES
Sum rules for 1/m corrections to the form factors of semileptonic B decays
[DE94-618548] p 4514 N94-37065

SUPERCOMPUTERS
Hardware implementation of a desktop supercomputer for high performance image processing
[AD-A280550] p 4489 N94-36731
A scalable high-performance I/O system
[DE94-011513] p 4498 N94-37519

SUPERCONDUCTING DEVICES
High temperature superconducting digital circuits and subsystems
[DE94-001207] p 4436 N94-36557
Microwave detection of a superconducting infrared sensor
[AD-D016297] p 4440 N94-37769

SUPERCONDUCTING FILMS
Electrically conductive, thermally insulating cryogenic current leads
[NASA-CASE-LAR-14964-1-CU] p 4437 N94-36781

Development of high Tc (greater than 100 K) Bi, Tl and Y-based materials as superconducting circuit elements
[NASA-CR-196276] p 4534 N94-37103
Critical-state flux-density profiles in type-2 superconducting thin-film strips and disks
[DE94-011199] p 4535 N94-37166
Superconducting TlCa2Ba2Cu3O9 thick films
[DE94-010436] p 4535 N94-37193
Activities of the Tandem Accelerator Center, University of Tsukuba
[DE94-748687] p 4522 N94-37237
The MBE growth and optical quality of BaTiO3 and SrTiO3 thin films on MgO
[DE94-011466] p 4538 N94-37570

SUPERCONDUCTING MAGNETS
Pulsed field magnets at the United States National High Magnetic Field Laboratory
[DE94-002624] p 4436 N94-36514
Fabrication and properties of Ag-clad Bi-2223 conductors and magnets
[DE94-011502] p 4438 N94-37111
Melt-processing of Y-Ba-Cu-O superconductors for improved levitation
[DE94-011503] p 4537 N94-37377
Permanent superconducting magnets for space applications
[NASA-CR-196293] p 4439 N94-37634

SUPERCONDUCTING SUPER COLLIDER
The 24/36/48 Cathode Strip Chamber layout for SSC GEM detector muon subsystem
[DE94-012676] p 4439 N94-37306

SUPERCONDUCTIVITY
High temperature superconducting digital circuits and subsystems
[DE94-001207] p 4436 N94-36557
Critical-state flux-density profiles in type-2 superconducting thin-film strips and disks
[DE94-011199] p 4535 N94-37166
ORNL superconducting technology program for electric power systems
[DE94-011471] p 4438 N94-37239
Midwest Superconductivity Consortium
[DE94-012716] p 4536 N94-37285

SUPERCONDUCTORS
Critical-state flux-density profiles in type-2 superconducting thin-film strips and disks
[DE94-011199] p 4535 N94-37166

SUPERFLUIDITY
Josephson acoustic radiation in superfluid helium
[AD-A280208] p 4533 N94-36742

SUPERLATTICES
Forward scattering of neutrons from polymeric and magnetic multilayers
[DE93-041158] p 4513 N94-36696

SUPERSATURATION
Hypobaric decompression sickness model development. Part 1: Diffusion of inert gas from a viscoelastic fluid (blood) into an expanding gas phase
[AD-A280298] p 4481 N94-37124

SUPERSONIC BOUNDARY LAYERS
Supersonic laminar flow control research
[NASA-CR-196280] p 4384 N94-37511

SUPERSONIC COMBUSTION RAMJET ENGINES
Experimental investigation of nozzle/plume aerodynamics at hypersonic speeds
[NASA-CR-195829] p 4382 N94-36687

SUPERSONIC FLOW
Supersonic laminar flow control research
[NASA-CR-196260] p 4384 N94-37511

SUPERSONIC JET FLOW
Mixing and noise benefit versus thrust penalty in supersonic jets using impingement tones
[NASA-TM-106583] p 4382 N94-36686

SUPERSONIC SPEED
An aerodynamic and static-stability analysis of the Hypersonic Applied Research Technology (HART) missile
[AD-A280631] p 4382 N94-36729

SUPERSONIC TRANSPORTS
Project report: Aircraft — atmospheric effects of stratospheric aircraft
[DE94-011759] p 4465 N94-37155
Jet aircraft engine exhaust emissions database development: Year 1990 and 2015 scenarios
[NASA-CR-4613] p 4466 N94-37252
Synthetic vision display evaluation studies
[NASA-CR-194963] p 4387 N94-37658

SUPPORT SYSTEMS
Training and operations support system (TOPS)
p 4545 N94-37344
NASA commercial technology. Agenda for change
[NASA-TM-109898] p 4546 N94-37765

SUPPORTS
Selectively lockable knee brace
[NASA-CASE-MFS-28991-1] p 4486 N94-36838
Stability analysis of an F/A-18 E/F cable mount m odel
[NASA-TM-108989] p 4386 N94-37636

SURFACE ACOUSTIC WAVE DEVICES
Real-time SAW measurements of NVR in cleanroom and in microenvironment
[DE94-011937] p 4389 N94-37159
New materials and multidimensional cluster analysis for SAW chemical sensor arrays
[DE94-012066] p 4409 N94-37161
SAW chemical sensor arrays using new thin-film materials
[DE94-011940] p 4411 N94-37365

SURFACE CRACKS
Exploratory study on H13 steel dies
[DE94-012118] p 4420 N94-37678

SURFACE ENERGY
Modelling of surfaces. Part 1: Monatomic metallic surfaces using equivalent crystal theory
[NASA-TM-106680] p 4419 N94-37459

SURFACE FINISHING
Strategic choices in surface treatments
[PB94-170669] p 4414 N94-36534
Robotic weld overlay coatings for erosion control
[DE94-013477] p 4417 N94-37116

SURFACE GEOMETRY
Automatic procedures for computing complete configuration geometry from individual component descriptions
[NASA-TM-4607] p 4382 N94-36942

SURFACE LAYERS
Surface-layer response over shrub-steppe canopy during springtime
[DE94-011235] p 4468 N94-37624

SURFACE PROPERTIES
First results from the Los Alamos plasma source ion implantation experiment
[DE94-003931] p 4414 N94-36461
EM-ANIMATE: A computer program for displaying and animating electromagnetic near-field and surface-current solutions: Video supplement to NASA Technical Memorandum 4539
[NASA-TM-4539-VIDEO-SUPPL] p 4492 N94-36518
Production of amorphous metal layers using ion implantation and investigation of the related modification of some surface properties
[DE94-617509] p 4414 N94-36541
Nonlinear optical spectroscopy for surface studies
[DE94-011623] p 4408 N94-37056
Atomic and electronic structure of metals and alloys: Rare earths, ultrathin films and surface alloys
[DE94-011581] p 4516 N94-37113
Laser probing of interfaces
[DE94-011300] p 4449 N94-37628

SURFACE REACTIONS
Gas-Phase and Surface Chemistry in Electronic Materials Processing. Materials Research Society Symposium proceedings, volume 334
[AD-A280586] p 4408 N94-36735
A photoemission study of Au, Ge, and O2 deposition on NH4F etched Si(111)
[DE94-013352] p 4519 N94-37553
Morphological aspects of surface reactions
[DE94-011208] p 4413 N94-37713
Diosmacycloalkanes as models for the formation of hydrocarbons from surface methylenes
[DE94-011211] p 4413 N94-37754

SURFACE ROUGHNESS
Rescaled box counting for the topological analysis of spatial data
[DE94-009820] p 4461 N94-36464
X-ray diffraction studies of evaporated gold thin films deposited on aluminum nitride substates
[AD-A280454] p 4536 N94-37228
Angle interferometer cross axis errors
[DE94-006190] p 4446 N94-37388

SURFACE TEMPERATURE
Correlation of analytical and experimental hot structure vibration results
[NASA-TM-104269] p 4386 N94-36644
Reference manual for the Thermal Analyst's Help Desk Expert System
[NASA-CR-194941] p 4397 N94-37504

SURFACE TREATMENT
Strategic choices in surface treatments
[PB94-170669] p 4414 N94-36534
The cyclic fatigue behaviour of adhesive joints
[AD-A280453] p 4456 N94-37186

SURFACE WATER
Atmospheric gas
[DE94-007439] p 4485 N94-37187

SURFACE WAVES
Investigation of ultrasonic surface wave interaction with porous saturated rocks
[DE94-013378] p 4469 N94-37177

SURFACTANTS
Chemiluminescent microemulsions
[AD-D016292] p 4413 N94-37761

SURGERY
Channel in hip implant stem
[NASA-CASE-MFS-28987-1] p 4486 N94-36840
Task-specific usability requirements for virtual information environments: Interface design and data representation for human operators of complex medical systems p 4483 N94-37262
On the feasibility of virtual environments in medicine p 4483 N94-37264

SURVEYS
California residential indoor air quality study. Volume 1: Methodology and descriptive statistics. Appendix
[PB94-166055] p 4464 N94-36995
Toward a new National Weather Service: National Weather Service employee feedback p 4474 N94-37467

SUSPENSION SYSTEMS (VEHICLES)
Study of Japanese electrodynamic-suspension maglev systems
[DE94-011486] p 4452 N94-37515

SWEAT COOLING
Modeling of outgassing and matrix decomposition in carbon-phenolic composites
[NASA-CR-196319] p 4405 N94-37471

SWEPT FORWARD WINGS
Forward sweep, low noise rotor blade
[NASA-CASE-LAR-14569-1] p 4386 N94-36767

SWITCHING
Determining the refractive index of a lambda/4 thin film on a thick substrate from a transmittance measurement
[DE93-019584] p 4523 N94-36693

SWITCHING CIRCUITS
Time-dependent simulations of filament propagation in photoconducting switches
[DE94-012146] p 4438 N94-37213
Neurocontrol of a broadband (ATM) Clos' switching network
[PB94-179389] p 4441 N94-37851

SYMMETRY
CP violation outside the standard model phenomenology for pedestrians
[DE94-002216] p 4511 N94-36512
Variational discrete symmetries
[DE94-618485] p 4507 N94-37062

SYNCHROTRON RADIATION
Physics Division annual review, 1 April 1992 - 31 March 1993
[DE94-002497] p 4512 N94-36513
Activities of the Photon Factory
[DE94-748682] p 4522 N94-37236
Guiding hard x rays with glass polycapillary fiber
[DE94-004949] p 4525 N94-37258
Arterial cross-section measurements from dual energy transvenous coronary angiography images
[DE94-011193] p 4482 N94-37444

SYNCHROTRONS
Electroweak physics at the Tevatron collider
[DE93-040927] p 4513 N94-36695
Physics with primary beams of the KEK-PS
[DE94-748635] p 4522 N94-37234

SYNTHESIS (CHEMISTRY)
Tert-butylalumoxanes: Synthetic analogs for methylalumoxane (MAO) and new catalytic routes to polyolefins and polyketones
[AD-A280511] p 4399 N94-37106
Cyclization of bis-urethanes as a new method for the synthesis of 5-substituted, 6-membered cyclic ureas
[AD-A280232] p 4399 N94-37134
Midwest Superconductivity Consortium
[DE94-012716] p 4536 N94-37285
Theoretical and experimental investigations of fullerene derivatives: C60H2, C60H4, C70H2 and C60CH22
[DE94-012727] p 4536 N94-37287
Copper-containing ceramic precursor synthesis: Solid-state transformations and materials technology
[NASA-TM-106556] p 4399 N94-37315
Iron hydrous titanium oxide catalysts for the dehydrogenation of ethylbenzene to styrene
[DE94-010381] p 4412 N94-37542
High T(sub c) copper-oxide superconductors comprising Tl-Sr-Ca-Cu-O
[AD-D016307] p 4538 N94-37776
Substituted silyl-terminated compounds and polymers thereof
[AD-D016310] p 4427 N94-37779
Carborane-(silane or siloxane)-unsaturated hydrocarbon based thermosetting polymers
[AD-D016311] p 4427 N94-37818
Double network elastomers and method of making same
[AD-D016323] p 4427 N94-37831

SYNTHETIC APERTURE RADAR
Radially combined 30 W, 14-16 GHz amplifier
[DE94-010078] p 4432 N94-36471
Imaging targets embedded in a lossy half space with Synthetic Aperture Radar
[DE94-010807] p 4435 N94-37391
SYSTEM FAILURES
Network survivability performance
[AD-A278746] p 4433 N94-36756
Network survivability performance (computer diskette)
[AD-M000332] p 4433 N94-36757
SYSTEMS ANALYSIS
An automated method for Low Level Windshear Alert System (LLWAS) data quality analysis
[AD-A280313] p 4472 N94-37126
SYSTEMS ENGINEERING
SOFIA: Aircraft system, aft telescope cavity configuration, phase 2. Volume 1: Executive summary
[NASA-CR-196362] p 4546 N94-36642
The Engineering Review Board p 4540 N94-36843
H infinity control for nonlinear and linear systems
[AD-A280450] p 4494 N94-37226
Virtual Interfaces: Research and Applications
[AGARD-CP-541] p 4482 N94-37261
Immersive virtual environments as trainer: System design from a cognitive stance p 4484 N94-37267
On the use of fuzzy logic assessment for high consequence implementation risk analysis
[DE94-011417] p 4507 N94-37564
Ordering design tasks based on coupling strengths
[NASA-TM-109137] p 4387 N94-37762
SYSTEMS INTEGRATION
The use of a tactile interface to convey position and motion perceptions p 4486 N94-37281
SYSTEMS MANAGEMENT
Distributed VIRtual System (DIVIRS) project
[NASA-CR-196262] p 4495 N94-37509
SYSTEMS STABILITY
Robust stabilization of marginally stable positive-real systems
[NASA-TM-109136] p 4500 N94-37058

T

TARGET ACQUISITION
Pointing and Tracking Systems
[AGARD-CP-539] p 4392 N94-36616
Laser designation pods optimized concept for day/night operations p 4393 N94-36620
Infrared search and track demonstrator programme p 4393 N94-36622
Multiple target track-while-scan in the airborne EO environment p 4394 N94-36629
Efficient contact determination between geometric models
[AD-A280244] p 4494 N94-37120
Distributed detection theory and data fusion
[AD-A280410] p 4434 N94-37183
TARGET RECOGNITION
Efficient contact determination between geometric models
[AD-A280244] p 4494 N94-37120
TECHNOLOGIES
JPRS report: Science and technology. Central Eurasia: Space
[JPRS-USP-94-004] p 4391 N94-37002
JPRS report: Science and technology. Central Eurasia: Space p 4391 N94-37003
JPRS report: Science and technology. Central Eurasia
[JPRS-UST-94-013] p 4509 N94-37006
JPRS report: Science and technology. Central Eurasia: Materials science
[JPRS-UMS-93-008] p 4404 N94-37010
TECHNOLOGY ASSESSMENT
LNG vehicle technology, economics, and safety assessment
[PB94-165487] p 4450 N94-36721
Review of advanced radiator technologies for spacecraft power systems and space thermal control
[NASA-TM-4555] p 4398 N94-36821
Conceptual design: TFE verification program
[DE94-012469] p 4398 N94-37433
Refrigeration and Air-Conditioning Technology Workshop
[DE94-010813] p 4431 N94-37452
Remote use of distributed robotics resources to enhance technology development and insertion
[DE94-009285] p 4502 N94-37785
TECHNOLOGY TRANSFER
Software engineering technology transfer: Understanding the process p 4492 N94-36502
ORNL superconducting technology program for electric power systems
[DE94-011471] p 4438 N94-37239
TECHNOLOGY UTILIZATION
Abstracts of 2nd International Conference on Lasers and their Applications
[DE94-617409] p 4448 N94-37169
Advanced Turbine Technology Applications Project (ATTAP)
[NASA-CR-195367] p 4452 N94-37763
NASA commercial technology. Agenda for change
[NASA-TM-109898] p 4546 N94-37765
TEFLON (TRADEMARK)
An amorphous fluoropolymer: Next generation optical coating candidate
[DE94-012386] p 4425 N94-37422
TELECOMMUNICATION
Network survivability performance
[AD-A278746] p 4433 N94-36756
Network survivability performance (computer diskette)
[AD-M000332] p 4433 N94-36757
TELEMETRY
Preliminary PANSAT ground station software design and use of an expert system to analyze telemetry
[AD-A280600] p 4392 N94-36726
TELEOPERATORS
Task-specific usability requirements for virtual information environments: Interface design and data representation for human operators of complex medical systems p 4483 N94-37262
Operator gaze position control interfaces: Investigation of psychophysical and operational parameters p 4485 N94-37273
Low cost software-based rendering and stereoscopic interfaces for teleoperation and virtual reality p 4486 N94-37279
TELEROBOTICS
Virtual Interfaces: Research and Applications
[AGARD-CP-541] p 4482 N94-37261
TELEVISION SYSTEMS
Low cost software-based rendering and stereoscopic interfaces for teleoperation and virtual reality p 4486 N94-37279
TEMPERATURE CONTROL
Review of advanced radiator technologies for spacecraft power systems and space thermal control
[NASA-TM-4555] p 4398 N94-36821
Microscopic image processing systems for measuring nonuniform film thickness profiles
[DE94-005336] p 4424 N94-37223
TEMPERATURE DEPENDENCE
A possible origin of EL6 chondrites from a high temperature-high pressure solar gas
[DE94-010467] p 4548 N94-36759
Effect of temperature on the electron attachment and detachment properties of c-C4F6
[DE94-012750] p 4518 N94-37383
Coupled Marangoni-Benard/Rayleigh-Benard instability with temperature dependent viscosity
[NASA-TM-106646] p 4444 N94-37507
TEMPERATURE EFFECTS
Design and analysis of high-field quasi-continuous magnets
[DE94-000762] p 4508 N94-36556
Correlation of analytical and experimental hot structure vibration results
[NASA-TM-104269] p 4386 N94-36644
Hot dynamic test rig for measuring hypersonic engine seal flow and durability
[NASA-TM-106507] p 4450 N94-36645
Ground and space flight experiments of the effects of light, sound and/or temperature on animals
[NASA-CR-196102] p 4478 N94-36986
Some effects of heat release in premixed flames
[DE94-011346] p 4409 N94-37199
A fully coupled thermal, chemical, mechanical cookoff model
[DE94-011432] p 4428 N94-37201
Measurement uncertainty and feasibility study of a flush airdata system for a hypersonic flight experiment
[NASA-TM-4627] p 4383 N94-37378
Effect of temperature on the electron attachment and detachment properties of c-C4F6
[DE94-012750] p 4518 N94-37383
Material and design considerations for the carbon armored ITER divertor
[DE94-737854] p 4530 N94-37415
A method for thermal analysis of spiral bevel gears
[NASA-TM-106612] p 4451 N94-37451
Laminated thin shell structures subjected to free vibration in a hygrothermal environment
[NASA-TM-106600] p 4456 N94-37456
Mechanical performance of austempered ductile iron
[AD-A280452] p 4420 N94-37758
TEMPERATURE GRADIENTS
Isotope scaling and eta(i) mode with impurities in tokamak plasmas
[DE94-012763] p 4529 N94-37361
TEMPERATURE MEASUREMENT
Laser-saturated fluorescence measurements in laminar sooting diffusion flames
[NASA-CR-191025] p 4508 N94-36643
Methodologies for thermal and mechanical testing of TMC materials p 4401 N94-36659
Fiber optic (flight quality) sensors for advanced aircraft propulsion
[NASA-CR-191195] p 4387 N94-37401
Study on the measurement uncertainty of noise properties of a millimeter wave amplifier
[PB94-170917] p 4510 N94-37632
TEMPERATURE PROFILES
Probing flame chemistry with MBMS, theory, and modeling
[DE94-011224] p 4413 N94-37623
TEMPERATURE SENSORS
Fiber optic (flight quality) sensors for advanced aircraft propulsion
[NASA-CR-191195] p 4387 N94-37401
TENSILE PROPERTIES
Properties of TMC processed by fibre coating and hiping p 4401 N94-36656
Metal matrix composites: Analysis of simple specimens and model components under creep and fatigue loading p 4402 N94-36661
Mechanical performance of austempered ductile iron
[AD-A280452] p 4420 N94-37758
TENSILE STRENGTH
Tensile strength of simulated and welded butt joints in W-Cu composite sheet
[NASA-TM-4584] p 4405 N94-37460
A comparison of graphite/epoxy tape laminates and 2-D braided composites mechanical properties
[NASA-CR-4610] p 4420 N94-37582
Size effect in composite materials and structures: Basic concepts and design considerations p 4460 N94-37808
TENSILE TESTS
Metal matrix composites: Analysis of simple specimens and model components under creep and fatigue loading p 4402 N94-36661
ASTM and VAMAS activities in titanium matrix composites test methods development p 4403 N94-36668
Methodologies for the thermomechanical characterization of continuous-fiber ceramic matrix composites: A review of test methods
[DE94-012111] p 4405 N94-37370
TENSION
On nature's scaling effects p 4459 N94-37803
TENSORS
Tensor-GMRES method for large sparse systems of nonlinear equations
[NASA-CR-196379] p 4505 N94-37655
TERMINAL GUIDANCE
Evaluation of GPS position and attitude determination for automated rendezvous and docking missions
[NASA-CR-4614] p 4397 N94-37506
TERMINOLOGY
Alternative fuel information: Glossary
[DE94-006889] p 4429 N94-37403
A graphic view of Geometric Dimensioning and Tolerancing
[DE94-011478] p 4435 N94-37736
TERNARY ALLOYS
Processing and mechanical properties of NiAl-based in-situ composites
[NASA-CR-195333] p 4416 N94-36954
TERRAIN ANALYSIS
Rescaled box counting for the topological analysis of spatial data
[DE94-009820] p 4461 N94-36464
TERRAIN FOLLOWING AIRCRAFT
Advanced information processing system: The Army Fault-Tolerant Architecture detailed design overview
[NASA-CR-194924] p 4497 N94-36962
TEST EQUIPMENT
Internally damped, self-arresting vertical drop-weight apparatus
[NASA-CASE-LAR-15003-1] p 4389 N94-36826
TEST FACILITIES
Engineering directorate technical facilities catalog
[NASA-TM-109895] p 4390 N94-37443
TETHERED BALLOONS
Three flights into thunderstorms with the revised Rocket Electric Field Sounding (REFS) payload
[AD-A280424] p 4473 N94-37217
TETHERING
Permanent superconducting magnets for space applications
[NASA-CR-196293] p 4439 N94-37634
TETRAHEDRONS
Microstructure and chemistry of MgO- and CoO-doped nickel-titanate spinels
[DE94-012741] p 4537 N94-37382

TETRAHYDROFURAN
Solution characterization of poly(isobornyl methacrylate) in tetrahydrofuran
[AD-A280497] p 4409 N94-37145

THALLIUM COMPOUNDS
Development of high Tc (greater than 100 K) Bi, Tl and Y-based materials as superconducting circuit elements
[NASA-CR-196276] p 4534 N94-37103
InTlSb for long-wavelength infrared photodetectors and arrays
[AD-A280207] p 4524 N94-37149
Effect of thermal annealing on grain boundary chemistry of polycrystalline TlBa2Ca2Cu3O(y) films
[DE94-011464] p 4538 N94-37569
High T(sub c) copper-oxide superconductors comprising Tl-Sr-Ca-Cu-O
[AD-D016307] p 4538 N94-37776

THEORETICAL PHYSICS
Physics Division annual review, 1 April 1992 - 31 March 1993
[DE94-002497] p 4512 N94-36513
High Energy Physics Division of research activities
[DE93-019681] p 4521 N94-36694
Quantum and quasi-classical analyses of high order emission processes
[DE93-041348] p 4513 N94-36697
Direct photoionization of excited helium
[DE94-618732] p 4516 N94-37097
Is it possible to assign physical meaning to field theory with higher derivatives?
[DE94-618466] p 4539 N94-37172
Activities of the Laboratory of Physics, Helsinki University of Technology
[PB94-175247] p 4509 N94-37301

THERAPY
On the feasibility of virtual environments in medicine p 4483 N94-37264

THERMAL ANALYSIS
Preliminary analysis for a Mach 8 crossflow transition experiment on the Pegasus (R) space booster
[NASA-TM-104272] p 4381 N94-36648
Methodologies for thermal and mechanical testing of TMC materials p 4401 N94-36659
United States Air Force Summer Research Program, 1993. Volume 6: Arnold Engineering Development Center, Frank J. Seiler Research Laboratory and Wilford Hall Medical Center
[AD-A278697] p 4551 N94-36982
Transient thermal and dynamic stresses in strongback-design blankets
[DE94-012639] p 4530 N94-37441
A method for thermal analysis of spiral bevel gears
[NASA-TM-106612] p 4451 N94-37451
Reference manual for the Thermal Analyst's Help Desk Expert System
[NASA-CR-194941] p 4397 N94-37504

THERMAL CONDUCTIVITY
Theory of anomalous transport in H-mode plasmas
[DE94-727546] p 4531 N94-37485

THERMAL CONTROL COATINGS
Modeling of thermal barrier coatings
[NASA-CR-195365] p 4421 N94-36637

THERMAL CYCLING TESTS
Hot dynamic test rig for measuring hypersonic engine seal flow and durability
[NASA-TM-106507] p 4450 N94-36645
Prediction of thermal and mechanical stress-strain responses of TMC's subjected to complex TMF histories p 4402 N94-36666
Carbon-carbon heat pipe testing and evaluation
[NASA-TM-106630] p 4405 N94-37318
Effects of ply thickness on thermal cycle induced damage and thermal strain p 4459 N94-37806

THERMAL DECOMPOSITION
Characterization and processing of sintered products from nano-crystalline powders generated by the RTDS method
[DE94-004765] p 4415 N94-36553
Thermal-oxidative pretreatment and evaluation of poly (hexafluoropropene oxide) fluids
[NASA-TM-106659] p 4424 N94-37300
Thermal decomposition reactions of HMX and RDX and their importance in predicting cookoff hazards
[DE94-011430] p 4429 N94-37413

THERMAL DIFFUSIVITY
Self-sustained turbulence and L-mode confinement in toroidal plasmas
[DE94-748497] p 4532 N94-37734

THERMAL EXPANSION
Modeling of thermal barrier coatings
[NASA-CR-195365] p 4421 N94-36637
Effects of ply thickness on thermal cycle induced damage and thermal strain p 4459 N94-37806

THERMAL FATIGUE
Prediction of thermal and mechanical stress-strain responses of TMC's subjected to complex TMF histories p 4402 N94-36666
Creep-fatigue interaction property of a nickel-base heat-resistant alloy Hastelloy XR in simulated HTGR helium gas environment
[DE94-737934] p 4418 N94-37416
Effects of ply thickness on thermal cycle induced damage and thermal strain p 4459 N94-37806

THERMAL INSULATION
Electrically conductive, thermally insulating cryogenic current leads
[NASA-CASE-LAR-14964-1-CU] p 4437 N94-36781
Development of processing techniques for advanced thermal protection materials
[NASA-CR-196261] p 4426 N94-37510

THERMAL PLASMAS
D-D fusion experiments using fast z-pinches
[DE94-010090] p 4526 N94-36448
Time-resolved probing of electron thermal transport in plasma produced by femtosecond laser pulses
[DE94-012061] p 4530 N94-37392

THERMAL PROTECTION
Development of processing techniques for advanced thermal protection materials
[NASA-CR-196261] p 4426 N94-37510
Active cooling from the sixties to NASP
[NASA-TM-109079] p 4456 N94-37541

THERMAL RESISTANCE
Characterisation of Fibre Reinforced Titanium Matrix Composites
[AD-A2775206] p 4400 N94-36649
Creep-fatigue interaction property of a nickel-base heat-resistant alloy Hastelloy XR in simulated HTGR helium gas environment
[DE94-737934] p 4418 N94-37416

THERMAL STABILITY
Advanced thermally stable, coal-derived, jet fuels development program. Experiment system and model development
[AD-A278968] p 4428 N94-36505
Process simulation and modeling for advanced intermetallic alloys
[AD-A280327] p 4416 N94-37030
Thermodynamics of minerals stable near the Earth's surface
[DE94-012479] p 4539 N94-37094
Organic nonlinear optical (NLO) polymers. 4: Thermally stable NLO polymers
[AD-A280196] p 4423 N94-37148
Interferometric JFTOT tube deposit measuring device
[AD-D016295] p 4430 N94-37768

THERMAL STRESSES
Advanced thermally stable, coal-derived, jet fuels development program. Experiment system and model development
[AD-A278968] p 4428 N94-36505
Correlation of analytical and experimental hot structure vibration results
[NASA-TM-104269] p 4386 N94-36644
Material and design considerations for the carbon armored ITER divertor
[DE94-737854] p 4530 N94-37415
Transient thermal and dynamic stresses in strongback-design blankets
[DE94-012639] p 4530 N94-37441
Residual stresses in a multi-pass weld in an austenitic stainless steel plate before and after thermal stress relief
[DE94-013278] p 4420 N94-37548
A simple evaluation of thermally-induced streses in the vicinity of the stitch in a through-thickness reinforced cross-ply laminate
[NASA-CR-196317] p 4406 N94-37653

THERMALIZATION (ENERGY ABSORPTION)
Positron implantation in solids
[DE94-013029] p 4537 N94-37499

THERMIONIC CONVERTERS
TFE verification program
[DE94-009870] p 4398 N94-37514

THERMIONIC EMITTERS
TFE verification program
[DE94-009870] p 4398 N94-37514

THERMOCHEMISTRY
Thermodynamics of minerals stable near the Earth's surface
[DE94-012479] p 4539 N94-37094
CHEETAH: A fast thermochemical code for detonation
[DE94-012586] p 4429 N94-37427

THERMOCOUPLES
Initial report on calorimetry for the Tore Supra Outboard pump Limiter
[DE94-011244] p 4531 N94-37626

THERMODYNAMIC EQUILIBRIUM
Stability and dynamics of spatio-temporal structures
[DE94-013035] p 4412 N94-37491

THERMODYNAMIC PROPERTIES
A possible origin of EL6 chondrites from a high temperature-high pressure solar gas
[DE94-010467] p 4548 N94-36759
Ability of the total strain version of strainrange partitioning to characterize thermomechanical fatigue behavior
[NASA-TM-4556] p 4455 N94-37102
Solution characterization of poly(isobornyl methacrylate) in tetrahydrofuran
[AD-A280497] p 4409 N94-37145
Azobenzene-containing polymers: Some optoelectronic properties
[AD-A280448] p 4424 N94-37185
Development of durable high-temperature catalysts for natural gas combustion: Catalytic materials (CATMAT (trade name)) properties database
[PB94-171824] p 4412 N94-37462

THERMODYNAMICS
A-TOUGH: A multimedia fluid-flow/energy-transport model for fully-coupled atmospheric-subsurface interactions
[DE94-004304] p 4472 N94-36739
United States Air Force Summer Research Program, 1993. Volume 5A: Wright Laboratory
[AD-A278696] p 4551 N94-36981
Thermodynamics of minerals stable near the Earth's surface
[DE94-012479] p 4539 N94-37094
Thermomechanical studies of tungsten heavy alloys
[AD-A280250] p 4417 N94-37122
Time-of-flight pulsed ion beam surface analysis as a means of in situ, real-time characterization of the growth of ferro-electric and conductive oxide heterostructures
[DE94-012628] p 4517 N94-37249
Modeling of outgassing and matrix decomposition in carbon-phenolic composites
[NASA-CR-196319] p 4405 N94-37471

THERMOGRAVIMETRY
Basic solutions to carbon/carbon oxidation: Science and technology
[AD-A280447] p 4404 N94-37232

THERMOMECHANICAL TREATMENT
Process simulation and modeling for advanced intermetallic alloys
[AD-A280327] p 4416 N94-37030
Fabrication and properties of Ag-clad Bi-2223 conductors and magnets
[DE94-011502] p 4438 N94-37111
Maintaining constant standards during the forging process p 4421 N94-37326

THERMOPHILES
Conversion of acetic acid to methane by thermophiles
[DE94-012478] p 4479 N94-37434

THERMOPLASTIC FILMS
Interfaces of high-protection performance polyaryls-coated zinc phosphated steels
[DE94-011732] p 4417 N94-37153

THERMOPLASTIC RESINS
Structural composite construction materials manufactured from municipal solid waste
[AD-A280635] p 4403 N94-36730

THERMOPLASTICITY
Micromechanical modeling of damage growth in titanium based metal-matrix composites p 4402 N94-36664

THERMOSETTING RESINS
Carborane-siloxane or silane-unsaturated hydrocarbon based polymers
[AD-D016220] p 4425 N94-37482
Synthesis of phthalonitrile resins containing ether and imide linkages with aromatic diamine curing agent
[AD-D016309] p 4427 N94-37778
Carborane-(silane or siloxane)-unsaturated hydrocarbon based thermosetting polymers
[AD-D016311] p 4427 N94-37818

THERMOSIPHONS
Determination of the dispersion constant in a constrained vapor bubble thermosyphon
[NASA-CR-196124] p 4442 N94-36992

THICK FILMS
Electrically conductive, thermally insulating cryogenic current leads
[NASA-CASE-LAR-14964-1-CU] p 4437 N94-36781
Superconducting TlCa2Ba2Cu3O9 thick films
[DE94-010436] p 4535 N94-37193

THICK PLATES
Residual stresses in a multi-pass weld in an austenitic stainless steel plate before and after thermal stress relief
[DE94-013278] p 4420 N94-37548

THICKNESS
Effects of ply thickness on thermal cycle induced damage and thermal strain p 4459 N94-37806

THIN FILMS
Irradiation effects in Fe-30 percent Ni alloy during Ar ion implantation
[DE94-619057] p 4415 N94-36564
Determining the refractive index of a lambda/4 thin film on a thick substrate from a transmittance measurement
[DE93-019584] p 4523 N94-36693
Diamond deposition and defect chemistry studied via solid state NMR
[AD-A280609] p 4533 N94-36727
Small-angle x ray scattering studies of microvoids in amorphous-silicon-based semiconductors
[DE94-006931] p 4533 N94-36745
Atomic and electronic structure of metals and alloys: Rare earths, ultrathin films and surface alloys
[DE94-011581] p 4516 N94-37113
Poly(p-phenylene) derivatives new high performance nonlinear optical polymers
[AD-A280248] p 4422 N94-37121
New materials and multidimensional cluster analysis for SAW chemical sensor arrays
[DE94-012066] p 4409 N94-37161
Critical-state flux-density profiles in type-2 superconducting thin-film strips and disks
[DE94-011199] p 4535 N94-37166
Substrate effects on the structure and optical properties of epitaxial PbTiO3 thin films prepared by metal-organic chemical vapor deposition
[DE94-010432] p 4535 N94-37192
Microscopic image processing systems for measuring nonuniform film thickness profiles
[DE94-005336] p 4424 N94-37223
X-ray diffraction studies of evaporated gold thin films deposited on aluminum nitride substates
[AD-A280454] p 4536 N94-37228
Time-of-flight pulsed ion beam surface analysis as a means of in situ, real-time characterization of the growth of ferro-electric and conductive oxide heterostructures
[DE94-012628] p 4517 N94-37249
SAW chemical sensor arrays using new thin-film materials
[DE94-011940] p 4411 N94-37365
Investigation of polycrystalline thin-film CuInSe2 solar cells based on ZnSe windows
[DE94-006936] p 4462 N94-37381
Scanning x-ray diffraction: A technique with high compositional resolution for studying phase formation in co-deposited thin films
[DE94-011496] p 4420 N94-37516
Residual stress and Raman spectra of laser deposited highly-tetrahedral-coordinated-amorphous-carbon films
[DE94-012067] p 4426 N94-37537
The MBE growth and optical quality of BaTiO3 and SrTiO3 thin films on MgO
[DE94-011468] p 4538 N94-37570

THIN WALLED SHELLS
Laminated thin shell structures subjected to free vibration in a hygrothermal environment
[NASA-TM-106600] p 4456 N94-37456

THIOLS
Bond selective chemistry beyond the adiabatic approximation
[DE94-012486] p 4408 N94-37095

THOMSON SCATTERING
Design of the divertor Thomson scattering system on D3-D
[DE94-012672] p 4527 N94-37081

THREAT EVALUATION
Sensor data fusion for air to air situation awareness beyond visual range p 4395 N94-36633

THREE DIMENSIONAL BODIES
The problems of the minimal surface and minimal lineal measure in three dimensions
[DE94-013002] p 4479 N94-37355

THREE DIMENSIONAL FLOW
Simulation of three-dimensional multi-phase flow characteristics in the deswirl section of the CDIF MHD power train
[DE94-012644] p 4443 N94-37176
Evaluation of parameterizations for pollutant transport and dispersion in an urban street canyon using a three-dimensional dynamic flow model
[DE94-012641] p 4467 N94-37429
Development of advanced Navier-Stokes solver
[NASA-CR-195094] p 4504 N94-37449
Unstructured grid methods for the simulation of 3D transient flows
[NASA-CR-196139] p 4444 N94-37525

THREE DIMENSIONAL MODELS
Finite-rate chemistry and transient effects in Direct Numerical Simulations of turbulent non-premixed flames
[DE94-005250] p 4410 N94-37222
Evaluation of parameterizations for pollutant transport and dispersion in an urban street canyon using a three-dimensional dynamic flow model
[DE94-012641] p 4467 N94-37429
A computational model for three-dimensional jointed media with a single joint set
[DE94-007582] p 4470 N94-37527
Three-dimensional gyrokinetic particle-in-cell simulation of plasmas on a massively parallel computer: LDRD Core Competency Project
[DE94-013367] p 4532 N94-37732

THRUST REVERSAL
Subsonic aerodynamic characteristic of semispan commercial transport model with wing-mounted advanced ducted propeller operating in reverse thrust --- conducted in the Langley 14 by 22 foot subsonic wind tunnel
[NASA-TP-3427] p 4384 N94-37505

THRUSTORS
Characteristics of ions emitted from high-current hollow cathodes
[NASA-CR-195372] p 4398 N94-37764

THUNDERSTORMS
Three flights into thunderstorms with the revised Rocket Electric Field Sounding (REFS) payload
[AD-A280424] p 4473 N94-37217

TILT ROTOR AIRCRAFT
Analysis of vertiport studies funded by the Airport Improvement Program (AIP)
[SCT-93RR-21] p 4390 N94-37424

TIME MEASUREMENT
SACS: A cache simulator incorporating timing analysis with buffer and memory management
[AD-A280472] p 4494 N94-37230
Chemical recognition software
[DE94-012918] p 4495 N94-37496
Techniques for real-time parallel processing: Sensor processing case studies
[AD-A280633] p 4499 N94-37760

TIME SERIES ANALYSIS
Embedded chaotic time series: Applications in prediction and spatio-temporal classification
[AD-A280690] p 4508 N94-37130
Index and bulk parameters for frequency-direction spectra measured at CERC Field Research Facility, September 1990 to August 1991
[AD-A280423] p 4476 N94-37216
Index and bulk parameters for frequency-direction spectra measured at CERC Field Research Facility, September 1991 to August 1992
[AD-A280455] p 4477 N94-37229

TIN ALLOYS
Use of rotation to suppress thermosolutal convection in directionally solidified binary alloys
[NASA-CR-196372] p 4415 N94-36811

TIN OXIDES
Low temperature atmospheric pressure chemical vapor deposition of group 14 oxide films
[DE94-013115] p 4425 N94-37317

TISSUES (BIOLOGY)
Three dimensional optic tissue culture and process
[NASA-CASE-MSC-22368-1] p 4478 N94-36765
Chemical and structural characterization of nitroaromatic adducts with hemoglobins
[AD-A280533] p 4480 N94-37089

TITAN
Infrared spectroscopy of Jupiter and Saturn
[NASA-CR-196294] p 4549 N94-36961

TITANIA
Morphological aspects of surface reactions
[DE94-011208] p 4413 N94-37713

TITANIUM
Characterisation of Fibre Reinforced Titanium Matrix Composites
[AD-A2775206] p 4400 N94-36649
Possibilities and pitfalls in aerospace applications of titanium matrix composites p 4400 N94-36650
Applications of Titanium Matrix Composite to large airframe structure p 4400 N94-36651
SCS-6 (tm) fiber reinforced titanium p 4400 N94-36652
Processing of titanium matrix composites p 4401 N94-36653
Composites based on titanium with external and internal reinforcement p 4401 N94-36654
Manufacture and properties of sigma fibre reinforced titanium p 4401 N94-36655
Methodologies for thermal and mechanical testing of TMC materials p 4401 N94-36659
Ultrasonic nondestructive characterization methods for the development and life prediction of titanium matrix composites p 4401 N94-36660
Metal matrix composites: Analysis of simple specimens and model components under creep and fatigue loading p 4402 N94-36661
Residual strength and life prediction techniques for Ti MMC p 4402 N94-36662
Micromechanical modeling of damage growth in titanium based metal-matrix composites p 4402 N94-36664
Crack growth under cycle loading in fibre reinforced titanium metal matrix composites p 4402 N94-36665
Pre-standardisation work on fatigue and fracture testing of titanium matrix composites p 4402 N94-36667
ASTM and VAMAS activities in titanium matrix composites test methods development p 4403 N94-36668
A methodology to predict damage initiation, damage growth and residual strength in titanium matrix composites
[NASA-TM-109135] p 4405 N94-37320

TITANIUM ALLOYS
Characterisation of Fibre Reinforced Titanium Matrix Composites
[AD-A2775206] p 4400 N94-36649
Composites based on titanium with external and internal reinforcement p 4401 N94-36654
Properties of TMC processed by fibre coating and hiping p 4401 N94-36656
Fibre-matrix interface properties in Ti-matrix composites: Chemical compatibility and micromechanical behaviour p 4401 N94-36657
Oxidation behavior of titanium aluminide matrix materials p 4401 N94-36658
Process/composite concurrent tailoring of SiC/Ti composites p 4402 N94-36663
Prediction of thermal and mechanical stress-strain responses of TMC's subjected to complex TMF histories p 4402 N94-36666
Development of mechanical testing methods for titanium matrix composites (traction-ogligo-cyclic fatigue) p 4403 N94-36669
Modelling and testing fibre reinforced titanium for design purposes p 4403 N94-36670
Process simulation and modeling for advanced intermetallic alloys
[AD-A280327] p 4416 N94-37030
Feasibility of (IMC)(sub d)-reinforced metal matrix composites
[AD-A280626] p 4404 N94-37044
Alternate melting and refining routes p 4421 N94-37323
Maintaining constant standards during the forging process p 4421 N94-37326

TITANIUM BORIDES
Feasibility of (IMC)(sub d)-reinforced metal matrix composites
[AD-A280626] p 4404 N94-37044

TITANIUM OXIDES
Substrate effects on the structure and optical properties of epitaxial PbTiO3 thin films prepared by metal-organic chemical vapor deposition
[DE94-010432] p 4535 N94-37192
Determination of interface structure and bonding at atomic resolution in the stem
[DE94-011466] p 4517 N94-37238
Numerical analysis of an impinging jet reactor for the CVD and gas-phase nucleation of titania
[NASA-TM-106619] p 4431 N94-37254
Bibliography of work on the photocatalytic removal of hazardous compounds from water and air
[DE94-006906] p 4467 N94-37405
Iron hydrous titanium oxide catalysts for the dehydrogenation of ethylbenzene to styrene
[DE94-010381] p 4412 N94-37542

TOKAMAK DEVICES
Design of the divertor Thomson scattering system on D3-D
[DE94-012672] p 4527 N94-37081
The role of heating and current drive in ITER
[DE94-012679] p 4527 N94-37082
Initial studies of reflectometer for ITER
[DE94-012476] p 4528 N94-37167
Towards nuclear fusion reactors
[DE94-748680] p 4528 N94-37235
Startup and shutdown of the PULSAR Tokamak Reactor
[DE94-013128] p 4528 N94-37292
Motional Stark effect upgrades on D3-D
[DE94-013146] p 4528 N94-37297
MARFE's in tokamak edge plasma: Pattern formation under nonlocal constraints
[DE94-012766] p 4529 N94-37309
ELMy-H mode as limit cycle and transient responses of H-modes in tokamaks
[DE94-727510] p 4529 N94-37358
Isotope scaling and eta(i) mode with impurities in tokamak plasmas
[DE94-012763] p 4529 N94-37361
A role of neutral hydrogen in CHS plasmas with reheat and collapse and comparison with JIPPT-IIU tokamak plasmas
[DE94-718985] p 4530 N94-37384
Material and design considerations for the carbon armored ITER divertor
[DE94-737854] p 4530 N94-37415

Recent DIII-D high power heating and current drive experiments
[DE94-012509] p 4530 N94-37436
Two-dimensional over-all neutronics analysis of the ITER device
[DE94-718963] p 4530 N94-37464
Improvement study of the divertor configuration of the Steady State Tokamak Reactor (SSTR)
[DE94-718961] p 4531 N94-37484
Research using small tokamaks
[DE94-621827] p 4531 N94-37493
Initial report on calorimetry for the Tore Supra Outboard pump Limiter
[DE94-011244] p 4531 N94-37626

TOLERANCES (MECHANICS)
Turbine disks: Lifing against defects and materials development p 4454 N94-37329

TOLUENE
California residential indoor air quality study. Volume 1: Methodology and descriptive statistics
[PB94-166048] p 4464 N94-36994

TOMOGRAPHY
Signal processing for the 1992 Barents Sea tomography experiment
[AD-A278580] p 4476 N94-36971
Density and composition analysis using focused MeV ion microbeam techniques
[DE94-012241] p 4517 N94-37210
The effects of proton-beam quality on the production of gamma rays for nuclear resonance absorption in nitrogen
[DE94-011609] p 4523 N94-37629
A note on analytic recovery of transition probabilities in three dimensional diffuse tomography
[DE94-011378] p 4506 N94-37719

TOPOGRAPHY
Four beam interferometer manual: Operating instructions for the INEL diffraction Moire interferometer
[DE94-010772] p 4453 N94-36452
Representing the influence of subgrid topography on hydrology
[DE94-004595] p 4474 N94-37379

TOPOLOGY
Rescaled box counting for the topological analysis of spatial data
[DE94-009820] p 4461 N94-36464
Note on certain rigid subshifts
[PB94-179058] p 4506 N94-37833
Localization of topological Pontryagin classes by propagation with finite speed
[PB94-180666] p 4506 N94-37852

TOROIDAL PLASMAS
Confinement improvement in H-mode-like plasmas in helical systems
[DE94-727619] p 4528 N94-37231
Towards nuclear fusion reactors
[DE94-748680] p 4528 N94-37235
MARFE's in tokamak edge plasma: Pattern formation under nonlocal constraints
[DE94-012766] p 4529 N94-37309
Isotope scaling and eta(i) mode with impurities in tokamak plasmas
[DE94-012763] p 4529 N94-37361
A role of neutral hydrogen in CHS plasmas with reheat and collapse and comparison with JIPPT-IIU tokamak plasmas
[DE94-718985] p 4530 N94-37384
Recent DIII-D high power heating and current drive experiments
[DE94-012509] p 4530 N94-37436
Theory of anomalous transport in H-mode plasmas
[DE94-727546] p 4531 N94-37485
Fast electron generation and transport in a turbulent, magnetized plasma
[DE94-012986] p 4531 N94-37730
Self-sustained turbulence and L-mode confinement in toroidal plasmas
[DE94-748497] p 4532 N94-37734

TORQUE
Variable stiffness torsion springs
[NASA-CASE-MFS-28930-1] p 4509 N94-36782
Dynamics of a split torque helicopter transmission
[NASA-TM-106410] p 4452 N94-37457

TORSION
Variable stiffness torsion springs
[NASA-CASE-MFS-28930-1] p 4509 N94-36782

TOTAL QUALITY MANAGEMENT
A survey of commonly applied methods for software process improvement
[AD-A278595] p 4493 N94-36974

TOXIC HAZARDS
Solid state fluorometer: Prototype development
[AD-A280321] p 4534 N94-37027

TRACE ELEMENTS
Accelerated line-by-line calculations for the radiative transfer of trace gases related to climate studies
[DE94-004404] p 4464 N94-36552

TRACKING (POSITION)
Pointing and Tracking Systems
[AGARD-CP-539] p 4392 N94-36616
Landing of an unmanned helicopter on a moving platform. High accuracy navigation and tracking p 4387 N94-36618
Advanced helmet tracking technology developments for Naval aviation p 4393 N94-36623
Advances in helmet trackers p 4394 N94-36624
High accuracy control algorithm application to a tracking turret p 4394 N94-36626
Aeroservoelastic stabilization considerations for pointing and tracking systems p 4394 N94-36627
Studies and simulations on sensor fusion and cueing for fighter application p 4395 N94-36632
Sensor data fusion for air to air situation awareness beyond visual range p 4395 N94-36633
Global Positioning System Synchronized Active Light Autonomous Docking System
[NASA-CASE-MFS-28853-1] p 4395 N94-36825
Signal processing for the 1992 Barents Sea tomography experiment
[AD-A278580] p 4476 N94-36971
Manual tracking performance using a virtual hand controller: A comparison study p 4484 N94-37271
A comparison of two examples of magnetic tracker systems p 4485 N94-37275

TRADEOFFS
On the use of fuzzy logic assessment for high consequence implementation risk analysis
[DE94-011417] p 4507 N94-37564

TRAFFIC
SIHTI: Energy and environmental technology
[DE94-763290] p 4464 N94-37007

TRAINING DEVICES
Evaluation of a tool for producing and presenting interactive videodisc job aids
[AD-A278599] p 4432 N94-36473
Assistance in instruction and training of air traffic controllers p 4483 N94-37265
Immersive virtual environments as trainer: System design from a cognitive stance p 4484 N94-37267

TRAINING SIMULATORS
Immersive virtual environments as trainer: System design from a cognitive stance p 4484 N94-37267

TRAJECTORY CONTROL
Advanced information processing system: Hosting of advanced guidance, navigation and control algorithms on AIPS using ASTER
[NASA-CR-194960] p 4499 N94-37583

TRAJECTORY OPTIMIZATION
Optimal control theory determination of feasible return-to-launch-site aborts for the HL-20 Personnel Launch System vehicle
[NASA-TP-3449] p 4396 N94-37260

TRAJECTORY PLANNING
Robot trajectory planning via dynamic programming
[DE94-008424] p 4501 N94-37529

TRANSFORMATIONS (MATHEMATICS)
Multitarget track initiation using a modified Hough transform p 4395 N94-36630
Variational discrete symmetries
[DE94-618485] p 4507 N94-37062
The canonical symmetry for integral systems
[DE94-618486] p 4504 N94-37375
Parallel tridiagonalization through two-step band reduction
[DE94-011512] p 4505 N94-37518

TRANSIENT RESPONSE
ELMy-H mode as limit cycle and transient responses of H-modes in tokamaks
[DE94-727510] p 4529 N94-37358

TRANSISTORS
Single event mirroring and sense amplifier designs for enhanced SE tolerance of DRAMs
[DE94-010397] p 4438 N94-37190
Role of burn-in during qualification testing
[DE94-007864] p 4439 N94-37513

TRANSITION METALS
Consequences of competing hybridization for magnetic ordering in correlated-electron lattices
[DE94-011648] p 4534 N94-37057

TRANSMISSION EFFICIENCY
Guiding hard x rays with glass polycapillary fiber
[DE94-004949] p 4525 N94-37258

TRANSMISSION LINES
A novel transition between rectangular waveguide and layered ridge dielectric waveguide
[NASA-TM-106661] p 4433 N94-36955

TRANSMISSIONS (MACHINE ELEMENTS)
Vibration signature analysis of a faulted gear transmission system
[NASA-TM-106623] p 4450 N94-36953
Dynamics of a split torque helicopter transmission
[NASA-TM-106410] p 4452 N94-37457

TRANSMITTANCE
Determining the refractive index of a lambda/4 thin film on a thick substrate from a transmittance measurement
[DE93-019584] p 4523 N94-36693
Three-stage attenuation using Glan-Thompson prisms
[AD-A280481] p 4525 N94-37350

TRANSMITTER RECEIVERS
Design and analysis of a mode B and mode JD satellite Earth station
[AD-A280417] p 4391 N94-37225

TRANSMUTATION
Characterization of nuclear transmutations in materials irradiated test facilities
[DE94-013309] p 4420 N94-37552

TRANSONIC WIND TUNNELS
Experimental uncertainty and drag measurements in the national transonic facility
[NASA-CR-4600] p 4389 N94-36945

TRANSPORT AIRCRAFT
Subsonic aerodynamic characteristic of semispan commercial transport model with wing-mounted advanced ducted propeller operating in reverse thrust --- conducted in the Langley 14 by 22 foot subsonic wind tunnel
[NASA-TP-3427] p 4384 N94-37505

TRANSPORT PROPERTIES
Computational chemistry research
[NASA-CR-196120] p 4408 N94-36989
Confinement improvement in H-mode-like plasmas in helical systems
[DE94-727619] p 4528 N94-37231
Midwest Superconductivity Consortium
[DE94-012716] p 4536 N94-37285
Theoretical studies of the transport properties in compound semiconductors
[NASA-CR-196109] p 4439 N94-37501
Effects of molecular transport on turbulence-chemistry interactions in a hydrogen-argon-air jet diffusion flame
[DE94-005107] p 4413 N94-37711
Self-sustained turbulence and L-mode confinement in toroidal plasmas
[DE94-748497] p 4532 N94-37734
Flux creep: Its dependence on current denisty and relation to critical current densities from transport and magnetic measurements
[DE94-011701] p 4440 N94-37738

TRANSPORT THEORY
Anomalous cross field flux in CHS
[DE94-727547] p 4529 N94-37359
Neutron transport methods on scalable shared memory multiprocessors
[DE94-012324] p 4498 N94-37419
Bounce resonance heating and transport in a magnetic mirror
[DE94-727545] p 4531 N94-37466
Theory of anomalous transport in H-mode plasmas
[DE94-727546] p 4531 N94-37485

TRANSPORTATION
LNG vehicle technology, economics, and safety assessment
[PB94-165487] p 4450 N94-36721
The implementation of Electronic Data Interchange (EDI) with defense transportation operations
[AD-A280568] p 4493 N94-37040

TRANSVERSE OSCILLATION
Is it possible to assign physical meaning to field theory with higher derivatives?
[DE94-618468] p 4539 N94-37172

TRAPPED PARTICLES
Spontaneous force optical traps
[AD-A280574] p 4514 N94-37041

TRAVELING WAVE TUBES
Evaluation of some slow-wave vane structures for aminiature traveling-wave tube at 30 GHz
[NASA-TM-106654] p 4437 N94-36819

TRIANGULATION
Linear-size nonobtuse triangulation of polygons
[DE94-010746] p 4505 N94-37620

TRIBOLOGY
Evaluation of the EHL film thickness and extreme pressure additives on gear surface fatigue life
[NASA-TM-106663] p 4451 N94-37319
Properties of perfluoropolyethers for space applications
[NASA-TM-106616] p 4426 N94-37520

TRIBUTARIES
Numerical simulation of nocturnal drainage flows in an idealized valley-tributary system
[DE94-011684] p 4472 N94-37115
The influence of tributaries on nocturnal valley flows
[DE94-011613] p 4473 N94-37242

TROPOSPHERE
Measurements and modeling of the effect of convective clouds on the upper tropospheric moisture budget
[NASA-TM-109894] p 4473 N94-37371
Tropospheric radiative forcing of CH4
[DE94-011628] p 4468 N94-37631
TUBERCULOSIS
Rapid susceptibility testing of Mycobacterium avium complex and Mycobacterium tuberculosis isolated from AIDS patients
[NASA-CR-196268] p 4478 N94-36996
TUBES
Modeling of forced CVI for tube fabrication
[DE94-012718] p 4410 N94-37286
First-principles determination of the polarizabilities of carbon tubules as a function of length
[DE94-013015] p 4537 N94-37356
TUNABLE LASERS
Diode-pumped, continuously tunable, 2.3 micron CW laser specification
[AD-D016312] p 4450 N94-37838
TUNGSTEN
Preradiation studies for non-thermal Z-pinch wire load experiments on Saturn
[DE94-013459] p 4527 N94-37072
Thermomechanical studies of tungsten heavy alloys
[AD-A280250] p 4417 N94-37122
TUNGSTEN ALLOYS
Thermomechanical studies of tungsten heavy alloys
[AD-A280250] p 4417 N94-37122
Examination of weldability of Ni-Cr-W superalloys
[DE94-719014] p 4418 N94-37385
TUNING
Tune modulation due to gradient ripple and the dynamic aperture
[DE94-011922] p 4524 N94-37157
TURBINE BLADES
Mars vertical axis wind machines. The design of a Darreus and a Giromill for use on Mars
[NASA-CR-196143] p 4462 N94-36807
A combined experiment/computational study of flow in turbine blade cooling passage
[NASA-CR-4584] p 4442 N94-36957
Process enhancements of superalloy material
p 4421 N94-37324
TURBOMACHINERY
Preliminary design for a reverse Brayton cycle cryogenic cooler
[NASA-CR-189341] p 4461 N94-36805
TURBULENCE
The alternative faces of turbulent flow
[TM-5-94] p 4442 N94-36934
Finite-rate chemistry and transient effects in Direct Numerical Simulations of turbulent non-premixed flames
[DE94-005250] p 4410 N94-37222
Evolution of turbulent fields in explosions
[DE94-010405] p 4444 N94-37390
Effects of molecular transport on turbulence-chemistry interactions in a hydrogen-argon-air jet diffusion flame
[DE94-005107] p 4413 N94-37711
Fast electron generation and transport in a turbulent, magnetized plasma
[DE94-012966] p 4531 N94-37730
Self-sustained turbulence and L-mode confinement in toroidal plasmas
[DE94-748497] p 4532 N94-37734
TURBULENCE MODELS
Evolution of turbulent fields in explosions
[DE94-010405] p 4444 N94-37390
TURBULENT BOUNDARY LAYER
Hypersonic shock/boundary-layer interaction database: New and corrected data
[NASA-CR-177638] p 4441 N94-36519
TURBULENT COMBUSTION
Some effects of heat release in premixed flames
[DE94-011346] p 4409 N94-37199
TURBULENT DIFFUSION
Short-tower sigma(theta) measurements in the Colorado Plateaus region
[DE94-007478] p 4463 N94-36478
Influences of flame-vortex interactions on formation of oxides of nitrogen in curved methane-air diffusion flamelets
[DE94-005105] p 4409 N94-37221
Spray combustion model improvement study, 1
[NASA-CR-196122] p 4410 N94-37250
Effects of molecular transport on turbulence-chemistry interactions in a hydrogen-argon-air jet diffusion flame
[DE94-005107] p 4413 N94-37711
TURBULENT FLOW
Preliminary analysis for a Mach 8 crossflow transition experiment on the Pegasus (R) space booster
[NASA-TM-104272] p 4381 N94-36648
The alternative faces of turbulent flow
[TM-5-94] p 4442 N94-36934
Simulation of three-dimensional multi-phase flow characteristics in the deswirl section of the CDIF MHD power train
[DE94-012644] p 4443 N94-37176
The stabilizing effect of compressibility in turbulent shear flow
[NASA-CR-194932] p 4444 N94-37605
TURBULENT JETS
Evolution of turbulent fields in explosions
[DE94-010405] p 4444 N94-37390
TURBULENT MIXING
Evolution of turbulent fields in explosions
[DE94-010405] p 4444 N94-37390
TURRET
High accuracy control algorithm application to a tracking turret p 4394 N94-36626
TWINNING
Substrate effects on the structure and optical properties of epitaxial PbTiO3 thin films prepared by metal-organic chemical vapor deposition
[DE94-010432] p 4535 N94-37192
TWO DIMENSIONAL FLOW
A method for flow simulation about complex geometries using both structured and unstructured grids
[NASA-TM-106633] p 4383 N94-37283
TWO DIMENSIONAL MODELS
MARFE's in tokamak edge plasma: Pattern formation under nonlocal constraints
[DE94-012766] p 4529 N94-37309
Atmospheric structure simulation: An ARMA model for smooth isotropic two-dimensional geophysical power spectra
[AD-A280476] p 4470 N94-37649
TWO PHASE FLOW
Simulation of three-dimensional multi-phase flow characteristics in the deswirl section of the CDIF MHD power train
[DE94-012644] p 4443 N94-37176
Flow visualization for Lagrangian particle methods
[DE94-010757] p 4443 N94-37195
Effects of two-phase flow on the deflagration of porous energetic materials
[DE94-011423] p 4411 N94-37412
TWO STAGE TURBINES
Experimental measurements and analytical analysis related to gas turbine heat transfer. Part 1: Time-averaged heat-flux and surface-pressure measurements on the vanes and blades of the SSME fuel-side turbine and comparison with prediction. Part 2: Phase-resolved surface-pressure and heat-flux measurements on the first blade of the SSME fuel-side turbine
[NASA-CR-196296] p 4442 N94-36969

U

U.S.S.R. SPACE PROGRAM
JPRS report: Science and technology. Central Eurasia: Space
[JPRS-USP-94-004] p 4391 N94-37002
ULLAGE
Cryogenic fluid management technologies for space transportation. Zero G thermodynamic vent system
[NASA-CR-193981] p 4430 N94-36806
ULTRAHIGH FREQUENCIES
TIPC user manual
[DE94-004470] p 4432 N94-36443
ULTRASONIC FLAW DETECTION
Ultrasonic nondestructive characterization methods for the development and life prediction of titanium matrix composites p 4401 N94-36660
ULTRASONIC RADIATION
Investigation of ultrasonic surface wave interaction with porous saturated rocks
[DE94-013378] p 4469 N94-37177
ULTRASONIC TESTS
Ultrasonic nondestructive characterization methods for the development and life prediction of titanium matrix composites p 4401 N94-36660
ULTRAVIOLET ASTRONOMY
Ultraviolet spectropolarimetry of high redshift quasars with the Hubble Space Telescope
[NASA-CR-196014] p 4546 N94-36690
ULTRAVIOLET SPECTROSCOPY
Poly(p-phenylene) derivatives new high performance nonlinear optical polymers
[AD-A280248] p 4422 N94-37121
UNDERWATER ACOUSTICS
Signal processing for the 1992 Barents Sea tomography experiment
[AD-A278580] p 4476 N94-36971
UNITED STATES
Math and science illiteracy: Social and economic impacts
[DE94-010801] p 4540 N94-37092
UNIVERSITIES
Activities of the Laboratory of Physics, Helsinki University of Technology
[PB94-175247] p 4509 N94-37301
UNIVERSITY PROGRAM
Beginning a dialogue on the changing environment for the physical and mathematical sciences
p 4509 N94-36948
Design and development of experimental facilities for short duration, low-gravity combustion and fire experiments
[NASA-CR-196107] p 4389 N94-36967
United States Air Force Summer Research Program, 1993. Volume 7: Armstrong Laboratory
[AD-A278655] p 4550 N94-36975
United States Air Force Summer Research Program, 1993. Volume 14: Rome Laboratory
[AD-A278656] p 4550 N94-36976
United States Air Force Summer Research Program, 1993. Volume 13: Phillips Laboratory
[AD-A278657] p 4550 N94-36977
United States Air Force Summer Research Program, 1993. Volume 16: Arnold Engineering Development Center, Frank J. Seiler Research Laboratory and Wilford Hall Medical Center
[AD-A278658] p 4550 N94-36978
United States Air Force Summer Research Program, 1993. Volume 3: Phillips Laboratory
[AD-A278694] p 4550 N94-36979
United States Air Force Summer Research Program, 1993. Volume 4: Rome Laboratory
[AD-A278695] p 4551 N94-36980
United States Air Force Summer Research Program, 1993. Volume 5A: Wright Laboratory
[AD-A278696] p 4551 N94-36981
United States Air Force Summer Research Program, 1993. Volume 6: Arnold Engineering Development Center, Frank J. Seiler Research Laboratory and Wilford Hall Medical Center
[AD-A278697] p 4551 N94-36982
United States Air Force Summer Research Program, 1993. Volume 8: Phillips Laboratory
[AD-A278698] p 4551 N94-36983
United States Air Force Summer Research Program, 1993. Volume 9: Rome Laboratory
[AD-A278699] p 4551 N94-36984
UNSTEADY FLOW
Experimental investigation of nozzle/plume aerodynamics at hypersonic speeds
[NASA-CR-195829] p 4382 N94-36687
On automating domain connectivity for overset grids
[NASA-CR-196113] p 4493 N94-36920
Unsteady flow field of large-amplitude pitching airfoils
[AD-A280444] p 4383 N94-37219
Development of advanced Navier-Stokes solver
[NASA-CR-195094] p 4504 N94-37449
Unstructured grid methods for the simulation of 3D transient flows
[NASA-CR-196139] p 4444 N94-37525
URANIUM OXIDES
Sintering of dioxide pellets in an oxidizing atmosphere (CO2)
[DE94-613046] p 4414 N94-36517
UREAS
Cyclization of bis-urethanes as a new method for the synthesis of 5-substituted, 6-membered cyclic ureas
[AD-A280232] p 4399 N94-37134
URETHANES
Cyclization of bis-urethanes as a new method for the synthesis of 5-substituted, 6-membered cyclic ureas
[AD-A280232] p 4399 N94-37134
USER MANUALS (COMPUTER PROGRAMS)
TIPC user manual
[DE94-004470] p 4432 N94-36443
Rotorwash analysis handbook. Volume 2: Appendixes
[SCT-93RR-17-VOL-2] p 4382 N94-36487
NIPER Lab WARDEN: Descriptive panels and diagrams for NIPER Lab WARDEN software, volume 2
[DE94-000126] p 4493 N94-36699
Eigensystem realization algorithm user's guide forVAX/VMS computers: Version 931216
[NASA-TM-109066] p 4493 N94-36818
An arbitrary grid CFD algorithm for configuration aerodynamics analysis. Volume 2: FEMNAS user guide
[NASA-CR-196135] p 4493 N94-36922
TRENDS: A flight test relational database user's guide and reference manual
[NASA-TM-108806] p 4381 N94-37332
Development of durable high-temperature catalysts for natural gas combustion: Catalytic materials (CATMAT (trade name)) properties database
[PB94-171824] p 4412 N94-37462
Reference manual for the Thermal Analyst's Help Desk Expert System
[NASA-CR-194941] p 4397 N94-37504

User's manual for SNL-SAND-2 code
[DE94-011744] p 4496 N94-37673

V

VACUUM
A nonconservative scheme for isentropic gas dynamics
[DE94-011488] p 4445 N94-37724
VACUUM MELTING
The influence of VAR processes and parameters on white spot formation in Alloy 718
[DE94-012071] p 4417 N94-37367
VALLEYS
Numerical simulation of nocturnal drainage flows in an idealized valley-tributary system
[DE94-011684] p 4472 N94-37115
The influence of tributaries on nocturnal valley flows
[DE94-011613] p 4473 N94-37242
VALVES
A dynamic model of a linear actuator based on polymer hydrogel
[DE94-010800] p 4408 N94-37091
VANADIUM ALLOYS
Transient thermal and dynamic stresses in strongback-design blankets
[DE94-012639] p 4530 N94-37441
Characterization of nuclear transmutations in materials irradiated test facilities
[DE94-013309] p 4420 N94-37552
VANES
Experimental measurements and analytical analysis related to gas turbine heat transfer. Part 1: Time-averaged heat-flux and surface-pressure measurements on the vanes and blades of the SSME fuel-side turbine and comparison with prediction. Part 2: Phase-resolved surface-pressure and heat-flux measurements on the first blade of the SSME fuel-side turbine
[NASA-CR-196296] p 4442 N94-36969
VAPOR DEPOSITION
SCS-6 (tm) fiber reinforced titanium
p 4400 N94-36652
Processing of titanium matrix composites
p 4401 N94-36653
Manufacture and properties of sigma fibre reinforced titanium p 4401 N94-36655
Diamond deposition and defect chemistry studied via solid state NMR
[AD-A280609] p 4533 N94-36727
Turning soot into diamonds with microwaves
[DE94-013426] p 4422 N94-37066
Substrate effects on the structure and optical properties of epitaxial PbTiO3 thin films prepared by metal-organic chemical vapor deposition
[DE94-010432] p 4535 N94-37192
Basic solutions to carbon/carbon oxidation: Science and technology
[AD-A280447] p 4404 N94-37232
Numerical analysis of an impinging jet reactor for the CVD and gas-phase nucleation of titania
[NASA-TM-106619] p 4431 N94-37254
Low temperature atmospheric pressure chemical vapor deposition of group 14 oxide films
[DE94-013115] p 4425 N94-37317
Preliminary soft x ray studies of beta-SiC
[DE94-013023] p 4537 N94-37498
Morphological aspects of surface reactions
[DE94-011208] p 4413 N94-37713
VAPOR PHASE EPITAXY
Optical spectroscopy of a nitrogen-hydrogen complex in ZnSe
[DE94-011622] p 4413 N94-37630
VAPOR PHASES
Hypobaric decompression sickness model development. Part 1: Diffusion of inert gas from a viscoelastic fluid (blood) into an expanding gas phase
[AD-A280298] p 4481 N94-37124
Numerical analysis of an impinging jet reactor for the CVD and gas-phase nucleation of titania
[NASA-TM-106619] p 4431 N94-37254
Photodissociation and spectroscopy of gas phase bimetallic clusters
[DE94-012607] p 4419 N94-37438
VAPOR TRAPS
Spontaneous force optical traps
[AD-A280574] p 4514 N94-37041
VAPORIZING
Supersonic bare metal cluster beams
[DE94-010790] p 4532 N94-36454
VAPORS
A-TOUGH: A multimedia fluid-flow/energy-transport model for fully-coupled atmospheric-subsurface interactions
[DE94-004304] p 4472 N94-36739
VARIABILITY
Variability of the California Current System off Point Sur, California from April 1988 to December 1990
[AD-A278579] p 4476 N94-36985
The role of horizontal variability in air-sea interaction
[AD-A280561] p 4476 N94-37047
VARNISHES
Atomic oxygen treatment for non-contact removal of organic protective coatings from painting surfaces
[NASA-TM-106650] p 4421 N94-36952
VASOCONSTRICTION
Homeostatic responses to prolonged cold exposure: Human cold acclimatization
[AD-A280234] p 4481 N94-37136
VECTOR PROCESSING (COMPUTERS)
A-TOUGH: A multimedia fluid-flow/energy-transport model for fully-coupled atmospheric-subsurface interactions
[DE94-004304] p 4472 N94-36739
VECTOR QUANTIZATION
Studies on image compression and image reconstruction
[NASA-CR-196304] p 4433 N94-36810
VEGETATION
Response of plants and ecosystems to CO2 and climate change
[DE94-011583] p 4466 N94-37376
Surface-layer response over shrub-steppe canopy during springtime
[DE94-011235] p 4468 N94-37624
VEGETATION GROWTH
Response of plants and ecosystems to CO2 and climate change
[DE94-011583] p 4466 N94-37376
VELOCITY DISTRIBUTION
Fast electron generation and transport in a turbulent, magnetized plasma
[DE94-012986] p 4531 N94-37730
VELOCITY MEASUREMENT
An automated method for Low Level Windshear Alert System (LLWAS) data quality analysis
[AD-A280313] p 4472 N94-37126
VENTING
Cryogenic fluid management technologies for space transportation. Zero G thermodynamic vent system
[NASA-CR-193981] p 4430 N94-36806
VENTS
Vent processes during the 1912 eruption at Novarupta, Katmai National Park, Alaska
[DE94-010740] p 4468 N94-36451
VERTICAL TAKEOFF AIRCRAFT
Analysis of vertiport studies funded by the Airport Improvement Program (AIP)
[SCT-93RR-21] p 4390 N94-37424
VERY HIGH FREQUENCIES
TIPC user manual
[DE94-004470] p 4432 N94-36443
VHF adaptive antenna development task
[AD-A280320] p 4434 N94-37127
VESTIBULES
Relation of motion sickness susceptibility to vestibular and behavioral measures of orientation
[NASA-CR-196121] p 4480 N94-37005
Attenuating the disorienting effects of head movement during whole-body rotation using a visual reference: Further tests of a predictive hypothesis p 4482 N94-37276
The use of a tactile interface to convey position and motion perceptions p 4486 N94-37281
VIBRATION
Dipole forbidden vibrational modes for NO and CO on Cu observed in the far IR
[DE94-003199] p 4408 N94-36559
Vibration signature analysis of a faulted gear transmission system
[NASA-TM-106623] p 4450 N94-36953
VIBRATION DAMPING
Correlation of analytical and experimental hot structure vibration results
[NASA-TM-104269] p 4386 N94-36644
A PDE-based methodology for modeling, parameter estimation and feedback control in structural and structural acoustic systems
[NASA-CR-194928] p 4500 N94-36924
Vibration suppression with approximate finite dimensional compensators for distributed systems: Computational methods and experimental results
[NASA-CR-194927] p 4500 N94-36928
Multirate flutter suppression system design for the Benchmark Active Controls Technology Wing
[NASA-CR-196112] p 4388 N94-36965
Modeling and control of intelligent flexible structures
[AD-A280478] p 4396 N94-37349
VIBRATION EFFECTS
Characterization of spacecraft and environmental disturbances on a SmallSat
[NASA-CR-194915] p 4396 N94-36990
VIBRATION MODE
Correlation of analytical and experimental hot structure vibration results
[NASA-TM-104269] p 4386 N94-36644
The dynamics of hydrogen atoms dissolved in Zr Cr2 alloy
[DE94-618756] p 4520 N94-37652
VIBRATION TESTS
An enhancement to the NA4 gear vibration diagnostic parameter
[NASA-TM-106553] p 4452 N94-37521
VIBRATIONAL SPECTRA
Diosmacycloalkanes as models for the formation of hydrocarbons from surface methylenes
[DE94-011211] p 4413 N94-37754
VIBRATIONAL STATES
Infrared spectroscopy of organic free radicals related to combustion processes
[DE94-012481] p 4409 N94-37168
Optical spectroscopy of a nitrogen-hydrogen complex in ZnSe
[DE94-011622] p 4413 N94-37630
VIDEO COMPRESSION
Studies on image compression and image reconstruction
[NASA-CR-196304] p 4433 N94-36810
Portable color multimedia training systems based on monochrome laptop computers (CBT-in-a-briefcase), with spinoff implications for video uplink and downlink in spaceflight operations
[NASA-TM-108460] p 4496 N94-37556
VIDEO DATA
Evaluation of a tool for producing and presenting interactive videodisc job aids
[AD-A278599] p 4432 N94-36473
VIDEO SIGNALS
Portable color multimedia training systems based on monochrome laptop computers (CBT-in-a-briefcase), with spinoff implications for video uplink and downlink in spaceflight operations
[NASA-TM-108460] p 4496 N94-37556
VIRTUAL REALITY
Virtual Interfaces: Research and Applications
[AGARD-CP-541] p 4482 N94-37261
Profile analysis of after-effects experienced during exposure to several virtual reality environments
p 4482 N94-37263
On the feasibility of virtual environments in medicine
p 4483 N94-37264
Immersive virtual environments as trainer: System design from a cognitive stance p 4484 N94-37267
Creation of a virtual world to study human spatial perception during sustained acceleration
p 4484 N94-37268
The DRA Virtual Cockpit Research Program
p 4484 N94-37269
Virtual reality evolution or revolution
p 4484 N94-37270
Manual tracking performance using a virtual hand controller: A comparison study p 4484 N94-37271
A comparison of two examples of magnetic tracker systems p 4485 N94-37275
Some side-effects of immersion virtual reality
p 4482 N94-37277
Low cost software-based rendering and stereoscopic interfaces for teleoperation and virtual reality
p 4486 N94-37279
VIRUSES
Recombinant protein production and insect cell culture and process
[NASA-CASE-MSC-22336-1] p 4478 N94-36751
VISCOELASTICITY
Hypobaric decompression sickness model development. Part 1: Diffusion of inert gas from a viscoelastic fluid (blood) into an expanding gas phase
[AD-A280298] p 4481 N94-37124
Some considerations for modeling the creep behavior of composite materials
[DE94-012112] p 4404 N94-37205
VISCOPLASTICITY
Micromechanical modeling of damage growth in titanium based metal-matrix composites p 4402 N94-36664
VISCOSITY
United States Air Force Summer Research Program, 1993. Volume 6: Arnold Engineering Development Center, Frank J. Seiler Research Laboratory and Wilford Hall Medical Center
[AD-A278697] p 4551 N94-36982
Evaluation of the EHL film thickness and extreme pressure additives on gear surface fatigue life
[NASA-TM-106663] p 4451 N94-37319
Momentum-energy transport from turbulence driven by parallel flow shear
[DE94-012765] p 4443 N94-37362

Coupled Marangoni-Benard/Rayleigh-Benard instability with temperature dependent viscosity
[NASA-TM-106646] p 4444 N94-37507

VISIBILITY
Composite helicopter accident profiles: Deficient crew/aircraft performance
[SCT-90RR-46] p 4385 N94-37604

VISUAL ACCOMMODATION
Visual accommodation to virtual image displays when knowledge of object distance conflicts with optical distance p 4485 N94-37278

VISUAL CONTROL
Interactive large screen: A multi-mode dialogue tool for future cockpits p 4484 N94-37266
A non-intrusive way to measure point-of-gaze p 4484 N94-37272
Operator gaze position control interfaces: Investigation of psychophysical and operational parameters p 4485 N94-37273
Gaze orientation under G(z)-load. Methodological aspects: Preliminary results p 4485 N94-37274
A comparison of two examples of magnetic tracker systems p 4485 N94-37275
Night vision goggles in Emergency Medical Service (EMS) helicopters
[SCT-93RR-22] p 4487 N94-37742

VISUAL PERCEPTION
Efficient contact determination between geometric models
[AD-A280244] p 4494 N94-37120
Creation of a virtual world to study human spatial perception during sustained acceleration p 4484 N94-37268
The DRA Virtual Cockpit Research Program p 4484 N94-37269

VISUAL STIMULI
The use of a tactile interface to convey position and motion perceptions p 4486 N94-37281

VISUAL TASKS
Behavioral performance in monkeys exposed to TEMPO high-peak-power microwave pulses at 3 GHz
[AD-A280551] p 4478 N94-37045
Assessment of night vision goggle workload: Flight test engineer's guide
[SCT-91RR-45] p 4487 N94-37743

VITERBI DECODERS
Error control techniques for satellite and space communications
[NASA-CR-196302] p 4433 N94-36931

VOICE COMMUNICATION
The Canadian network for the advancement of research, industry and education (CANARIE) p 4543 N94-37336

VOICE CONTROL
Interactive large screen: A multi-mode dialogue tool for future cockpits p 4484 N94-37266

VOICE DATA PROCESSING
Noise reduction for speech enhancement using non-linear wavelet processing
[AD-A280469] p 4434 N94-37141

VOLATILITY
Molecular beam surface analysis
[DE94-010773] p 4406 N94-36453

VOLCANOES
Vent processes during the 1912 eruption at Novarupta, Katmai National Park, Alaska
[DE94-010740] p 4468 N94-36451

VOLTERRA EQUATIONS
Multiquadric collocation methods in the numerical solution of Volterra integral equations with weakly singular kernels
[DE94-013000] p 4505 N94-37497

VOMITING
Profile analysis of after-effects experienced during exposure to several virtual reality environments p 4482 N94-37263

VON KARMAN EQUATION
Finite element approximation of an optimal control problem for the von Karman equations
[NASA-CR-194955] p 4505 N94-37540

VORTEX GENERATORS
Mars vertical axis wind machines: The design of a tornado vortex machine for use on Mars
[NASA-CR-196144] p 4462 N94-36823

VORTICES
Influences of flame-vortex interactions on formation of oxides of nitrogen in curved methane-air diffusion flamelets
[DE94-005105] p 4409 N94-37221

W

WAKES
Towards enhancing and delaying disturbances in free shear flows
[NASA-CR-194945] p 4445 N94-37606

WALL JETS
Evolution of turbulent fields in explosions
[DE94-010405] p 4444 N94-37390

WARFARE
Profile analysis of after-effects experienced during exposure to several virtual reality environments p 4482 N94-37263

WARNING SYSTEMS
An automated method for Low Level Windshear Alert System (LLWAS) data quality analysis
[AD-A280313] p 4472 N94-37126
Distributed detection theory and data fusion
[AD-A280410] p 4434 N94-37183
Terminal Doppler Weather Radar (TDWR) build 5 Test and Evaluation Master Plan (TEMP)
[AD-A280426] p 4434 N94-37218
Aircraft command in emergency situations prototype development users manual
[DOT/FAA/CT-94/24] p 4385 N94-37706

WASHINGTON
Analysis of deep seismic reflection and other data from the Southern Washington Cascades
[DE94-004075] p 4470 N94-37489

WASTE TREATMENT
Activities of the Chemical Technology Division
[DE94-013050] p 4410 N94-37357
The integrated performance evaluation program quality assurance guidance in support of EM environmental sampling and analysis activities
[DE94-013043] p 4468 N94-37731

WASTE UTILIZATION
Structural composite construction materials manufactured from municipal solid waste
[AD-A280635] p 4403 N94-36730
SIHTI: Energy and environmental technology
[DE94-763290] p 4464 N94-37007
Estimates of US biomass energy consumption 1992
[DE94-011458] p 4463 N94-37567

WATER
United States Air Force Summer Research Program, 1993. Volume 16: Arnold Engineering Development Center, Frank J. Seiler Research Laboratory and Wilford Hall Medical Center
[AD-A278658] p 4550 N94-36978
Investigation of ultrasonic surface wave interaction with porous saturated rocks
[DE94-013378] p 4469 N94-37177

WATER FLOW
Numerical simulation of nocturnal drainage flows in an idealized valley-tributary system
[DE94-011684] p 4472 N94-37115

WATER IMMERSION
Evaluation of flame-sprayed polymer coatings for civil works navigation structures
[AD-A280507] p 4422 N94-37104

WATER QUALITY
Determination of copper in tap water using solid-phase spectrophotometry
[NASA-TM-106480] p 4408 N94-36537

WATER TREATMENT
Bibliography of work on the photocatalytic removal of hazardous compounds from water and air
[DE94-006906] p 4467 N94-37405

WATER VAPOR
Two-channel microwave radiometer for observations of total column precipitable water vapor and cloud liquid water path
[DE94-007480] p 4471 N94-36479
Measurements and modeling of the effect of convective clouds on the upper tropospheric moisture budget
[NASA-TM-109894] p 4473 N94-37371
Tropospheric radiative forcing of CH4
[DE94-011628] p 4468 N94-37631

WATER WAVES
Index and bulk parameters for frequency-direction spectra measured at CERC Field Research Facility, September 1992 to August 1993
[AD-A280233] p 4476 N94-37135
Index and bulk parameters for frequency-direction spectra measured at CERC Field Research Facility, September 1990 to August 1991
[AD-A280423] p 4476 N94-37216
Index and bulk parameters for frequency-direction spectra measured at CERC Field Research Facility, September 1991 to August 1992
[AD-A280455] p 4477 N94-37229
Airborne ROWS data report for the high resolution experiment, June 1993
[NASA-TM-104609] p 4477 N94-37397

WATERWAYS
Index and bulk parameters for frequency-direction spectra measured at CERC Field Research Facility, September 1990 to August 1991
[AD-A280423] p 4476 N94-37216
Index and bulk parameters for frequency-direction spectra measured at CERC Field Research Facility, September 1991 to August 1992
[AD-A280455] p 4477 N94-37229

WAVE DIFFRACTION
Intensity of waves diffracted from symmetrical profile lamellar gratings
[DE94-611101] p 4433 N94-36753

WAVE DISPERSION
Unstable solitary-wave solutions of the generalized Benjamin-Bona-Mahony equation
[DE94-013302] p 4496 N94-37549
Self-sustained turbulence and L-mode confinement in toroidal plasmas
[DE94-748497] p 4532 N94-37734

WAVE EQUATIONS
Elimination of numerical dispersion in finite-difference modeling and migration by flux-corrected transport
[DE94-004159] p 4510 N94-36551

WAVE FRONT DEFORMATION
Adaptive optics for laser beamforming in the atmosphere p 4393 N94-36621

WAVE FRONTS
Wavefront simulator for evaluating RF communication array signal processors
[AD-D016281] p 4436 N94-37835

WAVE FUNCTIONS
Solving the two-dimensional Schroedinger equation in self-consistent basis
[DE94-621535] p 4504 N94-37174
MCHF calculations of isotope shifts. 1: Program implementation and test runs. 2: Large-scale active space calculations
[DE94-013036] p 4518 N94-37313
The angular and energy distributions of ejected electrons in electron-impact ionization of helium
[DE94-618748] p 4519 N94-37528

WAVE INTERACTION
Investigation of ultrasonic surface wave interaction with porous saturated rocks
[DE94-013378] p 4469 N94-37177

WAVE PROPAGATION
Propagation of radius-tailored laser pulses over extended distances in a uniform plasma
[AD-A280405] p 4528 N94-37182
Final report on spectral broadening by cross-phase modulation in linearly birefringent optical fibers
[DE94-010406] p 4524 N94-37191
Langmuir waves in the electron-positron plasma
[DE94-618779] p 4531 N94-37728

WAVE SCATTERING
Scattering theory for the quantum envelope of a classical system
[DE94-008530] p 4539 N94-36508
Scattering cross section of sound waves by the modal element method
[NASA-TM-106667] p 4510 N94-37308

WAVEGUIDES
Radially combined 30 W, 14-16 GHz amplifier
[DE94-010078] p 4432 N94-36471
A novel transition between rectangular waveguide and layered ridge dielectric waveguide
[NASA-TM-106661] p 4433 N94-36955

WAVELET ANALYSIS
Noise reduction for speech enhancement using non-linear wavelet processing
[AD-A280469] p 4434 N94-37141
Detection of the electrocardiogram P-wave using wavelet analysis
[DE94-010791] p 4481 N94-37197

WEAR RESISTANCE
Robotic weld overlay coatings for erosion control
[DE94-013477] p 4417 N94-37116

WEAR TESTS
Robotic weld overlay coatings for erosion control
[DE94-013477] p 4417 N94-37116

WEATHER FORECASTING
Toward a new National Weather Service: Weather for those who fly p 4472 N94-36947

WEATHER STATIONS
Toward a new National Weather Service: Weather for those who fly p 4472 N94-36947

WEATHERING
Evaluation of flame-sprayed polymer coatings for civil works navigation structures
[AD-A280507] p 4422 N94-37104

WEIBULL DENSITY FUNCTIONS
Statistical characterization of rare events p 4454 N94-37327
Statistical scaling relationships and size effects in the strength and creep rupture of fibrous composites p 4460 N94-37809

WEIGHT REDUCTION
Carbon-carbon heat pipe testing and evaluation
[NASA-TM-106630] p 4405 N94-37318

WELD STRENGTH
Mitigation of harmful effects of welds in zirconium alloy components
[DE94-619033] p 4414 N94-36543
WELDABILITY
Examination of weldability of Ni-Cr-W superalloys
[DE94-719014] p 4418 N94-37385
Tensile strength of simulated and welded butt joints in W-Cu composite sheet
[NASA-TM-4584] p 4405 N94-37460
WELDED JOINTS
Mitigation of harmful effects of welds in zirconium alloy components
[DE94-619033] p 4414 N94-36543
Examination of weldability of Ni-Cr-W superalloys
[DE94-719014] p 4418 N94-37385
Tensile strength of simulated and welded butt joints in W-Cu composite sheet
[NASA-TM-4584] p 4405 N94-37460
Residual stresses in a multi-pass weld in an austenitic stainless steel plate before and after thermal stress relief
[DE94-013278] p 4420 N94-37548
WELDING
Vent processes during the 1912 eruption at Novarupta, Katmai National Park, Alaska
[DE94-010740] p 4468 N94-36451
Examination of weldability of Ni-Cr-W superalloys
[DE94-719014] p 4418 N94-37385
WETTING
Investigation of ultrasonic surface wave interaction with porous saturated rocks
[DE94-013378] p 4469 N94-37177
WIDE ANGLE LENSES
Hubble Space Telescope Wide Field and Planetary Camera 2 instrument handbook, version 2.0
[NASA-CR-189368] p 4547 N94-36918
WIDEBAND COMMUNICATION
KONRAD: Wide band digital HF receiver
[PB94-184686] p 4435 N94-37813
WIDTH
Determination of the upsilon(1s) leptonic width
[DE94-618534] p 4516 N94-37096
WIND DIRECTION
Short-tower sigma(theta) measurements in the Colorado Plateaus region
[DE94-007478] p 4463 N94-36478
WIND EFFECTS
Numerical simulation of nocturna ainage flows in an idealized valley-tributary system
[DE94-011684] p 4472 N94-37115
Index and bulk parameters for frequency-direction spectra measured at CERC Field Research Facility, September 1992 to August 1993
[AD-A280233] p 4476 N94-37135
WIND MEASUREMENT
An automated method for Low Level Windshear Alert System (LLWAS) data quality analysis
[AD-A280313] p 4472 N94-37126
Terminal Doppler Weather Radar (TDWR) build 5 Test and Evaluation Master Plan (TEMP)
[AD-A280426] p 4434 N94-37218
WIND SHEAR
An automated method for Low Level Windshear Alert System (LLWAS) data quality analysis
[AD-A280313] p 4472 N94-37126
Terminal Doppler Weather Radar (TDWR) build 5 Test and Evaluation Master Plan (TEMP)
[AD-A280426] p 4434 N94-37218
WIND TUNNEL APPARATUS
Strength evaluation of socket joints
[NASA-CR-4608] p 4389 N94-37259
WIND TUNNEL CALIBRATION
Experimental uncertainty and drag measurements in the national transonic facility
[NASA-CR-4600] p 4389 N94-36945
WIND TUNNEL MODELS
NASA Lewis wind tunnel model systems criteria
[NASA-TM-106565] p 4390 N94-37522
Stability analysis of an F/A-18 E/F cable mount m odel
[NASA-TM-108989] p 4386 N94-37636
WIND TUNNEL STABILITY TESTS
Aerodynamic characteristics of the National Launch System (NLS) 1 1/2 stage launch vehicle
[NASA-TP-3488] p 4384 N94-37577
WIND TUNNEL TESTS
A shadowgraph study of Space Transportation System (STS): The Space Shuttle Launch Vehicle (SSLV)
[NASA-RP-1341] p 4382 N94-36741
Experimental uncertainty and drag measurements in the national transonic facility
[NASA-CR-4600] p 4389 N94-36945
Pressure-sensing performance of upright cylinders in a Mach 10 boundary-layer
[NASA-TM-4633] p 4383 N94-37395
Subsonic aerodynamic characteristic of semispan commercial transport model with wing-mounted advanced ducted propeller operating in reverse thrust --- conducted in the Langley 14 by 22 foot subsonic wind tunnel
[NASA-TP-3427] p 4384 N94-37505
NASA Lewis wind tunnel model systems criteria
[NASA-TM-106565] p 4390 N94-37522
Aerodynamic characteristics of the National Launch System (NLS) 1 1/2 stage launch vehicle
[NASA-TP-3488] p 4384 N94-37577
Stability analysis of an F/A-18 E/F cable mount m odel
[NASA-TM-108989] p 4386 N94-37636
WIND TURBINES
Mars vertical axis wind machines. The design of a Darreus and a Giromill for use on Mars
[NASA-CR-196143] p 4462 N94-36807
Mars vertical axis wind machines: The design of a tornado vortex machine for use on Mars
[NASA-CR-196144] p 4462 N94-36823
Fatigue case study and loading spectra for wind turbines
[DE94-010798] p 4457 N94-37622
WIND VELOCITY
An automated method for Low Level Windshear Alert System (LLWAS) data quality analysis
[AD-A280313] p 4472 N94-37126
WINDMILLS (WINDPOWERED MACHINES)
Mars vertical axis wind machines. The design of a Darreus and a Giromill for use on Mars
[NASA-CR-196143] p 4462 N94-36807
Mars vertical axis wind machines: The design of a tornado vortex machine for use on Mars
[NASA-CR-196144] p 4462 N94-36823
WINDPOWER UTILIZATION
Mars vertical axis wind machines. The design of a Darreus and a Giromill for use on Mars
[NASA-CR-196143] p 4462 N94-36807
Mars vertical axis wind machines: The design of a tornado vortex machine for use on Mars
[NASA-CR-196144] p 4462 N94-36823
1993 JSES (Japan Solar Energy Society)/JWEA (Japa n Wind Energy Association) Joint Conference and 1993 Japan-Korea Joint Conference on Solar Energy
[DE94-767725] p 4462 N94-37418
Fatigue case study and loading spectra for wind turbines
[DE94-010798] p 4457 N94-37622
WINDPOWERED GENERATORS
Mars vertical axis wind machines. The design of a Darreus and a Giromill for use on Mars
[NASA-CR-196143] p 4462 N94-36807
Mars vertical axis wind machines: The design of a tornado vortex machine for use on Mars
[NASA-CR-196144] p 4462 N94-36823
WINDSHIELDS
Canopy breaking device
[AD-D016294] p 4385 N94-37767
WING OSCILLATIONS
Multirate flutter suppression system design for the Benchmark Active Controls Technology Wing
[NASA-CR-196112] p 4388 N94-36965
WINTER
Cooling of the West Spitzbergen Current: Wintertime observations west of Svalbard
[AD-A280648] p 4475 N94-36762
WOOD
Estimates of US biomass energy consumption 1992
[DE94-011458] p 4463 N94-37567
WORDS (LANGUAGE)
A graphic view of Geometric Dimensioning and Tolerancing
[DE94-011478] p 4435 N94-37736
WORKING FLUIDS
Refrigeration and Air-Conditioning Technology Workshop
[DE94-010813] p 4431 N94-37452
WORKLOADS (PSYCHOPHYSIOLOGY)
Human factors for flight deck certification personnel
[AD-A280477] p 4487 N94-37347
Assessment of night vision goggle workload: Flight test engineer's guide
[SCT-91RR-45] p 4487 N94-37743
WORKSTATIONS
A comparison of queueing, cluster and distributed computing systems
[NASA-TM-109025] p 4497 N94-36932
WOVEN COMPOSITES
Development of nondestructive evaluation methods and prediction of effects of flaws on the fracture behavior of structural ceramics
[DE94-012466] p 4425 N94-37423

X

X RAY ANALYSIS
AEM and AES of radiation-induced segregation in proton-irradiated stainless steels
[DE94-012734] p 4418 N94-37398
Scanning x-ray diffraction: A technique with high compositional resolution for studying phase formation in co-deposited thin films
[DE94-011496] p 4420 N94-37516
X RAY ASTRONOMY
The BL LAC phenomenon: X-ray observations of transition objects and determination of the x-ray spectrum of a complete sample of flat-spectrum radio sources
[NASA-CR-195951] p 4546 N94-36688
X RAY DIFFRACTION
Processing, packaging, and characterization of electroceramic materials for phased array antennas
[AD-A280251] p 4432 N94-36743
Pair correlations in crystalline solid solutions
[DE94-012319] p 4535 N94-37212
X-ray diffraction studies of evaporated gold thin films deposited on aluminum nitride substates
[AD-A280454] p 4536 N94-37228
Scanning x-ray diffraction: A technique with high compositional resolution for studying phase formation in co-deposited thin films
[DE94-011496] p 4420 N94-37516
X RAY LASERS
Ionization balance and gain calculations for neon-like selenium x-ray laser plasmas
[DE94-012590] p 4530 N94-37437
X RAY SCATTERING
Small-angle x ray scattering studies of microvoids in amorphous-silicon-based semiconductors
[DE94-006931] p 4533 N94-36745
XAFS-like structure of resonant Raman scattering
[DE94-618410] p 4517 N94-37171
X RAY SOURCES
Coherent multiple-foil x-ray transition radiation
[DE93-040831] p 4525 N94-37486
X RAY SPECTRA
The BL LAC phenomenon: X-ray observations of transition objects and determination of the x-ray spectrum of a complete sample of flat-spectrum radio sources
[NASA-CR-195951] p 4546 N94-36688
On the shape of x ray spectra excited by heavy ions
[DE94-618747] p 4519 N94-37651
X RAY SPECTROSCOPY
Microstructure and chemistry of MgO- and CoO-doped nickel-titanate spinels
[DE94-012741] p 4537 N94-37382
Preliminary soft x ray studies of beta-SiC
[DE94-013023] p 4537 N94-37498
X RAYS
Guiding hard x rays with glass polycapillary fiber
[DE94-004949] p 4525 N94-37258
Preliminary soft x ray studies of beta-SiC
[DE94-013023] p 4537 N94-37498
Advanced laser driver for soft x-ray projection lithography
[DE94-011643] p 4449 N94-37722
X-31 AIRCRAFT
Controlling forebody asymmetries in flight: Experience with boundary layer transition strips
[NASA-TM-4595] p 4383 N94-36944
XENON
Characteristics of ions emitted from high-current hollow cathodes
[NASA-CR-195372] p 4398 N94-37764
XENON CHLORIDE LASERS
Metal-carbon nanostructures
[DE94-009177] p 4400 N94-36509

Y

YAG LASERS
Greater than 100 watt average power at 0.53 micron with 25 ns, 2.5 kHz repetition rate pulses from a single power oscillator
[DE94-011641] p 4447 N94-37114
High average power pulsed phase conjugate laser with birefringence correction
[DE94-012062] p 4447 N94-37160
Holmium quasi-two level laser
[AD-D016302] p 4449 N94-37772
Intracavity-pumped 2.1 micrometer Ho(3+):YAGl aser
[AD-D016308] p 4449 N94-37777
YAWING MOMENTS
Controlling forebody asymmetries in flight: Experience with boundary layer transition strips
[NASA-TM-4595] p 4383 N94-36944

YBCO SUPERCONDUCTORS
Activities of the Tandem Accelerator Center, University of Tsukuba
[DE94-748687] p 4522 N94-37237
Melt-processing of Y-Ba-Cu-O superconductors for improved levitation
[DE94-011503] p 4537 N94-37377
Permanent superconducting magnets for space applications
[NASA-CR-196293] p 4439 N94-37634
YIELD STRENGTH
Mechanical performance of austempered ductile iron
[AD-A280452] p 4420 N94-37758

Z

ZEOLITES
Direct catalytic decomposition of nitric oxide
[DE94-005025] p 4407 N94-36475
Thermodynamics of minerals stable near the Earth's surface
[DE94-012479] p 4539 N94-37094
Photochemistry without protons. Radical cation chemistry in zeolites
[DE94-012631] p 4412 N94-37439
ZETA PINCH
D-D fusion experiments using fast z-pinches
[DE94-010090] p 4526 N94-36448
Preradiation studies for non-thermal Z-pinch wire load experiments on Saturn
[DE94-013459] p 4527 N94-37072
ZINC SELENIDES
Investigation of polycrystalline thin-film CuInSe2 solar cells based on ZnSe windows
[DE94-006936] p 4462 N94-37381
Optical spectroscopy of a nitrogen-hydrogen complex in ZnSe
[DE94-011622] p 4413 N94-37630
ZIRCONIUM
Characterization and processing of sintered products from nano-crystalline powders generated by the RTDS method
[DE94-004765] p 4415 N94-36553
ZIRCONIUM ALLOYS
Mitigation of harmful effects of welds in zirconium alloy components
[DE94-619033] p 4414 N94-36543
Modelling irradiation creep of zirconium alloys
[DE94-619055] p 4414 N94-36544
Precipitation in Zr-2.5 Nb enhanced by proton irradiation
[DE94-619056] p 4415 N94-36563
The dynamics of hydrogen atoms dissolved in Zr Cr2 alloy
[DE94-618756] p 4520 N94-37652
ZIRCONIUM OXIDES
Superacid catalysis of light hydrocarbon conversion
[DE94-011132] p 4411 N94-37431

Typical Personal Author Index Listing

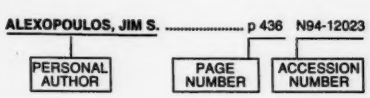

Listings in this index are arranged alphabetically by personal author. The page number helps you locate the citation in the abstract section. The accession number denotes the number by which the citation is identified.

A

ABRAMOV, V. V. ..... p 4511 N94-36504
ACOSTA, RAMON D. ..... p 4494 N94-37123
ADAMS, MARY S. ..... p 4382 N94-36942
p 4383 N94-36950
ADAMS, STUART J. ..... p 4498 N94-37500
ADAPALLI, SRIDHAR ..... p 4484 N94-37271
ADATI, K. ..... p 4530 N94-37384
ADDIS, R. P. ..... p 4465 N94-37093
ADELMAN, HOWARD M. ..... p 4386 N94-37256
ADIBNAZARI, SAEED ..... p 4456 N94-37125
AFANASEV, L. G. ..... p 4515 N94-37075
AGER, J. W., III ..... p 4413 N94-37630
AGGARWAL, ISHWAR D. ..... p 4526 N94-37774
AGRAWAL, GHASI R. ..... p 4438 N94-37196
AIHARA, H. ..... p 4513 N94-36695
AJMANI, KUMUD ..... p 4502 N94-36647
AKIBA, MASATO ..... p 4530 N94-37415
AKIYAMA, R. ..... p 4530 N94-37384
AL-MOHAMAD, ALI ..... p 4415 N94-36564
ALBERCA, LUIS F. ..... p 4469 N94-37215
ALBRECHT, G. F. ..... p 4447 N94-37114
p 4449 N94-37737
ALBROW, M. G. ..... p 4513 N94-36558
ALEXANDER, K. B. ..... p 4418 N94-37399
p 4538 N94-37570
ALEXOPOULOS, T. ..... p 4515 N94-37067
ALEYNIKOV, A. N. ..... p 4526 N94-36536
ALGER, T. W. ..... p 4448 N94-37244
ALHORN, DEAN C. ..... p 4509 N94-36782
ALLRED, R. E. ..... p 4411 N94-37365
ALLRED, RONALD E. ..... p 4409 N94-37161
ALLWINE, K. J. ..... p 4463 N94-36478
ALTAMIRANO, MARK M. ..... p 4525 N94-37350
ALTYNOV, V. A. ..... p 4519 N94-37651
AMBUR, DAMODAR R. ..... p 4389 N94-36826
AMEEN, S. ..... p 4475 N94-37790
AMIRKHANOV, I. V. ..... p 4504 N94-37175
AMOS, ANTHONY K. ..... p 4397 N94-37351
ANANT, KANWALDIP S. ..... p 4481 N94-37197
ANDERSON, A. M. ..... p 4482 N94-37276
ANDERSON, A. T. ..... p 4448 N94-37244
ANDERSON, DONALD M. ..... p 4475 N94-36761
ANDERSON, I. M. ..... p 4537 N94-37382
p 4537 N94-37400
ANDERSON, J. ..... p 4523 N94-37547
ANDERSON, L. E. ..... p 4480 N94-37625
ANDERSON, M. U. ..... p 4428 N94-37052
ANDERSON, S. ..... p 4410 N94-37296
ANDRAS, MARIA T. ..... p 4399 N94-37315
ANDREWS, ANGELA ..... p 4478 N94-36751
ANDRISANI, DOMINICK, II ..... p 4388 N94-36820
ANFIMOV, D. S. ..... p 4550 N94-37293
ANGELI, ROBERT J. ..... p 4452 N94-37766
ANNIS, CHARLES ..... p 4454 N94-37327
ANSCHUETZ, ROBERT R., II ..... p 4390 N94-37755
p 4391 N94-37756
ANTOLAK, A. J. ..... p 4517 N94-37210
ANTONELIS, T. ..... p 4441 N94-37851
ANTONSEN, T. M., JR. ..... p 4448 N94-37368
ANTUNEZ, E. ..... p 4443 N94-37050
APPELHANS, A. D. ..... p 4406 N94-36453
APPLIN, ZACHARY T. ..... p 4384 N94-37505
ARAJ, A. ..... p 4433 N94-36810
ARAKI, MASANORI ..... p 4530 N94-37415
ARBUZOV, A. B. ..... p 4515 N94-37066
p 4516 N94-37099
ARIMOTO, H. ..... p 4530 N94-37384
ARMITAGE, J. C. ..... p 4426 N94-37714
ARNOLD, P. A. ..... p 4448 N94-37244
ARNOLD, STEVEN M. ..... p 4455 N94-36561
ARNOTT, W. PATRICK ..... p 4431 N94-37090
ARZIGIAN, JAMES S. ..... p 4448 N94-37198
ASHBY, M. R. ..... p 4502 N94-37784
ASHIZAWA, MOTO ..... p 4422 N94-36968
ASPIN, W. M. ..... p 4394 N94-36624
ATAGI, L. M. ..... p 4425 N94-37317
ATEN, LAURIE A. ..... p 4478 N94-36765
ATMADJA, JULIANA ..... p 4476 N94-37216
ATWOOD, C. L. ..... p 4430 N94-36447
ATZMON, M. ..... p 4418 N94-37398
AUCIELLO, O. ..... p 4517 N94-37249
AUERNHEIMER, BRENT ..... p 4491 N94-36495
AUSTIN, R. H. ..... p 4449 N94-37733
AUSTIN, ROBERT D. ..... p 4493 N94-36974
AVALANI, B. ..... p 4496 N94-37551
AVALLE, M. ..... p 4395 N94-36632
AZMY, Y. Y. ..... p 4498 N94-37419
AZUMI, M. ..... p 4532 N94-37734

B

BABIKYAN, CAROL A. ..... p 4497 N94-36962
p 4498 N94-37500
BADER, S. D. ..... p 4509 N94-37517
BAER, M. R. ..... p 4400 N94-36456
p 4428 N94-37052
p 4428 N94-37201
BAI, G. R. ..... p 4535 N94-37192
BAILEY, JOHN ..... p 4492 N94-36501
BAILEY, S. ..... p 4477 N94-37397
BAJAJ, R. ..... p 4416 N94-37080
BAJER, V. N. ..... p 4514 N94-37065
BAJIS, KATIE ..... p 4541 N94-36846
BAKER, A. J. ..... p 4493 N94-36914
p 4493 N94-36922
BAKER, J. E. ..... p 4500 N94-37083
BAKER, KEVIN ..... p 4486 N94-36838
BAKUCKAS, J. G., JR. ..... p 4405 N94-37320
BALACHANDRAN, U. ..... p 4438 N94-37111
p 4537 N94-37377
BALDIN, B. YU. ..... p 4511 N94-36504
BALDWIN, G. T. ..... p 4526 N94-36448
BALL, RICHARD D. ..... p 4457 N94-37704
BALLINGALL, J. M. ..... p 4533 N94-36755
BALTRUSAITIS, R. M. ..... p 4522 N94-37303
BANKS, BRUCE A. ..... p 4421 N94-36952
BANKS, H. T. ..... p 4500 N94-36924
p 4500 N94-36928
p 4503 N94-36991
BANNIKOV, A. V. ..... p 4512 N94-36523
BARBIER, B. ..... p 4484 N94-37266
BARFKNECHT, ANDREW ..... p 4534 N94-37036
BARGER, RAYMOND L. ..... p 4382 N94-36942
p 4383 N94-36950
BARKER, L. KEITH ..... p 4501 N94-37589
BARKER, LINDA ..... p 4491 N94-36494
BARNABAS, M. V. ..... p 4412 N94-37439
BARNABAS, VIJAY ..... p 4396 N94-37257
BARNES, C. W. ..... p 4527 N94-37101
BARNES, D. C. ..... p 4529 N94-37316
BARRETT, C. ..... p 4424 N94-37227
BARRON, ANDREW ..... p 4399 N94-37315
BARRON, ANDREW R. ..... p 4399 N94-37106
p 4399 N94-37650
BARRY, RANDALL K. ..... p 4542 N94-36856
BARTHOLOMEW, JOHN W. ..... p 4409 N94-37161
BARTOLOTTA, P. A. ..... p 4403 N94-36668
BARU, S. E. ..... p 4516 N94-37096
BASILI, VICTOR R. ..... p 4489 N94-36485
BASORE, P. A. ..... p 4462 N94-37189
BATALLA, E. ..... p 4423 N94-37147
BATEMAN, J. E. ..... p 4445 N94-36531
BATES, F. ..... p 4478 N94-37045
BATES, J. K. ..... p 4411 N94-37380
BATES, T. ..... p 4468 N94-36451
BATHKE, C. G. ..... p 4528 N94-37292
BATILL, STEPHEN M. ..... p 4389 N94-36945
BATTLES, J. E. ..... p 4410 N94-37357
BAUGHCUM, STEVE ..... p 4465 N94-37155
BAUGHCUM, STEVEN L. ..... p 4467 N94-37607
BAUMEISTER, KENNETH J. ..... p 4510 N94-37308
BAUR, U. ..... p 4512 N94-36526
BEACH, R. J. ..... p 4447 N94-37114
p 4449 N94-37722
BEARD, JAMES ..... p 4392 N94-37026
BEDELL, K. S. ..... p 4534 N94-37057
p 4438 N94-37295
BEGIN, FRANCOIS ..... p 4395 N94-36634
BEHRENS, R., JR. ..... p 4429 N94-37413
BELDICA, C. ..... p 4459 N94-37804
BELFORTE, S. ..... p 4511 N94-36463
BELIAN, R. D. ..... p 4549 N94-37668
BELL, J. B. ..... p 4444 N94-37390
BELSER, F. C. ..... p 4439 N94-37306
BENCH, G. S. ..... p 4517 N94-37210
BENDER, SUSAN F. A. ..... p 4389 N94-37159
p 4424 N94-37204
BENGTSON, R. D. ..... p 4443 N94-37362
BENLLOCH, J. M. ..... p 4511 N94-36459
BENNETT, C. L. ..... p 4467 N94-37428
BENNETT, R. ..... p 4507 N94-37564
BENO, M. A. ..... p 4420 N94-37516
BENTLEY, J. ..... p 4417 N94-37304
p 4525 N94-37374
p 4537 N94-37382
p 4537 N94-37400
BENTON, E. R. ..... p 4416 N94-36993
BENTON, E. V. ..... p 4416 N94-36993
BERARDO, STEPHEN V. ..... p 4390 N94-37424
BERCAW, ROBERT W. ..... p 4398 N94-36951
BERG, D. ..... p 4523 N94-37547
BERG, MARTIN C. ..... p 4388 N94-36965
BERGMAN, KENNETH H. ..... p 4461 N94-36827
BERGMANN, J. W. ..... p 4455 N94-37331
BERMAN, E. ..... p 4547 N94-37555
p 4547 N94-37667
BERN, M. ..... p 4505 N94-37620
BERRY, G. F. ..... p 4465 N94-37100
BERRY, JOHN D. ..... p 4383 N94-36966
BICKFORD, RANDALL L. ..... p 4403 N94-36730
BIDWELL, S. W. ..... p 4475 N94-37790
BILLINGE, S. J. L. ..... p 4536 N94-37291
BILTOFT, P. ..... p 4523 N94-36693
BIRMAN, VICTOR ..... p 4403 N94-36956
BIRN, J. ..... p 4471 N94-37701
BISCHOF, C. ..... p 4505 N94-37518
BISCHOF, C. H. ..... p 4504 N94-37246
BISHOP, A. R. ..... p 4502 N94-36685
BISSON, S. E. ..... p 4473 N94-37371
BITTNER, T. ..... p 4477 N94-36481
BJORKEN, J. D. ..... p 4515 N94-37084
BJORKMAN, W. S. ..... p 4381 N94-37332
BLACK, D. ..... p 4523 N94-37547
BLAKE, D. M. ..... p 4467 N94-37405
BLANDER, M. ..... p 4548 N94-36759
BLINOV, A. E. ..... p 4516 N94-37096
BLINOV, V. E. ..... p 4516 N94-37096
BLODGETT, MARK P. ..... p 4401 N94-36660
BLOEBAUM, CHRISTINA L. ..... p 4387 N94-37762
BLOHM, M. ..... p 4469 N94-36738
BLOSSER, MAX L. ..... p 4456 N94-37541
BLUMBERG, MAURICE H. ..... p 4491 N94-36493
BODE, ARTHUR P. ..... p 4480 N94-36764
BODINI, ANGELO ..... p 4543 N94-37335
BOEHME, D. R. ..... p 4427 N94-37725
BOENIG, H. J. ..... p 4508 N94-36556
BOESPFLUG, E. P. ..... p 4412 N94-37542
BOGDANOFF, DAVID W. ..... p 4382 N94-36687
BOHM, J. ..... p 4512 N94-36523
BOLDYREV, ALEXANDER I. ..... p 4512 N94-36521
BOLIN, J. T. ..... p 4538 N94-37677

BOLLIG, JOHN p 4462 N94-36807
BOLTON, W. R. p 4465 N94-37154
BONA, J. L. p 4496 N94-37549
BONDI, M. J. p 4381 N94-37332
BOROVSKY, J. E. p 4549 N94-37668
p 4471 N94-37669
BOSSE, E. p 4395 N94-36631
BOTSIS, JOHN p 4459 N94-37804
BOURGAIN, J. p 4506 N94-37853
BOUWENS, J. p 4484 N94-37272
BOVERIE, B. p 4435 N94-37391
BOWDEN, J. W. p 4414 N94-36543
BOWEN, P. p 4402 N94-36665
BOWERS, M. W. p 4447 N94-37160
BOWMAN, RANDY R. p 4419 N94-37503
BOWMAN, STEVEN R. p 4449 N94-37772
BOYD, TIMOTHY J. p 4475 N94-36762
BOYLE, JAMES M. p 4504 N94-37247
BOYLE, L. L. p 4532 N94-36542
BOZZOLO, GUILLERMO p 4419 N94-37459
BRACH, DAVID p 4462 N94-36807
BRADLEY, C. R. p 4411 N94-37380
BRAGDON, CLIFFORD R. p 4390 N94-37424
BRANDENBURG, J. E. p 4396 N94-36445
BRANDRETH, M. p 4544 N94-37340
BRANSON, ROGER p 4391 N94-37756
BRAWN, I. P. p 4436 N94-36532
BREIZMAN, B. N. p 4526 N94-36536
BRENNER, RICHARD p 4499 N94-37583
BRIDGEWATER, A. W. p 4395 N94-36630
BRIGGS, STEVE J. p 4440 N94-37759
BRINDLE, JAMES H. p 4393 N94-36623
BRITCHER, COLIN P. p 4390 N94-37450
BRITTON, C. L., JR. p 4521 N94-37220
BROCK, B. C. p 4435 N94-37391
BROCK, D. p 4408 N94-37091
BROCKMEIER, N. F. p 4422 N94-37055
BRODSKY, S. J. p 4539 N94-37543
BROOKS, THOMAS F. p 4386 N94-36767
BROWN, C. D. p 4495 N94-37430
BROWN, D. E. p 4500 N94-36924
BROWN, G. G. p 4468 N94-37740
BROWN, JAMES H. p 4470 N94-37649
BROWNING, N. D. p 4517 N94-37238
p 4538 N94-37545
BRUNELLE, EUGENE J. p 4458 N94-37800
BRUNER, DORIS A. p 4525 N94-37350
BRUNO, KRISTIN J. p 4490 N94-36489
BRUTZMAN, DON p 4500 N94-37039
BRYAN, J. B. p 4446 N94-37388
BRYCE, E. A. p 4430 N94-36447
BUCHANAN, DENNIS J. p 4401 N94-36659
BUCHELNIKOVA, N. S. p 4531 N94-37726
BUCK, E. C. p 4411 N94-37380
BUCK, M. E. p 4462 N94-37189
BUEHLER, M. F. p 4415 N94-36553
BUGOS, R. p 4432 N94-36471
BUI-PHAM, M. N. p 4407 N94-36462
p 4407 N94-36482
BUJATTI, M. p 4432 N94-36471
BULUSU, S. p 4429 N94-37413
BURCH, J. L. p 4469 N94-36949
BURDICK, LISA p 4540 N94-36750
BURNS, JOHN A. p 4502 N94-36562
BURROWS, C. J. p 4547 N94-36918
BURROWS, CYNTHIA J. p 4399 N94-37134
BUSCHE, R. M. p 4478 N94-36720
BUSSARD, R. W. p 4529 N94-37316
BUTLER, BRETT p 4545 N94-37757
BUTLER, BRUCE D. p 4481 N94-37224
BUTLER, BRYAN P. p 4497 N94-36962
p 4498 N94-37500
BUTLER, L. J. p 4408 N94-37095
BUTLER, MARK C. p 4441 N94-36724
BUZULUTSKOV, A. F. p 4511 N94-36504
BYERS, J. A. p 4532 N94-37732
BYINGTON, MARSHALL p 4429 N94-37446

C

CAHILL, P. A. p 4536 N94-37287
CALDEIRA, K. p 4477 N94-37494
CALES, MICHAEL p 4421 N94-35952
CALHOON, W. H., JR. p 4413 N94-37711
CALISKAN, ARI G. p 4459 N94-37804
CALLCOTT, T. A. p 4537 N94-37498
CALM, J. M. p 4426 N94-37490
CAMBIER, JEAN-LUC p 4382 N94-36687
CAMPBELL, DAVID J. p 4491 N94-36494
CAMPBELL, L. J. p 4436 N94-36514
p 4508 N94-36556
CAMPO, E. p 4454 N94-37329
CAMPONESCHI, EUGENE THOMAS, JR. p 4459 N94-37802
CANABAL, FRANCISCO, III p 4486 N94-36840
CANN, C. D. p 4415 N94-36563
CAO, R. p 4519 N94-37553
CAO, Y. p 4427 N94-37854
CAPPS, C. D. p 4438 N94-37213
CARALP, M. p 4421 N94-37326
CARD, J. M. p 4409 N94-37221
CARDON, J. G. p 4398 N94-36445
CARDOSI, KIM M. p 4487 N94-37347
CARDWELL, DELMAR R. p 4478 N94-36765
CARLIN, DAUN p 4462 N94-36823
CARLIN, MIKE p 4462 N94-36823
CARLSTROM, T. N. p 4527 N94-37081
CARNEY, R. E. p 4436 N94-36532
CARPENTER, J. RUSSELL p 4392 N94-37386
CARTER, C. B. p 4537 N94-37382
CARTER, D. L. p 4446 N94-37388
CARTER, J. G. p 4518 N94-37383
CARTER, M. R. p 4467 N94-37428
CARTER, R. D. p 4418 N94-37398
CASSONE, VINCENT M. p 4481 N94-37140
CASTELO, VICTOR p 4544 N94-37343
CAUSEY, A. R. p 4414 N94-36544
CAVANAUGH, J. p 4494 N94-37061
CAYLOR, I. J. p 4475 N94-37790
CHABAL, Y. J. p 4408 N94-36559
CHAFFIN, MARK S. p 4383 N94-36966
CHAKRABARTI, S. p 4433 N94-36753
CHAKRAVORTY, J. N. p 4433 N94-36753
CHAMBERS, LIN HARTUNG p 4444 N94-37455
CHAMIS, C. C. p 4402 N94-36663
CHAMIS, CHRISTOS C. p 4457 N94-37704
CHAMPETIER, ROBERT J. p 4525 N94-37350
CHAN, K. C. D. p 4449 N94-37733
CHANG, B. p 4525 N94-37486
CHANG, H. L.M. p 4535 N94-37192
CHANG, J. J. p 4448 N94-37244
CHANG, R. P. H. p 4517 N94-37249
CHANG, S. L. p 4443 N94-37176
CHAPMAN, D. p 4482 N94-37444
CHAR, K. p 4436 N94-36557
CHEKANOV, N. A. p 4504 N94-37174
CHELETTE, TAMARA L. p 4484 N94-37268
CHELKOV, G. A. p 4512 N94-36523
CHEN, C. P. p 4410 N94-37250
CHEN, C.-J. p 4524 N94-37191
CHEN, E. P. p 4457 N94-37705
CHEN, GUI-QIANG p 4445 N94-37724
CHEN, J. H. p 4410 N94-37222
CHEN, P. C. p 4501 N94-37425
CHEN, Y. p 4533 N94-36745
CHEN, Y. L. p 4435 N94-37255
CHENG, BETTY H. C. p 4491 N94-36495
CHENG, PETER Y. p 4394 N94-36627
CHERKASSKY, V. S. p 4526 N94-36536
CHERNENKO, A. M. p 4550 N94-37293
CHERNOV, V. A. p 4517 N94-37171
CHERVYAKOV, A. M. p 4539 N94-37172
CHEVET, F. p 4421 N94-37326
CHIEN, K. Y. p 4444 N94-37390
CHIEN, TZE T. p 4394 N94-36625
CHILDRESS, S. R. p 4533 N94-36746
CHIN, H. N. S. p 4475 N94-37621
CHISHOLM, G. H. p 4434 N94-37206
CHISHOLM, M. F. p 4517 N94-37238
p 4538 N94-37545
CHIU, ING-TSAU p 4493 N94-36920
CHO, J. H. p 4440 N94-37738
CHOUDHARY, A. p 4496 N94-37551
CHOW, R. p 4523 N94-36693
p 4425 N94-37422
CHOY, F. K. p 4450 N94-36953
CHRISTENSEN, R. M. p 4479 N94-37355
CHRISTIAN, ELIOT p 4542 N94-36859
CHRISTODOULOU, N. p 4414 N94-36544
CHRISTOPHOROU, L. G. p 4518 N94-37383
CHU, CHIN-CHANG p 4427 N94-37829
CHU, WEI-KAN p 4425 N94-37317
CHUANG, C. C. p 4474 N94-37566
CHUANG, C.-H. p 4501 N94-37590
CHUNG, T.-C. p 4404 N94-37232
CHURAKOV, V. V. p 4511 N94-36504
CHURCH, H. W. p 4463 N94-36470
CLARK, ANNE L. p 4498 N94-37500
CLARK, DAVID A. p 4472 N94-37126
CLARK, R. p 4419 N94-37442
CLASEN, ROBERT J. p 4497 N94-36962
CLEM, J. R. p 4535 N94-37166
CLEMENTS, J. W. p 4439 N94-37306
CLEMMONS, JAMES I., JR. p 4447 N94-36946
CLEMMONS, T. G. p 4455 N94-37015
CLEVELAND, GARY p 4543 N94-37334
CLIFT, VAUGHAN L. p 4480 N94-36766
CLIFT, W. M. p 4427 N94-37725
CLODIUS, W. B. p 4432 N94-36443
CLOUGH, S. A. p 4464 N94-36552
COBB, B. L. p 4478 N94-37045
COBLEIGH, BRENT R. p 4383 N94-36944
COCKS, F. H. p 4461 N94-36511
CODISPOTI, LOUIS A. p 4475 N94-36446
COFFEY, H. T. p 4452 N94-37515
COHEN, B. I. p 4532 N94-37732
COLEMAN, C. E. p 4414 N94-36543
p 4415 N94-36563
COLEMAN, ELAINE p 4396 N94-37257
COLLIN, MARIE-FRANCE p 4499 N94-36535
COLLINS, J. P. p 4444 N94-37390
COLLINS, JOSHUA p 4431 N94-37254
COLOME, S. D. p 4464 N94-36994
p 4464 N94-36995
COMASKEY, B. p 4447 N94-37114
p 4449 N94-37737
COMASKEY, BRIAN p 4448 N94-37203
COMBS, W. E. p 4532 N94-36540
COMPTON, R. p 4537 N94-37369
COMPTON, R. N. p 4400 N94-36509
CONDON, STEVEN E. p 4490 N94-36491
CONNOLLY, J. F. p 4445 N94-36531
CONZETT, H. E. p 4520 N94-37717
COOK, J. p 4401 N94-36653
p 4402 N94-36667
COOK, JEFFREY p 4401 N94-36658
COOPER, A. p 4507 N94-37564
COOPER, B. R. p 4534 N94-37057
COOPER, G. p 4526 N94-36448
COSKREN, ROBERT J. p 4421 N94-36641
COSTELLO, DANIEL J., JR. p 4433 N94-36931
COTTER, GLADYS A. p 4544 N94-37338
COUNCE, D. M. p 4431 N94-37452
CRANE, CHRISTOPHER G. p 4399 N94-37134
CRANSTON, ROBERT p 4434 N94-37218
CRESS, D. p 4435 N94-37391
CRIMINALE, W. O. p 4445 N94-37606
CRIVELLI, LUIS p 4497 N94-36503
CROCE, F. p 4408 N94-37031
CROOKS, R. M. p 4411 N94-37365
CROOKS, RICHARD M. p 4409 N94-37161
CROSS, J. L. p 4381 N94-37332
CROW, J. E. p 4436 N94-36514
CROW, J. T. p 4527 N94-37072
CRUZ, G. E. p 4430 N94-36444
CSIGE, I. p 4416 N94-36993
CUCINOTTA, FRANCIS A. p 4481 N94-37282
CUDA, VINCE p 4396 N94-36990
CUELLAR, L. p 4393 N94-36621
CULBERTSON, JAMES C. p 4440 N94-37769
CURTIS, D. C. p 4473 N94-37217
CUSHING, STEVEN p 4385 N94-37013
CYR, D. R. p 4521 N94-37720
CZARNASKI, JOSEPH p 4534 N94-37027

D

DAHL, D. A. p 4406 N94-36453
DAMBRINE, B. p 4403 N94-36669
DAMCOTT, D. L. p 4418 N94-37398
DAMKROGER, B. K. p 4417 N94-37367
DANDREA, J. A. p 4478 N94-37045
DANE, C. B. p 4449 N94-37722
DANFORD, M. D. p 4420 N94-37578
DANG, DUC NHAN p 4407 N94-36529
DANZAN, S. p 4516 N94-37097
p 4517 N94-37173
DARAB, J. G. p 4415 N94-36553
DASARO, ERIC A. p 4475 N94-36762
DASGUPTA, S. p 4424 N94-37223
DASGUPTA, SUNANDO. p 4442 N94-36992
DASILVA, L. p 4530 N94-37437
DATSKOS, P. G. p 4518 N94-37383
DATYE, A. K. p 4410 N94-37296
DAVID, S. A. p 4420 N94-37548
DAVIDOFF, G. p 4497 N94-36441
DAVIDSON, FREDERIC M. p 4397 N94-36988
DAVIDSON, JOHN B. p 4388 N94-36820
p 4388 N94-37059
DAVIES, B. R. p 4502 N94-37785
DAVIS, JAMES L. p 4470 N94-37581
DAYDE, M. J. p 4497 N94-36547
DAYTON, JAMES A., JR. p 4437 N94-36819
DEAN, JEFFREY S. p 4500 N94-37043
DEASON, V. A. p 4453 N94-36452
DEATON, VIVIAN C. p 4386 N94-36644
DEBONIS, JAMES R. p 4383 N94-37283
DEBONS, F. E. p 4475 N94-36446
DECKER, HARRY J. p 4452 N94-37521
DEGNAN, FRANK p 4396 N94-37257
DEHAEMER, MICHAEL J. p 4422 N94-36968
DEHMANI, HASSAN p 4434 N94-37141
DELGENIO, A. D. p 4473 N94-37371
DELMORE, J. E. p 4406 N94-36453
DEMOURA, J. I. p 4520 N94-37652
DENAVIT, J. p 4528 N94-37207

DENBO, D. W. p 4545 N94-37348
DENDOOVEN, P. G. p 4446 N94-37723
DENHARTOG, D. J. p 4529 N94-37354
DEO, R. B. p 4458 N94-37799
DESJARDIN, M. p 4407 N94-36482
DESTLER, W. W. p 4448 N94-37368
DEVADIGA, SADASHIVA p 4446 N94-36812
DEVAULT, JON B. p 4422 N94-36968
DEVINE, K. D. p 4498 N94-37487
DEY, J. p 4514 N94-37063
DHOPLE, ARVIND M. p 4478 N94-36996
DIB, NIHAD I. p 4433 N94-36955
DICKENS, PHILLIP M. p 4497 N94-37411
DICKINSON, J. T. p 4424 N94-37184
DICKMANNS, E. D. p 4394 N94-36628
DIECKMAN, S. L. p 4425 N94-37423
DIETRICH, HARRY B. p 4538 N94-37770
DIETZ, N. L. p 4411 N94-37380
DILMANIAN, F. A. p 4525 N94-37258
DIMITS, A. M. p 4532 N94-37732
DINERSTEIN, HARRIET L. p 4547 N94-37825
DIPRINZIO, MARC D. p 4397 N94-37506
DIXIT, M. S. p 4426 N94-37714
DOCTOR, R. D. p 4465 N94-37100
DODGE, L. p 4411 N94-37409
DODSON, LORI J. p 4441 N94-36519
DOERRY, A. W. p 4435 N94-37391
DOHRMANN, C. R. p 4501 N94-37529
DOLIN, R. M. p 4495 N94-37245
DOMAS, P. A. p 4455 N94-37330
DOMENICO, T. p 4419 N94-37442
DOMINGUEZ, F. p 4426 N94-37537
DONG, J. Q. p 4529 N94-37361
p 4443 N94-37362
DONG, Q. Y. p 4537 N94-37498
DORAN, J. C. p 4472 N94-37048
p 4474 N94-37565
DORLAND, W. D. p 4529 N94-37361
DORMAN, D. R. p 4413 N94-37630
DOUBT, G. L. p 4414 N94-36543
DOUGHERTY, THOMAS K. p 4427 N94-37779
DOWDING, ROBERT J. p 4417 N94-37122
DOWGIALLO, E. J. p 4437 N94-37053
DOWLA, FARID U. p 4481 N94-37197
DOWNS, J. L. p 4468 N94-37624
DRAGEL, G. p 4419 N94-37442
DRAKE, B. p 4524 N94-37110
DRAVID, V. P. p 4538 N94-37545
DU, VINCE p 4478 N94-36986
DUBE, JOHN p 4462 N94-36807
DUBEAU, J. p 4426 N94-37714
DUDEK, H. J. p 4401 N94-36656
DUFF, I. S. p 4497 N94-36547
DUMAS, P. p 4408 N94-36559
DUMAY, A. C. M. p 4483 N94-37264
DUMESIC, J. A. p 4411 N94-37372
DUNBAR, RICK p 4540 N94-36750
p 4541 N94-36845
DUNCAN, DAVID B. p 4403 N94-36730
DUNCAN, DENISE p 4540 N94-36750
DUNCAN, MICHAEL A. p 4419 N94-37438
DUNCAN, MICHAEL D. p 4440 N94-37775
DUNCAN, WALTER C. p 4447 N94-36946
DUNLAP, B. p 4537 N94-37369
DUNN, ADRIAN J. p 4482 N94-37233
DUNN, SHANE A. p 4456 N94-37253
DUPONT, J. N. p 4417 N94-37116
DURAJ, STAN A. p 4399 N94-37315
DURAN, G. p 4461 N94-36476
DURSCH, H. W. p 4399 N94-37614
DUTTON, KEVIN E. p 4396 N94-37260
DUXSTAD, K. J. p 4413 N94-37630
DYER, DOUGLAS E. p 4499 N94-36722
DYHR, AMY p 4462 N94-36823
DYMENT, RICHARD J. p 4390 N94-37424
DYSHKANT, A. S. p 4511 N94-36504
DYSON, RODGER W. p 4502 N94-36647

E

EASTMENT, J. D. p 4432 N94-36567
EBBERS, C. A. p 4449 N94-37737
EBELING, CHARLES p 4397 N94-37580
EBIHARA, BEN p 4437 N94-36819
ECKLES, WILLIAM E. p 4399 N94-37315
EDERER, D. L. p 4537 N94-37498
EDWARDS, LEE p 4392 N94-37026
p 4396 N94-37257
EGGLESTON, ROBERT G. p 4484 N94-37271
EICHELBERGER, J. p 4468 N94-36451
EISERMAN, RICHARD p 4396 N94-37257
EKDAHL, C. p 4522 N94-37303
ELINGS, V. p 4524 N94-37110
ELLINGSON, W. A. p 4425 N94-37423
ELLIS, RUSSELL C. p 4543 N94-37042
ELORANTA, K. p 4506 N94-37833
EMERSON, J. A. p 4439 N94-37363
EMERSON, J. E. p 4537 N94-37377
EMERSON, S. p 4465 N94-37187
ENGELBERT, HANS-PETER p 4387 N94-36618
ENGELS, E., JR. p 4521 N94-37721
ERIKSON, JILL p 4478 N94-36986
ERIKSSON, G. p 4548 N94-36759
ERWIN, JIM p 4541 N94-36849
ESAREY, E. p 4528 N94-37182
ESKEN, ROBERT L. p 4484 N94-37268
ESTEROWITZ, LEON p 4448 N94-37481
p 4449 N94-37777
p 4450 N94-37838
ESTLANDER, A. p 4464 N94-37007
EVANS, N. D. p 4525 N94-37374
EVERETT, M. E. p 4395 N94-36633

F

FAEHL, R. J. p 4414 N94-36461
FALK, R. A. p 4438 N94-37213
FAN, SYLVIA p 4490 N94-36492
FANWICK, PHILLIP E. p 4399 N94-37315
FARHAT, CHARBEL p 4497 N94-36503
FARMER, MOSES p 4386 N94-37636
FAST, J. D. p 4465 N94-37093
FAVENESI, J. A. p 4455 N94-37015
FAVRE, J. P. p 4401 N94-36657
FEDOR, CHESTER p 4440 N94-37832
FEEST, E. A. p 4401 N94-36653
FEI, TONG p 4510 N94-36551
FEINSTEIN, S. p 4524 N94-37110
FELCHER, G. P. p 4513 N94-36696
FELDMAN, BARRY J. p 4449 N94-37772
FELDMAN, D. W. p 4449 N94-37733
FENG, DAN p 4505 N94-37655
FENG, X. p 4411 N94-37380
FERBER, M. K. p 4405 N94-37370
FERBER, MATTISON K. p 4404 N94-37205
FERGUSON, B. L. p 4421 N94-36637
FERGUSON, R. E. p 4444 N94-37390
FERGUSON, SAMUEL W. p 4381 N94-36466
p 4382 N94-36467
p 4390 N94-37424
FERNANDO, M. p 4456 N94-37186
FERRANTE, JOHN p 4419 N94-37459
FIELD, CHRISTOPHER T. p 4397 N94-36988
FIELD, E. C., JR. p 4464 N94-36973
FIELD, JAY E. p 4425 N94-37421
FIELDS, D. J. p 4467 N94-37428
FIGUEROA, FERNANDO p 4487 N94-37458
FILIATRE, E. p 4484 N94-37266
FILIPPOV, G. F. p 4539 N94-37079
FIRESTONE, ELAINE R. p 4475 N94-36958
FIRESTONE, JAMES K. p 4475 N94-36958
FISCHER, C. F. p 4518 N94-37313
FISHER, DAVID F. p 4383 N94-36944
FISHER, GARY p 4542 N94-36858
FISHERMAN, S. G. p 4404 N94-37044
FITZGERALD, T. J. p 4469 N94-37314
FITZGERALD, WENDY S. p 4478 N94-36765
FITZPATRICK, KEVIN C. p 4440 N94-37832
FLEETWOOD, D. M. p 4439 N94-37513
FLYTZANI-STEPHANOPOULOS, M. p 4407 N94-36475
FONCK, R. J. p 4529 N94-37354
FONG, R. W. L. p 4414 N94-36543
FOOTE, J. H. p 4527 N94-37081
FORBES, JOHN p 4486 N94-36838
FORD, W. E. p 4501 N94-37783
FORDON, KATHY J. p 4399 N94-37134
FORSHAW, J. R. p 4513 N94-36549
FORSTER, R. p 4523 N94-37547
FORTNER, J. A. p 4411 N94-37380
FOSTER, C. M. p 4535 N94-37192
FOSTER, I. p 4496 N94-37551
FOSTER, I. T. p 4498 N94-37568
FOSTER, KAREN p 4534 N94-37027
FOUSER, THOMAS J. p 4490 N94-36489
FRANCIS, KAREN p 4478 N94-36751
FRANCIS, KAREN M. p 4478 N94-36765
FRANK, A. L. p 4416 N94-36993
FRANK, LOUIS A. p 4470 N94-37470
FRANKS, R. M. p 4430 N94-36444
FRANZEN, J. p 4523 N94-37547
FRAZIER, WILLIAM E. p 4401 N94-36658
FREAR, D. R. p 4464 N94-37071
FREDERICO, T. p 4514 N94-37063
FREDIANI, ALDO p 4454 N94-37329
FREEMAN, R. C. p 4395 N94-36633
FREESLAND, DOUG p 4396 N94-36990
FREITAG, M. p 4509 N94-37517
FREUND, F. p 4438 N94-37241
FRIED, L. E. p 4429 N94-37427
FRIEDMANN, T. A. p 4426 N94-37537
FRISCH, H. J. p 4520 N94-37674
FUJIWARA, M. p 4530 N94-37384
FUKUYAMA, A. p 4528 N94-37231
p 4531 N94-37485
p 4532 N94-37734
FUKUYAMA, ATSUSHI p 4529 N94-37358
FURIHATA, SHIORI p 4518 N94-37387
FURNISH, M. D. p 4405 N94-37627

G

GAINES, JAMES R. p 4514 N94-36964
GALATOLO, ROBERTO p 4454 N94-37329
GALLOP, L. D. p 4446 N94-36760
GAME, DAVID p 4526 N94-37657
GAMES, RICHARD A. p 4499 N94-37760
GANGLOFF, RICHARD P. p 4415 N94-36809
GARCIA, M. D. p 4496 N94-37739
GARG, VIJAY K. p 4387 N94-37448
GARVEY, G. T. p 4520 N94-37671
GARVEY, J. p 4436 N94-36532
GATES, B. C. p 4411 N94-37431
GATRONE, R. C. p 4534 N94-37069
GAUGER, J. R. p 4481 N94-37353
GAUGLER, RAYMOND E. p 4387 N94-37448
GAVRILIK, O. M. p 4505 N94-37483
GE, YUNTAO p 4475 N94-36958
GEE, J. M. p 4462 N94-37189
GENEROLI, ROBERT M. p 4450 N94-36839
GENEROUS, CURTIS p 4540 N94-36750
GEORGE, E. P. p 4419 N94-37420
GHAN, S. J. p 4474 N94-37379
p 4474 N94-37566
GHOSH, V. J. p 4537 N94-37499
GIBSON, D. M. p 4525 N94-37258
GIERMAN, S. M. p 4449 N94-37733
GILCHRIST, JOHN p 4396 N94-37257
GILE, BRENDA E. p 4384 N94-37505
GILL, DEE R. p 4422 N94-36968
GILLEN, K. T. p 4536 N94-37287
GILMORE, JEROLD P. p 4394 N94-36625
GILMOUR, PHILLIP p 4534 N94-37103
GINANNI, J. p 4472 N94-36739
GLASS, MICHAEL W. p 4443 N94-37195
GLEASON, KAREN K. p 4533 N94-36727
GLEBOV, V. YU. p 4511 N94-36504
GLENDENNING, N. K. p 4548 N94-37049
GODDARD, J. W. F. p 4432 N94-36567
GODFREY, S. p 4512 N94-36527
GODWIN, D. S. p 4425 N94-37373
GOHR, LISA p 4462 N94-36807
GOKOGLU, SULEYMAN A. p 4431 N94-37254
GOLDIN, G. p 4413 N94-37711
GOLDSMITH, J. E. M. p 4473 N94-37371
GOLDSTEIN, J. C. p 4449 N94-37733
GOLDSTEIN, W. H. p 4530 N94-37437
GOMES, I. C. p 4420 N94-37552
GOMES, PAUL V. p 4428 N94-36972
GONCHAROV, P. I. p 4511 N94-36504
GONG, LESLIE p 4381 N94-36648
GOODWIN, THOMAS p 4478 N94-36751
GOODWIN, THOMAS J. p 4478 N94-36765
GORDON, EDWARD M. p 4399 N94-37315
GORDON, IAN p 4545 N94-37344
GORE, R. A. p 4496 N94-37782
GOREMYCHKIN, E. A. p 4534 N94-37054
GOSSEIN, C. p 4449 N94-37495
GOSZTOLA, D. p 4512 N94-36524
GOTSIS, PASCAL K. p 4456 N94-37456
GOTT, JACK p 4478 N94-36986
GOYAL, A. p 4538 N94-37569
GRABERT, GREGORY p 4534 N94-37103
GRABOWSKI, L. p 4421 N94-37328
GRAHAM, R. A. p 4428 N94-37052
GRAHAM, RONALD E. p 4431 N94-36943
GRAHAM, SUSAN L. p 4494 N94-37119
GRANATSTEIN, V. p 4448 N94-37368
GRANT, K. E. p 4468 N94-37631
GRAVES, SARA J. p 4491 N94-36496
GRAY, K. E. p 4420 N94-37516
GRAYBILL, R. p 4523 N94-37629
GRECO, MICHAEL p 4473 N94-37143
GREEN, D. p 4518 N94-37312
GREEN, D. W. p 4410 N94-37357
GREEN, DAVID L. p 4385 N94-37604
p 4487 N94-37741
p 4487 N94-37742
p 4487 N94-37743
GREEN, EDWARD J. p 4475 N94-36446
GREEN, L. W. p 4447 N94-36565
GREENBAUM, S. G. p 4408 N94-37031
GREENE, D. S. p 4449 N94-37495
GREENFIELD, P. p 4546 N94-36795
GREENWALD, A. p 4426 N94-37714

GRIBBLE, R. J. p 4414 N94-36461
GRIESEL, MARTHA ANN p 4490 N94-36489
GRIFFIN, P. J. p 4496 N94-37673
GRIFFITH, JAMES R. p 4427 N94-37773
GRIFFITHS, S. K. p 4428 N94-37202
GRIGG, D. p 4524 N94-37110
GRIGGS, D. P. p 4465 N94-37093
GRIMES, GLENN C. p 4458 N94-37801
GRIMSDALE, CHARLES p 4484 N94-37270
GRIMSTAD, GREGORY E. p 4385 N94-37706
GRODSKI, JULIUS J. p 4485 N94-37273
p 4486 N94-37279
GROENEWOLD, G. S. p 4406 N94-36453
GROSS, R. J. p 4428 N94-37201
GROSSMAN, A. S. p 4468 N94-37631
GROZIN, A. G. p 4521 N94-36748
p 4514 N94-36749
p 4514 N94-37065
GRUEN, D. M. p 4422 N94-37068
p 4517 N94-37249
GUEDRY, F. E. p 4482 N94-37276
p 4486 N94-37281
GUILL, FREDERICK C. p 4385 N94-37767
GULACSI, M. p 4438 N94-37295
GULATI, KUSH p 4438 N94-37190
GULLI, C. p 4486 N94-37280
GUNTHER, CHRISTIAN K. p 4420 N94-37582
GUO, D. p 4535 N94-37192
GUPTA, SANDEEP p 4500 N94-37058
GUPTILL, JAMES D. p 4456 N94-37456
GURBANI, V. p 4547 N94-37555
p 4547 N94-37667
GURLEY, G. p 4524 N94-37110
GURZHIEV, A. N. p 4511 N94-36504
GUSTAFSSON, BERTIL p 4496 N94-37656

H

HACK, W. p 4546 N94-36795
HACKEL, L. A. p 4449 N94-37722
HAERTLING, GENE p 4534 N94-37103
HAGERMAN, KAREN p 4422 N94-36968
HALBLEIB, J. A. p 4527 N94-37072
HALDAR, P. p 4438 N94-37111
HALFORD, GARY R. p 4455 N94-37102
HALL, DANA p 4492 N94-36500
HALL, SUSAN MAIN p 4491 N94-36497
HALLER, E. E. p 4413 N94-37630
HALLER, HENRY C. p 4390 N94-37522
HALSKI, P. J. p 4393 N94-36617
HAMADA, Y. p 4530 N94-37384
HAMMERMEISTER, D. p 4472 N94-36739
HAMMOUD, AHMAD N. p 4398 N94-36951
HAN, BONG-GYOON p 4479 N94-37156
HANADA, MASAYA p 4522 N94-37463
HANCE, DENNIS J. p 4391 N94-37225
HANCOX, N. L. p 4402 N94-36667
HANDROCK, J. L. p 4428 N94-37202
p 4428 N94-37243
HANDSCHUH, R. F. p 4450 N94-36953
HANDSCHUH, ROBERT F. p 4451 N94-37451
p 4452 N94-37521
HANEY, S. p 4527 N94-37082
HANGST, J. S. p 4523 N94-37619
HANKLA, A. K. p 4447 N94-37160
HANSMA, P. K. p 4514 N94-37034
p 4524 N94-37110
HANSON, HOWARD P. p 4476 N94-37038
HARADAM, D. P. p 4481 N94-37353
HARDGROVE, JOHN p 4534 N94-37027
HARGIS, P. H., JR. p 4495 N94-37496
HARLAN, C. J. p 4399 N94-37650
HARM, DEBORAH L. p 4482 N94-37263
HARMON, D. p 4402 N94-36662
HARMON, D. M. p 4403 N94-36668
HARMS, RICHARD p 4547 N94-37037
HARPER, RICHARD E. p 4497 N94-36962
p 4498 N94-37500
HARRIGAN, R. W. p 4502 N94-37785
HARRIS, CHRIS H. p 4497 N94-36962
HARRIS, J. W. p 4548 N94-37557
HARRIS, R. N. p 4545 N94-37563
HARRISON, G. F. p 4402 N94-36661
p 4421 N94-37328
HARRISON, TAN R. p 4404 N94-37232
HARTER, J. p 4402 N94-36662
HARTLEY, M. p 4403 N94-36669
HARTMAN, GEORGE A. p 4401 N94-36659
HATORI, TADATSUGU p 4531 N94-37466
HAUFLER, R. E. p 4400 N94-36509
HAUSER, R. K. p 4463 N94-36478
HAWLEY, M. p 4425 N94-37373
HAWSEY, R. A. p 4438 N94-37239
HAYDEN, H. L. p 4452 N94-37512
HE, J. L. p 4452 N94-37515
HEADLEY, T. J. p 4427 N94-37725
HEALY, M. D. p 4536 N94-37290
HEBSUR, MOHAN p 4403 N94-36752
HECKMAN, G. p 4470 N94-37530
p 4471 N94-37780
p 4471 N94-37781
HEGER, A. S. p 4496 N94-37739
HEIDELBERGER, PHILIP p 4497 N94-37411
HEIKKINEN, D. W. p 4517 N94-37210
HEINAENEN, K. p 4414 N94-36525
HEINBOCKEL, JOHN H. p 4522 N94-37508
HELMICK, L. S. p 4424 N94-37300
HELTON, J. W. p 4494 N94-37226
HENDERSON, C. C. p 4536 N94-37287
HENDERSON, CHARLES p 4442 N94-36960
HENDERSON, LESLIE J. p 4425 N94-37482
p 4427 N94-37818
HENDERSON, M. p 4496 N94-37519
HENDERSON, STEPHEN C. p 4467 N94-37607
HENDRICKS, J. S. p 4506 N94-36449
HENINS, I. p 4414 N94-36461
HENSHAW, JIM p 4400 N94-36652
HEPP, ALOYSIUS F. p 4399 N94-37315
HERCULES, D. M. p 4399 N94-37214
HERMAN, J. D. p 4545 N94-37563
HERNANDEZ, J. p 4467 N94-37428
HERRICK, J. p 4404 N94-37105
HERTEL, PETER S. p 4467 N94-37607
HESSE, M. p 4471 N94-37701
HETTICH, R. p 4537 N94-37369
HETTICH, R. L. p 4400 N94-36509
HEYMSFIELD, G. M. p 4475 N94-37790
HICKMAN, JAMES p 4534 N94-37027
HIETALA, V. M. p 4436 N94-36557
HIHN, JAIRUS M. p 4490 N94-36489
HILL, CAROL M. p 4408 N94-36537
HILL, LINDA p 4541 N94-36844
HILLNER, P. E. p 4514 N94-37034
HILTZ, FREDERICK F. p 4385 N94-37830
p 4385 N94-37839
HINCHCLIFFE, HEATHER p 4478 N94-36986
HINES, D. p 4477 N94-37397
HIRSCHMUGL, C. J. p 4408 N94-36559
HO, P. p 4533 N94-36755
HOANG, DAC LUC p 4414 N94-36541
HOBBS, M. L. p 4428 N94-37201
HOEHN, J. G., JR. p 4438 N94-37111
HOEKSTRA, P. p 4469 N94-36738
HOEPPNER, DAVID p 4456 N94-37125
HOEPPNER, DAVID W. p 4453 N94-37322
HOFFERT, M. I. p 4477 N94-37494
HOFFMAN, D. M. p 4425 N94-37317
HOFFMAN, R. C. p 4416 N94-37080
HOJO, HITOSHI p 4531 N94-37466
HOLCOMB, DARRELL H. p 4386 N94-36465
HOLCOMB, FRANKLIN H. p 4440 N94-37759
HOLDRIDGE, GEOFFREY M. p 4422 N94-36968
HOLLEY, DANIEL C. p 4478 N94-36986
HOLLOWAY, D. L. p 4425 N94-37423
HOLT, R. A. p 4414 N94-36544
HOM, KAM W. p 4492 N94-36518
HONG, WON E. p 4462 N94-36823
HONIG, J. N. p 4449 N94-37722
HOOKER, MATTHEW W. p 4437 N94-36781
HOOKER, STANFORD B. p 4475 N94-36958
HOOVER, ERIC p 4473 N94-37143
HOPKINS, DALE A. p 4403 N94-36956
HORAN, D. M. p 4398 N94-36445
HORTOLLAND, ISABELLE p 4485 N94-37274
HORTON, J. A. p 4419 N94-37420
HORTON, W. p 4529 N94-37361
p 4443 N94-37362
HORVATH, J. A. p 4439 N94-37306
HORWITZ, E. P. p 4534 N94-37069
HOSKING, F. M. p 4464 N94-37071
HOU, GENE J. W. p 4397 N94-37502
HOU, L. STEVEN p 4505 N94-37540
HOU, S. Y. p 4436 N94-36557
HOURAHAN, G. C. p 4425 N94-37373
HOWARD, RICHARD p 4395 N94-36825
HRUSKA, J. p 4470 N94-37530
p 4471 N94-37780
p 4471 N94-37781
HSU, WEN L. p 4427 N94-37725
HU, HENRY S. p 4427 N94-37773
HUANG, S. p 4450 N94-36953
HUBBARD, C. R. p 4420 N94-37548
HUBBE, J. M. p 4468 N94-37624
HUDSON, D. V., JR. p 4451 N94-37406
HUET, P. p 4539 N94-37366
HUFFMAN, B. T. p 4514 N94-36700
HUGUENIN, YVES p 4393 N94-36620
HUMPHREYS, D. R. p 4527 N94-37072
HUMPHRIES, S., JR. p 4522 N94-37303
HUNG, ERIC K. p 4434 N94-37162
HUNTER, JUDY p 4540 N94-36750
p 4540 N94-36843
HUNTER, JUDY F. p 4541 N94-36850
p 4544 N94-37338
HUNTLEY, M. S. p 4487 N94-37347
HUSS-LEDERMAN, S. p 4504 N94-37246
HWANG, K. C. p 4533 N94-36755
HWANG, M.-S. p 4508 N94-36718
p 4446 N94-36719
HWANG, R. N. p 4521 N94-37194
HYER, M. W. p 4406 N94-37653

I

IANNELLI, G. S. p 4493 N94-36914
ICE, G. E. p 4535 N94-37212
IDA, K. p 4530 N94-37384
IDEI, H. p 4530 N94-37384
IGUCHI, H. p 4530 N94-37384
IIJIMA, TORU p 4520 N94-37672
IJIRI, Y. p 4506 N94-37718
IMAN, R. L. p 4464 N94-37071
IMPEY, CHRIS D. p 4546 N94-36690
INESON, JUDITH p 4484 N94-37269
INGRAM, J. C. p 4406 N94-36453
INMAN, DANIEL J. p 4396 N94-37349
INOPIN, E. V. p 4504 N94-37174
INOUE, TAKASHI p 4522 N94-37463
IRIGARAY, I. p 4484 N94-37266
IRRGANG, K. D. p 4477 N94-36481
ITOH, K. p 4528 N94-37231
p 4531 N94-37485
p 4532 N94-37734
ITOH, KIMITAKA p 4529 N94-37358
ITOH, S. p 4528 N94-37231
p 4532 N94-37734
ITOH, S. I. p 4531 N94-37485
ITOH, SANAE p 4529 N94-37358
IVANOV, M. A. p 4515 N94-37075
IVANOV, V. V. p 4514 N94-37064
IWAI, SATOSHI p 4518 N94-37387
IYER, A. N. p 4438 N94-37111

J

JACKSON, G. L. p 4530 N94-37436
JACKSON, KAREN E. p 4457 N94-37796
p 4458 N94-37798
JACKSON, T. L. p 4445 N94-37606
JACKSON, WADE C. p 4460 N94-37811
JACOBS, MARC Q. p 4503 N94-37146
JACOBS, S. J. p 4536 N94-37287
JACOBS, T. D. p 4425 N94-37423
JACOBSON, E. M. p 4504 N94-37246
JACOBSON, G. F. p 4447 N94-37160
JACOBSON, J. p 4426 N94-37712
JANSON, WILLIAM P. p 4484 N94-37271
JAVEDANI, J. p 4529 N94-37316
JAVRISHVILI, A. K. p 4512 N94-36523
JAYARAM, R. p 4418 N94-37396
JEDRZEJEWSKI, R. p 4546 N94-36795
JEFFERY, ROSS p 4490 N94-36488
JELETIC, KELLYANN p 4489 N94-36486
JENKINS, M. G. p 4405 N94-37370
JENKINS, RICHARD C. p 4507 N94-36970
JENKINS, ROBERT W. p 4434 N94-37127
JENSE, G. J. p 4483 N94-37264
JESSON, D. E. p 4517 N94-37238
JIA,YUN-TENG p 4412 N94-37533
JIAO, RONG-ZHU p 4412 N94-37534
JIN, CHANG-MING p 4400 N94-36509
p 4537 N94-37369
JODHA, SIRI p 4476 N94-37038
JOENSSON, P. p 4518 N94-37313
JOHANSSON, M. F. p 4436 N94-36557
JOHNSEN, H. A. p 4427 N94-37725
JOHNSON, D. R. p 4466 N94-37288
JOHNSON, DANIEL L. p 4480 N94-37118
JOHNSON, DAVID H. p 4475 N94-36446
JOHNSON, DAVID RAY p 4416 N94-36954
JOHNSON, E. p 4426 N94-37714
JOHNSON, ERIC N. p 4388 N94-37059
JOHNSON, M. L. p 4446 N94-36822
JOHNSON, R. N. p 4452 N94-37512
JOHNSON, S. Y. p 4470 N94-37489
JOHNSON, STEVEN p 4383 N94-37395
JOHNSON, THOMAS A. p 4396 N94-36990
JOHNSON, W. S. p 4402 N94-36666
p 4403 N94-36668
p 4405 N94-37320
JONES, J. WAYNE p 4400 N94-36650
JONES, KENNETH M. p 4384 N94-37505
JONES, MAE p 4396 N94-37257
JONES, MARSHALL B. p 4482 N94-37263
JONES, S. J. p 4533 N94-36745
JONES, W. R., JR. p 4424 N94-37300

JONES, WILLIAM R., JR. p 4426 N94-37520
JOO, H. p 4502 N94-36455
JOSHI, SURESH M. p 4500 N94-37058
JOYCE, G. p 4528 N94-37182
JUHASZ, ALBERT J. p 4398 N94-36821
p 4405 N94-37318
JUMPER, G. Y. p 4473 N94-37217

K

KAHANA, S. H. p 4511 N94-36460
KAHLE, BREWSTER p 4545 N94-37345
KAMEDA, J. p 4418 N94-37410
KAMEYAMA, IKUYA p 4398 N94-37764
KAN, HAN-PIN p 4458 N94-37799
KANJILAL, S. K. p 4451 N94-37188
KANSA, E. J. p 4505 N94-37497
KAO, M. p 4419 N94-37420
KAPLAN, JOSEPH A. p 4497 N94-36932
KARASAKI, K. p 4506 N94-37718
KARBHARI, VISTASP M. p 4422 N94-36968
KARLEN, D. p 4426 N94-37714
KARNAUKHOV, V. M. p 4519 N94-37414
KARPUKHIN, V. V. p 4515 N94-37075
KARPUR, PRASANNA p 4401 N94-36660
KASTURI, RANGACHAR p 4446 N94-36812
KATEHI, LINDA P. B. p 4433 N94-36955
KAUFFMAN, R. P. p 4513 N94-36539
KAVANAGH, FRANK p 4437 N94-36819
KAYE, KAREN p 4540 N94-36842
p 4541 N94-36847
p 4542 N94-36854
KEARNS, J. J. p 4416 N94-37080
KEHOE, MICHAEL W. p 4386 N94-36644
KEICHER, D. M. p 4464 N94-37071
KELLAS, SOTIRIS p 4458 N94-37798
KELLER, TEDDY M. p 4425 N94-37482
p 4427 N94-37778
p 4427 N94-37818
KELLEY, J. B. p 4417 N94-37367
KELLEY, T. A. p 4432 N94-36443
KELLY, H. NEALE p 4456 N94-37541
KELLY, J. G. p 4496 N94-37673
KELLY, JON p 4462 N94-36807
p 4462 N94-36823
KEMMERER, R. A. p 4434 N94-37206
KEMP, WILLIAM T. p 4525 N94-37350
KEMPER, GEORGE B. p 4481 N94-37224
KEMPKA, STEVEN N. p 4443 N94-37195
KENIK, E. A. p 4417 N94-37304
p 4525 N94-37374
p 4418 N94-37398
KENNEDY, ROBERT S. p 4482 N94-37263
KENNY, SEAN P. p 4397 N94-37502
KENT, S. p 4523 N94-37547
KENT, S. M. p 4547 N94-37667
KEOUGH, B. K. p 4399 N94-37614
KERNEY, JOHN T. p 4423 N94-37179
KERSTEIN, A. R. p 4413 N94-37711
KHALSA, S. p 4476 N94-37038
KHEHNMEHDEHKH, L. p 4519 N94-37528
KHOREV, A. I. p 4401 N94-36654
KHOROMSKIJ, B. N. p 4503 N94-37098
KHRIPLOVICH, I. B. p 4509 N94-37078
KICHER, THOMAS P. p 4451 N94-37451
KIM, J. S. p 4521 N94-37200
KIM, Y. M. p 4410 N94-37250
KING, BELINDA B. p 4502 N94-36562
KING, T. p 4419 N94-37420
KINLOCH, A. J. p 4456 N94-37186
KINNEY, A. L. p 4546 N94-36794
KINROSS-WRIGHT, J. M. p 4449 N94-37733
KIRKHAM, R. R. p 4468 N94-37624
KLASSEN, R. J. p 4414 N94-36544
KLAVETTER, E. A. p 4428 N94-36505
KLIMYK, A. U. p 4505 N94-37483
KLUGER, Y. p 4522 N94-37310
KNACKE, ROGER F. p 4549 N94-36961
KNAPP, G. S. p 4420 N94-37516
KNEPTON, J. p 4478 N94-37045
KNIGHT, W. D. p 4512 N94-36516
KNOTT, T. W. p 4406 N94-37653
KNUDSON, R. p 4432 N94-36471
KNYAZEV, B. A. p 4526 N94-36536
KODALI, P. p 4414 N94-36461
KOENIG, G. W. p 4455 N94-37331
KOKA, K. p 4519 N94-37414
KOLOMITSEV, A. I. p 4525 N94-37258
KOMAROV, V. I. p 4515 N94-37075
KONG, S. H. p 4449 N94-37733
KOOCHESFAHANI, MANOOCHEHR M. p 4383 N94-37219
KOPELMAN, R. p 4525 N94-37532
KORINKO, J. J. p 4416 N94-37080
KOSIER, S. L. p 4532 N94-36540
KOSINOV, A. G. p 4539 N94-37079
KOSTRITSKIJ, A. V. p 4511 N94-36504
KOTERAS, J. R. p 4470 N94-37527
KOTULAK, JOHN C. p 4485 N94-37278
KOZLOWSKI, M. R. p 4425 N94-37422
KRALL, J. p 4528 N94-37182
KRANTZ, TIMOTHY L. p 4452 N94-37457
KRAUSS, A. R. p 4422 N94-37068
p 4517 N94-37249
KRAUSS, GEORGE p 4420 N94-37758
KRAUSS, T. M. p 4421 N94-36637
KREBS, A. E. p 4404 N94-37088
KREIDER, KEVIN L. p 4510 N94-37308
KREN, LAWRENCE A. p 4450 N94-36645
KRESIN, V. V. p 4512 N94-36516
KRESKOVSKY, J. P. p 4442 N94-36957
KRISHNAMURTHY, S. p 4401 N94-36660
KRISHNAN, RAMKI R. p 4383 N94-36950
KROEGER, D. M. p 4538 N94-37569
KRUMSHTEJN, Z. V. p 4512 N94-36523
KUHL, A. L. p 4444 N94-37390
KULANDER, K. C. p 4513 N94-36697
KULIKOV, A. V. p 4515 N94-37075
KUMAKURA, M. p 4519 N94-37417
KUNG, P. J. p 4440 N94-37738
KUNSMANN, H. p 4419 N94-37420
KURAEV, E. A. p 4515 N94-37066
p 4516 N94-37099
KURBATOV, V. S. p 4515 N94-37076
KURNIT, N. A. p 4447 N94-36510
p 4449 N94-37495
KUSH, A. K. p 4463 N94-37488
KWANG, ABEL p 4456 N94-37554
KWARCIANY, R. p 4523 N94-37547
KWEI, G. H. p 4536 N94-37291

L

LABARRERE, T. p 4483 N94-37265
LABAUGH, MODENNA p 4492 N94-36499
LABELLE, LINDA J. p 4390 N94-37424
LACKRITZ, HILARY S. p 4423 N94-37133
p 4423 N94-37151
p 4423 N94-37179
LAIDLER, J. J. p 4410 N94-37357
LAL, R. p 4524 N94-37110
LALA, JAYNARAYAN H. p 4497 N94-36962
p 4498 N94-37500
LAMB, P. J. p 4499 N94-37583
LAMBERT, RALPH E. p 4474 N94-37394
LAMBERT, T. J. p 4394 N94-36627
LANCTO, R. p 4455 N94-37015
LANDAU, Z. HARRY p 4432 N94-36743
LANDEN, O. L. p 4466 N94-37252
LANDIS, ABRAHAM L. p 4530 N94-37392
LANDY, R. J. p 4427 N94-37779
LANG, B. p 4393 N94-36617
LANGLOIS, GUY p 4505 N94-37518
LANGSTON, STEPHEN p 4545 N94-37344
LARA-CURZIO, E. p 4417 N94-37138
LARA-CURZIO, EDGAR p 4405 N94-37370
LARK, KRISTINE A. p 4404 N94-37205
LARNER, K. p 4421 N94-37324
LARSEN, JAMES M. p 4510 N94-36551
LASSEIGNE, D. G. p 4400 N94-36650
LAU, KREISLER S. p 4445 N94-37606
LAURICH, B. K. p 4427 N94-37779
LAVIERS, H. p 4536 N94-37290
LAWRENCE, GREGORY W. p 4461 N94-36511
LAWSON, B. D. p 4392 N94-36726
LAWSON, W. S. p 4482 N94-37276
LAWSON, WILLIAM S. p 4438 N94-37213
LAWTON, TERI B. p 4517 N94-37209
LAZARUS, E. A. p 4523 N94-36468
LEBO, M. R. p 4530 N94-37436
LECHTER, WILLIAM L. p 4416 N94-37080
LEE, EUN U. p 4538 N94-37776
LEE, H. H. p 4401 N94-36658
LEE, I. Y. p 4406 N94-37653
LEE, L. p 4467 N94-37429
LEE, R. J. p 4436 N94-36557
LEE, R. W. p 4402 N94-36667
LEE, S. W. p 4530 N94-37392
LEE, WOOJIN p 4435 N94-37255
LEFEBVRE, M. p 4408 N94-37091
LEGER, ALAIN p 4393 N94-36621
p 4485 N94-37274
p 4486 N94-37280
LEMEZEC, J. p 4545 N94-37346
LEO, A. J. p 4463 N94-37488
LEON, M. p 4511 N94-36457
LEONE, J. M., JR. p 4473 N94-37242
p 4475 N94-37621
LEPPAENEN, R. p 4510 N94-37632
LERCHE, R. A. p 4446 N94-37723
LEROYER, P. p 4486 N94-37280
LESNOV, A. N. p 4507 N94-37062
p 4504 N94-37375
LESTER, L. p 4533 N94-36755
LEUCHT, R. p 4401 N94-36656
LEUNG, H. p 4395 N94-36630
LEUNG, L. R. p 4474 N94-37379
p 4474 N94-37566
LEVIN, B. F. p 4417 N94-37116
LEVIN, EUGENE p 4408 N94-36989
LEVUSH, B. p 4448 N94-37368
LEWIS, BERNARD L. p 4435 N94-37771
LEWIS, MARK J. p 4443 N94-37128
LEWIS, P. J. p 4431 N94-37452
LI, DONG-QI p 4509 N94-37517
LI, G. X. p 4443 N94-37362
LI, H. p 4521 N94-37200
LI, J. p 4408 N94-37031
LI, Z. p 4535 N94-37192
LIANG, ALAN Y. p 4389 N94-37159
p 4424 N94-37204
LIEBETRAU, A. M. p 4466 N94-37211
LILIENTHAL, MICHAEL G. p 4482 N94-37263
LILJEGREN, J. C. p 4471 N94-36479
LIN, H. W. p 4502 N94-37784
LIN, MING C. p 4494 N94-37120
LIN, PAUL P. p 4431 N94-36943
LIN, TING-TING Y. p 4453 N94-37150
LIN, W-H. p 4424 N94-37300
LIN, Y. p 4517 N94-37249
LINDQUIST, M. R. p 4451 N94-37188
LINDSEY, E. L. p 4425 N94-37422
LINEHAN, J. C. p 4415 N94-36553
LIOU, MENG-SING p 4441 N94-36646
p 4502 N94-36647
LIPKIN, H. J. p 4511 N94-36512
LIPKIN, J. p 4428 N94-37202
LISSON, BRIAN p 4434 N94-37127
LITTLE, BRENDA p 4477 N94-36522
LITTLE, LINDA p 4490 N94-36492
LITVA, J. p 4395 N94-36630
LIU, A. H. p 4424 N94-37223
LIU, C. T. p 4419 N94-37420
LIU, JIA-RUI p 4425 N94-37317
LIU, JIAN-GUO p 4445 N94-37724
LIU, LEE-YIN p 4423 N94-37133
p 4423 N94-37151
LIU, S. p 4422 N94-37068
LIVENGOOD, C. D. p 4465 N94-37100
LKHAGVA, O. p 4516 N94-37097
p 4517 N94-37173
p 4519 N94-37528
LLACER, J. p 4524 N94-37165
LO, C. F. p 4384 N94-37511
LO, T. p 4395 N94-36630
LOEHLE, C. p 4461 N94-36484
LOMTADZE, T. A. p 4512 N94-36523
LONDON, R. p 4530 N94-37437
LONG, CHARLES E. p 4476 N94-37135
p 4476 N94-37216
p 4477 N94-37229
LOOMIS, G. E. p 4523 N94-36693
p 4425 N94-37422
LOPEZ, E. P. p 4464 N94-37071
LOPRESTI, C. A. p 4466 N94-37211
LOTTES, S. A. p 4443 N94-37176
LOVEDAY, J. p 4547 N94-37667
LOWELL, CARL F. p 4403 N94-36752
LOWELL, DOUGLAS D. p 4450 N94-36721
LUCCO, STEVEN p 4494 N94-37119
LUDDERS, J. RICHARD p 4390 N94-37424
LUHMANN, JANET G. p 4549 N94-37012
LUHMANN, N. C., JR. p 4528 N94-37167
LUJAN, RICHARD D. p 4389 N94-37159
p 4424 N94-37204
LUNIEWICZ, MICHAEL F. p 4394 N94-36625
LUO, J. p 4422 N94-37068
LUPOVICI, CHRISTIAN p 4544 N94-37341
LUPTON, R. p 4547 N94-37555
p 4547 N94-37667
LUTZ, A. E. p 4407 N94-36482
LUTZ, T. J. p 4531 N94-37626
LYCAS, JOHN p 4540 N94-36750
LYELL, M. J. p 4445 N94-37635
LYNN, K. G. p 4537 N94-37499
LYONS, M. L. p 4444 N94-37390
LYTTLE, T. W. p 4466 N94-37389

M

MA, J. p 4441 N94-37851
MACCABE, A. B. p 4498 N94-37487
MACDONALD, JAMES R. p 4491 N94-36496
MACGOWAN, B. J. p 4530 N94-37437
MACKAMUL, K. p 4461 N94-36476

MACKEIGAN, C. p 4544 N94-37340
MACKINNON, B. p 4547 N94-37555
MACLEAN, J. p 4394 N94-36629
MADACHY, RAY p 4490 N94-36492
MADAU, PIERO p 4547 N94-36963
MAGGIORA, DEBRA R. p 4467 N94-37607
MAGILL, S. R. p 4511 N94-36483
MAHALINGAM, S. p 4410 N94-37222
MAHDAVI, M. A. p 4530 N94-37436
MAHMOOD, S. M. p 4492 N94-36698
p 4493 N94-36699
MAHON, RITA p 4440 N94-37775
MAHONEY, KAMIN p 4462 N94-36807
p 4462 N94-36823
MAJUMDAR, SAURIN p 4530 N94-37441
MAKHALDIANI, N. V. p 4515 N94-37066
p 4516 N94-37099
MAKI, KOICHI p 4530 N94-37464
MAKROGLOU, A. p 4505 N94-37497
MALARET, E. R. p 4398 N94-36445
MALEY, M. P. p 4440 N94-37738
MALITSKY, N. p 4495 N94-37453
MALKAN, MATTHEW A. p 4546 N94-36690
MALLAT, J. p 4510 N94-37632
MALOY, JOSEPH E. p 4390 N94-37443
MANHARDT, PAUL D. p 4493 N94-36914
p 4493 N94-36922
MANOCHA, DINESH p 4494 N94-37120
MAO, J. p 4423 N94-37147
MARDER, A. R. p 4417 N94-37116
MARDER, B. M. p 4527 N94-37072
MARGETIS, S. p 4520 N94-37715
MARGOLIS, S. B. p 4411 N94-37412
MARK, J. p 4451 N94-37406
MARKHAM, HOWARD p 4541 N94-36952
MARQUE, F. p 4483 N94-37265
MARTENS, J. S. p 4436 N94-36557
MARTIN, ERIC J. p 4484 N94-37268
MARTIN, S. J. p 4428 N94-36505
MARTIN, STEPHEN J. p 4475 N94-36446
MARTINEZ, M. J. p 4445 N94-37726
MASON, GREGORY S. p 4388 N94-36965
MASON, MARK R. p 4399 N94-37650
MASOTTO, THOMAS K. p 4497 N94-36962
MASSENGILL, LLOYD W. p 4438 N94-37190
p 4438 N94-37196
MASUDA, S. R. p 4424 N94-37300
MATIKAS, THEODORE E. p 4401 N94-36660
MATLOCK, DAVID K. p 4420 N94-37758
MATOCHKIN, E. P. p 4531 N94-37728
MATSON, D. W. p 4415 N94-36553
MATTHEWS, D. p 4530 N94-37437
MAUCHE, C. W. p 4548 N94-37164
MAUDLIN, P. J. p 4457 N94-37670
MAUZY, A. p 4466 N94-37299
MAYER, G. p 4399 N94-37214
MAZURKEVICH, G. E. p 4503 N94-37098
MAZUROWSKI, J. p 4533 N94-36755
MCCAA, J. p 4474 N94-37566
MCCANDLISH, JANET E. p 4491 N94-36496
MCCARTNEY, L. N. p 4403 N94-36670
MCCARTY, G. D. p 4430 N94-36447
MCCARTY, JON G. p 4412 N94-37462
MCCAUGHAN, FRANCES E. p 4444 N94-37507
MCCLAIN, CHARLES R. p 4475 N94-36958
MCCOWN, A. p 4447 N94-36510
MCCOWN, A. W. p 4449 N94-37495
MCDANIEL, R. L. p 4537 N94-37377
MCDERMOTT, JOSEPH S. p 4422 N94-36968
MCDONALD, M. J. p 4502 N94-37785
MCFARLAND, ISABEL p 4423 N94-37151
MCGARRY, FRANK p 4489 N94-36486
p 4492 N94-36500
MCGIBBON, A. J. p 4517 N94-37238
p 4538 N94-37545
p 4412 N94-37546
MCGIBBON, M. M. p 4517 N94-37238
p 4538 N94-37545
MCGINN, W. D. p 4393 N94-36622
MCGRATH, D. B. p 4442 N94-36957
MCGUIGAN, M. G. p 4394 N94-36629
MCGUIRE, EILEEN p 4491 N94-36497
MCGUIRE, GARY E. p 4437 N94-37033
p 4437 N94-37035
p 4437 N94-37107
p 4437 N94-37108
MCINTYRE, DALE C. p 4389 N94-37159
p 4424 N94-37204
MCKEE, R. A. p 4538 N94-37570
MCKINNEY, W. R. p 4496 N94-37549
MCKNIGHT, CLIFF p 4544 N94-37342
MCLAUGHLIN, PHILIP G. p 4476 N94-36971
MCMANUS, HUGH L. p 4405 N94-37471
MCNUTT, P. p 4462 N94-37407
MCSWEEN, HARRY Y., JR. p 4548 N94-37004
MEADOWS, J. p 4523 N94-37547
MEERSON, B. p 4529 N94-37309
MEIER, JOHN G., III p 4493 N94-37040
MEISENHEIMER, T. L. p 4439 N94-37513
MELE, GARY p 4478 N94-36986
MENIETTI, J. DOUGLAS p 4550 N94-37251
MENON, S. p 4413 N94-37711
MENU, J. P. p 4486 N94-37280
MENYUK, C. R. p 4524 N94-37191
MERENKOV, N. P. p 4515 N94-37066
p 4516 N94-37099
MESURE, S. p 4487 N94-37812
METCALF, D. p 4461 N94-36476
METCALF, VERN L. p 4500 N94-36924
METWALLY, MUNIR p 4465 N94-37155
p 4466 N94-37252
MEVREL, R. p 4401 N94-36657
MEYER, DAVID W. p 4539 N94-36725
MEYER, R. P. p 4393 N94-36617
MICKLE, THU-HA T. p 4401 N94-36658
MIHUL, A. p 4519 N94-37414
MILEY, G. H. p 4529 N94-37316
MILLER, D. J. p 4420 N94-37516
MILLER, D. K. p 4545 N94-37563
MILLER, J. A. p 4407 N94-36462
p 4407 N94-36482
MILLER, J. D. p 4531 N94-37626
MILLER, JEFFREY H. p 4450 N94-36645
MILLER, KEITH W. p 4491 N94-36498
MILLER, M. K. p 4418 N94-37396
MILLER, MARK D. p 4417 N94-37138
MILLER, P. L. p 4404 N94-37088
MILLS, W. J. p 4416 N94-37080
MILSHTEJN, A. I. p 4514 N94-36747
MINARIK, STEVEN B. p 4436 N94-37835
MINGUET, PIERRE J. p 4420 N94-37582
MIRDAMADI, M. p 4402 N94-36666
MISLEVY, ROBERT J. p 4506 N94-36728
p 4506 N94-36732
p 4507 N94-37046
MITCHELL, ALEC p 4421 N94-37323
MITCHELL, DEBORAH p 4491 N94-36494
MITCHELL, S. p 4505 N94-37620
MITCHELL, S. C. p 4449 N94-37737
MITROFANOV, I. G. p 4550 N94-37293
MIYANO, K. E. p 4537 N94-37498
MOCK, R. C. p 4527 N94-37072
MOELLER, KAREN p 4478 N94-36986
MOES, TIMOTHY R. p 4383 N94-37378
MOESSER, MARK W. p 4456 N94-37125
MOIR, R. W. p 4528 N94-37307
MOLANDER, W. A. p 4448 N94-37240
MOLBURG, J. C. p 4465 N94-37100
MONAGHAN, RICHARD C. p 4381 N94-36648
MONTAZER, P. p 4472 N94-36739
MOOIJ, H. A. p 4484 N94-37272
MOONIER, P. p 4521 N94-36694
MOORE, C. p 4523 N94-37547
MOORE, FREDERICK G. p 4538 N94-37770
MOORE, THOMAS J. p 4405 N94-37460
MORAN, KENNETH J. p 4382 N94-36729
MORAN, M. J. p 4525 N94-37486
MORGAN, B. p 4402 N94-36661
MORGAN, K. p 4444 N94-37525
MORGAN, K. L. p 4432 N94-36567
MORI, SEIJI p 4530 N94-37464
MORI, Y. p 4518 N94-37360
MORIDIS, G. p 4443 N94-37050
MORITA, N. p 4519 N94-37417
MORITA, S. p 4530 N94-37384
MORIYAMA, KOUKI p 4531 N94-37484
MOROZ, V. I. p 4519 N94-37414
MORRIS, A. TERRY p 4501 N94-37589
MORRIS, HARRY p 4545 N94-37345
MORRIS, M. D. p 4503 N94-37073
MORRIS, ROBERT E. p 4430 N94-37768
MORSE, D. H. p 4517 N94-37210
MORSE, STEPHEN E. p 4485 N94-37278
MOSCOVICI, H. p 4506 N94-37852
MOSES, D. p 4427 N94-37854
MOSHIER, W. C. p 4404 N94-37088
MOTEVALLI, VAHID p 4389 N94-36967
MOTOWIDLO, L. R. p 4438 N94-37111
MOUNTZIARIS, T. J. p 4408 N94-36735
MOYER, CARL B. p 4450 N94-36721
MULLER, D. p 4515 N94-37087
MULLICK, SANJOY p 4423 N94-37133
MUNKS, CLIFFORD B. p 4536 N94-37228
MURPHY, KELLY p 4383 N94-37395
MURPHY, PATRICK C. p 4388 N94-37059
MYERS, NEILL p 4486 N94-36838
MYLES, K. M. p 4410 N94-37357
MYTNICHENKO, S. V. p 4517 N94-37171

N

NACHALIEL, E. p 4525 N94-37258
NAEGELI, D. p 4411 N94-37409
NAGLE, GAIL A. p 4497 N94-36962
p 4499 N94-37583
NAIR, A. D. p 4548 N94-37834
NAKAJIMA, HAJIME p 4418 N94-37385
p 4418 N94-37416
p 4419 N94-37465
NAKANE, YOSHIHIRO p 4518 N94-37387
NAKASONE, YUJI p 4419 N94-37465
NAKAYAMA, Y. p 4526 N94-36472
NALLANTHIGHAL, S. p 4393 N94-36622
NASIR, M. A. p 4435 N94-37255
NASIROV, T. Z. p 4504 N94-37175
NASTASI, M. p 4414 N94-36461
NATANSOHN, A. p 4423 N94-37147
p 4424 N94-37185
p 4424 N94-37227
NATER, R. p 4508 N94-36718
NATHAL, MICHAEL V. p 4419 N94-37503
NAVROTSKY, A. p 4539 N94-37094
NEBEL, R. A. p 4529 N94-37316
NEEL, F. p 4483 N94-37265
NELLIS, W. J. p 4407 N94-36458
NELSON, MICHAEL L. p 4497 N94-36932
NELSON, P. A. p 4442 N94-36817
NELSON, W. E. p 4495 N94-37496
NEMZEK, R. J. p 4549 N94-37668
p 4471 N94-37669
NESTERENKO, V. V. p 4539 N94-37172
NEUGEBAUER, G. L. p 4545 N94-37563
NEUMAN, B. CLIFFORD p 4495 N94-37509
NEVINS, W. M. p 4527 N94-37062
NEWBERG, H. p 4547 N94-37555
p 4547 N94-37667
NEWMAN, HARVEY S. p 4440 N94-37769
NG, H. K. p 4451 N94-37070
NGO, E. p 4432 N94-36743
NGUYEN, D. C. p 4449 N94-37733
NGUYEN, DUNG PHU CHI p 4396 N94-36990
NGUYEN, PHUC p 4407 N94-36529
NGUYEN, TAM p 4478 N94-36986
NGUYEN, TIEN DUNG p 4407 N94-36529
NGUYEN, VAN DACH p 4407 N94-36529
NICHOLS, W. R. p 4502 N94-36455
NICINSKI, T. p 4547 N94-37555
NICKLESS, B. p 4498 N94-37519
NICODEME, P. p 4394 N94-36626
NICOL, DAVID M. p 4497 N94-37411
NIELSEN, J. S. p 4523 N94-37619
NIETO, M. M. p 4512 N94-36515
NIKITENKO, S. G. p 4517 N94-37171
NIKONOV, E. G. p 4503 N94-37098
NILAN, MICHAEL S. p 4483 N94-37262
NILSON, D. G. p 4527 N94-37081
p 4528 N94-37297
NIMBLETT, F. p 4439 N94-37306
NISHINO, TORU p 4531 N94-37484
NOEBE, RONALD D. p 4419 N94-37503
NOLL, M. p 4393 N94-36619
NOONAN, C. A. p 4395 N94-36633
NORI, SEKHAR p 4433 N94-36810
NORMAN, D. M. p 4511 N94-36506
NORTON, J. R. p 4413 N94-37754
NOTA, A. p 4546 N94-36795
NUCCIO, V. F. p 4470 N94-37489
NYGREN, R. E. p 4531 N94-37626
NYSTROM, W. D. p 4529 N94-37316

O

OAKHAM, F. G. p 4426 N94-37714
OBRIEN, T. J. p 4441 N94-36550
OBRIEN, T. KEVIN p 4459 N94-37805
OCONNOR, K. p 4429 N94-37402
OCONNOR, KIM p 4478 N94-36751
p 4478 N94-36765
ODAY, M. E. p 4432 N94-36743
ODYNIEC, G. p 4519 N94-37558
OHAIR, JOHN R. p 4503 N94-36723
OHERN, T. J. p 4428 N94-36505
OHI, J. M. p 4451 N94-37406
OKHRIMENKO, I. P. p 4539 N94-37079
OKUMURA, SARAH p 4478 N94-36986
OKUMURA, YOSHIKAZU p 4522 N94-37463
OLEGO, D. J. p 4413 N94-37630
OLSEN, D. K. p 4492 N94-36698
p 4493 N94-36699
OLSEN, L. C. p 4462 N94-37381
OLSSON, PELLE p 4496 N94-37656
ONCINA, CARLOS A. p 4467 N94-37807
OPRISON, RICHARD p 4534 N94-37027

ORMSBY, RACHEL A. p 4397 N94-37504
ORONA, J. R. p 4545 N94-37563
ORTEGA, JAMES M. p 4442 N94-36960
ORZECHOWSKI, J. A. p 4493 N94-36914
p 4493 N94-36922
OSBORN, R. p 4534 N94-37054
OSBOURN, GORDON C. p 4409 N94-37161
OSCARSSON, F. p 4435 N94-37813
OSHAUGHNESSEY, D. M. p 4407 N94-36482
OSHEA, T. P. p 4463 N94-37488
OSOFSKY, MICHAEL S. p 4538 N94-37776
OSTEEN, LANCE B. p 4472 N94-37115
OSTENDORF, MARI p 4434 N94-37032
OSTERHELD, A. L. p 4530 N94-37437
OSTROFF, AARON J. p 4388 N94-37014
OTTESEN, D. K. p 4427 N94-37725
OUTKA, D. A. p 4427 N94-37725

P

PACIESAS, WILLIAM S. p 4547 N94-37702
PACIOREK, K. J. L. p 4424 N94-37300
PADDEN, W. J. p 4543 N94-37336
PADOVAN, JOE p 4456 N94-37554
PAFFETT, M. T. p 4410 N94-37296
PAINE, R. T. p 4410 N94-37284
PAJERSKI, ROSE p 4490 N94-36487
PALMER, REGINA p 4492 N94-36499
PALMER, W. D. p 4437 N94-37033
p 4437 N94-37035
PALMER, W. DEVEREUX p 4437 N94-37107
p 4437 N94-37108
PALMTAG, S. P. p 4506 N94-36449
PALSSON, B. O. p 4468 N94-37740
PAN, X. p 4422 N94-37068
PANCE, A. p 4436 N94-36557
PANCE, ALEKSANDAR p 4534 N94-37036
PANG, Y. p 4511 N94-36460
PANTANO, CARLO p 4404 N94-37232
PAPADOPOULOS, PERIKLES p 4382 N94-36687
PAPPA, RICHARD S. p 4493 N94-36818
PARADISO, J. p 4439 N94-37306
PARDO, B. T. p 4430 N94-36447
PARILLE, DONALD R. p 4421 N94-37324
PARIS, CECIL A. p 4396 N94-37009
PARK, H. M. p 4467 N94-37429
PARK, J.-H. p 4419 N94-37442
PARKIN, D. M. p 4436 N94-36514
PARRIS, P. A. p 4467 N94-37492
PARTRIDGE, R. A. p 4545 N94-37563
PARZEN, G. p 4524 N94-37157
p 4505 N94-37675
PASQUERO, G. p 4454 N94-37329
PATCH, S. K. p 4506 N94-37719
PAULISH, DANIEL J. p 4493 N94-36974
PAYNE, J. E. p 4536 N94-37311
PAYNE, JEFFREY E. p 4491 N94-36498
PAYNE, L. L. p 4536 N94-37311
PAZ-PUJALT, G. R. p 4408 N94-36735
PEARLSTEIN, ARNE J. p 4415 N94-36811
PEARSON, J. p 4509 N94-37517
PEASE, R. L. p 4532 N94-36540
PEDERSON, M. R. p 4537 N94-37356
PEEBLES, H. C. p 4464 N94-37071
PEIRO, J. p 4444 N94-37525
PEISEN, DEBORAH J. p 4390 N94-37424
PELLIEUX, L. p 4486 N94-37280
PELTON, A. p 4548 N94-36759
PEMBERTON, JANNA L. p 4477 N94-37229
PENNELL, W. T. p 4463 N94-36477
PENNER, J. E. p 4474 N94-37566
PENNYCOOK, S. J. p 4517 N94-37238
p 4538 N94-37545
p 4412 N94-37546
PERAIRE, J. p 4444 N94-37525
PEREZ, L. p 4398 N94-36445
PERNAMBUCO-WISE, P. p 4508 N94-36556
PETERKA, ROBERT J. p 4480 N94-37005
PETERSON, D. W. p 4439 N94-37363
PETERSON, GEORGE P. p 4398 N94-36821
PETERSON, JOANNA p 4462 N94-36807
PETRAVICK, D. p 4547 N94-37555
p 4547 N94-37667
PETRICK, M. p 4443 N94-37176
PETRIE, T. W. p 4530 N94-37436
PETROPOULOS, LAMBROS J. p 4481 N94-37124
PETROVA, T. p 4416 N94-37074
PETROVIC, J. J. p 4405 N94-37289
PETRUKHIN, V. I. p 4512 N94-36523
PETRUS, G. J. p 4421 N94-36637
PETRY, C. E. p 4546 N94-36690
PETTIT, F. S. p 4399 N94-37214
PETVIASHVILI, N. p 4529 N94-37309
PHILIPP, WARREN H. p 4408 N94-36537
PHILLIPS, J. p 4436 N94-36557
PHILLIPS, K. p 4427 N94-37725
PHIPPS, G. S. p 4447 N94-37051
PHOENIX, S. LEIGH p 4460 N94-37809
PIANETTA, P. p 4519 N94-37553
PIETILAE, S. p 4464 N94-37007
PINEDADEGYVEZ, JOSE p 4489 N94-36731
PINT, B. A. p 4418 N94-37399
PINTO, JOSEPH p 4450 N94-37838
PINTO, JOSEPH F. p 4448 N94-37481
PIPPIN, H. G. p 4399 N94-37614
PISKA, K. p 4512 N94-36523
PLATO, J. G. p 4449 N94-37733
PLAWSKY, J. L. p 4424 N94-37223
PLAWSKY, JOEL L. p 4442 N94-36992
PLEDECOCQ, B. p 4486 N94-37280
PLOMBON, J. J. p 4438 N94-37241
POE, CLARENCE C., JR. p 4460 N94-37811
POKORA, D. C. p 4384 N94-37577
POLIDORI, DAVE p 4462 N94-36807
POLITES, MICHAEL E. p 4509 N94-36782
POLITZER, P. A. p 4530 N94-37436
POLLACK, ROBERT H. p 4491 N94-36494
PONCHAK, GEORGE E. p 4433 N94-36955
POND, JEFFREY M. p 4440 N94-37769
PONOMAREV, I. Y. p 4525 N94-37258
PONTAU, A. E. p 4517 N94-37210
PONTEKORVO, D. B. p 4514 N94-37064
POPPEL, GARY L. p 4387 N94-37401
PORDES, R. p 4523 N94-37547
p 4547 N94-37555
PORTER, D. p 4469 N94-36738
POST, R. p 4402 N94-36662
POUKEY, J. W. p 4527 N94-37072
POULAIN, P. p 4394 N94-36626
POULSEN, O. p 4523 N94-37619
POUX, FREDERIC p 4485 N94-37274
POWARS, CHARLES A. p 4450 N94-36721
POWER, MICHAEL B. p 4399 N94-37315
PRAKASH, J. p 4437 N94-37053
PRASAD, CHUNCHU B. p 4389 N94-36826
PRATER, C. B. p 4524 N94-37110
PRATUCH, S. M. p 4439 N94-37306
PRESTON, R. F. p 4402 N94-36667
PREWETT, TACEY p 4478 N94-36751
PREWETT, TACEY L. p 4478 N94-36765
PRITCHARD, JOCELYN I. p 4386 N94-37256
PRIZANT, MARK J. p 4497 N94-36962
PROFFITT, MELISSA S. p 4388 N94-37014
PRUESS, K. p 4443 N94-37050
PUEBLA, CRISTIAN A. p 4390 N94-37163
PULLIAM, THOMAS H. p 4505 N94-37655
PURETZKY, A. A. p 4400 N94-36509
PUREZA, PABLO C. p 4526 N94-37774

Q

QI, LIN-KUN p 4412 N94-37533
QIU, Z. Q. p 4509 N94-37517
QUIMBY, HOWARD M. p 4402 N94-36664
QUINN, ROBERT D. p 4381 N94-36648
QUINTO, P. FRANK p 4384 N94-37505
QUONG, A. A. p 4537 N94-37356

R

RACE, TIMOTHY D. p 4422 N94-37104
RACK, H. J. p 4416 N94-37030
RADMACHER, M. p 4514 N94-37034
RADOVIC, LJUBISA p 4404 N94-37232
RAEISAENEN, A. p 4510 N94-37632
RAHKO, K. p 4441 N94-37851
RAINER, F. p 4425 N94-37422
RAISSON, G. p 4421 N94-37325
RAJAGOPAL, K. R. p 4444 N94-37544
RAJAN, P. K. p 4525 N94-37579
RAMAKRISHNAN, RAMACHANDRAN p 4525 N94-37579
RAMAN, GANESH p 4382 N94-36686
RAMBO, P. W. p 4528 N94-37207
p 4438 N94-37213
RAMSDELL, JOHN D. p 4499 N94-37760
RANDALL, RICHARD L. p 4491 N94-36493
RANDOLPH, LYNWOOD P. p 4542 N94-36855
RASH, LARRY C. p 4389 N94-37259
RASUMOV, A. V. p 4504 N94-37375
RAVIKUMAR, V. p 4538 N94-37545
RAYMOND, J. C. p 4548 N94-37164
RAZEGHI, MANIJEH p 4524 N94-37149
REAMES, F. M. p 4466 N94-37288
REASS, W. A. p 4414 N94-36461
REDEY, L. p 4437 N94-37053
REDMOND, E. L., II p 4506 N94-36449
REGAL, DAVID M. p 4387 N94-37658
REGAN, E. C. p 4482 N94-37277
REGHU, M. p 4427 N94-37854
REICHERT, P. p 4449 N94-37722
REIFF, PATRICIA H. p 4469 N94-37016
REINGOLD, EYAL M. p 4485 N94-37273
REINTJES, JOHN F. p 4440 N94-37775
REISTER, D. B. p 4503 N94-37073
REJ, D. J. p 4414 N94-36461
RESCHKE, M. F. p 4486 N94-37281
RESHETOV, A. p 4495 N94-37453
RESTREPO, J. M. p 4496 N94-37549
REYNOLDS, J. F. p 4466 N94-37376
RICCO, A. J. p 4411 N94-37365
RICCO, ANTONIO J. p 4409 N94-37161
RICE, B. W. p 4527 N94-37081
p 4528 N94-37297
RICE, EDWARD J. p 4382 N94-36686
RICHARDS, W. LANCE p 4381 N94-36648
RICHMAN, ROBERT M. p 4399 N94-37315
RICKEL, D. G. p 4508 N94-36556
RIDGEWAY, ROLAND p 4541 N94-36851
RIECKE, H. p 4412 N94-37491
RIOUAL, J.-L. p 4442 N94-36817
RISCHMILLER, FREDERICK W. p 4476 N94-36985
RISEBOROUGH, E. p 4395 N94-36631
RIZZO, T. G. p 4512 N94-36527
ROBBINS, MARK p 4478 N94-36986
ROBERTS, R. G. p 4513 N94-36549
ROBERTSON, J. G. p 4401 N94-36655
ROBINETT, R. D. p 4501 N94-37529
ROBINSON, S. L. p 4428 N94-37243
ROCHEFORT, P. A. p 4447 N94-36565
ROCHON, P. p 4423 N94-37147
p 4424 N94-37185
p 4424 N94-37227
RODRIGUE, GARRY H. p 4481 N94-37197
RODRIGUEZ, AGUSTIN M. p 4419 N94-37459
ROESELER, ARMIN p 4490 N94-36490
ROGERS, J. D. p 4508 N94-36556
ROGERS, JAMES L., JR. p 4387 N94-37762
ROGERS, R. D. p 4534 N94-37069
ROGERS, W. p 4441 N94-36550
ROHLFING, C. M. p 4536 N94-37287
ROHLICEK, J. R. p 4434 N94-37032
ROLAND, C. M. p 4427 N94-37831
ROLLINS, A. N. p 4534 N94-37069
ROOT, J. H. p 4414 N94-36543
ROSNER, DANIEL E. p 4431 N94-37254
ROTE, D. M. p 4452 N94-37515
ROTHBERG, EDWARD p 4499 N94-37854
ROUGHTON, JUDY H. p 4476 N94-37135
ROUSSEL-DUPRE, R. A. p 4432 N94-36643
ROVANG, RICHARD D. p 4405 N94-37318
RUBENCHIK, A. M. p 4510 N94-37536
RUBIANO, R. R. p 4425 N94-37317
RUDOLPH, ALAN p 4427 N94-37829
RUOFF, ARHTUR L. p 4537 N94-37435
RUPERT, A. H. p 4486 N94-37281
RUPERT, A. R. p 4482 N94-37276
RUPPERT, J. p 4505 N94-37620
RUSHANAN, JOSEPH J. p 4499 N94-37760
RUSS, S. M. p 4403 N94-36668
RUSS, STEPHAN M. p 4400 N94-36650
RUSSELL, S. J. p 4449 N94-37733
RUTLEDGE, SHARON K. p 4421 N94-36952
RYAN, KENNETH F. p 4417 N94-37122
RYDEN, R. p 4409 N94-37221

S

SABAT, MICHAEL L. p 4399 N94-37315
SADD, MARTIN H. p 4455 N94-36520
SAGAT, S. p 4414 N94-36543
SAILOR, W. C. p 4527 N94-37101
SAITO, TEIICHIRO p 4418 N94-37385
SALISBURY, MICHAEL S. p 4447 N94-37137
SALKELD, RICHARD W. p 4421 N94-37324
SALMELA, O. p 4477 N94-37855
SALTSMAN, JAMES F. p 4455 N94-37102
SAMPSON, WILLIAM T. p 4390 N94-37424
p 4487 N94-37742
SANCHEZ-CASTRO, C. p 4534 N94-37057
SANCHEZ, A. p 4502 N94-36685
SANDLER, D. p 4393 N94-36821
SANDOR, PATRICK B. p 4485 N94-37274
SANFORD, T. W. L. p 4527 N94-37072
SANGHERA, JASBINDER S. p 4526 N94-37774
SANTANGELO, P. G. p 4427 N94-37831
SANTOS, G. R. T. p 4414 N94-36517
SANUKI, H. p 4528 N94-37231
SARAVANOS, D. A. p 4402 N94-36663
SARAVANOS, DIMITRIS A. p 4403 N94-36956
SARIKOV, N. A. p 4504 N94-37175
SARKAR, S. p 4444 N94-37605
SAROFIM, A. F. p 4407 N94-36475
SATO, T. p 4526 N94-36472

SATOH, KAZUYOSHI ..... p 4530 N94-37415
SATOH, SATOSHI ..... p 4530 N94-37464
SAULT, A. G. ..... p 4412 N94-37542
SAWYER, BRIAN M. ..... p 4390 N94-37424
SAYOOD, KHALID ..... p 4433 N94-36810
SCHAFER, K. J. ..... p 4513 N94-36697
SCHAFFER, W. ..... p 4513 N94-36539
SCHARER, J. E. ..... p 4527 N94-37139
SCHEIDEMANN, A. ..... p 4512 N94-36516
SCHELLING, F. J. ..... p 4463 N94-36470
SCHIEHLEN, J. ..... p 4394 N94-36628
SCHIFFER, J. P. ..... p 4523 N94-37619
SCHILLIG, J. B. ..... p 4508 N94-36556
SCHINDLER, K. ..... p 4471 N94-37701
SCHLAGEL, T. J. ..... p 4511 N94-36460
SCHLAIN, ED ..... p 4473 N94-37143
SCHLIENGER, M. E. ..... p 4417 N94-37367
SCHLUMPF, F. ..... p 4515 N94-37086
SCHMIRLER, J. ERIC ..... p 4462 N94-36823
SCHNEIDER-MUNTAU, H. J. ..... p 4436 N94-36514
p 4508 N94-36556
SCHNEIDER, J. M. ..... p 4474 N94-37394
SCHNEIDER, J. W. ..... p 4421 N94-36474
SCHNEIDER, M. B. ..... p 4525 N94-37486
SCHNEIDER, STEVEN P. ..... p 4443 N94-37060
SCHOESSOW, P. ..... p 4521 N94-36694
SCHOONOVER, R. M. ..... p 4508 N94-36718
p 4446 N94-36719
SCHOR, ANDREI ..... p 4499 N94-37583
SCHORR, HERBERT ..... p 4495 N94-37509
SCHREIBER, ROBERT ..... p 4499 N94-37654
SCHREYER, HOWARD L. ..... p 4423 N94-37181
SCHRIMPF, R. D. ..... p 4532 N94-36540
SCHROEDER, JOHANNES ..... p 4387 N94-36618
SCHUBERT, W. K. ..... p 4462 N94-37189
SCHUDLICH, R. ..... p 4465 N94-37187
SCHULZ, FRITZ ..... p 4542 N94-36857
SCHULZE, C. ..... p 4482 N94-37444
SCHWANK, J. R. ..... p 4439 N94-37513
SCHWANTJE, ROBERT ..... p 4461 N94-36919
SCOTT, D. W. ..... p 4496 N94-37556
SCOTT, M. J. ..... p 4466 N94-37211
SEALS, ROBERT ..... p 4465 N94-37155
SEBELIUS, P. ..... p 4439 N94-37306
SECHI, F. ..... p 4432 N94-36471
SEGALL, BENJAMIN ..... p 4439 N94-37501
SEGALMAN, D. ..... p 4408 N94-37091
SEKAR, R. R. ..... p 4451 N94-37070
SEKI, YASUSHI ..... p 4530 N94-37464
p 4531 N94-37484
SELINDER, T. I. ..... p 4420 N94-37516
SELKIRK, E. B. ..... p 4447 N94-36565
SELVADURAY, GUNA S. ..... p 4426 N94-37510
SENGUPTA, L. C. ..... p 4432 N94-36743
SERGEY, G. ..... p 4547 N94-37555
p 4547 N94-37667
SETTLES, GARY S. ..... p 4441 N94-36519
SGASLIK, ACHIM ..... p 4381 N94-37352
SHABAT, A. B. ..... p 4507 N94-37062
SHADOAN, MIKE ..... p 4486 N94-36838
SHAFFER, L. ..... p 4535 N94-37212
SHAH, ASHWIN R. ..... p 4457 N94-37704
SHAMROTH, S. J. ..... p 4442 N94-36957
SHANEYFELT, M. R. ..... p 4439 N94-37513
SHANG, H. M. ..... p 4410 N94-37250
SHANNON, J. D. ..... p 4467 N94-37429
SHANNON, JACK D. ..... p 4467 N94-37440
SHAPIRO, E. G. ..... p 4510 N94-37536
SHAW, B. A. ..... p 4404 N94-37088
SHAW, W. J. ..... p 4472 N94-37048
p 4468 N94-37624
SHEA, M. A. ..... p 4470 N94-37530
p 4471 N94-37780
p 4471 N94-37781
SHEEHAN, KATHLEEN M. ..... p 4506 N94-36728
SHEK, M. L. ..... p 4537 N94-37498
SHELTON, KEVIN J. ..... p 4447 N94-36946
SHEN, Y. R. ..... p 4408 N94-37056
p 4449 N94-37628
SHEPARD, P. F. ..... p 4521 N94-37721
SHEPHERD, I. G. ..... p 4409 N94-37199
SHERWOOD, JAMES A. ..... p 4402 N94-36664
SHI, P. ..... p 4523 N94-37619
SHIMKAVEG, G. ..... p 4530 N94-37437
SHIMSKI, JOHN ..... p 4451 N94-37319
SHINN, JUDY L. ..... p 4416 N94-36993
SHIPSEY, I. ..... p 4426 N94-37714
SHIRKOV, G. D. ..... p 4515 N94-37077
SHUKLA, ARUN ..... p 4455 N94-36520
SIEGAL, M. P. ..... p 4426 N94-37537
SIEGENTHALER, U. ..... p 4477 N94-37494
SILAGADZE, Z. K. ..... p 4504 N94-37170
SILCOX, R. J. ..... p 4500 N94-36924
SILIN, I. N. ..... p 4515 N94-37076
SILLING, S. A. ..... p 4405 N94-37627
SIMARD, MARC-ALAIN ..... p 4395 N94-36634
SIMITSES, GEORGE J. ..... p 4457 N94-37797
SIMONEN, T. C. ..... p 4530 N94-37436
SIMONOV, V. I. ..... p 4532 N94-36548
SIMONS, JACK ..... p 4512 N94-36521
SIMPSON, GARY B. ..... p 4487 N94-37742
SIMPSON, M. L. ..... p 4521 N94-37220
SIMPSON, R. L. ..... p 4426 N94-37537
SIMS, J. R. ..... p 4508 N94-36556
SINGH, D. ..... p 4425 N94-37423
SINGH, J. P. ..... p 4425 N94-37423
SINOR, J. E. ..... p 4451 N94-37408
SIROCKY, PAUL J. ..... p 4450 N94-36645
SISTERSON, D. L. ..... p 4474 N94-37394
SIVERS, E. A. ..... p 4425 N94-37423
SKARDA, J. RAYMOND LEE ..... p 4444 N94-37507
SKARHA, J. E. ..... p 4518 N94-37298
SKELTON, EARL F. ..... p 4538 N94-37776
SLANE, S. ..... p 4408 N94-37031
SMALLEY, R. E. ..... p 4532 N94-36454
SMART, D. F. ..... p 4470 N94-37530
p 4471 N94-37780
p 4471 N94-37781
SMATHERS, H. W. ..... p 4398 N94-36445
SMID, I. ..... p 4530 N94-37415
SMITH, A. G. ..... p 4548 N94-37834
SMITH, A. W. ..... p 4410 N94-37286
SMITH, C. ..... p 4446 N94-36719
SMITH, C. W. ..... p 4549 N94-37668
SMITH, D. C. ..... p 4536 N94-37290
SMITH, D. L. ..... p 4420 N94-37552
SMITH, D. M. ..... p 4466 N94-37389
SMITH, DONALD ..... p 4490 N94-36487
SMITH, F. T. ..... p 4408 N94-36735
SMITH, PHILLIP J. ..... p 4473 N94-37294
SMITH, RALPH C. ..... p 4503 N94-36923
p 4500 N94-36924
p 4500 N94-36928
p 4503 N94-36991
SMITH, WILLIAM G. ..... p 4494 N94-37230
SMYTHE, WENDY ..... p 4396 N94-37257
SO, C. B. ..... p 4415 N94-36563
SOBIESZCZANSKI-SOBIESKI, JAROSLAW
p 4386 N94-37256
SOCORRORAMOS, A. J. ..... p 4492 N94-36546
SOEDER, RONALD H. ..... p 4390 N94-37522
SONDAK, DOUGLAS ..... p 4442 N94-36808
SOPCHYSHYN, F. C. ..... p 4447 N94-36565
SORENSEN, N. R. ..... p 4464 N94-37071
SOUKIEH, MOHAMAD ..... p 4415 N94-36564
SPARGO, BARRY J. ..... p 4427 N94-37829
SPARKS, C. J. ..... p 4535 N94-37212
SPAULDING, GLENN ..... p 4478 N94-36751
SPAULDING, GLENN F. ..... p 4478 N94-36765
SPECHT, E. D. ..... p 4538 N94-37569
p 4538 N94-37570
SPIELMAN, R. B. ..... p 4526 N94-36448
p 4527 N94-37072
SPOONER, S. ..... p 4420 N94-37548
SPRAGGE, M. K. ..... p 4425 N94-37422
SPRANGLE, P. ..... p 4528 N94-37182
SPRAY, S. ..... p 4507 N94-37564
SPRINGER, A. M. ..... p 4382 N94-36741
p 4384 N94-37577
SROMOVSKY, LAWRENCE A. ..... p 4549 N94-36689
STAHL, S. ..... p 4393 N94-36621
STALEY, R. J. ..... p 4436 N94-36532
STALLWORTH, P. E. ..... p 4408 N94-37031
STAMPE, DAVE M. ..... p 4485 N94-37273
p 4486 N94-37279
STANBERY, B. J. ..... p 4533 N94-36744
STANGE, A. ..... p 4512 N94-36526
STANLEY, W. D. ..... p 4470 N94-37489
STARK, MIKE ..... p 4492 N94-36501
STARR, T. L. ..... p 4410 N94-37286
STATHIS, JOHN ..... p 4490 N94-36488
STAVNES, MARK W. ..... p 4398 N94-36951
STEELE, H. S. ..... p 4449 N94-37495
STEINETZ, BRUCE M. ..... p 4450 N94-36645
STENGER, DAVID A. ..... p 4427 N94-37829
STEPHENSON, D. A. ..... p 4457 N94-37670
STEPHENSON, GEOFFREY A. ..... p 4543 N94-37337
STEPONKUS, P. L. ..... p 4479 N94-37248
STEPPE, JEAN M. ..... p 4501 N94-37526
STERN, HERVEY W. ..... p 4432 N94-36473
STERZINGER, GEORGE J. ..... p 4481 N94-36740
STEVENS, R. ..... p 4498 N94-37519
STEVENS, WALTER J. ..... p 4480 N94-37089
STEVENSON, R. ..... p 4457 N94-37670
STEWART, GREGORY D. ..... p 4431 N94-37254
STEWART, K. ..... p 4477 N94-37397
STEWART, R. E. ..... p 4530 N94-37437
STOCKUM, ROBERT W. ..... p 4389 N94-36826
STOHR, J. F. ..... p 4401 N94-36657
STOKES, G. M. ..... p 4463 N94-36477
STONEKING, W. R. ..... p 4531 N94-37730
STONEMAN, ROBERT ..... p 4450 N94-37838
STONEMAN, ROBERT S. ..... p 4449 N94-37777
STOUGHTON, C. ..... p 4547 N94-37555
p 4547 N94-37667
STOUT, M. G. ..... p 4457 N94-37670
STOVALL, JOHN R. ..... p 4387 N94-36933
STOWELL, S. ..... p 4432 N94-36743
STRAKHOVA, S. I. ..... p 4516 N94-37097
p 4517 N94-37173
STRAKHOVENKO, V. M. ..... p 4514 N94-36747
STRATTON, JOCK ..... p 4473 N94-37143
STREET, KENNETH W. ..... p 4408 N94-36537
STRIGHT, JAMES R. ..... p 4508 N94-37130
STROM, ULRICH ..... p 4440 N94-37769
STUART, G. C. ..... p 4426 N94-37714
STUBBS, DAVID A. ..... p 4401 N94-36660
STYLES, R. C. ..... p 4415 N94-36563
SUDARSHAN, E. C. G. ..... p 4539 N94-36507
p 4539 N94-36508
SUGAMA, TOSHIFUMI ..... p 4417 N94-37153
SUHREN, M. ..... p 4408 N94-36559
SUKHBAATAR, TS. ..... p 4516 N94-37097
p 4517 N94-37173
SULLIVAN, N. S. ..... p 4436 N94-36514
SUN, SHI-PING ..... p 4412 N94-37533
SUN, X. ..... p 4505 N94-37518
SUN, XIAOBAI ..... p 4504 N94-37246
SUN, XIAOLI ..... p 4397 N94-36988
SUNWOO, A. J. ..... p 4420 N94-37678
SUTHERLAND, H. J. ..... p 4457 N94-37622
SUZUKI, SATOSHI ..... p 4530 N94-37415
SVEC, W. A. ..... p 4478 N94-36555
SWANSON, R. A. C. ..... p 4435 N94-37736
SWANSON, S. ..... p 4468 N94-36451
SWANSON, STEPHEN R. ..... p 4460 N94-37810
SWEENEY, PAT ..... p 4473 N94-37143
SWEET, J. N. ..... p 4439 N94-37363
SWIERGIEL, ARTUR H. ..... p 4482 N94-37233
SWIFT, WALTER L. ..... p 4461 N94-36805
SYAMLAL, M. ..... p 4441 N94-36550
SYMBALISTY, E. M. D. ..... p 4432 N94-36443
SYMKO, OREST G. ..... p 4431 N94-37029
SZE, R. C. ..... p 4447 N94-36510
SZOKE, A. ..... p 4530 N94-37392
SZYMURSKI, S. R. ..... p 4425 N94-37373

T

TABER-DUDAS, ARDETH ..... p 4540 N94-36750
TADA, EISUKE ..... p 4530 N94-37464
TAJIMA, T. ..... p 4529 N94-37309
TAKAGI, A. ..... p 4518 N94-37360
TAKAGI, H. ..... p 4536 N94-37291
TAKATSU, HIDEYUKI ..... p 4530 N94-37464
TAKATSU, TAMAO ..... p 4418 N94-37385
TALAGA, R. ..... p 4521 N94-36694
TALLANT, D. R. ..... p 4426 N94-37537
TANABE, TATSUHIKO ..... p 4419 N94-37465
TANAKA, KAZUHIRO ..... p 4522 N94-37234
TANAKA, MASANOBU ..... p 4522 N94-37463
TANAKA, SHUN-ICHI ..... p 4518 N94-37387
TANG, J. ..... p 4519 N94-37550
TANG, YUAN-LIANG ..... p 4446 N94-36812
TANI, B. S. ..... p 4411 N94-37380
TANKERSLEY, LAWRENCE L. ..... p 4440 N94-37775
TANNER, STEPHEN P. ..... p 4408 N94-36537
TASKAR, N. R. ..... p 4413 N94-37630
TAUSWORTHE, ROBERT C. ..... p 4490 N94-36489
TAYLOR, J. ..... p 4446 N94-36719
TAYLOR, P. A. ..... p 4405 N94-37627
TAYLOR, S. C. ..... p 4426 N94-37714
TAYLOR, T. S. ..... p 4530 N94-37436
TENNE-SENS, U. A. ..... p 4434 N94-37127
TERAESRANTA, H. ..... p 4548 N94-37834
TERRY, J. ..... p 4519 N94-37553
TESMER, J. ..... p 4414 N94-36461
THAYER, K. J. ..... p 4512 N94-36513
THEE, PAUL L. ..... p 4535 N94-37129
THIESSEN, M. ..... p 4468 N94-37856
THIMMAPURAM, P. ..... p 4465 N94-37100
THOMAS, S. J. ..... p 4449 N94-37495
THOMPSON, D. C. ..... p 4449 N94-37495
THOMPSON, J. A. ..... p 4521 N94-37721
THOMPSON, NANCY ..... p 4386 N94-37636
THOMPSON, RICHARD ..... p 4413 N94-37761
THOMPSON, S. L. ..... p 4463 N94-36470
p 4446 N94-37388
THORN, W. F. ..... p 4473 N94-37217
THORNBERG, STEVE M. ..... p 4389 N94-37159
THORNBERG, STEVEN M. ..... p 4424 N94-37204
THROWER, PETER A. ..... p 4404 N94-37232
THURAI, M. ..... p 4432 N94-36567
p 4464 N94-36994
TIAN, Y. ..... p 4464 N94-36995
TIOURIRINE, T. N. ..... p 4529 N94-37316
TISONE, G. C. ..... p 4495 N94-37496

TOKAREVA, N. A. ..... p 4515 N94-37077
TOLSON, ROBERT H. ..... p 4397 N94-37506
TOME, C. ..... p 4414 N94-36544
TOMIO, L. ..... p 4514 N94-37063
TOMPKINS, STEPHEN S. ..... p 4459 N94-37806
TOPLIKAR, EDWARD G. ..... p 4422 N94-37121
p 4423 N94-37148
p 4423 N94-37179
TORNIKOSKI, M. ..... p 4548 N94-37834
TOTH, LOUIS E. ..... p 4538 N94-37776
TOWNSEND, D. P. ..... p 4450 N94-36953
TOWNSEND, DENNIS P. ..... p 4451 N94-37319
TRAHAN, M. W. ..... p 4495 N94-37496
TRAN, T. ..... p 4398 N94-36445
TRANTER, P. H. ..... p 4402 N94-36661
p 4421 N94-37328
TREADWELL, STEVEN ..... p 4497 N94-36962
TRIFUNAC, A. D. ..... p 4412 N94-37439
TROTT, W. ..... p 4428 N94-36505
TROXEL, STEVEN E. ..... p 4524 N94-37142
TRUSSELL, F. G. ..... p 4489 N94-36480
TSAO, A. ..... p 4504 N94-37246
TSE, D. G. N. ..... p 4442 N94-36957
TSKHADADZE, E. G. ..... p 4512 N94-36523
TSUJI, HIROKAZU ..... p 4418 N94-37385
p 4418 N94-37416
p 4419 N94-37465
TUCKER, C. J. ..... p 4393 N94-36622
TUEY, DICK ..... p 4541 N94-36848
TUINMAN, A. ..... p 4537 N94-37369
TUINMAN, A. A. ..... p 4400 N94-36509
TUNNELL, L. N. ..... p 4518 N94-37305
TURCICH, ELIZABETH ..... p 4434 N94-37218
TURITSYN, S. K. ..... p 4510 N94-37536
TURKOVICH, JOHN ..... p 4499 N94-37583
TURNER, JAMES C. ..... p 4505 N94-37540
TURNER, L. ..... p 4529 N94-37316
TURNER, R. M. ..... p 4395 N94-36631
TWEED, J. H. ..... p 4402 N94-36667
TYURIN, VICTOR M. ..... p 4544 N94-37339

U

UCCI, ANTHONY M. ..... p 4406 N94-37633
ULBRICHT, L. E. ..... p 4451 N94-37188
ULLAURI, JULIO C. ..... p 4388 N94-36733
UNGER, L. ..... p 4548 N94-36759
UNNINAYAR, SUSHEL ..... p 4461 N94-36827
UNSEREN, M. A. ..... p 4501 N94-37735

V

VAEKIPARTA, K. ..... p 4427 N94-37854
VALETT, JON D. ..... p 4490 N94-36491
VALIN, PIERRE ..... p 4395 N94-36634
VALLE, TONY ..... p 4545 N94-37757
VALTAOJA, E. ..... p 4548 N94-37834
VANALSTYNE, RICHARD ..... p 4466 N94-37252
VANBOCKSTAL, L. ..... p 4508 N94-36556
VANDEMARK, D. ..... p 4477 N94-37397
VANDEN AVYLE, J. A. ..... p 4417 N94-37367
VANDENBURG, J. W. ..... p 4496 N94-37673
VANDERGRAFT, J. ..... p 4469 N94-36738
VANN, CHARLES S. ..... p 4524 N94-37112
VANWINSUM, W. ..... p 4484 N94-37267
VANWOLFFELAAR, P. C. ..... p 4484 N94-37267
VARSHNEY, PRAMOD K. ..... p 4434 N94-37183
VASSEL, A. ..... p 4401 N94-36657
VAUSE, CHESTER A., III ..... p 4514 N94-36964
VELSKO, S. P. ..... p 4447 N94-37114
p 4449 N94-37737
VERTOGRADOV, L. S. ..... p 4512 N94-36523
VERVISCH, L. ..... p 4410 N94-37222
VIANCO, P. T. ..... p 4464 N94-37071
VIGNALE, GIOVANNI ..... p 4516 N94-37109
VINITSKIJ, S. I. ..... p 4504 N94-37174
VINNINS, M. F. ..... p 4446 N94-36760
VISSERS, D. R. ..... p 4437 N94-37053
VITRIA, J. ..... p 4524 N94-37165
VO, VAN THUAN ..... p 4407 N94-36529
VOAS, JEFFREY M. ..... p 4491 N94-36498
VOLKOV, A. A. ..... p 4511 N94-36504
VOLLTRAUER, H. ..... p 4461 N94-36476
VONMAYRHAUSER, ANNELIESE ..... p 4490 N94-36490
VOSSNACK, OLE E. ..... p 4516 N94-37158
VU, B. T. V. ..... p 4530 N94-37392
VU, HOANG LAM ..... p 4414 N94-36541
VUKELICH, SHARON ..... p 4421 N94-37324
p 4454 N94-37327

W

WADA, YASUHIRO ..... p 4441 N94-36646
WAGNER, J. C. ..... p 4506 N94-36449
WAGNER, J. S. ..... p 4495 N94-37496
WAGNER, PATRICIA ..... p 4477 N94-36522
WAGNER, R. ..... p 4521 N94-36694
WAGNER, ROBERT ..... p 4430 N94-37768
WAHBE, ROBERT ..... p 4494 N94-37119
WAI, P. K. A. ..... p 4524 N94-37191
WALDMAN, JEFFREY ..... p 4401 N94-36658
WALIGORA, SHARON ..... p 4492 N94-36501
WALKER, DAVID E. ..... p 4500 N94-36736
WALKER, F. J. ..... p 4538 N94-37570
WALKER, H. ..... p 4473 N94-37242
WALKER, J. R. ..... p 4532 N94-36542
WALKER, J. W. ..... p 4521 N94-37220
WALLETT, THOMAS M. ..... p 4437 N94-36819
WALLING, R. S. ..... p 4530 N94-37437
WALTER, K. C. ..... p 4414 N94-36461
WALTER, MANFRED A. ..... p 4389 N94-36826
WAN, GANG ..... p 4412 N94-37533
WANG, A. S. D. ..... p 4459 N94-37807
WANG, C. H. ..... p 4423 N94-37144
p 4409 N94-37145
WANG, MING L. ..... p 4423 N94-37181
WANG, X. L. ..... p 4420 N94-37548
WANG, XIN-NIAN ..... p 4520 N94-37716
WANG, YUFENG ..... p 4516 N94-37152
WANG, YUN ..... p 4500 N94-36924
p 4500 N94-36928
WANG, Z. L. ..... p 4538 N94-37569
WARD, CLAY A. ..... p 4466 N94-37252
WARD, R. L. ..... p 4425 N94-37422
WARM, B. ..... p 4393 N94-36619
WARN, C. ..... p 4522 N94-37303
WARREN, DAVID ..... p 4396 N94-37257
WARREN, DAVID R. ..... p 4392 N94-37026
WAS, G. S. ..... p 4418 N94-37398
WASIELEWSKI, M. R. ..... p 4477 N94-36481
p 4512 N94-36524
p 4477 N94-36554
p 4478 N94-36555
WATANABE, K. ..... p 4526 N94-36472
WATANABE, S. ..... p 4477 N94-36554
WATERS, WILLIAM A. ..... p 4389 N94-36826
WATERS, WILLIAM M. ..... p 4440 N94-37840
WATRING, D. A. ..... p 4446 N94-36822
WATSON, A. T. ..... p 4436 N94-36532
WATSON, GORDON K. ..... p 4405 N94-37460
WATSON, JIM ..... p 4545 N94-37757
WAYNANT, RONALD W. ..... p 4440 N94-37775
WAYNER, P. C., JR. ..... p 4424 N94-37223
WAYNER, PETER C., JR. ..... p 4442 N94-36992
WEBB, WAYNE ..... p 4546 N94-36690
WEBSTER, R. T. ..... p 4414 N94-36543
WEINSTEIN, ROY ..... p 4439 N94-37634
WEIRUP, D. L. ..... p 4517 N94-37210
WEISSHAAR, J. C. ..... p 4409 N94-37168
WELCH, D. O. ..... p 4537 N94-37499
WELCH, SHARON S. ..... p 4447 N94-36946
WELLER, ROBERT A. ..... p 4476 N94-37047
p 4473 N94-37180
WEN, XI-MENG ..... p 4412 N94-37533
WENAUS, T. J. ..... p 4439 N94-37306
WENDT, J. R. ..... p 4436 N94-36557
WENDT, R. G. ..... p 4404 N94-37088
WENZEL, H. ..... p 4513 N94-36528
WERLEY, K. A. ..... p 4528 N94-37292
WESTMORELAND, P. R. ..... p 4408 N94-36735
p 4413 N94-37623
WESTPHAL, TODD L. ..... p 4475 N94-36958
WETHERHOLD, ROBERT C. ..... p 4406 N94-37633
WEY, CHANGLIE ..... p 4508 N94-36643
WHEAT, S. R. ..... p 4498 N94-37487
WHINNERY, L. L. ..... p 4428 N94-37202
WHITE, A. R. ..... p 4513 N94-36538
WHITE, J. M. ..... p 4413 N94-37713
WHITELEY, S. R. ..... p 4436 N94-36557
WHITEMAN, C. D. ..... p 4463 N94-36478
WHITMORE, STEPHEN A. ..... p 4383 N94-37378
WHITSON, PEGGY A. ..... p 4480 N94-36766
WHITTENBEGER, JOHN D. ..... p 4403 N94-36752
WHITTINGTON, DAVID H. ..... p 4387 N94-37658
WICKLUND, A. B. ..... p 4518 N94-37298
WIECEK, MALGORZATA M. ..... p 4495 N94-37539
WIEDERRECHT, G. P. ..... p 4477 N94-36554
p 4478 N94-36555
WIEMAN, CARL ..... p 4514 N94-37041
WIERDA, M. ..... p 4484 N94-37267
WIGREN, C. ..... p 4519 N94-37553
WILEY, ROGER W. ..... p 4485 N94-37278
WILKINS, DICK J. ..... p 4422 N94-36968
p 4459 N94-37803
WILLETT, J. C. ..... p 4473 N94-37217
WILLIAMS, F. A. ..... p 4409 N94-37221
p 4411 N94-37412
WILLIAMS, J. L. ..... p 4540 N94-37092
WILLIAMS, M. ..... p 4485 N94-37275
WILLIAMS, RONALD H. ..... p 4421 N94-37324
WILLIAMS, T. J. ..... p 4532 N94-37732
WILLIAMSON, D. L. ..... p 4533 N94-36745
WILLIAMSON, R. L. ..... p 4417 N94-37367
WILLIS, J. O. ..... p 4440 N94-37738
WILSON, A. L. ..... p 4464 N94-36994
p 4464 N94-36995
WILSON, C. C. ..... p 4532 N94-36548
WILSON, CHARLES E. ..... p 4385 N94-37830
p 4385 N94-37839
WILSON, F. W. ..... p 4472 N94-37126
WILSON, JOHN W. ..... p 4416 N94-36993
p 4481 N94-37282
WILSON, TIMOTHY M. ..... p 4400 N94-36651
WILT, THOMAS E. ..... p 4455 N94-36561
WINGERSKY, MARILYN S. ..... p 4506 N94-36728
WINICK, ROBERT M. ..... p 4390 N94-37424
WINOKUR, P. S. ..... p 4439 N94-37513
WINSTONE, M. R. ..... p 4402 N94-36661
WINTENBERG, A. L. ..... p 4521 N94-37220
WISE, J. L. ..... p 4405 N94-37627
WISE, STEPHANIE A. ..... p 4437 N94-36781
WITKOWSKI, W. ..... p 4408 N94-37091
WOLF, STUART A. ..... p 4440 N94-37769
WOLK, J. A. ..... p 4413 N94-37630
WOO, C. H. ..... p 4414 N94-36544
WOOD, B. P. ..... p 4414 N94-36461
WOOD, BERNARD J. ..... p 4412 N94-37462
WOODBURY, DALE T. ..... p 4394 N94-36625
WOODS, M. ..... p 4515 N94-37085
WORLEY, P. H. ..... p 4498 N94-37568
WORRALL, DIANA M. ..... p 4546 N94-36688
WRAY, RICHARD B. ..... p 4387 N94-36933
WRIGHT, D. M. ..... p 4439 N94-37306
WRIGHT, MICHAEL E. ..... p 4422 N94-37121
p 4423 N94-37133
p 4423 N94-37148
p 4423 N94-37151
p 4423 N94-37179
WROBLEWSKI, D. ..... p 4528 N94-37297
WU, F. ..... p 4506 N94-37852
WU, S. J. ..... p 4439 N94-37302
WU, S. T. ..... p 4549 N94-36469
WUEBBLES, DONALD J. ..... p 4465 N94-37155
WUEST, C. R. ..... p 4439 N94-37306
WYATT, TERRY ..... p 4392 N94-37026

X

XIA, JIULIN ..... p 4423 N94-37144
XIAO, Q.-F. ..... p 4525 N94-37258
XU, CHUAN-JING ..... p 4411 N94-37365
XU, CHUANJING ..... p 4409 N94-37161
XU, MING ..... p 4496 N94-37551

Y

YAGI, M. ..... p 4528 N94-37231
p 4531 N94-37485
p 4532 N94-37734
YAMADA, H. ..... p 4530 N94-37384
YAMADA, HIROKO ..... p 4512 N94-36524
YAMAGISHI, T. ..... p 4529 N94-37359
YAMAMOTO, Y. ..... p 4529 N94-37316
YAMAUCHI, MASANORI ..... p 4523 N94-37727
YAMAZAKI, SEIICHIROU ..... p 4531 N94-37484
YAMAZAKI, T. ..... p 4519 N94-37417
YAMILOV, R. I. ..... p 4507 N94-37062
YAN, Y. ..... p 4495 N94-37453
YANG, DA-ZHU ..... p 4412 N94-37534
YANG, N. Y. C. ..... p 4427 N94-37725
YASHAR, F. ..... p 4524 N94-37110
YAZKOV, V. V. ..... p 4515 N94-37075
YEH, EUENG-NAN ..... p 4475 N94-36958
YEH, L. ..... p 4508 N94-36560
YEN, W. M. ..... p 4538 N94-37676
YOON, SEOKKWAN ..... p 4504 N94-37449
YORKE, JAMES ..... p 4507 N94-37028
YOSHII, MASAHITO ..... p 4522 N94-37234
YOU, H. ..... p 4535 N94-37192
YOUNG, ANDREW J. ..... p 4481 N94-37136
YOUNG, B. K. F. ..... p 4530 N94-37437
YOUNG, C. ..... p 4522 N94-37303
YOUNG, HARRY J. ..... p 4450 N94-36839
YU,ZENG-LIANG ..... p 4479 N94-37535

Z

ZACHARY, D. S. ..... p 4518 N94-37364
ZADJURA, MONA ..... p 4396 N94-37257
ZAK, B. D. ..... p 4463 N94-36470
ZAKRAJSEK, J. J. ..... p 4450 N94-36953
ZAKRAJSEK, JAMES J. ..... p 4452 N94-37521
ZAMAN, AFROZ ..... p 4435 N94-37255
ZANEVSKIJ, YU. V. ..... p 4482 N94-37729

ZANNER, F. J. ..... p 4417 N94-37367
ZAPATA, L. E. ..... p 4449 N94-37722
ZAPOTOCNY, T. H. ..... p 4466 N94-37288
ZAPOTOSKY, J. E. ..... p 4481 N94-37353
ZELKOWITZ, MARVIN V. ..... p 4492 N94-36502
ZHADAMBA, B. ..... p 4516 N94-37097
p 4517 N94-37173
ZHANG, HONG ..... p 4495 N94-37539
ZHANG, WEI-BE ..... p 4412 N94-37534
ZHANG, X. Q. ..... p 4409 N94-37145
ZHANG, YAN-PING ..... p 4407 N94-36475
ZHAO, D. ..... p 4459 N94-37804
ZHENG, ZONG-SHUANG ..... p 4425 N94-37317
ZHONG, S. ..... p 4474 N94-37565
ZHONG, W. ..... p 4537 N94-37377
ZIMIN, S. ..... p 4530 N94-37464
ZINDER, STEPHEN H. ..... p 4479 N94-37434
ZON, G, D. R. ..... p 4484 N94-37272
ZONDLAK, R. J. ..... p 4407 N94-36482
ZSCHACK, P. ..... p 4535 N94-37212
ZWEBEN, CARL ..... p 4480 N94-37808

CORPORATE SOURCE INDEX

Typical Corporate Source Index Listing

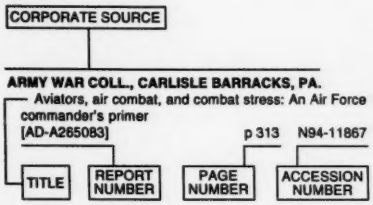

Listings in this index are arranged alphabetically by corporate source. The title of the document provides the user with a brief description of the subject matter. The report number helps to indicate the type of document cited (e.g., NASA report, translation, NASA contractor report). The accession number denotes the number by which the citation is identified. The page number helps you locate the citation in the abstract section. The titles are arranged under each corporate source in ascending accession number order.

A

ACADEMY OF SCIENCES OF THE UKRAINE, KIEV.
The asymptotics of matrix elements of Gaussian potential between the basis functions of three-dimensional harmonic oscillator
[DE94-618467] p 4539 N94-37079

ACADEMY OF SCIENCES (USSR), KIEV (USSR).
Representations of the q-deformed algebras U(q) (so(2,1)) and U(q) (so(3,1)
[DE94-616619] p 4505 N94-37483

ACADEMY OF SCIENCES (USSR), MOSCOW (USSR).
Collaboration in Crystallography: Proceedings of the 1st Joint Seminar of the ISIS-INCR Collaboration in Crystallography
[PB94-171097] p 4532 N94-36548
Composites based on titanium with external and internal reinforcement p 4401 N94-36654

ACADEMY OF SCIENCES (USSR), NOVOSIBIRSK (USSR).
Production of a positron and a bound electron by high-energy photon in a strong Coulomb field
[DE94-618501] p 4514 N94-36747
Methods of calculation of higher power corrections in QCD
[DE94-618511] p 4521 N94-36748
Introduction to the heavy quark effective theory, part 1
[DE94-618512] p 4514 N94-36749
Relaxation of the density matrix for an arbitrary spin in random external fields
[DE94-618457] p 4509 N94-37078
Determination of the upsilon(1s) leptonic width
[DE94-618534] p 4516 N94-37096
Wick-Cutkovsky model: An introduction
[DE94-618365] p 4504 N94-37170
XAFS-like structure of resonant Raman scattering
[DE94-618410] p 4517 N94-37171
Langmuir waves in the electron-positron plasma
[DE94-618779] p 4531 N94-37728

ACCELERATION CONSULTANTS, ALBUQUERQUE, NM.
BMAP dipole magnetic field analysis and orbit tracking/calculations of energy deposition in GaAs WHEBY detectors
[DE94-012080] p 4522 N94-37303

ACUREX CORP., MOUNTAIN VIEW, CA.
LNG vehicle technology, economics, and safety assessment
[PB94-165487] p 4450 N94-36721

ADVISORY GROUP FOR AEROSPACE RESEARCH AND DEVELOPMENT, NEUILLY-SUR-SEINE (FRANCE).
Pointing and Tracking Systems
[AGARD-CP-539] p 4392 N94-36616
Characterisation of Fibre Reinforced Titanium Matrix Composites
[AD-A2775206] p 4400 N94-36649
Virtual Interfaces: Research and Applications
[AGARD-CP-541] p 4482 N94-37261
Impact of Materials Defects on Engine Structures Integrity
[AGARD-R-790] p 4453 N94-37321
International High Speed Networks for Scientific and Technical Information
[AGARD-CP-544] p 4543 N94-37333
A guide to tenders and contracts alerting services
[AGARD-R-799] p 4540 N94-37447

AEA TECHNOLOGY, LONDON (ENGLAND).
UK methane emissions inventory: A scoping study on the use of ambient measurements to reduce uncertainties
[PB94-167855] p 4463 N94-36533
Processing of titanium matrix composites p 4401 N94-36653
Pre-standardisation work on fatigue and fracture testing of titanium matrix composites p 4402 N94-36667
Environmental risk management
[DE94-620987] p 4467 N94-37492

AEROJET DELFT CORP., AZUSA, CA.
Earth Observing System/Advanced Microwave Sounding Unit-A (EOS/AMSU-A) software management plan
[NASA-CR-189362] p 4461 N94-36919

AEROJET ELECTROSYSTEMS CO., AZUSA, CA.
Earth Observing System (EOS)/Advanced Microwave Sounding Unit A (AMSU-A) configuration management plan
[NASA-CR-189371] p 4494 N94-37061

AEROSPACE MEDICAL RESEARCH LABS., WRIGHT-PATTERSON AFB, OH.
Creation of a virtual world to study human spatial perception during sustained acceleration p 4484 N94-37268
Manual tracking performance using a virtual hand controller: A comparison study p 4484 N94-37271

AIR-CONDITIONING AND REFRIGERATION TECHNOLOGY INST., INC., ARLINGTON, VA.
Materials Compatibility and Lubricant Research on CFC-refrigerant substitutes
[DE94-012352] p 4425 N94-37373
Sealed tube comparisons of the compatibility of desiccants with refrigerants and lubricants
[DE94-012371] p 4425 N94-37421
Information on alternative refrigerants and lubricants: The ARTI refrigerant database
[DE94-009997] p 4426 N94-37490

AIR FORCE GEOPHYSICS LAB., HANSCOM AFB, MA.
Solar-Terrestrial Predictions, 4: Proceedings of aworkshop. Volume 3: Geomagnetic papers; ionospheric papers
[PB94-173192] p 4470 N94-37530
Solar-Terrestrial Predictions, 4: Proceedings of a workshop. Volume 1: Workshop overview papers; working group reports; User community reports; Regional Warning Center Reports
[PB94-173176] p 4471 N94-37780
Solar-Terrestrial Predictions, 4: Proceedings of a workshop. Volume 2: Solar papers; magnetospheric papers
[PB94-173184] p 4471 N94-37781

AIR FORCE INST. OF TECH., WRIGHT-PATTERSON AFB, OH.
Searching for plans using a hierarchy of learned macros and selective reuse
[AD-A280594] p 4499 N94-36722
Multirate time-frequency distributions
[AD-A280595] p 4503 N94-36723
Computational investigation of an improved cowl concept for hypersonic propulsive nozzles
[AD-A280596] p 4441 N94-36724
An aerodynamic and static-stability analysis of the Hypersonic Applied Research Technology (HART) missile
[AD-A280631] p 4382 N94-36729
Mixed H2/H-infinity optimization with multiple H infinity constraints
[AD-A280572] p 4388 N94-36733
H2 optimal control with H-infinity, mu, and L1 constraints
[AD-A280593] p 4500 N94-36736
A mean value analysis heuristic for analysis of aircraft sortie generation
[AD-A278578] p 4507 N94-36970
Global Picture Archiving and Communication Systems (GPACS): An overview
[AD-A280617] p 4543 N94-37042
Subgrouped real time recurrent learning neural networks
[AD-A280618] p 4500 N94-37043
The excitation mechanism of praseodymium-doped semiconductors
[AD-A280687] p 4535 N94-37129
Embedded chaotic time series: Applications in prediction and spatio-temporal classification
[AD-A280690] p 4508 N94-37130
Noise reduction for speech enhancement using non-linear wavelet processing
[AD-A280469] p 4434 N94-37141
A diffraction-based model of anisoplanatism effects in adaptive optic systems
[AD-A280491] p 4524 N94-37142
Calibration and initial testing of a new hydraulic simulator
[AD-A280632] p 4390 N94-37163
Design and analysis of a mode B and mode JD satellite Earth station
[AD-A280417] p 4391 N94-37225
Feature and model selection in feedforward neural networks
[AD-A280709] p 4501 N94-37526

AIR UNIV., MAXWELL AFB, AL.
Aircraft battle damage repair for the 1990's and beyond
[AD-A278635] p 4386 N94-36465

AKRON UNIV., OH.
Hierarchically parallelized constrained nonlinear solvers with automated substructuring
[NASA-CR-194474] p 4456 N94-37554

ALABAMA UNIV., HUNTSVILLE, AL.
A study of physical mechanisms for filament eruption and coronal mass ejection via numerical simulation
[NASA-CR-196087] p 4549 N94-36469
Spray combustion model improvement study, 1
[NASA-CR-196122] p 4410 N94-37250
Gamma ray astronomy
[NASA-CR-193970] p 4547 N94-37702

ALASKA UNIV., FAIRBANKS, AK.
Vent processes during the 1912 eruption at Novarupta, Katmai National Park, Alaska
[DE94-010740] p 4468 N94-36451

ALBANY INTERNATIONAL RESEARCH CORP., MANSFIELD, MA.
Flame resistant fibrous structures development
[NASA-CR-185700] p 4421 N94-36641

ALENIA AERONAUTICA, TURIN (ITALY).
Studies and simulations on sensor fusion and cueing for fighter application p 4395 N94-36632

ALLIANCE FOR TELECOMMUNICATIONS INDUSTRY SOLUTIONS, WASHINGTON, DC.
Network survivability performance
[AD-A278746] p 4433 N94-36756

Network survivability performance (computer diskette)
[AD-M000332] p 4433 N94-36757

ALLIED-SIGNAL AEROSPACE CO., KANSAS CITY, MO.
Replacement of silicone polymer A with silicone polymer B and the subsequent characterization of the new cellular silicone materials
[DE94-010105] p 4421 N94-36474

ALLISON ENGINE CO., INDIANAPOLIS, IN.
Advanced Turbine Technology Applications Project (ATTAP)
[NASA-CR-195367] p 4452 N94-37763

AMES LAB., IA.
Characterization of mechanical properties degradation using small punch testing technique
[DE94-011202] p 4418 N94-37410
Perfluorodiethoxymethane on nickel and nickel oxide surfaces
[DE94-011200] p 4426 N94-37712

ARGONNE NATIONAL LAB., IDAHO FALLS, ID.
Characterization of nuclear transmutations in materials irradiated test facilities
[DE94-013309] p 4420 N94-37552

ARGONNE NATIONAL LAB., IL.
Using Gopher on the Internet
[DE94-009736] p 4497 N94-36441
Rescaled box counting for the topological analysis of spatial data
[DE94-009820] p 4461 N94-36464
Femtosecond transient absorption studies of the light harvesting Chl a/b protein complex of Photosystem 2 in higher plants
[DE94-009684] p 4477 N94-36481
Deep inelastic scattering results from the first year of HERA operation
[DE94-004578] p 4511 N94-36483
CP violation outside the standard model phenomenology for pedestrians
[DE94-002216] p 4511 N94-36512
Physics Division annual review, 1 April 1992 - 31 March 1993
[DE94-002497] p 4512 N94-36513
Picosecond laser induced electric field modulation of carotenoid absorption bands
[DE94-009692] p 4512 N94-36524
Summary of the extensions of the Standard Model working group
[DE94-002217] p 4512 N94-36527
The Pomeron and Quantum Chromodynamics (QCD) with many light quarks
[DE94-001351] p 4513 N94-36538
Solvent effects on the energetics and dynamics of ultrafast electron transfer in chlorophyll-porphyrin-acceptor triads
[DE94-009693] p 4477 N94-36554
Femtosecond transient grating studies of electron transfer in porphyrin and chlorophyll donor-acceptor molecules
[DE94-009694] p 4478 N94-36555
High Energy Physics Division of research activities
[DE93-019681] p 4521 N94-36694
Forward scattering of neutrons from polymeric and magnetic multilayers
[DE93-041158] p 4513 N94-36696
A possible origin of EL6 chondrites from a high temperature-high pressure solar gas
[DE94-010467] p 4548 N94-36759
Sodium/nickel-chloride battery development
[DE94-011481] p 4437 N94-37053
Quadrupolar effects in PrCu2Si2
[DE94-011509] p 4534 N94-37054
Scoping economics for the commercial manufacture of metallocene catalysts
[DE94-011526] p 4422 N94-37055
Turning soot into diamonds with microwaves
[DE94-013426] p 4422 N94-37068
Comparison of the crystal structure and molecular models of N,N-diisobutyl-2- (octylphenylphosphinyl) acetamide (CMPO)
[DE94-013434] p 4534 N94-37069
Potential benefits of oxygen-enriched intake air in a vehicle powered by a spark-ignition engine
[DE94-013452] p 4451 N94-37070
The potential for control of carbon dioxide emissions from integrated gasification/combined-cycle systems
[DE94-012646] p 4465 N94-37100
Fabrication and properties of Ag-clad Bi-2223 conductors and magnets
[DE94-011502] p 4438 N94-37111
Simulation of three-dimensional multi-phase flow characteristics in the deswirl section of the CDIF MHD power train
[DE94-012644] p 4443 N94-37176
Substrate effects on the structure and optical properties of epitaxial PbTiO3 thin films prepared by metal-organic chemical vapor deposition
[DE94-010432] p 4535 N94-37192
Superconducting TlCa2Ba2Cu3O9 thick films
[DE94-010436] p 4535 N94-37193
An overview of the current status of resonance theory in reactor physics applications
[DE94-010465] p 4521 N94-37194
A two-level formal specification of a defense communications system
[DE94-012117] p 4434 N94-37206
The impact of HPF data layout on the design of efficient and maintainable parallel linear algebra libraries
[DE94-012382] p 4504 N94-37246
Automatic, self-adaptive control of unfold transformations
[DE94-012455] p 4504 N94-37247
Time-of-flight pulsed ion beam surface analysis as a means of in situ, real-time characterization of the growth of ferro-electric and conductive oxide heterostructures
[DE94-012628] p 4517 N94-37249
Activities of the Chemical Technology Division
[DE94-013050] p 4410 N94-37357
Melt-processing of Y-Ba-Cu-O superconductors for improved levitation
[DE94-011503] p 4537 N94-37377
Analytical electron microscopy examination of solid reaction products in long-term test of SRL 200 waste glasses
[DE94-005482] p 4411 N94-37380
Site Scientific Mission Plan for the Southern Great Plains CART site, January - June 1994
[DE94-012114] p 4474 N94-37394
Development of nondestructive evaluation methods and prediction of effects of flaws on the fracture behavior of structural ceramics
[DE94-012466] p 4425 N94-37423
Evaluation of parameterizations for pollutant transport and dispersion in an urban street canyon using a three-dimensional dynamic flow model
[DE94-012641] p 4467 N94-37429
Photochemistry without protons. Radical cation chemistry in zeolites
[DE94-012631] p 4412 N94-37439
Modeling atmospheric concentrations and deposition of Hg
[DE94-012633] p 4467 N94-37440
Transient thermal and dynamic stresses in strongback-design blankets
[DE94-012639] p 4530 N94-37441
Development of intermetallic coatings for fusion power applications
[DE94-012647] p 4419 N94-37442
Study of Japanese electrodynamic-suspension maglev systems
[DE94-011486] p 4452 N94-37515
Scanning x-ray diffraction: A technique with high compositional resolution for studying phase formation in co-deposited thin films
[DE94-011496] p 4420 N94-37516
Magnetic and structural instabilities of ferromagnetic and antiferromagnetic Fe/Cu(100)
[DE94-011504] p 4509 N94-37517
Parallel tridiagnoalization through two-step band reduction
[DE94-011512] p 4505 N94-37518
A scalable high-performance I/O system
[DE94-011513] p 4498 N94-37519
Unstable solitary-wave solutions of the generalized Benjamin-Bona-Mahony equation
[DE94-013302] p 4496 N94-37549
Electron-transfer reactions involving two harmonic potentials with a different force constant: The Zusman approach versus the spin-boson model
[DE94-013306] p 4519 N94-37550
A compilation system that integrates high performance FORTRAN and FORTRAN M
[DE94-013308] p 4496 N94-37551
Laser cooling of 24Mg+ in the ASTRID storage ring
[DE94-010445] p 4523 N94-37619
A nonconservative scheme for isentropic gas dynamics
[DE94-011488] p 4445 N94-37724
A graphic view of Geometric Dimensioning and Tolerancing
[DE94-011478] p 4435 N94-37736

ARIZONA UNIV., TUCSON, AZ.
Ultraviolet spectropolarimetry of high redshift quasars with the Hubble Space Telescope
[NASA-CR-196014] p 4546 N94-36690

ARMY AEROMEDICAL RESEARCH LAB., FORT RUCKER, AL.
Visual accommodation to virtual image displays when knowledge of object distance conflicts with optical distance p 4485 N94-37278

ARMY ARMAMENT RESEARCH, DEVELOPMENT AND ENGINEERING CENTER, WATERVLIET, NY.
Chromium/molybdenum alloy plating. Part 1: The electrodeposition of low contraction chromium/molybdenum alloys using unipolar (on/off) pulse plating
[AD-A280236] p 4417 N94-37138

ARMY AVIATION SYSTEMS COMMAND, HAMPTON, VA.
Navier-Stokes and potential theory solutions for ahelicopter fuselage and comparison with experiment
[NASA-TM-4566] p 4383 N94-36966

ARMY CONSTRUCTION ENGINEERING RESEARCH LAB., CHAMPAIGN, IL.
Evaluation of flame-sprayed polymer coatings for civil works navigation structures
[AD-A280507] p 4422 N94-37104
Understanding and managing power system harmonics
[AD-A280627] p 4440 N94-37759

ARMY PERSONNEL RESEARCH ESTABLISHMENT, FARNBOROUGH (ENGLAND).
Some side-effects of immersion virtual reality
p 4482 N94-37277

ARMY RESEARCH INST. OF ENVIRONMENTAL MEDICINE, NATICK, MA.
Homeostatic responses to prolonged cold exposure: Human cold acclimatization
[AD-A280234] p 4481 N94-37136

ARMY RESEARCH LAB., WATERTOWN, MA.
Processing, packaging, and characterization of electroceramic materials for phased array antennas
[AD-A280251] p 4432 N94-36743
Thermomechanical studies of tungsten heavy alloys
[AD-A280250] p 4417 N94-37122

ARMY VEHICLE STRUCTURES LAB., HAMPTON, VA.
Optimization for minimum sensitivity to uncertain parameters
[NASA-TM-109139] p 4386 N94-37256
Sub-ply level scaling approach investigated for graphite-epoxy composite beam columns
p 4458 N94-37798
Damage and strength of composite materials: Trends, predictions, and challenges p 4459 N94-37805

ATLANTIC RESEARCH CORP., GAINESVILLE, VA.
NASA reload program
[NASA-CR-193972] p 4429 N94-37446

ATMOSPHERIC AND ENVIRONMENTAL RESEARCH, INC., CAMBRIDGE, MA.
Accelerated line-by-line calculations for the radiative transfer of trace gases related to climate studies
[DE94-004404] p 4464 N94-36552

ATOMIC ENERGY COMMISSION, DAMASCUS (SYRIA).
Irradiation effects in Fe-30 percent Ni alloy during Ar ion implantation
[DE94-619057] p 4415 N94-36564

ATOMIC ENERGY OF CANADA LTD., CHALK RIVER (ONTARIO).
Phase transitions in crystalline solids 1
[DE94-619029] p 4532 N94-36542
Mitigation of harmful effects of welds in zirconium alloy components
[DE94-619033] p 4414 N94-36543
Modelling irradiation creep of zirconium alloys
[DE94-619055] p 4414 N94-36544
Precipitation in Zr-2.5 Nb enhanced by proton irradiation
[DE94-619056] p 4415 N94-36563
An externally heated copper vapour laser
[DE94-619484] p 4447 N94-36565

ATOMIC ENERGY ORGANIZATION OF IRAN, TEHERAN.
Abstracts of 2nd International Conference on Lasers and their Applications
[DE94-617409] p 4448 N94-37169

B

BETTIS ATOMIC POWER LAB., PITTSBURGH, PA.
A coarse-mesh nodal method-diffusive-mesh finite difference method
[DE94-010809] p 4502 N94-36455
Irradiation assisted stress corrosion cracking of HTH Alloy X-750 and Alloy 625
[DE94-012667] p 4416 N94-37080

BIO EN-GENE-ER ASSOCIATES, INC., WILMINGTON, DE.
Opportunities for innovation: Biotechnology
[PB94-157831] p 4478 N94-36720

BIRMINGHAM UNIV. (ENGLAND).
First results from a prototype level-1 calorimeter trigger system for LHC, RD 27 (UK) collaboration
[PB94-167475] p 4436 N94-36532
Crack growth under cycle loading in fibre reinforced titanium metal matrix composites p 4402 N94-36665

BOEING CO., SEATTLE, WA.
New plasma source of hydrides for epitaxial growth
[DE94-006918] p 4533 N94-36744
BOEING COMMERCIAL AIRPLANE CO., SEATTLE, WA.
World jet airplane inventory at year-end 1993
[PB94-164993] p 4384 N94-36530
Stratospheric emissions effects database development
[NASA-CR-4592] p 4467 N94-37607
Synthetic vision display evaluation studies
[NASA-CR-194963] p 4387 N94-37658
Aircraft command in emergency situations prototype development users manual
[DOT/FAA/CT-94/24] p 4385 N94-37706
BOEING DEFENSE AND SPACE GROUP, PHILADELPHIA, PA.
A comparison of graphite/epoxy tape laminates and 2-D braided composites mechanical properties
[NASA-CR-4610] p 4420 N94-37582
BOEING DEFENSE AND SPACE GROUP, SEATTLE, WA.
Evaluation of seals and lubricants used on the Long Duration Exposure Facility
[NASA-CR-4604] p 4399 N94-37614
BOSTON UNIV., MA.
An error-resistant linguistic protocol for air traffic control
[NASA-CR-196098] p 4385 N94-37013
Segment-based acoustic models for continuous speech recognition
[AD-A280332] p 4434 N94-37032
BRITISH AEROSPACE AIRCRAFT GROUP, BRISTOL (ENGLAND).
A comparison of two examples of magnetic tracker systems p 4485 N94-37275
BRITISH AEROSPACE DEFENCE LTD., PRESTON (ENGLAND).
Sensor data fusion for air to air situation awareness beyond visual range p 4395 N94-36633
BRITISH COLUMBIA UNIV., VANCOUVER.
Alternate melting and refining routes
p 4421 N94-37323
BRITISH PETROLEUM CO. LTD., SUNBURY-ON-THAMES (ENGLAND).
Manufacture and properties of sigma fibre reinforced titanium p 4401 N94-36655
BROOKHAVEN NATIONAL LAB., UPTON, NY.
The E2/M1 mixing ratio in the excitation of the Delta from polarized photo-reactions
[DE94-004235] p 4510 N94-36442
High baryon density from relativistic heavy ion collisions
[DE94-003894] p 4511 N94-36460
The t(anti t)(gamma) background to pp (yields) W(gamma) + X at the SSC
[DE94-001386] p 4512 N94-36526
Effective Lagrangian for gluons and Higgs pseudoscalars
[DE94-001381] p 4513 N94-36539
Dipole forbidden vibrational modes for NO and CO on Cu observed in the far IR
[DE94-003199] p 4408 N94-36559
Production of phi mesons in central Si+Au collisions at 14.6 A GeV/c
[DE94-011726] p 4516 N94-37152
Interfaces of high-protection performance polyaryls-coated zinc phosphated steels
[DE94-011732] p 4417 N94-37153
Tune modulation due to gradient ripple and the dynamic aperture
[DE94-011922] p 4524 N94-37157
Kaon correlation systematics in E859
[DE94-011927] p 4516 N94-37158
Guiding hard x rays with glass polycapillary fiber
[DE94-004949] p 4525 N94-37258
Comparison of oxygen and silicon induced reactions at 14.6 A(GeV/C)
[DE94-011923] p 4518 N94-37364
Arterial cross-section measurements from dual energy transvenous coronary angiography images
[DE94-011193] p 4482 N94-37444
Preliminary soft x ray studies of beta-SiC
[DE94-013023] p 4537 N94-37498
Positron implantation in solids
[DE94-013029] p 4537 N94-37499
Search for the H dibaryon by Xi(-) capture on the deuteron
[DE94-011733] p 4520 N94-37672
Symplectic tracking using point magnets and a reference orbit made of circular arcs and straight lines
[DE94-011919] p 4505 N94-37675
BULGARIAN ACADEMY OF SCIENCES, SOFIA.
Data compatibility for various Charpy-tests
[DE94-617534] p 4416 N94-37074

C

CAE ELECTRONICS LTD., SAINT LAURENT (QUEBEC).
Training and operations support system (TOPS)
p 4545 N94-37344
CALIFORNIA UNIV., BERKELEY, CA.
Josephson acoustic radiation in superfluid helium
[AD-A280208] p 4533 N94-36742
CALIFORNIA UNIV., BERKELEY. LAWRENCE BERKELEY LAB, CA.
Quantum harmonic Brownian motion in a general environment: A modified phase-space approach
[DE94-003249] p 4508 N94-36560
Electroweak physics at the Tevatron collider
[DE93-040927] p 4513 N94-36695
Absolute limit on rotation of gravitationally bound stars
[DE94-011367] p 4548 N94-37049
Large-scale three-dimensional geothermal reservoir simulation on PC's
[DE94-011374] p 4443 N94-37050
Nonlinear optical spectroscopy for surface studies
[DE94-011623] p 4408 N94-37056
High resolution electron diffraction analysis of structural changes associated with the photocycle of bacteriorhodopsin
[DE94-011800] p 4479 N94-37156
Recovering depth from focus using iterative image estimation techniques
[DE94-010994] p 4524 N94-37165
Some effects of heat release in premixed flames
[DE94-011346] p 4409 N94-37199
Suppression of beam-break-up in a standing wave free electron laser two-beam accelerator
[DE94-011348] p 4521 N94-37200
Development of low dielectric constant alumina-based ceramics for microelectronic substrates
[DE94-011360] p 4439 N94-37302
The Mesozoic Era of relativistic heavy ion physics and beyond
[DE94-011341] p 4548 N94-37557
Strangeness and the quark-gluon plasma: An experimenter's perspective
[DE94-011377] p 4519 N94-37558
Laser probing of interfaces
[DE94-011300] p 4449 N94-37628
Optical spectroscopy of a nitrogen-hydrogen complex in ZnSe
[DE94-011622] p 4413 N94-37630
Hadron production in S+nucleus collisions at 200 GeV/nucleon
[DE94-011344] p 4520 N94-37715
Pre-equilibrium parton dynamics: Proceedings
[DE94-011347] p 4520 N94-37716
The spin observables of electron-nucleon scattering from the formalism of nucleon-nucleon scattering
[DE94-011368] p 4520 N94-37717
A Lagrangian-Eulerian finite element method with adaptive gridding for advection-dispersion problems
[DE94-011372] p 4506 N94-37718
A note on analytic recovery of transition probabilities in three dimensional diffuse tomography
[DE94-011378] p 4506 N94-37719
Fast beam studies of free radical photodissociation
[DE94-011380] p 4521 N94-37720
CALIFORNIA UNIV., DAVIS, CA.
Fault tolerance in opto-electronic computing
[AD-A280219] p 4453 N94-37150
Initial studies of reflectometer for ITER
[DE94-012476] p 4528 N94-37167
Superacid catalysis of light hydrocarbon conversion
[DE94-011132] p 4411 N94-37431
CALIFORNIA UNIV., LA JOLLA, CA.
Guaranteed time observations support for Faint Object Spectrograph (FOS) on HST
[NASA-CR-196305] p 4547 N94-37037
CALIFORNIA UNIV., LOS ANGELES, CA.
An investigation of solar wind effects on the evolution of the Martian atmosphere
[NASA-CR-193424] p 4549 N94-37012
CALIFORNIA UNIV., SAN DIEGO, LA JOLLA, CA.
H infinity control for nonlinear and linear systems
[AD-A280450] p 4494 N94-37226
CALIFORNIA UNIV., SANTA BARBARA, CA.
Combined atomic force and scanning reflection interference contrast microscopy
[AD-A280341] p 4514 N94-37034
A new, optical-lever based atomic force microscope
[AD-A280524] p 4524 N94-37110
Solving ill-conditioned matrix equations in control
[AD-A280502] p 4503 N94-37146
CALSPAN-BUFFALO UNIV. RESEARCH CENTER, NY.
Experimental measurements and analytical analysis related to gas turbine heat transfer. Part 1: Time-averaged heat-flux and surface-pressure measurements on the vanes and blades of the SSME fuel-side turbine and comparison with prediction. Part 2: Phase-resolved surface-pressure and heat-flux measurements on the first blade of the SSME fuel-side turbine
[NASA-CR-196296] p 4442 N94-36969
CALSPAN CORP., ARNOLD AFS, TN.
Strength evaluation of socket joints
[NASA-CR-4608] p 4389 N94-37259
CANADA INST. FOR SCIENTIFIC AND TECHNICAL INFORMATION, OTTAWA (ONTARIO).
Electronic document delivery: Towards the virtual library p 4544 N94-37340
CARNEGIE-MELLON UNIV., PITTSBURGH, PA.
A survey of commonly applied methods for software process improvement
[AD-A278595] p 4493 N94-36974
Adaptable binary programs
[AD-A280243] p 4494 N94-37119
CASE WESTERN RESERVE UNIV., CLEVELAND, OH.
Theoretical studies of the transport properties in compound semiconductors
[NASA-CR-196109] p 4439 N94-37501
CENTRE D'ESSAIS EN VOL, BRETIGNY-SUR-ORGE (FRANCE).
Gaze orientation under G(z)-load. Methodological aspects: Preliminary results p 4485 N94-37274
CENTRE D'ETUDES DE LA NAVIGATION AERIENNE, TOULOUSE (FRANCE).
Assistance in instruction and training of air traffic controllers p 4483 N94-37265
CENTRE D'ETUDES ET DE RECHERCHES DE MEDECINE AEROSPATIALE, BRETIGNY SUR ORGE (FRANCE).
3D sound experimental approach: Methodology and preliminary results p 4486 N94-37280
CENTRE EUROPEEN RECHERCHE ET DE FORMATION ADVANCE EN CALCUL SCIENTIFIC, TOULOUSE (FRANCE).
Porting industrial codes and developing sparse linear solvers on parallel computers
[PB94-170503] p 4497 N94-36547
CENTRE NATIONAL DE LA RECHERCHE SCIENTIFIQUE, MARSEILLES (FRANCE).
Postural strategies for the continuous control of static and dynamic balance in man
[PB94-184678] p 4487 N94-37812
CENTRE TECHNIQUE DES INDUSTRIES MECANIQUES, SAINT ETIENNE (FRANCE).
Strategic choices in surface treatments
[PB94-170669] p 4414 N94-36534
COLEMAN RESEARCH CORP., COLUMBIA, MD.
Geophysical data fusion for subsurface imaging
[DE94-000056] p 4469 N94-36738
CHICAGO UNIV., CHICAGO, IL.
Bond selective chemistry beyond the adiabatic approximation
[DE94-012486] p 4408 N94-37095
CDF results on electroweak physics
[DE94-011750] p 4520 N94-37674
CHINA NUCLEAR INFORMATION CENTRE, BEIJING (CHINA).
The determination of hydrogen in sodium by vacuum extraction
[DE94-620278] p 4412 N94-37533
Study on extraction behavior of TRPO with different composition
[DE94-620287] p 4412 N94-37534
Studying of ion implantation effect on the biology in China
[DE94-620692] p 4479 N94-37535
CHRISTOPHER NEWPORT COLL., NEWPORT NEWS, VA.
Prospective communications research to support fly by light/power by wire
[NASA-CR-196369] p 4526 N94-37657
CINCINNATI UNIV., OH.
Design of scaled down structural models
p 4457 N94-37797
CLEMSON UNIV., SC.
Process simulation and modeling for advanced intermetallic alloys
[AD-A280327] p 4416 N94-37030
Development of high Tc (greater than 100 K) Bi, Tl and Y-based materials as superconducting circuit elements
[NASA-CR-196276] p 4534 N94-37103
COASTAL ENGINEERING RESEARCH CENTER, VICKSBURG, MS.
Index and bulk parameters for frequency-direction spectra measured at CERC Field Research Facility, September 1992 to August 1993
[AD-A280233] p 4476 N94-37135

Index and bulk parameters for frequency-direction spectra measured at CERC Field Research Facility, September 1990 to August 1991
[AD-A280423] p 4476 N94-37216
Index and bulk parameters for frequency-direction spectra measured at CERC Field Research Facility, September 1991 to August 1992
[AD-A280455] p 4477 N94-37229

COLORADO SCHOOL OF MINES, GOLDEN, CO.
Elimination of numerical dispersion in finite-difference modeling and migration by flux-corrected transport
[DE94-004159] p 4510 N94-36551
Small-angle x ray scattering studies of microvoids in amorphous-silicon-based semiconductors
[DE94-006931] p 4533 N94-36745
Mechanical performance of austempered ductile iron
[AD-A280452] p 4420 N94-37758

COLORADO STATE UNIV., FORT COLLINS, CO.
Assessing efficiency of software production for NASA-SEL data p 4490 N94-36490
Dioxacycloalkanes as models for the formation of hydrocarbons from surface methylenes
[DE94-011211] p 4413 N94-37754
Characteristics of ions emitted from high-current hollow cathodes
[NASA-CR-195372] p 4398 N94-37764

COLORADO UNIV., BOULDER, CO.
A transient FETI methodology for large-scale parallel implicit computations in structural mechanics, part 2
[NASA-CR-194823] p 4497 N94-36503
Turbulent transfer in the marine planetary boundary layer
[AD-A280549] p 4476 N94-37038
Spontaneous force optical traps
[AD-A280574] p 4514 N94-37041

COMMUNICATIONS RESEARCH CENTRE, OTTAWA (ONTARIO).
VHF adaptive antenna development task
[AD-A280320] p 4434 N94-37127

COMPUTATIONAL MECHANICS CO., KNOXVILLE, TN.
An arbitrary grid CFD algorithm for configuration aerodynamics analysis. Volume 1: Theory and validations
[NASA-CR-195918] p 4493 N94-36914
An arbitrary grid CFD algorithm for configuration aerodynamics analysis. Volume 2: FEMNAS user guide
[NASA-CR-196135] p 4493 N94-36922

COMPUTER SCIENCES CORP., GREENBELT, MD.
Proceedings of the Eighteenth Annual Software Engineering Workshop
[NASA-CR-189348] p 4489 N94-36484

COMPUTER TECHNOLOGY ASSOCIATES, INC., HAMPTON, VA.
Characterization of spacecraft and environmental disturbances on a SmallSat
[NASA-CR-194915] p 4396 N94-36990

CONDUCTUS, INC., SUNNYVALE, CA.
Submillimeter quasioptical Josephson junction oscillator with integrated tuning elements
[AD-A280380] p 4534 N94-37036

CONSEJO SUPERIOR DE INVESTIGACIONES CIENTIFICAS, MADRID (SPAIN).
Bulletin boards, electronic mail, conferencing, current use by scientists and engineers: Effects on libraries and information centres: Do they have a role?
p 4544 N94-37343

CORNELL UNIV., ITHACA, NY.
Effects of freezing and cold acclimation on the plasma membrane of isolated protoplasts
[DE94-012487] p 4479 N94-37248
Conversion of acetic acid to methane by thermophiles
[DE94-012478] p 4479 N94-37434
Studies of the III-V compounds in the megabar regime
[DE94-012488] p 4537 N94-37435
Statistical scaling relationships and size effects in the strength and creep rupture of fibrous composites
p 4460 N94-37809

CREARE, INC., HANOVER, NH.
Preliminary design for a reverse Brayton cycle cryogenic cooler
[NASA-CR-189341] p 4461 N94-36805

D

DAYTON UNIV., OH.
Operations and support cost modeling of conceptual space vehicles
[NASA-CR-196299] p 4397 N94-37580

DAYTON UNIV. RESEARCH INST., OH.
Methodologies for thermal and mechanical testing of TMC materials p 4401 N94-36659
Ultrasonic nondestructive characterization methods for the development and life prediction of titanium matrix composites p 4401 N94-36660

DEFENCE RESEARCH AGENCY, FARNBOROUGH, HAMPSHIRE (ENGLAND).
Metal matrix composites: Analysis of simple specimens and model components under creep and fatigue loading
p 4402 N94-36661
The DRA Virtual Cockpit Research Program
p 4484 N94-37269
Defects and their effects on the integrity of nickel based aeroengine discs p 4421 N94-37328

DEFENCE RESEARCH ESTABLISHMENT OTTAWA, OTTAWA (ONTARIO).
Radar tracking in multipath: Techniques for improved performance p 4395 N94-36631
Laboratory evaluation of the Standard Elektrik Lorenz (SEL) fibre-optic rate gyroscope
[AD-A280191] p 4446 N94-36760
Array element gain and phase estimation in the presence of interference
[AD-A280381] p 4434 N94-37162

DEFORMATION CONTROL TECHNOLOGY, INC., CLEVELAND, OH.
Modeling of thermal barrier coatings
[NASA-CR-195365] p 4421 N94-36637

DELAWARE UNIV., NEWARK, DE.
Superacid catalysis of light hydrocarbon conversion
[DE94-011132] p 4411 N94-37431
On nature's scaling effects p 4459 N94-37803

DEPARTMENT OF ENERGY, WASHINGTON, DC.
Alternative fuel information: Facts about CNG and LPG conversion
[DE94-006888] p 4429 N94-37402
Alternative fuel information: Glossary
[DE94-006889] p 4429 N94-37403
Alternative fuel information: State alternative fuel laws and incentives
[DE94-006892] p 4429 N94-37404
Proceedings of the Third Atmospheric Radiation Measurement (ARM) Science Team Meeting
[DE94-011194] p 4467 N94-37454
The integrated performance evaluation program quality assurance guidance in support of EM environmental sampling and analysis activities
[DE94-013043] p 4468 N94-37731

DEPARTMENT OF THE NAVY, WASHINGTON, DC.
Two-micron modelocked laser system
[AD-D016219] p 4448 N94-37481
Carborane-siloxane or silane-unsaturated hydrocarbon based polymers
[AD-D016220] p 4425 N94-37482
Chemiluminescent microemulsions
[AD-D016292] p 4413 N94-37761
Dual valve plate two-way pressure relief valve
[AD-D016293] p 4452 N94-37766
Canopy breaking device
[AD-D016294] p 4385 N94-37767
Interferometric JFTOT tube deposit measuring device
[AD-D016295] p 4430 N94-37768
Microwave detection of a superconducting infrared sensor
[AD-D016297] p 4440 N94-37769
Implanting impurities in semiconductors and semiconductor implanted with impurities
[AD-D016298] p 4538 N94-37770
MTI compatible coherent sidelobe canceller
[AD-D016300] p 4435 N94-37771
Holmium quasi-two level laser
[AD-D016302] p 4449 N94-37772
Fluorinated resins with low dielectric constant
[AD-D016303] p 4427 N94-37773
Method of forming waveguides with ion exchange of halogen ions
[AD-D016304] p 4526 N94-37774
Time-gated imaging through defense-scattering materials using stimulated Raman amplification
[AD-D016305] p 4440 N94-37775
High T(sub c) copper-oxide superconductors comprising Tl-Sr-Ca-Cu-O
[AD-D016307] p 4538 N94-37776
Intracavity-pumped 2.1 micrometer Ho(3+):YAGl aser
[AD-D016308] p 4449 N94-37777
Synthesis of phthalonitrile resins containing ether and imide linkages with aromatic diamine curing agent
[AD-D016309] p 4427 N94-37778
Substituted silyl-terminated compounds and polymers thereof
[AD-D016310] p 4427 N94-37779
Carborane-(silane or siloxane)-unsaturated hydrocarbon based thermosetting polymers
[AD-D016311] p 4427 N94-37818
Surface modification of polymers with self-assembled monolayers that promote adhesion, outgrowth and differentiation of biological cells
[AD-D016321] p 4427 N94-37829
Marker beacon case
[AD-D016322] p 4385 N94-37830
Double network elastomers and method of making same
[AD-D016323] p 4427 N94-37831
Crosspoint analog data selector
[AD-D016326] p 4440 N94-37832
Wavefront simulator for evaluating RF communication array signal processors
[AD-D016281] p 4436 N94-37835
Diode-pumped, continuously tunable, 2.3 micron CW laser specification
[AD-D016312] p 4450 N94-37838
System for broadcasting marker beacon signals and processing responses from seeking entities
[AD-D016313] p 4385 N94-37839
Phase shifter for directly sampled bandpass signals
[AD-D016320] p 4440 N94-37840

DEUTSCHE FORSCHUNGS- UND VERSUCHSANSTALT FUER LUFT- UND RAUMFAHRT, COLOGNE (GERMANY).
Properties of TMC processed by fibre coating and hiping p 4401 N94-36656

DIEHL G.M.B.H. UND CO., ROETHENBACH (GERMANY).
Pointing and tracking concept for a high energy laser weapon application p 4393 N94-36619

DIRECTION DES RECHERCHES, ETUDES ET TECHNIQUES, PARIS (FRANCE).
The 1st International Symposium on Organic Photochromism: Molecules and Systems
[PB94-179488] p 4399 N94-37531

DIVISION LTD., ALMONDSBURY, BRISTOL (ENGLAND).
Virtual reality evolution or revolution
p 4484 N94-37270

DORNIER-WERKE G.M.B.H., FRIEDRICHSHAFEN (GERMANY).
Landing of an unmanned helicopter on a moving platform. High accuracy navigation and tracking
p 4387 N94-36618

DOW CORNING CORP., CARROLLTON, KY.
Methyl chloride via oxyhydrochlorination of methane
[DE94-010691] p 4406 N94-36450

DRAPER (CHARLES STARK) LAB., INC., CAMBRIDGE, MA.
Inertial pseudo star reference unit
p 4394 N94-36625
Advanced information processing system: The Army Fault-Tolerant Architecture detailed design overview
[NASA-CR-194924] p 4497 N94-36962
Advanced information processing system: Authentication protocols for network communication
[NASA-CR-194923] p 4498 N94-37500
Advanced information processing system: Hosting of advanced guidance, navigation and control algorithms on AIPS using ASTER
[NASA-CR-194960] p 4499 N94-37583

DREXEL UNIV., PHILADELPHIA, PA.
Scaling effects of defects in fiber-reinforced composites p 4459 N94-37807

DUKE UNIV., DURHAM, NC.
Novel carbon-ion fuel cells
[DE94-010716] p 4461 N94-36511

DUNCAN TECHNOLOGIES, INC., NEWCASTLE, CA.
Structural composite construction materials manufactured from municipal solid waste
[AD-A280635] p 4403 N94-36730

E

E-SYSTEMS, INC., GREENVILLE, TX.
SOFIA: Aircraft system, aft telescope cavity configuration, phase 2. Volume 1: Executive summary
[NASA-CR-196362] p 4546 N94-36642

EAST CAROLINA UNIV., GREENVILLE, NC.
Evaluation of dried storage of platelets for transfusion: Physiologic integrity and hemostatic functionality
[AD-A280665] p 4480 N94-36764

EDGERTON, GERMESHAUSEN AND GRIER, INC., ALBUQUERQUE, NM.
Blast overpressure studies with animals and man
[AD-A280240] p 4480 N94-37118

EDGERTON, GERMESHAUSEN AND GRIER, INC., IDAHO FALLS, ID.
Four beam interferometer manual: Operating instructions for the INEL diffraction Moire interferometer
[DE94-010772] p 4453 N94-36452
Molecular beam surface analysis
[DE94-010773] p 4406 N94-36453

EDUCATIONAL TESTING SERVICE, PRINCETON, NJ.
Dealing with uncertainty about item parameters: Expected response functions
[AD-A280610] p 4506 N94-36728
Probability-based inference in cognitive diagnosis
[AD-A280553] p 4506 N94-36732
Virtual representation of IID observations in Bayesian belief networks
[AD-A280552] p 4507 N94-37046

EG AND G ENERGY MEASUREMENTS, INC., SANTA BARBARA, CA.
Data simulation for the Associated Particle Imaging system
[DE94-012664] p 4518 N94-37305
ELORET CORP., PALO ALTO, CA.
Experimental investigation of nozzle/plume aerodynamics at hypersonic speeds
[NASA-CR-195829] p 4382 N94-36687
EMA, MANSFIELD, TX.
Rotorwash analysis handbook. Volume 1: Development and analysis
[SCT-93RR-17-VOL-1] p 4381 N94-36466
Rotorwash analysis handbook. Volume 2: Appendixes
[SCT-93RR-17-VOL-2] p 4382 N94-36467
ENERGY INFORMATION ADMINISTRATION, WASHINGTON, DC.
Estimates of US biomass energy consumption 1992
[DE94-011458] p 4463 N94-37567
EUROPEAN ORGANIZATION FOR NUCLEAR RESEARCH, GENEVA (SWITZERLAND).
First results from a prototype level-1 calorimeter trigger system for LHC, RD 27 (UK) collaboration
[PB94-167475] p 4436 N94-36532
EUROPEAN SPACE AGENCY. ESRIN, FRASCATI (ITALY).
Global information networks: How they work
p 4543 N94-37335

F

FEDERAL AVIATION ADMINISTRATION, ATLANTIC CITY, NJ.
AWOS Data Acquisition System (ADAS) Operational Test and Evaluation (OT/E) integration and OT/E operational test report
[AD-A280492] p 4473 N94-37143
Terminal Doppler Weather Radar (TDWR) build 5 Test and Evaluation Master Plan (TEMP)
[AD-A280426] p 4434 N94-37218
FEDERAL AVIATION ADMINISTRATION, CAMBRIDGE, MA.
Human factors for flight deck certification personnel
[AD-A280477] p 4487 N94-37347
FEDERAL AVIATION ADMINISTRATION, WASHINGTON, DC.
Accomplishments under the Airport Improvement Program
[AD-A280661] p 4389 N94-36763
Criminal Acts Against Civil Aviation, 1993
[AD-A280694] p 4384 N94-37131
FERMI NATIONAL ACCELERATOR LAB., BATAVIA, IL.
Top quark search at CDF
[DE94-003643] p 4511 N94-36459
Measurement of the elastic, total and diffraction cross sections at tevatron energies
[DE94-004659] p 4511 N94-36463
A search for first generation scalar leptoquarks at radical s equal to 1.8 TeV with the D0 detector
[DE94-008846] p 4511 N94-36506
B-lifetime measurements at the tevatron
[DE94-003617] p 4513 N94-36528
Blois 5: Experimental summary
[DE94-001219] p 4513 N94-36558
B quark production cross sections and the b- (bar b) correlated production cross section at CDF
[DE94-000620] p 4514 N94-36700
Assess progress being made for the KTeV electromagnetic calorimeter crystal order in France
[DE94-009396] p 4533 N94-36746
Mass identified particle production and Bose Einstein correlations at 1800 GeV
[DE94-013418] p 4515 N94-37067
Prospects for measuring B(s) mixing at CDF
[DE94-013147] p 4518 N94-37298
Particle physics
[DE94-012944] p 4518 N94-37312
Fermilab's DART DA system
[DE94-013240] p 4523 N94-37547
The distributed development environment for SDSS software
[DE94-013238] p 4547 N94-37555
Sloan Digital Sky Survey
[DE94-011749] p 4547 N94-37667
FIAT AVIAZIONE S.P.A., TURIN (ITALY).
Turbine disks: Lifing against defects and materials development p 4454 N94-37329
FIBER MATERIALS, INC., BIDDEFORD, ME.
The development of short, high surface area activated carbon fibers
[AD-A280509] p 4404 N94-37105
FLORIDA INST. OF TECH., MELBOURNE, FL.
Rapid susceptibility testing of Mycobacterium avium complex and Mycobacterium tuberculosis isolated from AIDS patients
[NASA-CR-196268] p 4478 N94-36996
FORGE SOCIETE NATIONALE D'ETUDE ET DE CONSTRUCTION DE MOTEURS D'AVIATION, GENNEVILLIERS (FRANCE).
Maintaining constant standards during the forging process p 4421 N94-37326
FRANCE TELECOM NORTH AMERICA, NEW YORK, NY.
Information retrieval services on wide area networks: A vision of the future p 4545 N94-37346
FUEL CELL ENGINEERING CORP., DANBURY, CT.
MCFC product development test
[DE94-002005] p 4463 N94-37488

G

GAS RESEARCH INST., CHICAGO, IL.
LNG vehicle technology, economics, and safety assessment
[PB94-165487] p 4450 N94-36721
GEC-MARCONI AVIONICS LTD., BASILON, ESSEX (ENGLAND).
Infrared search and track demonstrator programme
p 4393 N94-36622
Multiple target track-while-scan in the airborne EO environment p 4394 N94-36629
GENERAL ACCOUNTING OFFICE, WASHINGTON, DC.
Space Shuttle: Incomplete data and funding approach increase cost risk for upgrade program. Report to Congressional Requesters
[GAO/NSIAD-94-23] p 4392 N94-37026
Space Station: Impact of the expanded Russian role on funding and research. Report to the Ranking Minority Member, Subcommittee on Oversight of Government Management, Committee on Governmental Affairs, US Senate
[GAO/NSIAD-94-220] p 4396 N94-37257
GENERAL ATOMIC CO., SAN DIEGO, CA.
Conceptual design: TFE verification program
[DE94-012469] p 4398 N94-37433
Recent DIII-D high power heating and current drive experiments
[DE94-012509] p 4530 N94-37436
TFE verification program
[DE94-009870] p 4398 N94-37514
GENERAL ELECTRIC CO., CINCINNATI, OH.
Substantiating powder metal life methodologies for engines p 4455 N94-37330
Fiber optic (flight quality) sensors for advanced aircraft propulsion
[NASA-CR-191195] p 4387 N94-37401
GENERAL ELECTRIC CO., SCHENECTADY, NY.
Superconducting TlCa2Ba2Cu3O9 thick films
[DE94-010436] p 4535 N94-37193
Coal-fueled diesel technology development: Fuel injection equipment for coal-fueled diesel engines
[DE94-004088] p 4452 N94-37512
GENERAL ELECTRIC CO. LTD., EDINBURGH (SCOTLAND).
Advances in helmet trackers p 4394 N94-36624
GEOLOGICAL SURVEY, DENVER, CO.
Analysis of deep seismic reflection and other data from the Southern Washington Cascades
[DE94-004075] p 4470 N94-37489
GEOLOGICAL SURVEY, WASHINGTON, DC.
Z39.50 and GILS model p 4542 N94-36859
GEOLOGICAL SURVEY OF CANADA, OTTAWA (ONTARIO).
Solar-Terrestrial Predictions, 4: Proceedings of aworkshop. Volume 3: Geomagnetic papers; ionospheric papers
[PB94-173192] p 4470 N94-37530
Solar-Terrestrial Predictions, 4: Proceedings of a workshop. Volume 1: Workshop overview papers; working group reports; User community reports; Regional Warning Center Reports
[PB94-173176] p 4471 N94-37780
Solar-Terrestrial Predictions, 4: Proceedings of a workshop. Volume 2: Solar papers; magnetospheric papers
[PB94-173184] p 4471 N94-37781
GEORGE WASHINGTON UNIV., HAMPTON, VA.
Evaluation of GPS position and attitude determination for automated rendezvous and docking missions
[NASA-CR-4614] p 4397 N94-37506
GEORGIA INST. OF TECH., ATLANTA, GA.
Robust stability of second-order systems
[NASA-CR-196384] p 4501 N94-37590
GEORGIA UNIV., AIKEN, SC.
Modeling of forced CVI for tube fabrication
[DE94-012718] p 4410 N94-37286
GEORGIA UNIV., ATHENS.
Photodissociation and spectroscopy of gas phase bimetallic clusters
[DE94-012607] p 4419 N94-37438
Optical studies of dynamical processes in disordered systems
[DE94-011945] p 4538 N94-37676
GOOD SAMARITAN HOSPITAL AND MEDICAL CENTER, PORTLAND, OR.
Relation of motion sickness susceptibility to vestibular and behavioral measures of orientation
[NASA-CR-196121] p 4480 N94-37005
GOSUDARSTVENNYI KOMITET PO ISPOLZOVANIYU ATOMNOI ENERGII, SERPUKHOV (USSR).
Angular dependence of parton-parton scattering extracted from hadron pair production in pp collisions at radicals equal to 11.5 GeV
[DE94-611174] p 4511 N94-36504
Variational discrete symmetries
[DE94-618485] p 4507 N94-37062
The canonical symmetry for integral systems
[DE94-618486] p 4504 N94-37375
GRONINGEN RIJKSUNIV. (NETHERLANDS).
Immersive virtual environments as trainer: System design from a cognitive stance p 4484 N94-37267

H

HARVARD-SMITHSONIAN CENTER FOR ASTROPHYSICS, AMADO, AZ.
Measurement and interpretation of crustal deformation rates associated with postglacial rebound
[NASA-CR-196300] p 4470 N94-37581
HARVARD UNIV., CAMBRIDGE, MA.
Tert-butylalumoxanes: Synthetic analogs for methylalumoxane (MAO) and new catalytic routes to polyolefins and polyketones
[AD-A280511] p 4399 N94-37106
Tert-butylalumoxanes: Synthetic analogs for methylalumoxane (MAO) and new catalytic routes to polyolefins and polyketones
[AD-A280532] p 4399 N94-37650
HAWAII UNIV., MANOA, HI.
Studies of the thermal and optical responses of H atoms in solid H2
[NASA-CR-196114] p 4514 N94-36964
HELSINKI UNIV. (FINLAND).
Mineralogy and metallurgical properties of iron ore sinter based on magnetite fines
[DE94-763309] p 4414 N94-36525
HELSINKI UNIV. OF TECHNOLOGY, ESPOO (FINLAND).
Activities of the Laboratory of Physics, Helsinki University of Technology
[PB94-175247] p 4509 N94-37301
Study on the measurement uncertainty of noise properties of a millimeter wave amplifier
[PB94-170917] p 4510 N94-37632
Note on certain rigid subshifts
[PB94-179058] p 4506 N94-37833
Neurocontrol of a broadband (ATM) Clos' switching network
[PB94-179389] p 4441 N94-37851
Pressure dependence of the conductivity and magnetoconductance in oriented iodine-doped polyacetylene
[PB94-184488] p 4427 N94-37854
Measuring the upper profile of sea ice in the Bay of Bothnia with a laser profilometer
[PB94-184561] p 4477 N94-37855
HELSINKI UNIV. OF TECHNOLOGY, KYLMAELAE (FINLAND).
Correlated radio and optical variations in a sample of AGN. A simultaneous radio-optical flare in BL lacertae
[PB94-179181] p 4548 N94-37834
HOUSTON UNIV., TX.
Permanent superconducting magnets for space applications
[NASA-CR-196293] p 4439 N94-37634
HUNTER COLL., NEW YORK, NY.
Sodium-23 NMR and complex impedance studies of gel electrolytes based on poly(acrylonitrile)
[AD-A280330] p 4408 N94-37031

I

IBM FEDERAL SYSTEMS DIV., GAITHERSBURG, MD.
Lessons learned applying CASE methods/tools to Ada software development projects p 4491 N94-36493
IIT RESEARCH INST., BARTLESVILLE, OK.
NIPER Lab WARDEN: Description and LabVIEW executable code of a general-purpose laboratory-automation program
[DE94-000125] p 4492 N94-36698

NIPER Lab WARDEN: Descriptive panels and diagrams for NIPER Lab WARDEN software, volume 2
[DE94-000126] p 4493 N94-36699

IIT RESEARCH INST., CHICAGO, IL.
ELF Communications System ecological monitoring program: Electromagnetic field measurements and engineering support
[AD-A280489] p 4481 N94-37353

ILLINOIS UNIV., CHICAGO, IL.
Strength characteristics and crack growth behavior of a composite with well aligned fibers p 4459 N94-37804

ILLINOIS UNIV., URBANA-CHAMPAIGN, IL.
Use of rotation to suppress thermosolutal convection in directionally solidified binary alloys
[NASA-CR-196372] p 4415 N94-36811
Baseline antenna design for space exploration initiative
[NASA-CR-196298] p 4435 N94-37255

IMPERIAL COLL. OF SCIENCE AND TECHNOLOGY, LONDON (ENGLAND).
The cyclic fatigue behaviour of adhesive joints
[AD-A280453] p 4456 N94-37186

IMPHY S.A., IMPHY (FRANCE).
The control of cleanness in powder metallurgy materials for turbine disks p 4421 N94-37325

INDUSTRY AND SCIENCE CANADA, OTTAWA (ONTARIO).
The Canadian network for the advancement of research, industry and education (CANARIE) p 4543 N94-37336

INSTITUT DES HAUTES ETUDES SCIENTIFIQUES, BURES-SUR-YVETTE (FRANCE).
Localization of topological Pontryagin classes by propagation with finite speed
[PB94-160666] p 4506 N94-37852
Eigenfunction bounds for compact manifolds with integrable geodesic flow
[PB94-160874] p 4506 N94-37853

INSTITUTE FOR COMPUTER APPLICATIONS IN SCIENCE AND ENGINEERING, HAMPTON, VA.
A note on the regularity of solutions of infinite dimensional Riccati equations
[NASA-CR-194898] p 4502 N94-36562
A Galerkin method for linear PDE systems in circular geometries with structural acoustic applications
[NASA-CR-194925] p 4503 N94-36923
A PDE-based methodology for modeling, parameter estimation and feedback control in structural and structural acoustic systems
[NASA-CR-194929] p 4500 N94-36924
Vibration suppression with approximate finite dimensional compensators for distributed systems: Computational methods and experimental results
[NASA-CR-194927] p 4500 N94-36928
Parameter estimation in a structural acoustic system with fully nonlinear coupling conditions
[NASA-CR-194926] p 4503 N94-36991
Parallelized direct execution simulation of message-passing parallel programs
[NASA-CR-194936] p 4497 N94-37411
A scalable parallel algorithm for multiple objective linear programs
[NASA-CR-194920] p 4495 N94-37539
Finite element approximation of an optimal control problem for the von Karman equations
[NASA-CR-194955] p 4505 N94-37540
The stabilizing effect of compressibility in turbulent shear flow
[NASA-CR-194932] p 4444 N94-37605
Towards enhancing and delaying disturbances in free shear flows
[NASA-CR-194945] p 4445 N94-37606

INSTITUTE FOR SCIENTIFIC AND TECHNICAL INFORMATION, VANDOEUVRE-LES-NANCY (FRANCE).
Providing electronic documents in Europe: Experience of INIST p 4544 N94-37341

INSTITUTE OF SOUND AND VIBRATION RESEARCH, SOUTHAMPTON (ENGLAND).
An algorithm for the automatic control of boundary layer flow
[ISVR-TR-233] p 4442 N94-36817

INSTITUTO DE FISICA TEORICA, SAO PAULO (BRAZIL).
Relativistic di-quark model of p p-bar yields K(+)K(-) reaction
[DE94-618519] p 4514 N94-37063

INSTITUTO DE PESQUISAS ENERGETICAS E NUCLEARES, SAO PAULO (BRAZIL).
Sintering of dioxide pellets in an oxidizing atmosphere (CO2)
[DE94-613046] p 4414 N94-36517
The dynamics of hydrogen atoms dissolved in Zr Cr2 alloy
[DE94-618756] p 4520 N94-37652

INTEGRATED ENVIRONMENTAL SERVICES, IRVINE, CA.
California residential indoor air quality study. Volume 1: Methodology and descriptive statistics
[PB94-166048] p 4464 N94-36994
California residential indoor air quality study. Volume 1: Methodology and descriptive statistics. Appendix
[PB94-166055] p 4464 N94-36995

INTERNATIONAL ATOMIC ENERGY AGENCY, VIENNA (AUSTRIA).
Microwave reflectometry for fusion plasma diagnostics
[DE94-620118] p 4527 N94-36566
Research using small tokamaks
[DE94-621827] p 4531 N94-37493

INTERNATIONAL CENTRE FOR THEORETICAL PHYSICS, TRIESTE (ITALY).
Intensity of waves diffracted from symmetrical profile lamellar gratings
[DE94-611101] p 4433 N94-36753

INTERNATIONAL SOCIETY FOR OPTICAL ENGINEERING, BELLINGHAM, WA.
Proceedings of SPIE: The International Society for Optical Engineering, Computational Vision Based on Neurobiology, volume 2054
[AD-A278731] p 4523 N94-36468

INTERNATIONAL SOFTWARE SYSTEMS, INC., AUSTIN, TX.
Proto code generation techniques
[AD-A280275] p 4494 N94-37123

IOWA STATE UNIV. OF SCIENCE AND TECHNOLOGY, AMES, IA.
Critical-state flux-density profiles in type-2 superconducting thin-film strips and disks
[DE94-011199] p 4535 N94-37166

IOWA UNIV., IOWA CITY, IA.
Plasma and radio waves from Neptune: Source mechanisms and propagation
[NASA-CR-196284] p 4550 N94-37251
Analysis of plasma measurements for the Geotail mission
[NASA-CR-196274] p 4470 N94-37470

J

JAPAN ATOMIC ENERGY RESEARCH INST., TOKYO (JAPAN).
Towards nuclear fusion reactors
[DE94-746680] p 4528 N94-37235
Examination of weldability of Ni-Cr-W superalloys
[DE94-719014] p 4418 N94-37385
Stopping power of charged particles from 10 eV/amu to 10 GeV/amu
[DE94-719024] p 4518 N94-37387
Material and design considerations for the carbon armored ITER divertor
[DE94-737854] p 4530 N94-37415
Creep-fatigue interaction property of a nickel-base heat-resistant alloy Hastelloy XR in simulated HTGR helium gas environment
[DE94-737934] p 4418 N94-37416
Production of high current H(-) beams in a cesium seeded volume negative ion source equipped with PG filter
[DE94-718962] p 4522 N94-37463
Two-dimensional over-all neutronics analysis of the ITER device
[DE94-718963] p 4530 N94-37464
Creep properties with short period excessive loadings on a nickel-base heat-resistant alloy Hastelloy XR
[DE94-718965] p 4419 N94-37465
Improvement study of the divertor configuration of the Steady State Tokamak Reactor (SSTR)
[DE94-718961] p 4531 N94-37484

JAPAN SOLAR ENERGY SOCIETY, TOKYO (JAPAN).
1993 JSES (Japan Solar Energy Society)/JWEA (Japan Wind Energy Association) Joint Conference and 1993 Japan-Korea Joint Conference on Solar Energy
[DE94-767725] p 4462 N94-37418

JET PROPULSION LAB., CALIFORNIA INST. OF TECH., PASADENA, CA.
Software forecasting as it is really done: A study of JPL software engineers p 4490 N94-36489
Applying formal methods and object-oriented analysis to existing flight software p 4491 N94-36495
Publications of the Jet Propulsion Laboratory, 1992
[NASA-CR-196125] p 4542 N94-37008

JOHNS HOPKINS UNIV., BALTIMORE, MD.
Receiver design, performance analysis, and evaluation for space-borne laser altimeters and space-to-space laser ranging systems
[NASA-CR-194747] p 4397 N94-36988

JOINT INST. FOR NUCLEAR RESEARCH, DUBNA (USSR).
Measurement and processing of gammas accompanying muon pairs in the reaction pi(-)C yields mu(+)mu(-) + gamma + X at 38 GeV
[DE94-617044] p 4512 N94-36523
Simple and efficient method of secondary vertex searching
[DE94-618542] p 4514 N94-37064
Radiative and rare mu and pi decays
[DE94-618549] p 4515 N94-37066
Wide aperture scintillation hodoscope with FEU-143 photomultipliers
[DE94-618211] p 4515 N94-37075
New method for minimizing regular functions with constraints on parameter region
[DE94-618340] p 4515 N94-37076
The mathematical simulation of physical processes in ECR multicharged ions sources
[DE94-618343] p 4515 N94-37077
Direct photoionization of excited helium
[DE94-618732] p 4516 N94-37097
Cost-effective computations with boundary interface operators in elliptic problems
[DE94-621506] p 4503 N94-37098
Five-lepton decay modes of muon and tau mesons
[DE94-621636] p 4516 N94-37089
Is it possible to assign physical meaning to field theory with higher derivatives?
[DE94-618468] p 4539 N94-37172
Resonance photoionization of the excited helium
[DE94-618733] p 4517 N94-37173
Solving the two-dimensional Schroedinger equation in self-consistent basis
[DE94-621535] p 4504 N94-37174
Numerical solution to the boundary-value problem for the Bethe-Salpeter equation with quadratically rising potential
[DE94-621606] p 4504 N94-37175
About existence of a baryon with the 3.52 GeV/c2 mass
[DE94-621641] p 4519 N94-37414
The angular and energy distributions of ejected electrons in electron-impact ionization of helium
[DE94-618748] p 4519 N94-37528
On the shape of x ray spectra excited by heavy ions
[DE94-618747] p 4519 N94-37651
Comparison of gaseous and semiconductor detectors for medical imaging
[DE94-621344] p 4482 N94-37729

JOINT PUBLICATIONS RESEARCH SERVICE, ARLINGTON, VA.
JPRS report: Central Eurasia. Aviation and cosmonautics, No. 4, April 1993
[JPRS-UAC-94-003] p 4391 N94-36999
JPRS report: Central Eurasia. Aviation and cosmonautics, No. 5, May 1993
[JPRS-UAC-94-004] p 4391 N94-37000
JPRS report: Central Eurasia. Aviation and cosmonautics, No. 6, June 1993
[JPRS-UAC-94-005] p 4391 N94-37001
JPRS report: Science and technology. Central Eurasia: Space
[JPRS-USP-94-004] p 4391 N94-37002
JPRS report: Science and technology. Central Eurasia: Space p 4391 N94-37003
JPRS report: Science and technology. Central Eurasia
[JPRS-UST-94-013] p 4509 N94-37006
JPRS report: Science and technology. Central Eurasia: Materials science
[JPRS-UMS-93-008] p 4404 N94-37010
JPRS report: Science and technology. Central Eurasia: Engineering and equipment
[JPRS-UEQ-93-007] p 4431 N94-37523
JPRS report: Science and technology. Central Eurasia: Engineering and equipment
[JPRS-UEQ-93-008] p 4432 N94-37524
JPRS report: Science and technology. Central Eurasia: Engineering and equipment
[JPRS-UEQ-93-005] p 4432 N94-37538

K

KAUPPA-JA TEOLLISUUSMINISTERIO, HELSINKI, UUDENMAA (FINLAND).
SIHTI: Energy and environmental technology
[DE94-763290] p 4464 N94-37007

KNOWLEDGE EXCHANGE TECHNOLOGIES LTD., STRASSEN (LUXEMBOURG).
Standards for data and document interchange p 4543 N94-37337

KRUG LIFE SCIENCES, INC., SAN ANTONIO, TX.
Hypobaric decompression sickness model development. Part 1: Diffusion of inert gas from a viscoelastic fluid (blood) into an expanding gas phase
[AD-A280298] p 4481 N94-37124

L

LAWRENCE LIVERMORE NATIONAL LAB., LIVERMORE, CA.
MODIL cryocooler producibility demonstration project results
[DE93-019213] p 4430 N94-36444
Fluids at high shock pressures and temperatures and some thoughts about future possibilities
[DE94-003625] p 4407 N94-36458
Low-energy electron collisions with metal clusters: Electron capture and cluster fragmentation
[DE94-003623] p 4512 N94-36516
Determining the refractive index of a lambda/4 thin film on a thick substrate from a transmittance measurement
[DE93-019584] p 4523 N94-36693
Quantum and quasi-classical analyses of high order emission processes
[DE93-041348] p 4513 N94-36697
Design of the divertor Thomson scattering system on D3-D
[DE94-012672] p 4527 N94-37081
The role of heating and current drive in ITER
[DE94-012679] p 4527 N94-37082
U-turn alternative to the large aperture switch
[DE94-011541] p 4524 N94-37112
Greater than 100 watt average power at 0.53 micron with 25 ns, 2.5 kHz repetition rate pulses from a single power oscillator
[DE94-011641] p 4447 N94-37114
Project report: Aircraft
[DE94-011759] p 4465 N94-37155
High average power pulsed phase conjugate laser with birefringence correction
[DE94-012082] p 4447 N94-37160
The winds of cataclysmic variables
[DE94-010897] p 4548 N94-37164
Final report on spectral broadening by cross-phase modulation in linearly birefringent optical fibers
[DE94-010406] p 4524 N94-37191
Detection of the electrocardiogram P-wave using wavelet analysis
[DE94-010791] p 4481 N94-37197
Suppression of beam-break-up in a standing wave free electron laser two-beam accelerator
[DE94-011348] p 4521 N94-37200
Diode array alternative to paint removal solid-state cw laser
[DE94-011482] p 4448 N94-37203
Time-step stability for self-consistent Monte Carlo device simulation
[DE94-012145] p 4528 N94-37207
A rejection method for selection of scattered states
[DE94-012232] p 4517 N94-37209
Time-dependent simulations of filament propagation in photoconducting switches
[DE94-012146] p 4438 N94-37213
Frequency doubling of copper lasers using temperature-tuned ADP
[DE94-011542] p 4448 N94-37240
The influence of tributaries on nocturnal valley flows
[DE94-011613] p 4473 N94-37242
New hollow-cathode electrode for high-power copper lasers
[DE94-011637] p 4448 N94-37244
Motional Stark effect upgrades on D3-D
[DE94-013146] p 4528 N94-37297
The 24/36/48 Cathode Strip Chamber layout for SSC GEM detector muon subsystem
[DE94-012676] p 4439 N94-37306
The logic behind thick, liquid-walled, fusion concepts
[DE94-012678] p 4528 N94-37307
The problems of the minimal surface and minimal lineal measure in three dimensions
[DE94-013002] p 4479 N94-37355
Angle interferometer cross axis errors
[DE94-006190] p 4446 N94-37388
Evolution of turbulent fields in explosions
[DE94-010405] p 4444 N94-37390
Time-resolved probing of electron thermal transport in plasma produced by femtosecond laser pulses
[DE94-012061] p 4530 N94-37392
An amorphous fluoropolymer: Next generation optical coating candidate
[DE94-012386] p 4425 N94-37422
CHEETAH: A fast thermochemical code for detonation
[DE94-012586] p 4429 N94-37427
Gaseous effluent monitoring and identification using an imaging Fourier transform spectrometer
[DE94-012627] p 4467 N94-37428
Ionization balance and gain calculations for neon-like selenium x-ray laser plasmas
[DE94-012590] p 4530 N94-37437
Coherent multiple-foil x-ray transition radiation
[DE93-040831] p 4525 N94-37486
Simple ocean carbon cycle models
[DE94-011745] p 4477 N94-37494
Multiquadric collocation methods in the numerical solution of Volterra integral equations with weakly singular kernels
[DE94-013000] p 4505 N94-37497
Effect of the stimulated Brillouin backscattering on self-focusing threshold
[DE94-008678] p 4510 N94-37536
Factors influencing the parameterization of anvil clouds within GCMs
[DE94-010794] p 4475 N94-37621
Tropospheric radiative forcing of CH4
[DE94-011628] p 4468 N94-37631
Exploratory study on H13 steel dies
[DE94-012118] p 4420 N94-37678
Advanced laser driver for soft x-ray projection lithography
[DE94-011643] p 4449 N94-37722
A freon-filled, holographic bubble chamber as a high energy photon burst spectrometer
[DE94-011645] p 4446 N94-37723
Three-dimensional gyrokinetic particle-in-cell simulation of plasmas on a massively parallel computer: LDRD Core Competency Project
[DE94-013367] p 4532 N94-37732
The 250 watt average power electro-quality Q-switched diode pumped power oscillator
[DE94-011644] p 4449 N94-37737
LEHIGH UNIV., BETHLEHEM, PA.
Robotic weld overlay coatings for erosion control
[DE94-013477] p 4417 N94-37116
LIBRARY OF CONGRESS, WASHINGTON, DC.
A concise introduction to MARC p 4542 N94-36856
LITTON DATA SYSTEMS, AGOURA HILLS, CA.
Analysis of a successful inspection program
p 4490 N94-36492
LOCKHEED ADVANCED DEVELOPMENT CO., SUNLAND, CA.
Experimental observations of scale effects on bonded and bolted joints in composite structures
p 4458 N94-37801
LOCKHEED ENGINEERING AND SCIENCES CO., HAMPTON, VA.
Reference manual for the Thermal Analyst's Help Desk Expert System
[NASA-CR-194941] p 4397 N94-37504
LOCKHEED ENGINEERING AND SCIENCES CO., HOUSTON, TX.
Space Generic Open Avionics Architecture (SGOAA) standard specification
[NASA-CR-188290] p 4387 N94-36933
LOCKHEED MISSILES AND SPACE CO., PALO ALTO, CA.
Origins of energetic ions in the Earth's magnetosheath
[NASA-CR-189359] p 4471 N94-37703
LORAL SYSTEMS, INC., ORLANDO, FL.
Advanced distributed simulation technology advanced rotary wing aircraft. Software programmer's manual visual system module
[AD-A280260] p 4390 N94-37755
Advanced distributed simulation technology advanced rotary wing aircraft. System/segment specification. Volume 4: Simulation system module RAH-66 Kit
[AD-A280261] p 4391 N94-37756
Advanced distributed simulation technology. SIMWORLD data base
[AD-A280262] p 4545 N94-37757
LOS ALAMOS NATIONAL LAB., NM.
TIPC user manual
[DE94-004470] p 4432 N94-36443
MCNP: Multigroup/adjoint capabilities
[DE94-010682] p 4506 N94-36449
Older muons are wiser: Using time information in (mu)LCR spectroscopy
[DE93-018556] p 4511 N94-36457
First results from the Los Alamos plasma source ion implantation experiment
[DE94-003931] p 4414 N94-36461
A high power microwave frequency modulated KrF laser
[DE94-009303] p 4447 N94-36510
Pulsed field magnets at the United States National High Magnetic Field Laboratory
[DE94-002624] p 4436 N94-36514
Generalized squeezed states from generalized coherent states
[DE94-002689] p 4512 N94-36515
Design and analysis of high-field quasi-continuous magnets
[DE94-000782] p 4508 N94-36556
Nonlinearity with disorder: Spatio-temporal complex behavior arising from length scales competition
[DE94-000675] p 4502 N94-36685
Consequences of competing hybridization for magnetic ordering in correlated-electron lattices
[DE94-011648] p 4534 N94-37057
Conceptual design for a fast neutron ionization chamber for fusion reactor plasma diagnostics
[DE94-013396] p 4527 N94-37101
Interchangeable spline reference guide
[DE94-012368] p 4495 N94-37245
Mechanical behavior of MoSi2 and MoSi2 composites
[DE94-013116] p 4405 N94-37289
Quantum confinement in GaP nanoclusters
[DE94-013119] p 4536 N94-37290
Structural ground-state of La2CuO4 in the LTO phase: Evidence of local disorder
[DE94-013126] p 4536 N94-37291
Startup and shutdown of the PULSAR Tokamak Reactor
[DE94-013128] p 4528 N94-37292
A high precision gamma ray spectrometer for the Mars 1994 mission
[DE94-013133] p 4550 N94-37293
Theory of metal insulator transition in strongly correlated electron systems
[DE94-013135] p 4438 N94-37295
The hydrogenolysis and isomerization of light hydrocarbons over Pt catalysts
[DE94-013142] p 4410 N94-37296
Mexico City air quality research initiative, volume 4
[DE94-013201] p 4466 N94-37299
BMAP dipole magnetic field analysis and orbit tracking/calculations of energy deposition in GaAs WHEBY detectors
[DE94-012080] p 4522 N94-37303
Non-equilibrium evolution of the disoriented chiral condensate in heavy-ion collisions
[DE94-012897] p 4522 N94-37310
Channel probe measurements for the American Sector Clutter Experiment, January 1994
[DE94-013086] p 4469 N94-37314
Inertial Electrostatic Confinement (IEC) devices
[DE94-013114] p 4529 N94-37316
Low temperature atmospheric pressure chemical vapor deposition of group 14 oxide films
[DE94-013115] p 4425 N94-37317
Selected case studies in modeling and simulation applied to environmentally conscious design and manufacturing
[DE94-007556] p 4466 N94-37389
NRL HF propagation measurements between Guadeloupe and Providenciales during the CRRES exercises
[DE94-012078] p 4435 N94-37393
Raman scattering of variable bandwidth KrF radiation in long air paths
[DE94-012912] p 4449 N94-37495
The effects of proton-beam quality on the production of gamma rays for nuclear resonance absorption in nitrogen
[DE94-011609] p 4523 N94-37629
Random and periodic substorms and their origins in the solar wind
[DE94-011693] p 4549 N94-37668
Substorm statistics: Occurrences and amplitudes
[DE94-011694] p 4471 N94-37669
Experimental and finite-element simulation results for a plane-strain punch-test using isotropic and anisotropic materials
[DE94-011711] p 4457 N94-37670
Neutrino-nucleon scattering
[DE94-011720] p 4520 N94-37671
Magnetotail dynamics: MHD simulations of driven and spontaneous dynamic changes
[DE94-011702] p 4471 N94-37701
Recent progress of the Los Alamos advanced free electron laser
[DE94-011654] p 4449 N94-37733
Flux creep: Its dependence on current denisty and relation to critical current densities from transport and magnetic measurements
[DE94-011701] p 4440 N94-37738
Fuzzy logic to improve efficiency of finite element and finite difference schemes
[DE94-011718] p 4496 N94-37739
Open architecture controllers for advanced manufacturing
[DE94-007572] p 4496 N94-37782
LOUGHBOROUGH UNIV. OF TECHNOLOGY (ENGLAND).
Electronic journals p 4544 N94-37342

LOUISIANA STATE UNIV., SHREVEPORT, LA.
Cerebral neurochemical mechanisms in stress and anxiety
[AD-A280473] p 4482 N94-37233
LOYOLA COLL., BALTIMORE, MD.
Advanced manufacturing technology for polymer composite structures in Japan p 4422 N94-36968

M

MAISON DE LA MECANIQUE, COURBEVOIE, ILE-DE-FRANCE (FRANCE).
Strategic choices in surface treatments
[PB94-170669] p 4414 N94-36534
MARTIN LABS., INC., HOUSTON, TX.
MarChem 93, the proceedings, the 1993 workshop on marine chemistry instrumentation
[AD-A279035] p 4475 N94-36446
MARTIN MARIETTA ASTRO SPACE, PHILADELPHIA, PA.
Size effect in composite materials and structures: Basic concepts and design considerations
p 4460 N94-37808
MARTIN MARIETTA CORP., DENVER, CO.
Software quality: Process or people
p 4492 N94-36499
MARTIN MARIETTA LABS., SYRACUSE, NY.
Low temperature materials
[AD-A278703] p 4533 N94-36755
MARYLAND UNIV., COLLEGE PARK, MD.
Proceedings of the Eighteenth Annual Software Engineering Workshop
[NASA-CR-189348] p 4489 N94-36484
The maturing of the quality improvement paradigm in the SEL p 4489 N94-36485
Software engineering technology transfer: Understanding the process p 4492 N94-36502
Theoretical investigations of chaotic dynamics
[AD-A280325] p 4507 N94-37028
A fundamental study of hypersonic unstarts
[AD-A280506] p 4443 N94-37128
Microwave generation for magnetic fusion energy applications
[DE94-012107] p 4448 N94-37368
MASSACHUSETTS INST. OF TECH., CAMBRIDGE.
Direct catalytic decomposition of nitric oxide
[DE94-005025] p 4407 N94-36475
Diamond deposition and defect chemistry studied via solid state NMR
[AD-A280609] p 4533 N94-36727
An automated method for Low Level Windshear Alert System (LLWAS) data quality analysis
[AD-A280313] p 4472 N94-37126
Modeling of outgassing and matrix decomposition in carbon-phenolic composites
[NASA-CR-196319] p 4405 N94-37471
MASSACHUSETTS INST. OF TECH., LEXINGTON.
Solid state research
[AD-A280573] p 4533 N94-36734
MASSACHUSETTS UNIV., AMHERST, MA.
Probing flame chemistry with MBMS, theory, and modeling
[DE94-011224] p 4413 N94-37623
MASSACHUSETTS UNIV., LOWELL, MA.
Micromechanical modeling of damage growth in titanium based metal-matrix composites p 4402 N94-36664
MATERIALS RESEARCH SOCIETY, PITTSBURG, PA.
Gas-Phase and Surface Chemistry in Electronic Materials Processing. Materials Research Society Symposium proceedings, volume 334
[AD-A280586] p 4408 N94-36735
MCAT INST., SAN JOSE, CA.
Turbulence modeling of free shear layers for high performance aircraft
[NASA-CR-196137] p 4442 N94-36808
Development of advanced Navier-Stokes solver
[NASA-CR-195094] p 4504 N94-37449
MCDONNELL-DOUGLAS AEROSPACE, LONG BEACH, CA.
Jet aircraft engine exhaust emissions database development: Year 1990 and 2015 scenarios
[NASA-CR-4613] p 4466 N94-37252
MCDONNELL-DOUGLAS AEROSPACE, SAINT LOUIS, MO.
ICAAS piloted simulation results p 4393 N94-36617
Aeroservoelastic stabilization considerations for pointing and tracking systems p 4394 N94-36627
MCDONNELL-DOUGLAS CORP., SAINT LOUIS, MO.
Applications of Titanium Matrix Composite to large airframe structure p 4400 N94-36651
MCMASTER UNIV., HAMILTON (ONTARIO).
Multitarget track initiation using a modified Hough transform p 4395 N94-36630
MICHIGAN STATE UNIV., EAST LANSING, MI.
Unsteady flow field of large-amplitude pitching airfoils
[AD-A280444] p 4383 N94-37219
MICHIGAN UNIV., ANN ARBOR, MI.
Submicrometer fiber-optic chemical sensors: Measuring pH inside single cells
[DE94-004160] p 4525 N94-37532
Biological determinants of photobioreactor design
[DE94-011665] p 4468 N94-37740
MICROELECTRONICS CENTER OF NORTH CAROLINA, RESEARCH TRIANGLE PARK, NC.
Field emitter array RF amplifier development project phase one, cathode technology development
[AD-A280334] p 4437 N94-37033
Field emitter array RF amplifier development project. Phase 1, option 1
[AD-A280377] p 4437 N94-37035
Field emitter array RF amplifier development project. Phase 1, option 1
[AD-A280513] p 4437 N94-37107
Field emitter array RF amplifier development project. Cathode technology development. Phase 1
[AD-A280515] p 4437 N94-37108
MIDWEST RESEARCH INST., CARY, NC.
Combustion characterization of methylal in reciprocating engines
[DE94-006949] p 4411 N94-37409
MIDWEST RESEARCH INST., GOLDEN, CO.
Amorphous silicon photovoltaic manufacturing technology, phase 2A
[DE94-006895] p 4461 N94-36476
Integrated gasification combined cycle and steam injection gas turbine powered by biomass joint-venture evaluation
[DE94-006905] p 4461 N94-36740
New plasma source of hydrides for epitaxial growth
[DE94-006918] p 4533 N94-36744
Small-angle x ray scattering studies of microvoids in amorphous-silicon-based semiconductors
[DE94-006931] p 4533 N94-36745
Investigation of polycrystalline thin-film CuInSe2 solar cells based on ZnSe windows
[DE94-006936] p 4462 N94-37381
Bibliography of work on the photocatalytic removal of hazardous compounds from water and air
[DE94-006906] p 4467 N94-37405
Fuel savings and emissions reductions from light duty fuel cell vehicles
[DE94-006909] p 4451 N94-37406
US manufacturers of commercially available stand-alone photovoltaic lighting systems
[DE94-006917] p 4462 N94-37407
Technical evaluation and assessment of CNG/LPG bi-fuel and flex-fuel vehicle viability
[DE94-006925] p 4451 N94-37408
Combustion characterization of methylal in reciprocating engines
[DE94-006949] p 4411 N94-37409
Comparative alternative/clean fuels provisions of the Clean Air Act Amendments of 1990 and the Energy Policy Act of 1992
[DE94-006887] p 4429 N94-37426
MISSOURI UNIV., COLUMBIA, MO.
Microscopic theory of the dielectric response of highly dispersive biological media
[AD-A280516] p 4516 N94-37109
MITRE CORP., BEDFORD, MA.
Techniques for real-time parallel processing: Sensor processing case studies
[AD-A280633] p 4499 N94-37760
MITRE CORP., WASHINGTON, DC.
Standards in the architectural effort
p 4541 N94-36852
MOOIJ AND ASSOCIATES, OEGSTGEEST (NETHERLANDS).
A non-intrusive way to measure point-of-gaze
p 4484 N94-37272
MORGANTOWN TECHNOLOGY CENTER, WV.
Multiphase flow with interphase exchanges (MFIX) documentation theory guide
[DE94-000087] p 4441 N94-36550
MOSCOW STATE UNIV. (RUSSIA).
Sum rules for 1/m corrections to the form factors of semileptonic B decays
[DE94-618548] p 4514 N94-37065
MOTOREN- UND TURBINEN-UNION MUENCHEN G.M.B.H., MUNICH (GERMANY).
Predicting defect behaviour p 4455 N94-37331

N

NATIONAL ACADEMY OF SCIENCES - NATIONAL RESEARCH COUNCIL, WASHINGTON, DC.
Cosmic rays: Physics and astrophysics. A research briefing
[NASA-CR-196118] p 4550 N94-36921
Toward a new National Weather Service: Weather for those who fly p 4472 N94-36947
Beginning a dialogue on the changing environment for the physical and mathematical sciences
p 4509 N94-36948
Science priorities for the human dimensions of global change p 4464 N94-36987
Toward a new National Weather Service: National Weather Service employee feedback
p 4474 N94-37467
NATIONAL AERONAUTICS AND SPACE ADMINISTRATION, WASHINGTON, DC.
NASA Access Mechanism: Lessons learned document
[NASA-TM-109924] p 4540 N94-36750
Modeling the Earth system in the Mission to Planet Earth era
[NASA-TM-109892] p 4461 N94-36827
NASA STI Program Coordinating Council Eleventh Meeting: NASA STI Modernization Plan
[NASA-TM-109415] p 4540 N94-36841
NASA STI modernization plan p 4540 N94-36842
The Engineering Review Board p 4540 N94-36843
RECON Replacement Project p 4541 N94-36844
Electronic SCAN (Selected Current Aerospace Notices) p 4541 N94-36845
Machine Translation Project p 4541 N94-36846
Multimedia p 4541 N94-36847
Electronic document interchange p 4541 N94-36848
Electronic document interchange p 4541 N94-36849
NASA Access Mechanism (NAM) p 4541 N94-36850
Network upgrades p 4541 N94-36851
NASA STI Program Coordinating Council Twelfth Meeting: Standards
[NASA-TM-109925] p 4541 N94-36853
STI Architectural Framework Working Group p 4542 N94-36854
OSI and TCP/IP p 4542 N94-36855
Government Information Locator Service (GILS). Draft report to the Information Infrastructure Task Force p 4542 N94-36860
Aeronautical engineering: A continuing bibliography with indexes (supplement 307)
[NASA-SP-7037(307)] p 4381 N94-37117
The virtual library: Coming of age p 4544 N94-37338
Aerospace medicine and biology: A continuing bibliography with indexes (supplement 392)
[NASA-SP-7011(392)] p 4482 N94-37445
NASA commercial technology. Agenda for change
[NASA-TM-109898] p 4546 N94-37765
NATIONAL AERONAUTICS AND SPACE ADMINISTRATION. AMES RESEARCH CENTER, MOFFETT FIELD, CA.
TRENDS: A flight test relational database user's guide and reference manual
[NASA-TM-108806] p 4381 N94-37332
NATIONAL AERONAUTICS AND SPACE ADMINISTRATION. GODDARD INST. FOR SPACE STUDIES, NEW YORK, NY.
Measurements and modeling of the effect of convective clouds on the upper tropospheric moisture budget
[NASA-TM-109894] p 4473 N94-37371
NATIONAL AERONAUTICS AND SPACE ADMINISTRATION. GODDARD SPACE FLIGHT CENTER, GREENBELT, MD.
Proceedings of the Eighteenth Annual Software Engineering Workshop
[NASA-CR-189348] p 4489 N94-36484
Process improvement as an investment: Measuring its worth p 4489 N94-36486
Recent SEL experiments and studies p 4490 N94-36487
The (mis)use of subjective process measures in software engineering p 4490 N94-36491
Profile of NASA software engineering: Lessons learned from building the baseline p 4492 N94-36500
Impact of Ada in the Flight Dynamics Division: Excitement and frustration p 4492 N94-36501
SeaWiFS technical report series. Volume 20: The SeaWiFS bio-optical archive and storage system (SeaBASS), part 1
[NASA-TM-104566-VOL-20-PT-1] p 4475 N94-36958
Airborne ROWS data report for the high resolution experiment, June 1993
[NASA-TM-104609] p 4477 N94-37397

NASA ER-2 Doppler radar reflectivity calibration for the CAMEX project
[NASA-TM-104611] p 4475 N94-37790

NATIONAL AERONAUTICS AND SPACE ADMINISTRATION. HUGH L. DRYDEN FLIGHT RESEARCH CENTER, EDWARDS, CA.

Controlling forebody asymmetries in flight: Experience with boundary layer transition strips
[NASA-TM-4595] p 4383 N94-36944
Measurement uncertainty and feasibility study of a flush airdata system for a hypersonic flight experiment
[NASA-TM-4627] p 4383 N94-37378
Pressure-sensing performance of upright cylinders in a Mach 10 boundary-layer
[NASA-TM-4633] p 4383 N94-37395

NATIONAL AERONAUTICS AND SPACE ADMINISTRATION. HUGH L. DRYDEN FLIGHT RESEARCH FACILITY, EDWARDS, CA.

Correlation of analytical and experimental hot structure vibration results
[NASA-TM-104269] p 4386 N94-36644
Preliminary analysis for a Mach 8 crossflow transition experiment on the Pegasus (R) space booster
[NASA-TM-104272] p 4381 N94-36648

NATIONAL AERONAUTICS AND SPACE ADMINISTRATION. LYNDON B. JOHNSON SPACE CENTER, HOUSTON, TX.

Recombinant protein production and insect cell culture and process
[NASA-CASE-MSC-22336-1] p 4478 N94-36751
Three dimensional optic tissue culture and process
[NASA-CASE-MSC-22368-1] p 4478 N94-36765
Method and apparatus for the collection, storage, and real time analysis of blood and other bodily fluids
[NASA-CASE-MSC-22463-1] p 4480 N94-36766
Preload release mechanism
[NASA-CASE-MSC-22327-1] p 4450 N94-36839
Profile analysis of after-effects experienced during exposure to several virtual reality environments
p 4482 N94-37263
The use of a tactile interface to convey position and motion perceptions p 4486 N94-37281
Progress in navigation filter estimate fusion and its application to spacecraft rendezvous
[NASA-TM-104794] p 4392 N94-37386
Engineering directorate technical facilities catalog
[NASA-TM-109895] p 4390 N94-37443

NATIONAL AERONAUTICS AND SPACE ADMINISTRATION. LANGLEY RESEARCH CENTER, HAMPTON, VA.

EM-ANIMATE: A computer program for displaying and animating electromagnetic near-field and surface-current solutions: Video supplement to NASA Technical Memorandum 4539
[NASA-TM-4539-VIDEO-SUPPL] p 4492 N94-36518
Prediction of thermal and mechanical stress-strain responses of TMC's subjected to complex TMF histories
p 4402 N94-36666
ASTM and VAMAS activities in titanium matrix composites test methods development
p 4403 N94-36668
A shadowgraph study of Space Transportation System (STS): The Space Shuttle Launch Vehicle (SSLV)
[NASA-RP-1341] p 4382 N94-36741
Forward sweep, low noise rotor blade
[NASA-CASE-LAR-14569-1] p 4386 N94-36767
Electrically conductive, thermally insulating cryogenic current leads
[NASA-CASE-LAR-14964-1-CU] p 4437 N94-36781
Eigensystem realization algorithm user's guide forVAX/VMS computers: Version 931216
[NASA-TM-109066] p 4493 N94-36818
Gain weighted eigenspace assignment
[NASA-TM-109130] p 4388 N94-36820
Internally damped, self-arresting vertical drop-weight apparatus
[NASA-CASE-LAR-15003-1] p 4389 N94-36826
A comparison of queueing, cluster and distributed computing systems
[NASA-TM-109025] p 4497 N94-36932
Automatic procedures for computing complete configuration geometry from individual component descriptions
[NASA-TM-4607] p 4382 N94-36942
Optical position measurement for a large gap magnetic suspension system: Design and performance analysis
[NASA-TP-3438] p 4447 N94-36946
Automatic computation of Euler-marching and subsonic grids for wing-fuselage configurations
[NASA-TM-4573] p 4383 N94-36950
Navier-Stokes and potential theory solutions for ahelicopter fuselage and comparison with experiment
[NASA-TM-4566] p 4383 N94-36966
LET spectra of fragmented 600-MeV/A iron beam on aluminum and polyethylene: A preliminary analysis
[NASA-TP-3436] p 4416 N94-36993
Design and evaluation of a Stochastic Optimal Feed-forward and Feedback Technology (SOFFT) flight control architecture
[NASA-TP-3419] p 4388 N94-37014
Robust stabilization of marginally stable positive-real systems
[NASA-TM-109136] p 4500 N94-37058
Predicting the effects of unmodeled dynamics on an aircraft flight control system design using eigenspace assignment
[NASA-TM-4548] p 4388 N94-37059
Ability of the total strain version of strainrange partitioning to characterize thermomechanical fatigue behavior
[NASA-TM-4556] p 4455 N94-37102
Issues concerning the updating of finite-element models from experimental data
[NASA-TM-109116] p 4456 N94-37253
Optimization for minimum sensitivity to uncertain parameters
[NASA-TM-109139] p 4386 N94-37256
Optimal control theory determination of feasible return-to-launch-site aborts for the HL-20 Personnel Launch System vehicle
[NASA-TP-3449] p 4396 N94-37260
Estimates of cellular mutagenesis from cosmic rays
[NASA-TP-3453] p 4481 N94-37282
A methodology to predict damage initiation, damage growth and residual strength in titanium matrix composites
[NASA-TM-109135] p 4405 N94-37320
Hypersonic, nonequilibrium flow over the FIRE 2 forebody at 1634 sec
[NASA-TM-109141] p 4444 N94-37455
Approximate analysis for repeated eigenvalue problems with applications to controls-structure integrated design
[NASA-TP-3439] p 4397 N94-37502
Subsonic aerodynamic characteristic of semispan commercial transport model with wing-mounted advanced ducted propeller operating in reverse thrust
[NASA-TP-3427] p 4384 N94-37505
Active cooling from the sixties to NASP
[NASA-TM-109079] p 4456 N94-37541
Technology demonstration of space intravehicular automation and robotics
[NASA-TM-109138] p 4501 N94-37589
Stability analysis of an F/A-18 E/F cable mount m odel
[NASA-TM-108989] p 4386 N94-37636
Ordering design tasks based on coupling strengths
[NASA-TM-109137] p 4387 N94-37762
Workshop on Scaling Effects in Composite Materials and Structures
[NASA-CP-3271] p 4457 N94-37796
Effects of ply thickness on thermal cycle induced damage and thermal strain p 4459 N94-37806
Impact force as a scaling parameter
p 4460 N94-37811

NATIONAL AERONAUTICS AND SPACE ADMINISTRATION. LEWIS RESEARCH CENTER, CLEVELAND, OH.

Determination of copper in tap water using solid-phase spectrophotometry
[NASA-TM-106480] p 4408 N94-36537
A coupled/uncoupled deformation and fatigue damage algorithm utilizing the finite element method
[NASA-TM-106526] p 4455 N94-36561
Hot dynamic test rig for measuring hypersonic engine seal flow and durability
[NASA-TM-106507] p 4450 N94-36645
A flux splitting scheme with high-resolution and robustness for discontinuities
[NASA-TM-106452] p 4441 N94-36646
Preconditioned implicit solvers for the Navier-Stokes equations on distributed-memory machines
[NASA-TM-106449] p 4502 N94-36647
Process/composite concurrent tailoring of SiC/Ti composites p 4402 N94-36663
Mixing and noise benefit versus thrust penalty in supersonic jets using impingement tones
[NASA-TM-106583] p 4382 N94-36686
NiAl-base composite containing high volume fraction of AlN for advanced engines
[NASA-CASE-LEW-15818-1] p 4403 N94-36752
Evaluation of some slow-wave vane structures for aminiature traveling-wave tube at 30 GHz
[NASA-TM-106654] p 4437 N94-36819
Review of advanced radiator technologies for spacecraft power systems and space thermal control
[NASA-TM-4555] p 4398 N94-36821
Neural network for positioning Space Station solar arrays
[NASA-TM-106656] p 4431 N94-36943
Operational environments for electrical power wiring on NASA space systems
[NASA-TM-106655] p 4398 N94-36951
Atomic oxygen treatment for non-contact removal of organic protective coatings from painting surfaces
[NASA-TM-106650] p 4421 N94-36952
Vibration signature analysis of a faulted gear transmission system
[NASA-TM-106623] p 4450 N94-36953
A novel transition between rectangular waveguide and layered ridge dielectric waveguide
[NASA-TM-106661] p 4433 N94-36955
Detection of delaminations in composite beams using piezoelectric sensors
[NASA-TM-106611] p 4403 N94-36956
Numerical analysis of an impinging jet reactor for the CVD and gas-phase nucleation of titania
[NASA-TM-106619] p 4431 N94-37254
A method for flow simulation about complex geometries using both structured and unstructured grids
[NASA-TM-106633] p 4383 N94-37283
Thermal-oxidative pretreatment and evaluation of poly (hexafluoropropene oxide) fluids
[NASA-TM-106659] p 4424 N94-37300
Scattering cross section of sound waves by the modal element method
[NASA-TM-106667] p 4510 N94-37308
Copper-containing ceramic precursor synthesis: Solid-state transformations and materials technology
[NASA-TM-106556] p 4399 N94-37315
Carbon-carbon heat pipe testing and evaluation
[NASA-TM-106630] p 4405 N94-37318
Evaluation of the EHL film thickness and extreme pressure additives on gear surface fatigue life
[NASA-TM-106663] p 4451 N94-37319
Prediction of film cooling on gas turbine airfoils
[NASA-TM-106653] p 4387 N94-37448
A method for thermal analysis of spiral bevel gears
[NASA-TM-106612] p 4451 N94-37451
Laminated thin shell structures subjected to free vibration in a hygrothermal environment
[NASA-TM-106600] p 4456 N94-37456
Dynamics of a split torque helicopter transmission
[NASA-TM-106410] p 4452 N94-37457
Modelling of surfaces. Part 1: Monatomic metallic surfaces using equivalent crystal theory
[NASA-TM-106680] p 4419 N94-37459
Tensile strength of simulated and welded butt joints in W-Cu composite sheet
[NASA-TM-4584] p 4405 N94-37460
Physical and mechanical metallurgy of NiAl
[NASA-TP-3398] p 4419 N94-37503
Coupled Marangoni-Benard/Rayleigh-Benard instability with temperature dependent viscosity
[NASA-TM-106646] p 4444 N94-37507
Properties of perfluoropolyethers for space applications
[NASA-TM-106616] p 4426 N94-37520
An enhancement to the NA4 gear vibration diagnostic parameter
[NASA-TM-106553] p 4452 N94-37521
NASA Lewis wind tunnel model systems criteria
[NASA-TM-106565] p 4390 N94-37522
Probabilistic assessment of space nuclear propulsion system nozzle
[NASA-TM-106539] p 4457 N94-37704

NATIONAL AERONAUTICS AND SPACE ADMINISTRATION. MARSHALL SPACE FLIGHT CENTER, HUNTSVILLE, AL.

Variable stiffness torsion springs
[NASA-CASE-MFS-28930-1] p 4509 N94-36782
Ampoule failure sensor time response testing: Experiments 2 and 3
[NASA-TM-108458] p 4446 N94-36822
Global Positioning System Synchronized Active Light Autonomous Docking System
[NASA-CASE-MFS-28853-1] p 4395 N94-36825
Selectively lockable knee brace
[NASA-CASE-MFS-28991-1] p 4486 N94-36838
Channel in hip implant stem
[NASA-CASE-MFS-28987-1] p 4486 N94-36840
Portable color multimedia training systems based on monochrome laptop computers (CBT-in-a-briefcase), with spinoff implications for video uplink and downlink in spaceflight operations
[NASA-TM-108460] p 4496 N94-37556
Aerodynamic characteristics of the National Launch System (NLS) 1 1/2 stage launch vehicle
[NASA-TP-3488] p 4384 N94-37577
The corrosion protection of several aluminum alloys by chromic acid and sulfuric acid anodizing
[NASA-TP-3490] p 4420 N94-37578

NATIONAL DEFENCE RESEARCH ESTABLISHMENT, STOCKHOLM (SWEDEN).

KONRAD: Wide band digital HF receiver
[PB94-184686] p 4435 N94-37813

NATIONAL DEFENCE RESEARCH ESTABLISHMENT, UMEA (SWEDEN).
Program GAUSSPLYM: A tool in Windows environment for studying continuous releases
[PB94-184603] p 4468 N94-37856
NATIONAL INST. FOR FUSION SCIENCE, NAGOYA (JAPAN).
Q-profile flattening due to nonlinear development of resistive kink mode and ensuing fast crash in sawtooth oscillations
[DE94-727625] p 4526 N94-36472
Confinement improvement in H-mode-like plasmas in helical systems
[DE94-727619] p 4528 N94-37231
ELMy-H mode as limit cycle and transient responses of H-modes in tokamaks
[DE94-727510] p 4529 N94-37358
Anomalous cross field flux in CHS
[DE94-727547] p 4529 N94-37359
A role of neutral hydrogen in CHS plasmas with reheat and collapse and comparison with JIPPT-IIU tokamak plasmas
[DE94-716985] p 4530 N94-37384
Bounce resonance heating and transport in a magnetic mirror
[DE94-727545] p 4531 N94-37466
Theory of anomalous transport in H-mode plasmas
[DE94-727546] p 4531 N94-37485
Self-sustained turbulence and L-mode confinement in toroidal plasmas
[DE94-748497] p 4532 N94-37734
NATIONAL INST. OF STANDARDS AND TECHNOLOGY, GAITHERSBURG, MD.
Determination of density of mass standards: Requirement and method
[PB94-163078] p 4508 N94-36718
Electronic balance and some gravimetric applications (the density of solids and liquids, pycnometry and mass)
[PB94-163052] p 4446 N94-36719
Open system environments p 4542 N94-36857
Open system environment procurement p 4542 N94-36858
Chemical and structural characterization of nitroaromatic adducts with hemoglobins
[AD-A280533] p 4480 N94-37089
NATIONAL LAB. FOR HIGH ENERGY PHYSICS, IBARAKI (JAPAN).
Physics with primary beams of the KEK-PS
[DE94-748635] p 4522 N94-37234
Activities of the Photon Factory
[DE94-748682] p 4522 N94-37236
Proceedings of the Workshop on Negative Ion Formation and Beam Handling
[DE94-748683] p 4518 N94-37360
NATIONAL LAB. FOR HIGH ENERGY PHYSICS, TSUKUBA (JAPAN).
Proceedings of the Workshop on TRISTAN Physics at High Luminosities
[DE94-737969] p 4523 N94-37727
NATIONAL LIBRARY OF CANADA, OTTAWA (ONTARIO).
An introduction to the Internet and its services p 4543 N94-37334
NATIONAL OCEANIC AND ATMOSPHERIC ADMINISTRATION, BOULDER, CO.
Solar-Terrestrial Predictions, 4: Proceedings of aworkshop. Volume 3: Geomagnetic papers; ionospheric papers
[PB94-173192] p 4470 N94-37530
Solar-Terrestrial Predictions, 4: Proceedings of a workshop. Volume 1: Workshop overview papers; working group reports; User community reports; Regional Warning Center Reports
[PB94-173176] p 4471 N94-37780
Solar-Terrestrial Predictions, 4: Proceedings of a workshop. Volume 2: Solar papers; magnetospheric papers
[PB94-173184] p 4471 N94-37781
NATIONAL OCEANOGRAPHIC DATA CENTER, WASHINGTON, DC.
NOAA polar satellite calibration: A system description
[NOAA-TR-NESDIS-77] p 4396 N94-37009
NATIONAL PHYSICAL LAB., TEDDINGTON (ENGLAND).
UK methane emissions inventory: A scoping study on the use of ambient measurements to reduce uncertainties
[PB94-167855] p 4463 N94-36533
Modelling and testing fibre reinforced titanium for design purposes p 4403 N94-36670
NAVAL AEROSPACE MEDICAL RESEARCH LAB., PENSACOLA, FL.
Behavioral performance in monkeys exposed to TEMPO high-peak-power microwave pulses at 3 GHz
[AD-A280551] p 4478 N94-37045
Attenuating the disorienting effects of head movement during whole-body rotation using a visual reference: Further tests of a predictive hypothesis p 4482 N94-37276
NAVAL AIR WARFARE CENTER, WARMINSTER, PA.
Advanced helmet tracking technology developments for Naval aviation p 4393 N94-36623
Oxidation behavior of titanium aluminide matrix materials p 4401 N94-36658
NAVAL POSTGRADUATE SCHOOL, MONTEREY, CA.
The influence of fin height and wall conductivity on integral-fin tubes during steam condensation
[AD-A280597] p 4539 N94-36725
Preliminary PANSAT ground station software design and use of an expert system to analyze telemetry
[AD-A280600] p 4392 N94-36726
Signal processing for the 1992 Barents Sea tomography experiment
[AD-A278580] p 4476 N94-36971
Validation and implementation of optical diagnostics for particle sizing in rocket motors
[AD-A278581] p 4428 N94-36972
Variability of the California Current System off Point Sur, California from April 1988 to December 1990
[AD-A278579] p 4476 N94-36985
Beyond intelligent vacuum cleaners
[AD-A280565] p 4500 N94-37039
The implementation of Electronic Data Interchange (EDI) with defense transportation operations
[AD-A280568] p 4493 N94-37040
Efficient contact determination between geometric models
[AD-A280244] p 4494 N94-37120
X-ray diffraction studies of evaporated gold thin films deposited on aluminum nitride substates
[AD-A280454] p 4536 N94-37228
SACS: A cache simulator incorporating timing analysis with buffer and memory management
[AD-A280472] p 4494 N94-37230
Planning German Army helicopter maintenance and mission assignment
[AD-A280483] p 4381 N94-37352
NAVAL RESEARCH LAB., BAY SAINT LOUIS, MS.
Indicators for sulfate-reducing bacteria in microbiologically influenced corrosion
[AD-A278914] p 4477 N94-36522
NAVAL RESEARCH LAB., WASHINGTON, DC.
UVPI imaging from the LACE satellite: The Low Cost Launch Vehicle (LCLV) rocket plume
[AD-A278785] p 4398 N94-36445
Propagation of radius-tailored laser pulses over extended distances in a uniform plasma
[AD-A280405] p 4528 N94-37182
NAVAL SURFACE WARFARE CENTER, ANNAPOLIS, MD.
The effects of specimen scale on the compression strength of composite materials p 4459 N94-37802
NAVY PERSONNEL RESEARCH AND DEVELOPMENT CENTER, SAN DIEGO, CA.
Evaluation of a tool for producing and presenting interactive videodisc job aids
[AD-A278599] p 4432 N94-36473
NEBRASKA UNIV., LINCOLN, NE.
Studies on image compression and image reconstruction
[NASA-CR-196304] p 4433 N94-36810
Holographic grating relaxation studies of probe diffusion in amorphous polymers
[AD-A280496] p 4423 N94-37144
Solution characterization of poly(isobornyl methacrylate) in tetrahydrofuran
[AD-A280497] p 4409 N94-37145
NEVADA UNIV. SYSTEM, RENO, NV.
Fundamentals studies of radial wave thermoacoustic engines
[AD-A280534] p 4431 N94-37090
NEW MEXICO UNIV., ALBUQUERQUE, NM.
Interaction effects of cracks, flaws and damage in ceramic
[AD-A280368] p 4423 N94-37181
Development of immobilized ligands for actinide separations
[DE94-012714] p 4410 N94-37284
NEW SOUTH WALES UNIV., KENSINGTON (AUSTRALIA).
Specification-based software sizing: An empirical investigation of function metrics p 4490 N94-36488
NICHOLS RESEARCH CORP., HUNTSVILLE, AL.
Fracture mechanics life analytical methods verification testing
[NASA-CR-4602] p 4455 N94-37015
NORDQUIST (BRUCE O.), TROY, OH.
The alternative faces of turbulent flow
[TM-5-94] p 4442 N94-36934
NORTHROP CORP., HAWTHORNE, CA.
Effects of scale in predicting global structural response p 4458 N94-37799
NORTHWESTERN UNIV., EVANSTON, IL.
InTISb for long-wavelength infrared photodetectors and arrays
[AD-A280207] p 4524 N94-37149
Stability and dynamics of spatio-temporal structures
[DE94-013035] p 4412 N94-37491
NOTRE DAME UNIV., IN.
Error control techniques for satellite and space communications
[NASA-CR-196302] p 4433 N94-36931
Experimental uncertainty and drag measurements in the national transonic facility
[NASA-CR-4600] p 4389 N94-36945

O

OAK RIDGE NATIONAL LAB., TN.
Metal-carbon nanostructures
[DE94-009177] p 4400 N94-36509
A method for obtaining a least squares fit of a hyperplane to uncertain data
[DE94-012498] p 4503 N94-37073
Adaptive learning of multi-sensor integration techniques with genetic algorithms
[DE94-012744] p 4500 N94-37083
Some considerations for modeling the creep behavior of composite materials
[DE94-012112] p 4404 N94-37205
Catalog of data bases and reports
[DE94-012230] p 4466 N94-37208
Pair correlations in crystalline solid solutions
[DE94-012319] p 4535 N94-37212
Testing new technology for the heavy ion experiment at CERN
[DE94-004747] p 4521 N94-37220
Determination of interface structure and bonding at atomic resolution in the stem
[DE94-011466] p 4517 N94-37238
ORNL superconducting technology program for electric power systems
[DE94-011471] p 4438 N94-37239
Modeling of forced CVI for tube fabrication
[DE94-012718] p 4410 N94-37286
Elemental mapping of segregation in stainless steels with an imaging filter
[DE94-012659] p 4417 N94-37304
Ionic properties of hydrogenated and fluorinated fullerenes
[DE94-012110] p 4537 N94-37369
Methodologies for the thermomechanical characterization of continuous-fiber ceramic matrix composites: A review of test methods
[DE94-012111] p 4405 N94-37370
Measurement of scanning electron microscope resolution
[DE94-012661] p 4525 N94-37374
Microstructure and chemistry of MgO- and CoO-doped nickel-titanate spinels
[DE94-012741] p 4537 N94-37382
Effect of temperature on the electron attachment and detachment properties of c-C4F6
[DE94-012750] p 4518 N94-37383
Atomic level characterization of defects in microalloyed NiAl: An atom probe investigation
[DE94-012732] p 4418 N94-37396
AEM and AES of radiation-induced segregation in proton-irradiated stainless steels
[DE94-012734] p 4418 N94-37398
The effect of reactive elements on the segregation behavior and microstructure of alpha-Al2O3 scales on beta-NiAl
[DE94-012739] p 4418 N94-37399
ALCHEMI formulated for delocalization and anti-site defects
[DE94-012740] p 4537 N94-37400
Neutron transport methods on scalable shared memory multiprocessors
[DE94-012324] p 4498 N94-37419
Mechanical behavior and phase stability of NiAl-based shape memory alloys
[DE94-012336] p 4419 N94-37420
Refrigeration and Air-Conditioning Technology Workshop
[DE94-010813] p 4431 N94-37452
Atomic resolution characterization of a SrTiO3 grain boundary in the STEM
[DE94-011469] p 4538 N94-37545
The application of maximum entropy to Z-contrast imaging in a stem
[DE94-011470] p 4412 N94-37546
Residual stresses in a multi-pass weld in an austenitic stainless steel plate before and after thermal stress relief
[DE94-013278] p 4420 N94-37548

Parallel Spectral Transform Shallow Water Model: A runtime-tunable parallel benchmark code
[DE94-011460] p 4498 N94-37568
Effect of thermal annealing on grain boundary chemistry of polycrystalline TlBa2Ca2Cu3O(y) films
[DE94-011464] p 4538 N94-37569
The MBE growth and optical quality of BaTiO3 and SrTiO3 thin films on MgO
[DE94-011468] p 4538 N94-37570
A new technique for dynamic load distribution when two manipulators mutually lift a rigid object, part 2
[DE94-010126] p 4501 N94-37735

OAK RIDGE Y-12 PLANT, TN.
Analysis spectral shapes from California and central United States ground motion
[DE94-010041] p 4469 N94-36758

OBSERVATORIO DEL EBRO, ROQUETAS (SPAIN).
Eurocap program: Ebre Station
[AD-A280418] p 4469 N94-37215

OFFICE NATIONAL D'ETUDES ET DE RECHERCHES AEROSPATIALES, PARIS (FRANCE).
Fibre-matrix interface properties in Ti-matrix composites: Chemical compatibility and micromechanical behaviour
p 4401 N94-36657

OHIO STATE UNIV., COLUMBUS.
Investigation of ultrasonic surface wave interaction with porous saturated rocks
[DE94-013378] p 4469 N94-37177

OLD DOMINION UNIV., NORFOLK, VA.
Large angle magnetic suspension test fixture
[NASA-CR-196138] p 4390 N94-37450
Theoretical studies of a molecular beam generator
[NASA-CR-196306] p 4522 N94-37508

OVERSET METHODS, INC., VACAVILLE, CA.
On automating domain connectivity for overset grids
[NASA-CR-196113] p 4493 N94-36920

OXFORD UNIV. (ENGLAND).
Design, implementaion and evaluation of a declarative object-oriented programming language
[PB94-169208] p 4492 N94-36546

P

PACIFIC NORTHWEST LAB., RICHLAND, WA.
ARM: A climate process observatory
[DE94-007473] p 4463 N94-36477
Short-tower sigma(theta) measurements in the Colorado Plateaus region
[DE94-007478] p 4463 N94-36478
Two-channel microwave radiometer for observations of total column precipitable water vapor and cloud liquid water path
[DE94-007480] p 4471 N94-36479
Characterization and processing of sintered products from nano-crystalline powders generated by the RTDS method
[DE94-004765] p 4415 N94-36553
On the development of boundary layer secondary circulations resulting from horizontally varying surface heat flux
[DE94-011234] p 4472 N94-37048
Climate uncertainty and the regional economic impacts of global climate change
[DE94-012242] p 4466 N94-37211
Interactive calculator for use with multi-dimensional netCDF files
[DE94-007477] p 4545 N94-37348
Representing the influence of subgrid topography on hydrology
[DE94-004595] p 4474 N94-37379
An experimental and numerical study of boundary layer structure over areas of inhomogeneous sensible heat fluxes
[DE94-011441] p 4474 N94-37565
A stratiform cloud parameterization for general circulation models
[DE94-011442] p 4474 N94-37566
Surface-layer response over shrub-steppe canopy during springtime
[DE94-011235] p 4468 N94-37624
Investigation of exposure to Extremely Low Frequency (ELF) magnetic and electric fields: Ongoing animals studies
[DE94-011239] p 4480 N94-37625

PACIFIC-SIERRA RESEARCH CORP., SANTA MONICA, CA.
Controlled atmospheric breakdown: Applications and research opportunities
[AD-A278584] p 4464 N94-36973

PARAMAX ELECTRONIC, INC., MONTREAL (QUEBEC).
Contact level fusion of radar and IRST contacts on almost electromagnetically silent platform
p 4395 N94-36634

PENNSYLVANIA STATE UNIV., ERIE, PA.
Infrared spectroscopy of Jupiter and Saturn
[NASA-CR-196294] p 4549 N94-36961

PENNSYLVANIA STATE UNIV., UNIVERSITY PARK, PA.
Hypersonic shock/boundary-layer interaction database: New and corrected data
[NASA-CR-177638] p 4441 N94-36519
A model-based approach for detection of runways and other objects in image sequences acquired using an on-board camera
[NASA-CR-196424] p 4446 N94-36812
Using nonequilibrium alloying techniques for corrosion inhibition in Gr/Al and Gr/Mg metal matrix composites
[AD-A280529] p 4404 N94-37088
Basic solutions to carbon/carbon oxidation: Science and technology
[AD-A280447] p 4404 N94-37232
Configurational evolution dynamics and stability during in-situ development of large orbiting spacecraft
[AD-A280482] p 4397 N94-37351

PHILLIPS LAB., HANSCOM AFB, MA.
Three flights into thunderstorms with the revised Rocket Electric Field Sounding (REFS) payload
[AD-A280424] p 4473 N94-37217
Atmospheric structure simulation: An ARMA model for smooth isotropic two-dimensional geophysical power spectra
[AD-A280476] p 4470 N94-37649

PHILLIPS LAB., KIRTLAND AFB, NM.
Three-stage attenuation using Glan-Thompson prisms
[AD-A280481] p 4525 N94-37350

PHYSICS AND ELECTRONICS LAB. TNO, THE HAGUE (NETHERLANDS).
On the feasibility of virtual environments in medicine
p 4483 N94-37264

PHYTRON INSTRUMENTS, INC., MOUNTAIN VIEW, CA.
A charge distribution analysis instrument for catalysis and material science applications
[DE94-011587] p 4438 N94-37241

PITTSBURGH UNIV., PITTSBURGH, PA.
Status review and accomplishments of the Materials Research Center at the University of Pittsburgh
[AD-A280422] p 4399 N94-37214
Numerical study of the flow of granular materials down an inclined plane
[DE94-010729] p 4444 N94-37544
Experimental particle physics at the University of Pittsburgh
[DE94-011636] p 4521 N94-37721

PRATT AND WHITNEY AIRCRAFT, WEST PALM BEACH, FL.
Statistical characterization of rare events
p 4454 N94-37327

PRINCETON UNIV., NJ.
Thermodynamics of minerals stable near the Earth's surface
[DE94-012479] p 4539 N94-37094

PURDUE UNIV., WEST LAFAYETTE, IN.
Holt film wall shear instrumentation for boundary layer transition research
[NASA-CR-196040] p 4443 N94-37060
Midwest Superconductivity Consortium
[DE94-012716] p 4536 N94-37285
The life cycles of intense cyclonic and anticyclonic circulation systems observed over oceans
[NASA-CR-196271] p 4473 N94-37294
Crystallographic studies of nitrogenase and hydrogenase
[DE94-011972] p 4538 N94-37677

Q

QUEENS UNIV., KINGSTON (ONTARIO).
Optically induced high efficiency gratings in azo polymer films
[AD-A280505] p 4423 N94-37147
Azobenzene-containing polymers: Some optoelectronic properties
[AD-A280448] p 4424 N94-37185
Thermal cis-trans isomerization rates of azobenzenes bound in the side chain of some copolymers and blends
[AD-A280451] p 4424 N94-37227

R

RAUTARUKKI OY, RAAHE, OULU (FINLAND).
Mineralogy and metallurgical properties of iron ore sinter based on magnetite fines
[DE94-763309] p 4414 N94-36525

RELIABLE SOFTWARE TECHNOLOGY CORP., RESTON, VA.
An empirical comparison of a dynamic software testability metric to static cyclomatic complexity
p 4491 N94-36498

RENSSELAER POLYTECHNIC INST., TROY, NY.
Determination of the dispersion constant in a constrained vapor bubble thermosyphon
[NASA-CR-196124] p 4442 N94-36892
Microscopic image processing systems for measuring nonuniform film thickness profiles
[DE94-005336] p 4424 N94-37223
Scaling, elasticity, and CLPT p 4458 N94-37800

RESEARCH AND DEVELOPMENT LABS., CULVER CITY, CA.
United States Air Force Summer Research Program, 1993. Volume 7: Armstrong Laboratory
[AD-A278655] p 4550 N94-36975
United States Air Force Summer Research Program, 1993. Volume 14: Rome Laboratory
[AD-A278656] p 4550 N94-36976
United States Air Force Summer Research Program, 1993. Volume 13: Phillips Laboratory
[AD-A278657] p 4550 N94-36977
United States Air Force Summer Research Program, 1993. Volume 16: Arnold Engineering Development Center, Frank J. Seiler Research Laboratory and Wilford Hall Medical Center
[AD-A278658] p 4550 N94-36978
United States Air Force Summer Research Program, 1993. Volume 3: Phillips Laboratory
[AD-A278694] p 4550 N94-36979
United States Air Force Summer Research Program, 1993. Volume 4: Rome Laboratory
[AD-A278695] p 4551 N94-36980
United States Air Force Summer Research Program, 1993. Volume 5A: Wright Laboratory
[AD-A278696] p 4551 N94-36981
United States Air Force Summer Research Program, 1993. Volume 6: Arnold Engineering Development Center, Frank J. Seiler Research Laboratory and Wilford Hall Medical Center
[AD-A278697] p 4551 N94-36982
United States Air Force Summer Research Program, 1993. Volume 8: Phillips Laboratory
[AD-A278698] p 4551 N94-36983
United States Air Force Summer Research Program, 1993. Volume 9: Rome Laboratory
[AD-A278699] p 4551 N94-36984

RESEARCH INST. FOR ADVANCED COMPUTER SCIENCE, MOFFETT FIELD, CA.
Computational chemistry research
[NASA-CR-196120] p 4408 N94-36989
Improved load distribution in parallel sparse Cholesky factorization
[NASA-CR-196380] p 4499 N94-37654
Tensor-GMRES method for large sparse systems of nonlinear equations
[NASA-CR-196379] p 4505 N94-37655
High-order centered difference methods with sharp shock resolution
[NASA-CR-196374] p 4496 N94-37656

REYNOLDS ELECTRICAL AND ENGINEERING CO., INC., LAS VEGAS, NV.
A-TOUGH: A multimedia fluid-flow/energy-transport model for fully-coupled atmospheric-subsurface interactions
[DE94-004304] p 4472 N94-36739

RHODE ISLAND UNIV., KINGSTON, RI.
Studies of the effect of microstructure on the dynamic behavior of granular and particulate media
[AD-A279012] p 4455 N94-36520

RICE UNIV., HOUSTON, TX.
Supersonic bare metal cluster beams
[DE94-010790] p 4532 N94-36454
Dynamics explorer data analysis
[NASA-CR-196141] p 4469 N94-37016

RISK ENGINEERING, INC., BOULDER, CO.
Analysis spectral shapes from California and central United States ground motion
[DE94-010041] p 4469 N94-36758

ROCKWELL INTERNATIONAL CORP., DOWNEY, CA.
Cryogenic fluid management technologies for space transportation. Zero G thermodynamic vent system
[NASA-CR-193981] p 4430 N94-36806

RUTHERFORD APPLETON LAB., CHILTON (ENGLAND).
Experimental characterisation of gas microstrip detectors. Part 1: Gain characteristics
[PB94-167087] p 4445 N94-36531
First results from a prototype level-1 calorimeter trigger system for LHC, RD 27 (UK) collaboration
[PB94-167475] p 4436 N94-36532
Particle physics experiments report, 1993
[PB94-169109] p 4521 N94-36545
Porting industrial codes and developing sparse linear solvers on parallel computers
[PB94-170503] p 4497 N94-36547
Collaboration in Crystallography: Proceedings of the 1st Joint Seminar of the ISIS-INCR Collaboration in Crystallography
[PB94-171097] p 4532 N94-36548

Direct photoproduction of jets in the k(T)-factorisation prescription
[PB94-171139] p 4513 N94-36549
Chilbolton Advanced Meteorological Radar: A tool for multi-disciplinary atmospheric research
[PB94-167467] p 4432 N94-36567

S

SAN DIEGO STATE UNIV., CA.
Response of plants and ecosystems to CO2 and climate change
[DE94-011583] p 4466 N94-37376
SAN JOSE STATE UNIV., CA.
Ground and space flight experiments of the effects of light, sound and/or temperature on animals
[NASA-CR-196102] p 4478 N94-36986
Development of processing techniques for advanced thermal protection materials
[NASA-CR-196261] p 4426 N94-37510
SANDIA NATIONAL LABS., ALBUQUERQUE, NM.
Advances in rapid prototyping
[DE94-010075] p 4430 N94-36447
D-D fusion experiments using fast z-pinches
[DE94-010090] p 4526 N94-36448
A mixture model for shock compression of porous multi-component reactive materials
[DE93-017638] p 4400 N94-36456
Rich methane/air flames: Burning velocities, extinction limits, and flammability limit
[DE94-004340] p 4407 N94-36462
Paleoclimate validation of a numerical climate model
[DE94-009287] p 4463 N94-36470
Radially combined 30 W, 14-16 GHz amplifier
[DE94-010078] p 4432 N94-36471
Software use control
[DE94-008429] p 4489 N94-36480
Rich flammability limits in CH3OH/CO/diluent mixtures
[DE94-004341] p 4407 N94-36482
Advanced thermally stable, coal-derived, jet fuels development program. Experiment system and model development
[AD-A278968] p 4426 N94-36505
Correlation of hot-carrier stress and ionization induced degradation in bipolar transistors
[DE94-007269] p 4532 N94-36540
High temperature superconducting digital circuits and subsystems
[DE94-001207] p 4436 N94-36557
A more exact analysis of Sandia Laser Tracker data
[DE94-011411] p 4447 N94-37051
DDT modeling and shock compression experiments of porous or damaged energetic materials
[DE94-011419] p 4428 N94-37052
Integrated environmentally compatible soldering technologies
[DE94-013456] p 4464 N94-37071
Preradiation studies for non-thermal Z-pinch wire load experiments on Saturn
[DE94-013459] p 4527 N94-37072
A dynamic model of a linear actuator based on polymer hydrogel
[DE94-010800] p 4408 N94-37091
Math and science illiteracy: Social and economic impacts
[DE94-010801] p 4540 N94-37092
UAV's in climate research: The ARM Unmanned Aerospace Vehicle Program
[DE94-011753] p 4465 N94-37154
Real-time SAW measurements of NVR in cleanroom and in microenvironment
[DE94-011937] p 4389 N94-37159
New materials and multidimensional cluster analysis for SAW chemical sensor arrays
[DE94-012066] p 4409 N94-37161
Progress on the emitter wrap-through silicon solar cell
[DE94-010382] p 4462 N94-37189
Single event mirroring and sense amplifier designs for enhanced SE tolerance of DRAMs
[DE94-010397] p 4438 N94-37190
Flow visualization for Lagrangian particle methods
[DE94-010757] p 4443 N94-37195
A proposed SEU tolerant DRAM cell
[DE94-010758] p 4438 N94-37196
Laser drilling of printed wiring boards: Sandia LDRD program
[DE94-011004] p 4448 N94-37198
A fully coupled thermal, chemical, mechanical cookoff model
[DE94-011432] p 4428 N94-37201
Processing solid propellants for recycling
[DE94-011433] p 4428 N94-37202
Development of high sensitivity techniques for characterizing outgassing of polymeric construction materials for microenvironments
[DE94-012068] p 4424 N94-37204
Density and composition analysis using focused MeV ion microbeam techniques
[DE94-012241] p 4517 N94-37210
Influences of flame-vortex interactions on formation of oxides of nitrogen in curved methane-air diffusion flamelets
[DE94-005105] p 4409 N94-37221
Finite-rate chemistry and transient effects in Direct Numerical Simulations of turbulent non-premixed flames
[DE94-005250] p 4410 N94-37222
Hydrogen storage for vehicular applications: Technology status and key development areas
[DE94-011626] p 4428 N94-37243
Theoretical and experimental investigations of fullerene derivatives: C60H2, C60H4, C70H2 and C60CH22
[DE94-012727] p 4536 N94-37287
First-principles determination of the polarizabilities of carbon tubules as a function of length
[DE94-013015] p 4537 N94-37356
Evaluating plastic assembly processes for high reliability applications using HAST and Assembly Test Chips
[DE94-010750] p 4439 N94-37363
SAW chemical sensor arrays using new thin-film materials
[DE94-011940] p 4411 N94-37365
The influence of VAR processes and parameters on white spot formation in Alloy 718
[DE94-012071] p 4417 N94-37367
Imaging targets embedded in a lossy half space with Synthetic Aperture Radar
[DE94-010807] p 4435 N94-37391
Bootstrap planning: Theory and application
[DE94-006466] p 4501 N94-37425
Policies for implementing network firewalls
[DE94-011030] p 4495 N94-37430
Experience with automatic, dynamic load balancing and adaptive finite element computation
[DE94-001422] p 4498 N94-37487
Chemical recognition software
[DE94-012918] p 4495 N94-37496
Role of burn-in during qualification testing
[DE94-007864] p 4439 N94-37513
A computational model for three-dimensional jointed media with a single joint set
[DE94-007582] p 4470 N94-37527
Robot trajectory planning via dynamic programming
[DE94-008424] p 4501 N94-37529
Residual stress and Raman spectra of laser deposited highly-tetrahedral-coordinated-amorphous-carbon films
[DE94-012067] p 4426 N94-37537
Iron hydrous titanium oxide catalysts for the dehydrogenation of ethylbenzene to styrene
[DE94-010381] p 4412 N94-37542
Integrated Engineering Information Technology, FY 1993 accomplishments
[DE94-011406] p 4545 N94-37563
On the use of fuzzy logic assessment for high consequence implementation risk analysis
[DE94-011417] p 4507 N94-37564
Linear-size nonobtuse triangulation of polygons
[DE94-010746] p 4505 N94-37620
Fatigue case study and loading spectra for wind turbines
[DE94-010798] p 4457 N94-37622
Initial report on calorimetry for the Tore Supra Outboard pump Limiter
[DE94-011244] p 4531 N94-37626
Micromechanical modeling of advanced materials
[DE94-011249] p 4405 N94-37627
User's manual for SNL-SAND-2 code
[DE94-011744] p 4496 N94-37673
Numerical simulation of dynamic fracture and failure in solids
[DE94-010379] p 4457 N94-37705
Effects of molecular transport on turbulence-chemistry interactions in a hydrogen-argon-air jet diffusion flame
[DE94-005107] p 4413 N94-37711
Analysis of anelastic flow and numerical treatment via finite elements
[DE94-012141] p 4445 N94-37726
What is an open architecture robot controller?
[DE94-007854] p 4501 N94-37783
Interactive Collaborative Environments (ICE): Platform independent X application sharing and multi-media over wide area networks
[DE94-008868] p 4502 N94-37784
Remote use of distributed robotics resources to enhance technology development and insertion
[DE94-009285] p 4502 N94-37785
SANDIA NATIONAL LABS., LIVERMORE, CA.
Effects of two-phase flow on the deflagration of porous energetic materials
[DE94-011423] p 4411 N94-37412
Thermal decomposition reactions of HMX and RDX and their importance in predicting cookoff hazards
[DE94-011430] p 4429 N94-37413
Compilation of diamond-like carbon properties for barriers and hard coatings
[DE94-012139] p 4427 N94-37725
SCIENCE APPLICATIONS INTERNATIONAL CORP., MCLEAN, VA.
Solid state fluorometer: Prototype development
[AD-A280321] p 4534 N94-37027
SCIENCE RESEARCH COUNCIL, CHILTON (ENGLAND).
First results from a prototype level-1 calorimeter trigger system for LHC, RD 27 (UK) collaboration
[PB94-167475] p 4436 N94-36532
Particle physics experiments report, 1993
[PB94-169109] p 4521 N94-36545
SCIENTIFIC RESEARCH ASSOCIATES, INC., GLASTONBURY, CT.
A combined experiment/computational study of flow in turbine blade cooling passage
[NASA-CR-4584] p 4442 N94-36957
SECURE SOLUTIONS, INC., LA JOLLA, CA.
Analysis of end-to-end encryption and traffic flow confidentiality options
[AD-A278612] p 4433 N94-36754
SEXTANT AVIONIQUE, SAINT MEDARD EN JALLES (FRANCE).
Interactive large screen: A multi-mode dialogue tool for future cockpits p 4484 N94-37266
SINOR (J. E.) CONSULTANTS, INC., NIWOT, CO.
Technical evaluation and assessment of CNG/LPG bi-fuel and flex-fuel vehicle viability
[DE94-006925] p 4451 N94-37408
SMITHSONIAN ASTROPHYSICAL OBSERVATORY, CAMBRIDGE, MA.
The BL LAC phenomenon: X-ray observations of transition objects and determination of the x-ray spectrum of a complete sampie of flat-spectrum radio sources
[NASA-CR-195951] p 4546 N94-36688
SOCIETE NATIONALE D'ETUDE ET DE CONSTRUCTION DE MOTEURS D'AVIATION, EVRY (FRANCE).
Development of mechanical testing methods for titanium matrix composites (traction-ogligo-cyclic fatigue) p 4403 N94-36669
SOFTECH, INC., ALEXANDRIA, VA.
Fusing modeling techniques to support domain analysis for reuse opportunities identification p 4491 N94-36497
SOUTH CAROLINA STATE COLL., ORANGEBURG, SC.
Applications of high transition temperature superconductors at the Savannah River Site
[DE94-012938] p 4536 N94-37311
SOUTHWEST RESEARCH INST., SAN ANTONIO, TX.
High Altitude Plasma Instrument (HAPI) data analysis
[NASA-CR-189360] p 4469 N94-36949
SOUTHWEST TEXAS STATE UNIV., SAN MARCOS, TX.
Highly fluorinated polymers
[NASA-CR-196270] p 4422 N94-37025
SPACE TELESCOPE SCIENCE INST., BALTIMORE, MD.
Hubble Space Telescope faint object spectrograph instrument handbook, version 5.0
[NASA-CR-189367] p 4546 N94-36794
Hubble Space Telescope faint object camera instrument handbook (Post-COSTAR), version 5.0
[NASA-CR-189365] p 4546 N94-36795
Hubble Space Telescope Wide Field and Planetary Camera 2 Instrument handbook, version 2.0
[NASA-CR-189368] p 4547 N94-36918
Hubble Space Telescope cycle 5. Phase 1: Proposal instructions, version 4.0
[NASA-CR-189364] p 4547 N94-36963
SPIRE CORP., BEDFORD, MA.
Gas microstrip detectors on resistive plastic substrates
[DE94-011336] p 4426 N94-37714
SR RESEARCH, TORONTO (ONTARIO).
Operator gaze position control interfaces: Investigation of psychophysical and operational parameters p 4485 N94-37273
Low cost software-based rendering and stereoscopic interfaces for teleoperation and virtual reality p 4486 N94-37279
SRI INTERNATIONAL CORP., MENLO PARK, CA.
Development of durable high-temperature catalysts for natural gas combustion: Catalytic materials (CATMAT (trade name)) properties database
[PB94-171824] p 4412 N94-37462
STANFORD LINEAR ACCELERATOR CENTER, CA.
Testing violation of CPT and quantum mechanics in the K(0) - bar-K(0) system
[DE94-012057] p 4539 N94-37365

A photoemission study of Au, Ge, and O2 deposition on NH4F etched Si(111)
[DE94-013352] p 4519 N94-37553

STANFORD RESEARCH INST., MENLO PARK, CA.
Hard diffraction and deep inelastic scattering
[DE94-013353] p 4515 N94-37084
Precise determination of the weak mixing angle from a measurement of ALR in e(+)e(-) yields Z0
[DE94-013355] p 4515 N94-37085
The form factors of the nucleons
[DE94-013357] p 4515 N94-37086
A study of jet handedness in hadronic Z0 decays
[DE94-013358] p 4515 N94-37087
Polarization phenomena in quantum chromodynamics
[DE94-010663] p 4539 N94-37543

STARMARK CORP., ARLINGTON, VA.
Composite helicopter accident profiles: Deficient crew/aircraft performance
[SCT-90RR-46] p 4385 N94-37604
Civil use of night vision devices: Evaluation pilot's guide, part 1
[SCT-91RR-43] p 4487 N94-37741
Assessment of night vision goggle workload: Flight test engineer's guide
[SCT-91RR-45] p 4487 N94-37743

STATE UNIV. OF NEW YORK, BUFFALO, NY.
Probability techniques for reliability analysis of composite materials
[NASA-CR-195294] p 4406 N94-37633

STATE UNIV. OF NEW YORK, STONY BROOK, NY.
Atomic and electronic structure of metals and alloys: Rare earths, ultrathin films and surface alloys
[DE94-011581] p 4516 N94-37113
Cyclization of bis-urethanes as a new method for the synthesis of 5-substituted, 6-membered cyclic ureas
[AD-A280232] p 4399 N94-37134

STONEHILL COLL., NORTH EASTON, MA.
An error-resistant linguistic protocol for air traffic control
[NASA-CR-196098] p 4385 N94-37013

SUPERCONDUCTING SUPER COLLIDER LAB., DALLAS, TX.
ZLIB++: Object-oriented numerical library for differential algebra
[DE94-010839] p 4495 N94-37453

SVERDRUP TECHNOLOGY, INC., BROOK PARK, OH.
Laser-saturated fluorescence measurements in laminar sooting diffusion flames
[NASA-CR-191025] p 4508 N94-36643

SYRACUSE UNIV., NY.
Distributed detection theory and data fusion
[AD-A280410] p 4434 N94-37183
Task-specific usability requirements for virtual information environments: Interface design and data representation for human operators of complex medical systems p 4483 N94-37262

SYSTEMS CONTROL TECHNOLOGY, INC., ARLINGTON, VA.
Rotorwash analysis handbook. Volume 1: Development and analysis
[SCT-93RR-17-VOL-1] p 4381 N94-36466
Rotorwash analysis handbook. Volume 2: Appendixes
[SCT-93RR-17-VOL-2] p 4382 N94-36467
Analysis of vertiport studies funded by the Airport Improvement Program (AIP)
[SCT-93RR-21] p 4390 N94-37424
Composite helicopter accident profiles: Deficient crew/aircraft performance
[SCT-90RR-46] p 4385 N94-37604
Civil use of night vision devices: Evaluation pilot's guide, part 1
[SCT-91RR-43] p 4487 N94-37741
Night vision goggles in Emergency Medical Service (EMS) helicopters
[SCT-93RR-22] p 4487 N94-37742
Assessment of night vision goggle workload: Flight test engineer's guide
[SCT-91RR-45] p 4487 N94-37743

T

TECHNOLOGY/SCIENTIFIC SERVICES, INC., DAYTON, OH.
Sensitivity and signal to noise ratio improvement of a one micron ladar system incorporating a neodymium doped optical fiber preamplifier. Laser radar testbed
[AD-A280235] p 4447 N94-37137

TENNESSEE TECHNOLOGICAL UNIV., COOKEVILLE, TN.
Design of a composite filter realizable on practical spatial light modulators
[NASA-CR-196297] p 4525 N94-37579

TENNESSEE UNIV., KNOXVILLE, TN.
Processing and mechanical properties of NiAl-based in-situ composites
[NASA-CR-195333] p 4416 N94-36954
Light stable isotope analysis of meteorites by ion microprobe
[NASA-CR-196096] p 4548 N94-37004

TENNESSEE UNIV. SPACE INST., TULLAHOMA, TN.
Supersonic laminar flow control research
[NASA-CR-196260] p 4384 N94-37511

TEXAS A&M UNIV., COLLEGE STATION, TX.
Hardware implementation of a desktop supercomputer for high performance image processing
[AD-A280550] p 4489 N94-36731
Melatonin, the pineal gland, and circadian rhythms
[AD-A280467] p 4481 N94-37140

TEXAS STATE UNIV., AUSTIN, TX.
On the interpretation of diamagnetic loop measurements for a current-carrying plasma column in a conducting chamber
[DE94-007107] p 4526 N94-36536

TEXAS UNIV., AUSTIN, TX.
Coherence and chaos
[DE94-008529] p 4539 N94-36507
Scattering theory for the quantum envelope of a classical system
[DE94-008530] p 4539 N94-36508
MARFE's in tokamak edge plasma: Pattern formation under nonlocal constraints
[DE94-012766] p 4529 N94-37309
Isotope scaling and eta(i) mode with impurities in tokamak plasmas
[DE94-012763] p 4529 N94-37361
Momentum-energy transport from turbulence driven by parallel flow shear
[DE94-012765] p 4443 N94-37362
Morphological aspects of surface reactions
[DE94-011208] p 4413 N94-37713
Far-infrared emission line spectroscopy of planetary nebulae from the KAO
[NASA-CR-196289] p 4547 N94-37825

TEXAS UNIV., HOUSTON, TX.
Cardiac pressure changes with venous gas embolism and decompression
[AD-A280412] p 4481 N94-37224

TEXTRON SPECIALTY MATERIALS, LOWELL, MA.
SCS-6 (tm) fiber reinforced titanium p 4400 N94-36652

THERMO ELECTRON TECHNOLOGIES CORP., SAN DIEGO, CA.
Adaptive optics for laser beamforming in the atmosphere p 4393 N94-36621

THOMSON-CSF, BAGNEUX (FRANCE).
High accuracy control algorithm application to a tracking turret p 4394 N94-36626

THOMSON RESEARCH PROJECTS, INC., LAKE MILLS, WI.
Mars vertical axis wind machines. The design of a Darreus and a Giromill for use on Mars
[NASA-CR-196143] p 4462 N94-36807
Mars vertical axis wind machines: The design of a tornado vortex machine for use on Mars
[NASA-CR-196144] p 4462 N94-36823

THOMSON-TRT DEFENSE, GUYANCOURT (FRANCE).
Laser designation pods optimized concept for day/night operations p 4393 N94-36620

TOKYO UNIV., TANASHI (JAPAN).
First observation of laser-induced resonant annihilation in metastable antiprotonic helium atoms
[DE94-748658] p 4519 N94-37417

TRW, INC., HUNTSVILLE, AL.
Integrating end-to-end threads of control into object-oriented analysis and design p 4491 N94-36496

TSENTRALNI AEROGIDRODINAMICHESKII INST., MOSCOW (USSR).
Problems of international exchange of scientific and technical information for a Russian aerospace research institute p 4544 N94-37339

TSUKUBA UNIV., IBARAKI (JAPAN).
Activities of the Tandem Accelerator Center, University of Tsukuba
[DE94-748687] p 4522 N94-37237

TULANE UNIV., NEW ORLEANS, LA.
Methodologies to determine forces on bones and muscles of body segments during exercise, employing compact sensors suitable for use in crowded space vehicles
[NASA-CR-196272] p 4487 N94-37458

U

UNISYS CORP., PAOLI, PA.
Software engineering with application-specific languages p 4491 N94-36494

UNITED KINGDOM ATOMIC ENERGY AUTHORITY, HARWELL (ENGLAND).
Processing of titanium matrix composites p 4401 N94-36653

UNIVERSITAET DER BUNDESWEHR MUENCHEN, NEUBIBERG (GERMANY).
Two-axis camera platform for machine vision p 4394 N94-36628

UNIVERSITY OF SOUTHERN CALIFORNIA, LOS ANGELES, CA.
Distributed VIRtual System (DIVIRS) project
[NASA-CR-196262] p 4495 N94-37509

UTAH STATE UNIV., LOGAN, UT.
Poly(p-phenylene) derivatives new high performance nonlinear optical polymers
[AD-A280248] p 4422 N94-37121
Literature review and preliminary studies of fretting and fretting fatigue including special applications to aircraft joints
[AD-A280310] p 4456 N94-37125
Organic NLO polymers. 2: Main-chain and guest-host Chi(2)NLO polymers: NLO-phore structure versus poling
[AD-A280230] p 4423 N94-37133
Organic nonlinear optical (NLO) polymers. 4: Thermally stable NLO polymers
[AD-A280196] p 4423 N94-37148
Organic NLO polymers. 5: Homopolymerization of indole based NLO-phore: A heterocycle Chi(2)NLO main-chain polymer
[AD-A280229] p 4423 N94-37151
Organometallic NLO polymers. 4: Organometallic main-chain, side-chain, and guest-host polymers: A study of their orientation and relaxation using second harmonic generation
[AD-A280347] p 4423 N94-37179

UTAH UNIV., SALT LAKE CITY, UT.
Isolated SO4-2 and PO4-3 anions do not exist
[AD-A278831] p 4512 N94-36521
Miniature thermoacoustic refrigerator
[AD-A280326] p 4431 N94-37029
History and prognosis of material discontinuity effects on engine components structural integrity p 4453 N94-37322
Scaling of impact damage in fiber composites p 4460 N94-37810

V

VANDERBILT UNIV., NASHVILLE, TN.
MCHF calculations of isotope shifts. 1: Program implementation and test runs. 2: Large-scale active space calculations
[DE94-013036] p 4518 N94-37313

VIETNAM NATIONAL ATOMIC ENERGY COMMISSION, HANOI.
Method of N-15 analysis by mass-spectroscopy on ion implanter MPB-200
[DE94-618203] p 4407 N94-36529
Production of amorphous metal layers using ion implantation and investigation of the related modification of some surface properties
[DE94-617509] p 4414 N94-36541

VIRGINIA POLYTECHNIC INST. AND STATE UNIV., BLACKSBURG, VA.
Feasibility of (IMC)(sub d)-reinforced metal matrix composites
[AD-A280626] p 4404 N94-37044
Modeling and control of intelligent flexible structures
[AD-A280478] p 4396 N94-37349
A simple evaluation of thermally-induced streses in the vicinity of the stitch in a through-thickness reinforced cross-ply laminate
[NASA-CR-196317] p 4406 N94-37653

VIRGINIA UNIV., CHARLOTTESVILLE, VA.
NASA-UVA Light Aerospace Alloy and Structures Technology Program (LA2ST)
[NASA-CR-196290] p 4415 N94-36809
Research in parallel computing
[NASA-CR-196267] p 4442 N94-36960

W

WAIS, INC., MENLO PARK, CA.
Wide area information servers: An executive information system for unstructured files p 4545 N94-37345

WALES UNIV., SWANSEA.
Unstructured grid methods for the simulation of 3D transient flows
[NASA-CR-196139] p 4444 N94-37525

WARREN SPRING LAB., STEVENAGE (ENGLAND).
UK methane emissions inventory: A scoping study on the use of ambient measurements to reduce uncertainties
[PB94-167855] p 4463 N94-36533

WASHINGTON STATE UNIV., PULLMAN, WA.
Defect initiation/growth and energy dissipation induced by deformation and fracture
[AD-A280411] p 4424 N94-37184
WASHINGTON STATE UNIV., RICHLAND, WA.
Investigation of polycrystalline thin-film CuInSe2 solar cells based on ZnSe windows
[DE94-006936] p 4462 N94-37381
WASHINGTON UNIV., SEATTLE, WA.
Cooling of the West Spitzbergen Current: Wintertime observations west of Svalbard
[AD-A280648] p 4475 N94-36762
Multirate flutter suppression system design for the Benchmark Active Controls Technology Wing
[NASA-CR-196112] p 4388 N94-36965
Atmospheric gas
[DE94-007439] p 4465 N94-37187
WEST VIRGINIA STATE COLL., CHARLESTON, VA.
Magnetic Earth Ionosphere Resonant Frequencies (NASA-MEIRF Project)
[NASA-CR-196303] p 4435 N94-37461
WEST VIRGINIA UNIV., MORGANTOWN, VA.
Project JOVE
[NASA-CR-196292] p 4445 N94-37635
WESTFIELD COLL., LONDON (ENGLAND).
First results from a prototype level-1 calorimeter trigger system for LHC, RD 27 (UK) collaboration
[PB94-167475] p 4436 N94-36532
WESTINGHOUSE ELECTRIC CORP., WEST MIFFLIN, PA.
Irradiation assisted stress corrosion cracking of HTH Alloy X-750 and Alloy 625
[DE94-012667] p 4416 N94-37080
WESTINGHOUSE HANFORD CO., RICHLAND, WA.
Jumper connector analysis
[DE94-010373] p 4451 N94-37188
WESTINGHOUSE SAVANNAH RIVER CO., AIKEN, SC.
Long-range mesoscale modeling of pollutant transport for the European Tracer EXperiment (ETEX)
[DE94-010820] p 4465 N94-37093
Numerical simulation of nocturnal drainage flows in an idealized valley-tributary system
[DE94-011684] p 4472 N94-37115
WISCONSIN UNIV., MADISON, WI.
Scientific and technical support for the Galileo net flux radiometer experiment
[NASA-CR-196009] p 4549 N94-36689
Basic studies in plasma wave interactions
[AD-A280465] p 4527 N94-37139
Infrared spectroscopy of organic free radicals related to combustion processes
[DE94-012481] p 4409 N94-37168
Modeling of trace constituent transport with the University of Wisconsin global isentropic-sigma model
[DE94-012729] p 4466 N94-37288
A fast spectroscopic diagnostic for the measurement of plasma impurity ion dynamics
[DE94-012985] p 4529 N94-37354
Thermodynamic and kinetic aspects of surface acidity
[DE94-012351] p 4411 N94-37372
Fast electron generation and transport in a turbulent, magnetized plasma
[DE94-012986] p 4531 N94-37730
WISCONSIN UNIV., MILWAUKEE, WI.
An investigation of molybdenum and molybdenum oxide catalyzed hydrocarbon formation reactions
[DE94-013700] p 4409 N94-37132
WOODS HOLE OCEANOGRAPHIC INST., MA.
Phytoplankton blooms and coastal physical processes
[AD-A280646] p 4475 N94-36761
The role of horizontal variability in air-sea interaction
[AD-A280561] p 4476 N94-37047
Experiment on rapidly intensifying cyclones over the Atlantic
[AD-A280365] p 4473 N94-37180
WORCESTER POLYTECHNIC INST., MA.
Design and development of experimental facilities for short duration, low-gravity combustion and fire experiments
[NASA-CR-196107] p 4389 N94-36967
WRIGHT LAB., WRIGHT-PATTERSON AFB, OH.
Possibilities and pitfalls in aerospace applications of titanium matrix composites p 4400 N94-36650
Residual strength and life prediction techniques for Ti MMC p 4402 N94-36662
Process enhancements of superalloy material
p 4421 N94-37324

Z

ZIRST, MEYLAN (FRANCE).
Adaptive multisensor fusion for the perception and interpretation of outdoor robot scenes
[PB94-170719] p 4499 N94-36535

Typical Contract Number Index Listing

AF PROJ. 2306 ..... p 92 N94-11866

CONTRACT NUMBER | PAGE NUMBER | ACCESSION NUMBER

Listings in this index are arranged alphanumerically by contract number. Under each contract number the accession numbers denoting documents that have been produced as a result of research done under that contract are arranged in ascending order. The page number helps to locate the citation in the abstract section. The accession number denotes the number by which the citation is identified.

AF PROJ. 2004 ..... p 4447 N94-37137
AF PROJ. 2302 ..... p 4400 N94-36650
AF-AFOSR-0091-90 ..... p 4503 N94-36991
AF-AFOSR-0155-91 ..... p 4397 N94-37351
AF-AFOSR-0166-91 ..... p 4494 N94-37226
AF-AFOSR-0181-91 ..... p 4396 N94-37349
AF-AFOSR-0203-91 ..... p 4516 N94-37109
AF-AFOSR-0240-91 ..... p 4503 N94-37146
AF-AFOSR-0244-90 ..... p 4481 N94-37140
AF-AFOSR-0353-89 ..... p 4527 N94-37139
AF-AFOSR-0417-89 ..... p 4383 N94-37219
AF-AFOSR-0419-91 ..... p 4423 N94-37181
AF-AFOSR-0441-91 ..... p 4399 N94-37214
AF-AFOSR-0493-92 ..... p 4459 N94-37804
ARPA ORDER 8162 ..... p 4437 N94-37108
DA PROJ. 1L1-61102-AH-45 ..... p 4451 N94-37451
DA PROJ. 1L1-62211-A-47-A ..... p 4450 N94-36953
p 4451 N94-37319
p 4452 N94-37457
p 4452 N94-37521
DA PROJ. 3M1-62787-A-878 ..... p 4480 N94-37118
DA PROJ. 3048 ..... p 4428 N94-36505
DAAH04-93-G-0516 ..... p 4408 N94-36735
DAAK60-93-C-0015 ..... p 4404 N94-37105
DAAL03-91-G-0237 ..... p 4505 N94-37540
DABT63-92-C-0026 ..... p 4494 N94-37119
DACA88-93-C-0013 ..... p 4403 N94-36730
DAJA45-93-C-0008 ..... p 4456 N94-37186
DAJA45-93-C-0041 ..... p 4469 N94-37215
DAMD17-88-C-8141 ..... p 4480 N94-37118
DE-AC02-76CH-00016 ..... p 4510 N94-36442
p 4511 N94-36460
p 4512 N94-36526
p 4513 N94-36539
p 4408 N94-36559
p 4516 N94-37152
p 4417 N94-37153
p 4524 N94-37157
p 4516 N94-37158
p 4525 N94-37258
p 4518 N94-37364
p 4482 N94-37444
p 4537 N94-37498
p 4537 N94-37499
p 4520 N94-37672
p 4505 N94-37675
DE-AC02-76CH-03000 ..... p 4511 N94-36459
p 4511 N94-36463
p 4511 N94-36506
p 4513 N94-36528
p 4513 N94-36558
p 4514 N94-36700
p 4533 N94-36746
p 4515 N94-37067
p 4518 N94-37298
p 4518 N94-37312
p 4523 N94-37547
p 4547 N94-37555
p 4547 N94-37667
p 4520 N94-37674
DE-AC02-83CH-10093 ..... p 4461 N94-36476
p 4461 N94-36740
p 4533 N94-36744
p 4533 N94-36745
p 4462 N94-37381
p 4429 N94-37402
p 4429 N94-37403
p 4429 N94-37404
p 4467 N94-37405
p 4451 N94-37406
p 4462 N94-37407
p 4451 N94-37408
p 4411 N94-37409
p 4429 N94-37426
DE-AC03-76SF-00098 ..... p 4508 N94-36560
p 4513 N94-36695
p 4548 N94-37049
p 4443 N94-37050
p 4408 N94-37056
p 4479 N94-37156
p 4524 N94-37165
p 4409 N94-37199
p 4521 N94-37200
p 4439 N94-37302
p 4518 N94-37364
p 4548 N94-37557
p 4519 N94-37558
p 4449 N94-37628
p 4413 N94-37630
p 4520 N94-37715
p 4520 N94-37716
p 4520 N94-37717
p 4506 N94-37718
p 4506 N94-37719
p 4521 N94-37720
DE-AC03-76SF-00515 ..... p 4515 N94-37084
p 4515 N94-37085
p 4515 N94-37086
p 4515 N94-37087
p 4539 N94-37366
p 4539 N94-37543
p 4519 N94-37553
DE-AC03-84ER-51044 ..... p 4528 N94-37297
DE-AC03-86SF-16298 ..... p 4398 N94-37433
p 4398 N94-37514
DE-AC03-89ER-51114 ..... p 4527 N94-37081
p 4530 N94-37436
DE-AC04-76DP-00613 ..... p 4421 N94-36474
DE-AC04-76DP-00789 ..... p 4400 N94-36456
p 4436 N94-36557
p 4410 N94-37222
p 4537 N94-37356
DE-AC04-76DR-00789 ..... p 4407 N94-36462
p 4465 N94-37154
p 4409 N94-37221
p 4473 N94-37371
p 4413 N94-37711
p 4427 N94-37725
DE-AC04-94AL-85000 ..... p 4430 N94-36447
p 4526 N94-36448
p 4463 N94-36470
p 4432 N94-36471
p 4489 N94-36480
p 4407 N94-36482
p 4428 N94-36505
p 4532 N94-36540
p 4447 N94-37051
p 4428 N94-37052
p 4464 N94-37071
p 4527 N94-37072
p 4408 N94-37091
p 4540 N94-37092
p 4389 N94-37159
p 4409 N94-37161
p 4462 N94-37189
p 4438 N94-37190
p 4443 N94-37195
p 4438 N94-37196
p 4448 N94-37198
p 4428 N94-37201
p 4428 N94-37202
p 4424 N94-37204
p 4517 N94-37210
p 4428 N94-37243
p 4536 N94-37287
p 4439 N94-37363
p 4411 N94-37365
p 4417 N94-37367
p 4435 N94-37391
p 4411 N94-37412
p 4429 N94-37413
p 4501 N94-37425
p 4495 N94-37430
p 4498 N94-37487
p 4495 N94-37496
p 4439 N94-37513
p 4470 N94-37527
p 4501 N94-37529
p 4426 N94-37537
p 4412 N94-37542
p 4545 N94-37563
p 4507 N94-37564
p 4505 N94-37620
p 4457 N94-37622
p 4531 N94-37626
p 4405 N94-37627
p 4496 N94-37673
p 4457 N94-37705
p 4445 N94-37726
p 4501 N94-37783
p 4502 N94-37784
p 4502 N94-37785
DE-AC05-76OR-00033 ..... p 4418 N94-37396
p 4538 N94-37545
p 4412 N94-37546
DE-AC05-84OR-21400 ..... p 4400 N94-36509
p 4503 N94-37073
p 4500 N94-37083
p 4404 N94-37205
p 4466 N94-37208
p 4535 N94-37212
p 4521 N94-37220
p 4517 N94-37236
p 4438 N94-37239
p 4410 N94-37286
p 4417 N94-37304
p 4537 N94-37369
p 4405 N94-37370
p 4525 N94-37374
p 4537 N94-37382
p 4518 N94-37383
p 4418 N94-37396
p 4418 N94-37398
p 4418 N94-37399
p 4537 N94-37400
p 4498 N94-37419
p 4419 N94-37420
p 4530 N94-37436
p 4431 N94-37452
p 4538 N94-37545
p 4412 N94-37546
p 4420 N94-37548
p 4498 N94-37568
p 4538 N94-37569
p 4538 N94-37570
p 4501 N94-37735
DE-AC05-84OS-21400 ..... p 4469 N94-36758
DE-AC05-85OR-21400 ..... p 4548 N94-37004
DE-AC06-76RL-01830 ..... p 4463 N94-36477
p 4463 N94-36478
p 4471 N94-36479
p 4415 N94-36553
p 4472 N94-37048
p 4466 N94-37211
p 4545 N94-37348
p 4474 N94-37379
p 4474 N94-37565
p 4474 N94-37566
p 4468 N94-37624
p 4480 N94-37625
DE-AC06-87RL-10930 ..... p 4451 N94-37188
DE-AC07-76ID-01570 ..... p 4453 N94-36452
p 4406 N94-36453
DE-AC08-93NV-11265 ..... p 4518 N94-37305
DE-AC08-94NV-11432 ..... p 4472 N94-36739
DE-AC09-76SR-00819 ..... p 4461 N94-36464
DE-AC09-89SR-18035 ..... p 4465 N94-37093

	p 4472	N94-37115
DE-AC11-89PN-38014	p 4416	N94-37080
DE-AC11-93PN-38195	p 4502	N94-36455
	p 4416	N94-37080
DE-AC21-88MC-23174	p 4452	N94-37512
DE-AC21-92MC-29106	p 4469	N94-36738
DE-AC22-91PC-90180	p 4444	N94-37544
DE-AC22-91PC-91030	p 4406	N94-36450
DE-AC22-93PC-92116	p 4411	N94-37431
DE-AC35-89ER-40486	p 4495	N94-37453
DE-AI32-92AL-82529	p 4435	N94-37393
DE-AT21-92MC-29267	p 4470	N94-37489
DE-FC03-86ER-52126	p 4530	N94-37436
DE-FC21-92MC-29237	p 4463	N94-37488
DE-FC22-83FE-60149	p 4492	N94-36698
	p 4493	N94-36699
DE-FG02-84ER-13183	p 4411	N94-37372
DE-FG02-84ER-13214	p 4479	N94-37248
DE-FG02-84ER-13299	p 4413	N94-37754
DE-FG02-85ER-13370	p 4479	N94-37434
DE-FG02-85ER-13437	p 4539	N94-37094
DE-FG02-85ER-53198	p 4529	N94-37354
	p 4531	N94-37730
DE-FG02-86ER-45239	p 4516	N94-37113
DE-FG02-87ER-13749	p 4469	N94-37177
DE-FG02-87ER-45320	p 4537	N94-37435
DE-FG02-89ER-14045	p 4424	N94-37223
DE-FG02-89ER-14079	p 4510	N94-36551
DE-FG02-90ER-45427	p 4536	N94-37285
DE-FG02-90ER-61085	p 4525	N94-37532
DE-FG02-91CE-23810	p 4425	N94-37373
	p 4425	N94-37421
	p 4426	N94-37490
DE-FG02-91ER-14192	p 4413	N94-37623
DE-FG02-91ER-40646	p 4521	N94-37721
DE-FG02-91ER-61221	p 4525	N94-37258
DE-FG02-92ER-14269	p 4409	N94-37132
DE-FG02-92ER-14303	p 4412	N94-37491
DE-FG02-92ER-14305	p 4408	N94-37095
DE-FG02-92ER-14306	p 4409	N94-37168
DE-FG02-92ER-20070	p 4538	N94-37677
DE-FG02-92ER-45475	p 4538	N94-37545
DE-FG02-92ER-61439	p 4466	N94-37288
DE-FG02-92ER-81463	p 4426	N94-37714
DE-FG02-93ER-40768	p 4511	N94-36460
DE-FG02-93ER-61549	p 4464	N94-36552
DE-FG03-86ER-60490	p 4466	N94-37376
DE-FG03-92ER-54185	p 4528	N94-37167
DE-FG03-93ER-14334	p 4413	N94-37713
DE-FG03-93ER-40757	p 4539	N94-36507
	p 4539	N94-36508
DE-FG04-86ER-13915	p 4410	N94-37284
DE-FG05-80ET-53088	p 4526	N94-36536
	p 4529	N94-37309
	p 4529	N94-37361
	p 4443	N94-37362
DE-FG05-85ER-13429	p 4532	N94-36454
DE-FG05-87ER-40319	p 4512	N94-36526
DE-FG05-87ER-52147	p 4448	N94-37368
DE-FG05-88ER-13867	p 4518	N94-37313
DE-FG05-88ER-53266	p 4443	N94-37362
DE-FG06-90ER-61037	p 4465	N94-37187
DE-FG06-92ER-14234	p 4468	N94-36451
DE-FG09-87ER-45291	p 4538	N94-37676
DE-FG09-90ER-14156	p 4419	N94-37438
DE-FG09-92SR-18273	p 4536	N94-37311
DE-FG22-91PC-91293	p 4407	N94-36475
DE-FG22-92PC-92542	p 4417	N94-37116
DE-FG22-93PC-93212	p 4468	N94-37740
DE-FG22-93PC-93219	p 4461	N94-36511
DE-FG49-93CE-15566	p 4438	N94-37241
DEN3-336	p 4452	N94-37763
DTFA01-87-C-00014	p 4381	N94-36466
	p 4382	N94-36467
	p 4385	N94-37604
	p 4487	N94-37742
DTFA01-91-Z-02036	p 4472	N94-37126
DTFA01-93-C-00030	p 4390	N94-37424
DTFA03-89-C-00051	p 4385	N94-37706
F19628-90-C-0002	p 4533	N94-36734
F19628-90-C-0003	p 4493	N94-36074
F19628-90-C-0100	p 4464	N94-36973
F19628-94-C-0001	p 4499	N94-37760
F30602-91-C-0012	p 4494	N94-37123
F33615-89-C-5612	p 4401	N94-36660
F33615-90-D-0014	p 4481	N94-37224
F33615-90-D-0606	p 4481	N94-37224
F33615-91-C-5806	p 4401	N94-36660
F33615-91-D-0652	p 4534	N94-37027
F33615-92-C-0018	p 4481	N94-37124
F33615-92-C-5663	p 4401	N94-36660
F40620-91-1-0209	p 4455	N94-36520
F49620-91-C-0044	p 4533	N94-36755
F49620-91-C-0093	p 4424	N94-37184
F49620-92-J-0006	p 4443	N94-37128
F49620-92-J-0033	p 4507	N94-37028
F49620-93-C-0037	p 4534	N94-37036
F49620-93-1-0122	p 4434	N94-37183
F49620-93-1-0125	p 4482	N94-37233
F49620-93-1-0198	p 4500	N94-36924
	p 4500	N94-36928
	p 4503	N94-36991
F49620-93-1-0311	p 4404	N94-37232
GA PROJ. 3450	p 4398	N94-37433
GA PROJ. 3466	p 4530	N94-37436
GRI 5091-260-2233	p 4412	N94-37462
GRI-5091-251-2347	p 4464	N94-36994
	p 4464	N94-36995
GRI-5091-292-2153	p 4450	N94-36721
MDA972-91-C-0028	p 4437	N94-37033
	p 4437	N94-37035
	p 4437	N94-37107
	p 4437	N94-37108
MDA972-92-J-1028	p 4494	N94-37119
MIPR-92MM2588	p 4480	N94-37089
NAGW-2295	p 4549	N94-37012
NAGW-2796	p 4549	N94-36961
NAGW-2800	p 4548	N94-37004
NAGW-2962	p 4444	N94-37525
NAGW-3143	p 4550	N94-37251
NAGW-3557	p 4550	N94-36921
NAGW-3782	p 4480	N94-37005
NAGW-9	p 4549	N94-36469
NAG1-1056	p 4390	N94-37450
NAG1-1108	p 4534	N94-37103
NAG1-1201	p 4443	N94-37060
NAG1-1280	p 4457	N94-37797
NAG1-1309	p 4526	N94-37657
NAG1-1327	p 4397	N94-37580
NAG1-1371	p 4446	N94-36812
NAG1-1397	p 4501	N94-37590
NAG1-1424	p 4522	N94-37508
NAG1-1516	p 4444	N94-37605
NAG1-1529	p 4442	N94-36960
NAG1-1600	p 4503	N94-36923
	p 4500	N94-36928
NAG1-343	p 4406	N94-37653
NAG1-536427	p 4497	N94-36503
NAG1-631	p 4422	N94-37025
NAG1-745	p 4415	N94-36809
NAG1-884	p 4491	N94-36498
NAG10-0106	p 4478	N94-36996
NAG2-372	p 4547	N94-37825
NAG2-564	p 4385	N94-37013
NAG2-781	p 4441	N94-36519
NAG2-783	p 4493	N94-36920
NAG2-827	p 4497	N94-36503
NAG2-848	p 4426	N94-37510
NAG2-881	p 4384	N94-37511
NAG3-1121	p 4415	N94-36811
NAG3-1142	p 4456	N94-37554
NAG3-1206	p 4398	N94-37764
NAG3-1399	p 4442	N94-36992
NAG3-581	p 4442	N94-36969
NAG3-862	p 4406	N94-37633
NAG3-876	p 4416	N94-36954
NAG5-1267	p 4435	N94-37461
NAG5-1612	p 4433	N94-36810
NAG5-1630	p 4547	N94-37037
NAG5-1724	p 4546	N94-36688
NAG5-1882	p 4546	N94-36688
NAG5-1930	p 4470	N94-37581
NAG5-2232	p 4397	N94-36988
NAG5-2371	p 4470	N94-37470
NAG5-557	p 4433	N94-36931
NAG5-775	p 4469	N94-37016
NAG8-149	p 4445	N94-37635
NAG8-295	p 4405	N94-37471
NAG8-915	p 4473	N94-37294
NAG9-710	p 4525	N94-37579
NAG9-720	p 4487	N94-37458
NANB2D1219	p 4478	N94-36720
NAS1-18224	p 4399	N94-37614
NAS1-18565	p 4497	N94-36962
	p 4498	N94-37500
	p 4499	N94-37583
NAS1-18842	p 4458	N94-37799
NAS1-18936	p 4396	N94-36990
NAS1-19000	p 4500	N94-36924
	p 4397	N94-37504
NAS1-19247	p 4420	N94-37582
	p 4399	N94-37614
NAS1-19345	p 4466	N94-37252
NAS1-19360	p 4467	N94-37607
	p 4387	N94-37658
NAS1-19385	p 4389	N94-37259
NAS1-19480	p 4502	N94-36562
	p 4503	N94-36923
	p 4500	N94-36924
	p 4500	N94-36928
	p 4503	N94-36991
	p 4497	N94-37411
NAS1-19672	p 4495	N94-37539
NAS2-12568	p 4505	N94-37540
	p 4444	N94-37605
	p 4445	N94-37606
NAS2-13599	p 4383	N94-36966
NAS2-13721	p 4493	N94-36914
	p 4493	N94-36922
	p 4546	N94-36642
	p 4498	N94-37654
	p 4505	N94-37655
	p 4496	N94-37656
NAS3-23709	p 4399	N94-37315
NAS3-24105	p 4508	N94-36643
NAS3-25209	p 4405	N94-37318
NAS3-25266	p 4398	N94-36951
	p 4457	N94-37704
NAS3-25776	p 4437	N94-36819
NAS3-25805	p 4387	N94-37401
NAS3-26251	p 4442	N94-36957
NAS3-26664	p 4421	N94-36637
NAS3-26776	p 4419	N94-37459
NAS3-27186	p 4382	N94-36686
	p 4398	N94-36951
NAS5-26555	p 4546	N94-36690
	p 4546	N94-36794
	p 4546	N94-36795
	p 4547	N94-36918
	p 4547	N94-36963
NAS5-31213	p 4471	N94-37703
NAS5-31281	p 4461	N94-36805
NAS5-32314	p 4461	N94-36919
	p 4494	N94-37061
NAS5-33030	p 4469	N94-36949
NAS8-38103	p 4455	N94-37015
NAS8-38609	p 4410	N94-37250
	p 4547	N94-37702
NAS8-38668	p 4429	N94-37446
NAS8-39202	p 4430	N94-36806
NAS9-17635	p 4421	N94-36641
NAS9-19100	p 4387	N94-36933
NAS9-592	p 4439	N94-37634
NCC1-104	p 4397	N94-37506
NCC1-156	p 4388	N94-36965
NCC1-177	p 4389	N94-36945
NCC2-431	p 4408	N94-36989
NCC2-487	p 4382	N94-36687
NCC2-505	p 4504	N94-37449
NCC2-539	p 4495	N94-37509
NCC2-593	p 4478	N94-36986
NCC2-663	p 4442	N94-36808
NCC2-679	p 4549	N94-36689
NCC2-710	p 4462	N94-36807
	p 4462	N94-36823
NCC3-162	p 4399	N94-37315
NCC3-19	p 4421	N94-36952
NCC3-208	p 4403	N94-36956
NCC3-216	p 4435	N94-37255
NCC3-218	p 4402	N94-36664
NCC3-233	p 4441	N94-36646
	p 4502	N94-36647
NCC3-246	p 4399	N94-37315
NCC3-248	p 4455	N94-36561
NCC3-249	p 4399	N94-37315
NCC3-281	p 4399	N94-37315
NCC3-312	p 4389	N94-36967
NCC3-55	p 4439	N94-37501
NGT-5-0377	p 4431	N94-37254
NR PROJ. RR0-4204	p 4506	N94-36728
	p 4506	N94-36732
NR PROJ. 03103	p 4477	N94-36522
NSERC-OGP-0137436	p 4505	N94-37540
NSF ASC-87-17773	p 4497	N94-36503
NSF CCR-92-09873	p 4491	N94-36495
NSF CDA-87-22788	p 4494	N94-37119
NSF DDM-93-09706	p 4387	N94-37762
NSF DMS-93-08605	p 4495	N94-37539
NSF EEC-91-47146	p 4420	N94-37758
NSF ENG-91-11333	p 4422	N94-36968
NSF INT-90-16771	p 4408	N94-36559
NSF OCE-93-13563	p 4464	N94-36987
NSF-CCR-92-01195	p 4497	N94-37411
NSG-5123	p 4492	N94-36502
N00014-84-K-0405	p 4476	N94-37038
N00014-87-K-0004	p 4475	N94-36762
N00014-88-K-0304	p 4506	N94-36728
	p 4506	N94-36732
	p 4507	N94-37046
N00014-88-K-0315	p 4399	N94-37134
N00014-89-J-1111	p 4475	N94-36761
N00014-89-J-1497	p 4512	N94-36521
N00014-89-J-3166	p 4416	N94-37030
N00014-90-J-1423	p 4473	N94-37180
N00014-90-J-1470	p 4476	N94-37047
N00014-90-J-1549	p 4482	N94-37276
N00014-90-J-1901	p 4533	N94-36727
N00014-91-J-1006	p 4514	N94-37041

N00014-91-J-1017 ..... p 4453 N94-37150
N00014-91-J-1196 ..... p 4404 N94-37088
N00014-91-J-1405 ..... p 4475 N94-36762
N00014-91-J-1625 ..... p 4422 N94-37121
p 4423 N94-37133
p 4423 N94-37148
p 4423 N94-37151
p 4423 N94-37179
N00014-91-J-1934 ..... p 4399 N94-37106
p 4399 N94-37650
N00014-91-J-2015 ..... p 4431 N94-37029
N00014-92-J-1244 ..... p 4480 N94-36764
N00014-92-J-1260 ..... p 4514 N94-37034
p 4524 N94-37110
N00014-92-J-1629 ..... p 4408 N94-37031
N00014-92-J-1778 ..... p 4434 N94-37032
N00014-92-J-1951 ..... p 4524 N94-37149
N00014-93-J-1131 ..... p 4431 N94-37090
N00014-93-1-0448 ..... p 4475 N94-36446
N00014-93-1-0539 ..... p 4404 N94-37044
N00014-93-1-0591 ..... p 4517 N94-37249
N00014-93-1-0615 ..... p 4423 N94-37147
p 4424 N94-37185
p 4424 N94-37227
N00014-94-1-0043 ..... p 4533 N94-36742
N00014-94-1-0511 ..... p 4408 N94-36735
N00014-94-1-0516 ..... p 4489 N94-36731
N0001494-MP-23031 ..... p 4477 N94-37397
N00039-93-C-0001 ..... p 4481 N94-37353
N00039-93-C-0099 ..... p 4433 N94-36754
N00600-93-C-2481 ..... p 4494 N94-37119
N61339-91-D-0001 ..... p 4390 N94-37755
p 4391 N94-37756
p 4545 N94-37757
PROJ. MM3-3130 ..... p 4478 N94-37045
PROJ. RR0-4204 ..... p 4507 N94-37046
PROJ. 91-16 ..... p 4496 N94-37556
RTOP 023-10-01-01 ..... p 4383 N94-36966
RTOP 199-45-16-11 ..... p 4416 N94-36993
p 4481 N94-37282
RTOP 225-99-00-01 ..... p 4397 N94-37506
RTOP 232-01-04-04 ..... p 4444 N94-37455
RTOP 232-02-02 ..... p 4398 N94-37764
RTOP 233-01-0A ..... p 4399 N94-37315
RTOP 233-01-0E ..... p 4421 N94-36952
RTOP 233-01-01-01 ..... p 4396 N94-36990
RTOP 233-01-01-05 ..... p 4500 N94-37058
p 4397 N94-37502
RTOP 233-01-01-12 ..... p 4493 N94-36818
p 4456 N94-37253
RTOP 233-02-0D ..... p 4424 N94-37300
p 4426 N94-37520
RTOP 233-02-08 ..... p 4405 N94-37318
RTOP 233-03-02-04 ..... p 4399 N94-37614
RTOP 233-03-03-02 ..... p 4501 N94-37589
RTOP 235-01-1C ..... p 4437 N94-36819
RTOP 307-51-00 ..... p 4433 N94-36955
RTOP 323-15-03 ..... p 4398 N94-36951
RTOP 422-00-00 ..... p 4461 N94-36919
p 4494 N94-37061
RTOP 460-28-16 ..... p 4475 N94-37790
RTOP 461-31-05-20 ..... p 4477 N94-37397
RTOP 477-50-00-01 ..... p 4397 N94-37504
RTOP 505-59-36-01 ..... p 4383 N94-36966
RTOP 505-59-36 ..... p 4381 N94-37332
RTOP 505-59-54-01 ..... p 4389 N94-36945
RTOP 505-59-70-03 ..... p 4492 N94-36518
RTOP 505-59-85-01 ..... p 4389 N94-37259
RTOP 505-62-10 ..... p 4452 N94-37457
RTOP 505-62-36 ..... p 4450 N94-36953
p 4451 N94-37319
p 4451 N94-37451
p 4452 N94-37521
RTOP 505-62-50 ..... p 4387 N94-37401
RTOP 505-62-52 ..... p 4508 N94-36643
p 4442 N94-36957
p 4510 N94-37308
p 4387 N94-37448
RTOP 505-62-84 ..... p 4390 N94-37522
RTOP 505-63-12 ..... p 4455 N94-36561
p 4405 N94-37460
RTOP 505-63-36-06 ..... p 4386 N94-37256
RTOP 505-63-5A ..... p 4421 N94-36637
RTOP 505-63-5B ..... p 4403 N94-36956
p 4455 N94-37102
p 4456 N94-37554
RTOP 505-63-50-04 ..... p 4405 N94-37320
RTOP 505-63-50-06 ..... p 4387 N94-37762
RTOP 505-63-50-09 ..... p 4457 N94-37796
RTOP 505-63-50-13 ..... p 4386 N94-37636
RTOP 505-63-50 ..... p 4386 N94-36644
RTOP 505-63-52 ..... p 4416 N94-36954
RTOP 505-64-30-01 ..... p 4388 N94-36820
p 4388 N94-37014
RTOP 505-64-52-01 ..... p 4388 N94-37059
RTOP 505-64-52-53 ..... p 4497 N94-36962
RTOP 505-68-40 ..... p 4498 N94-37500
RTOP 505-68-71 ..... p 4383 N94-37378
RTOP 505-70-00 ..... p 4383 N94-36944
RTOP 505-70-63-01 ..... p 4383 N94-37395
RTOP 505-70-91 ..... p 4456 N94-37541
RTOP 505-90-5K ..... p 4381 N94-36648
p 4441 N94-36646
p 4502 N94-36647
RTOP 505-90-52-01 ..... p 4502 N94-36562
p 4503 N94-36923
p 4500 N94-36924
p 4500 N94-36928
p 4503 N94-36991
p 4497 N94-37411
p 4495 N94-37539
p 4505 N94-37540
p 4444 N94-37605
p 4445 N94-37606
RTOP 505-90-53-02 ..... p 4497 N94-36932
RTOP 505-90-53 ..... p 4419 N94-37459
RTOP 506-43-61-02 ..... p 4399 N94-37614
RTOP 506-59-61-03 ..... p 4499 N94-37583
RTOP 506-59-61-04 ..... p 4447 N94-36946
p 4396 N94-37260
RTOP 509-10-11-01 ..... p 4382 N94-36942
p 4383 N94-36950
RTOP 510-01-50 ..... p 4419 N94-37503
p 4406 N94-37633
RTOP 510-02-12-09 ..... p 4420 N94-37582
RTOP 535-03-10-02 ..... p 4384 N94-37505
RTOP 537-01-22-01 ..... p 4466 N94-37252
p 4467 N94-37607
RTOP 537-02-22 ..... p 4382 N94-36686
RTOP 537-02-23 ..... p 4383 N94-37283
RTOP 537-04-20 ..... p 4456 N94-37456
RTOP 537-08-20-01 ..... p 4387 N94-37658
RTOP 552-00-00 ..... p 4489 N94-36484
RTOP 583-02-21 ..... p 4398 N94-36821
RTOP 584-04-11 ..... p 4457 N94-37704
RTOP 602-00-00 ..... p 4469 N94-36949
p 4471 N94-37703
RTOP 633-00-00 ..... p 4546 N94-36794
p 4546 N94-36795
p 4547 N94-36918
p 4547 N94-36963
RTOP 674-24-05 ..... p 4444 N94-37507
RTOP 778-32-21 ..... p 4452 N94-37763
RTOP 962-22-00 ..... p 4431 N94-37254
SBIR-02.07-5494 ..... p 4493 N94-36914
p 4493 N94-36922
SWRI PROJ. 15-3320 ..... p 4469 N94-36949
W-31-109-ENG-38 ..... p 4497 N94-36441
p 4461 N94-36464
p 4477 N94-36481
p 4511 N94-36483
p 4511 N94-36512
p 4512 N94-36513
p 4512 N94-36524
p 4512 N94-36527
p 4513 N94-36538
p 4477 N94-36554
p 4478 N94-36555
p 4521 N94-36694
p 4513 N94-36696
p 4548 N94-36759
p 4437 N94-37053
p 4534 N94-37054
p 4422 N94-37055
p 4422 N94-37068
p 4534 N94-37069
p 4451 N94-37070
p 4465 N94-37100
p 4438 N94-37111
p 4443 N94-37176
p 4504 N94-37246
p 4504 N94-37247
p 4517 N94-37249
p 4410 N94-37357
p 4518 N94-37364
p 4537 N94-37377
p 4411 N94-37380
p 4474 N94-37394
p 4425 N94-37423
p 4467 N94-37429
p 4412 N94-37439
p 4467 N94-37440
p 4530 N94-37441
p 4419 N94-37442
p 4452 N94-37515
p 4420 N94-37516
p 4509 N94-37517
p 4505 N94-37518
p 4498 N94-37519
p 4496 N94-37549
p 4519 N94-37550
p 4496 N94-37551
W-31109-ENG-38 ..... p 4420 N94-37552
p 4523 N94-37619
p 4445 N94-37724
p 4435 N94-37736
p 4535 N94-37192
p 4535 N94-37193
p 4521 N94-37194
p 4434 N94-37206
W-7405-ENG-36 ..... p 4432 N94-36443
p 4506 N94-36449
p 4511 N94-36457
p 4414 N94-36461
p 4447 N94-36510
p 4436 N94-36514
p 4512 N94-36515
p 4508 N94-36556
p 4502 N94-36685
p 4534 N94-37057
p 4527 N94-37101
p 4495 N94-37245
p 4405 N94-37289
p 4536 N94-37290
p 4536 N94-37291
p 4528 N94-37292
p 4550 N94-37293
p 4438 N94-37295
p 4410 N94-37296
p 4466 N94-37299
p 4522 N94-37303
p 4522 N94-37310
p 4469 N94-37314
p 4529 N94-37316
p 4425 N94-37317
p 4466 N94-37389
p 4435 N94-37393
p 4449 N94-37495
p 4523 N94-37629
p 4549 N94-37668
p 4471 N94-37669
p 4457 N94-37670
p 4520 N94-37671
p 4471 N94-37701
p 4449 N94-37733
p 4440 N94-37738
p 4496 N94-37739
p 4496 N94-37782
W-7405-ENG-48 ..... p 4430 N94-36444
p 4407 N94-36458
p 4512 N94-36516
p 4523 N94-36693
p 4513 N94-36697
p 4527 N94-37081
p 4527 N94-37082
p 4524 N94-37112
p 4447 N94-37114
p 4465 N94-37155
p 4447 N94-37160
p 4548 N94-37164
p 4524 N94-37191
p 4481 N94-37197
p 4521 N94-37200
p 4448 N94-37203
p 4528 N94-37207
p 4517 N94-37209
p 4517 N94-37210
p 4438 N94-37213
p 4448 N94-37240
p 4473 N94-37242
p 4448 N94-37244
p 4528 N94-37297
p 4439 N94-37306
p 4528 N94-37307
p 4479 N94-37355
p 4518 N94-37364
p 4446 N94-37388
p 4444 N94-37390
p 4530 N94-37392
p 4425 N94-37422
p 4429 N94-37427
p 4467 N94-37428
p 4530 N94-37436
p 4530 N94-37437
p 4525 N94-37486
p 4477 N94-37494
p 4505 N94-37497
p 4510 N94-37536
p 4475 N94-37621
p 4468 N94-37631
p 4420 N94-37678
p 4449 N94-37722
p 4446 N94-37723
p 4532 N94-37732
p 4449 N94-37737
W-7405-ENG-82 ..... p 4535 N94-37166
p 4418 N94-37410
p 4426 N94-37712

Typical Report Number Index Listing

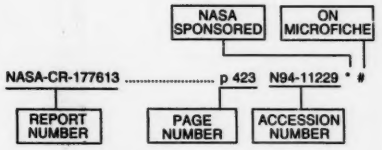

Listings in this index are arranged alphanumerically by report number. The accession number denotes the number by which the citation is identified. The page number helps to locate the citation in the abstract section. An asterisk (*) indicates that the item is a NASA report. A pound sign (#) indicates that the item is available on microfiche.

A-94042 p 4381 N94-37332 * #
A-94078 p 4441 N94-36519 * #

ACW-200A p 4473 N94-37143

AD-A2775206 p 4400 N94-36649 #
AD-A278578 p 4507 N94-36970
AD-A278579 p 4476 N94-36985
AD-A278580 p 4476 N94-36971
AD-A278581 p 4428 N94-36972
AD-A278584 p 4464 N94-36973
AD-A278595 p 4493 N94-36974
AD-A278599 p 4432 N94-36473
AD-A278612 p 4433 N94-36754
AD-A278635 p 4386 N94-36465
AD-A278655 p 4550 N94-36975
AD-A278656 p 4550 N94-36976
AD-A278657 p 4550 N94-36977
AD-A278658 p 4550 N94-36978
AD-A278694 p 4550 N94-36979
AD-A278695 p 4551 N94-36980
AD-A278696 p 4551 N94-36981
AD-A278697 p 4551 N94-36982
AD-A278698 p 4551 N94-36983
AD-A278699 p 4551 N94-36984
AD-A278703 p 4533 N94-36755
AD-A278731 p 4523 N94-36468
AD-A278746 p 4433 N94-36756
AD-A278785 p 4398 N94-36445
AD-A278831 p 4512 N94-36521
AD-A278914 p 4477 N94-36522
AD-A278968 p 4428 N94-36505
AD-A279012 p 4455 N94-36520
AD-A279035 p 4475 N94-36446
AD-A280191 p 4446 N94-36760 #
AD-A280196 p 4423 N94-37148
AD-A280207 p 4524 N94-37149
AD-A280208 p 4533 N94-36742 #
AD-A280219 p 4453 N94-37150
AD-A280229 p 4423 N94-37151
AD-A280230 p 4423 N94-37133
AD-A280232 p 4399 N94-37134
AD-A280233 p 4476 N94-37135
AD-A280234 p 4481 N94-37136
AD-A280235 p 4447 N94-37137
AD-A280236 p 4417 N94-37138
AD-A280240 p 4480 N94-37118
AD-A280243 p 4494 N94-37119
AD-A280244 p 4494 N94-37120
AD-A280248 p 4422 N94-37121
AD-A280250 p 4417 N94-37122
AD-A280251 p 4432 N94-36743 #
AD-A280260 p 4390 N94-37755 #
AD-A280261 p 4391 N94-37756 #
AD-A280262 p 4545 N94-37757 #
AD-A280275 p 4494 N94-37123
AD-A280298 p 4481 N94-37124
AD-A280310 p 4456 N94-37125
AD-A280313 p 4472 N94-37126
AD-A280320 p 4434 N94-37127
AD-A280321 p 4534 N94-37027
AD-A280325 p 4507 N94-37028
AD-A280326 p 4431 N94-37029
AD-A280327 p 4416 N94-37030 #
AD-A280330 p 4408 N94-37031
AD-A280332 p 4434 N94-37032
AD-A280334 p 4437 N94-37033
AD-A280341 p 4514 N94-37034 #
AD-A280347 p 4423 N94-37179
AD-A280357 p 4502 N94-36562 * #
AD-A280365 p 4473 N94-37180
AD-A280368 p 4423 N94-37181
AD-A280377 p 4437 N94-37035 #
AD-A280380 p 4534 N94-37036 #
AD-A280381 p 4434 N94-37162 #
AD-A280405 p 4528 N94-37182
AD-A280410 p 4434 N94-37183
AD-A280411 p 4424 N94-37184
AD-A280412 p 4481 N94-37224
AD-A280417 p 4391 N94-37225
AD-A280418 p 4469 N94-37215
AD-A280422 p 4399 N94-37214
AD-A280423 p 4476 N94-37216
AD-A280424 p 4473 N94-37217
AD-A280426 p 4434 N94-37218
AD-A280444 p 4383 N94-37219
AD-A280447 p 4404 N94-37232
AD-A280448 p 4424 N94-37185
AD-A280450 p 4494 N94-37226
AD-A280451 p 4424 N94-37227
AD-A280452 p 4420 N94-37758 #
AD-A280453 p 4456 N94-37186
AD-A280454 p 4536 N94-37228
AD-A280455 p 4477 N94-37229
AD-A280465 p 4527 N94-37139 #
AD-A280467 p 4481 N94-37140 #
AD-A280469 p 4434 N94-37141 #
AD-A280472 p 4494 N94-37230
AD-A280473 p 4482 N94-37233 #
AD-A280476 p 4470 N94-37649
AD-A280477 p 4487 N94-37347
AD-A280478 p 4396 N94-37349
AD-A280481 p 4525 N94-37350
AD-A280482 p 4397 N94-37351
AD-A280483 p 4381 N94-37352
AD-A280489 p 4481 N94-37353
AD-A280491 p 4524 N94-37142
AD-A280492 p 4473 N94-37143
AD-A280496 p 4423 N94-37144
AD-A280497 p 4409 N94-37145
AD-A280502 p 4503 N94-37146
AD-A280505 p 4423 N94-37147
AD-A280506 p 4443 N94-37128
AD-A280507 p 4422 N94-37104
AD-A280509 p 4404 N94-37105
AD-A280511 p 4399 N94-37106
AD-A280513 p 4437 N94-37107
AD-A280515 p 4437 N94-37108
AD-A280516 p 4516 N94-37109
AD-A280524 p 4524 N94-37110
AD-A280529 p 4404 N94-37088 #
AD-A280532 p 4399 N94-37650 #
AD-A280533 p 4480 N94-37089
AD-A280534 p 4431 N94-37090
AD-A280549 p 4476 N94-37038
AD-A280550 p 4489 N94-36731 #
AD-A280551 p 4478 N94-37045
AD-A280552 p 4507 N94-37046
AD-A280553 p 4506 N94-36732 #
AD-A280561 p 4476 N94-37047
AD-A280565 p 4500 N94-37039
AD-A280568 p 4493 N94-37040
AD-A280572 p 4388 N94-36733 #
AD-A280573 p 4533 N94-36734 #
AD-A280574 p 4514 N94-37041
AD-A280586 p 4408 N94-36735 #
AD-A280593 p 4500 N94-36736 #
AD-A280594 p 4499 N94-36722 #
AD-A280595 p 4503 N94-36723 #
AD-A280596 p 4441 N94-36724 #
AD-A280597 p 4539 N94-36725 #
AD-A280600 p 4392 N94-36726 #
AD-A280609 p 4533 N94-36727 #
AD-A280610 p 4506 N94-36728 #
AD-A280617 p 4543 N94-37042
AD-A280618 p 4500 N94-37043
AD-A280626 p 4404 N94-37044
AD-A280627 p 4440 N94-37759
AD-A280631 p 4382 N94-36729 #
AD-A280632 p 4390 N94-37163
AD-A280633 p 4499 N94-37760
AD-A280635 p 4403 N94-36730 #
AD-A280646 p 4475 N94-36761 #
AD-A280648 p 4475 N94-36762 #
AD-A280661 p 4389 N94-36763 #
AD-A280665 p 4480 N94-36764 #
AD-A280687 p 4535 N94-37129
AD-A280690 p 4508 N94-37130
AD-A280694 p 4384 N94-37131
AD-A280709 p 4501 N94-37526

AD-B17920 p 4526 N94-36472 #

AD-D016219 p 4448 N94-37481
AD-D016220 p 4425 N94-37482
AD-D016281 p 4436 N94-37835 #
AD-D016292 p 4413 N94-37761
AD-D016293 p 4452 N94-37766
AD-D016294 p 4385 N94-37767
AD-D016295 p 4430 N94-37768
AD-D016297 p 4440 N94-37769
AD-D016298 p 4538 N94-37770
AD-D016300 p 4435 N94-37771
AD-D016302 p 4449 N94-37772
AD-D016303 p 4427 N94-37773
AD-D016304 p 4526 N94-37774
AD-D016305 p 4440 N94-37775
AD-D016307 p 4538 N94-37776
AD-D016308 p 4449 N94-37777
AD-D016309 p 4427 N94-37778
AD-D016310 p 4427 N94-37779
AD-D016311 p 4427 N94-37818
AD-D016312 p 4450 N94-37838 #
AD-D016313 p 4385 N94-37839
AD-D016320 p 4440 N94-37840
AD-D016321 p 4427 N94-37829
AD-D016322 p 4385 N94-37830 #
AD-D016323 p 4427 N94-37831 #
AD-D016326 p 4440 N94-37832 #

AD-E201846 p 4464 N94-36973

AD-M000332 p 4433 N94-36757

ADST-94-W003283 p 4545 N94-37757 #

ADST/TR/94-003256 p 4390 N94-37755 #
ADST/TR/94-003276-VOL-4 p 4391 N94-37756 #

AECL-10757 p 4447 N94-36565 #
AECL-10823 p 4414 N94-36544 #
AECL-10877 p 4415 N94-36563 #
AECL-10882 p 4532 N94-36542 #
AECL-10950 p 4414 N94-36543 #

AECS-PH-S/FRSR-77 p 4415 N94-36564 #

AFIT/DS/AA/94-2 p 4500 N94-36736 #
AFIT/DS/AA/94-3 p 4382 N94-36729 #

AFIT/DS/ENG/94-03 p 4503 N94-36723 #
AFIT/DS/ENG/94J-01 p 4499 N94-36722 #
AFIT/DS/ENG/94J-04 p 4508 N94-37130
AFIT/DS/ENG/94J-05 p 4524 N94-37142

AFIT/DS/ENP/94-01 p 4535 N94-37129

AFIT/DS/ENS/94-1 p 4501 N94-37526

AFIT/ENG/GE/94J-01 p 4500 N94-37043

AFIT/GA/ENY/94J-1 ..... p 4390 N94-37163

AFIT/GAE/ENY/94J-04 ..... p 4388 N94-36733 #
AFIT/GAE/ENY/94J-1 ..... p 4441 N94-36724 #

AFIT/GCE/ENC/94J-1 ..... p 4434 N94-37141 #

AFIT/GCS/ENG/94J-02 ..... p 4543 N94-37042

AFIT/GE/ENG/94J-02 ..... p 4391 N94-37225

AFIT/GOR/ENS/94M-07 ..... p 4507 N94-36970

AFOSR-04-0348TR ..... p 4507 N94-37028
AFOSR-94-0231TR ..... p 4533 N94-36755
AFOSR-94-0267TR ..... p 4455 N94-36520
AFOSR-94-0347TR ..... p 4534 N94-37036 #
AFOSR-94-0349TR ..... p 4516 N94-37109
AFOSR-94-0352TR ..... p 4423 N94-37181
AFOSR-94-0353TR ..... p 4396 N94-37349
AFOSR-94-0354TR ..... p 4399 N94-37214
AFOSR-94-0355TR ..... p 4383 N94-37219
AFOSR-94-0357TR ..... p 4424 N94-37184
AFOSR-94-0358TR ..... p 4481 N94-37140 #
AFOSR-94-0359TR ..... p 4494 N94-37226
AFOSR-94-0360TR ..... p 4503 N94-37146
AFOSR-94-0361TR ..... p 4397 N94-37351
AFOSR-94-0362TR ..... p 4443 N94-37126
AFOSR-94-0364TR ..... p 4404 N94-37232
AFOSR-94-0365TR ..... p 4434 N94-37183
AFOSR-94-0366TR ..... p 4482 N94-37233 #
AFOSR-94-0368TR ..... p 4527 N94-37139 #

AGARD-CP-539 ..... p 4392 N94-36616 #
AGARD-CP-541 ..... p 4482 N94-37261 #
AGARD-CP-544 ..... p 4543 N94-37333 #

AGARD-R-790 ..... p 4453 N94-37321 #
AGARD-R-796 ..... p 4400 N94-36649 #
AGARD-R-799 ..... p 4540 N94-37447 #

AIAA PAPER 94-0083 ..... p 4441 N94-36646 * #
AIAA PAPER 94-0408 ..... p 4502 N94-36647 * #
AIAA PAPER 94-1754 ..... p 4403 N94-36956 * #
AIAA PAPER 94-1826 ..... p 4383 N94-36944 * #
AIAA PAPER 94-1930 ..... p 4383 N94-37378 * #
AIAA PAPER 94-2937 ..... p 4450 N94-36953 * #
AIAA PAPER 94-2955 ..... p 4382 N94-36686 * #
AIAA PAPER 94-4065 ..... p 4405 N94-37318 * #

AL/AO-TR-1993-0176 ..... p 4481 N94-37224

AL/CF-TR-1994-0029-PT-1 ..... p 4481 N94-37124

AL/OE-TR-1993-0162 ..... p 4534 N94-37027

ANL-HEP-CP-93-60 ..... p 4512 N94-36527 #
ANL-HEP-CP-93-70 ..... p 4513 N94-36538 #
ANL-HEP-CP-93-77 ..... p 4511 N94-36512 #
ANL-HEP-CP-93-99 ..... p 4511 N94-36483 #

ANL-HEP-TR-93-22 ..... p 4521 N94-36694 #

ANL-93/12 ..... p 4512 N94-36513 #
ANL-94/15 ..... p 4410 N94-37357 #

ANL/CHM/CP-81275 ..... p 4517 N94-37249 #
ANL/CHM/CP-81873 ..... p 4512 N94-36524 #
ANL/CHM/CP-81874 ..... p 4477 N94-36481 #
ANL/CHM/CP-81875 ..... p 4478 N94-36555 #
ANL/CHM/CP-81878 ..... p 4477 N94-36554 #
ANL/CHM/CP-82961 ..... p 4422 N94-37068 #

ANL/CHM/PP-77910 ..... p 4412 N94-37439 #
ANL/CHM/PP-81023 ..... p 4534 N94-37069 #
ANL/CHM/PP-81877 ..... p 4519 N94-37550 #

ANL/CMT/CP-79602 ..... p 4411 N94-37380
ANL/CMT/CP-82684 ..... p 4437 N94-37053 #

ANL/CMT/PP-73161 ..... p 4548 N94-36759 #

ANL/DIS/TM-13 ..... p 4434 N94-37206 #

ANL/ER/CP-81934 ..... p 4467 N94-37429 #
ANL/ER/CP-82908 ..... p 4467 N94-37440 #

ANL/ER/PP-74856 ..... p 4461 N94-36464 #

ANL/ES/CP-80868 ..... p 4465 N94-37100 #
ANL/ES/CP-81789 ..... p 4443 N94-37176 #
ANL/ES/CP-82657 ..... p 4422 N94-37055 #

ANL/ESD-20 ..... p 4452 N94-37515 #

ANL/ESD/TM-64 ..... p 4451 N94-37070 #

ANL/ET/CP-81391 ..... p 4530 N94-37441 #
ANL/ET/CP-81527 ..... p 4419 N94-37442 #
ANL/ET/CP-81945 ..... p 4438 N94-37111 #
ANL/ET/CP-81946 ..... p 4537 N94-37377
ANL/ET/CP-82303 ..... p 4425 N94-37423 #

ANL/IPD/CP-82431 ..... p 4497 N94-36441 #

ANL/ITD/RP-82647 ..... p 4535 N94-37193 #

ANL/MCS-TM-184 ..... p 4504 N94-37246 #

ANL/MCS/CP-82092 ..... p 4504 N94-37247 #
ANL/MCS/CP-82803 ..... p 4505 N94-37518 #
ANL/MCS/CP-82804 ..... p 4498 N94-37519 #
ANL/MCS/CP-82927 ..... p 4496 N94-37549 #
ANL/MCS/CP-82973 ..... p 4496 N94-37551 #

ANL/MCS/PP-74001 ..... p 4445 N94-37724 #

ANL/MSD/CP-79818 ..... p 4513 N94-36696 #
ANL/MSD/CP-81222 ..... p 4535 N94-37192 #
ANL/MSD/CP-82160 ..... p 4509 N94-37517 #
ANL/MSD/CP-82716 ..... p 4420 N94-37516
ANL/MSD/CP-82754 ..... p 4534 N94-37054 #

ANL/PHY/CP-82605 ..... p 4523 N94-37619 #

ANL/RA/CP-80550 ..... p 4521 N94-37194 #

ANL/TD/CP-82061 ..... p 4420 N94-37552 #
ANL/TD/CP-82680 ..... p 4435 N94-37736 #

ARCCB-TR-94011 ..... p 4417 N94-37138

ARL-CR-117 ..... p 4420 N94-37758 #

ARL-MR-157 ..... p 4386 N94-37256 * #

ARL-TR-291 ..... p 4452 N94-37457 * #
ARL-TR-389 ..... p 4452 N94-37521 * #
ARL-TR-447 ..... p 4417 N94-37122
ARL-TR-448 ..... p 4432 N94-36743 #
ARL-TR-457 ..... p 4451 N94-37451 * #
ARL-TR-475 ..... p 4450 N94-36953 * #
ARL-TR-477 ..... p 4451 N94-37319 * #

ARM-94-001 ..... p 4474 N94-37394 #

ASIPP-0036 ..... p 4479 N94-37535 #

ATC-207 ..... p 4472 N94-37126

ATCOM-TR-94-A-013 ..... p 4383 N94-36966 * #

AU-ARI-93-4 ..... p 4386 N94-36465

B-254253 ..... p 4392 N94-37026 #
B-257654 ..... p 4396 N94-37257 #

BNL-49448 ..... p 4513 N94-36539 #
BNL-49462 ..... p 4512 N94-36526 #
BNL-49557 ..... p 4408 N94-36559 #
BNL-49593 ..... p 4510 N94-36442 #
BNL-49626 ..... p 4511 N94-36460 #
BNL-49773 ..... p 4525 N94-37258 #
BNL-49799 ..... p 4505 N94-37675
BNL-49801 ..... p 4524 N94-37157 #
BNL-60186 ..... p 4537 N94-37499 #
BNL-60245 ..... p 4516 N94-37152 #
BNL-60249 ..... p 4516 N94-37158 #
BNL-60251 ..... p 4518 N94-37364 #
BNL-60347 ..... p 4417 N94-37153 #
BNL-60355 ..... p 4520 N94-37672 #
BNL-60381 ..... p 4537 N94-37498 #
BNL-60385 ..... p 4482 N94-37444 #

BUDKERINP-92-11 ..... p 4521 N94-36748 #
BUDKERINP-92-46 ..... p 4516 N94-37096
BUDKERINP-92-80 ..... p 4514 N94-37065 #
BUDKERINP-92-83 ..... p 4509 N94-37078 #
BUDKERINP-92-88 ..... p 4517 N94-37171 #
BUDKERINP-92-89 ..... p 4514 N94-36747 #
BUDKERINP-92-97-PT-1 ..... p 4514 N94-36749 #

CBP-72 ..... p 4521 N94-37200 #

CCMS-94-05 ..... p 4406 N94-37653 * #

CDRL-005 ..... p 4494 N94-37061 * #
CDRL-008 ..... p 4461 N94-36919 * #

CERC-94-5 ..... p 4476 N94-37216
CERC-94-6 ..... p 4476 N94-37135
CERC-94-7 ..... p 4477 N94-37229

CERL-FM-94/07 ..... p 4422 N94-37104

CERL-P1-01 ..... p 4403 N94-36730 #

CERL-TR-FE-94/10 ..... p 4440 N94-37759

CMC-TR2.1-94-VOL-1 ..... p 4493 N94-36914 * #
CMC-TR4.2-92-VOL-2 ..... p 4493 N94-36922 * #

CMU-CS-94-137 ..... p 4494 N94-37119

CMU/SEI-93-TR-27 ..... p 4493 N94-36974

CNIC-00746 ..... p 4479 N94-37535 #
CNIC-00758 ..... p 4412 N94-37534 #
CNIC-00759 ..... p 4412 N94-37533 #

COG-93-205 ..... p 4415 N94-36563 #
COG-93-376 ..... p 4414 N94-36543 #
COG-93-84 ..... p 4414 N94-36544 #

CONF-9203297 ..... p 4527 N94-36566 #
CONF-9207233 ..... p 4518 N94-37360 #
CONF-9209396 ..... p 4530 N94-37384 #
CONF-9209420 ..... p 4531 N94-37493 #
CONF-9209447 ..... p 4415 N94-36563 #
CONF-9211211-6 ..... p 4530 N94-37437 #
CONF-9212108 ..... p 4523 N94-37727 #
CONF-9301109-5 ..... p 4515 N94-37067 #
CONF-930173-14 ..... p 4516 N94-37152 #
CONF-930173-19 ..... p 4518 N94-37364 #
CONF-930173-20 ..... p 4516 N94-37158 #
CONF-930269-26 ..... p 4522 N94-37303 #
CONF-9303119-5 ..... p 4513 N94-36697 #
CONF-9303122-5-REV-1 ..... p 4475 N94-37621 #
CONF-9303122 ..... p 4467 N94-37454 #
CONF-9305282-2 ..... p 4511 N94-36460 #
CONF-9305311-1 ..... p 4511 N94-36459 #
CONF-9305325 ..... p 4416 N94-37074 #
CONF-930611 ..... p 4414 N94-36543 #
CONF-9306140-1 ..... p 4512 N94-36515 #
CONF-9306140-3 ..... p 4539 N94-36507 #
CONF-9306166 ..... p 4431 N94-37452 #
CONF-9306176-10 ..... p 4513 N94-36539 #
CONF-9306176-11 ..... p 4512 N94-36527 #
CONF-9306176-19 ..... p 4511 N94-36483 #
CONF-9306176-9 ..... p 4512 N94-36526 #
CONF-9306218-1 ..... p 4400 N94-36509 #
CONF-9306221-10 ..... p 4520 N94-37674 #
CONF-9306221-6 ..... p 4513 N94-36558 #
CONF-9306221-8 ..... p 4513 N94-36538 #
CONF-9306228-1 ..... p 4511 N94-36457 #
CONF-9306248-2 ..... p 4513 N94-36696 #
CONF-9306251-1 ..... p 4513 N94-36695 #
CONF-9306258-15 ..... p 4518 N94-37298 #
CONF-9306258-4 ..... p 4511 N94-36512 #
CONF-9306281-1 ..... p 4408 N94-36559 #
CONF-930637-15 ..... p 4520 N94-37672 #
CONF-930676-65 ..... p 4407 N94-36458 #
CONF-930676-9 ..... p 4400 N94-36456 #
CONF-9307143-1 ..... p 4514 N94-36700 #
CONF-9307155-3 ..... p 4537 N94-37499 #
CONF-930717-2 ..... p 4512 N94-36516 #
CONF-9307181-1 ..... p 4477 N94-37494 #
CONF-930761-5 ..... p 4511 N94-36463 #
CONF-930767-8 ..... p 4539 N94-37543 #
CONF-9308122-18 ..... p 4419 N94-37420 #
CONF-9308160-2 ..... p 4415 N94-36553 #
CONF-9308164-7 ..... p 4510 N94-36442 #
CONF-9308181 ..... p 4520 N94-37716 #
CONF-9308210-2 ..... p 4519 N94-37558
CONF-9308213 ..... p 4448 N94-37169 #
CONF-930824-31 ..... p 4525 N94-37258 #
CONF-930893-3 ..... p 4463 N94-37488 #
CONF-9309185-3 ..... p 4502 N94-36685 #
CONF-9309233-1 ..... p 4525 N94-37486 #
CONF-9309256-5 ..... p 4426 N94-37714 #
CONF-930926-2 ..... p 4508 N94-36556 #
CONF-9309292-1 ..... p 4513 N94-36528 #
CONF-930999-10 ..... p 4548 N94-37557
CONF-931009-25 ..... p 4535 N94-37212 #
CONF-9310135-4 ..... p 4474 N94-37379
CONF-9310164-11 ..... p 4467 N94-37428 #
CONF-9310169-3 ..... p 4437 N94-37053 #
CONF-9310191-2 ..... p 4426 N94-37490 #
CONF-9310193-11 ..... p 4523 N94-37619 #
CONF-9310239-2 ..... p 4547 N94-37667 #
CONF-9310313-1 ..... p 4521 N94-37194 #
CONF-9310316-1 ..... p 4548 N94-37164 #
CONF-9310322-1 ..... p 4527 N94-37082 #
CONF-931085-1 ..... p 4466 N94-37211 #
CONF-931107-37 ..... p 4482 N94-37444 #
CONF-931108-101 ..... p 4413 N94-37630
CONF-931108-10 ..... p 4414 N94-36461 #
CONF-931108-38 ..... p 4411 N94-37380
CONF-9311101-3 ..... p 4436 N94-36557 #

CONF-9311104-21 ..... p 4537 N94-37498 #
CONF-9311104-22 ..... p 4519 N94-37553 #
CONF-9311109-1 ..... p 4436 N94-36514 #
CONF-9311138-2 ..... p 4449 N94-37628 #
CONF-9311208-1 ..... p 4465 N94-37155 #
CONF-931178-2 ..... p 4530 N94-37436 #
CONF-931269 ..... p 4462 N94-37418 #
CONF-940115-26 ..... p 4463 N94-36478 #
CONF-940115-27 ..... p 4545 N94-37348 #
CONF-940115-32 ..... p 4466 N94-37288 #
CONF-940120-2 ..... p 4443 N94-37050 #
CONF-940122-4 ..... p 4535 N94-37166 #
CONF-940131-4 ..... p 4471 N94-36479 #
CONF-940131-6 ..... p 4463 N94-36477 #
CONF-940135-6 ..... p 4404 N94-37205 #
CONF-940136-2 ..... p 4498 N94-37487 #
CONF-940142-37 ..... p 4449 N94-37733 #
CONF-940142-38 ..... p 4521 N94-37200 #
CONF-940142-39 ..... p 4408 N94-37056 #
CONF-940168 ..... p 4467 N94-37492 #
CONF-940169-4 ..... p 4520 N94-37715 #
CONF-940173-3 ..... p 4520 N94-37671
CONF-940181-1 ..... p 4444 N94-37390 #
CONF-940182-1 ..... p 4548 N94-37049 #
CONF-940185-1 ..... p 4418 N94-37410 #
CONF-940216-2 ..... p 4518 N94-37305 #
CONF-940216-4 ..... p 4529 N94-37316 #
CONF-940226-7 ..... p 4449 N94-37737 #
CONF-940233-1 ..... p 4515 N94-37084 #
CONF-940277-1 ..... p 4474 N94-37566 #
CONF-940277-3 ..... p 4473 N94-37371 * #
CONF-940280-1 ..... p 4522 N94-37310 #
CONF-9403110-1 ..... p 4468 N94-37624 #
CONF-9403111-1 ..... p 4480 N94-37625 #
CONF-9403115-1 ..... p 4471 N94-37669 #
CONF-9403115-2 ..... p 4549 N94-37668 #
CONF-9403116-1 ..... p 4471 N94-37701 #
CONF-9403118-1 ..... p 4539 N94-37366 #
CONF-9403119-1 ..... p 4416 N94-37080 #
CONF-9403120-1 ..... p 4517 N94-37249 #
CONF-9403120-2 ..... p 4438 N94-37295 #
CONF-940327-1 ..... p 4515 N94-37087 #
CONF-940327-2 ..... p 4515 N94-37085 #
CONF-940362-3 ..... p 4468 N94-37624 #
CONF-940362-4 ..... p 4474 N94-37565 #
CONF-940362-5 ..... p 4472 N94-37048 #
CONF-940371-1 ..... p 4467 N94-37440 #
CONF-940397-1 ..... p 4407 N94-36482 #
CONF-940397-2 ..... p 4409 N94-37199 #
CONF-940407-20 ..... p 4498 N94-37419 #
CONF-940411-11 ..... p 4535 N94-37192 #
CONF-940411-15 ..... p 4420 N94-37516
CONF-940411-16 ..... p 4538 N94-37570 #
CONF-940411-17 ..... p 4537 N94-37369 #
CONF-940411-18 ..... p 4426 N94-37537 #
CONF-940411-20 ..... p 4537 N94-37356 #
CONF-940411-22 ..... p 4536 N94-37287 #
CONF-940411-23 ..... p 4536 N94-37290 #
CONF-940411-24 ..... p 4425 N94-37317 #
CONF-9404113-1 ..... p 4489 N94-36480 #
CONF-940412-5 ..... p 4405 N94-37370 #
CONF-9404133-1 ..... p 4430 N94-36447 #
CONF-9404135-1 ..... p 4447 N94-36510 #
CONF-9404135-2 ..... p 4449 N94-37722 #
CONF-9404135-3 ..... p 4447 N94-37114 #
CONF-9404138-1-VUGRAPHS ..... p 4497 N94-36441 #
CONF-9404141-1 ..... p 4518 N94-37383 #
CONF-9404144-1 ..... p 4457 N94-37622 #
CONF-9404145-1 ..... p 4495 N94-37430 #
CONF-9404162-2 ..... p 4495 N94-37496 #
CONF-9404169-1 ..... p 4550 N94-37293 #
CONF-940423-1 ..... p 4462 N94-37189 #
CONF-940433-3 ..... p 4412 N94-37542 #
CONF-940449-7 ..... p 4481 N94-37197 #
CONF-940449-8 ..... p 4506 N94-37719 #
CONF-940492-2 ..... p 4547 N94-37555 #
CONF-940492-3 ..... p 4523 N94-37547 #
CONF-940504-1 ..... p 4410 N94-37296 #
CONF-940510-6 ..... p 4389 N94-37159 #
CONF-940510-7 ..... p 4424 N94-37204 #
CONF-9405100-2 ..... p 4498 N94-37568 #
CONF-9405100-3 ..... p 4498 N94-37519 #
CONF-9405100-4 ..... p 4505 N94-37518 #
CONF-9405100-5 ..... p 4496 N94-37551 #
CONF-9405112-2 ..... p 4432 N94-36471 #
CONF-9405128-1 ..... p 4526 N94-36448 #
CONF-9405132-3 ..... p 4520 N94-37717 #
CONF-9405132-4 ..... p 4515 N94-37086 #
CONF-9405136-11 ..... p 4429 N94-37413 #
CONF-9405136-2 ..... p 4428 N94-37201 #
CONF-9405136-3 ..... p 4428 N94-37202 #
CONF-9405136-6 ..... p 4428 N94-37052 #
CONF-9405136-8 ..... p 4411 N94-37412 #
CONF-9405139-1 ..... p 4443 N94-37195 #
CONF-9405143-3 ..... p 4425 N94-37423 #
CONF-9405146-1 ..... p 4465 N94-37154 #
CONF-9405147-1 ..... p 4517 N94-37209 #
CONF-9405147-2 ..... p 4438 N94-37213 #
CONF-9405147-3 ..... p 4528 N94-37207 #
CONF-9405150-1 ..... p 4422 N94-37055 #
CONF-9405157-2 ..... p 4449 N94-37495 #
CONF-940524-5 ..... p 4517 N94-37210 #
CONF-940552-2 ..... p 4446 N94-37723 #
CONF-940552-7 ..... p 4527 N94-37081 #
CONF-940552-8 ..... p 4528 N94-37297 #
CONF-940553-30 ..... p 4463 N94-36470 #
CONF-940553-4 ..... p 4472 N94-36739 #
CONF-940582-1-REV-1 ..... p 4447 N94-37160 #
CONF-940582-4 ..... p 4448 N94-37244 #
CONF-940593-10 ..... p 4512 N94-36524 #
CONF-940593-6 ..... p 4477 N94-36481 #
CONF-940593-8 ..... p 4478 N94-36555 #
CONF-940593-9 ..... p 4477 N94-36554 #
CONF-940596-4 ..... p 4439 N94-37363
CONF-940598-1 ..... p 4405 N94-37289 #
CONF-940602-8 ..... p 4502 N94-36455 #
CONF-940613-8 ..... p 4451 N94-37186 #
CONF-9406160-1 ..... p 4507 N94-37564 #
CONF-9406162-1 ..... p 4505 N94-37620 #
CONF-9406163-1 ..... p 4443 N94-37176 #
CONF-9406166-1 ..... p 4409 N94-37161 #
CONF-9406167-1 ..... p 4417 N94-37153 #
CONF-9406168-1 ..... p 4425 N94-37422 #
CONF-9406170-1 ..... p 4504 N94-37247 #
CONF-940618-1 ..... p 4505 N94-37675
CONF-940618-3 ..... p 4524 N94-37157 #
CONF-940629-3 ..... p 4509 N94-37517 #
CONF-940629-4 ..... p 4534 N94-37054 #
CONF-940629-5 ..... p 4534 N94-37057 #
CONF-940630-8 ..... p 4528 N94-37292 #
CONF-940630-9 ..... p 4527 N94-37101 #
CONF-940632-16 ..... p 4465 N94-37100 #
CONF-940632-17 ..... p 4467 N94-37429 #
CONF-940646-2 ..... p 4540 N94-37092 #
CONF-940651-2 ..... p 4440 N94-37738 #
CONF-940651-3 ..... p 4438 N94-37111 #
CONF-940651-4 ..... p 4537 N94-37377
CONF-940663-1 ..... p 4417 N94-37367 #
CONF-940664-1 ..... p 4419 N94-37442 #
CONF-940664-2 ..... p 4528 N94-37307 #
CONF-940664-5 ..... p 4530 N94-37441 #
CONF-940664-9 ..... p 4420 N94-37552 #
CONF-940691-2 ..... p 4408 N94-37091 #
CONF-940692-4 ..... p 4420 N94-37548 #
CONF-940701-2 ..... p 4536 N94-37291 #
CONF-940711-1 ..... p 4407 N94-36462 #
CONF-940711-2 ..... p 4407 N94-36482 #
CONF-940711-3 ..... p 4413 N94-37711 #
CONF-940719-1 ..... p 4457 N94-37670 #
CONF-940719-4 ..... p 4496 N94-37549 #
CONF-940726-10 ..... p 4438 N94-37196 #
CONF-940726-11 ..... p 4438 N94-37190 #
CONF-940726-2 ..... p 4532 N94-36540 #
CONF-940726-8 ..... p 4439 N94-37513 #
CONF-940742-5 ..... p 4506 N94-37718 #
CONF-940753-10 ..... p 4418 N94-37399 #
CONF-940753-4 ..... p 4538 N94-37569 #
CONF-940753-5 ..... p 4538 N94-37545 #
CONF-940753-6 ..... p 4525 N94-37374 #
CONF-940753-7 ..... p 4537 N94-37382 #
CONF-940753-8 ..... p 4418 N94-37396 #
CONF-940753-9 ..... p 4418 N94-37398 #
CONF-940766-1 ..... p 4517 N94-37238 #
CONF-940766-2 ..... p 4412 N94-37546 #
CONF-940766-4 ..... p 4417 N94-37304 #
CONF-940766-6 ..... p 4537 N94-37400 #
CONF-940769-1 ..... p 4465 N94-37093 #
CONF-940769-2 ..... p 4472 N94-37115 #
CONF-940769-3 ..... p 4473 N94-37242 #
CONF-940771-1 ..... p 4457 N94-37705 #
CONF-940775-1 ..... p 4411 N94-37365 #
CONF-940782-1 ..... p 4422 N94-37068 #
CONF-940809-4 ..... p 4424 N94-37223 #
CONF-940814-1 ..... p 4435 N94-37391 #
CONF-940838-4 ..... p 4409 N94-37221 #
CONF-940838-5 ..... p 4410 N94-37222 #
CONF-940854-1 ..... p 4446 N94-37388 #
CONF-940859-14 ..... p 4502 N94-37785 #
CONF-940859-16-PT-2 ..... p 4501 N94-37735 #
CONF-940859-18 ..... p 4496 N94-37739 #
CONF-940859-21 ..... p 4500 N94-37083 #
CONF-940859-4 ..... p 4466 N94-37389 #
CONF-940859-5 ..... p 4496 N94-37782 #
CONF-940859-6 ..... p 4501 N94-37529 #
CONF-940859-9 ..... p 4502 N94-37784 #
CONF-940860-1 ..... p 4501 N94-37425 #
CONF-940869-1 ..... p 4501 N94-37783 #
CONF-940871-1 ..... p 4510 N94-37536 #
CONF-940889-2-REV-1 ..... p 4530 N94-37392 #

CRAD-9103-TR-9248 ..... p 4466 N94-37252 * #

CRC-93-003 ..... p 4434 N94-37127

CREARE-TN-508 ..... p 4461 N94-36805 * #

CUBRC-640II-PT-1/2 ..... p 4442 N94-36969 * #

CWP-142P ..... p 4510 N94-36551 #

DE93-017638 ..... p 4400 N94-36456 #
DE93-018556 ..... p 4511 N94-36457 #
DE93-019213 ..... p 4430 N94-36444 #
DE93-019584 ..... p 4523 N94-36693 #
DE93-019681 ..... p 4521 N94-36694 #
DE93-040831 ..... p 4525 N94-37486 #
DE93-040927 ..... p 4513 N94-36695 #
DE93-041158 ..... p 4513 N94-36696 #
DE93-041348 ..... p 4513 N94-36697 #
DE94-000056 ..... p 4469 N94-36738 #
DE94-000087 ..... p 4441 N94-36550 #
DE94-000125 ..... p 4492 N94-36698 #
DE94-000126 ..... p 4493 N94-36699 #
DE94-000620 ..... p 4514 N94-36700 #
DE94-000675 ..... p 4502 N94-36685 #
DE94-000762 ..... p 4508 N94-36556 #
DE94-001207 ..... p 4436 N94-36557 #
DE94-001219 ..... p 4513 N94-36558 #
DE94-001351 ..... p 4513 N94-36538 #
DE94-001381 ..... p 4513 N94-36539 #
DE94-001386 ..... p 4512 N94-36526 #
DE94-001422 ..... p 4498 N94-37487 #
DE94-002005 ..... p 4463 N94-37488 #
DE94-002216 ..... p 4511 N94-36512 #
DE94-002217 ..... p 4512 N94-36527 #
DE94-002497 ..... p 4512 N94-36513 #
DE94-002624 ..... p 4436 N94-36514 #
DE94-002689 ..... p 4512 N94-36515 #
DE94-003199 ..... p 4408 N94-36559 #
DE94-003249 ..... p 4508 N94-36560 #
DE94-003617 ..... p 4513 N94-36528 #
DE94-003623 ..... p 4512 N94-36516 #
DE94-003625 ..... p 4407 N94-36458 #
DE94-003643 ..... p 4511 N94-36459 #
DE94-003894 ..... p 4511 N94-36460 #
DE94-003931 ..... p 4414 N94-36461 #
DE94-004075 ..... p 4470 N94-37489 #
DE94-004088 ..... p 4452 N94-37512 #
DE94-004159 ..... p 4510 N94-36551 #
DE94-004160 ..... p 4525 N94-37532 #
DE94-004235 ..... p 4510 N94-36442 #
DE94-004304 ..... p 4472 N94-36739 #
DE94-004340 ..... p 4407 N94-36462 #
DE94-004341 ..... p 4407 N94-36482 #
DE94-004404 ..... p 4464 N94-36552 #
DE94-004470 ..... p 4432 N94-36443 #
DE94-004578 ..... p 4511 N94-36483 #
DE94-004595 ..... p 4474 N94-37379
DE94-004659 ..... p 4511 N94-36463 #
DE94-004747 ..... p 4521 N94-37220 #
DE94-004765 ..... p 4415 N94-36553 #
DE94-004949 ..... p 4525 N94-37258 #
DE94-005025 ..... p 4407 N94-36475 #
DE94-005105 ..... p 4409 N94-37221 #
DE94-005107 ..... p 4413 N94-37711 #
DE94-005250 ..... p 4410 N94-37222 #
DE94-005336 ..... p 4424 N94-37223 #
DE94-005482 ..... p 4411 N94-37380
DE94-006190 ..... p 4446 N94-37388 #
DE94-006466 ..... p 4501 N94-37425 #
DE94-006887 ..... p 4429 N94-37426 #
DE94-006888 ..... p 4429 N94-37402 #
DE94-006889 ..... p 4429 N94-37403 #
DE94-006892 ..... p 4429 N94-37404 #
DE94-006895 ..... p 4461 N94-36476 #
DE94-006905 ..... p 4461 N94-36740 #
DE94-006906 ..... p 4467 N94-37405 #
DE94-006909 ..... p 4451 N94-37406 #
DE94-006917 ..... p 4462 N94-37407 #
DE94-006918 ..... p 4533 N94-36744 #
DE94-006925 ..... p 4451 N94-37408 #
DE94-006931 ..... p 4533 N94-36745 #
DE94-006936 ..... p 4462 N94-37381
DE94-006949 ..... p 4411 N94-37409 #
DE94-007107 ..... p 4526 N94-36536 #
DE94-007289 ..... p 4532 N94-36540 #
DE94-007439 ..... p 4465 N94-37187 #
DE94-007473 ..... p 4463 N94-36477 #
DE94-007477 ..... p 4545 N94-37348 #
DE94-007478 ..... p 4463 N94-36478 #
DE94-007480 ..... p 4471 N94-36479 #
DE94-007556 ..... p 4466 N94-37389 #
DE94-007572 ..... p 4496 N94-37782 #
DE94-007582 ..... p 4470 N94-37527 #
DE94-007854 ..... p 4501 N94-37783 #
DE94-007864 ..... p 4439 N94-37513 #
DE94-008424 ..... p 4501 N94-37529 #
DE94-008429 ..... p 4489 N94-36480 #

DE94-008529 ..... p 4539 N94-36507 #
DE94-008530 ..... p 4539 N94-36508 #
DE94-008678 ..... p 4510 N94-37536 #
DE94-008846 ..... p 4511 N94-36506 #
DE94-008868 ..... p 4502 N94-37784 #
DE94-009177 ..... p 4400 N94-36509 #
DE94-009285 ..... p 4502 N94-37785 #
DE94-009287 ..... p 4463 N94-36470 #
DE94-009303 ..... p 4447 N94-36510 #
DE94-009396 ..... p 4533 N94-36746 #
DE94-009684 ..... p 4477 N94-36481 #
DE94-009692 ..... p 4512 N94-36524 #
DE94-009693 ..... p 4477 N94-36554 #
DE94-009694 ..... p 4478 N94-36555 #
DE94-009736 ..... p 4497 N94-36441 #
DE94-009820 ..... p 4461 N94-36464 #
DE94-009870 ..... p 4398 N94-37514 #
DE94-009997 ..... p 4426 N94-37490 #
DE94-010041 ..... p 4469 N94-36758 #
DE94-010075 ..... p 4430 N94-36447 #
DE94-010078 ..... p 4432 N94-36471 #
DE94-010090 ..... p 4526 N94-36448 #
DE94-010105 ..... p 4421 N94-36474 #
DE94-010126 ..... p 4501 N94-37735 #
DE94-010373 ..... p 4451 N94-37188 #
DE94-010379 ..... p 4457 N94-37705 #
DE94-010381 ..... p 4412 N94-37542 #
DE94-010382 ..... p 4462 N94-37189 #
DE94-010397 ..... p 4438 N94-37190 #
DE94-010405 ..... p 1444 N94-37390 #
DE94-010406 ..... p 4524 N94-37191 #
DE94-010432 ..... p 4535 N94-37192 #
DE94-010436 ..... p 4535 N94-37193 #
DE94-010445 ..... p 4523 N94-37619 #
DE94-010465 ..... p 4521 N94-37194 #
DE94-010467 ..... p 4548 N94-36759 #
DE94-010663 ..... p 4539 N94-37543 #
DE94-010682 ..... p 4506 N94-36449 #
DE94-010691 ..... p 4406 N94-36450 #
DE94-010716 ..... p 4461 N94-36511 #
DE94-010729 ..... p 4444 N94-37544 #
DE94-010740 ..... p 4468 N94-36451 #
DE94-010746 ..... p 4505 N94-37620 #
DE94-010750 ..... p 4439 N94-37363
DE94-010757 ..... p 4443 N94-37195 #
DE94-010758 ..... p 4438 N94-37196 #
DE94-010772 ..... p 4453 N94-36452 #
DE94-010773 ..... p 4406 N94-36453 #
DE94-010790 ..... p 4532 N94-36454 #
DE94-010791 ..... p 4481 N94-37197 #
DE94-010794 ..... p 4475 N94-37621 #
DE94-010798 ..... p 4457 N94-37622 #
DE94-010800 ..... p 4408 N94-37091 #
DE94-010801 ..... p 4540 N94-37092 #
DE94-010807 ..... p 4435 N94-37391 #
DE94-010809 ..... p 4502 N94-36455 #
DE94-010813 ..... p 4431 N94-37452 #
DE94-010820 ..... p 4465 N94-37093 #
DE94-010839 ..... p 4495 N94-37453 #
DE94-010897 ..... p 4548 N94-37164 #
DE94-010994 ..... p 4524 N94-37165 #
DE94-011004 ..... p 4448 N94-37198 #
DE94-011030 ..... p 4495 N94-37430 #
DE94-011132 ..... p 4411 N94-37431 #
DE94-011193 ..... p 4482 N94-37444 #
DE94-011194 ..... p 4467 N94-37454 #
DE94-011199 ..... p 4535 N94-37166 #
DE94-011200 ..... p 4426 N94-37712 #
DE94-011202 ..... p 4418 N94-37410 #
DE94-011208 ..... p 4413 N94-37713 #
DE94-011211 ..... p 4413 N94-37754 #
DE94-011224 ..... p 4413 N94-37623 #
DE94-011234 ..... p 4472 N94-37048 #
DE94-011235 ..... p 4468 N94-37624 #
DE94-011239 ..... p 4480 N94-37625 #
DE94-011244 ..... p 4531 N94-37626 #
DE94-011249 ..... p 4405 N94-37627 #
DE94-011300 ..... p 4449 N94-37628 #
DE94-011336 ..... p 4426 N94-37714 #
DE94-011341 ..... p 4548 N94-37557
DE94-011344 ..... p 4520 N94-37715 #
DE94-011346 ..... p 4409 N94-37199 #
DE94-011347 ..... p 4520 N94-37716 #
DE94-011348 ..... p 4521 N94-37200 #
DE94-011360 ..... p 4439 N94-37302 #
DE94-011367 ..... p 4548 N94-37049 #
DE94-011368 ..... p 4520 N94-37717 #
DE94-011372 ..... p 4506 N94-37718 #
DE94-011374 ..... p 4443 N94-37050 #
DE94-011377 ..... p 4519 N94-37558
DE94-011378 ..... p 4506 N94-37719 #
DE94-011380 ..... p 4521 N94-37720 #
DE94-011406 ..... p 4545 N94-37563 #
DE94-011411 ..... p 4447 N94-37051 #
DE94-011417 ..... p 4507 N94-37564 #
DE94-011419 ..... p 4428 N94-37052 #
DE94-011423 ..... p 4411 N94-37412 #
DE94-011430 ..... p 4429 N94-37413 #
DE94-011432 ..... p 4428 N94-37201 #
DE94-011433 ..... p 4428 N94-37202 #
DE94-011441 ..... p 4474 N94-37565 #
DE94-011442 ..... p 4474 N94-37566 #
DE94-011458 ..... p 4463 N94-37567 #
DE94-011460 ..... p 4498 N94-37568 #
DE94-011464 ..... p 4538 N94-37569 #
DE94-011466 ..... p 4517 N94-37238 #
DE94-011468 ..... p 4538 N94-37570 #
DE94-011469 ..... p 4538 N94-37545 #
DE94-011470 ..... p 4412 N94-37546 #
DE94-011471 ..... p 4438 N94-37239 #
DE94-011478 ..... p 4435 N94-37736 #
DE94-011481 ..... p 4437 N94-37053 #
DE94-011482 ..... p 4448 N94-37203 #
DE94-011486 ..... p 4452 N94-37515 #
DE94-011488 ..... p 4445 N94-37724 #
DE94-011496 ..... p 4420 N94-37516
DE94-011502 ..... p 4438 N94-37111 #
DE94-011503 ..... p 4537 N94-37377
DE94-011504 ..... p 4509 N94-37517 #
DE94-011509 ..... p 4534 N94-37054 #
DE94-011512 ..... p 4505 N94-37518 #
DE94-011513 ..... p 4498 N94-37519 #
DE94-011526 ..... p 4422 N94-37055 #
DE94-011541 ..... p 4524 N94-37112 #
DE94-011542 ..... p 4448 N94-37240 #
DE94-011581 ..... p 4516 N94-37113 #
DE94-011583 ..... p 4466 N94-37376
DE94-011587 ..... p 4438 N94-37241 #
DE94-011609 ..... p 4523 N94-37629 #
DE94-011613 ..... p 4473 N94-37242 #
DE94-011622 ..... p 4413 N94-37630
DE94-011623 ..... p 4408 N94-37056 #
DE94-011626 ..... p 4428 N94-37243 #
DE94-011628 ..... p 4468 N94-37631 #
DE94-011636 ..... p 4521 N94-37721 #
DE94-011637 ..... p 4448 N94-37244 #
DE94-011641 ..... p 4447 N94-37114 #
DE94-011643 ..... p 4449 N94-37722 #
DE94-011644 ..... p 4449 N94-37737 #
DE94-011645 ..... p 4446 N94-37723 #
DE94-011648 ..... p 4534 N94-37057 #
DE94-011654 ..... p 4449 N94-37733 #
DE94-011665 ..... p 4468 N94-37740 #
DE94-011684 ..... p 4472 N94-37115 #
DE94-011693 ..... p 4549 N94-37668 #
DE94-011694 ..... p 4471 N94-37669 #
DE94-011701 ..... p 4440 N94-37738 #
DE94-011702 ..... p 4471 N94-37701 #
DE94-011711 ..... p 4457 N94-37670 #
DE94-011718 ..... p 4496 N94-37739 #
DE94-011720 ..... p 4520 N94-37671
DE94-011726 ..... p 4516 N94-37152 #
DE94-011732 ..... p 4417 N94-37153 #
DE94-011733 ..... p 4520 N94-37672 #
DE94-011744 ..... p 4496 N94-37673 #
DE94-011745 ..... p 4477 N94-37494 #
DE94-011749 ..... p 4547 N94-37667 #
DE94-011750 ..... p 4520 N94-37674 #
DE94-011753 ..... p 4465 N94-37154 #
DE94-011759 ..... p 4465 N94-37155 #
DE94-011800 ..... p 4479 N94-37156 #
DE94-011919 ..... p 4505 N94-37675
DE94-011922 ..... p 4524 N94-37157 #
DE94-011923 ..... p 4518 N94-37364 #
DE94-011927 ..... p 4516 N94-37158 #
DE94-011937 ..... p 4389 N94-37159 #
DE94-011940 ..... p 4411 N94-37365 #
DE94-011945 ..... p 4538 N94-37676 #
DE94-011972 ..... p 4538 N94-37677 #
DE94-012057 ..... p 4539 N94-37366 #
DE94-012061 ..... p 4530 N94-37392 #
DE94-012062 ..... p 4447 N94-37160 #
DE94-012066 ..... p 4409 N94-37161 #
DE94-012067 ..... p 4426 N94-37537 #
DE94-012068 ..... p 4424 N94-37204 #
DE94-012071 ..... p 4417 N94-37367 #
DE94-012078 ..... p 4435 N94-37393 #
DE94-012080 ..... p 4522 N94-37303 #
DE94-012107 ..... p 4448 N94-37368 #
DE94-012110 ..... p 4537 N94-37369 #
DE94-012111 ..... p 4405 N94-37370 #
DE94-012112 ..... p 4404 N94-37205 #
DE94-012114 ..... p 4474 N94-37394 #
DE94-012117 ..... p 4434 N94-37206 #
DE94-012118 ..... p 4420 N94-37678 #
DE94-012139 ..... p 4427 N94-37725 #
DE94-012141 ..... p 4445 N94-37726 #
DE94-012145 ..... p 4528 N94-37207 #
DE94-012146 ..... p 4438 N94-37213 #
DE94-012230 ..... p 4466 N94-37208 #
DE94-012232 ..... p 4517 N94-37209 #
DE94-012239 ..... p 4473 N94-37371 * #
DE94-012241 ..... p 4517 N94-37210 #
DE94-012242 ..... p 4466 N94-37211 #
DE94-012319 ..... p 4535 N94-37212 #
DE94-012324 ..... p 4498 N94-37419 #
DE94-012336 ..... p 4419 N94-37420 #
DE94-012351 ..... p 4411 N94-37372 #
DE94-012352 ..... p 4425 N94-37373 #
DE94-012368 ..... p 4495 N94-37245 #
DE94-012371 ..... p 4425 N94-37421 #
DE94-012382 ..... p 4504 N94-37246 #
DE94-012386 ..... p 4425 N94-37422 #
DE94-012455 ..... p 4504 N94-37247 #
DE94-012466 ..... p 4425 N94-37423 #
DE94-012469 ..... p 4398 N94-37433 #
DE94-012476 ..... p 4528 N94-37167 #
DE94-012478 ..... p 4479 N94-37434 #
DE94-012479 ..... p 4539 N94-37094 #
DE94-012481 ..... p 4409 N94-37168 #
DE94-012486 ..... p 4408 N94-37095 #
DE94-012487 ..... p 4479 N94-37248 #
DE94-012488 ..... p 4537 N94-37435 #
DE94-012498 ..... p 4503 N94-37073 #
DE94-012509 ..... p 4530 N94-37436 #
DE94-012586 ..... p 4429 N94-37427 #
DE94-012590 ..... p 4530 N94-37437 #
DE94-012607 ..... p 4419 N94-37438 #
DE94-012627 ..... p 4467 N94-37428 #
DE94-012628 ..... p 4517 N94-37249 #
DE94-012631 ..... p 4412 N94-37439 #
DE94-012633 ..... p 4467 N94-37440 #
DE94-012639 ..... p 4530 N94-37441 #
DE94-012641 ..... p 4467 N94-37429 #
DE94-012644 ..... p 4443 N94-37176 #
DE94-012646 ..... p 4465 N94-37100 #
DE94-012647 ..... p 4419 N94-37442 #
DE94-012659 ..... p 4417 N94-37304 #
DE94-012661 ..... p 4525 N94-37374 #
DE94-012664 ..... p 4518 N94-37305 #
DE94-012667 ..... p 4416 N94-37080 #
DE94-012672 ..... p 4527 N94-37081 #
DE94-012676 ..... p 4439 N94-37306 #
DE94-012678 ..... p 4528 N94-37307 #
DE94-012679 ..... p 4527 N94-37082 #
DE94-012714 ..... p 4410 N94-37284 #
DE94-012716 ..... p 4536 N94-37285 #
DE94-012718 ..... p 4410 N94-37286 #
DE94-012727 ..... p 4536 N94-37287 #
DE94-012729 ..... p 4466 N94-37288 #
DE94-012732 ..... p 4418 N94-37396 #
DE94-012734 ..... p 4418 N94-37398 #
DE94-012739 ..... p 4418 N94-37399 #
DE94-012740 ..... p 4537 N94-37400 #
DE94-012741 ..... p 4537 N94-37382 #
DE94-012744 ..... p 4500 N94-37083 #
DE94-012750 ..... p 4518 N94-37383 #
DE94-012763 ..... p 4529 N94-37361
DE94-012765 ..... p 4443 N94-37362
DE94-012766 ..... p 4529 N94-37309 #
DE94-012897 ..... p 4522 N94-37310 #
DE94-012912 ..... p 4449 N94-37495 #
DE94-012918 ..... p 4495 N94-37496 #
DE94-012938 ..... p 4536 N94-37311 #
DE94-012944 ..... p 4518 N94-37312 #
DE94-012985 ..... p 4529 N94-37354 #
DE94-012986 ..... p 4531 N94-37730 #
DE94-013000 ..... p 4505 N94-37497 #
DE94-013002 ..... p 4479 N94-37355 #
DE94-013015 ..... p 4537 N94-37356 #
DE94-013023 ..... p 4537 N94-37498 #
DE94-013029 ..... p 4537 N94-37499 #
DE94-013035 ..... p 4412 N94-37491 #
DE94-013036 ..... p 4518 N94-37313 #
DE94-013043 ..... p 4468 N94-37731 #
DE94-013050 ..... p 4410 N94-37357 #
DE94-013086 ..... p 4469 N94-37314 #
DE94-013114 ..... p 4529 N94-37316 #
DE94-013115 ..... p 4425 N94-37317 #
DE94-013116 ..... p 4405 N94-37289 #
DE94-013119 ..... p 4536 N94-37290 #
DE94-013126 ..... p 4536 N94-37291 #
DE94-013128 ..... p 4528 N94-37292 #
DE94-013133 ..... p 4550 N94-37293 #
DE94-013135 ..... p 4438 N94-37295 #
DE94-013142 ..... p 4410 N94-37296 #
DE94-013146 ..... p 4528 N94-37297 #
DE94-013147 ..... p 4518 N94-37298 #
DE94-013201 ..... p 4466 N94-37299 #
DE94-013238 ..... p 4547 N94-37555 #
DE94-013240 ..... p 4523 N94-37547 #
DE94-013278 ..... p 4420 N94-37548 #
DE94-013302 ..... p 4496 N94-37549 #
DE94-013306 ..... p 4519 N94-37550 #
DE94-013308 ..... p 4496 N94-37551 #
DE94-013309 ..... p 4420 N94-37552 #
DE94-013352 ..... p 4519 N94-37553 #
DE94-013353 ..... p 4515 N94-37084 #

DE94-013355 ..... p 4515 N94-37085 #
DE94-013357 ..... p 4515 N94-37086 #
DE94-013358 ..... p 4515 N94-37087 #
DE94-013367 ..... p 4532 N94-37732 #
DE94-013378 ..... p 4469 N94-37177 #
DE94-013396 ..... p 4527 N94-37101 #
DE94-013418 ..... p 4515 N94-37067 #
DE94-013426 ..... p 4422 N94-37068 #
DE94-013434 ..... p 4534 N94-37069 #
DE94-013452 ..... p 4451 N94-37070 #
DE94-013456 ..... p 4464 N94-37071 #
DE94-013459 ..... p 4527 N94-37072 #
DE94-013477 ..... p 4417 N94-37116 #
DE94-013700 ..... p 4409 N94-37132 #
DE94-611101 ..... p 4433 N94-36753 #
DE94-611174 ..... p 4511 N94-36504 #
DE94-613046 ..... p 4414 N94-36517 #
DE94-616619 ..... p 4505 N94-37483
DE94-617044 ..... p 4512 N94-36523
DE94-617409 ..... p 4448 N94-37169 #
DE94-617509 ..... p 4414 N94-36541 #
DE94-617534 ..... p 4416 N94-37074 #
DE94-618203 ..... p 4407 N94-36529 #
DE94-618211 ..... p 4515 N94-37075 #
DE94-618340 ..... p 4515 N94-37076 #
DE94-618343 ..... p 4515 N94-37077 * #
DE94-618365 ..... p 4504 N94-37170 #
DE94-618410 ..... p 4517 N94-37171 #
DE94-618457 ..... p 4509 N94-37078 #
DE94-618467 ..... p 4539 N94-37079 #
DE94-618468 ..... p 4539 N94-37172 #
DE94-618485 ..... p 4507 N94-37062 #
DE94-618486 ..... p 4504 N94-37375
DE94-618501 ..... p 4514 N94-36747 #
DE94-618511 ..... p 4521 N94-36748 #
DE94-618512 ..... p 4514 N94-36749 #
DE94-618519 ..... p 4514 N94-37063 #
DE94-618534 ..... p 4516 N94-37096
DE94-618542 ..... p 4514 N94-37064 #
DE94-618548 ..... p 4514 N94-37065 #
DE94-618549 ..... p 4515 N94-37066 #
DE94-618732 ..... p 4516 N94-37097
DE94-618733 ..... p 4517 N94-37173 #
DE94-618747 ..... p 4519 N94-37651 #
DE94-618748 ..... p 4519 N94-37528 #
DE94-618756 ..... p 4520 N94-37652 #
DE94-618779 ..... p 4531 N94-37728 #
DE94-619029 ..... p 4532 N94-36542 #
DE94-619033 ..... p 4414 N94-36543 #
DE94-619055 ..... p 4414 N94-36544 #
DE94-619056 ..... p 4415 N94-36563 #
DE94-619057 ..... p 4415 N94-36564 #
DE94-619484 ..... p 4447 N94-36565 #
DE94-620118 ..... p 4527 N94-36566 #
DE94-620278 ..... p 4412 N94-37533 #
DE94-620287 ..... p 4412 N94-37534 #
DE94-620692 ..... p 4479 N94-37535 #
DE94-620987 ..... p 4467 N94-37492 #
DE94-621344 ..... p 4482 N94-37729 #
DE94-621506 ..... p 4503 N94-37098
DE94-621535 ..... p 4504 N94-37174 #
DE94-621606 ..... p 4504 N94-37175 #
DE94-621636 ..... p 4516 N94-37099 #
DE94-621641 ..... p 4519 N94-37414 #
DE94-621827 ..... p 4531 N94-37493 #
DE94-718961 ..... p 4531 N94-37484 #
DE94-718962 ..... p 4522 N94-37463 #
DE94-718963 ..... p 4530 N94-37464 #
DE94-718965 ..... p 4419 N94-37465 #
DE94-718985 ..... p 4530 N94-37384 #
DE94-719014 ..... p 4418 N94-37385 #
DE94-719024 ..... p 4518 N94-37387 #
DE94-727510 ..... p 4529 N94-37358 #
DE94-727545 ..... p 4531 N94-37466 #
DE94-727546 ..... p 4531 N94-37485 #
DE94-727547 ..... p 4529 N94-37359 #
DE94-727619 ..... p 4528 N94-37231 #
DE94-727625 ..... p 4526 N94-36472 #
DE94-737854 ..... p 4530 N94-37415 #
DE94-737934 ..... p 4418 N94-37416 #
DE94-737969 ..... p 4523 N94-37727 #
DE94-748497 ..... p 4532 N94-37734 #
DE94-748635 ..... p 4522 N94-37234 #
DE94-748668 ..... p 4519 N94-37417 #
DE94-748680 ..... p 4528 N94-37235 #
DE94-748682 ..... p 4522 N94-37236 #
DE94-748683 ..... p 4518 N94-37360 #
DE94-748687 ..... p 4522 N94-37237 #
DE94-763290 ..... p 4464 N94-37007 #
DE94-763309 ..... p 4414 N94-36525 #
DE94-767725 ..... p 4462 N94-37418 #

DOE/CE-15566/T2 ..... p 4438 N94-37241 #
DOE/CE-23810/25 ..... p 4426 N94-37490 #
DOE/CE-23810/38A ..... p 4425 N94-37421 #
DOE/CE-23810/38 ..... p 4425 N94-37373 #

DOE/CH-03000/T20 ..... p 4511 N94-36506 #
DOE/CH-10093/314 ..... p 4429 N94-37426 #
DOE/CH-10093/315 ..... p 4429 N94-37402 #
DOE/CH-10093/316 ..... p 4429 N94-37403 #
DOE/CH-10093/319 ..... p 4429 N94-37404 #

DOE/EIA-0548(92) ..... p 4463 N94-37567 #

DOE/EM-0160P ..... p 4468 N94-37731 #

DOE/ER-13183/9 ..... p 4411 N94-37372 #
DOE/ER-13214/8 ..... p 4479 N94-37248 #
DOE/ER-13299/10 ..... p 4413 N94-37754 #
DOE/ER-13370/T3 ..... p 4479 N94-37434 #
DOE/ER-13429/8 ..... p 4532 N94-36454 #
DOE/ER-13437/T3 ..... p 4539 N94-37094 #
DOE/ER-13749/T2 ..... p 4469 N94-37177 #
DOE/ER-13867/14 ..... p 4518 N94-37313 #
DOE/ER-13915/T4 ..... p 4410 N94-37284 #
DOE/ER-14045/8 ..... p 4424 N94-37223 #
DOE/ER-14079/30 ..... p 4510 N94-36551 #
DOE/ER-14156/9 ..... p 4419 N94-37438 #
DOE/ER-14192/3 ..... p 4413 N94-37623 #
DOE/ER-14234/2 ..... p 4468 N94-36451 #
DOE/ER-14289/2 ..... p 4409 N94-37132 #
DOE/ER-14303/2 ..... p 4412 N94-37491 #
DOE/ER-14305/2 ..... p 4408 N94-37095 #
DOE/ER-14306/2 ..... p 4409 N94-37168 #
DOE/ER-14334/T1 ..... p 4413 N94-37713 #
DOE/ER-20070/1 ..... p 4538 N94-37677 #
DOE/ER-40646/4 ..... p 4521 N94-37721 #
DOE/ER-40757/015 ..... p 4539 N94-36507 #
DOE/ER-40757/29 ..... p 4539 N94-36508 #
DOE/ER-45239/9 ..... p 4516 N94-37113 #
DOE/ER-45291/7 ..... p 4538 N94-37676 #
DOE/ER-45320/6 ..... p 4537 N94-37435 #
DOE/ER-45427/4 ..... p 4536 N94-37285 #
DOE/ER-52147/7 ..... p 4448 N94-37368 #
DOE/ER-53198/238 ..... p 4529 N94-37354 #
DOE/ER-53198/239 ..... p 4531 N94-37730 #
DOE/ER-54185/T1 ..... p 4528 N94-37167 #
DOE/ER-60490/T2 ..... p 4466 N94-37376
DOE/ER-61037/3 ..... p 4465 N94-37187 #
DOE/ER-61085/3 ..... p 4525 N94-37532 #
DOE/ER-61549/1 ..... p 4464 N94-36552 #

DOE/ET-53088/628 ..... p 4526 N94-36536 #
DOE/ET-53088/654 ..... p 4529 N94-37361
DOE/ET-53088/657 ..... p 4443 N94-37362
DOE/ET-53088/658 ..... p 4529 N94-37309 #

DOE/FTR-94009396 ..... p 4533 N94-36746 #

DOE/MC-23174/3672 ..... p 4452 N94-37512 #
DOE/MC-29106/3531 ..... p 4469 N94-36738 #
DOE/MC-29237/94/C0248 ..... p 4463 N94-37488 #
DOE/MC-29267/3655 ..... p 4470 N94-37489 #

DOE/METC-94-1004 ..... p 4441 N94-36550 #

DOE/NASA-0336-4 ..... p 4452 N94-37763 * #

DOE/NV-11432/1 ..... p 4472 N94-36739 #

DOE/PC-90180/T10 ..... p 4444 N94-37544 #
DOE/PC-91030/T8 ..... p 4406 N94-36450 #
DOE/PC-91293/8 ..... p 4407 N94-36475 #
DOE/PC-92116/T2 ..... p 4411 N94-37431 #
DOE/PC-92542/T6 ..... p 4417 N94-37116 #
DOE/PC-93212/T2 ..... p 4468 N94-37740 #
DOE/PC-93219/T1 ..... p 4461 N94-36511 #

DOE/SR-18273/2 ..... p 4536 N94-37311 #

DOT/FAA/CT-TN93/46 ..... p 4473 N94-37143
DOT/FAA/CT-TN94/2 ..... p 4434 N94-37218

DOT/FAA/CT-93/2 ..... p 4456 N94-37125
DOT/FAA/CT-94/24 ..... p 4385 N94-37706 #

DOT/FAA/PP-94-2 ..... p 4389 N94-36763 #

DOT/FAA/RD-93-31-VOL-1 ..... p 4381 N94-36466 #
DOT/FAA/RD-93-31-VOL-2 ..... p 4382 N94-36467 #
DOT/FAA/RD-93/37 ..... p 4390 N94-37424 #
DOT/FAA/RD-93/5 ..... p 4487 N94-37347
DOT/FAA/RD-94/18 ..... p 4487 N94-37741 #
DOT/FAA/RD-94/20 ..... p 4487 N94-37743 #
DOT/FAA/RD-94/21 ..... p 4487 N94-37742 #
DOT/FAA/RD-94/22 ..... p 4385 N94-37604 #

DOTVNTSC-FAA-93-4 ..... p 4487 N94-37347

DREO-1210 ..... p 4446 N94-36760 #
DREO-12111 ..... p 4434 N94-37162 #

E-7660 ..... p 4455 N94-37102 * #
E-7713 ..... p 4419 N94-37503 * #
E-7771 ..... p 4508 N94-36643 * #
E-7881 ..... p 4452 N94-37457 * #
E-8031-1 ..... p 4450 N94-36645 * #
E-8243 ..... p 4442 N94-36957 * #
E-8263 ..... p 4398 N94-36821 * #
E-8302 ..... p 4502 N94-36647 * #
E-8311 ..... p 4441 N94-36646 * #
E-8410 ..... p 4408 N94-36537 * #
E-8615 ..... p 4456 N94-37554 * #
E-8652 ..... p 4455 N94-36561 * #
E-8664 ..... p 4406 N94-37633 * #
E-8682 ..... p 4457 N94-37704 * #
E-8708 ..... p 4452 N94-37521 * #
E-8709 ..... p 4405 N94-37460 * #
E-8716 ..... p 4399 N94-37315 * #
E-8742 ..... p 4390 N94-37522 * #
E-8844 ..... p 4382 N94-36686 * #
E-8864 ..... p 4416 N94-36954 * #
E-8874 ..... p 4456 N94-37456 * #
E-8894 ..... p 4403 N94-36956 * #
E-8895 ..... p 4451 N94-37451 * #
E-8899 ..... p 4426 N94-37520 * #
E-8905 ..... p 4431 N94-37254 * #
E-8914 ..... p 4450 N94-36953 * #
E-8929 ..... p 4405 N94-37318 * #
E-8952 ..... p 4444 N94-37507 * #
E-8955 ..... p 4383 N94-37283 * #
E-8958 ..... p 4421 N94-36952 * #
E-8965 ..... p 4387 N94-37448 * #
E-8967 ..... p 4437 N94-36819 * #
E-8968 ..... p 4398 N94-36951 * #
E-8969 ..... p 4431 N94-36943 * #
E-8974 ..... p 4424 N94-37300 * #
E-8977 ..... p 4433 N94-36955 * #
E-8979 ..... p 4451 N94-37319 * #
E-8989 ..... p 4510 N94-37306 * #
E-9020-PT-1 ..... p 4419 N94-37459 * #
E-9033 ..... p 4421 N94-36837 * #
E-9037 ..... p 4452 N94-37763 * #
E-9055 ..... p 4398 N94-37764 * #

ECETR-1 ..... p 4434 N94-37183

EDR-16624 ..... p 4452 N94-37763 * #

EGG-APO-10944 ..... p 4453 N94-36452 #

EGG-CMRE-11006 ..... p 4406 N94-36453 #

EGG-11265-3007 ..... p 4518 N94-37305 #

ERP-1132 ..... p 4470 N94-37649

ESC-TR-93-201 ..... p 4493 N94-36974
ESC-TR-94-084 ..... p 4533 N94-36734 #

ETS-RM-94-13-ONR ..... p 4507 N94-37046

ETS-RR-94-28-ONR ..... p 4506 N94-36728 #
ETS-RR-94-3-ONR ..... p 4506 N94-36732 #

FNAL-TM-1887 ..... p 4518 N94-37312 #

FNAL/C-93-329-E ..... p 4511 N94-36459 #
FNAL/C-93/266 ..... p 4513 N94-36558 #
FNAL/C-93/274-E ..... p 4514 N94-36700 #
FNAL/C-93/301-E ..... p 4518 N94-37296 #
FNAL/C-93/319-E ..... p 4513 N94-36528 #
FNAL/C-93/337-E ..... p 4520 N94-37674 #
FNAL/C-93/358-E ..... p 4511 N94-36483 #
FNAL/C-94/084 ..... p 4547 N94-37667 #
FNAL/C-94/093 ..... p 4547 N94-37555 #
FNAL/C-94/103 ..... p 4523 N94-37547 #
FNAL/C-94/124-E ..... p 4515 N94-37067 #

FOA-C-30745-3.6 ..... p 4435 N94-37813
FOA-C-40326-4.5 ..... p 4468 N94-37856

FSU-HEP-930830 ..... p 4512 N94-36526 #

GA-A-21511 ..... p 4398 N94-37514 #
GA-A-21603 ..... p 4530 N94-37436 #

GA-A21590 ..... p 4398 N94-37433 #

GAO/NSIAD-94-220 ..... p 4398 N94-37257 #
GAO/NSIAD-94-23 ..... p 4392 N94-37026 #

GEM/TN-93-518 ..... p 4439 N94-37306 #

GRI-93/0224.1-VOL-1 ..... p 4464 N94-36994
GRI-93/0224.2-VOL-1-APP ..... p 4464 N94-36995
GRI-94/0051 ..... p 4450 N94-36721
GRI-94/0086 ..... p 4412 N94-37462 #

G5189.01.26-VOL-1 ..... p 4546 N94-36642 * #

H-1943 ..... p 4386 N94-36644 * #
H-1954 ..... p 4381 N94-36648 * #
H-1977 ..... p 4383 N94-37395 * #
H-1992 ..... p 4383 N94-36944 * #
H-2010 ..... p 4383 N94-37378 * #

IAE-0119 ..... p 4412 N94-37533 #

IAEA-CN-56/C-2-5 ..... p 4530 N94-37384 #

IC-93/267 ..... p 4433 N94-36753 #

ICASE-94-20 ..... p 4502 N94-36562 * #
ICASE-94-38 ..... p 4495 N94-37539 * #
ICASE-94-40 ..... p 4503 N94-36923 * #
ICASE-94-41 ..... p 4503 N94-36991 * #
ICASE-94-42 ..... p 4500 N94-36928 * #
ICASE-94-43 ..... p 4500 N94-36924 * #
ICASE-94-46 ..... p 4444 N94-37605 * #
ICASE-94-50 ..... p 4497 N94-37411 * #
ICASE-94-56 ..... p 4445 N94-37606 * #
ICASE-94-63 ..... p 4505 N94-37540 * #

ICOMP-93-49 ..... p 4502 N94-36647 * #
ICOMP-93-50 ..... p 4441 N94-36646 * #

IFSR-628 ..... p 4526 N94-36536 #
IFSR-654 ..... p 4529 N94-37361
IFSR-657 ..... p 4443 N94-37362
IFSR-658 ..... p 4529 N94-37309 #

IFT-P-056-93 ..... p 4514 N94-37063 #

IHEP-OMMS-92-52 ..... p 4511 N94-36504 #

IHEP-OTF-92-143 ..... p 4507 N94-37062 #
IHEP-OTF-92-146 ..... p 4504 N94-37375

IHES/M/93/44 ..... p 4506 N94-37852
IHES/M/93/49 ..... p 4506 N94-37853

INIS-BR-3209 ..... p 4414 N94-36517 #
INIS-BR-3257 ..... p 4520 N94-37652 #

INIS-JP-017 ..... p 4528 N94-37235 #

INIS-MF-13749 ..... p 4448 N94-37169 #
INIS-MF-13779 ..... p 4531 N94-37493 #
INIS-MF-13795 ..... p 4416 N94-37074 #
INIS-MF-13810 ..... p 4527 N94-36566 #
INIS-MF-13835 ..... p 4467 N94-37492 #

INS-1014 ..... p 4519 N94-37417 #

IP347 ..... p 4473 N94-37217

IS-M-780 ..... p 4535 N94-37166 #
IS-M-787 ..... p 4418 N94-37410 #

IS-T-1678 ..... p 4426 N94-37712 #

ISBN-92-835-0704-5 ..... p 4540 N94-37447 #
ISBN-92-835-0711-8 ..... p 4453 N94-37321 #
ISBN-92-835-0735-5 ..... p 4400 N94-36649 #
ISBN-92-835-0736-3 ..... p 4543 N94-37333 #
ISBN-92-835-0741-X ..... p 4392 N94-36616 #
ISBN-92-835-0746-0 ..... p 4482 N94-37261 #
ISBN-951-22-1833-X ..... p 4506 N94-37833 #
ISBN-951-22-1841-0 ..... p 4477 N94-37855
ISBN-951-22-1930-1 ..... p 4510 N94-37632 #
ISBN-951-47-8004-3 ..... p 4464 N94-37007 #

ISVR-TR-233 ..... p 4442 N94-36817 #

ITP-93-22E ..... p 4539 N94-37079 #
ITP-93-29E ..... p 4505 N94-37483

IYAF-92-33 ..... p 4504 N94-37170 #
IYAF-92-36 ..... p 4531 N94-37728 #

JAERI-M-93-130 ..... p 4531 N94-37484 #
JAERI-M-93-132 ..... p 4522 N94-37463 #
JAERI-M-93-141 ..... p 4530 N94-37464 #
JAERI-M-93-144 ..... p 4419 N94-37465 #
JAERI-M-93-149 ..... p 4530 N94-37415 #
JAERI-M-93-150 ..... p 4418 N94-37385 #
JAERI-M-93-152 ..... p 4518 N94-37387 #
JAERI-M-93-187 ..... p 4418 N94-37416 #

JINR-E-1-92-372 ..... p 4512 N94-36523
JINR-E-1-93-253 ..... p 4515 N94-37076 #
JINR-E-11-93-163 ..... p 4503 N94-37098
JINR-E-13-93-204 ..... p 4482 N94-37729 #
JINR-E-13-93-234 ..... p 4515 N94-37075 #

JINR-E-2-93-193 ..... p 4539 N94-37172 #
JINR-E-4-93-196 ..... p 4515 N94-37066 #
JINR-E-4-93-87 ..... p 4516 N94-37099 #

JINR-R-1-93-121 ..... p 4519 N94-37414 #
JINR-R-10-93-271 ..... p 4514 N94-37064 #
JINR-R-11-93-173 ..... p 4504 N94-37175 #
JINR-R-14-93-247 ..... p 4519 N94-37651 #
JINR-R-4-93-150 ..... p 4504 N94-37174 #
JINR-R-4-93-198 ..... p 4516 N94-37097
JINR-R-4-93-193 ..... p 4517 N94-37173 #
JINR-R-4-93-200 ..... p 4519 N94-37528 #
JINR-R-9-93-240 ..... p 4515 N94-37077 #

JPL-BIBL-39-33 ..... p 4542 N94-37008 * #

JPRS-UAC-94-003 ..... p 4391 N94-36999 #
JPRS-UAC-94-004 ..... p 4391 N94-37000 #
JPRS-UAC-94-005 ..... p 4391 N94-37001 #

JPRS-UEQ-93-005 ..... p 4432 N94-37538 #
JPRS-UEQ-93-007 ..... p 4431 N94-37523 #
JPRS-UEQ-93-008 ..... p 4432 N94-37524 #

JPRS-UMS-93-008 ..... p 4404 N94-37010 #

JPRS-USP-94-004 ..... p 4391 N94-37002 #

JPRS-UST-94-013 ..... p 4509 N94-37006 #

JP9311132 ..... p 4531 N94-37466 #
JP9311133 ..... p 4531 N94-37485 #

JSC-19295 ..... p 4390 N94-37443 * #

KCP-613-5266 ..... p 4421 N94-36474 #

KEK-PR-93-1 ..... p 4522 N94-37236 #

KEK-PROC-92-17 ..... p 4518 N94-37360 #
KEK-PROC-93-2 ..... p 4523 N94-37727 #

KEK-93-8 ..... p 4522 N94-37234 #

KTM/E-B-171 ..... p 4464 N94-37007 #

L-00993-168 ..... p 4492 N94-36518 *
L-17232 ..... p 4397 N94-37502 * #
L-17257 ..... p 4447 N94-36946 * #
L-17273 ..... p 4388 N94-37014 * #
L-17325 ..... p 4383 N94-36966 * #
L-17333 ..... p 4388 N94-37059 * #
L-17342 ..... p 4416 N94-36993 * #
L-17343 ..... p 4396 N94-37260 * #
L-17364 ..... p 4383 N94-36950 * #
L-17377 ..... p 4481 N94-37282 * #
L-17395 ..... p 4382 N94-36942 * #
L-17414 ..... p 4457 N94-37796 * #
L-1782 ..... p 4384 N94-37505 * #

LA-SUB-94-74 ..... p 4522 N94-37303 #
LA-SUB-94-79 ..... p 4435 N94-37393 #

LA-UR-93-2556 ..... p 4511 N94-36457 #
LA-UR-93-3390 ..... p 4508 N94-36556 #
LA-UR-93-3496 ..... p 4502 N94-36685 #
LA-UR-93-3553 ..... p 4436 N94-36514 #
LA-UR-93-3731 ..... p 4512 N94-36515 #
LA-UR-93-4218 ..... p 4414 N94-36461 #
LA-UR-94-1164 ..... p 4534 N94-37057 #
LA-UR-94-1197 ..... p 4449 N94-37733 #
LA-UR-94-1238 ..... p 4457 N94-37670 #
LA-UR-94-1297 ..... p 4496 N94-37739 #
LA-UR-94-1300 ..... p 4520 N94-37671
LA-UR-94-1378 ..... p 4471 N94-37669 #
LA-UR-94-1379 ..... p 4549 N94-37668 #
LA-UR-94-1418 ..... p 4440 N94-37738 #
LA-UR-94-1455 ..... p 4471 N94-37701 #
LA-UR-94-1525 ..... p 4449 N94-37495 #
LA-UR-94-1566 ..... p 4522 N94-37310 #
LA-UR-94-1657 ..... p 4536 N94-37291 #
LA-UR-94-1715 ..... p 4536 N94-37290 #
LA-UR-94-1730 ..... p 4405 N94-37289 #
LA-UR-94-1733 ..... p 4425 N94-37317 #
LA-UR-94-1739 ..... p 4529 N94-37316 #
LA-UR-94-1811 ..... p 4469 N94-37314 #
LA-UR-94-1823 ..... p 4528 N94-37292 #
LA-UR-94-1832 ..... p 4527 N94-37101 #
LA-UR-94-1853 ..... p 4438 N94-37295 #
LA-UR-94-1862 ..... p 4550 N94-37293 #
LA-UR-94-1871 ..... p 4410 N94-37296 #
LA-UR-94-586 ..... p 4496 N94-37782 #
LA-UR-94-688 ..... p 4466 N94-37389 #
LA-UR-94-802 ..... p 4447 N94-36510 #

LA-12644-M ..... p 4432 N94-36443 #

LA-12699-VOL-4 ..... p 4466 N94-37299 #
LA-12704 ..... p 4506 N94-36449 #
LA-12746-M ..... p 4495 N94-37245 #
LA-12777-MS ..... p 4523 N94-37629 #

LBL-32657 ..... p 4439 N94-37302 #
LBL-33448 ..... p 4508 N94-36560 #
LBL-34572 ..... p 4513 N94-36695 #
LBL-34831 ..... p 4520 N94-37716 #
LBL-34924 ..... p 4521 N94-37720 #
LBL-34997 ..... p 4413 N94-37630
LBL-35128 ..... p 4519 N94-37558
LBL-35158 ..... p 4524 N94-37165 #
LBL-35192 ..... p 4443 N94-37050 #
LBL-35224 ..... p 4506 N94-37718 #
LBL-35277 ..... p 4548 N94-37049 #
LBL-35281 ..... p 4506 N94-37719 #
LBL-35295 ..... p 4520 N94-37715 #
LBL-35305 ..... p 4449 N94-37628 #
LBL-35306 ..... p 4408 N94-37056 #
LBL-35316 ..... p 4520 N94-37717 #
LBL-35318 ..... p 4409 N94-37199 #
LBL-35324 ..... p 4521 N94-37200 #
LBL-35330 ..... p 4548 N94-37557
LBL-35448 ..... p 4479 N94-37156 #

LESC-30354-C ..... p 4387 N94-36933 * #

M-748 ..... p 4455 N94-37015 * #
M-751 ..... p 4384 N94-37577 * #
M-752 ..... p 4382 N94-36741 * #
M-753 ..... p 4420 N94-37578 * #

MCAT-94-004 ..... p 4504 N94-37449 * #
MCAT-94-12 ..... p 4442 N94-36808 * #

MCTR-0794-01 ..... p 4525 N94-37579 * #

MIT-9181AL ..... p 4533 N94-36727 #

ML-10448 ..... p 4475 N94-36446

MTR-93B0000186 ..... p 4499 N94-37760

NAMRL-1389 ..... p 4478 N94-37045

NAS 1.15:104269 ..... p 4386 N94-36644 * #
NAS 1.15:104272 ..... p 4381 N94-36648 * #
NAS 1.15:104566-VOL-20-PT-1 ... p 4475 N94-36958 * #
NAS 1.15:104609 ..... p 4477 N94-37397 * #
NAS 1.15:104611 ..... p 4475 N94-37790 * #
NAS 1.15:104794 ..... p 4392 N94-37386 * #
NAS 1.15:106410 ..... p 4452 N94-37457 * #
NAS 1.15:106449 ..... p 4502 N94-36647 * #
NAS 1.15:106452 ..... p 4441 N94-36646 * #
NAS 1.15:106480 ..... p 4408 N94-36537 * #
NAS 1.15:106526 ..... p 4455 N94-36561 * #
NAS 1.15:106539 ..... p 4457 N94-37704 * #
NAS 1.15:106553 ..... p 4452 N94-37521 * #
NAS 1.15:106556 ..... p 4399 N94-37315 * #
NAS 1.15:106565 ..... p 4390 N94-37522 * #
NAS 1.15:10657 ..... p 4450 N94-36645 * #
NAS 1.15:106583 ..... p 4382 N94-36686 * #
NAS 1.15:106600 ..... p 4456 N94-37456 * #
NAS 1.15:106611 ..... p 4403 N94-36956 * #
NAS 1.15:106612 ..... p 4451 N94-37451 * #
NAS 1.15:106616 ..... p 4426 N94-37520 * #
NAS 1.15:106619 ..... p 4431 N94-37254 * #
NAS 1.15:106623 ..... p 4450 N94-36953 * #
NAS 1.15:106630 ..... p 4405 N94-37318 * #
NAS 1.15:106633 ..... p 4383 N94-37283 * #
NAS 1.15:106646 ..... p 4444 N94-37507 * #
NAS 1.15:106650 ..... p 4421 N94-36952 * #
NAS 1.15:106653 ..... p 4387 N94-37448 * #
NAS 1.15:106654 ..... p 4437 N94-36819 * #
NAS 1.15:106655 ..... p 4398 N94-36951 * #
NAS 1.15:106656 ..... p 4431 N94-36943 * #
NAS 1.15:106659 ..... p 4424 N94-37300 * #
NAS 1.15:106661 ..... p 4433 N94-36955 * #
NAS 1.15:106663 ..... p 4451 N94-37319 * #
NAS 1.15:106667 ..... p 4510 N94-37308 * #
NAS 1.15:106680 ..... p 4419 N94-37459 * #
NAS 1.15:108458 ..... p 4446 N94-36822 * #
NAS 1.15:108460 ..... p 4496 N94-37556 * #
NAS 1.15:108806 ..... p 4381 N94-37332 * #
NAS 1.15:108989 ..... p 4386 N94-37636 * #
NAS 1.15:109025 ..... p 4497 N94-36932 * #
NAS 1.15:109066 ..... p 4493 N94-36818 * #
NAS 1.15:109079 ..... p 4456 N94-37541 * #
NAS 1.15:109116 ..... p 4456 N94-37253 * #
NAS 1.15:109130 ..... p 4388 N94-36820 * #
NAS 1.15:109135 ..... p 4405 N94-37320 * #
NAS 1.15:109136 ..... p 4500 N94-37058 * #
NAS 1.15:109137 ..... p 4387 N94-37762 * #
NAS 1.15:109138 ..... p 4501 N94-37589 * #
NAS 1.15:109139 ..... p 4386 N94-37256 * #

NAS 1.15:109141 ..... p 4444 N94-37455 * #
NAS 1.15:109415 ..... p 4540 N94-36841 * #
NAS 1.15:109892 ..... p 4461 N94-36827 * #
NAS 1.15:109894 ..... p 4473 N94-37371 * #
NAS 1.15:109895 ..... p 4390 N94-37443 * #
NAS 1.15:109898 ..... p 4546 N94-37765 * #
NAS 1.15:109924 ..... p 4540 N94-36750 * #
NAS 1.15:109925 ..... p 4541 N94-36853 * #
NAS 1.15:4548 ..... p 4388 N94-37059 * #
NAS 1.15:4555 ..... p 4398 N94-36821 * #
NAS 1.15:4556 ..... p 4455 N94-37102 * #
NAS 1.15:4566 ..... p 4383 N94-36966 * #
NAS 1.15:4573 ..... p 4383 N94-36950 * #
NAS 1.15:4584 ..... p 4405 N94-37460 * #
NAS 1.15:4595 ..... p 4383 N94-36944 * #
NAS 1.15:4607 ..... p 4382 N94-36942 * #
NAS 1.15:4627 ..... p 4383 N94-37378 * #
NAS 1.15:4633 ..... p 4383 N94-37395 * #
NAS 1.21:7011(392) ..... p 4482 N94-37445 *
NAS 1.21:7037(307) ..... p 4381 N94-37117 *
NAS 1.26:177638 ..... p 4441 N94-36519 * #
NAS 1.26:185700 ..... p 4421 N94-36641 * #
NAS 1.26:188290 ..... p 4387 N94-36933 * #
NAS 1.26:189341 ..... p 4461 N94-36805 * #
NAS 1.26:189348 ..... p 4489 N94-36484 * #
NAS 1.26:189359 ..... p 4471 N94-37703 * #
NAS 1.26:189360 ..... p 4469 N94-36949 * #
NAS 1.26:189362 ..... p 4461 N94-36919 * #
NAS 1.26:189364 ..... p 4547 N94-36963 * #
NAS 1.26:189365 ..... p 4546 N94-36795 * #
NAS 1.26:189367 ..... p 4546 N94-36794 * #
NAS 1.26:189368 ..... p 4547 N94-36918 * #
NAS 1.26:189371 ..... p 4494 N94-37061 * #
NAS 1.26:191025 ..... p 4508 N94-36643 * #
NAS 1.26:191195 ..... p 4387 N94-37401 * #
NAS 1.26:193424 ..... p 4549 N94-37012 * #
NAS 1.26:193970 ..... p 4547 N94-37702 * #
NAS 1.26:193972 ..... p 4429 N94-37446 * #
NAS 1.26:193981 ..... p 4430 N94-36806 * #
NAS 1.26:194474 ..... p 4456 N94-37554 * #
NAS 1.26:194747 ..... p 4397 N94-36988 * #
NAS 1.26:194823 ..... p 4497 N94-36503 * #
NAS 1.26:194898 ..... p 4502 N94-36562 * #
NAS 1.26:194915 ..... p 4396 N94-36990 * #
NAS 1.26:194920 ..... p 4495 N94-37539 * #
NAS 1.26:194923 ..... p 4498 N94-37500 * #
NAS 1.26:194924 ..... p 4497 N94-36962 * #
NAS 1.26:194925 ..... p 4503 N94-36923 * #
NAS 1.26:194926 ..... p 4503 N94-36991 * #
NAS 1.26:194927 ..... p 4500 N94-36928 * #
NAS 1.26:194928 ..... p 4500 N94-36924 * #
NAS 1.26:194932 ..... p 4444 N94-37605 * #
NAS 1.26:194936 ..... p 4497 N94-37411 * #
NAS 1.26:194941 ..... p 4397 N94-37504 * #
NAS 1.26:194945 ..... p 4445 N94-37606 * #
NAS 1.26:194955 ..... p 4505 N94-37540 * #
NAS 1.26:194960 ..... p 4499 N94-37583 * #
NAS 1.26:194963 ..... p 4387 N94-37658 * #
NAS 1.26:195094 ..... p 4504 N94-37449 * #
NAS 1.26:195294 ..... p 4406 N94-37633 * #
NAS 1.26:195333 ..... p 4416 N94-36954 * #
NAS 1.26:195365 ..... p 4421 N94-36637 * #
NAS 1.26:195367 ..... p 4452 N94-37763 * #
NAS 1.26:195372 ..... p 4398 N94-37764 * #
NAS 1.26:195829 ..... p 4382 N94-36687 * #
NAS 1.26:195918 ..... p 4493 N94-36914 * #
NAS 1.26:195951 ..... p 4546 N94-36688 * #
NAS 1.26:196009 ..... p 4549 N94-36689 * #
NAS 1.26:196014 ..... p 4546 N94-36690 * #
NAS 1.26:196040 ..... p 4443 N94-37060 * #
NAS 1.26:196087 ..... p 4549 N94-36469 * #
NAS 1.26:196096 ..... p 4548 N94-37004 * #
NAS 1.26:196098 ..... p 4385 N94-37013 * #
NAS 1.26:196102 ..... p 4478 N94-36986 * #
NAS 1.26:196107 ..... p 4389 N94-36967 * #
NAS 1.26:196109 ..... p 4439 N94-37501 * #
NAS 1.26:196112 ..... p 4388 N94-36965 * #
NAS 1.26:196113 ..... p 4493 N94-36920 * #
NAS 1.26:196114 ..... p 4514 N94-36964 * #
NAS 1.26:196118 ..... p 4550 N94-36921 * #
NAS 1.26:196120 ..... p 4408 N94-36989 * #
NAS 1.26:196121 ..... p 4480 N94-37005 * #
NAS 1.26:196122 ..... p 4410 N94-37250 * #
NAS 1.26:196124 ..... p 4442 N94-36992 * #
NAS 1.26:196125 ..... p 4542 N94-37008 * #
NAS 1.26:196135 ..... p 4493 N94-36922 * #
NAS 1.26:196137 ..... p 4442 N94-36808 * #
NAS 1.26:196138 ..... p 4390 N94-37450 * #
NAS 1.26:196139 ..... p 4444 N94-37525 * #
NAS 1.26:196141 ..... p 4469 N94-37016 * #
NAS 1.26:196143 ..... p 4462 N94-36807 * #
NAS 1.26:196144 ..... p 4462 N94-36823 * #
NAS 1.26:196260 ..... p 4384 N94-37511 * #
NAS 1.26:196261 ..... p 4426 N94-37510 * #
NAS 1.26:196262 ..... p 4495 N94-37509 * #
NAS 1.26:196267 ..... p 4442 N94-36960 * #
NAS 1.26:196268 ..... p 4478 N94-36996 * #
NAS 1.26:196270 ..... p 4422 N94-37025 * #
NAS 1.26:196271 ..... p 4473 N94-37294 * #
NAS 1.26:196272 ..... p 4487 N94-37458 * #
NAS 1.26:196274 ..... p 4470 N94-37470 * #
NAS 1.26:196276 ..... p 4534 N94-37103 * #
NAS 1.26:196284 ..... p 4550 N94-37251 * #
NAS 1.26:196289 ..... p 4547 N94-37825 * #
NAS 1.26:196290 ..... p 4415 N94-36809 * #
NAS 1.26:196292 ..... p 4445 N94-37635 * #
NAS 1.26:196293 ..... p 4439 N94-37634 * #
NAS 1.26:196294 ..... p 4549 N94-36961 * #
NAS 1.26:196296 ..... p 4442 N94-36969 * #
NAS 1.26:196297 ..... p 4525 N94-37579 * #
NAS 1.26:196298 ..... p 4435 N94-37255 * #
NAS 1.26:196299 ..... p 4397 N94-37580 * #
NAS 1.26:196300 ..... p 4470 N94-37581 * #
NAS 1.26:196302 ..... p 4433 N94-36931 * #
NAS 1.26:196303 ..... p 4435 N94-37461 * #
NAS 1.26:196304 ..... p 4433 N94-36810 * #
NAS 1.26:196305 ..... p 4547 N94-37037 * #
NAS 1.26:196306 ..... p 4522 N94-37508 * #
NAS 1.26:196317 ..... p 4406 N94-37653 * #
NAS 1.26:196319 ..... p 4405 N94-37471 * #
NAS 1.26:196362 ..... p 4546 N94-36642 * #
NAS 1.26:196369 ..... p 4526 N94-37657 * #
NAS 1.26:196372 ..... p 4415 N94-36811 * #
NAS 1.26:196374 ..... p 4496 N94-37656 * #
NAS 1.26:196379 ..... p 4505 N94-37655 * #
NAS 1.26:196380 ..... p 4499 N94-37654 * #
NAS 1.26:196384 ..... p 4501 N94-37590 * #
NAS 1.26:196424 ..... p 4446 N94-36812 * #
NAS 1.26:4584 ..... p 4442 N94-36957 * #
NAS 1.26:4592 ..... p 4467 N94-37607 * #
NAS 1.26:4600 ..... p 4389 N94-36945 * #
NAS 1.26:4602 ..... p 4455 N94-37015 * #
NAS 1.26:4604 ..... p 4399 N94-37614 * #
NAS 1.26:4608 ..... p 4389 N94-37259 * #
NAS 1.26:4610 ..... p 4420 N94-37582 * #
NAS 1.26:4613 ..... p 4466 N94-37252 * #
NAS 1.26:4614 ..... p 4397 N94-37506 * #
NAS 1.55:3271 ..... p 4457 N94-37796 * #
NAS 1.60:3398 ..... p 4419 N94-37503 * #
NAS 1.60:3419 ..... p 4388 N94-37014 * #
NAS 1.60:3427 ..... p 4384 N94-37505 * #
NAS 1.60:3436 ..... p 4416 N94-36993 * #
NAS 1.60:3438 ..... p 4447 N94-36946 * #
NAS 1.60:3439 ..... p 4397 N94-37502 * #
NAS 1.60:3449 ..... p 4396 N94-37260 * #
NAS 1.60:3453 ..... p 4481 N94-37282 * #
NAS 1.60:3488 ..... p 4384 N94-37577 * #
NAS 1.60:3490 ..... p 4420 N94-37578 * #
NAS 1.61-1341 ..... p 4382 N94-36741 * #
NAS 1.71:LAR-14569-1 ..... p 4386 N94-36767 * #
NAS 1.71:LAR-14964-1-CU ..... p 4437 N94-36781 * #
NAS 1.71:LAR-15003-1 ..... p 4389 N94-36826 * #
NAS 1.71:LEW-15818-1 ..... p 4403 N94-36752 * #
NAS 1.71:MFS-28853-1 ..... p 4395 N94-36825 * #
NAS 1.71:MFS-28930-1 ..... p 4509 N94-36782 * #
NAS 1.71:MFS-28987-1 ..... p 4486 N94-36840 * #
NAS 1.71:MFS-28991-1 ..... p 4486 N94-36838 * #
NAS 1.71:MSC-22327-1 ..... p 4450 N94-36839 * #
NAS 1.71:MSC-22336-1 ..... p 4478 N94-36751 * #
NAS 1.71:MSC-22368-1 ..... p 4478 N94-36765 * #
NAS 1.71:MSC-22463-1 ..... p 4480 N94-36766 * #

NASA-CASE-LAR-14569-1 ..... p 4386 N94-36767 * #
NASA-CASE-LAR-14964-1-CU ..... p 4437 N94-36781 * #
NASA-CASE-LAR-15003-1 ..... p 4389 N94-36826 * #

NASA-CASE-LEW-15818-1 ..... p 4403 N94-36752 * #

NASA-CASE-MFS-28853-1 ..... p 4395 N94-36825 * #
NASA-CASE-MFS-28930-1 ..... p 4509 N94-36782 * #
NASA-CASE-MFS-28987-1 ..... p 4486 N94-36840 * #
NASA-CASE-MFS-28991-1 ..... p 4486 N94-36838 * #

NASA-CASE-MSC-22327-1 ..... p 4450 N94-36839 * #
NASA-CASE-MSC-22336-1 ..... p 4478 N94-36751 * #
NASA-CASE-MSC-22368-1 ..... p 4478 N94-36765 * #
NASA-CASE-MSC-22463-1 ..... p 4480 N94-36766 * #

NASA-CP-3271 ..... p 4457 N94-37796 * #

NASA-CR-177638 ..... p 4441 N94-36519 * #
NASA-CR-185700 ..... p 4421 N94-36641 * #
NASA-CR-188290 ..... p 4387 N94-36933 * #
NASA-CR-189341 ..... p 4461 N94-36805 * #
NASA-CR-189348 ..... p 4489 N94-36484 * #
NASA-CR-189359 ..... p 4471 N94-37703 * #
NASA-CR-189360 ..... p 4469 N94-36949 * #
NASA-CR-189362 ..... p 4461 N94-36919 * #
NASA-CR-189364 ..... p 4547 N94-36963 * #
NASA-CR-189365 ..... p 4546 N94-36795 * #
NASA-CR-189367 ..... p 4546 N94-36794 * #
NASA-CR-189368 ..... p 4547 N94-36918 * #
NASA-CR-189371 ..... p 4494 N94-37061 * #
NASA-CR-191025 ..... p 4508 N94-36643 * #
NASA-CR-191195 ..... p 4387 N94-37401 * #
NASA-CR-193424 ..... p 4549 N94-37012 * #
NASA-CR-193970 ..... p 4547 N94-37702 * #
NASA-CR-193972 ..... p 4429 N94-37446 * #
NASA-CR-193981 ..... p 4430 N94-36806 * #
NASA-CR-194474 ..... p 4456 N94-37554 * #
NASA-CR-194747 ..... p 4397 N94-36988 * #
NASA-CR-194823 ..... p 4497 N94-36503 * #
NASA-CR-194898 ..... p 4502 N94-36562 * #
NASA-CR-194915 ..... p 4396 N94-36990 * #
NASA-CR-194920 ..... p 4495 N94-37539 * #
NASA-CR-194923 ..... p 4498 N94-37500 * #
NASA-CR-194924 ..... p 4497 N94-36962 * #
NASA-CR-194925 ..... p 4503 N94-36923 * #
NASA-CR-194926 ..... p 4503 N94-36991 * #
NASA-CR-194927 ..... p 4500 N94-36928 * #
NASA-CR-194928 ..... p 4500 N94-36924 * #
NASA-CR-194932 ..... p 4444 N94-37605 * #
NASA-CR-194936 ..... p 4497 N94-37411 * #
NASA-CR-194941 ..... p 4397 N94-37504 * #
NASA-CR-194945 ..... p 4445 N94-37606 * #
NASA-CR-194955 ..... p 4505 N94-37540 * #
NASA-CR-194960 ..... p 4499 N94-37583 * #
NASA-CR-194963 ..... p 4387 N94-37658 * #
NASA-CR-195094 ..... p 4504 N94-37449 * #
NASA-CR-195294 ..... p 4406 N94-37633 * #
NASA-CR-195333 ..... p 4416 N94-36954 * #
NASA-CR-195365 ..... p 4421 N94-36637 * #
NASA-CR-195367 ..... p 4452 N94-37763 * #
NASA-CR-195372 ..... p 4398 N94-37764 * #
NASA-CR-195829 ..... p 4382 N94-36687 * #
NASA-CR-195918 ..... p 4493 N94-36914 * #
NASA-CR-195951 ..... p 4546 N94-36688 * #
NASA-CR-196009 ..... p 4549 N94-36689 * #
NASA-CR-196014 ..... p 4546 N94-36690 * #
NASA-CR-196040 ..... p 4443 N94-37060 * #
NASA-CR-196087 ..... p 4549 N94-36469 * #
NASA-CR-196096 ..... p 4548 N94-37004 * #
NASA-CR-196098 ..... p 4385 N94-37013 * #
NASA-CR-196102 ..... p 4478 N94-36986 * #
NASA-CR-196107 ..... p 4389 N94-36967 * #
NASA-CR-196109 ..... p 4439 N94-37501 * #
NASA-CR-196112 ..... p 4388 N94-36965 * #
NASA-CR-196113 ..... p 4493 N94-36920 * #
NASA-CR-196114 ..... p 4514 N94-36964 * #
NASA-CR-196118 ..... p 4550 N94-36921 * #
NASA-CR-196120 ..... p 4408 N94-36989 * #
NASA-CR-196121 ..... p 4480 N94-37005 * #
NASA-CR-196122 ..... p 4410 N94-37250 * #
NASA-CR-196124 ..... p 4442 N94-36992 * #
NASA-CR-196125 ..... p 4542 N94-37008 * #
NASA-CR-196135 ..... p 4493 N94-36922 * #
NASA-CR-196137 ..... p 4442 N94-36808 * #
NASA-CR-196138 ..... p 4390 N94-37450 * #
NASA-CR-196139 ..... p 4444 N94-37525 * #
NASA-CR-196141 ..... p 4469 N94-37016 * #
NASA-CR-196143 ..... p 4462 N94-36807 * #
NASA-CR-196144 ..... p 4462 N94-36823 * #
NASA-CR-196260 ..... p 4384 N94-37511 * #
NASA-CR-196261 ..... p 4426 N94-37510 * #
NASA-CR-196262 ..... p 4495 N94-37509 * #
NASA-CR-196267 ..... p 4442 N94-36960 * #
NASA-CR-196268 ..... p 4478 N94-36996 * #
NASA-CR-196270 ..... p 4422 N94-37025 * #
NASA-CR-196271 ..... p 4473 N94-37294 * #
NASA-CR-196272 ..... p 4487 N94-37458 * #
NASA-CR-196274 ..... p 4470 N94-37470 * #
NASA-CR-196276 ..... p 4534 N94-37103 * #
NASA-CR-196284 ..... p 4550 N94-37251 * #
NASA-CR-196289 ..... p 4547 N94-37825 * #
NASA-CR-196290 ..... p 4415 N94-36809 * #
NASA-CR-196292 ..... p 4445 N94-37635 * #
NASA-CR-196293 ..... p 4439 N94-37634 * #
NASA-CR-196294 ..... p 4549 N94-36961 * #
NASA-CR-196296 ..... p 4442 N94-36969 * #
NASA-CR-196297 ..... p 4525 N94-37579 * #
NASA-CR-196298 ..... p 4435 N94-37255 * #
NASA-CR-196299 ..... p 4397 N94-37580 * #
NASA-CR-196300 ..... p 4470 N94-37581 * #
NASA-CR-196302 ..... p 4433 N94-36931 * #
NASA-CR-196303 ..... p 4435 N94-37461 * #
NASA-CR-196304 ..... p 4433 N94-36810 * #
NASA-CR-196305 ..... p 4547 N94-37037 * #
NASA-CR-196306 ..... p 4522 N94-37508 * #
NASA-CR-196317 ..... p 4406 N94-37653 * #
NASA-CR-196319 ..... p 4405 N94-37471 * #
NASA-CR-196362 ..... p 4546 N94-36642 * #
NASA-CR-196369 ..... p 4526 N94-37657 * #
NASA-CR-196372 ..... p 4415 N94-36811 * #
NASA-CR-196374 ..... p 4496 N94-37656 * #
NASA-CR-196379 ..... p 4505 N94-37655 * #
NASA-CR-196380 ..... p 4499 N94-37654 * #
NASA-CR-196384 ..... p 4501 N94-37590 * #
NASA-CR-196424 ..... p 4446 N94-36812 * #

NASA-CR-4584 ..... p 4442 N94-36957 * #
NASA-CR-4592 ..... p 4467 N94-37607 * #
NASA-CR-4600 ..... p 4389 N94-36945 * #
NASA-CR-4602 ..... p 4455 N94-37015 * #
NASA-CR-4604 ..... p 4399 N94-37614 * #
NASA-CR-4608 ..... p 4389 N94-37259 * #
NASA-CR-4610 ..... p 4420 N94-37582 * #
NASA-CR-4613 ..... p 4466 N94-37252 * #
NASA-CR-4614 ..... p 4397 N94-37506 * #

NASA-CU-28159 ..... p 4546 N94-37765 * #

NASA-RP-1341 ..... p 4382 N94-36741 * #

NASA-SP-7011(392) ..... p 4482 N94-37445 *
NASA-SP-7037(307) ..... p 4381 N94-37117 *

NASA-TM-104269 ..... p 4386 N94-36644 * #
NASA-TM-104272 ..... p 4381 N94-36648 * #
NASA-TM-104566-VOL-20-PT-1 .. p 4475 N94-36958 * #
NASA-TM-104609 ..... p 4477 N94-37397 * #
NASA-TM-104611 ..... p 4475 N94-37790 * #
NASA-TM-104794 ..... p 4392 N94-37386 * #
NASA-TM-106410 ..... p 4452 N94-37457 * #
NASA-TM-106449 ..... p 4502 N94-36647 * #
NASA-TM-106452 ..... p 4441 N94-36646 * #
NASA-TM-106480 ..... p 4408 N94-36537 * #
NASA-TM-106507 ..... p 4450 N94-36645 * #
NASA-TM-106526 ..... p 4455 N94-36561 * #
NASA-TM-106539 ..... p 4457 N94-37704 * #
NASA-TM-106553 ..... p 4452 N94-37521 * #
NASA-TM-106556 ..... p 4399 N94-37315 * #
NASA-TM-106565 ..... p 4390 N94-37522 * #
NASA-TM-106583 ..... p 4382 N94-36686 * #
NASA-TM-106600 ..... p 4456 N94-37456 * #
NASA-TM-106611 ..... p 4403 N94-36956 * #
NASA-TM-106612 ..... p 4451 N94-37451 * #
NASA-TM-106616 ..... p 4426 N94-37520 * #
NASA-TM-106619 ..... p 4431 N94-37254 * #
NASA-TM-106623 ..... p 4450 N94-36953 * #
NASA-TM-106630 ..... p 4405 N94-37318 * #
NASA-TM-106633 ..... p 4383 N94-37283 * #
NASA-TM-106646 ..... p 4444 N94-37507 * #
NASA-TM-106650 ..... p 4421 N94-36952 * #
NASA-TM-106653 ..... p 4387 N94-37448 * #
NASA-TM-106654 ..... p 4437 N94-36819 * #
NASA-TM-106655 ..... p 4398 N94-36951 * #
NASA-TM-106656 ..... p 4431 N94-36943 * #
NASA-TM-106659 ..... p 4424 N94-37300 * #
NASA-TM-106661 ..... p 4433 N94-36955 * #
NASA-TM-106663 ..... p 4451 N94-37319 * #
NASA-TM-106667 ..... p 4510 N94-37308 * #
NASA-TM-106680 ..... p 4419 N94-37459 * #
NASA-TM-108458 ..... p 4446 N94-36822 * #
NASA-TM-108460 ..... p 4496 N94-37556 * #
NASA-TM-108806 ..... p 4381 N94-37332 * #
NASA-TM-108959 ..... p 4386 N94-37636 * #
NASA-TM-109025 ..... p 4497 N94-36932 * #
NASA-TM-109066 ..... p 4493 N94-36818 * #
NASA-TM-109079 ..... p 4456 N94-37541 * #
NASA-TM-109116 ..... p 4456 N94-37253 * #
NASA-TM-109130 ..... p 4388 N94-36820 * #
NASA-TM-109135 ..... p 4405 N94-37320 * #
NASA-TM-109136 ..... p 4500 N94-37058 * #
NASA-TM-109137 ..... p 4387 N94-37762 * #
NASA-TM-109138 ..... p 4501 N94-37589 * #
NASA-TM-109139 ..... p 4386 N94-37256 * #
NASA-TM-109141 ..... p 4444 N94-37455 * #
NASA-TM-109415 ..... p 4540 N94-36841 * #
NASA-TM-109892 ..... p 4461 N94-36827 * #
NASA-TM-109894 ..... p 4473 N94-37371 * #
NASA-TM-109895 ..... p 4390 N94-37443 * #
NASA-TM-109898 ..... p 4546 N94-37765 * #
NASA-TM-109924 ..... p 4540 N94-36750 * #
NASA-TM-109925 ..... p 4541 N94-36853 * #
NASA-TM-4539-VIDEO-SUPPL .... p 4492 N94-36518 *
NASA-TM-4548 ..... p 4388 N94-37059 * #
NASA-TM-4555 ..... p 4396 N94-36821 * #
NASA-TM-4556 ..... p 4455 N94-37102 * #
NASA-TM-4566 ..... p 4383 N94-36966 * #
NASA-TM-4573 ..... p 4383 N94-36950 * #
NASA-TM-4584 ..... p 4405 N94-37460 * #
NASA-TM-4595 ..... p 4383 N94-36944 * #
NASA-TM-4607 ..... p 4382 N94-36942 * #
NASA-TM-4627 ..... p 4383 N94-37378 * #
NASA-TM-4633 ..... p 4383 N94-37395 * #

NASA-TP-3398 ..... p 4419 N94-37503 * #
NASA-TP-3419 ..... p 4388 N94-37014 * #
NASA-TP-3427 ..... p 4384 N94-37505 * #
NASA-TP-3436 ..... p 4416 N94-36993 * #
NASA-TP-3438 ..... p 4447 N94-36948 * #
NASA-TP-3439 ..... p 4397 N94-37502 * #
NASA-TP-3449 ..... p 4396 N94-37260 * #
NASA-TP-3453 ..... p 4481 N94-37262 * #
NASA-TP-3488 ..... p 4384 N94-37577 * #
NASA-TP-3490 ..... p 4420 N94-37578 * #

NATICK-TR-94/020 ..... p 4404 N94-37105

NAVY-CASE-74641 ..... p 4385 N94-37830 #
NAVY-CASE-74643 ..... p 4385 N94-37839
NAVY-CASE-75055 ..... p 4436 N94-37835 #
NAVY-CASE-75328 ..... p 4440 N94-37840
NAVY-CASE-75421 ..... p 4427 N94-37831 #
NAVY-CASE-75641 ..... p 4440 N94-37832 #
NAVY-CASE-75724 ..... p 4450 N94-37838 #
NAVY-CASE-75846 ..... p 4427 N94-37829

NEI-FI-217 ..... p 4414 N94-36525 #

NIFS-186 ..... p 4530 N94-37384 #
NIFS-219 ..... p 4532 N94-37734 #
NIFS-221 ..... p 4529 N94-37358 #
NIFS-225 ..... p 4531 N94-37466 #
NIFS-226 ..... p 4531 N94-37485 #
NIFS-227 ..... p 4529 N94-37359 #
NIFS-232 ..... p 4528 N94-37231 #
NIFS-238 ..... p 4526 N94-36472 #

NIPER-689-VOL-1 ..... p 4492 N94-36698 #
NIPER-689-VOL-2 ..... p 4493 N94-36699 #

NIST/GCR-93/633 ..... p 4478 N94-36720 #

NISTIR-5375 ..... p 4446 N94-36719
NISTIR-5378 ..... p 4508 N94-36718

NOAA-TR-NESDIS-77 ..... p 4396 N94-37009 #

NONP-DTIC-DK-94-14636 ..... p 4433 N94-36757

NONP-NASA-SUPPL-DK-94-19641 p 4441 N94-36519 * #

NONP-NASA-VT-94-12970 ..... p 4492 N94-36518 *

NPL-DQM-98 ..... p 4463 N94-36533

NPRDC-TR-94-8 ..... p 4432 N94-36473

NPS-CS-94-007 ..... p 4494 N94-37120

NREL/TP-411-6406 ..... p 4462 N94-37407 #
NREL/TP-411-6470-PHASE-2A ... p 4461 N94-36476 #
NREL/TP-425-6345 ..... p 4411 N94-37409 #
NREL/TP-425-6544 ..... p 4451 N94-37408 #
NREL/TP-430-6080 ..... p 4461 N94-36740 #
NREL/TP-430-6084 ..... p 4467 N94-37405 #
NREL/TP-451-6395 ..... p 4533 N94-36745 #
NREL/TP-451-6400 ..... p 4533 N94-36744 #
NREL/TP-451-6469 ..... p 4462 N94-37381
NREL/TP-463-6157 ..... p 4451 N94-37406 #

NRL/FR/8121-93-9545 ..... p 4398 N94-36445

NRL/MR/6790-94-7465 ..... p 4528 N94-37182

NRLD-BC-005-92-333 ..... p 4477 N94-36522

OMI-04-92-2 ..... p 4493 N94-36920 * #

ORNL-6797 ..... p 4431 N94-37452 #

ORNL/CDIAC-34/R4 ..... p 4466 N94-37208 #

ORNL/FTR-4875 ..... p 4521 N94-37220 #

ORNL/HTSPC-5 ..... p 4438 N94-37239 #

ORNL/SUB-85-55901/04 ..... p 4410 N94-37286 #

ORNL/TM-12686 ..... p 4503 N94-37073 #

PB94-157831 ..... p 4478 N94-36720 #
PB94-163052 ..... p 4446 N94-36719
PB94-163078 ..... p 4508 N94-36718
PB94-164993 ..... p 4384 N94-36530
PB94-165487 ..... p 4450 N94-36721
PB94-166048 ..... p 4464 N94-36994
PB94-166055 ..... p 4464 N94-36995
PB94-167067 ..... p 4445 N94-36531
PB94-167467 ..... p 4432 N94-36567
PB94-167475 ..... p 4436 N94-36532
PB94-167855 ..... p 4463 N94-36533
PB94-169109 ..... p 4521 N94-36545
PB94-169206 ..... p 4492 N94-36546
PB94-170503 ..... p 4497 N94-36547
PB94-170669 ..... p 4414 N94-36534
PB94-170719 ..... p 4499 N94-36535
PB94-170917 ..... p 4510 N94-37632 #
PB94-171097 ..... p 4532 N94-36548
PB94-171139 ..... p 4513 N94-36549
PB94-171824 ..... p 4412 N94-37462 #
PB94-173176 ..... p 4471 N94-37780 #
PB94-173184 ..... p 4471 N94-37781 #
PB94-173192 ..... p 4470 N94-37530 #
PB94-175247 ..... p 4509 N94-37301 #
PB94-179058 ..... p 4506 N94-37833 #
PB94-179181 ..... p 4548 N94-37834 #
PB94-179389 ..... p 4441 N94-37851
PB94-179488 ..... p 4399 N94-37531
PB94-180866 ..... p 4506 N94-37852
PB94-180874 ..... p 4506 N94-37853
PB94-184488 ..... p 4427 N94-37854
PB94-184561 ..... p 4477 N94-37855
PB94-184603 ..... p 4468 N94-37856
PB94-184678 ..... p 4487 N94-37812
PB94-184686 ..... p 4435 N94-37813

PL-TR-93-1041 ..... p 4525 N94-37350
PL-TR-93-2159 ..... p 4464 N94-36973
PL-TR-93-2182 ..... p 4473 N94-37217
PL-TR-93-2224 ..... p 4470 N94-37649

PNL-SA-22235 ..... p 4415 N94-36553 #
PNL-SA-22546 ..... p 4474 N94-37379
PNL-SA-22773 ..... p 4471 N94-36479 #
PNL-SA-23046 ..... p 4545 N94-37348 #
PNL-SA-23105 ..... p 4463 N94-36478 #
PNL-SA-23162 ..... p 4463 N94-36477 #
PNL-SA-23172 ..... p 4466 N94-37211 #
PNL-SA-23405 ..... p 4474 N94-37565 #
PNL-SA-23416 ..... p 4472 N94-37048 #
PNL-SA-23484 ..... p 4468 N94-37624 #
PNL-SA-23995 ..... p 4480 N94-37625 #
PNL-SA-24063 ..... p 4474 N94-37566 #

PRG-113 ..... p 4492 N94-36546

PUBL-4244 ..... p 4466 N94-37208 #

P9350017-STR3 ..... p 4437 N94-37033
P9350017-STR4 ..... p 4437 N94-37035 #

R/D-6869-MS-01 ..... p 4456 N94-37186
R/D-7131-EE-01 ..... p 4469 N94-37215

RAL-93-086 ..... p 4436 N94-36532
RAL-93-090-PT-1 ..... p 4445 N94-36531
RAL-94-009 ..... p 4521 N94-36545
RAL-94-011 ..... p 4432 N94-36567
RAL-94-019 ..... p 4497 N94-36547
RAL-94-028 ..... p 4513 N94-36549

REPT-S-200 ..... p 4510 N94-37632 #

REPT-102-94-007U ..... p 4433 N94-36754
REPT-10339 ..... p 4461 N94-36919 * #
REPT-1993:4 ..... p 4533 N94-36734 #
REPT-93549/1 ..... p 4489 N94-36731 #
REPT-94B00098 ..... p 4477 N94-37397 * #
REPT-94B00104-VOL-20-PT-1 ..... p 4475 N94-36958 * #
REPT-94B00110 ..... p 4475 N94-37790 * #
REPT-94003-SBIR-2-F ..... p 4534 N94-37036 #
REPT-9803-1 ..... p 4461 N94-36919 * #
REPT-9803-1 ..... p 4494 N94-37061 * #

RIACS-TP-94-07 ..... p 4496 N94-37656 * #
RIACS-TP-94-12 ..... p 4505 N94-37655 * #
RIACS-TP-94-13 ..... p 4499 N94-37654 * #

RPI/CHE/NASA-5-23390-4 ..... p 4442 N94-36992 * #

R94AEB175 ..... p 4387 N94-37401 * #

S-768 ..... p 4392 N94-37386 * #

SAIC-01-0262-01-1222 ..... p 4534 N94-37027

SAND-92-2625 ..... p 4470 N94-37527 #
SAND-93-1060C ..... p 4436 N94-36557 #
SAND-93-1395C ..... p 4400 N94-36456 #
SAND-93-1684C ..... p 4462 N94-37189 #
SAND-93-1922 ..... p 4531 N94-37626 #
SAND-93-2070C ..... p 4412 N94-37542 #
SAND-93-2172C ..... p 4498 N94-37487 #
SAND-93-2581C ..... p 4536 N94-37287 #
SAND-93-3822C ..... p 4408 N94-37091 #
SAND-93-3862C ..... p 4430 N94-36447 #
SAND-93-3897 ..... p 4545 N94-37563 #
SAND-93-3898C ..... p 4435 N94-37391 #
SAND-93-3957 ..... p 4496 N94-37673 #
SAND-93-4002C ..... p 4483 N94-36470 #
SAND-93-4039 ..... p 4484 N94-37071 #
SAND-94-0129 ..... p 4405 N94-37627 #
SAND-94-0240C ..... p 4409 N94-37161 #
SAND-94-0241C ..... p 4411 N94-37365 #
SAND-94-0247C ..... p 4457 N94-37705 #

SAND-94-0296C ..... p 4501 N94-37425 #
SAND-94-0320 ..... p 4445 N94-37726 #
SAND-94-0383 ..... p 4448 N94-37198 #
SAND-94-0448C ..... p 4439 N94-37513 #
SAND-94-0459C ..... p 4532 N94-36540 #
SAND-94-0478C ..... p 4389 N94-37159 #
SAND-94-0513C ..... p 4501 N94-37783 #
SAND-94-0533C ..... p 4438 N94-37196 #
SAND-94-0534C ..... p 4438 N94-37190 #
SAND-94-0596C ..... p 4502 N94-37785 #
SAND-94-0623C ..... p 4501 N94-37529 #
SAND-94-0694 ..... p 4527 N94-37072 #
SAND-94-0695C ..... p 4489 N94-36480 #
SAND-94-0709C ..... p 4432 N94-36471 #
SAND-94-0734C ..... p 4502 N94-37784 #
SAND-94-0766 ..... p 4447 N94-37051 #
SAND-94-0839C ..... p 4443 N94-37195 #
SAND-94-0912C ..... p 4439 N94-37363
SAND-94-0934C ..... p 4526 N94-36448 #
SAND-94-1019C ..... p 4426 N94-37537 #
SAND-94-1045C ..... p 4505 N94-37620 #
SAND-94-1078C ..... p 4457 N94-37622 #
SAND-94-1155C ..... p 4540 N94-37092 #
SAND-94-1188C ..... p 4428 N94-37052 #
SAND-94-1190C ..... p 4411 N94-37412 #
SAND-94-1191C ..... p 4429 N94-37413 #
SAND-94-1197C ..... p 4428 N94-37201 #
SAND-94-1198C ..... p 4428 N94-37202 #
SAND-94-1213C ..... p 4495 N94-37430 #
SAND-94-1267C ..... p 4417 N94-37367 #
SAND-94-1278C ..... p 4424 N94-37204 #
SAND-94-1347C ..... p 4507 N94-37564 #
SAND-94-1435C ..... p 4495 N94-37496 #
SAND-94-8219B ..... p 4427 N94-37725 #
SAND-94-8229 ..... p 4428 N94-37243 #
SAND-94-8483C ..... p 4407 N94-36462 #
SAND-94-8484C ..... p 4407 N94-36482 #
SAND-94-8501C ..... p 4409 N94-37221 #
SAND-94-8507C ..... p 4410 N94-37222 #
SAND-94-8510C ..... p 4413 N94-37711 #
SAND-94-8595C ..... p 4473 N94-37371 * #
SAND-94-8625C ..... p 4517 N94-37210 #
SAND-94-8640C ..... p 4465 N94-37154 #
SAND-94-8641C ..... p 4537 N94-37356 #

SCT-90RR-46 ..... p 4385 N94-37604 #
SCT-91RR-43 ..... p 4487 N94-37741 #
SCT-91RR-45 ..... p 4487 N94-37743 #
SCT-93RR-17-VOL-1 ..... p 4381 N94-36466 #
SCT-93RR-17-VOL-2 ..... p 4382 N94-36467 #
SCT-93RR-21 ..... p 4390 N94-37424 #
SCT-93RR-22 ..... p 4487 N94-37742 #

SEAS-UVA/528474/CS95/102 .... p 4442 N94-36960 * #

SEL-93-003 ..... p 4489 N94-36484 * #

SLAC-PUB-6450 ..... p 4539 N94-37543 #
SLAC-PUB-6477 ..... p 4515 N94-37084 #
SLAC-PUB-6493 ..... p 4515 N94-37085 #
SLAC-PUB-6502 ..... p 4515 N94-37086 #
SLAC-PUB-6511 ..... p 4515 N94-37087 #

SR-2 ..... p 4464 N94-36973

SRI-PYH-2976 ..... p 4412 N94-37462 #

SSCL-659 ..... p 4495 N94-37453 #

SSD-94M0038 ..... p 4430 N94-36806 * #

SU-SLAC-PUB-6466 ..... p 4519 N94-37553 #
SU-SLAC-PUB-6491 ..... p 4539 N94-37366 #

SU-SLAC/SSRL-0072 ..... p 4519 N94-37553 #

TKK-F-A719 ..... p 4427 N94-37854

TM-5-94 ..... p 4442 N94-36934 #

TR-14-ONR ..... p 4423 N94-37147
TR-15-ONR ..... p 4424 N94-37227
TR-15 ..... p 4423 N94-37148
TR-16-ONR ..... p 4424 N94-37185
TR-24 ..... p 4433 N94-36756
TR-24 ..... p 4433 N94-36757
TR-27-ONR ..... p 4423 N94-37144
TR-29-ONR ..... p 4409 N94-37145
TR-4-ONR ..... p 4399 N94-37650 #
TR-42 ..... p 4512 N94-36521

TSHUNE-0068 ..... p 4412 N94-37534 #

UAH-5-32753 ..... p 4410 N94-37250 * #

UCB-PTH-93/01 ..... p 4508 N94-36560 #

UCRL-CR-115942 ..... p 4524 N94-37191 #
UCRL-CR-116109-SUMM ..... p 4505 N94-37497 #
UCRL-CR-116392 ..... p 4479 N94-37355 #
UCRL-CR-117195 ..... p 4439 N94-37306 #

UCRL-ID-112216 ..... p 4430 N94-36444 #
UCRL-ID-114560 ..... p 4523 N94-36693 #
UCRL-ID-115752 ..... p 4429 N94-37427 #
UCRL-ID-116533 ..... p 4468 N94-37631 #
UCRL-ID-116758 ..... p 4524 N94-37112 #
UCRL-ID-117008 ..... p 4448 N94-37240 #
UCRL-ID-117029 ..... p 4448 N94-37203 #
UCRL-ID-117158 ..... p 4420 N94-37678 #
UCRL-ID-117214 ..... p 4532 N94-37732 #

UCRL-JC-112090 ..... p 4446 N94-37388 #
UCRL-JC-113294 ..... p 4513 N94-36697 #
UCRL-JC-113583-REV-1 ..... p 4475 N94-37621 #
UCRL-JC-114239 ..... p 4525 N94-37486 #
UCRL-JC-114619 ..... p 4467 N94-37428 #
UCRL-JC-114743 ..... p 4512 N94-36516 #
UCRL-JC-115052 ..... p 4407 N94-36458 #
UCRL-JC-115222 ..... p 4425 N94-37422 #
UCRL-JC-115423 ..... p 4527 N94-37082 #
UCRL-JC-115687-REV-1 ..... p 4447 N94-37160 #
UCRL-JC-115748 ..... p 4528 N94-37307 #
UCRL-JC-115855 ..... p 4481 N94-37197 #
UCRL-JC-115860 ..... p 4473 N94-37242 #
UCRL-JC-115923 ..... p 4444 N94-37390 #
UCRL-JC-115947-REV-1 ..... p 4530 N94-37392 #
UCRL-JC-116042 ..... p 4530 N94-37437 #
UCRL-JC-116184 ..... p 4446 N94-37723 #
UCRL-JC-116269 ..... p 4528 N94-37297 #
UCRL-JC-116270 ..... p 4527 N94-37081 #
UCRL-JC-116299 ..... p 4517 N94-37209 #
UCRL-JC-116300 ..... p 4528 N94-37207 #
UCRL-JC-116301 ..... p 4438 N94-37213 #
UCRL-JC-116517 ..... p 4477 N94-37494 #
UCRL-JC-116530 ..... p 4465 N94-37155 #
UCRL-JC-116700 ..... p 4448 N94-37244 #
UCRL-JC-116764 ..... p 4447 N94-37114 #
UCRL-JC-116818 ..... p 4510 N94-37536 #
UCRL-JC-116941 ..... p 4548 N94-37164 #
UCRL-JC-116999 ..... p 4449 N94-37737 #
UCRL-JC-117000 ..... p 4449 N94-37722 #

UCSB-TR-1 ..... p 4503 N94-37146

UILU-ENG-94-4008 ..... p 4415 N94-36811 * #

US-PATENT-APPL-SN-023426 ..... p 4452 N94-37766
US-PATENT-APPL-SN-035780 ..... p 4385 N94-37767
US-PATENT-APPL-SN-062856 ..... p 4478 N94-36751 * #
US-PATENT-APPL-SN-145352 ..... p 4436 N94-37835 #
US-PATENT-APPL-SN-169923 ..... p 4440 N94-37832 #
US-PATENT-APPL-SN-215793 ..... p 4437 N94-36781 * #
US-PATENT-APPL-SN-216559 ..... p 4385 N94-37830 #
US-PATENT-APPL-SN-216567 ..... p 4385 N94-37839
US-PATENT-APPL-SN-219318 ..... p 4427 N94-37831 #
US-PATENT-APPL-SN-220718 ..... p 4440 N94-37840
US-PATENT-APPL-SN-230571 ..... p 4450 N94-36839 * #
US-PATENT-APPL-SN-234034 ..... p 4427 N94-37829
US-PATENT-APPL-SN-235844 ..... p 4450 N94-37838 #
US-PATENT-APPL-SN-238044 ..... p 4386 N94-36767 * #
US-PATENT-APPL-SN-238767 ..... p 4403 N94-36752 * #
US-PATENT-APPL-SN-242546 ..... p 4478 N94-36765 * #
US-PATENT-APPL-SN-246460 ..... p 4509 N94-36782 * #
US-PATENT-APPL-SN-247189 ..... p 4480 N94-36766 * #
US-PATENT-APPL-SN-250141 ..... p 4389 N94-36826 * #
US-PATENT-APPL-SN-252032 ..... p 4486 N94-36838 * #
US-PATENT-APPL-SN-252615 ..... p 4486 N94-36840 * #
US-PATENT-APPL-SN-253635 ..... p 4413 N94-37761
US-PATENT-APPL-SN-283728 ..... p 4395 N94-36825 * #
US-PATENT-APPL-SN-499962 ..... p 4435 N94-37771
US-PATENT-APPL-SN-749825 ..... p 4538 N94-37770
US-PATENT-APPL-SN-841944 ..... p 4427 N94-37773
US-PATENT-APPL-SN-846633 ..... p 4440 N94-37769
US-PATENT-APPL-SN-860721 ..... p 4538 N94-37776
US-PATENT-APPL-SN-861213 ..... p 4440 N94-37775
US-PATENT-APPL-SN-906903 ..... p 4430 N94-37768
US-PATENT-APPL-SN-921776 ..... p 4427 N94-37778
US-PATENT-APPL-SN-926625 ..... p 4427 N94-37779
US-PATENT-APPL-SN-937765 ..... p 4526 N94-37774
US-PATENT-APPL-SN-968880 ..... p 4448 N94-37481
US-PATENT-APPL-SN-983194 ..... p 4425 N94-37482
US-PATENT-APPL-SN-991940 ..... p 4427 N94-37818
US-PATENT-APPL-SN-998347 ..... p 4449 N94-37772
US-PATENT-APPL-SN-998346 ..... p 4449 N94-37777

US-PATENT-CLASS-128-665 ..... p 4440 N94-37775
US-PATENT-CLASS-137-493.4 .... p 4452 N94-37766
US-PATENT-CLASS-244-129.1 .... p 4385 N94-37767
US-PATENT-CLASS-250-336.2 .... p 4440 N94-37769
US-PATENT-CLASS-252-700 ..... p 4413 N94-37761
US-PATENT-CLASS-342-384 ..... p 4435 N94-37771
US-PATENT-CLASS-356-382 ..... p 4430 N94-37768

US-PATENT-CLASS-372-20 ..... p 4448 N94-37481
US-PATENT-CLASS-372-41 ..... p 4449 N94-37777
US-PATENT-CLASS-372-68 ..... p 4449 N94-37772
US-PATENT-CLASS-437-22 ..... p 4538 N94-37770
US-PATENT-CLASS-505-1 ..... p 4538 N94-37776
US-PATENT-CLASS-522-99 ..... p 4427 N94-37818
US-PATENT-CLASS-528-170 ..... p 4427 N94-37778
US-PATENT-CLASS-528-38 ..... p 4427 N94-37779
US-PATENT-CLASS-560-221 ..... p 4427 N94-37773
US-PATENT-CLASS-65-3.14 ..... p 4526 N94-37774

US-PATENT-5,272,237 ..... p 4425 N94-37482
US-PATENT-5,272,708 ..... p 4448 N94-37481
US-PATENT-5,275,168 ..... p 4440 N94-37775
US-PATENT-5,282,492 ..... p 4452 N94-37766
US-PATENT-5,285,067 ..... p 4440 N94-37769
US-PATENT-5,287,376 ..... p 4449 N94-37772
US-PATENT-5,289,482 ..... p 4449 N94-37777
US-PATENT-5,292,779 ..... p 4427 N94-37818
US-PATENT-5,292,851 ..... p 4427 N94-37779
US-PATENT-5,292,854 ..... p 4427 N94-37778
US-PATENT-5,292,927 ..... p 4427 N94-37773
US-PATENT-5,293,218 ..... p 4430 N94-37768
US-PATENT-5,294,240 ..... p 4526 N94-37774
US-PATENT-5,294,557 ..... p 4538 N94-37770
US-PATENT-5,296,865 ..... p 4435 N94-37771
US-PATENT-5,298,197 ..... p 4413 N94-37761
US-PATENT-5,298,484 ..... p 4538 N94-37776
US-PATENT-5,301,904 ..... p 4385 N94-37767

USAMRDALC-01 ..... p 4480 N94-37089

USARIEM-TR-T94-11 ..... p 4481 N94-37136

UTTAC-60 ..... p 4522 N94-37237 #

UVA/528266/MSE94/116 ..... p 4415 N94-36809 * #

VAEC-B-020 ..... p 4407 N94-36529 #
VAEC-B-021 ..... p 4414 N94-36541 #

VPI-E-94-05 ..... p 4406 N94-37653 * #

WAPD-T-3030 ..... p 4502 N94-36455 #
WAPD-T-3034 ..... p 4416 N94-37080 #

WHC-SA-2111 ..... p 4451 N94-37188 #

WL-TR-94-1075 ..... p 4447 N94-37137
WL-TR-94-2003 ..... p 4428 N94-36505

WSRC-MS-94-0244 ..... p 4465 N94-37093 #
WSRC-MS-94-0251 ..... p 4472 N94-37115 #

WSS/CI-94-015 ..... p 4407 N94-36482 #

XC-ESC/MA ..... p 4533 N94-36734 #

Y/EN-5087 ..... p 4469 N94-36758 #

APPENDIX

NASA SCIENTIFIC AND TECHNICAL INFORMATION PROGRAM PRODUCTS AND SERVICES

The NASA Scientific and Technical Information (STI) Program provides for the collection and announcement of aerospace-related reports and literature obtained worldwide through agreements and exchanges. The result of the collection is the comprehensive NASA STI Database that covers aeronautics, space, and supporting disciplines.

The STI Database, documents generated or obtained by NASA, and products and services derived from or supporting the database are made available to the NASA research community and to the public. Descriptions and sources of these items are presented in the following pages.

Scientific and Technical Aerospace Reports (STAR) is an abstract journal, listing citations with abstracts for aerospace-related reports obtained from worldwide sources. *STAR* is issued on the first of each month, and announces current documents that have been entered into the NASA STI Database during the previous month. The reports are of the following types:

- NASA, NASA contractor, and NASA grantee reports;
- Reports issued by other U.S. Government agencies, domestic and foreign institutions, universities, and private firms;
- Translations in report form;
- NASA-owned patents and patent applications
- Other U.S. Government agency and foreign patents and patent applications
- Domestic and foreign dissertations and theses.

Journal, book, and conference literature, journal translations, and certain foreign dissertations having the same subject scope as *STAR* are announced in a companion journal, *NASA Open Volumes on Aerospace (NOVA). NOVA* is issued on the 15th of each month and is available from the NASA Center for AeroSpace Information, at the address below.

ELIGIBILITY AND REGISTRATION FOR NASA STI PRODUCTS AND SERVICES

Organizations of the type listed below that have registered with NASA can receive products and services.

- NASA offices and installations, contractors, subcontractors, grantees, and consultants;
- Other U.S. Government agencies and their contractors;
- Libraries in the United States that have arrangements with NASA to maintain collections of NASA documents for public reference;
- Other organizations in the United States having a need for NASA documents in work related to aeronautics and space research;
- Organizations abroad that have established reciprocal documents exchange arrangements with NASA.

The central service points—central points of document acquisition and control within qualified organizations—or individuals are eligible to register for NASA STI products and services. Domestic organizations or individuals may be eligible to receive various classes of NASA publications and services and should address their requests for registration or further information to:

ATTN: Registration Services
NASA Center for AeroSpace Information
800 Elkridge Landing Road
Linthicum Heights, MD 21090-2934
301-621-0390

Organizations abroad should direct requests to:

National Aeronautics and Space Administration
Scientific and Technical Information Program (JTT)
International STI Program
Washington, DC 20546-0001
USA
703-271-5640

SUBJECT SCOPE

The subject scope of *STAR* and *NOVA* includes all aspects of aeronautics and space research and development, supporting basic and applied research, and applications. Aerospace aspects of Earth resources, energy development, conservation, oceanography, environmental protection, urban transportation, and other topics of high national priority are also covered.

HOW TO USE *STAR* SUBJECT CATEGORIES

Abstracts in *STAR* are categorized by 10 major subject divisions that are divided further into 76 specific subject categories. The subject divisions and categories are listed in the Table of Contents together with a note for each that defines its scope and provides any cross-references. For example:

16 SPACE TRANSPORTATION

Includes passenger and cargo space transportation, e.g., shuttle operations; and space rescue techniques. For related information see also *03 Air Transportation and Safety* and *18 Spacecraft Design, Testing and Performance.* For space suits see *54 Man/System Technology and Life Support.*

CROSS-REFERENCES

Individual *STAR* abstracts are not ordinarily cross-referenced, except for certain conference reports or book translations that have had separate abstracts written for their component papers or chapters. Citations and abstracts of the components follow immediately after those of the parent document. When the subject content of a component differs sufficiently from the general content of the parent, a cross-reference citation also is printed at the end of the category to which it normally would have been assigned if it were independent.

DOCUMENTS ON MICROFICHE

Documents available on microfiche are designated by a pound sign (#) following the accession number.

LIMITED REPRODUCIBILITY

A note of limited reproducibility appears in the citation, if there are factors affecting the reproducibility of more than 20% of the document. These factors include faint or broken type, color photographs, black and white photographs, foldouts, dot matrix print, or some other factor that limits the reproducibility of the document. This notation also appears on the microfiche header.

NASA PATENTS AND PATENT APPLICATIONS

Patents and patent applications owned by NASA are announced in *STAR* under appropriate subject categories and are referenced in the *STAR* indexes. In the Report Number Index, patents are indexed by the NASA Case Number, and the U.S. Patent Class. Patent applications are indexed by the NASA Case Number and the U.S. Patent Application Serial Number.

Printed copies of patents (which are not microfiched) are available for purchase from the U.S. Patent and Trademark Office.

When ordering patents, the U.S. Patent Number should be used, and payment must be remitted in advance, by money order or check payable to the Commissioner of Patents and Trademarks. Prepaid purchase coupons for ordering are also available from the U.S. Patent and Trademark Office.

NASA patent application specifications are sold in both paper copy and microfiche by the NASA Center for AeroSpace Information (CASI). The N accession number should be used in ordering either paper copy or microfiche from CASI.

The patents and patent applications announced in *STAR* are owned by NASA and are available for royalty-free licensing. Requests for licensing terms and further information should be addressed to:

National Aeronautics and Space Administration
Associate General Counsel for Intellectual Property
Code GP
Washington, DC 20546-0001

SOURCES FOR DOCUMENTS

One or more sources from which a document announced in *STAR* is available to the public is ordinarily given on the last line of the citation. The most commonly indicated sources and their acronyms or abbreviations are listed below, and their addresses are listed on page A-6. If the publication is available from a source other than those listed, the publisher and his address will be displayed on the availability line or in combination with the corporate source line.

Avail: CASI. Sold by the NASA Center for AeroSpace Information. Prices for hard copy (HC) and microfiche (MF) are indicated by a price code following the letters HC or MF in the *STAR* citation. Current values for the price codes are given in the tables on page A-7.

NOTE ON ORDERING DOCUMENTS: When ordering publications from CASI, use the N accession number or other report number. It is also advisable to cite the title and other bibliographic identification.

Avail: SOD (or GPO). Sold by the Superintendent of Documents, U.S. Government Printing Office, in hard copy.

Avail: BLL (formerly NLL): British Library Lending Division, Boston Spa, Wetherby, Yorkshire, England. Photocopies available from this organization at the price shown. (If none is given, inquiry should be addressed to the BLL.)

Avail: DOE Depository Libraries. Organizations in U.S. cities and abroad that maintain collections of Department of Energy reports, usually in microfiche form, are listed in *Energy Research Abstracts*. Services available from the DOE and its depositories are described in a booklet, *DOE Technical Information Center - Its Functions and Services* (TID-4660), which may be obtained without charge from the DOE Technical Information Center.

Avail: ESDU. Pricing information on specific data, computer programs, and details on Engineering Sciences Data Unit (ESDU) topic categories can be obtained from ESDU International Ltd. Requesters in North America should use the Virginia address while all other requesters should use the London address, both of which are on page A-6.

Avail: Fachinformationszentrum Karlsruhe. Gesellschaft für wissenschaftlich-technische Information mbH 76344 Eggenstein-Leopoldshafen, Germany.

Avail: HMSO. Publications of Her Majesty's Stationery Office are sold in the U.S. by Pendragon House, Inc. (PHI), Redwood City, CA. The U.S. price (including a service and mailing charge) is given, or a conversion table may be obtained from PHI.

Avail: Issuing Activity, or Corporate Author, or no indication of availability. Inquiries as to the availability of these documents should be addressed to the organization shown in the citation as the corporate author of the document.

Avail: NASA Public Document Rooms. Documents so indicated may be examined at or purchased from the National Aeronautics and Space Administration (JBD-4), Public Documents Room (Room 1H23), Washington, DC 20546-0001, or public document rooms located at NASA installations, and the NASA Pasadena Office at the Jet Propulsion Laboratory.

Avail: NTIS. Sold by the National Technical Information Service. Initially distributed microfiche under the NTIS SRIM (Selected Research in Microfiche) are available. For information concerning this service, consult the NTIS Subscription Section, Springfield, VA 22161.

Avail: Univ. Microfilms. Documents so indicated are dissertations selected from *Dissertation Abstracts* and are sold by University Microfilms as xerographic copy (HC) and microfilm. All requests should cite the author and the Order Number as they appear in the citation.

Avail: US Patent and Trademark Office. Sold by Commissioner of Patents and Trademarks, U.S. Patent and Trademark Office, at the standard price of $1.50 each, postage free. (See discussion of NASA patents and patent applications on page A-3.)

Avail: (US Sales Only). These foreign documents are available to users within the United States from the National Technical Information Service (NTIS). They are available to users outside the United States through the International Nuclear Information Service (INIS) representative in their country, or by applying directly to the issuing organization.

Avail: USGS. Originals of many reports from the U.S. Geological Survey, which may contain color illustrations, or otherwise may not have the quality of illustrations preserved in the microfiche or facsimile reproduction, may be examined by the public at the libraries of the USGS field offices whose addresses are listed on page A-6. The libraries may be queried concerning the availability of specific documents and the possible utilization of local copying services, such as color reproduction.

FEDERAL DEPOSITORY LIBRARY PROGRAM

In order to provide the general public with greater access to U.S. Government publications, Congress established the Federal Depository Library Program under the Government Printing Office (GPO), with 53 regional depositories responsible for permanent retention of material, inter-library loan, and reference services. At least one copy of nearly every NASA and NASA-sponsored publication, either in printed or microfiche format, is received and retained by the 53 regional depositories. A list of the regional GPO libraries, arranged alphabetically by state, appears on page A-8. These libraries are *not* sales outlets. A local library can contact a regional depository to help locate specific reports, or direct contact may be made by an individual.

PUBLIC COLLECTION OF NASA DOCUMENTS

An extensive collection of NASA and NASA-sponsored publications is maintained by the British Library Lending Division, Boston Spa, Wetherby, Yorkshire, England for public access. The British Library Lending Division also has available many of the non-NASA publications cited in *STAR*. European requesters may purchase facsimile copy or microfiche of NASA and NASA-sponsored documents, those identified by both the symbols # and * from ESA — Information Retrieval Service European Space Agency, 8-10 rue Mario-Nikis, 75738 CEDEX 15, France.

SUBMITTING DOCUMENTS

All users of this abstract service are urged to forward reports to be considered for announcement in *STAR*. This will aid NASA in its efforts to provide the fullest possible coverage of all scientific and technical publications that might support aeronautics and space research and development. If you have prepared relevant reports (other than those you will transmit to NASA, DOD, or DOE through the

usual contract- or grant-reporting channels), please send them for consideration to the NASA Center for AeroSpace Information, 800 Elkridge Landing Road, Linthicum Heights, MD 21090-2934.

Reprints of journal articles, book chapters, and conference papers are also welcome. These will be considered for announcement in *STAR's* companion journal, *NOVA*.

You may specify a particular source to be included in a report announcement if you wish; otherwise the report will be placed on a public sale at the NASA Center for AeroSpace Information. Copyrighted publications will be announced but not distributed or sold.

PURCHASE OF *STAR*

STAR is publicly available on annual subscription from the NASA Center for AeroSpace Information (CASI). The 1994 subscription price of $94.00/domestic, $117.00/foreign will be applied on a prorated basis, through 1994. 1995 *STAR* subscription prices are $100.00/domestic and $125.00/foreign. Single copy prices: $33.00/domestic, $41.00/foreign.

An annual, cumulative *STAR Index* is also available at $54.00/domestic, $65.00/foreign.

STAR is available to registered users on annual subscription from the NASA Center for AeroSpace Information, ATTN: Registration Services, 800 Elkridge Landing Road, Linthicum Heights, MD 21090-2934.

ADDRESSES OF ORGANIZATIONS

British Library Lending Division
Boston Spa, Wetherby, Yorkshire
England

Commissioner of Patents and Trademarks
U.S. Patent and Trademark Office
Washington, DC 20231

Department of Energy
Technical Information Center
P.O. Box 62
Oak Ridge, TN 37830

European Space Agency-
Information Retrieval Service ESRIN
Via Galileo Galilei
00044 Frascati (Rome) Italy

Engineering Sciences Data Unit International
P.O. Box 1633
Manassas, VA 22110

Engineering Sciences Data Unit
International, Ltd.
251-259 Regent Street
London, W1R 7AD, England

Fachinformationszentrum Karlsruhe
Gesellschaft für wissenschaftlich-technische
Information mbH
76344 Eggenstein-Leopoldshafen, Germany

Her Majesty's Stationery Office
P.O. Box 569, S.E. 1
London, England

NASA Center for AeroSpace Information
800 Elkridge Landing Road
Linthicum Heights, MD 21090-2934

National Aeronautics and Space Administration
Scientific and Technical Information Program
(JTT)
Washington, DC 20546-0001

National Technical Information Service
5285 Port Royal Road
Springfield, VA 22161

Pendragon House, Inc.
899 Broadway Avenue
Redwood City, CA 94063

Superintendent of Documents
U.S. Government Printing Office
Washington, DC 20402

University Microfilms
A Xerox Company
300 North Zeeb Road
Ann Arbor, MI 48106

University Microfilms, Ltd.
Tylers Green
London, England

U.S. Geological Survey Library National Center
MS 950
12201 Sunrise Valley Drive
Reston, VA 22092

U.S. Geological Survey Library
2255 North Gemini Drive
Flagstaff, AZ 86001

U.S. Geological Survey
345 Middlefield Road
Menlo Park, CA 94025

U.S. Geological Survey Library
Box 25046
Denver Federal Center, MS914
Denver, CO 80225

CASI PRICE TABLES

(Effective November 1, 1994)

STANDARD PRICE DOCUMENTS

PRICE CODE	NORTH AMERICAN PRICE	FOREIGN PRICE
A01	$ 6.00	$ 12.00
A02	9.00	18.00
A03	17.50	35.00
A04-A05	19.50	39.00
A06-A09	27.00	54.00
A10-A13	36.50	73.00
A14-A17	44.50	89.00
A18-A21	52.00	104.00
A22-A25	61.00	122.00
A99	Call For Price	Call For Price

MICROFICHE

PRICE CODE	NORTH AMERICAN PRICE	FOREIGN PRICE
A01	$ 9.00	$ 18.00
A02	12.50	25.00
A03	17.50	35.00
A04	19.50	39.00
A06	27.00	54.00
A10	36.50	73.00

IMPORTANT NOTICE

CASI Shipping and Handling Charges
U.S.—ADD $3.00 per TOTAL ORDER
Canada and Mexico—ADD $3.50 per TOTAL ORDER
All Other Countries—ADD $7.50 per TOTAL ORDER
Does NOT apply to orders
requesting CASI RUSH HANDLING.
CASI accepts most credit/charge cards.

NASA Center for AeroSpace Information
800 Elkridge Landing Road
Linthicum Heights, MD 21090-2934
Telephone: (301) 621-0390
E-mail: help@sti.nasa.gov
Fax: (301) 621-0134

FEDERAL REGIONAL DEPOSITORY LIBRARIES

ALABAMA

AUBURN UNIV. AT MONTGOMERY LIBRARY
Documents Dept.
7300 University Dr.
Montgomery, AL 36117-3596
(205) 244-3650 Fax: (205) 244-0678

UNIV. OF ALABAMA
Amelia Gayle Gorgas Library
Govt. Documents
Box 870266
Tuscaloosa, AL 35487-0266
(205) 348-6046 Fax: (205) 348-8833

ARIZONA

DEPT. OF LIBRARY, ARCHIVES, AND PUBLIC RECORDS
Federal Documents
Third Floor State Capitol
1700 West Washington
Phoenix, AZ 85007
(602) 542-4121 Fax: (602) 542-4400, 542-4500

ARKANSAS

ARKANSAS STATE LIBRARY
State Library Services
One Capitol Mall
Little Rock, AR 72201
(501) 682-2869

CALIFORNIA

CALIFORNIA STATE LIBRARY
Govt. Publications Section
914 Capitol Mall - P.O. Box 942837
Sacramento, CA 94237-0001
(916) 322-4572 Fax: (916) 324-8120

COLORADO

UNIV. OF COLORADO - BOULDER
Norlin Library
Govt. Publications
Campus Box 184
Boulder, CO 83309-0184
(303) 492-8834 Fax: (303) 492-2185

DENVER PUBLIC LIBRARY
Govt. Publications Dept. BS/GPD
1357 Broadway
Denver, CO 80203
(303) 571-2135

CONNECTICUT

CONNECTICUT STATE LIBRARY
231 Capitol Avenue
Hartford, CT 06106
(203) 566-4971 Fax: (203) 566-3322

FLORIDA

UNIV. OF FLORIDA LIBRARIES
Documents Dept.
Library West
Gainesville, FL 32611-2048
(904) 392-0366 Fax: (904) 392-7251

GEORGIA

UNIV. OF GEORGIA LIBRARIES
Govt. Documents Dept.
Jackson Street
Athens, GA 30602
(404) 542-8949 Fax: (404) 542-6522

HAWAII

UNIV. OF HAWAII
Hamilton Library
Govt. Documents Collection
2550 The Mall
Honolulu, HI 96822
(808) 948-8230 Fax: (808) 956-5968

IDAHO

UNIV. OF IDAHO LIBRARY
Documents Section
Moscow, ID 83843
(208) 885-6344 Fax: (208) 885-6817

ILLINOIS

ILLINOIS STATE LIBRARY
Reference Dept.
300 South Second
Springfield, IL 62701-1796
(217) 782-7596 Fax: (217) 524-0041

INDIANA

INDIANA STATE LIBRARY
Serials/Documents Section
140 North Senate Avenue
Indianapolis, IN 46204
(317) 232-3678 Fax: (317) 232-3728

IOWA

UNIV. OF IOWA LIBRARIES
Govt. Publications Dept.
Washington & Madison Streets
Iowa City, IA 52242
(319) 335-5926 Fax: (319) 335-5830

KANSAS

UNIV. OF KANSAS
Govt. Documents & Map Library
6001 Malott Hall
Lawrence, KS 66045-2800
(913) 864-4660 Fax: (913) 864-5380

KENTUCKY

UNIV. OF KENTUCKY LIBRARIES
Govt. Publications/Maps Dept.
Lexington, KY 40506-0039
(606) 257-3139 Fax: (606) 257-1563, 257-8379

LOUISIANA

LOUISIANA STATE UNIV.
Middleton Library
Govt. Documents Dept.
Baton Rouge, LA 70803
(504) 388-2570 Fax: (504) 388-6992

LOUISIANA TECHNICAL UNIV.
Prescott Memorial Library
Govt. Documents Dept.
305 Wisteria Street
Ruston, LA 71270-9985
(318) 257-4962 Fax: (318) 257-2447

MAINE

TRI-STATE DOCUMENTS DEPOS.
Raymond H. Fogler Library
Govt. Documents & Microforms Dept.
Univ. of Maine
Orono, ME 04469
(207) 581-1680

MARYLAND

UNIV. OF MARYLAND
Hornbake Library
Govt. Documents/Maps Unit
College Park, MD 20742
(301) 454-3034 Fax: (301) 454-4985

MASSACHUSETTS

BOSTON PUBLIC LIBRARY
Govt. Documents Dept.
666 Boylston Street
Boston, MA 02117
(617) 536-5400 ext. 226
Fax: (617) 267-8273, 267-8248

MICHIGAN

DETROIT PUBLIC LIBRARY
5201 Woodward Avenue
Detroit, MI 48202-4093
(313) 833-1440, 833-1409
Fax: (313) 833-5039

LIBRARY OF MICHIGAN
Govt. Documents Unit
P.O. Box 30007
Lansing, MI 48909
(517) 373-0640 Fax: (517) 373-3381

MINNESOTA

UNIV. OF MINNESOTA
Wilson Library
Govt. Publications Library
309 19th Avenue South
Minneapolis, MN 55455
(612) 624-5073 Fax: (612) 626-9353

MISSISSIPPI

UNIV. OF MISSISSIPPI
J.D. Williams Library
Federal Documents Dept.
106 Old Gym Bldg.
University, MS 38677
(601) 232-5857 Fax: (601) 232-5453

MISSOURI

UNIV. OF MISSOURI - COLUMBIA
Ellis Library
Govt. Documents
Columbia, MO 65201
(314) 882-6733 Fax: (314) 882-8044

MONTANA

UNIV. OF MONTANA
Maureen & Mike Mansfield Library
Documents Div.
Missoula, MT 59812-1195
(406)243-6700 Fax: (406) 243-2060

NEBRASKA

UNIV. OF NEBRASKA - LINCOLN
D.L. Love Memorial Library
Documents Dept.
Lincoln, NE 68588
(402) 472-2562

NEVADA

UNIV. OF NEVADA
Reno Library
Govt. Publications Dept.
Reno, NV 89557
(702) 784-6579 Fax: (702) 784-1751

NEW JERSEY

NEWARK PUBLIC LIBRARY
U.S. Documents Div.
5 Washington Street - P.O. Box 630
Newark, NJ 07101-0630
(201) 733-7812 Fax: (201) 733-5648

NEW MEXICO

UNIV. OF NEW MEXICO
General Library
Govt. Publications Dept.
Albuquerque, NM 87131-1466
(505) 277-5441 Fax: (505) 277-6019

NEW MEXICO STATE LIBRARY
325 Don Gaspar Avenue
Santa Fe, NM 87503
(505) 827-3826 Fax: (505) 827-3820

NEW YORK

NEW YORK STATE LIBRARY
Documents/Gift & Exchange Section
Federal Depository Program
Cultural Education Center
Albany, NY 12230
(518) 474-5563 Fax: (518) 474-5786

NORTH CAROLINA

UNIV. OF NORTH CAROLINA - CHAPEL HILL
CB#3912, Davis Library
BA/SS Dept. - Documents
Chapel Hill, NC 27599
(919) 962-1151 Fax: (919) 962-0484

NORTH DAKOTA

NORTH DAKOTA STATE UNIV. LIB.
Documents Office
Fargo, ND 58105
(701) 237-8886 Fax: (701) 237-7138
In cooperation with Univ. of North Dakota, Chester Fritz Library
Grand Forks

OHIO

STATE LIBRARY OF OHIO
Documents Dept.
65 South Front Street
Columbus, OH 43266
(614) 644-7051 Fax: (614) 752-9178

OKLAHOMA

OKLAHOMA DEPT. OF LIBRARIES
U.S. Govt. Information Div.
200 NE 18th Street
Oklahoma City, OK 73105-3298
(405) 521-2502, ext. 252, 253
Fax: (405) 525-7804

OKLAHOMA STATE UNIV.
Edmon Low Library
Documents Dept.
Stillwater, OK 74078
(405) 744-6546 Fax: (405) 744-5183

OREGON

PORTLAND STATE UNIV.
Millar Library
934 SW Harrison - P.O. Box 1151
Portland, OR 97207
(503) 725-3673 Fax: (503) 725-4527

PENNSYLVANIA

STATE LIBRARY OF PENN.
Govt. Publications Section
Walnut St. & Commonwealth Ave. - P.O. Box 1601
Harrisburg, PA 17105
(717) 787-3752

SOUTH CAROLINA

CLEMSON UNIV.
Cooper Library
Public Documents Unit
Clemson, SC 29634-3001
(803) 656-5174 Fax: (803) 656-3025
In cooperation with Univ. of South Carolina, Thomas Cooper Library, Columbia

TENNESSEE

MEMPHIS STATE UNIV. LIBRARIES
Govt. Documents
Memphis, TN 38152
(901) 678-2586 Fax: (901) 678-2511

TEXAS

TEXAS STATE LIBRARY
United States Documents
P.O. Box 12927 - 1201 Brazos
Austin, TX 78711
(512) 463-5455 Fax: (512) 463-5436

TEXAS TECH. UNIV. LIBRARY
Documents Dept.
Lubbock, TX 79409
(806) 742-2268 Fax: (806) 742-1920

UTAH

UTAH STATE UNIV.
Merrill Library & Learning Resources Center, UMC-3000
Documents Dept.
Logan, UT 84322-3000
(801) 750-2684 Fax: (801) 750-2677

VIRGINIA

UNIV. OF VIRGINIA
Alderman Library
Govt. Documents
Charlottesville, VA 22903-2498
(804) 824-3133 Fax: (804) 924-4337

WASHINGTON

WASHINGTON STATE LIBRARY
Document Section
MS AJ-11
Olympia, WA 98504-0111
(206) 753-4027 Fax: (206) 753-3546

WEST VIRGINIA

WEST VIRGINIA UNIV. LIBRARY
Govt. Documents Section
P.O. Box 6069
Morgantown, WV 26506
(304) 293-3640

WISCONSIN

ST. HIST. SOC. OF WISCONSIN LIBRARY
Govt. Publications Section
816 State Street
Madison, WI 53706
(608) 262-2781 Fax: (608) 262-4711
In cooperation with Univ. of Wisconsin - Madison, Memorial Library

MILWAUKEE PUBLIC LIBRARY
Documents Div.
814 West Wisconsin Avenue
Milwaukee, WI 53233
(414) 278-2167 Fax: (414) 278-2137

*U.S. GOVERNMENT PRINTING OFFICE:1994-387-253/00011

SCAN Goes Electronic!

*I*f you have NASA Mail or if you can access the Internet you can get biweekly issues of *SCAN* delivered to your desktop — absolutely *free*!

Electronic SCAN takes advantage of computer technology to alert you to the latest aerospace-related, worldwide scientific and technical information that has been published.

*N*o more waiting while the paper copy is printed and mailed to you. You can review *Electronic SCAN* the same day it is released! And you get all 191 — or any combination of — subject areas of announcements with abstracts to browse at your leisure. When you locate a publication of interest, you can print the announcement or electronically add it to your publication order list.

Electronic SCAN.
Timely.
Flexible.
Complete.
Free!

*S*tart your free access to *Electronic SCAN* today. Over 1,000 announcements of new reports, books, conference proceedings, journal articles . . . and more — delivered to your computer every two weeks.

*F*or instant access via Internet:

ftp.sti.nasa.gov
gopher.sti.nasa.gov
listserv@sti.nasa.gov

*F*or additional information:

e-mail: help@sti.nasa.gov
scan@sti.nasa.gov
(Enter this address on the "To" line. Leave the subject line blank and send. You will receive an automatic reply with instructions in minutes.)
phone: 301-621-0390
fax: 301-621-0134
write: NASA Access Help Desk
NASA STI Program
NASA Center for AeroSpace Information
800 Elkridge Landing Road
Linthicum Heights, MD 21090-2934

NASA STI PROGRAM
SCIENTIFIC & TECHNICAL INFORMATION

SCAN *and* Electronic SCAN *are products of the NASA Scientific & Technical Information Program.*

9/93

POSTMASTER
Address Correction Requested
(Sections 137 and 159 Post Manual)

National Aeronautics and
Space Administration
Code JTT
Washington, DC 20546-0001

Official Business
Penalty for Private Use, $300

BULK RATE
POSTAGE & FEES PAID
NASA
PERMIT No. G-27

NASA

POSTMASTER: If Undeliverable (Section 158 Postal Manual) Do Not Return

Please circulate this publication to other colleagues within your organization.

NASA STI PROGRAM
SCIENTIFIC &
TECHNICAL
INFORMATION

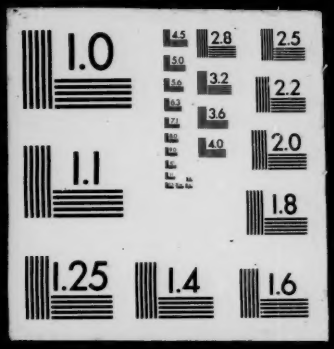
1.0
1.1
1.25
1.4
1.6
1.8
2.0
2.2
2.5
2.8
3.2
3.6
4.0
4.5
5.0
5.6
6.3
7.1
8.0
9.0
10.0
11.2
12.5
14.0
16.0